frontiers | Research Topics

Methods in gastrointestinal cancers

Edited by
Shuyun Rao, Imayavaramban Lakshmanan, Shantibhusan Senapati and Zhendong Jin

Published in
Frontiers in Oncology

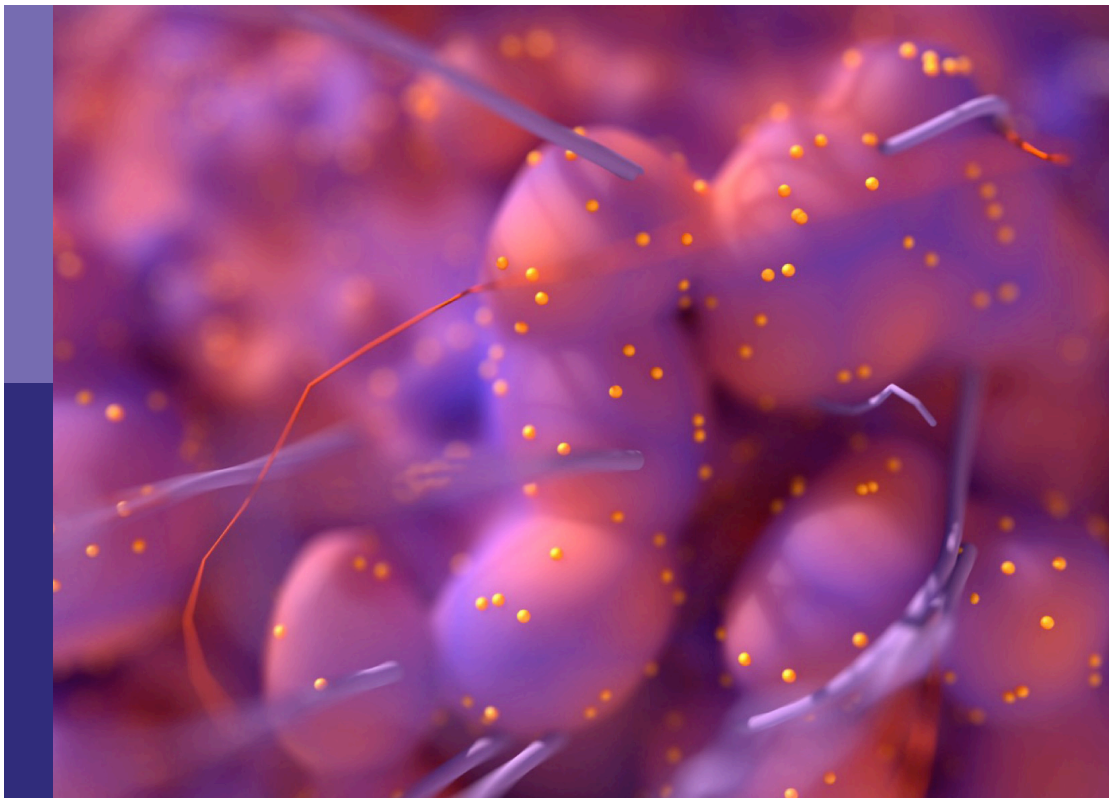

FRONTIERS EBOOK COPYRIGHT STATEMENT

The copyright in the text of individual articles in this ebook is the property of their respective authors or their respective institutions or funders. The copyright in graphics and images within each article may be subject to copyright of other parties. In both cases this is subject to a license granted to Frontiers.

The compilation of articles constituting this ebook is the property of Frontiers.

Each article within this ebook, and the ebook itself, are published under the most recent version of the Creative Commons CC-BY licence. The version current at the date of publication of this ebook is CC-BY 4.0. If the CC-BY licence is updated, the licence granted by Frontiers is automatically updated to the new version.

When exercising any right under the CC-BY licence, Frontiers must be attributed as the original publisher of the article or ebook, as applicable.

Authors have the responsibility of ensuring that any graphics or other materials which are the property of others may be included in the CC-BY licence, but this should be checked before relying on the CC-BY licence to reproduce those materials. Any copyright notices relating to those materials must be complied with.

Copyright and source acknowledgement notices may not be removed and must be displayed in any copy, derivative work or partial copy which includes the elements in question.

All copyright, and all rights therein, are protected by national and international copyright laws. The above represents a summary only. For further information please read Frontiers' Conditions for Website Use and Copyright Statement, and the applicable CC-BY licence.

ISSN 1664-8714
ISBN 978-2-8325-2340-7
DOI 10.3389/978-2-8325-2340-7

About Frontiers

Frontiers is more than just an open access publisher of scholarly articles: it is a pioneering approach to the world of academia, radically improving the way scholarly research is managed. The grand vision of Frontiers is a world where all people have an equal opportunity to seek, share and generate knowledge. Frontiers provides immediate and permanent online open access to all its publications, but this alone is not enough to realize our grand goals.

Frontiers journal series

The Frontiers journal series is a multi-tier and interdisciplinary set of open-access, online journals, promising a paradigm shift from the current review, selection and dissemination processes in academic publishing. All Frontiers journals are driven by researchers for researchers; therefore, they constitute a service to the scholarly community. At the same time, the *Frontiers journal series* operates on a revolutionary invention, the tiered publishing system, initially addressing specific communities of scholars, and gradually climbing up to broader public understanding, thus serving the interests of the lay society, too.

Dedication to quality

Each Frontiers article is a landmark of the highest quality, thanks to genuinely collaborative interactions between authors and review editors, who include some of the world's best academicians. Research must be certified by peers before entering a stream of knowledge that may eventually reach the public - and shape society; therefore, Frontiers only applies the most rigorous and unbiased reviews. Frontiers revolutionizes research publishing by freely delivering the most outstanding research, evaluated with no bias from both the academic and social point of view. By applying the most advanced information technologies, Frontiers is catapulting scholarly publishing into a new generation.

What are Frontiers Research Topics?

Frontiers Research Topics are very popular trademarks of the *Frontiers journals series*: they are collections of at least ten articles, all centered on a particular subject. With their unique mix of varied contributions from Original Research to Review Articles, Frontiers Research Topics unify the most influential researchers, the latest key findings and historical advances in a hot research area.

Find out more on how to host your own Frontiers Research Topic or contribute to one as an author by contacting the Frontiers editorial office: frontiersin.org/about/contact

Methods in gastrointestinal cancers

Topic editors

Shuyun Rao — Feinstein Institute for Medical Research, United States
Imayavaramban Lakshmanan — University of Nebraska Medical Center, United States
Shantibhusan Senapati — Institute of Life Sciences (ILS), India
Zhendong Jin — Second Military Medical University, China

Citation

Rao, S., Lakshmanan, I., Senapati, S., Jin, Z., eds. (2023). *Methods in gastrointestinal cancers*. Lausanne: Frontiers Media SA. doi: 10.3389/978-2-8325-2340-7

Table of contents

09 Editorial: Methods in gastrointestinal cancers
Yue Liu, Xinyue Wang, Jingyuan Wang, Chang Wu, Wanshun Li, Qiuyue Song and Zhendong Jin

11 Methods of a New Chronic Pancreatitis and Spontaneous Pancreatic Cancer Mouse Model Using Retrograde Pancreatic Duct Injection of Dibutyltin Dichloride
Deyu Zhang, Wanshun Li, Meiqi Wang, Hua Yin, Chuanchao Xia, Keliang Li and Haojie Huang

20 A Prediction Model Intended for Exploratory Laparoscopy Risk Stratification in Colorectal Cancer Patients With Potential Occult Peritoneal Metastasis
Yuanxin Zhang, Xiusen Qin, Yang Li, Xi Zhang, Rui Luo, Zhijie Wu, Victoria Li, Shuai Han, Hui Wang and Huaiming Wang

29 Colon Sparing Endoscopic Full-Thickness Resection for Advanced Colorectal Lesions: Is It Time for Global Adoption?
Zhong-Wei Wu, Chao-Hui Ding, Yao-Dong Song, Zong-Chao Cui, Xiu-Qian Bi and Bo Cheng

36 Neoadjuvant Chemoradiotherapy and Surgery for Esophageal Squamous Cell Carcinoma Versus Definitive Chemoradiotherapy With Salvage Surgery as Needed: The Study Protocol for the Randomized Controlled NEEDS Trial
Magnus Nilsson, Halla Olafsdottir, Gabriella Alexandersson von Döbeln, Fernanda Villegas, Giovanna Gagliardi, Mats Hellström, Qiao-Li Wang, Hemming Johansson, Val Gebski, Jakob Hedberg, Fredrik Klevebro, Sheraz Markar, Elizabeth Smyth, Pernilla Lagergren, Ghazwan Al-Haidari, Lars Cato Rekstad, Eirik Kjus Aahlin, Bengt Wallner, David Edholm, Jan Johansson, Eva Szabo, John V. Reynolds, CS Pramesh, Naveen Mummudi, Amit Joshi, Lorenzo Ferri, Rebecca KS Wong, Chris O'Callaghan, Jelena Lukovic, Kelvin KW Chan, Trevor Leong, Andrew Barbour, Mark Smithers, Yin Li, Xiaozheng Kang, Feng-Ming Kong, Yin-Kai Chao, Tom Crosby, Christiane Bruns, Hanneke van Laarhoven, Mark van Berge Henegouwen, Richard van Hillegersberg, Riccardo Rosati, Guillaume Piessen, Giovanni de Manzoni and Florian Lordick

47 The Key Role of microRNAs in Initiation and Progression of Hepatocellular Carcinoma
Suliman Khan, De-Yu Zhang, Ji-Yu Zhang, Mian Khizar Hayat, Jingli Ren, Safyan Nasir, Muhammad Fawad and Qian Bai

58 Research trends of artificial intelligence in pancreatic cancer: a bibliometric analysis
Hua Yin, Feixiong Zhang, Xiaoli Yang, Xiangkun Meng, Yu Miao, Muhammad Saad Noor Hussain, Li Yang and Zhaoshen Li

71 Role of intraoperative patients positioning in endoscopic full-thickness resection of large gastric tumors under general anesthesia
Li-Jun Zhou, Fei Xing, Dan Chen, Yan-Na Li and Shoaib Mohammad Rafiq

75 The clinical impact of endoscopic ultrasound-guided fine-needle aspiration on the patients with low-risk pancreatic cystic lesions
Shubo Pan, Jie Liu, Jiefang Guo, Qilin Zhu, Liangjing Wang and Xiaohua Shi

84 Application of deep learning in the real-time diagnosis of gastric lesion based on magnifying optical enhancement videos
Mingjun Ma, Zhen Li, Tao Yu, Guanqun Liu, Rui Ji, Guangchao Li, Zhuang Guo, Limei Wang, Qingqing Qi, Xiaoxiao Yang, Junyan Qu, Xiao Wang, Xiuli Zuo, Hongliang Ren and Yanqing Li

94 Hepatoid adenocarcinoma of the duodenal papilla with hepatic metastases: A case report and literature review
Lu Han, Naiqing Ding, Li Li, Xiao Wei, Jing Hu, Baorui Liu and Xiaoping Qian

101 The global research status and trends of the application of endoscopic ultrasonography in pancreatic tumors over the last decades: A bibliometric study
Chuanchao Xia, Hua Yin, Kecheng Zhang, Zhenhuan Wang, Xiaoli Yang and Haojie Huang

115 Multi-center verification of the influence of data ratio of training sets on test results of an AI system for detecting early gastric cancer based on the YOLO-v4 algorithm
Tao Jin, Yancai Jiang, Boneng Mao, Xing Wang, Bo Lu, Ji Qian, Hutao Zhou, Tieliang Ma, Yefei Zhang, Sisi Li, Yun Shi and Zhendong Yao

127 Advances in endoscopic resection techniques of small gastric tumors originating from the muscularis propria
Suliman Khan, Xiaona Cui, Safyan Nasir, Shoaib Mohammad Rafiq, Bo Qin and Qian Bai

132 Case report: New subtype of gastric adenocarcinoma arising from an *H. pylori* infection-negative stomach: Foveolar epithelium and mucous neck cell-mixed type adenocarcinoma
Xuemei Liu, Xinglong Wu, Jiaxing Zhu, Kazuyoshi Yagi, Yoichi Ajioka, Shuji Terai, Kenichi Mizuno, Hongping Li, Biguang Tuo and Lianjun Di

139 Patient-reported gastrointestinal symptoms following surgery for gastric cancer and the relative risk factors
Rui Xu, Qiong Gu, Shuomeng Xiao, Ping Zhao and Zhi Ding

147 Single-cell sequencing and establishment of an 8-gene prognostic model for pancreatic cancer patients
Xiao Yu, Qiyao Zhang, Shuijun Zhang, Yuting He and Wenzhi Guo

160 The reasonable therapeutic modality for biliary duct-to-duct anastomotic stricture after liver transplantation: ERCP or PTC?
Hu Bowen, Guo Wenzhi, Wen Peihao, Shi Jihua and Zhang Shuijun

168 The global research and emerging trends in autophagy of pancreatic cancer: A bibliometric and visualized study
Mingyang Song, Qin Lu, Min Xu, Yajie Li, Yawen Zhao, Chen Gong and Xilong Ou

184 Utility of dual-layer spectral-detector CT imaging for predicting pathological tumor stages and histologic grades of colorectal adenocarcinoma
Weicui Chen, Yongsong Ye, Daochun Zhang, Liting Mao, Lei Guo, Hanliang Zhang, Xiaohua Du, Weiwei Deng, Bo Liu and Xian Liu

196 Development and validation of lymph node ratio-based nomograms for primary duodenal adenocarcinoma after surgery
Jingxiang Shi, Sifan Liu, Jisen Cao, Shigang Shan, Jinjuan Zhang and Yijun Wang

209 Laparoscopic resection is not superior to endoscopic resection for relative small gastric gastrointestinal stromal tumors: A propensity score-matched study
De-Liang Li, Yang-Yang Zhou, Ji-Yu Zhang, Dan Liu, Li-Xia Zhao and Bing-Rong Liu

216 A framework for identification and classification of liver diseases based on machine learning algorithms
Huanfei Ding, Muhammad Fawad, Xiaolin Xu and Bowen Hu

223 Targeting the regulation of aberrant protein production pathway in gastrointestinal cancer treatment
Hiromichi Sato, Kazuki Sasaki, Tomoaki Hara, Shogo Kobayashi, Yuichiro Doki, Hidetoshi Eguchi, Taroh Satoh and Hideshi Ishii

229 The clinical outcomes of extended resections in patients with IV stage gallbladder cancers: A retrospective study from a large tertiary center
Kecheng Zhang, Hu Liu, Yongyang Zhao and Baohua Zhang

240 Robotic-assisted vs non-robotic traction techniques in endoscopic submucosal dissection for malignant gastrointestinal lesions
Zhao Meng, Zhanghua Huang, Bingli Deng, Liuming Ling, Yaowen Ning and Shoaib Mohammed Rafiq

245 Super-enhancers in esophageal carcinoma: Transcriptional addictions and therapeutic strategies
Yang Shi, Meiqi Wang, Dan Liu, Saif Ullah, Xing Ma, Huiyu Yang and Bingrong Liu

257 Advancing endoscopic traction techniques in endoscopic submucosal dissection
Suliman Khan, Faisal S. Ali, Saif Ullah, Xue- Huang and Hongyu Li

264 The role of the endoscopic grading of gastric intestinal metaplasia in assessing gastric cancer risk: A systematic review and meta-analysis
Shuangshuang Fang, Yuhan Fu, Sijing Du, Lin Wang, Xiangli Qing, Xiaoying Luo, Gengqing Song, Yang Yang and Wei Wei

272 Endoscopic resection of upper gastrointestinal lymphangioma: A single-center experience
Ziyu Shi, Xue Huang, Keliang Li, Qiuyue Tu, Dan Liu, Lixia Zhao, Huiyu Yang, Deliang Li, Yue Zhao, Jiyu Zhang, Muhan Li and Bingrong Liu

282 Study protocol for HGCSG1801: A multicenter, prospective, phase II trial of second-line FOLFIRI plus aflibercept in patients with metastatic colorectal cancer refractory to anti-EGFR antibodies
Hiroshi Nakatsumi, Yoshito Komatsu, Tetsuhito Muranaka, Satoshi Yuki, Yasuyuki Kawamoto, Kazuaki Harada, Masayoshi Dazai, Miki Tateyama, Yusuke Sasaki, Takuto Miyagishima, Yasushi Tsuji, Masaki Katagiri, Michio Nakamura, Susumu Sogabe, Kazuteru Hatanaka, Takashi Meguro, Tomoe Kobayashi, Atsushi Ishiguro, Osamu Muto, Yoshiaki Shindo, Masahito Kotaka, Takayuki Ando, Ryo Takagi, Naoya Sakamoto and Yu Sakata

289 The prognostic value and immunological role of angiogenesis-related patterns in colon adenocarcinoma
Weijie Sun, Ying Xu, Baolong Zhao, Min Zhao, Jiaying Chen, Yimin Chu and Haixia Peng

306 Integrated network pharmacology and experimental verification to investigate the mechanisms of YYFZBJS against colorectal cancer *via* CDK1/PI3K/Akt signaling
Jinxiao Li, Fangyuan Zhou, Luorui Shang, Na Liu, Yuhan Liu, Mengqi Zhang, Shuhan Wang and Shenglan Yang

322 Diagnosis and management of gastroenteropancreatic neuroendocrine neoplasms by nuclear medicine: Update and future perspective
Xing Ma, Ying Ding, Wenliang Li, Qiang Li and Hui Yang

327 Oncolytic virus: A catalyst for the treatment of gastric cancer
Junqing Wang, Linyong Du and Xiangjian Chen

349 Efficacy and feasibility of snare-assisted endoscopic resection of small submucosal gastric tumors: A retrospective analysis
Fei Zhao, Zhenzhen Liu, Anwei Wei, Wei Wang, Na Xu, and Xuanmei Pu

355 Cost-effectiveness analysis of sintilimab plus chemotherapy for advanced or metastatic esophageal squamous cell carcinoma
Maojin You, Yufan Huang, Zhongjie Cai, Qingfeng Wu, Wei Zhu, Ying He and Ruijia Chen

364 Application of machine learning techniques in real-world research to predict the risk of liver metastasis in rectal cancer
Binxu Qiu, Xiao hu Su, Xinxin Qin and Quan Wang

376 Tailoring the clinical management of colorectal cancer by ^{18}F-FDG PET/CT
Yang Shi, Meiqi Wang, Jiyu Zhang, Zheng Xiang, Can Li, Jingjing Zhang and Xing Ma

384 The reduction of ^{18}F-FDG uptake ability of tumor tissue after neoadjuvant chemoradiotherapy in locally advanced rectal cancer can effectively reflect the degree of tumor regression
Fengpeng Wu, Xiaoxiao Zhang, Congrong Yang, Kanghua Wang, Linlin Xiao, Chaoxi Zhou, Xinming Zhao and Guiying Wang

394 A system based on deep convolutional neural network improves the detection of early gastric cancer
Jie Feng, Shang rui Yu, Yao ping Zhang, Lina Qu, Lina Wei, Peng fei Wang, Li juan Zhu, Yanfeng Bao, Xiao gang Lei, Liang liang Gao, Yan hu Feng, Yi Yu and Xiao jun Huang

405 Constructing and validating of m6a-related genes prognostic signature for stomach adenocarcinoma and immune infiltration: Potential biomarkers for predicting the overall survival
Jing Yang, Zixuan Wu, Xiaoxi Wu, Siya Chen, Xinhua Xia and Jianguo Zeng

419 Artificial intelligence applicated in gastric cancer: A bibliometric and visual analysis *via* CiteSpace
Guoyang Zhang, Jingjing Song, Zongfeng Feng, Wentao Zhao, Pan Huang, Li Liu, Yang Zhang, Xufeng Su, Yukang Wu, Yi Cao, Zhengrong Li and Zhigang Jie

438 Comprehensive analysis of mixed neuroendocrine non-neuroendocrine neoplasms (MiNENs): A SEER database analysis of 767 cases
Huixin Song, Sen Yang, Yalu Zhang, Yuze Hua, Jorg Kleeff, Qiaofei Liu and Quan Liao

448 Lobaplatin-based prophylactic hyperthermic intraperitoneal chemotherapy for T4 gastric cancer patients: A retrospective clinical study
Yuxin Zhong, Wenzhe Kang, Haitao Hu, Weikun Li, Jing Zhang and Yantao Tian

455 A comparison of machine learning models and Cox proportional hazards models regarding their ability to predict the risk of gastrointestinal cancer based on metabolic syndrome and its components
Tao Thi Tran, Jeonghee Lee, Madhawa Gunathilake, Junetae Kim, Sun-Young Kim, Hyunsoon Cho and Jeongseon Kim

465 Effect of multimodal chemotherapy on survival of gastric cancer with liver metastasis – a population based analysis
Xinghui Li, Zhiqiang Chen, Yue Zhang, Hong Zhang, Haiyan Niu, Cheng Zheng, Xiaoying Jing, Hui Qiao, Guanhua Wang and Wenjun Yang

476 Analysis of risk factors for lymph node metastasis and prognosis study in patients with early gastric cancer: A SEER data-based study
Jinzhou Li, Ting Cui, Zeping Huang, Yanxi Mu, Yalong Yao, Wei Xu, Kang Chen, Haipeng Liu, Wenjie Wang and Xiao Chen

489 KRAS-specific antibody binds to KRAS protein inside colorectal adenocarcinoma cells and inhibits its localization to the plasma membrane
Kuen Kuen Lam, Yee Syuen Low, Michelle Lo, Michelle Wong, Choong Leong Tang, Emile Tan, Aik Yong Chok, Isaac Seow-En, Siew Heng Wong and Peh Yean Cheah

499 Tissue clearing and immunostaining to visualize the spatial organization of vasculature and tumor cells in mouse liver
Nicola Frenkel, Susanna Poghosyan, Jan Willem van Wijnbergen, Lotte van den Bent, Liza Wijler, André Verheem, Inne Borel Rinkes, Onno Kranenburg and Jeroen Hagendoorn

509 Predictive value of intratumoral-metabolic heterogeneity derived from ^{18}F-FDG PET/CT in distinguishing microsatellite instability status of colorectal carcinoma
Li Zhang, Yu Liu, Ying Ding, Yinqian Deng, Huanyu Chen, Fan Hu, Jun Fan, Xiaoli Lan and Wei Cao

frontiers | Frontiers in Oncology

TYPE Editorial
PUBLISHED 19 April 2023
DOI 10.3389/fonc.2023.1193964

Check for updates

OPEN ACCESS

EDITED AND REVIEWED BY
Liang Qiao,
Westmead Institute for Medical Research, Australia

*CORRESPONDENCE
Zhendong Jin
zhendongjin@126.com

†These authors share first authorship

SPECIALTY SECTION
This article was submitted to Gastrointestinal Cancers: Colorectal Cancer, a section of the journal Frontiers in Oncology

RECEIVED 26 March 2023
ACCEPTED 06 April 2023
PUBLISHED 19 April 2023

CITATION
Liu Y, Wang X, Wang J, Wu C, Li W, Song Q and Jin Z (2023) Editorial: Methods in gastrointestinal cancers.
Front. Oncol. 13:1193964.
doi: 10.3389/fonc.2023.1193964

COPYRIGHT
© 2023 Liu, Wang, Wang, Wu, Li, Song and Jin. This is an open-access article distributed under the terms of the Creative Commons Attribution License (CC BY). The use, distribution or reproduction in other forums is permitted, provided the original author(s) and the copyright owner(s) are credited and that the original publication in this journal is cited, in accordance with accepted academic practice. No use, distribution or reproduction is permitted which does not comply with these terms.

Editorial: Methods in gastrointestinal cancers

Yue Liu†, Xinyue Wang†, Jingyuan Wang†, Chang Wu, Wanshun Li, Qiuyue Song and Zhendong Jin*

Department of Gastroenterology, Changhai Hospital, Shanghai, China

KEYWORDS

detection, respectively artificial intelligence, early detection of cancer, artificial intelligence, gastrointestinal cancers

Editorial on the Research Topic
Methods in gastrointestinal cancers

As editors of this Research Topic, it was our pleasure to review a wide range of interesting and innovative articles in the field of methods in gastrointestinal cancers. In this Editorial, we summarize the findings and perspectives regarding the application of artificial intelligence (AI) in methods in gastrointestinal cancers.

Artificial intelligence is a new technology in which researchers design and create relevant algorithms, process relevant data, and draw corresponding conclusions without human assistance. We have summarized the perspectives detailed within each of the accepted articles about AI.

First, we consider the high incidence of gastric cancer (GC), which has increased the global burden. As it is frequently diagnosed at a late stage, gastric cancer has a high mortality rate. EUS, MRI, CT, PET-CT, and other imaging examination techniques are widely used in the diagnosis, treatment, and prognosis of gastric cancer. With the development of endoscopic technology and the increasing awareness of early screening among populations, the cure rate of most early gastric cancers has been significantly improved compared with the previous period, but the survival rate of advanced gastric cancer is still very low. Thus, for gastric cancer, early detection, diagnosis, and treatment play a very important role in reducing mortality and improving survival. However, owing to some objective reasons, such as the lack of professional knowledge and experience of endoscopists, the final diagnostic accuracy is biased. At the same time, through its continuous development, the diagnostic advantages of AI are constantly expanding compared with traditional imaging techniques. Thus, by reading the literature published on this topic, we have found that convolutional neural networks and deep learning are the current hot spots of AI in gastric cancer diagnosis and differential diagnosis. Feng et al. constructed an auxiliary EGC detection system based on DCNN and compared the diagnostic abilities of DCNN and endoscopists. DCNN has good diagnostic sensitivity and rapid diagnosis characteristics, the goal is to provide solutions. In the future, the use of AI technology may help endoscopists find more cancers earlier, thus greatly reducing the general incidence in the population. Considering the great potential for the clinical application of AI, imaging examination combined with AI will continue to be a research hot spot in the future.

Second, we consider pancreatic cancer (PC), which is common in the digestive system. PC is often only found when it is advanced; therefore, it has a high fatality rate and is known as the "king of cancers". Machine learning techniques have shown broad application potential in the diagnosis, differential diagnosis, treatment evaluation, and prediction of pancreatic diseases. For example, (1) the application of AI with malignant pancreatic tumors mainly established the machine learning model from Stephen, which integrated the free DNA fragment pattern of the whole genome, with detection sensitivity ranging from 57% to more than 99% and a specificity of 98%.[2] This research makes the early screening and diagnosis of pancreatic malignancies possible. (Yin et al.) The technology combined with AI can shorten diagnosis time and improve diagnosis accuracy compared with traditional CT/MRI and other imaging techniques. (Qiu et al.) In terms of treating malignant pancreatic tumors, the role played by AI is mainly focused on predicting the possibility of surgery and the prognosis of patients. With the continuous development of algorithm technology, it is possible to predict postoperative complications in patients. (4) EUS-FNA/B has played an important role in the diagnosis of pancreatic malignancies. The rapid development of AI means it can be combined with EUS-FNA/B to reduce or even avoid misdiagnosis caused by the inadequate diagnostic ability of physicians in some areas with underdeveloped technologies. In the future, as algorithms continue to improve, AI may be used as a screening tool for pancreatic EUS-FNA/B specimens. (5) AI can also be used in the treatment of malignant pancreatic tumors. Based on an in-depth analysis of clinical examinations and inspection results, it is possible to carry out personalized treatment for patients with malignant pancreatic tumors.

Third, we consider rectal cancer, which has one of the highest incidences of malignant tumors in the world. Owing to the lack of awareness of patients during physical examination, rectal cancer is often diagnosed late. Even after the radical resection of rectal cancer, some patients will still develop liver metastases. Rectal cancer with liver metastasis often has a poor prognosis and a low 5-year survival rate. Owing to its incidence increasing year by year, rectal cancer has become one of the major problems that threaten human health. The liver is the most common site of distant metastasis of rectal cancer. The presence or absence of liver metastases is often a major consideration in treatment regimens. Through a retrospective study, Qiu et al. developed an XGB-based machine learning model to predict the risk of liver metastases in rectal cancer, which used a machine learning algorithm that combined seven clinical and pathological features.

It will be fascinating to observe the development of AI. Although it may face many challenges in the future, AI has shown great potential for the diagnosis and treatment of diseases, including gastrointestinal cancer.

Author contributions

Article writing and draft manuscript preparation: YL, XYW, JYW. Article modification: CW, WSL, QYS. All authors contributed to the article and approved the submitted version.

Conflict of interest

The authors declare that the research was conducted in the absence of any commercial or financial relationships that could be construed as a potential conflict of interest.

Publisher's note

All claims expressed in this article are solely those of the authors and do not necessarily represent those of their affiliated organizations, or those of the publisher, the editors and the reviewers. Any product that may be evaluated in this article, or claim that may be made by its manufacturer, is not guaranteed or endorsed by the publisher.

frontiers | Frontiers in Oncology

ORIGINAL RESEARCH
published: 06 July 2022
doi: 10.3389/fonc.2022.947133

Methods of a New Chronic Pancreatitis and Spontaneous Pancreatic Cancer Mouse Model Using Retrograde Pancreatic Duct Injection of Dibutyltin Dichloride

Deyu Zhang[1], *Wanshun Li*[1], *Meiqi Wang*[2], *Hua Yin*[1], *Chuanchao Xia*[1], *Keliang Li*[2] *and Haojie Huang*[1]*

[1] Department of Gastroenterology, First Affiliated Hospital, Naval Medical University, Shanghai, China, [2] Academy of Medical Sciences, Zhengzhou University, Zhengzhou, China

OPEN ACCESS

Edited by:
Zhendong Jin,
Second Military Medical University, China

Reviewed by:
Xilong Ou,
Southeast University, China
Qiuxian Zheng,
Zhejiang University, China

***Correspondence:**
Haojie Huang
huanghaojie@smmu.edu.cn

Specialty section:
This article was submitted to Gastrointestinal Cancers: Hepato Pancreatic Biliary Cancers, a section of the journal Frontiers in Oncology

Received: 18 May 2022
Accepted: 08 June 2022
Published: 06 July 2022

Citation:
Zhang D, Li W, Wang M, Yin H, Xia C, Li K and Huang H (2022) Methods of a New Chronic Pancreatitis and Spontaneous Pancreatic Cancer Mouse Model Using Retrograde Pancreatic Duct Injection of Dibutyltin Dichloride. Front. Oncol. 12:947133. doi: 10.3389/fonc.2022.947133

The current study aimed to develop a new chronic pancreatitis and spontaneous pancreatic cancer model on C57/BL6 mouse through retrograde pancreatic duct injection of dibutyltin dichloride (DBTC) and explore its basic pathological changes as compared to the previous published chronic pancreatitis model through tail vein injection of DBTC with alcohol drinking. C57/BL6 mice were randomly divided into 3 groups: CG (control group; n = 15), VG (tail vein injection of DBTC (8 mg/kg) with 10% alcohol drinking group; n = 20), and PG (retrograde pancreatic duct injection of DBTC group (1 mg/kg); n = 30). Five mice in each group were sacrificed at a specific time point after the first treatment. The pathological section was observed. The activities of amylase, bilirubin, and hyaluronic acid in serum were determined. The expression of fibronectin, COL1A1, α-SMA, MMP-1, and TIMP-1 in the pancreas was assayed. Severe fibrosis of the pancreas with inflammatory cell infiltration could be observed on day 21 in the PG. In the VG, slight fibrosis of the pancreas with inflammatory cell infiltration was observed on day 28. There were significant differences in serum amylase, bilirubin, and hyaluronic acid levels between the PG and VG. The protein level of COL1A1 and α-SMA significantly increased in the PG. The mRNA expression of TIMP-1 is upregulated and the MMP-1 mRNA level is downregulated in the PG. Finally, typical neoplastic pathological change is significantly obvious in the PG. In conclusion, we established and validated a new chronic pancreatitis (CP) and spontaneous pancreatic cancer mouse model through retrograde injection of DBTC into the pancreatic duct. Previously reported mouse model through tail vein injection of DBTC with alcohol drinking could not cause obvious CP and neoplastic pathological change in mice.

Keywords: pancreatic cancer, DBTC, pancreatic disease, chronic pancreatitis, mouse model

INTRODUCTION

Chronic pancreatitis (CP) is a pancreatic disease mainly manifested by upper abdominal pain, diabetes, malnutrition, and diarrhea (1, 2). Additionally, CP is a significant pathogenic factor for pancreatic cancer. The main causes of CP are hereditary susceptibility, biliary tract obstruction, alcohol abuse, and hyperlipidemia (3, 4). The global morbidity of CP has surged to around 5 cases per 10,000 persons in 2019. It is vital for us to identify the underlying pathophysiology and to develop specific new therapeutic methods for CP and CP-induced pancreatic cancer (5).

The major pancreatic pathology of CP is characterized by extensive interstitial fibrosis, continuous inflammatory cell infiltration, and irreversible endocrine function damage. It has been shown that activated pancreatic stellate cells are the main source of pancreatic extracellular matrix proteins and the main effector cells of pancreatic fibrosis (6). Human CP tissue could be difficult to be acquired because surgery cannot be used to treat CP (5). In addition, chronic pancreatic inflammation is an obvious risk factor for the occurrence of pancreatic cancer, and the same fibro-inflammatory reaction is observed in pancreatic cancer, together with a loss of normal pancreatic cells.

Mouse models are commonly employed to study the progression of CP and pancreatic cancer, with genetic and pharmacological tools used to elucidate the cellular and cellular interactions within pancreatic tumors (7). The widely used CP and spontaneous pancreatic cancer mouse model is the intermittent intraperitoneal injection of caerulein. Caerulein, a peptide analog of cholecystokinin (CCK) and gastrin, stimulates pancreatic exocrine secretion and increases pancreatic proteolytic enzyme secretion to levels that cause injury of pancreatic acinar (8). In the 1990s, Van Laethem et al. reported the successful use of a 4-week intermittent intraperitoneal caerulein injection to induce a typical CP model (9). This method is consistent with the pathogenesis of CP and is widely used to investigate the pathogenesis and pathophysiological changes of CP (10). However, caerulein is expensive, so there is still a need for another effective CP and a spontaneous pancreatic cancer mouse model to corroborate the related research.

Tail injection of dibutyltin dichloride (DBTC) could be another feasible way to establish a CP mouse model. In early 1999, Merkord et al. illustrated that tail injection of DBTC with alcohol drinking could successfully induce CP in rats (11). However, the feasibility of the use of tail injection of DBTC in mice remains unclear, and some results seem to be contradictory. On the one hand, Zhang et al. reported the successful establishment of the CP mouse model through tail injection of DBTC with alcohol drinking (12). On the other hand, Lütt et al. illustrated that tail injection of DBTC with alcohol drinking could not induce CP in mice (13). Furthermore, only the caerulein-induced CP mouse model was confirmed to be used as a spontaneous pancreatic cancer mouse model. The viability of other CP models to be used as a spontaneous pancreatic cancer mouse model has not been clarified (14).

In our current study, a viable novel CP and spontaneous pancreatic cancer mouse model through retrograde injection of DBTC in pancreatic duct on mice was established and analyzed. In addition, we also analyzed the feasibility of the contradictory CP mouse model, which is a tail injection of DBTC with alcohol drinking, and we compared the efficacy and neoplastic changes between these two methods.

MATERIALS AND METHODS

Genetically Engineered Mice

LSL-K-Ras^{G12D} male mice, which possess the conditional knock-in mutant K-Ras^{G12D}, were obtained from Pro. Craig D. Logsdon (15). Ela-CreERT mice, which express tamoxifen-regulated CreERT specifically in pancreatic acinar cells under the control of a full-length elastase gene promoter, were developed in our laboratory as previously described (16). For targeted expression of K-Ras^{G12D} in pancreatic acinar cells, LSL-K-Ras^{G12D} mice were bred with Ela-CreERT mice to generate LSL-K-Ras/Ela-CreERT double-transgenic mice (acinar-Ras mice). Before experiments, tamoxifen was orally administered to these mice to activate Cre recombination in pancreatic acinar cells. The mice were raised in the Gastroenterology Laboratory of Changhai Hospital with standard food and a specified water supply.

Chronic Pancreatitis Induction

The mice were randomly divided into 3 groups: CG (control group), VG (tail vein injection group), and PG (retrograde pancreatic duct injection group) (n = 60). DBTC was solved in 60% ethanol, 20% glycerin, and 20% physiological saline. The DBTC concentration in the tail vein was 3.2 μg/μl. The DBTC concentration of retrograde pancreatic duct injection was 0.5 μg/μl. Mice in the VG were fed with 10% alcohol after DBTC injection in the tail vein. Control mice were only injected with solvent (60% ethanol, 20% glycerin, and 20% normal saline) through the retrograde pancreatic duct.

Preparation of Serum and Tissue Samples

Serum samples were collected from the inner canthus vein and stored at −80°C for the detection of amylase, hyaluronic acid, and bilirubin. The histological morphology of the pancreas was observed by H&E staining, and the degree of pancreatic fibrosis was observed by Masson staining. F4/80 and CD3 were detected by immunohistochemistry, and fibronectin (FN) was detected by immunofluorescence. COL1A1 and α-SMA contents were detected by Western blotting. The expression of matrix metalloproteinase-1 (MMP-1) mRNA and tissue inhibitor of metalloproteinases-1 (TIMP-1) mRNA was detected by real-time PCR.

Histological Analysis

The pancreas of mice was removed, then fixed with 4% paraformaldehyde, embedded in paraffin, and finally sectioned (5 μm). H&E and Masson staining processes were performed on

the sections of the specimens. The morphological changes in the pancreas and the degree of fibrosis were observed by light microscopy.

Western Blotting

Pancreatic tissues were collected and dissolved in radioimmunoprecipitation assay (RIPA) buffer and then incubated at 4°C. The solution was centrifuged at 14,000*g* for 10 min at 4°C, and the supernatant was collected. The protein concentration was determined by a standard protein assay kit. The samples were boiled at 98°C for 8 min. Equal amounts of protein (20 μg) were added to the chamber, then subjected to sodium dodecyl sulfate (SDS)–polyacrylamide gel electrophoresis, and blotted to polyvinylidene difluoride (PVDF) membranes. The membranes were blocked in 3% bovine serum albumin (BSA) for 30 min at 4°C and then incubated with an antibody against α-SMA (catalog # 56856, Cell Signaling Technology, Danvers, MA, USA) and COL1 (catalog # 66948, Cell Signaling Technology). The size of detected bands was quantified by using ImageJ software.

Immunohistochemistry

Paraffin-embedded pancreas tissue sections were dewaxed and rehydrated twice in PBS for 15 min. The sections were incubated with 0.3% H_2O_2 for 15 min to block endogenous peroxidases, washed twice in PBS, then incubated with 30 g/L of BSA for 10 min to prevent non-specific binding of antibodies, and then incubated with anti-CD3 (catalog # 78588, Cell Signaling Technology) or anti-F4/80 (catalog # 25514, Cell Signaling Technology). Finally, diaminobenzidine (DAB) was added as chromogen followed by hematoxylin. The images were observed by a light microscope, and the positive areas were analyzed by ImageJ software.

Immunofluorescence Assay

For immunofluorescence, slides of pancreas tissue were incubated with anti-FN (catalog # 72943, Cell Signaling Technology) and then counterstained with DAPI. Finally, the slides were observed by a fluorescence microscope.

Polymerase Chain Reaction

The RNA from pancreatic tissue was isolated with TRIzol reagent (Invitrogen, Carlsbad, CA, USA). The concentration of the RNA was analyzed by using a NanoDrop 1000 spectrophotometer (Thermo Fisher, Waltham, MA, USA) and then transcribed into cDNA by using a high-capacity cDNA reverse transcription kit (Life Technologies, Carlsbad, CA, USA) and amplified. Primer sequences, number of cycles, and annealing temperature are listed in **Table S1**. The expression levels were transformed into standard tubulin content, calculated by the $2^{-\Delta\Delta Ct}$ method.

RESULTS

Surgical Method and Pancreatic Weight Change

Surgical methods of retrograde pancreatic duct injection of DBTC (PG) are shown in **Figure 1A**. In brief, after general anesthesia and laparotomy, a fine catheter was inserted into the biliary duct to puncture the intestinal wall. Then, the clip was placed to block the distal biliary duct. A surgical suture was used to secure the proximal biliary duct with a fine catheter, and then infusion was started. Intraoperative photographs of retrograde pancreatic duct injection of DBTC (during infusion and after infusion) are shown in **Figures 1B, C**. The PG shows more significant pancreatic atrophy than the VG in **Figure 1D**.

Histological Change of Pancreas Between PG and VG

The histological features of the pancreas of mice in the PG were significantly changed to pancreatic atrophy, inflammatory cell infiltration, and pancreatic tissue fibrosis in 4 weeks (**Figure 2A**). After injection, pancreatic edema immediately appeared in the PG. On day 3, a partial inflammatory cell was observed, dominated by neutrophils and lymphocytes. On day 7, inflammatory cell infiltration became more obvious, and pancreatic cell necrosis also appeared. On day 14, the pancreas parenchyma showed obvious necrosis, with macrophages infiltrating and replacing part of the pancreatic duct epithelial cells. On day 28, pancreatic tissue was extensively replaced by interstitial fibers and connective tissue deposition. However, mice in the VG only showed mild pancreatic edema on day 14 (**Figure 2B**). On day 28, slight inflammatory cell infiltration and local fibrosis were observed. On day 42, although the degree of pancreatic tissue fibrosis was aggravated, it was still far less than that in the PG. Compared with the control group, Masson staining showed a significant increase in collagen deposition in the PG and only a slight increase in the VG, in each respective time point of our study.

Changes in Serum Amylase, Bilirubin, and Hyaluronic Acid Contents Between PG and VG

Amylase activity of mice in the PG after injection increased sharply within a day and then began to decline, but still higher than normal, and after 21 days, with extensive fibrosis of the pancreas and massive destruction, amylase activity decreased sharply, and the amylase activity of mice in the VG increased slightly from 1 to 14 days and then decreased after 14 days (**Figure 3A**). The bilirubin levels of mice in the VG and PG increased, indicating that the pathogenetic mechanism of CP was related to liver injury in mice (**Figure 3B**). Serum hyaluronic acid levels and bilirubin levels also increased (**Figure 3C**).

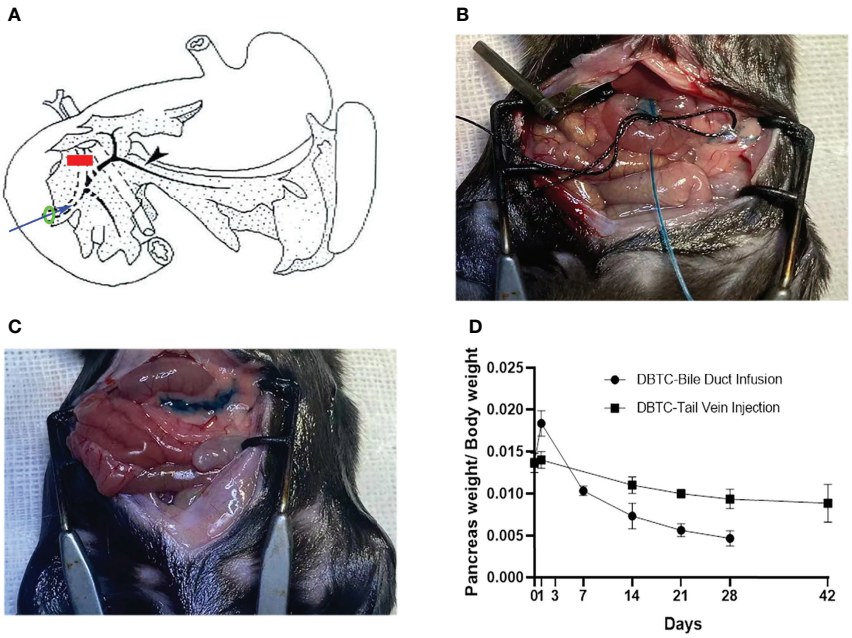

FIGURE 1 | **(A)** Schematic diagram of retrograde pancreatic duct injection of DBTC. Blue arrow, fine catheter to infuse DBTC solution; red line, clip to block distal biliary duct; black arrow, pancreatic duct; green ring, suture to secure biliary duct. **(B)** Intraoperative photographs of retrograde pancreatic duct injection of DBTC (during infusion). **(C)** Intraoperative photographs of retrograde pancreatic duct injection of DBTC (after infusion). Methylene blue (1%) is added to DBTC solution to trace pancreas parenchyma. **(D)** Percentage of pancreas weight/body weight in different groups. DBTC, dibutyltin dichloride.

Change in Inflammatory Cell Infiltration Between PG and VG

Figure 4 shows the results of T lymphocyte and macrophage infiltration. The results suggest that macrophages and T lymphocytes are the main inflammatory cell groups in DBTC-induced CP of the PG. For T lymphocytes, at day 1, T lymphocyte marker CD3 was not found in either the VG or PG. However, after 1 week, a slight T lymphocyte marker CD3 activity was observed in the PG (**Figure 4A**), indicating the presence of T lymphocyte infiltration, but not in the VG. The

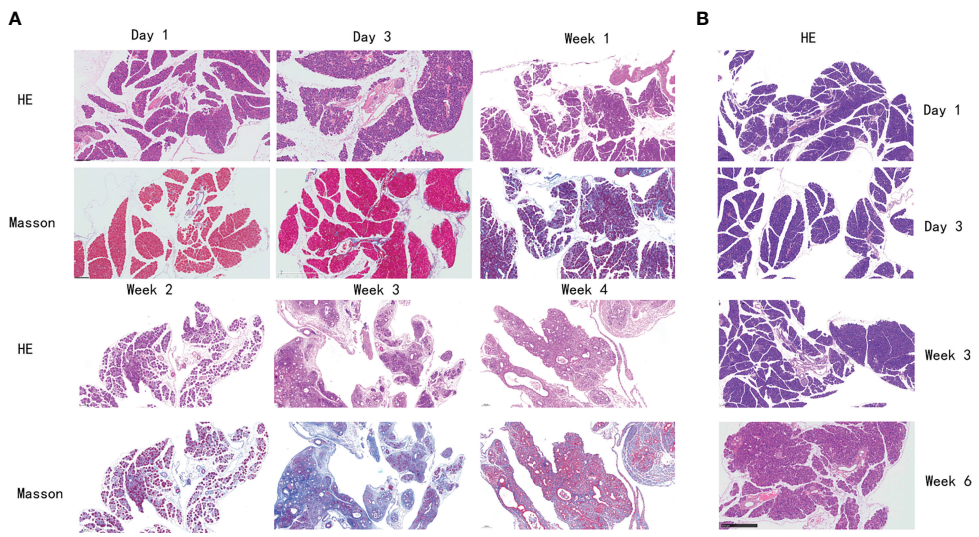

FIGURE 2 | Histological changes of the pancreas in mice with chronic pancreatitis. **(A)** Histological changes of mice in PG pancreas at different time points by H&E and Masson staining. **(B)** Histological changes of mice in VG pancreas at different time points by H&E staining. PG, retrograde pancreatic duct injection group; VG, tail vein injection group.

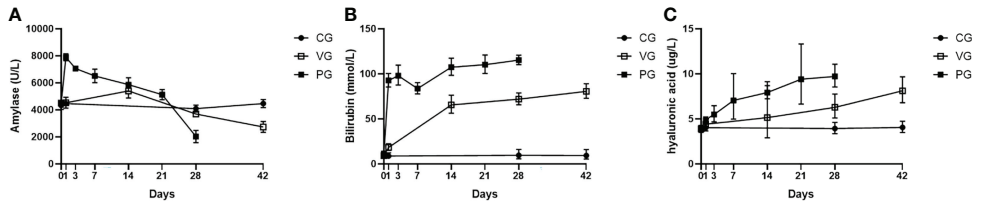

FIGURE 3 | Serum biochemical indices and pancreatic proportion of mice in CG, VG, and PG. **(A)** Serum amylase (U/L). **(B)** Bilirubin level in serum (mmol/L). **(C)** Hyaluronic acid (μg/L). PG, retrograde pancreatic duct injection group; VG, tail vein injection group; CG, control group.

number of T lymphocytes in the PG increased and remained elevated from day 21 to 28. However, few T lymphocytes were observed in the VG on day 14 (**Figure 4B**), and the number of infiltrated T lymphocytes remained much lower than in the PG throughout the observation period. For macrophages, mild macrophage infiltration was observed in the VG (**Figure 4C**) and PG (**Figure 4D**) on day 14, but as time went on, the number of macrophages in the PG increased faster than that in the VG,

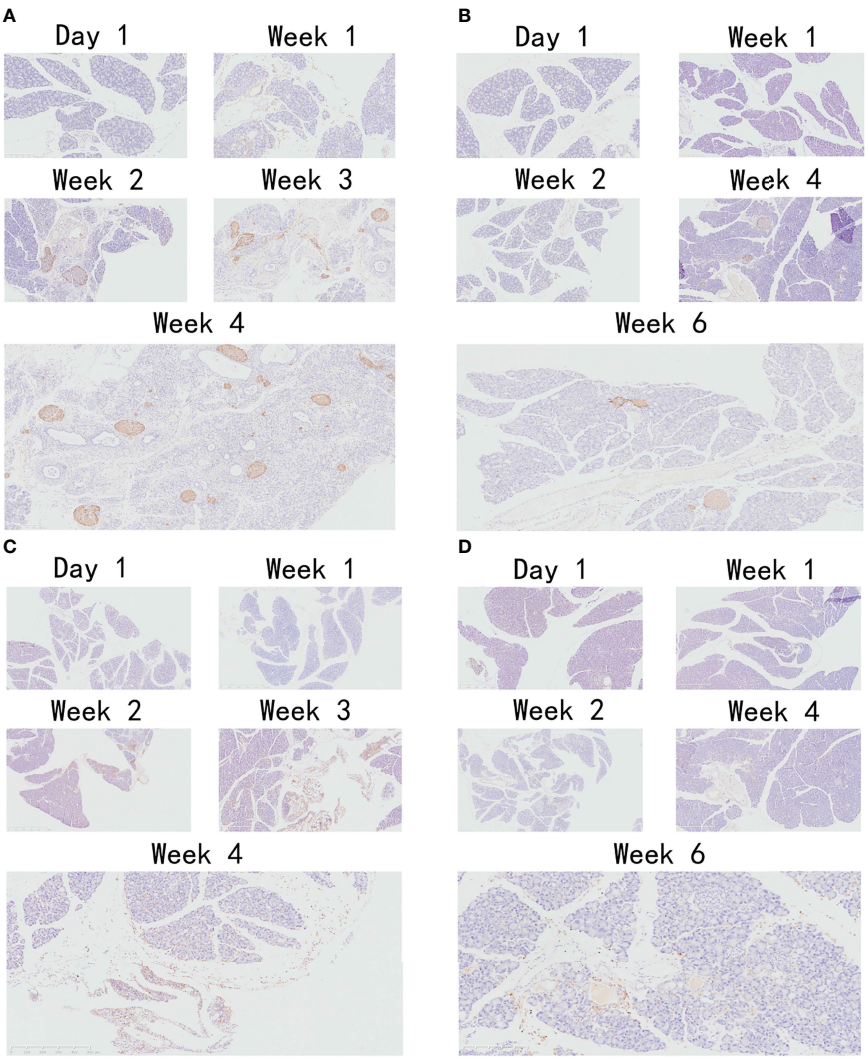

FIGURE 4 | Immunohistochemistry of T lymphocytes. **(A)** T lymphocytes were stained using an anti-mouse CD3 monoclonal antibody in PG. **(B)** T lymphocytes were stained using an anti-mouse CD3 monoclonal antibody in VG. **(C)** Macrophages were stained using an anti-mouse F4/80 monoclonal antibody in PG. **(D)** Macrophages were stained using an anti-mouse F4/80 monoclonal antibody in VG. PG, retrograde pancreatic duct injection group; VG, tail vein injection group.

and it was obvious that the number of macrophages in the PG at day 28 was much more than that in the VG at day 42.

Fibrotic Parameter Changes in Pancreas

Immunofluorescence was used to detect the distribution and expression of FN, a pivotal fibrosis index. On day 1, FN expression was observed neither in the VG nor in the PG. After 1 week, a moderate amount of FN expression was detected in the PG (**Figure 5A**) and increased throughout the observation period. However, only a moderate amount of FN was observed on day 42 in the VG (**Figure 5B**), indicating that the fibrosis level that appeared in the VG was so low that the mouse model cannot be established.

Changes in Fibrosis Indicator and Pancreatic Neoplastic Phenotype

An important feature of severe CP is the disorganized expression of metalloproteinase, including upregulated MMP-1 and downregulated TIMP-1. In our study, MMP-1 and TIMP-1 mRNAs were detected by real-time PCR (**Figures 6A, B**). The decreased rate of MMP-1 and TIMP-1 expression in the PG is sharper than that in the VG, suggesting that CP in the PG is much more severe than that in the VG. After the aforementioned multi-angle analysis, tail vein injection of DBTC with alcohol drinking (VG) has been proven to be unable to induce moderate CP. We further tested the protein level of other fibrotic factors, including COL1A1 and α-SMA, in the retrograde pancreatic duct injection group (PG). COL1A1 and α-SMA expression increased throughout the observation period and surged during the first 21 days (**Figure 6C**). Moreover, a pancreatic neoplastic pathological change could also be identified in 28 days in the PG (**Figures 6D–F**).

DISCUSSION

CP is a refractory pancreatic disease, mainly caused by biliary dysfunction or alcohol abuse. The pathological manifestation of CP is chronic inflammation in pancreatic parenchyma, atrophy of pancreatic acinar, and fibrous hyperplasia (17, 18). The incidence rate of CP shows a moderate escalation in the past 10 years due to larger alcohol consumption and increased rates of obesity worldwide (5). CP can eventually progress to pancreatic cancer. Therefore, the basic research of CP has attracted great attention from gastroenterologists and scientists. Several effective and reliable rodent models are needed to promote these studies. Additionally, the mouse model could be more flexible and useful than the rat model, because mice are easier to be raised and investigated, and mice have gallbladder in contrast to rats. This can improve the confidence and translational meaning of CP and pancreatic cancer basic research and medical treatment.

DBTC is a fat-soluble substance, and a moderate concentration of DBTC can cause necrosis of pancreatic duct epithelial cells and eventually block the pancreatic duct, resulting in pancreatitis *in vivo*. The blocked pancreatic duct can induce activated pancreatic stellate cells to produce cytokines, resulting in pancreatic fibrosis, and then CP symptoms emerge. This procedure could preferably mimic CP caused by biliary dysfunction in humans, and tail injection of DBTC with alcohol intake has been used in the rat CP model (19). A number of studies based on this rat CP model have been reported (20–22), suggesting the superior robustness of this model. However, DBTC injection has not been widely used in the mouse CP model. The highly toxic DBTC could be an important reason, and the dose used in the rat model could be lethal to mice, as one report has mentioned (23). One interesting

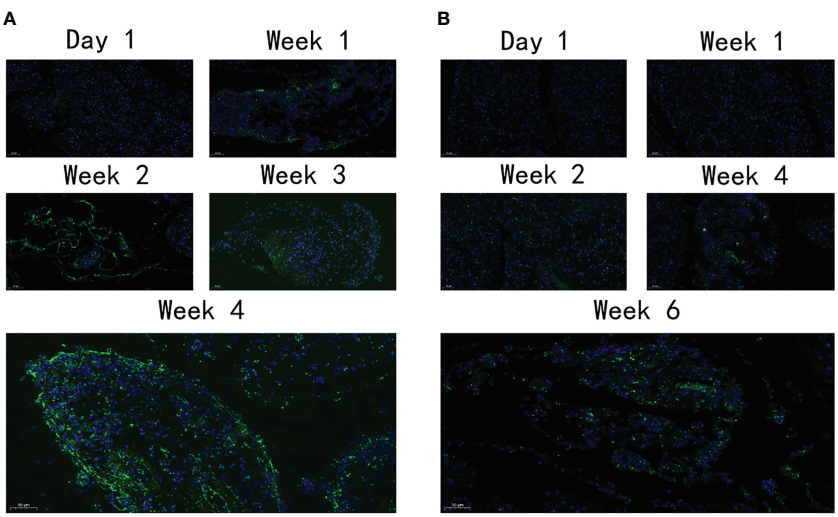

FIGURE 5 | The expression level of FN. **(A)** The expression of FN in PG at different time points. **(B)** The expression of FN in VG at different time points. FN, fibronectin; PG, retrograde pancreatic duct injection group; VG, tail vein injection group.

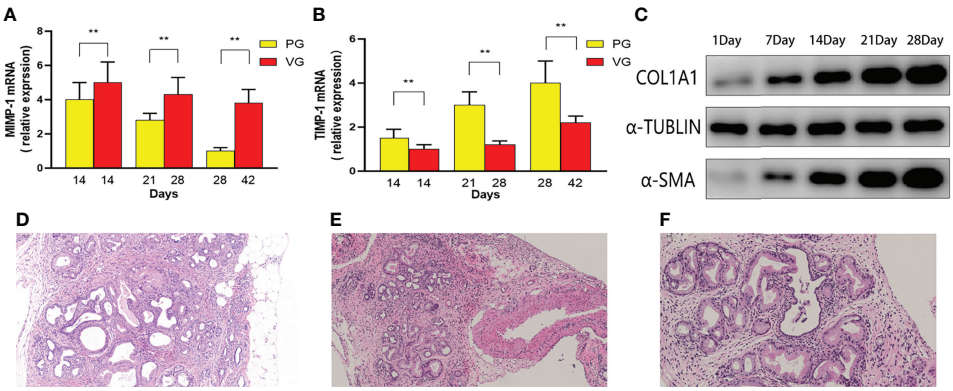

FIGURE 6 | The MMP-1 mRNA and TIMP-1 mRNA contents in mice of PG and VG changed at different time points. **(A)** Changes in MMP-1 mRNA expression (PG vs. VG). **(B)** Changes in TIMP-1 mRNA expression (PG vs. VG). **(C)** The expression levels of α-SMA and COL1 at different time points (PG). **(D–F)** Representative H&E images of PG 1 month after injection. PG, retrograde pancreatic duct injection group; VG, tail vein injection group.

question is whether it can successfully induce experimental CP through low-dose injection of DBTC in mice. In the Zhang et al. research, they reported that a low-dose injection of DBTC can induce a classical CP phenotype, including obvious pancreatic acinar atrophy and activation of pancreatic stellate cells and a large ratio of fibrous hyperplasia (12). However, in another research developed by Lütt et al., the researchers reported that the same dose of DBTC through tail injection could not induce an obvious CP phenotype in mice (13). Our finding strongly supports the prospective of Lütt et al.; 6 weeks after tail injection of DBTC with alcohol drinking, we were not able to observe a distinct pancreatic acinar atrophy and interstitial fibrous hyperplasia phenotype, and hyaluronic acid, bilirubin, and amylase contents did not significantly change. The injection dose of our research is consistent with that of a previous study (13). According to some previous studies, an increase in the tail injection dose of DBTC in mice (6–8 mg/kg) could trigger systemic toxicity (13, 23, 24). We can conclude that increasing the dose of DBTC to attempt to induce a CP phenotype can be unacceptable and that tail injection of DBTC with alcohol intake cannot induce an obvious CP-like pathological feature in mice. This finding would end the debate whether tail injection of DBTC with alcohol could induce CP and could be an ideal CP model in mouse.

Another highlight is a viable CP mouse model through retrograde pancreatic duct injection of DBTC has been established and validated in our current research. This mouse model showed great robustness for formatting classical CP pathological features in less than 4 weeks and a 100% survival rate. After 4 weeks, fibrosis in pancreas parenchyma and pancreatic acinar atrophy can be clearly observed in PG mice. The protein level of fibrosis biomarkers in the pancreas, including FN, COL1A1, and α-SMA, were found to be significantly increased. In addition, serum hyaluronic acid, bilirubin, and amylase contents show an ascending tendency in the initial 14 days. Then, with the progress of damage in pancreatic tissue with further loss of endocrine and exocrine functions, amylase levels began to decline while bilirubin and hyaluronic acid levels continued to rise after 14 days. Morphological changes in the pancreas also confirmed that retrograde injection of DBTC through the pancreatic duct can cause classic changes of CP, from pancreatic edema and pancreatic acinar cell necrosis in the initial term to persistent inflammation with pancreatic parenchymal interstitial fibrosis in the final term. The DBTC dose in the retrograde injection group (1 mg/kg) is much lower than that in the tail injection group (8 mg/kg). However, the pancreatic CP-like phenotype is much more significant, which may be attributed to the direct effect of DBTC retrograde injection on the pancreas.

CP is an obvious risk factor for pancreatic cancer (25). Nowadays, the major mouse model to study pancreatitis-induced spontaneous pancreatic cancer is a continuous injection of caerulein. Caerulein is a gastric regulatory molecule similar to CCK. It can stimulate excessive secretion of pancreatic acinar cells, impeding the separation of trypsinogen and lysosomal hydrolase in cells, and can be activated in a cathepsin B-dependent manner. Trypsin activity in turn leads to a series of cell damage. The inflammatory response caused by self-digestion of pancreatic tissue recruits inflammatory cells and releases inflammatory factors, which further cause severe local and even systemic inflammation. Continuous stimulation of the pancreas with caerulein would cause chronic inflammation with fibrosis and carcinogenesis, leading to spontaneous pancreatic cancer (26). This mouse model emphasized the role of excessive secretion of trypsin and cellular oxidative stress in the occurrence of pancreatic cancer. However, one important factor of CP is biliary obstruction, and a model of spontaneous pancreatic cancer is needed to mimic this pathology (4). A previous study has demonstrated that DBTC infusion could lead to acute pancreatitis through the obstruction of the biliary duct (11). In our current study, we proved that retrograde injection of DBTC through the pancreatic duct could induce reproducible spontaneous pancreatic neoplasm in mice with Kas mutation, which can be used as a spontaneous neoplasm mouse model in pancreatic cancer research as a supplementary method for caerulein-induced pancreatic cancer.

In conclusion, in this current study, we established and validated a new CP and spontaneous pancreatic neoplasm mouse model through retrograde injection of DBTC in the pancreatic duct. Moreover, we confirmed that tail injection of DBTC could not induce considerable CP or a neoplastic phenotype in mice.

DATA AVAILABILITY STATEMENT

The original contributions presented in the study are included in the article/**Supplementary Material**. Further inquiries can be directed to the corresponding author.

ETHICS STATEMENT

The animal study was reviewed and approved by The ethics committee of first Affiliated Hospital of Naval Medical University. Written informed consent was obtained from the owners for the participation of their animals in this study.

AUTHOR CONTRIBUTIONS

HH designed the project. DZ, WL, and MW exerted the experiment. MW, WL, and HY contributed to the main part of data analysis and prepared the main manuscript. DZ, MW, and KL revised the article and made suggestions to improve the article. DZ, WL, and MW have contributed equally to this work. Final approval of manuscript: All authors.

SUPPLEMENTARY MATERIAL

The Supplementary Material for this article can be found online at: https://www.frontiersin.org/articles/10.3389/fonc.2022.947133/full#supplementary-material

REFERENCES

1. Milosavljevic T, Kostic Milosavljevic M, Krstic M, Jovanovic I. Classification of Chronic Pancreatitis. *Digest Dis (Basel Switzerland)* (2010) 28(2):330–3. doi: 10.1159/000319409
2. Muniraj T, Aslanian HR, Farrell J, Jamidar PA. Chronic Pancreatitis, a Comprehensive Review and Update. Part I: Epidemiology, Etiology, Risk Factors, Genetics, Pathophysiology, and Clinical Features. *Disease-a-month DM* (2014) 60(12):530–50. doi: 10.1016/j.disamonth.2014.11.002
3. Ansari D, Andersson E, Andersson B, Andersson R. Chronic Pancreatitis: Potential Future Interventions. *Scand J Gastroenterol* (2010) 45(9):1022–8. doi: 10.3109/00365521003734174
4. Braganza JM, Lee SH, McCloy RF, McMahon MJ. Chronic Pancreatitis. *Lancet (London England)* (2011) 377(9772):1184–97. doi: 10.1016/S0140-6736(10)61852-1
5. Beyer G, Habtezion A, Werner J, Lerch M, Mayerle J. Chronic Pancreatitis. *Lancet* (2020) 396(10249):499–512. doi: 10.1016/S0140-6736(20)31318-0
6. Sparmann G, Merkord J, Jäschke A, Nizze H, Jonas L, Löhr M, et al. Pancreatic Fibrosis in Experimental Pancreatitis Induced by Dibutyltin Dichloride. *Gastroenterology* (1997) 112(5):1664–72. doi: 10.1016/s0016-5085(97)70049-0
7. Leal A, Liby K. Murine Models of Pancreatitis Leading to the Development of Pancreatic Cancer. *Curr Protoc Pharmacol* (2018) 83(1):e48. doi: 10.1002/cpph.48
8. Keppel Hesselink J. Rediscovery of Ceruletide, a CCK Agonist, as an Analgesic Drug. *J Pain Res* (2020) 13:123–30. doi: 10.2147/JPR.S232714
9. Van Laethem J, Robberecht P, Résibois A, Devière J. Transforming Growth Factor Beta Promotes Development of Fibrosis After Repeated Courses of Acute Pancreatitis in Mice. *Gastroenterology* (1996) 110(2):576–82. doi: 10.1053/gast.1996.v110.pm8566606
10. Yu J, Kim H. Oxidative Stress and Inflammatory Signaling in Cerulein Pancreatitis. *World J Gastroenterol* (2014) 20(46):17324–9. doi: 10.3748/wjg.v20.i46.17324
11. Merkord J, Weber H, Sparmann G, Jonas L, Hennighausen G. The Course of Pancreatic Fibrosis Induced by Dibutyltin Dichloride (DBTC). *Ann New York Acad Sci* (1999) 880:231–7. doi: 10.1111/j.1749-6632.1999.tb09527.x
12. Zhang H, Liu B, Xu X, Jiang T, Zhang X, Shi Y, et al. Pathophysiology of Chronic Pancreatitis Induced by Dibutyltin Dichloride Joint Ethanol in Mice. *World J Gastroenterol* (2016) 22(10):2960–70. doi: 10.3748/wjg.v22.i10.2960
13. Lütt F, Ehlers L, Nizze H, Jaster R. Different Characteristics of Chronic Dibutyltin Dichloride-Induced Pancreatitis and Cholangitis in Mouse and Rat. *Hepatobil Pancreatic Dis Int HBPD Int* (2020) 19(2):169–74. doi: 10.1016/j.hbpd.2019.10.007
14. Gitto S, Nakkina S, Beardsley J, Parikh J, Altomare D. Induction of Pancreatitis in Mice With Susceptibility to Pancreatic Cancer. *Methods Cell Biol* (2022) 168:139–59. doi: 10.1016/bs.mcb.2021.12.013
15. Huang H, Swidnicka-Siergiejko A, Daniluk J, Gaiser S, Yao Y, Peng L, et al. Transgenic Expression of PRSS1 Sensitizes Mice to Pancreatitis. *Gastroenterology* (2020) 158(4):1072–82.e7. doi: 10.1053/j.gastro.2019.08.016
16. Huang H, Liu Y, Daniluk J, Gaiser S, Chu J, Wang H, et al. Activation of Nuclear Factor-κb in Acinar Cells Increases the Severity of Pancreatitis in Mice. *Gastroenterology* (2013) 144(1):202–10. doi: 10.1053/j.gastro.2012.09.059
17. DiMagno EP. A Short, Eclectic History of Exocrine Pancreatic Insufficiency and Chronic Pancreatitis. *Gastroenterology* (1993) 104(5):1255–62. doi: 10.1016/0016-5085(93)90332-7
18. Ewald N, Hardt PD. Diagnosis and Treatment of Diabetes Mellitus in Chronic Pancreatitis. *World J Gastroenterol* (2013) 19(42):7276–81. doi: 10.3748/wjg.v19.i42.7276
19. Merkord J, Weber H, Jonas L, Nizze H, Hennighausen G. The Influence of Ethanol on Long-Term Effects of Dibutyltin Dichloride (DBTC) in Pancreas and Liver of Rats. *Hum Exp Toxicol* (1998) 17(3):144–50. doi: 10.1177/096032719801700304
20. Matsushita K, Mizushima T, Shirahige A, Tanioka H, Sawa K, Ochi K, et al. Effect of Taurine on Acinar Cell Apoptosis and Pancreatic Fibrosis in Dibutyltin Dichloride-Induced Chronic Pancreatitis. *Acta Med Okayama* (2012) 66(4):329–34. doi: 10.18926/AMO/48687
21. Zhou C, Lin-Li, Zhu X, Wen-Tang, Hu D, Dong Y, et al. Protective Effects of Edaravone on Experimental Chronic Pancreatitis Induced by Dibutyltin Dichloride in Rats. *Pancreatology* (2013) 13(2):125–32. doi: 10.1016/j.pan.2013.01.007
22. Hou X, Jin Z, Jiang F, Zhu J, Li Z. Expression of Smad7 and Smad Ubiquitin Regulatory Factor 2 in a Rat Model of Chronic Pancreatitis. *J Digest Dis* (2015) 16(7):408–15. doi: 10.1111/1751-2980.12253
23. Ueno S, Kashimoto T, Susa N, Ishii M, Chiba T, Mutoh K, et al. Comparison of Hepatotoxicity and Metabolism of Butyltin Compounds in the Liver of Mice, Rats and Guinea Pigs. *Arch Toxicol* (2003) 77(3):173–81. doi: 10.1007/s00204-002-0429-4
24. Ueno S, Susa N, Furukawa Y, Sugiyama M. Role of Cytochrome P450 in Hepatotoxicity Induced by Di- and Tributyltin Compounds in Mice. *Arch Toxicol* (1995) 69(9):655–8. doi: 10.1007/s002040050228
25. Kamisawa T, Wood LD, Itoi T, Takaori K. Pancreatic Cancer. *Lancet* (2016) 388(10039):73–85. doi: 10.1016/S0140-6736(16)00141-0
26. Lerch MM, Gorelick FS. Models of Acute and Chronic Pancreatitis. *Gastroenterology* (2013) 144(6):1180–93. doi: 10.1053/j.gastro.2012.12.043

Conflict of Interest: The authors declare that the research was conducted in the absence of any commercial or financial relationships that could be construed as a potential conflict of interest.

Publisher's Note: All claims expressed in this article are solely those of the authors and do not necessarily represent those of their affiliated organizations, or those of the publisher, the editors and the reviewers. Any product that may be evaluated in this article, or claim that may be made by its manufacturer, is not guaranteed or endorsed by the publisher.

Copyright © 2022 Zhang, Li, Wang, Yin, Xia, Li and Huang. This is an open-access article distributed under the terms of the Creative Commons Attribution License (CC BY). The use, distribution or reproduction in other forums is permitted, provided the original author(s) and the copyright owner(s) are credited and that the original publication in this journal is cited, in accordance with accepted academic practice. No use, distribution or reproduction is permitted which does not comply with these terms.

frontiers | Frontiers in Oncology

ORIGINAL RESEARCH
published: 13 July 2022
doi: 10.3389/fonc.2022.943951

A Prediction Model Intended for Exploratory Laparoscopy Risk Stratification in Colorectal Cancer Patients With Potential Occult Peritoneal Metastasis

Yuanxin Zhang[1†], Xiusen Qin[1,2†], Yang Li[1†], Xi Zhang[3], Rui Luo[1], Zhijie Wu[1], Victoria Li[4], Shuai Han[3], Hui Wang[1,2*] and Huaiming Wang[1,2*]*

[1] Department of Colorectal Surgery, The Sixth Affiliated Hospital, Sun Yat-sen University, Guangzhou, China, [2] Guangdong Provincial Key Laboratory of Colorectal and Pelvic Floor Disease, The Sixth Affiliated Hospital, Sun Yat-sen University, Guangzhou, China, [3] General Surgery Center, Department of Gastrointestinal Surgery, Zhujiang Hospital, Southern Medical University, Guangzhou, China, [4] Department of Secondary Education, Yew Chung International School, Kowloon Tong, Hong Kong, China

OPEN ACCESS

Edited by:
Zhendong Jin,
Second Military Medical University, China

Reviewed by:
Guoxiang Cai,
Shanghai Cancer Center, Fudan University, China
Mingyu Chen,
Sir Run Shaw Hospital, China

***Correspondence:**
Huaiming Wang
wanghm7@mail.sysu.edu.cn
Hui Wang
wang89@mail.sysu.edu.cn
Shuai Han
gzhanbo0624@smu.edu.cn

[†]These authors have contributed equally to this work

Specialty section:
This article was submitted to Gastrointestinal Cancers: Colorectal Cancer, a section of the journal Frontiers in Oncology

Received: *14 May 2022*
Accepted: *22 June 2022*
Published: *13 July 2022*

Citation:
Zhang Y, Qin X, Li Y, Zhang X, Luo R, Wu Z, Li V, Han S, Wang H and Wang H (2022) A Prediction Model Intended for Exploratory Laparoscopy Risk Stratification in Colorectal Cancer Patients With Potential Occult Peritoneal Metastasis. Front. Oncol. 12:943951. doi: 10.3389/fonc.2022.943951

Background: The early diagnosis of occult peritoneal metastasis (PM) remains a challenge due to the low sensitivity on computed tomography (CT) images. Exploratory laparoscopy is the gold standard to confirm PM but should only be proposed in selected patients due to its invasiveness, high cost, and port-site metastasis risk. In this study, we aimed to develop an individualized prediction model to identify occult PM status and determine optimal candidates for exploratory laparoscopy.

Method: A total of 622 colorectal cancer (CRC) patients from 2 centers were divided into training and external validation cohorts. All patients' PM status was first detected as negative on CT imaging but later confirmed by exploratory laparoscopy. Multivariate analysis was used to identify independent predictors, which were used to build a prediction model for identifying occult PM in CRC. The concordance index (C-index), calibration plot and decision curve analysis were used to evaluate its predictive accuracy and clinical utility.

Results: The C-indices of the model in the development and validation groups were 0.850 (95% CI 0.815-0.885) and 0.794 (95% CI, 0.690-0.899), respectively. The calibration curve showed consistency between the observed and predicted probabilities. The decision curve analysis indicated that the prediction model has a great clinical value between thresholds of 0.10 and 0.72. At a risk threshold of 30%, a total of 40% of exploratory laparoscopies could have been prevented, while still identifying 76.7% of clinically occult PM cases. A dynamic online platform was also developed to facilitate the usage of the proposed model.

Conclusions: Our individualized risk model could reduce the number of unnecessary exploratory laparoscopies while maintaining a high rate of diagnosis of clinically occult PM. These results warrant further validation in prospective studies.

Clinical Trial Registration: https://www.isrctn.com, identifier ISRCTN76852032

Keywords: exploratory laparoscopy, occult peritoneal metastasis, nomogram, colorectal cancer, decision curve analysis

INTRODUCTION

Despite recent improvements in cancer research, colorectal cancer (CRC) ranks second in mortality in both men and women worldwide (1). An important reason for the limited survival in CRC patients is the presence of distant metastasis. In particular, peritoneal metastases (PM) are associated with significantly shorter survival than metastases at other sites ($p < 0.001$) (2–4). The prediction of early PM plays an important role in the prognosis of CRC patients, because less aggressive cytoreductive surgery (CRS) is required for lower peritoneal cancer index (PCI) values and surgeons are also more likely to achieve complete (CC0) or near complete cytoreduction (CC1) (5). Both PCI and completeness of cytoreduction (CCR) are the indicators with the highest prognostic significance in the treatment of peritoneal carcinomatosis (6). All efforts should therefore be made to identify CRC patients with PM at the earliest stage.

Unfortunately, the early detection of colorectal PM is currently difficult due to the absence of typical symptoms and the low accuracy of noninvasive imaging methods for nodules smaller than 5 mm (7–9). Computed tomography (CT) is the most common noninvasive method to diagnose PM. CT detection of PM can only be suggested by omental caking, luminal narrowing, large nodules, and ascites (10). However, most of these PM-specific features usually exist at the late stage. Thus, CT detection of PM has high specificity but low sensitivity. This raises the problem that 10%-35% of CRCs with PM-negative status in CT readings were unexpectedly identified as PM-positive during subsequent surgery; also known as occult PM (11).

At present, diagnostic laparoscopy has been regarded as the most reliable tool to detect occult PM because it could provide direct visualization as well as histological confirmation, and could evaluate the extent of the disease, measured in terms of PCI (12–14). Meanwhile, some recent studies support the laparoscopy's safety and efficacy either in the excision of lesions or in the selection of potential PM candidates for CRS/HIPEC (15–19). However, the laparoscopic approach should only be proposed to the selected patients due to its invasive procedure, high cost and the possibility of port-site metastasis. Therefore, it is essential to develop an individualized prediction model to identify occult PM status and determine optimal candidates for exploratory laparoscopy.

We aimed to develop a prediction model for the noninvasive prediction of occult PM status in CRC patients and study of its utility for exploratory laparoscopy risk stratification.

Abbreviations: PM, peritoneal metastasis; CT, computed tomography; CRC, colorectal cancer; C-index, concordance index; ISRCTN, International Standard Randomised Controlled Trials Number; CRS, cytoreductive surgery; PCI, peritoneal cancer index; CCR, completeness of cytoreduction; CEA, carcinoembryonic antigen; CA125, carbohydrate antigen 125; CA19-9, carbohydrate antigen 19-9; dMMR, mismatch repair-deficient; NLR, neutrophil-to-lymphocyte ratio; PLR, platelet-to-lymphocyte ratio; LMR, lymphocyte-to-monocyte ratio; ROC, receiver operating characteristic; AUC, area under the ROC curve; DCA, decision curve analysis.

MATERIALS AND METHODS

Patients

The clinicopathological characteristics of CRC patients with or without occult PM were retrospectively selected from a 2-center cancer dataset between September 2007 and July 2019. All enrolled patients were initially diagnosed as PM-negative on CT imaging but later confirmed to have the actual PM status during laparoscopy. The patients were divided into the following two cohorts: a training cohort (n = 552 from center 1) and an external validation cohort (n = 70 from center 2). The study was registered at ISRCTN (No. ISRCTN76852032). The study received approval from the local Institutional Review Committee (No. 2020ZSLYEC–109). The requirement to obtain consent from patients was waived due to the retrospective nature of the study. The work has been reported in line with the STROCSS criteria (20).

Definitions and Variables

PM was defined as the dissemination of cancer cells in the abdominal or pelvic cavity, such as the greater omentum, ovaries, pelvic inlet, rectovesical (male) or rectouterine (female) pouch, and abdominal wall, or extensive carcinomatosis (21). These metastatic sites were determined to be malignant by pathological reviews of the biopsied or surgically resected specimens. All enrolled patients underwent enhanced CT examinations within two weeks before the operation. All CT images of patients were assessed and given a radiological diagnosis by at least two radiologists. A standardized exploration of the peritoneal cavity was conducted quadrant by quadrant using the endoscope, exploring the 13 regions of PCI as described by Sugarbaker (22). The procedures were only exploratory, and no extensive dissection was made (13, 23).

The baseline information of patients was extracted from the electronic dataset, including sex, age at diagnosis, primary tumor site, histological type, grade of differentiation, T stage, N stage, obstruction status, perforation status, carcinoembryonic antigen (CEA), carbohydrate antigen 125 (CA125) and carbohydrate antigen 19-9 (CA19-9) pretreatment levels, NRAS, KRAS, BRAF and PIK3CA gene mutation statuses, mismatch repair-deficient (dMMR) status, as well as systemic inflammatory markers such as the neutrophil-to-lymphocyte ratio (NLR), platelet-to-lymphocyte ratio (PLR) and lymphocyte-to-monocyte ratio (LMR).

Inclusion and Exclusion Criteria

The inclusion criteria were as follows: (1) patients were diagnosed with CRC by endoscopy-biopsy pathology, combined with CT and/or other examinations; (2) patients had only one malignant primary tumor; (3) patients did not undergo the previous resection of the primary tumor; and (4) patients underwent both enhanced CT and exploratory laparoscopy.

The exclusion criteria were as follows: (1) typical PM signs on CT; (2) other distant metastases; and (3) previous inflammatory diseases.

Construction of the Prediction Model

Univariate analysis was applied to assess the association between all included variables and occult PM. Statistical differences in the enrolled variables by PM status were assessed using the

independent T test or Mann–Whitney U test for continuous variables and the Chi-square test or Fisher's exact test for categorical variables.

Multivariate logistic regression analysis was adopted to identify independent risk factors for PM. According to the results of the multivariate analysis, a predictive nomogram was established to predict the risk of occult PM in CRC patients.

Evaluation of the Accuracy and Utility of the Model

The receiver operating characteristic (ROC) curve (24) and calibration curve (25) were both used to evaluate the predictive accuracy of the model. On the one hand, the value of the area under the ROC curve (AUC) is the same as that of the concordance index (C-index) in a logistic regression model. The maximum value of the AUC is 1.0, indicating perfect discrimination, whereas 0.5 indicates a random chance to correctly discriminate the outcome with the model. On the other hand, the calibration curve graphically shows the relationship between the predicted and actual risks for each outcome. A plot that perfectly fits the 45° reference line would indicate good agreement.

Decision curve analysis (DCA) is a method for appraising prediction models and visualizing the clinical consequences of a decision strategy. DCA was carried out to evaluate the prediction model's clinical application value by quantifying the net benefit and net reduction of each treatment strategy at different threshold probabilities (26, 27).

Statistical Analysis

All statistical analyses were conducted with SPSS (version 25.0; IBM Corp., Armonk, New York, USA) and R software (version 4.1.2; http://www.r-project.org). Univariate analysis was performed with SPSS. The following R packages were used to perform multivariate logistic regression analysis and build the ROC curve, nomogram, calibration plot, DCA curve and dynamic online platform: "rms", "pROC", "rmda", "dcurves", "rsconnect" and "DynNom". A two-sided P value <0.05 was used to indicate statistical significance.

RESULTS

Patient Characteristics

A total of 662 eligible CRC patients from the 2-center cancer dataset were enrolled in the analysis. The development and validation cohorts included 552 and 70 patients, respectively. The demographics and tumor characteristics of the cohorts were comparable, as shown in **Tables 1**, **2**. In clinical practice, not all CRC patients have information on the status of NRAS, KRAS, BRAF, PIK3CA and dMMR. According to the maximum Youden index, the corresponding optimal cutoff values for NLR, PLR and LMR were 2.5, 172.1 and 2.6, respectively. Patient characteristics, including age, tumor location, histological type, grade of differentiation, T stage, N stage, obstruction status, perforation status, serum CA125 level, NLR, PLR and LMR, were significantly associated with occult PM after univariate analysis in the development cohort ($P < 0.05$).

Construction and Validation of the Prediction Model

Multivariable analysis revealed that primary site, histological type, grade of differentiation, T stage, obstruction, serum CA125 and NLR were independent predictors of occult PM (**Figure 1**). Therefore, a predictive nomogram containing these variables was constructed (**Figure 2**). The Hosmer and Lemeshow test indicated a lack of significance ($P = 0.841$), demonstrating a good fit. In the training cohort, the AUC value of the prediction model was 0.850 (95% CI 0.815-0.885), and the ROC curve graphically showed that the model had better predictive performance than all univariate models alone (**Figure 3A**). The calibration curve of the model revealed good consistency between the prediction of occult PM and the actual situation observed (**Figure 3B**). A dynamic online platform (https://occult-pm.shinyapps.io/DynNomapp/) was developed to facilitate the usage of the proposed model (**Figure 4**). It can assist researchers and clinicians in more easily obtaining the risk probability of their patients by inputting their corresponding clinical variables, after which the web server will generate the output read in the form of figures and tables.

In the external validation cohort, the prediction model also yielded a high AUC of 0.794 (95% Cl, 0.690-0.899) (**Table 3**). This showed that the model could be applied to other independent patient populations.

Clinical Utility

Based on a range of threshold probabilities, DCA was used to evaluate the clinical application of the prediction model. This analysis indicated that when the threshold probability was in the range between 0.10 and 0.72, using the model to predict occult PM would provide more benefits than using either the "treat all with laparoscopy" or "treat none with laparoscopy" plans (**Figure 5A**). The cutoff value for the probability threshold was set at 30%, according to the maximum Youden index (**Table 3**). DCA confirmed that the prediction model could improve risk stratification among patients with negative findings on peritoneal CT imaging by applying diagnostic laparoscopy to all or none of the CRC patients. For example, at the 30% risk cutoff, the prediction model's net benefit was 60% (**Figure 5A**). We can state that if exploratory laparoscopy was performed when the patients' risk threshold was >30%, compared to "treat none with laparoscopy", the net benefit was equivalent to a net 60 true positive results per 100 patients without an increase in the number of false-positive results. Moreover, at a probability threshold of 30%, the net reduction in intervention was approximately 40 per 100 patients (**Figure 5B**). In other words, at this probability threshold, performing exploratory laparoscopy based on the model is equivalent to a strategy in which 40% of exploration could have been prevented without missing any occult PM cases.

DISCUSSION

The constructed model showed promising results with great predictive ability and clinical utility, improving exploratory

TABLE 1 | Characteristics of patients in the training and validation cohorts.

Characteristics	Training cohort			External-validation cohort		
	PM (+)	PM (-)	P value	PM (+)	PM (-)	P value
Sex			0.056			0.042*
Male	97 (28.4)	244 (71.6)		22 (48.9)	23 (51.1)	
Female	62 (29.4)	149 (70.6)		6 (24.0)	19 (76.0)	
Age at diagnosis			0.023*			0.075
< 60	99 (32.8)	203 (67.2)		20 (48.8)	21 (51.2)	
≥ 60	60 (24.0)	190 (76.0)		8 (27.6)	21 (72.4)	
Primary site			<0.001*			0.472
Right colon	63 (39.6)	96 (60.4)		11 (45.8)	13 (54.2)	
Left colon	70 (40.2)	104 (59.8)		17 (37.0)	29 (63.0)	
Rectum	26 (11.9)	193 (88.1)		–	–	
Histological type			<0.001*			0.367
AD	108 (23.3)	355 (76.7)		24 (37.5)	40 (62.5)	
MAD	38 (55.9)	30 (44.1)		2 (66.7)	1 (33.3)	
SRCC	13 (61.9)	8 (38.1)		2 (66.7)	1 (33.3)	
Differentiation			<0.001*			0.025*
Well/Moderate	82 (19.7)	335 (80.3)		21 (34.4)	40 (65.6)	
Poor/Undifferentiated	77 (57.0)	58 (43.0)		7 (77.8)	2 (22.2)	
T stage			<0.001*			0.472
T1-3	72 (21.7)	260 (78.3)		17 (37.0)	29 (63.0)	
T4	87 (39.5)	133 (60.5)		11 (45.8)	13 (54.2)	
N stage			0.014*			0.077
N0	31 (20.9)	117 (79.1)		12 (30.8)	27 (69.2)	
N1/N2	128 (31.7)	276 (68.3)		16 (51.6)	15 (48.4)	
Obstruction			<0.001*			0.024*
Negative	64 (16.7)	319 (83.3)		14 (30.4)	32 (69.6)	
Positive	95 (56.2)	74 (43.8)		14 (58.3)	10 (41.7)	
Perforation			0.041*			0.400
Negative	156 (28.5)	392 (71.5)		27 (39.1)	42 (60.9)	
Positive	3 (75.0)	1 (25.0)		1 (100)	0 (0)	
CEA			0.707			0.451
Nomal	74 (29.6)	176 (70.4)		13 (36.1)	23 (63.9)	
Elevated	85 (28.1)	217 (71.9)		14 (45.2)	17 (54.8)	
CA125			<0.001*			<0.001*
Nomal	81 (19.7)	330 (80.3)		7 (16.3)	36 (83.7)	
Elevated	78 (55.3)	63 (44.7)		21 (77.8)	6 (22.2)	
CA19-9			0.392			0.197
Nomal	102 (27.6)	267 (72.4)		19 (35.8)	34 (64.2)	
Elevated	57 (31.1)	126 (68.9)		7 (58.3)	5 (41.7)	
NLR			<0.001*			0.626
<2.5	55 (19.0)	235 (81.0)		15 (42.9)	20 (57.1)	
≥2.5	104 (39.7)	158 (60.3)		13 (37.1)	22 (62.9)	
PLR			<0.001*			0.329
<172.1	63 (20.7)	241 (79.3)		16 (45.7)	19 (54.3)	
≥172.1	96 (38.7)	152 (61.3)		12 (34.3)	23 (65.7)	
LMR			<0.001*			0.840
<2.6	89 (40.8)	129 (59.2)		10 (38.5)	16 (61.5)	
≥2.6	70 (21.0)	264 (79.0)		18 (40.9)	26 (59.1)	

PM, peritoneal metastasis; AD, adenocarcinoma; MAD, mucinous adenocarcinoma; SRCC, signet-ring cell carcinoma; CEA, carcinoembryonic antigen; CA125, carbohydrate antigen 125; CA19-9, carbohydrate antigen 19-9; NLR, neutrophil-lymphocyte ratio; PLR, platelet-lymphocyte ratio; LMR, lymphocyte-to-monocyte ratio.
*P was calculated from univariate association of characteristics with occult PM status in colorectal cancer cohort; *P value < 0.05.*

laparoscopy risk stratification among CRC patients with negative findings on peritoneal CT imaging. In the training cohort, by choosing a risk cutoff of 30%, a total of 40% of exploratory laparoscopies could have been prevented while still identifying 76.7% of clinically occult PM cases.

Although some CT-based prediction models, including deep learning algorithms and spectral photon-counting imaging, have been established to diagnose PM, they still showed false-negative outcomes in small nodules and the proportion of false negatives increased with decreasing lesion size (21, 28). Furthermore, the tedious steps of obtaining CT sequence images and importing them into algorithm would limit the clinical application of these models. We believe that the early detection of PM is crucial, especially for occult micrometastatic lesions, because these nodules are not rich in blood supply and are usually missed on routine imaging. Importantly, exploratory laparoscopy is still the gold standard to confirm PM. Therefore, on the one hand, occult PM status could be identified based on our easy-to-use and individualized model, and optimal candidates for exploratory laparoscopy could be determined. On the other hand, *via*

TABLE 2 | Demographics of NRAS, KRAS, BRAF, PIK3CA and dMMR status.

Characteristics	Training cohort			External-validation cohort		
	PM (+)	PM (-)	P value	PM (+)	PM (-)	P value
NRAS			0.036*			–
Wild	61 (27.4)	162 (72.6)		5 (45.5)	6 (54.5)	
Mutation	3 (75.0)	1 (25.0)		–	–	
KRAS			0.546			>0.999
Wild	37 (29.8)	87 (70.2)		3 (50.0)	3 (50.0)	
Mutation	27 (26.2)	76 (73.8)		2 (40.0)	3 (60.0)	
BRAF			0.293			–
Wild	58 (27.4)	154 (72.6)		6 (42.9)	8 (57.1)	
Mutation	6 (40.0)	9 (60.0)		–	–	
PIK3CA			0.938			–
Wild	56 (28.3)	142 (71.7)		5 (55.6)	4 (44.4)	
Mutation	8 (27.6)	21 (72.4)		–	–	
dMMR			0.537			0.079
No	60 (27.8)	156 (72.2)		16 (40)	24 (60)	
Yes	4 (36.4)	7 (63.6)		5 (83.3)	1 (16.7)	

dMMR, mismatch-repair deficiency.

*P was calculated from univariate association of characteristics with occult PM status in colorectal cancer cohort; *P value < 0.05.*

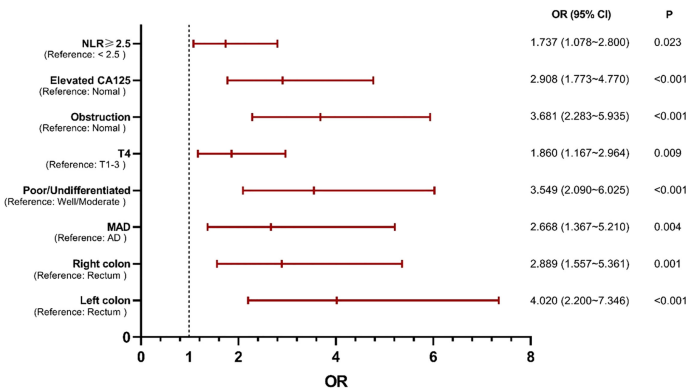

FIGURE 1 | Independent predictors of occult PM identified by multivariate analysis. NLR, neutrophil-to-lymphocyte ratio; MAD, mucinous adenocarcinoma; AD, adenocarcinoma.

exploratory laparoscopy, physicians could evaluate the feasibility of CRS depending on the PCI and CCR (13, 22).

The "seed and soil" theory is a highly recognized theoretical mechanism of PM, and it suggests that PM initiation depends on the synergy of the tumor cells (seed) and the peritoneal microenvironment (soil) (29). A recent study on hallmarks of cancer further recognized that the tumor microenvironment plays an integral role in tumorigenesis and malignant progression (30). Our research team has been engaged in studying the tumor microenvironment as a factor associated with colorectal PM. We found that enhancing cancer-associated fibroblast fatty acid catabolism within a metabolically challenging tumor microenvironment drives colon cancer PM (31). Inflammation should also be recognized as a part of the microenvironment that could potentiate malignancy. The whole process of PM consists of a long series of sequential, interrelated steps. Exfoliated tumor cells in the peritoneal cavity need to maintain their metastatic potential; they need to prevent programmed cell death, and need motility to reach the peritoneal surfaces with the capacity to subsequently attach to these surfaces (32–34). Finally, the capacity to invade the peritoneum and survive and proliferate in the new environment is required (35, 36). Interestingly, peritoneal infections could enhance the migration, invasion, and even proliferation capacities of tumor cells *in vitro* (37). Moreover, experimental work has demonstrated the intimate connection between the molecules driving these steps and the inflammatory cytokines released due to infection (38–40). Especially in the early stages of colorectal PM, a major pattern of chronic inflammation represented by a tumor microenvironment rich in TAM2 with upregulation of IL-6 and rewiring of signaling pathways linked to plasticity, stemness and metabolism has been observed (41). Thus, inflammation-based factors such as obstruction and NLR may suggest early-stage or occult PM.

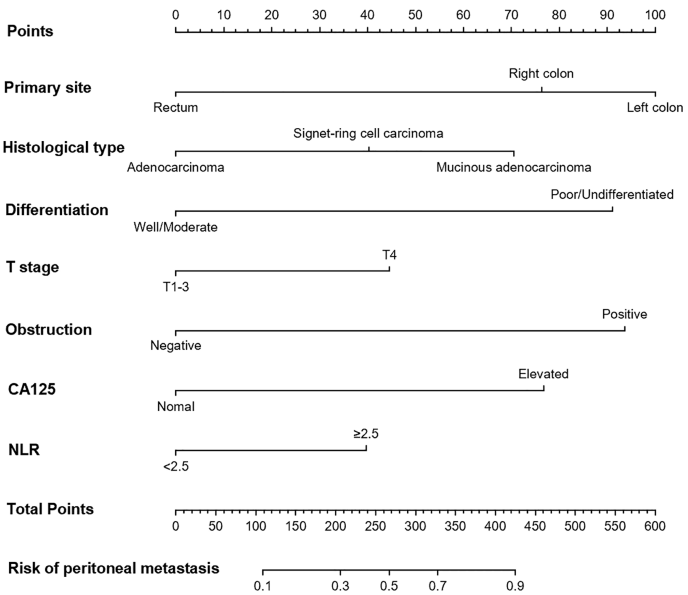

FIGURE 2 | Nomogram for predicting the possibility of occult PM in CRC patients.

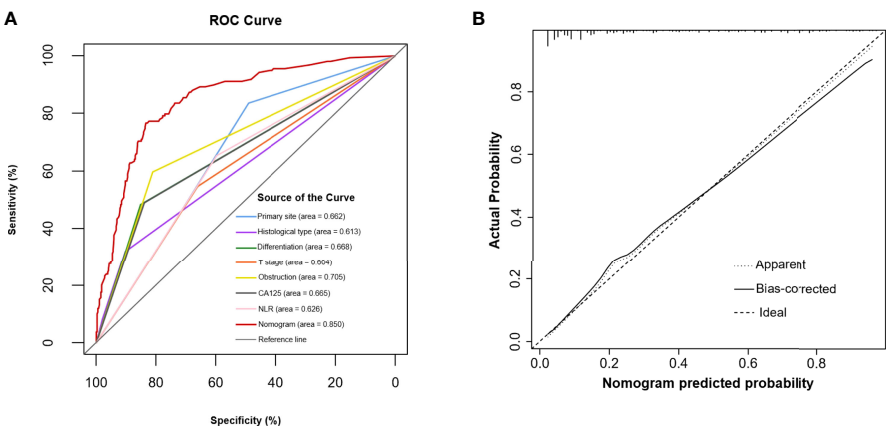

FIGURE 3 | **(A)** The predictive accuracy of the model was assessed by a ROC curve. **(B)** Calibration curve of the prediction model.

It is known that the major pathways of CRC cell dissemination are through direct transport, the lymphatic system and the circulatory system (42). N stage is traditionally believed to be the major milestone of tumor progression and is relevant to diverse metastatic sites. Interestingly, T4 neoplasms were significantly associated with PM, but the N stage was not an independent predictor for PM in this study. They are two variables that may have been confounded before. Advanced neoplasms present with rapid cell proliferation, increasing the interstitial fluid pressure in most solid tumors. Then, high pressure in the tumor increased the number of spontaneously shed tumor cells. This may lead to more tumor cells shedding into the lymphatics present in the tumor that can serve as a conduit for the tumor cells to metastasize to lymph nodes (43).

Several studies have reported that tumors carrying BRAF mutations exhibit a higher frequency of PM than tumors with a wild-type gene (2, 44). However, BRAF mutation was not significantly associated with occult PM in this study. The conflicting phenomenon may be that previous studies were designed to compare PM and non-PM, while our study was mainly based on comparing occult PM and non-PM. BRAF-mutant pmCRC was proven to exhibit a distinct pattern of metastatic spread (45, 46). Unlike an early-stage disease, these tumors are more likely to present with peritoneum-extensive metastasis, a pattern of metastatic spread that may contribute to the poor prognosis and survival of BRAF-mutant pmCRC patients. Only early-stage PM patients were enrolled in the

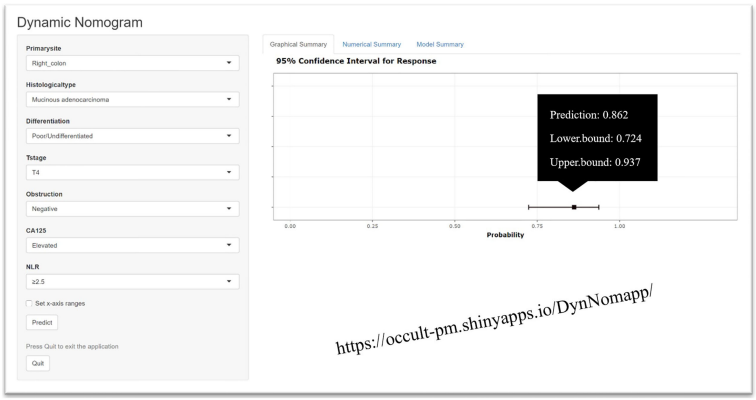

FIGURE 4 | Webserver display of the dynamic online platform.

TABLE 3 | Performance evaluation of the prediction model.

Parameter	Training cohort	External-validation cohort
TP	122	24
TN	328	29
FN	37	4
FP	65	13
Sensitivity	0.767	0.857
Specificity	0.835	0.690
AUC	0.850 (0.815-0.885)	0.794 (0.690-0.899)
Risk cutoff, %	30*	–

TP, true positive; TN, true negative; FN, false negative; FP, false positive; AUC, area under curve.
**The cutoff value for probability threshold was set according to the maximum Youden index.*

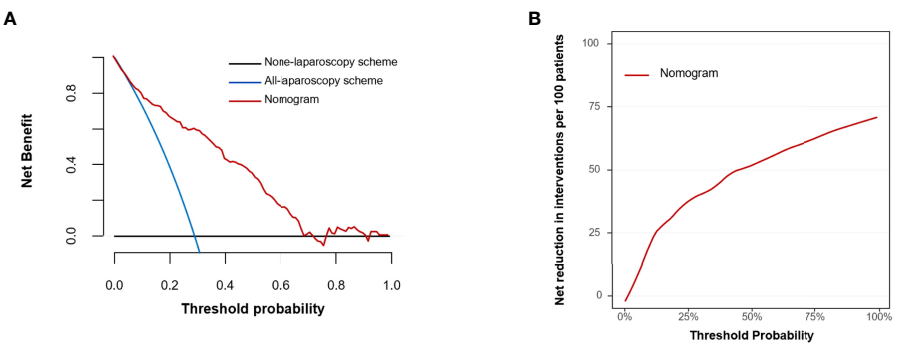

FIGURE 5 | Decision curve analysis for the prediction model. **(A)** Net benefit. **(B)** Net reduction.

cohort, and BRAF mutation was therefore noninformative in our model.

This study has some limitations. First, as with other retrospective studies, potential biases including case selection and model performance analysis, were inevitable. Second, although sequencing technology has become less expensive and tumor genotyping has become standard practice for pmCRC, the sample size of genes was relatively small, especially for mutation status, which may have limited its statistical power. Third, some studies found that the PCI score were underestimated for laparoscopy compared to laparotomy (13, 47). Even though it may underestimate PCI, exploratory laparoscopy accurately predicts the possibility of CCR. Finally, the threshold for exploratory laparoscopy should be determined after a physician and patient both weigh the harm of potentially unnecessary exploration and the benefit of confirming occult PM. Therefore, there is not a single risk threshold that can be used to determine who needs to undergo exploratory laparoscopy but rather a series of risk thresholds.

CONCLUSIONS

Our individualized risk model can be used to reduce the number of unnecessary exploratory laparoscopies in patients who are unlikely to harbor clinically occult PM while capturing most of the patients with clinically occult PM. These results warrant further validation in prospective studies.

DATA AVAILABILITY STATEMENT

The dataset used during the study is available from the corresponding author on a reasonable request.

ETHICS STATEMENT

This study was reviewed and approved by The Ethics Committees of The Sixth Affiliated Hospital of Sun Yat-sen University, No. 2020ZSLYEC-109. The requirement to obtain consent from patients was waived due to the retrospective nature of the study.

AUTHOR CONTRIBUTIONS

HW (9th author) designed the study. YZ, XQ, VL, HW (10th author) and SH contributed to the manuscript writing and revision. YL, ZW and XZ collected and summarized data. YZ and RL performed the statistical analysis and data interpretation. All authors read and approved the final draft.

FUNDING

This study was sponsored by the National Natural Science Foundation of China (Grant No. 82103084) and the Sun Yat-sen University Clinical Research 5010 Program (Grant No. 2019021). The funding body had no role in the design of the study, the collection, analysis, and interpretation of the data or writing the manuscript.

ACKNOWLEDGMENTS

The authors thank AJE Academic Services (www.aje.com) for English language editing and review services.

REFERENCES

1. World Health Organization. *International Agency for Research on Cancer. GLOBOCAN 2020: Estimated Cancer Incidence, Mortality and Prevalence Worldwide in 2020* . Available at: https://gco.iarc.fr/today.
2. Franko J, Shi Q, Meyers JP, Maughan TS, Adams RA, Seymour MT, et al. Prognosis of Patients With Peritoneal Metastatic Colorectal Cancer Given Systemic Therapy: An Analysis of Individual Patient Data From Prospective Randomised Trials From the Analysis and Research in Cancers of the Digestive System (ARCAD) Database. *Lancet Oncol* (2016) 17:1709–19. doi: 10.1016/S1470-2045(16)30500-9
3. Franko J, Shi Q, Goldman CD, Pockaj BA, Nelson GD, Goldberg RM, et al. Treatment of Colorectal Peritoneal Carcinomatosis With Systemic Chemotherapy: A Pooled Analysis of North Central Cancer Treatment Group Phase III Trials N9741 and N9841. *JCO* (2012) 30:263–7. doi: 10.1200/JCO.2011.37.1039
4. Klaver YLB, Simkens LHJ, Lemmens VEPP, Koopman M, Teerenstra S, Bleichrodt RP, et al. Outcomes of Colorectal Cancer Patients With Peritoneal Carcinomatosis Treated With Chemotherapy With and Without Targeted Therapy. *Eur J Surg Oncol* (2012) 38:617–23. doi: 10.1016/j.ejso.2012.03.008
5. Elias D, Glehen O, Pocard M, Quenet F, Goéré D, Arvieux C, et al. A Comparative Study of Complete Cytoreductive Surgery Plus Intraperitoneal Chemotherapy to Treat Peritoneal Dissemination From Colon, Rectum, Small Bowel, and Nonpseudomyxoma Appendix. *Ann Surg* (2010) 251:896–901. doi: 10.1097/SLA.0b013e3181d9765d
6. Glehen O, Kwiatkowski F, Sugarbaker PH, Elias D, Levine EA, De Simone M, et al. Cytoreductive Surgery Combined With Perioperative Intraperitoneal Chemotherapy for the Management of Peritoneal Carcinomatosis From Colorectal Cancer: A Multi-Institutional Study. *JCO* (2004) 22:3284–92. doi: 10.1200/JCO.2004.10.012
7. Elias D, Honoré C, Dumont F, Ducreux M, Boige V, Malka D, et al. Results of Systematic Second-Look Surgery Plus HIPEC in Asymptomatic Patients Presenting a High Risk of Developing Colorectal Peritoneal Carcinomatosis. *Ann Surg* (2011) 254:289–93. doi: 10.1097/SLA.0b013e31822638f6
8. Verwaal VJ, Zoetmulder FAN. Follow-Up of Patients Treated by Cytoreduction and Chemotherapy for Peritoneal Carcinomatosis of Colorectal Origin. *Eur J Surg Oncol* (2004) 30:280–5. doi: 10.1016/j.ejso.2003.12.003
9. Koh J-L, Yan TD, Glenn D, Morris DL. Evaluation of Preoperative Computed Tomography in Estimating Peritoneal Cancer Index in Colorectal Peritoneal Carcinomatosis. *Ann Surg Oncol* (2009) 16:327–33. doi: 10.1245/s10434-008-0234-2
10. Esquivel J, Chua TC, Stojadinovic A, Melero JT, Levine EA, Gutman M, et al. Accuracy and Clinical Relevance of Computed Tomography Scan Interpretation of Peritoneal Cancer Index in Colorectal Cancer Peritoneal Carcinomatosis: A Multi-Institutional Study. *J Surg Oncol* (2010) 102:565–70. doi: 10.1002/jso.21601
11. Dromain C, Leboulleux S, Auperin A, Goere D, Malka D, Lumbroso J, et al. Staging of Peritoneal Carcinomatosis: Enhanced CT vs. PET/Ct. *Abdom Imaging* (2008) 33:87–93. doi: 10.1007/s00261-007-9211-7
12. Bastiaenen VP, Klaver CEL, Kok NFM, de Wilt JHW, de Hingh IHJT, Aalbers AGJ, et al. Second and Third Look Laparoscopy in Pt4 Colon Cancer Patients for Early Detection of Peritoneal Metastases; the COLOPEC 2 Randomized Multicentre Trial. *BMC Cancer* (2019) 19:254. doi: 10.1186/s12885-019-5408-8
13. Najah H, Malgras B, Dohan A, Gronnier C, Eveno C, Pocard M. The Role of Single-Incision Laparoscopic Peritoneal Exploration in the Management of Patients With Peritoneal Metastases. *Surg Endosc* (2020) 34:2040–9. doi: 10.1007/s00464-019-06984-8
14. Goéré D. Incidence and Prognosis of Synchronous Colorectal Carcinomatosis: Evolution Since 1985? *Future Oncol* (2011) 7:1265–8. doi: 10.2217/fon.11.104
15. Marmor RA, Kelly KJ, Lowy AM, Baumgartner JM. Laparoscopy is Safe and Accurate to Evaluate Peritoneal Surface Metastasis Prior to Cytoreductive Surgery. *Ann Surg Oncol* (2016) 23:1461–7. doi: 10.1245/s10434-015-4958-5
16. Tabrizian P, Shrager B, Jibara G, Yang M-J, Romanoff A, Hiotis S, et al. Cytoreductive Surgery and Hyperthermic Intraperitoneal Chemotherapy for Peritoneal Carcinomatosis: Outcomes From a Single Tertiary Institution. *J Gastrointest Surg* (2014) 18:1024–31. doi: 10.1007/s11605-014-2477-5
17. Zarzavadjian le Bian A, Genser L, Denet C, Ferretti C, Laforest A, Ferraz J-M, et al. Safety and Feasibility of Repeat Laparoscopic Colorectal Resection: A Matched Case-Control Study. *Surg Endosc* (2020) 34:2120–6. doi: 10.1007/s00464-019-06995-5
18. Cai X, Duan L, Wang Y, Jiang W, Liang X, Yu H, et al. Laparoscopic Hepatectomy by Curettage and Aspiration: A Report of 855 Cases. *Surg Endosc* (2016) 30:2904–13. doi: 10.1007/s00464-015-4576-0
19. Cai XJ, Yu H, Liang X, Wang YF, Zheng XY, Huang DY, et al. Laparoscopic Hepatectomy by Curettage and Aspiration. Experiences of 62 Cases. *Surg Endosc* (2006) 20:1531–5. doi: 10.1007/s00464-005-0765-6

20. Agha R, Abdall-Razak A, Crossley E, Dowlut N, Iosifidis C, Mathew G, et al. STROCSS 2019 Guideline: Strengthening the Reporting of Cohort Studies in Surgery. *Int J Surg* (2019) 72:156–65. doi: 10.1016/j.ijsu.2019.11.002
21. Yuan Z, Xu T, Cai J, Zhao Y, Cao W, Fichera A, et al. Development and Validation of an Image-Based Deep Learning Algorithm for Detection of Synchronous Peritoneal Carcinomatosis in Colorectal Cancer. *Ann Surg* (2020) 275(4):e645–51. doi: 10.1097/SLA.0000000000004229
22. Jacquet P, Sugarbaker PH. Clinical Research Methodologies in Diagnosis and Staging of Patients With Peritoneal Carcinomatosis. *Cancer Treat Res* (1996) 82:359–74. doi: 10.1007/978-1-4613-1247-5_23
23. Najah H, Lo Dico R, Eveno C, Pocard M. Laparo-Endoscopic Single Site Surgery for Peritoneal Carcinomatosis Detection and Staging (With Video). *J Visc Surg* (2017) 154:133–4. doi: 10.1016/j.jviscsurg.2017.03.001
24. Mandrekar JN. Receiver Operating Characteristic Curve in Diagnostic Test Assessment. *J Thorac Oncol* (2010) 5:1315–6. doi: 10.1097/JTO.0b013e3181ec173d
25. On behalf of Topic Group 'Evaluating diagnostic tests and prediction models' of the STRATOS initiative, Van Calster B, McLernon DJ, van Smeden M, Wynants L, Steyerberg EW. Calibration: The Achilles Heel of Predictive Analytics. *BMC Med* (2019) 17:230. doi: 10.1186/s12916-019-1466-7
26. Mehralivand S, Shih JH, Rais-Bahrami S, Oto A, Bednarova S, Nix JW, et al. A Magnetic Resonance Imaging-Based Prediction Model for Prostate Biopsy Risk Stratification. *JAMA Oncol* (2018) 4:678–85. doi: 10.1001/jamaoncol.2017.5667
27. Vickers AJ, Elkin EB. Decision Curve Analysis: A Novel Method for Evaluating Prediction Models. *Med Decis Making* (2006) 26:565–74. doi: 10.1177/0272989X06295361
28. Thivolet A, Si-Mohamed S, Bonnot P-E, Blanchet C, Képénékian V, Boussel L, et al. Spectral Photon-Counting CT Imaging of Colorectal Peritoneal Metastases: Initial Experience in Rats. *Sci Rep* (2020) 10:13394. doi: 10.1038/s41598-020-70282-w
29. Fidler IJ. The Pathogenesis of Cancer Metastasis: The "Seed and Soil" Hypothesis Revisited. *Nat Rev Cancer* (2003) 3:453–8. doi: 10.1038/nrc1098
30. Hanahan D. Hallmarks of Cancer: New Dimensions. *Cancer Discovery* (2022) 12:31–46. doi: 10.1158/2159-8290.CD-21-1059
31. Peng S, Chen D, Cai J, Yuan Z, Huang B, Li Y, et al. Enhancing Cancer-Associated Fibroblast Fatty Acid Catabolism Within a Metabolically Challenging Tumor Microenvironment Drives Colon Cancer Peritoneal Metastasis. *Mol Oncol* (2021) 15:1391–411. doi: 10.1002/1878-0261.12917
32. Fermor B, Umpleby HC, Lever JV, Symes MO, Williamson RC. Proliferative and Metastatic Potential of Exfoliated Colorectal Cancer Cells. *J Natl Cancer Inst* (1986) 76:347–9.
33. Umpleby HC, Fermor B, Symes MO, Williamson RCN. Viability of Exfoliated Colorectal Carcinoma Cells. *Br J Surg* (2005) 71:659–63. doi: 10.1002/bjs.1800710902
34. Symes MO, Fermor B, Umpleby HC, Tribe CR, Williamson RC. Cells Exfoliated From Colorectal Cancers can Proliferate in Immune Deprived Mice. *Br J Cancer* (1984) 50:423–5. doi: 10.1038/bjc.1984.193
35. de Cuba EMV, Kwakman R, van Egmond M, Bosch LJW, Bonjer HJ, Meijer GA, et al. Understanding Molecular Mechanisms in Peritoneal Dissemination of Colorectal Cancer: Future Possibilities for Personalised Treatment by Use of Biomarkers. *Virchows Arch* (2012) 461:231–43. doi: 10.1007/s00428-012-1287-y
36. Klaver CEL, Wasmann KATGM, Verstegen M, van der Bilt JDW, Nagtegaal ID, van Ramshorst B, et al. Postoperative Abdominal Infections After Resection of T4 Colon Cancer Increase the Risk of Intra-Abdominal Recurrence. *Eur J Surg Oncol* (2018) 44:1880–8. doi: 10.1016/j.ejso.2018.09.016
37. Salvans S, Mayol X, Alonso S, Messeguer R, Pascual M, Mojal S, et al. Postoperative Peritoneal Infection Enhances Migration and Invasion Capacities of Tumor Cells *In Vitro*: An Insight Into the Association Between Anastomotic Leak and Recurrence After Surgery for Colorectal Cancer. *Ann Surg* (2014) 260:939–44. doi: 10.1097/SLA.0000000000000958
38. Coussens LM, Werb Z. Inflammation and Cancer. *Nature* (2002) 420:860–7. doi: 10.1038/nature01322
39. Aggarwal BB, Vijayalekshmi RV, Sung B. Targeting Inflammatory Pathways for Prevention and Therapy of Cancer: Short-Term Friend, Long-Term Foe. *Clin Cancer Res* (2009) 15:425–30. doi: 10.1158/1078-0432.CCR-08-0149
40. Wu Y, Zhou BP. Inflammation: A Driving Force Speeds Cancer Metastasis. *Cell Cycle* (2009) 8:3267–73. doi: 10.4161/cc.8.20.9699
41. Barriuso J, Nagaraju RT, Belgamwar S, Chakrabarty B, Burghel GJ, Schlecht H, et al. Early Adaptation of Colorectal Cancer Cells to the Peritoneal Cavity Is Associated With Activation of "Stemness" Programs and Local Inflammation. *Clin Cancer Res* (2021) 27:1119–30. doi: 10.1158/1078-0432.CCR-20-3320
42. Ceelen WP, Bracke ME. Peritoneal Minimal Residual Disease in Colorectal Cancer: Mechanisms, Prevention, and Treatment. *Lancet Oncol* (2009) 10:72–9. doi: 10.1016/S1470-2045(08)70335-8
43. Hayashi K, Jiang P, Yamauchi K, Yamamoto N, Tsuchiya H, Tomita K, et al. Real-Time Imaging of Tumor-Cell Shedding and Trafficking in Lymphatic Channels. *Cancer Res* (2007) 67:8223–8. doi: 10.1158/0008-5472.CAN-07-1237
44. Lipsyc M, Yaeger R. Impact of Somatic Mutations on Patterns of Metastasis in Colorectal Cancer. *J Gastrointest Oncol* (2015) 6:645–9. doi: 10.3978/j.issn.2078-6891.2015.045
45. Tran B, Kopetz S, Tie J, Gibbs P, Jiang Z-Q, Lieu CH, et al. Impact of BRAF Mutation and Microsatellite Instability on the Pattern of Metastatic Spread and Prognosis in Metastatic Colorectal Cancer. *Cancer* (2011) 117:4623–32. doi: 10.1002/cncr.26086
46. Yokota T, Ura T, Shibata N, Takahari D, Shitara K, Nomura M, et al. BRAF Mutation is a Powerful Prognostic Factor in Advanced and Recurrent Colorectal Cancer. *Br J Cancer* (2011) 104:856–62. doi: 10.1038/bjc.2011.19
47. Passot G, Dumont F, Goéré D, Arvieux C, Rousset P, Regimbeau J-M, et al. Multicentre Study of Laparoscopic or Open Assessment of the Peritoneal Cancer Index (BIG-RENAPE). *Br J Surg* (2018) 105:663–7. doi: 10.1002/bjs.10723

Conflict of Interest: The authors declare that the research was conducted in the absence of any commercial or financial relationships that could be construed as a potential conflict of interest.

Publisher's Note: All claims expressed in this article are solely those of the authors and do not necessarily represent those of their affiliated organizations, or those of the publisher, the editors and the reviewers. Any product that may be evaluated in this article, or claim that may be made by its manufacturer, is not guaranteed or endorsed by the publisher.

Copyright © 2022 Zhang, Qin, Li, Zhang, Luo, Wu, Li, Han, Wang and Wang. This is an open-access article distributed under the terms of the Creative Commons Attribution License (CC BY). The use, distribution or reproduction in other forums is permitted, provided the original author(s) and the copyright owner(s) are credited and that the original publication in this journal is cited, in accordance with accepted academic practice. No use, distribution or reproduction is permitted which does not comply with these terms.

frontiers | Frontiers in Oncology

PERSPECTIVE
published: 13 July 2022
doi: 10.3389/fonc.2022.967100

Colon Sparing Endoscopic Full-Thickness Resection for Advanced Colorectal Lesions: Is It Time for Global Adoption?

*Zhong-Wei Wu[1], Chao-Hui Ding[2], Yao-Dong Song[2], Zong-Chao Cui[2], Xiu-Qian Bi[2] and Bo Cheng[2]**

[1] Department of Gastrointestinal Surgery, The First Affiliated Hospital of Zhengzhou University, Zhengzhou, China,
[2] Department of Emergency Surgery, The First Affiliated Hospital of Zhengzhou University, Zhengzhou, China

The majority of colon lesions are <10 mm in size and are easily resected by endoscopists with appropriate basic training. Lesions ≥10 mm in size are difficult to remove technically and are associated with higher rates of incomplete resection. Currently, the main endoscopic approaches include endoscopic mucosal resection (EMR) for lesions without submucosal invasion, and endoscopic submucosal dissection (ESD) for relatively larger lesions involving the superficial submucosal layer. Both of these approaches have limitations, EMR cannot reliably ensure complete resection for larger tumors and recurrence is a key limitation. ESD reliably provides complete resection and an accurate pathological diagnosis but is associated with risk such as perforation or bleeding. In addition, both EMR and ESD may be ineffective in treating subepithelial lesions that extend beyond the submucosa. Endoscopic full-thickness resection (EFTR) is an emerging innovative endoscopic therapy which was developed to overcome the limitations of EMR and ESD. Advantages include enabling a transmural resection, complete resection of complex colorectal lesions involving the mucosa to the muscularis propria. Recent studies comparing EFTR with current resection techniques and radical surgery for relatively complicated and larger lesion have provided promising results. If the current trajectory of research and development is maintained, EFTR will likely to become a strong contender as an alternative standard of care for advanced colonic lesions. In the current study we aimed to address this need, and highlighted the areas of future research, while stressing the need for multinational collaboration provide the steppingstone(s) needed to bring EFTR to the mainstream.

Keywords: colon cancer, endoscopic therapy, endoscopic submucosal dissection, endoscopic full-thickness resection, gastrointestinal cancer

OPEN ACCESS

Edited by:
Zhendong Jin,
Second Military Medical University, China

Reviewed by:
Bin Zhang,
The Affiliated Hospital of Xuzhou Medical University, China
Yang Xi,
Huazhong University of Science and Technology, China

***Correspondence:**
Bo Cheng
edgar2017lw@126.com

Specialty section:
This article was submitted to Gastrointestinal Cancers: Colorectal Cancer, a section of the journal Frontiers in Oncology

Received: *12 June 2022*
Accepted: *20 June 2022*
Published: *13 July 2022*

Citation:
Wu Z-W, Ding C-H, Song Y-D, Cui Z-C, Bi X-Q and Cheng B (2022) Colon Sparing Endoscopic Full-Thickness Resection for Advanced Colorectal Lesions: Is It Time for Global Adoption? Front. Oncol. 12:967100. doi: 10.3389/fonc.2022.967100

INTRODUCTION

The flexible endoscope was originally designed as a diagnostic tool for examining the lumen of the gastrointestinal (GI) tract, now known as the 'first space' (1). The utility of expanding the operative field to this 'second space' has been highlighted by advances in interventional endoscopic techniques such as the development of a working channel, access to the peritoneal cavity and more recently,

access to extra-luminal organs such as the gallbladder and thyroid gland (2–4). Access to the submucosal layer – also known as the 'third space' – and to the subserosal layer – known as the 'fourth space' –has highlighted the potential of interventional endoscopy in reducing the need for invasive surgical interventions for the management of many luminal lesions (5).

Endoscopic mucosal resection (EMR) and endoscopic submucosal dissection (ESD) are two well established endoscopic resection techniques for lesions involving the mucosal and superficial submucosal layers (6, 7). However, EMR and ESD can be challenging as there is still a considerable rate of adverse events, particularly perforation and bleeding. Furthermore, larger lesions cannot reliably be removed resulting in incomplete resections, and dense fibrosis results in non-lifting, difficult-to-treat lesions (8, 9). ESD is technically challenging and burdened by longer procedure times and higher costs. It should therefore be restricted to lesions suspicious for high-grade dysplasia or early invasive cancer.

Endoscopic full-thickness resection (EFTR) is a latest addition to endoscopic resection techniques which is developed to overcome the limitations of EMR and ESD (10, 11). It involves the complete resection of the mucosa to the muscularis propria and is very useful for the treatment of difficult-to-resect lesions, e.g., recurrence with scar formation after previous endoscopic resections or even for associated lymph nodes resections (12). There are two approaches to EFTR i.e., exposed and non-exposed EFTR. In exposed EFTR, first the full-thickness resection is performed, with subsequent closure of the mucosal defect (mainly used for upper GI luminal subepithelial lesion). In non-exposed EFTR, serosa-to-serosa apposition is achieved, and then full thickness resection is completed with the assistance of a cap-mounted clip. However, it is challenging to safely and efficiently close the large defects resulting from EFTR. Successful closure of large defects is critical for the use of the EFTR procedures. Endoclips were used as the earliest treatment method for the endoscopic closure of GI perforations and are still a common tool for defect closure. Different types of endoclips with reliable rotation are available widely and are usually effective for the closure of small defects (<1 cm) but are less effective for the closure of larger defects (>1 cm).

Different suturing devices/systems have been developed for EFTR such as over-the-scope clips (OTSC) (Ovesco Endoscopy AG, Tubingen, Germany) and Overstitch (Apollo Endosurgery, Austin, TX, USA). OTSC is a clip-type full-thickness suturing device but is still unable to close defects larger than 2 cm. Several studies have reported the usefulness of the device for closure of fistulas, iatrogenic perforations and anastomotic leakage after surgery (13–16). The overstitch is not available worldwide and even in China. More recently Liu et al. designed the new technique of "Kissing Suture" for closing large GI wall defects that remained after EFTR. The successful use of the "Kissing Suture" method for endoscopic gastroplasty and NOTES gastroenterostomy (anastomose the jejunum and stomach) has been described in a human setting and has proven to be feasible and efficient (17–19). Since the introduction of EFTR with full-thickness resection device (FTRD) into clinical practices, there has been an increasing number of published studies on EFTR using the FTRD system in the colorectum (20, 21).

If the concerns of infection and intraperitoneal diffusion of tumor cells are solved, advanced complicated lesions such as gastrointestinal stromal tumors (GISTs) would be a good candidate for EFTR. Flexible endoscopy has opened up new frontiers for surgeons and endoscopists. As the armamentarium of interventional endoscopy expands and the ability of endoscopists to perform advanced interventions safely fosters an inevitable step forward that will involve the integration of new technology with innovative and creative thinking.

ENDOSCOPIC FULL-THICKNESS RESECTION

EMR for adenomas or early colorectal carcinomas with severe fibrosis have an increased risk of perforation and other adverse events. The perforation rate of ESD for lesions with severe submucosal fibrosis also remains high. Endoscopic full-thickness removal of luminal GI lesions is an efficient non-surgical development for en bloc resection for advanced adenomas (22, 23). Endoscopic resection of luminal GI neoplasms has traditionally been limited to the mucosa and submucosa due to the lack of adequate closure techniques. The introduction of the OTSC and the research on natural orifice transluminal endoscopic surgery (NOTES) paved the way for transmural endoscopic interventions (14, 24). In 2014, two groups separately reported the first clinical cases of EFTR using a OTSC device (25, 26). Since the approval of the FTRD (in 2014), multiple studies on colorectal EFTR have been published (27). Lesions <20 mm in diameter may be amenable to resection with an adapted OTSC cap, in which the lesion is pulled into the cap with retraction forceps resulting in invagination of the colon wall followed by OTSC deployment.

Zwager et al. reported the results of the Dutch colorectal EFTR registry where the data was prospectively collected from 20 hospitals and covered a total of 367 EFTR procedures (28). The procedure technical success was 83.9% and the R0 resection rate was 82.4%. Adverse events were noted in 9.3% of cases, with 2.7% of patients required emergency surgery. Recurrent or residual lesions rate was 6.4%. Interestingly, the Dutch colorectal EFTR data included a sizeable subgroup of patients (n = 221) undergoing EFTR for T1 carcinoma. A recent retrospective study described a high diagnostic value of EFTR for T1 carcinomas, allowing patients to be assigned to the best treatment strategy (29). The Dutch registry comprised 150 patients who had "secondary" EFTR after malignant polyps were not completely resected. According to Kuellmer et al., the vast majority of these patients were classified as "low risk" after EFTR, and surgery was therefore not deemed

necessary (30). According to both studies, EFTR of post-polypectomy scars appears to be a very good alternative in these cases.

Guo et al. presented 23 cases of exposed EFTR followed by defect closure using the OTSC method. The procedure technical success rate was 100% and delayed perforation was not observed at the 3-month mark (31). Tumor size ranged from 6–20 mm. Histopathological findings showed that one patient (4%) was high-risk GIST, 18 (78%) were very low-risk GIST, and 4 (17%) were leiomyomas. The main reported complication was localized peritonitis which occurred in two patients (9%). Zhou et al. and colleagues reported 26 EFTR cases for gastric GIST originating from the muscularis propria. R0 resection was achieved successfully in all tumors with a median size of 28 (range 12–45) mm. Full-thickness resected stomas was successfully closed using endoclips in all cases including the one where the defect was larger than 30 mm (32).

Recently, Liu et al. reported EFTR of colonic adenocarcinoma and lymphadenectomy in a 60-year-old man (33). Due to multiple prior abdominal surgeries, he was not considered a candidate for another intra-abdominal operation and therefore, endoscopic resection was recommended for him. A detachable balloon was inflated and placed in the transverse colon before the procedure to prevent contamination of the intraoperative field. EFTR of the colonic lesion was then completed successfully. An endoscope was introduced *via* the mucosal defect, to observer the lymph nodes. The lymph nodes were observed at 2-3 cm from the defect area and removed endoscopically. The large full-thickness defect was then closed using endoloops and endoclips **(Figure 1).** No adverse event was observed in the patient at the 12-month follow-up visit.

This case demonstrates the EFTR of a colorectal cancer and a lymphadenectomy. Although this case was striking, and the patient appears to be disease-free. The authors may simply gotten lucky in that the nodes were all easy to locate, they were adjacent to the original lesion, and could be resected easily. The majority of colorectal cancer surgeries involve an extended search for adenopathy and removal of all perilesional lymph nodes. It is easy to visualize how other benign or malignant lymph nodes could have gone unnoticed; if that were the case, there would have been far less to celebrate.

ENDOSCOPIC FULL-THICKNESS RESECTION – INDICATIONS, CLOSURE TECHNIQUES, COMPLICATIONS AND LIMITATIONS

In clinical practice, non-lifting lesions with extensive submucosal fibrosis and lesions involving difficult anatomical locations (appendiceal orifice or diverticula, and subepithelial tumors) are the main indications for EFTR. Moreover, EFTR is gaining attention as a credible diagnostic tool and alternative therapeutic option for T1 colorectal cancer, because it can provide high quality pathological specimens and precise histological risk assessment. GIST has been found to be a good indication for EFTR as well.

To date, several full-thickness endoscopic closure methods have been developed using endoclips with or without endoloops, as well several suturing devices, including the OTSC system or Overstitch is the most commonly using tool in clinical settings (34–38). The first published report of the use of endoclips to close perforations after resection of a gastric leiomyoma was in 1993 (39). Subsequently, multiple studies have demonstrated the successful use of endoclips for the closure of iatrogenic perforations resulting from EMR and ESD (40). Endoscopic clipping is now accepted as the most effective, popular, and widely available method for the closure of GI wall perforations (40, 41). Following the development and success of the use of endoclips, an endoscopic suturing methods for EFTR has been used to avoid the need for surgical intervention. However, endoclips can grasp only the mucosal layer, and closure of large defects is challenging if the defect size is larger than 1 cm, thus, there is a risk of leakage when using endoclip alone closure (42). To date, numerous studies have reported the successful use of the OTSC system and Overstitch for EFTR defect closure (31, 43). The major limitations of OTSC included limitation of maximum tumor

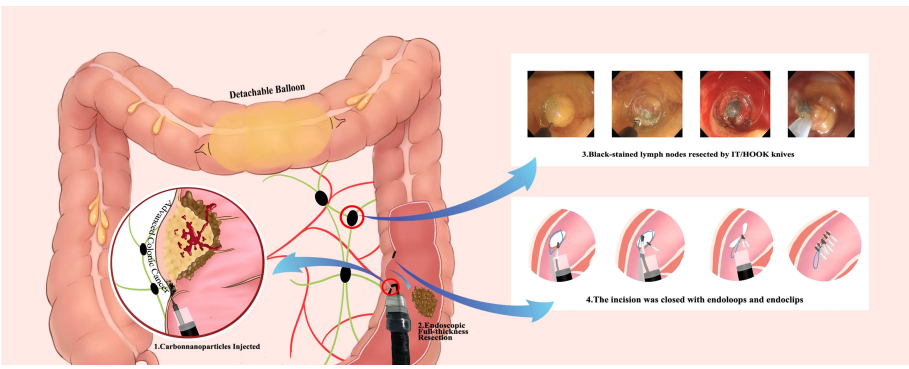

FIGURE 1 | Infographics of endoscopic full-thickness resection and lymphadenectomy for advanced colonic cancer as described by Liu et al.

size (up to 2 cm, due to the restraint of tissues that can be sufficiently pulled into the cap), tumor position (esophagus and duodenum due to limited workspace), and restricted maneuverability for defect closure. Additionally, in China, where the majority of the EFTR procedure has been performed in the world Overstitch is not available (34). To overcome the limitations of endoclips for large defect closure, endoscopists have designed several methods in combination with endoloops based on use of a double-channel endoscope, such as interrupted suture, clip-loop, endoscopic purse-string suture methods, and so on (35–37). None of these methods are suitable for defects larger than 4 cm (44). The use of a double-channel endoscope has disadvantages. First, a double channel endoscope is thicker, rigid, and heavier; therefore, it is difficult to manipulate. Second, the endoclip and endoloops are inserted through two different channels of the same endoscope, both move synchronously with the endoscope; thus, making it difficult for clipping the nylon loops around the edge of the defect. Third, it is necessary to change to the double-channel endoscope for defect closure, whereas the resection was made with a single-channel endoscope. Fourth, the double-channel endoscopes are not available in most of the endoscopy centers in China and other countries. Because of the technical limitations and difficulties of using a double-channel endoscope as well as endoscopic suturing devices, Liu et al. designed the "Kissing Suture" method for closing large GI wall defects that remained after EFTR. The ''Kissing Suture'' method requires a single-channel endoscope with endoloops and endoclips. The loop is placed in the defect area and uses two endoclips to anchor it to the two edges of the full-thickness layer or muscle layer of the defected wall. Tightening the loop changed the defect from linear-shaped to resemble the infinity symbol (∞). To the purpose of more rapid wound healing the defected edges are set in edges-to-edges apposition at the edge of submucosa-submucosa and mucosa-mucosa, respectively; and then endoclips are used to close the complete linear incision **(Figure 2).** Benefits of the "Kissing Suture" method included, it is easy to control the endoscope because the endoloops free from the endoscope and does not interfere with clipping. Additional, endoloops and endoclips can be used to reinforce the closure of the defect and prevent postoperative leak and peritonitis. However, the mucosa may invert while mucosa and submucosa are sutured together which could impair healing. From previous experience, defect closure with endoclips by the mucosa-mucosa apposition has been shown to be effective for quicker wound

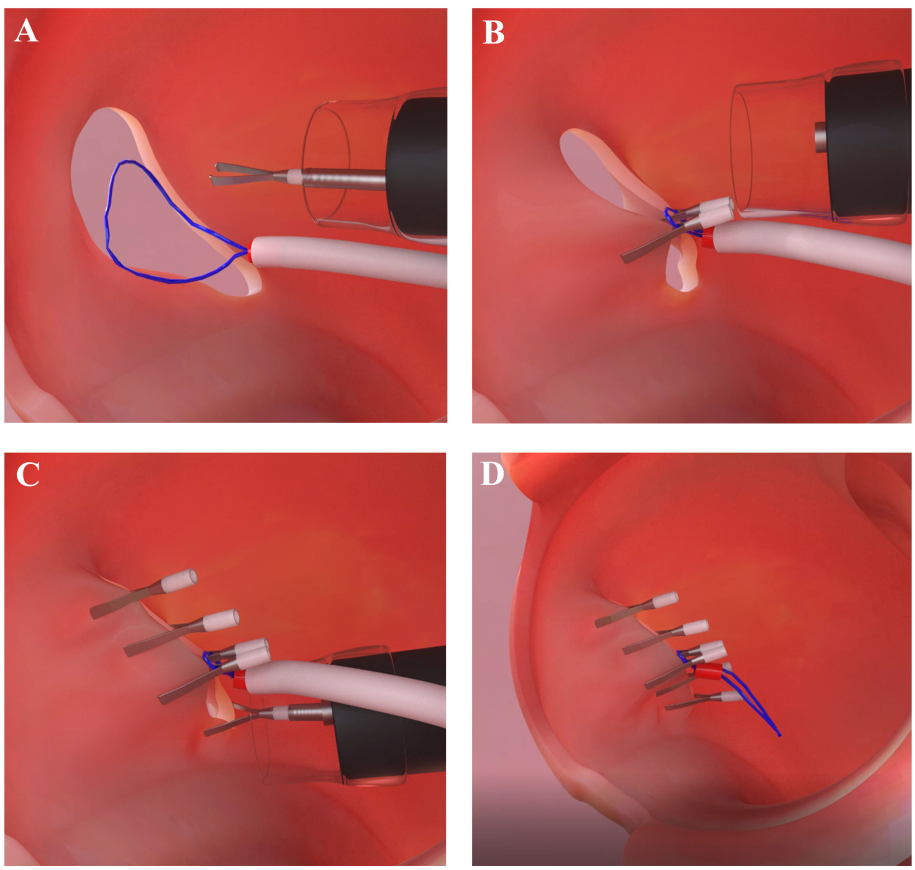

FIGURE 2 | Illustration of the ''Kissing Suture'' method. **(A)** Nylon loops along with endoclip is used to anchor the two edges of the defected wall. **(B)** Nylon loops is fixed along with endoclip. **(C)** Additional clips are used to complete the linear incision closure. **(D)** Overview of the defect closure using nylon loops and endoclips.

healing and prevention of ongoing leakage of air and digestive juices (17). The use of a single-channel endoscope with endoloops and endoclips has the advantage of being simple to manipulate, does not require specialized equipment, and there is no technical complexity. The "Kissing Suture" method has a potential future for the closure of large GI tract wall defect following EFTR, NOTES procedure, and for different kinds of perforation.

Bleeding and perforation are main EFTR complications. When bleeding occurs during the procedure, the use of dedicated hot coagulation forceps and/or hot biopsy forceps to stop it immediately are recommended. However, endoscopic clips should be used to ligate the bleeding vessels when large vessels are present, or the bleeding cannot be stopped using coagulation. To avoid perforation, use the dynamic submucosal injection approach for sessile and flat lesions to separate the lesion from muscularis propria with an adequate submucosal cushion, and take preventive measures if a deep resection is performed. It is critical to be able to recognize deep cuts or perforations since they must be closed immediately using endoclips.

DEVELOPMENT AND TRAINING FOR ENDOSCOPIC FULL-THICKNESS RESECTION

Gastroenterology fellows are trained to perform colonoscopy for diagnostic purposes in a straight forward fashion. It is essential to have a thorough understanding of EMR and ESD before attempting EFTR. EFTR expands upon these skills and transposes skills acquired from training in EMR or ESD (indications, proficiency in lesion identification, limitations, technique, and dealing with adverse events during the procedure). Although more advanced methods can be learned during ESD training, competency in the handling of adverse events such as perforation and bleeding is mandatory. Deconstruction of the steps involved in EFTR allows for task-oriented training. Adopting these basic principles, a credentialing process for competency in EFTR should be established as this will be essential for global adoption of this endoscopic modality.

Although there are a variety of artificial tissue and ex vivo models available, opportunities to practice on live animals that better imitate peristalsis, bleeding, and respiratory movement should be pursued. However, training specific to the colorectum remains challenging because live animal models such as porcine models do not provide adequate simulation of human colorectal tissue. Bovine specimens are good alternatives for the colorectum, particularly when training to use innovation such as the FTRD and other new resection tools. With the experience and improvements in endoscopic technology, the procedural difficulties observed with EFTR will be reduced as well. Additionally, patients with advanced adenomas who are poor surgical candidates may also benefit from EFTR.

FUTURE DIRECTION AND CONCLUSION

Traditionally, colectomy remains the treatment of choice for the management complex colorectal lesions. However, advanced endoscopic techniques have also been proposed in order to improve the accuracy of diagnosis, more precise risk assessment, and colon sparing resection of colorectal lesions. Advanced endoscopic resection techniques allow curative treatment of difficult colonic lesions and often avoids the need for surgery. However, determining the optimum resection technique (EMR, ESD or EFTR) for specific individual and lesions to maximize the efficacy, and safety while avoiding unnecessary surgical intervention remains a challenge. Although both EMR and ESD are effective and are currently preferred, a transmural approach for large lesions, if resources and expertise are available would be preferable.

Endoscopic full-thickness resection, a transmural approach, of luminal GI lesions is a new development that has been performed only in a limited manner and, in all fairness, can only be labeled as experimental. Nonetheless, interest and progress in this field are rapid and ongoing. Although EFTR technique is still developing and requires refinement, it is an outstanding procedure in terms of invasiveness. However, we should not be satisfied with the currently available numbers and retrospective studies. We must aim for large sample size prospective randomized controlled trials to compare the EFTR with other endoscopic methods with long-term follow-up data on recurrence rates and clinical outcomes. Development of reliable closure devices and establishment of appropriate indications will make EFTR more practical especially for advanced colonic lesions. This not only avoid patients to an unneeded, invasive intervention with its associated risks, but also reduces the financial burden on the patient, hospital system, and society. There is also a need for multinational collaboration and a consensus on training and credentialing pathway for EFTR, and on areas of future research necessary for widespread adoption of EFTR.

DATA AVAILABILITY STATEMENT

Publicly available datasets were analyzed in this study. This data can be found here: This is a perspective thought provoking article (not an original article). No original data was produced for this article. However, current data (non-original) collected for writing this article is available with corresponding author. It can be provided on request. (BC, E-mail: edgar2017lw@126.com).

ETHICS STATEMENT

The study protocol was reviewed and approved by the independent ethics committee of at the First Affiliated Hospital Zhengzhou University.

AUTHOR CONTRIBUTIONS

Study concept and design: Z-WW and BC. Manuscript writing: Z-WW, C-HD, Y-DS, and Z-CC. Acquisition of data: X-QB, C-HD, Y-DS, and Z-CC. Schematics drawn: Z-WW. Critical revision of manuscript: BC. All authors contributed to the article and approved the submitted version.

REFERENCES

1. Radhakrishnan A. Advances in Flexible Endoscopy. *Vet Clin North Am Small Anim Pract* (2016) 46(1):85–112. doi: 10.1016/j.cvsm.2015.08.003
2. Mori H, Kobayashi N, Kobara H, Nishiyama N, Fujihara S, Chiyo T, et al. Novel and Safer Endoscopic Cholecystectomy Using Only a Flexible Endoscope *via* Single Port. *World J Gastroenterol* (2016) 22(13):3558–63. doi: 10.3748/wjg.v22.i13.3558
3. Liu BR, Ullah S, Li DL, Liu D, Zhao LX, Yang W, et al. A Snare-Assisted Pure NOTES Retrograde Cholecystectomy Using a Single Channel Flexible Endoscope: A Pilot Experiment in a Porcine Model. *Surg Endosc* (2020) 34 (8):3706–10. doi: 10.1007/s00464-020-07561-0
4. Liu BR, Qiu XG, Li DL, Kong LJ, Ullah S, Li-Xia Z, et al. Flexible Endoscopic Transoral Thyroidectomy: A Pilot Study in a Porcine Model (With Video). *Gastrointest Endosc* (2021) 93(1):224–8. doi: 10.1016/j.gie.2020.07.033
5. Ullah S, Ali FS, Liu BR. Advancing Flexible Endoscopy to Natural Orifice Transluminal Endoscopic Surgery. *Curr Opin Gastroenterol* (2021) 37 (5):470–7. doi: 10.1097/MOG.0000000000000753
6. Nishizawa T, Yahagi N. Endoscopic Mucosal Resection and Endoscopic Submucosal Dissection: Technique and New Directions. *Curr Opin Gastroenterol* (2017) 33(5):315–9. doi: 10.1097/MOG.0000000000000388
7. Ono H, Yao K, Fujishiro M, Oda I, Uedo N, Nimura S, et al. Guidelines for Endoscopic Submucosal Dissection and Endoscopic Mucosal Resection for Early Gastric Cancer (Second Edition). *Dig Endosc* (2021) 33(1):4–20. doi: 10.1111/den.13883
8. Draganov PV, Wang AY, Othman MO, Fukami N. AGA Institute Clinical Practice Update: Endoscopic Submucosal Dissection in the United States. *Clin Gastroenterol Hepatol* (2019) 17(1):16–25. doi: 10.1016/j.cgh.2018.07.041
9. Ahmed Y, Othman M. EMR/ESD: Techniques, Complications, and Evidence. *Curr Gastroenterol Rep* (2020) 22(8):39. doi: 10.1007/s11894-020-00777-z
10. Rajan E, Wong Kee Song LM. Endoscopic Full Thickness Resection. *Gastroenterology* (2018) 154(7):1925–37.e2. doi: 10.1053/j.gastro.2018.02.020
11. Dalal I, Andalib I. Advances in Endoscopic Resection: A Review of Endoscopic Submucosal Dissection (ESD), Endoscopic Full Thickness Resection (EFTR) and Submucosal Tunneling Endoscopic Resection (STER). *Transl Gastroenterol Hepatol* (2022) 7:19. doi: 10.21037/tgh-2020-10
12. Li JW, Ang TL, Wang LM, Kwek ABE, Tan MTK, Fock KM, et al. Endoscopic Submucosal Dissection of Colorectal Neoplasms: An Audit of its Safety and Efficacy in a Single Tertiary Centre in Singapore. *Singapore Med J* (2019) 60 (10):526–31. doi: 10.11622/smedj.2019022
13. Piyachaturawat P, Mekaroonkamol P, Rerknimitr R. Use of the Over the Scope Clip to Close Perforations and Fistulas. *Gastrointest Endosc Clin N Am* (2020) 30(1):25–39. doi: 10.1016/j.giec.2019.08.002
14. Mosquera-Klinger G, Torres-Rincón R, Jaime-Carvajal J. Endoscopic Closure of Gastrointestinal Perforations and Fistulas Using the Ovesco Over-The-Scope Clip System at a Tertiary Care Hospital Center. *Rev Gastroenterol Mex (Engl Ed)* (2019) 84(2):263–6. doi: 10.1016/j.rgmxen.2018.10.005
15. Iabichino G, Eusebi LH, Palamara MA, Arena M, Pellicano R, Consolo P, et al. Performance of the Over-the-Scope Clip System in the Endoscopic Closure of Iatrogenic Gastrointestinal Perforations and Post-Surgical Leaks and Fistulas. *Minerva Gastroenterol Dietol* (2018) 64(1):75–83. doi: 10.23736/S1121-421X.17.02439-4
16. Wedi E, Gonzalez S, Menke D, Kruse E, Matthes K, Hochberger J, et al. One Hundred and One Over-the-Scope-Clip Applications for Severe Gastrointestinal Bleeding, Leaks and Fistulas. *World J Gastroenterol* (2016) 22(5):1844–53. doi: 10.3748/wjg.v22.i5.1844
17. Liu BR, Song JT, Qu B, Wen JF, Yin JB, Liu W, et al. Endoscopic Muscularis Dissection for Upper Gastrointestinal Subepithelial Tumors Originating From the Muscularis Propria. *Surg Endosc* (2012) 26:3141–8. doi: 10.1007/s00464-012-2305-5
18. Liu BR, Liu D, Zhao LX, Ullah S, Zhou YY, Zhang JY, et al. Endoscopic Gastroplasty as Therapy for Postoperative Gastric Distortion and Stenosis. *Endoscopy* (2019) 5:E105–7. doi: 10.1055/a-0837-0583
19. Liu BR, Liu D, Zhao LX, Ullah S, Zhang JP, Zhang JY, et al. Pure Natural Orifice Transluminal Endoscopic Surgery (NOTES) Nonstenting Endoscopic Gastroenterostomy: First Human Clinical Experience. *VideoGIE* (2019) 4:206–8. doi: 10.1016/j.vgie.2019.01.004
20. Meier B, Stritzke B, Kuellmer A, Zervoulakos P, Huebner GH, Repp M, et al. Efficacy and Safety of Endoscopic Full-Thickness Resection in the Colorectum: Results From the German Colonic FTRD Registry. *Am J Gastroenterol* (2020) 115(12):1998–2006. doi: 10.14309/ajg.0000000000000795
21. Li P, Ma B, Gong S, Zhang X, Li W. Efficacy and Safety of Endoscopic Full-Thickness Resection in the Colon and Rectum Using an Over-the-Scope Device: A Meta-Analysis. *Surg Endosc* (2021) 35(1):249–59. doi: 10.1007/s00464-020-07387-w
22. Albrecht H, Raithel M, Braun A, Nagel A, Stegmaier A, Utpatel K, et al. Endoscopic Full-Thickness Resection (EFTR) in the Lower Gastrointestinal Tract. *Tech Coloproctol* (2019) 23(10):957–63. doi: 10.1007/s10151-019-02043-5
23. Mori H, Kobara H, Nishiyama N, Masaki T. Current Status and Future Perspectives of Endoscopic Full-Thickness Resection. *Dig Endosc* (2018) 30 (Suppl 1):25–31. doi: 10.1111/den.13042
24. Rieder E, Martinec DV, Dunst CM, Swanström LL. A Novel Technique for Natural Orifice Endoscopic Full-Thickness Colon Wall Resection: An Experimental Pilot Study. *J Am Coll Surg* (2011) 213(3):422–9. doi: 10.1016/j.jamcollsurg.2011.05.015
25. Schmidt A, Damm M, Caca K. Endoscopic Full-Thickness Resection Using a Novel Over-the-Scope Device. *Gastroenterology* (2014) 147:740–2. doi: 10.1053/j.gastro.2014.07.045
26. Valli PV, Kaufmann M, Vrugt B, Bauerfeind P. Endoscopic Resection of a Diverticulum-Arisen Colonic Adenoma Using a Full-Thickness Resection Device. *Gastroenterology* (2014) 147:969–71. doi: 10.1053/j.gastro.2014.07.053
27. Schmidt A. Endoscopic Full-Thickness Resection in the Colorectum: Ready for Prime Time? *Endoscopy* (2020) 52(11):1024–5. doi: 10.1055/a-1191-3247
28. Zwager LW, Bastiaansen BAJ, Bronzwaer MES, van der Spek BW, Heine GDN, Haasnoot KJC, et al. Endoscopic Fullthickness Resection (eFTR) of Colorectal Lesions: Results From the Dutch Colorectal eFTR Registry. *Endoscopy* (2020) 52:1014–23. doi: 10.1055/a-1176-1107
29. van der Spek B, Haasnoot K, Meischl C, Heine D. Endoscopic Full-Thickness Resection in the Colorectum: A Single-Center Case Series Evaluating Indication, Efficacy and Safety. *Endosc Int Open* (2018) 6(10):E1227–34. doi: 10.1055/a-0672-1138
30. Kuellmer A, Mueller J, Caca K, Aepli P, Albers D, Schumacher B, et al. Endoscopic Full-Thickness Resection for Early Colorectal Cancer. *Gastrointest Endosc* (2019) 89(6):1180–89.e1. doi: 10.1016/j.gie.2018.12.025
31. Guo J, Liu Z, Sun S, Liu X, Wang S, Ge N, et al. Endoscopic Full-Thickness Resection With Defect Closure Using an Over-the-Scope Clip for Gastric Subepithelial Tumors Originating From the Muscularis Propria. *Surg Endosc* (2015) 29:3356–62. doi: 10.1007/s00464-015-4076-2
32. Zhou PH, Yao LQ, Qin XY, Cai MY, Xu MD, Zhong YS, et al. Endoscopic Full-Thickness Resection Without Laparoscopic Assistance for Gastric Submu Cosal Tumors Originated From the Muscularis Propria. *Surg Endosc* (2011) 25:2926–31. doi: 10.1007/s00464-011-1644-y
33. Liu BR, Liu D, Ullah S, Zhao L, Zheng Q, Ullah R, et al. Endoscopic Full-Thickness Resection and Endoscopic Lymphadenectomy for Advanced Colonic Cancer in an Inoperable Patient: First Human Clinical Experience. *Gastrointest Endosc* (2020) 91(2):451–2. doi: 10.1016/j.gie.2019.09.005
34. ASGE Technology Committee, Aslanian Committee Technology ASGE, Sethi HR, Bhutani A, Goodman MS, Krishnan AJ, K, et al. ASGE Guideline for Endoscopic Full-Thickness Resection and Submucosal Tunnel Endoscopic Resection. *VideoGIE* (2019) 4:343–50. doi: 10.1016/j.vgie.2019.03.010
35. Takeshita N, Ho KY. Endoscopic Closure for Full-Thickness Gastrointestinal Defects: Available Applications and Emerging Innovations. *Clin Endosc* (2016) 49:438–43. doi: 10.5946/ce.2016.104
36. Kukreja K, Chennubhotla S, Bhandari B, Arora A, Singhal S. Closing the Gaps: Endoscopic Suturing for Large Submucosal and Full-Thickness Defects. *Clin Endosc* (2018) 51:352–6. doi: 10.5946/ce.2017.117
37. Zeng CY, Li GH, Zhu Y, Zhou XJ, Lv NH, Chen YX, et al. Single-Channel Endoscopic Closure of Large Endoscopy Related Perforations. *Endoscopy* (2015) 47:735–8. doi: 10.1055/s-0034-1392043
38. Dellatore P, Bhagat V, Kahaleh M. Endoscopic Full Thickness Resection Versus Submucosal Tunneling Endoscopic Resection for Removal of

Submucosal Tumors: A Review Article. *Transl Gastroenterol Hepatol* (2019) 4:45. doi: 10.21037/tgh.2019.05.03
39. Binmoeller KF, Grimm H, Soehendra N. Endoscopic Closure of a Perforation Using Metallic Clips After Snare Excision of a Gastric Leiomyoma. *Gastrointest Endosc* (1993) 39:172–4. doi: 10.1016/S0016-5107(93)70060-7
40. Takamaru H, Saito Y, Yamada M, Tsuruki ES, Kinjo Y, Otake Y, et al. Clinical Impact of Endoscopic Clip Closure of Perforations During Endoscopic Submucosal Dissection for Colorectal Tumors. *Gastrointest Endosc* (2016) 84:494–502.e1. doi: 10.1016/j.gie.2016.01.014
41. Turan AS, Ultee G, Van Geenen EJM, Siersema PD. Clips for Managing Perforation and Bleeding After Colorectal Endoscopic Mucosal Resection. *Expert Rev Med Devices* (2019) 16:493–501. doi: 10.1080/17434440.2019.1618707
42. Inayat F, Aslam A, Grunwald MD, Hussain Q, Hurairah A, Iqbal S, et al. Omental Patching and Purse-String Endosuture Closure After Endoscopic Full-Thickness Resection in Patients With Gastric Gastrointestinal Stromal Tumors. *Clin Endosc* (2019) 52:283–7. doi: 10.5946/ce.2018.116
43. Kantsevoy SV, Bitner M, Hajiyeva G, Mirovski PM, Cox ME, Swope T, et al. Endoscopic Management of Colonic Perforations: Clips Versus Suturing Closure (With Videos). *Gastrointest Endosc* (2016) 84:487–92. doi: 10.1016/j.gie.2015.08.074
44. Zhang X, Modayil R, Criscitelli T, Stavropoulos SN. Endoscopic Resection for Subepithelial Lesions—Pure Endoscopic Full-Thickness Resection and Submucosal Tunneling Endoscopic Resection. *Transl Gastroenterol Hepatol* (2019) 4:39. doi: 10.21037/tgh.2019.05.01

Conflict of Interest: The authors declare that the research was conducted in the absence of any commercial or financial relationships that could be construed as a potential conflict of interest.

Publisher's Note: All claims expressed in this article are solely those of the authors and do not necessarily represent those of their affiliated organizations, or those of the publisher, the editors and the reviewers. Any product that may be evaluated in this article, or claim that may be made by its manufacturer, is not guaranteed or endorsed by the publisher.

Copyright © 2022 Wu, Ding, Song, Cui, Bi and Cheng. This is an open-access article distributed under the terms of the Creative Commons Attribution License (CC BY). The use, distribution or reproduction in other forums is permitted, provided the original author(s) and the copyright owner(s) are credited and that the original publication in this journal is cited, in accordance with accepted academic practice. No use, distribution or reproduction is permitted which does not comply with these terms.

frontiers | Frontiers in Oncology

METHODS
published: 13 July 2022
doi: 10.3389/fonc.2022.917961

Check for updates

Neoadjuvant Chemoradiotherapy and Surgery for Esophageal Squamous Cell Carcinoma Versus Definitive Chemoradiotherapy With Salvage Surgery as Needed: The Study Protocol for the Randomized Controlled NEEDS Trial

Magnus Nilsson[1,2], Halla Olafsdottir[1,3], Gabriella Alexandersson von Döbeln[1,3], Fernanda Villegas[4], Giovanna Gagliardi[4], Mats Hellström[5], Qiao-Li Wang[1], Hemming Johansson[5,6], Val Gebski[7], Jakob Hedberg[8], Fredrik Klevebro[1,2], Sheraz Markar[9,10], Elizabeth Smyth[11], Pernilla Lagergren[10,12], Ghazwan Al-Haidari[13], Lars Cato Rekstad[14], Eirik Kjus Aahlin[15], Bengt Wallner[16], David Edholm[17], Jan Johansson[18], Eva Szabo[19], John V. Reynolds[20], CS Pramesh[21], Naveen Mummudi[21], Amit Joshi[21], Lorenzo Ferri[22], Rebecca KS Wong[23,24], Chris O'Callaghan[25], Jelena Lukovic[23,24], Kelvin KW Chan[26], Trevor Leong[27], Andrew Barbour[28], Mark Smithers[28], Yin Li[29], Xiaozheng Kang[29], Feng-Ming Kong[30], Yin-Kai Chao[31], Tom Crosby[32], Christiane Bruns[33], Hanneke van Laarhoven[34], Mark van Berge Henegouwen[35], Richard van Hillegersberg[36], Riccardo Rosati[37], Guillaume Piessen[38], Giovanni de Manzoni[39] and Florian Lordick[40]*

[1] Division of Surgery, Department of Clinical Science, Intervention and Technology, Karolinska Institutet, Stockholm, Sweden, [2] Department of Upper Abdominal Diseases, Karolinska Comprehensive Cancer Center, Karolinska University Hospital, Stockholm, Sweden, [3] Thoracic Oncology Center, Karolinska Comprehensive Cancer Center, Karolinska University Hospital, Stockholm, Sweden, [4] Section of Radiotherapy Physics and Engineering, Department of Medical Radiation Physics and Nuclear Medicine, Karolinska Comprehensive Cancer Center, Karolinska University Hospital, Stockholm, Sweden, [5] Center for Clinical Cancer Studies, Karolinska Comprehensive Cancer Center, Karolinska University Hospital, Stockholm, Sweden, [6] Department of Oncology-Pathology, Karolinska Institutet, Stockholm, Sweden, [7] NHMRC Clinical Trials Centre, University of Sydney, Sydney, NSW, Australia, [8] Department of Surgical Sciences, Uppsala University Hospital, Uppsala, Sweden, [9] Nuffield Department of Surgery, University of Oxford, Oxford, United Kingdom, [10] Department of Molecular Medicine and Surgery, Karolinska Institutet, Stockholm, Sweden, [11] Department of Oncology, Cambridge University Hospitals National Health Service Foundation Trust, Cambridge, United Kingdom, [12] Department of Surgery and Cancer, Imperial College London, London, United Kingdom, [13] Department of Oncology, Oslo University Hospital, Oslo, Norway, [14] Department of Gastrointestinal Surgery, St. Olav's Hospital, Trondheim University Hospital, Trondheim, Norway, [15] Department of GI and HPB Surgery, University Hospital of Northern Norway, Tromsø, Norway, [16] Department of Surgical and Perioperative Sciences, Surgery, Umeå University, Umeå, Sweden, [17] Department of Surgery, Linköping University Hospital, Linköping, Sweden, [18] Department of Surgery, Skåne University Hospital, Lund, Sweden, [19] Department of Surgery, University Hospital of Örebro, Örebro, Sweden, [20] Department of Surgery, Trinity St James's Cancer Institute, Dublin, Ireland, [21] Tata Memorial Centre, Homi Bhabha National Institute, Mumbai, India, [22] Department of Thoracic Surgery, McGill University Health Centre, Montreal, QC, Canada, [23] Radiation Medicine Program, Princess Margaret Cancer Center, University Health Network, Toronto, ON, Canada, [24] Department of Radiation Oncology, University of Toronto, Toronto, ON, Canada, [25] Canadian Cancer Trials Group, Kingston, ON, Canada, [26] Sunnybrook Health Sciences Centre, University of Toronto, Toronto, ON, Canada, [27] Sir Peter MacCallum Department of Oncology, Peter MacCallum Cancer Centre, University of Melbourne, Melbourne, VIC, Australia, [28] Academy of Surgery, University of Queensland, Princess Alexandra Hospital, Brisbane, QLD, Australia, [29] Department of Thoracic Surgery, National Cancer Center/National Clinical Research Center for Cancer/Cancer Hospital, Chinese Academy of Medical Sciences and Peking Union Medical College, Beijing, China,

OPEN ACCESS

Edited by:
Zhendong Jin,
Second Military Medical University, China

Reviewed by:
Alessandro Gonfiotti,
University of Florence, Italy
Teng MAO,
Shanghai Jiao Tong University, China

***Correspondence:**
Magnus Nilsson
magnus.nilsson@ki.se

Specialty section:
This article was submitted to Gastrointestinal Cancers: Gastric & Esophageal Cancers, a section of the journal Frontiers in Oncology

Received: *11 April 2022*
Accepted: *08 June 2022*
Published: *13 July 2022*

Citation:
Nilsson M, Olafsdottir H, Alexanderssonvon Döbeln G, Villegas F, Gagliardi G, Hellström M, Wang Q-L, Johansson H, Gebski V, Hedberg J, Klevebro F, Markar S, Smyth E, Lagergren P, Al-Haidari G, Rekstad LC, Aahlin EK, Wallner B, Edholm D, Johansson J, Szabo E, Reynolds JV, Pramesh CS, Mummudi N, Joshi A, Ferri L, Wong RKS, O'Callaghan C, Lukovic J, Chan KKW, Leong T, Barbour A, Smithers M, Li Y, Kang X, Kong F-M, Chao Y-K, Crosby T, Bruns C, van Laarhoven H, van Berge Henegouwen M, van Hillegersberg R, Rosati R, Piessen G, de Manzoni G and Lordick F (2022) Neoadjuvant Chemoradiotherapy and Surgery for Esophageal Squamous Cell Carcinoma Versus Definitive Chemoradiotherapy With Salvage Surgery as Needed: The Study Protocol for the Randomized Controlled NEEDS Trial. Front. Oncol. 12:917961. doi: 10.3389/fonc.2022.917961

[30] Thoracic Oncology Center, HKU Shenzhen Hospital, Hong Kong University Li Ka Shing Medical School, Shenzhen, China, [31] Department of thoracic surgery, Chang Gung Memorial Hospital-Linkou, Chang Gung University, Taoyuan, Taiwan, [32] Department of Clinical Oncology, Velindre Cancer Centre, Cardiff, United Kingdom, [33] Department of General, Visceral and Cancer Surgery, University Hospital of Cologne, Cologne, Germany, [34] Department of Medical Oncology, Cancer Center Amsterdam, Amsterdam University Medical Centers, Amsterdam, Netherlands, [35] Department of Surgery, Cancer Center Amsterdam, Amsterdam University Medical Centers, University of Amsterdam, Amsterdam, Netherlands, [36] Departmentof Surgery, University Medical Center Utrecht, Utrecht, Netherlands, [37] Department of Gastrointestinal Surgery, San Rafaele Hospital, Vita Salute University, Milan, Italy, [38] Univ. Lille, CNRS, Inserm, CHU Lille, UMR9020-U1277 - CANTHER – Cancer Heterogeneity Plasticity and Resistance to Therapies, F-59000 Lille, France, [39] Upper GI Surgery Division, University of Verona, Verona, Italy, [40] University Cancer Center Leipzig, Leipzig University Medical Center, Leipzig, Germany

Background: The globally dominant treatment with curative intent for locally advanced esophageal squamous cell carcinoma (ESCC) is neoadjuvant chemoradiotherapy (nCRT) with subsequent esophagectomy. This multimodal treatment leads to around 60% overall 5-year survival, yet with impaired post-surgical quality of life. Observational studies indicate that curatively intended chemoradiotherapy, so-called definitive chemoradiotherapy (dCRT) followed by surveillance of the primary tumor site and regional lymph node stations and surgery only when needed to ensure local tumor control, may lead to similar survival as nCRT with surgery, but with considerably less impairment of quality of life. This trial aims to demonstrate that dCRT, with selectively performed salvage esophagectomy only when needed to achieve locoregional tumor control, is non-inferior regarding overall survival, and superior regarding health-related quality of life (HRQOL), compared to nCRT followed by mandatory surgery, in patients with operable, locally advanced ESCC.

Methods: This is a pragmatic open-label, randomized controlled phase III, multicenter trial with non-inferiority design with regard to the primary endpoint overall survival and a superiority hypothesis for the experimental intervention dCRT with regard to the main secondary endpoint global HRQOL one year after randomization. The control intervention is nCRT followed by preplanned surgery and the experimental intervention is dCRT followed by surveillance and salvage esophagectomy only when needed to secure local tumor control. *A target sample size of 1200 randomized patients is planned in order to reach 462 events (deaths) during follow-up.*

Clinical Trial Registration: www.ClinicalTrials.gov, identifier: NCT04460352.

Keywords: esophageal squamous cell carcinoma, neoadjuvant chemoradiotherapy, definitive chemoradiotherapy, locoregional surveillance, salvage esophagectomy

INTRODUCTION

Currently, esophageal cancer is the 7th most common cancer and the 6th most common cause of cancer deaths worldwide (1). Most esophageal cancers are diagnosed in advanced stages. Esophageal squamous cell carcinoma (ESCC) comprises more than 90% of cases of esophageal cancer worldwide, and despite the recent years' decrease in some Western countries, there are no signs of a global decrease in incidence (1).

Treatment with curative intent for locally advanced ESCC is controversial. Surgical resection of the esophagus was the first established treatment (2). Another alternative is definitive chemoradiotherapy (dCRT), which was first established in the early 1990s (3). Survival after surgical resection alone and after dCRT alone are similar, with five-year overall survival of around 25-30% (4, 5). A third curative treatment approach is esophagectomy preceded by neoadjuvant chemoradiotherapy (nCRT), which was shown to be superior to surgery alone in the CROSS trial, using a novel neoadjuvant chemoradiotherapy regimen consisting of weekly carboplatin and paclitaxel and a total radiation dose of 41.4 Gy, followed by esophagectomy (4). The CROSS trial showed an extraordinary 5-year overall survival after nCRT and surgery of 60% for ESCC, compared to only 33% for surgery alone (6). These outcomes after nCRT followed by planned surgery established the CROSS nCRT regimen with subsequent esophagectomy as a new standard of care for ESCC.

Importantly, observational studies indicate that dCRT, supplemented with salvage esophagectomy in cases of incomplete response or subsequent local recurrence, i.e. when needed for local tumor control, can reach survival levels equivalent to those seen with nCRT with subsequent mandatory esophagectomy (7, 8). The great advantage with this approach is that more than half of the patients will not need to undergo surgery and may consequently be able to avoid the deterioration of health-related quality of life (HRQOL) known to be associated with esophagectomy (9, 10). Based on these studies both nCRT with surgery, as well as dCRT with surveillance and salvage surgery when needed, are recommended treatment options for locally advanced ESCC in the European Society for Medical Oncology (ESMO) guidelines (11), although in many countries a majority of patients with operable ESCC are currently treated with nCRT and surgery, due to the more robust evidence available for this treatment (12–14).

To date, no adequately powered randomized trial comparing these two treatment alternatives has been published, or to our knowledge even been started or planned. The only two previous randomized trials addressing comparable research questions, both with recruitment in the time period around two decades ago, are today obsolete with regard to the compared interventions, both surgery and chemoradiotherapy. Furthermore, these did not include structured locoregional recurrence surveillance after dCRT (15, 16). In addition both these trials were underpowered with regard to overall survival endpoints. For these reasons a majority of operable curative intent patients with locally advanced ESCC in the world are more likely to be treated with nCRT followed by surgery (12–14).

Consequently, a large, pragmatic and direct intention-to-treat comparison between the two guideline-recommended treatment options for operable ESCC, nCRT with mandatory surgery vs dCRT with surgery only when needed to achieve local tumor control, is still lacking and strongly warranted. This trial, named NEoadjuvant chemoradiotherapy for Esophageal squamous cell carcinoma versus Definitive chemoradiotherapy with salvage Surgery as needed (NEEDS), could potentially change the current globally dominating practice from neoadjuvant nCRT with subsequent mandatory esophagectomy, to dCRT with subsequent surveillance and surgical resection performed only when needed.

METHODS

Study Objectives

Primary and Main Secondary Objective

The primary objective of the NEEDS trial is to demonstrate that dCRT with salvage esophagectomy as needed is non-inferior to nCRT followed by surgery regarding overall survival in patients with operable, locally advanced esophageal squamous cell carcinoma. The main secondary objective is to show superiority of dCRT with surgery only when needed, concerning global HRQOL one year after randomization

Secondary Objectives

- To study prespecified HRQOL endpoints relevant to esophageal cancer and effects of treatment for this disease, repeatedly during treatment and survivorship.
- To determine event free survival, loco-regional and distal relapse rates and histological response after chemoradiotherapy in the surgical specimen in the control arm.
- To investigate the overall health economic impact of each intervention. A cost-effectiveness analysis (CEA) will be conducted for all relevant endpoints comparing both interventions. Furthermore, the results of the trial-based CEA (e.g. patient-level resource use) will be used to build a decision analytic model and made publicly available to allow health care system-specific analysis by policy makers (e.g. country-specific costs or quality of life weights).
- To investigate the impact of each intervention on nutritional status during follow-up.
- To investigate whether any of the endpoints are affected by the type of radiological follow-up, CT or PET-CT, in patients treated with dCRT with salvage esophagectomy as needed.
- To investigate if there are any gender differences in any of the endpoints.
- To exploratively analyze putative tissue and liquid biomarkers in response to the different treatment strategies and long-term benefit. We aim to identify subgroups of patients who need trimodality treatment and those who have a good long-term outcome without esophagectomy.

Trial Design

The NEEDS trial is a pragmatic, open-label, randomized controlled phase III multicenter trial. Randomization (1:1) of eligible patients is performed before any anti-tumor treatment is given (**Figure 1**).

Study Setting

The NEEDS trial is an academic multicenter trial. To represent the global geographic incidence of ESCC the aim is to include patients from centers across most of the world´s continents, in order to maximize the generalizability of the results from the trial. Recruitment is so far planned in Sweden, Norway, Germany, Ireland, United Kingdom, France, Italy, Canada, India, China, Taiwan and Australia, and recruitment from several other countries are under discussion. The aim is to include around half of the patients in Asia and the other half in Western countries.

Eligibility Criteria

Inclusion Criteria

- Histopathologically confirmed ESCC in locally advanced stages cT1 N+ or cT2-4a any N, M0, according to the current (8th) version of the AJCC TNM classification.
- Technically resectable disease according to the local multidisciplinary team conference (MDT)/tumor board.

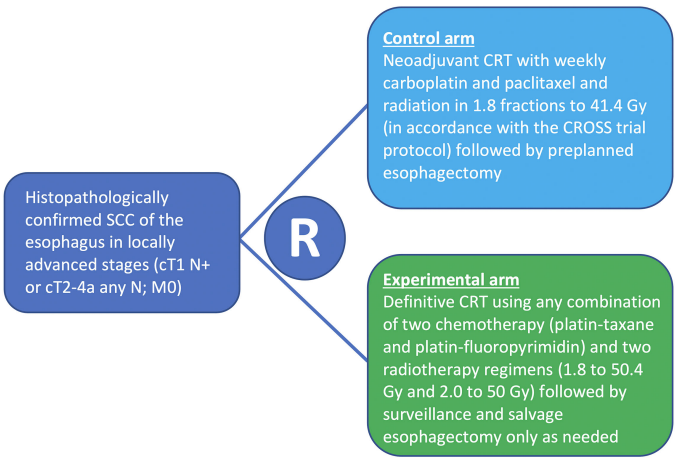

FIGURE 1 | NEEDS randomization overview.

- Age ≥ 18 years and ≤ 80 years.
- ECOG performance status 0-1.
    - Adequate organ function (assessed within 14 days prior to randomization):
    - White blood cell count (WBC) > 2 × 109/L.
    - Absolute neutrophil count (ANC) > 1.5 × 109/L.
    - Platelets ≥ 100 × 109/L.
    - Hemoglobin ≥ 9 g/dL.
    - Estimated glomerular filtration rate (eGFR) according to MDRD should be ≥ 60 ml/min.
    - Total bilirubin within normal limits (if the patient has documented Gilbert's disease ≤ 1.5 * ULN or direct bilirubin ≤ ULN).
    - Aspartate transaminase (AST) and alanine transaminase (ALT) ≤ 1.5ULN.
- Women of childbearing potential (WOCBP) must have a negative serum or urine pregnancy test (minimum sensitivity 25 IU/L or equivalent units of HCG) within 24 hours prior to randomization. Furthermore WOCBP should undergo monthly pregnancy testing during the study treatment and for a period of up to six months after termination of the study treatment. Home pregnancy tests are acceptable.
- Patients of childbearing/reproductive potential should use highly effective method of birth control measures during the study treatment period and for at least *six* months after the last study treatment. A highly effective method of birth control is defined as those which result in low failure rate (i.e. less than 1% per year) when used consistently and correctly and include combined hormonal contraception associated with inhibition of ovulation (oral, intravaginal, transdermal), progestogen-only hormonal contraception associated with inhibition of ovulation (oral, injectable, implantable), intrauterine device, intrauterine hormone-releasing system, bilateral tubal occlusion, vasectomized partner, and sexual abstinence.
- Female subjects who are breast feeding should discontinue nursing prior to the first dose of study treatment and until *six* months after the last study treatment.
- Male study participants should not father children during the study treatment and for at least six months after the last dose and should use effective contraceptive measures throughout this time period. Effective contraceptive measures include condoms, vasectomy, and sexual abstinence. Male study participants who wish to be fathers in the future should be offered counselling on sperm storage before starting any study treatment.
- Absence of any psychological, familial, sociological or geographical condition potentially hampering compliance with the study protocol and follow-up schedule; those conditions should be discussed with the patient before registration in the trial.
- Before patient registration/randomization, written informed consent must be given according to ICH/GCP/GDPR and national/local regulations.

Exclusion Criteria

- M1 according to the current (8th) version of the AJCC TNM classification.
- cT4b according to the current (8th) version of he AJCC TNM classification.
- Primary tumor not resectable without laryngectomy.
- Impaired renal, hepatic, cardiac, pulmonary or endocrine status that compromises the eligibility of the patient for multimodality treatment with chemoradiotherapy followed by esophagectomy.
- Subjects not considered likely to tolerate multimodality treatment with chemoradiotherapy followed by esophagectomy.
- Subjects with previous malignancies are excluded unless a complete remission or complete resection was achieved at

least 5 years prior to study entry. Adequately treated cervix uteri carcinoma in situ, and localized non-melanoma skin cancer are not exclusion criteria, regardless of time of diagnosis.

- Prior or concomitant treatment with radiotherapy or chemoradiotherapy with potential overlap of radiotherapy fields.
- Known uncontrollable hypersensitivity to the components of the chemotherapeutic agents used in the trial regimens.
- Inability to fully understand and digest information for study patients or to comply with study instructions due to language difficulty or cognitive failure such as dementia or severe psychiatric disorder.

Interventions

Control Intervention (Arm A)

The control intervention is concomitant nCRT followed by esophagectomy in accordance with the intervention arm in the CROSS trial (4). Radiotherapy is administered 1.8 Gy × 23 (total dose: 41.4 Gy) as detailed below. Chemotherapy, using a platinum-taxane regimen, is administered starting on the first day of radiotherapy: carboplatin area under the curve (AUC) 2mg/ml/min + paclitaxel 50mg/m^2 weekly × 5 (day 1, 8, 15, 22, 29).

Esophagectomy should be performed within 8 weeks of termination of chemoradiotherapy, unless the medical condition of the patient does not permit surgery within this timeframe.

Surveillance in Arm A

During the first two years, clinical status, symptoms and routine blood laboratory analyses (see below) will be followed up starting four to six weeks after surgery, then three months after surgery and then every third month up to two years after surgery. During years three to five after surgery, clinical status, symptoms and routine blood laboratory analyses (see below) will be followed every six months. Clinical follow-up visits can optionally be performed by telephone or using a video conference system. In addition, planned computerized tomography (CT) of neck, chest and abdomen will be performed at 9, 18, 36 and 60 months after surgery. The performance of PET-CT instead of CT is optional. Additional investigations should be performed on clinical suspicion of recurrence at any time. In the event of recurrence being diagnosed follow-up is terminated and the patient managed in accordance with local institutional treatment policy.

Experimental Intervention (Arm B)

The experimental intervention is concomitant dCRT, followed by surveillance, and esophagectomy only in case of residual or recurrent locoregional cancer. Radiotherapy can be administered using two alternative schemes, either 1.8 Gy × 28 (total dose: 50.4 Gy) or 2.0 Gy × 25 fractions (total dose: 50 Gy) as detailed below. Chemotherapy can be administered using any of the following regimens:

1. Platinum-Taxane Regimen (4)
   - Carboplatin AUC 2 mg/ml/min + paclitaxel 50mg/m^2 on day 1 weekly during the full course of radiotherapy (5 or 6 weeks, depending on the radiotherapy regimen used).
2. Platinum-Fluoropyrimidine Regimens (5, 17)
   - Cisplatin 75mg/m^2 on the first day of weeks 1 and 5 + 5-fluorouracil 1000 mg/m^2/day by continuous infusion on the first four days of weeks 1 and 5.
   - FOLFOX: Oxaliplatin 85 mg/m^2, calcium folinate 200 mg/m^2 and 5-fluorouracil 400 mg/m^2 on the first days of weeks 1, 3 and 5 + 5-fluorouracil 800 mg/m^2/day by continuous infusion on the first two days of weeks 1, 3 and 5.

There is no induction chemotherapy or adjuvant chemotherapy.

Surveillance in Arm B

Clinical status, symptoms and routine blood laboratory analyses (see below) will be assessed 4 weeks after completed dCRT, then every 3 months up to two years after completed dCRT. From two years and up to five years after dCRT, clinical status, symptoms and routine blood laboratory analyses (see below) will be followed up every six months. Clinical follow-up visits can optionally be performed by telephone or using a video conference system. In addition a CT of the neck, chest and abdomen will be performed at 4 weeks after completed dCRT and at 3, 6, 9, 12, 15, 18, 21, 24, 30, 36, 42, 48, 54 and 60 months after terminated dCRT. The performance of PET-CT instead of CT is optional.

In addition, upper endoscopy with multiple bite-on-bite biopsies from the original tumor area and from suspected residual or recurrent tumor will be performed at 3, 6, 9, 12, 15, 18, 21, 24, 30, 36, 42, 48, 54 and 60 months after terminated dCRT. Endoscopic ultrasonography (EUS) with fine needle aspiration (FNA) of suspected malignant lymph nodes is optional. Additional investigations should be performed on clinical suspicion of residual or recurrent disease at any time. For example clinical suspicion of residual disease is warranted in patients with persistent severe dysphagia 6 weeks after termination of dCRT. In the event of distant metastatic recurrence radiological and endoscopic follow-up is terminated and the patient managed in accordance with local institutional treatment policy.

Salvage Esophagectomy

Salvage esophagectomy is indicated in patients allocated to the experimental intervention (arm B), if there is either histopathological evidence of residual or recurrent cancer, or radiological signs of disease progression from one post dCRT surveillance CT or PET-CT to a subsequent one (even without histopathological proof). The verdict of disease progression should be made at the local multidisciplinary team conference of the study center in question. Another prerequisite for salvage esophagectomy is that the patient should be considered physiologically fit for surgery. The decision of whether the patient is fit for surgery is left at the discretion of the responsible surgeon, following the regular procedure of

operability assessment at each center based on conventional clinical assessment with optional support of any function tests considered useful.

Radiotherapy and Dose Planning

Fractionation Schedule

The radiotherapy in the trial also follows a pragmatic approach. The radiotherapy in Arm A will be given in 23 fractions of 1.8 Gy, 5 fractions a week (once daily), to a total dose of 41.4 Gy. The overall treatment time should not exceed 39 days (five and a half weeks). The radiotherapy in Arm B will follow either of two schedules: 28 fractions of 1.8 Gy, 5 fractions a week (once daily), to a total dose of 50.4 Gy, with overall treatment time not exceeding 46 days or 25 fractions of 2 Gy, 5 fractions a week (once daily), to a total dose of 50 Gy, with treatment time not exceeding 42 days (six weeks).

Treatment Preparation

For treatment preparation the patients should undergo CT simulation in treatment position with a slice thickness of maximum 3 mm. A 4D-CT can be used according to local routines. The use of intravenous contrast is recommended. The gastric filling should be standardized at simulation and at each treatment fraction according to local routines. This can be accomplished for example by two hours fasting prior to simulation and treatment. Positioning of the patient will be according to local routines and immobilization devices should be in accordance with the departmental policy.

Definition of target volumes

The principles of target delineation will be as follows: The gross tumor volume of the primary tumor (GTVT) and involved nodes (GTVN) should be delineated on a planning CT, taking all clinical, endoscopic, and radiological information (CT or PET-CT) into account. GTVT should include the entire circumference of the esophagus at the level of the tumor. The clinical target volume of the primary tumor (CTVT) includes a 3 cm margin in the cranio-caudal direction and 1 cm radial margin from GTVT with corrections for natural anatomic boundaries (such as heart, lungs, skeletal structures, kidneys, and liver) and oriented along the esophageal mucosa (not a simple geometric expansion). For tumors located in the gastro-esophageal junction a 2-cm distal margin of clinically uninvolved gastric mucosa is sufficient. The clinical target volume of involved nodes (CTVN) includes the GTVN plus a 0.5 cm margin in all directions, with corrections for natural anatomic boundaries. These two volumes should be joined to make the CTV (total), patchwork radiotherapy should be avoided, and different target volumes joined *via* the most probable lymphatic drainage. In case a 4D-CT or other robust motion management techniques are not available, the margins for motion management can be estimated to be 10 mm in the cranial and caudal direction and 3 mm in the radial directions and these should be included in the CTV (total), although the vertebral bodies should be entirely excluded. For proximal tumors, the cranial level of the CTV should not extend above the cricoid cartilage. The planning target volume (PTV) is applied according to local routines, commonly 5-10 mm. Organs at risk considered and delineated are the heart, the lungs, the spinal cord, and the kidneys.

In addition to these volumes patients in the experimental arm B will also be treated with elective lymph node irradiation (18). Elective lymph node irradiation will include the following regions for the respective tumor sites:

Proximal Tumors and Tumors Located in the Middle of Esophagus Mainly Above the Carina

Supraclavicular lymph nodes, analogous to level 4 in head and neck cancers (19) (**Supplementary Figure S1**). Levels 2-4 according to IASLC staging atlas (20) (**Supplementary Figure S2**) at the same levels as CTVT and CTVN: Paratracheal, pretracheal, mediastinal (anterior mediastinal, retrotracheal, posterior mediastinal and tracheobronchial), and para-esophageal lymph nodes.

Tumors Located in the Middle of Esophagus Mainly Below the Carina

Mediastinal, paratracheal, pretracheal and para-esophageal lymph nodes at the same levels as CTVT and CTVN, as well as paraaortic, paracardial, common hepatic, hepatogastric ligament, and celiac lymph nodes.

Distal Tumors

Paraaortic, paracardial, common hepatic, hepatogastric ligament, celiac, and para-esophageal lymph nodes (**Supplementary Figure S1**) at the same levels as CTVT and CTVN.

To encompass the para-esophageal lymph nodes, a radial margin of 1 cm from the outer esophageal wall is recommended.

Treatment Delivery

Radiotherapy will be delivered using 3D conformal radiotherapy (3DCRT), intensity modulated radiotherapy (IMRT) or volumetric arc therapy (VMAT). Concerning the dose distribution, 98% of the PTV should receive at least 95% of the prescribed dose. However, if this objective is unachievable, 95% of the PTV should receive at least 95% of the prescribed dose. The maximum dose within the PTV should not exceed 107% of the prescribed dose.When planning the radiotherapy treatment, the dose constraints in **Table 1** should be adhered to. Treatment position verification should be done in accordance with individual departmental policy.

Radiotherapy Modification for Treatment Delay

In case of missed treatment days, radiotherapy can be compensated at the discretion of the treating physician, though for patients randomized to Arm B (dCRT) the total radiation dose may be increased to a maximum EQD2 (equivalent total dose in 2Gy/fraction) of 55 Gy.

Modifications for Toxicity

In the event of radiation induced grade 4 esophagitis, both chemotherapy and radiotherapy should be withheld until the esophagitis has recovered to grade 3. Alternatively, the treatment

TABLE 1 | Dose constraints.

Structure	Priority	Constraints	Description
Spinal Cord	1	$D_{0.1cc}$ <45 Gy	The dose given to 0.1 cm^3 of the spinal cord should be less than 45 Gy. This constraint takes precedence over PTV coverage.
Total kidneys	2	V_{18Gy} <30%	The volume receiving 18 Gy should be less than 30%.
		D_{mean}< 18 Gy	The mean dose should be less than 18 Gy. Both constraints take precedence over PTV coverage.
Total lungs	3	D_{mean}< 20 Gy	The mean dose should be less than 20 Gy. This constraint takes precedence over PTV coverage.
	5	V_{20Gy} <20%	The volume receiving 20 Gy should be less than 20%
Heart	4	V_{30Gy} <30%	The volume receiving 30 Gy should be less than 30%.
		D_{mean}< 30 Gy	The mean dose should be less than 30 Gy.

can be discontinued at the discretion of the treating physician. Dosing modifications for chemotherapy are provided in **Supplementary Table S1.**

Radiotherapy Quality Assurance

The aim of the radiotherapy quality assurance (RT-QA) program is to ensure the consistency of radiotherapy treatment delivery across all participating centers as well as the verification of adherence to the protocol guidelines described above (21, 22). The RT-QA coordinating team is comprised of three medical physicists and three radiation oncologists based at the External Radiotherapy Department at the Karolinska University Hospital.

The RT-QA program is divided into two stages:

1. Pre-Study: All sites wishing to participate must submit a Facility Survey, perform a level 1 dosimetry audit, and complete two contouring benchmark exercises (one with a tumor located in the proximal and one in the distal esophagus) and two dose planning benchmark exercises with a proximal and a distal esophageal tumor respectively before patients can be included in the trial. These benchmark exercises must adhere to the radiotherapy guidelines described in the study protocol.
2. During study inclusion participating centers must send the radiotherapy data of each included patient to a specific online platform. The evaluation and monitoring procedure of the data is further divided into two levels. Level 1 consists of pre-treatment evaluation of contouring and dose planning of the first patient at each center. If major violations are identified in the contouring part, both re-delineation and re-planning will be requested. If violations are detected in the planning part, only re-planning will be requested. Once an acceptable quality level is achieved the centers progress to level 2. At this point, a retrospective evaluation of contouring and dose planning will be performed for one in every 5 patients, randomly selected, with feedback to centers regarding every evaluated patient.

In case of a loco-regional tumor recurrence (with or without simultaneous distant metastasis), the center is required to send the following DICOM data as soon as possible: diagnostic CT and, if available, the PET images, confirming the recurrence.

Surgical Quality Assurance

All centers participating in this trial are high volume centers, with highly experienced surgeons. Prior to the trial, participating surgeons will be asked to provide their annual and life-time volume of esophagectomies performed for cancer. For each participating center information regarding 30-day and 90-day mortality over the preceding three years will be collected. Centers will before entering the trial be requested to complete a questionnaire, to describe their intended and most commonly used operative approach based on tumor location and staging that may be encountered within the trial. This will allow an assessment of expected degree of heterogeneity in surgical approach and expected lymphadenectomy within the trial. Standard quality outcome metrics including data on estimated blood loss and perioperative complications will be collected for every operation within the trial. Two still photographs of the lymphadenectomy fields upon completion of lymphadenectomy (abdomen and thorax) will be saved at each participating site for every operation. Specifically, the abdominal photograph should include the upper pancreatic border with the dissection of stations 7, 8a, 9 and 11p. The thoracic photo should include dissection of the subcarinal area. The surgery quality assurance committee will form consensus on grading lymphadenectomy from these photographs by collectively assessing the first three cases from ten centers. After this, a randomly selected 10% of the included patients (selection stratified by center and country) will be assessed by two of the members of the surgery quality assurance committee. The photos will be scored on a Likert scale with four levels (excellent, good, fair and poor).

Outcomes

Primary and Main Secondary Endpoints

The primary endpoint of the NEEDS trial is overall survival (OS) with a minimum follow-up of two years. The main secondary endpoint is global HRQOL one year after randomization. The primary objective of treatment for localized esophageal cancer is cure and there are no known surrogate endpoints that can replace OS in a pragmatic trial aiming to establish best practice. However, the importance of patient reported HRQOL during survivorship qualifies HRQOL as a main secondary endpoint. The main secondary endpoint of HRQOL at one

year after randomization will be the global HRQOL score in the EORTC QLQ-C30 questionnaire.

Secondary Endpoints

- HRQOL will be assessed at baseline, and thereafter 6, 12, 24, 36 and 60 months after randomization using the EORTC HRQOL Questionnaire QLQ-C30 version 3.0 (23),the EORTC HRQOL esophagogastric-specific questionnaire EORTC QLQ-OG25 (24) and the EQ5D questionnaire (25). Predefined endpoints will be global HRQOL, physical function, dyspnea, diarrhea, dysphagia and anxiety at all assessed time-points.
- Event free survival (EFS), defined as time to relapse, initiation of any anti-tumor therapy beyond the study treatments (salvage surgery is considered a study treatment in the dCRT arm), or death, whichever comes first.
- Loco-regional and distant relapse rates, including the relation of relapse location to the radiation field (in-field or out-field).
- Histopathological response according to Mandard (26), as well as other pathological data in operated patients, i.e. ypTNM including total and metastatic lymph node count, and tumor free resection margins, R0 (according to the Royal College of Pathologist's definition of at least 1 mm without viable tumor cells) (27).
- Health economics will be assessed including patient-level medical resource use and societal costs due to sick-leave and other non-medical costs. Quality-adjusted life years (QALYs) will be calculated using EQ-5D, reported at baseline and 6, 12, 24, 36 and 60 months after randomization.
- Surgical complications according to the Esophagectomy Complications Consensus Group (ECCG) (28) and classified according to Clavien-Dindo (29) (Appendix 3)
- Treatment-related adverse events and toxicity coded by NCI CTCAE criteria version 5.0.
- Nutritional outcomes including weight change, dysphagia and appetite assessment.
- Gender stratified analyses of all endpoints.
- Exploratory analyses for putative tissue and liquid biomarkers for response to CRT and benefit from either of the two treatment strategies (optional per center).

Follow-Up

Included study subjects are followed up for five years. The follow-up and surveillance schemes for each study arm are described in detail above in the interventions section (**Figure 2**).

Randomization and Stratification

Randomization is performed online from within an electronic randomization system once all eligibility criteria have been verified and no exclusion criteria have been fulfilled. Treatment allocation is open-label among the two arms in a 1:1 ratio. Randomization is performed using minimization schemes with stratification for gender (male or female), age (< 70 yrs or ≥70 yrs), tumor site (upper, middle or lower third of the esophagus), performance status (ECOG 0 or 1), clinical nodal status (positive or negative/unknown), clinical primary tumor status (T4a or any other T) and trial center. The electronic randomization module is accessed from all participating sites.

Arm A

Months after surgery	1	3	6	9	12	15	18	21	24	30	36	42	48	54	60
Clinical examination	X	X	X	X	X	X	X	X	X[1]	X[1]	X[1]	X[1]	X[1]	X[1]	X[1]
Routine blood lab[2]	X	X	X	X	X	X	X	X	X	X	X	X	X	X	X
CT/PET-CT[3]				X			X				X				X

[1] After 24 months, clinical examination may be replaced by a telephone call or a video conference.
[2] Hemoglobin, platelets, leucocytes, CRP, Na, K, Ca, creatinine, AST, ALT, ALP, gamma-GT, albumin, bilirubin.
[3] PET-CT instead of CT is optional

Arm B

Months after dCRT	1	3	6	9	12	15	18	21	24	30	36	42	48	54	60
Clinical examination	X	X	X	X	X	X	X	X	X[1]	X[1]	X[1]	X[1]	X[1]	X[1]	X[1]
Routine blood lab[2]	X	X	X	X	X	X	X	X	X	X	X	X	X	X	X
CT/PET-CT[3]	X	X	X	X	X	X	X	X	X	X	X	X	X	X	X
Upper endoscopy[4]		X	X	X	X	X	X	X	X	X	X	X	X	X	X

[1] After 24 months, clinical examination may be replaced by a telephone call or a video conference.
[2] Hemoglobin, platelets, leucocytes, CRP, Na, K, Ca, creatinine, AST, ALT, ALP, gamma-GT, albumin, bilirubin.
[3] PET-CT instead of CT is optional
[4] Upper endoscopy with bite-on-bite biopsies +/- endoscopic ultrasound sonography with fine-needle-aspiration cytology

FIGURE 2 | Overview of scheduled cancer recurrence surveillance by treatment allocation.

Sample Size Calculation and Statistical Methods for Data Analysis

Sample Size Calculation

The study has a non-inferiority design to investigate whether dCRT followed by surveillance and salvage esophagectomy only as needed will not appreciably compromise mortality while potentially providing an improved HRQOL and reduced morbidity, compared to nCRT with planned esophagectomy. Based on data from the CROSS trial, the 5-year survival for patients receiving nCRT followed by surgery is 60% (6). For patients in the surveillance arm, a non-inferiority margin of 7.5% is considered to be clinically worthwhile as a trade-off for reduced surgical and post-surgical morbitity and improved HRQOL. The size of the non-inferiority margin was decided upon after discussions among professionals in the international esophageal cancer community, and representatives of the Swedish patient organization PALEMA. From clinical considerations, the assumption that surveillance would increase overall survival is remote and therefore a one-sided test for non-inferiority is assumed.

Assuming a 5-year accrual and 2-year follow-up duration, a sample size of 1200 patients will have 80% power with one-sided 95% confidence to declare non-inferiority with a margin of 7.5% (i.e. from 60% to 52.5% in the surveillance group) based on a 1:1 randomization. Based on these assumptions, the expected number of events is 462, corresponding to a hazard ratio of 1.26. The analysis will be according to the intention-to-treat (ITT) principle with no imputation for missing values.

Mean differences in HRQOL of 10 points or more will be considered clinically relevant.

Statistical Methods

The primary endpoint analysis of OS will be performed on the ITT population using differences in the 5-year survival proportion between treatments estimated by the method of Kaplan-Meier. Further analyses will include proportional hazards regression modelling accounting for stratification factors providing estimates of relative differences between treatment groups. Results will be presented as a figure including point estimates of the treatment effect, lower and upper 90% confidence limits and the non-inferiority margin (HR). The trigger for analysis will be based on the data maturity of the trial at 5-years. This is obtained as the ratio of the variance of the pooled (by treatment) Kaplan-Meier curve at 5-yrs to the variance of the 5-year Kaplan-Meier estimate had all patients been followed for 5-years (30). For the study to be analyzed this ratio would need to exceed 90% (ideally 95%).

The full analysis set (ITT population) comprises all randomized patients.

Additional proportional hazards regression models accounting including potential confounders (age, gender, tumor stage, primary tumorposition(proximal/mid/distal),typeofdCRT)willbeperformed.

For the secondary endpoint HRQOL mean differences between the treatment arms will be estimated using linear mixed regression models. Results from these models will be presented as mean differences together with 95% confidence intervals.

DISCUSSION

The NEEDS trial is the first adequately powered randomized trial to compare the two guideline recommended treatments options for ESCC (11); nCRT followed by planned esophagectomy vs. dCRT with surveillance and salvage esophagectomy only when needed for locoregional tumor control. Due to the lack of high-level evidence that dCRT and surgery only as needed is non-inferior to nCRT with surgery regarding survival, dCRT is in many countries most often used in frail patients who may not tolerate surgery (14, 31, 32). For this reason, there is an apparent need for a pragmatic, international multicenter trial which can generate results with a high degree of generalizability. The results will have the potential to change the current practice of operating most patients, to a new global practice allowing organ preservation for most patients, with non-inferior survival and superior quality of life.

The field of ESCC treatment is moving fast. It is expected that both nCRT followed by planned esophagectomy and also dCRT will be complemented by immunotherapies, at least in defined subsets of patients. In the context of the approval of immunotherapy by EMA following the Checkmate-577 study (33), the implementation of adjuvant immunotherapy with Nivolumab in resected patients with pathological residual disease in the resection specimen is in line with the FDA and EMA approvals. The Study Steering Committee had its second meeting 29 October 2021. Immunotherapy was discussed again and the decision was to pragmatically allow immunotherapy according to the approval status of the drug and clinical practice regulations in each country. As overall survival will definitely be affected, with or without imbalance between the study groups, a decision was taken to consider amending the primary endpoint from overall survival alone to two primary endpoints in the form of overall survival and HRQOL, either as a composite or separate endpoints. This will be finally discussed and decided at one of the next steering committee meetings. In the next years we will also see novel trial results from studies assessing the implementation of immunotherapy into dCRT of localized ESCC such as Skyscraper-07 (NCT04543617) and Keynote-975 (NCT04210115).

Clinical trials are usually described as explanatory or pragmatic. Explanatory trials measure efficacy, meaning the benefit of the treatment under ideal conditions. The aim then being to establish whether the treatment works, and this type of trial is usually undertaken during the initial development phase of an intervention (34). In explanatory trials participants are usually carefully selected to be homogeneous and treatments are very carefully standardized in an ideal experimental situation in order to establish proof of principle (34). Although explanatory trials are necessary to test whether new interventions work, they have limited generalizability to clinical practice, where patients are heterogeneous, and treatment usually is less standardized (34). Pragmatic trials, such as the NEEDS trial, measure effectiveness, meaning the benefit of treatment in clinical practice, and should therefore take place in a routine healthcare, or clinical practice setting (34).

For the same reason, pragmatic trials should normally use ITT, rather than per protocol (PP) analysis for primary outcomes. In a trial of interventions given over a period of time (for example nCRT/dCRT, surveillance and surgery) patients defined as having received an intervention per protocol, are usually a selection of the most successfully treated, potentially introducing bias into PP analyses. Consequently, in the NEEDS trial all analyses will be based on the ITT principle, although for the primary outcome - OS - an additional PP analysis will also be performed.

In conclusion the NEEDS trial is a randomized, pragmatic phase III trial comparing today's preferred standard of care, nCRT followed by planned esophagectomy, with the alternative therapy dCRT with surveillance and salvage esophagectomy only when needed for local tumor control, with a non-inferiority hypothesis for OS in locally advanced, operable ESCC. The objective is, if the study objectives of non-inferior OS and superior HRQOL are met, to guide a global change of practice from mandatory surgery to surgery only when really needed. The trial started inclusion in November 2020 and plans to include 1200 patients in several countries in Asia, Europe, Australia and North America, over the next 4-5 years.

DATA AVAILABILITY STATEMENT

The raw data supporting the conclusions of this article will be made available by the authors, without undue reservation.

ETHICS STATEMENT

The studies involving human participants were reviewed and approved by Etikprövningsmyndigheten. The patients/participants provided their written informed consent to participate in this study.

AUTHOR CONTRIBUTIONS

MN, RW and FL developed the concept. All authors developed the various aspects of the protocol. MN, HO, GA and FL wrote the manuscript. All authors reviewed manuscript and approved the final version. All authors contributed to the article and approved the submitted version.

FUNDING

The NEEDS trial is supported by a grant from the Swedish Research Council (grant number 2019-00423) aiming to cover central trial costs as well as overall trial costs in Sweden. Additional funding has been granted from the Swedish Cancer Society (grant number 200736) and from the Region of Stockholm (grant number 20200119). Local funding is being sought in all participating countries.

SUPPLEMENTARY MATERIAL

The Supplementary Material for this article can be found online at: https://www.frontiersin.org/articles/10.3389/fonc.2022.917961/full#supplementary-material

Supplementary Figure 1 | Supraclavicular lymph nodes are analogous to level 4 in head and neck cancers. The cranial border is defined by the cricoid cartilage. The anterior borders correspond to the sternocleidomastoid muscles. Cranially the posterior border is the posterior edge of the sternocleidomastoid muscle. Caudally the posterior border is the anterior edge of the scalene muscles and the apex of the lungs. The medial limit is the medial edge of the common carotid artery. The lateral limit is defined by the lateral edge of the sternocleidomastoid muscle cranially and the lateral edge of the scalene muscles caudally. The inferior border extends into the thoracic inlet.

Supplementary Figure 2 | Para-esophageal, paratracheal, pretracheal and mediastinal (anterior mediastinal, retrotracheal, posterior mediastinal and trachea-bronchial) lymph nodes. Above the carina, the CTV will encompass the entire trachea and extend radially to encompass the lower and upper paratracheal nodal stations which correspond to levels 2 and 4 in the IASLC staging atlas. Above the aortic arch the anterior border of the CTV is defined by the sternum and clavicular heads to encompass prevascular nodes (IASLC level 3). Above the level of the thoracic inlet, the trachea should be excluded from the CTV (unless the 1cm radial margin to the esophagus requires it). For distal tumors in which the CTV extends superiorly to the mediastinum only to respect the cranial margin to the primary tumor or to para-esophageal lymph node metastases, the superior nodal stations except for the para- esophageal lymph nodes need not to be included.

Supplementary Figure 3 | Paraaortic, hepatogastric ligament, celiac lymph nodes. Below the diaphragm the CTV should be extended inferiorly to the level of the origin of the celiac axis. The CTV will be bounded in the lateral aspect by the vertebral body on the right (usually Th12) and 0.5-1 cm beyond the lateral aspect of the aorta on the left, the vertebral body posteriorly and the pancreatic body anteriorly. Between the level of the gastro- esophageal junction and the celiac lymph nodes the lesser curvature nodes will be included. In this region the liver will define the right border and the stomach will define the left border. Anteriorly the CTV includes the fatty space between the lesser curvature and the liver.

Supplementary Table 1 | Guidelines for management of toxicity from chemotherapy graded according to CTCAE. *ULN, upper limit of normal.

REFERENCES

1. Bray F, Ferlay J, Soerjomataram I, Siegel RL, Torre LA, Jemal A. Global Cancer Statistics 2018: Globocan Estimates of Incidence and Mortality Worldwide for 36 Cancers in 185 Countries. *CA Cancer J Clin* (2018) 68 (6):394–424. doi: 10.3322/caac.21492
2. Lewis I. The Surgical Treatment of Carcinoma of the Oesophagus; With Special Reference to a New Operation for Growths of the Middle Third. *Br J Surg* (1946) 34:18–31. doi: 10.1002/bjs.18003413304
3. Herskovic A, Martz K, al-Sarraf M, Leichman L, Brindle J, Vaitkevicius V, et al. Combined Chemotherapy and Radiotherapy Compared With Radiotherapy Alone in Patients With Cancer of the Esophagus. *N Engl J Med* (1992) 326(24):1593–8. doi: 10.1056/NEJM199206113262403
4. van Hagen P, Hulshof MC, van Lanschot JJ, Steyerberg EW, van Berge Henegouwen MI, Wijnhoven BP, et al. Preoperative Chemoradiotherapy for Esophageal or Junctional Cancer. *N Engl J Med* (2012) 366(22):2074–84. doi: 10.1056/NEJMoa1112088
5. Conroy T, Galais MP, Raoul JL, Bouché O, Gourgou-Bourgade S, Douillard JY, et al. Definitive Chemoradiotherapy With Folfox Versus Fluorouracil and Cisplatin in Patients With Oesophageal Cancer (Prodige5/Accord17): Final Results of a Randomised, Phase 2/3 Trial. *Lancet Oncol* (2014) 15(3):305–14. doi: 10.1016/s1470-2045(14)70028-2
6. Shapiro J, van Lanschot JJB, Hulshof M, van Hagen P, van Berge Henegouwen MI, Wijnhoven BPL, et al. Neoadjuvant Chemoradiotherapy Plus Surgery Versus Surgery Alone for Oesophageal or Junctional Cancer (Cross): Long-Term Results of a Randomised Controlled Trial. *Lancet Oncol* (2015) 16 (9):1090–8. doi: 10.1016/S1470-2045(15)00040-6
7. Markar S, Gronnier C, Duhamel A, Pasquer A, Thereaux J, du Rieu MC, et al. Salvage Surgery After Chemoradiotherapy in the Management of Esophageal Cancer: Is It a Viable Therapeutic Option? *J Clin Oncol* (2015) 33(33):3866–73. doi: 10.1200/JCO.2014.59.9092
8. Vincent J, Mariette C, Pezet D, Huet E, Bonnetain F, Bouché O, et al. Early Surgery for Failure After Chemoradiation in Operable Thoracic Oesophageal Cancer. Analysis of the Non-Randomised Patients in Ffcd 9102 Phase Iii Trial: Chemoradiation Followed by Surgery Versus Chemoradiation Alone. *Eur J Cancer (Oxford Engl 1990)* (2015) 51(13):1683–93. doi: 10.1016/j.ejca.2015.05.027
9. O'Connell L, Coleman M, Kharyntiuk N, Walsh TN. Quality of Life in Patients With Upper Gi Malignancies Managed by a Strategy of Chemoradiotherapy Alone Versus Surgery. *Surg Oncol-Oxford* (2019) 30:33–9. doi: 10.1016/j.suronc.2019.05.021
10. Avery KNL, Metcalfe C, Barham CP, Alderson D, Falk SJ, Blazeby JM. Quality of Life During Potentially Curative Treatment for Locally Advanced Oesophageal Cancer. *Br J Surg* (2007) 94(11):1369–76. doi: 10.1002/bjs.5888
11. Lordick F, Mariette C, Haustermans K, Obermannova R, Arnold D, Committee EG. Oesophageal Cancer: Esmo Clinical Practice Guidelines for Diagnosis, Treatment and Follow-Up. *Ann Oncol* (2016) 27(suppl 5):v50–v7. doi: 10.1093/annonc/mdw329

12. Kalff MC, Gottlieb-Vedi E, Verhoeven RHA, van Laarhoven HWM, Lagergren J, Gisbertz SS, et al. Presentation, Treatment, and Prognosis of Esophageal Carcinoma in a Nationwide Comparison of Sweden and the Netherlands. *Ann Surg* (2021) 274(5):743–50. doi: 10.1097/SLA.0000000000005127
13. Habbous S, Yermakhanova O, Forster K, Holloway CMB, Darling G. Variation in Diagnosis, Treatment, and Outcome of Esophageal Cancer in a Regionalized Care System in Ontario, Canada. *JAMA Netw Open* (2021) 4(9): e2126090. doi: 10.1001/jamanetworkopen.2021.26090
14. Yang J, Liu X, Cao S, Dong X, Rao S, Cai K. Understanding Esophageal Cancer: The Challenges and Opportunities for the Next Decade. *Front Oncol* (2020) 10:1727. doi: 10.3389/fonc.2020.01727
15. Stahl M, Stuschke M, Lehmann N, Meyer HJ, Walz MK, Seeber S, et al. Chemoradiation With and Without Surgery in Patients With Locally Advanced Squamous Cell Carcinoma of the Esophagus. *J Clin Oncol* (2005) 23(10):2310–7. doi: 10.1200/JCO.2005.00.034
16. Bedenne L, Michel P, Bouche O, Milan C, Mariette C, Conroy T, et al. Chemoradiation Followed by Surgery Compared With Chemoradiation Alone in Squamous Cancer of the Esophagus: Ffcd 9102. *J Clin Oncol* (2007) 25 (10):1160–8. doi: 10.1200/JCO.2005.04.7118
17. Cooper JS, Guo MD, Herskovic A, Macdonald JS, Martenson JAJr., Al-Sarraf M, et al. Chemoradiotherapy of Locally Advanced Esophageal Cancer: Long-Term Follow-Up of a Prospective Randomized Trial (Rtog 85-01). Radiation Therapy Oncology Group. *JAMA* (1999) 281(17):1623–7. doi: 10.1001/jama.281.17.1623
18. Wu AJ, Bosch WR, Chang DT, Hong TS, Jabbour SK, Kleinberg LR, et al. Expert Consensus Contouring Guidelines for Intensity Modulated Radiation Therapy in Esophageal and Gastroesophageal Junction Cancer. *Int J Radiat Oncol Biol Phys* (2015) 92(4):911–20. doi: 10.1016/j.ijrobp.2015.03.030
19. Gregoire V, Ang K, Budach W, Grau C, Hamoir M, Langendijk JA, et al. Delineation of the Neck Node Levels for Head and Neck Tumors: A 2013 Update. Dahanca, Eortc, Hknpcsg, Ncic Ctg, Ncri, Rtog, Trog Consensus Guidelines. *Radiother Oncol* (2014) 110(1):172–81. doi: 10.1016/j.radonc.2013.10.010
20. Rusch VW, Asamura H, Watanabe H, Giroux DJ, Rami-Porta R, Goldstraw P. The Iaslc Lung Cancer Staging Project: A Proposal for a New International Lymph Node Map in the Forthcoming Seventh Edition of the Tnm Classification for Lung Cancer. *J Thorac Oncol* (2009) 4(5):568–77. doi: 10.1097/JTO.0b013e3181a0d82e
21. Ibbott G, Haworth A, Followill D. Quality Assurance for Clinical Trials. *Front Oncol* (2013) 3:1–11. doi: 10.3389/fonc.2013.00311
22. Moran JM, Molineu A, Kruse JJ, Oldham M, Jeraj R, Galvin JM, et al. Executive Summary of Aapm Report Task Group 113: Guidance for the Physics Aspects of Clinical Trials. *J Appl Clin Med Phys* (2018) 19(5):335–46. doi: 10.1002/acm2.12384
23. Aaronson NK, Ahmedzai S, Bergman B, Bullinger M, Cull A, Duez NJ, et al. The European Organization for Research and Treatment of Cancer Qlq-C30: A Quality-Of-Life Instrument for Use in International Clinical Trials in Oncology. *J Natl Cancer Inst* (1993) 85(5):365–76. doi: 10.1093/jnci/85.5.365
24. Lagergren P, Fayers P, Conroy T, Stein HJ, Sezer O, Hardwick R, et al. Clinical and Psychometric Validation of a Questionnaire Module, the Eortc Qlq-Og25, to Assess Health-Related Quality of Life in Patients With Cancer of the Oesophagus, the Oesophago-Gastric Junction and the Stomach. *Eur J Cancer* (2007) 43(14):2066–73. doi: 10.1016/j.ejca.2007.07.005
25. Herdman M, Gudex C, Lloyd A, Janssen M, Kind P, Parkin D, et al. Development and Preliminary Testing of the New Five-Level Version of Eq-5d (Eq-5d-5l). *Qual Life Res* (2011) 20(10):1727–36. doi: 10.1007/s11136-011-9903-x
26. Mandard AM, Dalibard F, Mandard JC, Marnay J, Henry-Amar M, Petiot JF, et al. Pathologic Assessment of Tumor Regression After Preoperative Chemoradiotherapy of Esophageal Carcinoma. Clinicopathologic Correlations. *Cancer* (1994) 73(11):2680–6. doi: 10.1002/1097-0142(19940601)73:11<2680::aid-cncr2820731105>3.0.co;2-c
27. Cancer Datasets and Tissue Pathways. *The Royal College of Pathologist* (2019). Available at: https://www.rcpath.org/profession/guidelines/cancer-datasets-and-tissue-pathways.html.
28. Low DE, Alderson D, Cecconello I, Chang AC, Darling GE, D'Journo XB, et al. International Consensus on Standardization of Data Collection for Complications Associated With Esophagectomy: Esophagectomy Complications Consensus Group (Eccg). *Ann Surg* (2015) 262(2):286–94. doi: 10.1097/SLA.0000000000001098
29. Dindo D, Demartines N, Clavien PA. Classification of Surgical Complications: A New Proposal With Evaluation in a Cohort of 6336 Patients and Results of a Survey. *Ann Surg* (2004) 240(2):205–13. doi: 10.1097/01.sla.0000133083.54934.ae
30. Gebski V, Garès V, Gibbs E, Byth K. Data Maturity and Follow-Up in Time-To-Event Analyses. *Int J Epidemiol* (2018) 47(3):850–9. doi: 10.1093/ije/dyy013
31. van der Wilk BJ, Eyck BM, Spaander MCW, Valkema R, Lagarde SM, Wijnhoven BPL, et al. Towards an Organ-Sparing Approach for Locally Advanced Esophageal Cancer. *Dig Surg* (2019) 36(6):462–9. doi: 10.1159/000493435
32. Shah MA, Kennedy EB, Catenacci DV, Deighton DC, Goodman KA, Malhotra NK, et al. Treatment of Locally Advanced Esophageal Carcinoma: Asco Guideline. *J Clin Oncol* (2020) 38(23):2677–94. doi: 10.1200/JCO.20.00866
33. Kelly RJ, Ajani JA, Kuzdzal J, Zander T, Van Cutsem E, Piessen G, et al. Adjuvant Nivolumab in Resected Esophageal or Gastroesophageal Junction Cancer. *N Engl J Med* (2021) 384(13):1191–203. doi: 10.1056/NEJMoa2032125
34. Sedgwick P. Explanatory Trials Versus Pragmatic Trials. *BMJ* (2014) 349: g6694. doi: 10.1136/bmj.g6694

Conflict of Interest: The authors declare that the research was conducted in the absence of any commercial or financial relationships that could be construed as a potential conflict of interest.

Publisher's Note: All claims expressed in this article are solely those of the authors and do not necessarily represent those of their affiliated organizations, or those of the publisher, the editors and the reviewers. Any product that may be evaluated in this article, or claim that may be made by its manufacturer, is not guaranteed or endorsed by the publisher.

Copyright © 2022 Nilsson, Olafsdottir, Alexandersson von Döbeln, Villegas, Gagliardi, Hellström, Wang, Johansson, Gebski, Hedberg, Klevebro, Markar, Smyth, Lagergren, Al-Haidari, Rekstad, Aahlin, Wallner, Edholm, Johansson, Szabo, Reynolds, Pramesh, Mummudi, Joshi, Ferri, Wong, O'Callaghan, Lukovic, Chan, Leong, Barbour, Smithers, Li, Kang, Kong, Chao, Crosby, Bruns, van Laarhoven, van Berge Henegouwen, van Hillegersberg, Rosati, Piessen, de Manzoni and Lordick. This is an open-access article distributed under the terms of the Creative Commons Attribution License (CC BY). The use, distribution or reproduction in other forums is permitted, provided the original author(s) and the copyright owner(s) are credited and that the original publication in this journal is cited, in accordance with accepted academic practice. No use, distribution or reproduction is permitted which does not comply with these terms.

frontiers | Frontiers in Oncology

REVIEW
published: 18 July 2022
doi: 10.3389/fonc.2022.950374

The Key Role of microRNAs in Initiation and Progression of Hepatocellular Carcinoma

Suliman Khan[1], De-Yu Zhang[2], Ji-Yu Zhang[2], Mian Khizar Hayat[3], Jingli Ren[4], Safyan Nasir[5], Muhammad Fawad[4,6] and Qian Bai[1]**

[1] Department of Cerebrovascular Diseases, the Second Affiliated Hospital of Zhengzhou University, Zhengzhou, China, [2] Department of Gastroenterology, the First Affiliated Hospital of Zhengzhou University, Zhengzhou, China, [3] Ministry of Education (MOE) Key Laboratory of Cell Activities and Stress Adopations, School of Life Sciences, Lanzhou University, Lanzhou, China, [4] Zhengzhou Key Laboratory of Big Data Analysis and Application, Henan Academy of Big Data, Zhengzhou University, Zhengzhou, China, [5] Allied District Headquarter Hospital, Faisalabad, Pakistan, [6] School of Mathematics and Statistics, Zhengzhou University, Zhengzhou, China

OPEN ACCESS

Edited by:
Zhendong Jin,
Second Military Medical University, China

Reviewed by:
Farooq Rashid,
Guangxi Veterinary Research Institute, China
Yao Huang,
Shanghai Jiao Tong University, China

***Correspondence:**
Muhammad Fawad
fawadkhn42@gmail.com
Qian Bai
baiqian@zzu.edu.cn

Specialty section:
This article was submitted to Gastrointestinal Cancers: Hepato Pancreatic Biliary Cancers, a section of the journal Frontiers in Oncology

Received: 22 May 2022
Accepted: 01 June 2022
Published: 18 July 2022

Citation:
Khan S, Zhang D-Y, Zhang J-Y, Hayat MK, Ren J, Nasir S, Fawad M and Bai Q (2022) The Key Role of microRNAs in Initiation and Progression of Hepatocellular Carcinoma. Front. Oncol. 12:950374. doi: 10.3389/fonc.2022.950374

Hepatocellular carcinoma (HCC) is the main type of primary liver malignancy and the fourth leading cause of cancer-related death worldwide. MicroRNAs (miRNAs), a type of non-coding RNA that regulates gene expression mainly on post-transcriptional level has a confirmed and important role in numerous biological process. By regulating specific target genes, miRNA can act as oncogene or tumor suppressor. Recent evidence has indicated that the deregulation of miR-NAs is closely associated with the clinical pathological features of HCC. However, the precise regulatory mechanism of each miRNA and its targets in HCC has yet to be illuminated. This study demonstrates that both oncogenic and tumor suppressive miRNAs are crucial in the formation and development of HCC. miRNAs influence biological behavior including proliferation, invasion, metastasis and apoptosis by targeting critical genes. Here, we summarize current knowledge about the expression profile and function of miRNAs in HCC and discuss the potential for miRNA-based therapy for HCC.

Keywords: hepatocellular carcinoma, microRNA, oncogene, tumor suppressor, therapy

INTRODUCTION

Hepatocellular carcinoma (HCC) is the fourth leading cause of cancer-related mortality and the seventh most frequent ma-lignancy worldwide (1). HCC accounts for approximately 90% of primary liver cancer, and is considered as one of the deadliest cancers. Infection of hepatitis B or C viruses, alcohol abuse, toxicants and metabolic disorders all increase the risk of liver cancer (2, 3). In addition, ingestion of the fungal metabolite aflatoxin B1, inhalation of smoke, and adeno-associated virus 2 also are associated with an increase in the incidence of HCC. Generally, patients with cirrhosis, and hu-man immunodeficiency virus infection or thalassemia are also at higher risk of HCC (4–6). Ac-cording to e-Medicine-Health, the 5-year survival rate of early stage HCC is 33%, vs. 2%-11% for advanced stage.

Despite the development of various treatment strategies such as antiviral therapies and clinical interventions, the prognosis of HCC remains poor. Thus, there is a need for developing advanced diagnostic and treatment options. During the last decade, researchers have focused on investigating the molecular underpinnings such as genomic aberrations, biomarkers and drug target sites. Among

the molecular entities, miRNAs play a crucial role in carcinogenesis and have enormous therapeutic potential, thus gaining serious attention during the last few years (7).

miRNAs regulate the global activity of cells by targeting a range of genes and proteins articulation. Increasing evidence demonstrates that miRNAs assume a key administrative role in Multiple Drug Resistance (MDR). Moreover, miRNAs have been considered as potential biomarkers and therapeutic targets (8).

miRNAs have been found frequently deregulated in HCC and specific miRNAs have been re-ported to be associated with the clinicopathological features including metastasis, recurrence, and prognosis of HCC (9). Moreover, compelling evidence suggested that miRNAs influence HCC development by targeting proliferation, apoptosis and metastasis of tumor cells. The proposed mechanisms by which miRNAs act as oncogenes or tumor suppressor genes were depicted in **Figure 1**. The up-regulated miRNAs and those down-regulated in HCC are shown in **Tables 1** and **2**. **Figure 2** shows a schematic overview of the deregulated miRNAs, their target genes and subsequent phenotypes of the resulting HCCs. The aim of this study is to systemically evaluate differentially expressed miRNAs in HCC patients which have been reported consistently through independent studies. Furthermore, we discuss the clinical applications of miRNAs in HCC diagnosis and treatment strategies.

DOWN-REGULATED MIRNAS IN HCC

miR-26a

miR-26a has been found to be downregulated during the progression and development of HCC. However, its expression level is not connected with tumor size or clinical stage of the HCC. Studies have indicated that overexpression of miR-26a stifles the expression of DNA methyltransferase 3b (DNMT3B), which act as an immediate target of miR-26a, suggesting a tumor suppressive effect of miR-26a. Notably, DNMT3B is significantly upregulated in HCC tis-sues (27, 28).

miR-98

MiR-98 functions as tumor suppressor or oncogene in different tumor by interacting with various target genes (29). MiR-98 has been found down-regulated in HCC tissues with its expression related to tumor size, metastasis, and portal vein tumor embolus (15). Zhou et al. reported that ectopic expression of miR-98 decreased the proliferation, migration, invasion and epithelial-mesenchymal transition (EMT) of HCC cells by inhibiting SALL4, thus suppress tumor generation. On the contrary, over expression of SALL4 reverses the suppressive effect of miR-98, resulting in accelerated proliferation, migration, invasion and EMT of HCC cells (30).

miR-101

Reduced expression of miR-101 has been reported in HCC tissues and cell lines (31), especially in HBV related HCC, suggesting a tumor suppressive role of miR-101 in HCC development (32). In addition, overexpression of miR-101 was associated with reduced the expression of DNA me-thyltransferase 3 alpha (DNMT3A) and vice versa. Moreover, miR-101 inhibits the expression of the FBJ murine osteosarcoma viral oncogene homolog (FOS) post-transcriptionally by binding to 3'UTR of FOS mRNA, thereby preventing HCC invasion and migration. Various studies have

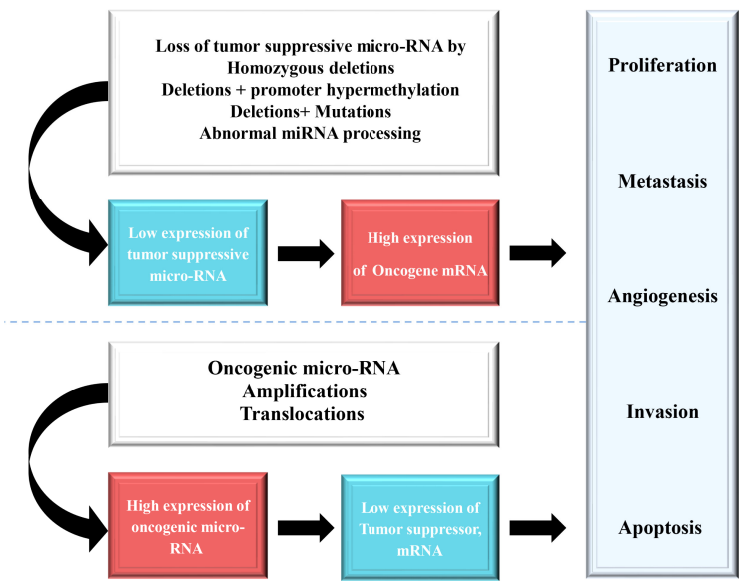

FIGURE 1 | The loss of function of tumor suppressive miRNAs result in an anomalous expression of the target tumor suppressor or oncogene, which contributes to tumor progression.

TABLE 1 | Up regulated miRNAs and their target genes in hepatocellular carcinoma.

miRNAs	Potential and Validated targets	Validated targets expressions	Functions of validated targets	References
miR-21	RHOB; PDCD4, RECK, PTEN	Down regulated	Proliferation, survival, invasiveness	(Cao et al., 2019) (10)
miR-27b	FBXW7	Down regulated	Apoptosis, growth arrest	(Sun et al., 2016) (8)
miR-4262	PDCD4	Down regulated	Enhance proliferation, decrease apoptosis.	(Lu et al., 2016) (11)
miR-935	c-Myc, cyclin D1, SOX7,	Down regulated	cell proliferation, cell motility, invasiveness	(Liu et al., 2016) (12)
mir-765	p-FOXO3a, p-AKT p21, INPP4B	Down regulated	cell proliferation, tumorigenicity	(Xie et al., 2016) (13)
miR-519a	cyclin D1, PI3K/Akt, p27, PTEN.	Down regulated	cell proliferation, cell cycle progression, Apoptosis, differentiation	(Tu et al., 2016) (14)
miR-1180	Cyclin D1, Myc, p-Rb, TNIP2.	Down regulated	cell proliferation, cell growth	(Zhou et al., 2016) (15)
miR-761	MFN2	Down regulated	Apoptosis, migration, invasion	(Zhou et al., 2016) (15)
miR-155-3p	FBXW7	Down regulated	cell proliferation, tumorigenesis	(Tang et al., 2016) (15)
miR-135a	MMP2, p-AKT, FOXO1.	Down regulated	Invasion, metastasis, cell migration	(Zeng et al., 2016) (15)
miR-107	CPEB3	Down regulated	cell proliferation, metastasis	(Zhou et al., 2014) (16)
miR-24-3p	SOX7, MT1M	Down regulated	Cell growth	(Dong et al., 2016) (17)
miR-103	PKC _α, AKAP12	Down regulated	Apoptosis, cell proliferation	(Xia et al., 2016) (18)
miR-222	p57, DDIT4, PTEN, Bmf, TIMP3, PPP2R2A, P27	Down regulated	Metastasis, Apoptosis, cell growth	(Yang et al., 2014) (19)

TABLE 2 | Down regulated miRNAs and their target genes in hepatocellular carcinoma.

miRNAs	Potential and Validated targets	Validated targets expressions in HCC	Functions of validated targets	References
miR-98	SALL4,	up regulated	proliferation, migration, invasion, chemo resistance	(Zhou et al., 2016) (15)
miR-101	Mcl-1; EED;DNMT3A; SOX9, EZH2	up regulated	proliferation, invasion, colony formation, cell cycle progression, tumorigenesis	(Xu et al., 2013) (20)
MiR-124	PIK3CA,SNAI2, ROCK2, EZH2 , STAT3	up regulated	proliferation, Apoptosis	(Lu et al., 2013) (21)
miR-133b	GPC3, TAGLN2, SOX9SIRT1	up regulated	proliferation, Apoptosis, invasion, tumorigenesis	(Tian et al., 2016) (22)
miR-502-3P	SET	up regulated	Cell proliferation, Migration, , invasion	(Jin et al., 2016) (23)
miR-613	DCLK1	up regulated	Tumorigenesis, proliferation, invasion	(Wang et al., 2016) (24)
miR-622	NF-κB , JNK, MAP4K4	up regulated	colony formation, proliferation, invasion, Apoptosis	(Song et al., 2015) (25)
miR-449a	POU2F1, FOS , Met ,ADAM10	up regulated	Cell proliferation, colony formation, migration, Invasion. differentiation	(Liu et al., 2016) (12)
miR-144	E2F3 , SMAD4	up regulated	Growth	
miR-634	Rab1A, DHX33	up regulated	cell growth, Colony formation	
miR-625	PTEN, p-Ak , p-HSP27, IGF2BP1	up regulated	Metastasis, Invasion	(Zhou et al., 2016) (15)
miR-26a	STAT3, IL-6	up regulated	Cell survival. Invasion, tumor growth	(Yang et al., 2013) (26)

concluded that miR-101 suppress HCC by targeting an oncogene known as enhancer of zeste homolog 2 (EZH2), myeloid cell leukemia sequence 1 (Mcl-1) and Nemo-like kinase (NLK) [17.18,19]. It is known that targeted disruption of NLK inhibits tumor cell growth by blocking cyclin D1 and CDK2 in human hepatocellular carcinoma (33). These studies have thus confirmed a key regulatory role of miR-101 in HCC progression.

miR-124

MiR-124 is down-regulated in HCC and is associated with decreased apoptosis and enhanced proliferation. It affects tumor progression with the involvement of STAT3 (34, 35). STAT3 has been reported to be activated significantly in HCC patients with poor prognosis. MiR-124 also suppresses ROCK2 and EZH2 on both the mRNA and protein levels, which in turn inhibits epithelial-

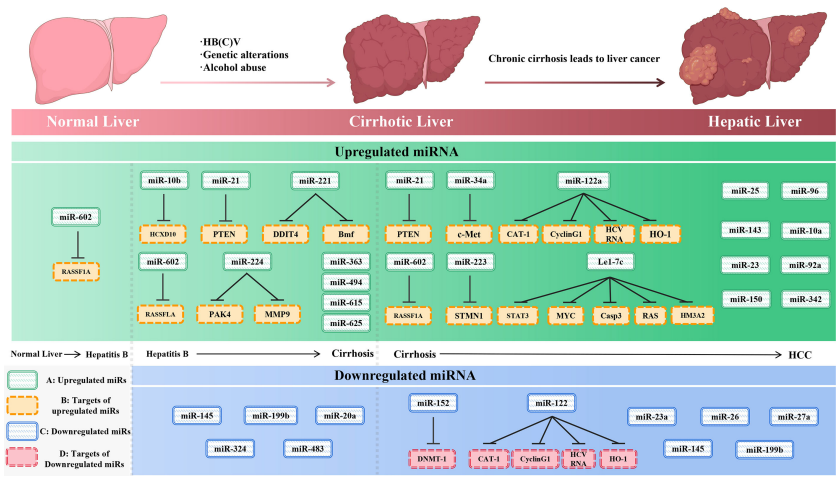

FIGURE 2 | The initiation and development of hepatocellular carcinoma (left) and the expression of miRNAs and their targets (right) during the development of liver cancer. **(A)**-upregulated miR-NAs, **(B)**-targets of upregulated miRNAs, **(C)**-downregulated miRNAs, and **(D)**-targets of downregulated miRNAs.

mesenchymal cell transition (36). Some reports have also indicated that miR-124 targets PIK3CA to inhibit cell proliferation (35).

miR-133b

miR-133b mostly acts as a tumor suppressor and is downregulated in HCC suggesting its involvement in cancer progression or development (37). It targets the Sirt1 gene which plays a key role in the development of different cancers. miR-133b if over-expressed, can attenuate cell proliferation and invasion, and increase apoptosis *via* the miR-133b/Sirt1/GPC3/Wnt β-catenin axis pathway (22).

miR-379

MiR-379 is differentially regulated in different tumors (i.e., it has been confirmed to be down-regulated in breast cancer and inhibit tumor progression and be over expressed and inhibit cell migration, invasion and EMT in HCC (38). MiR-379-5P functions through targeting focal adhesion kinase (FAK) 3'-UTR, thereby suppressing the AKT pathway. Activating AKT signaling or re-storing FAK expression can alter the tumor suppressing activity of miR-379-5P.

miR-502-3P

Down-regulation of miR-502-3P was found in both HCC cell lines and tissue samples. Over ex-pression of miR-502-3P dramatically inhibits proliferation, invasion, metastasis and adhesion in HCC. miR-502-3P directly targets SET which is a potent and specific inhibitor of protein phosphatase 2A (PP2A) and is associated with many cellular processes, such as cell cycle control, migration and apoptosis (39, 40). Moreover, miR-502-3p targets protein-coding genes such as SET and thus plays a crucial role in role in carcinoma development especially HCC. Interestingly, downregulation of miR-502-3P induces HCC, while its overexpression inhibits HCC invasion, proliferation, and metastasis, suggesting that targeting this miRNA can be suitable therapeutic option (23).

miR-193

Many studies have presented the role and importance of miR-193 family in cancer progression, metastasis, and development. The members of this family are miR-193a-3p, miR-193a-5p, miR-193b-3p, and miR-193b-5p, which play crucial role in disease biological processes. mir-193 interacts with different signaling molecules in order to induce suppression of tumor, therefore, it can be used as therapeutic options against HCC in order to make the treatment more effective (41). For instance, MiR-193a-5p has been reported to promote abnormal proliferation and limit apoptosis of HCC cells by targeting the downstream gene BMF, suggesting that miR-193a-5p/BMF axis could be potential therapeutic sites in HCC treatment (42).

miR-539

MiR-539 acts as a tumor suppressor, which is down-regulated in HCC tissues and cells. Many genes have been shown to be targeted by it including SPAG5, CARMA1, MMP-8, CDK4, and PHB2 (43). A study found that the delivery of miR-539 mimic significantly promoted apoptosis in HCC cells. Studies further showed that miR-539 resulted apoptotic death in HCC cells and tissues. MiR-539 reduced the expression of phosphorylation of STAT3 and anti-apoptotic proteins like Bcl-2 and Bcl-xL. While over-expression of STAT3 considerably reversed the apoptosis mediated by miR-539. Enforced expression of miR-539 eliminated the resistance of HCC cells to arsenic trioxide, which was also confirmed *in vivo* (44).

miR-613

miR-613 was initially reported to be implicated in lipid metabolism in HepG2 cells and macro-phages (45). miR-613

has been reported to suppress the proliferation and invasion of ovarian can-cer cells and prostate cancer cells (46). Recent studies have shown the link between miR-613 and tumorigenesis. DCLK1 was identified as a novel target of miR-613, which is frequently up-regulated in HCC and associated with tumorigenesis (47, 48). Targeting DCLK1 has been shown to suppress the growth of HCC xenograft tumors in nude mice models (24). Experimental studies revealed that miR-613 has the ability to negatively regulate the expression of DCLK1, which is based on its interaction within the 3′-UTR of DCLK1 (25).

miR-622

Numerous evidences indicate that miR-622 is frequently down-regulated in human tumors such as gastric cancer, colorectal cancer, pancreatic cancer, and glioma. Interestingly, studies have confirmed that over-expression of miR-622 slow down the growth of HCC xenograft tumors *in vivo*. Bioinformatics analysis and luciferase reporter assay discovered that miR-622 directly targeted the 3′-UTR of mitogen-activated protein 4 kinase 4 (MAP4K4) mRNA. Ectopic expression of miR-622 led to a significant reduction of MAP4K4 expression in HCC cells and xenograft tumors. MAP4K4 over-expression partially counteracted the impact of miR-622 on cell proliferation and apoptosis. Inhibition of JNK and NF-κB signaling simulated the anticancer effects of miR-622 in HCC cells (49).

miR-885-5p

In 2010, miR-885-5p was identified for the first time from a pheochromocytoma (50). miR-885-5p expression was elevated in patients with cirrhosis or HCC when compared with normal people (51). Both *in vitro* and *in vivo* studies showed that over-expression of miR-885-5p decreased metastasis of HCC cells, and vice versa. Additionally, it was revealed that miR-885-5p suppressed the activity of Wnt/β-catenin signaling pathway by targeting CTNNB1, which proposing miR-885-5p to be a promising negative regulator of HCC development (52).

UPREGULATED MIRNAS IN HCC

miR-21

miR-21 was significantly up-regulated in HCC tissues and cell lines, which is linked with the in-crease of tumor migration and invasion. The up-regulation of miR-21 can potentially decrease its targeted tumor suppressive factors and therefore promote the development of HCC. Various tar-gets of miR-21 have been experimentally confirmed, including PTEN, PDCD4, RECK, MARCKs, TPM1, and Cdc25A (53, 54). However, ectopic expression of these targets may have diverse functional effects on tumorigenesis. Additionally, it was shown that miR-21 was significantly over-expressed in HCC tissues and cells in expression profiling studies using miRNA microarrays. Inhibition of miR-21 increased the expression of the PTEN and decreased proliferation, migration and invasion of HCC cells.

miR-27b

miR-27b has been found to play an active role in many kinds of human tumors, which was found to be over-expressed in HCC. MiR-27b over-expression resulted in prominent increased proliferation and reduced apoptosis in Hep3B cells. *In vivo* studies showed that knockdown of miR-27b inhibited the growth of SMMC-7721 cells in mouse xenograft. Furthermore, it was confirmed that Fbxw7 was a direct target of miR-27b.

miR-24-3p and miR-103

Up-regulation of miR-24-3p and miR-103 was confirmed in HCC tissues, which played an important role in the initiation and progression of HCC by targeting metallothionein 1M (17). AKAP12 is an A-kinase scaffold protein whose down-regulation is linked to an increased risk of tumors including HCC (55). AKAP12 was realized as a tumor suppressor gene because of its capability to suppress growth rates and promote re-organization of the actin based cytoskeleton in v-Src-transformed fibroblasts. miR-103 acts a potential repressor of AKAP12 by directly targeting the 3′-UTR and therefore promotes HCC progression (18). Furthermore, AKAP12 can also binds to key signaling mediators such as PKC, PKA, calmodulin, F-actin, cyclins, Src and phospholipids in a spatiotemporal manner.

miR-107

In vitro and *in vivo* studies have demonstrated that over-expression of miR-107 contributes to proliferation in human HCC. Data showed that miR-107 acts as a tumor promoter in HCC by accelerating growth and metastasis. Notably, CPEB3 was identified as a novel and functional target of miR-107, which acts as a tumor suppressor in HCC. In addition, it was also showed that miR-107 regulates the pathogenesis of HCC partially through the CPEB3/EGFR pathway (16). MiR-107 was involved in a variety of pathological process including carcinogenesis, which was reported to accelerate the proliferation of gastric cancer cells.

miR-135a

In HCC, miR-135a transcribed by FOXM1 induces the development of portal vein tumor thrombus by inhibiting metastasis suppressor 1 (MTSS1) (56). A study determined miR-135a expression in HCC cells, normal liver cells, HCC tissues and adjacent normal live tissues and examined the effect of miR-135a on cell invasion and migration. miR-135a induced HCC cell metastasis and invasion by targeting the 3′-UTR of FOXO1 mRNA, consequently promoting Snail and MMP2 expression, inhibiting FOXO3a phosphorylation, and promoting AKT phosphorylation (57).

MiR-155-5p

miR-155-5p and miR-155-3p are different transcripts from the miR-155 host gene, in which miR-155-5p has been considered as the functional form. Previous studies found that miR-155-5p was significantly up-regulated in T cells. Functional manipulation of miR-155-5p expression revealed its important role in regulating Th17 development. Cell proliferation of HCC was enhanced by miR-155-5p both *in vitro* and *in vivo*. FBXW7 was identified as a

functional target of miR-155-5p and was involved in the effects of promoting HCC cells proliferation (58).

miR-519a

miR-519a belongs to the C19MC cluster, which plays a vital role in the pathogenesis of human cancers. Ectopic expression of miR519a increased the cell viability, proliferation and cell cycle progression in HCC cells. PTEN was confirmed to inhibit the progression of HCC by suppressing the PI3k/Akt pathway, and its insufficiency was closely associated with HCC development and progression (59). Studies have shown that the activation of PI3K/Akt signaling pathway pro-motes the progression of HCC and increases the malignant behavior of HCC. MiR-519a promotes HCC progression by activating the Akt signaling pathway and inhibiting PTEN (14).

miR-761

MiR-761 was found to be up-regulated in HCC tissues, which directly target Mitofusin-2 and inhibited its expression. However, a miR-761 inhibitor impaired mitochondrial function and effectively repressed tumor progression *in vitro* and *in vivo* by up-regulating Mitofusin-2.

miR-765

Abnormal expression of miR-765 frequently occur in a variety of human tumors and contributes to carcinogenesis by affecting various genes, therefore, it was considered as a potential target for cancer diagnosis and therapy. It has been demonstrated that miR-765 is over-expressed in HCC and its expression is correlated with HCC progression. MiR-765 promotes the progression of HCC by targeting and suppressing INPP4B. Suppression of INPP4B up-regulated p-AKT and Cyclin D1, while down-regulated p-FOXO3a and p21 in HCC. From these findings it was revealed that miR-765 acts as a potential onco-miR. INPP4B acts a tumor suppressor by regulating PI3K/Akt signaling pathway (13).

miR-935

miR-935 over-expression promotes cell proliferation, tumorigenesis and cell cycle progression, and vice versa. MiR-935 down-regulates the expression of sex determining region Y-Box 7 (SOX7) and increases C-Myc and cyclin D1, two G1/S transitional regulators (60). Certain evidences have shown that SOX7 may disrupt the transcriptional function of the β-catenin-TCF/LEF interaction and inhibit the activity of Wnt target genes including cyclin D1, c-Myc and COX-219. Several recent studies have shown that SOX7 acts as a tumor suppressor through the Wnt/β-catenin signaling pathway in various cancers (61).

miR-1180

Over-expression of miR-1180 promotes the proliferation of HCC by directly suppressing TNIP2, then it can up-regulate the NF-kB downstream target genes including cy-clin D1, Myc and p-Rb. Generally, it is accepted that TNIP2 played an essential role in the regulation of NF-kB pathway, which act as a transcription factor that facilitates a number of biological processes including cell proliferation. Previous studies have indicated that upregulation of miR-1180-3p induces HCC and is associated with poor prognosis, suggesting that it might be useful as a prognostic marker in the case of HCC. Moreover, targeting miR-1180 through inhibitors can decrease the risk of HCC or alleviate HCC progression and metastasis (62, 63).

miR-4262

MiR-4262 is over-expressed in HCC tissues and cell lines. Results showed that miR-4262 promotes cell proliferation by suppressing PDCD4 and promotes the accumulation of nuclear NF-kB/P65 by activating NF-kB pathway (11). PDCD4 functions as a tumor suppressor which regulates both transcription and translation in many cancers. It was confirmed that PDCD4 inhibits NF-kB dependent transcription in human glioblastoma cells by its direct interaction with p65 (64).

GENE ONTOLOGY AND KEGG ANALYSIS

Gene ontology and KEGG analysis was carried out for a number of genes. GO analysis showed that gene annotations are mainly in three aspects: biological processes (BP), molecular function (MF) and components (CC). In the biological process, the genes were mainly enriched in negative regulation of cellular process, intracellular signal transduction, negative regulation of macromolecule metabolic process, negative regulation of biological process and many more as shown in **Figure 3**. In the molecular function, the genes were mainly involved in protein binding, enzyme binding, molecular complex binding and other molecular functions. In the cell components, the expressed genes were mainly found in cytoplasm, nucleus, cytosol, organelle lumen, membrane enclosed lumen, intracellular organelle lumen and other cell components. These data showed that the genes exhibited different GO functions, implying the different roles of gene. In KEGG analysis, the genes were mainly involved in a number of pathways linked with pancreatic cancer, small cell lung cancer, prostate cancer, colorectal cancer and many other malignancies as shown in **Figure 4**.

MIRNAS CONFIRMED AS POTENTIAL THERAPEUTIC TARGETS AND DIAGNOSTIC MARKERS IN HCC

Differential and specific biomarkers are crucial for early detection and diagnosis of HCC, as well as the advancement of preventive screening. Nonetheless, current strategies are inadequate for detecting HCC in early stage. Advance in MRI and CT have incredibly improved the diagnostic efficacy of HCC. Serum alfa-fetoprotein (AFP) and des-gamma-carboxy prothrombin (DCP) levels have been utilized as HCC biomarkers. However, the exactness of AFP is modest with a sensitivity 39%– 65% and specificity 76%– 94%. However, 1/3 of HCC patients got missed diagnosis based on AFP and AFP levels can also be nonspecifically increased in patients with hepatitis and cirrhosis (65).

Numerous miRNAs are dysregulated in HCC and circulating miRNA levels are additionally influenced by HCC

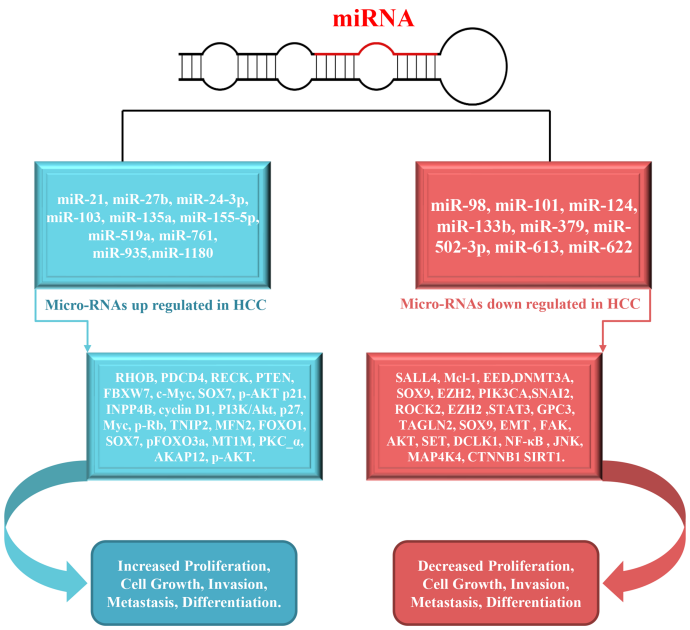

FIGURE 3 | Schematic overview of miRNAs involved in the metastasis, proliferation, migration and invasion in HCC. The inhibition of validated targets (left side) by specific miRNAs results in increased metastasis, proliferation, migration and invasion.

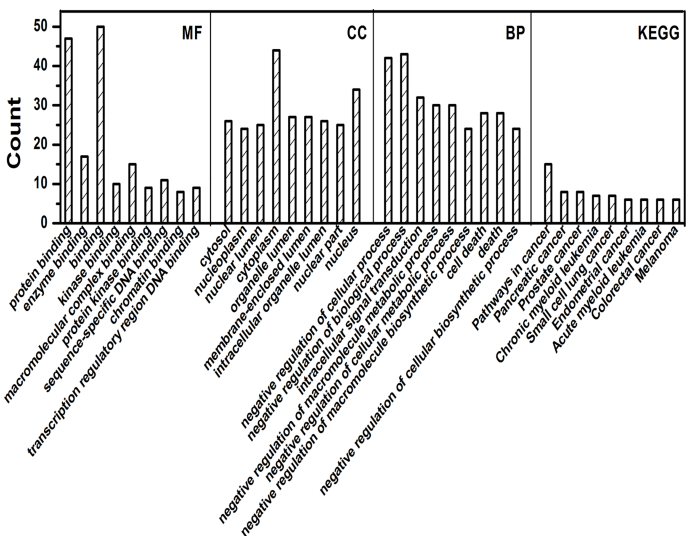

FIGURE 4 | GO and KEGG analysis by R package cluster Profiler. Enrichment analysis of Gene Ontology for targeted genes that include biological processes (BP), molecular function (MF), and cell fractions (CC) as well as KEGG pathways analysis.

progression. It is fascinating that circulating miR-21, miR-222, and miR-223 were observed to be up-regulated in HCC patients with HBV or HCV. Circulating miR-21 ex-pression was significantly higher in HCC patients than in those with perpetual hepatitis and healthy control. Receiver operating characteristic (ROC) investigation of miR-21 yielded an Area Under Curve (AUC) of 0.773 while separating HCC from perpetual hepatitis, and an AUC of 0.953 when separating HCC from healthy control. The values of miR-21 were better than AFP as biomarker in HCC. Meantime, serum levels of miR-1, miR-25, miR-92a, miR-206, miR-375, and miR let-7f were elevated in HCC patients.

miR-130b had the biggest AUC of 0.913, besides that, with an affectability of 87.7% and a specificity of 81.4% for distinguishing HCC. miR-15b had the affectability of 98.3% for identifying HCC, which is the most astounding one in all the miRNAs analyzed, despite its low specificity of 15.3%. The high affectability of miR-15b and miR-130b as HCC biomarkers may ensure patients with early stage HCC better prognosis. Similarly, serum miR-16 level was observed to be a more sensitive biomarker for HCC than AFP and DCP. The combination of miR-16, AFP, AFP-L3% and DCP yielded the optimum state of both affectability (92.4%) and specificity (78.5%) for HCC diagnosis, when investigation was limited to patients with tumors less than 3 cm. Moreover, a current meta-analysis in which eight investigations were incorporated demonstrated that the diagnostic value of miRNAs for HCC as follows: pooled affectability 0.87 (0.72–0.98), pooled specificity 0.90 (0.76–1.00), pooled positive probability proportion 8.7 (3.52– 97.45), pooled negative probability proportion 0.13 (0.02– 0.31), and pooled indicative chances proportion 86.69 (19.06– 2,646.00) (66).

miR-122, miR-125b, and miR-192 in serum are potential non-invasive biomarkers for identifying liver damage in patients. miR-122 act as a solid marker particularly to detect hepatitis B. Besides, when contrasted with ALT, miR-122 was found to reflect liver injury with a better AUC of 0.784. These discoveries recommended the capability of utilizing miR-122 as a delicate and enlightening biomarker for hepatitis B. In addition, miR-125b could be possibly utilized as a biomarker for HCV and miR-192 for drug-induced liver injury. The affectability and specificity of utilizing a single biomarker and combined biomarkers for liver disease has been investigated. The most extreme value of Youden's index come about after combination of miR-122 and miR-125b, in which affectability increased from73.41% to 83.89%, and specificity diminished from 83.05% to76.27%. Studies showed that the serum level of miR-122 was connected with ALT in HBV patients and even varied more sensitively than ALT (67). In this manner, miR-122 could be utilized as a more precise biomarker for HBV-related liver injury than ALT, a traditional biomarker of liver damage. This increased levels of miR-122 and miR-125b are related with less progression and better survival of HBV-induced liver injury patients. In general, the study provides clinical confirmation of circulating miR-122 as a biomarker for HBV patients, as well as the possibility of miR-125b and miR-192 as biomarkers for HCV and chemical related liver damage. Moreover, the combination of miR-122 and miR-125 demonstrated a higher affectability than ALT. Even though the affectability and strength of miRNAs as biomarkers for liver disease was reasonable, proper controls should be utilized. While evaluating the specificity of a miRNA for detecting HCC, it is important to make sure that examiners should be coordinated by age, sex, etiology and severity of illness.

MIRNA ACT AS TUMOR SUPPRESSOR

miR-493 was considered as a tumor suppressor in different human tumors by targeting on various molecules. In human bladder cancer cells, miR-493 reduces cell motility and movement capacity by targeting FZD4 and Rho C. miR-493 can also suppress tumor development, invasion and metastasis of lung cancer by regulating ERK, E2F1 and PI3K-AKT pathway. IGF1R and MKK7 were distinguished as immediate targets of miR-493, which suppress liver metastasis of colon tumor cells. miR-493 may stifle the tumorigenesis of HCC by modulating Wnt signaling path-way. While miR-493 is significantly down-regulated in HCC patients, restore of miR-493 could remarkably suppress the proliferation, invasion, migration and tumorigenicity of HCC cells *in vitro* and *in vivo*. miR-493 could down-regulate ANTXR1 and RSPO2 specifically and Wnt/b-catenin pathway was engaged with its anti-tumor capacity.

MIRNAS ACT AS THERAPEUTIC TARGETS

Recently, accumulated evidences have demonstrated that methodologies focused on regulation of miRNA expression could be a novel approach to malignancy treatment. Previous studies have shown that inhibition of miR-122 by modification of miRNA oligonucleotides was a promising strategy for minimizing miRNA action in non-human primates (68). Another investigation has exhibited that restoration of tumor suppressor miR-122 makes HCC cells more sensitive to sorafenib treatment by down-regulating of multidrug protection genes. Alternatively, suppression of oncogenic miR-221 brought about better survival and significant decrease in the number and size of tumors. Besides, HCC cells transfected with anti-miR-221 were more sensitive to chemo-therapy with joined interferon-α and 5-FU.

CONCLUSION AND FUTURE PERSPECTIVE

miRNAs play an important role in patho-physiological processes of the initiation and progression of HCC. Many miRNAs are abnormally expressed and play a vital role in HCC progression by specifically targeting at critical genes. Various reports have identified potential miRNA biomarkers, their target genes and the possible mechanisms that lead to hepatocarcinogenesis and advancement. MDR is a profoundly dilemma in tumor treatment process, which was realized to be regulated by a wide range of miRNAs. Along these lines, miRNAs could be utilized as ideal biomarkers for predicting chemotherapeutic reaction and potential targets in HCC treatment. For instance, miR-98 targets SALL4, miR-124 targets STAT3, miR-502-3P targets SET, miR-761 targets MFN2 and miR-222 targets P27. Among those some miRNAs even have multiple target genes that are involved in HCC progression. For example, miR-221 and miR-222 target p27, p57, Bmf, PTEN, TIMP3, DDIT4 and PPP2R2A. While miR-122 targets cyclin G1, ADAM10, AD-AM17, SRF, Igf1R and Bcl-w. As contrast, one target gene can be regulated by multiple miR-NAs simultaneously. These findings show that deregulated miRNAs

and their targets make up a complex interacting network, which influence HCC development and progression. Future re-search is needed to address and expand the therapeutic potential of miRNAs in inhibiting the progression of HCC. In addition, miRNAs may provide new perspectives and targets for the development and research of novel HCC treatment modalities.

AUTHOR CONTRIBUTIONS

Study concept and design: SK, QB, MF. Manuscript writing: SK, D-YZ, MH, JR, SN. Analysis and interpretation of data: MF, J-YZ, JR, SN. Acquisition of data: D-YZ, MH, JR, SN. Critical revision of manuscript and video: SK, QB, MF. Funding obtained: SK, QB, MF. All authors contributed to the article and approved the submitted version.

FUNDING

This study was financially supported by grants from Henan province innovation talents of science and technology plan (No. SB201901045) and hepatobiliary foundation of Henan Charity General Federation (No: GDXZ2019006).

REFERENCES

1. Morishita A, Oura K, Tadokoro T, Fujita K, Tani J, Masaki T, et al. MicroRNAs in the Pathogenesis of Hepatocellular Carcinoma: A Review. *Cancers (Basel)* (2021) 13(3):514. doi: 10.3390/cancers13030514
2. Craig AJ, von Felden J, Garcia-Lezana T, Sarcognato S, Villanueva A. Tumour Evolution in Hepatocellular Carcinoma. *Nat Rev Gastroenterol Hepatol* (2020) 17(3):139–52. doi: 10.1038/s41575-019-0229-4
3. Satriano L, Lewinska M, Rodrigues PM, Banales JM, Andersen JB. Metabolic Rearrangements in Primary Liver Cancers: Cause and Consequences. *Nat Rev Gastroenterol Hepatol* (2019) 16(12):748–66. doi: 10.1038/s41575-019-0217-8
4. Singal AG, Lampertico P, Nahon P. Epidemiology and Surveillance for Hepatocellular Carcinoma: New Trends. *J Hepatol* (2020) 72(2):250–61. doi: 10.1016/j.jhep.2019.08.025
5. Wang P, Cao J, Liu S, Pan H, Liu X, Sui A, et al. Upregulated microRNA-429 Inhibits the Migration of HCC Cells by Targeting TRAF6 Through the NF-κb Pathway. *Oncol Rep* (2017) 37(5):2883–90. doi: 10.3892/or.2017.5507
6. Huang XY, Yao JG, Huang HD, Wang C, Ma Y, Xia Q, et al. MicroRNA-429 Modulates Hepatocellular Carcinoma Prognosis and Tumorigenesis. *Gastroenterol Res Pract* (2013) 2013:804128. doi: 10.1155/2013/804128
7. Zhang H, Deng T, Ge S, Liu Y, Bai M, Zhu K, et al. Exosome circRNA Secreted From Adipocytes Promotes the Growth of Hepatocellular Carcinoma by Targeting Deubiquitination-Related USP7. *Oncogene*α (2019) 38(15):2844–59. doi: 10.1038/s41388-018-0619-z
8. Sun XF, Sun JP, Hou HT, Li K, Liu X, Ge QX, et al. MicroRNA-27b Exerts an Oncogenic Function by Targeting Fbxw7 in Human Hepatocellular Carcinoma. *Tumour Biol* (2016) 37(11):15325–32. doi: 10.1007/s13277-016-5444-9
9. Mayr C, Beyreis M, Wagner A, Pichler M, Neureiter D, Kiesslich T, et al. Deregulated MicroRNAs in Biliary Tract Cancer: Functional Targets and Potential Biomarkers. *BioMed Res Int* (2016) 2016:4805270. doi: 10.1155/2016/4805270
10. Cao LQ, Yang XW, Chen YB, Zhang DW, Jiang XF, Xue P. Exosomal miR-21 Regulates the TETs/PTENp1/PTEN Pathway to Promote Hepatocellular Carcinoma Growth. *Mol Cancer* (2019) 18(1):148. doi: 10.1186/s12943-019-1075-2
11. Lu S, Wu J, Gao Y, Han G, Ding W, Huang X. MicroRNA-4262 Activates the NF-κb and Enhances the Proliferation of Hepatocellular Carcinoma Cells. *Int J Biol Macromol* (2016) 86:43–9. doi: 10.1016/j.ijbiomac.2016.01.019
12. Liu F, Zhang S, Zhao Z, Mao X, Huang J, Wu Z, et al. MicroRNA-27b Up-Regulated by Human Papillomavirus 16 E7 Promotes Proliferation and Suppresses Apoptosis by Targeting Polo-Like Kinase2 in Cervical Cancer. *Oncotarget* (2016) 7 (15):19666–79. doi: 10.18632/oncotarget.7531
13. Xie BH, He X, Hua RX, Zhang B, Tan GS, Xiong SQ, et al. Mir-765 Promotes Cell Proliferation by Downregulating INPP4B Expression in Human Hepatocellular Carcinoma. *Cancer Biomark* (2016) 16(3):405–13. doi: 10.3233/CBM-160579
14. Tu K, Liu Z, Yao B, Han S, Yang W. MicroRNA-519a Promotes Tumor Growth by Targeting PTEN/PI3K/AKT Signaling in Hepatocellular Carcinoma. *Int J Oncol* (2016) 48(3):965–74. doi: 10.3892/ijo.2015.3309
15. Zhou X, Zhu HQ, Ma CQ, Li HG, Liu FF, Chang H, et al. MiR-1180 Promoted the Proliferation of Hepatocellular Car-Cinoma Cells by Repressing TNIP2 Expression. *BioMed Pharmacother* (2016) 79:315–20. doi: 10.1016/j.biopha.2016.02.025
16. Zhou C, Li G, Zhou J, Han N, Liu Z, Yin J. miR-107 Activates ATR/Chk1 Pathway and Suppress Cervical Cancer Invasion by Targeting MCL1. *PLoS One* (2014) 9(11):e111860. doi: 10.1371/journal.pone.0111860
17. Dong X, Ding W, Ye J, Yan D, Xue F, Xu L, et al. MiR-24-3p Enhances Cell Growth in Hepatocellular Carcinoma by Targeting Metallothionein 1M. *Cell Biochem Funct* (2016) 34(7):491–6. doi: 10.1002/cbf.3213
18. Xia W, Ni J, Zhuang J, Qian L, Wang P, Wang J. MiR-103 Regulates Hepatocellular Carcinoma Growth by Targeting AKAP12. *Int J Biochem Cell Biol* (2016) 71:1–11. doi: 10.1016/j.biocel.2015.11.017
19. Yang XW, Shen GZ, Cao LQ, Jiang X-F, Peng H-P, Shen G, et al. MicroRNA-1269 Promotes Proliferation in Human Hepatocellular Carcinoma via Downregulation of FOXO1. *BMC Cancer* (2014) 14:909. doi: 10.1186/1471-2407-14-909
20. Xu Y, An Y, Wang Y, Zhang C, Zhang H, Huang C, et al. miR-101 Inhibits Autophagy and Enhances Cisplatin-Induced Apoptosis in Hepatocellular Carcinoma Cells. *Oncol Rep* (2013) 29(5):2019–24. doi: 10.3892/or.2013.2338
21. Lu Y, Yue X, Cui Y, Zhang J, Wang K. MicroRNA-124 Suppresses Growth of Human Hepatocellular Carcinoma by Targeting STAT3. *Biochem Biophys Res Commun* (2013) 441(4):873–9. doi: 10.1016/j.bbrc.2013.10.157
22. Tian Z, Jiang H, Liu Y, Huang Y, Xiong X, Wu H, et al. MicroRNA-133b Inhibits Hepatocellular Carcinoma Cell Progres-Sion by Targeting Sirt1. *Exp Cell Res* (2016) 343(2):135–47. doi: 10.1016/j.yexcr.2016.03.027
23. Jin H, Yu M, Lin Y, Hou B, Wu Z, Li Z, Sun J. MiR-502-3P Suppresses Cell Proliferation, Migration, and Invasion in Hepatocellular Carcinoma by Targeting SET. *Onco Targets Ther* (2016) 9:3281–9. doi: 10.2147/OTT.S87183
24. Wang W, Zhang H, Wang L, Zhang S, Tang M. miR-613 Inhibits the Growth and Invasiveness of Human Hepatocellular Carcinoma *via* Targeting DCLK1. *Biochem Biophys Res Commun* (2016) 473(4):987–92. doi: 10.1016/j.bbrc.2016.04.003
25. Song WH, Feng XJ, Gong SJ, Chen JM, Wang SM, Xing DJ, et al. microRNA-622 Acts as a Tumor Suppressor in Hepatocellu-Lar Carcinoma. *Cancer Biol Ther* (2015) 16(12):1754–63. doi: 10.1080/15384047.2015.1095402
26. Yang X, Liang L, Zhang XF, Jia HL, Qin Y, Zhu XC, et al. MicroRNA-26a Suppresses Tumor Growth and Metastasis of Human Hepatocellular Carcinoma by Targeting Interleukin-6-Stat3 Pathway. *Hepatology* (2013) 58 (1):158–70. doi: 10.1002/hep.26305
27. Fu X, Meng Z, Liang W, Tian Y, Wang X, Han W, et al. miR-26a Enhances miRNA Biogenesis by Targeting Lin28B and Zcchc11 to Suppress Tumor Growth and Metastasis. *Oncogene*α (2014) 33(34):4296–306. doi: 10.1038/onc.2013.385
28. Li Y, Ren M, Zhao Y, Lu X, Wang M, Hu J, et al. MicroRNA-26a Inhibits Proliferation and Metastasis of Human Hepatocellular Carcinoma by Regulating DNMT3B-MEG3 Axis. *Oncol Rep* (2017) 37(6):3527–35. doi: 10.3892/or.2017.5579
29. Rizos E, Siafakas N, Katsantoni E, Skourti E, Salpeas V, Rizos I, Tsoporis JN, et al. Correction: Let-7, Mir-98 and Mir-181 as Bi-Omarkers for Cancer and Schizophrenia. *PLoS One* (2015) 10(8):e0135863. doi: 10.1371/journal.pone.0135863
30. Du Y, Li Y, Lv H, Zhou S, Sun Z, Wang M. miR-98 Suppresses Tumor Cell Growth and Metastasis by Targeting IGF1R in Oral Squamous Cell Carcinoma. *Int J Clin Exp Pathol* (2015) 8(10):12252–9.

31. Zheng F, Liao YJ, Cai MY, Liu TH, Chen SP, Wu PH, et al. Systemic Delivery of MicroRNA-101 Potently Inhibits Hepatocellular Carcinoma *In Vivo* by Repressing Multiple Targets. *PLoS Genet* (2015) 11(2):e1004873. doi: 10.1371/journal.pgen.1004873
32. Wei X, Xiang T, Ren G, Tan C, Liu R, et al. miR-101 is Down-Regulated by the Hepatitis B Virus X Protein and Induces Aberrant DNA Methylation by Targeting DNA Methyltransferase 3A. *Cell Signal* (2013) 25(2):439–46. doi: 10.1016/j.cellsig.2012.10.013
33. Jung KH, Kim JK, Noh JH, Eun JW, Bae HJ, Xie HJ, et al. Targeted Disruption of Nemo-Like Kinase Inhibits Tumor Cell Growth by Simultaneous Suppression of Cyclin D1 and CDK2 in Human Hepatocellular Carcinoma. *J Cell Biochem* (2010) 110(3):687–96. doi: 10.1002/jcb.22579
34. Wu LP, Wu J, Shang A, Yang M, Li L-L, Yu J, et al. miR-124 Inhibits Progression of Hepatocarcinoma by Targeting KLF4 and Promises a Novel Diagnostic Marker. *Artif Cells Nanomed Biotechnol* (2018) 46(sup1):159–67. doi: 10.1080/21691401.2017.1415918
35. Lang Q, Ling C. MiR-124 Suppresses Cell Proliferation in Hepatocellular Carcinoma by Target-Ing PIK3CA. *Biochem Biophys Res Commun* (2012) 426 (2):247–52. doi: 10.1016/j.bbrc.2012.08.075
36. Zheng F, Liao YJ, Cai MY, Liu YH, Liu TH, Chen SP, et al. The Putative Tumour Suppressor microRNA-124 Modulates Hepatocellular Carcinoma Cell Aggressiveness by Repressing ROCK2 and EZH2. *Gut*α (2012) 61 (2):278–89. doi: 10.1136/gut.2011.239145
37. El-Halawany MS, Ismail HM, Zeeneldin AA, Elfiky A, Tantawy M, Kobaisi MH, et al. Investigating the Pretreatment miRNA Expression Patterns of Advanced Hepatocellular Carcinoma Patients in Association With Response to TACE Treatment. *BioMed Res Int* (2015) 2015:649750. doi: 10.1155/2015/649750
38. Khan S, Brougham CL, Ryan J, Sahrudin A, O'Neill G, Wall D, et al. miR-379 Regulates Cyclin B1 Expression and is De-Creased in Breast Cancer. *PLoS One* (2013) 8(7):e68753. doi: 10.1371/journal.pone.0068753
39. Canela N, Rodriguez-Vilarrupla A, Estanyol JM, Diaz C, Pujol MJ, Agell N, et al. The SET Protein Regulates G2/M Transi-Tion by Modulating Cyclin B-Cyclin-Dependent Kinase 1 Activity. *J Biol Chem* (2003) 278(2):1158–64. doi: 10.1074/jbc.M207497200
40. Madeira A, Pommet JM, Prochiantz A, Allinquant B. SET Protein (TAF1beta, I2PP2A) is Involved in Neuronal Apoptosis Induced by an Amyloid Precursor Protein Cytoplasmic Subdomain. *FASEB J* (2005) 19(13):1905–7. doi: 10.1096/fj.05-3839fje
41. Khordadmehr M, Shahbazi R, Sadreddini S, et al. miR-193: A New Weapon Against Cancer. *J Cell Physiol* (2019) 234(10):16861–72. doi: 10.1002/jcp.28368
42. Wang JT, Wang ZH. Role of miR-193a-5p in the Proliferation and Apoptosis of Hepatocellular Carcinoma. *Eur Rev Med Pharmacol Sci* (2018) 22 (21):7233–9. doi: 10.26355/eurrev_201811_16257
43. Lv LY, Wang YZ, Zhang Q, et al. miR-539 Induces Cell Cycle Arrest in Nasopharyngeal Carci-Noma by Targeting Cyclin-Dependent Kinase 4. *Cell Biochem Funct* (2015) 33(8):534–40. doi: 10.1002/cbf.3152
44. Zhu C, Zhou R, Zhou Q, et al. microRNA-539 Suppresses Tumor Growth and Tumorigenesis and Overcomes Arsenic Trioxide Resistance in Hepatocellular Carcinoma. *Life Sci* (2016) 166:34–40. doi: 10.1016/j.lfs.2016.10.002
45. Zhong D, Zhang Y, Zeng YJ, et al. MicroRNA-613 Represses Lipogenesis in HepG2 Cells by Downregulating Lxrα. *Lipids Health Dis* (2013) 12:32. doi: 10.1186/1476-511X-12-32
46. Ren W, Li C, Duan W, et al. MicroRNA-613 Represses Prostate Cancer Cell Proliferation and Invasion Through Targeting Frizzled7. *Biochem Biophys Res Commun* (2016) 469(3):633–8. doi: 10.1016/j.bbrc.2015.12.054
47. Sureban SM, Madhoun MF, May R, Qu D, Ali N, Fazili J, et al. Plasma DCLK1 is a Marker of Hepatocellular Carci-Noma (HCC): Targeting DCLK1 Prevents HCC Tumor Xenograft Growth *via* a microRNA-Dependent Mechanism. *Oncotarget*α (2015) 6(35):37200–15. doi: 10.18632/oncotarget.5808
48. Chandrakesan P, Weygant N, May R, et al. DCLK1 Facilitates Intestinal Tumor Growth *via* Enhancing Pluripotency and Epithelial Mesenchymal Transition. *Oncotarget*α (2014) 5(19):9269–80. doi: 10.18632/oncotarget.2393
49. Afanasyeva EA, Mestdagh P, Kumps C, Vandesompele J, Ehemann V, Theissen J, et al. MicroRNA miR-885-5p Targets CDK2 and MCM5, Activates P53 and Inhibits Proliferation and Survival. *Cell Death Differ* (2011) 18(6):974–84. doi: 10.1038/cdd.2010.164
50. Gui J, Tian Y, Wen X, Zhang W, Zhang P, Gao J, et al. Serum microRNA Characterization Identifies miR-885-5p as a Potential Marker for Detecting Liver Pathologies. *Clin Sci (Lond)* (2011) 120(5):183–93. doi: 10.1042/CS20100297
51. Zhu J, Zheng Z, Wang J, Sun J, Wang P, Cheng X, et al. Different miRNA Expression Profiles Between Human Breast Cancer Tumors and Serum. *Front Genet* (2014) 5:149. doi: 10.3389/fgene.2014.00149
52. Meng F, Henson R, Wehbe-Janek H, Ghoshal K, Jacob ST, Patel T. MicroRNA-21 Regulates Expression of the PTEN Tumor Suppressor Gene in Human Hepatocellular Cancer. *Gastroenterology*α (2007) 133(2):647–58. doi: 10.1053/j.gastro.2007.05.022
53. Asangani IA, Rasheed SA, Nikolova DA, Leupold JH, Colburn NH, Post S, et al. MicroRNA-21 (miR-21) Post-Transcriptionally Downregulates Tumor Suppressor Pdcd4 and Stimulates Invasion, Intravasation and Metastasis in Colorectal Cancer. *Oncogene*α (2008) 27(15):2128–36. doi: 10.1038/sj.onc.1210856
54. Si ML, Hayashi Z M, Nomoto S, Kanda M, Okamura Y, Nishikawa Y, et al. miR-21-Mediated Tumor Growth. *Oncogene*α (2007) 26(19):2799–803. doi: 10.1038/sj.onc.1210083
55. Hayashi M, Nomoto S, Kanda M, Okamura Y, Nishikawa Y, Yamada S, et al. Identification of the A Kinase Anchor Protein 12 (AKAP12) Gene as a Candidate Tumor Suppressor of Hepatocellular Carcinoma. *J Surg Oncol* (2012) 105(4):381–6. doi: 10.1002/jso.22135
56. Liu S, Guo W, Shi J, Li N, Yu X, Xue J, et al. MicroRNA-135a Contributes to the Development of Portal Vein Tumor Thrombus by Promoting Metastasis in Hepatocellular Carcinoma. *J Hepatol* (2012) 56(2):389–96. doi: 10.1016/j.jhep.2011.08.008
57. Zeng YB, Liang XH, Zhang GX, Jiang N, Zhang T, Huang JY, et al. miRNA-135a Promotes Hepatocellular Carcinoma Cell Migration and Invasion by Targeting Forkhead Box O1. *Cancer Cell Int* (2016) 16:63. doi: 10.1186/s12935-016-0328-z
58. Tang B, Lei B, Qi G, Liang X, Tang F, Yuan S, et al. MicroRNA-155-3p Promotes Hepatocellular Carcinoma Formation by Suppressing FBXW7 Expression. *J Exp Clin Cancer Res* (2016) 35(1):93. doi: 10.1186/s13046-016-0371-6
59. Rahman MA, Kyriazanos ID, Ono T, Yamanoi A, Kohno H, Tsuchiya M, et al. Impact of PTEN Expression on the Outcome of Hepatitis C Virus-Positive Cirrhotic Hepatocellular Carcinoma Patients: Possible Relationship With COX II and Inducible Nitric Oxide Synthase. *Int J Cancer* (2002) 100 (2):152–7. doi: 10.1002/ijc.10458
60. Liu X, Li J, Yu Z, Li J, Sun R, Kan Q. miR-935 Promotes Liver Cancer Cell Proliferation and Migration by Targeting Sox7. *Oncol Res* (2017) 25(3):427–35. doi: 10.3727/096504016X14747300207374
61. Gautheron J, Luedde T. A Novel Player in Inflammation and Cancer: The Deubiquitinase CYLD Controls HCC Development. *J Hepatol* (2012) 57 (5):937–9. doi: 10.1016/j.jhep.2012.07.039
62. Zhou Z, Zhou X, Jiang Y, Qiu M, Liang X, Lin Q, et al. Clinical Significance of miR-1180-3p in Hepatocellular Carcinoma: A Study Based on Bioinformatics Analysis and RT-qPCR Validation. *Sci Rep* (2020) 10(1):11573. doi: 10.1038/s41598-020-68450-z
63. El-Nakeep S. Molecular and Genetic Markers in Hepatocellular Carcinoma: In Silico Analysis to Clinical Validation (Current Limitations and Future Promises). *World J Gastrointest Pathophysiol* (2022) 13(1):1–14. doi: 10.4291/wjgp.v13.i1.1
64. Matsuhashi S, Manirujjaman M, Hamajima H, Ozaki I. Control Mechanisms of the Tumor Suppressor PDCD4: Expression and Functions. *Int J Mol Sci* (2019) 20(9):2304. doi: 10.3390/ijms20092304
65. Tomimaru Y, Eguchi H, Nagano H, Wada H, Kobayashi S, Marubashi S, et al. Circulating microRNA-21 as a Novel Biomarker for Hepatocellular Carcinoma. *J Hepatol* (2012) 56(1):167–75. doi: 10.1016/j.jhep.2011.04.026
66. Zhang X, Zhang Z, Dai F, Shi B, Chen L, Zhang X, et al. Comparison of Circulating, Hepatocyte Specific Messenger RNA and microRNA as

Biomarkers for Chronic Hepatitis B and C. *PLoS One* (2014) 9(3):e92112. doi: 10.1371/journal.pone.0092112
67. Elmén J, Lindow M, Schütz S, et al. LNA-Mediated microRNA Silencing in non-Human Pri-Mates. *Natureα* (2008) 452(7189):896–9. doi: 10.1038/nature06783
68. Bai S, Nasser MW, Wang B, Hsu SH, Datta J, Kutay H, et al. MicroRNA-122 Inhibits Tumorigenic Properties of Hepato-Cellular Carcinoma Cells and Sensitizes These Cells to Sorafenib. *J Biol Chem* (2009) 284(46):32015–27. doi: 10.1074/jbc.M109.016774

Conflict of Interest: The authors declare that the research was conducted in the absence of any commercial or financial relationships that could be construed as a potential conflict of interest.

Publisher's Note: All claims expressed in this article are solely those of the authors and do not necessarily represent those of their affiliated organizations, or those of the publisher, the editors and the reviewers. Any product that may be evaluated in this article, or claim that may be made by its manufacturer, is not guaranteed or endorsed by the publisher.

Copyright © 2022 Khan, Zhang, Zhang, Hayat, Ren, Nasir, Fawad and Bai. This is an open-access article distributed under the terms of the Creative Commons Attribution License (CC BY). The use, distribution or reproduction in other forums is permitted, provided the original author(s) and the copyright owner(s) are credited and that the original publication in this journal is cited, in accordance with accepted academic practice. No use, distribution or reproduction is permitted which does not comply with these terms.

frontiers | Frontiers in Oncology

TYPE Original Research
PUBLISHED 02 August 2022
DOI 10.3389/fonc.2022.973999

Check for updates

OPEN ACCESS

EDITED BY
Zhendong Jin,
Second Military Medical University, China

REVIEWED BY
Li Tian,
Third Xiangya Hospital, Central South University, China
Junrong Liang,
Fourth Military Medical University, China

*CORRESPONDENCE
Zhaoshen Li
zhs_li@126.com
Li Yang
yanglixie_2008@126.com

†These authors have contributed equally to this work and share first authorship

SPECIALTY SECTION
This article was submitted to Gastrointestinal Cancers: Hepato Pancreatic Biliary Cancers, a section of the journal Frontiers in Oncology

RECEIVED 20 June 2022
ACCEPTED 13 July 2022
PUBLISHED 02 August 2022

CITATION
Yin H, Zhang F, Yang X, Meng X, Miao Y, Noor Hussain MS, Yang L and Li Z (2022) Research trends of artificial intelligence in pancreatic cancer: A bibliometric analysis. *Front. Oncol.* 12:973999. doi: 10.3389/fonc.2022.973999

COPYRIGHT
© 2022 Yin, Zhang, Yang, Meng, Miao, Noor Hussain, Yang and Li. This is an open-access article distributed under the terms of the Creative Commons Attribution License (CC BY). The use, distribution or reproduction in other forums is permitted, provided the original author(s) and the copyright owner(s) are credited and that the original publication in this journal is cited, in accordance with accepted academic practice. No use, distribution or reproduction is permitted which does not comply with these terms.

Research trends of artificial intelligence in pancreatic cancer: a bibliometric analysis

Hua Yin[1,2†], Feixiong Zhang[1†], Xiaoli Yang[1†], Xiangkun Meng[1], Yu Miao[1], Muhammad Saad Noor Hussain[3], Li Yang[1*] and Zhaoshen Li[2,4*]

[1]Department of Gastroenterology, General Hospital of Ningxia Medical University, Yinchuan, China, [2]Postgraduate Training Base in Shanghai Gongli Hospital, Ningxia Medical University, Shanghai, China, [3]Department of Anesthesia, Dar Ul Shafa Hospital Sialkot, Punjab, Pakistan, [4]Clinical Medical College, Ningxia Medical University, Yinchuan, China

Purpose: We evaluated the related research on artificial intelligence (AI) in pancreatic cancer (PC) through bibliometrics analysis and explored the research hotspots and current status from 1997 to 2021.

Methods: Publications related to AI in PC were retrieved from the Web of Science Core Collection (WoSCC) during 1997-2021. Bibliometrix package of R software 4.0.3 and VOSviewer were used to bibliometrics analysis.

Results: A total of 587 publications in this field were retrieved from WoSCC database. After 2018, the number of publications grew rapidly. The United States and Johns Hopkins University were the most influential country and institution, respectively. A total of 2805 keywords were investigated, 81 of which appeared more than 10 times. Co-occurrence analysis categorized these keywords into five types of clusters: (1) AI in biology of PC, (2) AI in pathology and radiology of PC, (3) AI in the therapy of PC, (4) AI in risk assessment of PC and (5) AI in endoscopic ultrasonography (EUS) of PC. Trend topics and thematic maps show that keywords " diagnosis ", "survival", "classification", and "management" are the research hotspots in this field.

Conclusion: The research related to AI in pancreatic cancer is still in the initial stage. Currently, AI is widely studied in biology, diagnosis, treatment, risk assessment, and EUS of pancreatic cancer. This bibliometrics study provided an insight into AI in PC research and helped researchers identify new research orientations.

KEYWORDS

Artificial intelligence, pancreatic cancer, AI, bibliometric, trends

Introduction

Pancreatic cancer (PC) is a common cancer of the digestive system. It is known as the "king of cancers" because of its high mortality rate. According to the World Cancer Report 2020, the 1-year survival rate of pancreatic cancer after diagnosis is 24%, and the 5-year survival rate is only 9% (1). However, for those with early-stage cancer whose tumor was confined to the primary site, the 5-year relative survival rate increased to 39.4 percent (2). Improving survival in patients with pancreatic cancer may require in-depth research on multiple aspects, including early diagnosis, health management and treatment (3, 4). In this process, a large amount of biomedical data will be generated. How to efficiently organize, integrate, understand and analyze these big data to provide help for medical professionals is a current scientific problem, and the emergence of artificial intelligence has solved this difficulty well.

Artificial intelligence (AI) is a branch of computer science that employs computers to imitate human brain processes and intelligent behaviors like learning, reasoning, thinking, and planning (5). With the advancement of machine learning techniques, particularly deep learning and neural networks, AI has shown promise in the diagnosis, treatment, and prognosis of pancreatic cancer (6). Support vector machine (SVM) algorithm was used to analyze RNA-SEQ data to identify biomarkers for early diagnosis of pancreatic ductal adenocarcinoma (PDAC) (7). Endoscopic ultrasonography (EUS) and computerized tomography (CT) images were analyzed by artificial neural network (ANN), convolutional neural network (CNN), and other artificial intelligence techniques in imaging diagnosis, which can better predict the diagnosis of pancreatic cancer and effectively reduce the influence of experience and subjective factors on accuracy (8–10). Furthermore, an AI model based on preoperative CT was able to accurately predict the occurrence of postoperative pancreatic fistula (POPF) clinical complications following pancreaticoduodenectomy (PD) surgery, especially at the intermediate risk level (11). The AI system could help surgeons optimize their preoperative strategies. AI is rapidly changing the field of medicine, and academic research on this topic in pancreatic cancer had proliferated in recent years, which also indicates the need for a comprehensive analysis of research patterns and trends of AI in pancreatic cancer. The importance of summarizing global research trends and hot spots is critical, yet no bibliometric analysis study exists in this field.

Bibliometric analysis is an interdisciplinary subject that uses information visualization methods to make quantitative analysis and summary of the indicators of authors, journals, countries, institutions, references and keywords of worldwide literatures in a certain field (12). In this way, we can understand the knowledge structure more systematically and intuitively, and identify the frontier or hot spot in a certain research field (13). Therefore, this study aims to conduct a comprehensive analysis of the publication about AI in PC, and provide an overall view and direction for future work to promote AI in pancreatic cancer research.

Materials and methods

Database and search strategy

We used the Web of Science Core Collection (WoSCC) as our data source. Since WoSCC covers the most vital data sources for bibliometric analysis, it was the most frequently used and accepted database in scientific or bibliometric studies, with a more consistent and standardized record in multidisciplinary literature research (14). All data were retrieved from WoSCC on May 20, 2022 to avoid the bias that could occur due to continuous updating of the WoSCC database. The search strategy was described as follows: TS=(artificial intelligence OR "computational intelligence" OR "deep learning" OR "computer aided" OR "machine learning" OR "support vector machine" OR "data learning" OR " artificial neural network" OR "digital image" OR "convolutional neural network" OR "evolutionary algorithms" OR "feature learning" OR "reinforcement learning" OR "big data" OR "image segmentation" OR "hybrid intelligent system" OR "hybrid intelligent system" OR "recurrent neural network" OR "natural language processing" OR " bayesian network " OR " bayesian learning" OR " random forest" OR "evolutionary algorithms" OR "multiagent system") AND TS=(pancreatic OR pancreas) AND TS=(neoplasm OR cancer OR tumor OR oncology OR carcinoma OR adenocarcinoma). The document type was restricted to articles and reviews, timespan was set from 1997 to 2021, and the publications' language was limited to English. In order to guarantee the representativeness of the included publications, the search results were filtered by title and abstract to exclude irrelevant articles. After 13 irrelevant literatures were excluded, 587 publications were finally extracted and exported in plain text format for analysis. The detailed retrieval process is shown in Figure 1.

Statistical analysis

The bibliometrix package of R software 4.0.3 was used to analyze the collected data. Publications, citations and collaborations of countries/regions, annual publications, and author publications were analyzed and the bar chart of annual publications was derived using Microsoft Excel 2019. In addition, the Bibliometrix package was

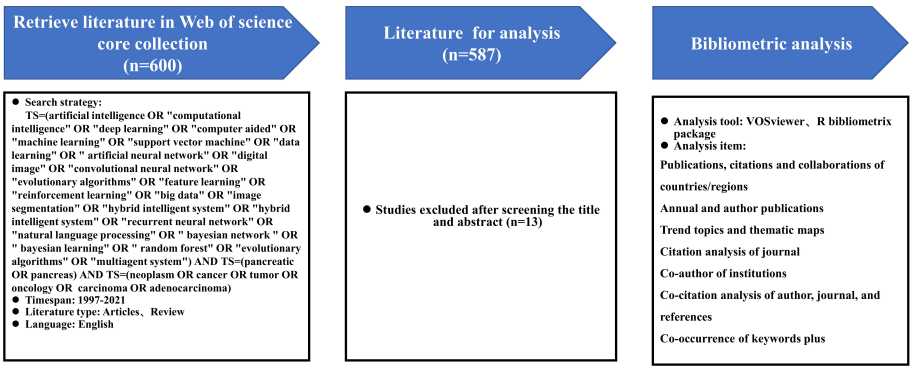

FIGURE 1
Procedures of bibliometric analysis: retrieval strategy, bibliometric analysis tools and items.

also used to generate trend topics and thematic maps. The quantity and quality of scientific researcher's academic production is evaluated by H-index that proposed by Hirsch (15). A scientist has index h if h of his or her the number of papers published over n years (Np) have at least h citations each and the other (Np – h) papers have ≤h citations each. VOSviewer (version 1.6.10) was used to visually analyze network maps of co-authors of institutions, co-citation of author/journal/references, citation of journal, and co-occurrence of keywords. Different clusters in the network map were represented by different colors and collaborations or co-citations were indicated by connection lines. The size of the circle indicates the number of documents, references, or keywords, while the thickness of the connection line indicates the strength of the link.

Result

Bibliometric analysis of annual publications

Between 1997 and 2021, the WoSCC core database discovered 587 publications on the topic of AI in pancreatic cancer. Figure 2 showed the trends of annual publications on research of AI in pancreatic cancer. Before 2017, the annual output of AI-related research on pancreatic cancer grew slowly, with only 25 publications published annually at most, indicating that it was in its infancy. But after 2018, the number of publications grew rapidly, reaching 188 in 2021,

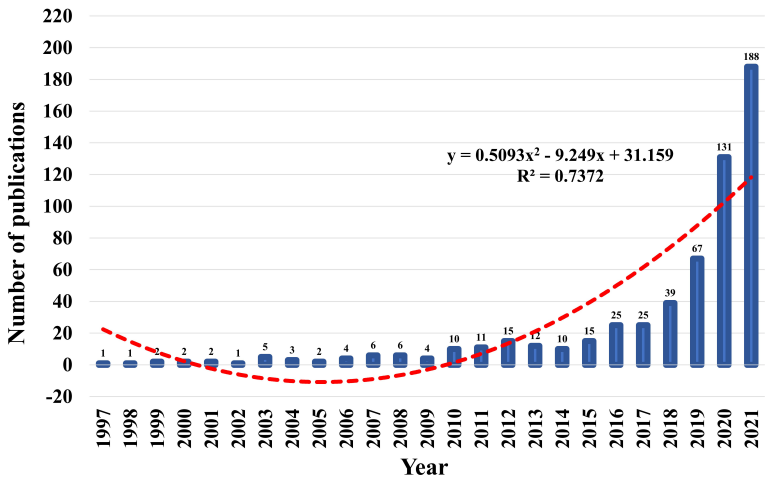

FIGURE 2
Trends of annual publications on research of AI in pancreatic cancer and the polynomial fitted curves (red dotted line).

seven times that of 2017. In the past 4 years, the cumulative number of published documents accounted for 72.4% of all publications. A polynomial model fitting (R2=0.7372) predicted a significant correlation between publication year and publication output, and the number of literatures in this field will continue to increase in the future, indicating that the application of AI in pancreatic cancer has become one of the current frontier fields.

The publishing performance of countries/regions

The research of AI in the field of PC was highlighted in 41countries across the world. The number of publications in each country was ranked to explore the global geographical distribution of publications in this field. In this study, it was found that the United States (181) was the most productive country, followed by China (154), Japan (33), Germany (29), and Korea (29), and the top 5 countries in total citations were the United States (4189), China (1785), Japan (596), Germany (466) and Italy (424). Table 1 showed the 15 countries with the highest publication volume and total citations. Figure 3 showed the country/region collaboration map worldwide. The Darker blues indicated higher collaboration rates. Countries that shared more than three papers were shown as link lines, and the wider the link line, the higher the rate of collaboration between the two countries. The highest number of collaborations was between the USA and China (30), followed by 12 and 8 collaborations between Germany and United Kingdom, and between USA and Germany, respectively. Supplementary Table S1 listed top 10 collaborative countries/regions.

Bibliometric analysis of institutions

There were 1030 institutions from different countries involved in the publications of AI in the field of PC research. The Johns Hopkins University, with 64 studies analyzed by bibliometrix package, Zhe Jiang University (46), Fu Dan University (45), Seoul National University (39), and Memorial Sloan-Ketterlin Cancer Center (32), were the top five institutions. Table 2 showed the top 15 institutions in terms of publications and citations. The co-authorship analysis showed that 51 institutions published more than five papers, and finally showed collaboration among 49 institutions after excluding two unrelated terms (Figure 4). In terms of linking strength, the leading five institutes included Johns Hopkins University (total link strength 34 times), Harvard Medical School (33), University of Pittsburgh (29), Memorial Sloan-Ketterlin Cancer Center (28), and The University of Texas MD Anderson Cancer Center (23).

Contributions of top journals and authors

A total of 321 journals published research in this field, including 45 journals with more than three publications (Figure 5A). The top 10 journals contributed 114 publications, accounting for nearly 19.4% of the 587 publications retrieved. Scientific Reports published the most literature (20 publications, 3.4%), followed by Frontiers in Oncology (18 publications), Cancers (12 publications), Clinical Cancer Research (10 publications), and Medical Physics (10 publications). More details were shown in Supplementary Table S2. We analyzed

TABLE 1 Top 15 countries/regions with highest publications and total citations on AI in pancreatic cancer.

Rank	Country	Publications	Rank	Country	Total Citations
1	USA	181	1	USA	4189
2	CHINA	154	2	CHINA	1785
3	JAPAN	33	3	JAPAN	596
4	GERMANY	29	4	GERMANY	466
5	KOREA	29	5	ITALY	424
6	ITALY	24	6	ROMANIA	405
7	INDIA	14	7	KOREA	333
8	NETHERLANDS	14	8	FRANCE	295
9	UNITED KINGDOM	14	9	CANADA	237
10	FRANCE	11	10	AUSTRALIA	232
11	CANADA	10	11	UNITED KINGDOM	232
12	AUSTRALIA	8	12	NETHERLANDS	204
13	ROMANIA	7	13	SWEDEN	138
14	SWEDEN	6	14	SINGAPORE	135
15	SWITZERLAND	6	15	CYPRUS	66

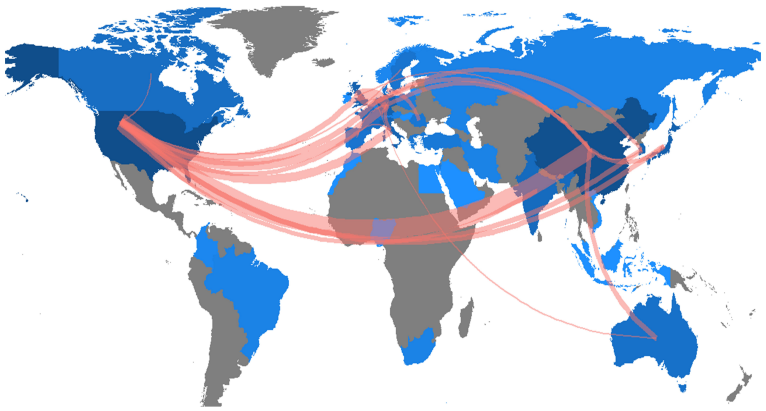

FIGURE 3
Country/region collaboration map. The Darker blues indicated higher collaboration rates, the wider the link line, the higher the rate of collaboration between the two countries. Countries with more than three shared papers were shown by connectors.

all the journals and found that 104 of them had more than 50 citations (Figure 5B). The top ten co-cited journals that published related papers were included in Supplementary Table S3. The most co-cited journal was Nature (467 citations), followed by Gastrointest Endoscopy (453 citations), Plos One (424 citations), Radiology (417 citations), and Clinical Cancer Research (412 citations).

In this study, 3747 authors participated in AI-PC related research, and 27 authors among them published more than five research publications. Table 3 listed the 10 most productive authors. Wang L, Li J, and Lu JP ranked in the top 3, with10, 9, and 9 articles, respectively. While author Hruban RH from Johns Hopkins University in the United States had the highest H-index. The H-index, proposed by Hirsch, combines the number of publications an author has published with the number of citations to better assess a scientist's impact.

Documents citation and references co-citation analyses

VOSviewer citation analysis showed that 44 of the 587 documents were cited more than 50 citations. The top three cited documents included "Molecular classification of human carcinomas by use of gene expression signatures" (520 citations) published in Cancer Research (16), followed by "Genome-wide cell-free DNA fragmentation in patients with cancer" (293 citations) published in Nature (17), and "Quantitative

TABLE 2 Top 15 publications and total citations institutions on research of AI in pancreatic cancer.

Rank	Affiliations	Publications	Affiliations	Citations
1	JOHNS HOPKINS UNIV	69	JOHNS HOPKINS UNIV	1034
2	ZHEJIANG UNIV	46	MEM SLOAN KETTERING CANC CTR	565
3	FUDAN UNIV	45	UNIV VIRGINIA	543
4	SEOUL NATL UNIV	39	UNIV CALIF SAN DIEGO	526
5	MEM SLOAN KETTERING CANC CTR	32	FUDAN UNIV	393
6	TECH UNIV MUNICH	31	NATL CANC CTR	346
7	UNIV TEXAS MD ANDERSON CANC CTR	29	LEIDEN UNIV	337
8	MAYO CLIN	25	UNIV AMSTERDAM	335
9	UNIV PENN	25	YALE UNIV	279
10	HARVARD MED SCH	23	STANFORD UNIV	268
11	SHANGHAI JIAO TONG UNIV	21	TECH UNIV MUNICH	264
12	SUN YAT SEN UNIV	21	UNIV TEXAS MD ANDERSON CANC CTR	248
13	YONSEI UNIV	20	UNIV PITTSBURGH	235
14	SICHUAN UNIV	19	SEOUL NATL UNIV	227
15	UNIV PITTSBURGH	19	MAYO CLIN	218

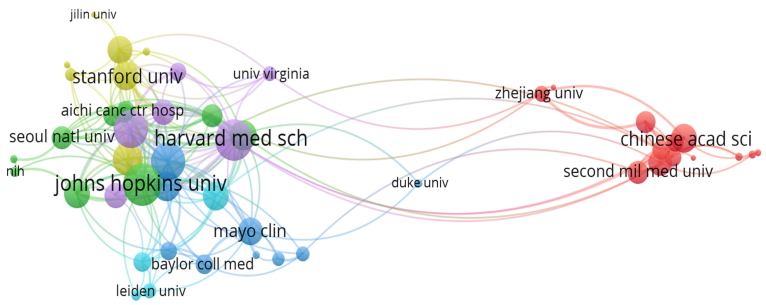

FIGURE 4
Analysis of co-authorship among institutions with more than five publications. Clusters were identified by color, the size of the circles represented the number of publications, and the thickness of the lines showed the strength of the association.

multiplex immunohistochemistry reveals myeloid-inflamed tumor-immune complexity associated with poor prognosis" (247 citations) published in Cell Reports (18). Table 4 listed the top ten documents with the highest citations.

Co-citation references analysis evaluated the link between documents that were cited together by other articles. The top ten references with the most citations in this field were also provided in Supplementary Table S4. Gillies RJ (2016, Radiology; 37 citations) (26), Breiman L (2001, Mach Learn; 37 citations) (27), and Rahib L (2014, Cancer Research 35 citations) (28) were the three references with the most citations.

Trends based on keywords co-occurrence analysis

The purpose of keywords co-occurrence analysis is to look into the relationship between keywords in a set of publications in order to uncover hot themes and help scholars better grasp current scientific concerns. The co-occurrence keywords in the WoSCC database were analyzed using VOSviewer. A total of 2805 keywords were investigated, 81 of which appeared more than ten times. Figure 6A showed the visual network map of keywords co-occurrence. Nodes in different colors represented different types of clusters, node size represented the occurrence of keywords, and a thick connection line showed a close relationship between two items. The top three keywords were "cancer" with 132 occurrences, "pancreatic cancer" with 103 occurrences, and "diagnosis" with 80 occurrences. Figure 6B was a density visualization map based on the frequency of keyword occurrences. Table 5 showed the number of occurrences, total link strength and theme description of each cluster. According to the results of cluster analysis, these keywords were divided into five clusters: cluster (1) AI in biology of pancreatic cancer; cluster (2) AI in pathology and radiology of pancreatic cancer; cluster (3) AI in therapy of pancreatic cancer; cluster (4) AI in risk assessment of pancreatic cancer; cluster (5) AI in endoscopic ultrasonography (EUS) of pancreatic cancer.

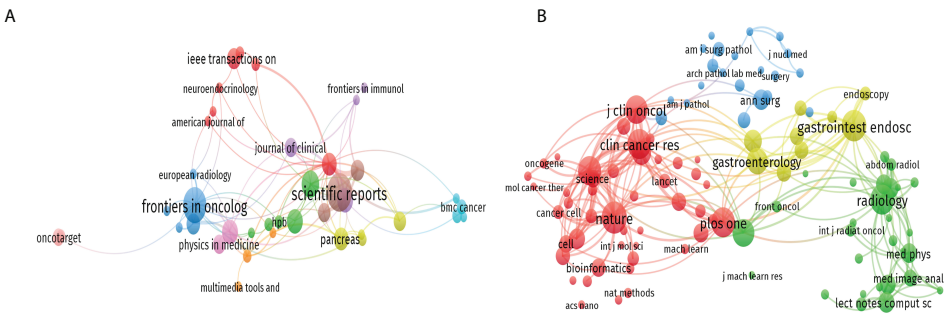

FIGURE 5
The citation and co-citation analysis of journal. **(A)** Network map of citation analysis of journals with more than three publications. **(B)** Network map of co-citation analysis of journals with more than fifty citations.

TABLE 3 Top 10 productive authors on AI in pancreatic cancer.

Rank	Author	Publications	H-index	Total Citations
1	WANG L	10	5	82
2	LI J	9	4	61
3	LU JP	9	3	40
4	HRUBAN RH	7	6	282
5	JANG JY	7	5	208
6	KIM Y	7	4	76
7	PARK S	7	4	118
8	WANG Y	7	4	45
9	ZHANG H	7	3	47
10	ZHANG J	7	3	51

Trend topics and thematic maps analysis

Considering that the analysis results of different bibliometric tools may differ, we compared the co-occurrence keywords map of VOSviewer with the trend topics and thematic maps of Bibliomtrix software to identify research hotspots in this field. Figure 7A was the trend topics map generated by Bibliometrix package by analyzing the keywords plus. The larger the circle is, the more frequently keywords appear. It can be seen that the hot spots in 2019 were mainly "classification", "management" and "expression", corresponding to cluster 1 and 4, followed by "diagnosis" and "survival" in 2020, corresponding to cluster 3. In 2021, the major hotspots were "differential-diagnosis", "computed tomography" and "EUS", corresponding to clusters 2 and 5. The thematic map formed by two-dimensional matrix can better predict future research directions. The thematic map of keywords plus was shown in Figure 7B. The horizontal axis of a thematic map reflects centrality, whereas the vertical axis represents density. As a result, four quadrants are created: motor-themes, which are essential and well-developed in the first quadrant (top right corner); the second quadrant (top left corner): highly specialized/niche themes that have grown in popularity but are less relevant to the field; Emerging or declining themes, which indicate certain developing or fading themes, are shown in the third quadrant (lower left corner); Quadrant 4 (lower right corner): basic themes that are significant to the field but are underdeveloped. In the map, bubbles marked by the most frequently occurring keywords represent clusters, and the size of bubbles is proportional to the frequency of occurrence (29). It was worth noting that the two clusters located in quadrant 4, which keywords "diagnosis", "survival", "classification", and "management" correspond to cluster 2, 3, 4 and 5 in the VOSviewer keyword network map, suggesting that they are the research frontiers in this field.

Discussion

AI has permeated the medical field at an accelerated pace in the past few years, particularly in pancreatic cancer. This study used bibliometrix package of R software and VOSviewer visualization software to perform bibliometric analysis of AI

TABLE 4 Top ten documents with the highest citations on research of AI in pancreatic cancer.

Rank	Papers	Author	Year/Journal	Total Citations
1	Molecular classification of human carcinomas by use of gene expression signatures	Su et al. (16)	2001 CANCER RES	520
2	Genome-wide cell-free DNA fragmentation in patients with cancer	Cristiano et al. (17)	2019 NATURE	293
3	Quantitative Multiplex Immunohistochemistry Reveals Myeloid-Inflamed Tumor-Immune Complexity Associated with Poor Prognosis	Tsujikawa et al. (18)	2017 CELL REP	247
4	Objective quantification of the Ki67 proliferative index in neuroendocrine tumors of the gastroentero pancreatic system: a comparison of digital image analysis with manual methods	Tang et al. (19)	2012 AM J SURG PATHOL	186
5	An Automatic Learning-Based Framework for Robust Nucleus Segmentation	Xing et al. (20)	2016 IEEE T MED IMAGING	173
6	Neural network analysis of dynamic sequences of EUS elastography used for the differential diagnosis of chronic pancreatitis and pancreatic cancer	Săftoiu et al. (21)	2008 GASTROINTEST ENDOSC	154
7	Adjuvant treatments for resected pancreatic adenocarcinoma: a systematic review and network meta-analysis	Liao et al. (22)	2013 LANCET ONCOL	150
8	Fast and robust online adaptive planning in stereotactic MR-guided adaptive radiation therapy (SMART) for pancreatic cancer	Bohoudi et al. (23)	2017 RADIOTHER ONCOL	148
9	Application of Artificial Intelligence to Gastroenterology and Hepatology	Le berre et al. (24)	2020 GASTROENTEROLOGY	137
10	Mirna expression profiles identify drivers in colorectal and pancreatic cancers	Piepoli et al. (25)	2012 PLOS ONE	120

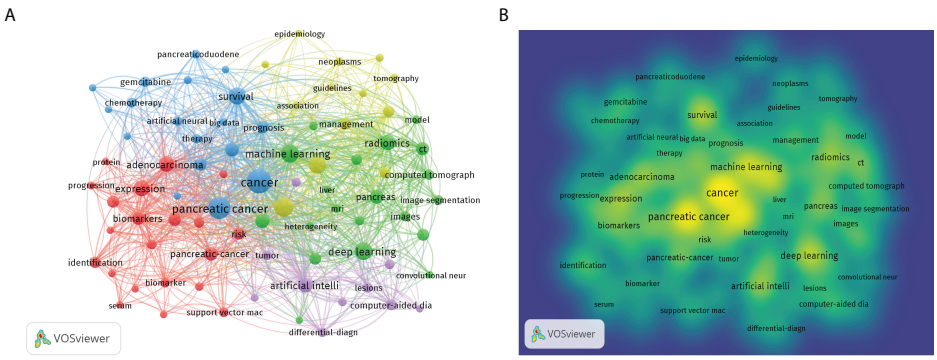

FIGURE 6
Bibliometric analysis of keywords by VOSviewer. **(A)** Map of Clusters based on keywords analysis. The size of the circle indicated occurrences of the keywords, different colors indicated the variety of clusters. **(B)** Keywords density visualization map. Different colors represented the frequency of keyword occurrences, and yellow indicated the highest frequency.

applied to pancreatic cancer research in the past 25 years, providing a comprehensive perspective for the field. We objectively and systematically described the application status, development trend, and future research hotspots of AI in pancreatic cancer, so as to help scholars quickly understand the research status in this field and provide valuable directions for topic selection activities. The first part of this study analyzed publications trends, countries, institutions, authors, and journals. Then, cluster analysis was carried out on the keywords to identify the research hotspots in this field.

According to the results of publication trends, the number of AI in pancreatic cancer publications had increased rapidly over the past four years, accounting for 74.2% of the total number of papers published, but the annual number of AI in pancreatic cancer publications was still lower than in other diseases (30), which indicated that this field was in its infancy and more countries and researchers will be involved in research in the future.

The two nations with the most publications of AI in pancreatic cancer were the United States and China. Citation counts were a common indicator of professional recognition of scientific work so citation analysis was widely used to evaluate the quality of research work. The number of citations and country collaborations in the United States far outnumbers those in other countries, and the university with the most publications and citations was also based in the United States, demonstrating that the United States holds a significant position in this field and leads the world. Despite the fact that China had a large number of publications, the low citations show that China has to increase the quality and influence of its research. This may also be related to the late start of AI in pancreatic cancer research in China, resulting in low international academic influence. Wang L from China was the most published author with ten publications, while the author with the highest H-index was Hruban RH from Johns Hopkins University in the United States, who worked on AI in pathology and radiology of pancreatic cancer. The total number of papers published by each author in this field is not high, which may be related to the initial stage of AI in pancreatic cancer research.

In theme trend and thematic map, we found that the keywords “diagnosis”, “survival”, “classification”, and “management” may be hot research topics for the future. Keyword Co-occurrence Analysis classifies these keywords into five clusters, and we’ll discuss research hotspots and trends for each cluster individually.

Cluster 1: AI in biology of pancreatic cancer

The biomarker CA199 was most widely used in the detection of pancreatic cancer, but its specificity and sensitivity were relatively low (70% and 5%, respectively) (31, 32). In the past 20 years, sequencing technologies had made significant progress, AI massive sequencing data was used to establish statistical model, the genetic and epigenetic patterns associated with gene expression and gene product, calculation was complex and highly specific three-dimensional shape of the protein molecules, had become the realistic choice of biomarkers for early diagnosis of pancreatic cancer (7, 33). Stephen et al. established a machine learning model that integrated the fragmentation patterns of cell-free DNA across the genome with detection sensitivity ranging from 57% to more than 99%, specificity of 98%, and a total area of 0.94 under the curve value in seven cancer types including pancreatic cancer (17). This study ranked second in the top 10 citation publications and offers a proof-of-concept technique for human cancer screening, early diagnosis, and monitoring. In addition, miRNAs were used in a machine learning method to assist early diagnosis of PDAC (34).

Cluster 2: AI in pathology and radiology of pancreatic cancer

In the field of medical image analysis, deep learning has demonstrated a stable and exceptional performance. Artificial intelligence (AI) has been frequently utilized in CT and MRI

TABLE 5 Highly frequent major keywords in each cluster.

Cluster	Main keywords	Total link strength	Occurrences	Theme description
Cluster1 (red)	protein	33	10	AI in biology of pancreatic cancer
	expression	176	51	
	exosomes	37	10	
	biomarkers	116	31	
	validation	64	20	
	discovery	39	11	
	immunohistochemistry	43	12	
cluster2 (green)	computed tomography	103	21	AI in pathology and radiology of pancreatic cancer
	computed-tomography	73	15	
	ct	166	35	
	image segmentation	55	17	
	radiomics	215	47	
	prediction	120	27	
	texture analysis	117	23	
	pathology	41	11	
cluster3 (blue)	cancer	469	132	AI in therapy of pancreatic cancer
	chemotherapy	64	18	
	immunotherapy	41	10	
	prognosis	132	28	
	survival	282	59	
	therapy	74	16	
	resection	59	12	
cluster4 (yellow)	classification	260	65	AI in health management of pancreatic cancer
	diagnosis	309	80	
	epidemiology	40	11	
	management	119	28	
	prognostic-factors	39	11	
	features	133	26	
cluster5 (purple)	chronic pancreatitis	49	12	AI in EUS of pancreatic cancer
	computer-aided diagnosis	103	23	
	differential-diagnosis	87	15	
	endoscopic ultrasonography	40	10	
	endoscopic ultrasound	47	14	
	fine-needle-aspiration	48	17	
	lesions	81	18	
	pancreatic adenocarcinoma	55	15	

imaging to identify pancreatic cancer and had showed notable benefits (35). Compared with radiologists, the convolutional neural network platform for CT-assisted diagnosis PC not only provided excellent diagnostic accuracy but also reduced the diagnosis time, indicating that AI has good clinical feasibility (10). MRI image segmentation by AI has been claimed to be more technically difficult than CT image segmentation (36). A convoluted neural network performed comparable to humans in recognizing the lesion, according to Liang et al (37). In hyperpolarized metabolic (HP)-magnetic resonance (MR) studies, AI was also employed to enhance the early detection of PDAC (38). To eliminate human bias in pathological specimen examination, AI approaches also performed well (39). The capacity of a multilayer perceptron neural network (MNN) to differentiate benign from malignant patients was developed and then assessed. In fact, the model had a 77 percent accuracy in classifying atypical fine-needle aspiration (FNA) biopsies as benign or malignant (40). Okon K et al. used neural network model to analyze the nuclear characteristics of patients undergoing surgery for pancreatic cancer, chronic pancreatitis and other tumors requiring pancreatic resection and the results showed that the correct rate of nuclear

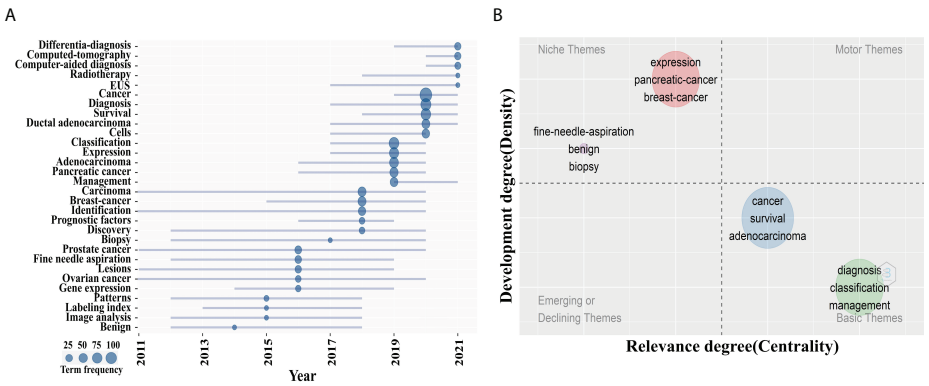

FIGURE 7
Theme analysis. **(A)** Trend topics map. The larger the circle is, the more occurrences keywords. **(B)** Thematic map of keywords plus. The x axis represented the centrality of a topic, which indicated the degree of interaction between network clusters in comparison to other clusters and provided information about its significance. The y axis showed the density that reflected the internal strength of a cluster network and may be considered as a measure of topic development. Keywords " diagnosis ", "survival", "classification", and "management" in quadrant 4 (Basic themes).

classification was 73% (41). Another study proposed a learning-based integrated framework for evaluating cell Ki-67 proliferation index, which had a higher accuracy than manual annotation and can provide indirect help for the diagnosis of pancreatic neuroendocrine tumors (42).

Cluster 3: AI in therapy of pancreatic cancer

The application of AI in the treatment of pancreatic cancer mainly focused on the prediction of pancreatic surgery risk, prognosis and chemotherapy response. AI can predict patient outcomes and postoperative complications by integrating multiple risk factors into the algorithm. Several researches applied an artificial intelligence system to create models and predict the occurrence of postoperative pancreatic fistula (POPF) following pancreaticoduodenectomy (11, 43, 44). The AI models established by Skawran et al. (45) and Kambkamba et al. (43) based on the imaging characteristics of preoperative CT and MRI respectively provided reliable predictability for the assessment of POPF. In assessing the prognosis of pancreatic cancer surgery, a subgroup of patients at low risk of mortality and morbidity in a study, Sahara et al. developed a predictive model based on machine learning to predict 30-day death following hepatopancreas surgery (46). The most important predictors of unexpected fatalities were age, sex, preoperative albumin level, preoperative platelet count, and disseminated malignancy. Palumbo et al. (47) used preoperative clinical and radiological data to build and verify a model for predicting early distant recurrence following upfront pancreaticoduodenectomy. This model proved to be useful in the treatment of pancreatic cancer patients. A study established a ML model to predict the risk of postoperative metastasis based on histological features of surgically removed pancreatic neuroendocrine tumor tissues (48). Zhang et al. developed a risk model using SVM, logistic regression, and lasso regression, which had a strong predictive effect on the likelihood of ICU admission and length of stay following PDAC surgery (49). In addition, one study presented a multiparameter analysis model to assess the predictive value of existing parameters and predicted long-term survival in patients with PDAC (50). AI also showed excellent performance in predicting chemotherapy response. For patients with pancreatic adenocarcinoma, a deep learning model can predict histological tumor response to neoadjuvant treatment, and the model was enhanced by include reductions in serum CA199 (51). Furthermore, the ANN dosage model was equivalent to the dose predicted by experts for pancreatic cancer stereotactic body radiation treatment (SBRT) (52). The use of artificial intelligence in the treatment of pancreatic cancer has shown to be promising. In the near future, Machine learning will play a greater role in pancreatic cancer treatment in the near future, thanks to thorough analyses of clinical factors, less-invasive biological samples, and radiological For patients with pancreatic adenocarcinoma, a deep learning model can predict histological tumor response to neoadjuvant treatment, and the model was enhanced by include reductions in serum CA199. Furthermore, the ANN dosage model was equivalent to the dose predicted by experts for pancreatic cancer stereotactic body radiation treatment (SBRT). The use of artificial intelligence in the treatment of pancreatic cancer has shown to be promising. Machine learning will play a greater role in pancreatic cancer treatment in the near future, thanks to thorough analyses of clinical factors, less-invasive biological samples, and radiological characteristics.

Cluster 4: AI in risk assessment of pancreatic cancer

Only a small percentage of patients (<15%) with pancreatic cancer had surgically resectable state after diagnosis (53), so

identifying individuals at high risk for PDAC or with early stage of resectable pancreatic cancer was critical to prognosis. The use of AI-based risk assessment models to pancreatic cancer is gaining traction. Appelbaum et al. used diagnostic codes collected from electronic health record (EHR) data to design and verify a prediction model that identified persons at high risk for PDAC up to a year before diagnosis (54). They also attempted to improve the performance of the model using independent multicenter datasets and additional laboratory test features. AI-based PC risk prediction models were established by analyzing patients with chronic pancreatitis of focal mass lesions and patients with prediabetes and new-onset diabetes, respectively (55, 56). The specificity of these models in identifying PC was up to 94.0%. PCLs (pancreatic cystic lesions) were well-known pancreatic cancer precancerous symptoms. To find characteristics that can be utilized as imaging biomarkers to detect high-risk PCLs, researchers applied quantitative image analysis mixed with machine learning and artificial intelligence (AI) technologies (57–60). This cost-effective method will aid in the differentiation of benign and malignant PCL, as well as advise therapeutic decisions for better utilization of medical resources.

Cluster 5: AI in EUS of pancreatic cancer

With promising results, AI has been applied to help endoscopists in the EUS assessment of pancreatic lesions (61–63). Zhu et al. collected EUS image characteristics from patients with PC and chronic pancreatitis and chose 16 features for SVM classification, with a sensitivity rate of 94% (8). For neural network analysis, Săftoiu employed dynamic sequences of EUS elastography and contrast-enhanced EUS recordings (21, 64). When CP and PC were differentiated, superior diagnostic results were obtained, according to their findings. AI was also employed to discriminate between benign and malignant cells during EUS-guided pancreatic fine-needle aspiration. Multilayer perceptron neural networks (MNNs) trained on segment pictures of cell clusters collected from FNA were as accurate as the cytologist who first inspected the section, according to one research (40). This model may be widely used as a screening tool for pancreatic FNA specimens. In the future, as clinical decision-making becomes increasingly complex, AI will play an important role in assisting clinicians in handling large amounts of EUS data. For EUS training and quality control, Zhang et al. used AI to construct a station classification model and segmentation model that included a pancreas, abdominal aorta and portal confluence. EUS's learning curve was reduced and quality control was enhanced because to this intelligence system (65).

Conclusion

The research of artificial intelligence in pancreatic cancer is still in its initial stages. AI is now being researched in pancreatic cancer biology, diagnosis, therapy, risk assessment, and EUS. The application of artificial intelligence effectively avoids human error and improves work efficiency. This bibliometrics study provides an insight into AI in PC research, concentrating on the present condition of the discipline. This viewpoint aids researchers in recognizing the field's hotspots and frontiers, as well as new research directions.

Data availability statement

The original contributions presented in the study are included in the article/Supplementary Material. Further inquiries can be directed to the corresponding authors.

Author contributions

The data was gathered by XM and YM. HY, FZ and XY analyzed the data and wrote the manuscript. MNH revised the language of the manuscript. ZL and LY conceived the study and reviewed the manuscript. All authors listed have made a substantial, direct, and intellectual contribution to the work and approved it for publication.

Funding

This research was supported by University-level project grant (Grant Number XM2019094).

Conflict of interest

The authors declare that the research was conducted in the absence of any commercial or financial relationships that could be construed as a potential conflict of interest.

Publisher's note

All claims expressed in this article are solely those of the authors and do not necessarily represent those of their affiliated organizations, or those of the publisher, the editors and the reviewers. Any product that may be evaluated in this article, or claim that may be made by its manufacturer, is not guaranteed or endorsed by the publisher.

Supplementary material

The Supplementary Material for this article can be found online at: https://www.frontiersin.org/articles/10.3389/fonc.2022.973999/full#supplementary-material

References

1. CP Wild, E Weiderpass and BW Stewart eds. *World cancer report: Cancer research for cancer prevention*. Lyon, France: International Agency for Research on Cancer (2020) p. pp 367–370.

2. Kenner B, Chari ST, Kelsen D, Klimstra DS, Pandol SJ, Rosenthal M, et al. Artificial intelligence and early detection of pancreatic cancer: 2020 summative review. *Pancreas* (2021) 50(3):251–79. doi: 10.1097/mpa.0000000000001762

3. Pereira SP, Oldfield L, Ney A, Hart PA, Keane MG, Pandol SJ, et al. Early detection of pancreatic cancer. *Lancet Gastroenterol Hepatol* (2020) 5(7):698–710. doi: 10.1016/s2468-1253(19)30416-9

4. Kenner BJ, Abrams ND, Chari ST, Field BF, Goldberg AE, Hoos WA, et al. Early detection of pancreatic cancer: Applying artificial intelligence to electronic health records. *Pancreas* (2021) 50(7):916–22. doi: 10.1097/mpa.0000000000001882

5. Ramesh AN, Kambhampati C, Monson JR, Drew PJ. Artificial intelligence in medicine. *Ann R Coll Surgeons Engl* (2004) 86(5):334–8. doi: 10.1308/147870804290

6. Hayashi H, Uemura N, Matsumura K, Zhao L, Sato H, Shiraishi Y, et al. Recent advances in artificial intelligence for pancreatic ductal adenocarcinoma. *World J Gastroenterol* (2021) 27(43):7480–96. doi: 10.3748/wjg.v27.i43.7480

7. Zhang ZM, Wang JS, Zulfiqar H, Lv H, Dao FY, Lin H. Early diagnosis of pancreatic ductal adenocarcinoma by combining relative expression orderings with machine-learning method. *Front Cell Dev Biol* (2020) 8:582864. doi: 10.3389/fcell.2020.582864

8. Zhu M, Xu C, Yu J, Wu Y, Li C, Zhang M, et al. Differentiation of pancreatic cancer and chronic pancreatitis using computer-aided diagnosis of endoscopic ultrasound (EUS) images: a diagnostic test. *PloS One* (2013) 8(5):e63820. doi: 10.1371/journal.pone.0063820

9. Tonozuka R, Itoi T, Nagata N, Kojima H, Sofuni A, Tsuchiya T, et al. Deep learning analysis for the detection of pancreatic cancer on endosonographic images: a pilot study. *J Hepato Biliary Pancreatic Sci* (2021) 28(1):95–104. doi: 10.1002/jhbp.825

10. Liu SL, Li S, Guo YT, Zhou YP, Zhang ZD, Li S, et al. Establishment and application of an artificial intelligence diagnosis system for pancreatic cancer with a faster region-based convolutional neural network. *Chin Med J* (2019) 132 (23):2795–803. doi: 10.1097/cm9.0000000000000544

11. Mu W, Liu C, Gao F, Qi Y, Lu H, Liu Z, et al. Prediction of clinically relevant pancreatico-enteric anastomotic fistulas after pancreatoduodenectomy using deep learning of preoperative computed tomography. *Theranostics* (2020) 10(21):9779–88. doi: 10.7150/thno.49671

12. Yu Y, Li Y, Zhang Z, Gu Z, Zhong H, Zha Q, et al. A bibliometric analysis using VOSviewer of publications on COVID-19. *Ann Trans Med* (2020) 8(13):816. doi: 10.21037/atm-20-4235

13. Musbahi A, Rao CB, Immanuel A. A bibliometric analysis of robotic surgery from 2001 to 2021. *World J Surg* (2022) 46(6):1314–24. doi: 10.1007/s00268-022-06492-2

14. Falagas ME, Pitsouni EI, Malietzis GA, Pappas G. Comparison of PubMed, scopus, web of science, and Google scholar: strengths and weaknesses. *FASEB J* (2008) 22(2):338–42. doi: 10.1096/fj.07-9492LSF

15. Hirsch JE. An index to quantify an individual's scientific research output. *Proc Natl Acad Sci United States America* (2005) 102(46):16569–72. doi: 10.1073/pnas.0507655102

16. Su AI, Welsh JB, Sapinoso LM, Kern SG, Dimitrov P, Lapp H, et al. Molecular classification of human carcinomas by use of gene expression signatures. *Cancer Res* (2001) 61(20):7388–93.

17. Cristiano S, Leal A, Phallen J, Fiksel J, Adleff V, Bruhm DC, et al. Genome-wide cell-free DNA fragmentation in patients with cancer. *Nature* (2019) 570 (7761):385–9. doi: 10.1038/s41586-019-1272-6

18. Tsujikawa T, Kumar S, Borkar RN, Azimi V, Thibault G, Chang YH, et al. Quantitative multiplex immunohistochemistry reveals myeloid-inflamed tumor-immune complexity associated with poor prognosis. *Cell Rep* (2017) 19(1):203–17. doi: 10.1016/j.celrep.2017.03.037

19. Tang LH, Gonen M, Hedvat C, Modlin IM, Klimstra DS. Objective quantification of the Ki67 proliferative index in neuroendocrine tumors of the gastroenteropancreatic system: a comparison of digital image analysis with manual methods. *Am J Surg Pathol*. (2012) 36(12):1761–70. doi: 10.1097/PAS.0b013e318263207c

20. Xing F, Xie Y, Yang L. An Automatic Learning-Based Framework for Robust Nucleus Segmentation. *IEEE Trans Med Imaging*. (2016) 35(2):550–66. doi: 10.1109/TMI.2015.2481436

21. Săftoiu A, Vilmann P, Gorunescu F, Gheonea DI, Gorunescu M, Ciurea T, et al. Neural network analysis of dynamic sequences of EUS elastography used for the differential diagnosis of chronic pancreatitis and pancreatic cancer. *Gastrointest Endosc* (2008) 68(6):1086–94. doi: 10.1016/j.gie.2008.04.031

22. Liao WC, Chien KL, Lin YL, Wu MS, Lin JT, Wang HP, et al. Adjuvant treatments for resected pancreatic adenocarcinoma: A systematic review and network meta-analysis. *Lancet Oncol*. (2013) 14(11):1095–103. doi: 10.1016/S1470-2045(13)70388-7

23. Bohoudi O, Bruynzeel AME, Senan S, Cuijpers JP, Slotman BJ, Lagerwaard FJ, et al. Fast and robust online adaptive planning in stereotactic MR-guided adaptive radiation therapy (SMART) for pancreatic cancer. *Radiother Oncol*. (2017) 125(3):439–44. doi: 10.1016/j.radonc.2017.07.028

24. Le Berre C, Sandborn WJ, Aridhi S, Devignes MD, Fournier L, Smaïl-Tabbone M, et al. Application of Artificial Intelligence to Gastroenterology and Hepatology. *Gastroenterology*. (2020) 158(1):76–94.e2. doi: 10.1053/j.gastro.2019.08.058

25. Piepoli A, Tavano F, Copetti M, Mazza T, Palumbo O, Panza A, et al. Mirna expression profiles identify drivers in colorectal and pancreatic cancers. *PLoS One*. (2012) 7(3):e33663. doi: 10.1371/journal.pone.0033663

26. Gillies RJ, Kinahan PE, Hricak H. Radiomics: Images are more than pictures, they are data. *Radiology* (2016) 278(2):563–77. doi: 10.1148/radiol.2015151169

27. Breiman L. Random forests. *Mach Learn* (2001) 45:5–32. doi: 10.1023/a:1010933404324

28. Rahib L, Smith BD, Aizenberg R, Rosenzweig AB, Fleshman JM, Matrisian LM. Projecting cancer incidence and deaths to 2030: the unexpected burden of thyroid, liver, and pancreas cancers in the united states. *Cancer Res* (2014) 74 (11):2913–21. doi: 10.1158/0008-5472.Can-14-0155

29. Zhu X, Hu J, Deng S, Tan Y, Qiu C, Zhang M, et al. Comprehensive bibliometric analysis of the kynurenine pathway in mood disorders: Focus on gut microbiota research. *Front Pharmacol* (2021) 12:687757. doi: 10.3389/fphar.2021.687757

30. Shen Z, Wu H, Chen Z, Hu J, Pan J, Kong J, et al. The global research of artificial intelligence on prostate cancer: A 22-year bibliometric analysis. *Front Oncol* (2022) 12:843735. doi: 10.3389/fonc.2022.843735

31. Datta J, Vollmer CMJr. Investigational biomarkers for pancreatic adenocarcinoma: where do we stand? *South Med J* (2014) 107(4):256–63. doi: 10.1097/smj.0000000000000088

32. Goonetilleke KS, Siriwardena AK. Systematic review of carbohydrate antigen (CA 19-9) as a biochemical marker in the diagnosis of pancreatic cancer. *Eur J Surg Oncol* (2007) 33(3):266–70. doi: 10.1016/j.ejso.2006.10.004

33. Marks DS, Colwell LJ, Sheridan R, Hopf TA, Pagnani A, Zecchina R, et al. Protein 3D structure computed from evolutionary sequence variation. *PloS One* (2011) 6(12):e28766. doi: 10.1371/journal.pone.0028766

34. Alizadeh Savareh B, Asadzadeh Aghdaie H, Behmanesh A, Bashiri A, Sadeghi A, Zali M, et al. A machine learning approach identified a diagnostic model for pancreatic cancer through using circulating microRNA signatures. *Pancreatology* (2020) 20(6):1195–204. doi: 10.1016/j.pan.2020.07.399

35. Barat M, Chassagnon G, Dohan A, Gaujoux S, Coriat R, Hoeffel C, et al. Artificial intelligence: a critical review of current applications in pancreatic imaging. *Japanese J Radiol* (2021) 39(6):514–23. doi: 10.1007/s11604-021-01098-5

36. Bobo MF, Bao S, Huo Y, Yao Y, Virostko J, Plassard AJ, et al. Fully convolutional neural networks improve abdominal organ segmentation. *Proc SPIE–the Int Soc Optical Eng* (2018) 10574:105742V. doi: 10.1117/12.2293751

37. Liang Y, Schott D, Zhang Y, Wang Z, Nasief H, Paulson E, et al. Auto-segmentation of pancreatic tumor in multi-parametric MRI using deep convolutional neural networks. *Radiother Oncol* (2020) 145:193–200. doi: 10.1016/j.radonc.2020.01.021

38. Enriquez JS, Chu Y, Pudakalakatti S, Hsieh KL, Salmon D, Dutta P, et al. Hyperpolarized magnetic resonance and artificial intelligence: Frontiers of imaging in pancreatic cancer. *JMIR Med Inf* (2021) 9(6):e26601. doi: 10.2196/26601

39. Cheng JY, Abel JT, Balis UGJ, McClintock DS, Pantanowitz L. Challenges in the development, deployment, and regulation of artificial intelligence in anatomic pathology. *Am J Pathol* (2021) 191(10):1684–92. doi: 10.1016/j.ajpath.2020.10.018

40. Momeni-Boroujeni A, Yousefi E, Somma J. Computer-assisted cytologic diagnosis in pancreatic FNA: An application of neural networks to image analysis. *Cancer Cytopathol* (2017) 125(12):926–33. doi: 10.1002/cncy.21915

41. Okoń K, Tomaszewska R, Nowak K, Stachura J. Application of neural networks to the classification of pancreatic intraductal proliferative lesions. *Anal Cell Pathol* (2001) 23(3-4):129–36. doi: 10.1155/2001/657268

42. Xing F, Su H, Neltner J, Yang L. Automatic ki-67 counting using robust cell detection and online dictionary learning. *IEEE Trans Bio Medical Eng* (2014) 61 (3):859–70. doi: 10.1109/tbme.2013.2291703

43. Kambakamba P, Mannil M, Herrera PE, Müller PC, Kuemmerli C, Linecker M, et al. The potential of machine learning to predict postoperative pancreatic fistula based on preoperative, non-contrast-enhanced CT: A proof-of-principle study. *Surgery* (2020) 167(2):448–54. doi: 10.1016/j.surg.2019.09.019

44. Han IW, Cho K, Ryu Y, Shin SH, Heo JS, Choi DW, et al. Risk prediction platform for pancreatic fistula after pancreatoduodenectomy using artificial intelligence. *World J Gastroenterol* (2020) 26(30):4453–64. doi: 10.3748/wjg.v26.i30.4453

45. Skawran SM, Kambakamba P, Baessler B, von Spiczak J, Kupka M, Müller PC, et al. Can magnetic resonance imaging radiomics of the pancreas predict postoperative pancreatic fistula? *Eur J Radiol* (2021) 140:109733. doi: 10.1016/j.ejrad.2021.109733

46. Sahara K, Paredes AZ, Tsilimigras DI, Sasaki K, Moro A, Hyer JM, et al. Machine learning predicts unpredicted deaths with high accuracy following hepatopancreatic surgery. *Hepatobil Surg Nutr* (2021) 10(1):20–30. doi: 10.21037/hbsn.2019.11.30

47. Palumbo D, Mori M, Prato F, Crippa S, Belfiori G, Reni M, et al. Prediction of early distant recurrence in upfront resectable pancreatic adenocarcinoma: A multidisciplinary, machine learning-based approach. *Cancers* (2021) 13(19):4938. doi: 10.3390/cancers13194938

48. Klimov S, Xue Y, Gertych A, Graham RP, Jiang Y, Bhattarai S, et al. Predicting metastasis risk in pancreatic neuroendocrine tumors using deep learning image analysis. *Front Oncol* (2020) 10:593211. doi: 10.3389/fonc.2020.593211

49. Zhang Y, Zhu S, Yuan Z, Li Q, Ding R, Bao X, et al. Risk factors and socio-economic burden in pancreatic ductal adenocarcinoma operation: a machine learning based analysis. *BMC Cancer* (2020) 20(1):1161. doi: 10.1186/s12885-020-07626-2

50. Kaissis GA, Jungmann F, Ziegelmayer S, Lohöfer FK, Harder FN, Schlitter AM, et al. Multiparametric modelling of survival in pancreatic ductal adenocarcinoma using clinical, histomorphological, genetic and image-derived parameters. *J Clin Med* (2020) 9(5):1250. doi: 10.3390/jcm9051250

51. Watson MD, Baimas-George MR, Murphy KJ, Pickens RC, Iannitti DA, Martinie JB, et al. Pure and hybrid deep learning models can predict pathologic tumor response to neoadjuvant therapy in pancreatic adenocarcinoma: A pilot study. *Am Surgeon* (2021) 87(12):1901–9. doi: 10.1177/0003134820982557

52. Campbell WG, Miften M, Olsen L, Stumpf P, Schefter T, Goodman KA, et al. Neural network dose models for knowledge-based planning in pancreatic SBRT. *Med Phys* (2017) 44(12):6148–58. doi: 10.1002/mp.12621

53. Pannala R, Basu A, Petersen GM, Chari ST. New-onset diabetes: a potential clue to the early diagnosis of pancreatic cancer. *Lancet Oncol* (2009) 10(1):88–95. doi: 10.1016/s1470-2045(08)70337-1

54. Appelbaum L, Cambronero JP, Stevens JP, Horng S, Pollick K, Silva G, et al. Development and validation of a pancreatic cancer risk model for the general population using electronic health records: An observational study. *Eur J Cancer (Oxford Engl 1990)* (2021) 143:19–30. doi: 10.1016/j.ejca.2020.10.019

55. Boursi B, Finkelman B, Giantonio BJ, Haynes K, Rustgi AK, Rhim AD, et al. A clinical prediction model to assess risk for pancreatic cancer among patients with prediabetes. *Eur J Gastroenterol Hepatol* (2022) 34(1):33–8. doi: 10.1097/meg.0000000000002052

56. Boursi B, Finkelman B, Giantonio BJ, Haynes K, Rustgi AK, Rhim AD, et al. A clinical prediction model to assess risk for pancreatic cancer among patients with new-onset diabetes. *Gastroenterology* (2017) 152(4):840–50.e3. doi: 10.1053/j.gastro.2016.11.046

57. Dmitriev K, Kaufman AE, Javed AA, Hruban RH, Fishman EK, Lennon AM, et al. Classification of pancreatic cysts in computed tomography images using a random forest and convolutional neural network ensemble. *Med Image Computing Computer Assisted Intervention* (2017) 10435:150–8. doi: 10.1007/978-3-319-66179-7_18

58. Wei R, Lin K, Yan W, Guo Y, Wang Y, Li J, et al. Computer-aided diagnosis of pancreas serous cystic neoplasms: A radiomics method on preoperative MDCT images. *Technol Cancer Res Treat* (2019) 18:1533033818824339. doi: 10.1177/1533033818824339

59. Yang J, Guo X, Ou X, Zhang W, Ma X. Discrimination of pancreatic serous cystadenomas from mucinous cystadenomas with CT textural features: Based on machine learning. *Front Oncol* (2019) 9:494. doi: 10.3389/fonc.2019.00494

60. Permuth JB, Choi J, Balarunathan Y, Kim J, Chen DT, Chen L, et al. Combining radiomic features with a miRNA classifier may improve prediction of malignant pathology for pancreatic intraductal papillary mucinous neoplasms. *Oncotarget* (2016) 7(52):85785–97. doi: 10.18632/oncotarget.11768

61. Dumitrescu EA, Ungureanu BS, Cazacu IM, Florescu LM, Streba L, Croitoru VM, et al. Diagnostic value of artificial intelligence-assisted endoscopic ultrasound for pancreatic cancer: A systematic review and meta-analysis. *Diagnost (Basel Switzerland)* (2022) 12(2). doi: 10.3390/diagnostics12020309

62. Das A, Nguyen CC, Li F, Li B. Digital image analysis of EUS images accurately differentiates pancreatic cancer from chronic pancreatitis and normal tissue. *Gastrointest Endosc* (2008) 67(6):861–7. doi: 10.1016/j.gie.2007.08.036

63. Ozkan M, Cakiroglu M, Kocaman O, Kurt M, Yilmaz B, Can G, et al. Age-based computer-aided diagnosis approach for pancreatic cancer on endoscopic ultrasound images. *Endosc Ultrasound* (2016) 5(2):101–7. doi: 10.4103/2303-9027.180473

64. Săftoiu A, Vilmann P, Dietrich CF, Iglesias-Garcia J, Hocke M, Seicean A, et al. Quantitative contrast-enhanced harmonic EUS in differential diagnosis of focal pancreatic masses (with videos). *Gastrointest Endosc* (2015) 82(1):59–69. doi: 10.1016/j.gie.2014.11.040

65. Zhang J, Zhu L, Yao L, Ding X, Chen D, Wu H, et al. Deep learning-based pancreas segmentation and station recognition system in EUS: development and validation of a useful training tool (with video). *Gastrointest Endosc* (2020) 92(4):874–85.e3. doi: 10.1016/j.gie.2020.04.071

frontiers | Frontiers in Oncology

TYPE Perspective
PUBLISHED 05 August 2022
DOI 10.3389/fonc.2022.985257

Check for updates

OPEN ACCESS

EDITED BY
Zhendong Jin,
Second Military Medical University, China

REVIEWED BY
Hafiz Abdul Waqas Ahmed,
Lady Reading Hospital, Pakistan
Ali Rizwan,
Capital Medical University, China

*CORRESPONDENCE
Li-Jun Zhou
529358809@qq.com

SPECIALTY SECTION
This article was submitted to Gastrointestinal Cancers: Gastric & Esophageal Cancers, a section of the journal Frontiers in Oncology

RECEIVED 03 July 2022
ACCEPTED 13 July 2022
PUBLISHED 05 August 2022

CITATION
Zhou L-J, Xing F, Chen D, Li Y-N and Rafiq SM (2022) Role of intraoperative patients positioning in endoscopic full-thickness resection of large gastric tumors under general anesthesia. *Front. Oncol.* 12:985257. doi: 10.3389/fonc.2022.985257

COPYRIGHT
© 2022 Zhou, Xing, Chen, Li and Rafiq. This is an open-access article distributed under the terms of the Creative Commons Attribution License (CC BY). The use, distribution or reproduction in other forums is permitted, provided the original author(s) and the copyright owner(s) are credited and that the original publication in this journal is cited, in accordance with accepted academic practice. No use, distribution or reproduction is permitted which does not comply with these terms.

Role of intraoperative patients positioning in endoscopic full-thickness resection of large gastric tumors under general anesthesia

Li-Jun Zhou*, Fei Xing, Dan Chen, Yan-Na Li and Shoaib Mohammad Rafiq

Department of Anesthesiology, Pain and Perioperative Medicine, the First Affiliated Hospital of Zhengzhou University, Zhengzhou, China

Full thickness endoscopic resection of large submucosal gastric tumors (>3 cm) is a big challenge for endoscopists. Issues include how to efficiently resect the lesion, obtain homeostasis, and suture the defect. There are no guidelines regarding the importance of patient position on the success of endoscopic resections in anesthetized patients. Typically, the patient is placed in left lateral position for the endoscopic therapy and during the procedure patient's position is changed to maintain the tumor above the gastric fluids to prevent gastric juices and tumor or tumor fragments from falling into the peritoneal cavity in the event of perforation. This study emphasized the importance of planning the procedure to ensure that the patient's position and anesthetist's concerns are met and allow optimal access to the lesion for endoscopic resection. Prior to sedation the patient should be positioned so that the tumor is in the up position which also prevents blood obscuring the operative field, helps detect bleeding points for immediately hemostasis. In addition, due to gravitational effect, the resected tumor will fall into the gastric cavity exposing the root of the tumor making resection easier and reduce procedure time. Preplanning avoids unnecessary readjustment of positioning and improves the ease and safety of the procedure.

KEYWORDS

Gastrointestinal Cancer, gastric tumors, submucosal tumors, endoscopic full-thickness resection, patient position, general anesthesia

Introduction

Endoscopic full-thickness resection techniques are now widely applied in the management of large gastric submucosal tumors (>3 cm) (1–3). Although, endoscopic full-thickness resection is considered a safe and minimally invasive method, many challenging factors remain to be solved (4, 5). Endoscopist's main focus is on the technical details of the resection including homeostasis and closure of the resulting defect (6, 7). To date, no study has focused on the critical effects of patient position on successful performance of these procedures and the left lateral positions and supine positions are considered the routine position for endoscopic procedures (8). In clinical practice, the tumor may be located anywhere in the stomach. When located on the dependent side it may be obscured by intragastric fluids which interfere with tumor resection, finding the tumor base, and achieving homeostasis.

Patient positioning for endoscopic procedures has not yet received much attention which contrasts with most other surgical procedures. However, the increasing requirement for general anesthesia for endoscopic resection procedures has led to the recognition of the need for patient positioning guidelines. The goal of optimal positioning is to provide the optimum access to the operative site while minimizing potential risks to the patient. Each position carries some degree of risk which is maximized in the anaesthetized patient who cannot make others aware of compromised conditions. Patients may also be transferred and positioned on operating tables whilst they are unconscious. The maneuvering and the final positioning have an impact on potential injuries sustained under anesthesia as endotracheal tubes, intravascular lines, and urinary catheters should be free to move and adequately secured before any movement. This all adds to challenges encountered by both the endoscopist and anesthetist attempting changing patient position during the procedure.

Because of the importance of keeping the tumor at a high position away from the dependent portion of the operative field, it is clear that the patient's position should vary according to the location of tumor. The optimal patient position can be left lateral, right lateral, prone, or even supine depending on the location of tumor. If unclear, the location of the tumor can be confirmed by CT before the procedure. This study discusses the influence of patient position on the success of large submucosal gastric tumor resections.

Importance of patient positioning for endoscopic resection

The left lateral position remains the standard (traditional) position for endoscopic therapy. In our early practice, we used the left lateral position as the routine position. However, in some cases, we noted that homeostasis was difficult because blood immediately covered the operating field obscuring the bleeding point resulting in a delay in achieving hemostasis. We also found that it was sometimes difficult to find the base of tumor when fluid covered the operating field.

After group discussion, it was recognized that it was possible to use the effects of gravity to overcome these difficulties. Ensuring that the tumor was located above the dependent part of the gastric cavity resulted in fluids and the tumor tending to move to the dependent portion away from the operative field. In addition, as resection proceeded the tumor fell into the gastric lumen allowing the base to be easily seen and bleeding points addressed. The solution was to initially position of the patient depending on the location of the tumor.

Liu et al. described a typical case of a 56-year-old women whose CT scan suggested a tumor on the posterior wall of greater curvature of the stomach (9). The endoscope was inserted into the stomach with the patient in the left lateral position. After washing the stomach, it was noted that watery fluids covered the tumor. The patient's position was changed to the prone position which produced an unobscured endoscopic field. The tumor was resected and the resected tumor fell into the gastric cavity away from the operative field allowing the defect to be closed using endoloops and endoclips without leakage of fluids into the peritoneal cavity (Figure 1).

According to our experience the combination of endoscopy and CT scan can usually provide the required information about the location of the tumor and the effects of patient position (10–12) allowing the patient position to be pre-planned. The supine position (include anterior lateral) and left lateral position is convenient for most patients requiring endoscopic full-thickness resections. For patients where the tumor is located on the posterior wall and greater curvature of gastric body and fundus, the prone position or right lateral is best. When in doubt and before the endoscopic resection is begun, water can be injected into the gastric cavity to confirm that the position chosen is ideal. If not the position can be changed allowing safe endoscopic full-thickness resection.

Importance of patient positioning from anesthetist's perspective

For surgical procedures, patients are placed on an operating table, and for the endoscopic treatment, on a trolley. There are well-established guidelines for patient positioning during surgical procedures, but no such guidelines are available for endoscopic therapies, especially when resecting large gastric tumors (13, 14). Advanced endoscopic techniques (eg, endoscopic submucosal dissection, endoscopic full-thickness resections, and peroral endoscopic myotomy) may have procedure times exceeding 60 minutes and in some cases

10.3389/fonc.2022.985257

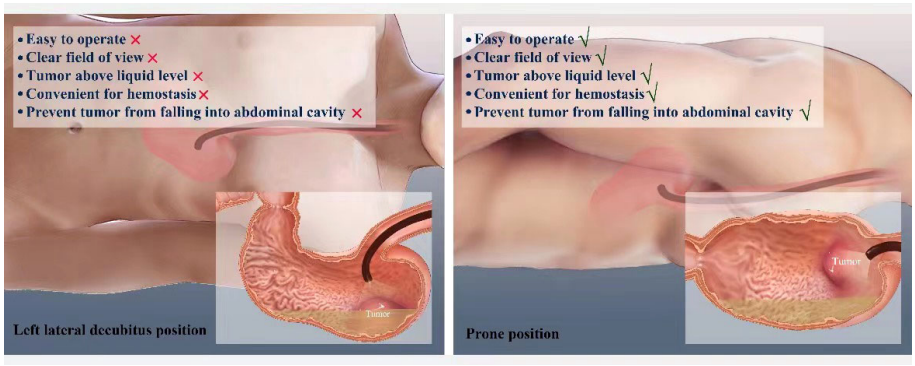

FIGURE 1
Graphical presentation of patient position variation during the Endoscopic full-thickness resection.

lasting several hours, and thus frequently require general anesthesia (15–17). When general anesthesia is intended, the airway is typically secured while the patient is still supine *via* an endotracheal tube. If the patient position needs to be adjusted during endoscopy therapy, extra care must be taken to secure and tape the endotracheal tube to prevent dislodgement while the patient is left lateral or prone or during position changes. Placing an anesthetized patient in the prone position requires the coordination of the entire staff (endoscopist, anesthetist, nurses). The primary duty of anesthesiologist is to coordinate the maneuver while maintaining inline stabilization of the cervical spine and monitoring the endotracheal tube. In order to prevent dislodging, the endotracheal tube should be disconnected from the circuit before shifting from supine to prone. Which, and how many, lines and monitors are disconnected during the shifting is up to the clinical judgment of the anesthesiologist. Ventilation and monitoring should be resumed as rapidly as possible. Patient positioning is critically important and should be preplanned by the endoscopist to avoid during the procedure changes in position and possible complication associated with it.

Frequently, the patient can assist in positioning prior to induction of anesthesia. However, the operating room team must move the patient while the patient is under general anesthesia. Additional staff will be needed for the transfer and positioning of patients with morbid obesity or unstable spine fractures. The anesthesiologist must be aware of any blood pressure alterations when the patient is moved following the induction of general anesthesia and must ensure a safe systemic blood pressure prior to any patient movement.

Future perspective and conclusion

Endoscopic full-thickness resection of large submucosal tumors is a recent development (18, 19). Most studies have focused on technical aspects such as how to resect the lesions, deal with homeostasis, and suturing of the defect (20–24). To our knowledge, no study has been primarily concerned with patient positioning for endoscopic full-thickness resections.

Patient position is a critical element for the successful endoscopic resection therapy of large submucosal gastric tumors. Prior to achieving any position, the patient must be transferred onto the endoscopy room trolley. The final position of the patient is of the utmost importance, but achieving these positions requires careful planning and collaboration. The overall plan for each patient position should be discussed prior to any procedure.

The ideal position depends on the location of the tumor and should be one in which the tumor is not covered by fluid and can fall into the gastric lumen away from the operative field. The combination of CT and endoscopic examination can help to make a primary plan for the patient's position. Even during procedure, one can inject water and observe the operative field and make sure that tumor is at higher level position.

Patient positioning should be individualized according the location of the tumor. Traditionally, the left lateral position and supine position are used for the tumor resections. After the stomach cleansing, the potential operative field (tumor) area to ascertain whether it is partially or fully covered with gastric fluids. If so, the patient's position is changed from left lateral to right lateral, supine or prone position depending on the location of the tumor so as to keep the tumor away from the dependent portion of the stomach. Typically, if the tumor is located in the lesser curvature of stomach, the left lateral position is used. For tumors located along the greater curvature. The right lateral position can be used with the supine position being used for tumors located in the anterior gastric wall and the prone position for tumors located in the posterior gastric wall.

Data availability statement

Publicly available datasets were analyzed in this study. This data can be found here: This is a perspective article. No original data was produced for this article. However, current data collected for writing this article is available with the corresponding author. It can be provided on request. (E-mail: 529358809@qq.com).

Ethics statement

This study was reviewed and approved by the independent ethics committee of the First Affiliated Hospital of Zhengzhou University. Written informed consent was obtained from all participants for their participation in this study.

Author contributions

Study concept and design: L-JZ, FX. Manuscript writing: L-JZ, FX. Analysis and interpretation of data: DC, Y-NL, SR. Administrative, technical or material support: DC, Y-NL, SR. Critical revision of manuscript: L-JZ, SR. All authors contributed to the article and approved the submitted version.

Conflict of interest

The authors declare that the research was conducted in the absence of any commercial or financial relationships that could be construed as a potential conflict of interest.

Publisher's note

All claims expressed in this article are solely those of the authors and do not necessarily represent those of their affiliated organizations, or those of the publisher, the editors and the reviewers. Any product that may be evaluated in this article, or claim that may be made by its manufacturer, is not guaranteed or endorsed by the publisher.

References

1. Jain D, Mahmood E, Desai A, Singhal S. Endoscopic full thickness resection for gastric tumors originating from muscularis propria. *World J Gastrointest Endosc* (2016) 8(14):489–95. doi: 10.4253/wjge.v8.i14.489

2. Antonino G, Alberto M, Michele A, Dario L, Fabio T, Mario T, et al. Efficacy and safety of gastric exposed endoscopic full-thickness resection without laparoscopic assistance: a systematic review. *Endosc Int Open* (2020) 8(9):E1173–82. doi: 10.1055/a-1198-4357

3. Zhang Y, Peng JB, Mao XL, Zheng HH, Zhou SK, Zhu LH, et al. Endoscopic resection of large (≥ 4 cm) upper gastrointestinal subepithelial tumors originating from the muscularis propria layer: a single-center study of 101 cases (with video). *Surg Endosc* (2021) 35(3):1442–52. doi: 10.1007/s00464-020-08033-1

4. Kaan HL, Ho KY. Endoscopic full thickness resection for gastrointestinal tumors - challenges and solutions. *Clin Endosc* (2020) 53(5):541–9. doi: 10.5946/ce.2019.161

5. Granata A, Martino A, Amata M, Ligresti D, Traina M. Gastrointestinal exposed endoscopic full-thickness resection in the era of endoscopic suturing: a retrospective single-center case series. *Wideochir Inne Tech Maloinwazyjne* (2021) 16(2):321–8. doi: 10.5114/wiitm.2021.104496

6. Sumiyama K, Gostout CJ. Novel techniques and instrumentation for EMR, ESD, and full-thickness endoscopic luminal resection. *Gastrointest Endosc Clin N Am* (2007) 17(3):471–85, v-vi. doi: 10.1016/j.giec.2007.05.009

7. Ge PS, Aihara H. Advanced endoscopic resection techniques: Endoscopic submucosal dissection and endoscopic full-thickness resection. *Dig Dis Sci* (2022) 67(5):1521–38. doi: 10.1007/s10620-022-07392-0

8. Meeusen V, Kim N, Elson J, Ma R, Newman F, Bendeich J, et al. Patient positioning guidelines for gastrointestinal endoscopic procedures. *Gastroenterol Nurs* (2021) 44(3):185–91. doi: 10.1097/SGA.0000000000000534

9. Zhao LX, Zheng QF, Wang K, Zhang JY, Song MY. Patient position: a critical variable for planning endoscopic full-thickness resection of gastric tumors. *China J Endosc* (2022) 28(1):72–6. doi: 10.12235/E20210114

10. Chen AH, Chan WH, Lee YH, Tseng JH, Yeh TS, Chiu CT, et al. Routine chest CT for staging of gastric cancer. *Br J Surg* (2019) 106(9):1197–203. doi: 10.1002/bjs.11186

11. Nostedt J, Gibson-Brokop L, Ghosh S, Seidler M, McCall M, Schiller D, et al. Evaluating the utility of computed tomography of the chest for gastric cancer staging. *Can J Surg* (2020) 63(1):E57–61. doi: 10.1503/cjs.000319

12. Wang J, Ao W, Mao G, Jia Y, Xie Z, Gu C, et al. Gastric calcifying fibrous tumors: Computed tomography findings and clinical manifestations. *Med (Baltimore)* (2021) 100(5):e23334. doi: 10.1097/MD.0000000000023334

13. Burlingame BL. Guideline implementation: Positioning the patient. *AORN J* (2017) 106(3):227–37. doi: 10.1016/j.aorn.2017.07.010

14. Powell E, Guidry J, Orengo I. Optimizing patient positioning during dermatologic surgery. *Cutis* (2021) 107(1):43–4. doi: 10.12788/cutis.0147

15. Meining A. Endoscopic full-thickness resection: the logical step toward more extended endoscopic oncologic resections? *Endoscopy* (2015) 47(2):101–2. doi: 10.1055/s-0034-1391372

16. Landin MD, Guerrón AD. Endoscopic mucosal resection and endoscopic submucosal dissection. *Surg Clin North Am* (2020) 100(6):1069–78. doi: 10.1016/j.suc.2020.07.004

17. Schaheen LW, Sanchez MV, Luketich JD. Peroral endoscopic myotomy for achalasia. *Thorac Surg Clin* (2018) 28(4):499–506. doi: 10.1016/j.thorsurg.2018.07.005

18. Liu BR, Liu D, Ullah S, Zhao L, Zheng Q, Ullah R, et al. Endoscopic full-thickness resection and endoscopic lymphadenectomy for advanced colonic cancer in an inoperable patient: first human clinical experience. *Gastrointest Endosc* (2020) 91(2):451–2. doi: 10.1016/j.gie.2019.09.005

19. Cai MY, Martin Carreras-Presas F, Zhou PH. Endoscopic full-thickness resection for gastrointestinal submucosal tumors. *Dig Endosc* (2018) 30 Suppl 1:17–24. doi: 10.1111/den.13003

20. de Moura DTH, Sachdev AH, Thompson CC. Endoscopic full-thickness defects and closure techniques. *Curr Treat Options Gastroenterol* (2018) 16(4):386–405. doi: 10.1007/s11938-018-0199-6

21. Granata A, Martino A, Ligresti D, Zito FP, Amata M, Lombardi G, et al. Closure techniques in exposed endoscopic full-thickness resection: Overview and future perspectives in the endoscopic suturing era. *World J Gastrointest Surg* (2021) 13(7):645–54. doi: 10.4240/wjgs.v13.i7.645

22. Modayil RJ, Zhang X, Khodorskiy D, Stavropoulos SN. Advanced resection and closure techniques for endoscopic full-thickness resection in the gastric fundus. *VideoGIE* (2020) 5(2):61–3. doi: 10.1016/j.vgie.2019.11.001

23. Lee JH, Kedia P, Stavropoulos SN, Carr-Locke D. AGA clinical practice update on endoscopic management of perforations in gastrointestinal tract: Expert review. *Clin Gastroenterol Hepatol* (2021) 19(11):2252–61.e2. doi: 10.1016/j.cgh.2021.06.045

24. Goto O, Koizumi E, Higuchi K, Noda H, Onda T, Omori J, et al. Cutting-edge technologies for gastrointestinal therapeutic endoscopy. *J Nippon Med Sch* (2021) 88(1):17–24. doi: 10.1272/jnms.JNMS.2021_88-109

frontiers | Frontiers in Oncology

TYPE Original Research
PUBLISHED 05 August 2022
DOI 10.3389/fonc.2022.961293

Check for updates

OPEN ACCESS

EDITED BY
Zhendong Jin,
Second Military Medical University, China

REVIEWED BY
Hua Yin,
Ningxia Medical University, China
Ying Xing,
72nd Group Army Hospital of the Chinese PLA, China
Qiong Luo,
Mengchao Hepatobiliary Hospital, China

*CORRESPONDENCE
Xiaohua Shi
sxhsz@sina.com

†These authors share first authorship

SPECIALTY SECTION
This article was submitted to Gastrointestinal Cancers: Hepato Pancreatic Biliary Cancers, a section of the journal Frontiers in Oncology

RECEIVED 04 June 2022
ACCEPTED 11 July 2022
PUBLISHED 05 August 2022

CITATION
Pan S, Liu J, Guo J, Zhu Q, Wang L and Shi X (2022) The clinical impact of endoscopic ultrasound-guided fine-needle aspiration on the patients with low-risk pancreatic cystic lesions. *Front. Oncol.* 12:961293. doi: 10.3389/fonc.2022.961293

COPYRIGHT
© 2022 Pan, Liu, Guo, Zhu, Wang and Shi. This is an open-access article distributed under the terms of the Creative Commons Attribution License (CC BY). The use, distribution or reproduction in other forums is permitted, provided the original author (s) and the copyright owner(s) are credited and that the original publication in this journal is cited, in accordance with accepted academic practice. No use, distribution or reproduction is permitted which does not comply with these terms.

The clinical impact of endoscopic ultrasound-guided fine-needle aspiration on the patients with low-risk pancreatic cystic lesions

Shubo Pan[1†], Jie Liu[1†], Jiefang Guo[2†], Qilin Zhu[1], Liangjing Wang[1] and Xiaohua Shi[1*]

[1]Department of Gastroenterology, Suzhou Science and Technology Town Hospital, Jiangsu, China, [2]Department of Endoscopy, Eastern Hepatobiliary Hospital, Second Military Medical University, Shanghai, China

Background and aims: Endoscopic ultrasound (EUS) is playing a more and more important role in the management of pancreatic cystic lesion (PCLs). The aim of our study was to evaluate the clinical impact of EUS and EUS guided fine needle aspiration (FNA) on patients with low-risk PCLs.

Materials and methods: Low-risk PCL patients who underwent EUS-FNA in 2 edoscopic centers were retrospectively collected and analyzed. The clinical impact of EUS-FNA on these patients was analyzed and the predictors for significance EUS-FNA (defined by diagnosis and treatment method change, new high-risk feature identified after imaging scans) were analyzed by logistic regression analyses.

Results: From July 2004 to February 2017, 186 patients with low-risk PCLs were included. The study cohort had a mean age of 52.4 ± 15.9 years (range: 19-86 years) with 89 (47.8%) male patients included. The clinical significance of EUS-FNAs was observed in 74 patients (39.8%). The presumed diagnoses of PCLs by imaging were changed in 51 (51/74, 68.9%) patients. Nineteen (19/74, 25.7%) new high-risk features were identified by EUS-FNA, and four patients (4/74, 5.4%) underwent surgery due to suspicious or malignant cytology. Based on multivariate analysis, large cyst size [odds ratio (OR): 1.12, 95% confidence interval (CI): 1.02–1.19, P = 0.033], young age (OR: 0.94, 95% CI: 0.91–0.99, P = 0.041) and BMI over 25 (OR: 3.15, 95% CI: 1.29–7.86, P = 0.013) were independent predictors of clinical significance for EUS-FNA. The optimal age and cyst size to predict significance EUS-FNA was 46.0 years and 2.3cm.

Conclusions: On the basis of a 2-center retrospective study, EUS-FNA was clinically significant in about 40% of low-risk PCLs, especially in young, large cyst size, and overweight patients.

KEYWORDS

endoscopic ultrasound, fine needle aspiration (FNA), pancreatic cystic lesion, cross sectional imaging, clinical significance, cytology, cyst fluid analysis

Introduction

Pancreatic cystic lesions (PCLs) are being incidentally detected at an increased rate due to the widespread use of cross-section imaging technologies (1). The incidence of PCLs ranged from 1.9% to 13.5% in different races, and there was a strong correlation between increasing age and the prevalence of PCLs (2).

PCLs represent a wide clinicopathologic spectrum. Most PCLs are benign, but mucinous neoplasm, including mucinous cystic neoplasm(MCNs) and intraductal papillary mucinous neoplasm (IPMNs) represent precursor lesions to invasive adenocarcinoma (3). Surgical resection plays a core role in the management of PCL. However, the surgical indications are varied between different guidelines (4–6). Furthermore, following these guidelines resulted in an inaccuracy in determining the true surgery candidates (7, 8). Therefore, objective indications obtained by advanced modality is needed to better manage PCLs.

Endoscopic ultrasound (EUS) and EUS-guided fine needle aspiration (FNA) play more and more important roles in the management of PCLs. EUS enables us to show more detailed cyst features, and the objects indicators in cyst fluid such as cytology, biochemical markers, and molecular bio-makers obtained by EUS-FNA can further help us identify the nature of PCLs (9). Similar with the recommendations for surgical indications, the indications for EUS and EUS-FNA also vary between different guidelines (4–6). In general, EUS is recommended only when a PCL has high risk factors. However, only 6% of PCLs had high risk features when identified (10). Although most PCL related pancreatic cancers occur in cysts with high risk features, the pancreatic cancer related mortality in low-risk cysts should not be ignored (11, 12).

Although EUS-FNA is an invasive procedure, it has been identified to be safe (13). The value of EUS in the vast majority of low risk PCLs is rare studied. Whether the EUS-FNA has clinical impact on low-risk PCLs is not determined yet.

To address the aforementioned issues, we conducted this 2-center retrospective study to explore the value of EUS and EUS-FNA in PCL patients who had no imaging high-risk features. The more precise indications to perform EUS-FNA in low-risk PCL patients are also explored in this study.

Materials and methods

Patients selection

From July 2004 to February 2017, the PCL patients who performed EUS-FNA in Eastern Hepatobiliary Hospital, Shanghai, China and Suzhou Science and Technology Town Hospital, Jiangsu province, China, were retrospectively analyzed. The indications for EUS-FNA in our study were as follow: (1) EUS performed before the indications were clarified in guidelines; (2) The cross-sectional imaging diagnoses were not determined; (3) We intended to perform EUS guided ethanol ablation after malignancy was excluded by EUS-FNA; (4) The patient himself requested further scans to alleviate anxiety. All patients had EUS under the supervision of an anesthesiologist, and prophylactic antibiotics were given to all patients prior to EUS-FNA. All of the procedures were carried out by experienced therapeutic endoscopists who completed more than 100 EUS scanning cases each year. EUS was performed using linear echoendoscopes (GIF-UCT260; Olympus Corporation, Japan or SP-900,Fuji Corporation, Japan). Cyst fluid were aspirated under EUS guidance using a 19-gauge or 22-gauge needle (NA-200H-8022; Olympus Corporation or Expect; Boston Scientific, Massachusetts, MA or Echo Tip Ultra; Cook Medical, IN). The morphology of the cyst was evaluated and recorded by endoscopists. The cystic fluid was evaluated by the "string sign" initially and then sent for cytology evaluation and assessment of the carcino-embryonic antigen (CEA), glucose (year after 2016), and amylase levels. We used elevated cyst fluid CEA levels >192ng/mL, a positive string sign or a cyst fluid glucose < 25 mg/dl to define mucinous cysts. The serous cyst was diagnosed by clear non-viscous cystic fluid with negative string sign and cystic fluid CEA levels <192ng/mL in multilobulated cyst. The pseudocyst was diagnosed by elevated amylase and lipase in cyst fluid with negative string sign and cystic fluid CEA

levels <5ng/mL. Cytology was considered as the golden standard for malignancy. All EUS-FNA were performed within 3 months after the cysts were identified.

The patient inclusion criterion were as follow: (1) Patients who underwent EUS-FNA and cyst fluid analyses in these 2 centers. (2) Before EUS-FNA, the cross-sectional imaging examinations were performed. (3) The detailed medical record and follow up data can be obtained. (4) Patients without high risk features recommended by Fukuoka guidelines (low-risk PCLs) (5). The exclusion criterion were as follow: (1) Patients who had one of the following clinical or radiologic high risk features (pancreatitis, size≥3 cm, enhancing nodule, main pancreatic duct dilatation, thick cyst wall, abrupt change in main pancreatic duct diameter with upstream parenchymal atrophy, lymphadenopathy, elevated serum CA 19-9, cyst growth ≥ 5 mm/2 years) (5). (2) The cyst fluid analyses were incomplete due to insufficient cyst fluid. (3) EUS performed by trainees. (4) The aforementioned PCL high risk features in EUS reports were incomplete. (5) The medical record or follow up data can not be obtained. The study was approved by the Institutional Review Board of both hospital.

Definition of clinical significance EUS

The primary aim of our study is to explore whether EUS or EUS-FNA has clinical significance in low-risk PCLs. All the low-risk PCLs included in our study will undergo surveillance according to the current guidelines.Therefore, we defined EUS as having clinical significance according to the following criterion: (1) The imaging diagnoses were inconsistent with the diagnoses after EUS-FNA; (2) EUS-FNA identified new high-risk features in accordance with the 2017 Fukuoka guidelines (5); and (3) The management approach was changed after EUS-FNA. That means the endoscopic or surgical treatment would be adopted after EUS-FNA.

The second aim of our study was to identify the more precise indications to perform EUS-FNA. Subjects were divided into 2 groups: the clinical significance group and clinical insignificance group.The demographic information, smoking and drinking status, body mass index (BMI), pancreatic cancer family history, presence of non-specific abdominal symptoms (abdominal pain, abdominal discomfort, weight loss), presence of diabetes mellitus, cross-sectional imaging findings (including size, location, single or multiple cyst morphology) were reviewed and analyzed.

Statistics analysis

Continuous variables with a normal distribution are represented by means and standard deviation (SD), while categorical variables are represented by numbers (%). The Student's unpaired t-test for normal distributed continuous variables and the Mann–Whitney U test for non-normally distributed variables were used to compare demographic data and imaging findings between the clinical significance and insignificance groups. For categorical data, we utilized the χ^2 test, and for cell counts less than 5, we used Fisher's exact test. The independent high risk factors related with clinical significance EUS were calculated using univariate analysis and logistic regression analysis. The optimal cutoff level of parameters were assessed by receiver operator characteristic (ROC) curve. A statistically significant P-value of less than 0.05 was used. Using the SPSS 22.0 software, the data was examined (SPSS, Chicago, Illinois, USA).

Results

Patients and cyst imaging characteristics

From July 2004 to February 2017, a total of 392 PCL patients performed EUS-FNA in the 2 centers. After the inclusion and exclusion criterion were applied to the study cohort, a total of 186 patients with low risk cysts were included in our study (Figure 1). The demographic data and cyst imaging characteristics were summarized in Table 1. The study cohort had a mean age of 52.4 ± 15.9 years (range: 19-86 years) with 89 (47.8%) male patients included. According to the cross-sectional imaging results, the mean cyst size was 2.15 ± 1.80 cm. Most cysts had size larger than 2cm (124/186, 66.7%). Sixty-one (32.8%) cysts located in the head of pancreas, 70 cysts (37.6%) located in the body of pancreas and 55 (29.6%) cysts located in the tail of pancreas. Most of the cysts (156/186, 83.9%) were presented with single cyst morphology on cross-sectional imaging. Analyzing their personal life history, 52 (28.0%) patients had smoking history, 25 (13.4%) patients had alcohol abuse history and 16 (8.6%) patients had pancreatic cancer family history. The mean BMI for the study cohort was 23.47 ± 3.22 with 60 patients (32.3%) had BMI over 25. Forty-five (24.2%) had DM and 76 (40.9%) had non-specific abdominal symptoms at the time of diagnosis.

The clinical significance of EUS-FNA on patients with low risk PCLs

The clinical significance EUS-FNAs were observed in 74 patients (39.8%). After EUS-FNA, the presumed diagnoses of PCLs by cross-sectional imaging were changed in 51(51/74, 68.9%) patients among the 74 patients. The most common diagnosis change was mucinous cysts (MCN and IPMN) turned out to be SCNs (36/51, 70.6%). Twelve SCNs(12/51, 23.5%) turned out to be mucinous cysts after EUS-FNA. Two SCNs (3.9%) and one MCN (2.0%) turned out to be pancreatic

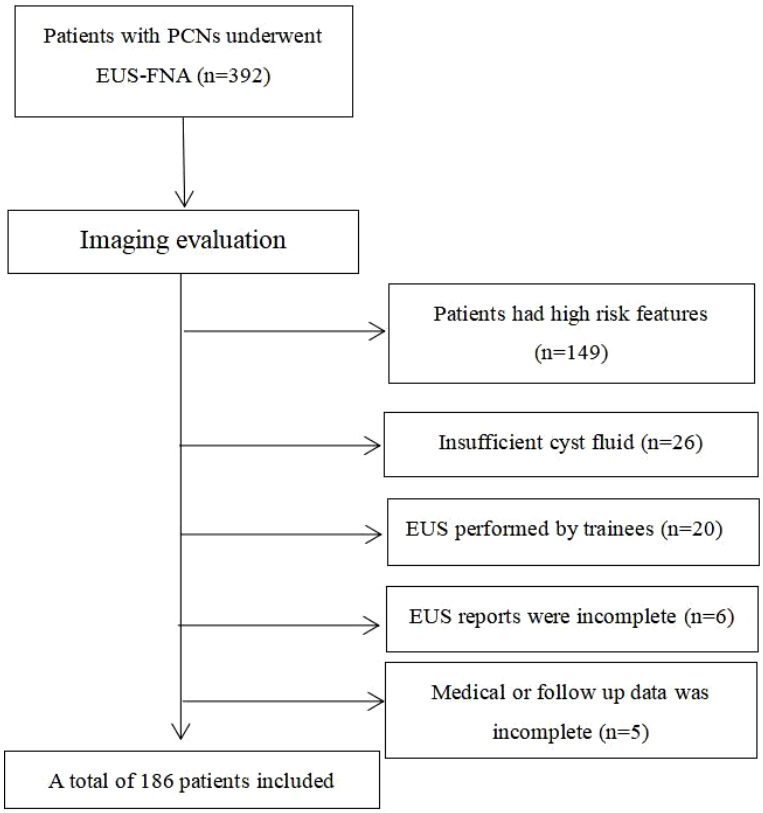

FIGURE 1
Patient selection flowchart (PCN, pancreatic cystic neoplasm; EUS-FNA, Endoscopic ultrasound guided fine needle aspiration).

TABLE 1 Clinical and imaging characteristics of 186 pancreatic cystic neoplasm patients.

Total case number	N=186
Age(yr)± SD	52.4 ± 15.9
Sex(M:F)	89:97
Diameter, mean ± SD(cm)	2.15 ± 1.80
Diameter ≤1.0cm, n%	7 (3.8)
1.0<Diameter ≤1.5cm, n%	29 (15.6)
1.5<Diameter ≤2.0cm, n%	36 (19.4)
2.0<Diameter ≤2.5cm, n%	48 (25.8)
2.5<Diameter ≤3.0cm, n%	76 (40.9)
Location of cysts: head/body/tail, n(%)	61/70/55
Single/multiple cyst morphology	156/30
Smoking history, n(%)	52 (28.0)
Alcohol abuse history, n(%)	25 (13.4)
BMI ± SD	23.47 ± 3.22
BMI over 25, n(%)	60 (32.3)
Pancreatic cancer family history, n(%)	16 (8.6)
Presence of DM, n(%)	45 (24.2)
Presence of non-specific abdominal symptoms, n(%)	76 (40.9)

SD, standard deviation; DM, diabetes mellitus; BMI, Body Mass Index.

neuroendocrine tumor (pNET). Besides, 19 (19/74, 25.7%) new high risk features were identified by EUS-FNA, including 10 mural nodules (10/19, 52.6%), 5 (5/19, 26.3%) main pancreatic duct dilation and 4 (4/19, 21.1%) cyst size >3cm. Among the 19 patients, 8 patients underwent endoscopic ethanol ablation due to new high risk features were identified. Moreover, 4 patients (4/74, 5.4%) underwent surgery due to suspicious or malignant cytology. Finally, 2 IPMN with malignant, 1 IPMN with high-grade intraepithelial neoplasia and 1 pNET were identified by pathological examinations.

Predictors of clinical significance EUS-FNA in patients with low-risk PCLs

The patients were divided into 2 groups, the clinical significance EUS-FNA group and clinical insignificance EUS-FNA group. Table 2 compares the clinical, demographic, and cystic characteristics of these two groups. Patients with a clinical significance EUS-FNA were younger (48.5 ± 12.7 vs 56.0 ± 13.6, P=0.034). The cyst size was larger in clinical significance EUS-FNA group than in clinical insignificance EUS-FNA group (2.36 ± 1.54cm vs 1.93 ± 1.36cm, P=0.043). The patients who had BMI over 25 is much more in clinical significance EUS-FNA group (32/74, 43.2% vs 28/112, 25.0%, P=0.029). Moreover, patients with pancreatic cancer family history was not fully significance common in clinical significance EUS-FNA group (10/74, 13.5% vs 6/106, 5.7%, P=0.052). The gender, tumor location, cyst morphology, smoking history, alcohol abuse history and presence of DM and presence of non-specific abdominal symptoms did not differ significantly between these two groups.

The age, cyst size, BMI over 25 and pancreatic cancer family history were included in multivariate analysis, the gender was adjusted. Large cyst size [odds ratio (OR): 1.12, 95% confident interval (CI): 1.02–1.19, P=0.033], young age (OR: 0.94, 95% CI: 0.91–0.99, P=0.041) and BMI over 25 (OR:3.15, 95% CI: 1.29-7.86, P=0.013) were independent predictors of clinical significance EUS-FNA (Table 3).

Moreover, according to ROC curve analyses, the optimal age to predict significance EUS-FNA was 46.0 years (Figure 2) and the optimal cyst size to predict significance EUS-FNA was 2.3cm (Figure 3).

Discussion

PCLs are rather prevalent. However, there is still a debate about how PCLs should be managed. The risk of malignancy should be carefully assessed. However, due to morphological overlap and the lack of unique imaging characteristics, a precise diagnosis of PCNs might be challenging (14, 15).

EUS and EUS based techniques are more and more common used in the management of PCLs (9). EUS is particularly useful for assessing diagnostic features and potential predictors of malignancy in PCLs. The performance of cytology in differentiating malignant and benign PCLs and the cystic fluid CEA level in differentiating mucinous and non-mucinous PCLs are sub-optimal (16). However, due to the low prevalence of malignancy in incidental PCLs and the invasive nature of the procedure, the indications to perform EUS-FNA tend to be conserved in current guidelines. Only a small percentage of patients will be recommended to perform EUS-FNA according to the recommendations. The vast majority of PCLs without high-risk features still harbor malignant PCLs. How to find these malignant patients is a clinical challenge with little focus on it. In this study, we identified EUS-FNA maybe useful in 39.8% low risk PCL patients. Additionally, we found that a cyst size larger than 2.3 cm, age<46 at the diagnosis, and BMI over 25 at the diagnosis are predictors of clinical significance EUS-FNA. Our study provides further

TABLE 2 Comparisons of the clinical and imaging feature between significance and insignificance EUS-FNA.

	Significance (n = 74)	Insignificance (n = 112)	P value
Age (yr)± SD	48.5 ± 12.7	56.0 ± 13.6	0.034
Sex (M:F)	36:38	53:59	0.860
Diameter, mean ± SD (cm)	2.36 ± 1.54	1.93 ± 1.36	0.043
Location of cysts: head/body/tail,n (%)	25/28/21	36/42/34	0.953
Single/multiple cyst morphology	59/15	97/15	0.212
Smoking history,n (%)	20 (27.0)	32 (28.6)	0.818
Alcohol abuse history,n (%)	9 (12.2)	16 (14.3)	0.678
BMI ± SD	24.06 ± 3.42	22.65 ± 3.01	0.108
BMI over 25, n (%)	32 (43.2)	28 (25)	0.029
Pancreatic cancer family history,n (%)	10 (13.5)	6 (5.4)	0.052
Presence of DM, n(%)	14 (18.9)	31 (27.7)	0.172
Presence of non-specific abdominal symptoms, n (%)	30 (40.5)	46 (41.1)	0.942

SD, standard deviation; DM, diabetes mellitus; BMI, Body Mass Index.

TABLE 3 Multivariate predictors for clinical significance EUS-FNA in low-risk PCLs patients.

Parameters	OR	95%CI	P value
Gender	2.36	0.56-6.89	0.689
Cyst size	1.12	1.02–1.19	0.033
Age	0.94	0.91-0.99	0.041
BMI over 25	3.15	1.29-7.86	0.013
Pancreatic cancer family history	1.89	0.92-2.45	0.085

BMI, Body mass index; OR, odds ratio; CI, confident interval.

evidence for the important role of EUS-FNA in the management of PCNs and identifies which patients with low-risk PCNs might benefit from EUS-FNA.

The value of EUS and EUS-FNA in patients with PCLs has been studied in many previous studies. According to the 2 studies by Allen et al. and Ferrone et al., EUS alone influences the management of 40% of PCNs discovered by chance (17, 18). The role of EUS-FNA was further explored. Ardengh et al. concluded that EUS-FNA has a management impact in almost 72% of incidental PCLs through a large prospective study. They deemed EUS-FNA had a major influence on the management strategy (19). In 2016, Rodríguez-D'Jesús et al. reported that EUS-FNA altered the diagnosis and management in 39% and 21% of patients with PCLs through a retrospective study. They concluded that EUS and EUS-FNA impact the diagnosis and management of patients with PCLs; therefore, both are necessary in the workup of these patients (20). In 2019, Chang et al. Conducted a large sample size retrospective study and reported that EUS-FNA changed the diagnosis in 45.7% PCLs patients and 54.5% patients with presumed branch duct (BD) IPMN and changed the management recommendation in 35.6% of patients with PCLs and 50.5% patients with BD-IPMN (21). Additional, they concluded EUS-FNA may be more useful in younger patients and in patients with a cyst size larger than 3cm (21). However, all the aforementioned studies did not focus on patients with low-risk PCLs. Due to the higher difficulty in

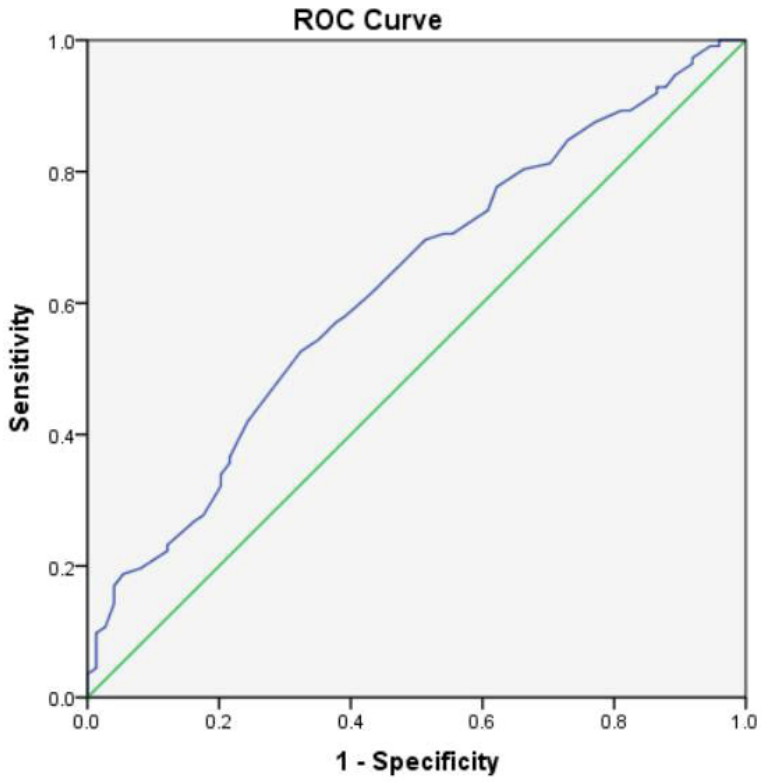

FIGURE 2
The ROC curve analysis to predict the optimal age for clinical significance EUS-FNA (the area under the curve=0.626).

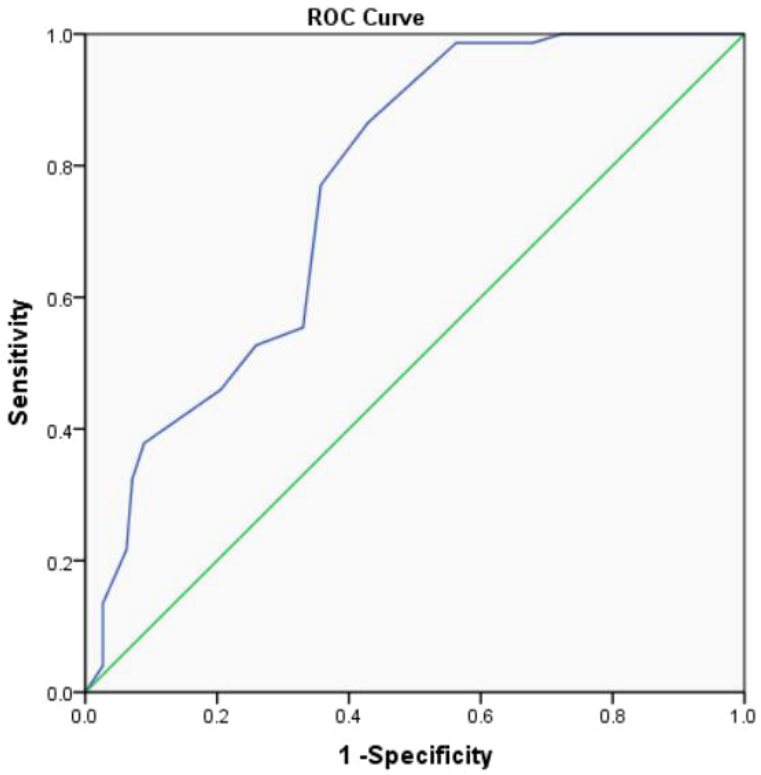

FIGURE 3
The ROC curve analysis to predict the optimal cyst size for clinical significance EUS-FNA (the area under the curve=0.765).

making accurate diagnosis in low-risk PCLs, we deemed the composition of the study cohort is one of the highlights of our study.

In the past, EUS-FNA for PCLs was reported to be associated with high incidence of complications. However, the situation changed recently. According to the recent meta-analysis (13, 22) and prospective randomized trial (23), we concluded that EUS-FNA is a safe procedure for diagnosing PCL that has a low risk of complications. The majority of side effects were minor, self-limiting, and did not necessitate medical attention. Extending the indications for EUS-FNA is logically possible and do not increase risk.

To make a definitive diagnosis for patients without adequaate pathological specimen seems impossible. The value of cytology obtained by EUS-FNA is limited in differentiating MCNs and SCNs with 42% sensitivity (24). Only about 35% of cytologic samples obtained by EUS-FNA were informative (25). Hence, the incidence of changing diagnoses after EUS-FNA is not included in our study. Instead, the clinical significance is adopted by us to assess the clinical impact of EUS-FNA on patients with low-risk PCLs. A more positive or conservative approach will be adopted after clinically significant EUS-FNA, including follow-up strategy and treatment strategy.

Many progresses have been described into the field of EUS-FNA for PCLs. For example, the intracystic Glucose level is reported to be more accurate than CEA level in diagnosing mucinous cysts (26, 27). The reported diagnostic yield for EUS-guided through the needle microforceps biopsy (EUS-TTNB) in diagnosing a specific cyst type was significantly higher with TTNB histology (72.5%) compared to that in FNA cytology (38.1%) (28). The *in vivo* imaging of the cyst epithelium can be visualized using EUS-guided needle-based confocal laser endomicroscopy (cCLE). Antonio et al. found that the diagnostic yield for nCLE at a US facility was 84.1%, much higher than the current "composite standard" (clinical, morphological, cyst fluid cytology, and chemical analyses) (29). However, the study cohort of our study is obtained between 2004 and 2017, when these techniques were not applied in clinical practise. Moreover, these techniques may not be applicable in most centers. Therefore, the conclusion of our study may be applicable to most centers.

There were certain limitations of our study. First, it was a retrospective review of a cohort of patients who underwent EUS-FNA. Follow-up data to determine which feature is associated with progression are lacking. Second, interobserver variability is unavoidable which may have caused bias. Third, the study's

sample size for each subgroup analysis was relatively small, which constrained the results. A big prospective cohort is clearly required.

Conclusion

On the basis of a 2 centers retrospective study, EUS-FNA was clinically significance in about 40% of low-risk PCLs, especially in young, large cyst size and overweight patients. Extending the indications of EUS-FNA may be reasonable based on the conclusion of our study. However, prospective study with large sample size is needed to further verify the findings of our study.

Data availability statement

The raw data supporting the conclusions of this article will be made available by the authors, without undue reservation.

Ethics statement

Written informed consent was obtained from the individual(s) for the publication of any potentially identifiable images or data included in this article.

Author contributions

SP: Data collection and statistical analysis. JL: Paper writing. JG: Design of the study and data collection. LW: Interpretation of data. QZ: Literature search. XS: Manuscript review design of the study. All authors contributed to the article and approved the submitted version.

Conflict of interest

The handling editor [ZJ] declared a shared parent affiliation with the author [JG] at the time of review.

The remaining authors declare that the research was conducted in the absence of any commercial or financial relationships that could be construed as a potential conflict of interest.

Publisher's note

All claims expressed in this article are solely those of the authors and do not necessarily represent those of their affiliated organizations, or those of the publisher, the editors and the reviewers. Any product that may be evaluated in this article, or claim that may be made by its manufacturer, is not guaranteed or endorsed by the publisher.

References

1. Vilas-Boas F, Macedo G. Pancreatic cystic lesions: New endoscopic trends in diagnosis. *J Clin Gastroenterol* (2018) 52(1):13–9. doi: 10.1097/MCG.0000000000000945

2. Zerboni G, Signoretti M, Crippa S, Falconi M, Arcidiacono PG, Capurso G. Systematic review and meta-analysis: Prevalence of incidentally detected pancreatic cystic lesions in asymptomatic individuals. *Pancreatology* (2019) 19(1):2–9. doi: 10.1016/j.pan.2018.11.014

3. Sakorafas GH, Sarr MG. Cystic neoplasms of the pancreas; what a clinician should know. *Cancer Treat Rev* (2005) 31(7):507–35. doi: 10.1016/j.ctrv.2005.09.001

4. European Study Group on Cystic Tumours of the Pancreas. European Evidence-based guidelines on pancreatic cystic neoplasms. *Gut* (2018) 67(5):789–804. doi: 10.1136/gutjnl-2018-316027

5. Tanaka M, Fernández-Del Castillo C, Kamisawa T, Jang JY, Levy P, Ohtsuka T, et al. Revisions of international consensus Fukuoka guidelines for the management of IPMN of the pancreas. *Pancreatology* (2017) 17(5):738–53. doi: 10.1016/j.pan.2017.07.007

6. Elta GH, Enestvedt BK, Sauer BG, Lennon AM. ACG clinical guideline: Diagnosis and management of pancreatic cysts. *Am J Gastroenterol* (2018) 113 (4):464–79. doi: 10.1038/ajg.2018.14

7. Wu J, Wang Y, Li Z, Miao H. Accuracy of Fukuoka and American gastroenterological association guidelines for predicting advanced neoplasia in pancreatic cyst neoplasm: A meta-analysis. *Ann Surg Oncol* (2019) 26(13):4522–36. doi: 10.1245/s10434-019-07921-8

8. Sun L, Wang W, Wang Y, Jiang F, Peng L, Jin G, et al. Validation of European evidence-based guidelines and American college of gastroenterology guidelines as predictors of advanced neoplasia in patients with suspected mucinous pancreatic cystic neoplasms. *J Gastroenterol Hepatol* (2020) 35(9):1644–51. doi: 10.1111/jgh.14973

9. Sun L, Huang H, Jin Z. Application of EUS-based techniques in the evaluation of pancreatic cystic neoplasms. *Endosc Ultrasound* (2021) 10(4):230–40. doi: 10.4103/EUS-D-20-00216

10. Sun L, Wang Y, Jiang F, Qian W, Shao C, Jin Z. Prevalence of pancreatic cystic lesions detected by magnetic resonance imaging in the Chinese population. *J Gastroenterol Hepatol* (2019) 34(9):1656–62. doi: 10.1111/jgh.14658

11. Kwok K, Chang J, Duan L, Huang BZ, Wu BU. Competing risks for mortality in patients with asymptomatic pancreatic cystic neoplasms: Implications for clinical management. *Am J Gastroenterol* (2017) 112(8):1330–6. doi: 10.1038/ajg.2017.141

12. Kim TH, Woo YS, Chon HK, Hwang JH, Yoo KS, Lee WJ, et al. Predictors of malignancy in "Pure" branch-duct intraductal papillary mucinous neoplasm of the pancreas without enhancing mural nodules on CT imaging: A nationwide multicenter study. *Gut Liver* (2018) 12(5):583–90. doi: 10.5009/gnl17582

13. Zhu H, Jiang F, Zhu J, Du Y, Jin Z, Li Z. Assessment of morbidity and mortality associated with endoscopic ultrasound-guided fine-needle aspiration for pancreatic cystic lesions: A systematic review and meta-analysis. *Dig Endosc* (2017) 29(6):667–75. doi: 10.1111/den.12851

14. de Jong K, van Hooft JE, Nio CY, Gouma DJ, Dijkgraaf MG, Bruno MJ, et al. Accuracy of preoperative workup in a prospective series of surgically resected cystic pancreatic lesions. *Scand J Gastroenterol* (2012) 47(8-9):1056–63. doi: 10.3109/00365521.2012.674970

15. Kadiyala V, Lee LS. Endosonography in the diagnosis and management of pancreatic cysts. *World J Gastrointest Endosc* (2015) 7(3):213–23. doi: 10.4253/wjge.v7.i3.213

16. Lee LS. Updates in diagnosis and management of pancreatic cysts. *World J Gastroenterol* (2021) 27(34):5700–14. doi: 10.3748/wjg.v27.i34.5700

17. Allen PJ, D'Angelica M, Gonen M, Jaques DP, Coit DG, Jarnagin WR, et al. A selective approach to the resection of cystic lesions of the pancreas: results from 539 consecutive patients. *Ann Surg* (2006) 244(4):572–82. doi: 10.1097/01.sla.0000237652.84466.54

18. Ferrone CR, Correa-Gallego C, Warshaw AL, Brugge WR, Forcione DG, Thayer SP, et al. Current trends in pancreatic cystic neoplasms. *Arch Surg* (2009) 144(5):448–54. doi: 10.1001/archsurg.2009.36

19. Ardengh JC, Lopes CV, de Lima-Filho ER, Kemp R, Dos Santos JS. Impact of endoscopic ultrasound-guided fine-needle aspiration on incidental pancreatic cysts. a prospective study. *Scand J Gastroenterol* (2014) 49(1):114–20. doi: 10.3109/00365521.2013.854830

20. Rodríguez-D'Jesús A, Fernández-Esparrach G, Boadas J, Busquets J, Fernández-Cruz L, Ferrer J, et al. Impact of endoscopic ultrasonography (EUS) and EUS-guided fine-needle aspiration on the management of pancreatic cystic lesions. *Eur J Gastroenterol Hepatol* (2016) 28(9):1094–9. doi: 10.1097/MEG.0000000000000678

21. Chang YT, Tung CC, Chang MC, Wu CH, Chen BB, Jan IS. Age and cystic size are associated with clinical impact of endoscopic ultrasonography-guided fine-needle aspiration on the management of pancreatic cystic neoplasms. *Scand J Gastroenterol* (2019) 54(4):506–12. doi: 10.1080/00365521.2019.1601254

22. Palomera-Tejeda E, Shah H, Attar BM, Bhurwal A, Vohra I, Mutneja HR. Prophylactic antibiotics do not prevent infectious complications of endoscopic ultrasound fine-needle aspiration of pancreatic cysts: A systematic review and meta-analysis. *Pancreas* (2021) 50(5):667–72. doi: 10.1097/MPA.0000000000001816

23. Colán-Hernández J, Sendino O, Loras C, Pardo A, Gornals JB, Concepción M, et al. Antibiotic prophylaxis is not required for endoscopic ultrasonography-guided fine-needle aspiration of pancreatic cystic lesions, based on a randomized trial. *Gastroenterology* (2020) 158(6):1642–9. doi: 10.1053/j.gastro.2020.01.025

24. Gillis A, Cipollone I, Cousins G, Conlon K. Does EUS-FNA molecular analysis carry additional value when compared to cytology in the diagnosis of pancreatic cystic neoplasm? a systematic review. *HPB (Oxford)* (2015) 17(5):377–86. doi: 10.1111/hpb.12364

25. Faias S, Cravo M, Pereira da Silva J, Chaves P, Dias Pereira A. Endoscopic ultrasound with fine needle aspiration is useful in pancreatic cysts smaller than 3 cm. *BMC Gastroenterol* (2020) 20(1):413. doi: 10.1186/s12876-020-01565-9

26. Smith ZL, Satyavada S, Simons-Linares R, Mok SRS, Martinez Moreno B, Aparicio JR, et al. Intracystic glucose and carcinoembryonic antigen in differentiating histologically confirmed pancreatic mucinous neoplastic cysts. *Am J Gastroenterol* (2022) 117(3):478–85. doi: 10.14309/ajg.0000000000001623

27. McCarty TR, Garg R, Rustagi T. Pancreatic cyst fluid glucose in differentiating mucinous from nonmucinous pancreatic cysts: a systematic review and meta-analysis. *Gastrointest Endosc* (2021) 94(4):698–712. doi: 10.1016/j.gie.2021.04.025

28. Crinò SF, Bernardoni L, Brozzi L, Barresi L, Malleo G, Salvia R, et al. Association between macroscopically visible tissue samples and diagnostic accuracy of EUS-guided through-the-needle microforceps biopsy sampling of pancreatic cystic lesions. *Gastrointest Endosc* (2019) 90(6):933–43. doi: 10.1016/j.gie.2019.05.009

29. Cheesman AR, Zhu H, Liao X, Szporn AH, Kumta NA, Nagula S, et al. Impact of EUS-guided microforceps biopsy sampling and needle-based confocal laser endomicroscopy on the diagnostic yield and clinical management of pancreatic cystic lesions. *Gastrointest Endosc* (2020) 91(5):1095–104. doi: 10.1016/j.gie.2019.12.022

frontiers | Frontiers in Oncology

TYPE Original Research
PUBLISHED 05 August 2022
DOI 10.3389/fonc.2022.945904

Check for updates

OPEN ACCESS

EDITED BY
Zhendong Jin,
Second Military Medical University, China

REVIEWED BY
Amit Dutta,
Christian Medical College &Hospital, India
Mohammad Hasan Olyaei,
Sadjad University of Technology, Iran

*CORRESPONDENCE
Yanqing Li
liyanqing@sdu.edu.cn

†These authors have contributed equally to this work and share first authorship

SPECIALTY SECTION
This article was submitted to Gastrointestinal Cancers: Gastric & Esophageal Cancers, a section of the journal Frontiers in Oncology

RECEIVED 17 May 2022
ACCEPTED 04 July 2022
PUBLISHED 05 August 2022

CITATION
Ma M, Li Z, Yu T, Liu G, Ji R, Li G, Guo Z, Wang L, Qi Q, Yang X, Qu J, Wang X, Zuo X, Ren H and Li Y (2022) Application of deep learning in the real-time diagnosis of gastric lesion based on magnifying optical enhancement videos. *Front. Oncol.* 12:945904. doi: 10.3389/fonc.2022.945904

COPYRIGHT
© 2022 Ma, Li, Yu, Liu, Ji, Li, Guo, Wang, Qi, Yang, Qu, Wang, Zuo, Ren and Li. This is an open-access article distributed under the terms of the Creative Commons Attribution License (CC BY). The use, distribution or reproduction in other forums is permitted, provided the original author (s) and the copyright owner(s) are credited and that the original publication in this journal is cited, in accordance with accepted academic practice. No use, distribution or reproduction is permitted which does not comply with these terms.

Application of deep learning in the real-time diagnosis of gastric lesion based on magnifying optical enhancement videos

Mingjun Ma[1,2,3†], Zhen Li[1,2,3†], Tao Yu[1,2,3†], Guanqun Liu[1,2,3], Rui Ji[1,2,3], Guangchao Li[1,2,3], Zhuang Guo[4], Limei Wang[1,2,3], Qingqing Qi[1,2,3], Xiaoxiao Yang[1,2,3], Junyan Qu[1,2,3], Xiao Wang[5], Xiuli Zuo[1,2,3], Hongliang Ren[6,7] and Yanqing Li[1,2,3*]

[1]Department of Gastroenterology, Qilu Hospital of Shandong University, Jinan, China, [2]Laboratory of Translational Gastroenterology, Qilu Hospital of Shandong University, Jinan, China, [3]Robot Engineering Laboratory for Precise Diagnosis and Therapy of Gastrointestinal Tumor, Qilu Hospital of Shandong University, Jinan, China, [4]Department of Gastroenterology, Shengli Oilfield Central Hospital, Dongying, China, [5]Department of Pathology, Qilu Hospital, Cheeloo College of Medicine, Shandong University, Jinan, China, [6]Department of Electronic Engineering, The Chinese University of Hong Kong, Hong Kong SAR, China, [7]Department of Biomedical Engineering, National University of Singapore, Singapore, Singapore

Background and aim: Magnifying image-enhanced endoscopy was demonstrated to have higher diagnostic accuracy than white-light endoscopy. However, differentiating early gastric cancers (EGCs) from benign lesions is difficult for beginners. We aimed to determine whether the computer-aided model for the diagnosis of gastric lesions can be applied to videos rather than still images.

Methods: A total of 719 magnifying optical enhancement images of EGCs, 1,490 optical enhancement images of the benign gastric lesions, and 1,514 images of background mucosa were retrospectively collected to train and develop a computer-aided diagnostic model. Subsequently, 101 video segments and 671 independent images were used for validation, and error frames were labeled to retrain the model. Finally, a total of 117 unaltered full-length videos were utilized to test the model and compared with those diagnostic results made by independent endoscopists.

Results: Except for atrophy combined with intestinal metaplasia (IM) and low-grade neoplasia, the diagnostic accuracy was 0.90 (85/94). The sensitivity, specificity, PLR, NLR, and overall accuracy of the model to distinguish EGC from non-cancerous lesions were 0.91 (48/53), 0.78 (50/64), 4.14, 0.12, and 0.84 (98/117), respectively. No significant difference was observed in the overall diagnostic accuracy between the computer-aided model and experts. A good level of kappa values was found between the model and experts, which meant that the kappa value was 0.63.

Conclusions: The performance of the computer-aided model for the diagnosis of EGC is comparable to that of experts. Magnifying the optical enhancement model alone may not be able to deal with all lesions in the stomach, especially when near the focus on severe atrophy with IM. These results warrant further validation in prospective studies with more patients. A ClinicalTrials.gov registration was obtained (identifier number: NCT04563416).

Clinical Trial Registration: ClinicalTrials.gov, identifier NCT04563416.

KEYWORDS

early gastric cancer, image-enhanced endoscopy, convolutional neural network, deep learning, tumor diagnosis

Introduction

Gastric cancer is the third most common cause of cancer-associated deaths worldwide, particularly in Asia (1). Early detection and treatment can cure the disease, with a 5-year survival rate greater than 90% (2). However, the sensitivity of conventional endoscopy with white-light imaging (C-WLI) in the diagnosis of early gastric cancers (EGCs) is only 40% (3). Magnifying image-enhanced endoscopy (M-IEE) techniques, such as magnifying narrow band imaging (M-NBI), have been developed. Two randomized controlled trials reported that white-light imaging combined with M-NBI can increase the sensitivity to 95% (4, 5). If an abrupt demarcation line (DL) is absent, the diagnosis of a non-cancerous lesion may be made with a 99% negative predictive value (NPV). Therefore, M-IEE may reduce the number of biopsies required to detect EGCs in screening endoscopy (6). The use of white-light imaging to detect suspected lesions and M-IEE techniques to diagnose EGC are recommended for screening endoscopy (7). However, because of the natural background of gastric inflammation, a benign lesion under M-IEE is easily confused with early cancer.

Magnifying optical enhancement (M-OE), an M-IEE technique, was developed by HOYA Co. (Tokyo, Japan). This technology combines digital signal processing and optical filters to clearly display a mucosal microsurface pattern (MSP) and microvessel pattern (MVP) (8). Nevertheless, differentiating EGCs from benign lesions is difficult for beginners with an accuracy of approximately 60% (9). Endoscopists often need to employ considerable effort to improve their diagnostic skills, and expertise with suboptimal interobserver agreement is crucial for the use of M-IEE (10).

Currently, artificial intelligence (AI) using deep machine learning has made a major breakthrough in gastroenterology; it uses the gradient descent method and backpropagation to automatically extract specific image features. The detection accuracy in identifying upper gastrointestinal cancer was 0.955 in C-WLI (11). Polyps can be identified in real time with 96% accuracy in screening colonoscopy (12). A multicenter study showed that C-WLI endoscopy can detect 80% of EGCs (13). AI shows an outstanding application in detection. Meanwhile, several studies verified the M-IEE diagnostic model through still images (14, 15). However, studies using EGC video verification are rare, which further simulated clinical practice. A recent study was able to distinguish tumors from adjacent tissues, using EGC videos (16). The comparison of EGC and various gastric benign lesions is missing. In this study, we included various disease phenotypes that need to be differentiated from EGC to develop an M-OE assistance model and test in unaltered full-length videos to ask whether the assistance model alone can meet the clinical need.

Abbreviations: C-WLI, white-light imaging; EGC, early gastric cancer; M-IEE, magnifying image-enhanced endoscopy; M-NBI, magnifying narrow band imaging; M-OE, magnifying optical enhancement; DL, demarcation line; IM, intestinal metaplasia; MSP, microsurface pattern; MVP, microvessel pattern; ROI, region of interest; TTROI, the total time of the region of interest; LGIN, mucosal low-grade neoplasia; CNN, convolutional neural network; PLR, positive likelihood ratio; NLR, negative likelihood ratio; ROC, receiver operating characteristic; AUC, area under the receiver operating characteristic curve.

Methods

This study complied with the Standards for the Reporting of Diagnostic Accuracy Studies initiative and the Declaration of Helsinki (17). It was approved by the Medical Ethics Committee of Qilu Hospital of Shandong University.

Preparation of image training sets

M-OE images between February 2016 and September 2019 were retrospectively obtained from one tertiary hospital to

develop an algorithm for the diagnosis of EGCs. All images were captured by magnifying endoscopy (EG-2990Zi; Pentax, Tokyo, Japan) and OE (EPK-I7000; Pentax, Tokyo, Japan) mode 1. The images of different types of devices came from different patients and were taken from different parts of the lesions. The images with the distal cap attachment were strictly selected. Only images that did not affect the judgment of lesions were retained, which the distal cap attachment accounts for no more than 25% of the image area.

Due to the fact that the diagnosis of advanced cancer and active ulcer is usually sufficient with the C-WLI endoscopy, the M-OE gastric images of advanced cancer, lymphoma, the active stage of ulcer, and artificial ulcer after endoscopic submucosal dissection were excluded. Poor-quality images resulting from less insufflation of air, post-biopsy bleeding, halation, blur, defocus, or mucus were also excluded. A single pathologist who was blinded to the endoscopic findings reviewed the histopathology. The pathological diagnostic criteria were based on the revised Vienna classification (18). C4 (mucosal high-grade neoplasia) and C5 (submucosal invasion by neoplasia) were diagnosed as cancer. C1 (negative for neoplasia), C2 (indefinite for neoplasia), and C3 [mucosal low-grade neoplasia (LGIN)] were diagnosed as non-cancerous lesions. Two experienced endoscopists who had performed M-OE for more than 3 years reviewed and manually labeled all images of pathologically proven EGC lesions. LGIN was discarded because a considerable number of LGIN were later confirmed as high-grade or even intramucosal carcinoma (19–21). For cases in which a discrepancy existed between pathological findings and endoscopic diagnosis, the pathologist and endoscopists would reassess and discuss to reach a joint decision. The M-OE images of EGCs should meet the following conditions: the presence of irregular or absence of MVP with a DL or the presence of irregular or absence of MSP with a DL (22). Finally, 952 M-OE EGC images from 126 patients and 3,442 M-OE non-cancerous images from 325 patients were selected. A total of 719 EGC images from 94 patients and 1,490 and 1,514 images of benign lesion and background mucosa, respectively, from 262 patients formed the training set (Table 1 and Figure 1). The rest of the patients and images formed the validation set.

Constructing a convolutional neural network algorithm

You Only Look Once version 4 is a popular and open-access model architecture worldwide (23). It has excellent performance in terms of accuracy and speed.

Images were divided into three categories: background mucosa, benign lesion, and EGC (Figure 2). Background mucosa is a mucosal image of the gastric fundus, cardia, and pyloric gland, which has no suspicious DL. The background images of atrophy and intestinal metaplasia (IM) were also included if there was no suspicious DL. A benign lesion means that the lesion needs to be distinguished from EGCs, such as erosion, localized IM, scarring, and localized atrophy. EGC refers to a cancerous lesion with MVP or MSP. The model automatically analyzes the input images and diagnoses the EGC with a blue rectangular frame and identifies benign lesions and background mucosa with green and red rectangular frames, respectively. For the convenience of statistical analysis, the images of the background mucosa and benign lesions were regarded as non-cancerous images.

An independent set of 671 validation images was prepared from 32 EGC patients and 63 non-cancerous patients, and the model showed 84% accuracy per image analysis. Moreover, 101 video segments recorded in the endoscopic system, 21 EGC video segments and 80 non-cancerous video segments, were used for validation. A total of 550 EGC images and 620 non-cancerous images that were transformed from the error recognition set were manually labeled and retrained.

Offline unaltered video test sets

A total of 117 full-length M-OE videos recorded using the endoscopy system were included in the test set. All patients had at least one biopsy. If more than one lesion was present in one patient, only the most serious lesion was evaluated.

Our CPU is Intel Core i5-8400, and the GPU is NVIDIA GeForce GTX 1080ti. The processing speed of the model is up to 30 frames/s, which meets the requirements of real-time recognition. (Supplementary Videos S1, S2) A video set may indicate different diagnostic results for the same lesion, which can be confusing, due to the model output diagnosis to each frame. In order to analyze the diagnostic performance, postprocessing based on videos was performed. The results of the video recognition were concentrated on the time axis, with the cancer tag upward and benign tag downward. The cancer tag would be prompted more frequently for the cancerous lesion. An engineer with no medical background marked out the region of interest (ROI) through automatic calculation by a computer. The

TABLE 1 Image composition of training set.

All cancer	719
EGCs with irregular MSP	571
EGCs with irregular MVP	148
Benign lesion	1,490
Localized intestinal	992
Localized atrophy and scaring	341
Erosion	157
Background mucosa	1,514
Gastric fundus	487
Gastric antrum	1,027

EGCs, early gastric cancer; MSP, microsurface pattern; MVP, microvessel pattern.

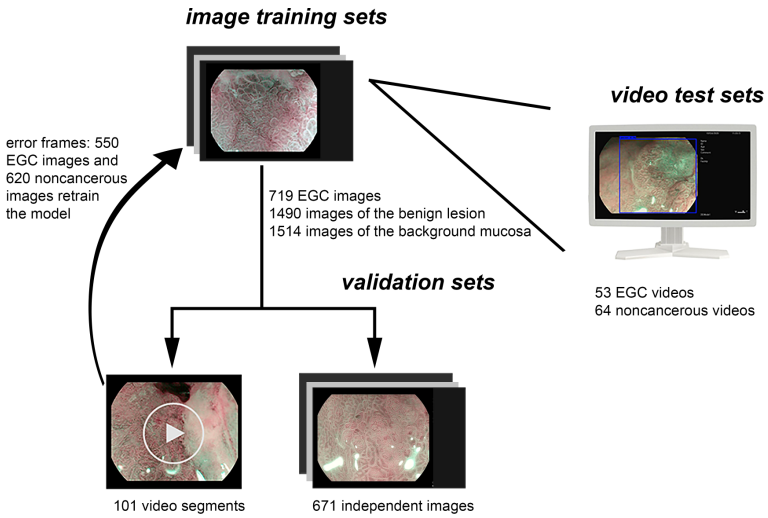

FIGURE 1
Data flow chart of the computer-aided system. Firstly, the model was developed using the training sets. Secondly, the model was evaluated by independent validation sets including videos and images, and the video frames with error were labeled and retrained the model. Finally, the model was tested using independent test video sets.

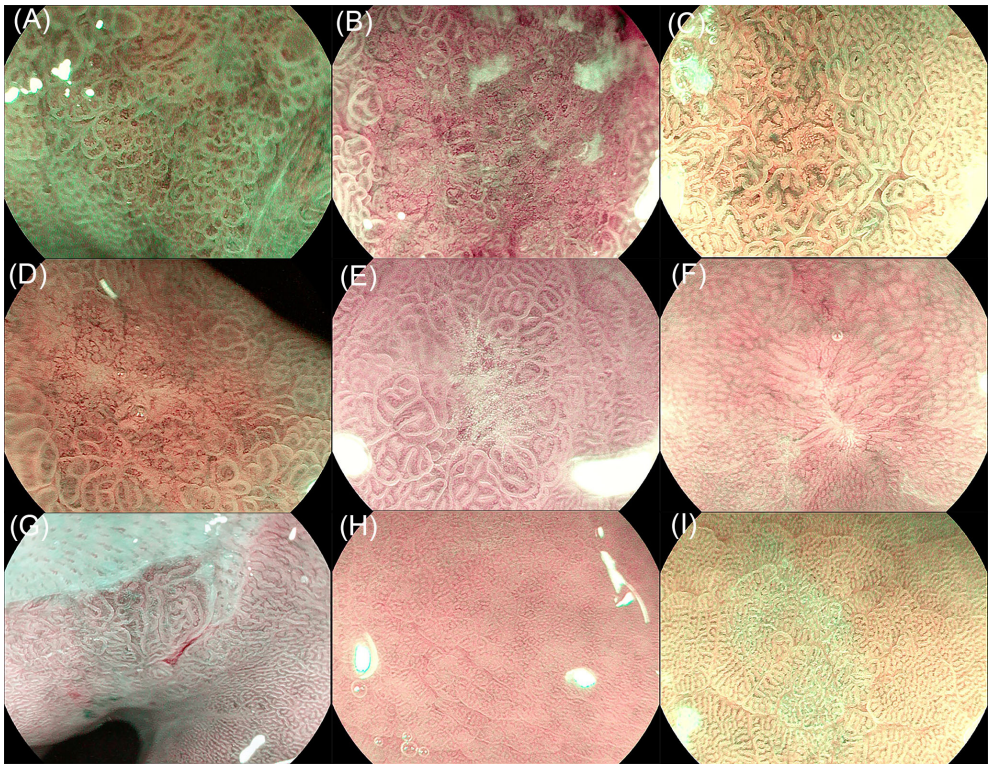

FIGURE 2
Image classification of the training set. **(A)** Early gastric cancer (EGC) with a mucosal microsurface pattern (MSP), **(B)** early gastric cancer (EGC) with microvessel pattern (MVP), **(C)** localized intestinal metaplasia, **(D)** localized atrophy, **(E)** erosion, **(F)** scaring, **(G)** cardia gland mucosa, **(H)** fundic gland mucosa, and **(I)** pyloric gland mucosa.

ROI started from any cancer recognition tag, and if there was no new cancer recognition tag within 3 s, it was regarded as the end of the ROI. Considering that the longer ROI indicates that the lesion is more likely to be EGC, the total time of the region of interest (TTROI) was recorded.

Evaluation of endoscopists and outcome measures

A total of 117 full-length videos were used to evaluate the model and experts. Five experts with more than 5 years of experience in magnifying endoscopy were evaluated. In the case of unknown pathology and no interference, the most serious lesion diagnosis was given for each patient.

In the test set, C4 and C5 were considered as cancers based on the gold standard of pathology. The performance of the model was evaluated through the test set. The receiver operating characteristic curve (ROC) was drawn according to the TTROI, and the best cutoff value was obtained. The diagnostic accuracy of each pathological type was analyzed. Sensitivity, specificity, positive likelihood ratio (PLR), negative likelihood ratio (NLR), and overall accuracy were calculated according to the cutoff value.

Statistical analysis

A Mann–Whitney U test was performed to calculate the statistical difference in the TTROI between cancerous and non-cancerous groups. The Pearson chi-square test was used to determine the statistical difference of no ROI between cancerous and non-cancerous groups. The two-paired McNemar test was performed to compare the accuracy between experts and the model. Kappa analysis was calculated to evaluate the interobserver agreement. Univariate analysis was performed for the pathological type with poor diagnostic accuracy. All statistical tests were two sided, and P<0.05 was considered statistically significant. Analyses were performed using R (version 4.0.2; Vienna, Austria) and SPSS (version 21.0; New York, U.S. IBM Corp).

Results

A total of 117 full-length videos for 10 h from 64 cases of non-cancerous lesions and 53 cases of EGC were used for the test. The clinical characteristics of the included patients are shown in Table 2.

Model performance

The TTROIs of the cancerous (median, 47 s; interquartile range, 12–90) and non-cancerous groups (median, 0 s; interquartile range, 0–0) were significantly different (P<0.0001). No ROIs of the cancerous (9.4%) and non-cancerous groups (78.1%) were significantly different (P<0.0001).

According to the TTROI, drawing the ROC curve, the area under the curve (AUC) was 0.874 and the best cutoff value was 1 s. Based on the cutoff value, a total of 5 cases of EGC and 14 cases of non-cancerous lesions were misidentified. Except for atrophy combined with IM and LGIN, the diagnostic sensitivity of different pathological types was almost 0.90 (Figure 3). The diagnostic sensitivity of atrophy combined with IM and LGIN were 0.63 and 0.43, respectively (Table 3). The sensitivity, specificity, PLR, NLR, and overall accuracy of the model to distinguish EGC from non-cancerous lesions were 0.91, 0.78, 4.14, 0.12, and 0.84, respectively.

Comparison with endoscopists

No significant difference was observed in the overall accuracy of the diagnosis between the computer-aided model and experts. Nevertheless, the diagnostic accuracy of the model for differential EGCs was significantly different from that of expert C (0.92 *vs.* 0.65, P < 0.01). Moreover, although the diagnostic performance of the

TABLE 2 Clinicopathologic characteristics of gastric mucosal lesions in the test set.

	Early gastric cancer (n=53)	Non-cancerous lesion (n=64)
Age, mean ± SD (range), years	63.3 ± 7.3 (48 – 78)	56.0 ± 10.2 (28 – 78)
Male sex, No. (%)	45 (84.9)	40 (62.5)
Location		
Cardia	12	6
Fundus	12	18
Angle	7	14
Antrum	22	26
Morphology		
0-I	1	
0-IIa	13	
0-IIb	10	
0-IIc	12	
0-IIa+IIc	12	
0-IIb+IIa	3	
0-IIb+IIc	2	
Pathology		
Inflammation		24
Atrophy		10
Intestinal		7
Atrophy + IM		16
Low-grade neoplasia		7
Poor differential EGCs	5	
Differential EGCs	48	

SD, standard deviation; IM, intestinal metaplasia; EGCs, early gastric cancers.

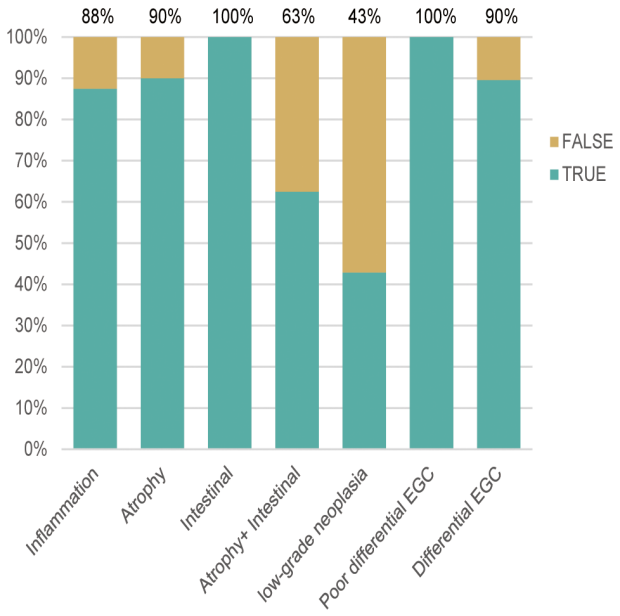

FIGURE 3
The diagnostic accuracy of different pathological types was approximately 0.90, except for atrophy combined with intestinal metaplasia (0.69) and low-grade neoplasia (0.43). EGC, early gastric cancer.

model for atrophy combined with IM seemed inferior to that of experts, there was no statistical difference between them (0.69 *vs.* 0.94, $P = 0.13$). A good level of kappa values was found between the model and experts, which were 0.62, 0.64, 0.53, 0.61, and 0.71 respectively (Table 4).

Influencing factors for the recognition of atrophy combined with intestinal metaplasia and low-grade neoplasia

We conducted a univariate analysis on factors that may lead to the false diagnosis of atrophy combined with IM (Table 5). The proportion of moderate, severe, and diffuse lesions increased in the error group, suggesting that severe diffuse atrophy combined with IM may be difficult to distinguish from EGC by using the computer-aided model.

There were seven LGINs in the unaltered full-length video data set, including four ESD-certified LGINs showing high-grade neoplasia in biopsy. Five of the seven LGINs were deemed as having obvious DL by experts, which was an important endoscopic characteristic for diagnosing EGC. Therefore, even the endoscopic experts showed poor diagnostic accuracy for LGIN lesions (0.43–0.57).

Discussion

We developed an M-OE model covering multiple gastric lesions, using unaltered full-length M-OE videos to evaluate

TABLE 3 Detailed results of the model diagnosis.

	Inflammation (95% CI)	Atrophy (95% CI)	IM(95% CI)	Atrophy+ IM (95% CI)	LGIN(95% CI)	Poor differential EGC (95% CI)	Differential EGC (95% CI)
Sensitivity	0.88 (0.82-0.93)	0.90 (0.85-0.95)	1.00 (1.00-1.00)	0.63 (0.54-0.71)	0.43 (0.34-0.52)	1.00 (1.00-1.00)	0.90 (0.84-0.95)
Specificity	0.83 (0.76-0.90)	0.83 (0.76-0.90)	0.83 (0.76-0.90)	0.87 (0.81-0.93)	0.86 (0.80-0.93)	0.83 (0.76-0.90)	0.80 (0.72-0.87)
PLR	5.09 (1.32-8.85)	5.35 (1.13-9.57)	5.79 (0.77-10.81)	4.86 (1.46-8.25)	3.14 (1.92-4.36)	5.89 (0.67-11.12)	4.42 (1.68-7.15)
NLR	0.15 (0.09-0.22)	0.12 (0.06-0.18)	0.00 (0.00-0.00)	0.43 (0.34-0.52)	0.66 (0.58-0.75)	0.00 (0.00-0.00)	0.13 (0.07-0.19)

CI, confidence interval; IM, intestinal metaplasia; EGC, early gastric cancer; LGIN, low-grade neoplasia; PLR, positive likelihood ratio; NLR, negative likelihood ratio.

TABLE 4 Diagnostic accuracy of the model versus experts.

	Inflammation (95% CI)	Atrophy (95% CI)	IM (95% CI)	Atrophy+ IM (95% CI)	LGIN (95% CI)	Poor differential EGC(95% CI)	Differential EGC(95% CI)	Total accuracy (95% CI)	Kappa
Model	0.88(0.69-0.96)	0.9(0.60-0.98)	1.00 (0.65-1.00)	0.69(0.44-0.86)	0.43(0.16-0.75)	1.00(0.57-1.00)	0.92(0.80-0.97)	0.84 (0.76-0.89)	
Expert A	0.92(0.74-0.98)	0.9(0.60-0.98)	1.00 (0.65-1.00)	0.94(0.72-0.99)*	0.43(0.16-0.75)	1.00(0.57-1.00)	0.9(0.78-0.95)	0.88 (0.81-0.93)	0.62
Expert B	0.92(0.74-0.98)	0.7(0.40-0.89)	0.86 (0.49-0.97)	0.63(0.39-0.82)	0.43(0.16-0.75)	1.00(0.57-1.00)	0.92(0.80-0.97)	0.83 (0.75-0.89)	0.64
Expert C	1(0.86-1.00)	0.9(0.60-0.98)	1.00 (0.65-1.00)	0.94(0.72-0.99)*	0.43(0.16-0.75)	1.00(0.57-1.00)	0.65(0.50-0.77)†	0.80 (0.72-0.87)	0.53
Expert D	0.83(0.64-0.93)	1(0.72-1.00)	1.00 (0.65-1.00)	0.94(0.72-0.99)*	0.57(0.25-0.84)	1.00(0.57-1.00)	0.79(0.66-0.88)	0.85 (0.77-0.90)	0.61
Expert E	0.92(0.74-0.98)	0.9(0.60-0.98)	1.00 (0.65-1.00)	0.94(0.72-0.99)*	0.43(0.16-0.75)	1.00(0.57-1.00)	0.92(0.80-0.97)	0.90 (0.83-0.94)	0.71

* P = 0.13, † P < 0.01; CI, confidence interval; IM, intestinal metaplasia; EGC, early gastric cancer; LGIN, low-grade neoplasia.

whether the M-OE model can meet the needs of clinical diagnosis. High diagnostic sensitivity was obtained for pathological subtypes, except atrophy combined with IM and LGIN. The overall accuracy is comparable to experts. Currently, three studies on the AI of magnifying EGC are available, all of which were verified by images (14, 15). Considering the variety of benign lesions under magnifying endoscopy, Hiroya et al. (24) included various types of benign lesions in the training set. However, their non-cancerous and cancerous images originated from the same patient. No biopsy pathology was performed; hence, they excluded any suspicious benign lesions to prevent the mixing of cancerous images. A recent video verification of EGC has shown similar results with us (16). However, they used the images of adjacent tissues as the control group and the adjacent tissue of the EGC is often the background mucosa, which could overestimate the performance of the model. In addition, the video clips they used may not represent clinical practice. It is difficult to adapt to multiple gastric lesions only by distinguishing between EGC and adjacent tissues. The distinction between cancer and benign lesions needs further verification. In order to achieve real-time clinical assistance, our study overcomes the shortcomings of the above studies and still achieves a high diagnostic ability through video verification in the case of multiple benign lesions.

We analyzed the statistical distribution of the TTROI and no ROI between cancerous and non-cancerous groups. In the

TABLE 5 Univariate analysis of diagnostic errors of atrophy combined with intestinal metaplasia.

	Correct (n=10)	Wrong (n=6)	P
Sex			0.869
Male	8 (80)	5 (83.3)	
Female	2 (20)	1 (16.7)	
Location			0.551
Upper	2 (20)	2 (33.3)	
Lower	8(80)	4 (66.7)	
Severity			0.037*
Moderate and severe	5(50)	6 (100)	
Mild	5 (50)	0 (0)	
Range			0.152
Diffuse	3 (30)	4 (66.7)	
Local	7 (70)	2 (33.3)	

*P < 0.05.

cancerous group, only five cases had no ROI and the median TTROI was 47 s, whereas in the non-cancerous group, 50 cases had no ROI and the median TTROI was 0 s. The TTROI and no ROI were significantly different (P<0.0001). Our model can well distinguish cancerous from non-cancerous groups, which achieve 0.91 sensitivity and minimize the missed diagnosis of EGC. The main reason for cancer recognition errors is differentiated carcinoma with a color similar to that of the background mucosa. We improve the robustness of the model by giving the model different images of benign gastric lesions. For different pathological types, most pathological types are close to 0.90 sensitivity and 0.80 specificity regardless of being benign or malignant.

The diagnostic accuracy of atrophy combined with IM and LGIN needs to be further improved, which causes low specificity. LGIN was also poorly recognized by experts. Since one-quarter of LGIN is diagnosed as EGC after the operation (19–21), a diagnostic resection of LGIN with DL is recommended in our center, which is consistent with the European guideline (18). Meanwhile, there is heterogeneity in the diagnosis of LGIN by pathologists. Therefore, we did not regard LGIN as a kind of lesion with deep learning features alone, to prevent dirty data from affecting the diagnostic efficiency of the model. We speculate that by constantly giving clear malignant and benign data, the final diagnostic efficiency will be generalized to the LGIN pathological entity. At present, the diagnostic accuracy of LGIN by the model is not inferior to that of experts.

Through the analysis of possible reasons for poor recognition of atrophy combined with IM, we found that the model is difficult to accurately diagnose severe and diffuse gastritis. Mistakes usually occur when the lesion is observed at near focus so that the DL of lesions is beyond the visual field, which indirectly indicates that the DL of lesions is an important feature of differentiating benign from malignant. In the practice of endoscopy, it is impossible to ensure that the DL of lesions is always in the endoscopic field, especially for magnifying endoscopy. Combining with the C-WLI detection model may solve this problem (25). Although it could produce false-positive prompts, our model can provide not only a diagnosis of the lesion but also the frame lesion location. In the actual test, endoscopists can make a secondary judgment on the suspicious lesions by the presence or absence of DL and actively discard some false-positive interferences. Therefore, we speculate higher specificity and PPV in practical applications. In any case, AI cannot replace endoscopists but only provide aid in clinical practice.

However, the NLR of our model is 0.12, which indicates that the model could rule out cancer robustly. Another strength is that the positive threshold is only 1 s. If the positive threshold is too high, overlong false-positive prompts will cause trouble for endoscopists in clinical practice. At the same time, the model has a good warning effect on suspected lesions, especially LGIN and severe atrophy combined with IM. The malignant risk of these two kinds of lesions is increased, so timely reminding endoscopists can evaluate these high-risk precancerous lesions more pertinently. Our model can adapt to the unaltered full-length video, which is undoubtedly progressive. Compared with the video clips, the model will encounter more situations that are biased toward clinical practice and needs a low negative likelihood ratio to adapt to long non-cancerous video segments. Of course, our model still needs to be verified online to evaluate the impact of the model on the observation of endoscopists.

This study had several limitations. First, it was conducted in a single center, and the test set is still relatively small. Second, the M-OE model only recognized MSP, MVP, and DL features, excluding C-WLI features. The C-WLI characteristics of the full-length video test will inevitably affect the diagnosis of endoscopists. It is necessary that the model could be applied to other endoscopy systems, especially NBI, which is the most commonly used image enhancement system. We will develop a united model including C-WLI and M-NBI in the future research. Third, the recognition ability of LGIN needs to be further improved. Last, the active ulcer was excluded in this study since the serious inflammatory background and the reactive hyperplasia of the mucosa surrounding the active ulcer would interfere with the model's diagnosis. Since the combination of C-WLI and M-OE is required to determine whether lesions are benign or malignant, the application of the model is limited.

Conclusion

We developed a new computer-aided system for the diagnosis of multiple gastric lesions in M-OE endoscopy, which is comparable to that of experts. The M-OE model alone may not be able to deal with all lesions in the stomach. Further development of our computer-aided system will combine the WLI model with the M-IEE models for automatic detection of lesions and accurate real-time diagnosis.

Data availability statement

The raw data supporting the conclusions of this article will be made available by the authors, without undue reservation.

Ethics statement

The studies involving human participants were reviewed and approved by Medical Ethics Committee of Qilu Hospital of Shandong University. The patients/participants provided their written informed consent to participate in this study.

Author contributions

Guarantor of the article: YL. Specific author contributions: MM, ZL, and TY should be considered joint first author. Conception and design: MM, ZL, YL, and TY. Analysis and interpretation of the data: MM, ZL, GQL, RJ, GCL, ZG, LW, QQ, and XW. Drafting of the article: MM. Critical revision for important intellectual content: XZ, HR, JQ, and XY. All authors contributed to the article and approved the submitted version.

Funding

This study was funded by the National Natural Science Foundation of China (81873550 and 81670489), Key Research and Development Program of Shandong Province (2018CXGC1209). This study is also funded by the Taishan Scholars Program of Shandong Province, Shandong Provincial Key Research and Development Program (Major Scientific and Technological Innovation Project) (2021CXGC010506), and Clinical Research Center of Shandong University (No. 2020SDUCRCC022).

Acknowledgments

The authors offer sincere gratitude to Xue-jun Shao, Yong-hang Lai, and Jian Feng for the technical support of the artificial intelligence algorithm and Suzette Pearl and Editage (www.editage.cn) for English polishing.

Conflict of interest

The authors declare that the research was conducted in the absence of any commercial or financial relationships that could be construed as a potential conflict of interest.

Publisher's note

All claims expressed in this article are solely those of the authors and do not necessarily represent those of their affiliated organizations, or those of the publisher, the editors and the reviewers. Any product that may be evaluated in this article, or claim that may be made by its manufacturer, is not guaranteed or endorsed by the publisher.

Supplementary material

The Supplementary Material for this article can be found online at: https://www.frontiersin.org/articles/10.3389/fonc.2022.945904/full#supplementary-material

References

1. Bray F, Ferlay J, Soerjomataram I, Siegel R, Torre L, Jemal A. Global cancer statistics 2018: Globocan estimates of incidence and mortality worldwide for 36 cancers in 185 countries. *CA: Cancer J Clin* (2018) 68(6):394–424. doi: 10.3322/caac.21492

2. Katai H, Ishikawa T, Akazawa K, Isobe Y, Miyashiro I, Oda I, et al. Five-year survival analysis of surgically resected gastric cancer cases in Japan: A retrospective analysis of more than 100,000 patients from the nationwide registry of the Japanese gastric cancer association (2001–2007). *Gastric Cancer* (2018) 21(1):144–54. doi: 10.1007/s10120-017-0716-7

3. Kato M, Kaise M, Yonezawa J, Toyoizumi H, Yoshimura N, Yoshida Y, et al. Magnifying endoscopy with narrow-band imaging achieves superior accuracy in the differential diagnosis of superficial gastric lesions identified with white-light endoscopy: A prospective study. *Gastrointest Endosc* (2010) 72(3):523–9. doi: 10.1016/j.gie.2010.04.041

4. Ezoe Y, Muto M, Uedo N, Doyama H, Yao K, Oda I, et al. Magnifying narrowband imaging is more accurate than conventional white-light imaging in diagnosis of gastric mucosal cancer. *Gastroenterology* (2011) 141(6):2017–25.e3. doi: 10.1053/j.gastro.2011.08.007

5. Yamada S, Doyama H, Yao K, Uedo N, Ezoe Y, Oda I, et al. An efficient diagnostic strategy for small, depressed early gastric cancer with magnifying narrow-band imaging: A post-hoc analysis of a prospective randomized controlled trial. *Gastrointest Endosc* (2014) 79(1):55–63. doi: 10.1016/j.gie.2013.07.008

6. Yao K, Doyama H, Gotoda T, Ishikawa H, Nagahama T, Yokoi C, et al. Diagnostic performance and limitations of magnifying narrow-band imaging in screening endoscopy of early gastric cancer: A prospective multicenter feasibility study. *Gastric Cancer* (2014) 17(4):669–79. doi: 10.1007/s10120-013-0332-0

7. Muto M, Yao K, Kaise M, Kato M, Uedo N, Yagi K, et al. Magnifying endoscopy simple diagnostic algorithm for early gastric cancer (Mesda-G). *Digest Endosc* (2016) 28(4):379–93. doi: 10.1111/den.12638

8. Neumann H, Fujishiro M, Wilcox C, Mönkemüller K. Present and future perspectives of virtual chromoendoscopy with I-scan and optical enhancement technology. *Digest Endosc* (2014) 26(S1):43–51. doi: 10.1111/den.12190

9. Nakanishi H, Doyama H, Ishikawa H, Uedo N, Gotoda T, Kato M, et al. Evaluation of an e-learning system for diagnosis of gastric lesions using magnifying narrow-band imaging: A multicenter randomized controlled study. *Endoscopy* (2017) 49(10):957–67. doi: 10.1055/s-0043-111888

10. Yoo C, Park M, Park S, Moon W, Kim H, Song J, et al. Observer variability in gastric neoplasm assessment using the vessel plus surface classification for magnifying endoscopy with narrow band imaging. *Clin Endosc* (2014) 47(1):74–8. doi: 10.5946/ce.2014.47.1.74

11. Luo H, Xu G, Li C, He L, Luo L, Wang Z, et al. Real-time artificial intelligence for detection of upper gastrointestinal cancer by endoscopy: A multicentre, case-control, diagnostic study. *Lancet Oncol* (2019) 20(12):1645–54. doi: 10.1016/s1470-2045(19)30637-0

12. Urban G, Tripathi P, Alkayali T, Mittal M, Jalali F, Karnes W, et al. Deep learning localizes and identifies polyps in real time with 96% accuracy in screening colonoscopy. *Gastroenterology* (2018) 155(4):1069–78.e8. doi: 10.1053/j.gastro.2018.06.037

13. Qu J, Li Z, Su J, Ma M, Xu C, Zhang A, et al. Development and validation of an automatic image-recognition endoscopic report generation system: A multicenter study. *Clin Trans Gastroenterol* (2020) 12(1):e00282. doi: 10.14309/ctg.0000000000000282

14. Li L, Chen Y, Shen Z, Zhang X, Sang J, Ding Y, et al. Convolutional neural network for the diagnosis of early gastric cancer based on magnifying narrow band imaging. *Gastric Cancer* (2020) 23(1):126–32. doi: 10.1007/s10120-019-00992-2

15. Horiuchi Y, Aoyama K, Tokai Y, Hirasawa T, Yoshimizu S, Ishiyama A, et al. Convolutional neural network for differentiating gastric cancer from gastritis using magnified endoscopy with narrow band imaging. *Dig Dis Sci* (2020) 65 (5):1355–63. doi: 10.1007/s10620-019-05862-6

16. Horiuchi Y, Hirasawa T, Ishizuka N, Tokai Y, Namikawa K, Yoshimizu S, et al. Performance of a computer-aided diagnosis system in diagnosing early gastric cancer using magnifying endoscopy videos with narrow-band imaging (with videos). *Gastrointest Endosc* (2020) 92(4):856–65.e1. doi: 10.1016/j.gie.2020.04.079

17. Bossuyt P, Reitsma J, Bruns D, Gatsonis C, Glasziou P, Irwig L, et al. Towards complete and accurate reporting of studies of diagnostic accuracy: The stard initiative. *Ann Internal Med* (2003) 138(1):40–4. doi: 10.7326/0003-4819-138-1-200301070-00010

18. Dixon M. Gastrointestinal epithelial neoplasia: Vienna revisited. *Gut* (2002) 51(1):130–1. doi: 10.1136/gut.51.1.130

19. Kim YJ, Park JC, Kim JH, Shin SK, Lee SK, Lee YC, et al. Histologic diagnosis based on forceps biopsy is not adequate for determining endoscopic treatment of gastric adenomatous lesions. *Endoscopy* (2010) 42(8):620–6. doi: 10.1055/s-0030-1255524

20. Miwa K, Doyama H, Ito R, Nakanishi H, Hirano K, Inagaki S, et al. Can magnifying endoscopy with narrow band imaging be useful for low grade adenomas in preoperative biopsy specimens? *Gastric Cancer* (2012) 15(2):170–8. doi: 10.1007/s10120-011-0093-6

21. Hwang JW, Bae YS, Kang MS, Kim JH, Jee SR, Lee SH, et al. Predicting pre- and post-resectional histologic discrepancies in gastric low-grade dysplasia: A comparison of white-light and magnifying endoscopy. *J Gastroenterol Hepatol* (2016) 31(2):394–402. doi: 10.1111/jgh.13195

22. Yao K, Anagnostopoulos G, Ragunath K. Magnifying endoscopy for diagnosing and delineating early gastric cancer. *Endoscopy* (2009) 41(5):462–7. doi: 10.1055/s-0029-1214594

23. J Redmon, S Divvala, R Girshick, A Farhadi eds. You only look once: Unified, real-time object detection. *Computer Vision and Pattern Recognition* (2016). p. 779–88. doi: 10.1109/CVPR.2016.91

24. Ueyama H, Kato Y, Akazawa Y, Yatagai N, Komori H, Takeda T, et al. Application of artificial intelligence using a convolutional neural network for diagnosis of early gastric cancer based on magnifying endoscopy with narrow-band imaging. *J Gastroenterol Hepatol* (2020) 21(4):653–60. doi: 10.1111/jgh.15190

25. Carpenter H, Talley N. Gastroscopy is incomplete without biopsy: Clinical relevance of distinguishing gastropathy from gastritis. *Gastroenterology* (1995) 108 (3):917–24. doi: 10.1016/0016-5085(95)90468-9

frontiers | Frontiers in Oncology

TYPE Case Report
PUBLISHED 08 August 2022
DOI 10.3389/fonc.2022.948892

Check for updates

OPEN ACCESS

EDITED BY
Zhendong Jin,
Second Military Medical University, China

REVIEWED BY
Taiki Hakozaki,
Tokyo Metropolitan Komagome Hospital, Japan
Pedro Guerra-Canchari,
National University of San Marcos, Peru

*CORRESPONDENCE
Xiaoping Qian
xiaopingqian@nju.edu.cn

SPECIALTY SECTION
This article was submitted to Gastrointestinal Cancers: Colorectal Cancer, a section of the journal Frontiers in Oncology

RECEIVED 20 May 2022
ACCEPTED 06 July 2022
PUBLISHED 08 August 2022

CITATION
Han L, Ding N, Li L, Wei X, Hu J, Liu B and Qian X (2022) Hepatoid adenocarcinoma of the duodenal papilla with hepatic metastases: A case report and literature review. *Front. Oncol.* 12:948892. doi: 10.3389/fonc.2022.948892

COPYRIGHT
© 2022 Han, Ding, Li, Wei, Hu, Liu and Qian. This is an open-access article distributed under the terms of the Creative Commons Attribution License (CC BY). The use, distribution or reproduction in other forums is permitted, provided the original author(s) and the copyright owner(s) are credited and that the original publication in this journal is cited, in accordance with accepted academic practice. No use, distribution or reproduction is permitted which does not comply with these terms.

Hepatoid adenocarcinoma of the duodenal papilla with hepatic metastases: A case report and literature review

Lu Han[1,2], Naiqing Ding[2], Li Li[2], Xiao Wei[2], Jing Hu[2], Baorui Liu[2] and Xiaoping Qian[1,2]*

[1]Nanjing Drum Tower Hospital Clinical College of Traditional Chinese and Western Medicine, Nanjing University of Chinese Medicine, Nanjing, China, [2]The Comprehensive Cancer Centre of Drum Tower Hospital, Medical School of Nanjing University, Nanjing, China

Hepatoid adenocarcinoma of the duodenum is a rare special type of adenocarcinoma, featured by hepatocyte components in primary adenocarcinoma of the duodenum. It has the characteristics of high malignancy, invasiveness, rapid progress, and poor prognosis. An abnormal elevation of serum alpha-fetoprotein (AFP) may occur in most cases. The diagnosis is mainly based on pathological morphology. Here, we reported a case of hepatic adenocarcinoma of the duodenum. The middle-aged female patient had an ampulla mass at diagnosis and received radical pancreaticoduodenectomy. The postoperative pathology was stage IIIA duodenal adenocarcinoma. At 1 month after surgery, she had multiple intrahepatic metastases and retroperitoneal lymph node metastasis; the AFP level was 300 ng/ml at that time. As she refused target therapy, two cycles of capecitabine-oxaliplatin (XELOX) chemotherapy were performed. However, the AFP elevated from 300 to 1,931.90 ng/ml, and the disease progressed rapidly. Immunohistochemistry (IHC) of tissue samples from presurgical endoscopic ultrasound guided fine needle aspiration (EUS-FNA), surgery, and liver biopsy showed positive AFP staining. Combining the abnormal elevation of serum AFP and microscopic pathological morphology, this case is diagnosed as hepatoid adenocarcinoma of the duodenum with liver metastasis. The physical condition of this patient was too poor to receive follow-up treatment. She died of the rapid disease progression with an overall survival time of 161 days. Considering that in most patients with hepatoid adenocarcinoma the abnormal elevation of serum AFP occurs preoperatively and returns to normal postoperatively rather than normal before surgery and increased after surgery, the primary lesion is located in the stomach rather than the intestine, and the patients are more often older men rather than middle-aged women; this case is rare particularly. Therefore, reporting this case with complete case data may be helpful to further study, so as to improve the understanding of this special type of malignant tumor.

KEYWORDS

hepatoid adenocarcinoma of the duodenum, hepatoid adenocarcinoma, alpha-fetoprotein (AFP), immunohistochemical, hepatic metastases

Introduction

In 1970, Bourreille et al. (1) reported a case of hepatic metastasis from gastric adenocarcinoma with elevated serum alpha-fetoprotein (AFP) for the first time. In 1985, Ishikura et al. (2) proposed the term "hepatoid adenocarcinoma (HAC)". HAC is a particular type of adenocarcinoma named for its similarity to the histological morphology and immunophenotype of hepatocellular carcinoma (HCC). It is a rare type with an estimated annual incidence rate of 0.58–0.83 per million people (2–4) and mostly happened in older men (5, 6). HAC is highly invasive and prone to liver metastasis, and prognosis is very poor, with an average overall survival rate of 10–18 months (7). HAC can be found in almost all malignant tumors of the digestive tract, especially in the stomach, accounting for about 63% of all HACs, possibly due to the fact that the stomach and liver are derived from the same part of the embryo (5, 8, 9). In addition, HAC can also occur in ovaries, lungs, bladder, etc. (10–12), and its onset is rare in the intestinal tract, especially in the duodenum. With the keywords hepatoid adenocarcinoma, duodenum, only three published papers were searched in the PubMed databases, and an article based on Surveillance, Epidemiology, and End Results (SEER) database found that the incidence of HAC of the gastrointestinal tract including the duodenum (excluding the stomach) in all HACs was only 5% (13). The scarcity of numbers reflects the rarity of HAC of the duodenum. Because the incidence of this special type of tumor is extremely low, its pathogenesis is not clear at present. Ishikura et al. (2) studied gastric HAC and found that the foregut derivatives of the primitive digestive tube were closely related to the production of AFP, which may be caused by the deviation in the cell differentiation process leading to tumor differentiation into hepatocytes. Sporadic cases of HAC originating from the intestinal tract have also been reported, most of which were accompanied by elevated serum AFP (14–16). Liming et al. (17) believe that one possibility is that the intestinal tract can produce a small amount of AFP during embryonic development, which promotes the appearance of tubular adenocarcinoma and hepatoid differentiation regions. In addition, it may be due to the existence of stem cells with bidirectional differentiation potential in the intestinal tract, which promotes glandular epithelium and hepatocyte differentiation (18, 19). Ziwei et al. (20) also believe that HAC cells resemble totipotent cells, which can proliferate in the early stage; this conjecture explains the generally poor prognosis.

The clinical manifestations of HAC patients are usually non-specific and mostly depend on the specific location of the primary tumor. For example, patients with colorectal cancer (CRC) may have abdominal pain, fever, or hematochezia. When a tumor occurs in the ampulla and nipple area of the duodenum, clinical manifestations such as yellow skin, yellow eyes, and yellow urine (such as in this case) can be seen. In most cases, patients have abnormally elevated serum AFP expression, but normal serum AFP expression (for example, in the early stage of diagnosis of this case) can also be seen.

Here, we introduce a middle-aged female patient diagnosed with hepatic adenocarcinoma of the duodenum with hepatic metastases; serum AFP was normal at the time of diagnosis but increased significantly with the progression of the disease. As the patient refused genetic testing and targeted therapy, she was treated with two cycles of XELOX chemotherapy and subsequently died due to rapid progression.

Case presentation

Diagnosis

Our patient is a 59-year-old woman with a history of hypertension and hyperglycemia for more than 15 years without previous history of alcohol consumption or smoking nor history of liver disease. She presented with intermittent fever without obvious inducement for 3 weeks (specific time points in Figure 1) with the highest temperature of 39°, accompanied by jaundice, occasional nausea, vomiting, and slight discomfort in the right upper abdomen. Biochemical examination revealed glutamic-pyruvate transaminase (ALT) levels of 198 U/L, glutamic-oxaloacetic transaminase (AST) 131 U/L, total bilirubin (TBil) 68 μmol/L, and direct bilirubin (DBil) 35.1 μmol/L. Blood routine examination revealed no obvious abnormalities. CT of the chest and abdomen showed no obvious active lesions in both lungs but gallbladder enlargement and dilatation of intrahepatic and extrahepatic bile ducts, common bile duct, and main pancreatic duct. MRI of the abdomen showed low biliary obstruction, and the obstruction level was located on the ampulla. Considering the possibility of inflammatory lesions, local hospitals gave anti-infection, fluid rehydration, liver protection, and other symptomatic treatment, but no obvious relief of symptoms.

Abdominal color ultrasound was performed at the general surgery department of our hospital on 19 October 2020. It showed that there is a mass in the ampullary region with dilation of intrahepatic and extrahepatic bile ducts and main pancreatic duct. Moreover, enlargement of the gallbladder was also shown. No obvious abnormality was observed in the liver. CT of pancreatic vascular reconstruction showed a mass in the ampulla, surrounded by enlarged lymph nodes, and was considered malignant. The intrahepatic and extrahepatic bile ducts and pancreatic ducts were dilated, the gallbladder was enlarged, and no obvious abnormalities of the liver and retroperitoneal lymph nodes were observed (Figures 2A, D). Tumor marker AFP was 5.00 ng/ml (normal range 0–10 ng/ml) (Table 1). The pathological result of EUS-FNA was moderately to poorly differentiated ampullary adenocarcinoma (Figure 3A); the immunohistochemistry (IHC) of EUS-FNA was AFP (+) (Figure 3B).

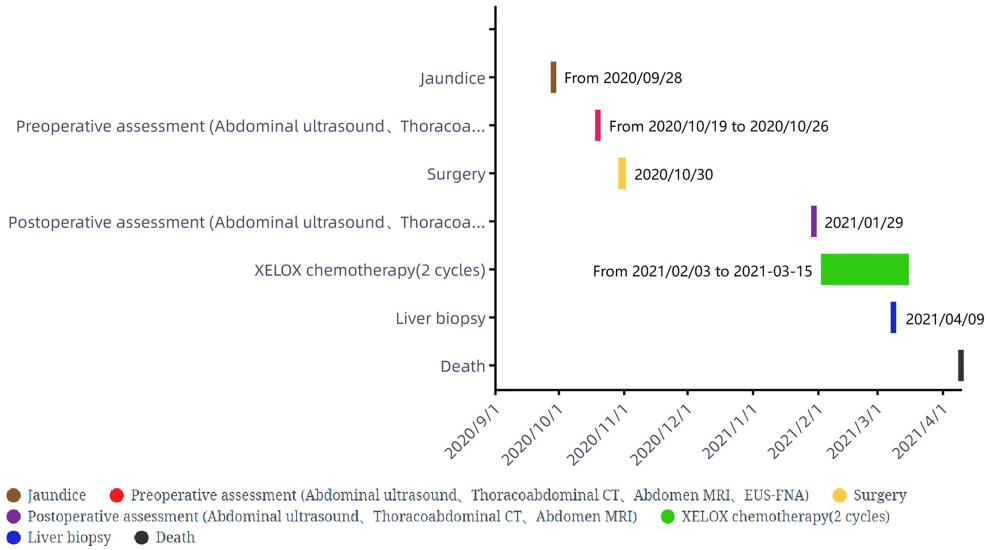

FIGURE 1
Time points corresponding to the diagnostic and therapeutic process.

Surgical intervention

After the patient was admitted to the hospital, the patient was evaluated with an Eastern Cooperative Oncology Group (ECOG) score result of 1. Physical examination revealed yellow skin and yellow sclera. The patient and family had no previous medical history of chronic viral hepatitis, bowel polyps, and inflammatory bowel disease (IBD). The patient underwent pancreaticoduodenectomy

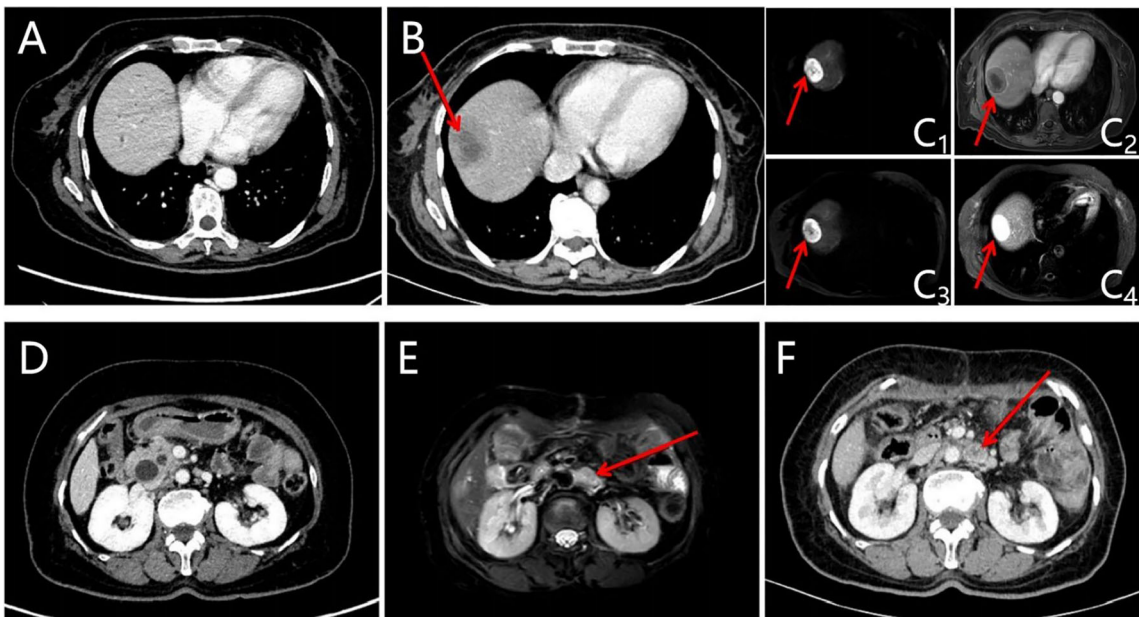

FIGURE 2
Images of the liver and retroperitoneal lymph node lesions were evaluated before and after the operation (new liver and retroperitoneal lymph node lesions after operation, shown by red arrows). **(A)** CT of liver before the operation; **(B)** CT of liver was evaluated at baseline after the operation; **(C)** MRI of the liver was evaluated at baseline after the operation (C_1: DWI-b50; C_2: T1WI; C_3: DWI-b800; C_4: T2WI); **(D)** CT of retroperitoneal lymph nodes before the operation; **(E)** CT of retroperitoneal lymph nodes was evaluated at baseline after the operation; **(F)** MRI of retroperitoneal lymph nodes was evaluated at baseline after the operation.

TABLE 1 Changes of Alpha-fetoprotein (AFP), Carcinoembryonic antigen (CEA) and Carbohydrate antigen 19-9 (CA19-9) levels at diagnosis, after the surgery, and after one cycle of chemotherapy.

Date	2020-10-18[a]	2021-01-29[b]	2021-03-04[c]
AFP (ng/ml)	5	330.9	1931.9
CEA (ng/ml)	54.31	22.56	25.62
CA19-9 (U/ml)	86.1	14.07	95.69

[a]Preoperative.
[b]after surgery.
[c]after one cycle of chemotherapy.

on 30 October 2020. Intraoperative exploration showed that there were no free ascites or metastatic nodules in the abdominal cavity, the liver had a normal size with cholestasis-like changes, and the gallbladder was swollen. A mass with a size of about 3 cm * 3 cm could be reached in the ampulla, and the texture was hard. Postoperative pathology (pancreaticoduodenectomy specimen) (Figure 3C) showed that the duodenal papilla had a poorly differentiated adenocarcinoma, the size of the mass was 4 cm * 2.5 cm * 1.2 cm, and the cancer tissue penetrated the duodenal muscle wall and invaded the pancreatic tissue. There is no definite cancer tissue invasion in the common bile duct. Vascular cancer embolus and perineural invasion can be seen. No cancer remains at the gastric margin, small intestinal margin, common bile duct margin, broken end margin of the pancreas, peripheral margin of the pancreas, and hook process margin of the pancreas. Cancer metastasis was found in 1/6 lymph nodes around the pancreas, and no cancer metastasis was found in 3 lymph nodes around the stomach, 1 lymph node around the intestine, and 2 lymph nodes around the common bile duct. Another 3 lymph nodes were sent, and no cancer metastasis was found. Pathological stage was IIIA (T4, N1, cM0); IHC: cancer cell expression CK(+), S100(-), Her2 (Sto)(++), COX2(+), VEGFR2(-), EGFR(++), Ki67(about 60%+), P16(focal +), CD56(-), PD-1(-), PD-L1(SP142)(the tumor cells -, interstitial immune cells about 5%+), MLH1(+), MSH2(+), MSH6 (+), PMS2(+), c-Met(+), CgA(-); AFP (+) (Figure 3D).

Baseline assessment

One month after surgery, CT and MRI scan showed multiple hepatic masses (Figures 2B, C) and retroperitoneal enlarged lymph nodes (Figures 2E, F), which were considered metastases. The patient refused to accept gene testing and targeted therapy, so one cycle of XELOX 3-week regimen chemotherapy was performed according to National Comprehensive Cancer Network (NCCN) guidelines for CRC.

Liver biopsy

After one cycle of chemotherapy, tumor marker AFP rose from 300 to 1,931.90 ng/ml (Table 1). In order to clarify the nature of the liver lesions, liver biopsy was performed. Microscopic observation showed that the tumor cells were distributed in plate shape, and abundant blood sinus structures were seen, adenocarcinoma area and hepatoid differentiation area coexist, polygonal tumor cells with larger volume and eosinophilic cytoplasm can be seen in the hepatoid differentiation area (Figure 4A). Liver biopsy pathology showed adenocarcinoma, poorly differentiated; IHC showed cancer cell expression Hept1 (-), CK19 (+++), CK7 (-), CDX-2 (focal +), Ki67 (70%+), CK20 (-), Villin (+++), Syn (focal +), CgA (focal +), CD56 (focal +); AFP (+), GPC-3 (+) (Figures 4B, C).

Combining the abnormal increase of serum AFP, microscopic pathological morphology and IHC features of tissue samples from

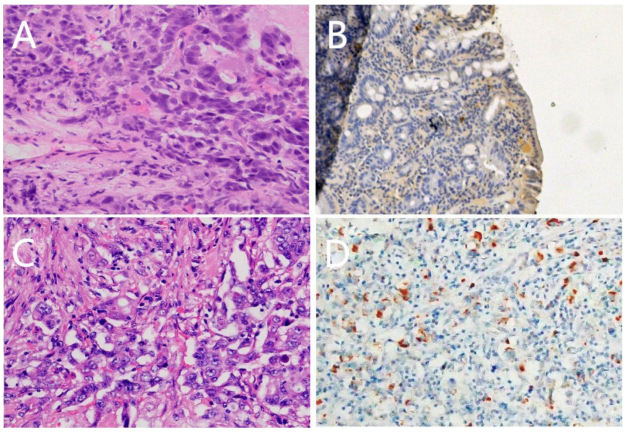

FIGURE 3
Pathological morphology **(A)** (HE ×400), expression of positive Alpha-fetoprotein(AFP) staining **(B)** (SP ×100) of tissue samples from presurgical endoscopic ultrasound-guided fine needle aspiration (EUS-FNA); Pathological morphology **(C)** (HE ×400), expression of positive Alpha-fetoprotein(AFP) staining **(D)** (SP ×100) of tissue samples fromsurgery.

presurgical EUS-FNS, surgery, and liver biopsy, this is a rare case of HAC of the duodenum with liver metastasis.

However, the disease progressed rapidly, and the patient died within 1 month after biopsy. The survival time was only 161 days. Patients and their families hope that the information they provide can help clinicians have a deeper understanding of this kind of diseases, thus helping more patients.

Discussion

This is a case report about the rare, highly malignant duodenum HAC. Because of the highly invasive and rapid progress nature of HAC, early diagnosis is particularly important. The diagnosis of HAC mainly depends on the pathological morphology; whatever the origin, most of them show similar morphological characteristics. Both adenocarcinoma and hepatoid differentiation areas can be observed in HAC. Adenocarcinoma areas are tubular in shape, and hepatoid differentiation areas have a similar arrangement to that of primary liver cancer. Furthermore, tumor cells in hepatoid differentiation areas have rich, eosinophilic or transparent staining cytoplasm, the nucleus is centered, mostly (quasi) circular or vacuolar, the nucleolus is large and obvious, mitotic images can be seen, and some of them have flake necrosis (21). Some scholars believe that the diagnosis of HAC can be established as long as the hepatoid differentiation area is found pathologically (22). However, the hepatoid differentiation area of HAC is mostly located in the deep part of the tumor, which makes the diagnosis extremely difficult. Important IHC markers included AFP, GPC-3, SALL4, and HSP70, among which the positive rate of AFP and GPC-3 was 85%~95% and 100%, respectively (22, 23). It is generally believed that AFP and GPC-3 are more specific markers in identifying hepatocyte differentiation areas and have been used as markers for the diagnosis of HAC routinely (24). In an analysis of 42 HAC cases reported by Zeng et al. (8), serum AFP levels were elevated in most patients with HAC, usually detected at extremely high levels (>1,000 ng/ml), while other serological biomarkers such as CEA and CA19-9 were consistently within the normal range, which were consistent with the clinical features of this patient. Abnormal elevation of serum AFP contributes to the objective diagnosis of the disease; however, the absence of a significant elevation of AFP could also be seen in some cases. The imaging features of HAC were not specific either, making it difficult to distinguish from other liver metastases (9). As HAC of the duodenum is rare and AFP staining is not included in routine IHC in CRC, it is difficult to conduct studies on large samples of this special type of tumor.

Gastric HAC is relatively more common than the others, so the research on this special type of tumor mostly focuses on gastric HAC. Clinical treatment of gastric HAC is usually preceded by radical gastrectomy. Radical gastrectomy combined with resection of liver metastases is feasible when liver metastasis is clearly identified and patient conditions permit. If radical resection of gastric lesions is not possible, surgical treatment is still recommended, and the surgical method should be changed to palliative gastrectomy. For patients with hepatic metastasis, palliative gastrectomy can be combined with other treatment methods, such as hepatic artery intubation chemotherapy (25). At present, there are no clear research results on the specific programs of postoperative adjuvant therapy (26). Simmet et al. (27) reported two cases of gastric HAC with hepatic metastasis, which achieved complete remission (CR) after first-line chemotherapy with cisplatin and etoposide, suggesting that cisplatin-based chemotherapy regimen may be the best choice for first-line chemotherapy for patients with gastric HAC. Due to the rarity of cases and lack of a large-sample randomized controlled study, the current clinical treatment strategy for patients with HAC of the duodenum is similar to that for CRC. Surgical treatment is the first choice, followed by chemotherapy and radiotherapy. It has been reported that the serum AFP level of HAC patients is correlated with prognosis. In most cases, the higher the level of serum AFP after the operation, the higher the rate of liver metastasis, and the worse prognosis (28). The reason may be that the increase of serum AFP can upregulate the expression of vascular endothelial growth factor receptor (VEGFR), which further leads to the formation of tumor emboli (29). However, whatever the level of AFP, the prognosis of patients with HAC is much worse than that of patients with normal adenocarcinoma. The average survival time is 10–18 months, and the 1-, 3-, and 5-year survival rates are 37.5%, 12.5%, and 8.3%, respectively (7).

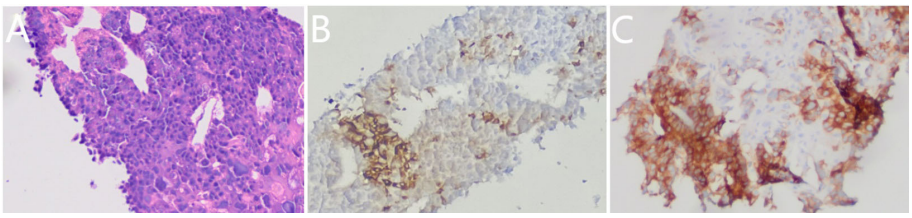

FIGURE 4
Pathological morphology **(A)** (HE ×100), expression of positive Alpha-fetoprotein(AFP) staining **(B)** (SP ×100) and positive glypican-3(GPC-3) staining **(C)** (SP ×100) in the liver metastases.

Most of the previously reported cases of HAC had a primary lesion in the stomach, and most of the cases showed abnormal elevation of serum AFP in the preoperative period; whereas in this case, the primary lesion was located in the duodenum, which is a rare site, and the elevation of serum AFP was observed in the postoperative period, which made the diagnosis of this case less precise. The reason for reporting this case is to draw the clinician's attention to the specific pathological type of HAC. When the pathological morphology of the tumor tissue tends to coexist with areas of adenocarcinoma and hepatoid differentiation, the possibility of HAC should be highly suspected and the accurate diagnosis should be identified as soon as possible. Moreover, the normal serum AFP at the time of diagnosis of the primary lesion cannot exclude the possibility of hepatocellular adenocarcinoma.

In conclusion, HAC of the duodenum is a rare special type of duodenal cancer with poor prognosis. It is often difficult to make a definite diagnosis in the early stage. The disease was not considered in the first EUS-FNA biopsy and pancreaticoduodenectomy; the diagnosis was made after the fast elevation of AFP and liver biopsy. It is suggested that for middle-aged and elderly patients, if the level of serum AFP increases and there is insufficient evidence for the diagnosis of hepatocellular carcinoma, HAC should be considered. Due to the low incidence rate, the treatment experience for this kind of disease is insufficient; targeted and effective standardized treatment remains to be explored.

In reviewing the paper, the following shortcomings remain, as there is no standard treatment regimen for this rare case, which is a common dilemma in the treatment of HAC. Focusing on this case, although the patient's symptoms were somewhat relieved by the systemic treatment described above, it is undeniable that the patient's survival was still relatively short and the exact mechanism of this is still to be explored in a pooled analysis of a large number of cases in order to find more effective treatment regimens.

Data availability statement

The original contributions presented in the study are included in the article/supplementary material. Further inquiries can be directed to the corresponding author.

Ethics statement

Written informed consent was obtained from the individual(s) for the publication of any potentially identifiable images or data included in this article.

Author contributions

ND and LL provided ideas for this case. XW, ND, LL, and BL drafted the manuscript and provided figures. LL, XW, JH, and XQ acquired, analyzed, and interpreted the data. ND, LL, XQ, and BL revised the manuscript critically for important intellectual content and agreed to be accountable for all aspects of the work in ensuring that questions related to the accuracy or integrity of any part of the work are appropriately investigated and resolved. All authors contributed to the article and approved the submitted version manuscript.

Funding

This study was supported by the Basic Research Project of Jiangsu Province (No. BK20211007).

Conflict of interest

The authors declare that the research was conducted in the absence of any commercial or financial relationships that could be construed as a potential conflict of interest.

Publisher's note

All claims expressed in this article are solely those of the authors and do not necessarily represent those of their affiliated organizations, or those of the publisher, the editors and the reviewers. Any product that may be evaluated in this article, or claim that may be made by its manufacturer, is not guaranteed or endorsed by the publisher.

References

1. Bourreille J, Metayer P, Sauger F, Matray F, Fondimare A. Existence of alpha feto protein during gastric-origin secondary cancer of the liver. *La Presse medicale* (1970) 78:1277–8.

2. Ishikura H, Fukasawa Y, Ogasawara K, Natori T, Tsukada Y, Aizawa M. An AFP-producing gastric carcinoma with features of hepatic differentiation. A case report. *Cancer* (1985) 56:840–8. doi: 10.1002/1097-0142(19850815)56:4<840::AID-CNCR2820560423>3.0.CO;2-E

3. Shen Z, Liu X, Lu B, Ye M. Hepatoid adenocarcinoma of the stomach: A case report of a rare type of gastri1c cancer. *Oncol Lett* (2016) 11:1077–80. doi: 10.3892/ol.2015.4023

4. Xiao C, Wu F, Jiang H, Teng L, Song F, Wang Q, et al. Hepatoid adenocarcinoma of the stomach: Nine case reports and treatment outcomes. *Oncol Lett* (2015) 10:1605–09. doi: 10.3892/ol.2015.3430

5. Su JS, Chen YT, Wang RC, Wu CY, Lee SW, Lee TY. Clinicopathological characteristics in the differential diagnosis of hepatoid adenocarcinoma: A literature review. *World J Gastroenterol* (2013) 19:321–7. doi: 10.3748/wjg.v19.i3.321

6. Inagawa S, Shimazaki J, Hori M, Yoshimi F, Adachi S, Kawamoto T, et al. Hepatoid adenocarcinoma of the stomach. *Gastric Cancer Off J Int Gastric Cancer Assoc Japanese Gastric Cancer Assoc* (2001) 4:43–52. doi: 10.1007/s101200100016

7. Zhihong H, Gengxu LIU. Clinical significance of AFP in diagnosis and monitoring of intestinal hepatoid adenocarcinoma. *J Hunan Normal University (Medical Science)* (2015) 12:49–51.

8. Zeng X, Zhang P, Xiao H, Wu X, Liu W, He J, et al. Clinicopathological features and prognosis of intestinal hepatoid adenocarcinoma: evaluation of a pooled case series. *Oncotarget* (2018) 9:2715–25. doi: 10.18632/oncotarget.23595

9. Yang J, Wang R, Zhang W, Zhuang W, Wang M, Tang C. Clinicopathological and prognostic characteristics of hepatoid adenocarcinoma of the stomach. *Gastroenterol Res Pract* (2014) 2014:140587. doi: 10.1155/2014/140587

10. Hou Z, Xie J, Zhang L, Dai G, Chen Y, He L. Hepatoid adenocarcinoma of the lung: A systematic review of the literature from 1981 to 2020. *Front Oncol* (2021) 11:702216. doi: 10.3389/fonc.2021.702216

11. Sinard J, Macleay LJr., Melamed J. Hepatoid adenocarcinoma in the urinary bladder. unusual localization of a newly recognized tumor type. *Cancer* (1994) 73:1919–25. doi: 10.1002/1097-0142(19940401)73:7<1919::AID-CNCR2820730724>3.0.CO;2-L

12. Hoshida Y, Nagakawa T, Mano S, Taguchi K, Aozasa K. Hepatoid adenocarcinoma of the endometrium associated with alpha-fetoprotein production. *Int J gynecological Pathol Off J Int Soc Gynecological Pathologists* (1996) 15:266–9. doi: 10.1097/00004347-199607000-00012

13. Wang W, Li G. Incidence and prognostic factors of hepatoid adenocarcinoma: A population-based analysis. *Trans Cancer Res* (2020) 9:5401–10. doi: 10.21037/tcr-20-1126

14. Tong L, Pan H, He J, Weng M, Zheng L. Hepatoid adenocarcinoma arising from heterotopic pancreas of the ileum: A case report. *Medicine* (2016) 95:e4067. doi: 10.1097/MD.0000000000004067

15. Ogbonna OH, Sakruti S, Sulieman M, Ali A, Shokrani B, Oneal P. Hepatoid adenocarcinoma of the duodenum: An unusual location. *Case Rep Oncol* (2016) 9:182–7. doi: 10.1159/000444746

16. Chen Y, Schaeffer DF, Yoshida EM. Hepatoid adenocarcinoma of the colon in a patient with inflammatory bowel disease. *World J Gastroenterol* (2014) 20:12657–61. doi: 10.3748/wjg.v20.i35.12657

17. Liming L, Wenpeng H, Huiping Z, Rui W, Pan W, Jianpo G. CT and clinical manifestations of hepatoid adenocarcinoma of stomach. *Chin J Med Imaging Technol* (2022) 38:713–6. doi: 10.13929/j.issn.1003-3289.2022.05.018

18. Borgonovo G, Razzetta F, Assalino M, Varaldo E, Puglisi M, Ceppa P. Rectal hepatoid carcinoma with liver metastases in a patient affected by ulcerative colitis. *Hepatobiliary pancreatic Dis Int HBPD Int* (2008) 7:539–43.

19. Cappetta A, Bergamo F, Mescoli C, Lonardi S, Rugge M, Zagonel V. Hepatoid adenocarcinoma of the colon: What should we target? *Pathol Oncol Res POR* (2012) 18:93–6. doi: 10.1007/s12253-011-9424-5

20. Ziwei XU, Chunyan Z, Yifei F, Yong W, Zan B, Yaoming S. Hepatoid adenocarcinoma misdiagnosed as primary liver cancer: A case report and literature review. *Chin J Colorectal Diseases(Electronic Edition)* (2019) 8:80–4.

21. Jixin Z, Lifang C, Quan Z, Hong C. Hepatoid adenocarcinoma of colon: A case report and literature review. *Chin J Clin Exp Pathol* (2013) 29:1366–8.

22. Metzgeroth G, Ströbel P, Baumbusch T, Reiter A, Hastka J. Hepatoid adenocarcinoma - review of the literature illustrated by a rare case originating in the peritoneal cavity. *Onkologie* (2010) 33:263–9. doi: 10.1159/000305717

23. Hishinuma M, Ohashi KI, Yamauchi N, Kashima T, Uozaki H, Ota S, et al. Hepatocellular oncofetal protein, glypican 3 is a sensitive marker for alpha-fetoprotein-producing gastric carcinoma. *Histopathology* (2006) 49:479–86. doi: 10.1111/j.1365-2559.2006.02522.x

24. Guoqing R, Ll Y, Xianglei H, Jianyu W, Wei W, Xin Z. Significance of combined expression of GPC3, HSP70, SALL4 and AFP in diagnosis of hepatoid adenocarcinoma of stomach. *Zhejiang Med* (2020) 42:780–2,6. doi: 10.12056/j.issn.1006-2785.2020.42.8.2019-2525

25. Mingjun Y, Xiaohui Y, Dezhong L. Research progress of hepatoid adenocarcinoma. *Chin J Cancer Prev Treat* (2020) 27:1940–4. doi: 10.16073/j.cnki.cjcpt.2020.23

26. Chao Y, Xiaofei A, Qin G. Clinical analysis of a case of AFP positive gastric cancer. *Chin J Integrated Traditional Western Med Digestion* (2015) 23:586–8. doi: 10.3969/j.issn.1671-038X.2015.08.21

27. Simmet V, Noblecourt M, Lizée T, Morvant B, Girault S, Soulié P, et al. Chemotherapy of metastatic hepatoid adenocarcinoma: Literature review and two case reports with cisplatin etoposide. *Oncol Lett* (2018) 15:48–54. doi: 10.3892/ol.2017.7263

28. Kong XX, Li XL, Tian Y, Ye QC, Xu XM, Liu Y, et al. The clinicopathological characteristics of alpha-Fetoprotein-Producing adenocarcinoma of the gastrointestinal tract-a single-center retrospective study. *Front Oncol* (2021) 11:635537. doi: 10.3389/fonc.2021.635537

29. Mukozu T, Nagai H, Matsui D, Kanekawa T, Sumino Y. Serum VEGF as a tumor marker in patients with HCV-related liver cirrhosis and hepatocellular carcinoma. *Anticancer Res* (2013) 33:1013–21.

frontiers | Frontiers in Oncology

TYPE Original Research
PUBLISHED 12 August 2022
DOI 10.3389/fonc.2022.980415

Check for updates

OPEN ACCESS

EDITED BY
Zhendong Jin,
Second Military Medical University, China

REVIEWED BY
Ting Tong,
Central South University, China
Yang Yanqi,
Sun Yat-sen Memorial Hospital, China

*CORRESPONDENCE
Haojie Huang
huanghaojie@smmu.edu.cn

†These authors have contributed equally to this work and share first authorship

SPECIALTY SECTION
This article was submitted to Gastrointestinal Cancers: Hepato Pancreatic Biliary Cancers, a section of the journal Frontiers in Oncology

RECEIVED 28 June 2022
ACCEPTED 25 July 2022
PUBLISHED 12 August 2022

CITATION
Xia C, Yin H, Zhang K, Wang Z, Yang X and Huang H (2022) The global research status and trends of the application of endoscopic ultrasonography in pancreatic tumors over the last decades: A bibliometric study. *Front. Oncol.* 12:980415. doi: 10.3389/fonc.2022.980415

COPYRIGHT
© 2022 Xia, Yin, Zhang, Wang, Yang and Huang. This is an open-access article distributed under the terms of the Creative Commons Attribution License (CC BY). The use, distribution or reproduction in other forums is permitted, provided the original author (s) and the copyright owner(s) are credited and that the original publication in this journal is cited, in accordance with accepted academic practice. No use, distribution or reproduction is permitted which does not comply with these terms.

The global research status and trends of the application of endoscopic ultrasonography in pancreatic tumors over the last decades: A bibliometric study

Chuanchao Xia[1†], Hua Yin[2†], Kecheng Zhang[3†], Zhenhuan Wang[4], Xiaoli Yang[2] and Haojie Huang[1*]

[1]Department of Gastroenterology, First Affiliated Hospital, Naval Medical University, Shanghai, China, [2]Department of Gastroenterology, General Hospital of Ningxia Medical University, Yinchuan, China, [3]Department of Biliary Tract Surgery, Eastern Hepatobiliary Surgery Hospital, Shanghai, China, [4]School of Biomedical Engineering and Technology, Tianjin Medical University, Tianjin, China

Background: To describe the development process and structural relationships of scientific achievements in endoscopic ultrasonography (EUS) in pancreatic tumors over the past decades and to reveal the key research topics using bibliometric analysis.

Methods: All relevant publications covering the research of EUS in pancreatic tumors from 1984 to 2021 were involved through the Web of Science Core Collection. R-bibliometrix was used to conduct the bibliometric analysis, and VOSviewer software was used to explore the hot spots and networks related to this field.

Results: Between 1984 and 2021, 4071 publications were involved. The number of annual publications increased from 1 to 310. The United States contributed the most publications to this field (n=1433, 35.20%), followed by Japan (n=827, 20.31%) and Germany (n=319, 7.84%). There was active cooperation between countries/regions. Gastrointestinal Endoscopy (GIE) was the most productive journal and the most influential journal. Professor Giovannini M, who produced the most publications, had a great influence on this research. The focus in this field was clarified by analyzing the top 10 citations and co-citations publications. Moreover, the analysis of the keywords showed Important topics: "Classification of pancreatic tumor disease" "Development of EUS in the diagnosis of pancreatic tumor diseases," and "Development of EUS in the treatment of pancreatic tumor diseases."

Conclusion: For the first time, bibliometric analysis was used to gain a deep understanding of the global trends of studies investigating EUS in pancreatic tumor diseases. The EUS field is rapidly evolving, and our study may be a critical reference for clinical researchers related to this field.

KEYWORDS

endoscopic ultrasonography (EUS), pancreatic tumors, bibliometric analysis, application, trend

Introduction

Flexible endoscopy was created in 1911, and ultrasound (US) followed in 1956. By combining ultrasonography and endoscopy, endoscopic ultrasonography (EUS) created an entirely new dimension in imaging (1). EUS was developed in the early 1980s, it places an ultrasound probe on the tip of the endoscope to directly observe the morphological structure and lesions of the mucosal surface as well as visualize the tube wall hierarchy, lesion origin, and infiltration depth using ultrasound technology. Due to the proximity of the US transducer to the lesion and the use of a high-frequency US probe, the picture resolution was improved (2).

The pancreas is a retroperitoneal organ, and traditional imaging diagnosis of pancreatic diseases is so inaccurate that malignant tumors are typically detected late in their progression, resulting in missed opportunities for surgery. Pancreatic neoplasms include benign pancreatic neoplasms and pancreatic malignancies, among which pancreatic cancer is one of the most deadly malignancies, with a fatality rate that is roughly equivalent to its incidence (3), and its five-year survival rate is still low. The aggressive biology, inefficient therapy, and advanced stages at the time of diagnosis all contribute to the disease's poor prognosis (4). As a result, detecting precursor lesions, early diagnosis, or effective treatment strategy may be a viable way for extending survival. Using EUS, images of the pancreas can be captured through the esophagus, stomach, and duodenum without being obstructed by gas, fat, or bone, and EUS also is allowed for tissue collection, making it the most widely used screening technology for early pancreatic tumors diagnosis (5, 6).

Lots of studies have shown that EUS and its related techniques, such as EUS elastography (EUS-EG), EUS-guided fine needle aspiration (EUS-FNA) and contrast-enhanced EUS (CE-EUS) are now considered to be the most sensitive imaging modality for the clinical diagnosis of pancreatic lesions, along with the detection of small cancers, the variability diagnosis of pancreatic solid or cystic lesions, and the staging of pancreatic lesions. Since the first clinical application of EUS in the 1980s, more than 30 years of development have changed various fields of gastroenterology. EUS has become a vital diagnostic and therapy tool, with more and more diagnostic and treatment recommendations recommending its use for inspection and treatment, particularly in pancreatic and gastrointestinal diseases (7).

It is expected that if we can analyze the recent research status of the application of EUS in pancreatic tumor diseases found in the literature that is presently available and explore the current research challenges and future research hotspots, we will be able to provide references for researchers interested in pancreatic tumors. Bibliometrics is the tool for achieving the aforementioned objectives. Using mathematical and statistical techniques, bibliometrics is the multidisciplinary study of all knowledge bearers, such as books, magazines, and other publications (8). It is a broad knowledge base that integrates philology, mathematics, and statistics with a focus on quantification. In addition to evaluating the contributions of various nations, institutions, journals, and scholars, bibliometric analysis can also describe a particular research area, foresee particular trends, and identify potential future research hotspots, all of which have a significant impact on disease prevention and treatment (9).

However, no study on the analysis of EUS in pancreatic tumors from a literature perspective exists, thus for the first time, we were able to acquire a comprehensive understanding of the global trends of studies examining EUS in pancreatic disease from multiple perspectives. Using the Web of Science (WOS), the goal of this study is to explore the content of the research literature on the application of EUS in pancreatic tumors. To provide a resource for clinical care and academic research in this area, we use the bibliometric strategies to conduct an extensive analysis of this field's research status throughout the previous decades, identify research trends, and predict probable future research hotspots.

Methods

Data source and collection

A comprehensive collection was conducted of all of the publications from the Web of Science Core Collection (WOSCC) from 1984 to 2021 with the following retrieval strategies:

[(endoscopic ultrasound) OR (endoscopic ultrasonography)] OR (EUS)] and [(Pancreatic cancer) or (PDAC) or (pancreatic tumor) or (pancreatic neoplasms) or (pancreatic cystic tumors)], and only "articles" was included. To avoid citation variations caused by frequent database updates, all related records were downloaded on May 4, 2022, and imported into relevant bibliometric tools for further analysis. All primary searches were independently performed by two authors (Xia and zhang), and their agreement showed considerable accordance. Figure 1 depicts the complete procedure of literature selection and screening.

Statistical analysis

We attempted to compile "The WOSCC Literature Analysis Report" to summarize publication features such as authors, nations, journals, institution status, annual publications, H index, and relations between authors or countries. By reviewing the most recent JCR (Journal Citation Reports) issue, a crucial tool for determining the academic effect of research, we obtained the most recent impact factor (IF) of the pertinent journals. The H-index is a statistic for evaluating an individual's contribution to scientific research (10). and the H-index, which reflects the academic influence of researchers or countries/regions, can be found on WOS.

We evaluated the number of publications and growth trends in various nations/areas using the bibliometrics online analytical platform. VOSviewer software was used to visualize keyword networks generated from related studies, allowing co-occurrence analysis to categorize terms into different clusters. The average year of appearance definition, which we used to gauge the relative novelty of terms, also colored each keyword when it first appeared.

Results

Annual output

According to the retrieval strategy, 6387 publications were included initially. 200 were excluded for unmatched document types, and 116 were excluded for published in 2022. In the end, 4071 "articles" were selected to perform analysis. The total number of publications worldwide was analyzed and an increasing trend in the total publishing has been demonstrated (from 1 in 1984 to 310 in 2021). The number of publications showed two stages: less before 2000 and more after 2000. The number of annual publications was more than 60 after 2000, more than 200 after 2014, and more than 300 in 2021 (the number was nearly 300 in 2018, and 2020). The annual publication outputs of the application of EUS in the pancreatic tumors field are shown in Figure 2. English was the most popular language in this subject, making up 94.92 percent of the total. German was the most prevalent non-English language, making up 2.11 percent of the total, followed by French (1.65%),

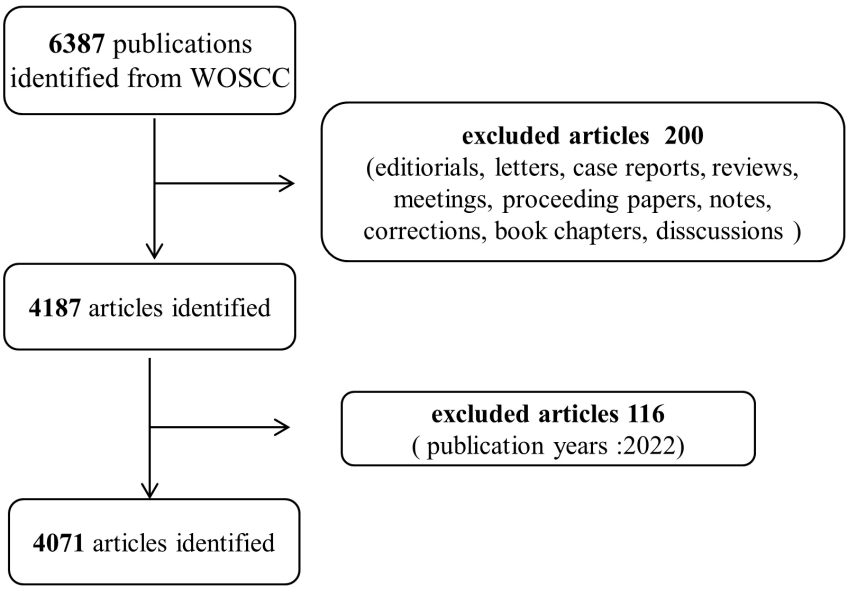

FIGURE 1
Flow diagram of literature selection and screening in this study.

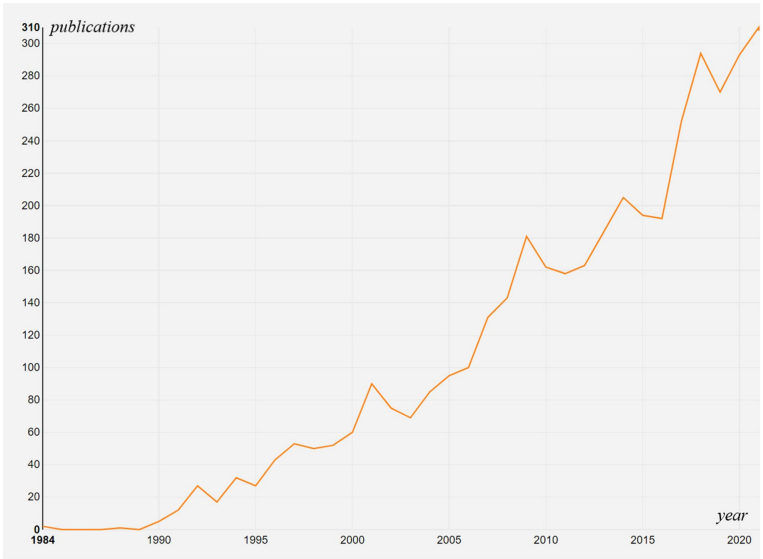

FIGURE 2
Times Cited and Publications Over Time.

Spanish (0.93%), and others such as Hungarian, Italian, Chinese, et al. are under 0.01%.

Country/region analysis

A total of 80 countries or regions participated in publishing articles on this research over the past few decades. The United States published the highest number of articles (n=1433, 35.20%), followed by Japan (n=827, 20.31%), Germany (n=319, 7.84%), France (n=280, 6.88%), Italy (n=264, 6.46%), China (n=225, 5.53%), South Korea (n=167, 4.10%), Spain (n=145, 3.56%), England (n=131, 3.22%), Netherlands (n=117, 2.87%). The top 10 countries/regions were showed in Figure 3. The outcomes of the cited frequency report from the WOSCC indicated that 4071 articles connected to this field were

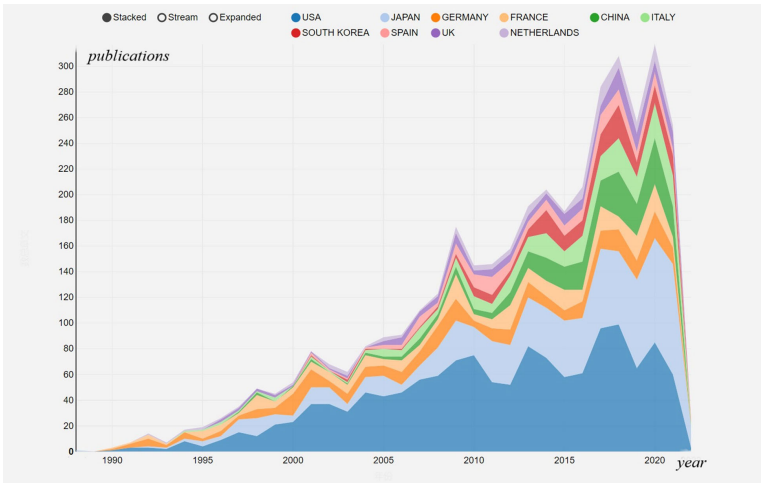

FIGURE 3
The contributions of different countries/regions to the research field.

referenced 119,150 times since 2001, and 90,462 times without self-citation. The average citation frequency per literature was 29.27, and the H-index was 141. The United States had the highest citation frequency (58,351 times, 51,569 times without self-citation). With an H-index of 116, the average number of citations per piece of literature was 49.72. With an H-index of 65, Japan's publications were mentioned 18,404 times (16,735 times without self-citation), placing it second among all nations.

We mapped the cooperation of countries and regions to have a better understanding of the extent of collaboration between them globally. Not only did the United States have the highest number of publications, but also had the closest international collaboration, which was shown by the U.S.'s prominent position in the co-occurrence network (Figure 4A). Active partnerships between nations and areas were shown on the visualization map; for instance, the USA had tight ties to Japan, Germany, France, and Italy (Figure 4B).

Journal analysis

Until 2021, a total of 607 scholarly journals had published articles on this research. There are 92 journals with more than 10 publications, 24 journals with more than 30, and 10 journals with more than 60, 5 journals with more than 100. The top 10 journals with the greatest contribution to this research accounted for 30.63% (1247/4071) of the total publications included in this study (Figure 5A). Gastrointestinal Endoscopy (GIE, IF2021 = 9.427, Q1) was the most productive journal contributing 341 scientific publications in this field, followed by Endoscopy (n=142, IF2020 = 10.093, Q1), Pancreas (n=140, IF2020 = 3.327, Q3), Pancreatology (n=124, IF2020 = 3.996, Q3), World Journal of Gastroenterology (n=111, IF2020 = 5.742, Q3). Moreover, the top 10 most influential journals were listed based on the H-index (Figure 5B). GIE, Endoscopy, American journal of gastroenterology, Pancreas and Clinical gastroenterology, and hepatology ranked top 5, which means that these academic journals probably have a significant influence on this field. In Figure 5C, we showed the close relations between these journals. Larger bubbles for GIE, Endoscopy, and Pancreas indicated more publications in those fields. Additionally, Endoscopy, the World Journal of Gastroenterology, Pancreas, and Pancreatology all had active citation agreements with GIE.

Author analysis

According to the number of publications, influential authors were evaluated. A total of 260 authors had published at least 10 articles, 60 authors with more than 20 articles, and 7 authors with more than 50 articles. The author with the most articles published among these was Giovannini M (n=66), followed by Yamao K (n=61), Brugge WR (n=59), and Palazzo L (n=58) (Figure 6A). Moreover, the citation number, h-index, and g-index were also used to evaluate the author's contributions. Citations in this field indicate that Brugge W ranked first (4388 citations), followed by Palazzo L (3896 citations) and Eloubeidi M (3237 citations) (Figure 6B).

The highest h-index was recorded by Eloubeidi M. (n=31), followed by publications from Brugge W (n=29) and Palazzo L (n=28) (Figure 6C). The publications' g-index from Eloubeidi M (n=50) was also first, followed by that from Palazzo L. (n=48) and Yamao K (n=47) (Figure 6D). Collaborations between the authors were depicted in the network map in Figure 6E.

Citation and co-citation of publications

The citation network map of Publications that have more than 200 citations was shown in Figure 7A. And the top 10 articles with the highest citations were shown in Table 1. There were 939 citations for the publication written by Brugge W et al. from the Journal of Gastroenterology in 2004, followed by the article published by Tanaka M et al. in the Journal of Pancreatology in 2017, with 647 citations, and Rosch T et al. in the Journal of New England Journal of Medicine in 1992, with 532 citations. The citation network map of references that were co-cited in more than 150 citations is shown in Figure 7B. With active co-cited corporations with "Varadarajulu S" and "Dewitt J," "Wiersema M" had the most publications among them all. In Table 2, the top 10 references with the most co-citations were presented. The top three references with the most citations were from Wiersema M [1997, 605 citations], Chang K [1997; 482 citations], and Brugge W [2004, 474 citations].

Analysis of keywords

We extracted keywords from the publications and analyzed co-occurrence *via* VOSviewer. A co-occurrence association was created between two keywords when they occurred in the same article. Strong co-occurring keywords can more precisely reveal research hotspots than a single term. A total of 100 keywords that were found to appear more than 50 times were used to construct the network visualization map (Figure 8A). And the top 10 keywords were diagnosis, cancer, management, pancreatic cancer, carcinoma, biopsy, tumors, pancreas, adenocarcinoma, lesions. The line that connects two terms in this keyword network map gets changed off as a sign. The number of occurrences was represented by the size of the bubble. The network visualization map's colors show the several clusters that the keywords formed. And in Figure 8B, each keyword was colored according to the moment when it emerged. The color of keywords served as a visual representation of when they first appeared, with blue implying an early introduction and yellow suggesting a more recent emergence.

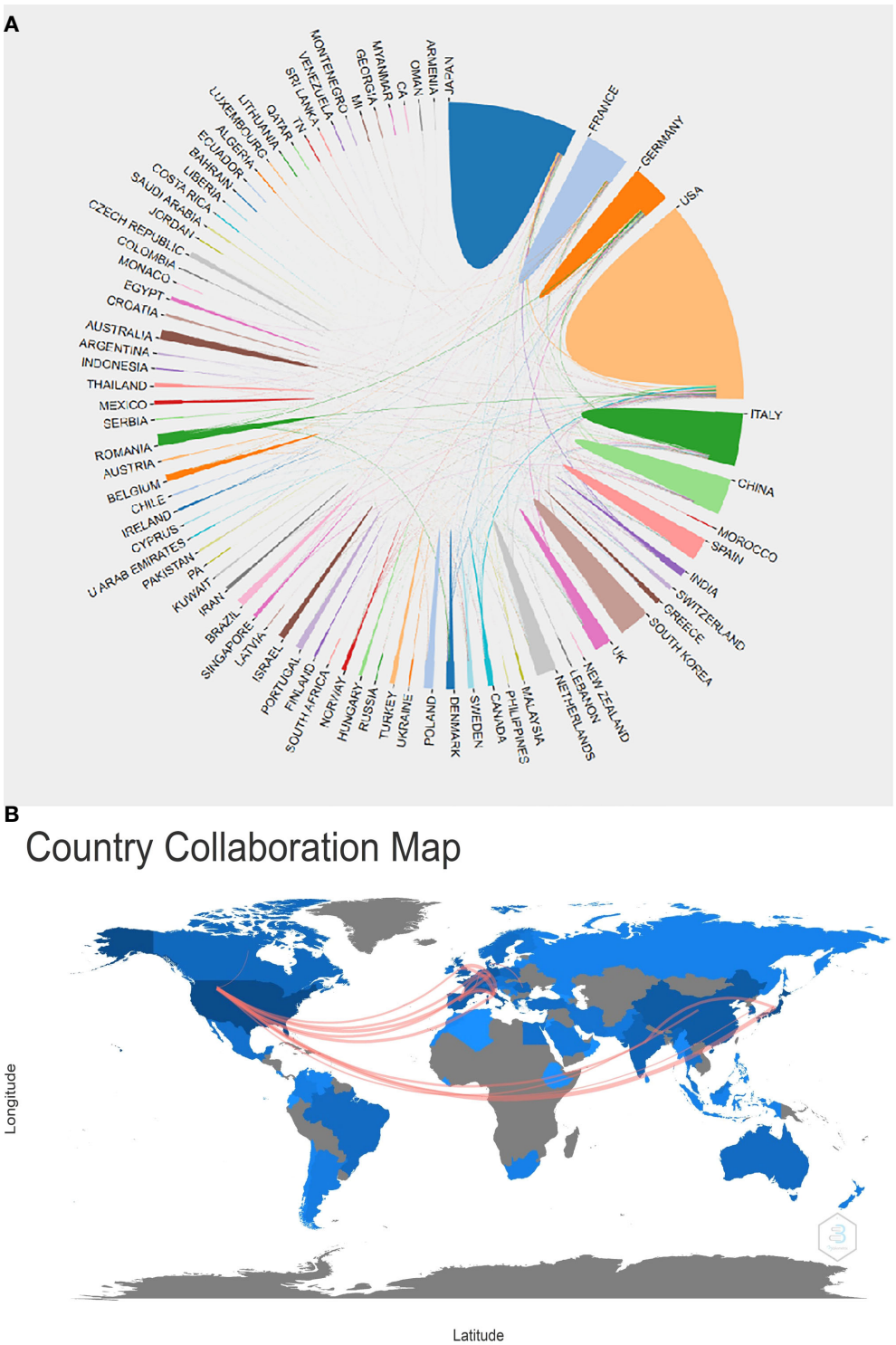

FIGURE 4
Country/region analysis. **(A)**The cooperation of countries/regions in this field from 1984 to 2021. **(B)** Country collaboration map in this field from 1984 to 2021.

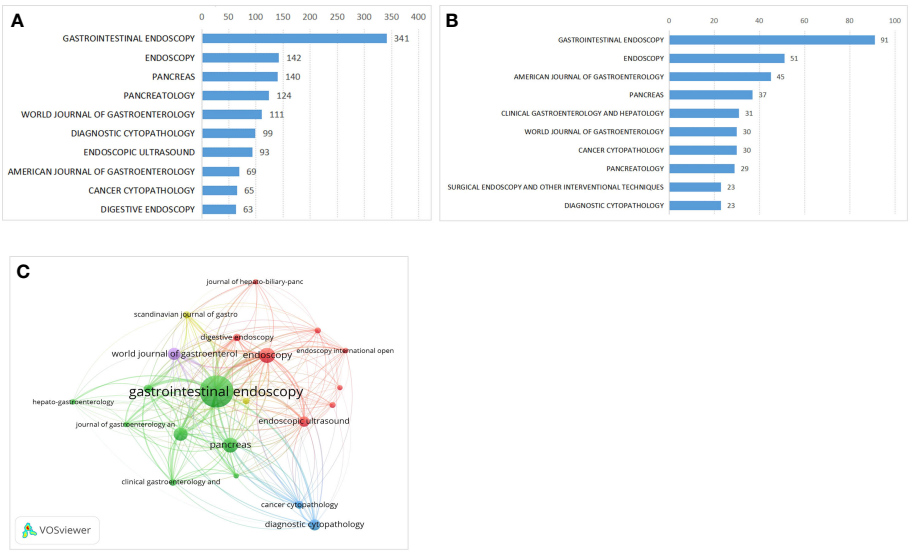

FIGURE 5
Journal distributions. **(A)** Top 10 journals of the publications, **(B)** Top 10 influential journals(H-Index). **(C)** The close relations between top 10 influential journals.

Discussion

Research trends

A bibliometric analysis was performed to introduce the development of EUS in pancreatic tumor diseases based on articles published from 1984 to 2021. In 1984, there was only one publication, which might because the area was still developing, but increased to 310 in 2020, especially in the last decade (2010-2021, the number of annual publications has exceeded 160), which reflects the hot research status in this field in recent years. Our investigation revealed a general upward trend in the annual production of this research, indicating that more people have been paying attention to it lately. The top five producing countries were the USA, Japan, Germany, France, and Italy, demonstrating their prominence in the field of this research. According to the country collaboration map, North America and Europe have produced the most articles among the top 20 nations, indicating that these two areas may have great potential for study and growth. These top contributing nations and regions were connected on the network map and nation collaboration map, demonstrating the research's global scope. This sort of international collaboration might promote academic exchange, draw better scientists to the topic, and speed up research on the application of EUS in pancreatic tumors.

Author analyses allow for a more thorough and unbiased assessment of researchers' contributions, the quality of their work, and their academic standing in a field of study. The 20 most productive authors in this area were also active scholars. Brugge W has the most citations, Eloubeidi M currently has the greatest h-index, and Giovannini M published the most publications. According to our study, the most well-known and respected authors in the field using these facts and indications may be identified. Notably, the majority of the authors were from organizations affiliated with universities and hospitals. Additionally, we evaluated the co-authorship of more than 20 papers and discovered that while there was some coordination and contact, it wasn't close. Therefore, author collaboration should be the main topic of future study. To put it another way, by identifying these leaders, we would be able to review the literature before starting new EUS-related research and quickly and accurately understand how this subject has developed.

As to the journals, the results showed that GIE, Endoscopy, Pancreas, Pancreatology, and World Journal of Gastroenterology were the most prevalent journals. The journals shown in the network map's co-citation frequency were closely related to one another in the field. This could guide new researchers who want to conduct their research and submit remarkable findings in this area. These journals mainly focus on clinical studies, and this research will mainly focus on the clinical field in the future.

Research status

The number of citations that an article obtains may be the most crucial bibliometric characteristic because it indicates how relevant and significant a study is in academic research. In this study, we analyzed the publications with citations from 1984 to

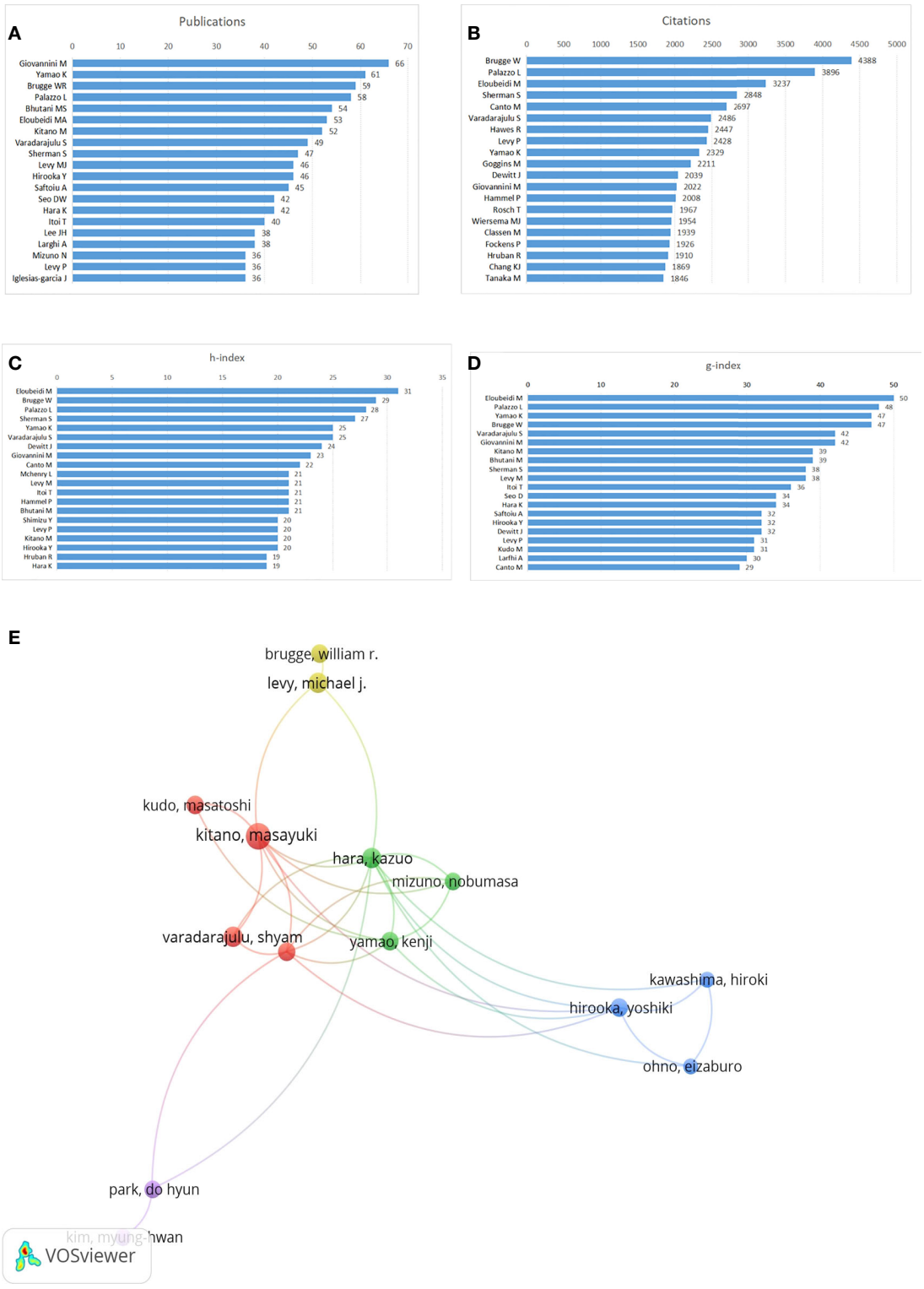

FIGURE 6
Author contributions. **(A)** Top 20 authors with the most publications, **(B)** Top 20 authors with the most ctiations, **(C)** h-index of publications from top 20 authors, **(D)** g-index of publications from top 20 authors, **(E)** Network map of co-authorship between authors with more than 30 publications.

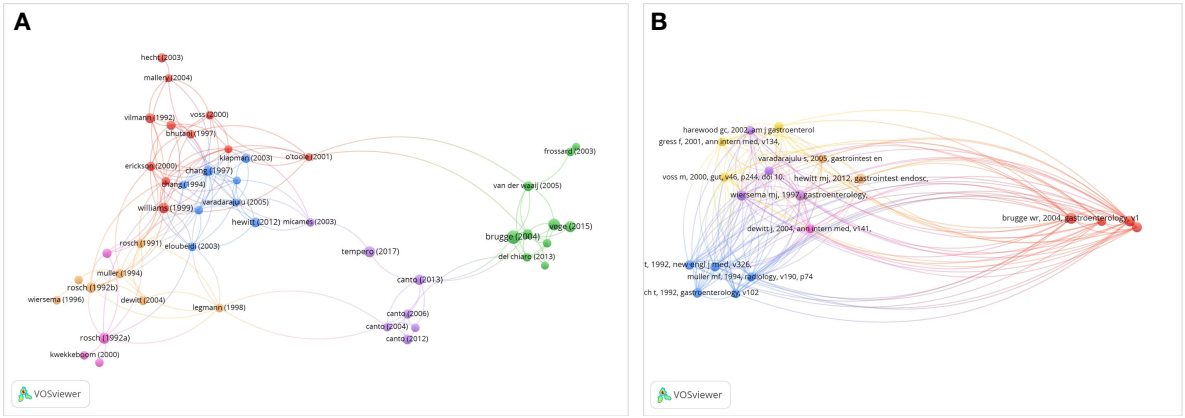

FIGURE 7
Network map of citation and co-citation publications. **(A)** Citation analysis of publications with more than 200 citations. **(B)** Co-citation analysis of references with more than 50 citations.

2021. And found that among the 4071 publications, 272 (6.69%) articles were cited more than 100 times. And the top 10 cited articles were listed in detail. Overall, eight of the top 10 publications were related to the diagnosis of EUS in pancreatic diseases, which indicated the vital function of EUS in the diagnosis of pancreatic diseases. According to keywords co-occurrence analysis, hotspots, subjects and trends are able to identify to guide researchers or clinicians to comprehend the

TABLE 1 Top 10 citation analysis of publications.

Rank	Author	Title	Source	Year	Country	Affiliation	Total Citation
1	Brugge W	Diagnosis of pancreatic cystic neoplasms: a report of the cooperative pancreatic cyst study	GASTROENTEROLOGY	2004	USA	Massachusetts General Hospital, Boston	934
2	Tanaka M	Revisions of international consensus Fukuoka guidelines for the management of IPMN of the pancreas	PANCREATOLOGY	2017	Japan	Shimonoseki City Hospital, Shimonoseki	647
3	Rosch T	Localization of pancreatic endocrine tumors by endoscopic ultrasonography	N ENGL J MED	1992	Germany	Technical University of Munich, Munich	532
4	Tempero M	Pancreatic Adenocarcinoma, Version 2.2017, NCCN Clinical Practice Guidelines in Oncology	J NATL COMPR CANCER NETW	2017	USA	University of California, San Francisco	529
5	Vege S	American gastroenterological association institute guideline on the diagnosis and management of asymptomatic neoplastic pancreatic cysts	GASTROENTEROLOGY	2015	USA	Mayo Clinic, Rochester	516
6	Williams D	Endoscopic ultrasound guided fine needle aspiration biopsy: a large single centre experience	GUT	1999	USA	Medical University of South Carolina, Charleston	484
7	Chang K	The clinical utility of endoscopic ultrasound-guided fine-needle aspiration in the diagnosis and staging of pancreatic carcinoma	GASTROINTEST ENDOSC	1997	USA	University of California, San Francisco	457
8	Canto M	International Cancer of the Pancreas Screening (CAPS) Consortium summit on the management of patients with increased risk for familial pancreatic cancer	GUT	2013	USA	Johns Hopkins University	443
9	Del Chiaro	European evidence-based guidelines on pancreatic cystic neoplasms	GUT	2018	USA	University of Colorado Cancer Center, Colorado	439
10	Hewitt M	EUS-guided FNA for diagnosis of solid pancreatic neoplasms: a meta-analysis	GASTROINTEST ENDOSC	2012	UK	Imperial College London, London	438

TABLE 2 Top 10 co-citation analysis of cited reference.

Rank	Author	Title	Source	Year	Country	Affiliation	Co-citations
1	Wiersema M	Endosonography-guided fine-needle aspiration biopsy: Diagnostic accuracy and complication assessment	GASTROENTEROLOGY	1997	USA	St Vincents Hosp, Indianapolis	605
2	Chang K	The clinical utility of endoscopic ultrasound-guided fine-needle aspiration in the diagnosis and staging of pancreatic carcinoma	GASTROINTEST ENDOSC	1997	USA	US Department of Veterans Affairs	482
3	Brugge W	Diagnosis of pancreatic cystic neoplasms: a report of the cooperative pancreatic cyst study	GASTROENTEROLOGY	2004	USA	Massachusetts General Hospital, Boston	474
4	Harewood G	Endosonography-guided fine needle aspiration biopsy in the evaluation of pancreatic masses	AM J GASTROENTEROL	2002	USA	Mayo Clinic, Rochester	461
5	Williams D	Endoscopic ultrasound guided fine needle aspiration biopsy: a large single centre experience	GUT	1999	USA	Medical University of South Carolina, Charleston	436
6	Rosch T	Endoscopic ultrasound in pancreatic tumor diagnosis	GASTROINTEST ENDOSC	1991	Germany	Technical University of Munich, Munich	433
7	Voss M	Value of endoscopic ultrasound guided fine needle aspiration biopsy in the diagnosis of solid pancreatic masses	GUT	2000	France	Beaujon Hospital, Clichy	425
8	Gress F	Endoscopic ultrasonography-guided fine-needle aspiration biopsy of suspected pancreatic cancer	ANN INTERN MED	2001	USA	Winthrop-University Hospital,Mineola	413
9	Eloubeidi M	Endoscopic ultrasound-guided fine needle aspiration biopsy of patients with suspected pancreatic cancer: Diagnostic accuracy and acute and 30-day complications	AM J GASTROENTEROL	2003	USA	Univ Alabama Birmingham,Birmingham	381
10	Palazzo L	Endoscopic ultrasonography in the diagnosis and staging of pancreatic adenocarcinoma. Results of a prospective study with comparison to ultrasonography and CT scan	ENDOSCOPY	1993	France	Beaujon Hospital, Clichy	359

development of related studies of EUS in pancreatic tumor diseases. In Figure 8, as was shown in the network map, the co-occurrences of keywords were analyzed and mainly clustered into three research subjects or trends. In this study, the hotpots of the progress of EUS in pancreatic diseases were as follows.

Classification of pancreatic tumor disease

Pancreatic tumor diseases were classified into benign tumors and malignant tumors. And benign included serous

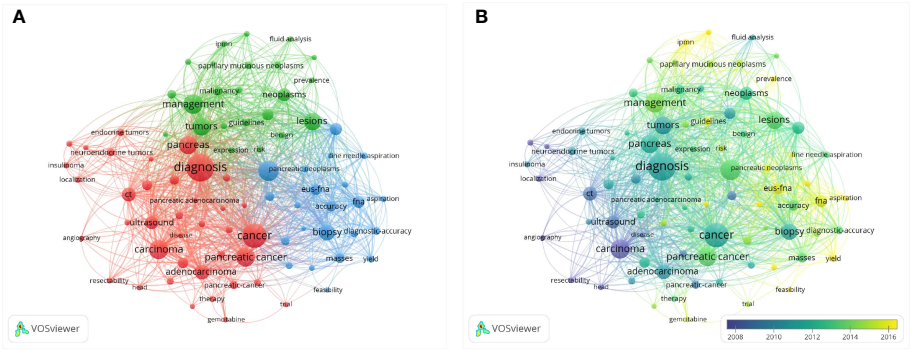

FIGURE 8
Co-occurrence analysis of keywords. **(A)** Network visualization map of keywords, **(B)** Overlay visualization map of keywords.

cystadenoma (SCN), pancreatic intraepithelial neoplasia (PanIN), mucinous cystic neoplasm (MCN), intraductal papillary mucinous neoplasm (IPMN), intraductal oncocytic papillary neoplasm (IOPN), intraductal tubulepapillary neoplasm (ITPN), and pancreatic neuroendocrine neoplasms (pNENs) (11). Among malignant tumors, pancreatic ductal adenocarcinoma (PDAC) has the highest incidence and malignancy, others included acinic cell carcinoma, pancreatic blastoma, and so on. Notably, endoscopic ultrasonography is crucial for the detection and management of both benign and malignant pancreatic tumors (12).

Development of EUS in the diagnosis of pancreatic tumor diseases

EUS can directly display the pancreatic tissue structure and the adjacent relationship of the surrounding organs. Compared with traditional imaging examination, EUS has a higher sensitivity and specificity in the diagnosis of pancreatic diseases and was recommended in guidelines. According to our study, the development of EUS in the diagnosis of pancreatic diseases were shown in detail.

In 1980, DiMagno. et al. (2) developed EUS for the evaluation of digestive diseases for the first time. As the whole pancreas can be visualized without any blind spots in the ultrasonographic images, EUS had gradually become an important diagnostic tool for pancreatic diseases. For the next decades, EUS was primarily used to aid in the diagnosis of pancreatic diseases. Strohm WD et al. (13) applied it to diagnose a pancreatic tumor in 1984 for the first time. However, on account of the lack of pathological confirmation of EUS, the clinical role of EUS had been restricted. But the advent of EUS-guided fine needle aspiration (EUS-FNA) offered a new diagnostic strategy for pancreatic tumor disease. In 1992, Peter et al. (14) successfully performed EUS-FNA on a patient with a pancreatic disease which could not be diagnosed by conventional methods, and obtained pancreatic tissue, which was suggested by pathology as mucinous cystic neoplasm. Pathological diagnosis, which cannot be obtained by EUS but could be acquired by EUS-FNA, is the gold standard for many diseases, which has promoted the development of EUS and made great progress. The method of EUS-FNA is not limited to pancreatic diseases, but applies to other lesions of the adjacent organs and structures.

In 1995, Kato et al. (15) in Japan first used the perfusion imaging approach in combination with EUS, an enhanced harmonic EUS has been developed, which was performed by injecting carbon dioxide through the angiographic catheter inserted into the celiac trunk or superior mesenteric artery during EUS circumferential scanning. Because of its advantages of high-resolution ultrasound and contrast-enhanced ultrasound, it is of great significance for distinguishing the characterization of solid and cystic pancreatic lesions, judging the stage of pancreatic cancer and vascular involvement (16). In 2002, Maurits J et al. (17) reported EUS-guided needle biopsy (EUS-TNB), which is similar to EUS-FNA but can obtain more reliable tissue for pathological diagnosis. In 2007, Janssen J et al. (EUS-EG 2007) reported the clinical use of EUS-elastography (EUS-EG) in pancreatic disease. EG is the technology that can image the differences of distortion between the soft tissue and the hard tissue in real-time. So it can study imaging of tumors and spreading diseases that cannot be detected by traditional ultrasound. Since then, EUS-EG has been widely used in the differential diagnosis of pancreatic solid mass, benign and malignant lymph nodes, gastrointestinal submucosal masses, and some other solid tumors. Endoscopic confocal laser endomicroscopy (CLE) is a new endoscopic confocal laser microscope that integrates traditional endoscopy under microscopic imaging technology, real-time histologic diagnosis in the endoscopic examination at the same time, through dynamic observation on the surface of the magnified 1000 times of particular organization cells, blood vessels, basement membrane, and stroma morphology and structure, and was called 'optical biopsy under endoscopy' (18). In 2011, Konda et al. (19) first applied this technique to evaluate the feasibility of nCLE of pancreatic lesions. Shortly afterward, the technique gradually matured and is mainly used in the differential diagnosis of pancreatic cystic lesions, solid pancreatic mass and enlarged lymph nodes.

Endoscopic ultrasonography (EUS) can perform personalized and real-time scanning of pancreatic lesions in the stomach or duodenal cavity at the nearest distance, and is one of the most sensitive methods for finding small pancreatic lesions. It can find lesions only 2mm in size, which has become one of the most accurate methods for locating pancreatic cancer and is conducive to the early detection of pancreatic cancer. Since its inception in the 1980s, this technique has played a huge role in the diagnosis of pancreatic diseases, especially with the development of assistive imaging, such as the CHE, EG, CLE and so on, and the development of EUS-FNA and EUS-FNB has brought the role of EUS to a new level. At present, EUS has been recommended as a critical diagnostic way in many clinical guidelines.

Development of EUS in the treatment of pancreatic tumor diseases

EUS not only can be used as a diagnostic tool for pancreatic diseases, but also has made significant breakthroughs in the transformation into minimally invasive intervention therapy with the continuous development of technological progress, and has become an important treatment method for pancreatic diseases.

EUS-guided ablation is a reliable treatment for patients with inoperable pancreatic diseases, high surgical risk, or rejection of surgery, mainly including ethanol ablation, mixed cryogenic ablation, radiofrequency ablation, photodynamic ablation, and laser ablation. EUS- radiofrequency ablation (RFA) is a novel tumor treatment method, which causes coagulation necrosis in surrounding tissues by releasing heat through a high-frequency current, and is widely used in the treatment of liver, lung and kidney tumors. Goldberg et al. (20) in 1999 reported the use of EUS-guided radiofrequency ablation for pancreatic diseases in porcine models for the first time. This study indicated that EUS-guided radiofrequency ablation can be used to produce coagulation necrosis in the porcine pancreas lesions. As technology continues to advance, it has become the most widely used way of ablation in the pancreas at present.

EUS-guided photodynamic ablation (PDT) is a tumor-specific ablative therapy that combines photosensitive drugs with EUS-guided light irradiation to produce oxygen-free radicals leading to cell death. Chan et al. (21) in 2003 first introduced the application of EUS-guided photodynamic therapy (PDT) in the pancreas. This study confirmed that EUS-PDT is safe and effective for advanced focal pancreatic cancer to a certain extent, but it remains to be further proved by further studies.

Pain is the most common complication in patients with pancreatic cancer, and peritoneal plexus block is a first-line adjuvant for the treatment of pain in patients with pancreatic cancer. Wiersema et al. (22) proposed in 1996 that EUS-celiac plexus neurolysis (CPN) could relieve the pain of patients with pancreatic patients. In addition, EUS-CPN can also improve the survival rate of patients with pancreatic cancer. Fuji-Lau et al. (23) showed in a case-control study that patients treated with EUS-CPN had a longer survival time compared with patients without. However, EUS-CPN does not eliminate pain, but only relieves it to some extent.

EUS-guided intratumoral fine-needle injection (EUS-FNI) is a relatively new targeted therapy that aims to maximize intratumoral drug concentration while minimizing systemic exposure and drug toxicity. As a result, it can be applied as a preoperative intervention to reduce tumor size or as a palliative care measure for unresectable tumors with obstructive symptoms. Currently, EUS-FNI can be used for a variety of interventions, including chemotherapy, immunotherapy, oncolytic virus therapy and tumor implantation. Chang et al. (24) in 2000 conducted the first clinical trial using EUS-FNI to directly inject anti-tumor agents into local cancer, which delivered allogeneic mixed lymphocyte cultures to unresectable pancreatic adenocarcinoma and the median survival of patients was 13.2 months with no operation-related complications. EUS-guided ethanol ablation is a novel alternative therapy for pancreatic cystic tumors and pancreatic neuroendocrine tumors in recent years, and its safety and feasibility have been reported in some studies (25, 26). EUS-FNI has precise localization and fewer adverse reactions, which can improve the clinical therapeutic effect of pancreatic masses.

Peripancreatic effusion is a common local complication after pancreatitis or pancreatic trauma. The fluid is divided into acute peripancreatic fluid accumulation, acute necrotic accumulation, pancreatic pseudocyst and walled-off necrosis (27). Pancreatic pseudocyst has clear cyst walls and few necrotic components, which usually appear 4 weeks after acute pancreatitis or pancreatic trauma, and a small part of them are secondary to chronic pancreatitis (28). The most common decompression indications of pancreatic pseudocyst are abdominal pain, infection, and biliary obstruction, and cysts (> 6cm in diameter) that continue to grow or remain unhealed for more than 6 weeks. Pancreatic abscesses and walled-off necrosis often need drainage intervention. Drainage is generally performed 4-6 weeks after the formation of peripancreatic effusion and full liquefaction of mature necrotic material in the capsule wall (29). In 1992, Grimm et al. (30) first proposed EUS-guided drainage therapy for pancreatic pseudocysts., which concluded that EUS-guided drainage is as effective as percutaneous drainage in the treatment of pancreatic pseudocysts.

Interstitial brachytherapy is an effective method for local control of pancreatic malignancies. Radioactive particles are implanted in and around the target tissue, exposing the target tissue to γ rays, resulting in local tissue damage and tumor ablation. Importantly, these radioactive seeds have a very low dose rate and penetration depth of no more than 1.7 cm, thus minimizing radiation exposure and damage to adjacent organs (31). Sun et al. (32) in 2005 showed for the first time in a pig model that the implantation of radioactive particles into pancreatic tissues guided by EUS is a safe and feasible brachytherapy method. The most popular radioactive particle is iodine-125, which has a half-life of 59.7 days and is suitable for fast-growing tumors such as pancreatic cancer.

Strengths and limitations

An objective quantitative analysis was made of the existing literatures by using bibliometrics. Researchers and clinicians' understanding of the worldwide presentation and patterns of EUS development in pancreatic tumors may be improved by these findings and recommendations. Our research has several advantages. First of all, this study for the first time used the bibliometrics analysis method with a deep insight to present the global development, status and trend of research on EUS in pancreatic tumor diseases. Secondly, our study uses widely used tools, which ensure the reliability of the data. Thirdly, bibliometric analysis is more thorough and objective than conventional literature evaluations. However, similar to other

bibliometric analyses, this study also has some limitations. First, we only searched articles in the WOS database; we did not search other databases like PubMed or Embase, thus some publications may have been missed. However, it is worth noting that the WOC is the one that is most frequently utilized in the bibliometric analysis. Secondly, there may be differences between bibliometric analysis results and actual research conditions. Our conclusions are based on research that has been published, however some crucial material might not have appeared in academic papers. Thirdly, there may not have been a thorough discussion in our research because some of the recently released significant articles may not have received enough attention from scholars. Despite these limitations, our study provides an elaborate global perspective on EUS of pancreatic tumor diseases research over the past five decades.

Conclusion

A thorough overview of the global research on EUS in pancreatic tumor diseases during the past decades was shown using bibliometric analysis. This topic is going through a period of tremendous development, and more scholars are becoming interested in it. Research results indicate that the USA contributed the most to productivity, and it connected closely with other countries, such as Japan, China, England, Germany, France, Italy, and Japan. And journals such as GIE, Endoscopy, Pancreas, Pancreatology and World Journal of Gastroenterology pay close attention to developments in the field. With the development of endoscopic technology and equipment, EUS has gradually developed from a simple diagnostic method to a significant part of interventional treatment of digestive system diseases, especially playing an important role in the diagnosis and treatment of pancreatic diseases. The topic of EUS in Pancreatic tumor diseases is worthy of continued follow-up by researchers, and we believe that this study contributes valuable information for researchers and clinicians.

Data availability statement

The original contributions presented in the study are included in the article/supplementary material. Further inquiries can be directed to the corresponding author.

Author contribution

CX: data collection and paper writing. HY: statistical analysis. KZ: interpretation of data. ZW and XY: literature search. HH: manuscript review. All authors contributed to the article and approved the submitted version.

Funding

Funded by the National Outstanding Youth Science Fund Project of National Natural Science Foundation of China (to H.J.H.), No. 82022008.

Conflict of interest

The authors declare that the research was conducted in the absence of any commercial or financial relationships that could be construed as a potential conflict of interest.

Publisher's note

All claims expressed in this article are solely those of the authors and do not necessarily represent those of their affiliated organizations, or those of the publisher, the editors and the reviewers. Any product that may be evaluated in this article, or claim that may be made by its manufacturer, is not guaranteed or endorsed by the publisher.

References

1. Cazacu IM, Luzuriaga Chavez AA, Saftoiu A, Vilmann P, Bhutani MS. A quarter century of EUS-FNA: Progress, milestones, and future directions. *Endosc Ultrasound* (2018) 7(3):141–60. doi: 10.4103/eus.eus_19_18

2. DiMagno EP, Buxton JL, Regan PT, Hattery RR, Wilson DA, Suarez JR, et al. Ultrasonic endoscope. *Lancet* (8169) 1980:1. doi: 10.1016/s0140-6736(80)91122-8

3. Xiao AY, Tan MLY, Wu LM, Asrani VM, Windsor JA, Yadav D, et al. Global incidence and mortality of pancreatic diseases: a systematic review, meta-analysis, and meta-regression of population-based cohort studies. *Lancet Gastroenterol Hepatol* (2016) 1(1):45–55. doi: 10.1016/s2468-1253(16)30004-8

4. Zhang Q, Zeng L, Chen Y, Lian G, Qian C, Chen S, et al. Pancreatic cancer epidemiology, detection, and management. *Gastroenterol Res Pract* (2016) 2016:8962321. doi: 10.1155/2016/8962321

5. Canto MI, Harinck F, Hruban RH, Offerhaus GJ, Poley JW, Kamel I, et al. International cancer of the pancreas screening (CAPS) consortium summit on the management of patients with increased risk for familial pancreatic cancer. *Gut* (2013) 62(3):339–47. doi: 10.1136/gutjnl-2012-303108

6. DaVee T, Coronel E, Papafragkakis C, Thaiudom S, Lanke G, Chakinala RC, et al. Pancreatic cancer screening in high-risk individuals with germline genetic mutations. *Gastrointest Endosc* (2018) 87(6):1443–50. doi: 10.1016/j.gie.2017.12.019

7. Saftoiu A, Hassan C, Areia M, Bhutani MS, Bisschops R, Bories E, et al. Role of gastrointestinal endoscopy in the screening of digestive tract cancers in Europe: European society of gastrointestinal endoscopy (ESGE) position statement. *Endoscopy* (2020) 52(4):293–304. doi: 10.1055/a-1104-5245

8. Agarwal P, Searls DB. Can literature analysis identify innovation drivers in drug discovery? *Nat Rev Drug Discovery* (2009) 8(11):865–78. doi: 10.1038/nrd2973

9. Sugimoto CR, Ahn YY, Smith E, Macaluso B, Larivière V. Factors affecting sex-related reporting in medical research: a cross-disciplinary bibliometric analysis. *Lancet* (2019) 393(10171):550–9. doi: 10.1016/s0140-6736(18)32995-7

10. Hirsch JE. An index to quantify an individual's scientific research output. *Proc Natl Acad Sci U S A* (2005) 102(46):16569–72. doi: 10.1073/pnas.0507655102

11. Nagtegaal ID, Odze RD, Klimstra D, Paradis V, Rugge M, Schirmacher P, et al. The 2019 WHO classification of tumours of the digestive system. *Histopathology* (2020) 76(2):182–8. doi: 10.1111/his.13975

12. Canakis A, Law R, Baron T. An updated review on ablative treatment of pancreatic cystic lesions. *Gastrointest Endosc* (2020) 91(3):520–6. doi: 10.1016/j.gie.2019.09.037

13. Strohm WD, Kurtz W, Hagenmüller F, Classen M. Diagnostic efficacy of endoscopic ultrasound tomography in pancreatic cancer and cholestasis. *Scand J Gastroenterol Suppl* (1984) 102:18–23.

14. Vilmann P, Jacobsen GK, Henriksen FW, Hancke S. Endoscopic ultrasonography with guided fine needle aspiration biopsy in pancreatic disease. *Gastrointest Endosc* (1992) 38(2):172–3. doi: 10.1016/s0016-5107(92)70385-x

15. Kato T, Tsukamoto Y, Naitoh Y, Hirooka Y, Furukawa T, Hayakawa T. Ultrasonographic and endoscopic ultrasonographic angiography in pancreatic mass lesions. *Acta Radiol* (1995) 36(4):381–7.

16. Worni M, Guller U, White RR, Castleberry AW, Pietrobon R, Cerny T, et al. Modest improvement in overall survival for patients with metastatic pancreatic cancer: a trend analysis using the surveillance, epidemiology, and end results registry from 1988 to 2008. *Pancreas* (2013) 42(7):1157–63. doi: 10.1097/MPA.0b013e318291fbc5

17. Janssen J, Schlörer E, Greiner L. EUS elastography of the pancreas: feasibility and pattern description of the normal pancreas, chronic pancreatitis, and focal pancreatic lesions. *Gastrointest Endosc* (2007) 65(7):971–8. doi: 10.1016/j.gie.2006.12.057

18. Anand K, Kahaleh M, Tyberg A. Use of needle-based confocal laser endomicroscopy in the diagnosis and management of pancreatic cyst lesions. *Endosc Ultrasound* (2018) 7(5):306–9. doi: 10.4103/eus.eus_46_18

19. Konda VJ, Aslanian HR, Wallace MB, Siddiqui UD, Hart J, Waxman I. First assessment of needle-based confocal laser endomicroscopy during EUS-FNA procedures of the pancreas (with videos). *Gastrointest Endosc* (2011) 74(5):1049–60. doi: 10.1016/j.gie.2011.07.018

20. Goldberg SN, Mallery S, Gazelle GS, Brugge WR. EUS-guided radiofrequency ablation in the pancreas: results in a porcine model. *Gastrointest Endosc* (1999) 50(3):392–401. doi: 10.1053/ge.1999.v50.98847

21. Chan HH, Nishioka NS, Mino M, Lauwers G, Brugge W. The use of endoscopic ultrasound (EUS)-guided photodynamic therapy (PDT) in the ablation of the pancreas: A pilot study. *Gastrointest Endosc* (2003) 57(5):AB242–2.

22. Wiersema MJ, Wiersema LM. Endosonography-guided celiac plexus neurolysis. *Gastrointest Endosc* (1996) 44(6):656–62. doi: 10.1016/s0016-5107(96)70047-0

23. Fujii-Lau LL, Bamlet WR, Eldrige JS, Chari ST, Gleeson FC, Abu Dayyeh BK, et al. Impact of celiac neurolysis on survival in patients with pancreatic cancer. *Gastrointest Endosc* (2015) 82(1):46–56.e2. doi: 10.1016/j.gie.2014.12.036

24. Chang KJ, Nguyen PT, Thompson JA, Kurosaki TT, Casey LR, Leung EC, et al. Phase I clinical trial of allogeneic mixed lymphocyte culture (cytoimplant) delivered by endoscopic ultrasound-guided fine-needle injection in patients with advanced pancreatic carcinoma. *Cancer* (2000) 88(6):1325–35. doi: 10.1002/(sici)1097-0142(20000315)88:6<1325::aid-cncr8>3.0.co;2-t

25. Gan SI, Thompson CC, Lauwers GY, Bounds BC, Brugge WR. Ethanol lavage of pancreatic cystic lesions: initial pilot study. *Gastrointest Endosc* (2005) 61(6):746–52. doi: 10.1016/s0016-5107(05)00320-2

26. Park DH, Choi JH, Oh D, Lee SS, Seo DW, Lee SK, et al. Endoscopic ultrasonography-guided ethanol ablation for small pancreatic neuroendocrine tumors: results of a pilot study. *Clin Endosc* (2015) 48(2):158–64. doi: 10.5946/ce.2015.48.2.158

27. Banks PA, Bollen TL, Dervenis C, Gooszen HG, Johnson CD, Sarr MG, et al. Classification of acute pancreatitis–2012: revision of the Atlanta classification and definitions by international consensus. *Gut* (2013) 62(1):102–11. doi: 10.1136/gutjnl-2012-302779

28. Halonen KI, Pettilä V, Leppäniemi AK, Kemppainen EA, Puolakkainen PA, Haapiainen RK. Multiple organ dysfunction associated with severe acute pancreatitis. *Crit Care Med* (2002) 30(6):1274–9. doi: 10.1097/00003246-200206000-00019

29. Seewald S, Ang TL, Teng KC, Soehendra N. EUS-guided drainage of pancreatic pseudocysts, abscesses and infected necrosis. *Dig Endosc* (2009) 21 Suppl 1:S61–5. doi: 10.1111/j.1443-1661.2009.00860.x

30. Grimm H, Binmoeller KF, Soehendra N. Endosonography-guided drainage of a pancreatic pseudocyst. *Gastrointest Endosc* (1992) 38(2):170–1. doi: 10.1016/s0016-5107(92)70384-8

31. Jin Z, Chang KJ. Endoscopic ultrasound-guided fiducial markers and brachytherapy. *Gastrointest Endosc Clin N Am* (2012) 22(2):325–x. doi: 10.1016/j.giec.2012.04.012

32. Sun S, Qingjie L, Qiyong G, Mengchun W, Bo Q, Hong X. EUS-guided interstitial brachytherapy of the pancreas: a feasibility study. *Gastrointest Endosc* (2005) 62(5):775–9. doi: 10.1016/j.gie.2005.06.050

frontiers | Frontiers in Oncology

TYPE Original Research
PUBLISHED 16 August 2022
DOI 10.3389/fonc.2022.953090

Check for updates

OPEN ACCESS

EDITED BY
Zhendong Jin,
Second Military Medical University, China

REVIEWED BY
Wenju Du,
University of Electronic Science and Technology of China, China
Bogdan Silviu Ungureanu,
University of Medicine and Pharmacy of Craiova, Romania

*CORRESPONDENCE
Zhendong Yao
815615317@qq.com
Yun Shi
13701536368@163.com

†These authors have contributed equally to this work and share first authorship

SPECIALTY SECTION
This article was submitted to Gastrointestinal Cancers: Gastric and Esophageal Cancers, a section of the journal Frontiers in Oncology

RECEIVED 25 May 2022
ACCEPTED 27 July 2022
PUBLISHED 16 August 2022

CITATION
Jin T, Jiang Y, Mao B, Wang X, Lu B, Qian J, Zhou H, Ma T, Zhang Y, Li S, Shi Y and Yao Z (2022) Multi-center verification of the influence of data ratio of training sets on test results of an AI system for detecting early gastric cancer based on the YOLO-v4 algorithm.
Front. Oncol. 12:953090.
doi: 10.3389/fonc.2022.953090

COPYRIGHT
© 2022 Jin, Jiang, Mao, Wang, Lu, Qian, Zhou, Ma, Zhang, Li, Shi and Yao. This is an open-access article distributed under the terms of the Creative Commons Attribution License (CC BY). The use, distribution or reproduction in other forums is permitted, provided the original author(s) and the copyright owner(s) are credited and that the original publication in this journal is cited, in accordance with accepted academic practice. No use, distribution or reproduction is permitted which does not comply with these terms.

Multi-center verification of the influence of data ratio of training sets on test results of an AI system for detecting early gastric cancer based on the YOLO-v4 algorithm

Tao Jin[1†], Yancai Jiang[1†], Boneng Mao[1†], Xing Wang[1], Bo Lu[2], Ji Qian[1], Hutao Zhou[1], Tieliang Ma[1], Yefei Zhang[3], Sisi Li[4], Yun Shi[3,5*] and Zhendong Yao[1*]

[1]Department of Gastroenterology, The Affiliated Yixing Hospital of Jiangsu University, Yixing, China, [2]Microsoft Ltd Co., Suzhou, China, [3]Department of Gastroenterology, The Second Affiliated Hospital of Soochow University, Suzhou, China, [4]Department of Gastroenterology, Civil Aviation Hospital of Shanghai, A Branch of Ruijin Hospital, Shanghai, China, [5]Department of Internal Medicine, Yixing Maternity and Child Health Care Hospital, Yixing, China

Objective: Convolutional Neural Network(CNN) is increasingly being applied in the diagnosis of gastric cancer. However, the impact of proportion of internal data in the training set on test results has not been sufficiently studied. Here, we constructed an artificial intelligence (AI) system called EGC-YOLOV4 using the YOLO-v4 algorithm to explore the optimal ratio of training set with the power to diagnose early gastric cancer.

Design: A total of 22,0918 gastroscopic images from Yixing People's Hospital were collected. 7 training set models were established to identify 4 test sets. Respective sensitivity, specificity, Youden index, accuracy, and corresponding thresholds were tested, and ROC curves were plotted.

Results: 1. The EGC-YOLOV4 system completes all tests at an average reading speed of about 15 ms/sheet; 2. The AUC values in training set 1 model were 0.8325, 0.8307, 0.8706, and 0.8279, in training set 2 model were 0.8674, 0.8635, 0.9056, and 0.9249, in training set 3 model were 0.8544, 0.8881, 0.9072, and 0.9237, in training set 4 model were 0.8271, 0.9020, 0.9102, and 0.9316, in training set 5 model were 0.8249, 0.8484, 0.8796, and 0.8931, in training set 6 model were 0.8235, 0.8539, 0.9002, and 0.9051, in training set 7 model were 0.7581, 0.8082, 0.8803, and 0.8763.

Conclusion: EGC-YOLOV4 can quickly and accurately identify the early gastric cancer lesions in gastroscopic images, and has good generalization.The proportion of positive and negative samples in the training set will affect the

overall diagnostic performance of AI.In this study, the optimal ratio of positive samples to negative samples in the training set is 1:1~ 1:2.

KEYWORDS

early gastric cancer (EGC), artificial intelligence (AI), convolutional neural network (CNN), ROC, YOLO, youden index

Background

Gastric cancer is the third leading cause of cancer-related mortality and one of the most common malignant tumors in the world. Over one million new cases of gastric cancer are diagnosed each year, resulting in over 780000 deaths (1, 2). The prognosis for people with gastric cancer varies according to the stage, with advanced gastric cancer patients having a poor prognosis. Patients with early gastric cancer, on the other hand, have a 5-year survival rate that exceeds 90%. This is because patients can be treated quickly following an endoscopic submucosal dissection (ESD).

In this view, endoscopy is widely regarded as the gold standard for early gastric cancer detection. However, the ability of endoscopic physicians to distinguish benign from malignant tissue *via* gastroscopy is highly dependent on their diagnostic competency, and inexperienced endoscopic physicians frequently misdiagnose patients. Atrophic gastritis is a precancerous condition that accounts for approximately 95% of stomach adenocarcinomas (3).

The morphological traits of early gastric cancer are difficult to distinguish from atrophic gastritis when using white light endoscopy. Endoscopic experts require extensive specialized training and a wide range of skills to successfully detect gastric cancer. Disparities in early gastric cancer detection rates across locations and hospital levels are related to differences in endoscopic physician expertise. Therefore, the most effective way to reduce stomach cancer mortality is to improve the effectiveness of early gastric cancer endoscopic diagnosis.

A growing number of researchers have developed an image recognition system based on a convolutional neural network for medical practice and disease screening, for example, the identification and classification of skin cancer (4, 5), radiation oncology (6), retinopathy (7), and histological classification of pathological biopsies (8).

Several studies that used CNN to train and recognize images of gastric cancer have yielded positive results (9–11). However, in this work, we used the YOLO-v4 algorithm (12)(Source code is at https://github.com/AlexeyAB/darknet.). The algorithm is a region-based CNN with high speed, adaptability, and a low rate of detection of background errors.

This multidisciplinary (AI and endoscopy) topic is attracting an increasing number of research institutes. While the field appears promising, it raises concerns about the flexibility and stability of these algorithms. When the algorithm design cannot be improved further, there is a tendency to seek new images and win through data volume.

In our previous work, we developed the EGC-YOLO with the YOLO-v3 algorithm (13) using nearly 40,000 gastroscopic images and achieved acceptable specificity and sensitivity in the test sets, but we want to go even further. In this study, we collected over 200,000 photos from four hospitals to see how proportion of positive and negative samples in the training set influenced EGC-YOLOV4 test performance.

Methods

Data sources and classification

We collected gastroscopic cases in Yixing People's Hospital between 2018 and 2021 and divided them into 2 categories based on pathological types, including images of early gastric cancer and images of non-gastric cancer (including moderate + heterosexual hyperplasia, severe heterosexual hyperplasia, and intramucosal carcinoma). There were 1200 early gastric cancer images and 219,718 non-gastric cancer images. There were a total of 220918 gastroscopic images obtained. The images were selected by four endoscopists, each with more than 10 years of experience in endoscopy and more than 10000 gastroscopy cases. In addition, 568 gastroscopic images (268 early gastric cancer images and 300 non-gastric cancer images) were obtained from the Department of Gastroenterology, Nanjing Drum Tower Hospital; 1340 images (403 images of early-stage gastric cancer and 937 images of non-gastric cancer) were obtained from the Department of Gastroenterology, The Second Affiliated Hospital of Soochow University; 4453 gastroscopic images (366 for early-stage gastric cancer and 4087 for non-gastric cancer) were obtained from The Endoscopy Center of Civil Aviation Hospital of Shanghai.

Data platform

We created an online test platform and data storage server specifically for this experiment, which has two modules. In the first module, each test worker can upload data and use the online image box selection and marking tool to mark and save each image. The platform website is https://image-exp.dev.zhishiq.com:8443/. In the second module, the results of all test sets were displayed immediately after the test. On each tested image, the sites suspected of having early gastric cancer lesions were marked with red boxes, which is very intuitive.

Research equipment and software

PYTHON programming language, LINUX OS system, GPU: NVIDIA RTX 2080TI+NVIDIA GTX 1080TI. Figure 1 depicts the construction of the EGC-YOLOV4.

Training set construction

A total of 220918 gastroscopic images, 1200 endoscopic images of early gastric cancer, and 219718 non-gastric cancer images were provided by Yixing People's Hospital. Hereinafter collectively referred to as training sources.

Training set 1: 1200 images of early gastric cancer were selected as positive samples from training sources, and 0 images of non-gastric cancer were randomly selected as negative samples from training sources, with a positive to negative ratio of 1:0.

Training set 2: 1200 images of early gastric cancer were selected as positive samples from training sources, and 1200 images of non-gastric cancer were randomly selected as negative samples from training sources, with a positive to negative ratio of 1:1.

Training set 3: 1200 images of early gastric cancer were selected as positive samples from training sources, and 2400 images of non-gastric cancer were randomly selected as negative samples from training sources, with a positive to negative ratio of 1:2.

Training set 4: 1200 images of early gastric cancer were selected as positive samples from training sources, and 4800 images of non-gastric cancer were randomly selected as negative samples from training sources, with a positive to negative ratio of 1:4.

Training set 5: 1200 images of early gastric cancer were selected as positive samples from training sources, and 9600 images of non-gastric cancer were randomly selected as negative samples from training sources, with a positive to negative ratio of 1:8.

Training set 6: 1200 images of early gastric cancer were selected as positive samples from training sources, and 19200 images of non-gastric cancer were randomly selected as negative samples from training sources, with a positive to negative ratio of 1:16.

Training set 7: 1200 images of early gastric cancer were selected as positive samples from training sources, and 38400

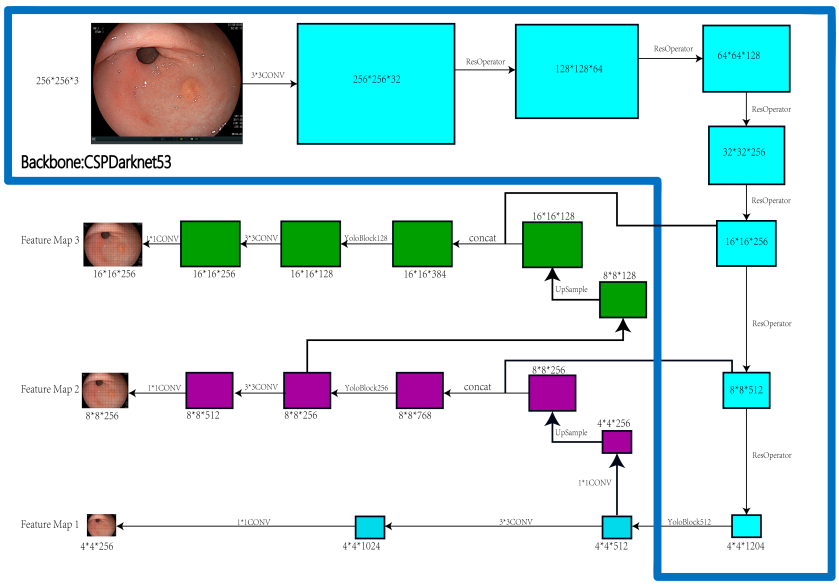

FIGURE 1
Steps and Architecture for EGC-YOLOV4.

images of non-gastric cancer were randomly selected as negative samples from training sources, with a positive to negative ratio of 1:32

Test set construction

Test set 1: This test set consists of a single external test set. All the 268 positive samples were gastroscopic images of early gastric cancer provided by the Department of Gastroenterology of Nanjing Drum Tower Hospital, whereas 300 negative samples were non-gastric cancer gastroscopic images provided by this hospital.

Test set 2: This test set consists of a single external test set. All the 366 positive samples were gastroscopic images of early gastric cancer from the Endoscopy Center of Gubei Branch of Shanghai Ruijin Hospital, whereas 4087 negative samples were randomly selected non-gastric cancer images.

Test set 3: This test set consists of a single external test set. All the 403 positive samples were gastroscopic images of early gastric cancer from the Department of Gastroenterology, The Second Affiliated Hospital of Soochow University, whereas 937 negative samples were non-gastric cancer images.

Test set 4: This test set consists of a mixed external test set. All the 717 positive samples were images randomly selected by the system after mixing images of early gastric cancer from the three hospitals mentioned above, whereas 1002 negative samples were images randomly selected by the system after mixing images of non-gastric cancer from the three hospitals.

Results

1. The training set 1 model

The training set 1 model was tested individually on test sets 1, 2, 3, and 4, respectively, with an average reading speed of 15 milliseconds/sheet. As shown in Figure 2, the measured AUC values were 0.8325, 0.8307, 0.8706, and 0.8279, respectively.

2. The training set 2 model

The training set 2 model was tested individually on test sets 1, 2, 3, and 4, respectively, with an average reading speed of 15 milliseconds/sheet. As shown in Figure 3, the measured AUC values were 0.8674, 0.8635, 0.9056, and 0.9249, respectively.

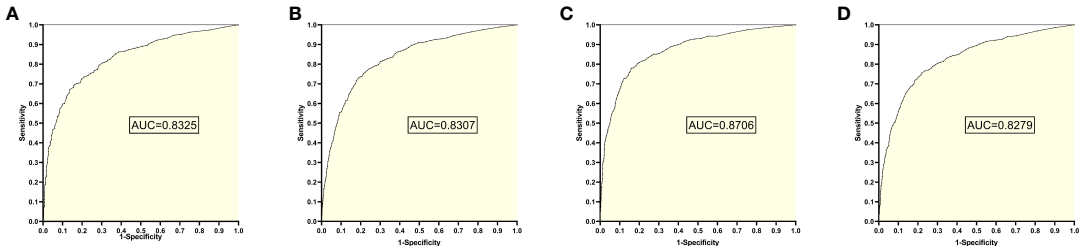

FIGURE 2
ROC curves and AUC values obtained from training set 1 model testing each test set: **(A)** results from test set 1; **(B)** results from test set 2; **(C)** results from test set 3; **(D)** results from test set 4.

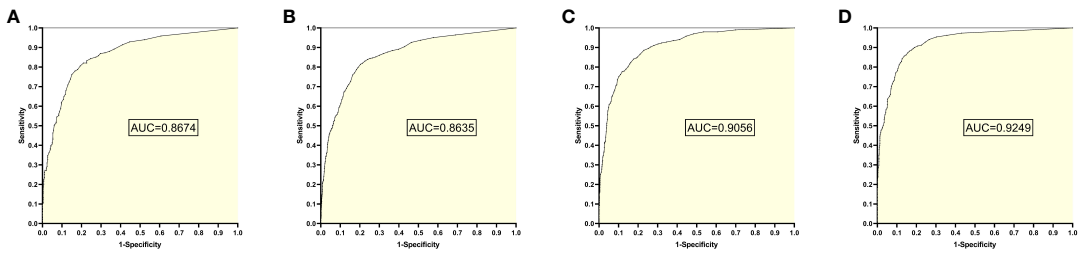

FIGURE 3
ROC curves and AUC values obtained from the training set 2 model testing each test set: **(A)** results from test set 1; **(B)** results from test set 2; **(C)** results from test set 3; **(D)** results from test set 4.

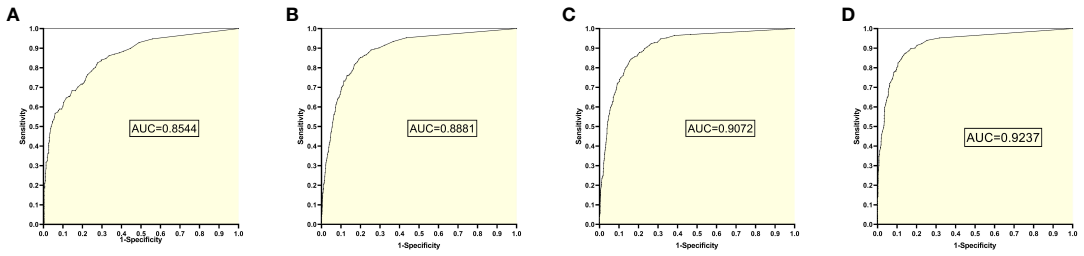

FIGURE 4
ROC Plot and AUC Values Obtained from Training Set 3 Model Testing Each Test Set: **(A)** Results from Test Set 1; **(B)** Results from Test Set 2; **(C)** Results from Test Set 3; **(D)** Results from Test Set 4.

3. The training set 3 model

The training set 3 model was tested separately for test sets 1, 2, 3, and 4, respectively, with an average reading speed of 14 milliseconds/sheet. As shown in Figure 4, the measured AUC values were 0.8544, 0.8881, 0.9072, and 0.9237, respectively.

4. The training set 4 model

The training set 4 model was tested separately for test sets 1, 2, 3, and 4, respectively, with an average reading speed of 14 milliseconds/sheet. As shown in Figure 5 ,the ROC curve was plotted with AUC values of 0.8271, 0.9020, 0.9102, and 0.9316, respectively.

5. The training set 5 model

The training set 5 model was tested individually on test sets 1, 2, 3, and 4, respectively, with an average reading speed of 14 milliseconds/sheet. As shown in Figure 6, the AUC values were 0.8249, 0.8484, 0.8796, and 0.8931, respectively.

6. The training set 6 model

The training set 6 model was tested individually on test sets 1, 2, 3, and 4, respectively, with an average reading speed of 15 ms/sheet. As shown in Figure 7, the AUC values were 0.8235, 0.8539, 0.9002, and 0.9051, respectively.

7. The training set 7 model

The training set 7 model was tested individually on test sets 1, 2, 3, and 4, respectively, with an average reading speed of 16 milliseconds/sheet. As shown in Figure 8, the AUC values were 0.7581, 0.8082, 0.8803, and 0.8763, respectively.

8. Change trend of AUC

According to the change trend of AUC in Figure 9, it can be found that the AUC first increases and then decreases with the increase of negative samples in the training set model. When the training set 2 model and training set 3 model are used for the test set, the AUC results of all test sets are greater than 0.85. Even when the ratio of positive samples to negative samples in the

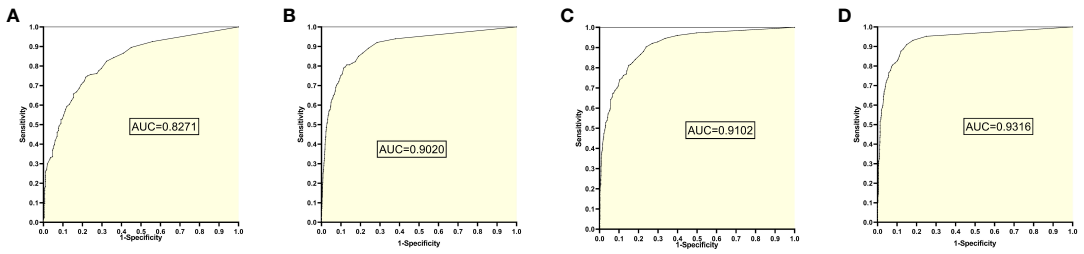

FIGURE 5
ROC curves and AUC values obtained from the training set 4 model testing each test set: **(A)** results from test set 1; **(B)** results from test set 2; **(C)** results from test set 3; **(D)** results from test set 4.

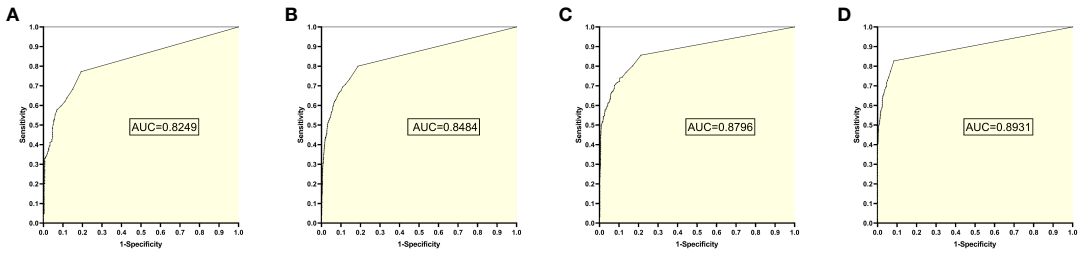

FIGURE 6
ROC curves and AUC values obtained by the training set 5 model testing each test set: **(A)** results from test set 1; **(B)** results from test set 2; **(C)** results from test set 3; **(D)** results from test set 4.

training set is at 1:1 ~ 1:2, EGC-YOLOV4 has good diagnostic performance for each test set (with the best generalization). Although Test Set 4 is a mixture of the first three independent external test sets with complicated internal data types, after testing, it was found that its maximum AUC once exceeded 0.90, and the highest AUC of all test results could be obtained. The Figure 8 AUC peak for test set 1 occurred in the training set 2 model, the AUC peak for test set 2 occurred in the training set 4 model, the AUC peak for test set 3 occurred in the training Figure 8 set 4 model, and the peak for test set 4 occurred in the training set 4 model.

9. Trends in sensitivity and specificity

The variation tendency in Figures 10–13 showed that when there were few negative samples in the training set model, the minimum value of specificity changed sharply with the threshold. When there were more negative samples in the training set, the minimum value of specificity increased significantly, and its stability was significantly improved, and it could finally be very steadily maintained above 0.9. The sensitivity always showed a monotonic decreasing trend with increasing threshold, and when the negative sample in the training set model increased significantly, the maximum value of sensitivity gradually decreased and finally was lower than 0.8.

Figures 10–13 are the curves of sensitivity, specificity, Youden index, and accuracy with threshold after testing test sets 1, 2, 3, and 4 with seven training set models, respectively.

10. Comparison of youden index and accuracy

In the test results of each group in this study, we listed the maximum Youden index and maximum accuracy rate of each group in Tables 1 and 2, and their corresponding sensitivity and specificity. It can be obviously found that the accuracy rate is always higher than Youden index under the same threshold value, but the corresponding sensitivity and specificity cannot be stably at a higher level at the same time when it reaches the maximum value, and some sensitivities are even less than 0.5. However, the Youden index better balances the importance of sensitivity and specificity in the actual diagnosis, that is, the corresponding sensitivity and specificity results can reach a good level at the same time when the Youden index is the largest, which ensures a low missed diagnosis rate while

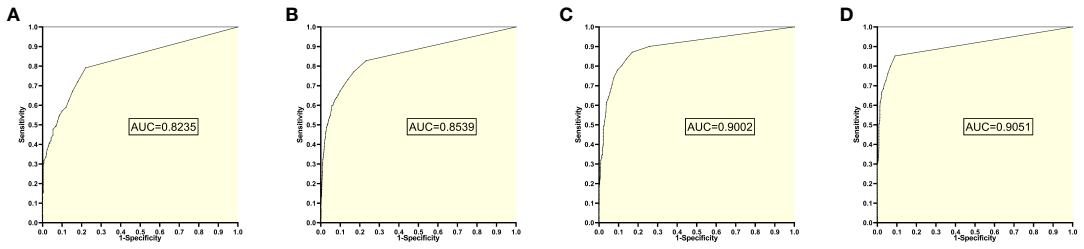

FIGURE 7
ROC curves and AUC values obtained from the training set 6 model testing each test set: **(A)** results from test set 1; **(B)** results from test set 2; **(C)** results from test set 3; **(D)** results from test set 4.

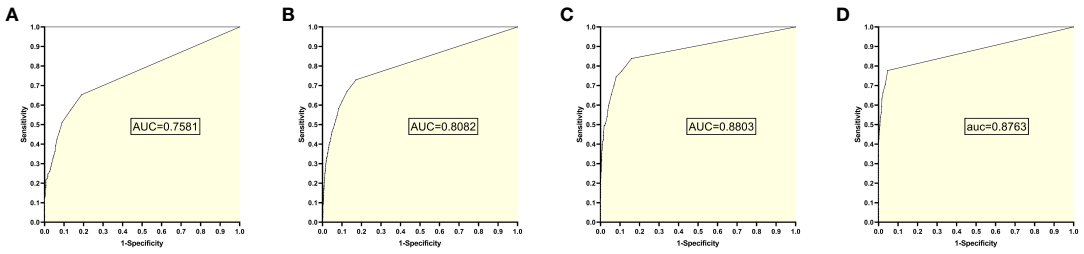

FIGURE 8
ROC curves and AUC values obtained from the training set 7 model testing each test set: **(A)** results from test set 1; **(B)** results from test set 2; **(C)** results from test set 3; **(D)** results from test set 4.

reducing misdiagnosis, so the Youden index is superior to the accuracy rate in the indication of threshold value.

Discussion

In this study, we constructed and developed the EGC-YOLOV4 system with the YOLO-v4 algorithm, trained AI according to different sample ratios using gastroscopic images from Yixing People's Hospital, obtained seven training set models, created four test sets with gastroscopic images from three different hospitals, and tested four test sets using seven training set models, respectively, which could efficiently and accurately screen for early gastric cancer in gastroscopic images. YOLO-v4 is capable of properly diagnosing gastroscopy pictures from various hospitals and has excellent generalizability. The percentage of positive and negative samples in the training set influences the overall diagnostic performance of AI, and an excessive number of negative samples decreases the diagnostic performance.

The rapid advancement of artificial intelligence's picture identification capability has given the area of medical illness diagnostics significant technological advantages. In clinical practice, the primary diagnostic procedures for gastric cancer are gastroscopy + mucosal pathological biopsy and imaging detection, which are employed for qualitative, localisation diagnosis and staging assessment, respectively. In the last two years, AI has conducted a number of studies in the area of gastroscopic image recognition, and more and more evidence indicates that a gastroscopic AI system may be used in clinical practice.

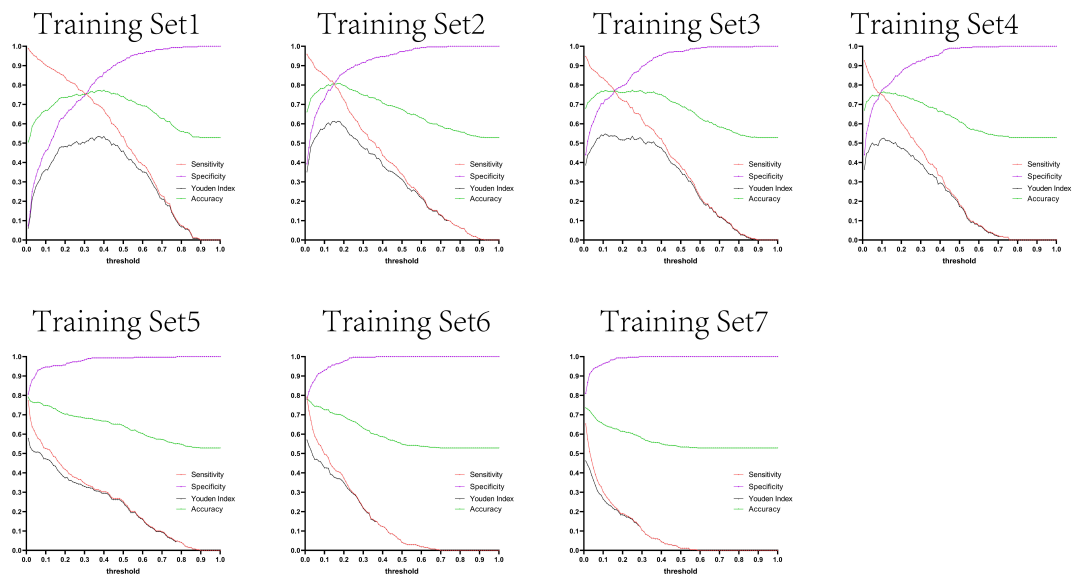

FIGURE 9
The trend lines graph of AUC value with the gradient of sample proportion in the training set models.

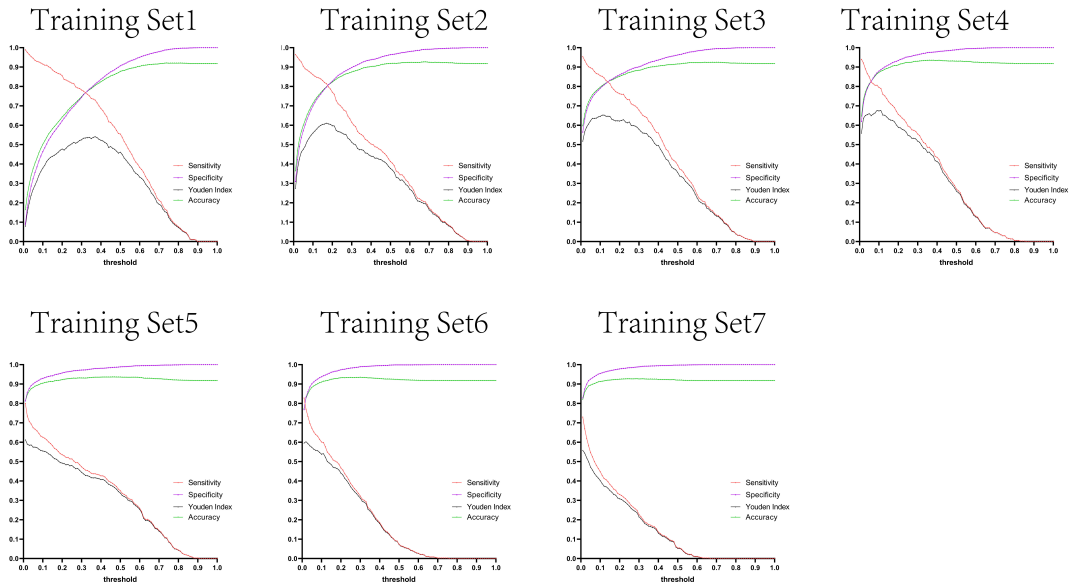

FIGURE 10
Curves of sensitivity, specificity, Youden index, and accuracy with threshold after test set 1 was tested separately by seven training set models.

Ishioka et al. (14), for instance, created a real-time AI system for recognizing gastric cancer picture frames in gastroscopic movies that has a sensitivity of 94.1 percent for discriminating stomach cancer. The gastric cancer diagnostic method developed by Hirasawa et al. (15) not only detects stomach cancer but also localizes it with a sensitivity of 92.2% and a positive predictive value of 30.6%. Tang et al. (16) developed a D-CNN model to predict gastric mucosal cancer using 3407 gastroscopic images from 666 gastric cancer patients as the training set and 228 gastroscopic images as the test set. The AUC of the AI model for distinguishing intramucosal cancer from advanced gastric cancer was found to be 0.942, with a sensitivity of 0.905 and a specificity of 0.853.Zhu et al. (17) constructed a CNN-CAD system based on the ResNet50 algorithm to determine the depth of gastric cancer invasion in

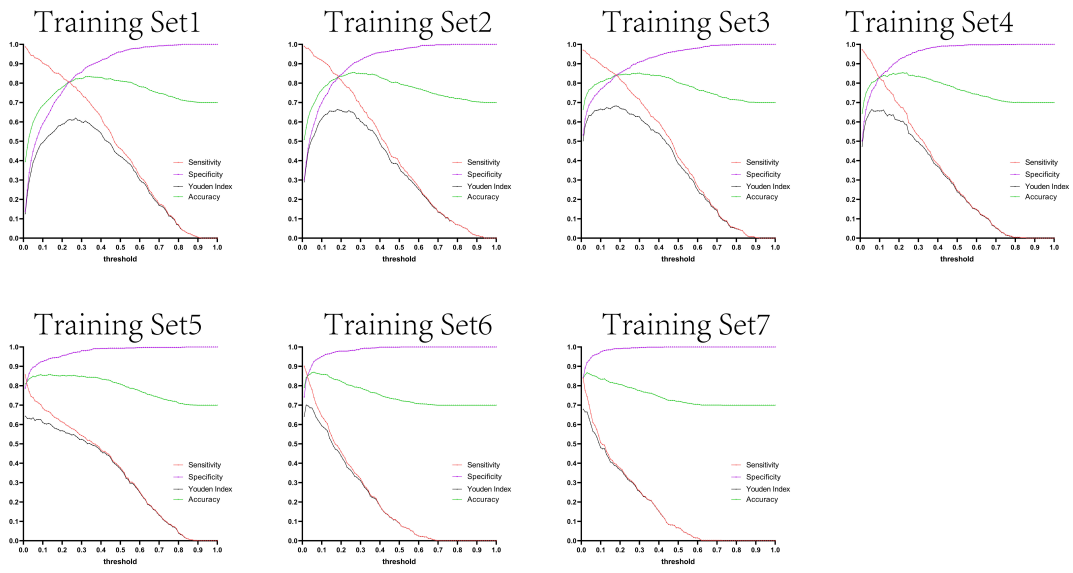

FIGURE 11
Curves of sensitivity, specificity, Youden index, and accuracy with threshold after test set 2 was tested separately by seven training set models.

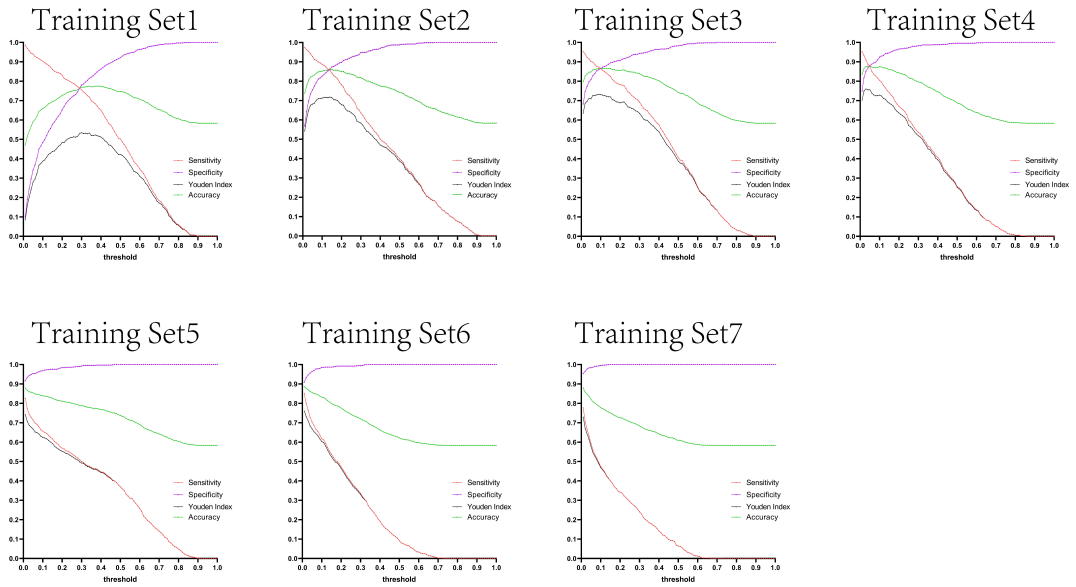

FIGURE 12
Curves of sensitivity, specificity, Youden index, and accuracy with threshold after test set 3 was tested separately by seven training set models.

order to screen patients undergoing endoscopic surgery. This system had an AUC of 0.94, sensitivity of 76.47 percent, specificity of 95.56 percent, overall accuracy of 89.16 percent, positive predictive value of 89.66 percent, and negative predictive value of 88.97 percent. This CNN-CAD method provides a high degree of accuracy and specificity for determining the depth of gastric cancer invasion, hence reducing the need for gastrectomy. Nagao et al. (18) used traditional white-light gastroscopy images,

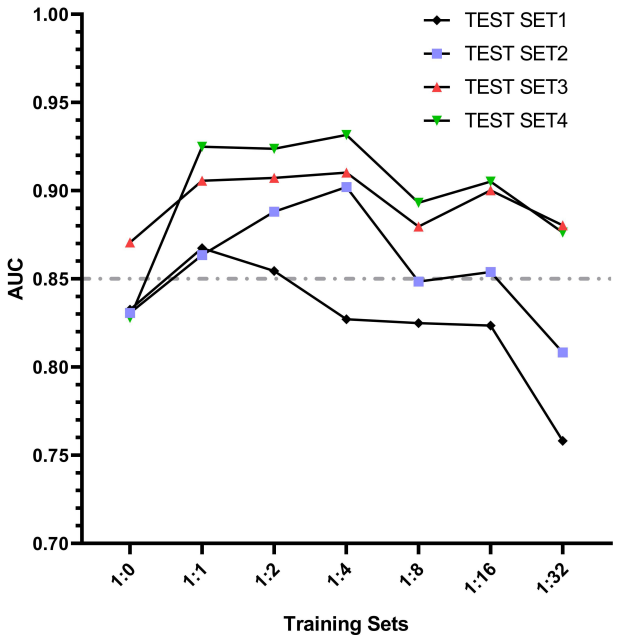

FIGURE 13
Curves of sensitivity, specificity, Youden index, and accuracy with threshold after test set 4 was tested separately by seven training set models.

TABLE 1 The results of testing four test sets for each of the seven training set models.

TRAINING SETS	TEST SETS	Youden index (max)	threshold	sensitivity	specificity
The training set 1 model	test set 1	0.534975	0.400	0.671642	0.863333
	test set 2	0.541106	0.370	0.729508	0.811598
	test set 3	0.620138	0.270	0.779156	0.840982
	test set 4	0.534972	0.300	0.754533	0.780439
The training set 2 model	test set 1	0.613184	0.17	0.779851	0.833333
	test set 2	0.61088	0.17	0.814208	0.796672
	test set 3	0.66403	0.18	0.841191	0.822839
	test set 4	0.718621	0.14	0.856346	0.862275
The training set 3 model	test set 1	0.547960	0.110	0.824627	0.723333
	test set 2	0.652434	0.120	0.844262	0.808172
	test set 3	0.682519	0.180	0.843672	0.838847
	test set 4	0.732363	0.090	0.873082	0.859281
The training set 4 model	test set 1	0.525870	0.110	0.742537	0.783333
	test set 2	0.686087	0.090	0.806011	0.870076
	test set 3	0.664165	0.060	0.903226	0.760939
	test set 4	0.760461	0.030	0.909344	0.851297
The training set 5 model	test set 1	0.579055	0.010000	0.772388	0.806667
	test set 2	0.613122	0.010000	0.800546	0.812576
	test set 3	0.643699	0.010000	0.856079	0.787620
	test set 4	0.743225	0.010000	0.827057	0.916168
The training set 6 model	test set 1	0.571045	0.010000	0.791045	0.780000
	test set 2	0.602643	0.020000	0.770492	0.832151
	test set 3	0.701277	0.020000	0.870968	0.830309
	test set 4	0.761344	0.010000	0.852162	0.909182
The training set 7 model	test set 1	0.462985	0.010000	0.652985	0.810000
	test set 2	0.557744	0.010000	0.729508	0.828236
	test set 3	0.679692	0.010000	0.838710	0.840982
	test set 4	0.729942	0.010000	0.776848	0.953094

Their maximal Youden index, their respective threshold values, as well as their sensitivity and specificity.

narrow-band imaging endoscopic images, and chromoendoscopy images to train AI to predict the depth of invasion of gastric cancer; the results demonstrated that the AI system could accurately predict the depth of invasion of gastric cancer.

Currently, the quality of endoscopic equipment and video collection devices in hospitals of all levels in China is inconsistent, high-definition acquisition cards are not widely used, and not all gastroscopic pictures can achieve 1080p resolution. Even though this field has great application potential, the stability and generalization of artificial intelligence in detecting endoscopic images from various medical institutions are still worth verifying, as overfitting issues frequently arise during the construction of AI systems, and how to obtain good generalization of AI systems is the most pressing issue at present. In order to deal with this issue, the training set we constructed in this study contains many images with varying resolutions to simulate the uneven image quality encountered in daily work. We then constructed four test sets with gastroscopic images from three different hospitals to test the diagnostic performance of each training set model separately and independently, and the results demonstrated that EGC-YOLOV4 could still demonstrate good diagnostic performance and was able to fully demonstrate its effectiveness.

People often train AI systems with more photos in the hopes of winning by volume when the algorithm architecture cannot be much further improved. But are AI systems that have been trained on more photos better tested? The findings of this investigation clearly refute this theory.The findings of this research show that an excessive number of negative samples in the training set reduces the diagnostic performance of AI, but an optimum number of negative samples may maximize AI power. The highest generalization performance in the EGC-YOLOV4 system is achieved by AI trained with a training set sample ratio from 1:1 to 1:2. To guarantee that the AI system performs the best in terms of diagnostic performance, it is thus a good idea to use pre-experiments to estimate the ratio of positive samples to negative samples in the most appropriate training set. We also discovered that when the same training set model was used for testing, the four test sets' optimal threshold values varied from

TABLE 2 The results of testing four test sets for each of the seven training set models.

TRAINING SETS	TEST SETS	Accuracy (max)	threshold	sensitivity	specificity
The training set 1 model	test set 1	0.772887	0.400	0.671642	0.863333
	test set 2	0.920728	0.740	0.161202	0.988745
	test set 3	0.833582	0.340	0.702233	0.890075
	test set 4	0.774869	0.340	0.718271	0.815369
The training set 2 model	test set 1	0.808099	0.170	0.779851	0.833333
	test set 2	0.926566	0.680	0.204918	0.991192
	test set 3	0.854478	0.260	0.751861	0.898613
	test set 4	0.860384	0.150	0.842399	0.873253
The training set 3 model	test set 1	0.772887	0.250	0.682836	0.853333
	test set 2	0.924545	0.640	0.204918	0.988989
	test set 3	0.851493	0.300	0.717122	0.909085
	test set 4	0.865620	0.100	0.864714	0.866267
The training set 4 model	test set 1	0.764085	0.110	0.742537	0.783333
	test set 2	0.935325	0.360	0.486339	0.975532
	test set 3	0.853731	0.220	0.672457	0.931697
	test set 4	0.878418	0.050	0.875872	0.880240
The training set 5 model	test set 1	0.790493	0.010000	0.772388	0.806667
	test set 2	0.936447	0.460000	0.387978	0.985564
	test set 3	0.856716	0.090000	0.702233	0.923159
	test set 4	0.878999	0.010000	0.827057	0.916168
The training set 6 model	test set 1	0.785211	0.010000	0.791045	0.780000
	test set 2	0.934651	0.300000	0.322404	0.989479
	test set 3	0.869403	0.060000	0.739454	0.925293
	test set 4	0.885398	0.010000	0.852162	0.909182
The training set 7 model	test set 1	0.735915	0.010000	0.652985	0.810000
	test set 2	0.927015	0.290000	0.248634	0.987766
	test set 3	0.867164	0.030000	0.744417	0.919957
	test set 4	0.879581	0.010000	0.776848	0.953094

Their maximal Accuracy, their respective threshold values, as well as their sensitivity and specificity.

one another, and in practice, a mature AI diagnostic software had to first set the threshold when screening for early gastric cancer. The determination of the specific set values of threshold had to be preset and corrected in accordance with various source datasets before AI testing, and the appropriate training set model had to be used.

Even though our study yielded favorable test results, there are still limitations, including: 1. In this research, during the process of manually labeling the lesion site of gastric cancer, all lesions are labeled in the shape of rectangular boxes, which is likely to result in a small amount of non-gastric cancer stomach mucosa inside the rectangular box. During the process of artificial intelligence system learning, this portion of non-gastric cancer mucosal images will be misidentified as early gastric cancer by AI, and their mucosal characteristics will be extracted, leading to the possibility that the trained artificial intelligence system will misdiagnose non-gastric cancer mucosa as gastric cancer. If the labeling tool can be modified to a polygonal lasso, it will precisely match the lesion mucosal border and optimize the decrease of the original lesion boundary. 2. Since this research only employed retrospective data and photos, further multicenter prospective studies might be conducted to remove selective bias and increase the study's reliability; 3. To analyze the trend of AI system performance when there are fewer negative samples than positive samples, we will add more sample proportion gradients in the design process of the training set model, such as 1:0.125, 1:0.25, and 1:0.5.

Data availability statement

The raw data supporting the conclusions of this article will be made available by the authors, without undue reservation.

Author contributions

Conceptualization, TJ, ZY and BL. Methodology, ZY. Software, BL. Formal analysis, ZY and BL. Investigation, TJ, YZ, SL, YJ, XW, YS, JQ, HZ, TM. Resources, BM. Data curation, BL. Writing—original draft preparation, ZY. Writing—review and editing, TJ, YJ.

Visualization, ZY, TJ, YJ and BL. Supervision, ZY and BM. Project administration, ZY. Funding acquisition, ZY and JQ. All authors have read and agreed to the publication of this manuscript.

Funding

This research was funded by the Foundation of Clinical Science and Technology of Wuxi, No. Q202062 and No. Q201924.

Acknowledgments

We thank Professor Weichang Chen for his constant advice and guidance regarding the design of this project and Professor Xiaoping Zou, who provided us with valuable gastroscopic images. Additional thanks go to Bo Lu for his contribution to the construction of EGC-YOLOV4 system. Finally, I wish to express my gratitude to the three hospitals (The Second Affiliated Hospital of Soochow University, Civil Aviation Hospital of Shanghai, and Nanjing Drum Tower Hospital) for providing us with endoscopic images.

Conflict of interest

Author BL is an employee of Microsoft Ltd, however, he was neither assigned or asked by Microsoft Ltd to participate in this research, nor did Microsoft Ltd have any interest in the current research or future application of this study. The author did not use any resource of Microsoft Ltd or work time to conduct this research.

The authors declare that the research was conducted in the absence of any commercial or financial relationships that could be construed as a potential conflict of interest.

Publisher's note

All claims expressed in this article are solely those of the authors and do not necessarily represent those of their affiliated organizations, or those of the publisher, the editors and the reviewers. Any product that may be evaluated in this article, or claim that may be made by its manufacturer, is not guaranteed or endorsed by the publisher.

References

1. Bray F, Ferlay J, Soerjomataram I, Siegel RL, Torre LA, Jemal A. Global cancer statistics 2018: GLOBOCAN estimates of incidence and mortality worldwide for 36 cancers in 185 countries. *CA-CANCER J Clin* (2020) 70:313. doi: 10.3322/caac.21609

2. Rawla P, Barsouk A. Epidemiology of gastric cancer: global trends, risk factors and prevention. *Przegląd Gastroenterologiczny* (2019) 14:26–38. doi: 10.5114/pg.2018.80001

3. Rugge M, Meggio A, Pravadelli C, Barbareschi M, Fassan M, Gentilini M, et al. Gastritis staging in the endoscopic follow-up for the secondary prevention of gastric cancer: a 5-year prospective study of 1755 patients. *Gut* (2018) 68:11–7. doi: 10.1136/gutjnl-2017-314600

4. Haggenmüller S, Maron RC, Hekler A, JS U, Barata C, Barnhill RL, et al. Skin cancer classification *via* convolutional neural networks: systematic review of studies involving human experts. *Eur J Cancer* (2021) 156:202–16. doi: 10.1016/j.ejca.2021.06.049

5. Maron RC, Haggenmüller S, von Kalle C, JS U, Meier F, Gellrich FF, et al. Robustness of convolutional neural networks in recognition of pigmented skin lesions. *Eur J Cancer* (2021) 145:81–91. doi: 10.1016/j.ejca.2020.11.020

6. Zhang Y, Yu H. Convolutional neural network based metal artifact reduction in X-ray computed tomography. *IEEE T Med Imaging* (2018) 37:1370–81. doi: 10.1109/TMI.2018.2823083

7. Al-Antary MT, Arafa Y. Multi-scale attention network for diabetic retinopathy classification. *IEEE Access* (2021) 9:54190–200. doi: 10.1109/ACCESS.2021.3070685

8. Yoshida H, Kiyuna T. Requirements for implementation of artificial intelligence in the practice of gastrointestinal pathology. *World J Gastroentero* (2021) 27:2818–33. doi: 10.3748/wjg.v27.i21.2818

9. Zhang L, Zhang Y, Wang L, Wang J, Liu Y. Diagnosis of gastric lesions through a deep convolutional neural network. *Digest Endosc* (2021) 33:788–96. doi: 10.1111/den.13844

10. Li L, Chen Y, Shen Z, Zhang X, Sang J, Ding Y, et al. Convolutional neural network for the diagnosis of early gastric cancer based on magnifying narrow band imaging. *Gastric Cancer* (2020) 23:126–32. doi: 10.1007/s10120-019-00992-2

11. Arribas J, Antonelli G, Frazzoni L, Fuccio L, Ebigbo A, van der Sommen F, et al. Standalone performance of artificial intelligence for upper GI neoplasia: a meta-analysis. *Gut* (2021) 70:1458–68. doi: 10.1136/gutjnl-2020-321922

12. Bochkovskiy A, Wang C-Y, Liao H-YM. *YOLOv4: Optimal speed and accuracy of object detection*. arXiv (2020).

13. Redmon J, Farhadi A. *YOLOv3: An incremental improvement*. arXiv (2018).

14. Ishioka M, Hirasawa T, Tada T. Detecting gastric cancer from video images using convolutional neural networks. *Dig Endosc* (2019) 31:e34–5. doi: 10.1111/den.13306

15. Hirasawa T, Aoyama K, Tanimoto T, Ishihara S, Shichijo S, Ozawa T, et al. Application of artificial intelligence using a convolutional neural network for detecting gastric cancer in endoscopic images. *Gastric Cancer* (2018) 21:653–60. doi: 10.1007/s10120-018-0793-2

16. Tang D, Zhou J, Wang L, Ni M, Chen M, Hassan S, et al. A novel model based on deep convolutional neural network improves diagnostic accuracy of intramucosal gastric cancer (With video). *Front Oncol* (2021) 11:622827. doi: 10.3389/fonc.2021.622827

17. Zhu Y, Wang QC, Xu MD, Zhang Z, Cheng J, Zhong YS, et al. Application of convolutional neural network in the diagnosis of the invasion depth of gastric cancer based on conventional endoscopy. *Gastrointest Endosc* (2019) 89:806–15. doi: 10.1016/j.gie.2018.11.011

18. Nagao S, Tsuji Y, Sakaguchi Y, Takahashi Y, Minatsuki C, Niimi K, et al. Highly accurate artificial intelligence systems to predict the invasion depth of gastric cancer: efficacy of conventional white-light imaging, nonmagnifying narrow-band imaging, and indigo-carmine dye contrast imaging. *Gastrointest Endosc* (2020) 92:866–73. doi: 10.1016/j.gie.2020.06.047

frontiers | Frontiers in Oncology

TYPE Perspective
PUBLISHED 25 August 2022
DOI 10.3389/fonc.2022.1001112

Check for updates

OPEN ACCESS

EDITED BY
Zhendong Jin,
Second Military Medical University, China

REVIEWED BY
Usman Ayub Awan,
The University of Haripur, Pakistan
Abdullah Shah,
Shaheed Benazir Bhutto University, Pakistan

*CORRESPONDENCE
Bo Qin
fccqinb@zzu.edu.cn
Qian Bai
baiqian@zzu.edu.cn

SPECIALTY SECTION
This article was submitted to Gastrointestinal Cancers: Gastric and Esophageal Cancers, a section of the journal Frontiers in Oncology

RECEIVED 22 July 2022
ACCEPTED 08 August 2022
PUBLISHED 25 August 2022

CITATION
Khan S, Cui X, Nasir S, Rafiq SM, Qin B and Bai Q (2022) Advances in endoscopic resection techniques of small gastric tumors originating from the muscularis propria.
Front. Oncol. 12:1001112.
doi: 10.3389/fonc.2022.1001112

COPYRIGHT
© 2022 Khan, Cui, Nasir, Rafiq, Qin and Bai. This is an open-access article distributed under the terms of the Creative Commons Attribution License (CC BY). The use, distribution or reproduction in other forums is permitted, provided the original author(s) and the copyright owner(s) are credited and that the original publication in this journal is cited, in accordance with accepted academic practice. No use, distribution or reproduction is permitted which does not comply with these terms.

Advances in endoscopic resection techniques of small gastric tumors originating from the muscularis propria

Suliman Khan[1], Xiaona Cui[2], Safyan Nasir[3], Shoaib Mohammad Rafiq[4], Bo Qin[5]* and Qian Bai[2]*

[1]Department of Cerebrovascular Diseases, the Second Affiliated hospital of Zhengzhou University, Zhengzhou, China, [2]Department of Anesthesiaology, the Second Affiliated hospital of Zhengzhou University, Zhengzhou, China, [3]Department of Medicine, Allied/District Headquarter Hospital Faisalabad, Faisalabad, Pakistan, [4]Department of Medicine, District Headquarter Hospital Gujranwala, Gujranwala, Pakistan, [5]Translational Medical Center, the First Affiliated Hospital of Zhengzhou University, Zhengzhou, China

Gastrointestinal stromal tumors are common gastrointestinal tumors typically originating from the muscularis propria layer of the stomach. Small gastric stromal tumors are usually detected incidentally during routine endoscopic examination. Although they may have malignant potentially, controversies remain regarding the need for endoscopic resection of small gastric stromal tumors originating from the muscularis propria. According to the guidelines of the European Society of Medical Oncology, all gastrointestinal stromal tumors >2 cm in size should be resected with endoscopic surveillance recommended for tumors <2 cm. Endoscopic resection including endoscopic mucosal dissection (EMD), endoscopic submucosal dissection (ESD), submucosal tunneling endoscopic resection and snare assisted endoscopic resection. However, EMD and ESD procedures may be accompanied with serious complications including perforation, bleeding, and abdominal infection. Snare-assisted endoscopic resection is an alternative approach and has the advantages of a shorter procedure time and a low rate of perforation or bleeding. This study summarizes the safety and feasibility of a novel snare-assisted endoscopic resection technique and highlights the pros and cons of the different endoscopic approaches currently used for subepithelia small gastric tumors.

KEYWORDS

gastric tumors, gastrointestinal stromal tumors, gastrointestinal endoscopy, snare assisted endoscopic resection, endoscopic mucosal resection, endoscopic submucosal dissection

Introduction

Small gastric stromal tumors are common, often asymptomatic and usually detected incidentally during upper gastrointestinal endoscopy (1–3). Widespread uses of digestive endoscopy and advances in endoscopic ultrasonography (EUS) have resulted in the diagnosis of small gastric submucosal tumors (4). These tumors are mostly gastrointestinal stromal tumors which have malignant potential. Minimally invasive endoscopic resection has become increasingly popular as a method for removal of small submucosal tumors.

According to the National Comprehensive Cancer Network (NCCN) guidelines, tumor resection is the first-line treatment for non-metastatic gastrointestinal stromal tumors. Larger gastrointestinal stromal tumors (>5 cm) often have more aggressive morphologic features and proliferation activity such that laparoscopic resection or surgery is recommended for complete resection (5, 6). However, it is still controversial for the treatment criteria of gastrointestinal stromal tumors (<2 cm) because of their uncertain malignant potential. Periodical surveillance and follow-up are recommended for tumors ≤2 cm, since they are considered of very low risk of malignancy and metastasis (7). However, several researchers have emphasized that small tumors have intermediate or high risk and should be resected to confirm the diagnosis and to avoid further risk of malignancy (8, 9).

Currently, the main endoscopic approaches for small gastrointestinal tumors include endoscopic mucosal dissection (EMD), endoscopic submucosal dissection (ESD), submucosal tunneling endoscopic resection, and snare assisted endoscopic resection (10–12). EMD is not ideal as it cannot reliably ensure complete resection for relatively larger tumors. ESD reliably provides complete resection and an accurate pathological diagnosis but is associated with a risk of perforation or bleeding and requires a relatively long procedure time (13, 14). The alternative is a snare-assisted endoscopic resection procedure which, compared to ESD, include a shorter procedure time, a low rate of perforation or bleeding, and increased cost effectiveness (15). This study summarizes the safety, feasibility and utility of the novel snare-assisted endoscopic resection technique for small gastric tumors originating from the muscularis propria compared to the well-established techniques of EMR and ESD.

Snare assisted endoscopic resection-accessories and technique

Instruments and accessories

A single-channel flexible endoscope such as the EVIS GIF-Q260J, Olympus, Tokyo, Japan is used to perform the procedure. Other equipment included a snare (Boston Scientific, Ref; M00562650), a transparent cap (Olympus, Model No: D-201-11804), endoscopic clips (ROCC-D-26-195, Micro-Tech (Nanjing) Co., Ltd, Chinaor HX-610-135, Olympus), and a virtual input & output (VIO) electrosurgical generator (ICC 200 EA INT; ERBE, Tübingen, Germany). The endoscope and all accessories are sterilized by soaking in paracetic acid prior to use.

Description of technique

Routine bowel preprations are performed before the procedure. After stomach cleansing using a saline solution, a single channel flexible endoscope with a transparent cap and a snare attached on the tip of the endoscope is introduced into the stomach. The lesion is observed and sucked into the transparent cap after which the snare is used to ligate the base of the tumor. The wire of the snare is tightened and a high frequency (35W) current is applied to resect the lesion. After the lesion is removed, any bleeding is controlled with electro coagulation forceps. Endoclips are then used to close the wound site and the resected specimen is sent for histopathologic examination (Figure 1).

Snare assisted endoscopic resection- indications and limitations

Controversies remain concerning the specific indications for endoscopic resection for small gastric tumors originating from muscularis propria. Based on current experience, patients with intraluminal submucosal tumors without ulceration, and maximal tumor diameter of 2 cm measured by endoscopic ultrasonography (EUS) or computed tomography (CT), and no evidence of lymph node involvement or distant metastasis are candidates for snare-assisted endoscopic resection (16, 17). Differentiation between potentially malignant gastrointestinal stromal tumors and other benign or non-neoplastic lesions is extremely difficult using image methods, especially for small lesions. In addition, some studies have reported that small gastric stromal tumors (<2 cm) may be of intermediate or high risk. Pang et al. reported a series with tumor size <2 cm in which 9 patients (3.9%) were in the intermediate risk group and 2 patients (0.9%) were in the high risk group (18). Yang et al. reported a series in which 7 cases (2.5%) were of intermediate risk and 10 cases (3.6%) and high risk in gastric stromal tumors <2 cm (19). Gao et al. reported that EUS-suspected gastrointestinal stromal tumors larger than 9.5 mm may be associated with significant progression (20).

In our center 62 patients (21 men and 41 women) with small gastric submucosal tumors were managed with a snare-assisted endoscopic resection. The mean age was 53.7 ± 11 years (range

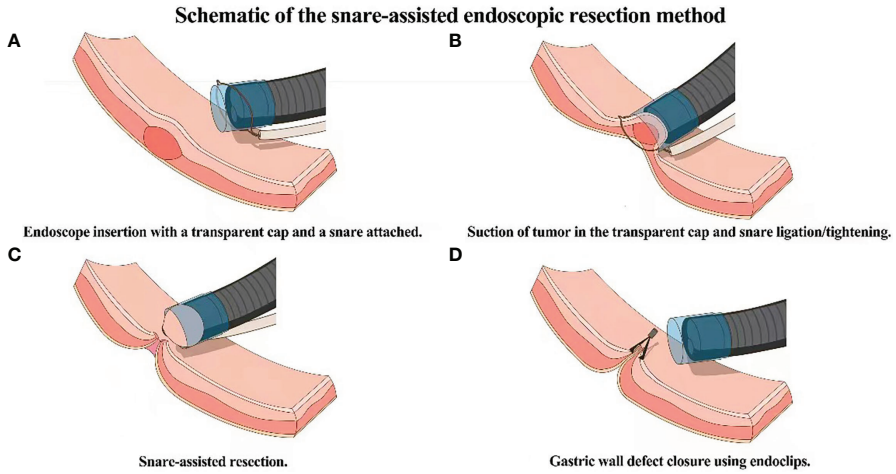

FIGURE 1
Schematic of the snare-assisted endoscopic resection method. **(A)** Endoscope entery into the stomach with a transparent cap and snare attached on the tip. **(B)** Suction of the tumor into the transparent cap and snare ligation. **(C)** Resection of the tumor. **(D)** Closure of the wound using endoclips.

28-73 years old). The mean tumor size was 0.64 ± 0.16 cm (median 0.60, range 0.31-0.97 cm). The technical success rate was 100%. The mean procedure time was 19.8 ± 9 minutes (median 20, range 9-30 min). There were no complications during or after the procedure. Due the small amount of mucosal damage wound clips were not required in 23 (37%) patients. Twenty-five (40.3%) of the tumors were located in the fundus near the cardia, 32 (51.6%) were located in the body and 5 (8%) were in the antrum. During 3-22 months of follow up, no recurrence or metastasis have occurred.

The snare-assisted endoscopic resection methods have several limitations. First, this method might not be suitable for gastric tumors located in the gastric cardia. When dissecting tumors located in the gastric cardia, the small size of the gastric cardia limits the performance of this method. Second, the direction of the traction can be provided on the oral side only. However, in most cases, this traction direction is sufficient for resection of tumors located in the fundus and corpus. Third, perforation cannot be completely avoided in all cases. Dissection of gastric tumors with a wide base will cause a wide defect in the stomach wall and likely result in a greater perforation rate. However, further investigation is needed to explore the risk factors associated with the perforation rate when using this method.

Other endoscopic approaches-techniques, safety and associated complications

Endoscopic methods other than snare-assisted endoscopic resection include, EMD, ESD, endoscopic submucosal excavation, submucosal tunneling endoscopic resection, and endoscopic full-thickness resection (21–23). All the procedures are performed under anesthesia with tracheal intubation.

Endoscopic Submucosal Dissection Technique: The endoscopic submucosal dissection mainly includes three steps: (i) identifying and marking the tumor boundaries; (ii) injecting saline mixed with indigo carmine into the submucosal layer; (iii) incising the mucosal layer with hook knife and dissecting the tumor using an IT knife.

Endoscopic Mucosal Dissection Technique: The endoscopic mucosal Resection technique is an improvement in the ESD procedure. The procedure includes. (i) Marking the tumor boundaries and injecting the solution into the submucosal layer; (ii) Incising the mucosal layer longitudinally; (iii) Dissecting the submucosal and muscular tissue to expose and remove the tumor completely; (iv) Checking the wound and clipping the incision.

EMD or ESD can be used successfully to treat gastric stromal tumors originating from the superficial muscularis propria layer, but when the tumor originates from the deep muscularis propria layer or has a tight connection with the underlying muscularis propria layer or serosal layer, the complete resection rate decreases and the rate of complications increases (24). If a small gastrointestinal stromal tumor is deemed to have a high potential for malignancy and postoperative recurrence, surgical resection is the best option to achieve sufficiently deep and lateral margins (25).

In a large-scale study of ESD treatment of 144 patients with muscularis propria tumors, the complete resection rate was 92.4% and no recurrence was detected. Several studies have demonstrated that endoscopic full-thickness resection can be the

diagnostic and definitive treatment for these tumors, with a success rate of 90% and low incidence of complications (26, 27). Therefore, for tumors <2 cm, besides periodic follow-up using EUS, endoscopic resection may be a good option. Endoscopic full-thickness resection allows en bloc resection by resecting the tumor and the surrounding serosal layer, but primary closure may be difficult, and perforation, serious bleeding and peritonitis may occur, which contraindicates its use for small muscularis tumors (28).

Endoscopic resection of muscularis propria tumors in different locations of the gastrointestinal tract can encounter difficulties; therefore, these tumors should be treated *via* different endoscopic approaches. For example, the complications rate for ESD/EFTR varies among the different locations of the stomach with the fundus being regarded as a difficult area for endoscopic resection (29). Perforation associated with endoscopic treatment is a serious complication that could confer an increase rate of mortality and major morbidity. Perioperative bleeding is another major complication of endoscopic resection of upper gastrointestinal tumors. The incidence of perioperative bleeding reported by recent studies ranges from 0 to 38.7%, which shows a high degree of variability (30, 31).

Conclusion and future direction

Advancement in endoscopic resection techniques including development of EMD and ESD has resulted in increased use of endoscopy for treatment of small gastric submucosal tumors. The selection of a particular technique depends on the size and location of the tumor. Overall, numerous studies have confirmed that these approaches are effective in terms of safety, and outcomes. Although both EMD and ESD are effective and are generally preferred for larger and deep lesions an approach that reduces procedure time, costs, and reduces hospital stay would be preferred. The snare-assisted method for the removal of gastric submucosal tumors smaller than 2 cm has the advantages of short procedure time, rare complications, short hospital stay and rapid post-procedural recovery. This is a simple and effective method for the treatment of small gastric submucosal tumors and achieves clinical success rates equal to or better than achieved with other endoscopic resection techniques (e.g., EMR and ESD) with advantages of efficacy, quickly and cost effectiveness.

The management of small gastric stromal tumors, particularly originating from the muscularis propria of the stoamch, is evolving towards an ultra minimally invasive approach. Where available, snare-assisted endoscopic resection can reduce procedure time, hospital stay, and cost of small gastric stromal tumors management. Specific treatment algorithms for snare assisted endoscopic resection, as are established for EMR and ESD, are needed. There is also a need for multinational collaboration and a consensus on training and credentialing pathway for snare assisted endoscopic resection technqiue, and on areas of future research necessary for widespread adoption.

Data availability statement

Publicly available datasets were analyzed in this study. This data can be found here: The data can be provided on request to the corresponding author. (Qian Bai, email: baiqian@zzu.edu.cn.)

Ethics statement

The studies involving human participants were reviewed and approved by the ethics committe of the Second Affiliated Hospital of Zhengzhou University. The patients/participants provided their written informed consent to participate in this study.

Author contributions

Study concept and design: SK, QB, BQ. Manuscript writing: SK, SN, SR. Analysis and interpretation of data: XC, SN. SR. Acquisition of data: XC, SN. Critical revision of manuscript and video: SK, QB. Funding obtained: SK, QB. All authors contributed to the article and approved the submitted version.

Funding

This study was financially supported by grants from Henan province innovation talents of science and technology plan (No. SB201901045) and hepatobiliary foundation of Henan Charity General Federation (No: GDXZ2019006).

Conflict of interest

The authors declare that the research was conducted in the absence of any commercial or financial relationships that could be construed as a potential conflict of interest.

Publisher's note

All claims expressed in this article are solely those of the authors and do not necessarily represent those of their affiliated organizations, or those of the publisher, the editors and the reviewers. Any product that may be evaluated in this article, or claim that may be made by its manufacturer, is not guaranteed or endorsed by the publisher.

References

1. Joensuu H, Hohenberger P, Corless CL. Gastrointestinal stromal tumour. *Lancet* (2013) 382(9896):973–83. doi: 10.1016/S0140-6736(13)60106-3

2. Akahoshi K, Oya M, Koga T, Shiratsuchi Y. Current clinical management of gastrointestinal stromal tumor. *World J Gastroenterol* (2018) 24(26):2806–17. doi: 10.3748/wjg.v24.i26.2806

3. Wang M, Xue A, Yuan W, Gao X, Fu M, Fang Y, et al. Clinicopathological features and prognosis of small gastric gastrointestinal stromal tumors (GISTs). *J Gastrointest Surg* (2019) 23(11):2136–43. doi: 10.1007/s11605-018-04070-3

4. Goto O, Kambe H, Niimi K, Mochizuki S, Asada-Hirayama I, Minatsuki C, et al. Discrepancy in diagnosis of gastric submucosal tumor among esophagogastroduodenoscopy, CT, and endoscopic ultrasonography: a retrospective analysis of 93 consecutive cases. *Abdom Imaging* (2012) 37 (6):1074–8. doi: 10.1007/s00261-012-9928-9

5. Mei L, Du W, Idowu M, von Mehren M, Boikos SA. Advances and challenges on management of gastrointestinal stromal tumors. *Front Oncol* (2018) 8:135. doi: 10.3389/fonc.2018.00135

6. Gertsen EC, van Boxel GI, Brosens LAA, Ruurda JP, van Hillegersberg R. Minimally invasive resection of Large gastric gastrointestinal stromal tumors. *Dig Surg* (2020) 37(6):441–6. doi: 10.1159/000510386

7. Zhu L, Khan S, Hui Y, Zhao J, Li B, Ma S, et al. Treatment recommendations for small gastric gastrointestinal stromal tumors: positive endoscopic resection. *Scand J Gastroenterol* (2019) 54(3):297–302. doi: 10.1080/00365521.2019.1578405

8. Li B, Chen T, Qi ZP, Yao LQ, Xu MD, Shi Q, et al. Efficacy and safety of endoscopic resection for small submucosal tumors originating from the muscularis propria layer in the gastric fundus. *Surg Endosc* (2019) 33(8):2553–61. doi: 10.1007/s00464-018-6549-6

9. Mazer L, Worth P, Visser B. Minimally invasive options for gastrointestinal stromal tumors of the stomach. *Surg Endosc* (2021) 35(3):1324–30. doi: 10.1007/s00464-020-07510-x

10. Ko EJ, Bang BW, Kwon KS, Shin YW, Kim HK. Endoscopic enucleation is effective and relatively safe in small gastric subepithelial tumors originating from muscularis propria. *Dig Dis Sci* (2019) 64(2):524–31. doi: 10.1007/s10620-018-5348-1

11. Du C, Linghu E. Submucosal tunneling endoscopic resection for the treatment of gastrointestinal submucosal tumors originating from the muscularis propria layer. *J Gastrointest Surg* (2017) 21(12):2100–9. doi: 10.1007/s11605-017-3579-7

12. Nishizawa T, Yahagi N. Endoscopic mucosal resection and endoscopic submucosal dissection: technique and new directions. *Curr Opin Gastroenterol* (2017) 33(5):315–9. doi: 10.1097/MOG.0000000000000388

13. Ahmed Y, Othman M. EMR/ESD: Techniques, complications, and evidence. *Curr Gastroenterol Rep* (2020) 22(8):39. doi: 10.1007/s11894-020-00777-z

14. Pimentel-Nunes P, Libânio D, Bastiaansen BAJ, Bhandari P, Bisschops R, Bourke MJ, et al. Endoscopic submucosal dissection for superficial gastrointestinal lesions: European society of gastrointestinal endoscopy (ESGE) guideline - update 2022. *Endoscopy* (2022) 54(6):591–622. doi: 10.1055/a-1811-7025

15. Zhu H, Shi D, Song H, Zhou M, Sun D, Li R, et al. Snare-assisted endoscopic resection of gastric subepithelial tumors originating from the muscularis propria layer: a multicenter study. *Surg Endosc* (2020) 34(9):3827–32. doi: 10.1007/s00464-019-07147-5

16. Hu J, Liu W, Chen Z, Lin D, Su M, Lan P, et al. A novel snare traction-assisted method during endoscopic resection for upper gastrointestinal submucosal tumors. *J Laparoendosc Adv Surg Tech A.* (2021) 31(4):416–22. doi: 10.1089/lap.2020.0462

17. Karaca C, Daglilar ES, Soyer OM, Gulluoglu M, Brugge WR. Endoscopic submucosal resection of gastric subepithelial lesions smaller than 20 mm: a comparison of saline solution-assisted snare and cap band mucosectomy techniques. *Gastrointest Endosc* (2017) 85(5):956–62. doi: 10.1016/j.gie.2016.09.016

18. Yang Z, Feng X, Zhang P, Chen T, Qiu H, Zhou Z, et al. Clinicopathological features and prognosis of 276 cases of primary small (≤ 2 cm) gastric gastrointestinal stromal tumors: a multicenter data review. *Surg Endosc* (2019) 33(9):2982–90. doi: 10.1007/s00464-018-6564-7

19. Pang T, Zhao Y, Fan T, Hu Q, Raymond D, Cao S, et al. Comparison of safety and outcomes between endoscopic and surgical resections of small (≤ 5 cm) primary gastric gastrointestinal stromal tumors. *J Cancer* (2019) 10(17):4132–41. doi: 10.7150/jca.29443

20. Gao Z, Wang C, Xue Q, Wang J, Shen Z, Jiang K, et al. The cut-off value of tumor size and appropriate timing of follow-up for management of minimal EUS-suspected gastric gastrointestinal stromal tumors. *BMC Gastroenterol* (2017) 17 (1):8. doi: 10.1186/s12876-016-0567-4

21. Nishida T, Goto O, Raut CP, Yahagi N. Diagnostic and treatment strategy for small gastrointestinal stromal tumors. *Cancer* (2016) 122(20):3110–8. doi: 10.1002/cncr.30239

22. Mullady DK, Tan BR. A multidisciplinary approach to the diagnosis and treatment of gastrointestinal stromal tumor. *J Clin Gastroenterol* (2013) 47(7):578–85. doi: 10.1097/MCG.0b013e3182936c87

23. Ko WJ, Cho JY. Current techniques for treating gastrointestinal stromal tumors in the upper gastrointestinal tract. *Clin Endosc* (2016) 49(3):226–8. doi: 10.5946/ce.2016.061

24. Zhang Q, Gao LQ, Han ZL, Li XF, Wang LH, Liu SD, et al. Effectiveness and safety of endoscopic resection for gastric GISTs: a systematic review. *Minim Invasive Ther Allied Technol* (2018) 27(3):127–37. doi: 10.1080/13645706.2017.1347097

25. Li L, Linghu E, Chai N. Endoscopic resection: Comparable with surgical resection for treating small-sized gastric GI stromal tumors? *Gastrointest Endosc* (2020) 91(6):1411–2. doi: 10.1016/j.gie.2020.01.046

26. Yang J, Ni M, Jiang J, Ren X, Zhu T, Cao S, et al. Comparison of endoscopic full-thickness resection and cap-assisted endoscopic full-thickness resection in the treatment of small (≤1.5 cm) gastric GI stromal tumors. *Gastrointest Endosc* (2022) 95(4):660–70.e2. doi: 10.1016/j.gie.2021.10.026

27. Ge N, Hu JL, Yang F, Yang F, Sun SY. Endoscopic full-thickness resection for treating small tumors originating from the muscularis propria in the gastric fundus: An improvement in technique over 15 years. *World J Gastrointest Oncol* (2019) 11(11):1054–64. doi: 10.4251/wjo.v11.i11.1054

28. Schmidt A, Bauder M, Riecken B, von Renteln D, Muehleisen H, Caca K, et al. Endoscopic full-thickness resection of gastric subepithelial tumors: a single-center series. *Endoscopy* (2015) 47(2):154–8. doi: 10.1055/s-0034-1390786

29. Lee JM, Yoo IK, Hong SP, Cho JY, Cho YK. A modified endoscopic full thickness resection for gastric subepithelial tumors from muscularis propria layer: Novel method. *J Gastroenterol Hepatol* (2021) 36(9):2558–61. doi: 10.1111/jgh.15505

30. Zhang Y, Meng Q, Zhou XB, Chen G, Zhu LH, Mao XL, et al. Feasibility of endoscopic resection without laparoscopic assistance for giant gastric subepithelial tumors originating from the muscularis propria layer (with video). *Surg Endosc* (2022) 36(5):3619–28. doi: 10.1007/s00464-022-09019-x

31. Khoo CY, Goh BKP, Eng AKH, Chan WH, Teo MCC, Chung AYF, et al. Laparoscopic wedge resection for suspected large (≥5 cm) gastric gastrointestinal stromal tumors. *Surg Endosc* (2017) 31(5):2271–9. doi: 10.1007/s00464-016-5229-7

frontiers | Frontiers in Oncology

TYPE Case Report
PUBLISHED 29 August 2022
DOI 10.3389/fonc.2022.970231

Check for updates

OPEN ACCESS

EDITED BY
Zhendong Jin,
Second Military Medical University, China

REVIEWED BY
Hideyuki Konishi,
Kyoto Prefectural University, Japan
Kazuhiro Kamada,
Kyoto Prefectural University of Medicine, Japan

*CORRESPONDENCE
Lianjun Di
462908604@qq.com
Biguang Tuo
tuobiguang@aliyun.com

†These authors have contributed equally to this work and share corresponding authorship

SPECIALTY SECTION
This article was submitted to Gastrointestinal Cancers: Gastric and Esophageal Cancers, a section of the journal Frontiers in Oncology

RECEIVED 15 June 2022
ACCEPTED 01 August 2022
PUBLISHED 29 August 2022

CITATION
Liu X, Wu X, Zhu J, Yagi K, Ajioka Y, Terai S, Mizuno K, Li H, Tuo B and Di L (2022) Case report: New subtype of gastric adenocarcinoma arising from an *H. pylori* infection-negative stomach: Foveolar epithelium and mucous neck cell-mixed type adenocarcinoma.
Front. Oncol. 12:970231.
doi: 10.3389/fonc.2022.970231

COPYRIGHT
© 2022 Liu, Wu, Zhu, Yagi, Ajioka, Terai, Mizuno, Li, Tuo and Di. This is an open-access article distributed under the terms of the Creative Commons Attribution License (CC BY). The use, distribution or reproduction in other forums is permitted, provided the original author(s) and the copyright owner(s) are credited and that the original publication in this journal is cited, in accordance with accepted academic practice. No use, distribution or reproduction is permitted which does not comply with these terms.

Case report: New subtype of gastric adenocarcinoma arising from an *H. pylori* infection-negative stomach: Foveolar epithelium and mucous neck cell-mixed type adenocarcinoma

Xuemei Liu[1], Xinglong Wu[2], Jiaxing Zhu[1], Kazuyoshi Yagi[3], Yoichi Ajioka[4], Shuji Terai[5], Kenichi Mizuno[5], Hongping Li[1], Biguang Tuo[1*†] and Lianjun Di[1*†]

[1]Department of Gastroenterology, Digestive Disease Hospital, Affiliated Hospital of Zunyi Medical University, Zunyi, China, [2]Department of Pathology, Affiliated Hospital of Zunyi Medical University, Zunyi, China, [3]Uonuma Institute of Community Medicine, Graduate School of Medical and Dental Sciences, Niigata University, Niigata, Japan, [4]Division of Molecular and Diagnostic Pathology, Graduate School of Medical and Dental Sciences, Niigata University, Niigata, Japan, [5]Division of Gastroenterology & Hepatology, Graduate School of Medical and Dental Sciences, Niigata University, Niigata, Japan

The characteristics of *Helicobacter pylori* (*H. pylori*) infection-negative gastric cancer have not been well documented because of its rarity, despite several types of *H. pylori* infection-negative gastric cancers being reported. In this report, we describe a case of early gastric cancer that developed without *H. pylori* infection with characteristic magnifying narrow-band imaging and novel histological findings. The difficulty in making an accurate diagnosis and differential diagnosis is highlighted, with the goal of providing more clinical experience for the diagnosis of *H. pylori* infection-negative gastric cancer.

KEYWORDS

***H. pylori* infection-negative stomach, new subtype of gastric cancer, mixed foveolar epithelium and mucous neckcell-type adenocarcinoma, bidirectional differentiation, rareness**

Introduction

Helicobacter pylori (*H. pylori*) infection causes chronic atrophic gastritis and progresses to gastric cancer (GC) (1), which is considered one of the most serious healthcare problems worldwide (2). Previously, the prevalence of *H. pylori* infection-negative gastric cancer (HPINGC) was very low, at 0.42%–5.4% of all cases of GCs (3–5). However, *H. pylori* eradication therapy is now becoming widespread, and the morbidity of *H. pylori* infection is decreasing. Therefore, it is expected that HPINGC will become a comparatively more common disease in the near future. Over the last 10 years, several types of HPINGC, including intraepithelial signet ring cell carcinoma and fundic gland type, foveolar epithelial type, cardiac gland type, pyloric gland type, and mixed type GC, classified by the Mizutani group, have been reported (3–5). Herein, we report a case of a 48-year-old woman with a new subtype of gastric adenocarcinoma: mixed foveolar epithelium and mucous neck cell-type adenocarcinoma in *H. pylori* infection-negative mucosa.

Case report

A 48-year-old woman visited our hospital after experiencing epigastric pain for approximately 1 month. There was no obvious cause of the paroxysmal dull abdominal pain and no history of loss of appetite, postprandial vomiting, or gastrointestinal bleeding. The physical examination was normal. The ^{14}C urea breath test (UBT) and serum *H. pylori* antibody results were negative, and she had no history of *H. pylori* eradication. Routine laboratory investigations were unremarkable.

Esophagogastroduodenoscopy showed a yellow and elevated lesion in the upper part of the greater curvature, and the background mucosa showed a regular arrangement of collecting venules (RAC), which was specific to the normal corpus mucosa with no atrophic changes (Figure 1A). The lesion presented as a defined light brownish area under narrow-band imaging (NBI) (Figure 1B). Magnifying endoscopy with NBI (ME-NBI) revealed an expanded and

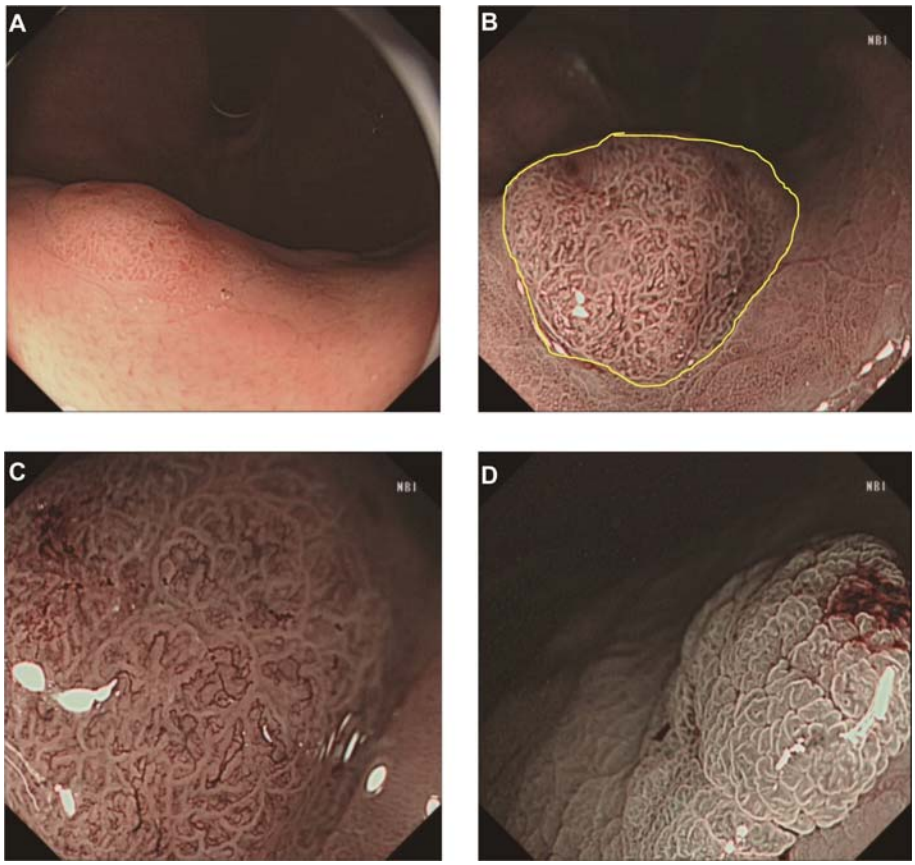

FIGURE 1
Endoscopic images. Esophagogastroduodenoscopy showed a yellowish and elevated lesion in the upper part of the greater curvature of the *H. pylori*-negative background **(A)**. NBI showed a defined light brownish elevated area **(B)**. Magnifying narrow-band imaging revealed an expanded and thinned white zone with changed polarity, as well as dilated and irregular microvascular architecture. The granular microsurface structure of this lesion was stained with acetic acid **(D)**. The yellow dotted line indicates the extent of the lesion diagnosed as cancer by histopathology.

thinned white zone with altered polarity and a dilated and irregular microvascular architecture (Figure 1C). The granular microsurface structure was detected by acetic acid staining, which was completely different from the surrounding fundic gland mucosa (Figure 1D). The initial suspected diagnosis was *H. pylori*-negative early GC based on all the above observations. This elevated lesion was diagnosed as differentiated gastric mucosal cancer that was 2 cm in diameter without ulceration or deep invasion signs, was defined as cT1a(M) by the eCura system, and met endoscopic submucosal dissection (ESD) indications (6). Therefore, diagnostic ESD was performed. Histopathologic examination of the resected specimen showed that the surrounding mucosa of the elevated lesion was a normal gastric fundic gland (Figures 2A,B); however, the superficial part of the elevated lesion had cellular atypia, and the nuclei were large and hyperchromatic with multiple layers (Figures 2A–D). These cells were Muc5AC positive (Figure 3C). Furthermore, under the atypia surface, tumor cells showed a pyloric gland-like morphology (Figures 2C, D), which was positively stained for MUC6 but negatively stained for PG1 and H^+-K^+-ATPase. Both layers, namely, the superficial part and the undersurface, displayed negativity for MUC2 and CD10 (Figures 3D–H). The Ki-67 labeling index was high in the superficial part and low in the undersurface, and P53 was positive in the superficial part (Figures 3A, B). Therefore, the final pathological diagnosis was early mixed foveolar epithelium and mucous neck cell-type gastric adenocarcinoma that was 7 × 5 mm in size (Figure 4). The postoperative course was uneventful, and she has been asymptomatic with no recurrence for 18 months.

Discussion

Currently, the prevalence of *H. pylori* infection is gradually decreasing with improvements in living conditions and eradication therapy, causing a decline in *H. pylori* infection-related GC. However, the frequency of HpNGC may show a relative increase. HpNGC is an adenocarcinoma that occurs in the stomach without active or previous *H. pylori* infection. Although various types of HpNGC have been reported (3–5), the main causal factors and diagnostic criteria have not yet been definitively established. Therefore, it is essential to recognize different types of HpNGC.

First, the definition of *H. pylori* infection negativity should be determined. Endoscopic, pathological, and clinical assessments are recommended as the criteria for the diagnosis of the gastric mucosa background without *H. pylori* infection, including negativity for *H. pylori* by endoscopic or pathological findings, negative UBT or serum IgG test, and no *H. pylori* eradication history. For endoscopic diagnosis, the lack of mucosal atrophy and the presence of RAC indicate *H. pylori* negativity. Additionally, linear erythema and fundic gland polyps are included as signs of *H. pylori* infection negativity. With pathological methods, biopsy specimens taken from the stomach are evaluated according to the updated Sydney System by pathologists. Combining endoscopic detection with

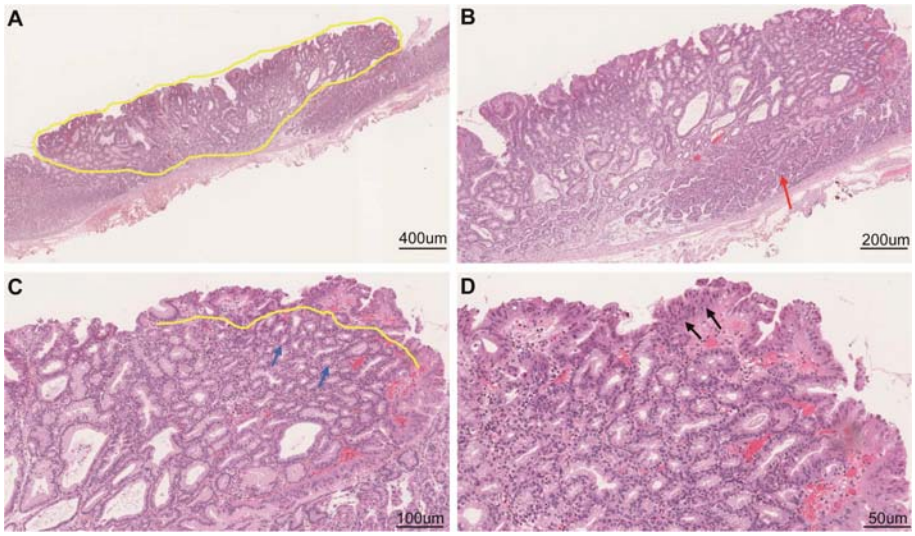

FIGURE 2
Histological examination of the resected specimen. Low-power field **(A)** and high-power field **(B–D)** of hematoxylin and eosin staining. Tumor cells were similar to mucous neck cells **(C)** and foveolar epithelium **(D)**. Scale bars represent 400 μm **(A)**, 200 μm **(B)**, 100 μm **(C)**, and 50 μm **(D)**. The yellow dotted line indicates the extent and size of the diagnosed cancer; the red arrow indicates a normal gastric corpus gland; the black arrows indicate sufficiently high cellular atypia in the surficial part; and the yellow line and blue arrows indicate that the undersurface part is the cancerous lesion.

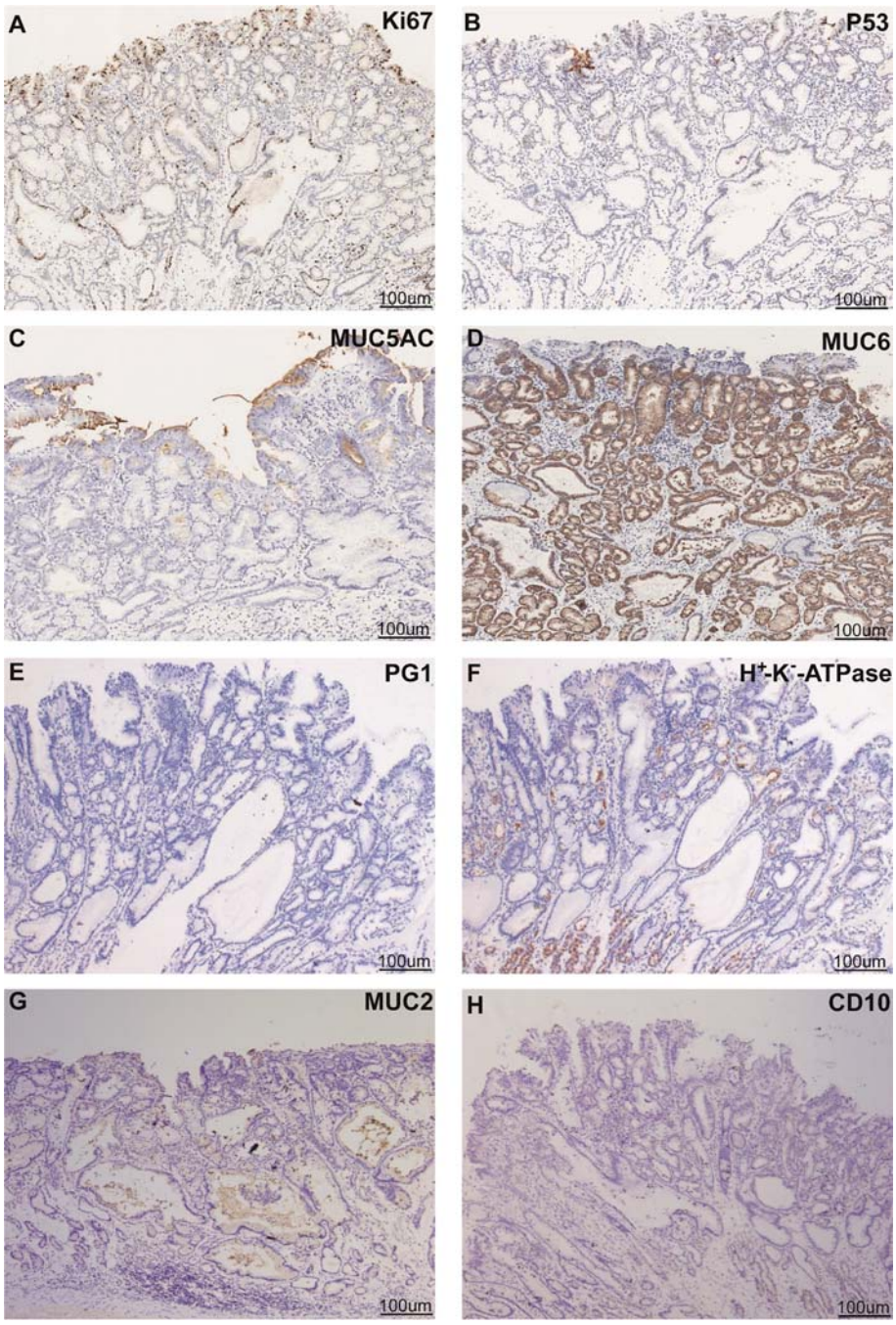

FIGURE 3
Phenotypic marker expression by immunohistochemistry staining with Ki67 **(A)**, P53 **(B)**, MUC5AC **(C)**, MUC6 **(D)**, PG1 **(E)**, proton pump (H^+ -K^+-ATPase) **(F)**, MUC2 **(G)**, and CD10 **(H)**. Scale bars represent 100 μm. Black arrows indicate different positively stained parts.

pathological findings can diagnose not only current *H. pylori* infection but also any past infection by evaluating atrophic changes and intestinal metaplasia (7, 8). With clinical methods, *H. pylori* negativity is confirmed by two or more tests, such as the UBT, serum or urine antibody test, and stool antigen test, because each test may give a false-negative result for *H. pylori* infection. Clinical methods can diagnose current infection with *H. pylori* but cannot distinguish between infection-naïve patients and patients with past infection (9). Together, the minimum criteria for *H. pylori* negativity require negative findings from two or more methods that include endoscopic or pathological findings and negative UBT or serum IgG tests, as well as no eradication history.

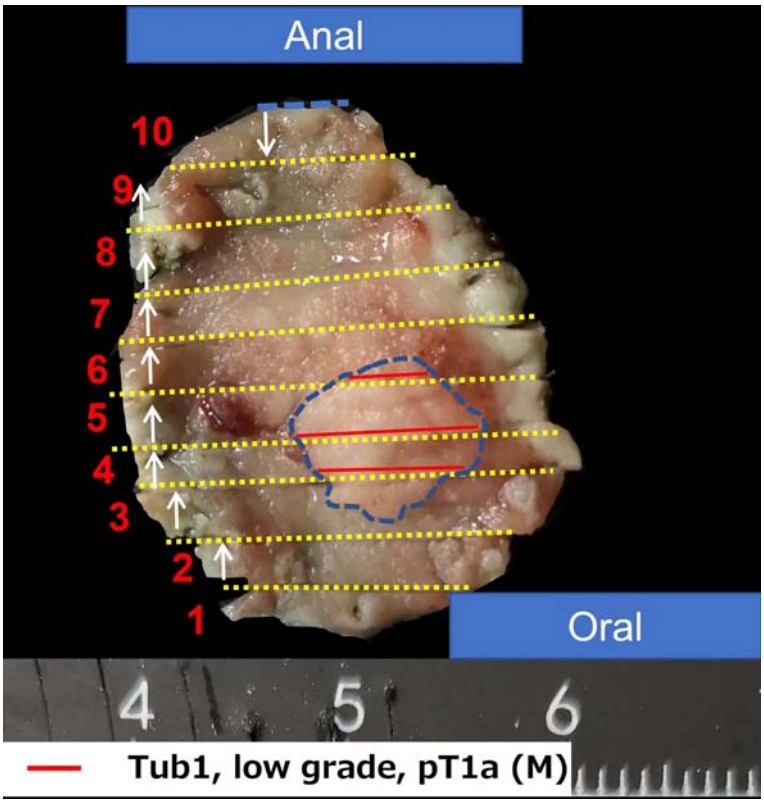

FIGURE 4
Pathological recovery diagrams. New subtype of gastric adenocarcinoma arising from an *H. pylori*-uninfected stomach: foveolar epithelium and mucous neck cell-mixed type adenocarcinoma, pT1a (M), Ly0, V0, pUL0, pHM0, and pVM0. The specimen was 2 × 2.5 cm and type 0-IIa, and the cancerous lesion was 7 × 5 mm with red marking in the blue circle.

Previously, six types of HpNGC were reported, namely, intraepithelial signet ring cell carcinoma (SRCC), fundic gland type, foveolar epithelial type, cardiac gland type, pyloric gland type, and mixed type GC (3–5). However, the variety of cells of origin may account for their varied appearance. Generally, SRCC presents as a discolored flat or depressed lesion in the lower or middle part of the stomach in relatively young female patients (5). Compared with SRCC in *H. pylori* infection-positive stomach tissue that presents in all layers, *H. pylori*-negative SRCC is generally located in the proliferative zone, as its pathological growth pattern has less invasion (10). The fundic gland type is usually located in the middle and upper part of the stomach in comparably older patients, and the predominant gross type is submucosal tumor-like. ME-NBI shows arborizing-like vessels and dilated crypts, which are defined as differentiated-type adenocarcinoma with chief cell differentiation that positively stains for H^+/K^+ ATPase, a parietal cell marker, and/or pepsinogen-I, a chief cell marker (11). The foveolar epithelial type is believed to develop from surface mucosal cells, and the gross type consists of lateral spread with some degree of elevation, villous or papillary surfaces, and a raspberry-like appearance of the non-atrophic gastric mucosa (12, 13). Unlike the undifferentiated type or fundic gland type, the field of cancerization is superficial, resulting in the appearance of defined demarcation, with MUC5AC positivity by immunohistochemistry (IHC). The cardiac gland type appears to originate from the cardiac gland, which displays depressed and red lesions, and perturbed ductal structures are observed in NBI-ME. The pyloric gland type is derived from the pyloric region with positive staining for CD10 and chromogranin A. The mixed type is believed to originate from various cell types, including foveolar epithelial cells, fundic gland cells, pyloric gland cells, or intestinal-type cells.

In this case, the tumor was located in the upper gastric corpus and developed in the fundic gland mucosa without *H. pylori* infection (Figure 1). The gross type as well as the microstructure and microvascular architecture in ME-NBI were similar to those of normal GC. Therefore, the final judgment was strongly dependent on the histological examination and IHC analysis. Histologically, the superficial part of the lesion had MUC5AC-positive staining, showed sufficiently high cellular atypia, and appeared smoothly connected to the lower part of the lesion with MUC6 positivity. However, the whole lesion was stained negatively for CD10 and MUC2. Thus, the final diagnosis was gastric-type adenocarcinoma. It is known that tumor cells have the ability to mimic the

morphology and function of mucosal epithelial cells where they co-occur. This adenocarcinoma is characterized by its existence above the fundic glands and composition of chief cells, parietal cells, and mucous neck cells. Tumors continuously occur from these mucous neck cells and form MUC6-positive parts. Furthermore, it develops to the foveolar part and forms MUC5AC-positive parts. Therefore, the whole cancerous lesion showed bidirectional differentiation, a foveolar-type epithelium to the surface, and mucous neck cells to the bottom. Since this bidirectional differentiation is a basic characteristic of the gastric mucosa, this tumor merely imitated this characteristic. This structure is different from the previously reported HpNGC.

In addition, this lesion is necessary to distinguish it from adenocarcinoma arising from pyloric gland adenoma. First, this lesion does not show typical endoscopic and histological findings of adenocarcinoma arising from pyloric gland adenoma (14, 15). The cancerous area is a superficial epithelial area showing MUC5AC. The subepithelial component of pyloric adenoma shows low atypical glands as adenoma, which indicates MUC6. A very important issue is that $MUC6^+$ glands are not only related to pyloric glands but also associated with mucous neck cells of fundic glands. In this case, tumors developed in the fundic gland mucosa without *H. pylori* infection, and it is more reasonable to regard $MUC6^+$ cells as mucous neck cells than those of the pyloric gland. Therefore, this case shows high atypical glands as cancer in the subepithelial MUC6 component. This lesion does not belong to adenocarcinoma arising from pyloric gland adenoma. Therefore, we propose the new entry of this cancer as HpNGC.

In summary, we report a rare case of early GC in an *H. pylori* infection-negative patient with the following characteristic clinicopathological findings: (1) elevated shape with an expanded and thinned white zone, as well as a dilated and irregular microvascular architecture in ME-NBI, and (2) histological differentiation toward mixed foveolar and mucous neck cell mucosa. In the future, the accumulation of cases may clarify the clinicopathological characteristics, but the current study does seem to describe a novel type of HpNGC.

Data availability statement

The original contributions presented in the study are included in the article/supplementary material. Further inquiries can be directed to the corresponding authors.

Ethics statement

The studies involving human participants were reviewed and approved by the Ethics Committee of Zunyi Medical University [2020] 2-515. The patients/participants provided their written informed consent to participate in this study. Written informed consent was obtained from the individual(s) for the publication of any potentially identifiable images or data included in this article.

Author contributions

Analysis of the results and the writing of the manuscript: XL. Collection of data: XL, KY, YA, ST, KM, and HL. Analysis of the results and pathological pictures: XW and JZ. Design and implementation of the research and revision of the manuscript: BT and LD. All authors contributed to the article and approved the submitted version.

Funding

This research was supported by the National Natural Science Foundation of China (81860103 and 82070536 to XL and 81572438 to BT) and the Guizhou Province International Science and Technology Cooperation (Gastroenterology) Base (Qian Ke He Platform Talents-HZJD [2021] 001 to XL).

Conflict of interest

The authors declare that the research was conducted in the absence of any commercial or financial relationships that could be construed as a potential conflict of interest.

Publisher's note

All claims expressed in this article are solely those of the authors and do not necessarily represent those of their affiliated organizations, or those of the publisher, the editors and the reviewers. Any product that may be evaluated in this article, or claim that may be made by its manufacturer, is not guaranteed or endorsed by the publisher.

References

1. Correa P. Human gastric carcinogenesis: a multistep and multifactorial process–first American cancer society award lecture on cancer epidemiology and prevention. *Cancer Res* (1992) 52:6735–40.

2. Yamaoka Y, Graham DY. Helicobacter pylori virulence and cancer pathogenesis. *Future Oncol* (2014) 10:1487–500. doi: 10.2217/fon.14.29

3. Kato S, Matsukura N, Tsukada K, Matsuda N, Mizoshita T, Tsukamoto T, et al. Helicobacter pylori infection-negative gastric cancer in Japanese hospital patients: incidence and pathological characteristics. *Cance Sci* (2007) 98:790–4. doi: 10.1111/j.1349-7006.2007.00478.x

4. Matsuo T, Ito M, Takata S, Tanaka S, Yoshihara M, Chayama K. Low prevalence of helicobacter pylori-negative gastric cancer among Japanese. *Helicobacter* (2011) 16:415–9. doi: 10.1111/j.1523-5378.2011.00889.x

5. Mizutani T, Araki H, Saigo C, Takada J, Kubota M, Ibuka T, et al. Endoscopic and pathological characteristics of helicobacter pylori infection-

negative early gastric cancer. *Digestive diseases* (2020) 38:474–83. doi: 10.1159/000506120

6. Hatta W, Gotoda T, Koike T, Masamune A. History and future perspectives in Japanese guidelines for endoscopic resection of early gastric cancer. *Dig Endosc* (2020) 32:180–90. doi: 10.1111/den.13531

7. Nagata N, Shimbo T, Akiyama J, Nakashima R, Kim HH, Yoshida T, et al. Predictability of gastric intestinal metaplasia by mottled patchy erythema seen on endoscopy. *Gastroenterol Res* (2011) 4:203–9. doi: 10.4021/gr357w

8. Toyokawa T, Suwaki K, Miyake Y, Nakatsu M, Ando M. Eradication of helicobacter pylori infection improved gastric mucosal atrophy and prevented progression of intestinal metaplasia, especially in the elderly population: a long-term prospective cohort study. *J Gastroenterol hepatology* (2010) 25:544–7. doi: 10.1111/j.1440-1746.2009.05995.x

9. Vaira D, Holton J, Menegatti M, Ricci C, Gatta L, Geminiani A, et al. Review article:invasive and non-invasive tests for helicobacter pylori infection. *Alimentary Pharmacol Ther* (2000) 14:13–22. doi: 10.1046/j.1365-2036.2000.00096.x

10. Horiuchi Y, Fujisaki J, Yamamoto N, Shimizu T, Miyamoto Y, Tomida H, et al. Biological behavior of the intramucosal helicobacter pylori-negative undifferentiated-type early gastric cancer: comparison with helicobacter pylori-positive early gastric cancer. *Gastric cancer* (2016) 19:160–5. doi: 10.1007/s10120-014-0452-1

11. Ueyama H, Matsumoto K, Nagahara A, Hayashi T, Yao T, Watanabe S. Gastric adenocarcinoma of the fundic gland type (chief cell predominant type). *Endoscopy* (2014) 46:153–7. doi: 10.3748/wjg.v22.i48.10523

12. Yamada A, Kaise M, Inoshita N, Toba T, Nomura K, Kuribayashi Y, et al. Characterization of helicobacter pylori-naïve early gastric cancers. *Digestion* (2018) 98:127–34. doi: 10.1159/000487795

13. Shibagaki K, Fukuyama C, Mikami H, Izumi D, Yamashita N, Mishiro T, et al. Gastric foveolar-type adenomas endoscopically showing a raspberry-like appearance in the helicobacter pylori -uninfected stomach. *Endoscopy Int Open* (2019) 7:E784–e791. doi: 10.1055/a-0854-3818

14. Vieth M, Kushima R, Borchard F, Stolte M. Pyloric gland adenoma: a clinico-pathological analysis of 90 cases. *Virchows Archiv* (2003) 442:317–21. doi: 10.1007/s00428-002-0750-6

15. Kushima R, Vieth M, Borchard F, Stolte M, Mukaisho K, Hattori T. Gastric-type well-differentiated adenocarcinoma and pyloric gland adenoma of the stomach. *Gastric cancer* (2006) 9:177–84. doi: 10.1007/s10120-006-0381-8

frontiers | Frontiers in Oncology

TYPE Original Research
PUBLISHED 14 September 2022
DOI 10.3389/fonc.2022.951485

Check for updates

OPEN ACCESS

EDITED BY
Shantibhusan Senapati,
Institute of Life Sciences (ILS), India

REVIEWED BY
Ilker Sengul,
Giresun University, Turkey
Keduovinuo Keditsu,
Putuonuo Nursing Home, India
Alessandro Puzziello,
University of Salerno, Italy

*CORRESPONDENCE
Zhi Ding
dzscch@sina.com

SPECIALTY SECTION
This article was submitted to Gastrointestinal Cancers: Gastric and Esophageal Cancers, a section of the journal Frontiers in Oncology

RECEIVED 24 May 2022
ACCEPTED 23 August 2022
PUBLISHED 14 September 2022

CITATION
Xu R, Gu Q, Xiao S, Zhao P and Ding Z (2022) Patient-reported gastrointestinal symptoms following surgery for gastric cancer and the relative risk factors.
Front. Oncol. 12:951485.
doi: 10.3389/fonc.2022.951485

COPYRIGHT
© 2022 Xu, Gu, Xiao, Zhao and Ding. This is an open-access article distributed under the terms of the Creative Commons Attribution License (CC BY). The use, distribution or reproduction in other forums is permitted, provided the original author(s) and the copyright owner(s) are credited and that the original publication in this journal is cited, in accordance with accepted academic practice. No use, distribution or reproduction is permitted which does not comply with these terms.

Patient-reported gastrointestinal symptoms following surgery for gastric cancer and the relative risk factors

Rui Xu, Qiong Gu, Shuomeng Xiao, Ping Zhao and Zhi Ding*

Department of Gastrointestinal Surgery, Sichuan Cancer Hospital and Institute, Sichuan Cancer Center, School of Medicine, University of Electronic Science and Technology of China, Chengdu, China

Purpose: The study aims to assess the incidence of short-term patient-reported postoperative gastrointestinal symptoms (PGISs) after gastric cancer surgery and explore the relative risk factors for the symptoms.

Methods: Patients with radical gastrectomy were included for this retrospective and observational study. Symptoms extracted from the MD Anderson Symptom Inventory Gastrointestinal Cancer Module (MDASI-GI) were collected in postdischarge week (PDW) 1 and postoperative month (POM) 1. The distributing states of symptoms were analyzed in PDW1 and POM1. Logistic regression models were used to identify risk factors for PGISs.

Results: Among 356 patients with complete interviews, 156 (43.8%) patients reported abdominal distention in PDW1, which was significantly higher than patients in POM1 [103 (28.9%), $p < 0.001$]. Pain (15.2% vs. 9.8%), dysphagia (5.6% vs. 7.0%), diarrhea (3.7% vs. 3.4%), and vomiting (2.5% vs. 2.8%) had no significant differences between PDW1 and POM1. Logistic models found that risk factors for PGISs were total gastrectomy [odds ratio (OR): 1.948; 95% CI: 1.097–3.459; $p = 0.023$] and disturbed sleep (OR: 3.116; 95% CI: 1.831–5.303; $p < 0.001$) in PDW1 and female gender (OR: 1.726; 95% CI: 1.071–2.782; $p = 0.025$), total gastrectomy (OR: 1.729; 95% CI: 1.055–2.834; $p = 0.030$), and disturbed sleep (OR: 3.533; 95% CI: 1.757–7.106; $p < 0.001$) in POM1.

Conclusions: The main symptom after gastric cancer surgery was abdominal distention. The relative risk factors for gastrointestinal symptoms after gastric cancer surgery were total gastrectomy and disturbed sleep. Timely symptom intervention may improve the quality of life of postgastrectomy patients.

KEYWORDS

surgery, gastrectomy, gastric cancer, symptom, risk factor

Abbreviations: PGISs, postoperative gastrointestinal symptoms; MDASI-GI, MD Anderson Symptom Inventory Gastrointestinal Cancer Module; PDW, postdischarge week; POM, postoperative month; GC, gastric cancer; PRO, patient-reported outcome; TNM, tumor–node–metastasis.

Introduction

Gastric cancer (GC) is the fifth most common type of cancer and the third leading cause of cancer deaths worldwide (1). In China, GC is still an upper gastrointestinal malignancy with high morbidity and mortality (2). At present, radical gastrectomy is the first-line treatment for GC that can prolong patients' survival time (3, 4). As surgery for GC gradually shifts toward minimally invasive approaches that can minimize trauma and postoperative complications and accelerate recovery (5, 6), postoperative gastrointestinal symptoms (PGISs) such as abdominal distention, pain, and vomiting continue to exist that affect quality of life (7).

In recent years, more attention is being given to the patient's subjective feelings as part of the recovery process (8). However, postoperative symptoms are not directly observable unless the patient reports them to the clinician (9). Patient-reported outcome (PRO) report is an important tool to assess the patient's physical health, functional status, and posttreatment feeling without interpretation bias from the medical personnel (10, 11). Many studies assumed that PROs reflect more accurately on the patient's perspective and assist clinicians to improve the quality of life of patients (12, 13).

PGIS is one of the common postoperative symptoms of GC. Gastrointestinal symptoms could increase patient distress and contribute to changes in functional status, treatment failure, depression, anxiety, and poor quality of life (14). In order to promote postoperative recovery and improve patients' quality of life, this study aims to understand short-term patient-reported PGISs and explore relative risk factors of PGISs.

Methods

Participants

This study included patients with GC who underwent radical gastrectomy with D2 lymphadenectomy in the Department of Gastrointestinal Surgery of Sichuan Cancer Hospital in China between January 2020 and December 2021. Informed consent was taken from all of the participants in this study. The inclusion criteria were as follows: 1) age 18 year and above; 2) GC tumor–node–metastasis (TNM) stage c/pT1-4NxM0; 3) under standard radical gastrectomy (total, proximal, and distal gastrectomy). Exclusion criteria included: 1) previous abdominal radiotherapy; 2) preoperative chemotherapy; 3) pulmonary, cardiovascular, and renal disease; 4) mental illness; 5) diabetes.

Data collection

The electronic medical record system provided age, gender, surgical data, and TNM stage according to the eighth edition of "TNM Classification of Malignant Tumors" by the American Joint Committee on Cancer/Union for International Cancer Control (15). The double-tract reconstruction was used in proximal gastrectomy. Roux-en-Y anastomosis of the esophagus and jejunum was performed in total gastrectomy. Multiple anastomotic methods were applied to distal gastrectomy, such as Billroth I, Billroth II, and Billroth II plus Braun anastomosis and Roux-en-Y anastomosis of the remnant stomach and jejunum. PGISs and sleep status were reported by patients, and each patient was interviewed by a healthcare provider who was trained in qualitative interviewing. The interviews were qualitative one-to-one interviews, which were conducted postdischarge week (PDW) 1 and postoperative month (POM) 1. Each interview lasted for 20 min per patient. PGISs (pain, abdominal distention, diarrhea, vomiting, dysphagia) and disturbed sleep were asked during the interview. All of the symptoms were extracted from the MD Anderson Symptom Inventory Gastrointestinal Cancer Module (MDASI-GI), a valid reliable questionnaire for assessing symptom severity and interference with function in gastrointestinal cancer (16, 17).

Data analysis

Demographic data, clinical data, and symptoms were presented as numbers and percentages. The t test and chi-square test were used to examine the quantitative and categorical data, respectively.

We performed univariate analyses using gender (women vs. men), approach of operations (open surgery vs. laparoscopic surgery), type of gastrectomy (total vs. proximal vs. distal), TNM stage (stages I–II vs. stage III), and sleep status (disturbed vs. non-disturbed), and PGISs were taken as the dependent variable. Those variables with p-values ≤0.05 were entered into the multivariate logistic analyses to determine the risk factors for PGISs.

Statistical analyses were performed using SPSS 20.0 software (IBM Corp., Armonk, NY, USA). A two-sided p-value <0.05 was considered significant.

Results

Patient characteristics

A total of 356 cases of postoperative patients with GC were involved in the study. There were 249 (69.9%) men and 107 (30.1%) women, and over 50% of the patients were aged ≤60 years (50.3%). Fifty (14%) patients underwent open surgery, and 306 (86%) patients underwent laparoscopic surgery. Of patients included in the study, 215 (60.4%) patients were staged with TNM I–II, and 141 (39.6%) patients were staged with TNM III. Baseline demographic and clinical features are summarized in Table 1.

Postoperative gastrointestinal symptoms

A total of 252 (70.8%) patients reported PGISs in PDW1, comprising abdominal distention (156, 43.8%), pain (54, 15.2%), dysphagia (20, 5.6%), diarrhea (13, 3.7%), and vomiting (9, 2.5%). Of the 356 patients, 185 (52.0%) patients reported PGISs about abdominal distention (103, 28.9%), pain (35, 9.8%), dysphagia (25, 7.0%), diarrhea (12, 3.4%), and vomiting (10, 2.8%) in POM1. The ratio of abdominal distention symptom reported in POM1 was lower than that in PDW1 (28.9% vs. 43.8%, $p < 0.001$). However, similar numbers of other PGISs were reported at two points in time (Figure 1).

The relations between postoperative gastrointestinal symtoms and clinical features

In POM1, the ratio of PGISs in men was less than that in women (48.2% vs. 60.7%, $p < 0.001$). In Table 2, compared with patients who underwent distal gastrectomy, the ratio of dysphagia was significantly higher in patients with total gastrectomy in PDW1 and POM1 (all $p < 0.001$) and the ratio of dysphagia was also significantly higher in patients with proximal gastrectomy in PDW1 ($p = 0.002$) and POM1 ($p = 0.003$).

TABLE 1 Demographics and clinical characteristics.

Variables	Number (%)
Age (years)	
≤60	179 (50.3)
>60	177 (49.7)
Gender	
Men	249 (69.9)
Women	107 (30.1)
Surgical approach	
Open surgery	50 (14.0)
Laparoscopic surgery	306 (86.0)
Type of gastrectomy	
Total	100 (28.1)
Proximal	30 (8.4)
Distal	226(63.5)
T stage	
T1	90 (25.3)
T2	59 (16.6)
T3	108 (30.3)
T4	99 (27.8)
N stage	
N0	155 (43.5)
N1	64 (18.0)
N2	69 (19.4)
N3	68 (19.1)
TNM stage	
I–II	215 (60.4)
III	141 (39.6)

The relations between postoperative gastrointestinal symtoms and sleep status

As Table 3 shows, patients with disturbed sleep reported PGISs more than patients with non-disturbed sleep in PDW1 and POM1 (all $p < 0.001$).

Risk factors for postoperative gastrointestinal symtoms

The multivariate logistic regression model identified that variables significantly associated with PGISs in PDW1 included total gastrectomy [odds ratio (OR): 1.948; 95% CI: 1.097–3.459; $p = 0.023$], disturbed sleep (OR: 3.116; 95% CI: 1.831–5.303; $p < 0.001$), and female gender (OR: 1.726; 95% CI: 1.071–2.782; $p = 0.025$) and total gastrectomy (OR: 1.729; 95% CI: 1.055–2.834; $p = 0.030$) and disturbed sleep (OR: 3.533; 95% CI: 1.757–7.106; $p < 0.001$) in POM1 (Table 4).

Discussion

Gastrointestinal symptoms are particularly common after abdominal surgery (18, 19). To our knowledge, this is the first study to alone observe short-term PGISs in GC. Five symptoms extracted from MDASI-GI were reported by patients through interviews. In this study, we found that abdominal distension is the main PGIS (43.8% vs. 28.9%), followed by pain (15.2% vs. 9.8%), dysphagia (5.6% vs. 3.4%), diarrhea (3.7% vs. 3.4%), and vomiting (2.5% vs. 2.8%) in PDW1 and POM1. Furthermore, with the recovery process, abdominal distension symptom was significantly relieved within 1 month after surgery, and other symptoms were also relieved but without statistical differences. Abdominal distension is the most common symptom after GC surgery and often associated with gastrointestinal dysfunction; studies found (18) that operation, analgesia, and inflammatory reaction could lead to the occurrence and development of gastrointestinal dysfunction. Therefore, the proportion of abdominal distension in early postoperative period was high, but with the recovery of gastrointestinal function, its ratio will decrease significantly. Previous studies showed that PGISs could increase the risk of postoperative complications, prolong the time of hospitalization, delay the follow-up adjuvant treatment, and reduce the quality of life (20, 21). PRO can provide the real

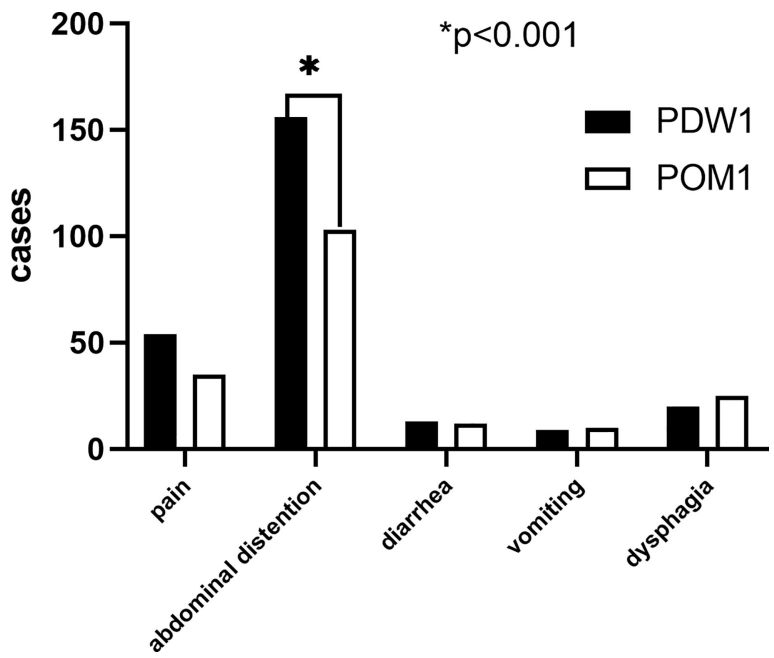

FIGURE 1
Frequency of postoperative gastrointestinal symptoms in the 356 patients. *$p < 0.001$.

feeling of patients after surgery, so that clinicians can carry out the necessary intervention to accelerate postoperative rehabilitation and improve the quality of life.

In this study, we found that the incidence of dysphagia symptom was higher in patients with total and proximal gastrectomy. This is consistent with studies from Lee et al. (22) and Choi et al. (23) suggesting that the dysphagia symptom was worse in the total gastrectomy group. Because of the disharmony and inconsistency of contraction and peristalsis between the esophagus and jejunum, patients with total or proximal gastrectomy sometimes suffer from dysphagia when eating. In addition, patients who underwent distal gastrectomy have a normal cardiac structure, so less dysphagia symptom is reported. According to multivariate models, total gastrectomy was considered as a risk factor for PGISs ($p < 0.05$). To reduce the burden of PGISs, surgeons should make the decision of total gastrectomy with caution and give professional dietary guidance after surgery.

The occurrence and development of PGISs are often related to many factors. Ana et al. (24) considered that gender is the influencing factor of gastrointestinal symptoms in patients with advanced cancer. Nolte et al. (25) found that the quality of life also varies by gender. In this study, we found that the ratio of women with PGISs was more than that of men in POM1 (60.7% vs. 48.2%, $p < 0.001$); this result clearly showed that the recovery of the gastrointestinal tract in women was slow after surgery. In fact, women are not only more emotionally sensitive than men but also more likely to think negatively (26, 27). In addition, Chinese male patients may show higher tolerance to their own symptoms due to the influence of traditional culture. Thus, our clinicians should keep in mind that gender will affect PROs and help them adjust their moods.

Moreover, we found that sleep status affected the occurrence of PGISs, and patients with disturbed sleep suffered from PGISs more than those without sleep disturbance ($p < 0.001$). Evidence has indicated that sleep disturbance occurred more frequently among cancer survivors (28), especially in GC (29), which reduces the quality of life and increases the incidence of complications (30). Patients who underwent gastrectomy always have psychosocial distresses such as fear of recurrence, difficulty in resuming social life, and concerns about family and finances (31), which can affect sleep status and then aggravate PGISs. In this study, we found that the risk of increased ratios of PGISs with disturbed sleep was 3.116 times that of patients with non-disturbed sleep in PDW1 (OR: 3.116; 95% CI: 1.831–5.303; $p < 0.001$) and 3.533 times in POM1 (OR: 3.533; 95% CI: 1.757–7.106; $p < 0.001$). Clinically, the sleep status and psychological status of patients are often ignored by surgeons. Therefore, clinicians need to pay more attention to sleep conditioning and psychological comfort.

In order to improve patients' symptoms and enhance the quality of life of patients, timely intervention is very important.

TABLE 2 The relations between PGISs and clinical characteristics.

Variables	PDW1						POM1					
	Non-PGISs	Abdominal distention	Pain	Diarrhea	Vomiting	Dysphagia	Non-PGISs	Abdominal distention	Pain	Diarrhea	Vomiting	Dysphagia
Age (years)												
≤60	47 (26.3)	80 (44.7)	28 (15.6)	8 (4.5)	7 (3.9)	9 (5.0)	77 (43.0)	57 (31.8)	20 (11.2)	6 (3.4)	8 (4.5)	11 (6.1)
>60	57 (32.2)	76 (42.9)	26 (14.7)	5 (2.8)	2 (1.1)	11 (6.2)	94 (53.1)	46 (26.0)	15 (8.5)	6 (3.4)	2 (1.1)	14 (7.9)
Gender												
Men	78 (31.3)	108 (43.4)	37 (14.9)	9 (3.6)	5 (2.0)	12 (4.8)	129 (51.8)[#]	71 (28.5)	19 (7.6)	9 (3.6)	5 (2.0)	16 (6.4)
Women	26 (24.3)	48 (44.9)	17 (15.9)	4 (3.7)	4 (3.7)	8 (7.5)	42 (39.3)	32 (29.9)	16 (15.0)	3 (2.8)	5 (4.7)	9 (8.4)
Surgical approach												
Open surgery	16 (32.0)	19 (38.0)	8 (16.0)	2 (4.0)	2 (4.0)	3 (6.0)	24 (48.0)	14 (28.0)	6 (12.0)	2 (4.0)	1 (2.0)	3 (6.0)
Laparoscopic surgery	88 (28.8)	137 (44.8)	46 (15.0)	11 (3.6)	7 (2.3)	17 (5.6)	147 (48.0)	89 (29.1)	29 (9.5)	10 (3.3)	9 (2.9)	22 (7.2)
Type of gastrectomy												
Total	21 (21.0)	45 (45.0)	14 (14.0)	5 (5.0)	1 (1.0)	14 (14.0)*	39 (39.0)	29 (29.0)	8 (8.0)	7 (7.0)	2 (2.0)	15 (15.0)*
Proximal	8 (26.7)	11 (36.7)	5 (16.7)	1 (3.3)	1 (3.3)	4 (13.3)[†]	14 (46.7)	8 (26.7)	2 (6.7)	0 (0.0)	1 (3.3)	5 (16.7)[‡]
Distal	75 (33.2)	100 (44.2)	35 (15.5)	7 (3.1)	7 (3.1)	2 (0.9)	118 (52.5)	66 (29.2)	25 (11.1)	5 (2.2)	7 (3.1)	5 (2.2)
TNM stage												
I–II	61 (28.4)	97 (45.1)	35 (16.3)	8 (3.7)	7 (3.3)	7 (3.3)	111 (51.6)	61 (28.4)	22 (10.2)	6 (2.8)	5 (2.3)	10 (4.7)
III	43 (30.5)	59 (41.8)	19 (13.5)	5 (3.5)	2 (1.4)	13 (9.2)	60 (42.6)	42 (29.8)	13 (9.2)	6 (4.3)	5 (3.5)	15 (10.6)

PDW, postdischarge week; POM, postoperative month; PGISs, postoperative gastrointestinal symptoms.
[#]$p < 0.001$ compared with women; *$p < 0.001$ compared with distal gastrectomy; [†]$p = 0.002$ compared with distal gastrectomy; [‡]$p = 0.003$ compared with distal gastrectomy.

10.3389/fonc.2022.951485

TABLE 3 The relations between PGISs and sleep status.

	PDW1		*p*-value	POM1		*p*-value
	Non-PGISs	PGISs		Non-PGISs	PGISs	
Sleep status			**<0.001**			**<0.001**
Disturbed	23 (16.1)	120 (83.9)		12 (24.0)	38 (76.0)	
Non-disturbed	81 (38.0)	132 (62.0)		159 (52.0)	147 (48.0)	

PDW, postdischarge week; POM, postoperative month; PGISs, postoperative gastrointestinal symptoms. The bold values mean that there are statistically significant.

TABLE 4 Multivariate logistic regression analysis of risk factors for PGISs.

Relative factors	PDW1	Multivariate analysis			POM1	Multivariate analysis		
	N	OR	95%CI	*P*- value	n	OR	95%CI	*P*- value
Gender								
Women	81	1.299	0.759-2.224	0.340	65	1.726	1.071-2.782	**0.025**
Men	171	Ref.			120	Ref.		
Surgical approach								
Open surgery	34	0.868	0.445-1.695	0.679	26	0.884	0.475-1.647	0.698
Laparoscopic surgery	218	Ref.			159	Ref.		
Type of gastrectomy								
Total	79	1.948	1.097-3.459	**0.023**	61	1.729	1.055-2.834	**0.030**
Partial	173	Ref.			124	Ref.		
TNM stage								
I–II	154	1.182	0.722-1.937	0.506	104	0.727	0.463-1.140	0.165
III	98	Ref.			81	Ref.		
Sleep status								
Disturbed	120	3.116	1.831-5.303	**<0.001**	38	3.533	1.757-7.106	**<0.001**
Non-disturbed	132	Ref.			147	Ref.		

PDW, postdischarge week; POM, postoperative month; PGISs, postoperative gastrointestinal symptoms. The bold values mean that there are statistically significant.

Comprehensive health education was proven to be an effective method, which could markedly improve patients' quality of life through disease awareness-raising activities, guidance on behavior and lifestyle, rehabilitation management, and psychological counseling (32). Drug therapy is also an option. Previous studies have found that auricular-plaster therapy of traditional Chinese medicine can improve postoperative gastrointestinal dysfunction and the quality of life (33).

This study has several limitations. Firstly, patients and healthcare providers were from the same department; patients' reported symptoms would be biased. Secondly, few patients underwent open surgery, which may lead us to underestimate the incidence of PGISs. However, minimally invasive surgical approaches to the treatment of GC have become increasingly more common (34). Finally, we only observed the main symptoms; other symptoms reported by patients were not included, which may lead to selection bias. Further research needs to be continued.

Conclusions

The main symptom after GC surgery was abdominal distention. The relative risk factors for gastrointestinal symptoms after GC surgery were total gastrectomy and disturbed sleep. Timely symptom intervention may improve the quality of life of postgastrectomy patients.

Data availability statement

The original contributions presented in the study are included in the article/supplementary material. Further inquiries can be directed to the corresponding author.

Ethics statement

Ethical review and approval was not required for the study on human participants in accordance with the local legislation

and institutional requirements. Written informed consent for participation was not required for this study in accordance with the national legislation and the institutional requirements.

Author contributions

RX and ZD designed the study; QG and SX collected the data; RX drafted the manuscript; PZ, ZD, and SX undertook the statistical analysis. All authors read and approved the final manuscript.

Funding

This work was supported by the Sichuan Provincial Science and Technology Project (No. 2020YFS0430; No. 2018SZ0263).

Conflict of interest

The authors declare that the research was conducted in the absence of any commercial or financial relationships that could be construed as a potential conflict of interest.

Publisher's note

All claims expressed in this article are solely those of the authors and do not necessarily represent those of their affiliated organizations, or those of the publisher, the editors and the reviewers. Any product that may be evaluated in this article, or claim that may be made by its manufacturer, is not guaranteed or endorsed by the publisher.

References

1. Bray F, Ferlay J, Soerjomataram I, Siegel RL, Torre LA, Jemal A. Global cancer statistics 2018: GLOBOCAN estimates of incidence and mortality worldwide for 36 cancers in 185 countries]. *CA Cancer J Clin* (2018) 68:394–424. doi: 10.3322/caac.21492

2. Cui H, Cao B, Liu G, Xi H, Chen Z, Liang W, et al. Comparison of short-term outcomes and quality of life in totally laparoscopic distal gastrectomy and totally robotic distal gastrectomy for clinical stage I-III gastric cancer: study protocol for a multi-institutional randomised clinical trial. *BMJ Open* (2021) 11:e043535. doi: 10.1136/bmjopen-2020-043535

3. Xu R, Xiao S, Ding Z, Zhao P. Does early postoperative enteral ecoimmunonutrition enhance intestinal function in gastric cancer? *Asia Pac J Clin Nutr* (2020) 29:469–75. doi: 10.6133/apjcn.202009_29(3).0004

4. Zheng J, Xue Y, Li C. Short-term efficacy and quality of life of gastric cancer patients undergoing radical gastrectomy assisted by external vision. *Comput Math Methods Med* (2021) 2021:4256347. doi: 10.1155/2021/4256347

5. Li GX. Shifting paradigm toward minimally invasive gastrectomy for gastric cancer–china's contribution. *Zhonghua Wei Chang Wai Ke Za Zhi* (2021) 24:657–61. doi: 10.3760/cma.j.cn.441530-20210728-00301

6. Berlth F, Knospe L, Jansen-Winkeln B, Hadzijusufovic E, Tagkalos E, Niebisch S, et al. Status of minimally invasive gastrectomy: Current advancements: robotic surgery and intraoperative imaging for gastric cancer]. *Chirurg* (2021) 92:528–34. doi: 10.1007/s00104-021-01391-z

7. Eom BW, Lee J, Lee IS, Son YG, Ryu KW, Kim SG, et al. Development and validation of a symptom-focused quality of life questionnaire (KOQUSS-40) for gastric cancer patients after gastrectomy. *Cancer Res Treat* (2021) 53:763–72. doi: 10.4143/crt.2020.1270

8. Hu X, Zhao F, Yu H, Luo Y, Liu J, Zhang Y. GC-PROM: validation of a patient-reported outcomes measure for Chinese patients with gastric cancer. *BMC Cancer* (2020) 20:41. doi: 10.1186/s12885-020-6518-z

9. Lee L, Tran T, Mayo NE, Carli F, Feldman LS. What does it really mean to "recover" from an operation? *Surgery* (2014) 155:211–6. doi: 10.1016/j.surg.2013.10.002

10. Fiore JFJr, Figueiredo S, Balvardi S, Lee L, Nauche B, Landry T, et al. How do we value postoperative recovery?: a systematic review of the measurement properties of patient-reported outcomes after abdominal surgery. *Ann Surg* (2018) 267:656–69. doi: 10.1097/SLA.0000000000002415

11. US Department of Health and Human Services FDA Center for Drug Evaluation and Research, US Department of Health and Human Services FDA Center for Biologics Evaluation and Research and US Department of Health and Human Services FDA Center for Devices and Radiological Health. Guidance for industry: patient-reported outcome measures: use in medical product development to support labeling claims: draft guidance. *Health Qual Life Outcomes* (2006) 4:79. doi: 10.1186/1477-7525-4-79

12. Schütte K, Schulz C, Middelberg-Bisping K. Impact of gastric cancer treatment on quality of life of patients. *Best Pract Res Clin Gastroenterol* (2021) 50-51:101727. doi: 10.1016/j.bpg.2021.101727

13. Hu Y, Zaydfudim VM. Quality of life after curative resection for gastric cancer: Survey metrics and implications of surgical technique. *J Surg Res* (2020) 251:168–79. doi: 10.1016/j.jss.2020.02.005

14. Cherwin CH. Gastrointestinal symptom representation in cancer symptom clusters: a synthesis of the literature. *Oncol Nurs Forum* (2012) 39:157–65. doi: 10.1188/12.ONF.157-165

15. Ji X, Bu ZD, Yan Y, Li ZY, Wu AW, Zhang LH, et al. The 8th edition of the American joint committee on cancer tumor-node-metastasis staging system for gastric cancer is superior to the 7th edition: results from a Chinese monoinstitutional study of 1663 patients. *Gastric Cancer* (2018) 21:643–52. doi: 10.1007/s10120-017-0779-5

16. Wang XS, Williams LA, Eng C, Mendoza TR, Shah NA, Kirkendoll KJ, et al. Validation and application of a module of the m. d. Anderson symptom inventory for measuring multiple symptoms in patients with gastrointestinal cancer (the MDASI-GI). *Cancer* (2010) 116:2053–63. doi: 10.1002/cncr.24920

17. Li N, Lu J, Xia D, Jiang X, Wen X, Qin X, et al. Serum biomarkers predict adjuvant chemotherapy-associated symptom clusters in radical resected colorectal cancer patients. *J Gastrointest Oncol* (2022) 13:197–209. doi: 10.21037/jgo-21-904

18. Tan S, Wu G, Yu W, Li N. Research advance in causes of postoperative gastrointestinal dysfunction. *Zhonghua Wei Chang Wai Ke Za Zhi* (2016) 19:351–5. doi: 10.3760/cma.j.issn.1671-0274.2016.03.029

19. Wang L, Ding K, Yang D, Zhao X. Management strategies of postoperative gastrointestinal tract dysfunction:a review of 210 cases. *Asian J Surg* (2022) 45:479–80. doi: 10.1016/j.asjsur.2021.08.065

20. Zhang S, Guo W, Jiao Y, Guo X, Xu L, Gao H. Systematic review and meta-analysis of the effect of transcutaneous electrical acupoint stimulation on gastrointestinal function after laparoscopic surgery. *Ann Palliat Med* (2021) 10:11840–8. doi: 10.21037/apm-21-3046

21. Chen Y, Dong C, Lian G, Li D, Yin Y, Yu W, et al. Dexamethasone on postoperative gastrointestinal motility: A placebo-controlled, double-blinded, randomized controlled trial. *J Gastroenterol Hepatol* (2020) 35:1549–54. doi: 10.1111/jgh.15020

22. Lee JH, Lee HJ, Choi YS, Kim TH, Huh YJ, Suh YS, et al. Postoperative quality of life after total gastrectomy compared with partial gastrectomy: Longitudinal evaluation by European organization for research and treatment of cancer-OG25 and STO22. *J Gastric Cancer* (2016) 16:230–9. doi: 10.5230/jgc.2016.16.4.230

23. Choi JH, Han SU, Yang HK, Kim YW, Ryu KW, Park JM, et al. The pattern of postoperative quality of life following minimally invasive gastrectomy for gastric

cancer: a prospective cohort from Korean multicenter robotic gastrectomy trial. *Ann Surg Treat Res* (2020) 99:275–84. doi: 10.4174/astr.2020.99.5.275

24. Ana J, Rosario M, Alberto A, Virginia M, Yolanda V, Beatriz M, et al. Symptom clusters in advanced cancer. *J Pain Symptom Manage* (2011) 42(1):24–31. doi: 10.1016/J.JPAINSYMMAN.2010.10.266

25. Nolte S, Liegl G, Petersen MA, Aaronson NK, Costantini A, Fayers PM, et al. General population normative data for the EORTC QLQ-C30 health-related quality of life questionnaire based on 15,386 persons across 13 European countries, Canada and the unites states. *Eur J Cancer* (2019) 107:153–63. doi: 10.1016/j.ejca.2018.11.024

26. Linden W, Vodermaier A, Mackenzie R, Greig D. Anxiety and depression after cancer diagnosis: prevalence rates by cancer type, gender, and age. *J Affect Disord* (2012) 141:343–51. doi: 10.1016/j.jad.2012.03.025

27. Belov OO, Dronenko VG, Rybinska VA, Tkach AA, Shevchuk TV. Gender features of depressive and anxious manifestations of the lung cancer patients. *Wiad Lek* (2022) 75:393–6. doi: 10.36740/WLek202202112

28. Garland SN, Johnson JA, Savard J, Gehrman P, Perlis M, Carlson L, et al. Sleeping well with cancer: a systematic review of cognitive behavioral therapy for insomnia in cancer patients. *Neuropsychiatr Dis Treat* (2014) 10:1113–24. doi: 10.2147/NDT.S47790

29. Yoon HS, Yang JJ, Song M, Lee HW, Lee Y, Lee KM, et al. Short sleep duration and its correlates among cancer survivors in Korea: the Korea national health and nutrition examination surveys. *Asian Pac J Cancer Prev* (2015) 16:4705–10. doi: 10.7314/apjcp.2015.16.11.4705

30. Schulte FSM, Chalifour K, Eaton G, Garland SN. Quality of life among survivors of adolescent and young adult cancer in Canada: A young adults with cancer in their prime (YACPRIME) study. *Cancer* (2021) 127:1325–33. doi: 10.1002/cncr.33372

31. Rastogi S, Tevaarwerk AJ, Sesto M, Van Remortel B, Date P, Gangnon R, et al. Effect of a technology-supported physical activity intervention on health-related quality of life, sleep, and processes of behavior change in cancer survivors: A randomized controlled trial. *Psychooncology* (2020) 29:1917–26. doi: 10.1002/pon.5524

32. Gao Q, Li H, Zou Y, Hou B, Liu L. Effectiveness of a comprehensive post-operative health education program in improving quality of life after gastric cancer surgery. *Ann Palliat Med* (2020) 9:921–6. doi: 10.21037/apm.2020.04.14

33. Zhang Y, Wang X, Yang H. Effect of traditional Chinese medicine nursing on postoperative patients with gastric cancer and its impact on quality of life. *Am J Transl Res* (2021) 13(5):5589–95.

34. Costantino CL, Mullen JT. Minimally invasive gastric cancer surgery. *Surg Oncol Clin N Am* (2019) 28:201–13. doi: 10.1016/j.soc.2018.11.007

frontiers | Frontiers in Oncology

TYPE Original Research
PUBLISHED 28 September 2022
DOI 10.3389/fonc.2022.1000447

Check for updates

OPEN ACCESS

EDITED BY
Zhendong Jin,
Second Military Medical University, China

REVIEWED BY
Liqi Sun,
Second Military Medical University
Farooq Rashid,
Chongqing Public Health Medical Center, China

*CORRESPONDENCE
Wenzhi Guo
fccguowz@zzu.edu.cn
Yuting He
fccheyt1@zzu.edu.cn

†These authors have contributed equally to this work

SPECIALTY SECTION
This article was submitted to Gastrointestinal Cancers: Hepato Pancreatic Biliary Cancers, a section of the journal Frontiers in Oncology

RECEIVED 22 July 2022
ACCEPTED 05 September 2022
PUBLISHED 28 September 2022

CITATION
Yu X, Zhang Q, Zhang S, He Y and Guo W (2022) Single-cell sequencing and establishment of an 8-gene prognostic model for pancreatic cancer patients.
Front. Oncol. 12:1000447.
doi: 10.3389/fonc.2022.1000447

COPYRIGHT
© 2022 Yu, Zhang, Zhang, He and Guo. This is an open-access article distributed under the terms of the Creative Commons Attribution License (CC BY). The use, distribution or reproduction in other forums is permitted, provided the original author(s) and the copyright owner(s) are credited and that the original publication in this journal is cited, in accordance with accepted academic practice. No use, distribution or reproduction is permitted which does not comply with these terms.

Single-cell sequencing and establishment of an 8-gene prognostic model for pancreatic cancer patients

Xiao Yu[1,2,3,4†], Qiyao Zhang[1,2,3,4†], Shuijun Zhang[1,2,3,4], Yuting He[1,2,3,4*] and Wenzhi Guo[1,2,3,4*]

[1]Department of Hepatobiliary and Pancreatic Surgery, The First Affiliated Hospital of Zhengzhou University, Zhengzhou, China, [2]Key Laboratory of Hepatobiliary and Pancreatic Surgery and Digestive Organ Transplantation of Henan Province, The First Affiliated Hospital of Zhengzhou University, Zhengzhou, China, [3]Open and Key Laboratory of Hepatobiliary & Pancreatic Surgery and Digestive Organ Transplantation at Henan Universities, The First Affiliated Hospital of Zhengzhou University, Zhengzhou, China, [4]Henan Key Laboratory of Digestive Organ Transplantation,The First Affiliated Hospital of Zhengzhou University, Zhengzhou, China

Background: Single-cell sequencing (SCS) technologies enable analysis of gene structure and expression data at single-cell resolution. However, SCS analysis in pancreatic cancer remains largely unexplored.

Methods: We downloaded pancreatic cancer SCS data from different databases and applied appropriate dimensionality reduction algorithms. We identified 10 cell types and subsequently screened differentially expressed marker genes of these 10 cell types using FindAllMarkers analysis. Also, we evaluated the tumor immune microenvironment based on ESTIMATE and MCP-counter. Statistical enrichment was evaluated using Gene Ontology and Kyoto Encyclopedia of Genes and Genomes pathway analysis. We used all candidate gene sets in KEGG database to perform gene set enrichment analysis. We used LASSO regression to reduce the number of genes in the pancreatic risk model by R package *glmnet*, followed by rtPCR to validate the expression of the signature genes in different pancreatic cancer cell lines.

Results: We identified 15 cell subpopulations by dimension reduction and data clustering. We divided the 15 subpopulations into 10 distinct cell types based on marker gene expression. Then, we performed functional enrichment analysis for the 352 marker genes in pancreatic cancer cells. Based on RNA expression data and prognostic information from TCGA and GEO datasets, we identified 42 prognosis-related genes, including 5 protective genes and 37 high-risk genes, which we used to identified two molecular subtypes. C1 subtype was associated with a better prognosis, whereas C2 subtype was associated with a worse prognosis. Moreover, chemokine and chemokine receptor genes were differentially expressed between C1 and C2 subtypes. Functional and pathway enrichment uncovered functional differences between C1 and C2 subtype. We identified eight genes that could serve as potential biomarkers for prognosis prediction in pancreatic cancer patients. These genes were used to establish an 8-gene pancreatic cancer prognostic model.

Conclusions: We established an 8-gene pancreatic cancer prognostic model. This model can meaningfully predict prognosis and treatment response in pancreatic cancer patients.

KEYWORDS

single-cell sequencing, pancreatic cancer, chemokines, immune microenvironment, prognostic model

Introduction

Pancreatic cancer is one of the most lethal malignancies and is associated with a high mortality rate (1–3). Pancreatic ductal adenocarcinoma (PDAC) is derived from the pancreatic ductal epithelium and accounts for about 90% of pancreatic cancer (4, 5). The lethality of pancreatic cancer is largely due to its difficulty to diagnose early and a lack of effective treatments. Despite improved surgical techniques and the use of neoadjuvant and adjuvant chemotherapies, the prognosis of pancreatic cancer remains stubbornly poor. Though immunotherapies have shown preliminary effectiveness in pancreatic cancer treatment, they are still at the preclinical stage (6). Therefore, it is urgent and imperative to explore the mechanisms of pancreatic cancer progression to identify new therapeutic modalities, especially immunotherapy.

The continuous development of sequencing technology has significantly improved RNA sequencing (RNA-seq) methods and techniques (7). However, bulk RNA-seq is the whole observation and detection of a population of cells. As the analysis represents the average expression of a population of cells, bulk RNA-seq fails to capture cellular heterogeneity (8, 9). The genetic information of cells with the same phenotype may differ significantly, and many rare cell populations are lost in the overall characterization. The emergence and advancement of single-cell sequencing (SCS) in the last decade have enabled precision genetic analysis of tumors (10, 11). SCS provides an abundance of molecular information, making it possible to characterize a variety of rare or previously unidentified cell populations within tumors (12, 13). SCS is a highly impactful tool that can facilitate the early diagnosis, tracking, and individualized treatment of cancers. SCS has been widely used to uncover molecular mechanisms and characterize rare subpopulations in many cancers, including lung cancer (14), breast cancer (15), gastric cancer (16), and colorectal cancer. In colorectal cancer, macrophages and dendritic cells were significantly associated with myeloid-targeting immunotherapies (17). SCS also revealed rare targetable genes that could be informative to develop lung cancer treatment (18, 19). However, SCS has been under-utilized in pancreatic cancer studies.

In the present study, we downloaded pancreatic cancer SCS data as well as corresponding clinical data from Gene Expression Omnibus (GEO) database, Cancer Genome Atlas (TCGA) expression data collection, and International Cancer Genome Consortium (ICGC). Based on these data, we identified 2 molecular subtypes of HCC with significant immunological differences. Then, we performed appropriate gene selection using dimensionality reduction algorithms. We examined molecular and immune signatures and constructed a polygenic risk score model. Our 8-gene model may serve as a promising biomarker to predict pancreatic cancer patient prognosis and immunotherapy efficacy.

Methods

Data acquisition and preprocessing

We downloaded the SCS data GSE156405 from GEO (http://www.ncbi.nlm.nih.gov/geo/) database. We retained scRNA-seq data from five patients with needle biopsy. We download pancreatic cancer gene expression spectrum data and clinical information from TCGA database (https://portal.gdc.cancer.gov/).

PACA-AU data was obtained from the ICGC database (https://dcc.icgc.org/). We obtained GSE21501, GSE28735, GSE57495, GSE62452, GSE71729, and GSE85916 datasets from the GEO database (https://www.ncbi.nlm.nih.gov/geo/). Subsequently, preserved pancreatic cancer sample data of six datasets (GEO) were combined and eliminated batch effects using removeBatchEffect (20).

Dimensionality reduction

The scRNA-seq data were processed as described below:

1) Single-cell analysis was performed on five samples from GSE156405.

2) Set thresholds such that each gene was expressed in a minimum of three cells and each cell expressed a minimum of 250 genes.
3) The percentage of mitochondria and rRNA was calculated by PercentageFeatureSet function (21).
4) Cells were filtered such that each cell used in subsequent analysis expressed more than 500 and fewer than 6000 genes, had less than 30% mitochondrial gene expression, and a minimum unique molecular identifier (UMI) of 1000.
5) The FindVariableFeatures function was used to find hypervariable genes (21).

Definition and analysis of cell subsets

The cells were clustered by FindNeighbors and FindClusters (21). We obtained immune cell markers associated with pancreatic cancer from previous studies, including stellate cell (*ADIRF*), fibroblasts (*COL1A1*, *COL1A2*, and *DCN*), T cells (*CD2*, *CD3D*, *CD3E*, and *CD3G*), B cells (*CD79A* and *CD79B*), neutrophils (*CSF3R*, *S100A8*, and *S100A9*), mast cells (*GATA2*, *TPSAB1*, and *TPSB2*), NK cells (*KLRF1*, *FGFBP2*, and *KLRC1*), macrophage (*CD163* and *CD68*), pDC (*LILRA4*) and pancreatic cancer cells (*KRT19* and *TM4SF1*) (22–24). FindAllMarkers was used to select marker genes of each subpopulation (logFC =0.5, Minpct=0.35). Prognostic genes were clustered by ConsensusClusterPlus in the RNA-seq cohort (25). The optimal number of clusters was determined according to the cumulative distribution function (CDF).

DEGs identification and functional enrichment analysis

The *limma* package in R was used to identify differentially expressed genes (DEGs) associated with tumorigenesis by comparing gene expression levels between pancreatic cancer tissues and normal tissues. Statistical enrichment was evaluated using Gene Ontology (GO) and Kyoto Encyclopedia of Genes and Genomes (KEGG) pathway analysis. GO enrichment analyses included biological process (BP), molecular function (MF), and cellular component (CC).

Cell score

CIBERSORT was used to calculate the immune cell fraction for each tumor subtype in the RNA-seq and GEO datasets. The MCP counter was used to evaluate the immune microenvironment, and the expression levels of immune cell marker genes were used to evaluate the degree of immune cell infiltration.

LASSO regression and immune score

LASSO regression (developed by Tibshirani) can develop a refined model by constructing a penalty function (26, 27). It is a biased estimation with complex collinearity. In our study, we used LASSO regression to reduce the number of genes in the risk model by R package *glmnet* (28). Then, we performed a 10-fold cross-validation for model building. The ESTIMATE database was utilized to calculate immune cell score. CIBERSORT is a deconvolution algorithm that calculates the proportion of cells *via* processing of bulk RNA-seq data.

Statistical analysis

We used SPSS 23.0 (SPSS, Inc., Chicago, IL) for statistical analysis. R package *Survival CoxPH* function was used to conduct a univariate Cox proportional risk regression model. Multivariate Cox regression analysis was performed on the prognosis-related genes identified by LASSO. The R package *timeROC* was used to perform receiver operating characteristic (ROC) analysis on the prognosis classification of the RiskScore. Differences were considered statistically significant at $P < 0.05$ (*$P < 0.05$; **$P < 0.01$; ***$P < 0.001$; ****$P < 0.0001$)

Results

Single-cell data for dimensionality reduction and clustering

All data processing and analysis workflows were shown in Figure S1. We performed log-normalization to normalize data from five pancreatic cancer samples (Figure 1A). Through data integration, scaling, and PCA dimensionality reduction, we identified 15 distinct subpopulations (Figure 1B). The 15 subpopulations were re-grouped into 10 different cell types according immune cell marker gene expression (Figure 1C). We screened differentially expressed marker genes of the 10 cell types by FindAllMarkers analysis. The top five marker genes in each cell subpopulation were presented in Figure 1D **(positive=TRUE)**. Furthermore, we performed functional enrichment analysis using the 352 marker genes in pancreatic cancer cells. GO and KEGG pathway enrichment analyses were performed on the 352 DEGs using WebGestaltR tools (P<0.05) (29). According to GO functional annotation, 256 clusters were annotated significantly in the BP category (Figure 2A). A total of

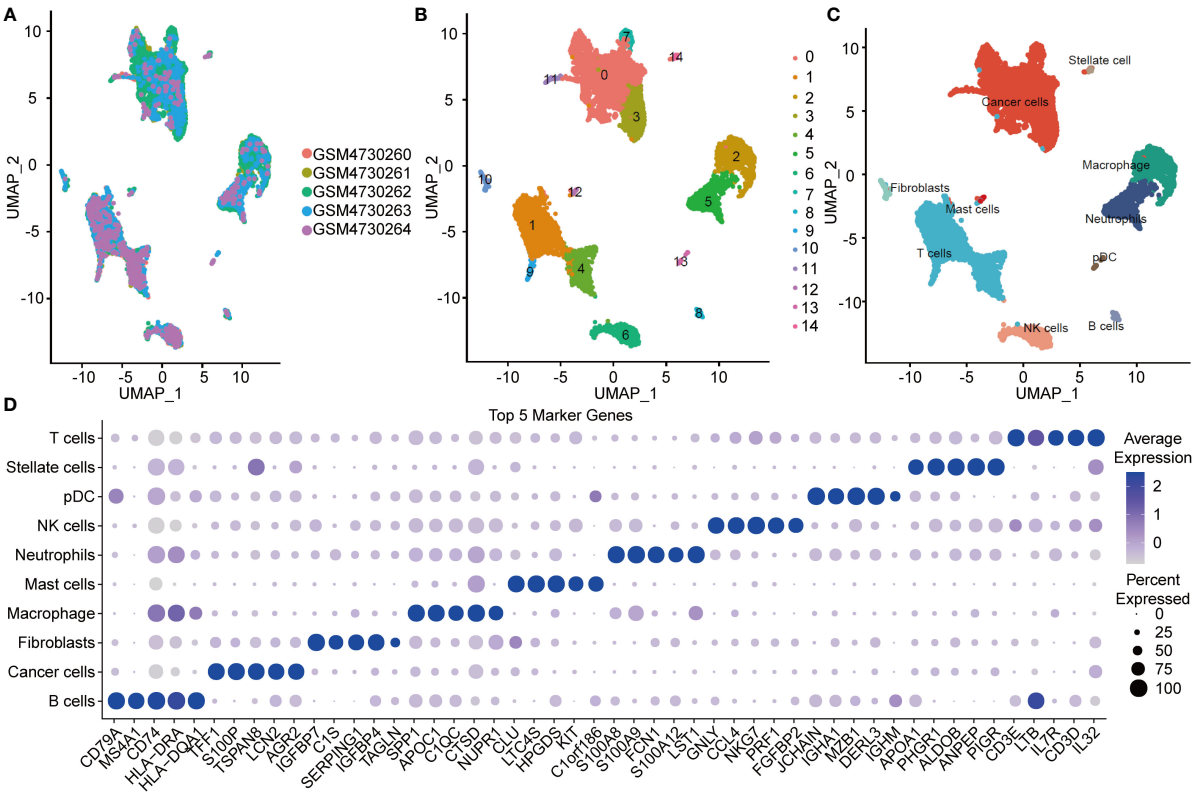

FIGURE 1
UMAP plot and maker genes of cell population. **(A)** UMAP plot of SCS in five samples. **(B)** UMAP of the 14 subgroups after clustering. **(C)** UMAP of subpopulation after cell annotation. **(D)** Top five marker genes in the cell population.

161 GO terms were annotated in the CC category (Figure 2B). Lastly, 38 clusters with significant differences were annotated in the MF category (Figure 2C). Thirty-three DEGs were annotated in the KEGG pathway (Figure 2D). The results showed that intercellular junctions and extracellular matrix interactions were significantly enriched.

Construction of pancreatic cancer molecular subtypes

The above analyses revealed cancer cells represented a large proportion of the cells sequenced from pancreatic cancer patients, as they were the main principal components. We further identified prognosis-related marker genes and constructed new molecular subtypes of pancreatic cancer based on them. We identified 5 protective genes and 37 high risk genes through univariate analysis in RNA-seq and GEO datasets ($p < 0.05$, HR > 1) (Figure 3A). Pancreatic cancer samples in RNA-seq were clustered by using 42 prognostic associated genes. CDF Delta area curve revealed the clustering result is relatively stable when the clustering number is two. Therefore, we defined 2 molecular subtypes (k=2) (Figures 3B, C). C1 subtype had a relatively better prognosis, whereas C2 subtype was associated with a worse prognosis. Similar results were also observed in the GEO cohort (Figures 3D, E), which further confirmed the prognostic significance of the molecular subtype classification.

Cell type differences between C1 and C2 subtypes

To assess cell differences between C1 and C2 subtypes, we probed our SCS data and by examining differentially expressed marker genes in different molecular subtypes. Using our RNA-seq data and the GEO database, we calculated the immune cell score of each subtype and compared the resulting score between the C1 and C2 subtypes. The results showed the cancer cell score of the C2 subtype was significantly increased compared with the cancer cell score in C1 subtype (Figures 4A, B). T and B cell scores in C1 subtype were significantly higher than in the C2 subtype.

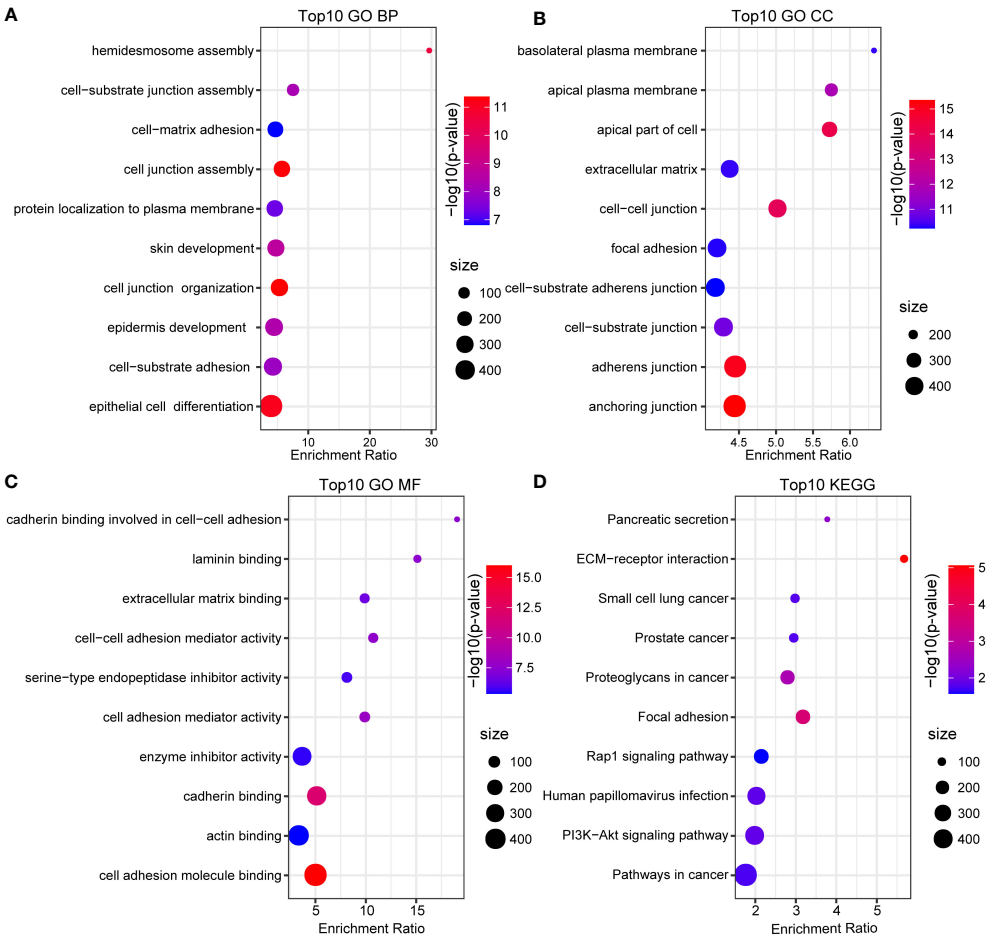

FIGURE 2
GO and KEGG annotation. **(A)** BP annotation of the maker genes in cancer cells. **(B)** CC annotation of the maker genes in cancer cells. **(C)** MF annotation of the maker genes in cancer cells. **(D)** KEGG annotation of the maker gene in cancer cells.

C1 and C2 subtype immune signatures

To further explore immune microenvironment differences between the two subgroups, we evaluated the degree of immune cell infiltration in pancreatic· cancer cohorts using immune cell marker gene expression. The immune cell marker genes were derived from previous studies (30). The tumor immune microenvironment was also evaluated based on ESTIMATE and MCP-counter. The discrepancy of immune cells between the RNA-seq and GEO cohort was shown in Figures 5A–F. ESTIMATE, MCP-counter, and single sample gene set enrichment analysis (ssGSEA) revealed significant differences between most immune cells. The distribution of immune infiltration in RNA-seq was consistent with the GEO cohort. These results revealed the consistency of molecular characteristics and molecular subtype stability. We presented ssGSEA immune scores by heatmaps to illustrate differences in the immune microenvironment, (Figures 4C, D). Taken together, these findings demonstrated a significant difference in immune microenvironment score between C1 and C2 subtypes.

Immune checkpoints and chemokines

The development and use of immune checkpoint targeting immunotherapies in the personalized treatment of pancreatic cancer has become increasingly common. Therefore, we evaluated the distribution of immune checkpoint gene expression in the RNA-seq and GEO datasets. We found 32 (69.57%) of the 46 checkpoint genes were aberrantly expressed in the RNA-seq dataset, and most of them were overexpressed in the C2 subtype, which has the worst prognosis (Figures S2A, S2B). In the GEO dataset, 28 (68.29%) of the 41 checkpoint

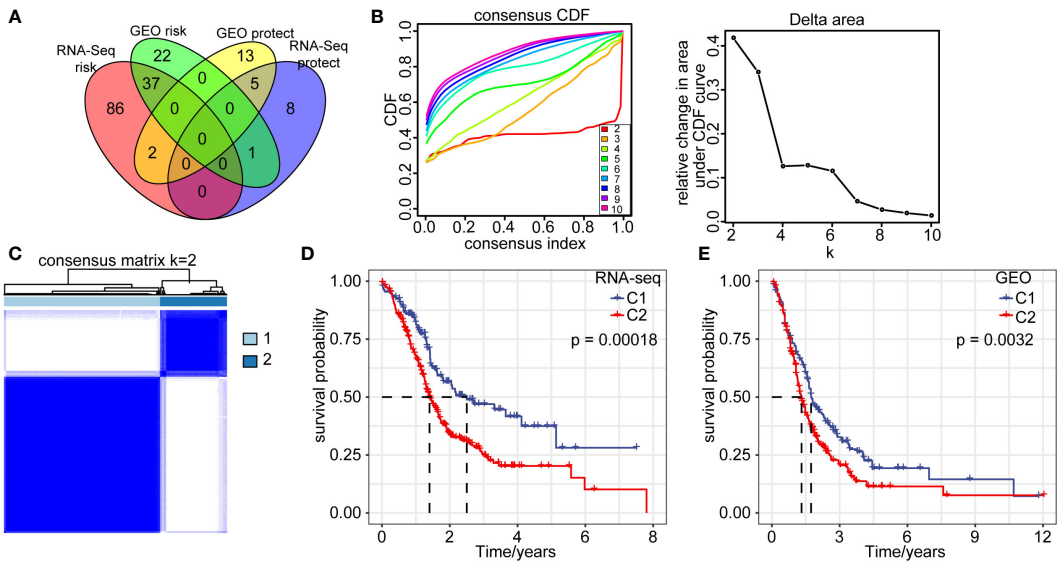

FIGURE 3
Molecular signatures of cancer cells. **(A)** Venn diagram overlap of 352 marker genes in cancer cells from two cohorts by single factor analysis. **(B)** CDF curve and CDF delta area of RNA-seq queue sample. **(C)** Heatmap of RNA-seq sample clustering (consensus k=2). **(D)** Overall survival curves of C1 and C2 subtype in RNA-seq dataset. **(E)** Overall survival curves of C1 and C2 subtype in GEO database.

genes were aberrantly expressed. Consistent with the RNA-seq dataset, most of them were overexpressed in the C2 subtype (Figures S2C, S2D).

Chemokines play essential roles in cancer progression and may facilitate immune cell migration into the tumor microenvironment, further affecting cancer progression and therapeutic response. Here, we analyzed the expression of chemokines in C1 and C2 subtype. In the RNA-seq data, 25 out of 41 chemokines were differentially expressed between the subtypes (Figure S3A), which suggest that the degree of immune cell infiltration in C1 and C2 subtypes may differ. In the GEO cohort, 22 out of 37 chemokines were differentially expressed between C1 and C2 subtype (Figure S3B). Such differences may contribute to rapid tumor progression and poor immunotherapy efficacy. Additionally, we evaluated chemokine receptor gene expression in the two subtypes. A total of 13 out of 18 chemokine receptor genes were differentially expressed in RNA-seq database (Figure S3C). In the GEO database, 11 of the 17 chemokine receptor genes were differentially expressed (Figure S3D). Chemokines and chemokine receptor relative gene expression maintained was consistent between C1 and C2 subtypes in both the RNA-seq and GEO datasets. Most were highly expressed in the C2 subtype, which is associated with a worst prognosis. These results also were illustrated as heat maps (Figures S3E, S3F).

Functional and pathway enrichment analyses

To verify the functional differences between the C1 and C2 subtypes, we performed GO functional enrichment analysis of DEGs between the C1 and C2 subtypes in the RNA-seq dataset. Regarding GO function annotations of DEGs, 553 annotations with significant differences were observed in BP, including epithelial cell differentiation, angiogenesis, and regulation of signaling receptor activity (Figure S4A). A total of 124 GO CC terms were annotated (Figure S4B). The most significant difference between the C1 and C2 subtypes was plasma membrane protein complex. A total of 58 genes were significantly annotated in MF (Figure S4C). Additionally, KEGG pathway analysis was adapted for gene set enrichment analysis (GSEA) of C1 and C2 subtypes ($p < 0.05$, and FDR < 0.25) (Figure S4D) (31).

To continue exploring the C1 and C2 subtypes, we performed gene set enrichment analysis (GSEA) using all candidate gene sets in KEGG database. Several cancer-related pathways, such as base excision repair, P53 signaling pathway, and pancreatic cancer were significantly enriched in the C2 subtype according to the RNA-seq dataset (Figures 6A, B). Importantly, the enrichment results from the GEO dataset were consistent with the RNA-seq results (Figures 6C, D).

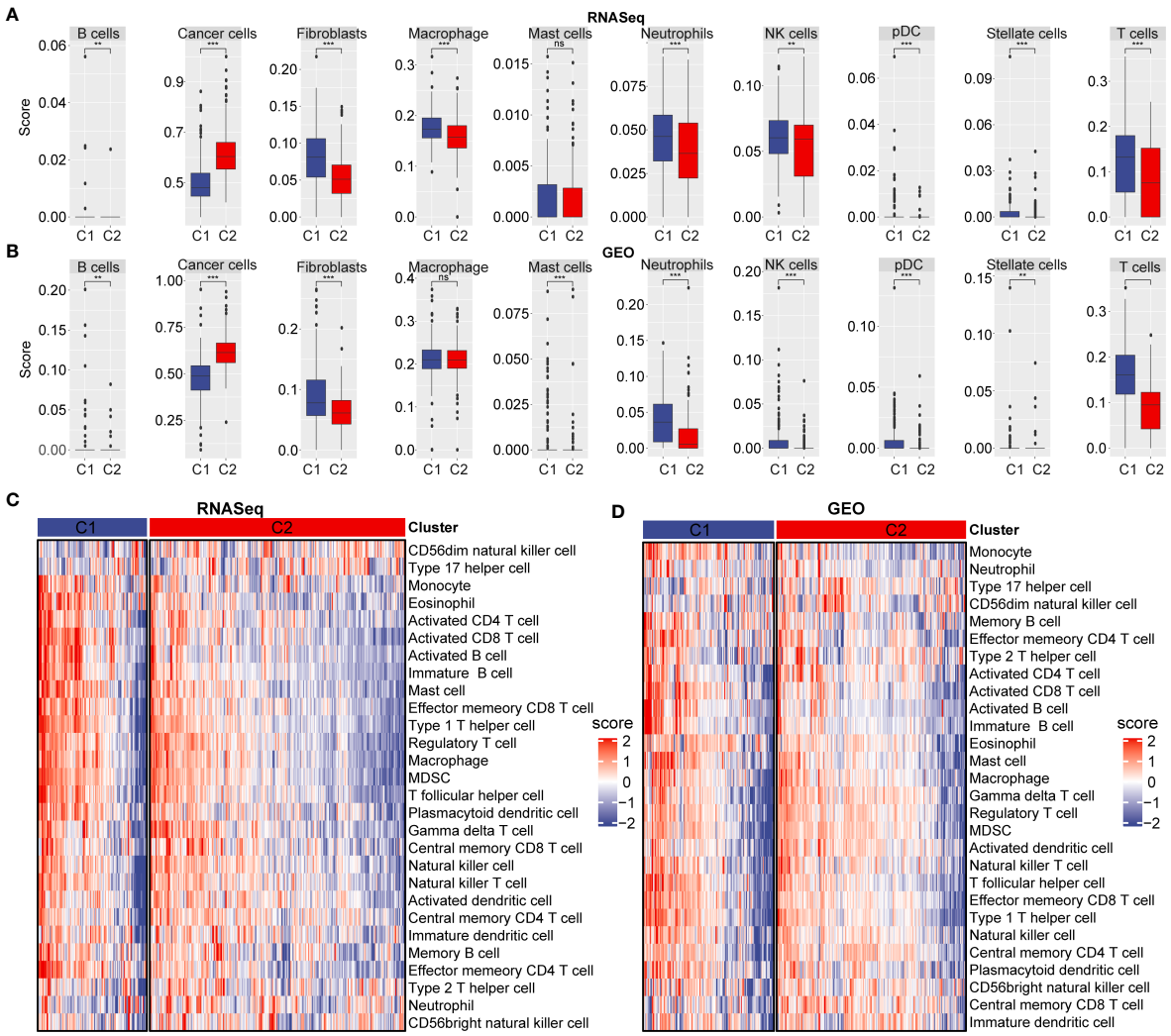

FIGURE 4
Immune cell scores and heat map of immune microenvironment score. **(A)** Cell score between C1 and C2 subtype in RNA-seq dataset. **(B)** Cell score between C1 and C2 subtype in GEO database. **(C)** Differences in heat map distribution of ssGSEA immune microenvironment score in subtypes. **(D)** Heatmap distribution differences of ssGSEA immune microenvironment score in GEO dataset in subtypes. $^{**}p < 0.01$; $^{***}p < 0.001$; ns, no significant.

Mutational signature and immune cell type classification

Also, we used the TCGA dataset to analyze gene mutations in the C1 and C2 subtypes. We found that subtype was markedly correlated with gene mutations in pancreatic cancer. We noted a higher percentage of KRAS, TP53, SMAD4, and CDKN2A mutations in the C2 subtype (Figure 7A). Similarly, data from ICGC-AU showed that the mutation frequency of KRAS was significantly lower in the C1 subtype than in the C2 subtype (Figure 7B).

Six infiltrating immune cell types have been identified in human cancer: IC1 (wound healing), IC2 (INF-R dominant), IC3 (inflammation), IC4 (lymphocyte depletion), IC5 (immunologically silenced), and IC6 (TGF-beta dominant). As expect, IC1, IC2, and IC6 are associated with poor prognosis. In TCGA, most pancreatic cancer patients belonged to IC1, IC2, and IC3 immune subtypes (Figure 7C), though the IC5 immune subtype is not included in TCGA data. Survival analysis revealed these immune subtypes were not significantly associated with overall survival in pancreatic cancer (Figure 7D). We also observed significant differences in the distribution of these immune subtypes in C1 and C2 subtypes (Figure 7E). IC3 was the major infiltrating immune cell type of the C1 subtype, whereas IC1 become the predominant immune cell type of the C2 subtype.

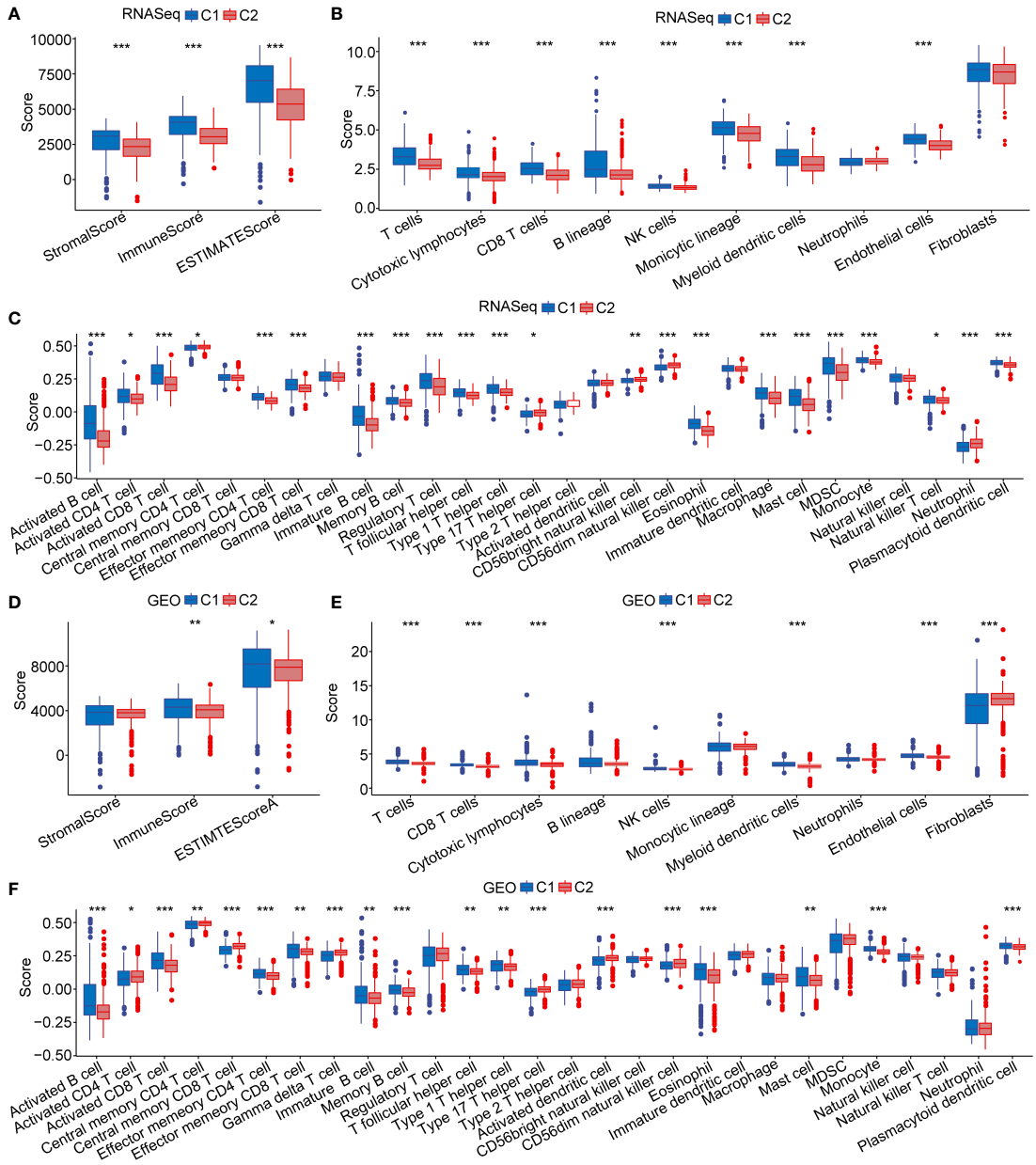

FIGURE 5
Immune microenvironment score. **(A–C)** The distribution of immune microenvironment score in RNA-seq dataset. **(D–F)** The distribution of immune microenvironment score in GEO database. *$p < 0.05$; **$p < 0.01$; ***$p < 0.001$.

Tumor Immune Dysfunction and Exclusion (TIDE) analysis

We used the TIDE software (http://tide.dfci.harvard.edu/) to evaluate potential clinical effects of immunotherapy in the C1 and C2 subtypes. A higher TIDE prediction score indicates an increased chance of immune escape, which indicates immunotherapy may be less beneficial for these patients. In the RNA-seq dataset, exclusion scores were remarkably elevated in the C2 subtype and dysfunction scores were higher in the C1 subtype. However, TIDE scores between the C1 and C2 subtypes were not significantly different (Figures 8A–C). The exclusion and dysfunction scores in the GEO dataset were consistent with the RNA-seq dataset. Although, the TIDE score was increased in the C2 subtype compared to the C1 subtype (Figures 8D–F). This result was consistent with previous immune checkpoints and immune microenvironment analysis.

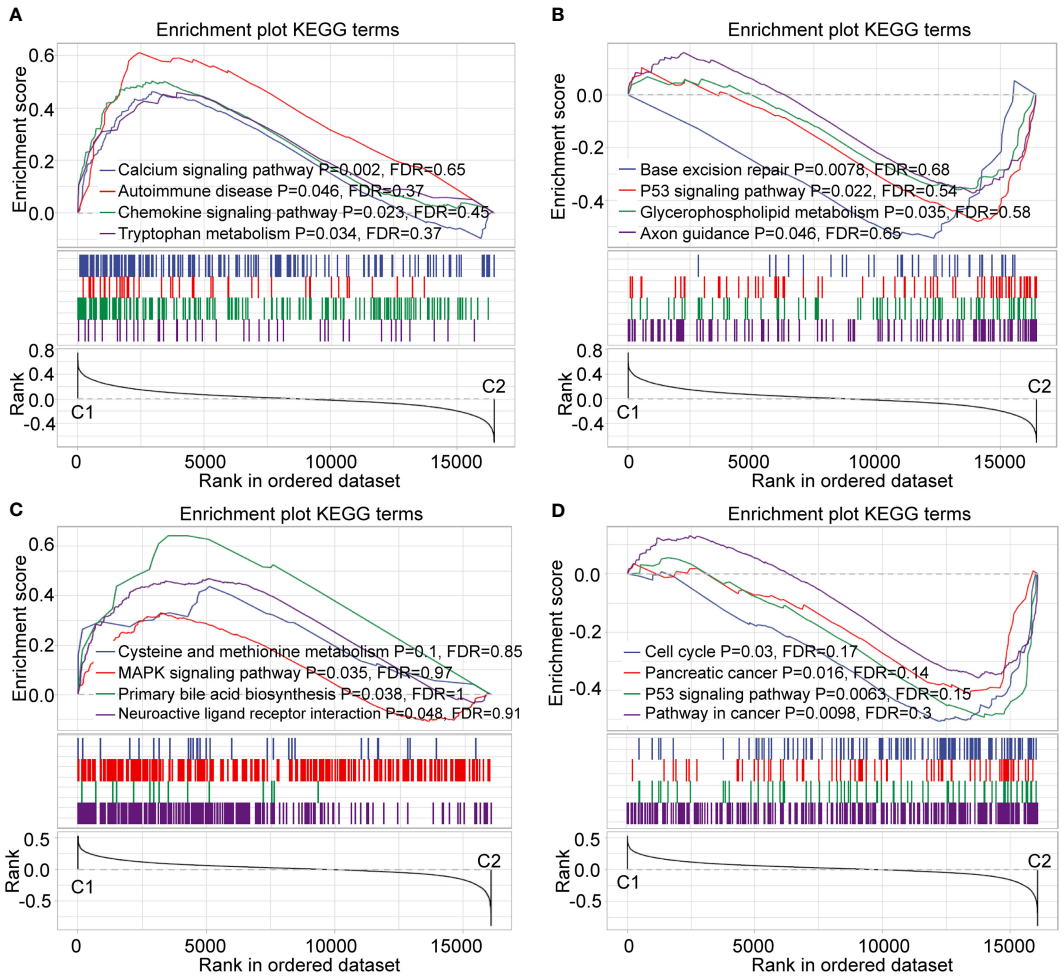

FIGURE 6
Enrichment analysis of GSEA pathway. **(A, B)** GSEA of C1 and C2 subtype in RNA-seq dataset. **(C, D)** GSEA of C1 and C2 subtype in the GEO dataset.

Prognostic model

Using the GEO dataset, we identified 42 genes that can predict cancer prognosis. We randomly sampled the GEO dataset with a sampling ratio of Train: test = 7:3. Then, we applied LASSO regression (lambda= 0.046) to obtain 11 prognosis-related genes (Figure 9A). To further reduce the number of genes, we used stepAIC, which reduced the number of genes to eight (*EPS8*, *DSG2*, *RHOD*, *ITGB6*, *ANKRD37*, *SELENBP1*, *FOXA3*, *ALDH1A1*) and determined the corresponding risk coefficients (Figure 9B) (32). Finally, we arrived at an 8-gene prognostic model for pancreatic cancer patients. We calculated the risk score of each sample in both the GEO training dataset and validation dataset and divided the samples into high and low risk groups using the median as cutoff. A higher score predicted poorer prognosis in pancreatic cancer patients. Kaplan Meier (KM) curves and ROC curves were displayed in Figures 9C, D. The corresponding AUC in 1-year, 2-year, and 3-year were 0.65, 0.71, and 0.75, respectively. Moreover, we validated our model in GEO validation, TCGA, and ICGC datasets (Figures 9E, F).

Discussion

SCS technologies have been increasingly used in disease research over the past decade (33–35). SCS can reveal gene structure and expression status at single-cell resolution, which facilitated the exploration of biological processes and disease mechanisms with unprecedented precision (36, 37). In our study, we classified and defined two pancreatic cancer subtypes by analyzing SCS data from multiple public databases. We observed sequenced cells form 10 cell subgroups, including stellate cells, fibroblasts, T cells, B cells, neutrophils, mast cells, NK cells, macrophages, pDCs, and

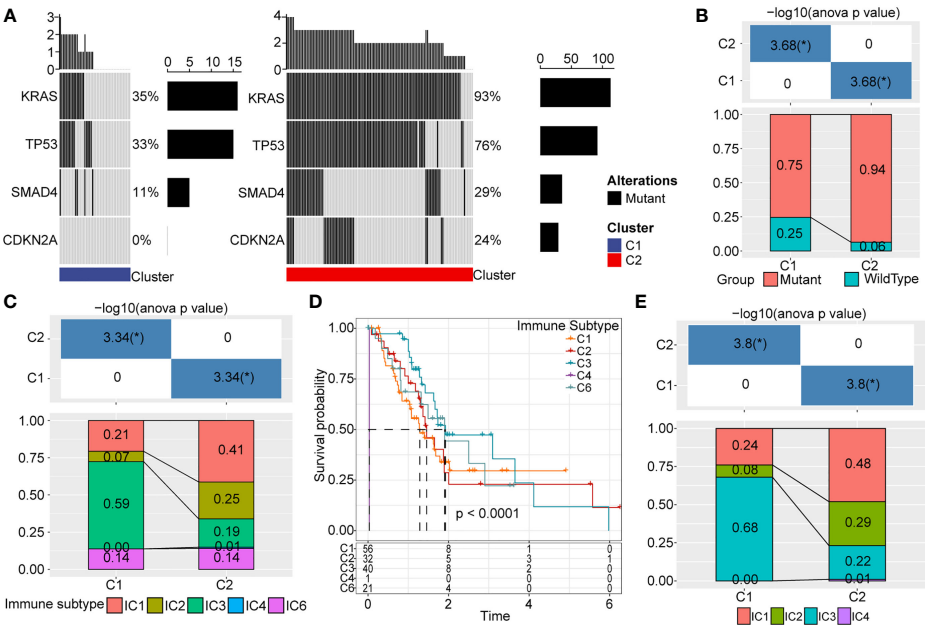

FIGURE 7
Gene mutations and distribution of immune subtypes. **(A)** Somatic mutations analysis of DEGs in two molecular subtypes. **(B)** Mutation frequency differences of KRAS among different subtypes in ICGC cohort. **(C)** Sankey between molecular types and immune subtypes. **(D)** Survival curve of existing immune subtypes. **(E)** Distribution of immune subtypes among different molecular types. *p < 0.05.

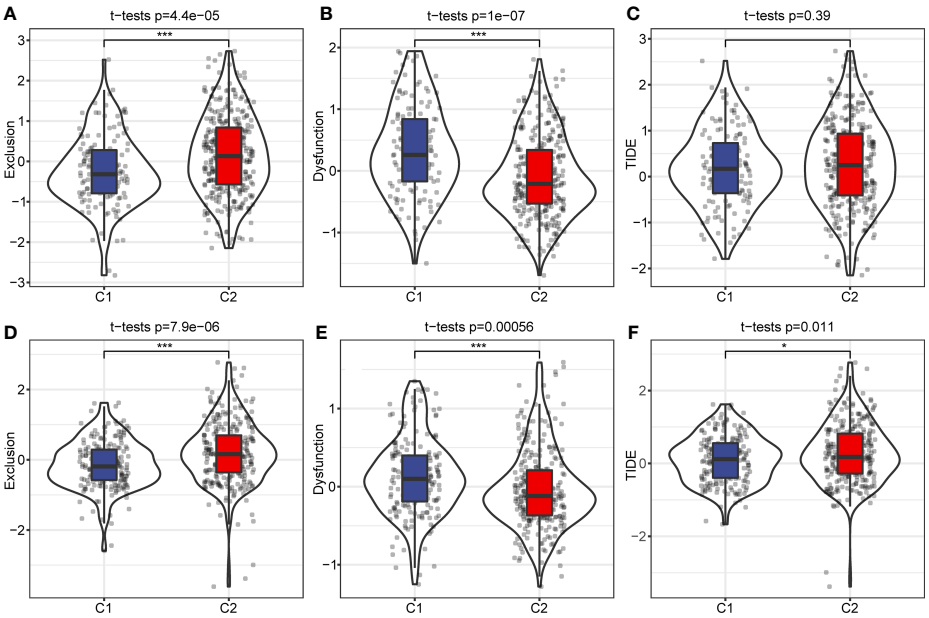

FIGURE 8
TIDE analysis of immune therapy. **(A)** Exclusion scores among different molecular subtypes in RNA-seq dataset. **(B)** C1 and C2 subtype dysfunction scores in the RNA-seq dataset. **(C)** TIDE score of different molecular subtypes in RNA-seq data. **(D)** Differences of Exclusion scores among different molecular subtypes of the GEO dataset. **(E)** C1 and C2 subtype Exclusion scores in the GEO dataset. **(F)** TIDE score of different molecular subtypes in the GEO dataset. *$p < 0.05$; ***$p < 0.001$.

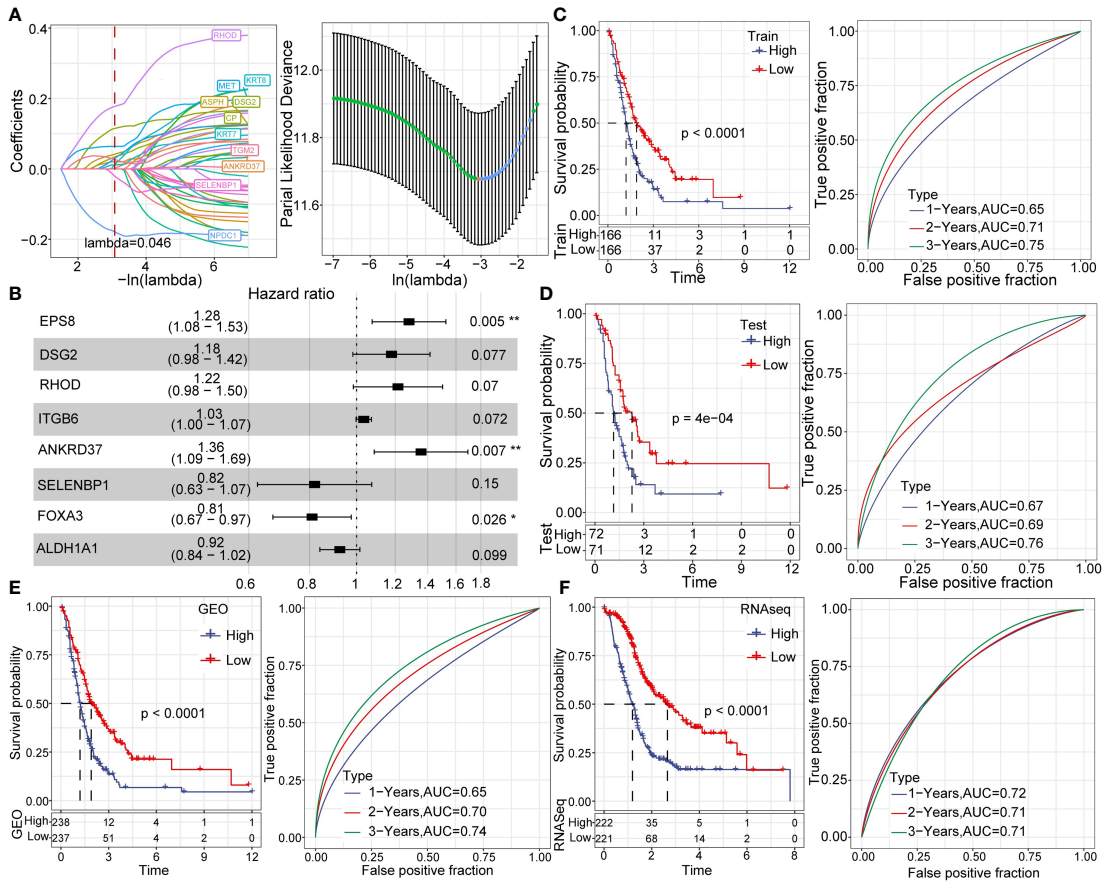

FIGURE 9
Establishment and analysis of prognostic models. **(A)** LASSO coefficient profiles of 42 prognostic genes in the GSE dataset. **(B)** Multivariate analysis of the risk model genes. **(C)** KM and ROC analysis of the risk model in the GEO dataset. **(D)** KM and ROC analysis of the risk model in the GEO validation dataset. **(E)** KM and ROC analysis of the risk model in the complete GEO dataset. **(F)** KM and ROC analysis of the risk model in complete the RNA-seq dataset. *p < 0.05; **p < 0.01.

pancreatic cancer cells. These subgroups can be identified by expression of specific marker genes. Researchers have found immune cells of the various lymphoid and myeloid lineages by SCS (38). These immune cell subsets facilitated the formation of an immunosuppressive microenvironment in pancreatic cancer. We further explored the molecular and immune signatures of different cell subsets. Furthermore, we used TIDE software to evaluate potential clinical immunotherapy efficacy in the C1 and C2 subtypes. C2 had a higher TIDE score, which suggests patients with this subtype would benefit less from immunotherapy. Nevertheless, we need to note that the mechanism(s) of immune cell exclusion and dysfunction may well be different in different tumor types. Therefore, this conclusion still needs to be verified by more precise molecular and animal experiments.

Pancreatic cancer has an extremely poor prognosis, which is largely attributed to its difficulty to diagnose early (39–41). Given this limited therapeutic window, it is of great interest to establish gene models that can effectively predict pancreatic cancer prognosis. Hosein et al. (38) observed macrophage heterogeneity in pancreatic cancer at different stages using single-cell RNA-seq. Specifically, they revealed macrophages express different genes at different times and play different functional roles. Studies have yet to relate marker genes with cell subgroup in pancreatic cancer.

We identified 10 different cell types using data clustering and dimension reduction. Then, we performed functional enrichment analysis for 352 marker genes in pancreatic cancer cells. Notably, we found some marker genes were markedly correlated with pancreatic cancer progression. These finding indicate the prognostic risk model may provide clinical treatment guidance. Specifically, we found *EPS8*, *DSG2*, *RHOD*, *ITGB6*, *ANKRD37*, *SELENBP1*, *FOXA3*, and *ALDH1A1* could be potential biomarkers to accurately predict the prognosis of pancreatic cancer patients. Therefore, we established a prognostic model based on these eight genes. The

prognostic risk model was a worthy prognostic indicator, as evidenced by its ability to accurately indicate prognosis in three external datasets (GEO validation, TCGA, and ICGC datasets). Similar with our findings, serval studies have demonstrated *EPS8*, *DSG2*, *ITGB6* were aberrantly expressed in pancreatic cancer, breast cancer, pituitary tumor, and gastric cancer (42, 43). Hütz et al. (43) found silenced *DSG2* facilitated pancreatic cancer cell migration and invasion. *EPS8* increased polyubiquitination by downregulating ALDH7A1 protein expression in pancreatic cancer. Zhuang et al. (44) observed that *ITGB6* was significantly upregulated and closely associated with overall survival in pancreatic cancer. These findings have important significance for prognosis prediction and subsequent treatment of pancreatic cancer patients. The risk model could predict the patient prognosis and may inform the use of individualized therapies in pancreatic cancer patients.

Conclusion

Based on pancreatic cancer SCS data from the GEO, TCGA and ICGC databases, we identified a new molecular subtype of HCC with distinct molecular and immune signatures. Meanwhile, we established a risk model based on 8 prognosis-related genes, which has stable and effective prognosis prediction performance.

Data availability statement

We downloaded the SCS data GSE156405 from GEO (http://www.ncbi.nlm.nih.gov/geo/) database. We retained scRNA data from five patients with needle biopsy. We download pancreatic cancer gene expression spectrum data and clinical information from TCGA database (https://portal.gdc.cancer.gov/). PACA-AU data was obtained from the ICGC database (https://dcc.icgc.org/). TCGA and ICGC datasets were combined to RNA-seq. Then, batch effects were eliminated using removeBatchEffect. We obtained GSE21501, GSE28735, GSE57495, GSE62452, GSE71729, and GSE85916 datasets from the GEO database (https://www.ncbi.nlm.nih.gov/geo/).

Author contributions

WG, SZ, and YH designed and guided the study. XY and QZ analyzed the data and wrote the manuscript. XY drew the figures. All authors read and approved the final manuscript.

Funding

This work was supported by Leading Talents of Zhongyuan Science and Technology Innovation (214200510027), Henan Provincial Medical Science and Technology Research Plan (SBGJ2018002 and SBGJ202102117), Henan Medical Science and Technology Joint Building Program (LHGJ20210324), Outstanding Foreign Scientist Studio in Henan Province (GZS2020004), and the Gandan Xiangzhao Research Fund (GDXZ2022002).

Conflict of interest

The authors declare that the research was conducted in the absence of any commercial or financial relationships that could be construed as a potential conflict of interest.

Publisher's note

All claims expressed in this article are solely those of the authors and do not necessarily represent those of their affiliated organizations, or those of the publisher, the editors and the reviewers. Any product that may be evaluated in this article, or claim that may be made by its manufacturer, is not guaranteed or endorsed by the publisher.

Supplementary material

The Supplementary Material for this article can be found online at: https://www.frontiersin.org/articles/10.3389/fonc.2022.1000447/full#supplementary-material

References

1. Berger AC, Garcia MJr., Hoffman JP, Regine WF, Abrams RA, Safran H, et al. Postresection Ca 19-9 predicts overall survival in patients with pancreatic cancer treated with adjuvant chemoradiation: A prospective validation by rtog 9704. *J Clin Oncol Off J Am Soc Clin Oncol* (2008) 26(36):5918–22. doi: 10.1200/jco.2008.18.6288

2. Azmi AS, Li Y, Aboukameel A, Muqbil I, Philip PA, Mohammad RM. DNA-Methylation-Caused downregulation of mir-30 contributes to the high expression of Xpo1 and the aggressive growth of tumors in pancreatic ductal adenocarcinoma. *Cancers* (2019) 11(8):1101. doi: 10.3390/cancers11081101

3. Lin QJ, Yang F, Jin C, Fu DL. Current status and progress of pancreatic cancer in China. *World J Gastroenterol* (2015) 21(26):7988–8003. doi: 10.3748/wjg.v21.i26.7988

4. Huang C, Iovanna J, Santofimia-Castaño P. Targeting fibrosis: The bridge that connects pancreatitis and pancreatic cancer. *Int J Mol Sci* (2021) 22(9):4970. doi: 10.3390/ijms22094970

5. Gandhi NS, Feldman MK, Le O, Morris-Stiff G. Imaging mimics of pancreatic ductal adenocarcinoma. *Abdom. Radiol (New York)* (2018) 43(2):273–84. doi: 10.1007/s00261-017-1330-1

6. Morrison AH, Byrne KT, Vonderheide RH. Immunotherapy and prevention of pancreatic cancer. *Trends Cancer* (2018) 4(6):418–28. doi: 10.1016/j.trecan.2018.04.001

7. Hong M, Tao S, Zhang L, Diao LT, Huang X, Huang S, et al. Rna sequencing: New technologies and applications in cancer research. *J Hematol Oncol* (2020) 13 (1):166. doi: 10.1186/s13045-020-01005-x

8. Kinker GS, Greenwald AC, Tal R, Orlova Z, Cuoco MS, McFarland JM, et al. Pan-cancer single-cell rna-seq identifies recurring programs of cellular heterogeneity. *Nat Genet* (2020) 52(11):1208–18. doi: 10.1038/s41588-020-00726-6

9. Papalexi E, Satija R. Single-cell rna sequencing to explore immune cell heterogeneity. *Nat Rev Immunol* (2018) 18(1):35–45. doi: 10.1038/nri.2017.76

10. Han X, Zhou Z, Fei L, Sun H, Wang R, Chen Y, et al. Construction of a human cell landscape at single-cell level. *Nature* (2020) 581(7808):303–9. doi: 10.1038/s41586-020-2157-4

11. Bian S, Hou Y, Zhou X, Li X, Yong J, Wang Y, et al. Single-cell multiomics sequencing and analyses of human colorectal cancer. *Sci (New York NY)* (2018) 362 (6418):1060–3. doi: 10.1126/science.aao3791

12. van Dijk EL, Auger H, Jaszczyszyn Y, Thermes C. Ten years of next-generation sequencing technology. *Trends Genet TIG* (2014) 30(9):418–26. doi: 10.1016/j.tig.2014.07.001

13. Zheng C, Zheng L, Yoo JK, Guo H, Zhang Y, Guo X, et al. Landscape of infiltrating T cells in liver cancer revealed by single-cell sequencing. *Cell* (2017) 169 (7):1342–56.e16. doi: 10.1016/j.cell.2017.05.035

14. Guo X, Zhang Y, Zheng L, Zheng C, Song J, Zhang Q, et al. Global characterization of T cells in non-Small-Cell lung cancer by single-cell sequencing. *Nat Med* (2018) 24(7):978–85. doi: 10.1038/s41591-018-0045-3

15. Kim C, Gao R, Sei E, Brandt R, Hartman J, Hatschek T, et al. Chemoresistance evolution in triple-negative breast cancer delineated by single-cell sequencing. *Cell* (2018) 173(4):879–93.e13. doi: 10.1016/j.cell.2018.03.041

16. Zhang M, Hu S, Min M, Ni Y, Lu Z, Sun X, et al. Dissecting transcriptional heterogeneity in primary gastric adenocarcinoma by single cell rna sequencing. *Gut* (2021) 70(3):464–75. doi: 10.1136/gutjnl-2019-320368

17. Bauer K, Michel S, Reuschenbach M, Nelius N, von Knebel Doeberitz M, Kloor M. Dendritic cell and macrophage infiltration in microsatellite-unstable and microsatellite-stable colorectal cancer. *Familial. Cancer* (2011) 10(3):557–65. doi: 10.1007/s10689-011-9449-7

18. Bischoff P, Trinks A, Obermayer B, Pett JP, Wiederspahn J, Uhlitz F, et al. Single-cell rna sequencing reveals distinct tumor microenvironmental patterns in lung adenocarcinoma. *Oncogene* (2021) 40(50):6748–58. doi: 10.1038/s41388-021-02054-3

19. Chen Z, Zhao M, Li M, Sui Q, Bian Y, Liang J, et al. Identification of differentially expressed genes in lung adenocarcinoma cells using single-cell rna sequencing not detected using traditional rna sequencing and microarray. *Lab invest. J Tech Methods Pathol* (2020) 100(10):1318–29. doi: 10.1038/s41374-020-0428-1

20. Phipson B, Lee S, Majewski IJ, Alexander WS, Smyth GK. Robust hyperparameter estimation protects against hypervariable genes and improves power to detect differential expression. *Ann Appl Stat* (2016) 10(2):946–63. doi: 10.1214/16-AOAS920

21. Stuart T, Butler A, Hoffman P, Hafemeister C, Papalexi E, Mauck WM 3rd, et al. Comprehensive integration of single-cell data. *Cell* (2019) 177(7):1888–902 e21. doi: 10.1016/j.cell.2019.05.031

22. Peng J, Sun BF, Chen CY, Zhou JY, Chen YS, Chen H, et al. Single-cell rna-seq highlights intra-tumoral heterogeneity and malignant progression in pancreatic ductal adenocarcinoma. *Cell Res* (2019) 29(9):725–38. doi: 10.1038/s41422-019-0195-y

23. Su C, Lv Y, Lu W, Yu Z, Ye Y, Guo B, et al. Single-cell rna sequencing in multiple pathologic types of renal cell carcinoma revealed novel potential tumor-specific markers. *Front Oncol* (2021) 11:719564. doi: 10.3389/fonc.2021.719564

24. Lee JJ, Bernard V, Semaan A, Monberg ME, Huang J, Stephens BM, et al. Elucidation of tumor-stromal heterogeneity and the ligand-receptor interactome by single-cell transcriptomics in real-world pancreatic cancer biopsies. *Clin Cancer Res an Off J Am Assoc Cancer Res* (2021) 27(21):5912–21. doi: 10.1158/1078-0432.Ccr-20-3925

25. Wilkerson MD, Hayes DN. Consensusclusterplus: A class discovery tool with confidence assessments and item tracking. *Bioinformatics* (2010) 26 (12):1572–3. doi: 10.1093/bioinformatics/btq170

26. Wurm MJ, Rathouz PJ, Hanlon BM. Regularized ordinal regression and the ordinalnet r package. *J Stat softw.* (2021) 99(6):1–42. doi: 10.18637/jss.v099.i06

27. Shen R, Wang S, Mo Q. Sparse integrative clustering of multiple omics data sets. *Ann Appl Stat* (2013) 7(1):269–94. doi: 10.1214/12-aoas578

28. Friedman J, Hastie T, Tibshirani R. Regularization paths for generalized linear models *Via* coordinate descent. *J Stat Softw.* (2010) 33(1):1–22. doi: 10.18637/jss.v033.i01

29. Liao Y, Wang J, Jaehnig EJ, Shi Z, Zhang B. Webgestalt 2019: Gene set analysis toolkit with revamped uis and apis. *Nucleic Acids Res* (2019) 47(W1): W199–205. doi: 10.1093/nar/gkz401

30. Şenbabaoğlu Y, Gejman RS, Winer AG, Liu M, Van Allen EM, de Velasco G, et al. Tumor immune microenvironment characterization in clear cell renal cell carcinoma identifies prognostic and immunotherapeutically relevant messenger rna signatures. *Genome Biol* (2016) 17(1):231. doi: 10.1186/s13059-016-1092-z

31. Liberzon A, Birger C, Thorvaldsdóttir H, Ghandi M, Mesirov JP, Tamayo P. The molecular signatures database (Msigdb) hallmark gene set collection. *Cell Syst* (2015) 1(6):417–25. doi: 10.1016/j.cels.2015.12.004

32. Zhang Z. Variable selection with stepwise and best subset approaches. *Ann Transl Med* (2016) 4(7):136. doi: 10.21037/atm.2016.03.35

33. Armand EJ, Li J, Xie F, Luo C, Mukamel EA. Single-cell sequencing of brain cell transcriptomes and epigenomes. *Neuron* (2021) 109(1):11–26. doi: 10.1016/j.neuron.2020.12.010

34. Hwang B, Lee JH, Bang D. Single-cell rna sequencing technologies and bioinformatics pipelines. *Exp Mol Med* (2018) 50(8):1–14. doi: 10.1038/s12276-018-0071-8

35. Hedlund E, Deng Q. Single-cell rna sequencing: Technical advancements and biological applications. *Mol aspects Med* (2018) 59:36–46. doi: 10.1016/j.mam.2017.07.003

36. Zhang K, Hocker JD, Miller M, Hou X, Chiou J, Poirion OB, et al. A single-cell atlas of chromatin accessibility in the human genome. *Cell* (2021) 184 (24):5985–6001.e19. doi: 10.1016/j.cell.2021.10.024

37. Navin N, Kendall J, Troge J, Andrews P, Rodgers L, McIndoo J, et al. Tumour evolution inferred by single-cell sequencing. *Nature* (2011) 472(7341):90–4. doi: 10.1038/nature09807

38. Hosein AN, Huang H, Wang Z, Parmar K, Du W, Huang J, et al. Cellular heterogeneity during mouse pancreatic ductal adenocarcinoma progression at single-cell resolution. *JCI Insight* (2019) 5(16):e129212. doi: 10.1172/jci.insight.129212

39. Ilic M, Ilic I. Epidemiology of pancreatic cancer. *World J Gastroenterol* (2016) 22(44):9694–705. doi: 10.3748/wjg.v22.i44.9694

40. Zhou B, Xu JW, Cheng YG, Gao JY, Hu SY, Wang L, et al. Early detection of pancreatic cancer: Where are we now and where are we going? *Int J Cancer* (2017) 141(2):231–41. doi: 10.1002/ijc.30670

41. Chen H, Zhuo Q, Ye Z, Xu X, Ji S. Organoid model: A new hope for pancreatic cancer treatment? *Biochim Biophys Acta Rev Cancer* (2021) 1875 (1):188466. doi: 10.1016/j.bbcan.2020.188466

42. Li Z, Sun Y, Xu J, Yang H, Liu X, Tian Y, et al. Integrin-B6 serves as a potential prognostic serum biomarker for gastric cancer. *Front Oncol* (2021) 11:770997. doi: 10.3389/fonc.2021.770997

43. Tan M, Meng J, Sun X, Fu X, Wang R. Eps8 supports pancreatic cancer growth by inhibiting Bmi1 mediated proteasomal degradation of Aldh7a1. *Exp Cell Res* (2021) 407(1):112782. doi: 10.1016/j.yexcr.2021.112782

44. Zhuang H, Zhou Z, Ma Z, Li Z, Liu C, Huang S, et al. Characterization of the prognostic and oncologic values of itgb superfamily members in pancreatic cancer. *J Cell Mol Med* (2020) 24(22):13481–93. doi: 10.1111/jcmm.15990

frontiers | Frontiers in Oncology

TYPE Original Research
PUBLISHED 29 September 2022
DOI 10.3389/fonc.2022.1035722

Check for updates

OPEN ACCESS

EDITED BY
Zhendong Jin,
Second Military Medical University, China

REVIEWED BY
Hafiz Abdul Waqas Ahmed,
Lady Reading Hospital, Pakistan
Yao Huang,
Shanghai Jiao Tong University, China

*CORRESPONDENCE
Zhang Shuijun
zhangshuijun@zzu.edu.cn

SPECIALTY SECTION
This article was submitted to Gastrointestinal Cancers: Hepato Pancreatic Biliary Cancers, a section of the journal Frontiers in Oncology

RECEIVED 03 September 2022
ACCEPTED 12 September 2022
PUBLISHED 29 September 2022

CITATION
Bowen H, Wenzhi G, Peihao W, Jihua S and Shuijun Z (2022) The reasonable therapeutic modality for biliary duct-to-duct anastomotic stricture after liver transplantation: ERCP or PTC?.
Front. Oncol. 12:1035722.
doi: 10.3389/fonc.2022.1035722

COPYRIGHT
© 2022 Bowen, Wenzhi, Peihao, Jihua and Shuijun. This is an open-access article distributed under the terms of the Creative Commons Attribution License (CC BY). The use, distribution or reproduction in other forums is permitted, provided the original author(s) and the copyright owner(s) are credited and that the original publication in this journal is cited, in accordance with accepted academic practice. No use, distribution or reproduction is permitted which does not comply with these terms.

The reasonable therapeutic modality for biliary duct-to-duct anastomotic stricture after liver transplantation: ERCP or PTC?

Hu Bowen[1,2,3], Guo Wenzhi[1,2,3], Wen Peihao[1,2,3], Shi Jihua[1,2,3] and Zhang Shuijun[1,2,3]*

[1]Department of Hepatobiliary and Pancreatic Surgery, First Affiliated Hospital of Zhengzhou University, Zhengzhou, China, [2]Henan Key Laboratory of Digestive Organ Transplantation, Zhengzhou, China, [3]Henan Research Centre for Organ Transplantation, Zhengzhou, China

Objective: To compare the initial success rate, feasibility, and effectiveness of endoscopic retrograde cholangiopancreatography (ERCP) versus percutaneous transhepatic cholangiography (PTC) for anastomotic biliary stricture after liver transplantation (LT).

Methods: We retrospectively analyzed the data collected during January 2015 to December 2021 from liver transplantation recipients who developed anastomotic biliary stricture after liver transplantation and treated by ERCP and/or PTC. The success rate, complications and patients' survival rate of ERCP and PTC procedures was evaluated.

Results: Forty-eight patients who underwent LT and were confirmed to have the anastomotic biliary stricture were enrolled. Overall, 48/48 patients underwent single or multiple ERCP procedures as the first line therapy; 121 therapeutic ERCPs (3.36 ± 2.53 ERCPs per patient) were performed in 36/48 patients successfully. All the 12 patients who failed ERCP tend to have special bile duct conditions such as overlong, angle shaped, and/or extremely narrowed bile duct and underwent PTC as an alternative treatment. The initial success rate of ERCP was 75% (36/48) while the success rate of ERCP for the 12 patients with special bile duct was 0% (0/12). PTC was an effective second-line treatment for those 12 patients who failed ERCP, and 58.33% (7 of 12 cases) were treated successfully. The average procedure time in PTC group was significantly lower than ERCP group (t=2.292, P=0.027). The feasibility of ERCP was associated with the anatomical shape of bile duct and the severity of the stricture site. Finally, the cumulative survival rate was 100% (12/12) in PTC group compared to 86.11% (31/36) in ERCP group (χ^2 =0.670, P=0.413).

Conclusion: ERCP is the gold standard method for the diagnosis and effective intervention for the management of biliary complications after LT. However, its use in certain types of biliary complications (e.g., patients with severe anastomotic biliary stricture and those with overlong and angle shaped bile ducts) is not promising and associated with significant risk of complications. PTC and other interventions should be studied along with ERCP for patients for

whom ERCP may not work. The feasibility and efficacy of primary management can be predicted by the noninvasive imaging examinations like Magnetic Resonance Cholangiopancreatography (MRCP) before the procedure, which may help with the choice of the most reasonable therapeutic modality and avoiding unnecessary financial burden and complications.

KEYWORDS

biliary complications, anastomotic biliary stricture, ERCP, PTC, liver transplantation

Introduction

Hepatocellular carcinoma (HCC) represents an important cause of morbidity and mortality. It is the sixth most common cancer and the fourth leading cause of cancer related death worldwide (1). HCC is increasingly act as a primary indication for liver transplantation. In general, liver transplantation is considered as the best treatment option for early-stage HCC, since it simultaneously treats the tumor and the underlying liver disease (the main risk factor for the development of new tumors). Thus, the number of patients transplanted for HCC are increasing, with a rate of 15-50% in all the liver transplantations performed in the world (2, 3). Although liver transplantation remains an outstanding therapy for HCC, biliary tract complications still remain a common problem following liver transplantation, which has been known as the "Achilles heel" of liver transplantation despite improved surgical technique and experience (4, 5).

Biliary complications after liver transplantation mainly include anastomotic stricture, non-anastomotic stricture, and bile leakage, although other complications such as bile duct stones, sphincter of oddi dysfunction, and progression of primary biliary disease can occur (6–8). These complications are commonly managed by endoscopic retrograde cholangiopancreatography (ERCP), which is considered as the gold standard and first line choice for most kinds of biliary complications after liver transplantation (9–12).

Although ERCP is considered safe and effective, the success rates of ERCP treatment is unsatisfactory, which ranges from 60% to 70% for anastomotic strictures and from 25% to 33% for non-anastomotic strictures (13, 14). For the reason that non-anastomotic biliary stricture has complicated etiology therefore it is quite difficult to be illuminated and managed, we just focused on anastomotic stricture in this study. In addition, the need for multiple ERCPs and post-ERCP complications is relatively high after liver transplantation. The patients for whom ERCP failed should be managed by other alternate techniques. PTC or bilioenteric anastomosis surgery are considered as the second-line therapy for these patients (15–17). However, the success rate, feasibility and effectiveness of PTC has not been well documented. Therefore, the aim of this study is to compare ERCP and PTC therapies in patients with anastomotic stricture.

Materials and methods

Patients and data collection

We retrospectively reviewed the study population consisted of 1264 consecutive patients who had undergone liver transplantation. After excluding those who received living donor liver, splitting donor liver, pediatric donor liver, re-transplantation, combined organ transplantation, and T-tube placement, we identified 1171 adult patients who received whole liver Donation after Citizen Death (DCD) at the First Affiliated Hospital of Zhengzhou University. Finally, we included 48 patients who developed anastomotic biliary stricture and underwent ERCP as a primary therapy for the management. No organ was obtained or used from executed prisoners in this study. All recipients received a duct-to-duct anastomosis of the bile duct without T-tube.

The study protocol was approved by the Institutional Review Board of the first affiliated hospital of Zhengzhou university and all methods were performed in accordance to relevant guidelines and regulations. Informed written consent was obtained from each patient before performing all procedures. We recorded the relevant demographic details (age, gender), etiology, biliary complications after liver transplantation, number of ERCPs and PTCs per patient, post-ERCP and PTC complications, and complementary or alternative treatments to ERCP (e.g., PTC and/or surgery) (Figure 1). Liver function of all the included patients were recorded and analyzed before and after the procedures. The baseline characteristics of included patients are shown in Table 1 and Figure 2.

Interventions

All ERCPs were performed by experienced endoscopists with a volume of 300 to 500 ERCP procedures annually. Based

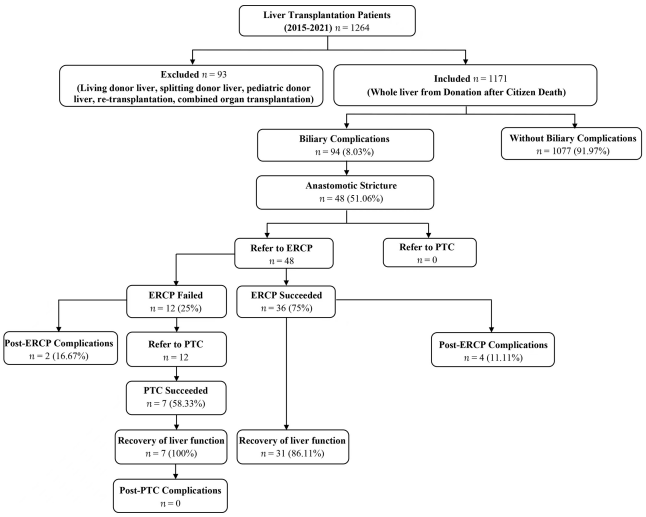

FIGURE 1
Schematic of study design and procedural data of liver transplantation patients.

TABLE 1 Baseline characteristics of 1171 liver transplantation patients.

	Biliary complication n = 94	Without Biliary complication n = 1077	Z/χ^2	*P* value
Age (years), Median (P25, P75)	50 (25, 57)	49 (43, 56)	0.689	0.491
Gender				
Male (%)	68 (72.3)	914 (84.9)	10.020	0.002
Female (%)	26 (27.7)	163 (15.1)		
Indications for liver transplantation (%), (n=1171)				
Hepatocellular carcinoma (HCC)	36.2%	424		
Hepatitis B cirrhosis	34.2%	400		
Alcoholic cirrhosis	7.9%	93		
Other disease	7.2%	84		
Autoimmune (AIH, PBC, PSC)	5.9%	69		
Acute liver failure	3.7%	43		
Hepatitis C cirrhosis	1.7%	20		
Wilson disease	1.1%	13		
Hilar cholangiocarcinoma	0.9%	10		
Hepatitis B and C cirrhosis	0.7%	8		
Cholangiocellular carcinoma	0.5%	6		
Amyloid polyneuropathy	0.1%	1		
Biliary complications (%), (n=94)				
Anastomotic stricture	51.06%	48		
Non-anastomotic stricture	13.83%	13		
Bile duct stone	12.77%	12		
Bile leakage	8.51%	8		
Sphincter of oddi dysfunction	7.45%	7		
Progression of primary biliary disease	6.38%	6		

AIH, autoimmune hepatitis; PBC, primary biliary cholangitis; PSC, primary sclerosing cholangitis. Other disease, Budd-Chiari, Polycystic liver, Cryptogenic cirrhosis.

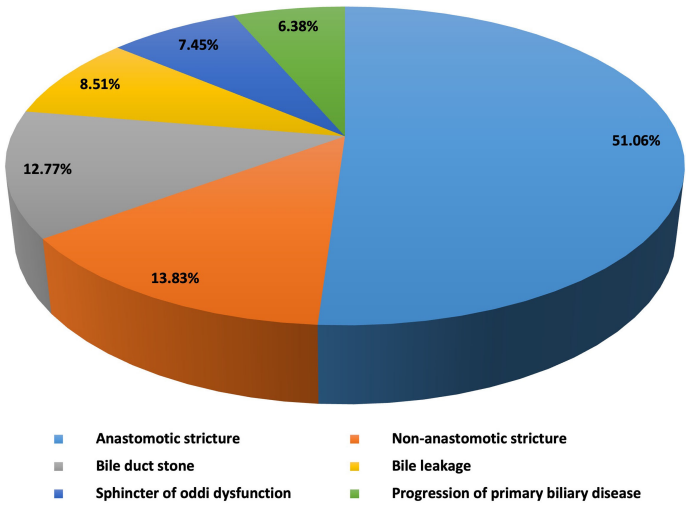

FIGURE 2
Baseline characteristics (etiology) of included patients.

on the radiological findings and the clinical characteristics of the patients, the type of ERCP treatment (ENBD or ERBD) and the diameter, size, number, and frequency of stent replacement were determined by the endoscopist.

An anastomotic stricture was defined as a dominant, short narrowing at the site of anastomosis and the contrast medium pass through narrowly or cannot pass through the stricture site on MRCP or ERCP imaging. ERCP procedure was considered to be accomplished successfully when the guide wire pass through the stricture site and a biliary stent was placed across the stricture site successfully during the ERCP procedure. ERCP was failed when the ERCP procedure was not completed according to the original plan (i.e., the guide wire cannot pass through the stricture site successfully). Patients who failed ERCP were managed by alternative or complementary treatment options such as PTC, surgery, or both.

Statistical analysis

The statistical analysis was performed using IBM SPSS Statistics 24.0. Descriptive statistics were employed to report findings, continuous variables were reported as means with standard deviation (SD) or median, and interquartile range (IQR). Categorical variables were reported as a percentage (%). The comparison of the differences in major characteristics between biliary complication and non-biliary complication groups was examined by t-tests, Wilcoxon Mann–Whitney test, or chi-square test as appropriate. A Kaplan-Meier survival analysis was also conducted. The statistical significance level was 0.05 for a two-tailed test.

Results

We identified 1171 cases (age, mean ± SD: 49.40 ± 10.26 years; range 18-75), 83.86% men. Ninety-four of 1171 (8%) patients developed biliary complications during a follow-up of 81.6 months (mean ± SD: 38.20 ± 25.31 months). The main reported biliary complications were anastomotic strictures in 51.06% (48/94) patients (Figure 3). Therapeutic ERCP was performed in 48/48 patients as a first line therapy. Overall, 121 therapeutic ERCPs (mean 3.36 ± 2.53 ERCPs per patient) were performed in 36/48 patients with biliary anastomotic stricture who gained success from ERCP. The initial success rate of ERCP was 75% (36/48). Twelve patients who failed ERCP were found to have special bile duct conditions such as overlong, angle shaped, and/or extremely narrowed bile duct on MRCP and ERCP examination, and later were allocated to PTC procedure as a second line therapy. The success rate of ERCP in patients with special bile duct was 0% (0/12), while the initial success rate of PTC in patients with special bile duct was 58.33% (7/12). Totally only 8 therapeutic PTCs (mean 1.14 ± 0.38 PTCs per patient) were performed in 7/12 patients who gained success from PTC, which was significantly lower than ERCP group (t=2.292, P=0.027). Five of 12 (41.67%) patients with special bile ducts who failed PTC received biliary enteric anastomosis as their final therapy.

Six patients suffered post-ERCP complications consist of cholangitis in 3, pancreatitis in 2 and bile leakage in 1 patient. Unfortunately, 5 of 36 patients who gained ERCP successfully died before the endpoint date of our study, of which 4 (80%) patients suffered from post-ERCP complications. We believed that complications caused by ERCP maybe one of the risk factors leading to mortality of these patients. However, there could be

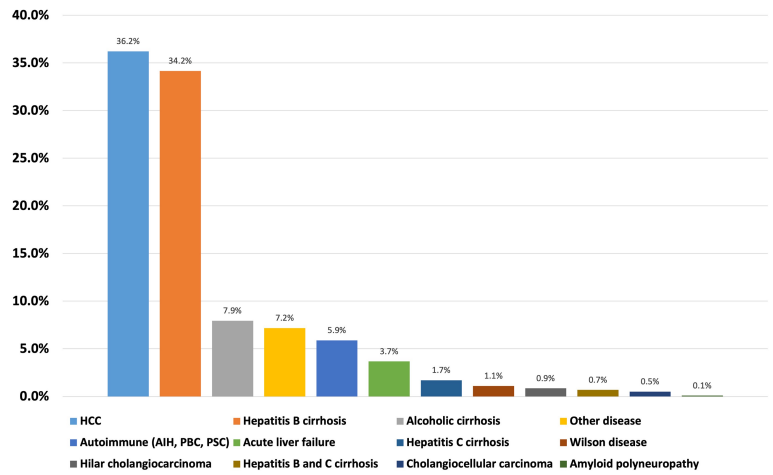

FIGURE 3
Biliary complications ratios after liver transplantation.

other risk factors such as liver function cannot be alleviated by ERCP procedure and therefore led to multi-organ functional disturbance ultimately. Importantly, the 12 patients with special bile duct conditions of which 7 received PTC successfully and 5 received biliary enteric anastomosis did not have any complications nor morbidity until our study endpoint.

The liver function of patients who underwent ERCP and PTCD were examined and analyzed before and after the procedure. In PTC group, all the patients 7/7 (100%) who underwent successful PTC gained recovery of liver function. On the other hand, in ERCP group, only 31/36 (86.11%) patients who received successful ERCP gained the recovery of liver function and the remaining 5/36 patients died finally. Those 5/36 patients whose liver function failed to recover after successful ERCP procedure may cause by the occlusion of the single plastic stent etc. Therefore, it is suggested that ERCP may not be the best choice for every patient suffered from biliary anastomotic stricture, especially for those with special bile duct conditions that failed ERCP. PTC is more efficient than ERCP for those patients with overlong, angle shaped or severe stricture bile duct that failed ERCP procedure (58.33% vs 0%).

The cumulative survival rate of the 36 patients who underwent successful ERCP was 86.11% (mean: 63.71, 95% CI: 56.35-71.08 months) compared to 100% (mean: 73.30, 95% CI: 73.30-73.30 months) of those underwent PTC (χ^2 =0.670, P=0.413) (Figure 4). Patients underwent PTC had better overall survival compared to the patients who underwent ERCP successfully.

Discussion

Biliary tract complications are commonly recognized clinically and considered as an important cause of morbidity and mortality after liver transplantation with an estimated incidence of 5% to 35% worldwide (3–7). Benign biliary strictures after transplantation can be classified into anastomotic and non-anastomotic strictures, which play an important role in graft and patient survival. For the reason that non-anastomotic biliary stricture has complicated etiology and is quite difficult to be illuminated and well managed, we just focused on anastomotic stricture in this study. Currently, biliary stricture is commonly managed by the gold standard and first line therapy ERCP for its efficient and minimally invasive character. However, other procedures including PTC intervention or surgery can also be considered if the condition cannot be managed by ERCP successfully (13–16). ERCP is a highly effective therapy for biliary complications after liver transplantation, but in some cases, the initial therapy may fail because of the inability of guide wire to pass through the stricture. In this study, we mainly evaluated the success rate, complications rate, patient's survival rate, and efficacy of ERCP and PTC procedures for anastomotic stricture.

The overall incidence of biliary strictures ranges from 10%-37% after liver transplantation, and anastomotic stricture comprises the majority of biliary strictures (8, 10, 16, 17). In our study, we found that 64.89% of the biliary complications was biliary stricture; of which 78.69% were anastomotic stricture, which was in accordance with previous studies. Several previous studies confirmed that ERCP and biliary stenting is a successful treatment in the majority of patients, which is considered to be more minimally invasive and convenient compared to both PTC and surgical treatment. Nevertheless, there are some procedure failures and also some contraindications, such as a minimal time between the liver transplantation surgery and ERCP procedure (8–10, 18, 19).

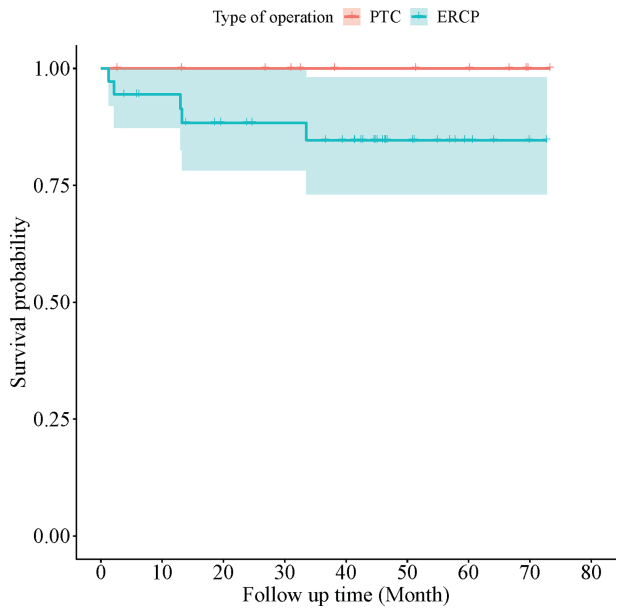

FIGURE 4
Kaplan-Meier survival analysis in 36 ERCP patients and 12 PTC patients.

We have observed that ERCP failed in patients with overlong, angle shaped bile duct and severe anastomotic biliary stricture, which didn't not allow the contrast medium and guide wire to pass through during ERCP (Figures 5A1, B1). However, PTC got success under these circumstances. On the other hand, ERCP is appropriate in patients with simple and moderate anastomotic biliary stricture, which allows the guide wire to pass through (Figures 5C1, 5B2). Most patients with anastomotic stricture require multiple endoscopic sessions at a frequency of every 2-3 months and the placement of single or multiple stents of 7-11.5 Fr for at least 12-24 months to prevent stent occlusion and other post-ERCP complications. In this study, we used a single plastic stent (TTSO-8.5-8, Cook, USA), however, some recent studies indicate that multiple plastic stents

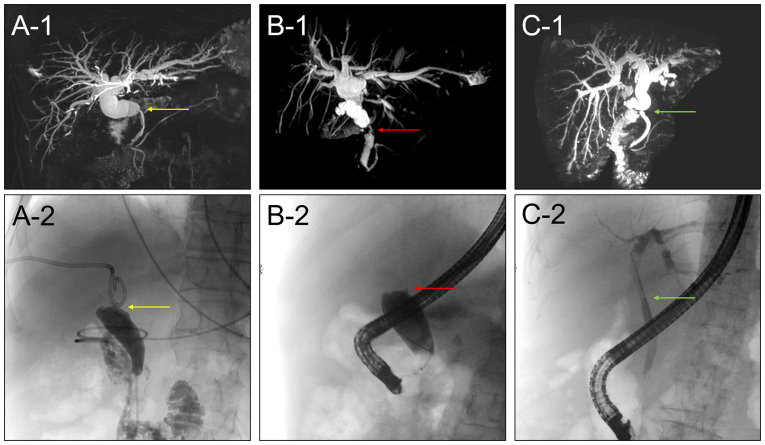

FIGURE 5
(A1) MRCP image showed the anastomotic biliary stricture with overlong and angle shaped bile duct. **(A2)** ERCP failed in patients with overlong and angle shaped bile duct. **(B1)** MRCP image showed the severe anastomotic biliary stricture. **(B2)** ERCP failed in patients with severe anastomotic biliary stricture. **(C1)** MRCP image showed a simple and moderate anastomotic biliary stricture. **(C2)** ERCP succeed in patients with simple and moderate anastomotic biliary stricture.

or metallic stents are comparatively more efficient, suggesting that the type of stent might be one of the factors affecting the efficiency of ERCP and the need for multiple ERCPs (20–22). Another endoscopic approach, defined by the placement of a fully covered self-expandable metal stent across the stenosis, has been reported to be effective; however, the high migration rate remains to be a major concern (23, 24). Further studies are needed before a definitive conclusion is drawn on which type of stent placement is the best choice for anastomotic biliary stricture after liver transplantation. However, we believed that the type of stent could be directly correlated with the success rate and post-ERCP complications. We have realized that stent placement is suitable for anastomotic stricture, while endoscopic nasal biliary drainage (ENBD) could be preferred for leakage patients. Nevertheless, further investigations are deemed necessary to evaluate the suitability of stent placement or ENBD for leakage patients.

PTC is usually reserved for severe anastomotic biliary stricture or overlong and angle shaped bile duct which cannot be traversed by ERCP and for patients who have undergone Roux-en-Y reconstruction after liver transplantation (Figures 5A2, C2). Although usually successful, PTC therapy is regarded as a second-line alternative therapy because of its invasive character, which may cause the discomfort and inconvenience for the patients. Gwon et al. (25) recently developed a technique using the dual catheter placement technique, namely 2 drainage catheters inserted *via* a single percutaneous tract. They achieved clinical success in 98.7% of 79 patients with anastomotic stricture. Our study showed that PTC was successful in 58.33% (7/12) cases where ERCP was totally failed. This is considerable success rate of 58.33% compared to 0% of ERCP for the 12 patients with special bile duct condition who failed the ERCP. So we believed that for the patients with severe stricture or angle shaped bile duct, PTC could be the primarily alternative therapy to ERCP. PTC treatment instead of ERCP will not only avoid need for multiple ERCPs and post ERCP complications but also have potential to reduce the patients' visit to the hospital and extra financial burden. The feasibility of primary management can be predicted by the MRCP imaging findings, which may help with the choice of the therapeutic modality at the first place itself. If MRCP findings showed the severe stricture or the bile duct is too long, or there is an angulation at the stricture site, we recommend PTC as the first line therapy. However, this study has several limitations including retrospective nature of the study, lack of control group, small sample size, and short follow up time. We believe that it is important to share initial results with fellow colleague so they would know what to expect and what more can be done to improve the technique.

In conclusion, ERCP is the gold standard for the diagnosis and effective intervention for the management of most kinds of biliary complications after liver transplantation. ERCP should be preferred, whenever feasible with the aim to avoid surgical intervention and resolve the patients' problems. However, its use in some cases was not promising and the need for multiple ERCPs is relatively high; therefore, it should not be the best option for certain kinds of biliary complications (e.g., patients with severe anastomotic biliary stricture and/or overlong and angle shaped bile duct). Beside this, a high proportion of these patients will need PTC/surgery as their final therapy. PTC and other interventions should be studied along with ERCP for patients for whom ERCP may not work. The feasibility of primary management can be predicted by the cholangiographic findings like MRCP, which may help with the choice of the therapeutic modality and avoid unnecessary complications after ERCP and extra financial cost. Further prospective, multicenter studies are needed to confirm these results.

Data availability statement

The raw data supporting the conclusions of this article will be made available by the authors, without undue reservation.

Ethics statement

The studies involving human participants were reviewed and approved by The First Affiliated Hospital of Zhengzhou University. The patients/participants provided their written informed consent to participate in this study.

Author contributions

Study concept and design: HB, ZS. Analysis and interpretation of data: HB, GW, WP, SJ. Acquisition of data: WP, SJ. Administrative, technical or material support: HB, GW, WP, SJ. Critical revision of the manuscript: ZS. All authors contributed to the article and approved the submitted version.

Funding

1. Hepatobiliary foundation of Henan Charity General Federation (No: GDXZ2019006). 2. Youth Project of the National Natural Science Foundation of China (82103282).

Conflict of interest

The authors declare that the research was conducted in the absence of any commercial or financial relationships that could be construed as a potential conflict of interest.

Publisher's note

All claims expressed in this article are solely those of the authors and do not necessarily represent those of their affiliated organizations, or those of the publisher, the editors and the reviewers. Any product that may be evaluated in this article, or claim that may be made by its manufacturer, is not guaranteed or endorsed by the publisher.

References

1. Santopaolo F, Lenci I, Milana M, Manzia TM, Baiocchi L. Liver transplantation for hepatocellular carcinoma: Where do we stand? *World J Gastroenterol* (2019) 25(21):2591–602. doi: 10.3748/wjg.v25.i21.2591

2. Adam R, Karam V, Delvart V, O'Grady J, Mirza D, Klempnauer J, et al. Evolution of indications and results of liver transplantation in europe. A report from the European liver transplant registry (ELTR). *J Hepatol* (2012) 57(3):675–88. doi: 10.1016/j.jhep.2012.04.015

3. de Villa V, Lo CM. Liver transplantation for hepatocellular carcinoma in Asia. *Oncologist* (2007) 12(11):1321–31. doi: 10.1634/theoncologist.12-11-1321

4. Verdonk RC, Buis CI, Porte RJ, Haagsma EB. Biliary complications after liver transplantation: A review. *Scand J Gastroenterol Suppl* (2006) 243):89–101. doi: 10.1080/00365520600664375

5. Wojcicki M, Milkiewicz P, Silva M. Biliary tract complications after liver transplantation: A review. *Dig Surg* (2008) 25(4):245–57. doi: 10.1159/000144653

6. Balderramo D, Navasa M, Cardenas A. Current management of biliary complications after liver transplantation: Emphasis on endoscopic therapy. *Gastroenterol Hepatol* (2011) 34(2):107e15. doi: 10.1016/j.gastrohep.2010.05.008

7. Guichelaar MM, Benson JT, Malinchoc M, Krom RA, Wiesner RH, Charlton MR. Risk factors for and clinical course of non-anastomotic biliary strictures after liver transplantation. *Am J Transplant* (2003) 3(7):885–90. doi: 10.1034/j.1600-6143.2003.00165.x

8. DaVee T, Geevarghese SK, Slaughter JC, Yachimski PS. Refractory anastomotic bile leaks after orthotopic liver transplantation are associated with hepatic artery disease. *GastrointestEndosc* (2017) 85(5):984–92. doi: 10.1016/j.gie.2016.08.050

9. Martins FP, Kahaleh M, Ferrari AP. Management of liver transplantation biliary stricture: Results from a tertiary hospital. *World J GastrointestEndosc* (2015) 7(7):747–57. doi: 10.4253/wjge.v7.i7.747

10. Egea Valenzuela J, JijónCrespín R, Serrano Jiménez A, Alberca de Las Parras F. Endoscopic retrograde cholangiopancreatography in the management of biliary complications after orthotopic liver transplantation. *Rev EspEnferm Dig* (2019) 111 (12):909–13. doi: 10.1055/s-0039-1681874

11. Crismale JF, Ahmad J. Endoscopic management of biliary issues in the liver transplant patient. *GastrointestEndosc Clin N Am* (2019) 29(2):237–56. doi: 10.1016/j.giec.2018.11.003

12. Ranjan P, Bansal RK, Mehta N, Lalwani S, Kumaran V, Sachdeva MK. Endoscopic management of post-liver transplant billiary complications: A prospective study from tertiary centre in India. *Indian J Gastroenterol* (2016) 35 (1):48–54. doi: 10.1007/s12664-016-0625-4

13. Seven G, Çınar K, Idilman R, Tüzüner A, Hazinedaroğlu S, Karayalçın S, et al. Endoscopic treatment of biliary complications following liver transplantation. *Turk J Gastroenterol* (2014) 25(2):156–61. doi: 10.5152/tjg.2014.4055

14. Dolay K, Soylu A, Aygun E. The role of ERCP in the management of bile leakage: Endoscopic sphincterotomy versus biliary stenting. *J Laparoendosc Adv Surg Tech A* (2010) 20(5):455–9. doi: 10.1089/lap.2009.0308

15. Macías-Gómez C, Dumonceau JM. Endoscopic management of biliary complications after liver transplantation: An evidence-based review. *World J GastrointestEndosc* (2015) 7(6):606–16. doi: 10.4253/wjge.v7.i6.606

16. Chang JH, Lee I, Choi MG, Han SW. Current diagnosis and treatment of benign biliary strictures after living donor liver transplantation. *World J Gastroenterol* (2016) 22(4):1593–606. doi: 10.3748/wjg.v22.i4.1593

17. Ahmed S, Schlachter TR, Hong K. Percutaneous transhepatic cholangioscopy. *Tech Vasc Interv Radiol* (2015) 18(4):201–9. doi: 10.1053/j.tvir.2015.07.003

18. Nam K, Lee SK, Song TJ, Park DH, Lee SS, Seo DW, et al. Percutaneous transhepatic cholangioscopy for biliary complications after liver transplantation: A single center experience. *J Hepatobiliary Pancreat Sci* (2016) 23(10):650–7. doi: 10.1002/jhbp.388

19. Shin M, Joh JW. Advances in endoscopic management of biliary complications after living donor liver transplantation: Comprehensive review of the literature. *World J Gastroenterol* (2016) 22(27):6173–91. doi: 10.3748/wjg.v22.i27.6173

20. Siriwardana HPP, Siriwardena AK. Systematic appraisal of the role of metallic endobiliary stents in the treatment of benign bile duct stricture. *Ann Surg* (2005) 242:10–9. doi: 10.1097/01.sla.0000167761.70021.4d

21. Dumonceau JM. Systematic appraisal of the role of metallic endobiliary stents in the treatment of benign bile duct stricture. *Ann Surg* (2006) 244(1):164–5. doi: 10.1097/01.sla.0000226477.17984.28

22. Kahaleh M, Behm B, Clarke BW, Brock A, Shami VM, De La Rue SA. Temporary placement of covered self-expandable metal stents in benign biliary strictures: A new paradigm? (with video). *GastrointestEndosc* (2008) 67:446–54. doi: 10.1016/j.gie.2007.06.057

23. Costamagna G. Covered self-expanding metal stents in benign biliary strictures: Not yet a "new paradigm" but a promising alternative. *GastrointestEndosc* (2008) 67(3):455–7. doi: 10.1016/j.gie.2007.10.006

24. Mahajan A, Ho H, Sauer B, Phillips MS, Shami VM. Temporary placement of fully covered self-expandable metal stents in benign biliary strictures: Midterm evaluation (with video). *GastrointestEndosc* (2009) 70(2):303–9. doi: 10.1016/j.gie.2008.11.029

25. Gwon DI, Sung KB, Ko GY, Yoon HK, Lee SG. Dual catheter placement technique for treatment of biliary anastomotic strictures after liver transplantation. *Liver Transpl* (2011) 17:159–66. doi: 10.1002/lt.22206

frontiers | Frontiers in Oncology

TYPE Original Research
PUBLISHED 03 October 2022
DOI 10.3389/fonc.2022.987026

Check for updates

OPEN ACCESS

EDITED BY
Zhendong Jin,
Second Military Medical University, China

REVIEWED BY
Jindong Zhang,
Peking University Third Hospital, China
Hafiz Abdul Waqas Ahmed,
Lady Reading Hospital, Pakistan

*CORRESPONDENCE
Xilong Ou
ouxilong2021@163.com
Chen Gong
gongchen@suda.edu.cn

†These authors have contributed equally to this work and share first authorship

SPECIALTY SECTION
This article was submitted to Gastrointestinal Cancers: Hepato Pancreatic Biliary Cancers, a section of the journal Frontiers in Oncology

RECEIVED 05 July 2022
ACCEPTED 15 September 2022
PUBLISHED 03 October 2022

CITATION
Song M, Lu Q, Xu M, Li Y, Zhao Y, Gong C and Ou X (2022) The global research and emerging trends in autophagy of pancreatic cancer: A bibliometric and visualized study. *Front. Oncol.* 12:987026. doi: 10.3389/fonc.2022.987026

COPYRIGHT
© 2022 Song, Lu, Xu, Li, Zhao, Gong and Ou. This is an open-access article distributed under the terms of the Creative Commons Attribution License (CC BY). The use, distribution or reproduction in other forums is permitted, provided the original author(s) and the copyright owner(s) are credited and that the original publication in this journal is cited, in accordance with accepted academic practice. No use, distribution or reproduction is permitted which does not comply with these terms.

The global research and emerging trends in autophagy of pancreatic cancer: A bibliometric and visualized study

Mingyang Song[1†], Qin Lu[1†], Min Xu[2], Yajie Li[3], Yawen Zhao[1], Chen Gong[4*] and Xilong Ou[1*]

[1]Department of Gastroenterology, Zhongda Hospital, School of Medicine, Southeast University, Nanjing, China, [2]Department of Human Anatomy, School of Medicine, Southeast University, Nanjing, China, [3]Department of Gerontology, Zhongda Hospital, School of Medicine, Southeast University, Nanjing, China, [4]Department of Gastroenterology, Taicang Affiliated Hospital of Soochow University, The First People's Hospital of Taicang, Jiangsu, China

Objective: To present the global research features and hotspots, and forecast the emerging trends by conducting a bibliometric analysis based on literature related to autophagy of pancreatic cancer from 2011 to 2022.

Methods: The literature data regarding autophagy of pancreatic cancer were retrieved and downloaded from the Web of Science Core Collection (WOSCC) from Clarivate Analytics on June 10th, 2022. VOSviewer (version 1.6.18) was used to perform the bibliometric analysis.

Results: A total of 616 studies written by 3993 authors, covered 45 countries and 871 organizations, published in 263 journals and co-cited 28152 references from 2719 journals. China (n=260, 42.2%) and the United States (n=211, 34.3%) were the most frequent publishers and collaborated closely. However, publications from China had a low average number of citations (25.35 times per paper). The output of University of Texas MD Anderson Cancer Center ranked the first with 26 papers (accounting for 4.2% of the total publications). *Cancers* (n=23, 3.7%; Impact Factor = 6.639) published most papers in this field and was very pleasure to accept related researches. Daolin Tang and Rui Kang published the most papers (n=18, respectively). The research hotspots mainly focused on the mechanisms of autophagy in tumor onset and progression, the role of autophagy in tumor apoptosis, and autophagy-related drugs in treating pancreatic cancer (especially combined therapy). The emerging topics were chemotherapy resistance mediated by autophagy, tumor microenvironment

related to autophagy, autophagy-depended epithelial-mesenchymal transition (EMT), mitophagy, and the role of autophagy in tumor invasion.

Conclusion: Attention has been increasing in autophagy of pancreatic cancer over the past 12 years. Our results undoubtedly provide scholars with new clues and ideas in this field.

KEYWORDS

pancreatic cancer, autophagy, bibliometric study, apoptosis, gemcitabine, chemotherapy resistance

Introduction

Pancreatic cancer remains the most aggressive and fatal among all malignancies, with a dismal 5-year relative survival rates of only 11%. Approximately 62,210 new pancreatic cancer cases are expected in the US in 2022 (1). Pancreatic ductal adenocarcinoma (PDAC) is the majority (90%) of pancreatic cancers. Most patients with pancreatic cancer are not suitable for curative surgery because of an advanced or metastatic stage at the time of diagnosis (2). Over the past decade, even the most advanced diagnostic tools, perioperative management, and systemic anti-tumor therapy for advanced disease have been developed but only modest improvements in patient outcomes (3). Therefore, early diagnosis, mechanisms of tumorigenesis, and anti-tumor strategies of pancreatic cancer have always been research hotspots.

Autophagy is an evolutionarily conserved catabolic mechanism that damaged organelles, aggregated proteins, cytoplasmic macromolecules, or pathogen are delivered to lysosomes for degradation, providing macromolecular precursors and energy, and ultimately recycled back into the cytosol for reuse (4–12). Based on diverse cellular functions, autophagy broadly encompasses three types: macroautophagy, microautophagy, and chaperone-mediated autophagy (13). Macroautophagy is the main autophagy process (hereafter autophagy) in which the autophagosome is newly formed by a double-membrane vesicle to sequester a variety of cellular cargo and transport this autophagic material to lysosomes for subsequent degradation (14, 15). Autophagy can be selective and non-selective depending on the way of sequestration of degradation targets. Non-selective autophagy is responsible for randomly engulfing cytoplasmic components into phagophores (the precursors to autophagosomes), whereas selective autophagy identifies and removes specific components. Selective autophagic degradation processes include mitophagy for damaged and/or superfluous mitochondria, aggrephagy for protein aggregates, ferritinophagy for the iron-sequestering protein ferritin, xenophagy for intracellular pathogens and the like (16–19). By contrast, microautophagy is responsible for directly engulfing cellular cargo by lysosomes (20). Finally, chaperone-mediated autophagy involves the direct translocation of specific cytosolic proteins (and possibly DNA and RNA) across the lysosomal membrane with the assistance of HSC70 and other co-chaperones (21, 22). In virtually all eukaryotic cells, autophagy occurs at a low basal level in physiological condition to maintain cellular homeostasis or regulate cellular functions (23, 24). Given the catabolic degradation function of autophagy, it is not surprising that dysregulation of autophagy has been associated with numerous human diseases, including cancers, neurodegenerative diseases, autoimmune disorders, and inflammatory diseases (25, 26). A total of 18,881 autophagy-related articles were published before 2019 and relevant research has dramatically risen in the past decade (27). Among which, the relationship between autophagy and cancer is one of the research hotspots. In 2011, Yang et al. reported that pancreatic cancers have a distinct dependence on autophagy (28). Then, hundreds of research articles have been published on autophagy of pancreatic cancer. Thus, it is urgently needed to collect and analyze the vast quantities of literatures on this topic.

Bibliometrics is a quantitative science based on large volumes of literatures. It can use of mathematical and statistical methods to comprehensively analyze the authors, keywords, journals, countries, institutions, citations, and their associations of selected publications, thus providing an objective evaluation of the dynamics and emerging trends in a research field or discipline (29). The visualization of bibliometric analysis can demonstrate the results in different forms and contribute to data interpretation, which make the results more intuitive and comprehensive (29, 30). This method has been widely used to assess various research domains, including medicine (31–33).

Previous bibliometric studies has focused on the research of autophagy (27), mitophagy (34), pancreatic cancer (35), tumor

microenvironment of pancreatic cancer (36), and pancreatic neuroendocrine tumors (37). As a novel perspective, we conducted a bibliometric analysis based on literature related to autophagy of pancreatic cancer from 2011 to 2022. This study aims to present the global research features and hotspots, and forecast the emerging trends in that field, which may provide researchers with new clues and ideas in the field of autophagy and pancreatic cancer.

Materials and methods

Data screening and collection

Web of Science Core Collection (WOSCC) is the most frequently used database in bibliometric analysis (31). We retrieved and downloaded literature data in the WOSCC from Clarivate Analytics on June 10th, 2022. Primary search terms were "pancreatic cancer", "pancreatic carcinoma", "pancreatic ductal adenocarcinoma" and "autophagy" and detailed search strategy is provided in Supplemental File S1. The retrieval time was set from January 1st, 2011 to June 9th, 2022. The language was limited to English and the literature type we searched for was restricted to article or review article. Two authors (MY S and Q L) independently screened the search results and removed the paper that did not related to autophagy of pancreatic cancer by reading the title, abstract, and if necessary, the whole article. Different viewpoints would be resolved by negotiation or reviewed by an experienced corresponding author (XL O). The literature data was finally exported with the record content of "Full Record and Cited References" and downloaded in plain text format.

Data analysis and visualization

We used VOSviewer (version 1.6.18) to perform the bibliometric analysis based on the literature data. The annual output of publications related to autophagy of pancreatic cancer was plotted using GraphPad Prism (version 6.0.4).

VOSviewer is a free JAVA-based computer program developed by Van Eck and Waltman, which is used for constructing and generating bibliometric maps visually. It provides a variety of easy-to-interpret visualization maps, including network visualization, overlay visualization, and density visualization (38). In VOSviewer, the co-authorship network map of countries/organizations/authors, the overlay visualization map of the citation analysis of sources, the density map of the co-citation analysis of cited authors and the co-occurrence analysis of all keywords were built. The data analyzing flow chart can be seen from Figure 1.

Results

Publication outputs and trend

According to our search strategy, a total of 616 publications on autophagy of pancreatic cancer were remained for bibliometric analysis, including 479 articles (77.8%) and 137 reviews (22.2%). The annual number of publications on the autophagy of pancreatic cancer from 2011 to 2022 (June 9th, 2022) is presented in Figure 2. Generally, the number of publications increased year by year and it dramatically raised from 11 in 2011 to 101 (including 66 articles and 35 reviews) in

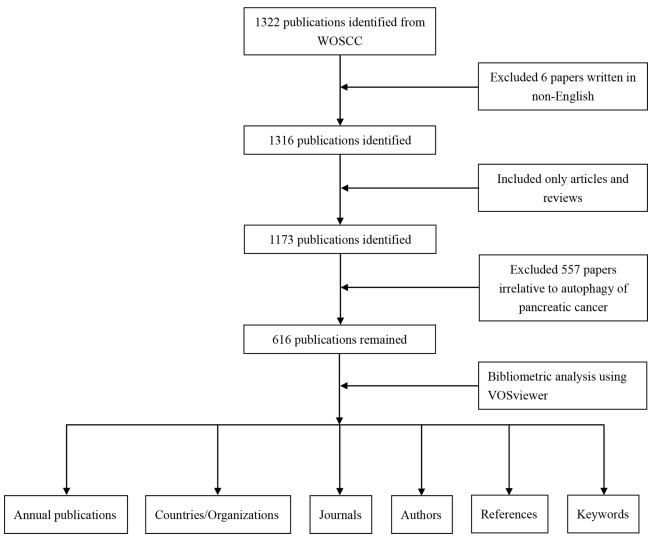

FIGURE 1
Flow chart of the data collection and analysis for research on autophagy of pancreatic cancer.

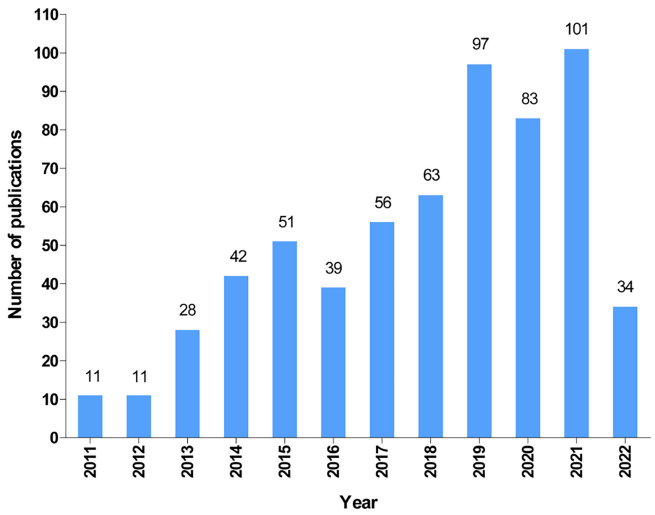

FIGURE 2
The annual output of autophagy and pancreatic cancer from 2011 to 2022.

2021, suggesting a gradually increased attention to autophagy of pancreatic cancer over the past 12 years. Moreover, as of June 9th, 2022, a total of 34 papers (including 31 articles and 3 reviews) have been published.

Countries and organizations

All included publications in the field covered 45 countries and 871 organizations. The output of China ranked the first with 260 (accounting for 42.2% of the total publications), followed by the United States (n=211, 34.3%), Italy (n=40, 6.5%), Germany (n=37, 6.0%) and Japan (n=37, 6.0%) (Table 1). However, among the top 10 countries, publications from China had a low average number of citations (25.35 times per paper), while the United States (63.9 times) was in first place by the average number of citations, followed by Italy (62.4 times), Germany (49.08 times), England (39.95 times) and France (39.18 times). Besides, a co-authorship network map of countries was built (Figure 3A) as the cooperation between different countries can be considered as a measure of international cooperation. Only the countries with a minimum of five publications were included and 25 countries were subsequently identified. China collaborated closely with the United States. The United States cooperated with 23 countries, ranked first, followed by Germany (n=12), Spain (n=11), China (n=10), Italy (n=10), and England (n=10).

The top 11 active organizations based on publication number were listed in Table 2. The production from these organizations ranged 12 to 26 publications, accounting for 28.7% (177/616) of the total publications. Organizations from China and the United States account for 6 and 5 respectively. University of Texas MD Anderson Cancer Center contributed the most publications (n=26, 4.2%) with 2657 citations, followed by Fudan University (n=18, 2.9%) with 645

TABLE 1 The top 10 productive countries in the field of autophagy and pancreatic cancer.

Rank	Country	Publications	Percentage	Total citations	Average citation
1	China	260	42.2%	6592	25.35
2	United States	211	34.3%	13482	63.9
3	Italy	40	6.5%	2456	62.4
4	Germany	37	6.0%	1816	49.08
5	Japan	37	6.0%	1069	28.89
6	France	28	4.5%	1097	39.18
7	South Korea	22	3.6%	526	23.91
8	England	19	3.1%	759	39.95
9	Spain	18	2.9%	452	25.11
10	Canada	13	2.1%	340	26.15

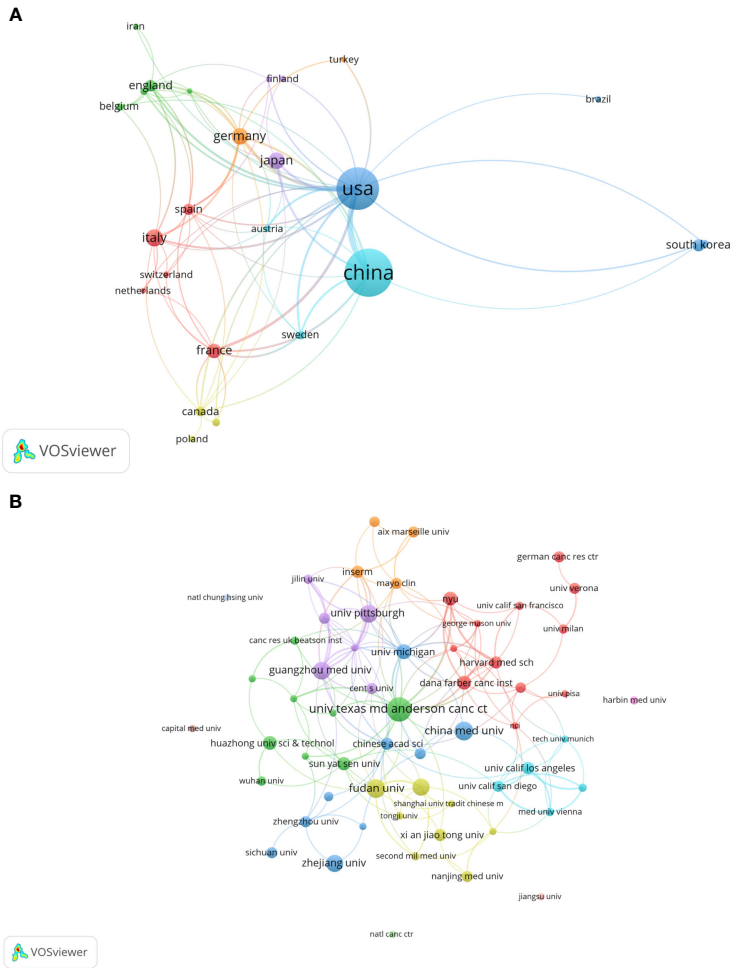

FIGURE 3
A visual map for VOSviewer network of countries and organizations related to autophagy of pancreatic cancer. **(A)** Country cooperation analysis. The total link strength was 241; the layout parameters: Attraction: 2, Repulsion: 1; **(B)** Organization cooperation analysis. The total link strength was 266; the layout parameters: Attraction: 4, Repulsion: -1. The circle size means the number of publications; the thickness of the line means the strength of the connection.

TABLE 2 The top 11 productive organizations published literature related to autophagy of pancreatic cancer.

Rank	Organization	Country	Publications	Total citations	Average citation
1	University of Texas MD Anderson Cancer Center	United States	26	2657	102.19
2	Fudan University	China	18	645	35.83
3	China Medical University	China	18	310	17.22
4	Guangzhou Medical University	China	17	1183	69.59
5	University of Pittsburgh	United States	17	1316	77.41
6	Zhejiang University	China	16	214	13.38
7	Shanghai Jiao Tong University	China	16	218	13.63
8	University of Michigan	United States	13	1683	129.46
9	New York University	United States	12	1621	135.08
10	Dana-Farber Cancer Institute	United States	12	2035	169.58
10	Huazhong University of Science and Technology	China	12	268	22.33

citations and China Medical University (n=18, 2.9%) with 310 citations. Publications from China organizations had also a low average number of citations. Notably, among the top 11 organizations, Dana-Farber Cancer Institute published a relatively low number of 12 papers related to autophagy of pancreatic cancer from 2011 to 2022. But it had the highest average number of citations (169.58 times). Five documents were set as a minimum for each organization to be analyzed; therefore, 58 of 871 organizations were included for network analysis (Figure 3B). The cooperation between organizations was a little stronger than that between countries based on the total link strength.

Analysis of journals and co-cited journals

A total of 263 academic journals published the 616 publications on autophagy of pancreatic cancer between 2011 to 2022. As is displayed in Table 3, the top 12 most frequent journals were distributed 153 papers, accounting 24.8% for all the obtained publications. The most productive journal has been *Cancers* with 23 papers (3.7% of the total), followed by *Oncotarget* (19, 3.0%), *Frontiers in Oncology* (15, 2.4%), *Autophagy* (13, 2.1%), and *International Journal of Molecular Sciences* (13, 2.1%). The top 3 journals with the highest total number of citations were *Autophagy* (982 citations), *Oncotarget* (841 citations), and *Gastroenterology* (713 citations). Among the top 12 journals, 66.7% (8/12) had an Impact Factor (IF) of more than five, and 66.7% (8/12) were at the Q1 JCR division. Besides, the journals (n=31) published a minimum of five publications were included in the overlay visualization map (Figure 4). The yellow nodes represented the emerging journals in recent 3 years. *Cancers* (IF=6.639, Q1), *Frontiers in Cell and Developmental Biology* (IF=6.684, Q2), *Biomedicine & Pharmacotherapy* (IF=6.53, Q1), and *Cells* (IF=6.6, Q2) were emerging journals publishing papers in the field of autophagy and pancreatic cancer.

Among 2719 co-cited journals, 14 journals had citations more than 500. As is shown in Table 4, *Nature* had the most co-citations up to 1415 times, followed by *Cancer Research* (1267 times), *Autophagy* (1238 times), and *Cell* (1116 times). Among the top 10 co-cited journals, 80% (8/10) had an IF of more than ten, 90% (9/10) were at the Q1 JCR division, and 80% (8/10) were from the United States.

Analysis of authors and co-cited authors

A total of 3,993 authors contributed the 616 included publications. The top author is defined as one who has published at least 5 papers and received over 600 citations. Finally, ten top authors were identified (Table 5). By the number of papers, Daolin Tang and Rui Kang published the most papers (n=18, respectively), followed by Alec C Kimmelman (n=16), Michael T Lotze (n=9), and Haoqiang Ying (n=7). Papers published by Alec C Kimmelman who comes from New York University had the highest total number of citations (3288 times). Notably, top authors all come from the United States. The authors (n=142) who had published with a minimum of three publications were entered into co-authorship network analysis of authors (Figure 5A). There were strong collaborations among authors who were in the same cluster/color, such as Daolin Tang, Rui Kang, and Michael T Lotze. However, sparse connection was observed among different clusters, indicating little cooperation between research groups.

A total of 20,319 authors were co-cited at least once. There were 50 authors who had been co-cited with a minimum of 40 times. They were included to make the density visualization which can intuitively display the most co-cited authors (Figure 5B). Specifically, SH Yang (n=227) was the most frequent co-cited authors, followed by N Mizushima (n=222) and RL Siegel (n=176). The remaining seven top authors were co-cited from 104 to 140 (Table 5).

TABLE 3 The top 12 productive journals associated with autophagy of pancreatic cancer.

Rank	Journal	Count	Percentage	Total citations	IF (2020)	JCR division (2020)	Country
1	Cancers	23	3.7%	300	6.639	Q1	Switzerland
2	Oncotarget	19	3.0%	841	None	None	United States
3	Frontiers in Oncology	15	2.4%	211	6.244	Q2	Switzerland
4	Autophagy	13	2.1%	982	16.016	Q1	United States
5	International Journal of Molecular Sciences	13	2.1%	197	5.924	Q1	United States
6	Journal of Experimental & Clinical Cancer Research	12	1.9%	365	11.161	Q1	Italy
7	Oncology Reports	11	1.8%	282	3.906	Q3	Greece
8	Cell Death & Disease	10	1.6%	430	8.469	Q1	England
9	Scientific Reports	10	1.6%	370	4.38	Q1	England
10	Gastroenterology	9	1.5%	713	22.682	Q1	United States
10	Cancer Letters	9	1.5%	223	8.679	Q1	Netherlands
10	Plos One	9	1.5%	271	3.24	Q2	United States

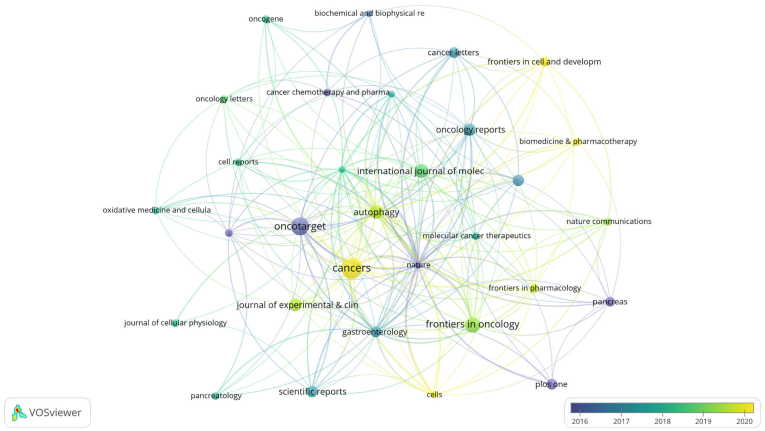

FIGURE 4
The overlay visualization map of journals associated with research on autophagy of pancreatic cancer. The layout parameters: Attraction: 4, Repulsion: -1. The circle size means the number of publications; the circle colors mean the average published year.

Analysis of papers and co-cited references

Among the 616 papers in our study, 100 papers were cited more than 50 times. The most cited papers were summarized in Table 6. Four original articles by Shenghong Yang et al. (28), Andrea Viale et al. (39), Wen Hou et al. (40), and Cristovão M Sousa (41), with 957, 699, 594, and 531 citations, respectively, were ranked first, second, third and fourth. The remaining six studies [Mathias T Rosenfeldt 2013 (42); Rushika M Perera 2015 (43); Kirsten L Bryant 2014 (44), Jennifer A Kashatus 2015 (45), Annan Yang 2014 (46), and Conan G Kinsey 2019 (47)] were cited between 266 to 485 times. Also, four top cited articles were published in *Nature*.

The results showed a total of 28,152 references were co-cited from 1 to 197. As is shown in Table 7, the most co-cited paper in the field of autophagy and pancreatic cancer by Shenghong Yang et al. (28), Mathias T Rosenfeldt et al. (42), and Annan Yang et al. (46), with 197, 96, and 86 citations, respectively, were ranked first, second, and third. The remaining eight top papers were co-cited from 54 to 73. Notably, the top 1 cited and co-cited paper was the same article published in *Genes & Development* by Shenghong Yang et al. in 2011 (28), entitled "Pancreatic cancers

TABLE 4 The most co-cited journals associated with autophagy of pancreatic cancer.

Rank	Journal	Total citations	IF (2020)	JCR division (2020)	Country
1	Nature	1415	49.962	Q1	England
2	Cancer Research	1267	12.701	Q1	United States
3	Autophagy	1238	16.016	Q1	United States
4	Cell	1116	41.584	Q1	United States
5	Journal of Biological Chemistry	865	5.157	Q2	United States
6	Proceedings of the National Academy of Sciences of the United States of America	825	11.205	Q1	United States
7	Clinical Cancer Research	723	12.531	Q1	United States
8	Genes & Development	708	11.361	Q1	United States
9	Oncogene	695	9.867	Q1	England
10	Cancer Cell	665	31.743	Q1	United States

TABLE 5 The top 10 authors and most co-cited authors in the field of autophagy and pancreatic cancer.

Rank	Author	Count	Total citations	Institution	Location	Rank	Co-cited author	Total citations
1	Daolin Tang	18	1326	UT Southwestern Medical Center	United States	1	SH Yang	227
1	Rui Kang	18	1326	UT Southwestern Medical Center	United States	2	N Mizushima	222
3	Alec C Kimmelman	16	3288	New York University	United States	3	RL Siegel	176
4	Michael T Lotze	9	923	University of Pittsburgh	United States	4	JY Guo	140
5	Haoqiang Ying	7	1799	University of Texas MD Anderson Cancer Center	United States	5	R Kang	128
6	Herbert J Zeh	6	778	University of Pittsburgh	United States	6	E White	125
7	Xiaoxu Wang	6	2244	Dana-Farber Cancer Institute	United States	7	DJ Klionsky	125
8	Anirban Maitra	6	687	Johns Hopkins University	United States	8	B Levine	122
9	Yangchun Xie	5	796	University of Pittsburgh	United States	9	MT Rosenfeldt	112
10	Joseph D Mancias	5	827	Dana-Farber Cancer Institute	United States	10	A Yang	104

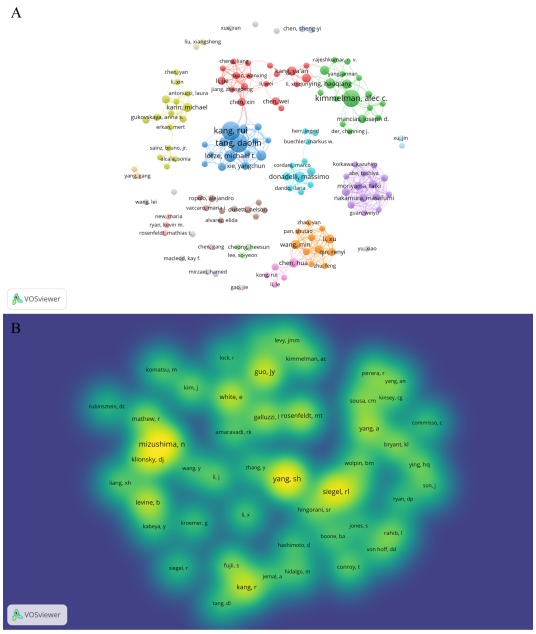

FIGURE 5
Authors and co-cited authors in the field of autophagy and pancreatic cancer. **(A)** The co-authorship network analysis of authors. The layout parameters: Attraction: 3, Repulsion: -1. The circle size means the number of publications; the thickness of the line means the strength of the connection; the circle colors mean different clusters; **(B)** The density map of co-cited authors. The layout parameters: Attraction: 2, Repulsion: 1. The color brightness means the frequency of occurrence.

TABLE 6 The most cited papers in the field of autophagy and pancreatic cancer.

Rank	Title	First author	Source	Type	Publication year	Total citations
1	pancreatic cancers require autophagy for tumor growth	Shenghong Yang	Genes & Development	Article	2011	957
2	Oncogene ablation-resistant pancreatic cancer cells depend on mitochondrial function	Andrea Viale	Nature	Article	2014	699
3	Autophagy promotes ferroptosis by degradation of ferritin	Wen Hou	Autophagy	Article	2016	594
4	Pancreatic stellate cells support tumour metabolism through autophagic alanine secretion	Cristovão M Sousa	Nature	Article	2016	531
5	p53 status determines the role of autophagy in pancreatic tumour development	Mathias T Rosenfeldt	Nature	Article	2013	485
6	Transcriptional control of autophagy-lysosome function drives pancreatic cancer metabolism	Rushika M Perera	Nature	Article	2015	453
7	KRAS: feeding pancreatic cancer proliferation	Kirsten L Bryant	Trends in Biochemical Sciences	Review	2014	413
8	Erk2 phosphorylation of Drp1 promotes mitochondrial fission and MAPK-driven tumor growth	Jennifer A Kashatus	Molecular Cell	Article	2015	347
9	Autophagy is critical for pancreatic tumor growth and progression in tumors with p53 alterations	Annan Yang	Cancer Discovery	Article	2014	305
10	Protective autophagy elicited by RAF→MEK→ERK inhibition suggests a treatment strategy for RAS-driven cancers	Conan G Kinsey	Nature Medicine	Article	2019	266

TABLE 7 The most co-cited papers in the field of autophagy and pancreatic cancer.

Rank	Title	First author	Source	Type	Publication year	Total citations
1	Pancreatic cancers require autophagy for tumor growth	Shenghong Yang	Genes & Development	Article	2011	197
2	p53 status determines the role of autophagy in pancreatic tumour development	Mathias T Rosenfeldt	Nature	Article	2013	96
3	Autophagy is critical for pancreatic tumor growth and progression in tumors with p53 alterations	Annan Yang	Cancer Discovery	Article	2014	86
4	Activated Ras requires autophagy to maintain oxidative metabolism and tumorigenesis	Jessie Yanxiang Guo	Genes & Development	Article	2011	73
5	Autophagy is activated in pancreatic cancer cells and correlates with poor patient outcome	Satoshi Fujii	Cancer Science	Article	2008	70
6	Pancreatic stellate cells support tumour metabolism through autophagic alanine secretion	Cristovão M Sousa	Nature	Article	2016	66
7	Transcriptional control of autophagy-lysosome function drives pancreatic cancer metabolism	Rushika M Perera	Nature	Article	2015	66
8	Projecting cancer incidence and deaths to 2030: the unexpected burden of thyroid, liver, and pancreas cancers in the United States	Lola Rahib	Cancer Research	Article	2014	61
9	Cancer statistics, 2019	Rebecca L Siegel	CA-A Cancer Journal for Clinicians	Article	2019	56
10	Autophagy Sustains Pancreatic Cancer Growth through Both Cell-Autonomous and Nonautonomous Mechanisms	Annan Yang	Cancer Discovery	Article	2018	54
10	Phase II and pharmacodynamic study of autophagy inhibition using hydroxychloroquine in patients with metastatic pancreatic adenocarcinoma	Brian M Wolpin	Oncologist	Article	2014	54

require autophagy for tumor growth", indicating a wide influence and a highly proven peer recognition in the field.

Analysis of keyword co-occurrence

The co-occurrence analysis of all keywords showed a total of 2668 keywords were extracted. The keywords with the same meaning were merged (Supplemental File S2), such as pancreatic cancer, cancer cells, beclin 1, etc. Table 8 listed the top 20 high-frequency co-occurrence keywords. These keywords may reveal the hotspots in the field of autophagy and pancreatic cancer. The most co-occurrence keyword was autophagy (n=419 co-occurrences), followed by pancreatic cancer (n=360), apoptosis (n=146), cancer (n=146), expression (n=111), growth (n=102), gemcitabine (n=101), inhibition (n=97), activation (n=80), cells (n=75), etc. According to Price's Law, the keywords appeared over 15 times were used to build a network map to visualize keyword clusters (Figure 6A) and 69 keywords were finally identified. The network was divided into five clusters with different colors and it is highly homogeneous between the items in the same color. There were 24 items in cluster 1 (red), including activation, cancer, cells, growth, inhibition, metabolism, pathway, progression, degradation, inflammation, mechanisms, tumorigenesis, AMPK, beclin 1, mice, KRAS, p53, p62, phosphorylation, stress, etc. There were 13 items in cluster 2 (green), including tumor microenvironment, epithelial-mesenchymal transition, down-regulation, NF-kappa-B, stem-cells, tumor-suppressor, etc. There were 12 items in cluster 3 (blue), including apoptosis, cell death, death, endoplasmic-reticulum stress, *in-vitro*, induction, mitophagy, mTOR, oxidative stress, etc. There were 11 items in cluster 4 (yellow), including gemcitabine, survival, resistance, chemoresistance, chemotherapy, chloroquine, combination, hydroxychloroquine, hypoxia, therapy, etc. There were 9 items in cluster 5 (purple), including expression, proliferation, tumor-growth, identification, prognosis, invasion, metastasis, migration, and promotes.

The overlay visualization map of the 69 keywords is showed in Figure 6B. The research focus can be intuitively observed by the evolution of high-frequency keywords over time. The yellow nodes represented the emerging keywords near 2019. Among which, the most co-occurrence keywords were resistance (n=49 co-occurrences), followed by tumor microenvironment (n=23), epithelial-mesenchymal transition (EMT) (n=22), mitophagy (n=21), and invasion (n=21). These keywords may become the future research hotspots in the field of autophagy and pancreatic cancer.

Discussion

In this study, we used VOSviewer software to perform a bibliometric analysis based on the literature related to autophagy of pancreatic cancer in WoSCC database from 2011 to 2022 (June 9th, 2022). A total of 616 studies were written by 3993 authors, covered 45 countries and 871 organizations, published in 263 journals and co-cited 28152 references from 2719 journals. Most of which are original articles (77.8%). An average of 45.70 references each publication were noted. The primary aim of the current study was to explore the global research features and hotspots and forecast the emerging trends which may be helpful to researchers in autophagy of pancreatic cancer field.

Overall, the annual publication output has dramatically increased from 11 in 2011 up to 101 in 2021 which reveals that attention has been increasing in autophagy of pancreatic cancer field over the past 12 years. Autophagy plays an important role in tumor pathogenesis and contributes to tumor growth (48, 49). The article published in *Genes & Development* (IF=11.361) by Shenghong Yang et al, in 2011 which confirmed that pancreatic cancers actually require autophagy for tumorgenic growth has been cited and co-cited the most frequently (28), indicating Shenghong Yang is an accomplished scholar in this field and his study is considered as the most fundamental and important study. Besides, it

TABLE 8 The top 20 keywords related to autophagy of pancreatic cancer.

Rank	keyword	Count	Rank	keyword	Count
1	autophagy	419	11	cancer cells	64
2	pancreatic cancer	360	12	progression	61
3	apoptosis	146	13	survival	55
3	cancer	146	13	metabolism	55
5	expression	111	15	proliferation	51
6	growth	102	15	therapy	51
7	gemcitabine	101	15	pathway	51
8	inhibition	97	15	ductal adenocarcinoma	51
9	activation	80	19	resistance	49
10	cells	75	20	death	48

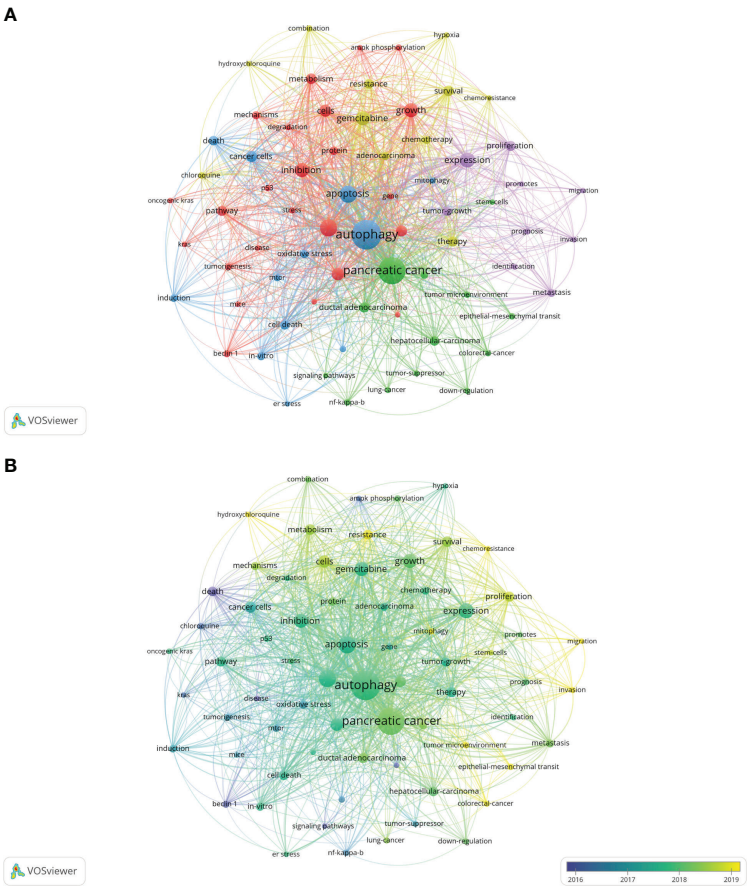

FIGURE 6
Keywords related to autophagy of pancreatic cancer. **(A)** Network visualization of keywords drawn by VOSviewer. The layout parameters: Attraction: 2, Repulsion: 1. The circle size means the frequency of occurrence; the circle colors mean different clusters; **(B)** Overlay visualization of keywords drawn by VOSviewer. The layout parameters: Attraction: 2, Repulsion: 1. The circle size means the frequency of occurrence; the circle colors mean the average published year.

pointed chloroquine and its derivatives are powerful inhibitors of autophagy which could be used to treat pancreatic cancer patients (28). Therefore, more attention on the research of autophagy and pancreatic cancer field will be triggered (50).

As far as countries for publication of papers are considered, a bibliometric analysis of autophagy showed that China and the United States were the most productive countries (27). Again, one bibliometric study on mitophagy (34) and the other bibliometric study on pancreatic cancer research (35) arrived the same conclusion. Our results also showed that China and the United States were the most frequent publishers in the field of autophagy and pancreatic cancer. 76.5% of the total publications was contributed by China and the United States, far more than any other country. This phenomenon could be called “Matthew effect”. In the network visualization map, extensive cooperation was observed between countries with a minimum of five publications, indicating a widespread trans-national communication in the research of autophagy and pancreatic cancer. Specifically, China and the United States collaborated closely. The United States can play as the central role in the cooperation network map with its cooperation with 23 countries. Despite the United States, Germany, Spain, China, Italy, and England can also be suggested as minor cores as they cooperated with 12, 11, 10, 10, and 10 countries, respectively. However, China had a lower average number of citations than United States, Italy, Germany, England, France and Japan, and none of the top 10 cited and top 11 co-cited papers were written by Chinese scholars, implying the quality of studies written by Chinese scholars needs further improvement. In terms of organizations, China and the United States contributed six and five of the top 11 organizations, respectively. The number of average citations per papers of top 11 organizations was generally consistent with that of countries. Among which, Dana-Farber Cancer Institute had the highest average number of citations (169.58 times) among the top 11 organizations, and two high-frequency cited authors (Xiaoxu Wang and Joseph D

Mancias) were from this institution, showing the high influence of its published articles. Besides, cooperation between countries were found to be a little sparser than those between agencies, indicating that international cooperation should be strengthened in this field. Notably, University of Texas MD Anderson Cancer Center, the most productive organization, collaborated most closely with many United States universities and research institutions, and also with Universities from China, such as China Medical University, Fudan University, Sun Yat-Sen University, Xi'an Jiaotong University, and Tongji University, showing that the United States and China collaborated closely between organizations.

When it comes to journals and co-cited journals, our results showed the journals published the most papers related to autophagy of pancreatic cancer were *Cancers* (n=23), *Oncotarget* (n=19), *Frontiers in Oncology* (n=15), *Autophagy* (n=13), and *International Journal of Molecular Sciences* (n=13). Among the top 12 journals, 66.7% had an IF of more than five, and 66.7% were at the Q1 JCR division. *Nature* (n=1415 times), *Cancer Research* (n=1267 times), *Autophagy* (n=1238 times), and *Cell* (n=1116 times) were the most high-frequency co-cited journals. Among the top 10 co-cited journals, 80% had an IF of more than ten, 90% were at the Q1 JCR division. These data indicated many high-quality and high-impact journals were particularly interested in and play a significant role in the field of autophagy and pancreatic cancer. Besides, it is worth noting that *Cancers*, the most productive journal, was also an emerging journal in recent 3 years, implying this journal was very pleasure to accept the researches in this field. Despite the most productive journals, *Frontiers in Cell and Developmental Biology* (IF=6.684, Q2), *Biomedicine & Pharmacotherapy* (IF=6.53, Q1), and *Cells* (IF=6.6, Q2) were the emerging journals that accepted related papers in recent 3 years. These results will also assist future scholars in selecting journals when submitting manuscripts associated to autophagy of pancreatic cancer.

A high citation frequency indicating a wide influence and a highly proven peer recognition in the field. In this bibliometric analysis, the top 10 most-cited papers were as follows (Table 6): Shenghong Yang et al. published "pancreatic cancers require autophagy for tumor growth (28)" in *Genes & Development* in 2011, which was the most cited paper (957 citations). This study reported that pancreatic cancers have a distinct dependence on autophagy. The second cited paper, "Oncogene ablation-resistant pancreatic cancer cells depend on mitochondrial function", was published by Andrea Viale et al. (39) in *Nature* in 2014. This study illuminated a therapeutic strategy of combined targeting of the KRAS pathway and mitochondrial respiration to treat pancreatic cancer. The third cited paper, "Autophagy promotes ferroptosis by degradation of ferritin" was published by Wen Hou et al. (40) in *Autophagy* in 2016. This study found autophagy promotes ferroptosis by degradation of ferritin which provide novel insight into the interplay between autophagy and regulated cell death. The fourth cited paper was published by Cristovão M Sousa et al. (41) in *Nature* in 2016. It reported pancreatic stellate cells (PSCs)-derived alanine is an alternative fuel source that can sustain the growth of cancer cells in the tumor microenvironment. And alanine release in PSC is dependent on PSC autophagy which is mediated by cancer cells. The fifth cited paper was published by Mathias T Rosenfeldt et al. (42) in *Nature* in 2013. It showed the progression of pancreatic cancer is intrinsically associated with the status of p53 (a tumor suppressor gene). Inhibition of autophagy promotes cancer onset instead of blocking cancer progression in mouse model with oncogenic KRAS but without p53. The sixth cited paper was published by Rushika M Perera et al. (43) in *Nature* in 2015. This article reported MiT/TFE-dependent autophagy-lysosome activation is essential for pancreatic cancer growth, which is a novel hallmark of malignant tumor. The seventh cited paper was published by Turtle et al. (44) Kirsten L Bryant in *Trends in Biochemical Sciences* in 2014. This is a review presented oncogenic KRAS plays a critical role in controlling tumor metabolism by increasing autophagy and orchestrating other multiple metabolic changes. The eighth cited paper was published by Jennifer A Kashatus et al. (45) in *Molecular Cell* in 2015. This article illuminated the activation of Ras or MAPK pathway (the downstream biological process) leads to Mek-dependent phosphorylation of the GTPase Drp1 and subsequent mitochondrial fission. Inhibition of Drp1 or its phosphorylation blocks pancreatic cancer growth. The ninth cited paper was published by Annan Yang et al. (46) in *Cancer Discovery* in 2014. This article reported autophagy plays a central role in pancreatic cancer and showed that autophagy inhibition may have therapeutical effect on pancreatic cancer, independent of p53 status. The tenth cited paper was published by Conan G Kinsey et al. (47) in *Nature Medicine* in 2019. This article represented trametinib combined with hydroxychloroquine may be a new strategy to treat RAS-driven cancers. Besides, the most co-cited papers were listed in Table 7. These most co-cited studies have a major impact on autophagy of pancreatic cancer field. The first, second, third, sixth and seventh co-cited papers are the same as the first, fifth, ninth, fourth and sixth cited paper listed in Table 6. The eighth and ninth co-cited papers are about the epidemiology of cancers. The remaining 4 top co-cited articles are mainly about the role of autophagy in pancreatic cancer. Keywords represent the major topic of papers. To explore the global research features and hotspots, we constructed a co-occurrence analysis of all keywords in the field of autophagy and pancreatic cancer by VOSviewer. As autophagy broadly consists of macroautophagy, microautophagy, and chaperone-mediated autophagy, we individually searched for publications concerning the three types. The publication numbers were 18, 0, and 7, respectively. The content of the remaining publications was indistinguishable. Macroautophagy has been studied the most. The keywords appeared over 15 times were clustered into five main categories in the network visualization map (Figure 6A) which can intuitively show the direction and scope in this field. After reviewing and summarizing relevant researches, we found the keywords in cluster 1 (red) and cluster 5 (purple) mainly focused on the regulation mechanisms of autophagy in pancreatic cancer onset and

progression. Among which, expression, growth, and inhibition could represent the research hotspots. In the top cite and co-cited papers, Shenghong Yang et al. reported pancreatic cancers required autophagy for tumor growth in 2011 (28), which is considered as the most fundamental and important study in this field. The other article published in *Genes & Development* by Jessie Yanxiang Guo et al. in 2011, reported activated oncogene HRAS or KRAS could increase basal autophagy which was essential to maintain human cancer cell survival in starvation and in oncogenesis (51). As KRAS mutation was found in 70~95% of PDAC patients (52), researches on the regulation of autophagy in Ras-expressing pancreatic cancer cells were rapidly increasing. Notably, Mathias T Rosenfeldt et al. showed Inhibition of autophagy promotes cancer onset instead of blocking cancer progression in mouse model with oncogenic KRAS but without p53 (42), suggesting a dual role of autophagy in pancreatic cancer progression (53, 54). In the transcriptional program, Rushika M Perera et al. presented MiT/TFE-dependent autophagy-lysosome activation is essential for pancreatic cancer growth, which is a novel hallmark of malignant tumor (43). Besides, Di Malta, C. et al. found transcriptional activation of Rag guanosine triphosphatases could control the mechanistic target of rapamycin complex 1 and regulate anabolic pathways related to nutrient metabolism, leading to excessive cell proliferation and tumor growth (55). Researches have also shown that autophagy supports the growth of pancreatic cancer through both cell-autonomous and nonautonomous pathways (56). These studies provide us insights into the role of autophagy in pancreatic cancer, which may be used to treat this malignant cancer in future. The keywords in cluster 2 (green) were mainly associated with the relationship between autophagy and tumor microenvironment as well as that between autophagy and EMT in pancreatic cancer. Notably, tumor microenvironment and EMT were the emerging keywords in recent years, indicating they may become the future hotspots in the field of autophagy and pancreatic cancer. Hypoxic tumor microenvironment is characterized as a hallmark of pancreatic cancer (57). Increased autophagy flux may mediate the survival of pancreatic cancer stem cells (CSCs) under a hypoxic tumor microenvironment. The inhibition of autophagy converts survival signaling to suicide and finally suppresses cancer development in mouse models (58). Besides, a top cited and co-cited paper published in Nature by Cristovão M Sousa et al. in 2016, reported PSCs-derived alanine is an alternative fuel source that can sustain the growth of cancer cells in the tumor microenvironment. And alanine release in PSC is dependent on PSC autophagy which is mediated by cancer cells (41). Despite of CSC and PSC, immune cells, endothelial cells, and fibroblasts may also promote tumor progression through the metabolic crosstalk with malignant cells in the tumor microenvironment (59), the role of autophagy in tumor microenvironment needs further study. In terms of EMT, it is a trans-differentiation process in which epithelial cells acquire mesenchymal features that promote the invasion and metastasis of cancers (60). Enhanced autophagy induced by HIF-1 alpha was reported to promote EMT and the metastatic ability of pancreatic CSCs (61). In RAS-mutated pancreatic cancer cells, the inhibition of autophagy activated the SQSTM1/p62-mediated NF-kappa-B pathway, subsequently enhancing EMT which finally promoted cancer invasion (62). This broadens the horizon for the research of the dual role of autophagy in pancreatic cancer. The keywords in cluster 3 (blue) were mainly related to the role of autophagy in the apoptosis of pancreatic cancer cells. Apoptosis represents a type of programmed cell death that can remove the damaged cells orderly and efficiently (63). Targeting apoptosis is a common therapy strategy for PDAC. However, the cancer cells can establish various mechanisms to reduce apoptosis, including autophagy (64). For example, mitochondrial uncoupling protein 2 (UCP2) plays an essential role in tumorigenesis and development. UCP2 induces autophagy through enhancing Beclin 1 and inhibiting the AKT-MTOR pathway, leading to anti-apoptosis effects or inhibiting other types of cell death in a reactive oxygen species (ROS)-dependent mechanism (65), implying an anti-apoptosis role of autophagy. Eicosapentaenoic acid, a common omega-3 fatty acid, can not only induce autophagy but impair its anti-apoptosis ability in pancreatic cancer cells (66). Ubiquitin specific peptidase 22 (USP22) is an epigenetic regulator, it was reported USP22 induced autophagy by activating MAPK1, thereby promoting cell proliferation and gemcitabine resistance in pancreatic cancer cell lines (67). As discussed above, CSCs and PSCs sustain tumor growth depend on autophagy. Studies have reported inhibiting autophagy also triggers apoptosis in CSCs and PSCs (58, 68). These studies indicate that chemotherapy combined the regulation of autophagy could be a potential future direction in treating pancreatic cancers. Besides, mitophagy is an emerging keyword in this cluster. It is reported mitophagy involved the cell death and modulation of metabolism in pancreatic cancer. Again, mitophagy plays a double-edged action in the regulation of the antitumor efficacy of certain cytotoxic agents (69). The keywords in cluster 4 (yellow) were mainly about the autophagy regulation in the treatment of pancreatic cancer. Autophagy is an essential catabolic mechanism in pancreatic cancer onset and progression. The inhibitions of autolysosome formation, a lysosomotropic agent named chloroquine (CQ) and a V-ATPase inhibitor named bafilomycin A_1, were reported to suppress tumorigenic growth of pancreatic cancers alone (28). However, a phase II and pharmacodynamic study showed hydroxychloroquine (HCQ, an inhibitor of autophagy) monotherapy did not result in a consistent autophagy inhibition as evaluated by peripheral lymphocytes LC3-II levels and achieved negligible benefits in previously treated patients with metastatic pancreatic cancer (70). The dual role of autophagy in pancreatic cancer makes it difficult to be a therapeutic target alone (54). Therefore, most studies focused on combination therapy for treating pancreatic cancer by inhibiting [e.g., CQ or bafilomycin A_1 (28), DQ661 (71)] or inducing [Quercetin (72), Demethylzeylasteral (73)] autophagy to increase therapeutic efficacy of gemcitabine or other antitumor drugs. As mentioned above, activation of autophagy has led to gemcitabine resistance by inhibiting apoptosis in the treatment of PDAC patients. A recent randomized phase II preoperative study reported resectable pancreatic adenocarcinoma patients treated by gemcitabine and

nab-paclitaxel with HCQ resulted in an evidence of autophagy inhibition and immune activity and achieved greater pathologic tumor response and lower CA199 levels than patients treated by gemcitabine and nab-paclitaxel alone (74). Alternatively, autophagy induction may result in an antitumor efficacy through autophagy-mediated metabolic stress or injury. For instance, combined therapy with Demethylzeylasteral and gemcitabine induces autophagic cell death and demethylzeylasteral could increases the chemosensitivity to gemcitabine in treating pancreatic cancer (73). These results suggest autophagy-related drugs play a complex role in pancreatic cancer chemotherapy. As discussed above, the current research related to autophagy of pancreatic cancer mainly about basic research and clinical application. The focus of scholars has gradually switched from basic research to clinical application. The hot topics in current research have always been the mechanisms of autophagy in tumor onset and progression, the role of autophagy in tumor apoptosis, and autophagy-related drugs in treating pancreatic cancer (especially combined therapy). The emerging topics mainly focused on chemotherapy resistance mediated by autophagy, tumor microenvironment related to autophagy, autophagy-depended EMT, mitophagy, and the role of autophagy in tumor invasion, that may become the main future direction in the field of autophagy and pancreatic cancer.

Our study first conducted a bibliometric analysis related to autophagy of pancreatic cancer, providing an objective and intuitive evaluation of the research features and hotspots and forecasting the emerging trends in that field. Admittedly, this study has some limitations. First, we collected the literature data only from WOSCC database and the related papers from other sources may be neglected. Secondly, the literature language was limited to English, that may result in the source of bias. Thirdly, since the total number of citations depends on various factors (e.g., time of publication, journal, research area), the number of citations may not accurately represent the impact of a paper, and some recent landmark papers may have been omitted.

Conclusion

This study showed research activities were multiplying in the field of autophagy and pancreatic cancer. China and the United States were the most frequent publishers and collaborated closely in this field. *Cancers* published most papers in this field and was very pleasure to accept the related researches. We have also listed the most cited and co-cited papers and authors. Importantly, the mechanisms of autophagy in tumor onset and progression, the role of autophagy in tumor apoptosis, and autophagy-related drugs in treating pancreatic cancer (especially combined therapy) were the research hotspots. The emerging topics were chemotherapy resistance mediated by autophagy, tumor microenvironment related to autophagy, autophagy-depended EMT, mitophagy, and the role of autophagy in tumor invasion. These results undoubtedly provide scholars with new clues and ideas in the field of autophagy and pancreatic cancer.

Data availability statement

The original contributions presented in the study are included in the article/Supplementary Material. Further inquiries can be directed to the corresponding authors.

Author contributions

XLO and CG designed the project. MYS, QL and XLO collected the literature data. MYS, QL and MX contributed to the main part of data analysis and prepared the main manuscript. MX, YJL and YWZ revised the article and made suggestions to improve the article. YJL and YWZ prepared the figures and tables. Final approval of manuscript: All authors.

Funding

This work was supported by the National Natural Science Foundation of China (No. 81802378) and the Gusu Health Talents Training Project (No. GSWS2021058).

Conflict of interest

The authors declare that the research was conducted in the absence of any commercial or financial relationships that could be construed as a potential conflict of interest.

Publisher's note

All claims expressed in this article are solely those of the authors and do not necessarily represent those of their affiliated organizations, or those of the publisher, the editors and the reviewers. Any product that may be evaluated in this article, or claim that may be made by its manufacturer, is not guaranteed or endorsed by the publisher.

Supplementary material

The Supplementary Material for this article can be found online at: https://www.frontiersin.org/articles/10.3389/fonc.2022.987026/full#supplementary-material

References

1. Siegel RL, Miller KD, Fuchs HE, Jemal A. Cancer statistics, 2022. *CA Cancer J Clin* (2022) 72(1):7–33. doi: 10.3322/caac.21708

2. Neoptolemos JP, Kleeff J, Michl P, Costello E, Greenhalf W, et al. Therapeutic developments in pancreatic cancer: current and future perspectives. *Nat Rev Gastroenterol Hepatol* (2018) 15(6):333–48. doi: 10.1038/s41575-018-0005-x

3. Mizrahi JD, Surana R, Valle JW, Shroff RT. Pancreatic cancer. *Lancet* (2020) 395(10242):2008–20. doi: 10.1016/S0140-6736(20)30974-0

4. Cuervo AM. Autophagy: in sickness and in health. *Trends Cell Biol* (2004) 14 (2):70–7. doi: 10.1016/j.tcb.2003.12.002

5. Goswami SK, Das DK. Autophagy in the myocardium: Dying for survival? *Exp Clin Cardiol* (2006) 11(3):183–8.

6. Klionsky DJ. Autophagy: from phenomenology to molecular understanding in less than a decade. *Nat Rev Mol Cell Biol* (2007) 8(11):931–7. doi: 10.1038/nrm2245

7. Levine B. Cell biology: autophagy and cancer. *Nature* (2007) 446(7137):745–7. doi: 10.1038/446745a

8. Levine B, Klionsky DJ. Development by self-digestion: molecular mechanisms and biological functions of autophagy. *Dev Cell* (2004) 6(4):463–77. doi: 10.1016/s1534-5807(04)00099-1

9. Levine B, Kroemer G. Autophagy in the pathogenesis of disease. *Cell* (2008) 132(1):27–42. doi: 10.1016/j.cell.2007.12.018

10. Mizushima N, Yoshimori T, Ohsumi Y. The role of atg proteins in autophagosome formation. *Annu Rev Cell Dev Biol* (2011) 27:107–32. doi: 10.1146/annurev-cellbio-092910-154005

11. Rogov V, Dötsch V, Johansen T, Kirkin V. Interactions between autophagy receptors and ubiquitin-like proteins form the molecular basis for selective autophagy. *Mol Cell* (2014) 53(2):167–78. doi: 10.1016/j.molcel.2013.12.014

12. Shintani T, Klionsky DJ. Autophagy in health and disease: a double-edged sword. *Science* (2004) 306(5698):990–5. doi: 10.1126/science.1099993

13. Mizushima N. A brief history of autophagy from cell biology to physiology and disease. *Nat Cell Biol* (2018) 20(5):521–7. doi: 10.1038/s41556-018-0092-5

14. Marinković M, Šprung M, Buljubašić M, Novak I. Autophagy modulation in cancer: Current knowledge on action and therapy. *Oxid Med Cell Longev* (2018) 2018:8023821. doi: 10.1155/2018/8023821

15. Nakatogawa H. Mechanisms governing autophagosome biogenesis. *Nat Rev Mol Cell Biol* (2020) 21(8):439–58. doi: 10.1038/s41580-020-0241-0

16. Jin M, Liu X, Klionsky DJ. SnapShot: Selective autophagy. *Cell* (2013) 152(1-2):368–8. doi: 10.1016/j.cell.2013.01.004

17. Gatica D, Lahiri V, Klionsky DJ. Cargo recognition and degradation by selective autophagy. *Nat Cell Biol* (2018) 20(3):233–42. doi: 10.1038/s41556-018-0037-z

18. Johansen T, Lamark T. Selective autophagy: ATG8 family proteins, LIR motifs and cargo receptors. *J Mol Biol* (2020) 432(1):80–103. doi: 10.1016/j.jmb.2019.07.016

19. Kirkin V. History of the selective autophagy research: How did it begin and where does it stand today? *J Mol Biol* (2020) 432(1):3–27. doi: 10.1016/j.jmb.2019.05.010

20. Schuck S. Microautophagy - distinct molecular mechanisms handle cargoes of many sizes. *J Cell Sci* (2020) 133(17):jcs246322. doi: 10.1242/jcs.246322

21. Kaushik S, Cuervo AM. The coming of age of chaperone-mediated autophagy. *Nat Rev Mol Cell Biol* (2018) 19(6):365–81. doi: 10.1038/s41580-018-0001-6

22. Fujiwara Y, Wada K, Kabuta T. Lysosomal degradation of intracellular nucleic acids-multiple autophagic pathways. *J Biochem* (2017) 161(2):145–54. doi: 10.1093/jb/mvw085

23. Dikic I, Elazar Z. Mechanism and medical implications of mammalian autophagy. *Nat Rev Mol Cell Biol* (2018) 19(6):349–64. doi: 10.1038/s41580-018-0003-4

24. Levine B, Kroemer G. Biological functions of autophagy genes: A disease perspective. *Cell* (2019) 176(1-2):11–42. doi: 10.1016/j.cell.2018.09.048

25. Mizushima N, Levine B. Autophagy in human diseases. *N Engl J Med* (2020) 383(16):1564–76. doi: 10.1056/NEJMra2022774

26. Mizushima N, Levine B, Cuervo AM, Klionsky DJ. Autophagy fights disease through cellular self-digestion. *Nature* (2008) 451(7182):1069–75. doi: 10.1038/nature06639

27. Hong T, Feng X, Tong W, Xu W. Bibliometric analysis of research on the trends in autophagy. *PeerJ* (2019) 7:e7103. doi: 10.7717/peerj.7103

28. Yang SH, Wang XX, Contino G, Liesa M, Sahin E, et al. Pancreatic cancers require autophagy for tumor growth. *Genes Dev* (2011) 25(7):717–29. doi: 10.1101/gad.2016111

29. Donthu N, Kumar S, Mukherjee D, Pandey N, Lim WM. How to conduct a bibliometric analysis: An overview and guidelines. *J Business Res* (2021) 133:285–96. doi: 10.1016/j.jbusres.2021.04.070

30. Liu Y, Xu Y, Cheng X, Lin Y, Jiang S, et al. Research trends and most influential clinical studies on anti-PD1/PDL1 immunotherapy for cancers: A bibliometric analysis. *Front Immunol* (2022) 13:862084. doi: 10.3389/fimmu.2022.862084

31. Zhang J, Song L, Xu L, Fan Y, Wang T, et al. Knowledge domain and emerging trends in ferroptosis research: A bibliometric and knowledge-map analysis. *Front Oncol* (2021) 11:686726. doi: 10.3389/fonc.2021.686726

32. Shen J, Shen H, Ke L, Chen J, Dang X, et al. Knowledge mapping of immunotherapy for hepatocellular carcinoma: A bibliometric study. *Front Immunol* (2022) 13:815575. doi: 10.3389/fimmu.2022.815575

33. Thompson DF, Walker CK. A descriptive and historical review of bibliometrics with applications to medical sciences. *Pharmacotherapy* (2015) 35 (6):551–9. doi: 10.1002/phar.1586

34. Chen J, Li X, Jia Y, Xia Z, Ye J. Publication trends on mitophagy in the world and China: A 16-year bibliometric analysis. *Front Cell Dev Biol* (2021) 9:793772. doi: 10.3389/fcell.2021.793772

35. Wang K, Herr I. Machine-Learning-Based bibliometric analysis of pancreatic cancer research over the past 25 years. *Front Oncol* (2022) 12:832385. doi: 10.3389/fonc.2022.832385

36. Wu K, Liu Y, Liu L, Peng Y, Pang H, et al. Emerging trends and research foci in tumor microenvironment of pancreatic cancer: A bibliometric and visualized study. *Front Oncol* (2022) 12:810774. doi: 10.3389/fonc.2022.810774

37. Shi H, Chen H, Qian B, Huang Z, Tan P, et al. The 100 most cited articles on pancreatic neuroendocrine tumors from 2000 to 2020: a bibliometric analysis. *Jpn J Clin Oncol* (2022) 52(3):251–9. doi: 10.1093/jjco/hyab205

38. van Eck NJ, Waltman L. Software survey: VOSviewer, a computer program for bibliometric mapping. *Scientometrics* (2010) 84(2):523–38. doi: 10.1007/s11192-009-0146-3

39. Viale A, Pettazzoni P, Lyssiotis CA, Ying HQ, Sanchez N, et al. Oncogene ablation-resistant pancreatic cancer cells depend on mitochondrial function. *Nature* (2014) 514(7524):628–+. doi: 10.1038/nature13611

40. Hou W, Xie YC, Song XX, Sun XF, Lotze MT, et al. Autophagy promotes ferroptosis by degradation of ferritin. *Autophagy* (2016) 12(8):1425–8. doi: 10.1080/15548627.2016.1187366

41. Sousa CM, Biancur DE, Wang XX, Halbrook CJ, Sherman MH, et al. Pancreatic stellate cells support tumour metabolism through autophagic alanine secretion. *Nature* (2016) 536(7617):479–+. doi: 10.1038/nature19084

42. Rosenfeldt MT, O'Prey J, Morton JP, Nixon C, MacKay G, et al. p53 status determines the role of autophagy in pancreatic tumour development. *Nature* (2013) 504(7479):296–+. doi: 10.1038/nature12865

43. Perera R, Stoykova S, Nicolay BN, Ross KN, Fitamant J, et al. Transcriptional control of autophagy-lysosome function drives pancreatic cancer metabolism. *Nature* (2015) 524(7565):361–U251. doi: 10.1038/nature14587

44. Bryant KL, Mancias JD, Kimmelman AC, Der CJ. KRAS: feeding pancreatic cancer proliferation. *Trends Biochem Sci* (2014) 39(2):91–100. doi: 10.1016/j.tibs.2013.12.004

45. Kashatus JA, Nascimento A, Myers LJ, Sher A, Byrne FL, et al. Erk2 phosphorylation of Drp1 promotes mitochondrial fission and MAPK-driven tumor growth. *Mol Cell* (2015) 57(3):537–51. doi: 10.1016/j.molcel.2015.01.002

46. Yang A, Rajeshkumar NV, Wang XX, Yabuuchi S, Alexander BM, et al. Autophagy is critical for pancreatic tumor growth and progression in tumors with p53 alterations. *Cancer Discov* (2014) 4(8):905–13. doi: 10.1158/2159-8290.cd-14-0362

47. Kinsey CG, Camolotto SA, Boespflug AM, Guillen KP, Foth M, et al. Protective autophagy elicited by RAF -> MEK -> ERK inhibition suggests a treatment strategy for RAS-driven cancers. *Nat Med* (2019) 25(4):620–+. doi: 10.1038/s41591-019-0367-9

48. Poillet-Perez L, White E. Role of tumor and host autophagy in cancer metabolism. *Genes Dev* (2019) 33(11-12):610–9. doi: 10.1101/gad.325514.119

49. Ishaq M, Ojha R, Sharma AP, Singh SK. Autophagy in cancer: Recent advances and future directions. *Semin Cancer Biol* (2020) 66:171–81. doi: 10.1016/j.semcancer.2020.03.010

50. Li J, Chen X, Kang R, Zeh H, Klionsky DJ, et al. Regulation and function of autophagy in pancreatic cancer. *Autophagy* (2021) 17(11):3275–96. doi: 10.1080/15548627.2020.1847462

51. Guo JY, Chen HY, Mathew R, Fan J, Strohecker AM, et al. Activated ras requires autophagy to maintain oxidative metabolism and tumorigenesis. *Genes Dev* (2011) 25(5):460–70. doi: 10.1101/gad.2016311

52. Buscail L, Bournet B, Cordelier P. Role of oncogenic KRAS in the diagnosis, prognosis and treatment of pancreatic cancer. *Nat Rev Gastroenterol Hepatol* (2020) 17(3):153–68. doi: 10.1038/s41575-019-0245-4

53. Levy JMM, Towers CG, Thorburn A. Targeting autophagy in cancer. *Nat Rev Cancers* (2017) 17(9):528–42. doi: 10.1038/nrc.2017.53

54. Görgülü K, Diakopoulos KN, Kaya-Aksoy E, Ciecielski KJ, Ai J, et al. The role of autophagy in pancreatic cancer: From bench to the dark bedside. *Cells* (2020) 9(4):1063. doi: 10.3390/cells9041063

55. Di Malta C, Siciliano D, Calcagni A, Monfregola J, Punzi S, et al. Transcriptional activation of RagD GTPase controls mTORC1 and promotes cancer growth. *Science* (2017) 356(6343):1188–92. doi: 10.1126/science.aag2553

56. Yang AN, Herter-Sprie G, Zhang HK, Lin EY, Biancur D, et al. Autophagy sustains pancreatic cancer growth through both cell-autonomous and nonautonomous mechanisms. *Cancer Discov* (2018) 8(3):276–87. doi: 10.1158/2159-8290.cd-17-0952

57. Brown JM, Giaccia AJ. The unique physiology of solid tumors: opportunities (and problems) for cancer therapy. *Cancer Res* (1998) 58(7):1408–16.

58. Rausch V, Liu L, Apel A, Rettig T, Gladkich J, et al. Autophagy mediates survival of pancreatic tumour-initiating cells in a hypoxic microenvironment. *J Pathol* (2012) 227(3):325–35. doi: 10.1002/path.3994

59. Andersen HB, Ialchina R, Pedersen SF, Czaplinska D. Metabolic reprogramming by driver mutation-tumor microenvironment interplay in pancreatic cancer: new therapeutic targets. *Cancer Metastasis Rev* (2021) 40(4):1093–114. doi: 10.1007/s10555-021-10004-4

60. Chen HT, Liu H, Mao MJ, Tan Y, Mo XQ, et al. Crosstalk between autophagy and epithelial-mesenchymal transition and its application in cancer therapy. *Mol Cancers* (2019) 18(1):101. doi: 10.1186/s12943-019-1030-2

61. Zhu HT, Wang DQ, Zhang LR, Xie XD, Wu YY, et al. Upregulation of autophagy by hypoxia-inducible factor-1 alpha promotes EMT and metastatic ability of CD133(+) pancreatic cancer stem-like cells during intermittent hypoxia. *Oncol Rep* (2014) 32(3):935–42. doi: 10.3892/or.2014.3298

62. Wang Y, Xiong H, Liu D, Hill C, Ertay A, et al. Autophagy inhibition specifically promotes epithelial-mesenchymal transition and invasion in RAS-mutated cancer cells. *Autophagy* (2019) 15(5):886–99. doi: 10.1080/15548627.2019.1569912

63. Fuchs Y, Steller H. Programmed cell death in animal development and disease. *Cell* (2011) 147(4):742–58. doi: 10.1016/j.cell.2011.10.033

64. Kang R, Tang D, Schapiro NE, Livesey KM, Farkas A, et al. The receptor for advanced glycation end products (RAGE) sustains autophagy and limits apoptosis, promoting pancreatic tumor cell survival. *Cell Death Differ* (2010) 17(4):666–76. doi: 10.1038/cdd.2009.149

65. Dando I, Pacchiana R, Pozza ED, Cataldo I, Bruno S, et al. UCP2 inhibition induces ROS/Akt/mTOR axis: Role of GAPDH nuclear translocation in genipin/everolimus anticancer synergism. *Free Radic Biol Med* (2017) 113:176–89. doi: 10.1016/j.freeradbiomed.2017.09.022

66. Fukui M, Kang KS, Okada K, Zhu BT. EPA, An omega-3 fatty acid, induces apoptosis in human pancreatic cancer cells: Role of ROS accumulation, caspase-8 activation, and autophagy induction. *J Cell Biochem* (2013) 114(1):192–203. doi: 10.1002/jcb.24354

67. Liang JX, Ning Z, Gao W, Ling J, Wang AM, et al. Ubiquitin–specific protease 22–induced autophagy is correlated with poor prognosis of pancreatic cancer. *Oncol Rep* (2014) 32(6):2726–34. doi: 10.3892/or.2014.3508

68. Zhang X, Schönrogge M, Eichberg J, Wendt EHU, Kumstel S, et al. Blocking autophagy in cancer-associated fibroblasts supports chemotherapy of pancreatic cancer cells. *Front Oncol* (2018) 8:590. doi: 10.3389/fonc.2018.00590

69. Xie Y, Liu J, Kang R, Tang D. Mitophagy in pancreatic cancer. *Front Oncol* (2021) 11:616079. doi: 10.3389/fonc.2021.616079

70. Wolpin BM, Rubinson DA, Wang XX, Chan JA, Cleary JM, et al. Phase II and pharmacodynamic study of autophagy inhibition using hydroxychloroquine in patients with metastatic pancreatic adenocarcinoma. *Oncologist* (2014) 19(6):637–8. doi: 10.1634/theoncologist.2014-0086

71. Rebecca VW, Nicastri MC, McLaughlin N, Fennelly C, McAfee Q, et al. A unified approach to targeting the lysosome's degradative and growth signaling roles. *Cancer Discovery* (2017) 7(11):1266–83. doi: 10.1158/2159-8290.cd-17-0741

72. Lan CY, Chen SY, Kuo CW, Lu CC, Yen GC. Quercetin facilitates cell death and chemosensitivity through RAGE/PI3K/AKT/mTOR axis in human pancreatic cancer cells. *J Food Drug Anal* (2019) 27(4):887–96. doi: 10.1016/j.jfda.2019.07.001

73. Wang F, Tian X, Zhang Z, Ma Y, Xie X, et al. Demethylzeylasteral (ZST93) inhibits cell growth and enhances cell chemosensitivity to gemcitabine in human pancreatic cancer cells *via* apoptotic and autophagic pathways. *Int J Cancers* (2018) 142(9):1938–51. doi: 10.1002/ijc.31211

74. Zeh HJ, Bahary N, Boone BA, Singhi AD, Miller-Ocuin JL, et al. A randomized phase II preoperative study of autophagy inhibition with high-dose hydroxychloroquine and Gemcitabine/Nab-paclitaxel in pancreatic cancer patients. *Clin Cancer Res* (2020) 26(13):3126–34. doi: 10.1158/1078-0432.ccr-19-4042

frontiers | Frontiers in Oncology

TYPE Original Research
PUBLISHED 03 October 2022
DOI 10.3389/fonc.2022.1002592

Check for updates

OPEN ACCESS

EDITED BY
Imayavaramban Lakshmanan,
University of Nebraska Medical Center,
United States

REVIEWED BY
Simone Vicini,
Sapienza University of Rome, Italy
David Reisman,
University of South Carolina,
United States

*CORRESPONDENCE
Xian Liu
liuxian74@hotmail.com

†These authors have contributed equally to this work and share first authorship

SPECIALTY SECTION
This article was submitted to Gastrointestinal Cancers: Colorectal Cancer, a section of the journal Frontiers in Oncology

RECEIVED 25 July 2022
ACCEPTED 09 September 2022
PUBLISHED 03 October 2022

CITATION
Chen W, Ye Y, Zhang D, Mao L, Guo L, Zhang H, Du X, Deng W, Liu B and Liu X (2022) Utility of dual-layer spectral-detector CT imaging for predicting pathological tumor stages and histologic grades of colorectal adenocarcinoma.
Front. Oncol. 12:1002592.
doi: 10.3389/fonc.2022.1002592

COPYRIGHT
© 2022 Chen, Ye, Zhang, Mao, Guo, Zhang, Du, Deng, Liu and Liu. This is an open-access article distributed under the terms of the Creative Commons Attribution License (CC BY). The use, distribution or reproduction in other forums is permitted, provided the original author(s) and the copyright owner(s) are credited and that the original publication in this journal is cited, in accordance with accepted academic practice. No use, distribution or reproduction is permitted which does not comply with these terms.

Utility of dual-layer spectral-detector CT imaging for predicting pathological tumor stages and histologic grades of colorectal adenocarcinoma

Weicui Chen[1†], Yongsong Ye[1†], Daochun Zhang[2], Liting Mao[1], Lei Guo[1], Hanliang Zhang[1], Xiaohua Du[3], Weiwei Deng[4], Bo Liu[1] and Xian Liu[1*]

[1]Department of Radiology, The Second Affiliated Hospital of Guangzhou University of Chinese Medicine, Guangzhou, China, [2]Taizhou Hospital of Zhejiang Province affiliated to Wenzhou Medical University, Taizhou, China, [3]Department of Pathology, The Second Affiliated Hospital of Guangzhou University of Chinese Medicine, Guangzhou, China, [4]Clinical and Technical Support, Philips Healthcare, Shanghai, China

Objectives: To assess the utility of Dual-layer spectral-detector CT (DLCT) in predicting the pT stage and histologic grade for colorectal adenocarcinoma (CRAC).

Methods: A total of 131 patients (mean 62.7 ± 12.9 years; 72 female, 59 male) with pathologically confirmed CRAC (35 pT1-2, 61 pT3, and 35 pT4; 32 high grade and 99 low grade), who received dual-phase DLCT were enrolled in this retrospective study. Normalized iodine concentration (NIC), slope of the spectral HU curve (λHU), and effective atomic number (Eff-Z) were measured for each lesion by two radiologists independently. Intraobserver reliability and interobserver agreement were assessed. The above values were compared between three pT-stage and two histologic-grade groups. The correlation between the pT stages and above values were assessed. Receiver operating characteristic (ROC) curves were calculated to evaluate the diagnostic efficacy.

Results: Intra-class correlation coefficients were ranged from 0.856 to 0.983 for all measurements. Eff-Z [7.21(0.09) vs 7.31 (0.10) vs 7.35 (0.19)], NIC_{AP} [0.11 (0.05) vs 0.15 (0.08) vs 0.15 (0.08)], NIC_{VP} [0.27 (0.06) vs 0.34 (0.11) vs 0.35 (0.12)], λHU_{AP} [1.20 (0.45) vs 1.93 (1.18) vs 2.37 (0.91)], and λHU_{VP} [2.07 (0.68) vs 2.35 (0.62) vs 3.09 (1.07)] were significantly different among pT stage groups (all $P<0.001$) and exhibited a positive correlation with pT stages ($r= 0.503$, 0.455, 0.394, 0.512, 0.376, respectively, all $P<0.001$). Eff-Z [7.37 (0.10) vs 7.28 (0.08)], NIC_{AP}[0.20 (0.10) vs 0.13 (0.08)], NIC_{VP}[0.35 (0.07) vs 0.31 (0.11)], and λHU_{AP} [2.59 (1.11) vs 1.63 (0.75)] in the high-grade group were markedly higher than those in the low-grade group (all $P<0.05$). For discriminating the advanced- from early-stage CARC, the AUCs of Eff-Z, NIC_{AP}, NIC_{VP}, λHU_{AP}, and λHU_{VP} were 0.83, 0.80, 0.79, 0.86, and 0.68, respectively (all $P<0.001$). For

discriminating the high- from low-grade CARC, the AUCs of Eff-Z, NIC_{AP}, NIC_{VP}, and λHU_{AP} were 0.81, 0.81, 0.64, and 0.81, respectively (all $P<0.05$).

Conclusions: The quantitative parameters derived from DLCT may provide new markers for assessing pT stages and histologic differentiation in patients with CRAC.

KEYWORDS

colorectal neoplasms, tomography, X-ray computed, pathology, neoplasm staging

Highlights

- CRAC with higher quantitative parameters was associated with more aggressive characteristics.
- Eff-Z, NIC_{AP}, and λHU_{AP} demonstrated moderate positive correlations with the pT stages (r= 0.503, 0.455, 0.512, respectively).
- Eff-Z, NIC_{AP}, and λHU_{AP} exhibited excellent diagnostic capability for predicting advanced-stage or high-grade CRAC (all AUCs≥0.80).

Introduction

Colorectal cancer (CRC) is the third most common cancer and the second-largest cause of cancer-related death globally. In recent years, the incidence and mortality rates of CRC have shown an increasing trend in people aged under 50 years (1, 2). Tumor-node-metastasis (TNM) stage and histologic grade are significant predictors of survival for patients with CRC (3, 4). Patients with locally advanced colorectal cancer (pathological T3/T4) had a decreased 5-year survival rate compared with those at the early stage (5). In addition, poorly differentiated CRC shows an increased risk of recurrence and a progressively poor prognosis (3, 4).

Abbreviations: AP, Arterial phase; CRC, Colorectal cancer; CRAC, Colorectal adenocarcinoma; CEA, Carcinoembryonic antigen; CA, Carbohydrate antigen; DLCT, Dual-layer spectral-detector computed tomography; EUS, Endoscopic ultrasonography; Eff-Z, Effective atomic number; IC, Iodine concentration; ICC, Intraclass correlation coefficient; IQR, Interquartile range; MDCT, Multi detector row computed tomography; MVD, Micro vessel density; NCCN, National comprehensive cancer network; NIC, Normalized iodine concentration; ROC, Receiver operating characteristic; SD, Standard deviation; TNM, Tumor node metastasis; VP, Venous phase; VMI, Virtual mono-energetic images; λHU, HU curve.

The choice of therapeutic strategies for CRC patients3is highly dependent on the preoperative stage and tumor ocation. According to the National Comprehensive Cancer Network (NCCN) Clinical Practice Guidelines, neoadjuvant chemoradiotherapy followed by surgery is the preferred modality for locally advanced rectal cancer (below the peritoneal reflection) (5). Although neoadjuvant chemotherapy is not currently a standard treatment for colon cancer, it still has many potential advantages for T3/T4 tumors, including tumor downstaging, reduction in high-risk features of resected tumors, and achieving R0 (margin negative) resection (6–9). Additionally, the Asian Guidelines recommend central lymphadenectomy in selected T2 and all T3/T4 colon cancers (10, 11). Therefore, the correct preoperative identification of advanced-stage CRC would be valuable for determining the most appropriate treatment decision, particularly for high-risk patients, such as those with poor histologic differentiation.

Various imaging modalities have been used for evaluating tumor stage qualitatively, including endoscopic ultrasonography (EUS), multi-detector row computed tomography (MDCT), and magnetic resonance imaging (MRI). The assessment of tumor stage with EUS is well validated, but EUS has two significant limitations: over-staging T2 tumors and inapplicability to stenotic tumors (12). MDCT has been recommended by many current guidelines due to its rapid scanning and thin slices. However, the diagnostic performance is unsatisfactory for tumor staging between radiological stage and pathological results, with an overall consistent rate of 60% ~70% (13–15). Compared to MDCT, MRI has excellent soft-tissue resolution (16). Nevertheless, it is still rather difficult to differentiate fibrosis-induced desmoplastic reaction (pathological T2) from fibrosis-containing tumor cells (pathological T3) (17, 18). Furthermore, the accuracy of analysis with the above imaging modalities depend on the experience of the radiologists, lacking objective and quantitative indicators.

Recently, dual-layer spectral-detector CT (DLCT) has been developed as a novel imaging technology for characterizing different materials by their energy-dependent attenuation properties. In contrast to dual-source or fast kV switching techniques, DLCT employs two layers of detectors

to absorb and differentiate high and low energy simultaneously with perfect spatial and temporal alignment. This detector-based spectral separation technique can keep the data intact and improve the accuracy of energy spectrum analysis without altering clinical workflow or increasing radiation exposure (19, 20). Previous studies have suggested that DLCT can enhance the visualization of colorectal lesions, distinguish intra- and extra-luminal iodine or calcium from ingested material, and improve computed tomography (CT) virtual colonography *via* electronic cleansing (21–23). For instance, Obmann MM et al. showed that DLCT could improve polyp conspicuity and reader confidence in a CT colonography phantom, superior to a conventional 120-KVp CT (21). In Wang and colleagues' research, iodine concentration (IC) and normalized IC (NIC) derived from DLCT were verified to be helpful in assessing local colonic wall thickening caused by colon neoplasia (22). Spectral data appear to be promising for evaluating the pathological prognostic factors of gastrointestinal tumors and providing a differential diagnosis. We hypothesized that the poorly differentiated or advanced stages CRC may present with relatively higher quantitative parameters derived from DLCT due to the numerous tumor angiogenesis or increased tumor heterogeneity. However, evidence of DLCT's efficacy in differentiating pathological tumor (pT) stage and histologic grade for CRC is still lacking.

Therefore, this study aimed to explore the correlation between the DLCT quantitative parameters and the prognostic factors in colorectal adenocarcinoma (CRAC), further investigating the diagnostic performance of those parameters in the differentiation of advanced-stage from early-stage and high-grade from low-grade CRAC.

Materials and methods

Participants

In this study, 131 CRAC patients demonstrated by pathology were retrospectively enrolled between May 2021 and March 2022. All patients signed informed consent forms according to our institutional guidelines. The inclusion criteria were the following: (a) the presence of tubular adenocarcinoma in the colon or rectum as supported by pathology; (b) complete pathological information, including pT staging and histologic grade; (c) complete clinical information,including carcinoembryonic antigen (CEA) and carbohydrate antigen (CA) 19-9 levels. The exclusion criteria were the following: (a) received preoperative chemotherapy or radiation therapy; (b) poor image quality with motion or metal artifacts; (c) time interval between CT examination and surgery > 1 week. Figure 1 provides a flowchart showing the patient-selection process.

Dual-layer spectral-detector CT imaging protocol

CT was performed using a DLCT (IQon spectral CT, Philips Healthcare, Best, the Netherlands) with a nonenhanced and dual-phase contrast-enhanced scan in a craniocaudal direction and the supine position. The patients were injected with a nonionic contrast agent (ultrafast 370, Bayer Healthcare, Guangzhou, China) intravenously by a high-pressure injector at a rate of 2.5 mL/s, with a total dose of 80~120ml (1.5 ml/kg of body weight). Arterial phase (AP) images were triggered by bolus-tracking when the attenuation in the abdominal aorta reached 150 HU. Venous phase (VP) images were acquired 40 seconds after the AP. The scan range comprised the upper edge, including the diaphragm, and the lower, surpassing the symphysis pubis.

The scanning parameters were as follows: tube voltage, 120 kV; tube current, automated modulation with Dose Right Index 22; collimation, 0.6 × 64 mm; rotation time, 0.4 seconds; helical pitch, 1.1.

Image generation and quantitative analysis

The conventional images and quantitative spectral analysis were performed using IntelliSpace Portal software (Version 10.0; Philips Healthcare). The spectral-based image data were post-processed to generate different image types: (a) iodine density images (iodine map); (b) effective atomic number (Eff-Z) images; (c) virtual mono-energetic images (VMI). All the images were reconstructed with 1mm slice thickness and 1 mm interval.

Two radiologists with more than ten years of experience in gastrointestinal imaging (YY and LM), to whom the clinical and pathological information were not disclosed, evaluated the data independently according to the following steps. First, the 40keV VMI axial images obtained in the arterial and VP were selected to identify tumor margin. Second, a freehand ROI was manually drawn around the edge of the tumor, avoiding fat, necrosis, vessels, and calcification.

The above measurements were performed on each slice of the entire tumor, and the average values of all the ROIs were calculated to minimize the measurement bias. Third, CT values of lesions at 40 and 100keV, and IC of the lesion, abdominal aorta, or external iliac artery were measured on the corresponding spectral images obtained at arterial and VP. The Eff-Z value of tumors was measured on Eff-Z images (pre-contrast phase).

The NIC of tumor and slope of the spectral HU curve (λHU) were calculated at arterial and VP, respectively, according to the following formulas:

$$NIC = IC_{tumor}/IC_{artery}$$

$$\lambda HU = (\text{CT value 40keV} - \text{CT value 100keV})/60.$$

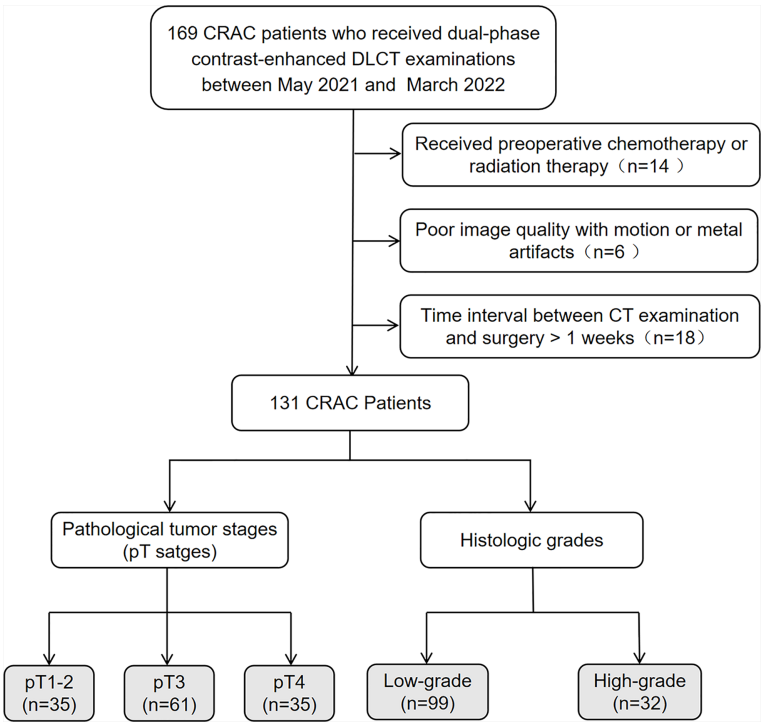

FIGURE 1
Flowchart of patient selection. CRAC, colorectal adenocarcinoma; DLCT, dual-layer spectral-detector CT.

All original measured data were tested for consistency. The final results were expressed as the average values of the obtained data.

Histopathologic analyses

All patients were operated upon within one week after the DLCT examination. The tumor specimens were further assessed with both HE and immunohistochemical staining by a gastrointestinal pathologist with 12 years of experience in the field (XHD). The evaluation of TNM stages and pathological factors was based on the eighth edition of the American Joint Committee on Cancer Staging system. Tumour grade was classified as grade 1 (well differentiated, greater than 95% gland formation), grade 2 (moderately differentiated, 50% ~95% gland formation), or grade 3 (poorly differentiated, less than 50% gland formation). According to two tiered grading system of WHO criteria, the tumors were classified as either low- (G1 and G2) or high-grade CRAC (G3).

Statistical analysis

Intraobserver reliability and interobserver agreement were determined using the intra-class correlation coefficient (ICC). ICCs are considered to provide adequate reliability if they are higher than 0.75. The normal distribution of quantitative variables was assessed using the Kolmogorov-Smirnov test. Continuous variables are presented as mean ± standard deviation (SD) or median with interquartile range (IQR), as appropriate. The Chi-square test was used to evaluate the enumeration data. The Student's t-test, one-way analysis of variance (ANOVA), Mann-Whitney U test, or Kruskal-Wallis ANOVA test was used to compare the quantitative parameters between two groups by histologic grades (high and low) and three groups by pT stages (pT1-2, pT3, and pT4). The Bonferroni method was used to correct the *p*-value for multiple comparisons. Spearman correlation analysis was performed to assess the correlation between the pT stages and DLCT parameters quantitatively: weakly correlated: 0~0.40, moderately correlated: 0.41~0.75, strongly correlated: 0.76~1.00. A receiver operating characteristic (ROC) curve was generated to evaluate the diagnostic efficacy of each parameter for differentiating advanced- (pT3/4) from early-stage (pT1/2) and high- from low-grade CRAC. A comparison of ROC curves was applied to test the significance of differences between the area under ROC curves (AUCs).

Statistical analyses were performed using SPSS Statistics 22.0 and MedCalc12.7.2 software. All tests were two sided, and *p*-values lower than 0.05 were considered significant.

Results

Comparison of patients' clinical-pathological characteristics between different pT stages and histologic grades

One hundred and thirty-one patients (male 59, female 72; median age 62.7 ± 12.9 years, range 25~91 years) without distant metastasis were enrolled in the study. According to the postoperative pathological results, the distribution of primary tumor (pT stage) was: pT1-2 (n=35), pT3 (n=61), and pT4 (n=35). Due to inaccurate assessment of preoperative tumor staging, the patients with pT3~4 rectal adenocarcinoma received surgery directly instead of preoperative chemotherapy or radiation therapy. Thirty-two patients had low-grade tumors, and 99 patients had high-grade tumors.

There was a significant difference in the aspect of pN stage among different pT stages and histological grades (all $P<0.05$). CA19-9 and CEA levels markedly varied among different pT stages (all $P<0.05$).

The patients' clinical-pathological characteristics between different pT stages and histologic grades are shown in Table 1.

Intraobserver reliability and interobserver agreement

The intraobserver reliability and interobserver agreement of DLCT parameter measurement were excellent. The range of 95%

TABLE 1 Clinical pathological characteristics on 131 CRAC.

Variables	All patients	pT Stages			*P* Value	Histologic Grade		*P* Value
		pT1-2	pT3	pT4		High	Low	
No. of patients	131	35	61	35		32	99	
Age (years), mean ± SD	62.7 ± 12.9	61.7 ± 10.4	61.7 ± 14.0	65.2 ± 130	0.388	60.6 ± 11.7	63.3 ± 13.2	0.306
Gender, No. (%)					0.758			0.061
Female	55.0 (72/131)	51.4 (18/35)	54.1 (33/61)	60.0 (21/35)		40.6 (13/32)	59.6 (59/99)	
Male	45.0 (59/131)	48.6 (17/35)	45.9 (28/61)	40.0 (14/35)		59.4 (19/32)	40.4 (40/99)	
CA19-9 level, No. (%)					<0.001			0.078
Normal	45.0(59/131)	80.0 (28/35)	32.8 (20/61)	31.4 (11/35)		25.0 (8/32)	42.4 (42/99)	
Abnormal	55.0 (72/131)	20.0 (7/35)	67.2 (41/61)	68.6 (24/35)		75.0 (24/32)	57.6 (57/99)	
CEA level, No. (%)					<0.001			0.467
Normal	42.0 (55/131)	88.6 (31/35)	29.51 (18/61)	17.1 (6/35)		31.3 (10/32)	38.4 (38/99)	
Abnormal	58.0 (76/131)	11.4 (4/35)	70.5 (43/61)	82.9 (29/35)		68.8 (22/32)	61.6 (61/99)	
Tumor location, No. (%)					0.037			0.247
Right colon	21.4 (28/131)	14.3 (5/35)	19.7 (12/61)	31.4 (11/35)		25.0 (8/32)	20.2 (20/99)	
Left colon	41.2 (54/131)	28.6 (10/35)	45.9 (28/61)	45.7 (16/35)		50.0 (16/32)	38.4 (38/99)	
Rectum	37.4 (49/131)	57.1 (20/35)	34.4 (21/61)	22.9 (8/35)		25.0 (8/32)	41.4 (41/99)	
Upper Rectum	18.3 (24/131)	34.3 (12/35)	13.1 (8/61)	11.4 (4/35)		9.4 (3/32)	20.2 (20/99)	
Middle Rectum	11.5 (15/131)	20.0 (7/35)	11.5 (7/61)	2.9 (1/35)		6.3 (2/32)	18.2 (18/99)	
Low Rectum	7.6 (10/131)	8.6 (3/35)	9.8 (6/61)	8.6 (3/35)		9.4 (3/32)	3.0 (3/99)	
pN stage, No. (%)					0.001			<0.001
pN0	49.6 (65/131)	65.7 (23/35)	52.5 (32/61)	28.6 (10/35)		12.5 (4/32)	53.5 (53/99)	
pN1	25.2 (33/131)	31.4 (11/35)	21.3 (13/61)	25.7 (9/35)		37.5 (12/32)	19.2 (19/99)	
pN2	25.2 (33/131)	52.9 (1/35)	26.2 (16/61)	45.7 (16/35)		50.0 (16/32)	27.3 (27/99)	
pT stage, No. (%)					/			0.686
pT1-2	26.7 (35/131)	/	/	/		12.5 (4/32)	19.2 (19/99)	
pT3	46.6 (61/31)	/	/	/		56.3 (18/32)	52.5 (52/99)	
pT4	26.7 (35/131)	/	/	/		31.3 (10/32)	28.3 (28/99)	
Histologic grade, No. (%)					0.238			/
High	24.4 (32/131)	17.1 (6/35)	31.2 (19/61)	20.0 (7/35)		/	/	
Low	75.6 (99/131)	82.9 (29/35)	68.9 (42/61)	80.0 (28/35)		/	/	

CRAC, colorectal adenocarcinoma; pT, pathological tumor; CEA, carcino-embryonicantigen; CA19-9, carbohydrate antigen 19-9; pN, pathological lymph node.
Staging of tumors was in accordance with American Joint Committee on Cancer TNM classification;grading of tumors was based on the WHO grading criteria.
Normally distributed data were analyzed by Student's t test or ANOVA, and were expressed as means ± standard deviations.

confidence interval (CI) for intraobserver reliability were 0.877 to 0.992. The range of 95% CI for intreobserver agreement were 0.739 to 0.983 (Table 2).

Comparison of DLCT parameter values between different pT stages and histologic grades

Based on the Kolmogorov-Smirnov test, all of the quantitative parameters showed non-normal distributions (all $P<0.05$).The Eff-Z values of tumors at the pT1-2, pT3, and pT4 stages were significantly different [7.21(0.09) vs 7.31 (0.10) vs 7.35 (0.19), $P<0.001$, respectively]. The NIC_{AP} and λHU_{AP} values of the tumors were significantly different among pT1-2, pT3, and pT4 stages [0.11 (0.05) vs 0.15 (0.08) vs 0.15 (0.08); 1.20 (0.45) vs 1.93 (1.18) vs 2.37 (0.91), $P<0.001$, respectively]. The NIC_{VP} and λHU_{VP} values of the tumors were significantly different among pT1-2, pT3, and pT4 stages [0.27 (0.06) vs 0.34 (0.11) vs 0.35 (0.12); 2.07 (0.68) vs 2.35 (0.62) vs 3.09 (1.07), $P<0.001$, respectively]. Tumors at the pT4 stage demonstrated higher Eff-Z, NIC_{AP}, λHU_{AP}, and NIC_{VP} values than pT1-2 tumors, and higher λHU_{VP} values than pT1-2 and pT3 tumors (Table 3, Table S1, Figures 2–4).

The Eff-Z, NIC_{AP}, λHU_{AP} and NIC_{VP} values were significantly different between high- and low-grade CRAC [7.37 (0.10) vs 7.28 (0.08), $P<0.001$; 0.20 (0.10) vs 0.13 (0.08), $P<0.001$; 2.59 (1.11) vs 1.63 (0.75), $P<0.001$; 0.35 (0.07) vs 0.31 (0.11), $P=0.015$]. High- and low-grade tumors showed no difference in λHU_{VP} values [2.40 (0.82) vs 2.35 (0.84), $P=0.902$] (Table 3, Figures 2–4).

Correlation between DLCT parameters and pT stages

The Eff-Z, NIC_{AP}, and λHU_{AP} values demonstrated a moderate positive correlation with the pT stages ($r=0.503$, $P<0.001$; $r=0.455$, $P<0.001$; $r=0.512$, $P<0.001$, respectively). The NIC_{VP} and λHU_{VP} values showed a weak correlation with the pT stages ($r=0.394$, $P<0.001$; $r=0.376$, $P<0.001$, respectively) (Table 3).

TABLE 2 Intraobserver reliabilty and interobserver agreement of DLCT parameter measurement.

Parameter	Intraobserver Reliability (ICC, 95%CI)	Interobserver Agreement (ICC, 95%CI)
Eff-Z	0.921 (0.885~0.952)	0.969 (0.937~0.985)
AP		
CT40keV (HU)	0.962 (0.942~0.976)	0.912 (0.826~0.957)
CT100keV (HU)	0.983 (0.978~0.987)	0.890 (0.771~0.947)
IC_{tumor} (ug/ml)	0.980 (0.952~0.992)	0.856 (0.739~0.923)
IC_{artery} (ug/ml)	0.975 (0.937~0.990)	0.934 (0.876~0.956)
VP		
CT40keV (HU)	0.971 (0.929~0.988)	0.954 (0.905~0.978)
CT100keV (HU)	0.948 (0.877~0.980)	0.900 (0.791~0.952)
IC_{tumor} (ug/ml)	0.959 (0.900~0.984)	0.923 (0.850~0.960)
IC_{artery} (ug/ml)	0.975 (0.947~0.992)	0.966 (0.934~0.983)

DLCT, dual-layer spectral-detector CT; ICC, intra-class correlation coefficients; CI, confidence interval; Eff-Z, effective atomic number; AP, arterial phase; IC, iodine concentration; VP, venous phase.

TABLE 3 Comparison DLCT parameter values between different pT stages and histologic grades, and the correlations with pT stages.

Parameter	pT Stages			*P* Value	*r*	*P* Value	Histologic Grade		*P* Value
	pT1-2 (n = 35)	pT3 (n = 61)	pT4 (n = 35)				High (n = 32)	Low (n = 99)	
Eff-Z	7.21 (0.09)	7.31 (0.10)	7.35 (0.19)	<0.001	0.503	<0.001	7.37 (0.10)	7.28 (0.08)	<0.001
NIC_{AP}	0.11 (0.05)	0.15 (0.08)	0.15 (0.08)	<0.001	0.455	<0.001	0.20 (0.10)	0.13 (0.08)	<0.001
λHU_{AP}	1.20 (0.45)	1.93 (1.18)	2.37 (0.91)	<0.001	0.512	<0.001	2.59 (1.11)	1.63 (0.75)	<0.001
NIC_{VP}	0.27 (0.06)	0.34 (0.11)	0.35 (0.12)	<0.001	0.394	<0.001	0.35 (0.07)	0.31 (0.11)	0.015
λHU_{VP}	2.07 (0.68)	2.35 (0.62)	3.09 (1.07)	<0.001	0.376	<0.001	2.40 (0.82)	2.35 (0.84)	0.902

DLCT, dual-layer spectral-detector CT; pT, pathological stage; Eff-Z, effective atomic number; NIC, normalized iodine concentration; AP, arterial phase; VP, venous phase; λHU, slope of the spectral HU curve.
Non-normally distributed data were analyzed by Mann-Whitney U test or Kruskal-Wallis H test, and were expressed as medians (interquartile ranges).

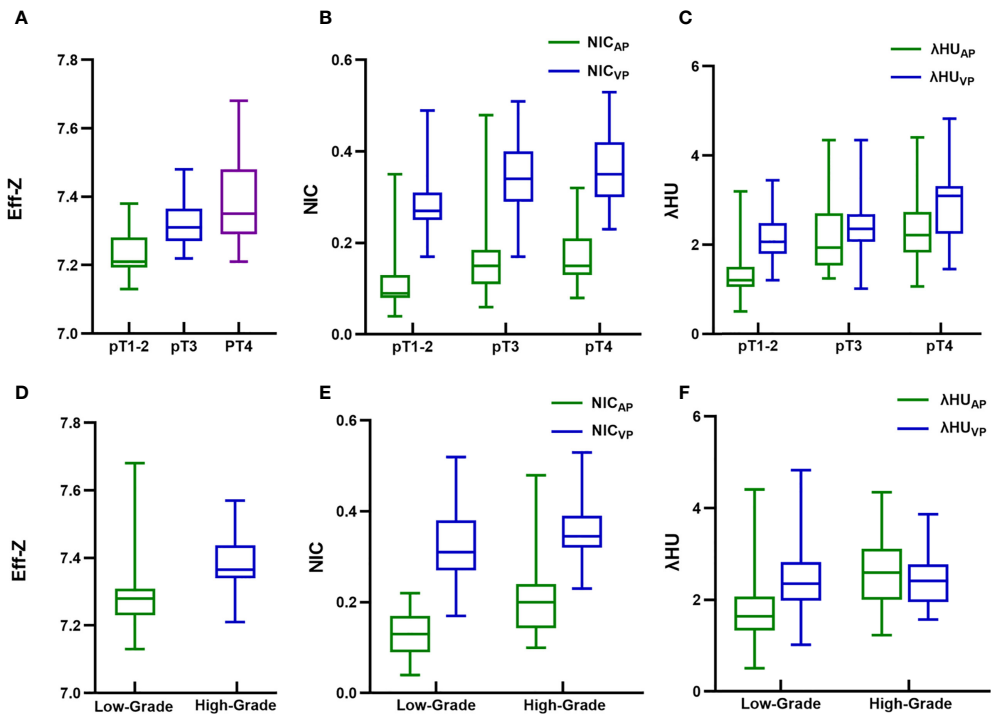

FIGURE 2
Box and whisker plots of **(A)** effective atomic number (Eff-Z) in pre-contrast phase, **(B)** normalized iodine concentration (NIC) in arterial and venous phase (VP), **(C)** spectral HU curve (λHU) in arterial and VP of different pathological tumor (pT) stage colorectal adenocarcinoma (CRAC); **(D)** Eff-Z in pre-contrast phase, **(E)** NIC in arterial and VP, **(F)** λHU in arterial and VP of high- and low-grade CRAC. Boxes show the upper and lower quartiles, and horizontal lines within boxes indicate median values. Whiskers represent the 95th and fifth percentiles. High- and low-grade CRAC showed no difference in λHU from VP (P>0.05), whereas differences in the rest of quantitative parameter values were observed between different pT stages and histologic grades (all P<0.05).

Diagnostic performance of Eff-Z, NIC$_{AP}$, λHU$_{AP}$, NIC$_{VP}$, and λHU$_{VP}$ values for discriminating advanced- from early-stage CRAC

For discriminating the advanced- from early-stage CRAC, the AUCs of the Eff-Z, NIC$_{AP}$, and λHU$_{AP}$ values were 0.826 [(95% CI: 0.750~0.887), P<0.001], 0.803 [(95% CI: 0.724~0.867), P<0.001], and 0.859 [(95% CI: 0.787~0.913), P<0.001], respectively. The AUCs of NIC$_{VP}$, and λHU$_{VP}$ were 0.793 [(95% CI: 0.713~0.859), P<0.001] and 0.682 [(95% CI: 0.595~0.760), P<0.001], respectively. Further pairwise comparisons showed that the AUCs of the Eff-Z, λHU$_{AP}$, and NIC$_{VP}$ values were significantly higher than that of λHU$_{VP}$ (all P<0.05) (Table 4, Table S2, Figure 5A).

According to the AUC, the cut-off values of the mean Eff-Z, NIC$_{AP}$, and λHU$_{AP}$ were 7.26 (with 81.25% sensitivity, 74.29% specificity), 0.10 (with 89.58% sensitivity, 60.00% specificity), and 1.50 (83.33% sensitivity, 77.14% specificity), respectively. The cut-off value for the NIC$_{VP}$ and λHU$_{VP}$ were 0.32 (with 60.42% sensitivity, 85.71% specificity) and 2.10 (with 75.00% sensitivity, 54.29% specificity) (Table 4, Figure 5A).

Diagnostic performance of Eff-Z, NIC$_{AP}$, λHU$_{AP}$, and NIC$_{VP}$ values for discriminating high- from low-grade CRAC

For discriminating high- from low-grade CRAC, the AUCs of the Eff-Z, NIC$_{AP}$, λHU$_{AP}$ and NIC$_{VP}$ were 0.812 [(95% CI: 0.735~0.875), P<0.001], 0.805 [(95% CI: 0.726~0.869), P<0.001], 0.815 [(95% CI: 0.738~0.877), P<0.001], and 0.643 [(95% CI: 0.555~0.725), P<0.001], respectively. Further pairwise comparisons showed that the AUCs of the Eff-Z, λHU$_{AP}$, and NIC$_{AP}$ values were significantly higher than that of NIC$_{VP}$ (all P<0.01) (Table 5, Table S3, Figure 5B).

The cut-off values of the mean Eff-Z, NIC$_{AP}$, λHU$_{AP}$ and NIC$_{VP}$ were 7.31 (with 90.62% sensitivity, 76.77% specificity), 0.16 (with 68.75% sensitivity, 74.75% specificity), 1.86 (93.75%

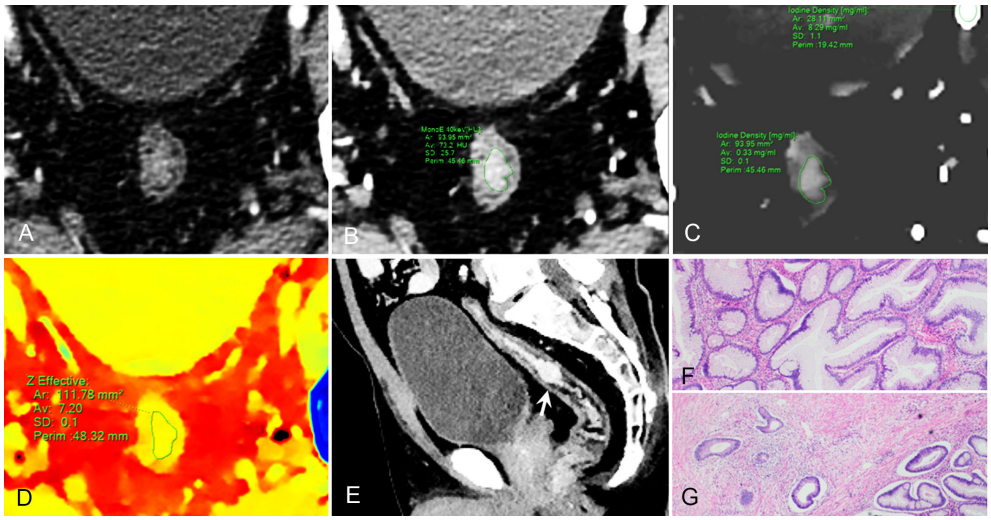

FIGURE 3
59-year-old man with pathological tumor stage 2 and grade 1 rectal adenocarcinoma, who underwent preoperative dual-layer spectral-detector CT. **(A)** Axial arterial phase (AP) contrast-enhanced image shows irregular wall thickening of the rectum. **(B)** 40 keV virtual mono-energetic image (VMI) in AP shows apparent contrast enhancement between the lesion and surrounding tissue. **(C)** Iodine map in AP shows the lesion with an iodine concentration (IC) value of 0.33 mg/ml; the external iliac artery at the same slice with an IC value of 8.29 mg/ml; a normalized iodine concentration(NIC) value of lesion was 0.04 in AP. **(D)** Effective atomic number (Eff-Z) images in the pre-contrast phase shows the colorful lesion with an Eff-Z value of 7.20. **(E)** Sagittal reconstruction 40 keV VMI shows the tumor located in upper rectum (arrow). **(F)** H E staining demonstrates the tumor is mostly composed of gland-forming elements (×40). **(G)** The tumor cells invade the muscularis propria (×40).

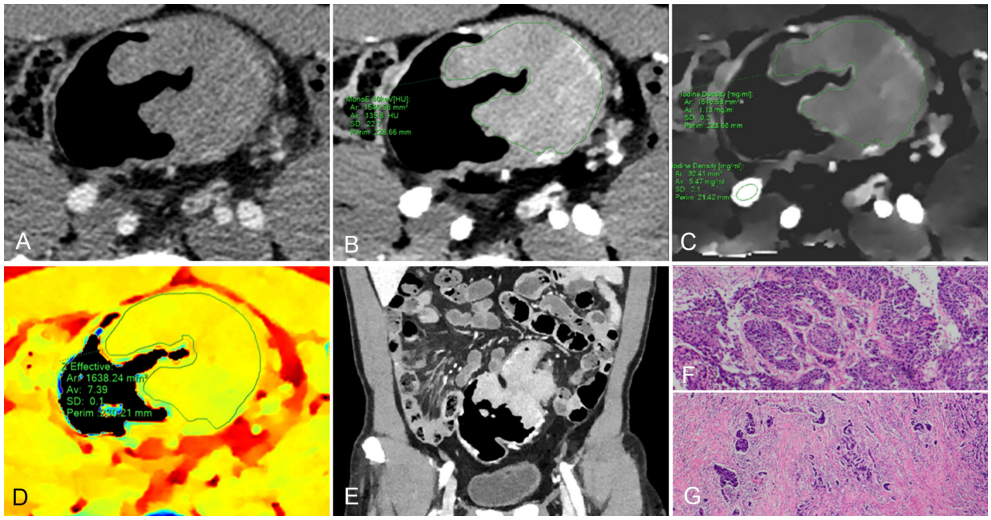

FIGURE 4
61-year-old man with pathological tumor stage 3 and grade 3 colon adenocarcinoma, who underwent preoperative dual-layer spectral-detector CT. **(A)** Axial arterial phase (AP) contrast-enhanced image shows an irregular mass of the descending colon. **(B)** 40 keV virtual mono-energetic image (VMI) in AP shows apparent contrast enhancement between the lesion and surrounding tissue. **(C)** Iodine map in AP shows the lesion with an iodine concentration (IC) value of 1.13 mg/ml; the external iliac artery at the same slice with an IC value of 5.47 mg/ml; a normalized iodine concentration (NIC) value of lesion was 0.21 in AP. **(D)** Effective atomic number (Eff-Z) images in the pre-contrast phase shows the colorful lesion with an Eff-Z value of 7.39. **(E)** Coronal reconstruction 40 keV VMI shows the tumor located in descending colon. **(F)** H E staining demonstrates the tumor with a minor glandular component (×40). **(G)** The tumor cells invade beyond the muscularis propria (×40).

TABLE 4 Performance of DLCT parameters in differentiating advanced- from early-stage CRAC.

Parameter	AUC	Cutoff	Sensitivity (%)	Specificity (%)	Youden index J	95% CI	*P* Value
Eff-Z	0.826	7.26	81.25	74.29	0.555	0.750~0.887	<0.001
NIC_{AP}	0.803	0.10	89.58	60.00	0.496	0.724~0.867	<0.001
λHU_{AP}	0.859	1.50	83.33	77.14	0.605	0.787~0.913	<0.001
NIC_{VP}	0.793	0.32	60.42	85.71	0.461	0.713~0.859	<0.001
λHU_{VP}	0.682	2.10	75.00	54.29	0.293	0.595~0.760	<0.001

CRAC, colorectal adenocarcinoma; AUC, area under curve; CI, confidence interval; Eff-Z, effective atomic number; NIC, normalized iodine concentration; AP, arterial phase; VP, venous phase; λHU, slope of the spectral HU curve.

sensitivity, 64.65% specificity), and 0.31 (with 78.12% sensitivity, 52.53% specificity), respectively (Table 5, Figure 5B).

Discussion

Pathological tumor stage and histologic differentiation are the most critical factors for CRAC prognosis (3, 24) and may wanrrant different management approaches (6–11). In this study, we evaluated and compared the relationship between quantitative parameters derived from DLCT and pathological tumor stages and histologic differentiation in patients with CRAC. We found that CRAC with higher quantitative parameters (Eff-Z, NIC_{AP}, λHU_{AP}, NIC_{VP}) was associated with more aggressive characteristics (advanced pT stage, poor histologic differentiation), and exhibited a positive correlation with pT stage. Eff-Z, NIC_{AP}, and λHU_{AP} values could successfully distinguish advanced- from early-stage tumors and high- from low-grade CRAC.

To derive the imaging measures, the ROIs were created on each CT slice of the entire tumor. This approach may well reflect the characteristic and heterogeneity of the CRAC. Besides, considering that the physiological distributions of IC in individuals would affect the iodine perfusion (25, 26), we compared the gender and age in the two groups (pT-stage and histologic-grade subgroups) to reduce the bias caused by the two factors. We found no significant differences regarding the gender and age in these two groups.

We observed that the quantitative parameters (Eff-Z in pre-contrast phase, λHU_{AP}) increased significantly in the advanced pT stage or high-grade CRAC. Eff-Z, which describes the nature of material or compound interactions with radiation (27, 28), can discriminate and reflect the characteristics of material more accurately than attenuation in HU (29). The Eff-Z of cancerous tissue differs from healthy tissue because of the different trace element concentrations in tumor tissues (30). In most tumors, Eff-Z is consistently higher than healthy tissue, as verified by many studies (31, 32). Additionally, Eff-Z can reflect material heterogeneity. λHU describes the attenuation changes of different materials as a function of the energy spectrum of x-ray photons, which is associated with material composition, density, and interactions between photon energies and material

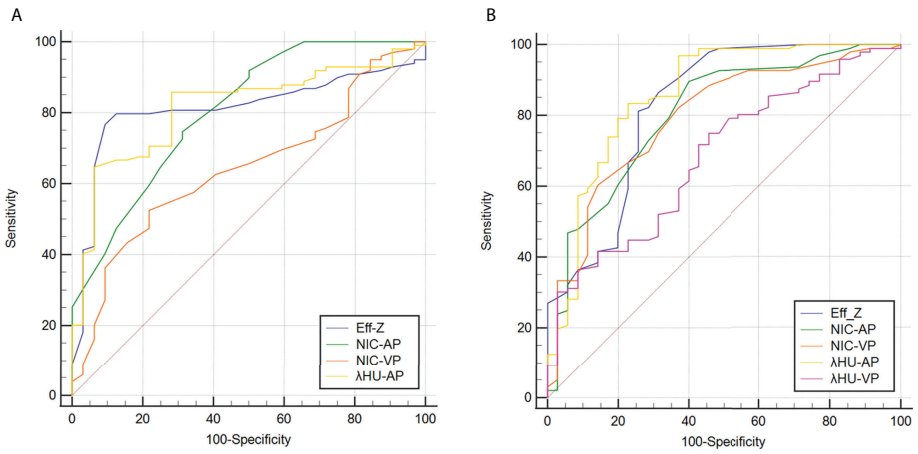

FIGURE 5
Receiver operating characteristic curves for predicting high-grade **(A)** and advanced-stage and **(B)** CRAC. Details of the area under the curves of each metric are shown in the results section. CRAC, colorectal adenocarcinoma.

TABLE 5 Performance of DLCT parameters in differentiating high- from low-grade CRAC.

Parameter	AUC	Cutoff	Sensitivity (%)	Specificity (%)	Youden index J	95% CI	*P* Value
Eff-Z	0.812	7.31	90.62	76.77	0.674	0.735~0.875	<0.001
NIC_{AP}	0.805	0.16	68.75	74.75	0.435	0.726~0.869	<0.001
λHU_{AP}	0.815	1.86	93.75	64.65	0.584	0.738~0.877	<0.001
NIC_{VP}	0.643	0.31	78.12	52.53	0.307	0.555~0.725	0.0067

CRAC, colorectal adenocarcinoma; AUC, area under curve; CI, confidence interval; Eff-Z, effective atomic number; NIC, normalized iodine concentration; AP, arterial phase; VP, venous phase; λHU, slope of the spectral HU curve.

(33, 34). We hypothesized the higher Eff-Z in the plain phase and λHU_{AP} values in aggressive CRAC (e.g., advanced T stage, high grade) may be attributed to increased tumor heterogeneity, where tumor tissue exhibited nuclear pleomorphism and abnormal elemental composition. The spectral curve of the lesion was also affected by the iodinated contrast agent. Higher iodine intake within the tumor leads to a steeper spectrum HU curve slope due to more tissue attenuation of X-rays (35). Besides, it is worth noting that Eff-Z value in the tumor tissue is changed by contrast material after enhancement. The addition to a tumor with a high atomic number element, such as iodine, shifts the linear attenuation coefficients and effective atomic number of that tumor significantly.

Many studies have suggested that IC can reflect blood volume, microvascular permeability, and tissue neovascularization (36–39). In this study, to minimize technical or physiological variabilities, such as injection rate and dose of contrast agent, and individual cardiac output differences, we used NIC values to assess the lesion iodine content. We found that both NIC in AP and VP are significantly higher in the advanced pT stage or high-grade CRAC. According to the acquisition time of our abdomen CT, the AP was triggered by bolus-tracking when the attenuation in the abdominal aorta reached 150 HU, and the VP followed at intervals of 40 seconds. Hence, the AP NIC mainly reflects the degree of neovascularization in CRAC, while the VP NIC represent the microcirculation of the tumor and distribution of contrast media within interstitial spaces (40). Neovascularization is of utmost importance for tumor growth and invasion. Studies have demonstrated an increased microvessel density (MVD) in tumors with poor histologic differentiation and poor prognoses (41, 42). MVD is a surrogate marker that reflects tumor angiogenesis and has a significant positive correlation with IC (43). Advanced-stage or high-grade CRAC presents increased angiogenesis and abnormal microvascular permeability, leading to higher NIC values. Our results agreed with those of Cao et al. and Gong et al., who used rapid kV switching dual-energy CT (Discovery 750 HD, GE) to evaluate the colon cancer differentiation degree (44, 45). They showed that the IC and NIC of high-grade colon cancer were significantly higher than that of low-grade colon cancer; Therefore, quantitative parameters of iodine concentration can provide helpful information in distinguishing low- from high-grade colorectal cancer.

We found that the quantitative parameters (Eff-Z in pre-contrast phase, both NIC and λHU in AP) manifested good diagnostic performances in diagnosing pathological tumor stage and histologic grades in CRAC (all the AUCs≥0.80). Notably, we found that the most valuable quantitative parameters were obtained in the AP rather than the VP, in accordance with Li R and colleagues' results, who found that the NIC value in the AP gave a relatively high diagnostic performance in discriminating poorly differentiated from well-differentiated gastric cancers (46). Previous studies have shown that the AP IC has the strongest correlations with quantitative volume perfusion CT parameters (47), potentially explaining why the AP parameters had the highest discriminating power for differentiating the above pathological factors in CRAC. Conversely, the ability of some metrics to discriminate tumor stages or histologic grades of CRAC was unsatisfactory, such as λHU_{VP} and NIC_{VP}, with an AUC of 0.68 and 0.64, respectively. The following two reasons might interpret the results. First, these quantitative parameters obtained in the VP can't reflect the tumour's blood supply or heterogeneity accurately. Second, the sample size was relatively small. Expanding the sample size may improve the diagnostic performance of the two parameters.

The present study had some limitations. First, ROI included the entire tumour, but it may not completely match the microscopic histological sample. Second, other rare histologic types were not included, such as mucinous adenocarcinoma, signet ring cell and undifferentiated carcinomas. Future research with more cases of different types is essential to draw broader conclusion. Third, this study was a retrospective and single-center design; hence, we need to perform further prospective clinical trials to validate our results. Finally, because the sample size was imbalanced, the research will be expanded in the future to confirm the accuracy of the results.

In conclusion, DLCT is a potential modality for performing non-invasive evaluations of pT stages and histologic grades in CRAC preoperatively. CRAC with higher values of Eff-Z, NIC_{AP}, λHU_{AP}, and $NIC_{VP,}$ are associated with more aggressive characteristics and worse prognosis. Eff-Z, NIC_{AP}, and λHU_{AP} exhibited excellent diagnostic capability for predicting

advanced-stage or high-grade CRAC (all the AUCs≥0.80). The findings indicate that DLCT quantitative parameters may lead to better guidance of surgical and oncological treatment planning for patients with CRAC.

Data availability statement

The original contributions presented in the study are included in the article/Supplementary Material. Further inquiries can be directed to the corresponding author.

Ethics statement

The studies involving human participants were reviewed and approved by the institutional review board of the second affiliated hospital of guangzhou university of chinese medicine. The patients/participants provided their written informed consent to participate in this study. Written informed consent was obtained from the individual(s) for the publication of any potentially identifiable images or data included in this article.

Author contributions

WC: Data curation, Writing- Original draft preparation. YY: Writing - Review & Editing. DZ: Data curation, Writing- Original draft preparation. LM: Data curation, Writing- Original draft preparation. LG: Writing- Original draft preparation, Formal analysis. HZ: Data curation, Funding acquisition. XD: Investigation, Resources. WD: Data Curation. BL: Supervision. XL: Conceptualization, Methodology, Writing -Review & Editing. All authors contributed to the article and approved the submitted version.

Funding

This work was supported by the National Nature Science of Foundation of China[Grant No.82202259] and Youth Talent Project of The Second Affiliated Hospital of Guangzhou University of Chinese Medicine [Grant No. ZY2022YL05].

Conflict of interest

The authors declare that the research was conducted in the absence of any commercial or financial relationships that could be construed as a potential conflict of interest.

Publisher's note

All claims expressed in this article are solely those of the authors and do not necessarily represent those of their affiliated organizations, or those of the publisher, the editors and the reviewers. Any product that may be evaluated in this article, or claim that may be made by its manufacturer, is not guaranteed or endorsed by the publisher.

Supplementary material

The Supplementary Material for this article can be found online at: https://www.frontiersin.org/articles/10.3389/fonc.2022.1002592/full#supplementary-material

References

1. Siegel RL, Miller KD, Jemal A. Cancer statistics, 2022. *CA Cancer J Clin* (2022) 72(1):7–33. doi: 10.3322/caac.21708

2. Ferlay J, Colombet M, Soerjomataram I, Mathers C, Parkin DM, Piñeros M, et al. Estimating the global cancer incidence and mortality in 2018: GLOBOCAN sources and methods. *Int J Cancer* (2019) 144(8):1941–53. doi: 10.1002/ijc.31937

3. Marks KM, West NP, Morris E, Quirke P. Clinicopathological, genomic and immunological factors in colorectal cancer prognosis. *Br J Surg* (2018) 105(2):e99-e109. doi: 10.1002/bjs.10756

4. Compton CC. Colorectal carcinoma: diagnostic, prognostic, and molecular features. *Mod Pathol* (2003) 16(4):376–88. doi: 10.1097/01.MP.0000062859.46942.93

5. Benson AB, Venook AP, Al-Hawary MM, Cederquist L, Chen YJ, Ciombor KK, et al. NCCN guidelines insights: Colon cancer, version 2. *2018 J Natl Compr Canc Netw* (2018) 16(4):359–69. doi: 10.6004/jnccn.2018.0021

6. Kim S, Huh JW, Lee WY, Yun SH, Kim HC, Cho YB, et al. Oncologic outcomes of pathologic T4 and T3 colon cancer patients diagnosed with clinical T4 stage disease using preoperative computed tomography scan. *Surg Oncol* (2022) 41:101749. doi: 10.1016/j.suronc.2022.101749

7. Foxtrot Collaborative G. Feasibility of preoperative chemotherapy for locally advanced, operable colon cancer: the pilot phase of a randomised controlled trial. *Lancet Oncol* (2012) 13(11):1152–60. doi: 10.1016/S1470-2045(12)70348-0

8. Cheong CK, Nistala KRY, Ng CH, Syn N, Chang HSY, Sundar R, et al. Neoadjuvant therapy in locally advanced colon cancer: a meta-analysis and systematic review. *J Gastrointest Oncol* (2020) 11(5):847–57. doi: 10.21037/jgo-20-220

9. de Gooyer JM, Verstegen MG, 't Lam-Boer J, Radema SA, Verhoeven RHA, Verhoef C, et al. Neoadjuvant chemotherapy for locally advanced T4 colon cancer: A nationwide propensity-score matched cohort analysis. *Dig Surg* (2020) 37(4):292–301. doi: 10.1159/000503446

10. Pellino G, Warren O, Mills S, Rasheed S, Tekkis PP, Kontovounisios C. Comparison of Western and Asian guidelines concerning the management of colon cancer. *Dis Colon Rectum* (2018) 61(2):250–9. doi: 10.1097/DCR.0000000000001012

11. Hashiguchi Y, Muro K, Saito Y, Ito Y, Ajioka Y, Hamaguchi T, et al. Japanese Society for cancer of the colon and rectum (JSCCR) guidelines 2019 for the treatment of colorectal cancer. *Int J Clin Oncol* (2020) 25(1):1–42. doi: 10.1007/s10147-019-01485-z

12. Cho E, Nakajima M, Yasuda K, Ashihara T, Kawai K. Endoscopic ultrasonography in the diagnosis of colorectal cancer invasion. *Gastrointest Endosc* (1993) 39(4):521–7. doi: 10.1016/s0016-5107(93)70163-7

13. Nerad E, Lahaye MJ, Maas M, Nelemans P, Bakers FC, Beets GL, et al. Diagnostic accuracy of CT for local staging of colon cancer: A systematic review and meta-analysis. *AJR Am J Roentgenol* (2016) v207(5):984–95. doi: 10.2214/AJR.15.15785

14. Fernandez LM, Parlade AJ, Wasser EJ, Dasilva G, de Azevedo RU, Ortega CD, et al. How reliable is CT scan in staging right colon cancer? *Dis Colon Rectum* (2019) 62(8):960–4. doi: 10.1097/DCR.0000000000001387

15. Liu LH, Zhou GF, Zhou JJ, Rao SX, Zeng MS. Impact of visceral adipose tissue on the accuracy of T-staging by CT in colon cancer. *Eur J Radiol* (2021) 134:109400. doi: 10.1016/j.ejrad.2020.109400

16. Horvat N, Carlos Tavares Rocha C, Clemente Oliveira B, Petkovska I, Gollub MJ. MRI Of rectal cancer: Tumor staging, imaging techniques, and management. *Radiographics* (2019) 39(2):367–87. doi: 10.1148/rg.2019180114

17. Taylor FG, Swift RI, Blomqvist L, Brown G. A systematic approach to the interpretation of preoperative staging MRI for rectal cancer. *AJR Am J Roentgenol* (2008) 191(6):1827–35. doi: 10.2214/AJR.08.1004

18. Beets-Tan RG, Beets GL, Vliegen RF, Kessels AG, Van Boven H, De Bruine A, et al. Accuracy of magnetic resonance imaging in prediction of tumour-free resection margin in rectal cancer surgery. *Lancet* (2001) 357(9255):497–504. doi: 10.1016/s0140-6736(00)04040-x

19. van Ommen F, de Jong HWAM, Dankbaar JW, Bennink E, Leiner T, Schilham AMR. Dose of CT protocols acquired in clinical routine using a dual-layer detector CT scanner: A preliminary report. *Eur J Radiol* (2019) 112:65–71. doi: 10.1016/j.ejrad.2019.01.011

20. Rassouli N, Etesami M, Dhanantwari A, Rajiah P. Detector-based spectral CT with a novel dual-layer technology: principles and applications. *Insights Imaging* (2017) 8(6):589–98. doi: 10.1007/s13244-017-0571-4

21. Obmann MM, An C, Schaefer A, Sun Y, Wang ZJ, Yee J, et al. Improved sensitivity and reader confidence in CT colonography using dual-layer spectral CT: A phantom study. *Radiology* (2020) 297(1):99–107. doi: 10.1148/radiol.2020200032

22. Wang G, Fang Y, Wang Z, Jin Z. Quantitative assessment of radiologically indeterminate local colonic wall thickening on iodine density images using dual-layer spectral detector CT. *Acad Radiol* (2021) 28(10):1368–74. doi: 10.1016/j.acra.2020.06.012

23. Taguchi N, Oda S, Imuta M, Yamamura S, Yokota Y, Nakaura T, et al. Dual-energy computed tomography colonography using dual-layer spectral detector computed tomography: Utility of virtual monochromatic imaging for electronic cleansing. *Eur J Radiol* (2018) 108:7–12. doi: 10.1016/j.ejrad.2018.09.011

24. Sun Q, Liu T, Liu P, Luo J, Zhang N, Lu K, et al. Perineural and lymphovascular invasion predicts for poor prognosis in locally advanced rectal cancer after neoadjuvant chemoradiotherapy and surgery. *J Cancer* (2019) 10 (10):2243–9. doi: 10.7150/jca.31473

25. Zopfs D, Reimer RP, Sonnabend K, Rinneburger M, Hentschke CM, Persigehl T, et al. Intraindividual consistency of iodine concentration in dual-energy computed tomography of the chest and abdomen. *Invest Radiol* (2021) 56 (3):181–7. doi: 10.1097/RLI.0000000000000724

26. Zopfs D, Graffe J, Reimer RP, Schäfer S, Persigehl T, Maintz D, et al. Quantitative distribution of iodinated contrast media in body computed tomography: data from a large reference cohort. *Eur Radiol* (2021) 31(4):2340–8. doi: 10.1007/s00330-020-07298-3

27. Murty RC. Effective atomic numbers of heterogeneous materials. *Nature* (1965) 207:398–9. doi: 10.1038/207398a0

28. Yamashita Y, Kimura M, Kitahara M, Takumi H. Measurement of effective atomic numbers using energy-resolved computed tomography. *J Nucl Sci Technol* (2014) 51:1256–63. doi: 10.1080/00223131.2014.919881

29. Hua CH, Shapira N, Merchant TE, Klahr P, Yagil Y. Accuracy of electron density, effective atomic number, and iodine concentration determination with a dual-layer dual-energy computed tomography system. *Med Phys* (2018) 45 (6):2486–97. doi: 10.1002/mp.12903

30. Taylor ML. Quantification of differences in the effective atomic numbers of healthy and cancerous tissues: a discussion in the context of diagnostics and dosimetry. *Med Phys* (2012) 39(9):5437–45. doi: 10.1118/1.4742849

31. Naga Raju GJ, John Charles M, Bhuloka Reddy S, Sarita P, Seetharami Reddy B, Rama Lakshmi PVB, et al. Trace elemental analysis in cancer-afflicted tissues of penis and testis by PIXE technique. *Nucl Instruments Methods Phys Res Section B: Beam Interact Mater Atoms* (2005) 229:457–64. doi: 10.1016/j.nimb.2004.12.120

32. Bhuloka Reddy S, John Charles M, Ravi Kumar M, Seetharami Reddy B, Anjaneyulu CH, Naga GJ, et al. Trace elemental analysis of carcinoma kidney and stomach by PIXE method. *Nucl Instruments Methods Phys Res Section B: Beam Interact Mater Atoms* (2002) 207:345–55. doi: 10.1016/S016-583X(02)01292-2

33. Wang X, Meier D, Taguchi K, Wagenaar DJ, Patt BE, Frey EC. Material separation in x-ray CT with energy resolved photon-counting detectors. *Med Phys* (2011) 38(3):1534–46. doi: 10.1118/1.3553401

34. McKetty MH. The AAPM/RSNA physics tutorial for residents. *X-ray Attenuation Radiographics* (1998) 18(1):151–163; quiz 149. doi: 10.1148/radiographics.18.1.9460114

35. Wu J, Lv Y, Wang N, Zhao Y, Zhang P, Liu Y, et al. The value of single-source dual-energy CT imaging for discriminating microsatellite instability from microsatellite stability human colorectal cancer. *Eur Radiol* (2019) 29(7):3782–90. doi: 10.1007/s00330-019-06144-5

36. Pelgrim GJ, van Hamersvelt RW, Willemink MJ, Schmidt BT, Flohr T, Schilham A, et al. Accuracy of iodine quantification using dual energy CT in latest generation dual source and dual layer CT. *Eur Radiol* (2017) 27(9):3904–12. doi: 10.1007/s00330-017-4752-9

37. Zhang LJ, Wu S, Wang M, Lu L, Chen B, Jin L, et al. Quantitative dual energy CT measurements in rabbit VX2 liver tumors: Comparison to perfusion CT measurements and histopathological findings. *Eur J Radiol* (2012) 81(8):1766–75. doi: 10.1016/j.ejrad.2011.06.057

38. van Assen M, Lavra F, Schoepf UJ, Jacobs BE, Williams BT, Thompson ZM, et al. Iodine quantification based on rest / stress perfusion dual energy CT to differentiate ischemic, infarcted and normal myocardium. *Eur J Radiol* (2019) 112:136–43. doi: 10.1016/j.ejrad.2019.01.017

39. Delgado Sánchez-Gracián C, Oca Pernas R, Trinidad López C, Santos Armentia E, Vaamonde Liste A, Vázquez Caamaño M, et al. Quantitative myocardial perfusion with stress dual-energy CT: iodine concentration differences between normal and ischemic or necrotic myocardium. *Initial Exp Eur Radiol* (2016) 26(9):3199–207. doi: 10.1007/s00330-015-4128-y

40. Li Q, Li X, Li XY, Huo JW, Lv FJ, Luo TY. Spectral CT in lung cancer: Usefulness of iodine concentration for evaluation of tumor angiogenesis and prognosis. *AJR Am J Roentgenol* (2020) 215(3):595–602. doi: 10.2214/AJR.19.22688

41. Marcon J, Graser A, Horst D, Casuscelli J, Spek A, Stief CG, et al. Papillary vs clear cell renal cell carcinoma. differentiation and grading by iodine concentration using DECT-correlation with microvascular density. *Eur Radiol* (2020) 30(1):1–10. doi: 10.1007/s00330-019-06298-2

42. Kim JW, Jeong YY, Chang NK, Heo SH, Shin SS, Lee JH, et al. Perfusion CT in colorectal cancer: comparison of perfusion parameters with tumor grade and microvessel density. *Korean J Radiol* (2012) 13 Suppl 1:S89–97. doi: 10.3348/kjr.2012.13.S1.S89

43. den Uil SH, van den Broek E, Coupé VMH, Vellinga TT, Delis-van Diemen PM, Bril H, et al. Prognostic value of microvessel density in stage II and III colon cancer patients: a retrospective cohort study. *BMC Gastroenterol* (2019) 19(1):146. doi: 10.1186/s12876-019-1063-4

44. Cao Y, Zhang G, Bao H, Ren J, Wang Z, Zhang J, et al. Development of a dual-energy spectral computed tomography-based nomogram for the preoperative discrimination of histological grade in colorectal adenocarcinoma patients. *J Gastrointest Oncol* (2021) 12(2):544–55. doi: 10.21037/jgo-20-368

45. Gong HX, Zhang KB, Wu LM, Baigorri BF, Yin Y, Geng XC, et al. Dual energy spectral CT imaging for colorectal cancer grading: A preliminary study. *PloS One* (2016) 11(2):e0147756. doi: 10.1371/journal.pone.0147756

46. Li R, Li J, Wang X, Liang P, Gao J. Detection of gastric cancer and its histological type based on iodine concentration in spectral CT. *Cancer Imaging* (2018) 18(1):42. doi: 10.1186/s40644-018-0176-2

47. Thaiss WM, Haberland U, Kaufmann S, Spira D, Thomas C, Nikolaou K, et al. Iodine concentration as a perfusion surrogate marker in oncology: Further elucidation of the underlying mechanisms using volume perfusion CT with 80 kVp. *Eur Radiol* (2016) 26(9):2929–36. doi: 10.1007/s00330-015-4154-9

frontiers | Frontiers in Oncology

TYPE Original Research
PUBLISHED 04 October 2022
DOI 10.3389/fonc.2022.962381

Check for updates

OPEN ACCESS

EDITED BY
Zhendong Jin,
Second Military Medical University, China

REVIEWED BY
Shiva Basnet,
Southern University of Science and Technology, China
Mehmet Levhi Akin,
Istinye University, Turkey

*CORRESPONDENCE
Yijun Wang
wangyijun_carl@163.com
Jinjuan Zhang
15522242886@163.com

SPECIALTY SECTION
This article was submitted to Gastrointestinal Cancers: Colorectal Cancer, a section of the journal Frontiers in Oncology

RECEIVED 06 June 2022
ACCEPTED 20 September 2022
PUBLISHED 04 October 2022

CITATION
Shi J, Liu S, Cao J, Shan S, Zhang J and Wang Y (2022) Development and validation of lymph node ratio-based nomograms for primary duodenal adenocarcinoma after surgery. *Front. Oncol.* 12:962381. doi: 10.3389/fonc.2022.962381

COPYRIGHT
© 2022 Shi, Liu, Cao, Shan, Zhang and Wang. This is an open-access article distributed under the terms of the Creative Commons Attribution License (CC BY). The use, distribution or reproduction in other forums is permitted, provided the original author(s) and the copyright owner(s) are credited and that the original publication in this journal is cited, in accordance with accepted academic practice. No use, distribution or reproduction is permitted which does not comply with these terms.

Development and validation of lymph node ratio-based nomograms for primary duodenal adenocarcinoma after surgery

Jingxiang Shi[1,2,3,4], Sifan Liu[5], Jisen Cao[1,4], Shigang Shan[1,4], Jinjuan Zhang[1,4]* and Yijun Wang[1,4]*

[1]Department of Hepatobiliary Surgery, The Third Central Hospital of Tianjin, Tianjin, China, [2]Tianjin Key Laboratory of Extracorporeal Life Support for Critical Diseases, The Third Central Hospital of Tianjin, Tianjin, China, [3]Artificial Cell Engineering Technology Research Center, The Third Central Hospital of Tianjin, Tianjin, China, [4]Tianjin Institute of Hepatobiliary Disease, The Third Central Hospital of Tianjin, Tianjin, China, [5]School of Statistics, Tianjin University of Finance and Economics, Tianjin, China

Background: The prediction models for primary duodenal adenocarcinoma (PDA) are deficient. This study aimed to determine the predictive value of the lymph node ratio (LNR) in PDA patients and to establish and validate nomograms for predicting overall survival (OS) and cancer-specific survival (CSS) for PDAs after surgical resection.

Methods: We extracted the demographics and clinicopathological information of PDA patients between 2004 and 2018 from the Surveillance, Epidemiology and End Results database. After screening cases, we randomly divided the enrolled patients into training and validation groups. X-tile software was used to obtain the best cut-off value for the LNR. Univariate and multivariate Cox analyses were used in the training group to screen out significant variables to develop nomograms. The predictive accuracy of the nomograms was evaluated by the concordance index (C-index), calibration curves, area under the receiver operating characteristic curve (AUC) and decision curve analysis (DCA). Finally, four risk groups were created based on quartiles of the model scores.

Results: A total of 978 patients were included in this study. The best cut-off value for the LNR was 0.47. LNR was a negative predictive factor for both OS and CSS. Age, sex, grade, chemotherapy and LNR were used to construct the OS nomogram, while age, grade, chemotherapy, the number of lymph nodes removed and LNR were incorporated into the CSS nomogram. The C-index, calibration curves and AUC of the training and validation sets revealed their good predictability. DCA showed that the predictive value of the nomograms was superior to that of the American Joint Committee on Cancer (AJCC) TNM staging system (8th edition). In addition, risk stratification demonstrated that patients with higher risk correlated with poor survival.

Conclusions: The LNR was an adverse prognostic determinant for PDAs. The nomograms provided an accurate and applicable tool to evaluate the prognosis of PDA patients after surgery.

KEYWORDS

lymph node ratio, nomogram, primary duodenal adenocarcinoma, overall survival, cancer-specific survival

Introduction

Primary duodenal adenocarcinoma (PDA), which arises from duodenal mucosal glandular epithelial cells, is a rare malignant tumour (1). According to epidemiological investigation, its incidence is no more than 0.5 in 100,000, accounting for only 0.5% of all gastrointestinal tumours (2, 3). The majority of PDAs occur in the second portion of the duodenum, followed by the first portion (4). Due to the adjacency of anatomical position and the same surgical approach, cancers from the head of pancreas, the distal common bile duct, the ampulla of Vater and the descending portion of the duodenum called "periampullary carcinoma" have often been studied together (5). However, the biological features and prognosis of these tumours are different. Therefore, it is necessary to study PDA as a unique entity.

Surgical resection is the main curative treatment for PDAs (6). Pancreaticoduodenectomy or segmental resection is performed in most cases (7). One meta-analysis demonstrated that surgery might greatly improve survival compared with nonsurgery (5-year overall survival rate, 43.4% vs 2.5%) (8). Poultsides et al. (9) pointed out that the 5-year overall survival (OS) rate after resection of PDA was 48%. Another study indicated that the 5-year cancer-specific survival (CSS) rate after surgery was 43% (3). However, due to the low incidence of this disease and the small sample size of clinical research, there are few studies on prediction models for PDA patients after surgery.

The lymph node ratio (LNR), which refers to the proportion of positive lymph nodes in the total examined nodes, has shown its importance for the prognostic prediction of several malignancies in recent years. Zhou et al. (10) pointed out that the LNR was an important prognostic factor for non-small-cell lung cancer. Macedo et al. (11) indicated that the LNR was a better prognostic tool than the TNM system in colorectal cancer. Our previous study demonstrated that it was an important predictor of poor survival in pancreatic neuroendocrine tumours (12). However, there are no published reports about nomograms for predicting the survival of PDA patients combined with LNR data.

In this study, based on data from the Surveillance, Epidemiology, and End Results (SEER) database, we identified the effect of the LNR on the prognosis of patients with PDA. We further established and validated nomograms to predict 1-, 3-, and 5-year OS and CSS rates for PDAs after surgery.

Materials and methods

Data collection

The SEER database is a population-based database supported by the National Cancer Institute in the USA and contains a large amount of evidence-based medical data (13). We used SEER*Stat software (version 8.3.9.2) to extract data from the SEER database. The Incidence SEER Research Plus Data, 18 Registries, Nov 2020 Sub (2000–2018) dataset was selected for analysis (username for log in: 15881-Nov2020). Patients diagnosed with PDA between 2004 and 2018 were confirmed retrospectively. The selection parameters in the software were as follows: Site and Morphology, "Primary Site – labelled" (C17.0-Duodenum) and "ICD-O-3 Hist/behav" (8140/3, 8143/3, 8144/3, 8210/3, 8211/3, 8220/3, 8221/3, 8255/3, 8260/3-8263/3, 8310/3, 8323/3, 8480/3, 8481/3, 8574/3, 8576/3). The extracted demographic variables included age, sex, patient ID, year of diagnosis, race and marital status. The corresponding clinicopathological variables were as follows: histologic type, grade, diagnostic confirmation, American Joint Committee on Cancer (AJCC) TNM staging system, T stage, N stage, M stage, tumour size, surgery at the primary site, scope of regional lymph node surgery, radiation recode, chemotherapy recode, regional nodes examined, positive regional nodes, survival months, SEER cause-specific death classification, vital status recode, first malignant primary indicator and sequence number.

Data processing

The exclusion criteria were as follows: 1) patients who did not undergo surgery; 2) patients who did not have regional

lymph nodes removed during surgery; 3) patients who had multiple primary tumours; and 4) missing or unknown clinical information.

We treated age as a continuous variable and other factors as categorical variables. Patients who were single, separated, divorced or widowed were regarded as unmarried. Tumour grade was defined as Grade I (well differentiated), Grade II (moderately differentiated), Grade III (poorly differentiated) and Grade IV (undifferentiated or anaplastic) according to the SEER tumour grade system. The TNM staging system was adjusted based on the eighth edition of AJCC. OS was defined as the time from the date of diagnosis to the date of death by any cause or last follow-up, and CSS was defined as the time from the date of diagnosis to the date of death caused by PDA (12).

Construction and validation of the nomograms

The enrolled patients were randomly assigned to a training set and a validation set at a ratio of 7:3. For the training cohort, the "survival" package in R software was used for univariate and multivariate Cox regression analysis to screen significant variables (14). After that, the "rms" package was used to construct nomograms based on the results of multivariate analysis (14). The validation cohort was treated as an external validation of the nomograms.

We calculated the concordance index (C-index) and the area under the receiver operating characteristic curve (AUC) of the training and validation groups to evaluate the discrimination ability of the nomograms (15). Calibration curves were plotted to assess the calibration ability (16). In addition, we used decision curve analysis (DCA) to evaluate the clinical usefulness of the nomograms (17). Furthermore, DCA was performed to compare the AJCC staging system (8th edition), LNR and the nomograms.

Statistical analysis

Statistical analyses were performed as described in our previous study (12). Continuous variables were reported as the mean with standard deviation. Categorical variables were presented as frequencies and percentages. X-tile software was used to determine the optimal cut-off value of the LNR (18). Survival curves (for both OS and CSS) were generated using the Kaplan–Meier method, and the differences in groups were analysed using the log-rank test. Variables with $P < 0.2$ in univariate analysis were considered for generating multivariate analysis. Factors with $P < 0.05$ in multivariate analysis were entered into the nomograms. Corresponding 95% confidence intervals (CIs) and hazard ratios (HRs) were calculated. We used Pearson's correlation to detect collinearity among the variables. A correlation coefficient < 0.7 between two variables was regarded as no multicollinearity (19). $P < 0.05$ was defined as statistically significant. All statistical tests were performed using R statistical software (version 4.1.2, https://www.r-project.org, Vienna, Austria).

Results

Patient characteristics

From 2004 to 2018, a total of 978 eligible patients from the SEER database were included in this study. Among them, 685 cases were randomly allocated to the training group, while 293 cases were allocated to the validation group. The study procedure is shown in Figure 1. The demographic and clinicopathological characteristics of the enrolled patients are summarized in Table 1. For the overall group, the median age was 65 years, and the median follow-up time was 38 months (range, 1-179 months). By the end of the last follow-up, 326 patients (47.6%) had died from PDA, and 56 patients (8.2%) had died from other causes in the training set. For the validation set, the numbers were 138 (47.1%) and 26 (8.9%), respectively. The 1-, 3-, and 5-year OS rates for the training group and the validation group were 75.8%, 55.3%, 47.9% and 76.8%, 53.6%, 47.4%. The corresponding 1-, 3-, and 5-year CSS rates for the two groups were 79.1%, 61.0%, 54.5% and 80.9%, 60.8%, 55.3%, respectively. There were no significant differences between the two groups. The best cut-off value for the LNR was 0.47. Thus, we divided the total patients into three groups (LNR1: 0, LNR2: ≤ 0.47 and LNR3: > 0.47). Patients with a lower LNR were associated with better OS and CSS (Figures 2A, B).

Nomogram construction

For the training cohort, the following variables were included in the univariate analysis: age, sex, race, marital status, grade, tumour size, T stage, N stage, M stage, radiotherapy, chemotherapy, the number of lymph nodes removed and LNR. The factors with significant differences were incorporated into the multivariate Cox regression analysis. The multivariate analyses identified that age, sex, grade, chemotherapy and LNR were significantly associated with OS and that age, grade, chemotherapy, the number of lymph nodes removed and LNR were significantly associated with CSS (Tables 2, 3). Therefore, nomograms for predicting the 1-, 3-, and 5-year OS and CSS rates were established based on these variables (Figures 3A, B). Each variable was given a score on the points scale. The survival probability of a patient can be easily calculated by adding the scores of each selected factor. There was no collinearity among the screened variables for the overall dataset, the training or the validation sets (Supplementary Figure S1).

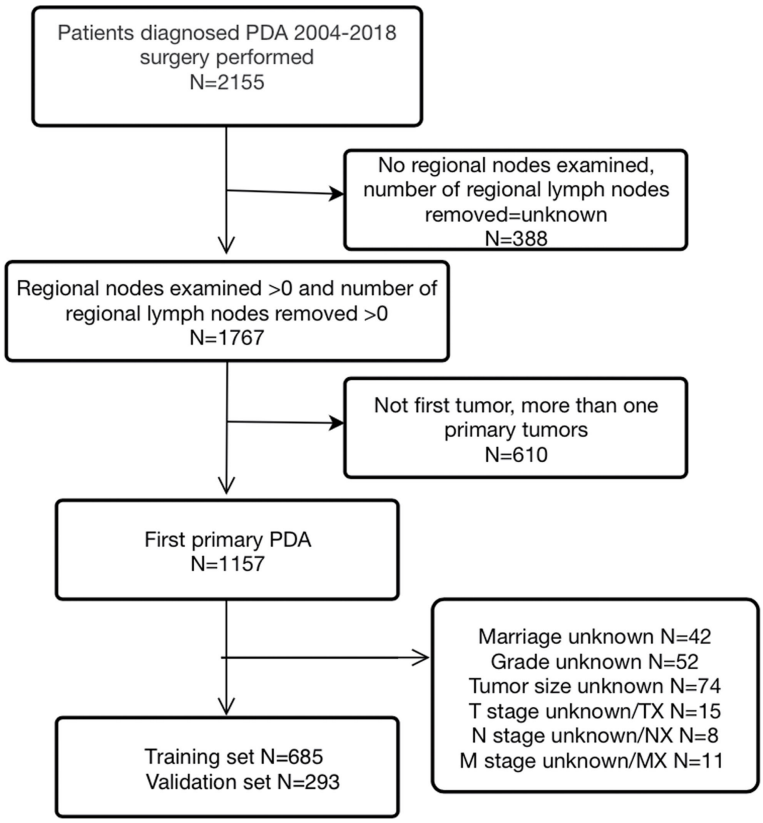

FIGURE 1
The flow chart of included patients.

Nomogram validation

We performed internal and external verification of the two nomograms. In the internal validation, the C-index for OS prediction was 0.697 (95% CI, 0.670 to 0.724), while for CSS, it was 0.700 (95% CI, 0.671 to 0.729). In the external validation, the C-index for OS prediction was 0.669 (95% CI, 0.629 to 0.709), while for CSS, it was 0.674 (95% CI, 0.626 to 0.722). The calibration curves of the OS nomogram showed high consistency between the predicted and observed survival probability in both the training (Figure 4A) and validation (Figure 4E) cohorts. Similarly, the calibration plots of the CSS nomogram were close to the standard curves in the two sets (Figures 5A, E). The AUC values for predicting 1-, 3-, and 5-year OS rates were 0.767, 0.717 and 0.704 in the training group (Supplementary Figure S2A) and 0.705, 0.722 and 0.715 in the validation group (Supplementary Figure S2B). With regard to the 1-, 3-, and 5-year CSS rates, the AUC values were 0.762, 0.733 and 0.703 in the training group (Supplementary Figure S2C) and 0.764, 0.715 and 0.706 in the validation group (Supplementary Figure S2D). For both the training and validation sets, the DCA curves for OS (Figures 4B–D, F–H) and CSS (Figures 5B-D, F-H) indicated

TABLE 1 Patient demographics and clinicopathological characteristics.

Variables	Training group	Validation group
Age (year)	64.72 ± 12.75	65.85 ± 12.00
Sex		
Female	315 (46.0)	144 (49.1)
Male	370 (54.0)	149 (50.9)
Race		
White	529 (77.2)	215 (73.4)
Black	96 (14.0)	54 (18.4)
Others	60 (8.8)	24 (8.2)
Marriage		
Married	445 (65.0)	185 (63.1)
Unmarried	240 (35.0)	108 (36.9)
Grade		
I	57 (8.3)	21 (7.2)
II	355 (51.8)	165 (56.3)
III	263 (38.4)	104 (35.5)
IV	10 (1.5)	3 (1.0)
Tumour size (cm)		

(Continued)

TABLE 1 Continued

Variables	Training group	Validation group
≤2	94 (13.7)	32 (10.9)
2-4	293 (42.8)	125 (42.7)
>4	298 (43.5)	136 (46.4)
T stage		
T1	36 (5.3)	18 (6.1)
T2	42 (6.1)	27 (9.2)
T3	257 (37.5)	109 (37.2)
T4	350 (51.1)	139 (47.4)
N stage		
N0	245 (35.8)	128 (43.7)
N1	318 (46.4)	127 (43.3)
N2	122 (17.8)	38 (13.0)
M stage		
M0	630 (92.0)	273 (93.2)
M1	55 (8.0)	20 (6.8)
Radiotherapy		
Yes	89 (13.0)	45 (15.4)
No	596 (87.0)	248 (84.6)
Chemotherapy		
Yes	348 (50.8)	156 (53.2)
No	337 (49.2)	137 (46.8)
Lymph nodes removed		
<15	367 (53.6)	145 (49.5)
≥15	318 (46.4)	148 (50.5)
AJCC TNM stage		
I	54 (7.9)	30 (10.2)
IIA	101 (14.7)	55 (18.8)
IIB	87 (12.7)	39 (13.3)
IIIA	284 (41.5)	116 (39.6)
IIIB	104 (15.2)	33 (11.3)
IV	55 (8.0)	20 (6.8)
LNR		
0	262 (38.2)	115 (39.2)
≤0.47	324 (47.3)	134 (45.7)
>0.47	99 (14.5)	44 (15.0)

LNR, lymph node ratio.

that our nomograms exhibited optimal net benefit with a wider range of threshold probability compared to the AJCC staging system (8th edition), and LNR had good prediction ability regarding patient prognosis.

Risk stratification

Finally, we performed risk stratification for PDA patients based on the two established nomograms. They were categorized into four groups according to the scores for OS (Min-89.9, 89.9-111.4, 111.4-136.9, 136.9-Max) or the scores for CSS (Min-100.2, 100.2-126.3, 126.3-159.7, 159.7-Max). The Kaplan–Meier survival curves showed that statistically significant differences in OS (Figures 6A, B) and CSS (Figures 6C, D) were observed among the four different risk groups in both the training and validation sets.

Discussion

PDA is a rare gastrointestinal malignancy. Patients are usually diagnosed at an advanced stage due to a lack of specific symptoms, which leads to adverse prognoses (3). Considering the low prevalence of this disease and the limited number of clinical studies, there is no consensus on prognostic factors. Therefore, we used a large dataset collected by the SEER program to identify the factors affecting the survival of PDA patients after surgery. Furthermore, we developed nomograms to predict OS and CSS for these patients. Given the significance of LNR, we analysed it separately and integrated it into the nomograms according to the multivariate Cox regression analysis. The relatively high C-indices and values of AUC in the training and validation sets demonstrated that the nomograms displayed good ability in predicting OS and CSS. The calibration curves showed excellent agreement between the predicted and actual survival, which further ensured their accuracy and reliability.

It is well established that lymph node status (yes/no presence of metastatic node) is an important prognostic determinant in PDA patients after operation. Sakamoto et al. (20) suggested that lymph node metastasis was a negative predictive factor for OS. Meijer et al. (21) reported that lymph node involvement correlated with poor survival. However, lymph node status ignores the different prognoses of lymph node-positive cases, which may lead to confusion in such patients. To overcome this limitation, LNR emerged as a substitute for lymph node status. Its effect on survival has been confirmed by many neoplasms, such as gastric, pancreatic, and ampullary cancer (22–24). With respect to PDA, Jensen et al. (25) pointed out that LNR > 0.2 was associated with increased mortality. Tran et al. (26) indicated that the LNR was an important predictor of lower OS. Liang et al. (27) identified that LNR > 0.4 was associated with decreased survival. Another study showed that patients with high LNR levels had shorter OS (9). Our study, in accordance with previous reports, demonstrated that LNR was an adverse independent prognostic factor for both OS and CSS. Furthermore, LNR may eliminate the variation in dissection techniques by different surgeons and the variation in specimen examination by different pathologists and is more accurate than lymph node status for prognosis prediction.

Apart from LNR, the proposed nomograms contain several other predictors, such as age, sex, grade, chemotherapy and the

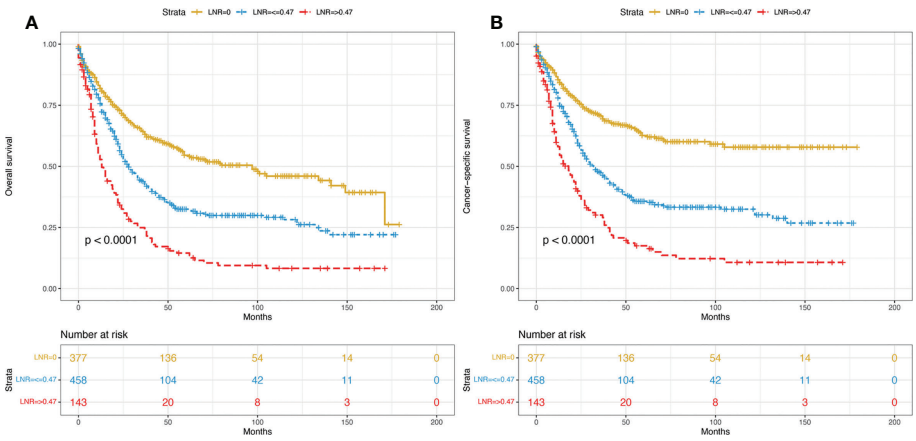

FIGURE 2
Kaplan–Meier curves of OS **(A)** and CSS **(B)** for all included patients stratified by LNR. OS, overall survival; CSS, cancer-specific survival; LNR, lymph node ratio.

TABLE 2 Univariate and multivariate analysis of overall survival (OS) in the training set.

	Univariate analysis		Multivariate analysis	
	HR (95% CI)	*P*	HR (95% CI)	*P*
Age (year)	1.03 (1.02-1.04)	<0.001	1.02 (1.01-1.03)	<0.001
Sex				
Female	0.74 (0.60-0.90)	0.003	0.79 (0.64-0.97)	0.022
Male	Reference		Reference	
Race				
White	Reference			
Black	0.95 (0.71-1.29)	0.750		
Others	1.23 (0.86-1.76)	0.252		
Marriage				
Married	Reference			
Unmarried	1.12 (0.91-1.39)	0.275		
Grade				
I, II	Reference		Reference	
III, IV	1.43 (1.17-1.75)	<0.001	1.44 (1.17-1.78)	0.009
Tumour size (cm)				
≤2	Reference			
2-4	1.18 (0.87-1.60)	0.290		
>4	1.05 (0.77-1.43)	0.756		
T stage				
T1	Reference			
T2	0.75 (0.41-1.39)	0.368		
T3	0.91 (0.57-1.45)	0.695		
T4	0.93 (0.59-1.48)	0.766		
N stage				
N0	Reference			

(Continued)

TABLE 2 Continued

	Univariate analysis		Multivariate analysis	
	HR (95% CI)	*P*	HR (95% CI)	*P*
N1	0.97 (0.77-1.21)	0.768		
N2	1.14 (0.86-1.51)	0.369		
M stage				
M0	Reference			
M1	0.95 (0.65-1.38)	0.780		
Radiotherapy				
Yes	0.71 (0.52-0.97)	0.033	1.06 (0.75-1.50)	0.729
No	Reference		Reference	
Chemotherapy				
Yes	0.68 (0.55-0.83)	<0.001	0.49 (0.38-0.62)	<0.001
No	Reference		Reference	
Lymph nodes removed				
<15	Reference		Reference	
≥15	0.73 (0.59-0.90)	0.003	0.82 (0.65-1.02)	0.079
LNR				
0	Reference		Reference	
≤0.47	1.66 (1.31-2.09)	<0.001	2.40 (1.85-3.12)	<0.001
>0.47	3.08 (2.31-4.11)	<0.001	3.67 (2.67-5.03)	<0.001

LNR, lymph node ratio.

TABLE 3 Univariate and multivariate analysis of cancer-specific survival (CSS) in the training set.

	Univariate analysis		Multivariate analysis	
	HR (95% CI)	*P*	HR (95% CI)	*P*
Age (year)	1.03 (1.02-1.03)	<0.001	1.02 (1.01-1.03)	<0.001
Sex				
Female	0.81 (0.65-1.01)	0.062	0.90 (0.72-1.12)	0.336
Male	Reference		Reference	
Race				
White	Reference			
Black	0.95 (0.69-1.31)	0.755		
Others	1.16 (0.78-1.71)	0.460		
Marriage				
Married	Reference			
Unmarried	1.10 (0.87-1.37)	0.437		
Grade				
I, II	Reference		Reference	
III, IV	1.69 (1.36-2.09)	<0.001	1.68 (1.34-2.11)	<0.001
Tumour size (cm)				
≤2	Reference		Reference	
2-4	1.41 (0.99-2.00)	0.050	1.40 (0.99-1.99)	0.059
>4	1.19 (0.84-1.69)	0.332	1.20 (0.84-1.71)	0.310
T stage				

(Continued)

10.3389/fonc.2022.962381

TABLE 3 Continued

	Univariate analysis		Multivariate analysis	
	HR (95% CI)	*P*	HR (95% CI)	*P*
T1	Reference			
T2	1.01 (0.51-1.97)	0.987		
T3	0.96 (0.56-1.64)	0.876		
T4	1.14 (0.67-1.94)	0.621		
N stage				
N0	Reference			
N1	1.06 (0.83-1.35)	0.651		
N2	1.19 (0.87-1.62)	0.280		
M stage				
M0	Reference			
M1	1.00 (0.68-1.49)	0.987		
Radiotherapy				
Yes	0.76 (0.54-1.05)	0.094	1.03 (0.72-1.48)	0.857
No	Reference		Reference	
Chemotherapy				
Yes	0.76 (0.61-0.94)	0.012	0.49 (0.38-0.64)	<0.001
No	Reference		Reference	
Lymph nodes removed				
<15	Reference		Reference	
≥15	0.73 (0.58-0.91)	0.006	0.77 (0.60-0.98)	0.034
LNR				
0	Reference		Reference	
≤0.47	1.98 (1.52-2.57)	<0.001	2.92 (2.18-3.90)	<0.001
>0.47	3.66 (2.67-5.03)	<0.001	4.25 (3.01-6.00)	<0.001

LNR, lymph node ratio.

number of lymph nodes removed. Our research identified that older age was strongly associated with worse survival, as shown in other reports (3, 4, 28). Similar to the conclusion of Wang et al. (29), the mortality rate of women was lower than that of men. Moreover, histologic grade, which reflects the biological characteristics of tumour tissue, was also an important prognostic factor for PDA patients in our study. This was consistent with previous reports (3, 28, 30, 31). Ecker et al. (32) indicated that PDA patients with lymph node positivity after surgery could gain survival benefits from adjuvant chemotherapy. A similar effect was observed in our research. In addition, this study demonstrated that the number of lymph nodes examined ≥ 15 was associated with improved survival, which was also in accordance with the results of some investigations (20, 33, 34). The possible reason is that the number of lymph nodes removed affects not only the accuracy of N staging but also the therapeutic effect of lymphadenectomy to eradicate potentially hidden lesions in lymph nodes (20).

In the present study, we constructed and validated nomograms to predict 1-, 3-, and 5-year OS and CSS for PDA patients after surgery. The nomograms have the following advantages. First, their prediction ability was superior to that of the AJCC TNM staging system (8th edition). This is because our nomograms integrated not only clinicopathological variables but also demographic variables, which were more accurate than the TNM staging system. DCA curves confirmed this. Second, the variables used in the nomograms are easily obtained in clinical work. Therefore, by using the variable scores, clinicians may precisely assess the risk factors for patients and develop subsequent individualized treatment. A clear risk stratification of patients in different stages was demonstrated by survival curves. Third, the SEER database is a large and open database. Its information comes from 18 states in the US. Thus, the extracted data were rich, detailed and multicentric. Our results should be more applicable to the general population than studies from a single centre.

However, this study has several limitations. First, our nomograms were constructed based on the SEER database. SEER only includes information from American patients, which may not represent patients from all over the world. Second, some important parameters, such as surgical margin status, vascular invasion, chemotherapy regimens and radiation

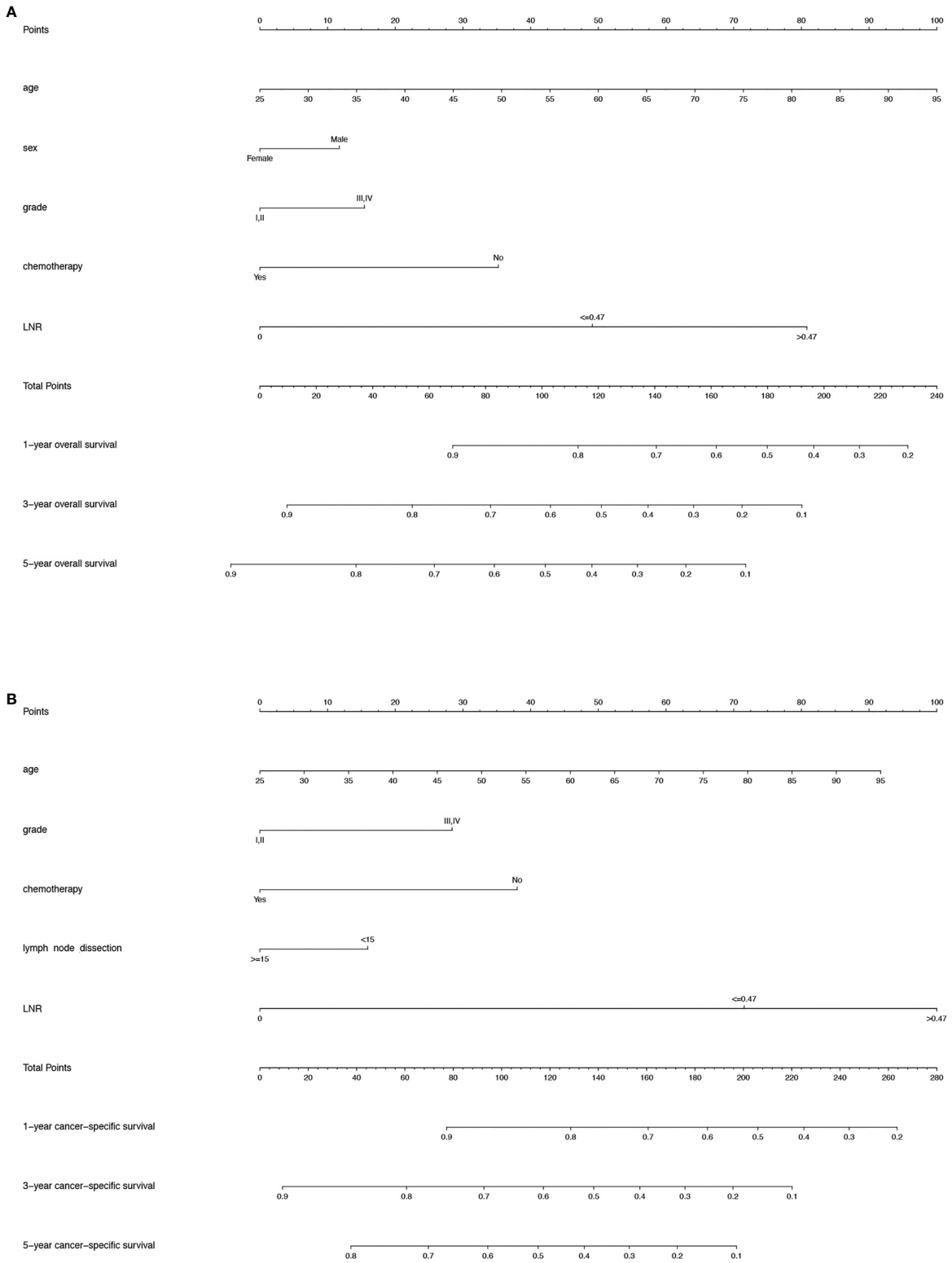

FIGURE 3
(A) Nomogram predicting the 1-, 3- and 5-year OS rates for PDA patients after surgery. **(B)** Nomogram predicting the 1-, 3- and 5-year CSS rates for PDA patients after surgery. OS, overall survival; PDA, primary duodenal adenocarcinoma; CSS, cancer-specific survival.

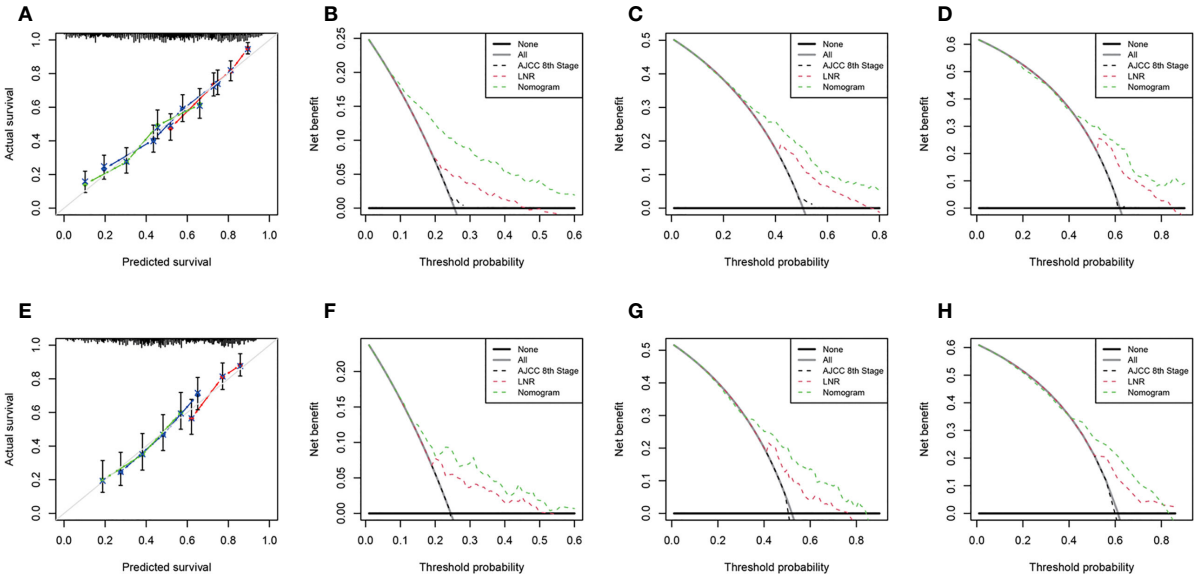

FIGURE 4
Calibration curves for OS prediction in the training cohort **(A)** and the validation cohort **(E)**. Decision curve analysis of the AJCC 8th edition staging system, nomogram and LNR for the 1- **(B)**, 3- **(C)** and 5-year **(D)** OS rates of PDA patients from the training cohort. Decision curve analysis of the AJCC 8th edition staging system, nomogram and LNR for the 1- **(F)**, 3- **(G)** and 5-year **(H)** OS rates of PDA patients from the validation cohort. OS, overall survival; LNR, lymph node ratio; PDA, primary duodenal adenocarcinoma. For calibration curves, red, blue and green lines represent 1, 3, and 5 years, respectively.

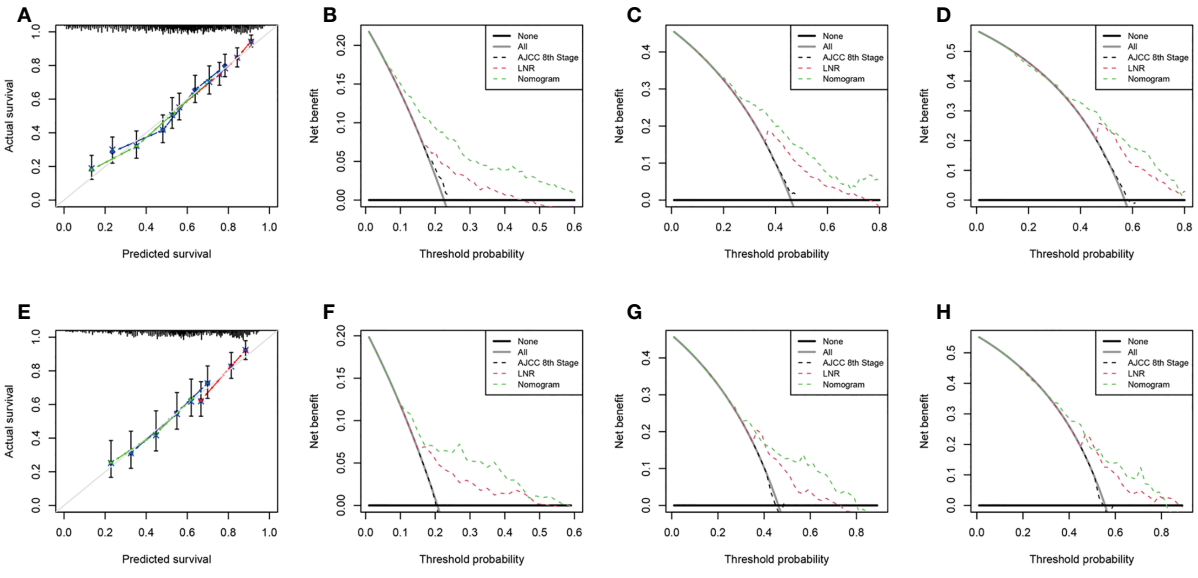

FIGURE 5
Calibration curves for CSS prediction in the training cohort **(A)** and the validation cohort **(E)**. Decision curve analysis of the AJCC 8th edition staging system, nomogram and LNR for the 1- **(B)**, 3- **(C)** and 5-year **(D)** CSS rates of PDA patients from the training cohort. Decision curve analysis of the AJCC 8th edition staging system, nomogram and LNR for the 1- **(F)**, 3- **(G)** and 5-year **(H)** CSS rates of PDA patients from the validation cohort. CSS, cancer-specific survival; LNR, lymph node ratio; PDA, primary duodenal adenocarcinoma. For calibration curves, red, blue and green lines represent 1, 3, and 5 years, respectively.

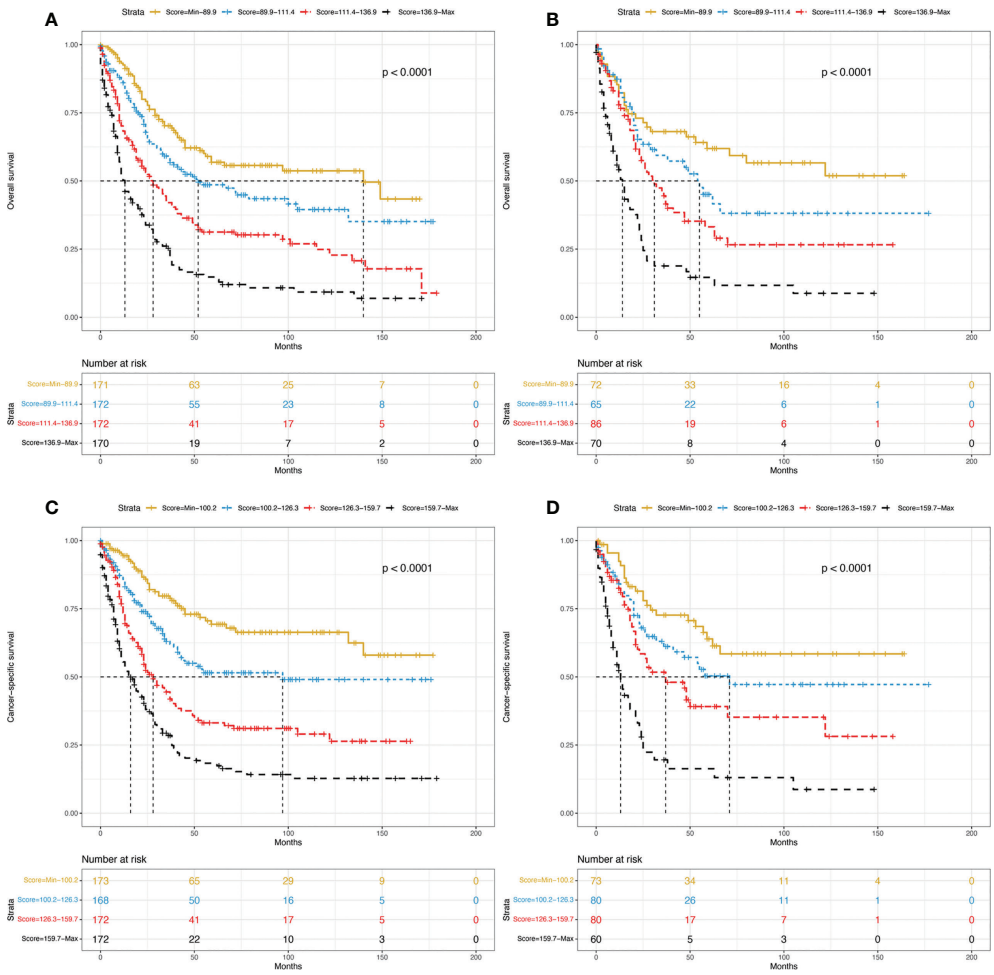

FIGURE 6
Kaplan–Meier curves of OS for the training group **(A)** and validation group **(B)** stratified by different risk scores. Kaplan–Meier curves of CSS for the training group **(C)** and validation group **(D)** stratified by different risk scores. OS, overall survival; CSS, cancer-specific survival.

dose/technology, were unavailable in the SEER dataset. This may have an impact on some results.

In conclusion, this study demonstrated that the LNR is an independent risk indicator for PDAs. Based on the SEER database, we constructed nomograms to predict OS and CSS for PDAs after surgery. These nomograms could assist clinicians in making individualized predictions of patient survival and providing improved treatment suggestions.

Data availability statement

The original contributions presented in the study are included in the article/Supplementary Material. Further inquiries can be directed to the corresponding authors.

Author contributions

All authors helped to perform the research; JS: performed the literature search and wrote the manuscript. SL and JC: performed data collection. SL and SS: contributed to statistical analysis. JZ and YW: contributed to revising the manuscript and study supervision. All authors contributed to the article and approved the submitted version.

Funding

This work was supported by the Tianjin Health Bureau under Grant (No. 2014KR04) and the Key Research Project of Tianjin Health and Family Planning Commission (No. 15KG114).

Acknowledgments

The authors sincerely thank the Surveillance, Epidemiology, and End Results (SEER) program for providing high-quality open resources for researchers.

Conflict of interest

The authors declare that the research was conducted in the absence of any commercial or financial relationships that could be construed as a potential conflict of interest.

Publisher's note

All claims expressed in this article are solely those of the authors and do not necessarily represent those of their affiliated organizations, or those of the publisher, the editors and the reviewers. Any product that may be evaluated in this article, or claim that may be made by its manufacturer, is not guaranteed or endorsed by the publisher.

Supplementary material

The Supplementary Material for this article can be found online at: https://www.frontiersin.org/articles/10.3389/fonc.2022.962381/full#supplementary-material

References

1. Li TY, Chen QC, Zhao H, Zhang YF, Zhao JJ, Cai JQ. Prognostic factors for overall survival in patients with primary duodenal adenocarcinoma. *Ann Palliat Med* (2021) 10:2781–90. doi: 10.21037/apm-20-1280

2. Jiang QL, Huang XH, Chen YT, Zhang JW, Wang CF. Prognostic factors and clinical characteristics of patients with primary duodenal adenocarcinoma: A single-center experience from China. *BioMed Res Int* (2016) 2016:6491049. doi: 10.1155/2016/6491049

3. Zhu Z, Zhong F. Comparative analysis of outcomes and clinicopathological characteristics of duodenal adenocarcinoma: A SEER analysis. *Cancer Invest* (2020) 38:543–8. doi: 10.1080/07357907.2020.1824260

4. Zhang S, Cui Y, Zhong B, Xiao W, Gong X, Chao K, et al. Clinicopathological characteristics and survival analysis of primary duodenal cancers: A 14-year experience in a tertiary centre in south China. *Int J Colorectal Dis* (2011) 26:219–26. doi: 10.1007/s00384-010-1063-x

5. He C, Mao Y, Wang J, Duan F, Lin X, Li S. Nomograms predict long-term survival for patients with periampullary adenocarcinoma after pancreatoduodenectomy. *BMC Cancer* (2018) 18:327. doi: 10.1186/s12885-018-4240-x

6. Sun H, Liu Y, Lv L, Li J, Liao X, Gong W. Prognostic factors and clinical characteristics of duodenal adenocarcinoma with survival: A retrospective study. *Front Oncol* (2021) 11:795891. doi: 10.3389/fonc.2021.795891

7. Solaini L, Jamieson NB, Metcalfe M, Abu Hilal M, Soonawalla Z, Davidson BR, et al. Outcome after surgical resection for duodenal adenocarcinoma in the UK. *Br J Surg* (2015) 102:676–81. doi: 10.1002/bjs.9791

8. Li D, Si X, Wan T, Zhou Y. Outcomes of surgical resection for primary duodenal adenocarcinoma: A systematic review. *Asian J Surg* (2019) 42:46–52. doi: 10.1016/j.asjsur.2018.04.005

9. Poultsides GA, Huang LC, Cameron JL, Tuli R, Lan L, Hruban RH, et al. Duodenal adenocarcinoma: clinicopathologic analysis and implications for treatment. *Ann Surg Oncol* (2012) 19:1928–35. doi: 10.1245/s10434-011-2168-3

10. Zhou J, Lin Z, Lyu M, Chen N, Liao H, Wang Z, et al. Prognostic value of lymph node ratio in non-small-cell lung cancer: A meta-analysis. *Jpn J Clin Oncol* (2020) 50:44–57. doi: 10.1093/jjco/hyz120

11. Macedo F, Sequeira H, Ladeira K, Bonito N, Viana C, Martins S. Metastatic lymph node ratio as a better prognostic tool than the TNM system in colorectal cancer. *Future Oncol* (2021) 17:1519–32. doi: 10.2217/fon-2020-0993

12. Shi J, Liu S, Cao J, Shan S, Ren C, Zhang J, et al. Prognostic nomogram based on the metastatic lymph node ratio for $T_{1\text{-}4}N_{0\text{-}1}M_0$ pancreatic neuroendocrine tumors after surgery. *Front Oncol* (2022) 12:899759. doi: 10.3389/fonc.2022.899759

13. Wang N, Yang J, Lyu J, Liu Q, He H, Liu J, et al. A convenient clinical nomogram for predicting the cancer-specific survival of individual patients with small-intestine adenocarcinoma. *BMC Cancer* (2020) 20:505. doi: 10.1186/s12885-020-06971-6

14. Li H, He Y, Huang L, Luo H, Zhu X. The nomogram model predicting overall survival and guiding clinical decision in patients with glioblastoma based on the SEER database. *Front Oncol* (2020) 10:1051. doi: 10.3389/fonc.2020.01051

15. Huang H, Fang W, Lin Y, Zheng Z, Wang Z, Chen X, et al. Predictive model for overall survival and cancer-specific survival in patients with esophageal adenocarcinoma. *J Oncol* (2021) 2021:4138575. doi: 10.1155/2021/4138575

16. Liu Q, Li W, Xie M, Yang M, Xu M, Yang L, et al. Development and validation of a SEER-based prognostic nomogram for cervical cancer patients below the age of 45 years. *Bosn J Basic Med Sci* (2021) 21:620–31. doi: 10.17305/bjbms.2020.5271

17. Fitzgerald M, Saville BR, Lewis RJ. Decision curve analysis. *JAMA* (2015) 313:409–10. doi: 10.1001/jama.2015.37

18. Camp RL, Dolled-Filhart M, Rimm DL. X-Tile: a new bio-informatics tool for biomarker assessment and outcome-based cut-point optimization. *Clin Cancer Res* (2004) 10:7252–9. doi: 10.1158/1078-0432.CCR-04-0713

19. Schober P, Boer C, Schwarte LA. Correlation coefficients: Appropriate use and interpretation. *Anesth Analg* (2018) 126:1763–8. doi: 10.1213/ANE.0000000000002864

20. Sakamoto T, Saiura A, Ono Y, Mise Y, Inoue Y, Ishizawa T, et al. Optimal lymphadenectomy for duodenal adenocarcinoma: Does the number alone matter? *Ann Surg Oncol* (2017) 24:3368–75. doi: 10.1245/s10434-017-6044-7

21. Meijer LL, Alberga AJ, de Bakker JK, van der Vliet HJ, Le Large TYS, van Grieken NCT, et al. Outcomes and treatment options for duodenal adenocarcinoma: A systematic review and meta-analysis. *Ann Surg Oncol* (2018) 25:2681–92. doi: 10.1245/s10434-018-6567-6

22. Nakamura S, Kanda M, Ito S, Mochizuki Y, Teramoto H, Ishigure K, et al. Accurate risk stratification of patients with node-positive gastric cancer by lymph node ratio. *World J Surg* (2020) 44:4184–92. doi: 10.1007/s00268-020-05739-0

23. Peng JS, Morris-Stiff G, Ali NS, Wey J, Chalikonda S, El-Hayek KM, et al. Neoadjuvant chemoradiation is associated with decreased lymph node ratio in borderline resectable pancreatic cancer: A propensity score matched analysis. *Hepatobiliary Pancreat Dis Int* (2021) 20:74–9. doi: 10.1016/j.hbpd.2020.08.001

24. Lino-Silva LS, Gómez-Álvarez MA, Salcedo-Hernández RA, Padilla-Rosciano AE, López-Basave HN. Prognostic importance of lymph node ratio after resection of ampullary carcinomas. *J Gastrointest Oncol* (2018) 9:1144–9. doi: 10.21037/jgo.2018.07.04

25. Jensen KK, Storkholm JH, Chen I, Burgdorf SK, Hansen CP. Long-term results after resection of primary duodenal adenocarcinoma: A retrospective cohort study. *Int J Surg* (2022) 100:106599. doi: 10.1016/j.ijsu.2022.106599

26. Tran TB, Qadan M, Dua MM, Norton JA, Poultsides GA, Visser BC. Prognostic relevance of lymph node ratio and total lymph node count for small bowel adenocarcinoma. *Surgery* (2015) 158:486–93. doi: 10.1016/j.surg.2015.03.048

27. Liang TJ, Wang BW, Liu SI, Chou NH, Tsai CC, Chen IS, et al. Number of involved lymph nodes is important in the prediction of prognosis for primary duodenal adenocarcinoma. *J Chin Med Assoc* (2012) 75:573–80. doi: 10.1016/j.jcma.2012.08.002

28. Jiang S, Zhao R, Li Y, Han X, Liu Z, Ge W, et al. Prognosis and nomogram for predicting postoperative survival of duodenal adenocarcinoma: A retrospective study in China and the SEER database. *Sci Rep* (2018) 8:7940. doi: 10.1038/s41598-018-26145-6

29. Wang N, Bu Q, Liu Q, Yang J, He H, Liu J, et al. Effect of marital status on duodenal adenocarcinoma survival: A surveillance epidemiology and end results population analysis. *Oncol Lett* (2019) 18:1904–14. doi: 10.3892/ol.2019.10475

30. Malleo G, Tonsi A, Marchegiani G, Casarotto A, Paiella S, Butturini G, et al. Postoperative morbidity is an additional prognostic factor after potentially curative pancreaticoduodenectomy for primary duodenal adenocarcinoma. *Langenbecks Arch Surg* (2013) 398:287–94. doi: 10.1007/s00423-012-0978-9

31. Kato Y, Takahashi S, Kinoshita T, Shibasaki H, Gotohda N, Konishi M. Surgical procedure depending on the depth of tumor invasion in duodenal cancer. *Jpn J Clin Oncol* (2014) 44:224–31. doi: 10.1093/jjco/hyt213

32. Ecker BL, McMillan MT, Datta J, Mamtani R, Giantonio BJ, Dempsey DT, et al. Efficacy of adjuvant chemotherapy for small bowel adenocarcinoma: A propensity score-matched analysis. *Cancer* (2016) 122:693–701. doi: 10.1002/cncr.29840

33. Cloyd JM, Norton JA, Visser BC, Poultsides GA. Does the extent of resection impact survival for duodenal adenocarcinoma? Analysis of 1,611 cases. *Ann Surg Oncol* (2015) 22:573–80. doi: 10.1245/s10434-014-4020-z

34. Sarela AI, Brennan MF, Karpeh MS, Klimstra D, Conlon KC. Adenocarcinoma of the duodenum: importance of accurate lymph node staging and similarity in outcome to gastric cancer. *Ann Surg Oncol* (2004) 11:380–6. doi: 10.1245/ASO.2004.05.021

frontiers | Frontiers in Oncology

TYPE Original Research
PUBLISHED 13 October 2022
DOI 10.3389/fonc.2022.1015916

Check for updates

OPEN ACCESS

EDITED BY
Zhendong Jin,
Second Military Medical University, China

REVIEWED BY
Bin Zhang,
The Affiliated Hospital of Xuzhou Medical University, China
Xiaoli Yang,
General Hospital of Ningxia Medical University, China

*CORRESPONDENCE
Bing-Rong Liu
fccliubr@zz.edu.cn

SPECIALTY SECTION
This article was submitted to Gastrointestinal Cancers: Gastric and Esophageal Cancers, a section of the journal Frontiers in Oncology

RECEIVED 10 August 2022
ACCEPTED 06 September 2022
PUBLISHED 13 October 2022

CITATION
Li D-L, Zhou Y-Y, Zhang J-Y, Liu D, Zhao L-X and Liu B-R (2022) Laparoscopic resection is not superior to endoscopic resection for relative small gastric gastrointestinal stromal tumors: A propensity score-matched study. *Front. Oncol.* 12:1015916. doi: 10.3389/fonc.2022.1015916

COPYRIGHT
© 2022 Li, Zhou, Zhang, Liu, Zhao and Liu. This is an open-access article distributed under the terms of the Creative Commons Attribution License (CC BY). The use, distribution or reproduction in other forums is permitted, provided the original author(s) and the copyright owner(s) are credited and that the original publication in this journal is cited, in accordance with accepted academic practice. No use, distribution or reproduction is permitted which does not comply with these terms.

Laparoscopic resection is not superior to endoscopic resection for relative small gastric gastrointestinal stromal tumors: A propensity score-matched study

De-Liang Li, Yang-Yang Zhou, Ji-Yu Zhang, Dan Liu, Li-Xia Zhao and Bing-Rong Liu*

Department of Gastroenterology and Hepatology, The First Affiliated Hospital of Zhengzhou University, Zhengzhou, China

Background and Aim: Endoscopic resection (ER) and laparoscopic resection (LAP) have been recommended for the treatment of gastric gastrointestinal stromal tumors (GISTs) less than 2 cm. However, the therapeutic approach for gastric GISTs between 2 and 5 cm in diameter is still under debate. In this retrospective study, we aimed to evaluate the feasibility, efficacy, and safety of ER for gastric GISTs (2–5 cm) compared with LAP.

Methods: From January, 2011 to January, 2018, 197 patients with GISTs at our institution with tumor diameter between 2 and 5 cm were included in our study. Clinical baseline characteristics, histopathological results, and perioperative outcomes were collected and compared in all the patients. Propensity score matching (PSM) methods were used to balance baseline characteristics.

Results: There was no significant difference in age (p = 0.246), gender (p = 0.572), tumor location (p = 0.333), pathological risk classification (p = 0.543), Ki-67 index (p = 0.212), and follow-up time (p = 0.831) in the ER and LAP groups. However, significance difference was found in times to liquid diet intake (4.45 ± 1.2 vs. 5.40 ± 1.5 days, p = 0.013) and hospital stays (7.72 ± 1.1 vs. 10.01 ± 1.3 days, p < 0.001). During the follow-up period, there was one recurrence in the ER group vs. two recurrences in the LAP group. After PSM, the tumor size was balanced between the two groups with 49 patients in each group. The times to liquid diet intake (4.18 ± 1.3 vs. 5.16 ± 1.6 days, p = 0.042) and hospital stay days (7.12 ± 1.1 vs. 9.94 ± 1.3, p < 0.0001) were still short in the ER group.

Conclusions: ER is more associated with a quick postoperative recovery than LAP. ER could be an alternative approach for gastric GISTs (2–5 cm). However, the long-term follow-up outcomes are still unclear and random control trials are needed.

KEYWORDS

endoscopic resection, laparoscopic resection, gastric GISTs, tumors, comparison

Introduction

Gastrointestinal stromal tumors (GISTs) are the most common mesenchymal lesions, accounting for 1% of gastrointestinal (GI) tumors (1). It can present throughout the GI tract, predominately in the stomach and small intestine (2–4). The clinical incidence of GISTs is about 1 per 100,000 annually with 54% men and 46% women (1). GISTs show a wide variety of clinical manifestations due to potential malignancy, the prognosis of which is difficult to predict and related to tumor size, mitotic index, KI-67, proliferative index, etc. (5).

With the development of the endoscopic technique, the detective rate of GISTs obviously increased (6). For small GISTs (<2 cm), endoscopic surveillance and follow-up are recommended. For non-metastatic GISTs with size >2 cm, tumor resection is the first-line treatment according to the National Comprehensive Cancer Network (NCCN) guidelines. GISTs have a low rate of lymphatic metastasis; local resection without lymphadenectomy is admitted. Large GISTs (>5 cm) appear to be more aggressive in morphologic features and proliferation activity, so laparoscopic resection (LAP) or surgery is more beneficial for complete resection. However, it is still controversial for the treatment criteria of relatively small GISTs (2–5 cm). Recently, the safety and effectivity of endoscopic resection (ER) have been proven in many studies (7, 8). Compared to LAP, ER is more minimally invasive, although in some cases has limited procedure space. Only a few reports have referred the outcome of ER for gastric GIST (2–5 cm) (9), and little is known about the clinical outcomes of ER procedures in comparison with LAP for gastric GISTs (2–5 cm). Therefore, this retrospective study aimed to compare the safety and feasibility of ER and LAP for gastric GISTs 2–5 cm in diameter in our center.

Materials and methods

Patients

This retrospective study was conducted in the first affiliated hospital of Zhengzhou University from January, 2011 to January, 2018. Patients who underwent curative resection and were confirmed with gastric GISTs by postoperative histopathological examinations were included in our study. Among these patients, 197 patients with tumor between 2 and 5 cm in diameter treated by ER were randomly matched (1:1) using propensity score matching (PSM) methods to patients who underwent LAP. The match criteria were as follows: 1) average age difference between groups <5 years; 2) gender consistency; 3) mean tumor maximum diameter difference between groups <0.5 cm; and 4) consistency of whether neoadjuvant imatinib was administered.

Baseline characteristics and clinicopathological data were obtained from the electronic medical database of our hospital, including age, sex, clinical symptoms, tumor locations, tumor size, and histopathological results. Operation-related outcomes were also collected, including operative duration, intraoperative and postoperative adverse events, time to oral intake, and length of postoperative stay. The median follow-up period, recurrence rate, and overall survival time were also recorded and compared. Informed consents were signed from all the inclusion patients after explaining each treatment management and the possible risks. This study was approved by the Institutional Review Board of The First Affiliated Hospital of Zhengzhou University.

Surgical procedures

Procedures were performed under anesthesia with tracheal intubation. Endoscopic resection includes endoscopic submucosal dissection (ESD) and endoscopic full-thickness resection (EFTR). The ESD procedure mainly included three steps as follows: (i) identifying and marking the tumor boundaries; (ii) injecting the saline water mixed with indigo carmine to the submucosal layer; and (iii) incising the mucosal layer with a hook knife and dissecting the tumor using the IT knife.

EFTR enables the resection of tumors that originated from the muscularis propria or serosal layer. The technique mainly has five steps: (i) marking the dots around the tumor using argon plasma coagulation; (ii) injecting the saline water into the submucosal layer; (iii) incising and dissecting the mucosa; (iv) resecting on full thickness; and (v) clipping the incision.

The LAP procedure includes the following steps: (i) Establish an initial access site and use carbon dioxide to create the pneumoperitoneum at a pressure of 12 mmHg. (ii) Four additional trocars are placed in an inverted trapezoidal setting in both procedures. (iii) Before resection, check out the overall abdominal situation. (iv) The wedge resection or gastrectomy is performed according to the tumor size and location. (v) Make sure that the gastric-wall defect is closed with a laparoscopic linear stapler or hand-sewn.

Histopathological evaluation

The resected specimens were fixed and sent to the pathological department. Hematoxylin and eosin (HE) and

immunohistochemicals were applied in all specimens, including the cell type, the mitotic index (MI), and the risk and related immunohistochemical markers.

Follow-up strategy

All patients received telephone follow-up or outpatient services within 1 month after being discharged to determine whether short-term complications occurred. Regular outpatient follow-up was performed according to the following strategy: 3, 6, and 12 months and yearly thereafter. Endoscopy and computed tomography (CT) were performed on every outpatient follow-up. Endoscopic examination was performed to assess the healing of the wound, and computed tomography (CT) evaluated the extent of the tumor. Recurrence was confirmed by CT scans and endoscopic ultrasound (EUS) was applied if necessary.

Statistical analysis

The main observational indicators included patient clinicopathological characters, perioperative results, and follow-up outcomes. Data were analyzed using SPSS 22.0 (International Business Machines Corporation, Chicago, IL, USA). Continuous data are shown as mean and standard deviation. Categorical data are expressed as frequency. Statistical differences between groups were performed using Student's *t*-test for continuous data and chi-square test or Fisher's exact test for categorical data. $p < 0.05$ was considered statistically significant.

Results

Clinical baseline data

The patients with GISTs who underwent surgical treatment in our hospital were retrospectively analyzed. According to the inclusion and exclusion criteria, 197 cases were finally included in this study with 74 cases in the ER group and 123 cases in the LAP group. The average age of the patients in the ER group was 59.5 years, and the ratio of male to female patients was 30:44; the average age of the patients in the laparoscopic group was 57.6 years, and the ratio of male to female patients was 57:66. The most common location distribution of tumors was the gastric fundus in both groups. There was no significant difference in age (59.50 vs. 57.57, $p = 0.246$), gender ($p = 0.572$), and tumor location ($p = 0.333$) between the two groups, but there was a statistically significant difference in tumor size (27.59 mm vs. 33.24 mm, $p < 0.001$).

Operative and pathological outcomes

All the 197 patients underwent tumor resection successfully. The ER group had significant advantages in postoperative fasting time and postoperative hospital stay, which were significantly shorter than those in the laparoscopic group (4.45 ± 1.2 days vs. 5.40 ± 1.5 days, $p = 0.013$; 7.72 ± 1.1 days vs. 10.01 ± 1.3, $p < 0.001$). There was no significant difference in operation time (98.80 ± 12.0 min vs. 110.79 ± 15.5 min, $p = 0.110$).

According to histological outcomes, 11, 26, 10, and 11 patients were identified to have very low-, low-, middle-, and high-risk GISTs in the ER group, respectively. In the LAP group, 16, 54, 37, and 16 patients were identified to have very low-, low-, middle-, and high-risk GISTs, respectively. The risk classifications had no difference between the two groups ($p = 0.543$). Moreover, 33, 29, and 12 patients were identified to have a Ki-67 index of <5%, 5%–10%, and >10% in the ER group, respectively. In the LAP group, 39, 63, and 21 patients were identified to have a Ki-67 index of <5%, 5%–10%, and >10%, respectively. The Ki-67 index had no significant difference between the two groups ($p = 0.212$).

Postoperative compilations

Six complications in 74 cases were found in the ER group, namely five cases of perforation and one case of pleural effusion. Eight complications in 123 cases in the LAP group were found, namely three cases of bleeding, two cases of intestinal obstruction, one case of perforation, one case of incision fat liquefaction, and one case of unstable vital signs. The postoperative complication rate had no difference between the two groups ($p = 0.853$).

In the ER group, two cases were converted to laparoscopic treatment during the operation, and 10 cases in the laparoscopic group were converted to open surgery due to the inability to resect the tumor entirely (Table 2).

Follow-up

A total of 197 patients were followed up by gastroscopy and CT scans. The mean follow-up times were 54.27 ± 12.6 and 55.96 ± 13.5 months, respectively. Ten patients in the LAP group were treated by imatinib, but only one patient received imatinib therapy. During the follow-up period, there was one recurrence in the ER group and two recurrences in the LAP group.

Propensity score matching analysis

Because the difference in tumor size between the two groups was obvious, it was considered a confounder. Propensity score matching (PSM) (1:1) was performed on the two groups of cases, and 49 pairs were successfully matched. A total of 98 matched patients were statistically analyzed, and there were no significant differences in age (58.82 vs. 57.31, p = 0.462), gender (p = 0.682), tumor location, (p = 0.727), and tumor size (29.78 mm vs. 29.53 mm, p = 0.897) between the two groups (Table 1).

There were two complications in 49 cases in the ER group, namely two cases of perforation. There were two complications in 49 cases in the laparoscopic group, namely one case of bleeding and one case of perforation. In the ER group, two cases were converted to laparoscopic treatment during the operation, and three cases in the LAP group were converted to open surgery due to inability to resect the tumor entirely (Table 2). The postoperative complications had no difference between the two groups (p = 1.00). However, the postoperative hospital stay (p < 0.01) and the time to first oral intake (p < 0.001) were still shorter in the ER group. Moreover, one patient experienced recurrence in each group (p = 1.00).

Discussion

Gastrointestinal stromal tumors (GISTs), the most common mesenchymal neoplasms, have been shown to be derived from interstitial Cajal cells (1). With a wide variety of clinical manifestations, it can be present throughout the GI tract, predominantly in the stomach (50%–60%). The incidence of GISTs is about 1 per 100,000 annually, which is still a threat to human health due to the potential malignance existing in all the GISTs.

Complete resection is still the first-line treatment for non-metastasis GISTs (10). Most GISTs rarely have lymphatic metastasis, so local resection without lymphadenectomy is admitted. Endoscopic surveillance and follow-up are currently recommended for GISTs larger than 2 cm. Sometimes it burdens patients emotionally and financially, so tumor resection is often selected. Large GISTs (>5 cm) appear to be more aggressive in morphologic features and proliferation activity, so laparoscopic resection (LAP) or even more surgery is more beneficial for complete resection. However, it is still controversial about the treatment criteria for relatively small GISTs (2–5 cm). With the development of laparoscopic and endoscopic techniques, these minimally invasive operations can achieve both surgical negative margin and an intact capsule of the GISTs. Few studies have

TABLE 1 Baseline characteristics of patients with gastric GISTs (2–5 cm) undergoing ER or LAP in the cohort.

Variable	Before matching			After matching		
	ER (n=74)	LAP (n=123)	P	ER (n=49)	LAP (n=49)	P
Age average±SD, year	59.50±13.45	57.57±12.15	0.246	58.82±14.13	57.31±16.13	0.462
Gender			00.572			0.682
Male	30	57		29	31	
Female	44	66		20	18	
Tumor size mean mm	27.59	33.24	<0.001	29.78	29.53	0.897
Location			0.333			0.727
Cardia	2	4		1	1	
Gastric fundus	48	73		34	31	
Gastric body	23	41		14	16	
Gastric antrum	1	5		0	1	
Risk classification			0.543			
Very low	11	16				
Low	26	54				
Middle	10	37				
High	11	16				
Ki-67			0.212			
<5	33	39				
05-10	29	63				
>10	12	21				
Follow-up			0.831			
Time average±SD, month	54.27±12.6	55.96±13.5		51.55 (30-98)	57.90 (33-93)	
Recurrence	1	2		1	1	

SD, standard deviation; ER, endoscopic resection; LAP, laparoscopic resection.

TABLE 2 Therapeutic outcomes of included patients.

Variable	Before matching			After matching		
	ER (n = 74)	LAP (n = 123)	P	ER (n = 49)	LAP (n = 49)	P
Operation time average ± SD, min	98.80 ± 12.0	110.79 ± 15.5	0.11	94.55 (39-211)	105.9 (30-250)	0.235
Transfer operation approach	2	10		2	3	
Time to liquid diet average ± SD, days	4.45 ± 1.2	5.40 ± 1.5	0.013	4.18 ± 1.3	5.16 ± 1.6	0.042
Hospital stay average ± SD, days	7.72 ± 1.1	10.01 ± 1.3	<0.001	7.12 ± 1.1	9.94 ± 1.3	<0.001
Adverse events			0.853			0.001
Bleeding	0	3		0	1	
Perforation	5	1		2	1	
Pleural effusion	1	1		0	0	
Intestinal obstruction	0	2		0	0	
Others	0	1		0	0	
Postoperative imatinib therapy	1	10		1	5	

made a comparison of the safety and effectiveness between laparoscopic resection and endoscopic resection. In this study, we thoroughly examined two types of minimally invasive resection treatment for gastric GISTs with diameters ranging from 2 to 5 cm.

Through previous review of literature, guidelines, and a summary of clinical experience, we determined that the tumor diameter is an important factor affecting the selection of approach (11). It has certain effects on operation time, postoperative recovery, and even disease prognosis. By comparing the clinical baseline data of the two groups, it was found that the tumor size in the endoscopic group was significantly lower than that in the laparoscopic group, so we included "tumor diameter" into the PSM variable for analysis. The location of the tumor also affects the choice of surgery to some extent (11). In the laparoscopic group, 10 cases were converted to open surgery, of which five cases were located in the lesser curvature of the gastric body (near the posterior wall of the gastric angle), four cases were located in the greater curvature of the fundus, and one case was located in the greater curvature of the gastric body. We therefore included "tumor location" in the analysis.

Considering that too many covariates will result in too much loss of the output data of this study, we only included patient age and gender in the variable analysis. In the end, 49 cases in the endoscopic treatment group and 49 cases in the laparoscopic treatment group were successfully matched. After matching, there were no significant differences in patient age, gender, tumor size, and tumor diameter between the two groups. In terms of operation-related indicators, the postoperative fasting time and postoperative hospital stay of the endoscopic group were significantly shorter than those of the laparoscopic group, which showed the minimally invasive advantages of endoscopic treatment, consistent with the results of Wang et al. In terms of operation time, the advantage of the endoscopic group is not obvious, and there is no statistical difference between the two groups. Considering that the data range included in this study is between, 2011 and, 2018, it represents the continuous development of domestic endoscopic technology on the basis of ESD. In the past 10 years, the performance of operations, endoscopic care cooperation, and suturing technology has been unstable, and it has not reached the maturity of laparoscopic technology in the same period; these cases were not operated on by the same endoscopist.

In terms of complications, no difference was observed between the two groups. However, Pang et al. compared endoscopic (n = 268) and surgical (including open and laparoscopic resection, n = 141) resection of small GISTs (<5 cm) in, 2019 (8). They discovered that endoscopic resection was always associated with a lower incidence of complications even after a propensity score matching analysis (3.6% vs. 13.1%, p = 0.026), suggesting endoscopic resection as a safe and promising alternative treatment for gastric GIST. Other previous studies in the past decades found that endoscopy had a similar or higher incidence of complications compared with laparoscopy; the conclusion was consistent with ours (12, 13). Therefore, whether ER has the advantage of safety should be verified in future studies, but the advantage of promoting quick recovery has no doubt in our study cohort.

The majority of the lesions may be endoscopically removed with a full capsule when seen macroscopically. The burnt edge on the capsule, however, may lead to a pathological diagnosis of R1 resection when examined under a microscope. Even in the hands of seasoned professionals, this is sometimes unavoidable and is not seen as learning-curve-related. Fortunately, research has shown that patients who receive R0 and R1 resection do not significantly vary in terms of relapse-free survival (RFS) (14, 15). Thus, despite resection margin involvement, endoscopic resection for stomach GISTs was still seen as a viable option (16), and the margin status was not analyzed in our study.

During the follow-up period, one patient died due to recurrence and metastasis in the endoscopic group but none in the laparoscopic group. There was one case of recurrence and metastasis in the endoscopic group and two cases of recurrence and metastasis in the laparoscopic group. The pathological results of these three patients suggested that they were all high-risk types. The recurrence rate was similar between the two groups. However, one study did find a high local recurrence rate (5.8%) after endoscopic enucleation of 86 GISTs, especially in large tumors (17), though complete endoscopic resection was achieved in all cases in this study. Our results also showed that patients in the ER group had smaller tumors than those in the surgical group. It may have been expected that endoscopic resection should also have advantages in OS and RFS than in surgical resection, but this was not the case. This may be due to the small sample size and short follow-up period. Long-term outcomes of GISTs still require confirmation in more prospective studies or multicenter studies.

This study has some limitations. It is a single-center retrospective study with a relatively small sample size, and there is a certain selection bias in the sample data. Therefore, it is necessary to further verify the above results through a multicenter prospective study. Endoscopic treatment is becoming more and more mature, and data over a longer time span could be collected for comprehensive analysis. The evaluation of patients' satisfaction with perioperative management was not included in this study, and it is recommended to add this indicator in future research.

Conclusion

In conclusion, in this retrospective study, the clinical baseline data of the two groups of patients were unevenly distributed. After propensity score matching, there was no statistical difference in age, gender, tumor size, and tumor diameter between the two groups. The matched endoscopic group was significantly better than the laparoscopic group in terms of postoperative fasting time and postoperative hospital stay. During the average follow-up of 55.12 months, there was no significant difference in the postoperative long-term efficacy between the two groups. Endoscopic resection treatment is safe and feasible for primary gastric stromal tumors with a diameter of 2–5 cm, and further research needs to be confirmed by multicenter prospective trials.

Data availability statement

The original contributions presented in the study are included in the article/supplementary material. Further inquiries can be directed to the corresponding author.

Ethics statement

This study was reviewed and approved by The First Affiliated Hospital of Zhengzhou University. The patients/participants provided their written informed consent to participate in this study.

Author contributions

Study concept and design: D-LL, B-RL. Manuscript writing: D-LL, Y-YZ. Technical and material support: Y-YZ, J-YZ, DL, L-XZ. Data collection: Y-YZ, J-YZ, DL, L-XZ. Revision of manuscript: B-RL. All authors contributed to the article and approved the submitted version.

Funding

1. Zhongyuan talent program (NO: ZYYCYU202012113) 2. The key R&D program of Henan Province (No., 222102310038) 3. Henan key medical laboratory: Innovative technology for minimally invasive treatment of digestive endoscope.

Conflict of interest

The authors declare that the research was conducted in the absence of any commercial or financial relationships that could be construed as a potential conflict of interest.

Publisher's note

All claims expressed in this article are solely those of the authors and do not necessarily represent those of their affiliated organizations, or those of the publisher, the editors and the reviewers. Any product that may be evaluated in this article, or claim that may be made by its manufacturer, is not guaranteed or endorsed by the publisher.

References

1. Li J, Shen L. The current status of and prospects in research regarding gastrointestinal stromal tumors in china. *Cancer* (2020) 126(S9):2048–53. doi: 10.1002/cncr.32684

2. Rubin BP, Singer S, Tsao C, Duensing A, Lux ML, Ruiz R, et al. Kit activation is a ubiquitous feature of gastrointestinal stromal tumors. *Cancer Res* (2001) 61 (22):8118–21.

3. Rubin B, Heinrich M, Corless C. Gastrointestinal stromal tumour. *Lancet (Lond Engl)* (2007) 369(9574):1731–41. doi: 10.1016/S0140-6736(07)60780-6

4. von Mehren M, Joensuu H. Gastrointestinal stromal tumors. *J Clin Oncol Off J Am Soc Clin Oncol* (2018) 36(2):136–43. doi: 10.1200/JCO.2017.74.9705

5. Demetri GD, Benjamin RS, Blanke CD, Blay JY, Casali P, Choi H, et al. Nccn task force report: Management of patients with gastrointestinal stromal tumor (gist)–update of the nccn clinical practice guidelines. *J Natl Compr Cancer Network JNCCN* (2007) 126(S9):S1–29: quiz S30. doi: 10.6004/jnccn.2007.2002

6. Mei L, Du W, Idowu M, von Mehren M, Boikos SA, et al. Advances and challenges on management of gastrointestinal stromal tumors. *Front Oncol* (2018) 8. doi: 10.3389/fonc.2018.00135

7. Liu S, Zhou X, Yao Y, Shi K, Yu M, Ji F, et al. Resection of the gastric submucosal tumor (g-smt) originating from the muscularis propria layer: Comparison of efficacy, patients' tolerability, and clinical outcomes between endoscopic full-thickness resection and surgical resection. *Surg Endoscopy* (2020) 34(9):4053–64. doi: 10.1007/s00464-019-07311-x

8. Pang T, Zhao Y, Fan T, Hu Q, Raymond D, Cao S, et al. Comparison of safety and outcomes between endoscopic and surgical resections of small (≤ 5 cm) primary gastric gastrointestinal stromal tumors. *J Cancer* (2019) 10(17):4132–41. doi: 10.7150/jca.29443

9. Chen L, Zhang Q, Li FY, Yang L, Zhang DC, Wang LJ, et al. Comparison of treatment outcomes between laparoscopic and endoscopic surgeries for relatively small gastric gastrointestinal stromal tumors. *Surg Oncol* (2018) 27(4):737–42. doi: 10.1016/j.suronc.2018.10.002

10. Patel S, Reichardt P. An updated review of the treatment landscape for advanced gastrointestinal stromal tumors. *Cancer* (2021) 127(13):2187–95. doi: 10.1002/cncr.33630

11. Yadav SC, Menon S, Bakshi G, Katdare A, Ramadwar M, Desai SB, et al. Gastrointestinal stromal tumor presenting with lower urinary tract symptoms - a series of five cases with unusual clinical presentation. *Indian J Urol IJU J Urological Soc India* (2021) 37(4):357–60. doi: 10.4103/iju.iju_267_21

12. Wang C, Gao Z, Shen K, Cao J, Shen Z, Jiang K, et al. Safety and efficiency of endoscopic resection versus laparoscopic resection in gastric gastrointestinal stromal tumours: a systematic review and meta-analysis. *Eur J Surg.Oncol* (2020) 46:667–74. doi: 10.1016/j.ejso.2019.10.030

13. Lei T, Tan F, Liu H, Ouyang M, Zhou H, Liu P, et al. Endoscopic or surgical resection for patients with 2–5 cm gastric gastrointestinal stromal tumors: a single-center 12-year experience from China. *Cancer Manag Res* (2020) 12:7659–70. doi: 10.2147/CMAR.S266898

14. Zhu Y, Xu MD, Xu C, Zhang XC, Chen SY, Zhong YS, et al. Microscopic positive tumor margin does not increase the rate of recurrence in endoscopic resected gastric mesenchymal tumors compared to negative tumor margin. *Surg Endosc* (2020) 34:159–69. doi: 10.1007/s00464-019-06744-8

15. McCarter MD, Antonescu CR, Ballman KV, Maki RG, Pisters PW, Demetri GD, et al. Microscopically positive margins for primary gastrointestinal stromal tumors: analysis of risk factors and tumor recurrence. *J Am Coll Surg* (2012) 215:53–9;discussion 59-60. doi: 10.1016/j.jamcollsurg.2012.05.008

16. Liu YB, Liu XY, Fang Y, Chen TY, Hu JW, Chen WF, et al. Comparison of safety and short-term outcomes between endoscopic and laparoscopic resections of gastric gastrointestinal stromal tumors with a diameter of 2-5 cm. *J Gastroenterol Hepatol* (2022) 37(7):1333–41. doi: 10.1111/jgh.15834

17. Wang Y, Li Y, Luo H, Yu H. Efficacy analysis of endoscopic submucosal excavation for gastric gastrointestinal stromal tumors. *Zhonghua Wei Chang Wai Ke Za Zhi* (2014) 17(4):352–5.

frontiers | Frontiers in Oncology

TYPE Original Research
PUBLISHED 14 October 2022
DOI 10.3389/fonc.2022.1048348

Check for updates

OPEN ACCESS

EDITED BY
Zhendong Jin,
Second Military Medical University, China

REVIEWED BY
Hafiz Abdul Waqas Ahmed,
Lady Reading Hospital, Pakistan
Usman Ayub Awan,
The University of Haripur, Pakistan

*CORRESPONDENCE
Bowen Hu
fcchubw@zzu.edu.cn
Muhammad Fawad
Fawadkhn42@gmail.com
Xiaolin Xu
xiaolin.xu@zju.edu.cn

SPECIALTY SECTION
This article was submitted to Gastrointestinal Cancers: Hepato Pancreatic Biliary Cancers, a section of the journal Frontiers in Oncology

RECEIVED 19 September 2022
ACCEPTED 26 September 2022
PUBLISHED 14 October 2022

CITATION
Ding H, Fawad M, Xu X and Hu B (2022) A framework for identification and classification of liver diseases based on machine learning algorithms. *Front. Oncol.* 12:1048348. doi: 10.3389/fonc.2022.1048348

COPYRIGHT
© 2022 Ding, Fawad, Xu and Hu. This is an open-access article distributed under the terms of the Creative Commons Attribution License (CC BY). The use, distribution or reproduction in other forums is permitted, provided the original author(s) and the copyright owner(s) are credited and that the original publication in this journal is cited, in accordance with accepted academic practice. No use, distribution or reproduction is permitted which does not comply with these terms.

A framework for identification and classification of liver diseases based on machine learning algorithms

Huanfei Ding[1], Muhammad Fawad[2*], Xiaolin Xu[2*] and Bowen Hu[1*]

[1]The First Affiliated Hospital of Zhengzhou University, Zhengzhou, China, [2]School of Public Health and Second Affiliated Hospital, Zhejiang University School of Medicine, Hangzhou, China

Hepatocellular carcinoma (HCC) is one of the most commonly seen liver disease. Most of HCC patients are diagnosed as Hepatitis B related cirrhosis simultaneously, especially in Asian countries. HCC is the fifth most common cancer and the second most common cause of cancer-related death in the World. HCC incidence rates have been rising in the past 3 decades, and it is expected to be doubled by 2030, if there is no effective means for its early diagnosis and management. The improvement of patient's care, research, and policy is significantly based on accurate medical diagnosis, especially for malignant tumor patients. However, sometimes it is really difficult to get access to advanced and expensive diagnostic tools such as computed tomography (CT), magnetic resonance imaging (MRI) and positron emission tomography (PET-CT)., especially for people who resides in poverty-stricken area. Therefore, experts are searching for a framework for predicting of early liver diseases based on basic and simple examinations such as biochemical and routine blood tests, which are easily accessible all around the World. Disease identification and classification has been significantly enhanced by using artificial intelligence (AI) and machine learning (ML) in conjunction with clinical data. The goal of this research is to extract the most significant risk factors or clinical parameters for liver diseases in 525 patients based on clinical experience using machine learning algorithms, such as regularized regression (RR), logistic regression (LR), random forest (RF), decision tree (DT), and extreme gradient boosting (XGBoost). The results showed that RF classier had the best performance (accuracy = 0.762, recall = 0.843, F1-score = 0.775, and AUC = 0.999) among the five ML algorithms. And the important orders of 14 significant risk factors are as follows: Total bilirubin, gamma-glutamyl transferase (GGT), direct bilirubin, hemoglobin, age, platelet, alkaline phosphatase (ALP), aspartate transaminase (AST), creatinine, alanine aminotransferase (ALT), cholesterol, albumin, urea nitrogen, and white blood

cells. ML classifiers might aid medical organizations in the early detection and classification of liver disease, which would be beneficial in low-income regions, and the relevance of risk factors would be helpful in the prevention and treatment of liver disease patients.

KEYWORDS

hepatocellular carcinoma, hepatitis B cirrhosis, classification, artificial intelligence, liver disease

Introduction

Despite advances in both the diagnostic and management of patients with liver disease, the access for early diagnosis based on basic and cost effective clinical parameters like biochemical and blood routine test is frequently unavailable, which has a large impact on the clinical outcomes and quality of life for patients suffering from liver disease. In addition, it is really difficult to get access to advanced and expensive diagnostic tools such as computed tomography (CT), magnetic resonance imaging (MRI) and positron emission tomography (PET-CT)., especially for people who resides in poverty-stricken area and can't afford these expensive tests.

Hepatocellular carcinoma (HCC) is the fifth most common cancer worldwide, and chronic HBV and HCV infection remains the major etiological contributor of HCC cases globally. WHO estimated that 257 million people (3.5% of the global population) are chronically infected with HBV infection as of the year 2015 (1, 2). The establishment of HBV chronicity depends on the age of exposure. The children younger than age 2 have 90% greater risk of HBV infection than adults (3, 4). Therefore, most chronic HBV infections are acquired vertically (i.e., mother to child transmission) at birth or feeding stage. Universal birth-dose HBV vaccination reduces the prevalence of chronic HBV in newborns (5); thus, most patients with chronic HBV were born in the pre-vaccination era.

Patients with chronic HBV are at risk of liver disease such as cirrhosis and HCC. The incidence of these liver diseases parallels the prevalence of chronic HBV (6), and therefore, the global distributions of chronic HBV and HCC mirror each other (7–10). It is estimated that chronic HBV is etiologically implicated in as many as 50% to 80% of all HCC cases, especially in HBV endemic areas (where chronic HBV prevalence is greater than 8%) (10, 11). The lifetime risk of chronic HBV carriers to develop cirrhosis and/or HCC is 15% to 40% (12, 13). The relative risk ratio of HCC in patients with chronic HBV ranged from 14 to 223 compared with that in noncarriers (14–16). The risk is substantially increased in those patients with liver cirrhosis (17). According to a systematic review in Asia, the incidence rates of HCC were 0.2, 0.6, and 3.7 per 100 person-years in inactive carriers, noncirrhotic chronic HBV, and cirrhotic chronic HBV, respectively (18).

The diagnosis of liver disease or condition depends on the information that includes risk factors that make accurate diagnosis difficult. These risk factors include resource and organizational limits, conflicts, ambiguity, and uncertainty. Many symptoms are vague and vary from person to person. Several diagnostic tests are costly, seldom performed, and often do not provide a black-and-white result. In addition, cognitive bias and improper use of heuristics are common occurrences during the diagnostic phase among physicians. This study intends to present a framework to aid medical professionals and other interested researchers in properly diagnosing liver disease, utilizing comprehensive assessment criteria. The outcomes of this research will aid physicians in making more precise judgments about liver disease identification.

Materials and methods

Patients

The study population consisted of 525 retrospectively reviewed consecutive patients who were suspected to have liver disease at The Affiliated Hospital of Zhengzhou University. We demonstrated the performance of the selected classifier models on the 525 patient's liver disease data. The 525 patients' liver disease data are divided into training and validation subsets. The training sample was used to train a model, and validation was used for model testing. In addition, we compare the classifier models using statistical measures to obtain the best classifier model. Based on the best classifier model, we identified significant factors contributing to liver disease. All results were performed in the R programming language.

Regularized regression (RR) classifier

RR is a classification approach that uses a penalized regression with coefficient estimates biased towards zero to regress the category of interest on text features. In other words, to avoid the problem of

overfitting, this approach prevents us from learning a more complex or flexible model. Ridge, lasso, and elastic net are frequently used penalty parameters for RR. The elastic net is a generalization of the ridge and lasso penalties that combines the two penalties used in the present study (19). The elastic net technique learns from the shortcomings of the lasso and ridge regression methods to improve the RR classifier.

Logistic regression (LR) classifier

The Logistic classifier algorithm is based on LR (20) and used to determine the relationship between a categorical target variable and several input variables. To make predication, as with inputs, it requires actual values based on the probability of an input belonging to a particular class. The probability is determined using a sigmoid function that incorporates the exponential function. LR is frequently used in machine learning due to its high efficiency and low computing resource requirements (21).

Decision tree (DT) classifier

The DT aims to develop a model that predicts the target variable by learning simple decision rules inferred from the input features. DT is the form of a tree that consists of a series of decisions and choices. They determine the class of a variable based on its features. Generally, these classes reside on the last branches of a DT. It may be binary or multi-class classifiers. Multiple rules with binary outcomes are used to build a set of tests that determine the class of a variable based on its features. DTs are an example of a divide and conquer method since they split the variables repeatedly until a final decision is reached (22). Due to their understandability and simplicity, DT is one of the most popular machine learning algorithms (23).

Random forest (RF) classifier

RFs, also known as random decision forests, consist of many random DTs. RFs developed a model using a random sampling of the actual data and a random subset of features (24). This randomness contributes to the model being more resilient than a DT and less prone to overfitting on the training data (25). Each tree provides a classification, which we call a "vote" for that class. The classification with the highest votes is chosen by the forest (over all the trees in the forest) (26).

Extreme gradient boosting (XGBoost) classifier

XGBoost offers a parallel tree-boosting approach that efficiently and precisely addresses various data science issues. The Extreme Gradient boost is a powerful and scalable classification algorithm developed by Chen and Guestrin (27). The fundamental concept of Extreme Gradient boost is the gradient boosting decision tree, which produces the final predictions from the combined prediction of many DTs. In Extreme Gradient boost, each new tree is constructed sequentially, attempting to correct the errors of the previous trees until the number of DTs specifies the threshold.

Performance measures for classification algorithm

After completing the training phase, all the models were tested on the test dataset. The performance of classification algorithms is evaluated through statistical indicators. This study uses four performance indicators: accuracy, precision, recall, F1-score, and area under curve (AUC). The performance measurements utilized in this article are detailed in the following section. Accuracy indicates how closely the measured value corresponds to a known value, while precision provides the accuracy of the model in terms of those predicted to be positive. A recall defines the number of real positives the model collected after being labeled as positive (true positive). The F1 provides a ratio between precision and recall. The receiver operating characteristics (ROC) is a probability curve, whereas AUC reflects the degree of separability. The ROC curve represents the relationship between sensitivity (true positive rate) and specificity (false positive rate) (28, 29).

Results

The collected parameters of liver disease patients included age, gender, albumin, ALP, ALT, AST, total bilirubin, cholinesterase, cholesterol, creatinine, GGT, urine protein, white blood cells, red blood cells, hemoglobin, platelet, direct bilirubin, and urea nitrogen used in the study are displayed in Figure 1. The study consists of 472 male and 53 female patients with an average age of 49.31 years. Among the 525 patients with liver disease, 256 had Hepatitis B cirrhosis, and 269 had Hepatocellular carcinoma.

The findings of the classifier models for testing data based on performance metrics are provided in Table 1. The results highlighted in bold emphasize that a particular classifier model performed significantly better than the other classifier models. The RF classifier obtains the highest accuracy (0.762) among all classifier models, while the RR classifier has the second highest accuracy (0.743). However, the RR classifier had the highest precision (0.731), and the LR classifier had the second-highest precision (0.725). According to Table 1, the classifiers with the best performance in terms of recall are RF, followed by DT. It is also observed from Table 1 that the RF classifier yields the best

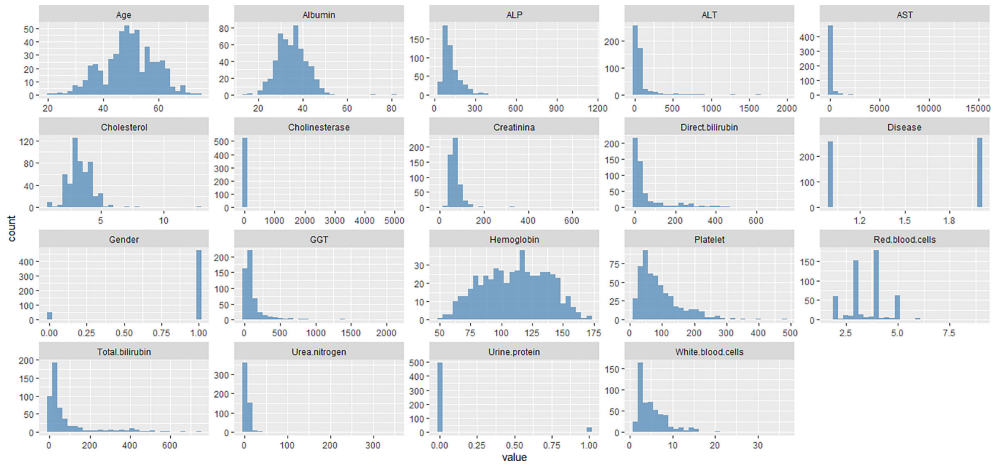

FIGURE 1
Depicts the visual inspection of patient characteristics used in the study.

results in terms of F1-score and AUC, followed by RR and XGBoost classifiers, respectively. Overall, the findings based on performance metrics reveal that the RF has the best classier model for liver disease.

After finding the optimum classier model, next we determine the variables importance based on the RF model, as presented in Figure 2. Variable importance describes the degree to which a model utilizes a certain variable to generate accurate predictions. Variables of high importance are drivers of the output, and their values have a substantial effect on the output values, while variables with little relevance may be excluded from a model to make it easier and quicker to fit and predict. Based on the mean decrease Gini and clinical experience using the RF algorithm, the final 14 important variables are Total bilirubin, GGT, direct bilirubin, hemoglobin, age, platelet, ALP, AST, creatinine, ALT, cholesterol, albumin, urea nitrogen, and white blood cells.

Discussion

HCC is the most common liver disease. HCC etiologies vary based on geography, lifestyle, and advanced medical care facilities availability. Although, NAFLD/NASH and excessive alcohol intake are the important risk factors leading to the development of HCC. However, at present, most of the HCC cases are caused by chronic infection from HBV or HCV (30). With the rising rates of obesity and diabetes mellitus as well as the declining levels of alcohol intake and viral hepatitis infection in many areas, It is expected that NAFLD/NASH will become the most important risk factor for HCC (31). Consequently, it is crucial and should be emphasized on surveillance and early diagnosis of HCC in at-risk populations. Universal unified prevention measures, education on high-risk behaviors, and screening programs for blood donors are crucial to prevent and reduce HBV and HCV induced HCC. However, vaccination is the key to prevent HBV-related HCC. Current antiviral therapies for HBV and HCV infection can only decrease HCC but cannot entirely eradicate it (32). Treatment of HCC has improved substantially over the last decades, with several curative options. Novel therapies, such as radioembolization with 90Y-labeled glass beads, and medications, such as sorafenib and regorafenib, have shown improvements in survival rates. However, there are serval areas where still improvement is needed (33). Additional studies are needed to improve prevention strategies and advance management of

TABLE 1 Performance measure of classifier machine learning models.

Model	Accuracy	Precision	Recall	F1-score	AUC
Regularised regression	0.743	0.731	0.745	0.738	0.815
Logistic regression	0.733	0.725	0.725	0.725	0.819
Random forest	0.762	0.717	0.843	0.775	0.999
Extreme Gradient boosting	0.724	0.704	0.745	0.724	0.989
Decision tree	0.657	0.615	0.784	0.690	0.878

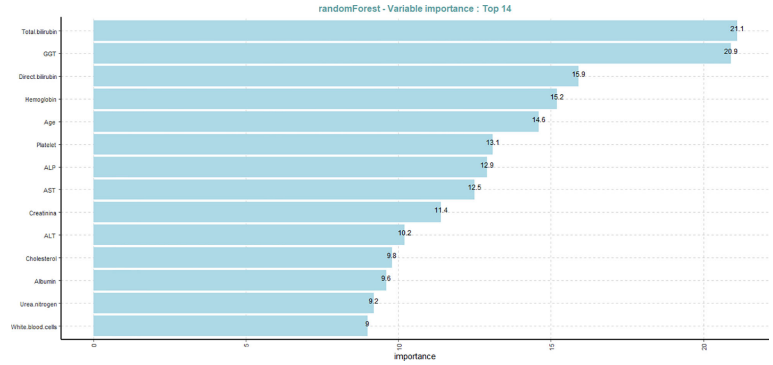

FIGURE 2
Variable importance plot of the 14 risk factors of liver disease based on the random forest classier.

patients with HCC, especially in the field of tumor regression therapies.

In 2015, nearly 1 million persons died because of complications of chronic HBV. In contrast to the reductions in mortality from other important infections, such as HIV, tuberculosis, and malaria, the mortality from chronic HBV-related complications increased over the past decade (1). Specifically, HBV cirrhosis-related deaths were 241,700 in 1990 compared with 312,400 in 2010. The numbers of deaths from chronic HBV-related HCC were 210,200 in 1990 compared with 341,400 in 2010. Deaths from HBV-associated HCC occur at a younger age in sub-Saharan Africa (median age 38.9) than in the Western Pacific region (median age 54.5) (34).

Even though several risk factors were etiologically illustrated for HCC, there are still dead zone in this field in terms of the unsatisfactory prognosis for HCC. For the reason that sometimes patients cannot get access to advanced and costly diagnostic tools such as CT, MRI and PET-CT etc., especially for people who has the problem of economics. Therefore, the results of our study imply a framework for early diagnosis of liver diseases based on basic tests like biochemical and blood routine test, which is easily accessible for almost all people all over the word. This study used more powerful machine learning classifier models with 18 liver disease parameters filtrated by clinical experience. The classifier models were compared based on the accuracy, precision, recall, F1-score, and AUC measures. We found that the RF classifier outperformed RR, LR, extreme gradient boosting, and DT in terms of accuracy, recall, F1-score, and AUC measures. In contrast, the RR classifier achieved the highest precision among all other classifier models. Overall, the findings of this research demonstrate that the RF model performed the best for the classification of liver disease. Furthermore, the variable importance plot revealed the most significant clinical factors that contributed the most to liver disease based on the RF model. Further, including other risk factors might also aid classification algorithms in accurately identifying liver disease in a patient. Studies conducted based on various age groups and topologies might assist in highlighting the contributions of several risk factors in the identification of liver disease. Future work should concentrate on these areas in order to increase model accuracy.

Conclusion

In this study, we applied ML classification algorithms to accurately detect liver disease in 525 with 18 risk factors filtered by clinical experience. The performance of ML classification algorithms is determined based on accuracy, precision, recall, F1-score, and AUC measures. Our findings show that the RF classifier model is the best-performing algorithm for liver disease classification among all RR, LR, DT, and XGBoost classifiers. Further, we identified the 14 important risk factors based on the RF classifier that has contributed the most to liver disease in 525 patients. The outcomes of this study will aid medical professionals and researchers in making better conclusions about identifying liver disease, which could also guide or improve the treatment of patients who do not have a clinical diagnosis.

Data availability statement

The raw data supporting the conclusions of this article will be made available by the authors, without undue reservation.

Ethics statement

The studies involving human participants were reviewed and approved by The First Affiliated Hospital of Zhengzhou University. The patients/participants provided their written informed consent to participate in this study.

Author contributions

Study Concept and Design: MF, HD, and XX; Manuscript Writing: MF, HD, and BH; Data Collection: BH; Analysis of Data: MF and XX; Critical revision of the Manuscript: BH, HD, and XX. All authors contributed to the article and approved the submitted version.

Funding

This study was financially supported by grants from Hepatobiliary foundation of Henan Charity General Federation (No: GDXZ2022003) and Hepatobiliary foundation of Henan Charity General Fedration (No: GDXZ2019006).

Conflict of interest

The authors declare that the research was conducted in the absence of any commercial or financial relationships that could be construed as a potential conflict of interest.

Publisher's note

All claims expressed in this article are solely those of the authors and do not necessarily represent those of their affiliated organizations, or those of the publisher, the editors and the reviewers. Any product that may be evaluated in this article, or claim that may be made by its manufacturer, is not guaranteed or endorsed by the publisher.

References

1. Organization WH. *Global hepatitis report 2017: Executive summary*. World Health Organization (2017). Available at: https://www.who.int/publications/i/item/9789241565455.

2. Seeff LB, Beebe GW, Hoofnagle JH, Norman JE, Buskell-Bales Z, Waggoner JG, et al. A serologic follow-up of the 1942 epidemic of post-vaccination hepatitis in the united states army. *New Engl J Med* (1987) 316(16):965–70. doi: 10.1056/NEJM198704163161601

3. Stevens CE, Beasley RP, Tsui J, Lee W-C. Vertical transmission of hepatitis b antigen in Taiwan. *New Engl J Med* (1975) 292(15):771–4. doi: 10.1056/NEJM197504102921503

4. Organization WH. *Immunization, vaccines and biologicals: Hepatitis b* (2017). Available at: https://www.who.int/teams/immunization-vaccines-and-biologicals/diseases/hepatitis.

5. Tu T, Bühler S, Bartenschlager R. Chronic viral hepatitis and its association with liver cancer. *Biol Chem* (2017) 398(8):817–37. doi: 10.1515/hsz-2017-0118

6. Kew MC. The hepatitis-b virus and hepatocellular carcinoma. *Semin Liver Dis* (1981) 1(1):59–67. doi: 10.1055/s-2008-1063930

7. Ferlay J, Soerjomataram I, Dikshit R, Eser S, Mathers C, Rebelo M, et al. Cancer incidence and mortality worldwide: Sources, methods and major patterns in globocan 2012. *Int J Cancer* (2015) 136(5):E359–E86. doi: 10.1002/ijc.29210

8. Schweitzer A, Horn J, Mikolajczyk RT, Krause G, Ott JJ. Estimations of worldwide prevalence of chronic hepatitis b virus infection: A systematic review of data published between 1965 and 2013. *Lancet* (2015) 386(10003):1546–55. doi: 10.1016/S0140-6736(15)61412-X

9. Yuen M-F, Hou J-L, Chutaputti A. Hepatocellular carcinoma in the Asia pacific region. *J Gastroenterol Hepatol* (2009) 24(3):346–53. doi: 10.1111/j.1440-1746.2009.05784.x

10. Parkin DM. The global health burden of infection-associated cancers in the year 2002. *Int J Cancer* (2006) 118(12):3030–44. doi: 10.1002/ijc.21731

11. Fattovich G, Stroffolini T, Zagni I, Donato F. Hepatocellular carcinoma in cirrhosis: Incidence and risk factors. *Gastroenterology* (2004) 127(5):S35–50. doi: 10.1053/j.gastro.2004.09.014

12. Lok AS, Chronic Hepatitis B. *New Engl J Med* (2002) 346(22):1682–3. doi: 10.1056/NEJM200205303462202

13. Beasley RP, Lin C-C, Hwang L-Y, Chien C-S. Hepatocellular carcinoma and hepatitis b virus: A prospective study of 22 707 men in Taiwan. *Lancet* (1981) 318 (8256):1129–33. doi: 10.1016/S0140-6736(81)90585-7

14. Shi J, Zhu L, Liu S, Xie Wf.A meta-analysis of case–control studies on the combined effect of hepatitis b and c virus infections in causing hepatocellular carcinoma in China. *Br J Cancer* (2005) 92(3):607–12. doi: 10.1038/sj.bjc.6602333

15. Donato F, Boffetta P, Puoti M. A meta-analysis of epidemiological studies on the combined effect of hepatitis b and c virus infections in causing hepatocellular carcinoma. *Int J Cancer* (1998) 75(3):347–54. doi: 10.1002/(SICI)1097-0215(19980130)75:3<347::AID-IJC4>3.0.CO;2-2

16. Yang JD, Kim WR, Coelho R, Mettler TA, Benson JT, Sanderson SO, et al. Cirrhosis is present in most patients with hepatitis b and hepatocellular carcinoma. *Clin Gastroenterol Hepatol* (2011) 9(1):64–70. doi: 10.1016/j.cgh.2010.08.019

17. Fattovich G, Bortolotti F, Donato F. Natural history of chronic hepatitis b: Special emphasis on disease progression and prognostic factors. *J Hepatol* (2008) 48 (2):335–52. doi: 10.1016/j.jhep.2007.11.011

18. Lozano R, Naghavi M, Foreman K, Lim S, Shibuya K, Aboyans V, et al. Global and regional mortality from 235 causes of death for 20 age groups in 1990 and 2010: A systematic analysis for the global burden of disease study 2010. *Lancet* (2012) 380(9859):2095–128. doi: 10.1016/S0140-6736(12)61728-0

19. Zou H, Hastie T. Regularization and variable selection *Via* the elastic net. *J R Stat Society: Ser B (Statistical Methodology)* (2005) 67(2):301–20. doi: 10.1111/j.1467-9868.2005.00503.x

20. Le Cessie S, Van Houwelingen JC. Ridge estimators in logistic regression. *J R Stat Soc Ser C (Applied Statistics)* (1992) 41(1):191–201. doi: 10.2307/2347628

21. Moreno-Ibarra M-A, Villuendas-Rey Y, Lytras MD, Yáñez-Márquez C, Salgado-Ramírez J-C. Classification of diseases using machine learning algorithms: A comparative study. *Mathematics* (2021) 9(15):1817. doi: 10.3390/math9151817

22. Quinlan JR. Induction of decision trees. *Mach Learn* (1986) 1(1):81–106. doi: 10.1007/BF00116251

23. Wu X, Kumar V, Ross Quinlan J, Ghosh J, Yang Q, Motoda H, et al. Top 10 algorithms in data mining. *Knowledge Inf Syst* (2008) 14(1):1–37. doi: 10.1007/s10115-007-0114-2

24. Breiman L. Random forests. *Mach Learn* (2001) 45(1):5–32. doi: 10.1023/A:1010933404324

25. Hastie T, Tibshirani R, Friedman J. Random forests. In: *The elements of statistical learning: Data mining, inference, and prediction*. New York, NY: Springer New York (2009). p. 587–604.

26. Yang R, Xiong X, Wang H, Li W. Explainable machine learning model to prediction egfr mutation in lung cancer. *Front Oncol* (2022) 12. doi: 10.3389/fonc.2022.924144

27. Chen T, Guestrin C. (2016). Xgboost: A scalable tree boosting system, in: *Proceedings of the 22nd ACM SIGKDD International Conference on Knowledge Discovery and Data Mining; San Francisco, California, USA: Association for Computing Machinery*, . pp. 785–94.

28. Hashmi MF, Katiyar S, Keskar AG, Bokde ND, Geem ZW. Efficient pneumonia detection in chest xray images using deep transfer learning. *Diagnostics* (2020) 10(6):417. doi: 10.3390/diagnostics10060417

29. Elsayad AM, Nassef AM, Al-Dhaifallah M, Elsayad KA. Classification of biodegradable substances using balanced random trees and boosted C5.0 decision trees. *Int J Environ Res Public Health* (2020) 17(24):9322 doi: 10.3390/ijerph17249322.

30. Ghouri YA, Mian I, Rowe JH. Review of hepatocellular carcinoma: Epidemiology, etiology, and carcinogenesis. *J carcinogenesis* (2017) 16(1). doi: 10.4103/jcar.JCar_9_16

31. McGlynn KA, London WT. The global epidemiology of hepatocellular carcinoma: Present and future. *Clinics Liver Dis* (2011) 15(2):223–43. doi: 10.1016/j.cld.2011.03.006

32. Lu T, Seto W-K, Zhu R-X, Lai C-L, Yuen M-F. Prevention of hepatocellular carcinoma in chronic viral hepatitis b and c infection. *World J gastroenterology: WJG* (2013) 19(47):8887–94. doi: 10.3748/wjg.v19.i47.8887

33. Bruix J, Qin S, Merle P, Granito A, Huang Y-H, Bodoky G, et al. Regorafenib for patients with hepatocellular carcinoma who progressed on sorafenib treatment (Resorce): A randomised, double-blind, placebo-controlled, phase 3 trial. *Lancet* (2017) 389(10064):56–66. doi: 10.1016/S0140-6736(16)32453-9

34. de Martel C, Maucort-Boulch D, Plummer M, Franceschi S. World-wide relative contribution of hepatitis b and c viruses in hepatocellular carcinoma. *Hepatology* (2015) 62(4):1190–200. doi: 10.1002/hep.27969

frontiers | Frontiers in Oncology

TYPE Opinion
PUBLISHED 21 October 2022
DOI 10.3389/fonc.2022.1018333

Check for updates

OPEN ACCESS

EDITED BY
Imayavaramban Lakshmanan,
University of Nebraska Medical Center,
United States

REVIEWED BY
Ya Cui,
University of California, Irvine,
United States

*CORRESPONDENCE
Hideshi Ishii
hishii@gesurg.med.osaka-u.ac.jp

SPECIALTY SECTION
This article was submitted to Gastrointestinal Cancers: Hepato Pancreatic Biliary Cancers, a section of the journal Frontiers in Oncology

RECEIVED 13 August 2022
ACCEPTED 15 September 2022
PUBLISHED 21 October 2022

CITATION
Sato H, Sasaki K, Hara T, Kobayashi S, Doki Y, Eguchi H, Satoh T and Ishii H (2022) Targeting the regulation of aberrant protein production pathway in gastrointestinal cancer treatment. *Front. Oncol.* 12:1018333. doi: 10.3389/fonc.2022.1018333

COPYRIGHT
© 2022 Sato, Sasaki, Hara, Kobayashi, Doki, Eguchi, Satoh and Ishii. This is an open-access article distributed under the terms of the Creative Commons Attribution License (CC BY). The use, distribution or reproduction in other forums is permitted, provided the original author(s) and the copyright owner(s) are credited and that the original publication in this journal is cited, in accordance with accepted academic practice. No use, distribution or reproduction is permitted which does not comply with these terms.

Targeting the regulation of aberrant protein production pathway in gastrointestinal cancer treatment

Hiromichi Sato[1,2], Kazuki Sasaki[1], Tomoaki Hara[2], Shogo Kobayashi[1], Yuichiro Doki[1], Hidetoshi Eguchi[1], Taroh Satoh[1] and Hideshi Ishii[2]*

[1]Department of Gastrointestinal Surgery, Osaka University Graduate School of Medicine, Suita, Japan, [2]Department of Medical Data Science, Center of Medical Innovation and Translational Research, Osaka University Graduate School of Medicine, Suita, Japan

KEYWORDS

SRP, RAPP, 7SL1, therapy, gastrointestinal cancer

Introduction

Recent single-cell level sequence analysis in pancreatic cancer, which is a representative of intractable gastrointestinal cancers, revealed that the tumor tissue comprised of not only epithelial malignant cancer cells but also stromal activated fibroblasts and infiltrated immune cells. This indicates that various changes in gene expression occur in cells, including changes in cell-to-cell communication, to form a microenvironment that is characteristic of cancer (1–6). Epithelial malignant cancer cells harbor "big 4" driver mutations, that is, substitutions or alterations of nucleotides in KRAS proto-oncogene, GTPase (KRAS), tumor protein P53 (TP53), and cyclin-dependent kinase inhibitor 2A (CDKN2A), and mothers against decapentaplegic homolog 4 (SMAD4) commonly occurs in pancreatic ductal adenocarcinoma (PDAC) (https://portal.gdc.cancer.gov), which can be useful for predicting survival in patients with resected PDAC (7). Conversely, numerous gene expression alterations, due to cancer-specific transcription, RNA processing, and translations, are demonstrated by mesenchymal components, which include activated fibroblasts, vascular endothelial cells, and immune cells (8, 9). Importantly, this cancer-specific alterations induce the production of abnormal peptides and proteins with deleterious degenerations, which led to anti-apoptotic and pro-survival signals in cell-to-cell communication among tumor-component cells, contributing to biologically malignant phenotypes such as epithelial-to-mesenchymal transition phenotypes, invasion, and metastasis (8, 9). Thus, the aberrant protein production is important for the development of cancer-specific

therapeutic approaches. Eventually, studies on mutation-prone tumors indicated that the mismatch-repair status predicted the clinical benefit of immune checkpoint blockade with anti-programmed cell death 1 reagents (10–12), suggesting that genetic mutations and resultant production of aberrant peptides or proteins may sensitize the response to cancer therapy. Recent studies have emerged that the importance of the regulation of aberrant protein production (RAPP) in many secretary and membrane proteins (13–16), playing a role in epithelial cancer cell and activated fibroblast or immune cell communication, the process associated with patient survival (6). In this article, we focused on the mechanism of RAPP in gastrointestinal cancer, especially pancreatic cancer, and explored the possibility of an innovative approach against intractable cancers.

RAPP in cancer

The process of RAPP is mediated by a signal recognition particle (SRP), a ubiquitous initiator of protein translation (17), which is composed of six protein subunits arranged on a noncoding RNA, 7SL1 (16). The Alu domain is associated with SRP9 (9 kDa; encoded at the cytogenetic band 1q42.12) and SRP14 (14 kDa; encoded at the cytogenetic band 15q22) proteins, whereas the signal recognition domain is bounded by SRP19 (19 kDa; encoded at the cytogenetic band 5q22.2), SRP54 (54 kDa; encoded at the cytogenetic band 14q13.2), SRP68 (68 kDa; encoded at the cytogenetic band 17q25.1), and SRP72 (72 kDa; encoded at the cytogenetic band 4q12) proteins (16). Given that an SRP is a complex composed of multiple proteins encoded by multiple regions, it is suggested that it is responsible for a finely regulated mechanism (16, 17). This mechanism is also conserved across species, of which disruption can lead to various human diseases (16, 17). Here, we focused on the role of SRP in gastrointestinal cancers.

SRP

Studies on the Alu-domain associated with SRP9 and SRP14 indicated that they are involved in several human cancers and can be used as diagnostic markers. The proteomic expression analysis of human colorectal cancer showed the upregulation of SRP9 with hypoxic adaptation of the tumor microenvironment of heterogeneous primary human tumor tissues (18), suggesting the role of SRP9 in RAPP in cancer. Interestingly, in adenosine-to-inosine RNA editing, 10 recurrent nonsynonymous RNA editing candidates were identified in nine genes, including the gene for SRP9 (19), indicating that the mechanism of those genes not directly encoded in the genomic DNA is implicated in colorectal cancer. The nucleotide sequence analysis of non-Hodgkin B-cell lymphoma, a hematopoietic malignancy, allowed the identification of an aberrant fusion gene of SRP9 conjoined with epoxide hydrolase 1 (EPHX1, encoded at the cytogenetic band 1q42.12) (20), suggesting that the mechanism that converts epoxides from the degradation of aromatic compounds to trans-dihydrodiols resulting in secretion from cells may be involved in this disease. The study of dysregulated RNA binding proteins identified 11 candidates of RNA binding proteins, including SRP14, which are involved in the hepatitis B virus (HBV)-related hepatocellular carcinoma prognosis (21), indicating that RAPP may be involved in the mechanism such as the HBV lifecycle and the progression of this disease. The study of pancreatic cancer PSN-1 cells indicated that the knockdown of SRP72 resulted in a significant increase in sensitization to radiation therapy as measured by colony formation assays, indicating that SRP72 is a marker of radiotherapy resistance against cancer (22).

7SL1

Previous studies indicated that 7SL1, a noncoding RNA that binds to proteins to execute potent post-transcriptional regulation, is upregulated in cancer cells (23). It was demonstrated that 7SL1 binds to the 3'-untranslated region (UTR) of mRNA of tumor suppressor TP53 and that the interaction of 7SL1 with TP53 mRNA reduced the translation of p53 protein. On the other hand, the silencing of 7SL1 resulted in the increased binding of embryonic lethal, abnormal vision, *Drosophila* (ELAV)-like 1, Hu Antigen R (HuR) to TP53 mRNA, an interaction that led to the promotion of p53 translation, which reveals the competitive mechanism of 7SL1 and HuR for binding to TP53 3'-UTR (23). HuR selectively binds to adenylate-uridylate-(AU)-rich elements (AREs) found in the 3'-UTRs of various mRNAs. Given that AREs stimulate the degradation of mRNAs, HuR plays a role in stabilizing ARE-containing mRNAs by inhibiting degradation (24). The HuR is highly expressed in many cancers, including pancreatic cancer, functions as the post-transcriptional regulator of core metabolic enzymes, and is critical for survival under acute glucose deprivation in pancreatic cancer cells (25). In hepatocellular carcinoma, Wilms tumor 1-associating protein (WTAP) is significantly upregulated, and avian erythroblastosis virus E26 (V-Ets) oncogene homolog-1 (ETS1) was identified as the downstream effector of WTAP, suggesting that WTAP-guided m6A modification contributes to the progression of hepatocellular carcinoma *via* the HuR-ETS1-cyclin dependent kinase inhibitor 1A (p21)/cyclin dependent kinase inhibitor 1B (p27) axis (26). In pancreatic cancer, the role of mRNA modification at m6A in polo-like kinase 1 in cell cycle homeostasis was demonstrated (27), although the involvement of HuR and 7SL1 was elusive, suggesting that 7SL1 is involved, at least partially, in the process of antagonizing to p53 (Figure 1).

A study on forkhead box P3 (FOXP3), a transcription factor that is crucial for the development and inhibitory function of regulatory T-cells (Treg), indicated that overexpression of FOXP3 resulted in the repression of the transcription of 7SL1, whereas the

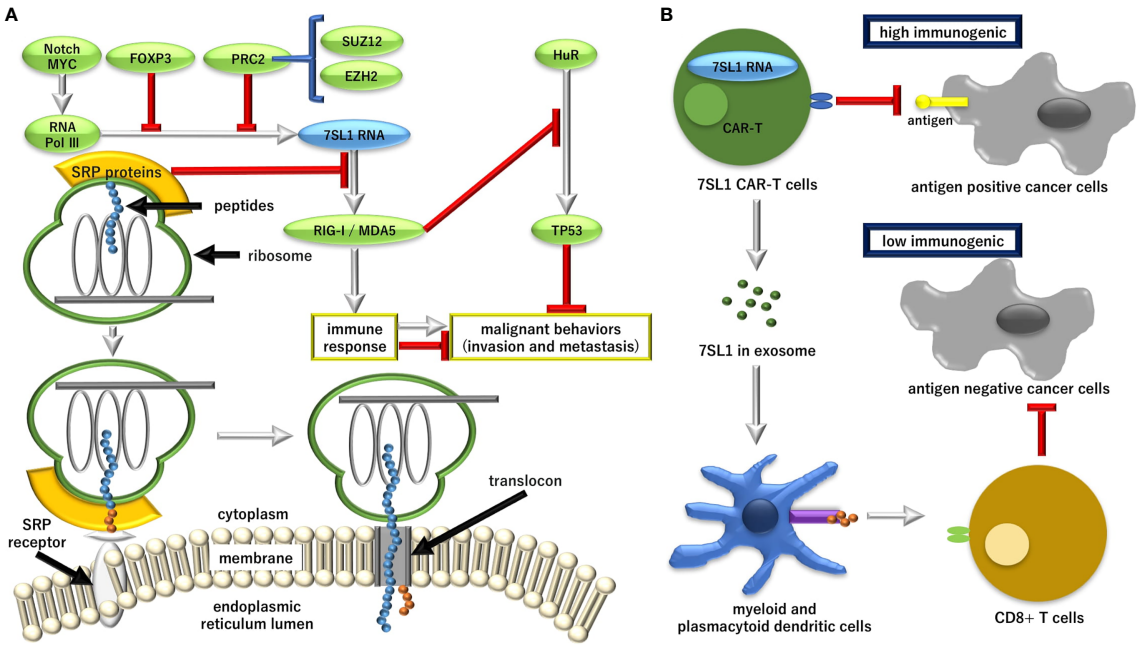

FIGURE 1
The role of endogenous immune stimulatory noncoding RNA 7SL1 in the pathway for the regulation of the aberrant protein production (RAPP) and its possible application in cancer therapy. **(A)** Transcriptional regulation of 7SL1 and the downstream mechanism for tumor suppressor tumor protein P53 (TP53). MYC, proto-oncogene, basic helix-loop-helix (BHLH) transcription factor (MYC); FOXP3, forkhead box P3; PRC2, polycomb repression complex 2; SUZ12, SUZ12 polycomb repressive complex 2 subunit; EZH2, enhancer of zeste 2 polycomb repressive complex 2 subunit; Pol II, RNA polymerase II; Pol III, RNA polymerase III; SRP, signal recognition particle; RIG-1, retinoic acid-inducible gene 1 protein; MDA5, melanoma differentiation-associated gene 5; HuR, embryonic lethal, abnormal vision, *Drosophila* (ELAV)-like 1, Hu antigen R. **(B)** Although the unshielded 7SL1-mediated stimulation of tumor tissues can result in disease progression, the exosomal delivery of 7SL1 or its combination with engineering chimeric antigen receptor (CAR)-T cells can stimulate an anti-tumor effect and lead to a favorable disease outcome. Ag, antigen.

knockdown of FOXP3 showed the upregulation of 7SL1 RNA transcription (28). The mechanism was confirmed by chromatin immuno-precipitation analysis and reporter assay (28). The study showed that FOXP3 promoted the expression of TP53 at the translational levels through repressing 7SL1 RNA (28). However, considering the recent study that indicated that Treg is chemoattracted to the tumor microenvironment by chemokine gradients such as C-C motif chemokine receptor 4 (CCR4)-C-C motif chemokine ligand 17 (CCL17)/CCL22, CCR8-CCL1, CCR10-CCL28, and CXCR3-CCL9/10/11, it is demonstrated that Treg cells are activated and inhibit antitumor immune responses, suggesting that strategies to deplete Treg cells and the control of Treg cell functions to increase antitumor immune responses are required in cancer immunotherapy (29), which demonstrates the multifaceted role of Treg in cancer. Given that FOXP3 unlikely represents the effect on 7SL1 exclusively in Treg cells, whether 7SL1 is an appropriate target to control Treg remains to be investigated.

Although a role of the polycomb repressive complex 2 (PRC2) component, working on the enhancer of zeste 2 polycomb repressive complex 2 subunit (EZH2)-mediated epigenetic control of RNA polymerase II (Pol II) transcribed coding gene transcription, has been well-established, a recent study on EZH2-mediated epigenetic regulation of RNA polymerase III (Pol III) transcription indicated that EZH2 is involved in the repression of Pol III transcription of tRNA(Tyr), 5S rRNA, and 7SL1 RNA genes *via* the interaction with transcriptional factor complex IIIC (TFIIIC) as well as SUZ12 polycomb repressive complex 2 subunit (SUZ12) (30), suggesting that basic mechanisms common to cells, which are specific mechanisms to cancer, are involved in 7SL1 regulation. Thus, it is necessary to study the upstream regulation of 7SL1 transcription in cells, which responds to various stimuli such as hypoxia and hyponutrition that are characterized by the extracellular tumor microenvironment.

Damage-associated molecular patterns in cancer-associated fibroblasts-to-cancer cell interactions

In a single-cell sequence analysis (1–6), it was well-recognized that interactions between cancer cells and CAFs in

stroma generate signals for cancer progression, inflammatory responses, and therapeutic outcomes (31–33). Previous reports have indicated that the arrangement of SRPs in 7SL1 is necessary to execute a physiological function of PARP in DAMPs (34). Reportedly, SRP dysfunction resulted in the induction of invasion and metastasis of cancer cells, which is associated with the evacuation from host's immune response. A previous study elucidated that SRPs and 7SL1 are involved in the process of such signal, which revealed the importance of endogenous RNA response acting as damage-associated molecular patterns (35). In this study, it was demonstrated that triggering of notch receptor 1-MYC proto-oncogene and basic helix-loop-helix (BHLH) transcription factor (MYC) signaling in the stroma of breast cancer results in the activation of Pol III-driven increase in 7SL1, which is normally shielded by SRP9 and SRP 14 (35). The induced 7SL1 transcription resulted in an alteration of its stoichiometry with SRP9 and SRP 14, which led to the generation of unshielded 7SL1 in the stromal exosomes (35). Moreover, the unshielded 7SL1 can drive an inflammatory response. The unshielded 7SL1 activates the retinoic acid-inducible gene 1 protein (RIG-I), a pattern recognition receptor usually reserved for viral infections, to enhance tumor growth, metastasis, and therapy resistance, suggesting that the regulation of RNA unshielding can couple stromal activation with deployment of DAMPs of RNA, which is closely associated with the aggressive features of cancer (35). This also indicates the potential of 7SL1 as a target of cancer therapy, considering the immunogenic property of this endogenous non-coding RNA. The significant roles of exosome-mediated RNA transfer was demonstrated in a breast cancer study, indicating that CAFs orchestrate an intricate crosstalk with cancer cells by utilizing exosomes (36). The significance in gastrointestinal cancer warrants further investigation.

Application to chimeric antigen receptor-T therapy

Recently, it was demonstrated that the immune stimulatory property can be utilized for the development of CAR-T cell therapy (37). The vector-mediated gene transfer of 7SL1 activated the RIG-I/melanoma differentiation-associated gene 5 (MDA5) signaling and promoted the expansion and effector-memory differentiation of CAR-T cells (37). MDA5 binds to RNAs with a modified DExD/H-box helicase core and a C-terminal domain, thus leading to a proinflammatory response that includes interferons (38, 39). RN7SL1 restricts myeloid-derived suppressor cell development, decreases transforming growth factor beta 1 (TGFB) in myeloid cells, and fosters dendritic cell subsets, which led to the endogenous expansion of effector-memory and tumor-specific T cells (37, 40). It is suggested that the unshielded form of 7SL1 can be used in peptide antigens to enhance anti-tumor efficacy (Figure 1).

Discussion

Despite advances in surgery, standard radiation therapy, and chemotherapy, immunotherapy was added as a fourth treatment to cancer, as the discovery of immune modulation through immune check points and exploration of new combinations of cancer multimodality therapies led to overcoming long-term resistance and tumor recurrence (41). Cancer is a genetic disease involving numerous mutations (42–44), and the evidence that the mismatch-repair status predicted the clinical benefit of immune checkpoint blockade with pembrolizumab is important (10–12), as this suggests that the quantity or quality of gene mutations may influence susceptibility to immune checkpoint inhibitor therapy. Furthermore, the effect of immunotherapy can be maximized by regulating gene mutations and the consequent amino acid mutation neoantigen to eradicate cancer (45–47). If inducing a hot state in which cell-to-cell interactions are activated immunologically is possible, immune checkpoint inhibitors can not only be applied, but cancer-specific antigens can also be identified and used as vectors or employed as CAR-T therapy (48, 49). Nevertheless, methods to induce immunologically cold tumors into hot ones remain to be developed, and further investigations are necessary for application in a clinical setting.

The RAPP pathway study revealed the immune stimulatory property of endogenous non-coding RNA, 7SL1, which is a component of SRPs. A previous study suggests several important implications. First, given that the co-deploy peptide antigen with 7SL1 can exert an efficient anti-tumor effect (36), this approach may be useful to treat intractable solid tumors such as mutation-prone gastrointestinal cancer. Second, considering that unshielded 7SL1 in exosomes can be transferred in the tumor microenvironment (34), it is possible that the cell-to-cell communication is assessed by an RNA study in liquid biopsy as a companion diagnostic tool. Third, as radiotherapy can induce inflammatory microenvironment remodeling (50), the combination of RAPP pathway-mediated stimulatory cancer therapy with radiation may be useful to induce the immune response to convert an immune cold into a hot tumor, and multiple protocols have been developed (51). Fourth, nucleotide-mediated immune stimulation may be expanded as an anti-cancer therapy. Eventually, the intratumoral injection of the seasonal flu shot can generate systemic CD8+ T cell-mediated antitumor immunity and sensitizes resistant tumors to the checkpoint blockade, suggesting that it converts immunologically cold tumors to hot tumors and serves as an immunotherapy for cancer (52). To optimize the effect of treatment for intractable cancer, further studies to accumulate evidence are warranted.

Author contributions

HS, KS, and HI conceptualized the study objectives and obtained the funding, wrote the manuscript. TH, SK, YD, HE,

and TS outlined content of the manuscript. TS suggested which disease information should be addressed in the manuscript. All authors have read and approved the final manuscript version for publication.

Funding

This work was supported in part by a Grant-in-Aid for Scientific Research from the Ministry of Education, Culture, Sports, Science and Technology (19K22658; 20H00541; 22H03146; 22K19559), and Japan Agency for Medical Research and Development (AMED) (17cm0106414h0002; JP19lm0203007; JP20lm0203007; JP21lm0203007). Partial support was received from Princess Takamatsu Cancer Research Fund and Mitsubishi Foundation to HI.

Acknowledgments

Authors are thankful to every lab member.

Conflict of interest

Partial institutional endowments were received from Taiho Pharmaceutical Co., Ltd. (Tokyo, Japan), Hirotsu Bio Science Inc. (Tokyo, Japan); Kinshu-kai Medical Corporation (Osaka, Japan); Kyowa-kai Medical Corporation (Osaka, Japan); IDEA Consultants Inc. (Tokyo, Japan); Unitech Co. Ltd. (Chiba, Japan).

The remaining authors declare that the research was conducted in the absence of any commercial or financial relationships that could be construed as a potential conflict of interest.

Publisher's note

All claims expressed in this article are solely those of the authors and do not necessarily represent those of their affiliated organizations, or those of the publisher, the editors and the reviewers. Any product that may be evaluated in this article, or claim that may be made by its manufacturer, is not guaranteed or endorsed by the publisher.

References

1. Elyada E, Bolisetty M, Laise P, Flynn WF, Courtois ET, Burkhart RA, et al. Cross-species single-cell analysis of pancreatic ductal adenocarcinoma reveals antigen-presenting cancer-associated fibroblasts. *Cancer Discov* (2019) 9 (8):1102–23. doi: 10.1158/2159-8290.CD-19-0094

2. Lin W, Noel P, Borazanci EH, Lee J, Amini A, Han IW, et al. Single-cell transcriptome analysis of tumor and stromal compartments of pancreatic ductal adenocarcinoma primary tumors and metastatic lesions. *Genome Med* (2020) 12 (1):80. doi: 10.1186/s13073-020-00776-9

3. Chen K, Wang Q, Li M, Guo H, Liu W, Wang F, et al. Single-cell RNA-seq reveals dynamic change in tumor microenvironment during pancreatic ductal adenocarcinoma malignant progression. *EBioMedicine* (2021) 66:103315. doi: 10.1016/j.ebiom.2021.103315

4. Peng J, Sun BF, Chen CY, Zhou JY, Chen YS, Chen H, et al. Single-cell RNA-seq highlights intra-tumoral heterogeneity and malignant progression in pancreatic ductal adenocarcinoma. *Cell Res* (2019) 29(9):725–38. doi: 10.1038/s41422-019-0195-y

5. Schlesinger Y, Yosefov-Levi O, Kolodkin-Gal D, Granit RZ, Peters L, Kalifa R, et al. Single-cell transcriptomes of pancreatic preinvasive lesions and cancer reveal acinar metaplastic cells' heterogeneity. *Nat Commun* (2020) 11(1):4516. doi: 10.1038/s41467-020-18207-z

6. Chijimatsu R, Kobayashi S, Takeda Y, Kitakaze M, Tatekawa S, Arao Y, et al. Establishment of a reference single-cell RNA sequencing dataset for human pancreatic adenocarcinoma. *iScience* (2022) 25(8):104659. doi: 10.1016/j.isci.2022.104659

7. McIntyre CA, Lawrence SA, Richards AL, Chou JF, Wong W, Capanu M, et al. Alterations in driver genes are predictive of survival in patients with resected pancreatic ductal adenocarcinoma. *Cancer* (2020) 126(17):3939–49. doi: 10.1002/cncr.33038

8. Hanahan D, Weinberg RA. The hallmarks of cancer. *Cell* (2000) 100(1):57–70. doi: 10.1016/s0092-8674(00)81683-9

9. Hanahan D, Weinberg RA. Hallmarks of cancer: The next generation. *Cell* (2011) 144(5):646–74. doi: 10.1016/j.cell.2011.02.013

10. Le DT, Uram JN, Wang H, Bartlett BR, Kemberling H, Eyring AD, et al. PD-1 blockade in tumors with mismatch-repair deficiency. *N Engl J Med* (2015) 372 (26):2509–20. doi: 10.1056/NEJMoa1500596

11. Le DT, Durham JN, Smith KN, Wang H, Bartlett BR, Aulakh LK, et al. Mismatch repair deficiency predicts response of solid tumors to PD-1 blockade. *Science* (2017) 357(6349):409–13. doi: 10.1126/science.aan6733

12. Ciombor KK, Goldberg RM. Hypermutated tumors and immune checkpoint inhibition. *Drugs* (2018) 78(2):155–62. doi: 10.1007/s40265-018-0863-0

13. Popp MW-L, Maquat LE. Defective secretory-protein mrnas take the rapp. *Trends Biochem Sci* (2014) 39(4):154–6. doi: 10.1016/j.tibs.2014.02.001

14. Karamyshev AL, Patrick AE, Karamysheva ZN, Griesemer DS, Hudson H, Tjon-Kon-Sang S, et al. Inefficient SRP interaction with a nascent chain triggers a mrna quality control pathway. *Cell* (2014) 156(1-2):146–57. doi: 10.1016/j.cell.2013.12.017

15. Karamyshev AL, Karamysheva ZN. Lost in translation: Ribosome-associated mRNA and protein quality controls. *Front Genet* (2018) 9:431. doi: 10.3389/fgene.2018.00431

16. Kellogg MK, Tikhonova EB, Karamyshev AJ. Signal recognition particle in human diseases. *Front Genet* (2022) 13:898083. doi: 10.3389/fgene.2022.898083

17. Lütcke H. Signal recognition particle (SRP), a ubiquitous initiator of protein translocation. *Eur J Biochem* (1995) 228(3):531–50. doi: 10.1111/j.1432-1033.1995.tb20293.x

18. Rho JH, Qin S, Wang JY, Roehrl MH. Proteomic expression analysis of surgical human colorectal cancer tissues: Up-regulation of PSB7, PRDX1, and SRP9 and hypoxic adaptation in cancer. *J Proteome Res* (2008) 7(7):2959–72. doi: 10.1021/pr8000892

19. Lee S-H, Kim H-P, Kang J-K, Song S-H, Han S-W, Kim T-Y. Identification of diverse adenosine-to-Inosine RNA editing subtypes in colorectal cancer. *Cancer Res Treat* (2017) 49(4):1077–87. doi: 10.4143/crt.2016.301

20. Matsumoto Y, Tsukamoto T, Chinen Y, Shimura Y, Sasaki N, Nagoshi H, et al. Detection of novel and recurrent conjoined genes in non-Hodgkin b-cell lymphoma. *J Clin Exp Hematop* (2021) 61(2):71–7. doi: 10.3960/jslrt.20033

21. Li M, Liu Z, Wang J, Liu H, Gong H, Li S, et al. Systematic analysis identifies a specific RNA-binding protein-related gene model for prognostication and risk-adjustment in HBV-related hepatocellular carcinoma. *Front Genet* (2021) 12:707305. doi: 10.3389/fgene.2021.707305

22. Prevo R, Tiwana GS, Maughan TS, Buffa FM, McKenna WG, Higgins GS. Depletion of signal recognition particle 72kDa increases radiosensitivity. *Cancer Biol Ther* (2017) 18(6):425–32. doi: 10.1080/15384047.2017.1323587

23. Abdelmohsen K, Panda AC, Kang M-J, Guo R, Kim J, Grammatikakis I, et al. 7SL RNA represses P53 translation by competing with hur. *Nucleic Acids Res* (2014) 42(15):10099–111. doi: 10.1093/nar/gku686

24. Brody JR, Dixon DA. Complex hur function in pancreatic cancer cells. *Wiley Interdiscip Rev RNA* (2018) 9(3):e1469. doi: 10.1002/wrna.1469

25. Burkhart RA, Pineda DM, Chand SN, Romeo C, Londin ER, Karoly ED, et al. HuR is a post-transcriptional regulator of core metabolic enzymes in pancreatic cancer. *RNA Biol* (2013) 10(8):1312–23. doi: 10.4161/rna.25274

26. Chen Y, Peng C, Chen J, Chen D, Yang B, He B, et al. WTAP facilitates progression of hepatocellular carcinoma *via* m6A-HuR-Dependent epigenetic silencing of ETS1. *Mol Cancer* (2019) 18(1):127. doi: 10.1186/s12943-019-1053-8

27. Tatekawa S, Tamari K, Chijimatsu R, Konno M, Motooka D, Mitsufuji S, et al. N(6)-methyladenosine methylation-regulated polo-like kinase 1 cell cycle homeostasis as a potential target of radiotherapy in pancreatic adenocarcinoma. *Sci Rep* (2022) 12(1):11074. doi: 10.1038/s41598-022-15196-5

28. Yang Y, Cheng J, Ren H, Zhao H, Gong W, Shan C. Tumor FOXP3 represses the expression of long noncoding RNA 7SL. *Biochem Biophys Res Commun* (2016) 472(3):432–6. doi: 10.1016/j.bbrc.2015.12.082

29. Ohue Y, Nishikawa H, Regulatory T. (Treg) cells in cancer: Can treg cells be a new therapeutic target? *Cancer Sci* (2019) 110(7):2080–9. doi: 10.1111/cas.14069

30. Liu C, Li S, Dai X, Ma J, Wan J, Jiang H, et al. PRC2 regulates RNA polymerase III transcribed non-translated RNA gene transcription through EZH2 and SUZ12 interaction with tfiiic complex. *Nucleic Acids Res* (2015) 43(13):6270–84. doi: 10.1093/nar/gkv574

31. Biffi G, Tuveson DA. Diversity and biology of cancer-associated fibroblasts. *Physiol Rev* (2021) 101(1):147–76. doi: 10.1152/physrev.00048.2019

32. Chen Y, McAndrews KM, Kalluri R. Clinical and therapeutic relevance of cancer-associated fibroblasts. *Nat Rev Clin Oncol* (2021) 18(12):792–804. doi: 10.1038/s41571-021-00546-5

33. Chen X, Song E. Turning foes to friends: Targeting cancer-associated fibroblasts. *Nat Rev Drug Discovery* (2019) 18(2):99–115. doi: 10.1038/s41573-018-0004-1

34. Krysko DV, Garg AD, Kaczmarek A, Krysko O, Agostinis P, Vandenabeele P. Immunogenic cell death and damps in cancer therapy. *Nat Rev Cancer* (2012) 12 (12):860–75. doi: 10.1038/nrc3380

35. Nabet BY, Qiu Y, Shabason JE, Wu TJ, Yoon T, Kim BC, et al. Exosome rna unshielding couples stromal activation to pattern recognition receptor signaling in cancer. *Cell* (2017) 170(2):352–66.e13. doi: 10.1016/j.cell.2017.06.031

36. Boelens MC, Wu TJ, Nabet BY, Xu B, Qiu Y, Yoon T, et al. Exosome transfer from stromal to breast cancer cells regulates therapy resistance pathways. *Cell* (2014) 159(3):499–513. doi: 10.1016/j.cell.2014.09.051

37. Johnson LR, Lee DY, Eacret JS, Ye D, June CH, Minn AJ. The immunostimulatory RNA RN7SL1 enables car-T cells to enhance autonomous and endogenous immune function. *Cell* (2021) 184(19):4981–95.e14. doi: 10.1016/j.cell.2021.08.004

38. Kato H, Takeuchi O, Sato S, Yoneyama M, Yamamoto M, Matsui K, et al. Differential roles of MDA5 and RIG-I helicases in the recognition of RNA viruses. *Nature* (2006) 441(7089):101–5. doi: 10.1038/nature04734

39. Dias Junior AG, Sampaio NG, Rehwinkel JA. Balancing act: MDA5 in antiviral immunity and autoinflammation. *Trends Microbiol* (2019) 27(1):75–85. doi: 10.1016/j.tim.2018.08.007

40. Nutt WS, Srivastava S. Special delivery! car-T cells transport RN7SL1 to the tumor microenvironment. *Trends Mol Med* (2021) 27(11):1019–21. doi: 10.1016/j.molmed.2021.09.002

41. Hegde PS, Chen DS. Top 10 challenges in cancer immunotherapy. *Immunity* (2020) 52(1):17–35. doi: 10.1016/j.immuni.2019.12.011

42. Devarakonda S, Rotolo F, Tsao M-S, Lanc I, Brambilla E, Masood A, et al. Tumor mutation burden as a biomarker in resected non–Small-Cell lung cancer. *J Clin Oncol* (2018) 36(30):2995–3006. doi: 10.1200/JCO.2018.78.1963

43. Chan TA, Yarchoan M, Jaffee E, Swanton C, Quezada SA, Stenzinger A, et al. Development of tumor mutation burden as an immunotherapy biomarker: Utility for the oncology clinic. *Ann Oncol* (2019) 30(1):44–56. doi: 10.1093/annonc/mdy495

44. Lindeboom RGH, Vermeulen M, Lehner B, Supek F. The impact of nonsense-mediated mrna decay on genetic disease, gene editing and cancer immunotherapy. *Nat Genet* (2019) 51(11):1645–51. doi: 10.1038/s41588-019-0517-5

45. Bonaventura P, Shekarian T, Alcazer V, Valladeau-Guilemond J, Valsesia-Wittmann S, Amigorena S, et al. Cold tumors: A therapeutic challenge for immunotherapy. *Front Immunol* (2019) 10:168. doi: 10.3389/fimmu.2019.00168

46. Kakoti S, Sato H, Laskar S, Yasuhara T, Shibata A. DNA Repair and signaling in immune-related cancer therapy. *Front Mol Biosci* (2020) 7:205. doi: 10.3389/fmolb.2020.00205

47. Liu Y-T, Sun Z-J. Turning cold tumors into hot tumors by improving T-cell infiltration. *Theranostics* (2021) 11(11):5365–86. doi: 10.7150/thno.58390

48. Martinez M, Moon EK. CAR T cells for solid tumors: New strategies for finding, infiltrating, and surviving in the tumor microenvironment. *Front Immunol* (2019) 10:128. doi: 10.3389/fimmu.2019.00128

49. Ma S, Li X, Wang X, Cheng L, Li Z, Zhang C, et al. Current progress in CAR-T cell therapy for solid tumors. *Int J Biol Sci* (2019) 15(12):2548–60. doi: 10.7150/ijbs.34213

50. McLaughlin M, Patin EC, Pedersen M, Wilkins A, Dillon MT, Melcher AA, et al. Inflammatory microenvironment remodelling by tumour cells after radiotherapy. *Nat Rev Cancer* (2020) 20(4):203–17. doi: 10.1038/s41568-020-0246-1

51. Galon J, Bruni D. Approaches to treat immune hot, altered and cold tumours with combination immunotherapies. *Nat Rev Drug Discovery* (2019) 18 (3):197–218. doi: 10.1038/s41573-018-0007-y

52. Newman JH, Chesson CB, Herzog NL, Bommareddy PK, Aspromonte SM, Pepe R, et al. Intratumoral injection of the seasonal flu shot converts immunologically cold tumors to hot and serves as an immunotherapy for cancer. *Proc Natl Acad Sci USA* (2020) 117(2):1119–28. doi: 10.1073/pnas.1904022116

frontiers | Frontiers in Oncology

TYPE Original Research
PUBLISHED 24 October 2022
DOI 10.3389/fonc.2022.1032737

Check for updates

OPEN ACCESS

EDITED BY
Zhendong Jin,
Second Military Medical University, China

REVIEWED BY
Liqi Sun,
Second Military Medical University, China
Qiong Luo,
Mengchao Hepatobiliary Hospital, China
Hua Yin,
Ningxia Medical University, China

*CORRESPONDENCE
Baohua Zhang
zhbh_ehbh@163.com

†These authors have contributed equally to this work and share first authorship

SPECIALTY SECTION
This article was submitted to Gastrointestinal Cancers: Hepato Pancreatic Biliary Cancers, a section of the journal Frontiers in Oncology

RECEIVED 31 August 2022
ACCEPTED 03 October 2022
PUBLISHED 24 October 2022

CITATION
Zhang K, Liu H, Zhao Y and Zhang B (2022) The clinical outcomes of extended resections in patients with IV stage gallbladder cancers: A retrospective study from a large tertiary center.
Front. Oncol. 12:1032737.
doi: 10.3389/fonc.2022.1032737

COPYRIGHT
© 2022 Zhang, Liu, Zhao and Zhang. This is an open-access article distributed under the terms of the Creative Commons Attribution License (CC BY). The use, distribution or reproduction in other forums is permitted, provided the original author(s) and the copyright owner(s) are credited and that the original publication in this journal is cited, in accordance with accepted academic practice. No use, distribution or reproduction is permitted which does not comply with these terms.

The clinical outcomes of extended resections in patients with IV stage gallbladder cancers: A retrospective study from a large tertiary center

Kecheng Zhang†, Hu Liu†, Yongyang Zhao† and Baohua Zhang*

Department of Biliary Tract Surgery, Shanghai Eastern Hepatobiliary Surgery Hospital, Shanghai, China

Background and aim: The role of extended resections in patients with clinical stage IV gallbladder cancer (GBC) remains unclear. This study retrospectively analyzed the clinical outcomes of patients who underwent extended resections for IV GBC.

Methods: Patients who were diagnosed with IV stage GBCs and underwent extended resections in Eastern Hepatobiliary Surgery Hospital, Shanghai, China, were retrospectively included in our study. Extended resection was defined as a major hepatectomy (resection of ≥3 liver segments), a pancreatoduodenectomy, or both. The clinical outcomes (baseline characteristics, preoperative variables, intraoperative variables, pathological outcomes, and follow-up data) were obtained and analyzed. The factors associated with major postoperative complications and long-term survival were analyzed by logistic regression analyses.

Results: From January 2011 to June 2017, 74 patients were included in our study. There were 33 (44.6%) males and the median age was 62.5 years (interquartile range [IQR], 56.0-67.0 years). According to pathological specimens, the median tumor size was 7cm (IQR, 6-8cm), 73(98.6%) of them received R0 resection and 72 (97.2%) of them were IV A stage GBC. Three perioperative deaths (5.4%) occurred, and major postoperative complications occurred for 15 patients (20.3%). Among them, 61 patients (82.4%) experienced recurrence and 17 patients (23.0%) were still alive after a median follow-up period of 52 months. The disease free survival time was 9 months (95% confidence interval [CI], 7.8-10.2 months) and the overall survival was 18.0 months (95% CI, 15.2-20.8 months). Longer hospital stay days [odds ratio, (OR) =1.979, 95%CI:1.038-1.193, P=0.003), initial symptoms with abdominal pain (OR=21.489, 95%CI=1.22-37.57, P=0.036), more blood transfusion volume during hospitalization (OR=1.036, 95%CI:1.021-1.058, P=0.005), and intraoperative hemorrhage (OR=18.56, 95%C:3.54-47.65, P=0.001) were independently associated with postoperative complications. Moreover,

locally recurrence (OR=1.65, 95%CI:1.17-1.96, P=0.015), and more adjuvant chemotherapy cycles (OR=1.46, 95%CI:1.13-1.76, P=0.026) were independently associated with long-term survival.

Conclusion: Our retrospective study identified that extended resections can be safely and efficaciously performed on stage IV GBC patients in selected cases and performed by experienced surgeons.

KEYWORDS

gallbladder carcinoma, extended resection, advanced stage, adverse events, long-term survival, recurrence

Introduction

Gallbladder cancer (GBC) is not common, but the malignancy nature of the cancer is highly aggressive. The incidence rate is less than 2/100,000 worldwide, with broad regional diversity (1, 2). The incidence of gallbladder cancer in China accounted for 0.4%~3.8% of all the biliary tract diseases, the disease 6th among digestive tract tumors (3, 4). Due to the lack of clinical symptoms in the early stages and the anatomical peculiarity of the absence of a submucosal layer, GBC is often diagnosed at an advanced stage (5). As a result, the prognosis for GBC is relatively poor, with the 5-year survival rate only reaching 5% in China (6).

The only curative treatment is complete surgical resection (7). However, only about one-tenth to one-fifth of patients are surgical candidates when diagnosed and they often underwent radical resections. But the prognosis of GBC after resection remains unfavorable (8, 9). Especially for patients with an advanced stage of GBC, the reported median overall survival (OS) period was only about 1 year after radical resection (10).

To achieve R0 resection, extended resections have been described in the treatment of advanced GBC. Comparing to radical resections, the extended resections have more extensive excision. These surgical methods include major hepatectomy, pancreatoduodenectomy (PD), and hepatectomy combined with PD (11–15). The survival benefits of extended resections for advanced GBC were inconsistent in these studies, but the reported post-operative adverse event rate is unexpectedly high (>50%). However, almost all published studies combined T3 and T4 GBC with a small sample size. The evidence level is not that high and we should not only follow the conclusions from these studies. More data is needed to show the actual clinical outcomes for stage IV GBC patients who underwent extended resections.

The objective of this study is to analyze the results of extended resections for patients with stage IV stage GBC with a study cohort in a large volume center. The primary aim is post-operative survival. The second aim is to explore the factors associated with long-term survival and postoperative major complications.

Materials and methods

Study cohort

From January 2011 to June 2017, patients who were diagnosed with IV A stage GBCs and underwent extended resections in the department of biliary surgery, Eastern Hepatobiliary Surgery Hospital, Shanghai, China, were retrospectively included in our study. The following inclusion criteria were applied: (1) patients pathologically diagnosed with GBC; (2) patients whose full electronic medical records and imaging records could be obtained; and (3) patients whose follow-up data could be obtained. Exclusion criteria included (1) specimens obtained from reresections; (2) concomitant other neoplasms on final pathology (e.g., primary liver cancer, cholangiocarcinoma); and (3) patients with unavailable pathological and follow-up data.(4) patients were incidentally diagnosed with GBC. The selection procedure of the study participants is presented in Figure 1. The Institutional Review Board of our hospital approved the study protocol.

The grade of T4 stage was according to the American Joint Committee on Cancer (AJCC) 8th edition. In our study, if a patient was staged with IV A, he/she had T4 (invasion of the portal vein or main hepatic artery, or direct invasion of two or more extrahepatic organs or structures), N0-1 (one to three regional lymph nodes had metastases) and M0. If a patient was staged with IV B, he/she had any T, N2 (more than four regional lymph nodes had metastases), and M0 (patients with M1 will not receive surgical resection).

The decision on surgical treatment was made by a multidisciplinary hepatopancreatobiliary team. The choices of surgical procedures depended on the location and extent of

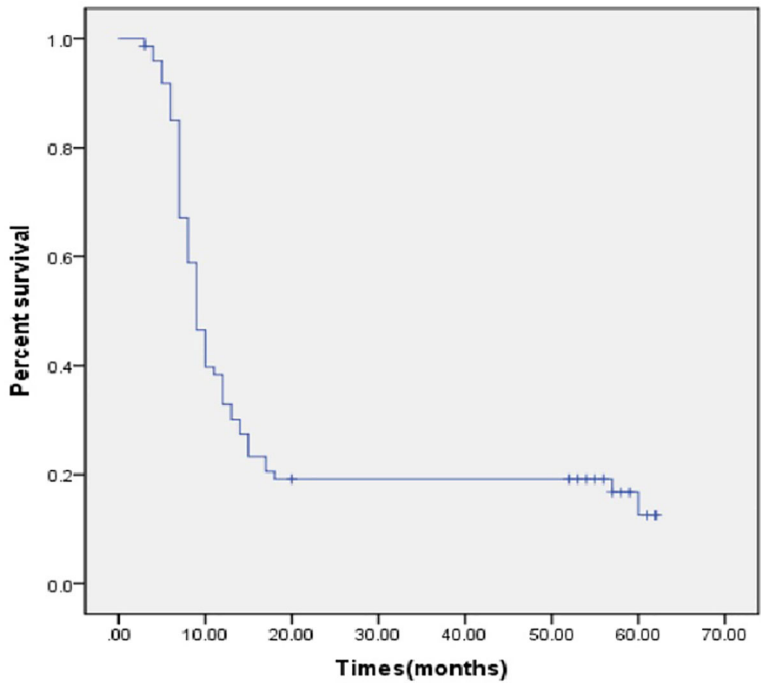

FIGURE 1
Disease free survival in months.

diseases obtained by imaging modalities. All the operations were performed by experienced surgeons. Long-term survival was defined as survival for 2 years or longer.

Perioperative management and chemotherapy strategy

Routine preoperative exams were carried out before surgery to rule out any surgical contraindications. The electrocardiograph, lung function, coagulation function, liver function, renal function, electrolyte, and hemoglobin were among the standard tests performed. One hour before the surgery, antibiotic prophylaxis (third generation cephalosporin or ciprofloxacin) was routinely used. After preoperative evaluations, all the patients were supposed to have good surgical tolerance (American Society of Anesthesiologists grade II or above). Informed consent was provided by every patient. All operations were performed by experienced surgeons.

After surgery, antibiotics (third generation cephalosporin) were routinely used and lasted for a week. Blood examinations were performed to determine whether infections and electrolyte disturbances existed. Total parenteral nutrition was performed before the recovery of intestinal function. Plain CT was performed if any clinically significant symptoms occurred to exclude postoperative complications.

Adjuvant chemotherapy will be recommended for patients after surgical resection if they can tolerate it. Most of the regimens used for post-operative adjuvant chemotherapy were oxaliplatin+ S-1/capecitabine. Post-operative adjuvant radiation was not routinely performed in our hospital.

If a patient experiences a recurrence, chemotherapy with palliative intent will be recommended. The most frequently used regimen was S-1/capecitabine.

Variable definitions

Various indicators were included in our study to fully illustrate the impact of extended resections on patients with stage IV GBC.

First, the baseline characteristics, including age, sex, body mass index (BMI), initial symptoms, hospital stay days, and surgical methods. Major hepatectomy (resection of three or more segments of the liver), PD, or both, with or without en bloc resection of the duodenum, colon, or stomach, were the surgical methods used in our study (14). Enlarged lymph node dissection and biliary anastomosis were performed in each case.

Second, the preoperative variables, including total bilirubin, alanine aminotransferase (ALT), carcinoembryonic antigen (CEA), carbohydrate antigen 19-9 (CA19-9) and the history of biliary drainage [through Endoscopic

Retrograde Cholangiopancreatography (ERCP) or percutaneous transhepaticcholangial drainage (PTCD)].

Third, the intraoperative variables, including operation duration, intraoperative blood loss, blood transfusion volume, and intraoperative complications.

Fourth, the pathological outcomes included tumor size, location (gallbladder neck, body and bottom), differentiated degree, margin status, and peripheral tissue invasion status. Peripheral tissue invasion status consisted of perineural invasion, vascular invasion, cancerization of ducts, lymphatic metastasis, and common bile duct invasion.

Fifth, the follow-up data, including perioperative deaths (within 30 days after surgery), post- operative major complications, post-operative adjuvant chemotherapy history, disease-free survival (DFS) rate, and overall survival (OS) rate. The number of months between the date of extended resection or the date of the final follow-up examination was used to determine DFS. Recurrence was defined as a local or metastatic tumor confirmed by radiology or histology during postoperative follow-up. The OS calculation took into account all types of fatalities. Most of the regimens used for post-operative adjuvant chemotherapy were oxaliplatin+ S-1/capecitabine. Post-operative adjuvant radiation was not routinely performed in our hospital. Major complications were defined as Clavien-Dindo grade III or higher (16).

Statistical analysis

Continuous variables are presented as median (interquartile range), and categorical data are presented as number (%). Survival was reported using Kaplan-Meier methods. The differences between groups were compared by student's t-test, Mann-Whitney U test, chi-square test, and Fisher's exact test. Logistic regression analysis was used to identify factors associated with long-term survival and decreased adverse events. Variables of potential significance ($P < 0.10$) were entered into the Logistic regression model. All models were adjusted for age and sex, and the results were presented as an odds ratio (OR) with a 95% confidence interval (CI). All p values of 0.05 or lower were considered statistically significant. All statistical analyses were performed using SPSS version 22.0 (IBM Corporation, Armonk, NY, USA).

Results

Baseline characteristics

Between January 2011 and June 2017, 345 patients underwent extended resection with curative intent in our hospital. After inclusion and exclusion criteria were applied to the study cohort, 74 stage IV GBC patients were finally included in our study.

Among the 74 patients, there were 33 (44.6%) males and 41 (55.4%) females. At the time of diagnosis, the median age was 62.5 years (interquartile range [IQR], 56.0-67.0 years). The median BMI was 23.27 (IQR, 21.47-24.90) with 28 patients(37.8%) having a BMI over 24. The median hospital stay day was 23 days (IQR,18-31 days). The initial presenting symptoms were jaundice (n = 38), abdominal pain (n = 49), nausea (n = 2), weight loss (n = 1), back pain (n = 1), and no symptoms (n=1). 18 (24.3%) of them had multiple presenting symptoms. The median hospital stay day was 23 days (IQR, 18-31 days). 56 patients (75.7%) underwent major hepatectomy, 1 patient (1.4%) underwent PD, and 17 patients (23.0%) underwent major hepatectomy combined with PD (Table 1).

Perioperative variables

At presentation, the median value of CA19-9 was 287 ku/L (IQR 64.8- 880.8 ku/L), and 65 (87.8%) of them had elevated CA19-9 value (>37 ku/L). The median value of CEA was 3.35 ng/mL(IQR 2.30 - 5.45 ng/mL), and only 22 (29.7%) of them had elevated CEA value (>5 ng/mL). At presentation, the median total bilirubin level was 55.25 umol/l (IQR, 11.25 - 202.5 umol/L), and 47 (63.5%) of them had elevated total bilirubin levels(>18 umol/L). The median value of ALT was 69 U/L(IQR 20.75 - 162 U/L), and 50 (67.6%) of them had elevated ALT value (>40 U/L). 32 (43.2%) of them underwent preoperative biliary drainage (25 patients through PTCD and 7 patients through ERCP)(Table 1).

For intraoperative variables, the median operation duration was 330 mins (IQR, 292.5-412.5 mins) including operation duration, the median intraoperatve blood loss was 400ml (IQR, 250ml-725ml), and the median blood transfusion volume during hospitalization was 800ml (IQR, 0-1600ml). Intraoperative complications occurred for 4 patients (5.4%), and all the complications were hemorrhagic (Table 1).

Pathological outcomes

According to pathological specimens, the median tumor size was 7 cm (IQR, 6-8 cm). 12 (16.2%), 13 (17.6%) and 28 (37.8%) tumors originated from the bottom, body, and neck of the gallbladder. The location of tumors could not be identified in 21 (28.4%) patients due to the deep invasiveness of the tumors. Most of them were moderately differentiated (n = 67, 90.5%), 5 (6.8%) were identified as being poorly differentiated, and 2 (2.7%) were identified as being well differentiated.

After resection, only 1 patient (1.4%) received R1 resection due to the margin status being positive. The other 73 patients were identified to have received R0 resection and their margin status was all negative. But, contrary to the good results of the margin status, 36 patients (48.6%) had perineural invasion, 59 patients (79.7%) had vascular invasion, 11 patients (14.9%) had invasion of the common bile duct, and only 4 patients (5.4%)

TABLE 1 The baseline characteristics and perioperative variables of gallbladder cancer patients who underwent extended resection.

Variables	Total (n=74)	%
Age, median(IQR)	62.5	56.0-67.0
Gander, male	33	44.6
BMI, median(IQR)	23.27	21.47-24.90
>24	28	37.8
Hospital stays, median days(IQR)	23	18-31
Initial presenting symptoms		
jaundice	38	51.4
abdominal pain	49	66.2
nausea	2	2.7
weight loss	1	1.4
back pain	1	1.4
no symptom	1	1.4
Type of surgery		
major hepatectomy	56	75.7
PD	1	1.4
major hepatectomy+PD	17	23.0
CA19-9 level, median, ku/L(IQR)	287	64.8- 880.8
>37 ku/L	65	87.8
CEA level, median, ng/mL(IQR)	3.35	2.30 - 5.45
>5 ng/mL	22	29.7
Total bilirubin levels, median, umol/L(IQR)	55.25	11.25 - 202.5
>18 umol/L	47	63.5
ALT, median, U/L(IQR)	69	20.75 - 162
>40 U/L	50	67.6
Preoperative biliary drainage		
PTCD	25	33.8
ERCP	7	9.5
Operation duration, median min(IQR)	330	292.5-412.5
Intraoperatve blood loss, median ml (IQR)	400	250-725
Blood transfusion volume, median ml (IQR)	800	0-1600
Intraoperative hemorrhage	4	5.4

IQR, interquartile range; PD, pancreatoduodenectomy; BMI, body mass index; CEA, carcinoembryonic antigen; ALT, alaninetransaminase; PTCD, percutaneous transhepaticcholangial drainage; ERCP, Endoscopic Retrograde Cholangiopancreatography.

had cancerization of the duct. According to pathological specimens, 25 patients (33.8%) had N1 lymphatic metastases, 2 patients (2.7%) had N2 lymphatic metastases, and the other patients had N0 lymphatic metastases. Finally, 72 patients were staged as IV A GBC and 2 patients were staged as IV B GBC. Histology showed adenocarcinoma (n = 67), squamous-cell carcinoma (n = 4), adenosquamous carcinoma (n = 2), and neuroendocrine tumor (n = 1) (Table 2).

Long-term follow-up data

Three perioperative deaths (5.4%) occurred, two due to sepsis and one due to liver failure. Major postoperative

TABLE 2 The pathological outcomes and long-term follow up data of gallbladder cancer patients who underwent extended resection.

Variables	Total (n=74)	%
Tumor size, median cm (IQR)	7	6-8
Tumor location		
Bottom	12	16.2
Body	13	17.6
Neck	28	37.8
Uncertain	21	28.4
Tumor differentiation		
Well	5	6.8
Moderately	67	90.5
Poorly	2	2.7
Margin status		
negative	73	98.6
positive	1	1.4
Peripheral tissue invasion status		
perineural invasion	36	48.6
vascular invasion	59	79.7
common bile duct invasion	11	14.9
cancerization of duct	4	5.4
Lymphatic metastasis status		
N0	47	63.5
N1	25	33.8
N2	2	2.7
GBC staging		
IV A	72	97.3
IV B	2	2.7
Types of histology		
adenocarcinoma	67	90.5
squamous-cell carcinoma	4	5.5
adenosquamous carcinoma	2	2.7
neuroendocrine tumor	1	1.3
Major postoperative complications	15	20.3
infection	9	12.2
delayed gastric emptying	4	5.5
biliary fistula	1	1.3
others	4	5.5
Recurrence sites	61	82.4
locally	36	48.6
distant	25	33.8
Adjuvant chemotherapy cycles, median n (IQR)	6.0	3.0-9.0

IQR, interquartile range; GBC, Gallbladder cancer.

complications occurred for 15 patients (20.3%), including infection(n = 9), delayed gastric emptying (n = 4), biliary fistula (n = 1), and others (n = 4). The median number of adjuvant chemotherapy cycles was 6.0 (IQR 3.0–9.0).

Recurrence occurred for 61 patients (82.4%) after a median disease-free interval of 9 months (95% confidence interval [CI], 7.8–10.2 months, Figure 1). Imaging data showed that there were 36 cases that had local recurrence and 25 cases had distant

recurrence (on the peritoneum, n = 12, in the lung, n = 10, other locations, n = 3).

All the deaths were tumor-related. After a median follow-up period of 52 months, 26 patients (35.1%) survived beyond 2 years, and 17 patients (23.0%) were still alive at the time of last follow-up. The median OS was 18.0 months (95% CI, 15.2-20.8 months, Figure 2) and the median OS was 18.0 months (95% CI, 16.0–20.0 months) when the perioperative deaths were excluded.

Factors associated with postoperative complications in patients with GBC who underwent extended resections

A logistic regression model was established to identify factors associated with postoperative complications. The baseline characteristics, perioperative variables, and intraoperative variables were included in the univariate analysis. The differences in variables between the patients with or without postoperative complications were compared and presented in Supplementary Table 1 (without age and gender adjusted) and Table 3 (with age and gender adjusted), and the patients who experienced perioperative death were excluded (n = 3). Finally, a total of 14 GBC patients (14/71, 19.7%) experienced postoperative complications after extended resections.

Based on univariate analysis, longer hospital stay days (*P*=0.013), initial symptoms with abdominal pain (*P*=0.024), more intraoperatve blood loss (*P*=0.099), more blood transfusion volume during hospitalization (*P*=0.016) and intraoperative hemorrhage (*P*=0.001) were closely correlated with postoperative complications. These factors were included in the multivariate logistic regression analysis (Table 3).

Based on multivariate logistic regression analysis, longer hospital stay days (OR=1.979, 95%CI:1.038-1.193, *P*=0.003), initial symptoms with abdominal pain (OR=21.489, 95% CI=1.22-37.57, *P*=0.036), more blood transfusion volume during hospitalization (OR=1.036, 95%CI:1.021-1.058, *P*=0.005), and intraoperative hemorrhage (OR=18.56, 95% C:3.54-47.65, *P*=0.001) were independently associated with postoperative complications after age and gender were adjusted (Table 3).

Factors associated with long-term survival in patients with GBC who underwent extended resections

Patients who survived longer than 2 years were defined as long-term survivors in our study. All the variables were included in the univariate analysis. The differences in variables between

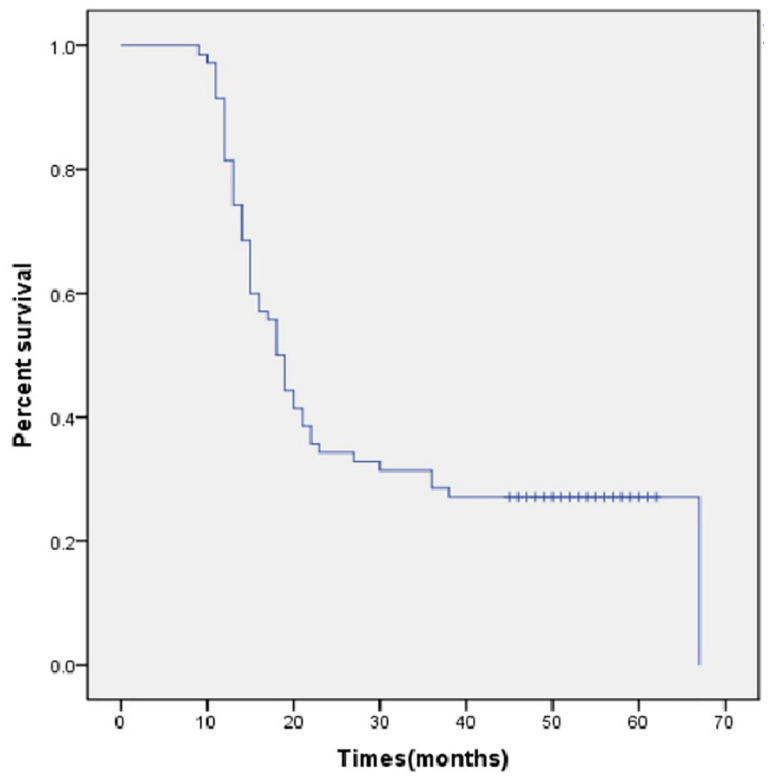

FIGURE 2
Overall survival in months.

TABLE 3 Univariate and multivariable analyses of risk factors for postoperative complications.

Parameters	With complications (n=14)	Without complications (n=57)	p value for univariate analyses	Adjusted OR (95% CI)	p value for multivariate analyses
Age,mean ± SD,year	63.4 ± 7.1	62.0 ± 8.4	0.578	1.640(0.336-7.999)	0.540
Male, n%	6(42.6)	26(45.6)	0.853	1.058(0.951-1.177)	0.299
Hospital stay days, mean ± SD	38.3 ± 14.8	24.1 ± 9.6	0.013	1.979(1.038-1.193)	0.003
BMI, mean ± SD	23.3 ± 3.2	23.3 ± 2.7	0.939		
Initial presenting symptoms, n%					
jaundice	5(35.7)	31(54.4)	0.211		
abdominal pain	13(92.9)	35(61.4)	0.024	21.489(1.22-37.57)	0.036
Type of surgery, n%					
major hepatectomy	10(71.4)	45(78.9)	0.546		
major hepatectomy+PD	4(28.6)	12(21.1)			
CA19-9 level, mean ± SD	408.7 ± 432.1	585.4 ± 710.8	0.378		
CEA level, mean ± SD	11.3 ± 24.8	7.0 ± 9.6	0.538		
Total bilirubin levels, mean ± SD	129.8 ± 149.5	107.4 ± 121.8	0.558		
ALT levels, mean ± SD	137.8 ± 163.1	104.5 ± 106.4	0.351		
Preoperative biliary drainage, n%	6(42.9)	25(43.9)	0.865		
Operation duration, mean ± SD	375 ± 38.7	329.8 ± 79.2	0.280		
Intraoperatve blood soss, mean ± SD	614.3 ± 293.1	460.5 ± 319.8	0.099	1.001(0.998-1.004)	0.514
Blood transfusion volume, mean ± SD	2332.1 ± 2773.2	1126.3 ± 2689.7	0.016	1.036(1.021-1.058)	0.005
Intraoperative hemorrhage,n%	4(28.6)	0(0)	0.001	18.56(3.54-47.65)	0.001
Tumor size, mean ± SD	7.05 ± 1.37	7.53 ± 2.68	0.371		
Tumor location					
Bottom	7(12.3)	3(21.4)	0.378		
Body	10(17.5)	3(21.4)	0.736		
.Neck	23(40.4)	5(35.7)	0.750		
Uncertain	17(29.8)	3(21.4)	0.531		

IQR, interquartile range; PD, pancreatoduodenectomy; BMI, body mass index; CEA, carcinoembryonic antigen; ALT, alaninetransaminase.

the patients with or without postoperative complications were compared and presented in Supplementary Table 2 (without age and gender adjusted) and Table 4 (with age and gender adjusted). The analysis of margin status was excluded because only one patient had positive margin status.

Based on univariate analysis, histology types of adenocarcinoma (P=0.048), locally recurrence (P=0.012), and more adjuvant chemotherapy cycles (P=0.016) were closely correlated with long-term survival. These factors were included in the multivariate logistic regression analysis (Table 4).

Based on multivariate logistic regression analysis, locally recurrence (OR=1.65, 95%CI:1.17-1.96, P=0.015), and more adjuvant chemotherapy cycles (OR=1.46, 95%CI:1.13-1.76, P=0.026) were independently associated with long-term survival after age and gender were adjusted (Table 4).

Discussion

This retrospective study investigated the clinical outcomes of extended resections in patients with stage IV GBC. To date, this study has the largest sample size on this issue. Our study cohort identified that extended resections can be safely and efficaciously performed on stage IV GBC patients in large volume centers. Despite a reported median disease-free survival of 9 months and a median OS of 18.0 months, 35% of the patients survived beyond 2 years, and 23% were still alive after a median follow-up time of 52 months. About one-fifth of patients experienced major postoperative complications, and the perioperative deaths were less than 5%. Moreover, we identified that longer hospital stay days, initial symptoms with abdominal pain, more blood transfusion volume during hospitalization, and

TABLE 4 Univariate and multivariable analyses of risk factors for long-term survival.

Parameters	Long-term survival (n=26)	Short-term survival (n=48)	p value for univariate analyses	Adjusted OR (95% CI)	p value for multivariate analyses
Age,mean ± SD,year	60.7 ± 7.7	63.0 ± 8.1	0.246	0.626(0.228-1.722)	0.364
Male, n%	13(50.0)	20(41.7)	0.491	0.967(0.908-1.030)	0.297
Hospital stay days, mean ± SD	26.3 ± 13.5	27.4 ± 11.9	0.726		
BMI, mean ± SD	23.4 ± 2.6	23.2 ± 2.8	0.705		
Initial presenting symptoms, n%					
jaundice	12(46.2)	26(54.2)	0.510		
abdominal pain	17(65.4)	32(66.7)	0.911		
Type of surgery, n% (n=73)					
major hepatectomy	21(80.8)	35(74.5)*	0.542		
major hepatectomy+PD	5(19.2)	12(25.5)			
CA19-9 level, mean ± SD	517.8 ± 667.0	594.5 ± 679.3	0.640		
CEA level, mean ± SD	5.7 ± 8.3	8.9 ± 15.7	0.341		
Total bilirubin levels, mean ± SD	109.9 ± 118.8	117.1 ± 133.1	0.819		
ALT levels, mean ± SD	144.9 ± 159.8	92.1 ± 82.5	0.125		
Preoperative biliary drainage, n%	10(38.5)	22(45.8)	0.541		
Operation duration, mean ± SD	337.8 ± 80.3	340.3 ± 73.9	0.936		
Intraoperatve blood soss, mean ± SD	530.8 ± 342.7	488.5 ± 319.6	0.591		
Blood transfusion volume, mean ± SD	1409.6 ± 1867.2	1459.4 ± 3091.3	0.941		
Intraoperative hemorrhage,n %	0(0)	4(8.3)	0.291		
Tumor size, mean ± SD	7.02 ± 1.97	7.49 ± 2.84	0.461		
Tumor location					
Bottom	3(11.5)	9(18.8)	0.354		
Body	4(15.4)	9(18.8)	0.618		
Neck	13(50)	15(31.3)	0.112		
Uncertain	6(23.1)	15(31.3)	0.356		
Tumor differentiation					
Well	1(3.8)	4(8.3)	0.651		
Moderately	24(92.3)	43(89.6)	0.702		
Poorly	1(3.8)	1(2.1)	1.00		
Peripheral tissue invasion status					
perineural invasion	11(42.3)	25(52.1)	0.422		
vascular invasion	21(80.8)	38(79.2)	0.931		
common bile duct invasion	6(23.1)	5(10.4)	0.144		
cancerization of duct	1(3.8)	3(6.3)	0.756		
Lymphatic metastasis status					
N0	17(65.4)	30(62.5)	0.806		
N1	7(26.9)	18(37.5)	0.358		
N2	2(7.7)	0	0.12		
GBC staging					
IV A	24(92.3)	48(100)	0.12		
IV B	2(7.7)	0(0)			
Types of histology					

(Continued)

TABLE 4 Continued

Parameters	Long-term survival (n=26)	Short-term survival (n=48)	p value for univariate analyses	Adjusted OR (95% CI)	p value for multivariate analyses
adenocarcinoma	22(84.6)	45(93.8)	**0.048**	0.32(0.10-1.691)	0.180
squamous-cell carcinoma	2(7.7)	2(4.2)	0.522		
adenosquamous carcinoma	1(3.8)	1(2.1)	0.655		
neuroendocrine tumor	1(3.8)	0(0)	0.351		
Major postoperative complications	15	20.3			
infection	2(7.7)	4(8.3)	0.923		
delayed gastric emptying	1(3.8)	3(6.3)	0.662		
biliary fistula	0(0)	1(2.1)	1.00		
others	1(3.8)	3(6.3)	0.662		
Recurrence sites (n=61)					
locally	16(76.2)	17(42.5)	**0.012**	1.65(1.17-1.96)	0.015
distant	5(23.8)	23(57.5)			
Adjuvant chemotherapy cycles, mean ± SD	8.20 ± 2.52	4.50 ± 3.50	**0.016**	1.46(1.13-1.76)	0.026

SD, Standard deviation; GBC, Gallbladder cancer; IQR, interquartile range; PD, pancreatoduodenectomy; BMI, body mass index; CEA, carcinoembryonic antigen; ALT, alaninetransaminase.
Bold values: P<0.1 and were included in multivariate analyses.
* only one case underwent PD in short-term survival group and was not included in analysis.

intraoperative hemorrhage were independently associated with major postoperative complications and local recurrence, and more adjuvant chemotherapy cycles were associated with long-term survival.

The value of extended resections for advanced GBC remains controversial. Results from previous studies were inconsistent. Two Japanese retrospective studies showed no survival benefit for advanced bile duct cancer and GBC patients who underwent hepatopancreaticoduodenectomy. No patient survived beyond 2 years, and the R0 resection rate was only 20% (17, 18). In a study from the Memorial Sloan Kettering Cancer Center (11), perioperative mortality rate was14% (5 of 36 patients) for major hepatectomies. Recurrence occurred for 24 patients (73%) and R0 resection margins were achieved for 91% of the patients. Most importantly, the 5-year survival rate was 27%. The R0 resection rate and 5-year survival rate were comparable with our study. They concluded that major hepatectomy combined with PD is appropriate in certain cases. However, the surgical indications were still not clear. Another study by Fong et al. (19) concluded that radical resection can provide long-term survival, even for large tumors with extensive liver invasion. However, the multi-variable analysis in that study showed that the extent of liver resection was not a risk factor for long-term survival. Due to the emerging evidence from previous studies, we conducted this study to explore the impact of extended resections for stage IV GBC. We believe our study can significantly help establish the role of extended resections in the management of stage IV GBC.

Searching the prognosis data about the advanced GBC patients who did not receive surgical resections, a Netherland population-based study that the 1-year survival rate for patients with advanced unresected GBC is less than 10% (20). The median OS of all patients who had unresected GBC treated with palliative chemotherapy was 6.4 months (14). Moreover, in a large scale randomized controlled ABC-02 trial (gemcitabine + cisplatin vs gemcitabine alone for unresected biliary tract cancer), no patient survived beyond 3 years (21). In our study, the 2 year survival rate was 35.1%, the estimated 5-year survival rate was about 20% and median OS was 18 months. The prognosis of advanced GBC patients was significantly improved by extended resection. However, more prospective randomized controlled studies are needed to further confirm the conclusion.

Almost all the patients reached R0 resection in our study. The R0 resection was higher than in previous studies. The first reason may be due to the careful patient selection preoperatively. The contrast-enhanced CT and MRI images will be carefully reviewed by radiologists and surgeons. Large tumors with extensive liver invasion will not perform extended resections. Second, the aim of the surgery is R0 resections. If the surgeon found there was no possibility to reach R0 resection during operation. The surgery will not continue and only a biopsy will be performed. Third, the surgeons who were qualified to perform extended resection were all rich in experience. On average, they perform more than 200 biliary and pancreatic surgeries every year. Therefore, most of them were IV A stage GBC and a high R0 resection rate was achieved in our study cohort.

Reducing the major postoperative complications is a way to improve prognosis. We identified that longer hospital stay days,

more blood transfusion volume during hospitalization, and intraoperative hemorrhage were independently associated with major postoperative complications. These factors were interrelated. More blood transfusions are required when intraoperative hemorrhage occurs. The complications due to hypovolemia require more hospital days for recovery. Therefore, more detailed intraoperative procedures are required to prevent intraoperative hemorrhage and finally reduce the major postoperative complications. Moreover, the initial symptoms of abdominal pain were also identified as a risk factor for major postoperative complications. The abdominal pain caused by extensive nerve invasion requires a larger resection area and finally causes intraoperative hemorrhage. However, the assumption should be verified in further studies.

For effective patient selection, prognostic factors for long-term survival should be identified. In our study, no pathological outcomes were associated with poor prognosis. However, poor survival in other studies was associated with preoperative tumor biomarker level, perivascular invasion, and invasion of the liver parenchyma (18, 22–24). All clinical stages of GBC were included in these studies with the small sample size. The IV stage GBCs were already aggressive tumors; therefore, these factors may not influence prognosis. Adjuvant chemotherapy is acknowledged as the first line treatment after surgical resection in most cancers. The recent BILCAP trial concluded that adjuvant capecitabine can improve OS for patients with resected biliary tract cancer (25). Another recent study found that individuals with resected GBC who had adjuvant chemoradiation treatment had considerably lower recurrence rates and improved OS than those that underwent surgery alone. Notably, individuals with N0 disease did not appear to benefit from adjuvant therapy. Therefore, this effect was only shown in patients with positive lymph node status (26).However, the role of adjuvant chemotherapy in advanced GBC after surgical resection is still not clear. Our study showed more adjuvant chemotherapy cycles were associated with long-term survival. However, no comparison group was set in our study. Further prospective randomized control is needed to clarify the true value of adjuvant chemotherapy and the optimal regimens.

Our study had several limitations. First, it was a retrospective review of a cohort of patients in a single center, so some selection bias may exist. The small sample size made it impossible to draw statistical conclusions about prognostic factors for prolonged survival, especially the pathological outcomes. Second, due to the retrospective nature, the postoperative quality of life was not analyzed. Third, the high morbidity and mortality rates associated with extensive resections should be weighed against the apparent survival benefit. Therefore, further prospective randomized control with a larger cohort of patients is needed to clarify the true value of extended resections.

Conclusion

Our retrospective study identified that extended resections can be safely and efficaciously performed on stage IV GBC patients in large volume centers. The median disease-free survival was 9 months and the median OS was 18.0 months, 35% of the patients survived beyond 2 years, and 23% were still alive after a median follow-up time of 52 months. About one-fifth of patients experienced major postoperative complications, and the perioperative deaths were less than 5%. Longer hospital stay days, initial symptoms with abdominal pain, more blood transfusion volume during hospitalization, and intraoperative hemorrhage were independently associated with major postoperative complication and locally recurrence and more adjuvant chemotherapy cycles were associated with long-term survival. Therefore, extended resections for patients with IVA stage GBC should be considered in selected patients and performed by experienced surgeons.

Data availability statement

The raw data supporting the conclusions of this article will be made available by the authors, without undue reservation.

Ethics statement

Written informed consent was obtained from the individual (s), and minor(s)' legal guardian/next of kin, for the publication of any potentially identifiable images or data included in this article.

Author contributions

KZ: Data collection, statistical analysis and interpretation of data. HL: Paper writing. BZ: Design of the study, data collection and literature search. YZ: Manuscript review design of the study. All authors contributed to the article and approved the submitted version.

Funding

This study was supported by Mengchao talents foundation from Eastern Hepatobiliary Surgery Hospital.

Conflict of interest

The authors declare that the research was conducted in the absence of any commercial or financial relationships that could be construed as a potential conflict of interest.

Publisher's note

All claims expressed in this article are solely those of the authors and do not necessarily represent those of their affiliated organizations, or those of the publisher, the editors and the reviewers. Any product that may be evaluated in this article, or claim that may be made by its manufacturer, is not guaranteed or endorsed by the publisher.

Supplementary material

The Supplementary Material for this article can be found online at: https://www.frontiersin.org/articles/10.3389/fonc.2022.1032737/full#supplementary-material

References

1. Lazcano-Ponce EC, Miquel JF, Munoz N, Herrero R, Ferrecio C, Wistuba II, et al. Epidemiology and molecular pathology of gallbladder cancer. *CA Cancer J Clin* (2001) 51(6):349–64. doi: 10.3322/canjclin.51.6.349

2. Stinton LM, Shaffer EA. Epidemiology of gallbladder disease: cholelithiasis and cancer. *Gut Liver* (2012) 6(2):172–87. doi: 10.5009/gnl.2012.6.2.172

3. Xie W, Yang T, Zuo J, Ma Z, Yu W, Hu Z, et al. Chinese And global burdens of gastrointestinal cancers from 1990 to 2019. *Front Public Health* (2022) 10:941284. doi: 10.3389/fpubh.2022.941284

4. Hundal R, Shaffer EA. Gallbladder cancer: epidemiology and outcome. *Clin Epidemiol* (2014) 6:99–109. doi: 10.2147/CLEP.S37357

5. Torre LA, Siegel RL, Islami F, Bray F, Jemal A. Worldwide burden of and trends in mortality from gallbladder and other biliary tract cancers. *Clin Gastroenterol Hepatol* (2018) 16(3):427–37. doi: 10.1016/j.cgh.2017.08.017

6. Branch of Biliary Surgery, Chinese Surgical Society and Chinese Committee of Biliary Surgeons. Guideline for the diagnosis and treatment of gallbladder carcinoma (2019 edition). *Zhonghua Wai Ke Za Zhi* (2020) 58(4):243–51. doi: 10.3760/cma.j.cn112139-20200106-00014

7. Taner CB, Nagorney DM, Donohue JH. Surgical treatment of gallbladder cancer. *J Gastrointest Surg* (2004) 8(1):83–89, 89. doi: 10.1016/j.gassur.2003.09.022

8. Dou C, Zhang C, Zhang C, Liu J. Propensity score analysis of outcomes following laparoscopic or open radical resection for gallbladder cancer in T2 and T3 stages. *J Gastrointest Surg* (2022) 26(7):1416–24. doi: 10.1007/s11605-022-05288-y

9. Li L, Ren T, Liu K, Li ML, Geng YJ, Yang Y, et al. Development and validation of a prognostic nomogram based on the systemic immune-inflammation index for resectable gallbladder cancer to predict survival and chemotherapy benefit. *Front Oncol* (2021) 11:692647. doi: 10.3389/fonc.2021.692647

10. Chen C, Geng Z, Shen H, Song H, Zhao Y, Zhang G, et al. Long-term outcomes and prognostic factors in advanced gallbladder cancer: Focus on the advanced T stage. *PloS One* (2016) 11(11):e166361. doi: 10.1371/journal.pone.0166361

11. D'Angelica M, Dalal KM, DeMatteo RP, Fong Y, Blumgart LH, Jarnagin WR. Analysis of the extent of resection for adenocarcinoma of the gallbladder. *Ann Surg Oncol* (2009) 16(4):806–16. doi: 10.1245/s10434-008-0189-3

12. Mizuno T, Ebata T, Yokoyama Y, Igami T, Yamaguchi J, Onoe S, et al. Major hepatectomy with or without pancreatoduodenectomy for advanced gallbladder cancer. *Br J Surg* (2019) 106(5):626–35. doi: 10.1002/bjs.11088

13. Yamamoto Y, Sugiura T, Okamura Y, Ito T, Ashida R, Uemura S, et al. Is combined pancreatoduodenectomy for advanced gallbladder cancer justified? *Surgery* (2016) 159(3):810–20. doi: 10.1016/j.surg.2015.09.009

14. Kuipers H, de Savornin LE, van Dooren M, Braat AE, Daams F, van Dam R, et al. Extended resections for advanced gallbladder cancer: Results from a nationwide cohort study. *Ann Surg Oncol* (2021) 28(2):835–43. doi: 10.1245/s10434-020-08858-z

15. Reddy SK, Marroquin CE, Kuo PC, Pappas TN, Clary BM. Extended hepatic resection for gallbladder cancer. *Am J Surg* (2007) 194(3):355–61. doi: 10.1016/j.amjsurg.2007.02.013

16. Dindo D, Demartines N, Clavien PA. Classification of surgical complications: a new proposal with evaluation in a cohort of 6336 patients and results of a survey. *Ann Surg* (2004) 240(2):205–13. doi: 10.1097/01.sla.0000133083.54934.ae

17. Sakamoto Y, Nara S, Kishi Y, Esaki M, Shimada K, Kokudo N, et al. Is extended hemihepatectomy plus pancreaticoduodenectomy justified for advanced bile duct cancer and gallbladder cancer? *Surgery* (2013) 153(6):794–800. doi: 10.1016/j.surg.2012.11.024

18. Kaneoka Y, Yamaguchi A, Isogai M, Harada T, Suzuki M. Hepatoduodenal ligament invasion by gallbladder carcinoma: histologic patterns and surgical recommendation. *World J Surg* (2003) 27(3):260–5. doi: 10.1007/s00268-002-6702-0

19. Fong Y, Jarnagin W, Blumgart LH. Gallbladder cancer: comparison of patients presenting initially for definitive operation with those presenting after prior noncurative intervention. *Ann Surg* (2000) 232(4):557–69. doi: 10.1097/00000658-200010000-00011

20. Witjes CD, van den Akker SA, Visser O, Karim-Kos HE, de Vries E, Ijzermans JN, et al. Gallbladder cancer in the Netherlands: incidence, treatment and survival patterns since 1989. *Dig Surg* (2012) 29(2):92–8. doi: 10.1159/000336217

21. Weigt J, Malfertheiner P. Cisplatin plus gemcitabine versus gemcitabine for biliary tract cancer. *Expert Rev Gastroenterol Hepatol* (2010) 4(4):395–7. doi: 10.1586/egh.10.45

22. Yamaguchi R, Nagino M, Oda K, Kamiya J, Uesaka K, Nimura Y. Perineural invasion has a negative impact on survival of patients with gallbladder carcinoma. *Br J Surg* (2002) 89(9):1130–6. doi: 10.1046/j.1365-2168.2002.02184.x

23. Chakravarty KD, Yeh CN, Jan YY, Chen MF. Factors influencing long-term survival in patients with T3 gallbladder adenocarcinoma. *Digestion* (2009) 79(3):151–7. doi: 10.1159/000210131

24. Noshiro H, Chijiiwa K, Yamaguchi K, Shimizu S, Sugitani A, Tanaka M. Factors affecting surgical outcome for gallbladder carcinoma. *Hepatogastroenterology* (2003) 50(52):939–44.

25. Primrose JN, Fox RP, Palmer DH, Malik HZ, Prasad R, Mirza D, et al. Capecitabine compared with observation in resected biliary tract cancer (BILCAP): a randomised, controlled, multicentre, phase 3 study. *Lancet Oncol* (2019) 20(5):663–73. doi: 10.1016/S1470-2045(18)30915-X

26. Hakeem AR, Papoulas M, Menon KV. The role of neoadjuvant chemotherapy or chemoradiotherapy for advanced gallbladder cancer - a systematic review. *Eur J Surg Oncol* (2019) 45(2):83–91. doi: 10.1016/j.ejso.2018.08.020

frontiers | Frontiers in Oncology

TYPE Review
PUBLISHED 25 October 2022
DOI 10.3389/fonc.2022.1062357

Check for updates

OPEN ACCESS

EDITED BY
Zhendong Jin,
Second Military Medical University, China

REVIEWED BY
Suliman Khan,
Second Affiliated Hospital of Zhengzhou University, China
Mingyang Song,
Southeast University, China

*CORRESPONDENCE
Zhao Meng
815412701@qq.com

SPECIALTY SECTION
This article was submitted to Gastrointestinal Cancers: Hepato Pancreatic Biliary Cancers, a section of the journal Frontiers in Oncology

RECEIVED 05 October 2022
ACCEPTED 11 October 2022
PUBLISHED 25 October 2022

CITATION
Meng Z, Huang Z, Deng B, Ling L, Ning Y and Rafiq SM (2022) Robotic-assisted vs non-robotic traction techniques in endoscopic submucosal dissection for malignant gastrointestinal lesions. *Front. Oncol.* 12:1062357. doi: 10.3389/fonc.2022.1062357

COPYRIGHT
© 2022 Meng, Huang, Deng, Ling, Ning and Rafiq. This is an open-access article distributed under the terms of the Creative Commons Attribution License (CC BY). The use, distribution or reproduction in other forums is permitted, provided the original author(s) and the copyright owner(s) are credited and that the original publication in this journal is cited, in accordance with accepted academic practice. No use, distribution or reproduction is permitted which does not comply with these terms.

Robotic-assisted vs non-robotic traction techniques in endoscopic submucosal dissection for malignant gastrointestinal lesions

Zhao Meng[1]*, Zhanghua Huang[1], Bingli Deng[1], Liuming Ling[1], Yaowen Ning[1] and Shoaib Mohammed Rafiq[2]

[1]Department of Gastroenterology, The Second People's Hospital of Qinzhou, Qinzhou, Guangxi, China, [2]Department of Emergency and Trauma Center, District Headquarter Teaching Hospital, Gujranwala, Pakistan

Endoscopic submucosal dissection is an effective approach with higher en bloc resection and complete resection rate for superficial gastrointestinal (GI) lesions. However, endoscopic submucosal dissection is technically challenging and associated with several adverse events, such as bleeding or perforations. The single channel flexible endoscope's intrinsic limitations in preserving visualization of the submucosal dissection plane as compared to laparoscopic surgery are the most common cause of complications during the endoscopic submucosal dissection technique. As a result, traction techniques were created as the endoscope's second helping hand in order to improve the effectiveness of the endoscopic submucosal dissection method. Trainees can master endoscopic submucosal dissection methods more quickly by using traction techniques. The anatomical location of the lesion plays a major role in determining which traction technique should be employed. An appealing way of traction is robot-assisted endoscopic submucosal dissection, and various types of endoscopic robots that allow bimanual operation are currently being developed. The advent of robot-assisted endoscopic technology ushers in a new era of endoscopic submucosal dissection, and with it come its own unique challenges that remain to be elucidated. Future research and development efforts are needed to focus on pathways and curriculums for trainees to master the currently available traction techniques and provide avenues for the development of newer traction modalities. In this article, we discuss evolution, characteristics, technological improvements and clinical comparisons of both robotic and non-robotic endoscopic traction techniques used in endoscopic submucosal dissection.

KEYWORDS

endoscopic submucosal dissection, robotic assisted traction, non-robotic traction, endoscopic traction, gastrointestinal cancer

Introduction

Endoscopic submucosal dissection (ESD) has become the widely accepted and minimally invasive therapy of choice for superficial gastrointestinal (GI) tumors (1–3). ESD is an efficient therapeutic endoscopic procedure with a high en bloc resection rate and lower local recurrence rate compared to endoscopic mucosal resection (4, 5). However, ESD is technically challenging because it is associated with prolonged procedure time and several adverse events. The most common complications of ESD are perforation and bleeding (6, 7). In addition, it also requires stricter access conditions and longer learning curve than endoscopic mucosal resection which limits the worldwide popularity, especially in the United States and Western Countries (8, 9).

The major cause of complications in ESD procedure is that the visibility of the dissection plane is not secured because of the mucosal flap (10). Appropriate tissue tension and clear visibility of the tissue to be dissected using traction are essential for effective and safe ESD procedure. Although, the use of a transparent cap and reduplicative submucosal injection before the next resection is beneficial to obtain clear visibility of the submucosal layer. However, the supporting capacity of cap is limited and repeated injections prolong the procedure time. Another simple method is to change the patient's position during the procedure for adequate tissue tension, but when the lesion is in the upper GI tract, the optimal position is limited. Although expert and experienced endoscopists can perform the endoscopic resection using superior dexterity gained from rich experience, unskilled endoscopists commonly find it technically demanding and difficult to complete the resection without good visibility of the dissection plane. The lack of a controllable second hand in ESD is a major difference compared with laparoscopic surgery which has three ports to assist the procedure.

Inspired by the surgical pull and push techniques, traction technology arisen and was applied as a "second-hand" for endoscope (11). With the assistant of some accessories, it can not only provide a clear view of submucosal tissue and vessel for operation but also gets adequate tissue tension, which facilitates ESD to be more effective and safer. In recent years, traction techniques have developed rapidly, including clip-with-snare traction, clip-with-line traction, magnetic anchor traction, percutaneous traction, external forceps traction, and internal-traction method (12–15). Although, these techniques are effective for simple counter traction, but they are still restricted in terms of being able to regulate the direction of the traction, change the submucosal layer's tension, and re-grasping of the tissue. Some of these techniques are also invasive and only effective in certain regions of the GI tract. Endoscopic use of flexible robotic arms may aid the operator in getting over the ESD procedure's technical challenges (16). Robot-assisted ESD is a desirable traction technique, and several kinds of endoscopic robots that permit bimanual operation are currently being developed. A new era of endoscopic surgery with robot assistance has begun. The goal of this study is to compare robotic and non-robotic endoscopic traction techniques in endoscopic submucosal dissection, as well as to review their development and characteristics.

Non-robotic endoscopic traction

Double-scope technique

In the double-scope traction technique, a second small-caliber endoscope is inserted along with the main endoscope after circumferential resection. By passing a share, net, or forceps through the second endoscope's channel, and deploying the instrument of interest on the desired edge of tissue undergoing resection, traction can be applied (17). The primary endoscope is responsible for ESD. The double-scope method is not feasible for deep intubation of the GI tract, and hence is generally used for colorectal or gastric ESD (18). Additional limitations of the double-scope method include friction from the two endoscopes, requirement of two endoscopists, and difficulty in resection of large lesions due to insufficient space for maneuvering and operability.

Double-channel scope traction (the R-Scope)

The double-channel endoscope (also known as the R-scope; Olympus) has two movable instrument channels: one moves grasping forceps vertically for lesion counter traction; the other swings a cutting knife horizontally for dissection (19, 20). The R-scope is heavier and more difficult to operate than a single-channel endoscope. Maneuvering two tools simultaneously through the double-channel-scope is technically challenging and time-consuming. The learning curve for efficient use and troubleshooting common problems that one may face while using the R-scope also needs to be elucidated.

Robot-assisted traction techniques

EndoSamurai

The EndoSamurai (Olympus Medical Systems Corp, Tokyo, Japan) consists of an endoscopic shaft and two independent arms with built-in working channels for interchanging surgical tools (21, 22). These independent arms are parallel to the endoscope shaft and can be opened after introduction of the

scope to the site of interest. A third working channel is available within the endoscopic shaft. However, this working channel allows relatively less triangulation compared to the two independent arms, which translates into suboptimal tissue counter traction. The EndoSamurai system requires an overtube for the insertion of the scope, and two endoscopists are needed for operation, (one at the scope and one controlling the command console for the two working channel arms. The EndoSamurai system allows five degrees of freedom. The complexity of controlling a multi-channel therapeutic endoscope needs further study, as does elucidation of a learning curve. Additionally, retraction of larger organs can be difficult which limits the potential for resection with clear margins. Furthermore, no human studies exist to date and the feasibility of this system *in vivo* remains to be seen.

ANUBIScope

The ANUBIS project was a result of collaboration between Storz and Institut de Recherche contre les Cancers de l'Appareil Digestif (IRCAD). The ANUBIScope consists of a four-way articulating flexible endoscopic shaft with two "wings" which are closed during introduction of the scope, acting as a tulip shaped blunt trocar to prevent luminal injury (23, 24). These "wings" house two 4.2 mm working channels, whereas a third 3.4 mm working channel is housed in the endoscope shaft. Similar to the EndoSamuai system, tissue retraction in a retroflexed position has been reported to be difficult with the ANUBIScope and remains an area of further experimentation. Additionally, the ANUBIScope requires cooperation and synchronized workflow between two physicians. The STRAS/ANUBIScope system is a robotic version of the ANUBIScope which has a tele-operated interface that obviates the need for a second physician and has been successfully used to perform ESD in porcine models with a favorable safety profile. Nonetheless, further study is needed before adoption of this system in human subjects.

Master and slave trans-endoluminal robot

The MASTER system consists of a master controller, a telesurgical workstation to independently control endoscopically deployed surgical tools for ESD, and a custom-designed therapeutic endoscope with two working channels. It should be performed by two operators, the endoscopist maneuvering the endoscope and the surgeon controlling the master robotic controller. Gastric ESD assisted by MASTER has been reported in several studies (25, 26). The MASTER system has been tested for EFTR as well as NOTES hepatic wedge resection with favorable preliminary results in terms of procedure time, maneuverability, degrees of freedom, ease of use and the cognitive load while performing procedures. More recently, a randomized, controlled, ex vivo study comparing conventional ESD to robot-assisted ESD (RESD) showed that RESD resulted in a higher en bloc resection rate with a shorter procedure time and a lower perforation rate. Robotic traction techniques, however, are currently in their infancy, and further experimental studies are needed to explore the safety and efficacy profile of these modalities.

Conclusion and future perspective

Endoscopic submucosal dissection is a landmark technique in the development of endoscopic therapy and has been rapidly promoted. Although endoscopic submucosal dissection is an effective therapy for superficial lesions in the GI tract, it is challenging and requires a high degree of skill levels, which might hinder its execution and raise the possibility of complications (27, 28). The current ESD procedure carries the high risk of complications such as bleeding and perforation resulting from blind dissection. This is because a standard endoscope has inherent limitations in maintaining visualization of the submucosal dissection plane due to its one-handed operation capacity. A long period of training is required for endoscopists because they must undergo extensive training before they can perform ESD in a secure and expert manner. Variety of non-robotic traction techniques have been emerged to overcome these limitations with the goal of achieving proper counter traction. These traction techniques can achieve good, clear visualization of the submucosal layer using only a few, easy-to-configure components. However, they are constrained by the fact that the direction of traction cannot be changed, and the modification process is difficult because re-grasping is not allowed (29–31). Moreover, the tension of traction can reduce over time in some of these techniques. Robot-assisted traction in endoscopic submucosal dissection is another attempt to mitigate this difficulty.

Various endoscopic robot systems with twin arms that can be operated bimanually are currently available in the market. Robotic systems have shown success in therapeutic endoscopic operations, but the development of specially tailored endoscopes and tools had delayed their widespread clinical use. According to several investigations, it is theoretically possible to do endoscopic submucosal dissection using a simple robot that enables the endoscopist to dynamically apply counter traction. In comparison to conventional non-robotic procedures, robotic-assisted traction could significantly shorten the duration of the

surgery and obtain a greater rate of direct vision dissection. Robotic-assisted traction is simple to implement into clinical practice and decreases the learning curve of endoscopic submucosal dissection for beginners. Additionally, it enables the endoscopist to carry out standard endoscopic submucosal dissection. Consequently, further research into the robotic-assisted traction strategy is necessary.

Authors contributions

Study concept and design: ZM, ZH. Manuscript writing: ZM, ZH, SR. Collection, analysis and interpretation of data: BD, LL, YN. Critical revision of manuscript: ZM, SR. All authors contributed to the article and approved the submitted version.

Conflict of interest

The authors declare that the research was conducted in the absence of any commercial or financial relationships that could be construed as a potential conflict of interest.

Publisher's note

All claims expressed in this article are solely those of the authors and do not necessarily represent those of their affiliated organizations, or those of the publisher, the editors and the reviewers. Any product that may be evaluated in this article, or claim that may be made by its manufacturer, is not guaranteed or endorsed by the publisher.

References

1. Aadam AA, Abe S. Endoscopic submucosal dissection for superficial esophageal cancer. *Dis Esophagus* (2018) 31(7). doi: 10.1093/dote/doy021

2. Landin MD, Guerrón AD. Endoscopic mucosal resection and endoscopic submucosal dissection. *Surg Clin North Am* (2020) 100(6):1069–78. doi: 10.1016/j.suc.2020.07.004

3. Ono H, Yao K, Fujishiro M, Oda I, Uedo N, Nimura S, et al. Guidelines for endoscopic submucosal dissection and endoscopic mucosal resection for early gastric cancer (second edition). *Dig Endosc* (2021) 33(1):4–20. doi: 10.1111/den.13883

4. Inoue T, Nakagawa K, Yamasaki Y, Shichijo S, Kanesaka T, Maekawa A, et al. Underwater endoscopic mucosal resection versus endoscopic submucosal dissection for 20-30 mm colorectal polyps. *J Gastroenterol Hepatol* (2021) 36(9):2549–57. doi: 10.1111/jgh.15494

5. Vaganov YE, Nagudov MA, Khomyakov EA, Achkasov SI. Endoscopic submucosal dissection versus endoscopic mucosal resection for colorectal tumors: a systematic review and meta-analysis. *Khirurgiia (Mosk)* (2021) 9):77–84. doi: 10.17116/hirurgia202109177

6. Akahoshi K, Kubokawa M, Inamura K, Akahoshi K, Shiratsuchi Y, Tamura S. Current challenge: Endoscopic submucosal dissection of superficial non-ampullary duodenal epithelial tumors. *Curr Treat Options Oncol* (2020) 21(12):98. doi: 10.1007/s11864-020-00796-y

7. Kotzev AI, Yang D, Draganov PV. How to master endoscopic submucosal dissection in the USA. *Dig Endosc* (2019) 31(1):94–100. doi: 10.1111/den.13240

8. Oyama T, Yahagi N, Ponchon T, Kiesslich T, Berr F. How to establish endoscopic submucosal dissection in Western countries. *World J Gastroenterol* (2015) 21(40):11209–20. doi: 10.3748/wjg.v21.i40.11209

9. Draganov PV, Coman RM, Gotoda T. Training for complex endoscopic procedures: how to incorporate endoscopic submucosal dissection skills in the West? *Expert Rev Gastroenterol Hepatol* (2014) 8(2):119–21. doi: 10.1586/17474124.2014.864552

10. Kishida Y, Kakushima N, Kawata N, Tanaka M, Takizawa K, Imai K, et al. Complications of endoscopic dilation for esophageal stenosis after endoscopic submucosal dissection of superficial esophageal cancer. *Surg Endosc* (2015) 29(10):2953–9. doi: 10.1007/s00464-014-4028-2

11. Fukami N. What we want for ESD is a second hand! traction method. *Gastrointest Endosc* (2013) 78(2):274–6. doi: 10.1016/j.gie.2013.04.192

12. Abe S, Wu SYS, Ego M, Takamaru H, Sekiguchi M, Yamada M, et al. Efficacy of current traction techniques for endoscopic submucosal dissection. *Gut Liver* (2020) 14(6):673–84. doi: 10.5009/gnl19266

13. Esaki M, Ihara E, Gotoda T. Endoscopic instruments and techniques in endoscopic submucosal dissection for early gastric cancer. *Expert Rev Gastroenterol Hepatol* (2021) 15(9):1009–20. doi: 10.1080/17474124.2021.1924056

14. Nagata M. Advances in traction methods for endoscopic submucosal dissection: What is the best traction method and traction direction? *World J Gastroenterol* (2022) 28(1):1–22. doi: 10.3748/wjg.v28.i1.1

15. Nagata M. Internal traction method using a spring-and-loop with clip (S-O clip) allows countertraction in gastric endoscopic submucosal dissection. *Surg Endosc* (2020) 34(8):3722–33. doi: 10.1007/s00464-020-07590-9

16. Kim SH, Kim BG, Choi HS, Hong D, Jang SH, Hong K, et al. Endoscopic submucosal dissection using a detachable assistant robot: a comparative *in vivo* feasibility study (with video). *Surg Endosc* (2021) 35(10):5836–41. doi: 10.1007/s00464-021-08510-1

17. Chou CK, Tsai KF, Tseng CH, Lee CT, Yang KH, Chang MC, et al. Novel colorectal endoscopic submucosal dissection with double-endoscope and snare-based traction. *Dis Colon Rectum* (2022) 65(7):936–45. doi: 10.1097/DCR.0000000000002355

18. Zhang Q, Xing TY, Wang Z. A snare combined with endoclips to assist in endoscopic submucosal dissection for intraepithelial neoplasia in the entire colon and rectum. *Scand J Gastroenterol* (2019) 54(1):114–21. doi: 10.1080/00365521.2018.1549270

19. Tang SJ, Naga YM, Zhang S. Double-channel double-grasper technique in over-the-scope clip deployment. *VideoGIE* (2020) 5(4):141–3. doi: 10.1016/j.vgie.2019.12.010

20. Neuhaus H, Costamagna G, Devière J, Fockens P, Ponchon T, Rösch T, et al. Endoscopic submucosal dissection (ESD) of early neoplastic gastric lesions using a new double-channel endoscope (the "R-scope"). *Endoscopy* (2006) 38(10):1016–23. doi: 10.1055/s-2006-944830

21. Yeung BP, Gourlay T. A technical review of flexible endoscopic multitasking platforms. *Int J Surg* (2012) 10(7):345–54. doi: 10.1016/j.ijsu.2012.05.009

22. Yasuda K, Kitano S, Ikeda K, Sumiyama K, Tajiri H. Assessment of a manipulator device for NOTES with basic surgical skill tests: a bench study. *Surg Laparosc Endosc Percutan Tech* (2014) 24(5):e191–5. doi: 10.1097/SLE.0b013e31828fa24a

23. Zorn L, Nageotte F, Zanne P, Legner A, Dallemagne B, Marescaux J, et al. A novel telemanipulated robotic assistant for surgical endoscopy: Preclinical application to ESD. *IEEE Trans BioMed Eng* (2018) 65(4):797–808. doi: 10.1109/TBME.2017.2720739

24. Iwasa T, Nakadate R, Onogi S, Okamoto Y, Arata J, Oguri S, et al. A new robotic-assisted flexible endoscope with single-hand control: endoscopic submucosal dissection in the ex vivo porcine stomach. *Surg Endosc* (2018) 32(7):3386–92. doi: 10.1007/s00464-018-6188-y

25. Phee SJ, Low SC, Huynh VA, Kencana AP, Sun ZL, Yang K. Master and slave transluminal endoscopic robot (MASTER) for natural orifice transluminal endoscopic surgery (NOTES). *Annu Int Conf IEEE Eng Med Biol Soc* (2009) 2009:1192–5. doi: 10.1109/IEMBS.2009.5333413

26. Takeshita N, Phee SJ, Chiu PW, Ho KY. Global evaluative assessment of robotic skills in endoscopy (GEARS-e): objective assessment tool for master and slave transluminal endoscopic robot. *Endosc Int Open* (2018) 6(8):E1065–9. doi: 10.1055/a-0640-3123

27. Santos JB, Nobre MRC, Oliveira CZ, Safatle-Ribeiro AV, Kawaguti F, Martins B, et al. Risk factors for adverse events of colorectal endoscopic

submucosal dissection: a systematic review and meta-analysis. *Eur J Gastroenterol Hepatol* (2021) 33(1S Suppl 1):e33–41. doi: 10.1097/MEG.0000000000001994

28. Kamigaichi Y, Oka S, Tanaka S, Nagata S, Kunihiro M, Kuwai T, et al. Factors for conversion risk of colorectal endoscopic submucosal dissection: A multicenter study. *Surg Endosc* (2022) 36(8):5698–709. doi: 10.1007/s00464-022-09250-6

29. Liu X, Yu X, Wang Y, Yu J, Liu X, Liu Z, et al. Effectiveness of a novel traction device in endoscopic submucosal dissection for colorectal lesions. *Surg Endosc* (2022). doi: 10.1007/s00464-022-09228-4

30. Yamasaki Y, Takeuchi Y, Uedo N, Kanesaka T, Kato M, Hamada K, et al. Efficacy of traction-assisted colorectal endoscopic submucosal dissection using a clip-and-thread technique: A prospective randomized study. *Dig Endosc* (2018) 30 (4):467–76. doi: 10.1111/den.13036

31. Bordillon P, Pioche M, Wallenhorst T, Rivory J, Legros R, Albouys J, et al. Double-clip traction for colonic endoscopic submucosal dissection: a multicenter study of 599 consecutive cases (with video). *Gastrointest Endosc* (2021) 94(2):333–43. doi: 10.1016/j.gie.2021.01.036

frontiers | Frontiers in Oncology

TYPE Review
PUBLISHED 27 October 2022
DOI 10.3389/fonc.2022.1036648

Check for updates

OPEN ACCESS

EDITED BY
Zhendong Jin,
Second Military Medical University, China

REVIEWED BY
Muhammad Azhar Nisar,
Tulane University, United States
Xiaoqun Dong,
Brown University, United States

*CORRESPONDENCE
Bingrong Liu
fccliubr@zzu.edu.cn
Huiyu Yang
huiyuyang@126.com
Xing Ma
fccmax@zzu.edu.cn

†These authors have contributed equally to this work

SPECIALTY SECTION
This article was submitted to Gastrointestinal Cancers: Gastric and Esophageal Cancers, a section of the journal Frontiers in Oncology

RECEIVED 04 September 2022
ACCEPTED 10 October 2022
PUBLISHED 27 October 2022

CITATION
Shi Y, Wang M, Liu D, Ullah S, Ma X, Yang H and Liu B (2022) Super-enhancers in esophageal carcinoma: Transcriptional addictions and therapeutic strategies.
Front. Oncol. 12:1036648.
doi: 10.3389/fonc.2022.1036648

COPYRIGHT
© 2022 Shi, Wang, Liu, Ullah, Ma, Yang and Liu. This is an open-access article distributed under the terms of the Creative Commons Attribution License (CC BY). The use, distribution or reproduction in other forums is permitted, provided the original author(s) and the copyright owner(s) are credited and that the original publication in this journal is cited, in accordance with accepted academic practice. No use, distribution or reproduction is permitted which does not comply with these terms.

Super-enhancers in esophageal carcinoma: Transcriptional addictions and therapeutic strategies

Yang Shi[1,2†], Meiqi Wang[3†], Dan Liu[1,2], Saif Ullah[1,2], Xing Ma[4*], Huiyu Yang[1,2*] and Bingrong Liu[1,2*]

[1]Department of Gastroenterology, The First Affiliated Hospital of Zhengzhou University, Zhengzhou, China, [2]State Key Laboratory of Esophageal Cancer Prevention and Treatment, Zhengzhou University, Zhengzhou, China, [3]Academy of Medical Sciences Zhengzhou University, Zhengzhou, China, [4]Department of Nuclear Medicine, The Affiliated Cancer Hospital of Zhengzhou University & Henan Cancer Hospital, Zhengzhou, China

The tumorigenesis of esophageal carcinoma arises from transcriptional dysregulation would become exceptionally dependent on specific regulators of gene expression, which could be preferentially attributed to the larger non-coding *cis*-regulatory elements, *i.e.* super-enhancers (SEs). SEs, large genomic regulatory entity in close genomic proximity, are underpinned by control cancer cell identity. As a consequence, the transcriptional addictions driven by SEs could offer an Achilles' heel for molecular treatments on patients of esophageal carcinoma and other types of cancer as well. In this review, we summarize the recent findings about the oncogenic SEs upon which esophageal cancer cells depend, and discuss why SEs could be seen as the hallmark of cancer, how transcriptional dependencies driven by SEs, and what opportunities could be supplied based on this cancer-specific SEs.

KEYWORDS

super-enhancers, esophageal carcinoma, core regulatory circuitry, transcriptional dependence, histone acetylation

Introduction

Esophageal carcinoma is the fourth most common gastrointestinal cancer worldwide. The incidence and mortality rates of esophageal carcinoma accounts for 11.75% and 14.99%, respectively (1). According to statistics from the International Researches Agency of Cancer (IRAC), the mortality rate of the cancer would increase 69% in China by 2040, while the main histological type is squamous cell carcinoma (ESCC) (2, 3). The standard-of-care regimens consisted of surgery, platinum-based chemotherapy, radiotherapy, and PD-1/PD-L1 blockade therapy (4, 5), which have improved the survival rate and patient's

quality of life. However, chemoradiotherapy resistance, postoperative recurrence and unresectable advanced lesions are still impeding the long-term survival of these patients. Given that the limited actionable drivers in ESCC, more effective avenues based on the clarification of the carcinogenesis are required. Recently, it is widely recognized that the disease-associated variations are bound up with enhancer regions, especially super-enhancers (SEs), which undoubtedly provides novel insights into therapeutic maneuvers.

Enhancers refer to non-coding part of genome that activate genes expression independent of orientation, distance, and location regarding its transcription start sites (TSSs). These regulatory elements always provide binding sites for multiple transcription factors (TFs) that can also be transcribed to produce non-coding enhancer RNAs (eRNAs). More recently, cluster of enhancers located genomic proximity were identified as the unique transcriptional single entity, known as SEs. SEs are underpinned by highly abundant and orchestrated interactions with transcription apparatus and active enhancer marks (Acetylation at lysine 27, H3K27ac & Monomethylation at lysine 4, H3K4me1). Notably, SEs have been demonstrated to dictate cell identity and disease and play a key role in carcinogenesis in a broad spectrum of tumors. Recently, it has been proposed that SEs have the potential to serve as valuable prognostic and therapeutic targets in cancer.

During the past decade, various types of cancer pathogenesis have been proved to be closely associated with SEs, such as oncogenes activation, dysregulated signaling pathways, and genetic mutations. Generally, cancer-specific SEs assembly are not presented in the corresponding non-cancerous tissues, such as C-Myc, INSM1 (6) and TAL1 (7). Broadly, these SEs activate the tumorigenic signaling pathways, promoting oncogenic transcriptions, and enriched in key TFs binding motifs. Fortunately, the sensitivity of SEs to perturbation has shown the promising therapeutic vulnerability in various types of cancer, including breast cancer (8), nasopharyngeal carcinoma (9), small cell lung cancer (10), medulloblastoma (11) and esophageal carcinoma (12). The critical oncogenes of ESCC, *e.g. TP63*, *SOX2*, *KLF5* and *ALDH3A1*, have been shown to participate in core regulatory circuitry (CRC) driven by SEs (12). Besides, the pharmacological inhibition of cyclin dependent kinase 7 (CDK7), bromodomain-containing protein 4 (BRD4) and histone deacetylases (HDACs), has been applied in esophageal carcinoma treatment (13).

Therefore, not surprisingly, deregulation of SEs is fundamental mechanism of cancer, which offers an Achilles heel for diagnostic and therapeutic maneuvers (14). This review attempts to discuss SEs' fundamental characteristics and roles in esophageal carcinoma, which would pave the way for SE-based diagnostic and therapeutic maneuvers.

Super-enhancers: identification, organization and functions

Identification of super-enhancers

Enhancers were firstly recognized as the *cis*-regulatory elements from simian virus 40 (SV40), which could prominently promote rabbit β-globulin transcription in HeLa cells (15, 16). In general, enhancers activate cell-type-specific gene expression regardless of their distance, position, and orientation with respective to the cognate promoter (17, 18). The elements of enhancer are bound up with critical TFs through their tissue-specific recognition motifs, thereby functioning as the platform to integrate signaling pathways and further dictate cell lineages (19). Mechanistically, the enrichment of master TFs on enhancers results in recruiting of the subunit of the Mediator complex (Med1), RNA polymerase II (Pol II), and the basal transcription apparatus, which is organized by looping between enhancers and their cognate promoters. Additionally, enhancer regions are mainly overlapped with DNase hypersensitive sites (DHS), and the active state of enhancers are dependent on the following combinations of histone modifications: enrichment with H3K27ac, H3K4me1, and deficiency of Trimethylation at lysine 4 (H3K4me3) (Table 1) (20).

TABLE 1 Histone modification markers and the related functional state of the regulatory elements.

Regulatory elements Surrogate Markers	Promoters	Enhancers	Super-enhancers
DHS	+	+	+
BRD4	+	+	+++
MED1	+	+	+++
H3K4me3	+	–	–
H3K4me1	–	+	+
H3K27ac	++	++	+++

DHS, DNase hypersensitive sites; BRD4, Bromodomain-containing protein 4; MED1, subunit of the Mediator complex; H3K4me3, Trimethylation at lysine 4; H3K4me1, Monomethylation at lysine 4; H3K27ac, Acetylation at lysine 27.

SEs were firstly identified as the unique cluster of enhancers in close genomic proximity, which were densely occupied by master TFs Oct4/Pou5f1, Sox2, Nanog (OSN), Klf4, Esrrb, and Med1 in murine embryonic stem cells (mESCs) (21, 22). The Rank Ordering of Super-Enhancers (ROSE) algorithm had been proposed to separate typical-enhancers (TEs) from SEs, whose constituent enhancers were stitched together within 12.5 kb genomic regions enriched by input-normalized level of Med1 signal.

Structural features of super-enhancers

Liquid-liquid phase separation (LLPS) is a physicochemical process by which membraneless organelles are generated in eukaryotic cells, which could compartmentalize biochemical reactions within the dense phase (23–25). It has been demonstrated that SEs are phase-separated assemblies accumulated by exceptionally high densities of master TFs, co-activators, and RNA Pol II, dictating the roles in cell identity and disease, including cancers (26). The intrinsically disordered regions (IDRs) of the co-activators (BRD4 & Med1), driven by high-valency and weak-affinity interactions, are responsible for the formation of the phase-separated condensates at SEs, which could bring those *cis*-elements and the cognate promoter in close three-dimensional (3D) proximity and then facilitate SEs activation (Figure 1). This physical interaction between enhancer and promoter both involving in TEs and SEs are mediated by cohesin-associated CTCF (CCCTC-binding factor) loops. Additionally, the ubiquitously expressed TF Yin Yang 1 (YY1) has been also identified as the structural regulators contributing to this loop structure (27). The disruption of this structure is likely to result in activation of oncogenes outside the neighborhood by deletion of CTCF binding site, which are consistent with a tendency of liquid phase condensates to undergo fusion.

Functional properties of super-enhancers

The main features of SEs had been summarized as following Richard A. Young *et al.* and colleagues: (i) high-density occupancy of master TFs, co-activators and chromatin remodelers (Table 1), (ii) large genomic spanning, (iii) ability to exceptionally activate transcription, (iv) sensitivity to perturbation and (v) dictate cell identity and disease (28). Based on these observations, the oncogenic role of SEs usually caused by genetic variations are proposed to drive the transcriptional addiction in cancer.

The transcriptional activities of SEs exhibit an order-of-magnitude higher than TEs and the individual constituent enhancers within SEs, which also showing highly context-dependent manner under rigorous genetic regulation (29).

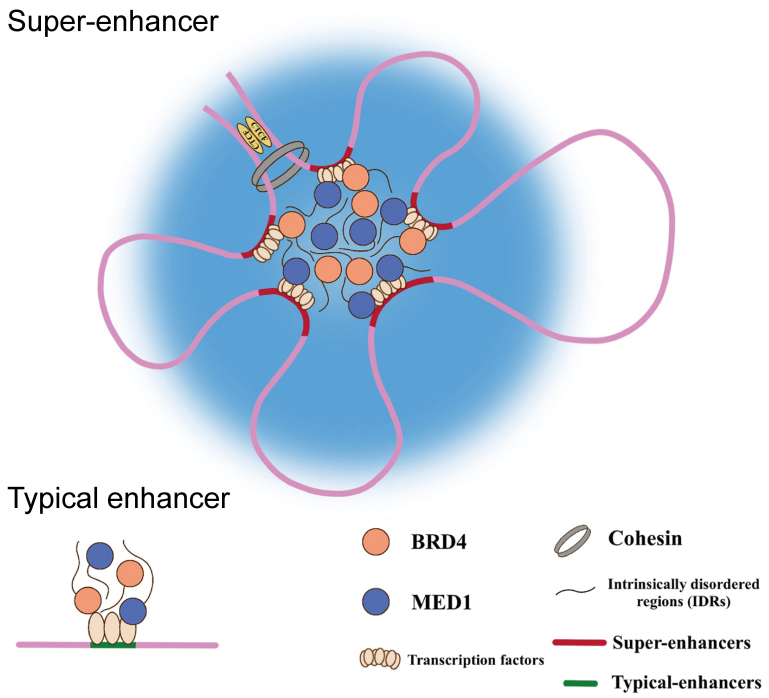

FIGURE 1
Schematic diagram of the phase-separated condensates at super-enhancers.

And more interestingly, the cooperativity of SEs constituents is neither additively nor synergistically, suggesting that the "*modus operandi*" of each component under highly precise and complex regulation by other component (30).

Establishment of oncogenic super-enhancers in esophageal carcinoma

Generally, inappropriate SEs are acquired *de novo* during tumorigenesis compared with the counterpart normal tissues, which driving expression of the critical oncogenes. The malignant transformation and maintenance underpinned by tumorigenic SEs could be seen as one of the core tenets of cancer biology (28, 31, 32). Mechanically, the formation of oncogenic SEs may stem from (i) focal amplification, (ii) genomic rearrangements, (iii) single nucleotide polymorphisms (SNPs), (iv) disruption of topological associating domain (TADs).

Genetic variations harboring super-enhancers constituents

Somatic copy number alterations (SCNAs) are common mechanism of oncogenesis driven by SEs. For example, focal amplification peak harboring SEs identified by profiling of H3K27ac in esophageal carcinoma (chr13:73880413-74042621, about ~162 kb), which subsequently proven to activate the oncogene *KLF5* expression. And these cancer-specific focal amplification peaks enriched in SEs have also been identified in several types of cancers, including head and neck squamous cell carcinoma, colorectal carcinoma, and liver hepatocellular carcinoma as well (33). Additionally, genomic rearrangements could change the natural genomic context resulting in close proximity between oncogene promoter and their SEs, which ectopically activates gene expression (34). This phenomenon is also described as "enhancer hijacking", by which oncogenic SEs formed in colorectal carcinoma, medulloblastoma, and acute myeloid leukemia as well (11, 35, 36). Besides, SNPs have been reported to promote tumorigenesis by disrupting the activities of SEs, including acquired oncogenic or abrogating protective allele within master TFs binding sites (37, 38).

These genomic variants provide novel insights into the carcinogenesis of esophageal carcinoma, which deserves further investigation.

Hijacking of super-enhancers by topological associating domain disruption

TADs have been recognized as the self-interacting genomic region, which demonstrates higher interconnection frequency than the outer regions (39). It has become clear that the main function of TADs is to insulate promoters from distal enhancers or SEs, which conducted by binding of insulator CCCTC-binding factor (CTCF) in cooperation with cohesin complex at their TAD boundaries (40). Although TADs structures are conserved in mammalian, disruption of TADs boundaries caused by genetic or epigenetic could be convenient for abnormal interactions between enhancer/SEs and promoters, which is undoubtedly could be laid the foundation for tumorigenesis.

It has been reported that TADs boundaries disruption could be caused by recurrent mutations of CTCF and cohesin binding sites, which were identified in esophageal carcinoma as well as other types of cancers, including liver hepatocellular carcinoma, colorectal carcinoma, and gastric carcinoma (41, 42). Furthermore, the boundaries disruption is also exemplified by epigenetic dysregulation in glioma by increasing hypermethylation in CTCF site followed by its reduced binding activity (43). Modification of 3D genome by TADs disruption could activate oncogene expression driven by inadvertent SEs-promoter looping, which might be utilized as the novel candidates for targeting the oncogenic SEs in esophageal carcinoma.

Principles of SEs-driven oncogenic transcription dependencies

Transcriptional core regulatory circuitries

The ESC master TFs OSN have previously been demonstrated to bind to their own genes or those of the others in mESCs, which forms an autoregulatory feed-froward loop, *i.e.*, CRC (44, 45). The constituents of this interconnected loop were subsequently extended with the other core TFs, Klf4 and Esrrb, both of which prominent for the maintenance of ESC state (Figure 2A) (21). Thus, CRC plays a critical role in the reprogram of somatic cell into induced pluripotent stem cells (iPSCs), and its dysregulation is undoubtedly involved in cancer (12, 46).

Trio-occupancy of OSN has also been well-studied in hESCs (human ESCs), which dominates the pluripotency contributing to human fibroblasts differentiated into the induced pluripotent identity. And this model has been complemented for additional seven key TFs by "CRC Mapper" algorithm, including FOXO1, ZIC3, NR5A1, RARG, MYB, RORA, and SOX21 (Figure 2B) (47). The principle of CRC identification by "CRC Mapper" has been characterized as the following three properties: TFs (i) encoded by SEs-assigned genes, (ii) binding to SEs of their own genes, (iii) forming fully interconnected feed-froward loops with other TFs by binding to their SEs.

In accordance with this strategy, cancer-type and -subtype specificity of CRC models have been identified in esophageal

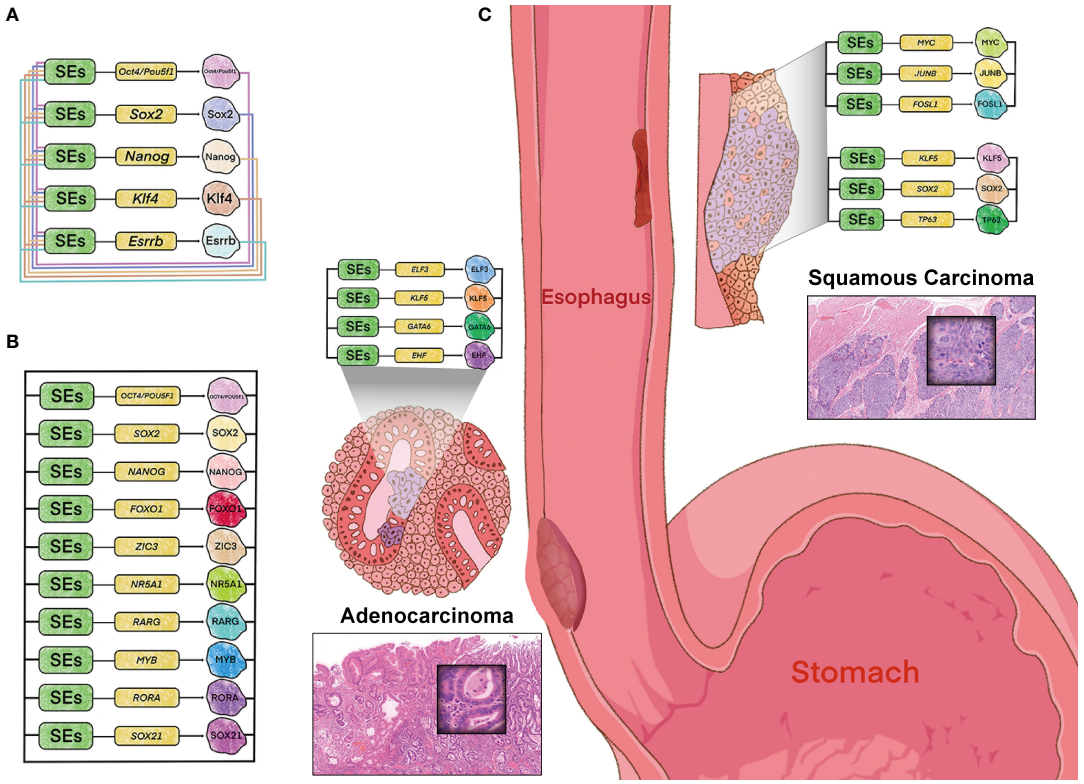

FIGURE 2
Model of core regulatory circuitry and its implications in esophageal tumorigenesis. **(A)** CRC model in murine embryonic stem cells. **(B)** CRC model in human embryonic stem cells identified by "CRC Mapper" algorithm. **(C)** Histopathology- and cell-type-specific CRC in esophageal carcinoma, including adenocarcinoma (left) and squamous cell carcinoma (right). Hematoxylin-eosin stain (magnification x 100).

cancer and other malignancies. For example, KLF5 has been proven to be collaborated with ELF3, GATA6 and EHF in EAC (46), while cooperated with TP63 and SOX2 in ESCC to form CRC (12), respectively (Figure 2C). And SOX2 has also been identified co-regulated with KLF4, EGR1 and NOTCH1 in Glioblastoma (48). These cancer-type and -subtype specific CRCs driven by SEs orchestrate the oncogenic transcriptional addiction, while offers therapeutic vulnerabilities due to perturbation sensitivity of their own SEs. These tissue-specific and cancer-specific CRCs driven by SEs orchestrate the oncogenic transcriptional addiction, which offers therapeutic vulnerabilities consistent with the perturbation sensitivity of their own SEs.

Furthermore, cell-type-specific CRC observed in types of cancers is in line with tumor heterogeneity, one of the hallmarks of malignancy. For example, the other CRC (MYC/JUNB/FOSL1) has been identified in ESCC, different with the KLF5/SOX2/TP63 circuitry (Figure 2C). This heterogeneity of CRC coincides with the two major genomic molecular subtypes in ESCC, which are presumably dominated by the two CRCs respectively. And different CRCs have also been identified in other types of cancers, including medulloblastomas and acute myeloid leukemia (49, 50). The heterogeneity of CRC highlights cell-type-specific property of SEs, which sheds light on the novel therapeutic possibilities.

Concentration of oncogenic signaling pathways on super-enhancers

The constituents within SEs have been demonstrated to be heavily loaded with terminal TFs of the Wnt, Tgfb-1, and Lif signaling pathways in mESCs, showing the preferential affections upon SE-assigned genes compared with genes regulated by TEs (51). Therefore, SEs could serve as a platform to converging multiple signaling pathways, dictating the development and disease state of cells, especially oncogenesis (52). For example, EAC-specific SEs has been proposed to be loaded with tumor-promoting TFs LIF, which contributes its malignant features by activating STAT3 and PI3K/AKT signaling pathways (46). Similarly, the cancer-subtype-specific SEs are densely bound up with its specific master TFs TP63 in ESCC, which participates in the formation of CRC and promotes cancer cell proliferation *via* PI3K/AKT signaling pathways (12, 53, 54).

These findings have also been clarified in other types of cancer, e.g., colorectal carcinoma (51), pancreatic carcinoma (55) and osteosarcoma (56). Taken together, these lines of evidence have been proposed that these oncogenic SEs occupied by key TFs pertaining to the critical signaling pathways upon which cancer cell depend, which offers the therapeutic vulnerabilities for esophageal carcinoma.

The occupancy of CDK7 at super-enhancers in esophageal carcinoma

The cyclin-dependent kinases (CDKs) of mammals comprise two main subfamilies with unique properties associated with cell cycle (CDKs 1-6 & 14-18) and transcriptional regulation (CDKs 7-13 & 19-20) (57). The unique functional repertoire of CDK7, the critical component of CDKs, is based on the regulation of transcription and cell cycle progression. Generally, CDK7 could activate transcriptional initiation and elongation by combining with transcription factor II H (TFIIH), while it could also control cell cycle progression by virtue of forming CDK-activating kinase (CAK) (58, 59).

Studies have demonstrated that the dysregulation of CDK7 was involved in various types of cancers and considered to be positively correlated with the aggressive clinicopathological features of these cancers, including esophageal cancer, hepatocellular carcinoma, gastric cancer, and colorectal cancer (13, 60–62). In ESCC, an immunohistochemical (IHC) analysis demonstrated that elevated expression of CDK7 was observed in over 80% samples which was associated with high tumor grade and poor prognosis. Notably, inhibited proliferation and decreased chemotherapeutic resistance have been observed when CDK7 gene was silenced (63). Besides, the level of CDK7 was higher in ESCC tissues with lymph node metastases compared to control group and positively correlated with tumor metastasis and patients' overall survival (64).

The overabundance of CDK7 within SEs regions offer the opportunities of blockade therapies in a lineage-specific cancer cell manner. THZ1, a covalent inhibitor of CDK7, was proposed to have a preferential impact on a plethora of oncogenes driven by SEs and could cause the disruption of specific transcriptional programs. For example, Chipumuro et al. found that this inhibitor could suppress the transcription of amplified *Mycn* to suppress the neuroblastoma cells proliferation and the sensitivity to THZ1 was related to preferentially decreased expression of SE-driven oncogenes (65). Subsequent studied showed that esophageal cancer, lung cancer and prostate cancer were sensitive to THZ1 treatment at low nanomolar range (10, 13, 66). Additionally, THZ1 could also cause downregulation of SEs-associated functional long noncoding RNAs acting as competing endogenous (ce-lncRNAs), such as HOTAIR, XIST, SNHG5, and LINC00094 (67), which are associated with expression of cancer hallmark genes. Notably, LINC00094, as a novel oncogenic lncRNA could be activated by master TFs, *e.g.*, TCF3 and KLF5, and positively correlate with poor prognosis. Upon inhibiting these TFs by THZ1, the level of LINC00094 is downregulated, which could cause tumor regression in ESCC. Thus, these studies have demonstrated THZ1 could be utilized as the crosshair of cancer drug discovery (57).

Similar to CDK7, CDK9 is mainly responsible for oncogenic transcription, *e.g.*, as *MCL-1* and *C-Myc*, by binding to elongation complex (p-TEFb) (68) and knocking down CDK9 has shown an excellent antineoplastic activity in hematologic and solid tumors. SNS-032, a selective inhibitor against CDK family as well can inhibit transcription initiation and elongation by targeting both CDK7 and CKD9, with the IC50 values of 62 and 4 nM, respectively (69–71). It could suppress the lung and lymph node metastasis as well as inhibit ESCC proliferation (72). These findings indicate that SNS-032 play an antineoplastic role in ESCC and is expected to enter clinical trials to validate its efficacy, especially in those with metastasis.

The occupancy of BRD4 at super-enhancers in esophageal carcinoma

The bromo domain and extra-terminal domain (BET) family contain BRD2, BRD3, BRD4, and testis-specific BRDT, which are characterized by acetylation recognition and transcription regulation (73). The well-known member of the BET family, BRD4 was initially recognized as the component of Mediator complex, and subsequently the general regulator for RNA Pol II by virtue of recruitment with transcriptional elongation factor P-TFEb. Consistently, the genomic profiling of BRD4 demonstrated that it is mainly enriched at active enhancers and promoters, which is not surprisingly complicated in critical cellular processes, such as embryogenesis (74) and cancer development (75–82). More importantly, the tumorigenic transcriptional activation of BRD4 are preferentially to regulate SE associated oncogenes, such as *C-Myc* and *BCL2* (83, 84)

Emerging evidence have demonstrated that inhibition of BRD4 occupancy result in SEs disruption and subsequently suppress its related oncogenes expression (73). Up till now, about 20 BRD4 inhibitors have been entered into clinical trials, some of which showed valuable therapeutics for several cancers, including hematological malignancies and non-small cell lung cancer (85). The critical oncogenes within these cancers showed highly sensitivity to JQ1, one of the promising anti-tumor BET inhibitors (22, 86). For instance, JQ1 has been demonstrated to inhibit ESCC proliferation by inhibiting *C-Myc* amplification (86). For another, it could also block recruitment of BRD4 on the

promoter of aurora kinases A and B (AURKA/B) to trigger cellular senescence, which provided a novel action manner of BRD4 in esophageal carcinoma (87). In esophageal adenocarcinoma (EAC), high expression of *YAP1* has been reported to be observed and positively associated with poor prognosis. JQ1 is capable of blocking BRD4 binding to the *YAP1* promoter and suppress Hippo/YAP1 signaling (88), which could be synergistically enhanced when traditional chemotherapeutic agents, *e.g.*, docetaxel, are added both *in vitro* and *in vivo* (88). Notably, cell cycle arrest, especially in G1 phase, has been observed in all the studies above. These studies also indicated that JQ1 might be a promising drug in esophageal carcinoma treatment.

Although a variety of small-molecule BET inhibitors have been entered in clinical researches, however, the off-target and side-effects cannot be neglected (89). Proteolysis targeting chimeric (PROTAC) technology have been utilized as an effective degradation tool over the years, which can ubiquitinate the disease-causing proteins by hijacking E3 ligases to achieve the anti-tumor effects (90). Compared to the general small-molecule inhibitors, the hetero-bifunctional molecule based on PROTAC technology demonstrated degradation of BET protein at low nanomolar dose with negligible side-effects (91). The first oral PROTACs (ARV-110, NCT03888612 & ARV-471, NCT04072952) have achieved encouraging benefit for prostate and breast cancer treatment in clinical trials (92). The newly developed GNE987, and PROTAC pan-BET degrader, have been showing good potency against several cancers, including hematological malignancies (93, 94), neuroblastoma (95), and prostate carcinoma (96). Additionally, MZ1, a PROTAC BET degrader, was previously identified unexpectedly degradation of BRD4 over other members of BET family, such as BRD2 and BRD3 (97). However, MZ1 have been proposed to suppress ESCC migration by degrading BRDT, initially recognized as testis-specific protein, rather than BRD2, BRD3 and BRD4. The migratory inhibition of ESCC by MZ1 resulted from down-regulation of *ΔNp63* target genes enriched within SEs (98).

The enrichment of histone acetylation at super-enhancers in esophageal carcinoma

Histone H3K27ac has been proposed to separate the active enhancers from poised enhancers occupied by H3K4me1 alone (99). The occupancy of H3K27ac facilitates the chromatin accessibility, which is responsible for exceptionally higher enrichment of master TFs, co-activators, and transcriptional machinery on SEs. Therefore, the dysregulated H3K27ac within SEs region could drive the oncogenesis in several types of cancer.

Histone acetylation is a relative steady-state controlled by two families of enzymes: histone acetyltransferases (HATs) and histone deacetylases (HDACs) (100, 101). Numerous studies have demonstrated that the disturbed equilibrium of histones acetylation is closely related with the tumorigenicity of esophageal carcinoma (Table 2). Furthermore, the tumor-promoting genes activated by hyperacetylation have also been identified in esophageal carcinoma (Table 3). The dysregulated histone acetylation of esophageal carcinoma could be accounted for the oncogenesis driven by SEs, which densely bound up with the active enhancer marker H3K27ac.

Based on this knowledge, the aberrant histone acetylation has been addressed as the alternative avenues for cancer treatment, especially those driven by oncogenic SEs. For example, the aberrantly expressed gene *SIRT7*, NAD-dependent deacetylase, was activated by SEs in non-alcoholic fatty liver disease (NAFLD)-associated hepatocellular carcinoma (HCCs). Depletion of *SIRT7* associated SE could suppress the tumorigenicity both *in vitro* and *in vivo* (110). And several types

TABLE 2 The correlations between dysregulated HDACs (and/or HATs) and the advanced oncogenic features of esophageal carcinoma.

Ref.	Sample info.			Targets	Malignant characteristics
	Pathol.	No.	Cell lines		
Langer R et al. (102)	EAC	180	N/A	HDAC2↑	Lymph node metastasis↑+ Pathological Differentiation (poor) (Human Tissues)
Zeng, et al. (103)	ESCC	86	EC/CUHK1, KYSE30/140/150/180	HDAC4↑	Clinical Stage (advanced) + Pathological Differentiation (poor) + OS & PFS (poor) (Human Tissues) Proliferation↑+ Migration↑(*in vitro*)
Xue, et al. (104)	ESCC	167	Eca-109	HAT1↑	Pathological Differentiation (poor) (Human Tissues) Proliferation↑(*in vitro*)
Feng, et al. (105)	ESCC	N/A	Eca-109, EC9706	HDAC7↑	Epithelial-mesenchymal transition↑(*in vitro* & *in vivo*)
Li, et al. (106)	ESCC	N/A	EC9706	HDAC6↑	Proliferation↑+ Migration↑(*in vitro*)

EC, Esophageal carcinoma; EAC, Esophageal adenocarcinoma; ESCC, Esophageal squamous cell carcinoma; HDACs, Histone deacetylases; HATs, Histone acetyltransferases; OS, Overall Survival; PFS, Progress-free Survival.

TABLE 3 The associations between dysregulated histone acetylation modifications and advanced oncogenic features.

Ref.	Sample info.			Targets		Malignant characteristics
	Pathol.	No.	Cell lines	Marker	Genes	
Zhang R et al. (107)	ESCC	90	Eca-109, TE-1	H3K27ac↑	CCAT1↑	Lymph node metastasis↑+ Clinical Stage (advanced) + OS (poor) (Human Tissues) Proliferation↑+ Migration↑(*in vitro* & *in vivo*)
Hu et al. (108)	ESCC	N/A	EC9706, KYSE150	H3K9ac↑	KLF4↑	Proliferation↓(*in vitro*)
Liang et al. (109)	ESCC	115	Eca-109, KYSE150/450	H3K27ac↑	LAMC2↑	Lymph node metastasis↑+ Clinical Stage (advanced) + OS (poor) (Human Tissues) Migration↑+ Invasion↑(*in vitro*)

of HDAC inhibitors (HDACis) have been shown as the promising therapeutic strategies against esophageal carcinoma (Table 4). Therefore, the recruitment of exceptionally high histone acetylation modification, especially H3K27ac, within the oncogenic SEs could contribute their vulnerabilities to HDACis for patients of esophageal carcinoma.

Conclusive remark

The concept of SEs and their function in physiology and disease has been established in the last decade. To date, there is no doubt that SEs acquired *de novo* are one of the hallmarks of esophageal carcinoma, and the available studies conclude the characteristics of the oncogenic SEs in esophageal carcinoma: (i) they are acquired based on genetic variants or TADs boundaries disruption, (ii) they drive the transcriptional additions depend on CRCs and convergence of tumorigenic signaling pathways, (iii) they could be targeted by inhibition of BRD4, CDK7, and histone acetylation, which exceptionally enriched within these *cis*-elements. However, there are still several unresolved points regarding SEs in esophageal carcinoma: (i) how the individual *bona fide* constituents selectively respond to targeted inhibition pertaining to the disproportionately enriched factors, (ii) how 3D genome structure of the SEs are influenced by the tumor-promoting signaling pathways, (iii) what are the critical transitions of SEs landscape during the process of precancerous lesions to cancer, (iv) what are the main differences of SEs profiling between squamous cell carcinoma and adenocarcinoma, (v) what are the clinical benefits based on the combinations of traditional treatments and novel therapeutic avenues targeting the subtype-specific or cell-type-specific CRCs. These insights about SEs-driven transcriptional dependencies in esophageal carcinoma, may shed light on the potential clinical application of the cancer-specific SEs.

TABLE 4 The molecular mechanism of histone deacetylase inhibitors against esophageal carcinoma.

Ref.	Sample info.		HDACis				Malignant Features
	Pathol.	Cell lines	Type	Names	Targets	Genes	
Hoshino et al. (111)	ESCC	T.Tn, TE-2	Cyclic Peptides	Romidepsin	HDAC1/2	PRDX1↑+ CDKN1A↑	Proliferation↓+ Apoptosis↑ (*in vitro* & *in vivo*)
Murakami, et al. (112)	ESCC	T.Tn, TE-2	Cyclic Peptides	CHAP31	Pan-HDAC (except HDAC6)	cleaved Caspase-9↑+ Bax/Bcl-2↑	Apoptosis↑ (*in vitro* & *in vivo*)
Tzao, et al. (113)	ESCC	KYSE70/150/510	Hydroxymates	SAHA	Pan-HDAC	CDKs↓+ E-cadherin↑	Proliferation↓ + Migration↓+ Invasion↓ (*in vitro* & *in vivo*)
Shoji, et al. (114)	ESCC	TE-9/10/11/14	Short-chain fatty acids	Valproic acid	HDAC1	RAD51↓	Radiosensitivity↑(*in vitro*)
Shi, et al. (115)	ESCC	TE-1, KYSE510	Hydroxymates	LMK-235	HDAC4/5	TNS3↓	Proliferation↓ (*in vitro* & *in vivo*)
Ma, et al. (116)	ESCC	EC9706, KYSE70	Benzamide	MS-275	HDAC1/3	PI3K/Akt/mTOR↓	Proliferation↓+ Apoptosis↑ (*in vitro* & *in vivo*)
Feingold, et al. (117)	EAC	NCI-SB-Esc1/2/3, OE33, Flo-1	Benzamide	MS-275	HDAC1/3	TXNIP↑	DNA damage↑+ Apoptosis↑(*in vitro*)

HDACis, Histone deacetylase inhibitors.

Author contributions

BL, HY, and XM formulated the study concept and design; YS wrote the original manuscript draft; MW, DL, provided the technical and material support; SU, critically revised the manuscript. All authors contributed to the article and approved the submitted version.

Funding

This study was supported by the Zhongyuan talent program (ZYYCYU202012113).

Acknowledgments

We apologize to the authors whose study could not be cited for the limited spaces. We would like to thank Jiyu Zhang for his delicate and exquisite schematic graphs. And we also thank Zhixin Li for his comments on this manuscript.

Conflict of interest

The authors declare that the research was conducted in the absence of any commercial or financial relationships that could be construed as a potential conflict of interest.

Publisher's note

All claims expressed in this article are solely those of the authors and do not necessarily represent those of their affiliated organizations, or those of the publisher, the editors and the reviewers. Any product that may be evaluated in this article, or claim that may be made by its manufacturer, is not guaranteed or endorsed by the publisher.

References

1. Ferlay J, Colombet M, Soerjomataram I, Parkin DM, Piñeros M, Znaor A, et al. Cancer statistics for the year 2020: An overview. *Int J Cancer* (2021) 149:778–89. doi: 10.1002/ijc.33588

2. Sung H, Ferlay J, Siegel RL, Laversanne M, Soerjomataram I, Jemal A, et al. Global cancer statistics 2020: Globocan estimates of incidence and mortality worldwide for 36 cancers in 185 countries. *CA Cancer J Clin* (2021) 71(3):209–49. doi: 10.3322/caac.21660

3. Wei W, Zeng H, Zheng R, Zhang S, An L, Chen R, et al. Cancer registration in China and its role in cancer prevention and control. *Lancet Oncol* (2020) 21(7): e342–e9. doi: 10.1016/s1470-2045(20)30073-5

4. Qiao Y, Zhao C, Li X, Zhao J, Huang Q, Ding Z, et al. Efficacy and safety of camrelizumab in combination with neoadjuvant chemotherapy for escc and its impact on esophagectomy. *Front Immunol* (2022) 13:953229. doi: 10.3389/fimmu.2022.953229

5. Li ZC, Sun YT, Lai MY, Zhou YX, Qiu MZ. Efficacy and safety of pd-1 inhibitors combined with chemotherapy as first-line therapy for advanced esophageal cancer: A systematic review and network meta-analysis. *Int Immunopharmacol* (2022) 109:108790. doi: 10.1016/j.intimp.2022.108790

6. Perk J, Iavarone A, Benezra R. Id family of helix-Loop-Helix proteins in cancer. *Nat Rev Cancer* (2005) 5(8):603–14. doi: 10.1038/nrc1673

7. Mansour MR, Abraham BJ, Anders L, Berezovskaya A, Gutierrez A, Durbin AD, et al. Oncogene Regulation. An oncogenic super-enhancer formed through somatic mutation of a noncoding intergenic element. *Sci (New York NY)* (2014) 346 (6215):1373–7. doi: 10.1126/science.1259037

8. Betancur PA, Abraham BJ, Yiu YY, Willingham SB, Khameneh F, Zarnegar M, et al. A Cd47-associated super-enhancer links pro-inflammatory signalling to Cd47 upregulation in breast cancer. *Nat Commun* (2017) 8:14802. doi: 10.1038/ncomms14802

9. Ke L, Zhou H, Wang C, Xiong G, Xiang Y, Ling Y, et al. Nasopharyngeal carcinoma super-Enhancer-Driven Etv6 correlates with prognosis. *Proc Natl Acad Sci United States America* (2017) 114(36):9683–8. doi: 10.1073/pnas.1705236114

10. Christensen CL, Kwiatkowski N, Abraham BJ, Carretero J, Al-Shahrour F, Zhang T, et al. Targeting transcriptional addictions in small cell lung cancer with a covalent Cdk7 inhibitor. *Cancer Cell* (2014) 26(6):909–22. doi: 10.1016/j.ccell.2014.10.019

11. Northcott PA, Lee C, Zichner T, Stutz AM, Erkek S, Kawauchi D, et al. Enhancer hijacking activates Gfi1 family oncogenes in medulloblastoma. *Nature* (2014) 511(7510):428–34. doi: 10.1038/nature13379

12. Jiang Y-Y, Jiang Y, Li C-Q, Zhang Y, Dakle P, Kaur H, et al. Tp63, Sox2, and Klf5 Establish a Core Regulatory Circuitry That Controls Epigenetic and Transcription Patterns in Esophageal Squamous Cell Carcinoma Cell Lines. *Gastroenterology* (2020) 159(4). doi: 10.1053/j.gastro.2020.06.050

13. Jiang Y-Y, Lin D-C, Mayakonda A, Hazawa M, Ding L-W, Chien W-W, et al. Targeting super-Enhancer-Associated oncogenes in oesophageal squamous cell carcinoma. *Gut* (2017) 66(8):1358–68. doi: 10.1136/gutjnl-2016-311818

14. Sengupta S, George RE. Super-Enhancer-Driven transcriptional dependencies in cancer. *Trends In Cancer* (2017) 3(4):269–81. doi: 10.1016/j.trecan.2017.03.006

15. Banerji J, Rusconi S, Schaffner W. Expression of a beta-globin gene is enhanced by remote Sv40 DNA sequences. *Cell* (1981) 27(2 Pt 1):299–308.

16. Benoist C, Chambon P. *In vivo* sequence requirements of the Sv40 early promotor region. *Nature* (1981) 290(5804):304–10. doi: 10.1038/290304a0

17. Buecker C, Wysocka J. Enhancers as information integration hubs in development: Lessons from genomics. *Trends genetics: TIG* (2012) 28(6):276–84. doi: 10.1016/j.tig.2012.02.008

18. Schaffner W. Enhancers, enhancers - from their discovery to today's universe of transcription enhancers. *Biol Chem* (2015) 396(4):311–27. doi: 10.1515/hsz-2014-0303

19. Calo E, Wysocka J. Modification of enhancer chromatin: What, how, and why? *Mol Cell* (2013) 49(5):825–37. doi: 10.1016/j.molcel.2013.01.038

20. Gross DS, Garrard WT. Nuclease hypersensitive sites in chromatin. *Annu Rev Biochem* (1988) 57:159–97. doi: 10.1146/annurev.bi.57.070188.001111

21. Whyte WA, Orlando DA, Hnisz D, Abraham BJ, Lin CY, Kagey MH, et al. Master transcription factors and mediator establish super-enhancers at key cell identity genes. *Cell* (2013) 153(2):307–19. doi: 10.1016/j.cell.2013.03.035

22. Loven J, Hoke HA, Lin CY, Lau A, Orlando DA, Vakoc CR, et al. Selective inhibition of tumor oncogenes by disruption of super-enhancers. *Cell* (2013) 153 (2):320–34. doi: 10.1016/j.cell.2013.03.036

23. Janmey PA, Hvidt S, Käs J, Lerche D, Maggs A, Sackmann E, et al. The mechanical properties of actin Gels. Elastic modulus and filament motions. *J Biol Chem* (1994) 269(51):32503–13. doi: 10.1016/S0021-9258(18)31663-6

24. Banani SF, Lee HO, Hyman AA, Rosen MK. Biomolecular condensates: Organizers of cellular biochemistry. *Nat Rev Mol Cell Biol* (2017) 18(5):285–98. doi: 10.1038/nrm.2017.7

25. Shin Y, Brangwynne CP. Liquid phase condensation in cell physiology and disease. *Science (New York NY)* (2017) 357(6357):eaaf4382. doi: 10.1126/science.aaf4382

26. Sabari BR, Dall'Agnese A, Boija A, Klein IA, Coffey EL, Shrinivas K, et al. Coactivator condensation at super-enhancers links phase separation and gene control. *Science* (2018) 361(6400):eaar3958. doi: 10.1126/science.aar3958

27. Weintraub AS, Li CH, Zamudio AV, Sigova AA, Hannett NM, Day DS, et al. Yy1 is a structural regulator of enhancer-promoter loops. *Cell* (2017) 171(7):1573–88.e28. doi: 10.1016/j.cell.2017.11.008

28. Hnisz D, Abraham BJ, Lee TI, Lau A, Saint-Andre V, Sigova AA, et al. Super-enhancers in the control of cell identity and disease. *Cell* (2013) 155(4):934–47. doi: 10.1016/j.cell.2013.09.053

29. Pott S, Lieb JD. What are super-enhancers? *Nat Genet* (2015) 47(1):8–12. doi: 10.1038/ng.3167

30. Proudhon C, Snetkova V, Raviram R, Lobry C, Badri S, Jiang T, et al. Active and inactive enhancers cooperate to exert localized and long-range control of gene regulation. *Cell Rep* (2016) 15(10):2159–69. doi: 10.1016/j.celrep.2016.04.087

31. Hanahan D, Weinberg RA. The hallmarks of cancer. *Cell* (2000) 100(1):57–70. doi: 10.1016/S0092-8674(00)81683-9

32. Hanahan D, Weinberg RA. Hallmarks of cancer: The next generation. *Cell* (2011) 144(5):646–74. doi: 10.1016/j.cell.2011.02.013

33. Zhang X, Choi PS, Francis JM, Imielinski M, Watanabe H, Cherniack AD, et al. Identification of focally amplified lineage-specific super-enhancers in human epithelial cancers. *Nat Genet* (2016) 48(2):176–82. doi: 10.1038/ng.3470

34. Herz HM. Enhancer deregulation in cancer and other diseases. *BioEssays: News Rev Molecular Cell Dev Biol* (2016) 38(10):1003–15. doi: 10.1002/bies.201600106

35. Groschel S, Sanders MA, Hoogenboezem R, de Wit E, Bouwman BAM, Erpelinck C, et al. A single oncogenic enhancer rearrangement causes concomitant Evi1 and Gata2 deregulation in leukemia. *Cell* (2014) 157(2):369–81. doi: 10.1016/j.cell.2014.02.019

36. Weischenfeldt J, Dubash T, Drainas AP, Mardin BR, Chen Y, Stutz AM, et al. Pan-cancer analysis of somatic copy-number alterations implicates Irs4 and Igf2 in enhancer hijacking. *Nat Genet* (2017) 49(1):65–74. doi: 10.1038/ng.3722

37. Oldridge DA, Wood AC, Weichert-Leahey N, Crimmins I, Sussman R, Winter C, et al. Genetic predisposition to neuroblastoma mediated by a Lmo1 super-enhancer polymorphism. *Nature* (2015) 528(7582):418–21. doi: 10.1038/nature15540

38. Kandaswamy R, Sava GP, Speedy HE, Beà S, Martín-Subero JI, Studd JB, et al. Genetic predisposition to chronic lymphocytic leukemia is mediated by a bmf super-enhancer polymorphism. *Cell Rep* (2016) 16(8):2061–7. doi: 10.1016/j.celrep.2016.07.053

39. Dixon JR, Selvaraj S, Yue F, Kim A, Li Y, Shen Y, et al. Topological domains in mammalian genomes identified by analysis of chromatin interactions. *Nature* (2012) 485(7398):376–80. doi: 10.1038/nature11082

40. Zuin J, Dixon JR, van der Reijden MI, Ye Z, Kolovos P, Brouwer RW, et al. Cohesin and ctcf differentially affect chromatin architecture and gene expression in human cells. *Proc Natl Acad Sci United States America* (2014) 111(3):996–1001. doi: 10.1073/pnas.1317788111

41. Katainen R, Dave K, Pitkänen E, Palin K, Kivioja T, Välimäki N, et al. Ctcf/Cohesin-binding sites are frequently mutated in cancer. *Nat Genet* (2015) 47(7):818–21. doi: 10.1038/ng.3335

42. Hnisz D, Weintraub AS, Day DS, Valton AL, Bak RO, Li CH, et al. Activation of proto-oncogenes by disruption of chromosome neighborhoods. *Sci (New York NY)* (2016) 351(6280):1454–8. doi: 10.1126/science.aad9024

43. Flavahan WA, Drier Y, Liau BB, Gillespie SM, Venteicher AS, Stemmer-Rachamimov AO, et al. Insulator dysfunction and oncogene activation in idh mutant gliomas. *Nature* (2016) 529(7584):110–4. doi: 10.1038/nature16490

44. Boyer LA, Lee TI, Cole MF, Johnstone SE, Levine SS, Zucker JP, et al. Core transcriptional regulatory circuitry in human embryonic stem cells. *Cell* (2005) 122(6):947–56. doi: 10.1016/j.cell.2005.08.020

45. Loh YH, Wu Q, Chew JL, Vega VB, Zhang W, Chen X, et al. The Oct4 and nanog transcription network regulates pluripotency in mouse embryonic stem cells. *Nat Genet* (2006) 38(4):431–40. doi: 10.1038/ng1760

46. Chen L, Huang M, Plummer J, Pan J, Jiang YY, Yang Q, et al. Master transcription factors form interconnected circuitry and orchestrate transcriptional networks in oesophageal adenocarcinoma. *Gut* (2020) 69(4):630–40. doi: 10.1136/gutjnl-2019-318325

47. Saint-André V, Federation AJ, Lin CY, Abraham BJ, Reddy J, Lee TI, et al. Models of human core transcriptional regulatory circuitries. *Genome Res* (2016) 26(3):385–96. doi: 10.1101/gr.197590.115

48. Riddick G, Kotliarova S, Rodriguez V, Kim HS, Linkous A, Storaska AJ, et al. A core regulatory circuit in glioblastoma stem cells links mapk activation to a transcriptional program of neural stem cell identity. *Sci Rep* (2017) 7:43605. doi: 10.1038/srep43605

49. Lin CY, Erkek S, Tong Y, Yin L, Federation AJ, Zapatka M, et al. Active medulloblastoma enhancers reveal subgroup-specific cellular origins. *Nature* (2016) 530(7588):57–62. doi: 10.1038/nature16546

50. Assi SA, Imperato MR, Coleman DJL, Pickin A, Potluri S, Ptasinska A, et al. Subtype-specific regulatory network rewiring in acute myeloid leukemia. *Nat Genet* (2019) 51(1):151–62. doi: 10.1038/s41588-018-0270-1

51. Hnisz D, Schuijers J, Lin CY, Weintraub AS, Abraham BJ, Lee TI, et al. Convergence of developmental and oncogenic signaling pathways at transcriptional super-enhancers. *Mol Cell* (2015) 58(2):362–70. doi: 10.1016/j.molcel.2015.02.014

52. Jia Q, Chen S, Tan Y, Li Y, Tang F. Oncogenic super-enhancer formation in tumorigenesis and its molecular mechanisms. *Exp Mol Med* (2020) 52(5):713–23. doi: 10.1038/s12276-020-0428-7

53. Ye S, Lee KB, Park MH, Lee JS, Kim SM. P63 regulates growth of esophageal squamous carcinoma cells *Via* the akt signaling pathway. *Int J Oncol* (2014) 44(6):2153–9. doi: 10.3892/ijo.2014.2374

54. Hu H, Xia SH, Li AD, Xu X, Cai Y, Han YL, et al. Elevated expression of P63 protein in human esophageal squamous cell carcinomas. *Int J Cancer* (2002) 102(6):580–3. doi: 10.1002/ijc.10739

55. Zhu X, Zhang T, Zhang Y, Chen H, Shen J, Jin X, et al. A super-enhancer controls tgf- B signaling in pancreatic cancer through downregulation of Tgfbr2. *Cell signalling* (2020) 66:109470. doi: 10.1016/j.cellsig.2019.109470

56. Lu B, He Y, He J, Wang L, Liu Z, Yang J, et al. Epigenetic profiling identifies lif as a super-Enhancer-Controlled regulator of stem cell-like properties in osteosarcoma. *Mol Cancer Research: MCR* (2020) 18(1):57–67. doi: 10.1158/1541-7786.Mcr-19-0470

57. Fisher RP. Cdk7: A kinase at the core of transcription and in the crosshairs of cancer drug discovery. *Transcription* (2019) 10(2):47–56. doi: 10.1080/21541264.2018.1553483

58. Coin F, Egly JM. Revisiting the function of Cdk7 in transcription by virtue of a recently described tfiih kinase inhibitor. *Mol Cell* (2015) 59(4):513–4. doi: 10.1016/j.molcel.2015.08.006

59. Schachter MM, Merrick KA, Larochelle S, Hirschi A, Zhang C, Shokat KM, et al. A Cdk7-Cdk4 T-loop phosphorylation cascade promotes G1 progression. *Mol Cell* (2013) 50(2):250–60. doi: 10.1016/j.molcel.2013.04.003

60. Huang JR, Qin WM, Wang K, Fu DR, Zhang WJ, Jiang QW, et al. Cyclin-dependent kinase 7 inhibitor Thz2 inhibits the growth of human gastric cancer in vitro and in vivo. *Am J Trans Res* (2018) 10(11):3664–76.

61. Wang C, Jin H, Gao D, Wang L, Evers B, Xue Z, et al. A crispr screen identifies Cdk7 as a therapeutic target in hepatocellular carcinoma. *Cell Res* (2018) 28(6):690–2. doi: 10.1038/s41422-018-0020-z

62. Zhou Y, Lu L, Jiang G, Chen Z, Li J, An P, et al. Targeting Cdk7 increases the stability of snail to promote the dissemination of colorectal cancer. *Cell Death Differ* (2019) 26(8):1442–52. doi: 10.1038/s41418-018-0222-4

63. Zhang J, Yang X, Wang Y, Shi H, Guan C, Yao L, et al. Low expression of cyclinh and cyclin-dependent kinase 7 can decrease the proliferation of human esophageal squamous cell carcinoma. *Digestive Dis Sci* (2013) 58(7):2028–37. doi: 10.1007/s10620-013-2597-x

64. Zhang J, Zhu J, Yang L, Guan C, Ni R, Wang Y, et al. Interaction with Ccnh/Cdk7 facilitates Ctbp2 promoting esophageal squamous cell carcinoma (Escc) metastasis *Via* upregulating epithelial-mesenchymal transition (Emt) progression. *Tumour biology: J Int Soc Oncodevelopmental Biol Med* (2015) 36(9):6701–14. doi: 10.1007/s13277-015-3354-x

65. Chipumuro E, Marco E, Christensen CL, Kwiatkowski N, Zhang T, Hatheway CM, et al. Cdk7 inhibition suppresses super-Enhancer-Linked oncogenic transcription in mycn-driven cancer. *Cell* (2014) 159(5):1126–39. doi: 10.1016/j.cell.2014.10.024

66. Rasool RU, Natesan R, Deng Q, Aras S, Lal P, Sander Effron S, et al. Cdk7 inhibition suppresses castration-resistant prostate cancer through Med1 inactivation. *Cancer Discov* (2019) 9(11):1538–55. doi: 10.1158/2159-8290.Cd-19-0189

67. Wang QY, Peng L, Chen Y, Liao LD, Chen JX, Li M, et al. Characterization of super-enhancer-associated functional lncRNAs acting as ceRNAs in ESCC. *Mol Oncol* (2020) 14(9):2203–30. doi: 10.1002/1878-0261.12726

68. Tong Z, Mejia A, Veeranki O, Verma A, Correa AM, Dokey R, et al. Targeting CDK9 and MCL-1 by a new CDK9/p-TEFb inhibitor with and without 5-fluorouracil in esophageal adenocarcinoma. *Ther Adv Med Oncol* (2019) 11:1758835919864850. doi: 10.1177/1758835919864850

69. Zhang J, Liu S, Ye Q, Pan J. Transcriptional inhibition by Cdk7/9 inhibitor sns-032 abrogates oncogene addiction and reduces liver metastasis in uveal melanoma. *Mol Cancer* (2019) 18(1):140. doi: 10.1186/s12943-019-1070-7

70. Chen R, Wierda WG, Chubb S, Hawtin RE, Fox JA, Keating MJ, et al. Mechanism of action of sns-032, a novel cyclin-dependent kinase inhibitor, in chronic lymphocytic leukemia. *Blood* (2009) 113(19):4637–45. doi: 10.1182/blood-2008-12-190256

71. Wu Y, Chen C, Sun X, Shi X, Jin B, Ding K, et al. Cyclin-dependent kinase 7/9 inhibitor sns-032 abrogates Fip1-Like-1 platelet-derived growth factor receptor A and bcr-abl oncogene addiction in malignant hematologic cells. *Clin Cancer research: an Off J Am Assoc Cancer Res* (2012) 18(7):1966–78. doi: 10.1158/1078-0432.Ccr-11-1971

72. Zeng H, Yang H, Song Y, Fang D, Chen L, Zhao Z, et al. Transcriptional inhibition by Cdk7/9 inhibitor sns-032 suppresses tumor growth and metastasis in esophageal squamous cell carcinoma. *Cell Death Dis* (2021) 12(11):1048. doi: 10.1038/s41419-021-04344-w

73. French CA. Small-molecule targeting of bet proteins in cancer. *Adv Cancer Res* (2016) 131:21–58. doi: 10.1016/bs.acr.2016.04.001

74. Toyama R, Rebbert ML, Dey A, Ozato K, Dawid IB. Brd4 associates with mitotic chromosomes throughout early zebrafish embryogenesis. *Developmental dynamics : an official publication of the American Association of Anatomists* (2008) 237(6):1636–44. doi: 10.1002/dvdy.21576

75. Donati B, Lorenzini E, Ciarrocchi A. Brd4 and cancer: Going beyond transcriptional regulation. *Mol Cancer* (2018) 17(1):1–13. doi: 10.1186/s12943-018-0915-9

76. Zuber J, Shi J, Wang E, Rappaport AR, Herrmann H, Sison EA, et al. Rnai screen identifies Brd4 as a therapeutic target in acute myeloid leukaemia. *Nature* (2011) 478(7370):524–8. doi: 10.1038/nature10334

77. Dawson MA, Prinjha RK, Dittmann A, Giotopoulos G, Bantscheff M, Chan WI, et al. Inhibition of bet recruitment to chromatin as an effective treatment for mll-fusion leukaemia. *Nature* (2011) 478(7370):529–33. doi: 10.1038/nature10509

78. Ceribelli M, Kelly PN, Shaffer AL, Wright GW, Xiao W, Yang Y, et al. Blockade of oncogenic ikb kinase activity in diffuse Large b-cell lymphoma by bromodomain and extraterminal domain protein inhibitors. *Proc Natl Acad Sci United States America* (2014) 111(31):11365–70. doi: 10.1073/pnas.1411701111

79. Wu Q, Liu F, Ge M, Laster KV, Wei L, Du R, et al. Brd4 drives esophageal squamous cell carcinoma growth by promoting Rcc2 expression. *Oncogene* (2022) 41(3):347–60. doi: 10.1038/s41388-021-02099-4

80. Chen X, Ma Q, Shang Z, Niu Y. Super-enhancer in prostate cancer: Transcriptional disorders and therapeutic targets. *NPJ Precis Oncol* (2020) 4 (1):31. doi: 10.1038/s41698-020-00137-0

81. Crawford NP, Alsarraj J, Lukes L, Walker RC, Officewala JS, Yang HH, et al. Bromodomain 4 activation predicts breast cancer survival. *Proc Natl Acad Sci United States America* (2008) 105(17):6380–5. doi: 10.1073/pnas.0710331105

82. Shimamura T, Chen Z, Soucheray M, Carretero J, Kikuchi E, Tchaicha JH, et al. Efficacy of bet bromodomain inhibition in kras-mutant non-small cell lung cancer. *Clin Cancer research: an Off J Am Assoc Cancer Res* (2013) 19(22):6183–92. doi: 10.1158/1078-0432.Ccr-12-3904

83. Delmore JE, Issa GC, Lemieux ME, Rahl PB, Shi J, Jacobs HM, et al. Bet bromodomain inhibition as a therapeutic strategy to target c-myc. *Cell* (2011) 146 (6):904–17. doi: 10.1016/j.cell.2011.08.017

84. Peirs S, Frismantas V, Matthijssens F, Van Loocke W, Pieters T, Vandamme N, et al. Targeting bet proteins improves the therapeutic efficacy of bcl-2 inhibition in T-cell acute lymphoblastic leukemia. *Leukemia* (2017) 31(10):2037–47. doi: 10.1038/leu.2017.10

85. Lu T, Lu W, Luo C. A patent review of Brd4 inhibitors (2013-2019). *Expert Opin Ther patents* (2020) 30(1):57–81. doi: 10.1080/13543776.2020.1702645

86. Wang J, Liu Z, Wang Z, Wang S, Chen Z, Li Z, et al. Targeting c-myc: Jq1 as a promising option for c-Myc-Amplified esophageal squamous cell carcinoma. *Cancer Lett* (2018) 419:64–74. doi: 10.1016/j.canlet.2018.01.051

87. Xu JL, Yuan YJ, Lv J, Qi D, Wu MD, Lan J, et al. Inhibition of Brd4 triggers cellular senescence through suppressing aurora kinases in oesophageal cancer cells. *J Cell Mol Med* (2020) 24(22):13036–45. doi: 10.1111/jcmm.15901

88. Song S, Li Y, Xu Y, Ma L, Pool Pizzi M, Jin J, et al. Targeting hippo coactivator Yap1 through bet bromodomain inhibition in esophageal adenocarcinoma. *Mol Oncol* (2020) 14(6):1410–26. doi: 10.1002/1878-0261.12667

89. Yang Y, Wu Z, Chen P, Zheng P, Zhang H, Zhou J. Proteolysis-targeting chimeras mediate the degradation of bromodomain and extra-terminal domain proteins. *Future med Chem* (2020) 12(18):1669–83. doi: 10.4155/fmc-2017-0264

90. Wan Y, Yan C, Gao H, Liu T. Small-molecule protacs: Novel agents for cancer therapy. *Future Med Chem* (2020) 12(10):915–38. doi: 10.4155/fmc-2019-0340

91. Raina K, Crews CM. Chemical inducers of targeted protein degradation. *J Biol Chem* (2010) 285(15):11057–60. doi: 10.1074/jbc.R109.078105

92. Qi SM, Dong J, Xu ZY, Cheng XD, Qin JJ. Protac: An effective targeted protein degradation strategy for cancer therapy. *Front Pharmacol* (2021) 12:692574. doi: 10.3389/fphar.2021.692574

93. Sang X, Zhang Y, Fang F, Gao L, Tao Y, Li X, et al. Brd4 protac degradation agent gne-987 inhibits acute myeloid leukemia by targeting super enhancers. (2021). doi: 10.21203/rs.3.rs-1204848/v1

94. Sang X, Zhang Y, Fang F, Gao L, Tao Y, Li X, et al. BRD4 inhibitor GNE-987 exerts anticancer effects by targeting super-enhancer-related gene LYL1 in acute myeloid leukemia. *J Immunol Res* (2022) 2022:7912484. doi: 10.1155/2022/7912484

95. Chen YL, Li XL, Li G, Tao YF, Zhuo R, Cao HB, et al. BRD4 inhibitor GNE987 exerts anti-cancer effects by targeting super-enhancers in neuroblastoma. *Cell biosci* (2022) 12(1):33. doi: 10.1186/s13578-022-00769-8

96. Hu R, Wang WL, Yang YY, Hu XT, Wang QW, Zuo WQ, et al. Identification of a selective Brd4 protac with potent antiproliferative effects in ar-positive prostate cancer based on a dual Bet/Plk1 inhibitor. *Eur J Med Chem* (2022) 227:113922. doi: 10.1016/j.ejmech.2021.113922

97. Zengerle M, Chan KH, Ciulli A. Selective small molecule induced degradation of the bet bromodomain protein Brd4. *ACS Chem Biol* (2015) 10 (8):1770–7. doi: 10.1021/acschembio.5b00216

98. Wang X, Kutschat AP, Yamada M, Prokakis E, Böttcher P, Tanaka K, et al. Bromodomain protein brdt directs Δnp63 function and super-enhancer activity in a subset of esophageal squamous cell carcinomas. *Cell Death Differ* (2021) 28 (7):2207–20. doi: 10.1038/s41418-021-00751-w

99. Creyghton MP, Cheng AW, Welstead GG, Kooistra T, Carey BW, Steine EJ, et al. Histone H3k27ac separates active from poised enhancers and predicts developmental state. *Proc Natl Acad Sci United States America* (2010) 107 (50):21931–6. doi: 10.1073/pnas.1016071107

100. Kurdistani SK, Grunstein M. Histone acetylation and deacetylation in yeast. *Nat Rev Mol Cell Biol* (2003) 4(4):276–84. doi: 10.1038/nrm1075

101. Seto E, Yoshida M. Erasers of histone acetylation: The histone deacetylase enzymes. *Cold Spring Harbor Perspect Biol* (2014) 6(4):a018713. doi: 10.1101/cshperspect.a018713

102. Langer R, Mutze K, Becker K, Feith M, Ott K, Höfler H, et al. Expression of class I histone deacetylases (Hdac1 and Hdac2) in oesophageal adenocarcinomas: An immunohistochemical study. *J Clin Pathol* (2010) 63(11):994–8. doi: 10.1136/jcp.2010.080952

103. Zeng L-S, Yang X-Z, Wen Y-F, Mail S-J, Wang M-H, Zhang M-Y, et al. Overexpressed Hdac4 is associated with poor survival and promotes tumor progression in esophageal carcinoma. *Aging (Albany NY)* (2016) 8(6):1236–49. doi: 10.18632/aging.100980

104. Xue L, Hou J, Wang Q, Yao L, Xu S, Ge D. Rnai screening identifies Hat1 as a potential drug target in esophageal squamous cell carcinoma. *Int J Clin Exp Pathol* (2014) 7(7):3898–907.

105. Feng Y, Ma Z, Pan M, Xu L, Feng J, Zhang Y, et al. Wnt5a promotes the metastasis of esophageal squamous cell carcinoma by activating the Hdac7/Snail signaling pathway. *Cell Death Dis* (2022) 13(5):480. doi: 10.1038/s41419-022-04901-x

106. Li N, Tie X-J, Liu P-J, Zhang Y, Ren H-Z, Gao X, et al. Effects of down-regulation of Hdac6 expression on proliferation, cell cycling and migration of esophageal squamous cell carcinoma cells and related molecular mechanisms. *Asian Pacific J Cancer Prevention: APJCP* (2013) 14(2):685–9. doi: 10.7314/APJCP.2013.14.2.685

107. Zhang E, Han L, Yin D, He X, Hong L, Si X, et al. H3k27 acetylation activated-long non-coding rna Ccat1 affects cell proliferation and migration by regulating Spry4 and Hoxb13 expression in esophageal squamous cell carcinoma. *Nucleic Acids Res* (2017) 45(6):3086–101. doi: 10.1093/nar/gkw1247

108. Hu C, Liu M, Zhang W, Xu Q, Ma K, Chen L, et al. Upregulation of Klf4 by methylseleninic acid in human esophageal squamous cell carcinoma cells: Modification of histone H3 acetylation through Hat/Hdac interplay. *Mol Carcinog* (2015) 54(10):1051–9. doi: 10.1002/mc.22174

109. Liang Y, Chen X, Wu Y, Li J, Zhang S, Wang K, et al. Lncrna Casc9 promotes esophageal squamous cell carcinoma metastasis through upregulating Lamc2 expression by interacting with the creb-binding protein. *Cell Death Differ* (2018) 25(11):1980–95. doi: 10.1038/s41418-018-0084-9

110. Wu F, Xu L, Tu Y, Cheung OKW, Szeto LLM, Mok MTS, et al. Sirtuin 7 super-enhancer drives epigenomic reprogramming in hepatocarcinogenesis. *Cancer Lett* (2022) 525:115–30. doi: 10.1016/j.canlet.2021.10.039

111. Hoshino I, Matsubara H, Hanari N, Mori M, Nishimori T, Yoneyama Y, et al. Histone deacetylase inhibitor Fk228 activates tumor suppressor Prdx1 with apoptosis induction in esophageal cancer cells. *Clin Cancer Research: an Off J Am Assoc Cancer Res* (2005) 11(21):7945–52. doi: 10.1158/1078-0432.Ccr-05-0840

112. Murakami K, Matsubara H, Hoshino I, Akutsu Y, Miyazawa Y, Matsushita K, et al. Chap31 induces apoptosis only *Via* the intrinsic pathway in human esophageal cancer cells. *Oncology* (2010) 78(1):62–74. doi: 10.1159/000292362

113. Tzao C, Jin JS, Chen BH, Chung HY, Chang CC, Hsu TY, et al. Anticancer effects of suberoylanilide hydroxamic acid in esophageal squamous cancer cells in vitro and in vivo. *Dis esophagus: Off J Int Soc Dis Esophagus* (2014) 27(7):693–702. doi: 10.1111/dote.12127

114. Shoji M, Ninomiya I, Makino I, Kinoshita J, Nakamura K, Oyama K, et al. Valproic acid, a histone deacetylase inhibitor, enhances radiosensitivity in

esophageal squamous cell carcinoma. *Int J Oncol* (2012) 40(6):2140–6. doi: 10.3892/ijo.2012.1416

115. Shi Y, Xiang Z, Yang H, Khan S, Li R, Zhou S, et al. Pharmacological targeting of Tns3 with histone deacetylase inhibitor as a therapeutic strategy in esophageal squamous cell carcinoma. *Aging* (2021) 13(11):15336–52. doi: 10.18632/aging.203091

116. Ma S, Liu T, Xu L, Wang Y, Zhou J, Huang T, et al. Histone deacetylases inhibitor Ms-275 suppresses human esophageal squamous cell carcinoma cell growth and progression *Via* the Pi3k/Akt/Mtor pathway. *J Cell Physiol* (2019) 234 (12):22400–10. doi: 10.1002/jcp.28805

117. Feingold PL, Surman DR, Brown K, Xu Y, McDuffie LA, Shukla V, et al. Induction of thioredoxin-interacting protein by a histone deacetylase inhibitor, entinostat, is associated with DNA damage and apoptosis in esophageal adenocarcinoma. *Mol Cancer Ther* (2018) 17(9):2013–23. doi: 10.1158/1535-7163.Mct-17-1240

frontiers | Frontiers in Oncology

TYPE Review
PUBLISHED 01 November 2022
DOI 10.3389/fonc.2022.1059636

Check for updates

OPEN ACCESS

EDITED BY
Zhendong Jin,
Second Military Medical University, China

REVIEWED BY
Yao Huang,
Shanghai Jiao Tong University, China
Hafiz Abdul Waqas Ahmed,
Lady Reading Hospital, Pakistan

*CORRESPONDENCE
Hongyu Li
511268085@qq.com

SPECIALTY SECTION
This article was submitted to Gastrointestinal Cancers: Hepato Pancreatic Biliary Cancers, a section of the journal Frontiers in Oncology

RECEIVED 01 October 2022
ACCEPTED 10 October 2022
PUBLISHED 01 November 2022

CITATION
Khan S, Ali FS, Ullah S, Huang X- and Li H (2022) Advancing endoscopic traction techniques in endoscopic submucosal dissection.
Front. Oncol. 12:1059636.
doi: 10.3389/fonc.2022.1059636

COPYRIGHT
© 2022 Khan, Ali, Ullah, Huang and Li. This is an open-access article distributed under the terms of the Creative Commons Attribution License (CC BY). The use, distribution or reproduction in other forums is permitted, provided the original author(s) and the copyright owner(s) are credited and that the original publication in this journal is cited, in accordance with accepted academic practice. No use, distribution or reproduction is permitted which does not comply with these terms.

Advancing endoscopic traction techniques in endoscopic submucosal dissection

Suliman Khan[1], Faisal S. Ali[2], Saif Ullah[3], Xue- Huang[3] and Hongyu Li[4]*

[1]The Second Affiliated Hospital of Zhengzhou University, Zhengzhou, China, [2]Gastroenterology, Hepatology, and Nutrition Department, University of Texas Health Science Center at Houston, Houston, TX, United States, [3]Department of Gastroenterology, The First Affiliated Hospital of Zhengzhou University, Changxing, Zhengzhou, China, [4]Department of Gastroenterology, The People's Hospital of Changxing Country, Zhejiang Province, China

Traction techniques have emerged as a desirable "second-hand" while performing endoscopic submucosal dissection (ESD), enabling adequate visualization of submucosal tissue and vasculature, which allows for safe and efficient dissection. Multiple traction techniques have been developed over the years, and these can be broadly divided into internal and external traction techniques. This arsenal of techniques allows for traction that is personalized to the location of the lesion undergoing ESD. Mastering traction techniques requires structured training, and understanding of the benefits and pitfalls of each technique. Future research and development efforts need to focus on pathways and curriculums for trainees to master the currently available endoscopic traction techniques and provide avenues for the development of newer traction modalities.

KEYWORDS

gastrointestinal cancer, endoscopic submucosal dissection, traction, endoscopic training, interventional endoscopy

Introduction

Endoscopic submucosal dissection (ESD) is increasingly being adopted as the management modality of choice for early superficial gastrointestinal (GI) tumors (1–3). ESD enables resection of challenging lesions, including en-bloc resection of lesions larger than 20 mm, which translates into a higher curative resection and lower local recurrence rate (4). Despite these benefits, the applicability of ESD is limited owing to its technical complexity

and potential for serious adverse events. For trainees, performing ESD entails a steeper learning curve. In the West, the applicability of ESD is further limited by lack of infrastructure to deal with the numerous obstacles faced by endoscopists when attempting to establish an ESD center (5, 6). Nonetheless, the techniques and tools for ESD continue to advance and evolve, predominantly in Japan and China.

Over the years, ESD has seen advancements in the approach to visualization and identification of the submucosal layer, such as use of a transparent cap and reduplicative submucosal injection before proceeding further with resection (7). However, the supporting capacity of transparent cap is limited, and repeated injections prolong procedure time. In recent years, tissue traction has emerged as an appealing "second-hand" while performing ESD (8). Inspired by the surgical pull and push techniques, traction not only provides clear view of submucosal tissue and vessels, but also provides adequate tissue tension during ESD. Traction techniques have been evolving since they first came to limelight. The various traction techniques currently in practice have advantages and pitfalls, depending on the location and size of the lesion (9).

Traction techniques can broadly be categorized into internal and external endoscopic traction technique (Figure 1). This article aims to summarize the evolution and characteristics of traction techniques, while highlighting the pros and cons of various approaches to traction.

External traction techniques

Early in the course of endoscopic mucosal resection (EMR), double-scope traction, percutaneous traction, and magnetic anchor traction techniques were employed for the resection of early gastric cancer in human and animal experiments (10). Subsequently, these traction modalities evolved and were implemented to improve the feasibility of ESD.

Percutaneous technique

The percutaneous-traction technique has mostly been utilized in animal trials (11). A laparoscopic port with a trocar is inserted directly into the gastric lumen after endoscopic determination of the proper port position. Snare forceps are subsequently inserted through the gastric port to grasp and pull the lesion to advance ESD, providing traction independent of the endoscope. The percutaneous-traction method carries a high risk of pneumoperitoneum and peritonitis. The incidence and severity of delayed adverse events also remains to be studied. Furthermore, the percutaneous-traction method is not advisable for lesions of the esophagus, the anterior gastric wall, lesions located in the high fundus of the stomach, and colorectal lesions, as this may increase the risk of adverse events.

Magnetic-anchor technique

Two prospective clinical trials have demonstrated the feasibility of magnetic-anchor-guided ESD of gastric lesions (12, 13). After placing an internal magnetic anchor at the target lesion, traction can be applied by a high-power electromagnet placed outside the body (Figure 2A). As one would expect, the magnetic force and consequently, the traction generated by this technique, depends on the patient's abdominal wall thickness. The adverse effect profile of deploying a magnetic traction system for ESD also needs to be further elucidated to better understand its clinical utility.

Clip-line technique

The most widely used and simplest traction techniques employ endoscopic clips. Since 2008, a variety of clip traction techniques have emerged (14, 15).

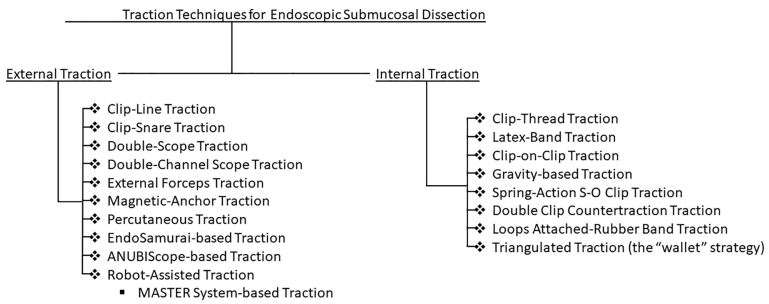

FIGURE 1
Flowchart of explored endoscopic traction techniques for endoscopic submucosal dissection.

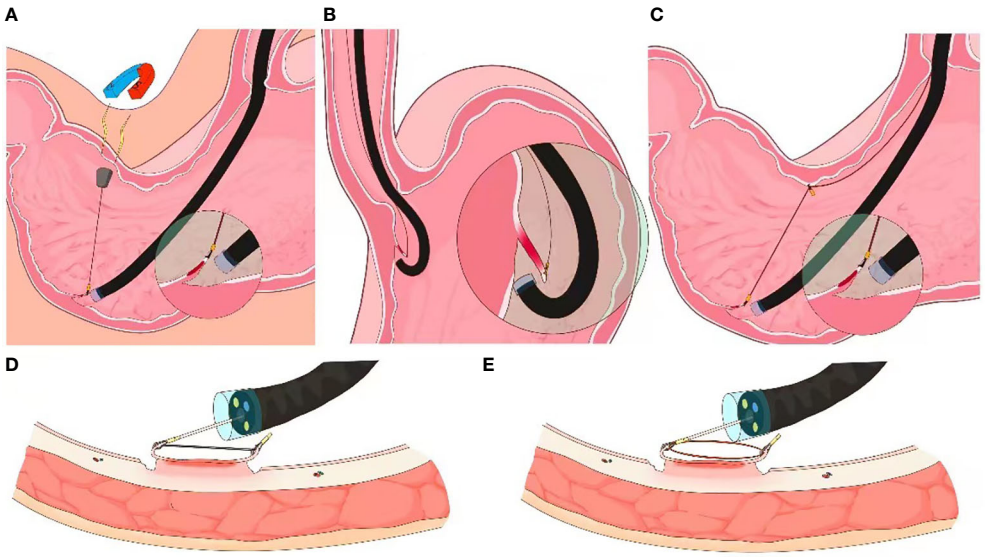

FIGURE 2
External endoscopic resection techniques. **(A)** Schematic of magnet-anchor traction technique ((from Gotoda et al). **(B)** Schematic of clip-line traction technique. **(C)** Schematic of pulley clip-line traction technique **(D, E)** Schematics of clip-snare traction technique.

Jeon et al' first described the clip-line traction technique in 2009 (16). A clip with dental floss or suture attached to its tail end is mounted on the endoscope. The clip is then advanced with the endoscope and deployed at the desired edge of the luminal lesion; controlled traction is achieved as the endoscopy technician or assistant manually pulls on the free end of the thread (Figure 2B**).** This is among the preferred techniques for trainees due to its relative ease of adoptability (14). The clip-line traction technique has also been used for other endoscopic interventions, such as endoscopic submucosal excavation (ESE), endoscopic full thickness resection (EFTR), and submucosal tunneling endoscopic resection (STER), where it has been shown to reduce the procedure time. However, this technique is limited by the degree of force that can be applied to the clip-line; there is a risk of clip dislodgement with excessive traction.

The clip-line technique can be modified into a pulley traction technique by deploying a second clip at the contralateral mucosa, thereby altering the direction of traction (Figure 2C**).** The pully technique is unsuitable for lesions within the esophagus, the cardia and the pylorus of stomach (17).

Clip-snare technique

The clip-snare traction technique entails pre-looping of a snare at the tip of the endoscope before introducing it into the GI tract. First demonstrated by Yoshida et al. and later be Ota et al., this technique is more commonly known as the clip-snare method with a pre-looping technique (CSM-PLT; Figures 2D, E) (18, 19). A clip is subsequently inserted through the working channel of the endoscope and attached to the mucosal flap of the lesion. The snare is then loosened, advanced forward and tightened to grasp the clip. Compared to a silk thread or a dental floss, the snare has a stable sheath to provide traction by pulling or pushing the clip in forward as well as retroflexed endoscope views. Moreover, the snare and the endoscope can be maneuvered independently for flexible movement. By deploying additional, adjacent clips, this technique can be modified to provide multi-point traction (20).

External forceps traction technique

Imaeda et al. first demonstrated the external forceps traction technique (21). After a circular incision of the lesion, the endoscope was retrieved to introduce grasping forceps with the assistance of a second forceps passing through the accessory channel of the endoscope. The grasping forceps were then anchored at the margin of the lesion like a lock. Traction is then applied, not only by pulling or pushing but also by rotation. Furthermore, when traction is not appropriate the lesion could also be released and regressed. This method has only been attempted in cases of early rectal cancer[46]. It should be noted that it is difficult to insert and

control forceps-produced traction when operating on deep-seated colonic lesions.

Internal traction techniques

Clip-based traction techniques

Chen et al. were among the first to demonstrate an internal traction technique; two clips were deployed on opposite ends of the lesion while performing ESD (22). Hot biopsy forceps were subsequently used to pull the small loop between two clips to achieve traction. The internal traction technique evolved thereafter in diverse forms, most notably the Sakamoto-Osada clip (S-O clip) based traction technique. The S-O clip was originally developed for colonic ESD by Sakamoto et al. (23). Subsequently, multiple variations of this system have been developed and reported, including the latex-band traction technique (a nylon thread looped with a latex band which is grasped by an endoclip; the nylon thread is maneuvered to apply traction); the clip and ring shaped thread traction technique (hemoclips with attached ring shaped thread are deployed at the oral and anal edges of the lesion; a third clip grasps the thread and is fixed to the opposite mucosal wall, creating a triangulated traction system. Alternatively, a single clip may be deployed on the desired edge of resected tissue and a second clip deployed on the contralateral mucosa to create internal traction); the loops-attached rubber band traction technique (a circular rubber band connected to many smaller nylon loops which are grasped with a clip when being deployed at the site of interest); the spring-action S-O clip technique (a 7 mm x 1.8 mm spring attached to a metal clip on one end for anchoring at the ESD site and a double nylon loop on one end to be grasped by a clip for contralateral anchoring); the double-clip counter-traction technique using a rubber band (two clips connected by a rubber band), and the wallet strategy (hemoclips with attached rubber bands are deployed at the oral and anal edges of the lesion; a third clip grasps rubber bands of both clips and is fixed to the opposite mucosal wall, creating a triangulated traction system.

Nomura et al. have reported a simplified clip-on-clip method (first clip is deployed at the ESD site of interest; second clip is deployed at the base of the first clip; a third clip is deployed on the contralateral mucosa while grasping the second clip from the free space available between its grasping teeth (Figure 3)**);** this technique is beneficial when performing ESD in narrow luminal regions such as the rectosigmoid colon (24). This technique also carries the advantage of providing traction independent of the endoscope. However, it is difficult to control the traction direction and the stability of this technique can be questionable at times; if the clips are placed suboptimally, adequate traction cannot be applied, and an additional clip is sometimes needed.

Gravity based traction

In recent years, data on feasibility of gravity-based traction has emerged, mostly in the context of colorectal ESD. A magnetic bead or a sinker is attached to the edge of the lesion which can be pulled by gravity. Altering patients' position to identify the ideal site for traction has been reported as an adjunct to facilitate adequate gravity-based traction (25).

Traction by location

Traction in the esophagus

The esophagus is a straight narrow tube extending from the pharynx to the cardia of the stomach. It has a special anatomy without a serosal layer and moves with respiration and heartbeats. Traction devices are seldom applied in the esophagus due its narrow lumen. Whenever needed, the clip-with-line traction technique is advisable. In a multicenter randomized controlled trial, Yoshida et al' demonstrated the superiority of the clip-line assisted ESD over conventional ESD in terms of procedure time (44.5min vs 60.5min) and should be considered the first choice for esophageal cancers≥20mm (18). The external forceps method is another option for esophageal ESD. Motohashi et al. and Hirota et al. have reported traction techniques modified from the above technique, which needs an overtube with a side-channel for forceps introduction, or an Impact Shooter® mounted on the scope (25, 26). Although this requires special devices, the direction of traction can be changed by rotating the angle of the overtube. The feasibility and potential efficacy of these traction modalities needs to be validated in larger randomized trials.

Traction in the stomach

The stomach is a J-shaped organ with varying sizes, and consists of four layers with a fibrous serosa. It is divided into 5 regions: cardia, fundus, body, antrum, and pylorus. Sufficient space and elasticity allow for a lot of traction.

Clip-line assisted ESD has been reported to significantly shorten procedure time without compromising safety while performing resection of gastric lesions (27). Further prospective, randomized and controlled study of this technique revealed that the procedure time reduction is most pronounced when performing ESD in the greater curvature of the upper or middle stomach with a low risk of perforation (28). The CSM-PLT technique has also been used for gastric ESD and has been reported to reduce procedure time compared to conventional ESD. Preliminary study of employing the clip-snare traction technique for gastroesophageal ESD has also been

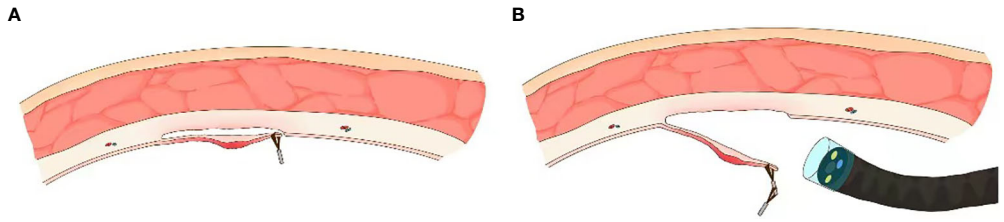

FIGURE 3
Internal endoscopic traction technique. **(A)** Schematic of S-O clip based internal traction technique (from Matsumoto et al). **(B)** Schematic of clip-on-clip method (from Nomura et al).

reported. Similarly, S-O clip-based internal traction technique has also been used and has been reported to increase procedure speed by 25% without additional risk of adverse events (29).

External forceps-based traction technique for gastric ESD proves to be cumbersome when dealing with lesions in the cardia, lesser curvature or the posterior wall of the upper gastric body due to restricted endoscopic retroflexion (30).

There are innovative traction techniques that have been introduced in the extensive space of the stomach for ESD, such as the EndoLifter and steerable grasper with a sheath (31). The former consists of a retractable grasping forceps attached to a transparent cap by a hinge that allows simultaneous grasping, retracting, and lifting of the mucosa. The steerable grasper is fixed on the endoscope with tape, and enables bidirectional rotation upto 100 degrees. Technical feasibility and safety of these traction techniques has been demonstrated in porcine stomach models where they provide dynamic and controlled traction at various locations. Further randomized trials are warranted to accelerate translation of these techniques for human use.

Traction in the colon and rectum

The colorectum is a long structure with several angulation segments, always accompanied by peristalsis. Colorectal ESD remains challenging due to procedural complexity, long procedure time, and high adverse events.

A novel clip-line traction technique has been designed by Yamasaki et al'., which obviates the need for withdrawal and reinsertion of the endoscope; a thread is tied to the teeth of a clip which is subsequently introduced into the lumen through the working channel of an endoscope. This technique has been utilized in a randomized controlled trail and was reported to significantly shorten procedure time compared with conventional-ESD (30). However, for lesions in the proximal colon, the efficacy of this technique dampened; it was difficult to control the force of traction applied to tissue. Yamada et al. used the CSM-PLT traction technique in a small number of patients for colorectal ESD; compared to conventional ESD, CSM-PLT reduced mean procedure time (31).

Multiple S-O clip-based traction techniques have been successfully utilized for traction during colorectal ESD, including the loops-attached rubber band traction technique, the spring-action S-O clip technique, the latex-band traction technique, the double-clip counter-traction technique, as well as the wallet strategy (both with rubber bands and ring-shaped thread). Employing the ring shaped thread for triangular traction has been shown to reduce dissection time compared to conventional ESD in a randomized trial (80 versus 130 minutes) by Mori et al. (32). As previously mentioned, the clip-on-clip traction technique is beneficial when performing ESD in narrow luminal regions such as the rectosigmoid colon (33).

Conclusion and future perspective

ESD is a landmark advancement in therapeutic endosocpy and continues to rapidly evolve. The steep learning curve, long procedure time, and potential for serious adverse events have been challenging for trainees during the learning and application of ESD. The advent of traction techniques has decreased procedure times consistently without increasing the risk of adverse events. The various traction techniques presented above indeed facilitate the advancement and application of ESD, especially for trainees. Factors that should be considered comprehensively before choosing a traction technique include the anatomical location of lesion, the anticipated procedure time, the traction direction, the device needed (for resection as well as traction) and by extension, the type of endoscope needed, the safety of the traction technique being considered, and the cost. Ones

experience with traction should also be considered. Notably, the use of traction techniques is not limited to ESD, and can be employed for emerging endoscopic technologies and other anatomical sites. Future research may focus on technological advancements and development of a structural curriculum for trainees which accommodates the increasing level of complexity of various traction techniques.

Author contributions

Study design and concept, SK, FA, and HL. Manuscript writing, FA, SU, and SK. Data collection and analysis, XH, FA, and HL. Critical revision of the manuscript, HL. All authors contributed to the article and approved the submitted version.

Conflict of interest

The authors declare that the research was conducted in the absence of any commercial or financial relationships that could be construed as a potential conflict of interest.

Publisher's note

All claims expressed in this article are solely those of the authors and do not necessarily represent those of their affiliated organizations, or those of the publisher, the editors and the reviewers. Any product that may be evaluated in this article, or claim that may be made by its manufacturer, is not guaranteed or endorsed by the publisher.

References

1. Landin MD, Guerrón AD. Endoscopic mucosal resection and endoscopic submucosal dissection. *Surg Clin North Am* (2020) 100(6):1069–78. doi: 10.1016/j.suc.2020.07.004

2. Ge PS, Aihara H. Advanced endoscopic resection techniques: Endoscopic submucosal dissection and endoscopic full-thickness resection. *Dig Dis Sci* (2022) 67(5):1521–38. doi: 10.1007/s10620-022-07392-0

3. Draganov PV, Wang AY, Othman MO, Fukami N. AGA institute clinical practice update: Endoscopic submucosal dissection in the united states. *Clin Gastroenterol Hepatol* (2019) 17(1):16–25.e1. doi: 10.1016/j.cgh.2018.07.041

4. Nishizawa T, Yahagi N. Endoscopic mucosal resection and endoscopic submucosal dissection: technique and new directions. *Curr Opin Gastroenterol* (2017) 33(5):315–9. doi: 10.1097/MOG.0000000000000388

5. Ma MX, Bourke MJ. Endoscopic submucosal dissection in the West: Current status and future directions. *Dig Endosc.* (2018) 30(3):310–20. doi: 10.1111/den.12960

6. Friedel D, Stavropoulos SN. Introduction of endoscopic submucosal dissection in the West. *World J Gastrointest Endosc* (2018) 10(10):225–38. doi: 10.4253/wjge.v10.i10.225

7. Wang J, Lin S, Qiao W, Liu S, Zhi F. Clinical outcomes of cap-assisted endoscopic resection for small rectal subepithelial tumors. *Gastroenterol Hepatol* (2021) 44(6):418–23. doi: 10.1016/j.gastrohep.2020.08.016

8. Abe S, Wu SYS, Ego M, Takamaru H, Sekiguchi M, Yamada M, et al. Efficacy of current traction techniques for endoscopic submucosal dissection. *Gut Liver* (2020) 14(6):673–84. doi: 10.5009/gnl19266

9. Xia M, Zhou Y, Yu J, Chen W, Huang X, Liao J. Short-term outcomes of traction-assisted versus conventional endoscopic submucosal dissection for superficial gastrointestinal neoplasms: a systematic review and meta-analysis of randomized controlled studies. *World J Surg Oncol* (2019) 17(1):94. doi: 10.1186/s12957-019-1639-z

10. Tsuji K, Yoshida N, Nakanishi H, Takemura K, Yamada S, Doyama H. Recent traction methods for endoscopic submucosal dissection. *World J Gastroenterol* (2016) 22(26):5917–26. doi: 10.3748/wjg.v22.i26.5917

11. von Delius S, Karagianni A, von Weyhern CH, Feussner H, Schuster T, Schmid RM, et al. Percutaneously assisted endoscopic surgery using a new PEG-minitrocar for advanced endoscopic submucosal dissection (with videos). *Gastrointest Endosc* (2008) 68(2):365–9. doi: 10.1016/j.gie.2008.02.093

12. Matsuzaki I, Hattori M, Yamauchi H, Goto N, Iwata Y, Yokoi T, et al. Magnetic anchor-guided endoscopic submucosal dissection for colorectal tumors (with video). *Surg Endosc* (2020) 34(2):1012–8. doi: 10.1007/s00464-019-07127-9

13. Gotoda T, Oda I, Tamakawa K, Ueda H, Kobayashi T, Kakizoe T. Prospective clinical trial of magnetic-anchor-guided endoscopic submucosal dissection for large early gastric cancer (with videos). *Gastrointest Endosc* (2009) 69(1):10–5. doi: 10.1016/j.gie.2008.03.1127

14. Jin P, Fu KI, Yu Y, He YQ, Wei Z, Wang X, et al. Traction using a clip-with-line is a preferred method for trainees in performing esophageal endoscopic submucosal dissection: an animal model study. *Therap Adv Gastroenterol* (2017) 10(4):343–51. doi: 10.1177/1756283X16687926

15. Kobara H, Kobayashi N, Nishiyama N, Tada N, Fujihara S, Masaki T. Simplified submucosal tunneling biopsy using clip-With-Line traction and closure for gastric subepithelial lesion. *Diagnostics (Basel)* (2020) 10(9):690. doi: 10.3390/diagnostics10090690

16. Jeon WJ, You IY, Chae HB, Park SM, Youn SJ. A new technique for gastric endoscopic submucosal dissection: peroral traction-assisted endoscopic submucosal dissection. *Gastrointest Endosc* (2009) 69(1):29–33. doi: 10.1016/j.gie.2008.03.1126

17. Shichijo S, Matsuno K, Takeuchi Y, Uedo N, Ishihara R. Pulley traction-assisted colonic endoscopic submucosal dissection affords good visibility of submucosal layer. *VideoGIE* (2018) 3(11):358–60. doi: 10.1016/j.vgie.2018.08.007

18. Yoshida N, Doyama H, Ota R, Takeda Y, Nakanishi H, Tominaga K, et al. Effectiveness of clip-and-snare method using pre-looping technique for gastric endoscopic submucosal dissection. *World J Gastrointest Endosc* (2016) 8(12):451–7. doi: 10.4253/wjge.v8.i12.451

19. Ota R, Doyama H, Tsuji K, Yamada S. Deep colonic endoscopic submucosal dissection using a modified clip and snare method incorporating a pre-looping technique. *BMJ Case Rep* (2015) 2015:bcr2014207918. doi: 10.1136/bcr-2014-207918

20. Sooklal S, Raja S, Jang S, Robertson S, Bhatt A. Endoscopic submucosal dissection of a large pedunculated gastric polyp causing gastric outlet obstruction using clip-snare traction technique. *VideoGIE* (2020) 5(9):407–8. doi: 10.1016/j.vgie.2020.05.003

21. Imaeda H, Iwao Y, Ogata H, Ichikawa H, Mori M, Hosoe N, et al. A new technique for endoscopic submucosal dissection for early gastric cancer using an external grasping forceps. *Endoscopy* (2006) 38(10):1007–10. doi: 10.1055/s-2006-925264

22. Chen PJ, Chu HC, Chang WK, Hsieh TY, Chao YC. Endoscopic submucosal dissection with internal traction for early gastric cancer (with video). *Gastrointest Endosc* (2008) 67(1):128–32. doi: 10.1016/j.gie.2007.07.021

23. Sakamoto N, Osada T, Shibuya T, Beppu K, Matsumoto K, Shimada Y, et al. The facilitation of a new traction device (S-O clip) assisting endoscopic submucosal dissection for superficial colorectal neoplasms. *Endoscopy* (2008) 40(Suppl 2):E94–5. doi: 10.1055/s-2007-995603

24. Nomura T, Kamei A, Sugimoto S, Oyamada J. Colorectal endoscopic submucosal dissection using a clip-on-clip traction method. *Endoscopy* (2018) 50(8):E197–8. doi: 10.1055/a-0605-2868

25. Ye L, Yuan X, Pang M, Bethge J, Ellrichmann M, Du J, et al. Magnetic bead-assisted endoscopic submucosal dissection: a gravity-based traction method for treating large superficial colorectal tumors. *Surg Endosc* (2019) 33(6):2034–41. doi: 10.1007/s00464-019-06799-7

26. Hirota M, Kato M, Yamasaki M, Kawai N, Miyazaki Y, Yamada T, et al. A novel endoscopic submucosal dissection technique with robust and adjustable tissue traction. *Endoscopy* (2014) 46(6):499–502. doi: 10.1055/s-0034-1364879

27. Kinoshita J, Iguchi M, Maekita T, Wan K, Shimokawa T, Fukatsu K, et al. Traction method versus conventional endoscopic submucosal dissection for gastric epithelial neoplasms: A randomized controlled trial. *Med (Baltimore)* (2022) 101 (13):e29172. doi: 10.1097/MD.0000000000029172

28. Yoshida M, Takizawa K, Suzuki S, Koike Y, Nonaka S, Yamasaki Y, et al. Conventional versus traction-assisted endoscopic submucosal dissection for gastric neoplasms: a multicenter, randomized controlled trial (with video). *Gastrointest Endosc* (2018) 87(5):1231–40. doi: 10.1016/j.gie.2017.11.031

29. Hashimoto R, Hirasawa D, Iwaki T, Yamaoka H, Nihei K, Tanaka I, et al. Usefulness of the s-O clip for gastric endoscopic submucosal dissection (with video). *Surg Endosc* (2018) 32(2):908–14. doi: 10.1007/s00464-017-5765-9

30. Yamasaki Y, Takeuchi Y, Uedo N, Kato M, Hamada K, Aoi K, et al. Traction-assisted colonic endoscopic submucosal dissection using clip and line: A feasibility study. *Endosc Int Open* (2016) 4(1):E51–5.

31. Yamada S, Doyama H, Ota R, Takeda Y, Tsuji K, Tsuji S, et al. Impact of the clip and snare method using the prelooping technique for colorectal endoscopic submucosal dissection. *Endoscopy* (2016) 48(3):281–5.

32. Mori H, Kobara H, Nishiyama N, Fujihara S, Matsunaga T, Masaki T. Novel effective and repeatedly available ring-thread counter traction for safer colorectal endoscopic submucosal dissection. *Surg Endosc* (2017) 31(7):3040–7. doi: 10.1007/s00464-016-5326-7

33. Nomura T, Matsuzaki I, Sugimoto S, Oyamda J, Kamei A, Kobayashi M. Clip-on-clip closure method for a mucosal defect after colorectal endoscopic submucosal dissection: a prospective feasibility study. *Surg Endosc* (2020) 34 (3):1412–6. doi: 10.1007/s00464-019-07195-x

frontiers | Frontiers in Oncology

TYPE Systematic Review
PUBLISHED 08 November 2022
DOI 10.3389/fonc.2022.1018248

Check for updates

OPEN ACCESS

EDITED BY
Zhendong Jin,
Medical University, China

REVIEWED BY
Gianluca Esposito,
Sapienza University Of Rome, Italy
Jun-Hyung Cho,
Soonchunhyang University Hospital Seoul, South Korea

*CORRESPONDENCE
Gengqing Song
songgavin2010@gmail.com
Yang Yang
pfdks@sina.com
Wei Wei
weiwei3816@mail.cintcm.ac.cn

SPECIALTY SECTION
This article was submitted to Gastrointestinal Cancers: Gastric and Esophageal Cancers, a section of the journal Frontiers in Oncology

RECEIVED 24 August 2022
ACCEPTED 17 October 2022
PUBLISHED 08 November 2022

CITATION
Fang S, Fu Y, Du S, Wang L, Qing X, Luo X, Song G, Yang Y and Wei W (2022) The role of the endoscopic grading of gastric intestinal metaplasia in assessing gastric cancer risk: A systematic review and meta-analysis. *Front. Oncol.* 12:1018248. doi: 10.3389/fonc.2022.1018248

COPYRIGHT
© 2022 Fang, Fu, Du, Wang, Qing, Luo, Song, Yang and Wei. This is an open-access article distributed under the terms of the Creative Commons Attribution License (CC BY). The use, distribution or reproduction in other forums is permitted, provided the original author(s) and the copyright owner(s) are credited and that the original publication in this journal is cited, in accordance with accepted academic practice. No use, distribution or reproduction is permitted which does not comply with these terms.

The role of the endoscopic grading of gastric intestinal metaplasia in assessing gastric cancer risk: A systematic review and meta-analysis

Shuangshuang Fang[1], Yuhan Fu[2], Sijing Du[1], Lin Wang[1], Xiangli Qing[1,3], Xiaoying Luo[1], Gengqing Song[4]*, Yang Yang[1]* and Wei Wei[1]*

[1]Department of Gastroenterology, Beijing Key Laboratory of Functional Gastrointestinal Disorders Diagnosis and Treatment of Traditional Chinese Medicine, Wangjing Hospital, China Academy of Chinese Medical Sciences, Beijing, China, [2]Department of Internal Medicine, MetroHealth Medical Center/Case Western Reserve University, Cleveland, OH, United States, [3]Department of Clinical Medicine, Chengdu University of Traditional Chinese Medicine, Chengdu, China, [4]Department of Gastroenterology and Hepatology, MetroHealth Medical Center/Case Western Reserve University, Cleveland, OH, United States

Background and aim: Patients with gastric intestinal metaplasia (IM) are at increased risk of gastric cancer (GC). The endoscopic grading of gastric intestinal metaplasia (EGGIM) with high-definition endoscopes has shown the potential to facilitate GC risk stratification. However, a comprehensive review and meta-analysis of published articles are lacking. We conducted a meta-analysis to access the value of EGGIM in the assessment of histological IM.

Materials: Studies were selected from PubMed, Medline, Embase, and Cochrane (last selection, Jun 2022). We extracted relevant data to calculate the accuracy of EGGIM compared with the operative link of gastric intestinal metaplasia (OLGIM) and to calculate pooled odds ratio (OR) with a 95% confidence interval (CI) assessing GC risk with different grading.

Results: Four diagnostic studies and three case-control clinical trials were included in the analysis, which included 665 patients and 738 patients, respectively. Compared with OLGIM III/IV, EGGIM(5-10) had a pooled sensitivity and specificity of 0.92(95%CI 0.86-0.96) and 0.90(95%CI 0.88-0.93), and the area under the curve(AUC) was 0.9702. In assessing early GC, the pooled OR of patients with EGGIM(5-10) was 7.46(95%CI 3.41-16.31) compared with that of EGGIM(0-4).

Conclusions: EGGIM is highly consistent with OLGIM, and patients with EGGIM (5-10) are at a higher risk for early GC. Some heterogeneity in the current research suggests that we need to carry out more strict control of confounding factors.

Systematic Review Registration: [https://www.crd.york.ac.uk/PROSPERO/display_record.php?RecordID=248691], (**Prospero registration number:** 248691)

KEYWORDS

endoscopic grading of gastric intestinal metaplasia, EGGIM, intestinal metaplasia, accuracy, Sensitivity

Introduction

Gastric cancer (GC) is the fifth most commonly diagnosed cancer worldwide and the fourth most common cause of cancer-related death (1). More than 95% of GC are adenocarcinomas (2). According to Lauren's classification, gastric adenocarcinomas can be classified into diffuse and intestinal types based on histology (3). The intestinal type is the most common type of gastric adenocarcinoma (4), which develops through a multistep process from gastritis, atrophy, intestinal metaplasia (IM), dysplasia to intestinal-type GC (5). Among those steps, IM is widely recognized as a precancerous stomach mucosal lesion, and patients with IM are at increased risk for intestinal-type GC.

Operative Link on Gastric Intestinal Metaplasia (OLGIM) is a grading standard to risk stratify IM, which involves five biopsy specimens: two from the antrum two from the corpus, and one from the angle of the stomach. Patients with OLGIM stage III-IV are at an increased risk of early gastric neoplasia (HR 20.7; 95% CI 5.04 to 85.6) and may develop early gastric neoplasia within two years (6). A meta-analysis that included three case-control studies reported a 3.99-fold odds ratio(95%CI 3.05 to 5.21) for GC of OLGIM stage III-IV (7). Although studies have supported that OLGIM can effectively risk-stratify GC (8–10), there are still some limitations. There are chances that biopsies may miss certain gastric mucosal lesions because they can present multifocally. Furthermore, the histopathology risk stratification tool can bring an extra burden to the healthcare system (11).

In recent years, image-enhanced endoscopy (IEE), including narrow-band imaging (NBI), linked color imaging (LCI), and blue laser imaging (BLI), has improved the performance of endoscopy (12). IEE can present a better characterization of the mucosal pattern, which is more accurate for endoscopists to make diagnoses based on images. Above this foundation, the endoscopic grading of gastric intestinal metaplasia (EGGIM) score system using IEE technology has been proposed to assess the GC risk based on endoscopic visualization of IM, which shows high concordance with OLGIM. EGGIM is performed by endoscopic evaluation of greater and lesser curvature of the antrum, angulus, and greater and lesser curvature of corpus. Each area was scored according to the extent of intestinal metaplasia (0, no intestinal metaplasia; 1, an area less than or equal to 30%; 2, a size greater than 30%), with a total score of 10 (8). Several studies have shown its potential to facilitate GC risk stratification. However, a comprehensive review and meta-analysis of published articles are lacking.

In this study, we conducted a systematic review and meta-analysis to explore the value of the EGGIM system in the assessment of histological IM and the risk classification of early gastric cancer.

Materials and methods

Study design

We performed a systematic search for diagnostic studies and case-control studies that evaluate the diagnostic accuracy of the EGGIM system using the OLGIM system or GC incidence as a gold standard. The protocol for this study has previously been registered with PROSPERO (registration no. 248691). The protocol followed the Preferred Reporting Items for Systematic Reviews and Meta-Analyses (PRISMA) (13) guidelines.

Search strategy

Four scientific databases (PubMed, Medline, Embase, and Cochrane) were searched by two researchers (WL and QXL) independently from their inception through Oct 14, 2021. Eligible articles published after this date were added manually. The last elicitation date was Jun 25, 2022. The references of identified articles

were also checked to retrieve potential missed articles. The detailed search strategy is shown in Supplementary Materials 1. Variables were combined with "Endoscopic grading of gastric intestinal metaplasia" or "EGGIM". Titles and abstracts were read to exclude irrelevant records. Articles not excluded were read through by two reviewers. Disagreements were resolved with a third reviewer (DSJ).

Inclusion/exclusion criteria

The inclusion criteria were as follows: 1) Diagnostic studies whose primary or secondary outcome was the evaluation of the accuracy of EGGIM using OLGIM as a gold standard, or case-control studies using EGGIM to stratify GC risk. 2) True positive (TP), true negative (TN), false positive (FP), false negative (FN), or the number of GC events were included in the paper. 3) The papers were published in English. We excluded study types, including letters, reviews, expert opinions, study protocols, animal studies, preclinical trials, and studies with fewer than 10 cases.

Data extraction and quality evaluation

Two reviewers (YY and DSJ) read the included articles and extracted data independently. The following variables were collected: the first author, publication year, country, study period, sample size, gender, the experience of endoscopists, endoscopic technology, and details of the measurement data. All collected data were double-checked by a third reviewer (FSS). Two reviewers(FSS and WL) scored the included diagnostic studies independently for risk of basis according to Quality Assessment of Diagnostic Accuracy Studies (QUADAS-2) (14) and scored the included case-control studies independently for risk of basis according to The Newcastle–Ottawa Scale (NOS) (15). Disagreements were resolved with a third reviewer(WW).

Data synthesis and statistical analysis

Meta-DiSc 1.4 and RevMan 5.4.1 (Cochrane, London, UK) were used to analyze the data. Heterogeneity was assessed with Cochrane's Q test and Higgins's I^2 statistics. A fixed-effects model was used when heterogeneity was absent (I^2 <50% or $p > 0.1$) and a random-effects model was used if heterogeneity existed (50% <I^2 <80% or $p < 0.05$). When heterogeneity was substantial (I^2 >80% or $p < 0.01$), a descriptive analysis was used, and subgroup analyses implement for different image-enhanced technology when the necessary data were available. All P-values were two-tailed, and P values < 0.05 were deemed to be statistically significant.

Results

We identified a total of 435 studies. Four diagnostic studies with 665 patients (8, 10, 16, 17) and three case-control studies with 728 patients met the selection criteria (9, 18, 19) (Figure 1).

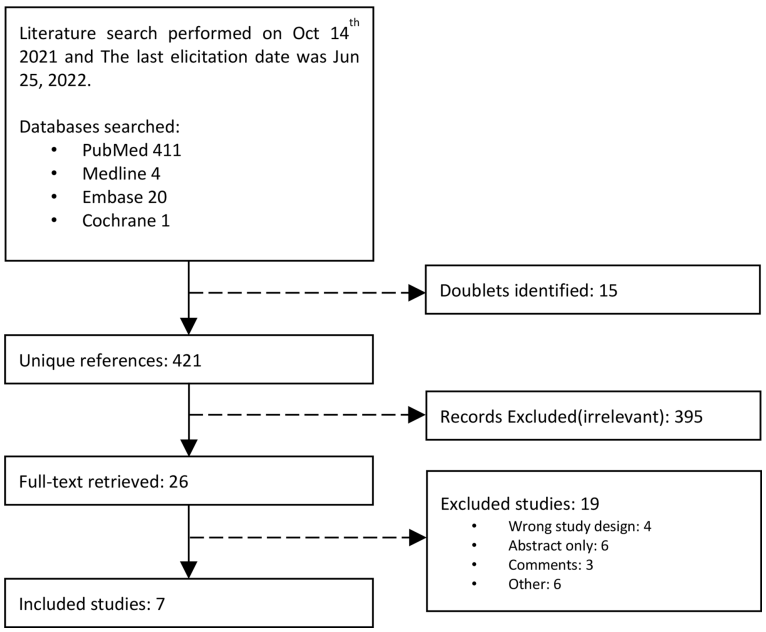

FIGURE 1
Flow diagram of literature research.

Table 1 summarizes the characteristics of the studies included in the meta-analysis. Two of the diagnostic studies compared NBI-assisted EGGIM with OLGIM and the other two comparisons were made LCI and BLI respectively. One case-control study compared NBI-assisted EGGIM with OLGIM to classify GC and non-GC patients; one used LCI and one used multiple IEE technologies risks stratify early gastric neoplasia. Most of the trials were conducted in Portugal, of which two were multinational studies and the remaining three were conducted in China and Japan. Four studies stipulate endoscopists' experience. Two studies required endoscopists who have operated more than 100 NBI per year, one study required endoscopists who performed 200 LCI per year, and the other study required endoscopists who have experience in performing more than 5000 upper endoscopies.

Quality assessment

The assessment of the risk of bias and applicability concerns for the four diagnostic studies are presented in Table 2. The survey conducted by Rui Castro et al. (17) was determined to have a high risk of bias in patient selection and reference standards since they failed to enroll consecutive patients and to include all cases in the analysis. The remaining studies were deemed to have a low risk of bias and applicability concern because the cases were included consecutively, EGGIM was graded before the pathological examination, and the pathologists were blinded when determining the gold standard OLGIM.

According to the NOS assessment, three case-control studies (9, 18, 19) obtained 6 stars, which represents acceptable study quality shown in Table 3.

EGGIM compared to OLGIM

Compared with OLGIM III/IV, EGGIM(5-10) obtained a pooled sensitivity and specificity of 0.92(95%CI 0.86-0.96) and 0.90(95%CI 0.88-0.93), and the area under the curve(AUC) was 0.9702 (Figure 2).

TABLE 1 Characteristics of studies included in the meta-analysis.

First Author	Year	Country	Study Period	Study design	Sample Size	Gender	Characteristics of endoscopists	Endoscopic Technology
Guanpo Zhang	2020	China	May, 2020-July, 2020	Diagnostic study	277	56.32% male	Three endoscopists with LCI experience more than 200 high-resolution endoscopy [HRE]-LCI per year.	LCI
Rui Castro	2019	Portugal	Sep, 2018-Nov, 2019	Diagnostic study	37	Unclear	Unclear	BLI
Gianluca Esposito	2018	Italy, Portugal	Jan, 2016-Sep, 2017	Diagnostic study	250	37.6% male	Four fully trained endoscopists with NBI experience (>100 HR-NBI per year).	NBI
Pedro Pimentel Nunes	2016	Portugal, Italy, Romania, UK, USA	Jan, 2014-Mar, 2015	Diagnostic study	101	42%male	In each center, one or more endoscopists with NBI experience (more than 100 HRE-NBI per year) performed the endoscopy.	NBI
Pedro Marcos	2019	Portugal	2012-2017	Case control	186	55.6% male	Data were collected from patients' endoscopy reports.	NBI
Masashi Kawamura	2021	Japan	Apr, 2017-Mar, 2019	Case control	380	62.1% male	Endoscopists who had experience of >5000 upper endoscopies in 10 Japanese facilities performed endoscopic procedures.	IEE
Jin Zheng	2022	China	Jan, 2018-Dec, 2021	Case control	162	57%male	Data were collected from patients' endoscopy reports.	LCI

LCI, linked color imaging; BLI, blue laser imaging; HR-NBI, high-resolution narrow-band imaging; NBI, narrow-band imaging; IEE, image-enhanced endoscopy.

TABLE 2 Assessment of risk of bias and applicability concern for all included diagnostic studies.

	Patient selection		Index test (EGGIM)		Reference standard (OLGIM)		Flow & timing
First author	Bias	Applicability	Bias	Applicability	Bias	Applicability	Bias
Guanpo Zhang	Low	Low	Low	Low	Low	Low	Low
Rui Castro	High	Low	Low	Low	High	Low	Low
Gianluca Esposito	Low	Low	Low	Low	Low	Low	Low
Pedro Pimentel Nunes	Low	Low	Low	Low	Low	Low	Low

EGGIM, endoscopic grading of gastric intestinal metaplasia; OLGIM, operative link of gastric intestinal metaplasia.

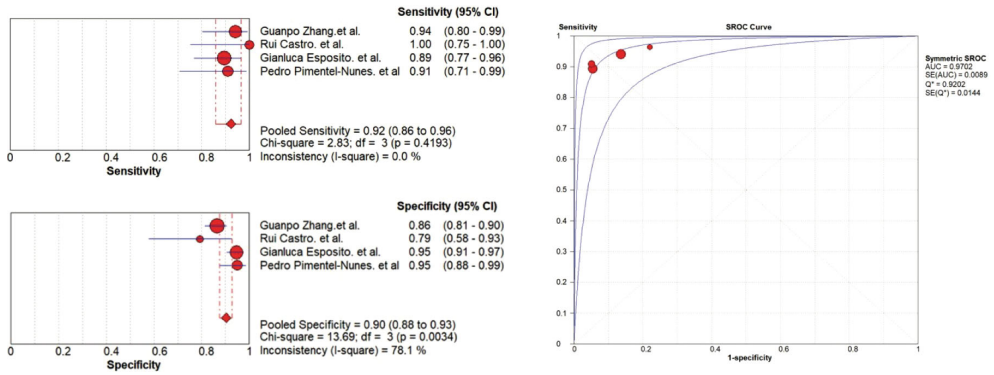

FIGURE 2
Diagnostic accuracy analysis of EGGIM(5-10) compared to OLGIM III/IV.

The results showed heterogeneity in the specificity(P=0.0034, I^2 =78.1%), between the studies, which means there are differences in the diagnosis of true negatives between studies. Rui Castro et al. (13) who compared BLI with OLGIM reported five false positives among 37 patients(13.51%), and Guanpo Zhang et al. (16) who used LCI reported 33 false positives among 277 patients(11.91%). However, two studies (8, 10) that compared NBI with OLGIM reported a lower false positives rate, 11 out of 250 (4.40%) and 4 out of 101 (3.96%) were false positives, respectively.

EGGIM for gastric cancer risk stratification

A high EGGIM score (5-10) has a significantly higher risk for GC compared with a low EGGIM score (0-4), with an odds ratio of 7.46 (95%CI 2.06-23.05; P=0.04, I^2 = 68%) (Figure 3).

Discussion

The OLGIM system based on histological examination to assess GC risk has been reported in the Kyoto global consensus (20). However, the clinical utility of OLGIM remains controversial especially in low-risk populations since it requires 5 biopsies. The frequency of OLGIM assessment remains low in daily clinical practice (21). The extent of mucosal lesions positively correlates with GC risk (22), and pathological assessment usually focuses on local areas of the stomach and fails to assess the whole stomach. Furthermore, endoscopic risk stratification tools, such as the Kimura-Takemoto classification, are highly correlated with pathological atrophy, and multi-point biopsies are not required (23). Therefore, endoscopic risk stratification tools play a significant role in gastric cancer risk stratification compared with histology-based risk assessment tools.

Our meta-analysis evaluated the effectiveness of EGGIM as a GC risk stratification tool. EGGIM was compared with the gold standard- the pathology-based OLGIM system. We found that EGGIM was in high concordance with OLGIM with an AUC of 0.9702, and patients with EGGIM (5-10 points) had a 7.46-fold higher risk of developing early GC than those with EGGIM (0-4 points). The EGGIM system as a tool for endoscopic GC risk stratification may be helpful for daily clinical practice.

Meta-analysis of the EGGIM system compared with OLGIM shows heterogeneity in specificity between different studies. The results suggest that there are differences in the number of false-positive cases in the various studies. The EGGIM system overestimated the GC risk for some patients with OLGIM stages 0-II. On the other hand, the EGGIM system has a high sensitivity with no apparent heterogeneity, indicating that EGGIM can

TABLE 3 Assessment of risk of bias and applicability concern for all included case-control studies.

First author	Is the case definition adequate	Representativeness of the case	Selection of control	Definition of controls	Comparability of cases and controls based on the design or analysis	Ascertainment of exposure	Same method of ascertainment for cases and controls	Non-response rate	Total score
Pedro Marcos	★	★	☆	★	★★	☆	★	☆	6
Masashi Kawamura	★	★	☆	★	★☆	★	★	☆	6
Jin Zheng	★	★	☆	★	★☆	★	★	☆	6

★ means the study in accordance with this entry; ☆ means the study failed to match this entry.

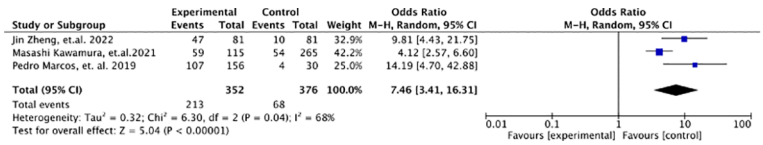

FIGURE 3
EGGIM(5-10) pooled analysis for early gastric cancer.

identify high-risk patients well. Therefore, EGGIM can identify the high-risk population with an acceptable rate of false positives, which can serve as the first step in risk stratification. An endoscopic-guided biopsy will improve the efficiency of GC screening and reduce the need for pathological examinations.

In addition to EGGIM, Kimura-Takemoto's endoscopic atrophy classification, which assesses the transition of the fundic-pyloric border (24), is widely used in GC risk stratification. It was consistent with the Operative link for gastritis assessment(OLGA) (25–27). Patients with Kimura-Takemoto endoscopic atrophy classification stages O2-O3 had a higher risk of gastric cancer HR=9.3 (95%CI 1.7-174, *P*=0.007) (28). Kimura-Takemoto's endoscopic atrophy classification assesses the border of atrophy, and EGGIM assesses the extent of intestinal metaplasia in five gastric sites. Both Kimura-Takemoto classification and EGGIM can predict GC risk, and the combination of the two may be able to improve the accuracy and consistency of GC risk stratification.

The Kyoto classification risk scoring system, which adds observations of intestinal metaplasia, Fhypertrophic fold enlargement, and nodularity to the Kimura-Takemoto system, is also widely used to assess GC risk (29, 30). The study by Masashi Kawamura et al. (19) found that OLGIM stage III/IV, high EGGIM score (5-10), and Kimura-Takemoto open type were risk factors for GC in multivariate analysis; however, the Kyoto classification risk scoring system combined with endoscopic features are not significant(*P*=0.315). The Kyoto classification risk scoring system based on white light endoscopy may result in a lower diagnostic power than IEE. Meanwhile, it incorporates multiple endoscopic features that may fail to provide new risk predictors. Further studies are recommended to explore the clinical utility of these endoscopic features. We hope these endoscopic and pathological risk assessment tools would be complementary to each other and optimally applied in practice.

There are some limitations of this meta-analysis. First, the number of included studies was small, with only 4 diagnostic studies and 3 case-control studies. Second, the specificity of EGGIM compared to OLGIM is heterogeneous, and there is a heterogeneity of EGGIM in predicting GC risk. Due to insufficient literature, subgroup analysis could not be performed for the operating physicians, the endoscopic techniques, etc. The EGGIM stage in one of the included case-control studies (9) was based on the reports, and there may be a significant bias in the evaluation of the EGGIM. Rui Castro's study (17) did not report the essential characteristics of the included patients and the endoscopist's experience, which reduced the study's reliability.

Conclusion

In summary, our meta-analysis is the first one to synthesize multiple studies to assess the effectiveness of EGGIM. The results showed that EGGIM was a reliable tool for gastric cancer risk stratification. Even though EGGIM carries a false-positive rate, it can still be complementary to pathological biopsy in risk stratification. In addition, with the development of endoscopic technology, endoscopic diagnosis of GC precancerous mucosa has shown great potential, and a unified diagnostic standard may be helpful to promote its application in daily practice. Finally, further prospective studies on endoscopic GC risk stratification systems such as EGGIM are needed to clarify their clinical utility.

Data availability statement

The original contributions presented in the study are included in the article/Supplementary Material. Further inquiries can be directed to the corresponding authors.

Author contributions

SF: Conceptualization, Methodology, Software, Validation, Formal analysis, Investigation, Data curation, Writing – original draft, Supervision. YF: Investigation, Writing. SD: Validation, Visualization. LW: Investigation, Data curation. XQ: Investigation, Data curation. XL: Investigation, Data curation. GS: Supervision, Project administration,. YY: Supervision, Project administration, Data curation. WW: Conceptualization, Methodology, Supervision, Project administration, Funding acquisition. All authors contributed to the article and approved the submitted version.

Funding

National Traditional Chinese Medicine Inheritance and Innovation Team Project (No. ZYYCXTD-C-202210). Scientific and technological innovation project of China Academy of Chinese Medical Science (No. CI2021A01008 and CI2021A01820). Science Research Program for TCM Industry (No. 201507001-09).

Conflict of interest

The authors declare that the research was conducted in the absence of any commercial or financial relationships that could be construed as a potential conflict of interest.

Publisher's note

All claims expressed in this article are solely those of the authors and do not necessarily represent those of their affiliated organizations, or those of the publisher, the editors and the reviewers. Any product that may be evaluated in this article, or claim that may be made by its manufacturer, is not guaranteed or endorsed by the publisher.

Supplementary material

The Supplementary Material for this article can be found online at: https://www.frontiersin.org/articles/10.3389/fonc.2022.1018248/full#supplementary-material

References

1. Sung H, Ferlay J, Siegel RL, Laversanne M, Soerjomataram I, Jemal A, et al. Global cancer statistics 2020: GLOBOCAN estimates of incidence and mortality worldwide for 36 cancers in 185 countries. *CA: A Cancer J Clin* (2021) 71(3):209–49. doi: 10.3322/caac.21660

2. de Martel C, Georges D, Bray F, Ferlay J, Clifford GM. Global burden of cancer attributable to infections in 2018: a worldwide incidence analysis. *Lancet Global Health* (2020) 8(2):e180–90. doi: 10.1016/S2214-109X(19)30488-7

3. Lauren P. The two histological main types of gastric carcinoma: diffuse and so-called intestinal-type carcinoma. An attempt at a histo-clinical classification. *Acta pathol microbiol Scandinavica* (1965) 64:31–49. doi: 10.1111/apm.1965.64.1.31

4. Ajani JA, Lee J, Sano T, Janjigian YY, Fan D, Song S. Gastric adenocarcinoma. *Nat Rev Dis primers* (2017) 3:17036. doi: 10.1038/nrdp.2017.36

5. Piazuelo MB, Correa P. Gastric cáncer: Overview. *Colombia Med (Cali Colombia)* (2013) 44(3):192–201.

6. Lee JWJ, Zhu F, Srivastava S, Tsao SK, Khor C, Ho KY, et al. Severity of gastric intestinal metaplasia predicts the risk of gastric cancer: a prospective multicentre cohort study (GCEP). *Gut* (2022) 71(5):854–63. doi: 10.1136/gutjnl-2021-324057

7. Yue H, Shan L, Bin L. The significance of OLGA and OLGIM staging systems in the risk assessment of gastric cancer: a systematic review and meta-analysis. *Gastric cancer : Off J Int Gastric Cancer Assoc Japanese Gastric Cancer Assoc* (2018) 21(4):579–87. doi: 10.1007/s10120-018-0812-3

8. Pimentel-Nunes P, Libânio D, Lage J, Abrantes D, Coimbra M, Esposito G, et al. A multicenter prospective study of the real-time use of narrow-band imaging in the diagnosis of premalignant gastric conditions and lesions. *Endoscopy* (2016) 48(8):723–30. doi: 10.1055/s-0042-108435

9. Marcos P, Brito-Gonçalves G, Libânio D, Pita I, Castro R, Sá I, et al. Endoscopic grading of gastric intestinal metaplasia on risk assessment for early gastric neoplasia: can we replace histology assessment also in the West? *Gut* (2020) 69(10):1762–8. doi: 10.1136/gutjnl-2019-320091

10. Esposito G, Pimentel-Nunes P, Angeletti S, Castro R, Libânio D, Galli G, et al. Endoscopic grading of gastric intestinal metaplasia (EGGIM): a multicenter validation study. *Endoscopy* (2019) 51(6):515–21. doi: 10.1055/a-0808-3186

11. Quach DT, Hiyama T, Gotoda T. Identifying high-risk individuals for gastric cancer surveillance from western and eastern perspectives: Lessons to learn and possibility to develop an integrated approach for daily practice. *World J Gastroenterol* (2019) 25(27):3546–62. doi: 10.3748/wjg.v25.i27.3546

12. East JE, Vleugels JL, Roelandt P, Bhandari P, Bisschops R, Dekker E, et al. Advanced endoscopic imaging: European society of gastrointestinal endoscopy (ESGE) technology review. *Endoscopy* (2016) 48(11):1029–45. doi: 10.1055/s-0042-118087

13. Moher D, Liberati A, Tetzlaff J, Altman DG, PRISMA Group. Preferred reporting items for systematic reviews and meta-analyses: the PRISMA statement. *PloS Med* (2009) 6(7):e1000097. doi: 10.1371/journal.pmed.1000097

14. Whiting PF, Rutjes AWS, Westwood ME, Mallett S, Deeks JJ, Reitsma JB, et al. QUADAS-2: a revised tool for the quality assessment of diagnostic accuracy studies. *Ann Internal Med* (2011) 155(8):529–36. doi: 10.7326/0003-4819-155-8-201110180-00009

15. Stang A. Critical evaluation of the Newcastle-Ottawa scale for the assessment of the quality of nonrandomized studies in meta-analyses. *Eur J Epidemiol* (2010) 25(9):603–5. doi: 10.1007/s10654-010-9491-z

16. Zhang G, Zheng J, Zheng L, Yu S, Jiang C, Lin W, et al. Gastric intestinal metaplasia assessment between linked color imaging based on endoscopy and pathology. *Scandinavian J Gastroenterol* (2021) 56(1):103–10. doi: 10.1080/00365521.2020.1849385

17. Castro R, Rodriguez M, Libânio D, Esposito G, Pita I, Patita M. Reliability and accuracy of blue light imaging for staging of intestinal metaplasia in the stomach. *Scand J Gastroenterol* (2019) 54(11):1301–05. doi: 10.1055/s-0039-1681615

18. Zheng J, Zhang G, Gao C, Xu G, Lin W, Jiang C, et al. Linked color imaging-based endoscopic grading of gastric intestinal metaplasia and histological gastritis staging in the assessment of gastric cancer risk. *Scandinavian J Gastroenterol* (2022) 14:1–7. doi: 10.1080/00365521.2022.2085061

19. Kawamura M, Uedo N, Koike T, Kanesaka T, Hatta W, Ogata Y, et al. Kyoto Classification risk scoring system and endoscopic grading of gastric intestinal metaplasia for gastric cancer: Multicenter observation study in Japan. *Digest Endosc* (2022) 34(3):508–16. doi: 10.1111/den.14114

20. Sugano K, Tack J, Kuipers EJ, Graham DY, El-Omar EM, Miura S, et al. Kyoto Global consensus report on helicobacter pylori gastritis. *Gut* (2015) 64 (9):1353–67. doi: 10.1136/gutjnl-2015-309252

21. Shah SC, Piazuelo MB, Kuipers EJ, Li D. AGA clinical practice update on the diagnosis and management of atrophic gastritis: Expert review. *Gastroenterology* (2021) 161(4):1325–1332.e7. doi: 10.1053/j.gastro.2021.06.078

22. Gawron AJ, Shah SC, Altayar O, Davitkov P, Morgan D, Turner K, et al. AGA technical review on gastric intestinal metaplasia-natural history and clinical outcomes. *Gastroenterology* (2020) Vol. 158:705–731.e5. doi: 10.1053/j.gastro.2019.12.001

23. Quach DT, Hiyama T, Gotoda T. Do subjects with mild or moderate atrophic gastritis or intestinal metaplasia confined to the antrum benefit from gastric cancer surveillance? *Gut England* (2020) Vol. 69:968–9. doi: 10.1136/gutjnl-2019-318720

24. Kimura K. Chronological transition of the fundic-pyloric border determined by stepwise biopsy of the lesser and greater curvatures of the stomach. *Gastroenterology* (1972) 63(4):584–92. doi: 10.1016/S0016-5085(19)33241-X

25. Ebigbo A, Marienhagen J, Messmann H. Regular arrangement of collecting venules and the kimura-takemoto classification for the endoscopic diagnosis of helicobacter pylori infection: Evaluation in a Western setting. *Digest endoscopy : Off J Japan Gastroenterol Endosc Soc* (2021) 33(4):587–91. doi: 10.1111/den.13808

26. Kim SJ, Choi CW, Kang DH, Kim HW, Park SB. Comparison of biannual and annual endoscopic gastric cancer surveillance after endoscopic resection. *Surg endosc* (2022) 36(3):1806–13. doi: 10.1007/s00464-021-08460-8

27. Maric L, Castaneda D, Singh H, Bejarano P, Jimenez Cantisano B, Castro FJ, et al. Kimura-takemoto classification: A tool to predict gastric intestinal metaplasia progression to advanced gastric neoplasia. *Digest Dis Sci* (2022) 67(8):4092–99. doi: 10.1007/s10620-021-07212-x

28. Shichijo S, Hirata Y, Niikura R, Hayakawa Y, Yamada A, Ushiku T, et al. Histologic intestinal metaplasia and endoscopic atrophy are predictors of gastric cancer development after helicobacter pylori eradication. *Gastrointest endosc* (2016) 84(4):618–24. doi: 10.1016/j.gie.2016.03.791

29. Toyoshima O, Nishizawa T, Yoshida S, Sakaguchi Y, Nakai Y, Watanabe H, et al. Endoscopy-based Kyoto classification score of gastritis related to pathological topography of neutrophil activity. *World J gastroenterol* (2020) 26(34):5146–55. doi: 10.3748/wjg.v26.i34.5146

30. Toyoshima O, Nishizawa T, Koike K. Endoscopic Kyoto classification of helicobacter pylori infection and gastric cancer risk diagnosis. *World J gastroenterol* (2020) 26(5):466–77. doi: 10.3748/wjg.v26.i5.466

frontiers | Frontiers in Oncology

TYPE Methods
PUBLISHED 09 November 2022
DOI 10.3389/fonc.2022.1030039

Check for updates

OPEN ACCESS

EDITED BY
Zhendong Jin,
Second Military Medical University, China

REVIEWED BY
Andee Dzulkarnaen Zakaria,
Universiti Sains Malaysia, Malaysia
Farooq Rashid,
Guangxi Veterinary Research Institute, China

*CORRESPONDENCE
Bingrong Liu
fccliubr@zzu.edu.cn

†These authors have contributed equally to this work and share first authorship

This article was submitted to Gastrointestinal Cancers: Gastric and Esophageal Cancers, a section of the journal Frontiers in Oncology

SPECIALTY SECTION
RECEIVED 28 August 2022
ACCEPTED 24 October 2022
PUBLISHED 09 November 2022

CITATION
Shi Z, Huang X, Li K, Tu Q, Liu D, Zhao L, Yang H, Li D, Zhao Y, Zhang J, Li M and Liu B (2022) Endoscopic resection of upper gastrointestinal lymphangioma: A single-center experience.
Front. Oncol. 12:1030039.
doi: 10.3389/fonc.2022.1030039

COPYRIGHT
© 2022 Shi, Huang, Li, Tu, Liu, Zhao, Yang, Li, Zhao, Zhang, Li and Liu. This is an open-access article distributed under the terms of the Creative Commons Attribution License (CC BY). The use, distribution or reproduction in other forums is permitted, provided the original author(s) and the copyright owner(s) are credited and that the original publication in this journal is cited, in accordance with accepted academic practice. No use, distribution or reproduction is permitted which does not comply with these terms.

Endoscopic resection of upper gastrointestinal lymphangioma: A single-center experience

Ziyu Shi[1†], Xue Huang[2†], Keliang Li[1], Qiuyue Tu[1], Dan Liu[1], Lixia Zhao[1], Huiyu Yang[1], Deliang Li[1], Yue Zhao[1], Jiyu Zhang[1], Muhan Li[1] and Bingrong Liu[1*]

[1]Department of Gastroenterology, The First Affiliated Hospital of Zhengzhou University, Zhengzhou, China, [2]Academy of Medical Science, Zhengzhou University, Zhengzhou, China

Objective: Lymphagioma, which in most cases as benign tumors, occurs in head, neck, axilla, and mediastinum. Lymphangioma is exceedingly rare in the upper gastrointestinal tract including esophagus, stomach, and duodenum. However, the clinical characteristics, natural history, and recurrence rate after endoscopic resection remain unclear. This study aims to evaluate the characteristic findings and assess the efficacy of endoscopic techniques in the management of this disease.

Methods: In this systematic retrospective analysis, we evaluated all 24 cases of upper gastrointestinal lymphangioma resected by endoscopic mucosal resection (EMR) or endoscopic submucosal dissection (ESD) and diagnosed by histopathology at our hospital from January 2012 to May 2021. We analyzed the results of endoscopy, endoscopic ultrasonography (EUS), CT, histologic examination, and follow-up assessments.

Results: 9 male and 15 female patients with esophageal lymphangioma were enrolled in this study, with a mean age of 54.17 ± 11.60 years (range 30-71 years). The lesions' size varied from 2.20 to 40.10 mm, with the median size of 7.83 mm. All patients were evaluated preoperatively, whose endoscopic appearance typically appears as dilated lymphatic channels beneath the surface epithelium of the protrude mucosal or sub-mucosal lesion. Endoscopic ultrasonography revealed the presence of a honeycomb-like or grid-like mass with a heterogeneous echo pattern, and a clear boundary between the lesion and the muscularis propria layer may be helpful for the primary diagnosis of this disease. 22 patients underwent EMR and 2 patient were treated with ESD. Histologic examination revealed that the lesions contained many dilated lymphatic vessels, which confirmed the initial diagnosis of lymphangioma in all patients. No major adverse events were found during the operation or a median follow-up of 43 months (range 13–92).

Conclusions: Endoscopic ultrasonography has important clinical value for the primary diagnosis of lymphangioma in the upper gastrointestinal tract. This

study also suggests that endoscopic resection should be considered as a more minimally invasive, safe, feasible, and effective therapeutic option comparing to laparoscopic surgery.

KEYWORDS

endoscopic ultrasonography (EUS), en bloc resection, clinical outcomes, vascular tumor, upper gastrointestinal lymphangioma

Introduction

Described for the first time by Koch in 1913, lymphangiomas are benign congenital malformations of the lymphatic system and consist of dilated lymphatic vessels (1). As a type of tumor mostly appears as submucosal lesion, the incidence of lymphangiomas is 1.2–2.8%, and those tumors occur most frequently in head, neck, axilla, and mediastinum (1, 2). Lymphangiomas can be found at any age of life, of which approximately 50% are present at birth and 90% are diagnosed before the age of 2, and both genders are equally affected (3, 4). Within the gastrointestinal tract, the small bowel mesentery is the most common site involved, followed by retroperitoneal sites (5, 6). Lymphangiomas exceedingly rarely involve the upper gastrointestinal tract including esophagus, stomach, and duodenum (7, 8). These tumors are usually asymptomatic and found incidentally because the clinical presentation is highly polymorphic and nonspecific, contributing little to establish the diagnosis (9, 10). As a minimally invasive technique, endoscopic resection has come to play a pivotal role in the management of upper gastrointestinal lymphangioma (UGL) (11, 12). However, studies involving a mass of UGLs are lacking, and many questions need to be answered regarding the clinical characteristics, natural history and recurrence rate after resection (13). In this systematic retrospective analysis, we evaluated all cases of UGL diagnosed and resected endoscopically at our hospital from January 2012 to May 2021. We analyzed the results of endoscopy, endoscopic ultrasonography (EUS), computed tomography (CT), histologic examination, and follow-up assessments to clarify the characteristic findings and assess the efficacy of endoscopic techniques in the management of this disease as well as its related complications, diagnostic difficulties, and therapeutic problems.

Materials and equipment

We report a systematic retrospective study from January 2012 to May 2021 concerning 24 patients who underwent EMR or ESD procedure for UGL in a tertiary hospital (The First Affiliated Hospital of Zhengzhou University, China). This retrospective study was approved by the Ethics Committee of this hospital.

The preparation, procedure, possible costs, and potential complications were explained to the patients or their family members in advance and all signed informed consent were provided by the participants. Before endoscopic treatment under general anesthesia, each patient had been evaluated by CT scans reviewed by two radiologists with more than 5-year experience. In addition, EUS was performed preoperatively in all 24 cases and each was reviewed by an experienced endoscopist who had performed more than 100 EUS examinations. Information about age, gender, clinical manifestation, CT scan results, lesion size, location, origin layer based on EUS, and complications was recorded.

The main endoscopic equipment and accessories include: Endoscopes (GIF-QF260J; Olympus Medical Science, Japan), Hook knife (KD-620LR; Olympus Medical Science, Tokyo, Japan), Insulation-tip knife (KD-611L; Olympus Medical Science, Tokyo, Japan), Snare with maximum insertion diameter of 1.8 mm (SD-221L-25; Olympus Medical Science, Japan), and Hemoclips (HXROCC-D-26-195-C, MICRO-TECH, China; HX-610-090 L, Olympus Medical Science, Tokyo, Japan).

Methods

Procedures

All patients were hospitalized and received general anesthesia during the operation. After the evaluation for patients, EMR or ESD was performed at the discretion of the endoscopist who will consider the preoperative examinations and intraoperative results. If the tumor was small and originated from the mucosal layer, the EMR was chosen. On the contrary, for large lymphangiomas originated from the submucosal layer without involving the muscle layer, the ESD was the superior option.

EMR procedure En bloc resection was defined as the tumor was excised in a whole piece, whose capsule was intact. First, a

solution of adrenaline and saline was injected into the submucosal space under the lesion with the injection needle to prevent complications such as perforation and bleeding. Then a snare was inserted through the main channel to capture and fix the lesion which was then removed using electric coagulation. Finally, hemostasis was obtained with endoscopic electric coagulation.

ESD procedure First, circumferential marking was made using an insulated-tip knife at a distance of 0.5 to 1.0 cm from the lesion border. Then, a solution of adrenaline and saline was injected to lift the submucosa to enhance surgical safety as well as prevent further complications. After a circumferential mucosal incision was performed by endoscopic hook knife, the transparent cap assisted in stripping the lesion. Finally, the tumor was completely and uneventfully en bloc resected by foreign forceps and then hemostasis was obtained.

Histopathological assessment

For all patients after the endoscopic resection procedure was performed, the specimens were stretched smoothly by pins on a corkboard and fixed with 10% formalin for later pathological examination. Every specimen was diagnosed by 2 expert gastrointestinal pathologists, providing a final confirmation.

Follow-up

The evidence of postoperative complications including fever, dyspnea, hematemesis, and chest or abdominal pain was recorded. Each of the patients was discharged successfully and they were followed up by endoscopy and/or detailed telephone interviews. The interview's outline was clinical symptoms, outcomes of treatment, and tests performed at their local hospitals.

Statistical analysis

The statistical analyses were performed using IBM SPSS Statistics v23.0 (Statistical Package for the Social Sciences, Inc, Chicago, IL, United States). The mean ± SD was done as quantitative variables and percentage (%) as qualitative variables.

Results

Baseline characteristics

The data from the clinical assessment, treatment, and follow-up were analyzed retrospectively. From January 2012 to May 2021, more than 100 patients were diagnosed with Upper Gastrointestinal Lymphangioma by histopathological examination, 24 patients of whom underwent EMR or ESD procedures for UGL in the First Affiliated Hospital of Zhengzhou University. The average age at diagnosis was 54.17 ± 11.60 years (range 30-71 years). There were 9 (37.50%) males and 15 (62.50%) females with a sex ratio equal to 0.6. Clinically, the presentation was highly polymorphic. Most patients presented with multiple symptoms including abdominal pain (n = 9), abdominal discomfort (n = 5), regurgitation (n = 5), bloating (n = 3), foreign body sensation (n = 2). The main symptom for esophageal lymphangioma was abdominal discomfort (n = 4), while that for duodenal and gastric lymphangioma was abdominal pain (n = 6). Lymphangiectasia was histologically confirmed in one patient seven months before the endoscopic resection of the lymphangioma. The baseline characteristics of the 24 patients are shown in Table 1.

Imaging features

The UGL was unique in 23 patients (95.80%), whereas 1 patient had more than one UGL. 25 lesions found in 24 patients were diagnosed by the endoscope and/or endoscopic ultrasonography before operation (Figure 1). Endoscopic appearance typically appears as dilated lymphatic channels beneath the surface epithelium of the protrude mucosal or sub-mucosal lesion (Figures 2, 3, 4). As related to the ultrasound features of the lesions, their size ranged from 2.2 to 40 mm with a median size of 7.8 mm. The most common site was esophagus (n=14; 58.33%) and duodenum (n=9, 37.50%), followed by stomach (n=1, 4.20%). As for esophageal lesions, they were located 17 to 35 cm distal to the incisor. At pre-operative EUS, 5 (20.83%) originated from the mucosal layer, 13 (54.17%) from the submucosal layer, and 6 (25.00%) from the muscular mucosa layer. Of the 24 patients who underwent EUS, 14 (58.33%) patients showed hypoechogenicity (Figure 5); 4 (16.67%) patients showed higher echo (Figure 6), 5 (20.83%) showed slightly mixed echogenicity (Figure 7), and 1 (4.17%) showed equal echogenicity. Of the 20 patients who underwent CT scans, lesions that presented as uneven density were shown in different locations in 9 (37.5%) patients, whereas CT was normal in 11 (45.8%) patients. Imaging data are shown in Table 2.

Treatment and pathological manifestations

All lesions were successfully resected endoscopically including 23 (91.67%) by endoscopic mucosal resection (EMR) and 2 (8.33%) by endoscopic submucosal dissection (ESD) (Table 2). Histologic examination revealed that the lesions contained many irregularly dilated lymphatic vessels, lined with flattened endothelial cells without atypia, and with

TABLE 1 Baseline characteristics.

Case	Gender	Age	Site	Size (mm)	Chief Complains	Endoscopic Appearance	Treatment	Follow-up time (M)
1	Female	58	Esophagus	5.7	Bloating	Submucosal mass	EMR	92
2	Female	47	Esophagus	10	Bloating	Nodule	EMR	73
3	Female	49	Esophagus	5.3	Abdominal pain	Mucosal prominence	EMR	67
4	Female	62	Esophagus	5	Abdominal pain	Protuberance	EMR	58
5	Female	41	Esophagus	3.9	Abdominal discomfort	Hemispherical protuberance	EMR	56
6	Male	62	Esophagus	6	Regurgitation	Mucosal prominence	EMR	48
7	Male	71	Esophagus	6.7	Abdominal pain	Submucosal mass	EMR	46
8	Female	61	Esophagus	6.2	Abdominal discomfort	Protuberance	EMR	45
9	Female	53	Esophagus	2.2	Abdominal discomfort	Submucosal mass	EMR	44
10	Male	65	Esophagus	5	Foreign body sensation	Submucosal mass	EMR	40
11	Male	61	Esophagus	7	Regurgitation	Hemispherical protuberance	EMR	34
12	Male	30	Esophagus	5.1	Abdominal discomfort	Submucosal mass	EMR	33
13	Male	56	Esophagus	4.8	Regurgitation	Nodule	EMR	29
14	Female	42	Esophagus	40	Foreign body sensation	Submucosal mass	ESD	26
15	Male	69	Duodenum	6.8	Abdominal pain	Nodule	EMR	55
16	Female	55	Duodenum	6.1	Abdominal pain	White protuberance	EMR	52
17	Male	60	Duodenum	3	Regurgitation	White diminutive nodule	EMR	51
18	Female	64	Duodenum	3	Regurgitation	Yellowish nodule with white spots	EMR	45
19	Female	69	Duodenum	6	Abdominal pain	Submucosal mass	EMR	33
20	Female	31	Duodenum	8	Abdominal pain	Yellowish submucosal mass	EMR	32
21	Female	33	Duodenum	5	Abdominal discomfort	Mucosal prominence with white spots	EMR	26
22	Female	48	Duodenum	10	Abdominal pain	Submucosal mass with white spots	EMR	20
23	Female	58	Duodenum	22.9	Bloating	Protuberance with white spots	ESD	13
24	Male	55	Stomach	4.1	Abdominal pain	Nodule	EMR	16

abundant lymphoid tissue. All those typical findings confirmed the initial diagnosis of lymphangioma in all patients. During and after operation, adverse events occurred in 3 (1 with active gastrointestinal bleeding during the operation and 2 with high fever after wards). All patients recovered.

Follow–up and recurrence

After the follow-up period ranged from 13 to 92 months (median 43 months), 1 patient was lost to follow-up because of the long period, and 23 survived to whom the last visit was used as the endpoint of follow-up. They all received gastroduodenoscopy and all patients were in good health, and neither recurrence nor death was observed.

Discussion

As most benign congenital malformations, lymphangiomas most commonly occur in childhood in head, neck, axilla, and mediastinum (9). Only a minority of cases are observed in adult patients and are diagnostically challenging. In addition, lymphangiomas have been extremely rarely reported in the upper gastrointestinal tract, including the esophagus, stomach, and duodenum (7, 8). Esophageal lymphangioma was first reported by Watson-Williams in 1934, and Brady and Milligan were the first persons to diagnose it by endoscopy (14). Possible etiologies are malformation of lymphatic vessels and the obstruction of lymphatic flow by inflammation or injury (15). And the acquired failure of lymphatic channels is more likely associated with the adult manifestations, possibly related to inflammatory conditions or physical trauma such as those result from surgical or radiation therapies (16). While the congenital and acquired causes are not mutually exclusive, a congenital impairment in communication between mesenchymal slits and the venous system may put patients at greater risk of drainage blocking in response to trauma (16, 17). Except for lymphangiectasia was histologically confirmed in one patient seven months before the endoscopic resection of the lymphangioma, no precipitating etiology could be identified in the current adult cases described in our research. In addition, there was no obvious connection between UGL and family tumor history in our study.

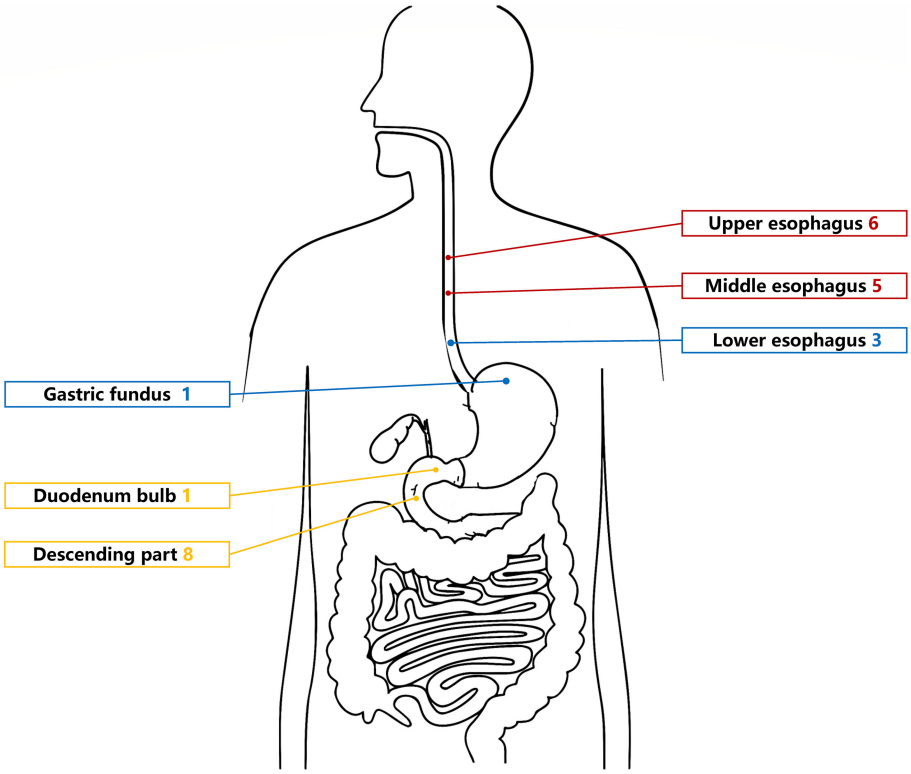

FIGURE 1
Site of lymphangiomas in the upper gastrointestinal tract.

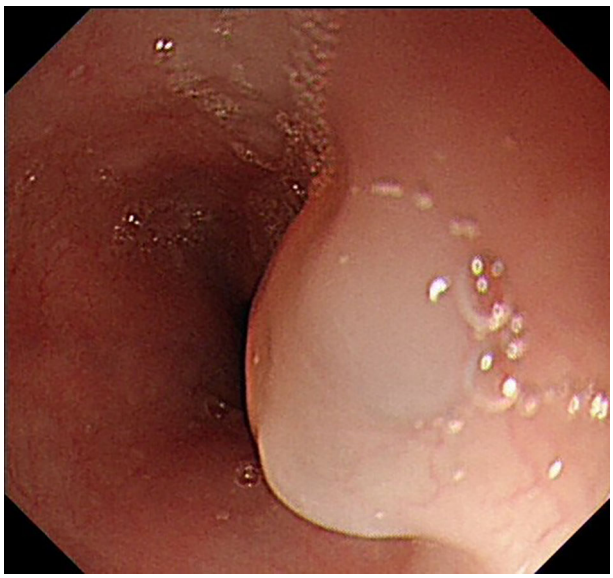

FIGURE 2
Endoscopic appearance of lymphangioma in the esophagus.

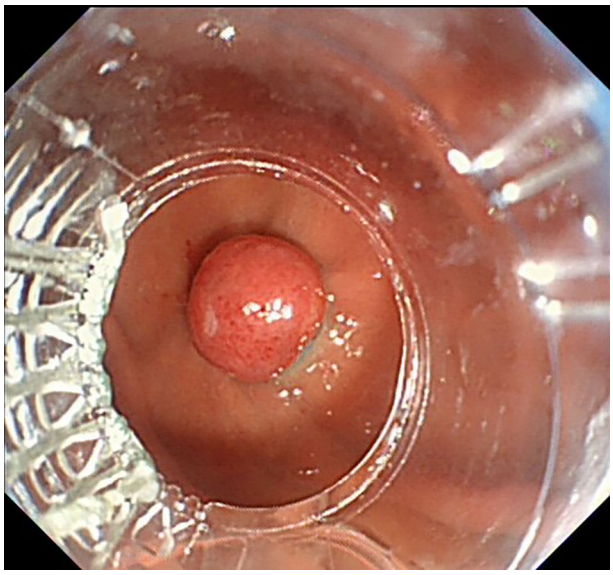

FIGURE 3
Nodular lymphangioma in the gastric fundus.

To date, only 75 UGLs have been described in English and Chinese language publications since 1934 based on our review, including 31 cases of esophageal lymphangioma, 27 cases of gastric lymphangioma, and 17 cases of duodenal lymphangioma (5, 18–21). Considering almost half of those cases reported later than 2000, it suggests increased use of upper endoscopy and rising awareness of endoscopists on upper gastrointestinal lesions (18, 19, 21). To the best of our knowledge, the present study including 24 patients is the largest scale of research referring to this rare clinical entity in the upper gastrointestinal tract. Cheng et al. (18) found that the esophageal tumors most frequently locate in the distal esophagus, while in Chinese patients, esophageal lymphangioma showed a predilection of upper- and middle-esophagus location. The former study has been confirmed in our research consisting of 6 patients with upper-esophageal

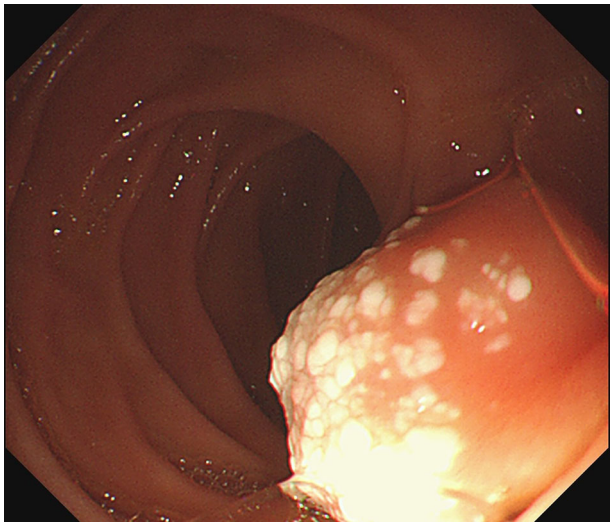

FIGURE 4
Mucosal prominence with white spots was the endoscopic appearance of the duodenal lesion.

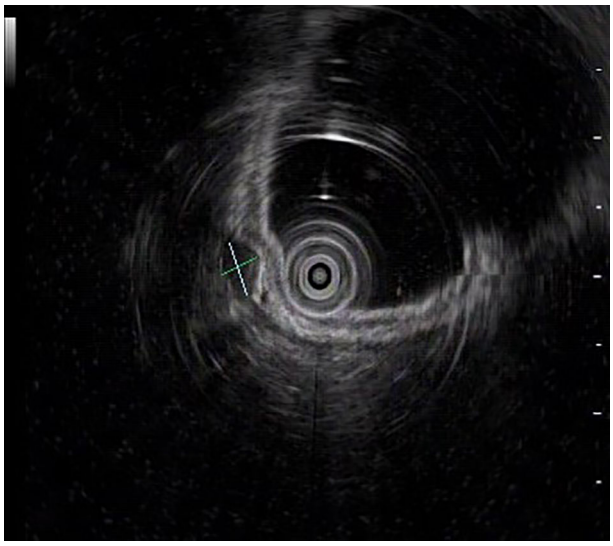

FIGURE 5
EUS image shows the gastric lesion with hypoechogenicity.

lesions and 5 patients with middle-esophageal lesions in all 14 Chinese patients with esophageal lymphangiomas. For duodenal lymphangiomas, the most common site was the duodenum descending part (21), which was also shown in our study. Compared to other gastric parts, previous studies reported that the most common location was the gastric body and antrum (19, 22, 23). Some authors have suggested that it is slightly more common in males than in females compared to our study, but no sex predominance has been confirmed until now (5).

The clinical presentation of these lesions depends on their size and location, and symptoms were diverse regardless of the age of presentation and sites. As most of these UGLs were detected incidentally, previous studies also reported that UGLs were associated more frequently (45%) with non-specific signs and symptoms such as vomiting, dyspepsia, abdominal pain, or

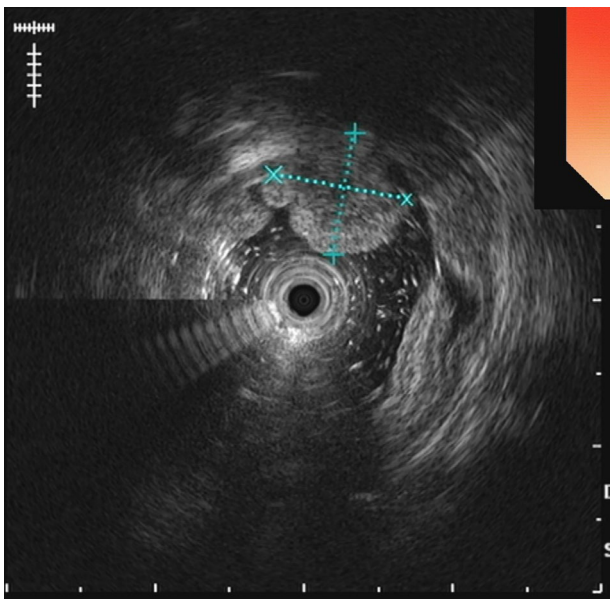

FIGURE 6
EUS examination demonstrates duodenal lymphangioma with hyperechogenicity.

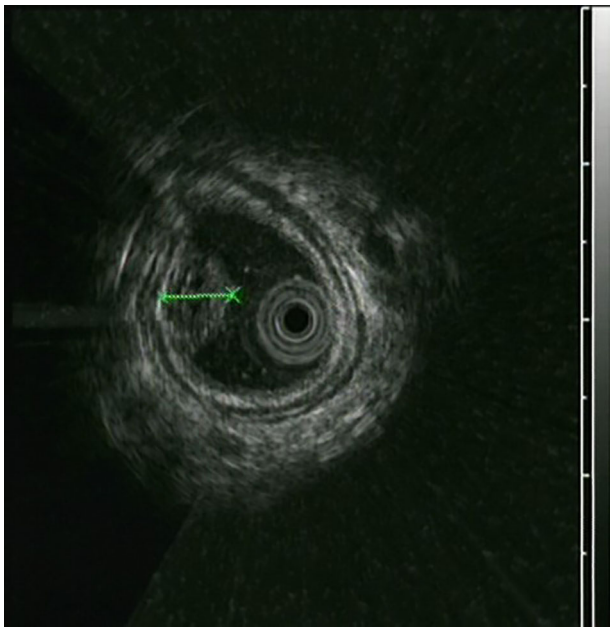

FIGURE 7
The esophageal lymphangioma was characterized by a heterogeneous echo.

were incidental findings (24, 25). And these non-specific signs and symptoms were consistent with our results.

An accurate preoperative diagnosis of UGLs, especially in an adult patient is uncommon owing to its rarity and diverse clinical and radiological features (16, 18). The imaging examination such as computed tomography seems not very helpful in the diagnosis of UGLs. In recent years, with the wide application of EUS which could provide valuable information, EUS became one of the most important diagnostic modalities for vascular tumors arising from the gastrointestinal tract (11, 24). However, the EUS features of gastric lymphangioma are not well demonstrated, possibly owing to its rarity (26). In endoscopy, most UGLs are recognized as polyps, and EUS is used to confirm the size and origin of the lesion (27). The classical characteristics of UGLs under EUS manifest a honeycomb- or grid-like multi-microcystic echo pattern and the lesion may involve lamina propria and submucosal layer. Sometimes, the echo pattern varies according to the size of dilated lymphatic vessels (2, 7, 18). In our experience, endoscopic appearance typically appears as dilated lymphatic channels beneath the surface epithelium of the protrude mucosal or sub-mucosal lesion. We find EUS an excellent initial diagnostic tool, and the presence of a honeycomb-like or grid-like mass with a heterogeneous echo pattern and a clear boundary between the lesion and the muscularis propria layer could be helpful for the primary diagnosis of UGL. As a result, EUS is recommended to all patients with UGLs before final endoscopic or surgery resection.

According to the previous research, complete en bloc resections usually contribute to excellent outcomes and prognoses for patients (28, 29). Many studies have illustrated that endoscopic resection is suitable for smaller lymphangiomas, while laparoscopic surgery is the recommended management for larger tumor involving the muscularis propria or the lesion is suspected malignant (11, 20, 25). In our study, all UGLs were successfully resected endoscopically including 22 (91.67%) by EMR and 2 (8.33%) by ESD. In addition to adverse events occurred in 3 patients who finally recovered, there were no other cases of recurrence during the follow-up period. As a truly minimally invasive technique, endoscopic treatment preserves the integrity of the anatomy and the original function of the organ (30). Hence, we recommend endoscopic resection both for yielding a final histological diagnosis and to prevent them from growing too large for endoscopic management.

It is extremely challenging for the diagnosis of relatively small gastrointestinal lymphangiomas, and histological examination is essential for a definitive diagnosis (26).Margaret et al. reported that it was hard to distinguish lymphangioma because of the histologic overlap with lymphangiectasia of the gastrointestinal mucosa (31). Compared with lymphangiectasia, he demonstrated the most reliable histologic features of lymphangioma as the presence of smooth muscle surrounding the lymphatic spaces and complete circumferential lining of spaces by endothelial-type cells (31, 32). Other types of vascular tumors include haemangiolymphangioma and haemangioma (33). Haemangiolymphangiomas are masses with mucosal and submucosal proliferations of capillary-type

TABLE 2 Endoscopic characteristics.

Patients	N (%)
Number of lesions	25
Single	23 (95.83%)
Multiple	1 (4.17%)
Locations	
Esophagus	14 (58.33%)
Upper esophagus	6 (25.00%)
Middle esophagus	5 (20.83%)
Lower esophagus	3 (12.50%)
Duodenum	9(37.50%)
Duodenum bulb	1 (4.17%)
duodenum descending part	8 (33.33%)
Stomach	1 (4.17%)
Size of lesions mean±SD(range)/mm	7.83±7.76 (2.20-40.10)
≤5mm	9 (37.50%)
>5,≤10mm	13 (54.16%)
>10mm	2 (8.33%)
Origin based on preoperative EUS	
Mucosa	5 (20.83%)
Submucous	13 (54.17%)
Muscularis mucosa	6 (25.00%)
Echogenicity based on preoperative EUS	
Hypo	14(58.33%)
Hyper	4 (16.67%)
Equal	1 (4.17%)
Mixed	5 (20.83%)
CT scan	
Yes	9 (37.50%)
No	11 (45.83%)
Unexamined	4 (16.67%)
Endoscopic treatment	
EMR	22 (91.67%)
ESD	2 (8.33%)

blood vessels, and of lymphatic-type vessels. And the cavity contained red blood cells or lymphatic fluid (34). While haemangiomas consist of clustered vascular hyperplasia in the submucosa, lumen irregularity, partial dilation (12). Other studies concluded that the typical features of lymphangiomas are the presence of alternating lymphoid tissue, lymphatic space, and chylous or serous fluid within an irregularly dilated lymphatic channel (16, 20, 25). The histological analysis of the resected mass from our patient provided a clear result for this differential diagnosis that the lesions contained many irregularly dilated lymphatic vessels, lined with flattened endothelial cells without atypia, and with abundant lymphoid tissue.

In conclusion, there were no typical signs of UGL for its clinical manifestations vary in both location and size. EUS has important clinical value for the primary diagnosis lymphangioma in the upper gastrointestinal tract. Because of the endoscopic resection's low technical complexity and complications for managements of patients with UGLs, this study suggests that this method should be considered as a minimally invasive, safe, feasible, and effective therapeutic option comparing to laparoscopic surgeries. Further studies are needed to confirm our findings.

Data availability statement

The raw data supporting the conclusions of this article will be made available by the authors, without undue reservation.

Ethics statement

The studies involving human participants were reviewed and approved by The Ethics Committee of The First Affiliated Hospital of Zhengzhou University. The patients/participants provided their written informed consent to participate in this study.

Author contributions

ZS, KL, DL, BL: Guarantors of the integrity of the entire study. BL, ZS, XH and QT: Study concepts. ZS, QT and ML: Study design. HY, JZ and YZ: Literature research. ZS, QT and KL: Data acquisition. QT and ML: Data analysis and statistical analysis. ZS, XH and KL: Manuscript preparation. DLL and JZ: Manuscript editing. BL and DL: Manuscript review. All authors contributed to the article and approved the submitted version.

Funding

This research was supported by the Key R&D Program of Henan Province (No. 222102310038).

Conflict of interest

The authors declare that the research was conducted in the absence of any commercial or financial relationships that could be construed as a potential conflict of interest.

Publisher's note

All claims expressed in this article are solely those of the authors and do not necessarily represent those of their affiliated organizations, or those of the publisher, the editors and the reviewers. Any product that may be evaluated in this article, or claim that may be made by its manufacturer, is not guaranteed or endorsed by the publisher.

References

1. Zhou Q, Zheng JW, Mai HM, Luo QF, Fan XD, Su LX, et al. Treatment guidelines of lymphatic malformations of the head and neck. *Oral Oncol* (2011) 47 (12):1105–9. doi: 10.1016/j.oraloncology.2011.08.001

2. Arashiro M, Satoh K, Osawa H, Yoshizawa M, Nakano H, Ajibe H, et al. Endoscopic submucosal dissection of esophageal lymphangioma: A case report with a review of the literature. *Clin J Gastroenterol* (2010) 3(3):140–3. doi: 10.1007/s12328-010-0150-4

3. Kennedy TL. Cystic hygroma-lymphangioma: A rare and still unclear entity. *Laryngoscope* (1989) 99(10 Pt 2 Suppl 49):1–10. doi: 10.1288/00005537-198910001-00001

4. Hancock BJ, St-Vil D, Luks FI, Di Lorenzo M, Blanchard H. Complications of lymphangiomas in children. *J Pediatr Surg* (1992) 27(2):220–4. doi: 10.1016/0022-3468(92)90316-Y

5. Rana A, Katzman PJ, Pegoli W, Qualia C. An unusual cause of abdominal pain: duodenal cystic lymphangioma. *Gastroenterol Hepatol (N Y)* (2013) 9(3):192–5.

6. Cui J, Huang LY, Lin SJ, Yi LZ, Wu CR, Zhang B. Small intestinal vascular malformation bleeding: A case report with imaging findings. *World J Gastroenterol* (2014) 20(38):14076–8. doi: 10.3748/wjg.v20.i38.14076

7. Gale EAM. Endoscopic submucosal dissection of a giant esophageal lymphangioma. *Endoscopy* (2018) 50(07):E181–E3. doi: 10.1055/a-0605-2443

8. Sriram P, Weise C, Seitz U, Brand B. Lymphangioma of the major duodenal papilla presenting as acute pancreatitis: Treatment by endoscopic snare papillectomy. *J Gastrointest Endoscopy* (2000) 51(6):733–6. doi: 10.1067/mge.2000.106111

9. Ali HA, Zeriouh B, Bouzayan L, Jabi R, Bouziane M. Giant cystic lymphangioma of the stomach: A case report. *Ann Med Surg (Lond)* (2021) 61:8–12. doi: 10.1016/j.amsu.2020.12.010

10. Saers T, Parusel M, Brockmann M, Krakamp B. Lymphangioma of the esophagus. *Gastrointest Endosc* (2005) 62(1):181–4. doi: 10.1016/S0016-5107(04)02844-5

11. Zhao ZF, Kuang L, Zhang N, Ma SR, Yang Z, Han X, et al. Endoscopic diagnosis and treatment of esophageal cavernous lymphangioma. *Surg Laparosc Endosc Percutan Tech* (2013) 23(3):299–302. doi: 10.1097/SLE.0b013e31828b8810

12. Hu PF, Chen H, Wang XH, Wang WJ, Su N, Shi B. Small intestinal hemangioma: Endoscopic or surgical intervention? a case report and review of literature. *World J Gastrointest Oncol* (2018) 10(12):516–21. doi: 10.4251/wjgo.v10.i12.516

13. Matsuda T, Hiki N, Nunobe S, Aikou S, Hirasawa T, Yamamoto Y, et al. Feasibility of laparoscopic and endoscopic cooperative surgery for gastric submucosal tumors (with video). *Gastrointest Endosc* (2016) 84(1):47–52. doi: 10.1016/j.gie.2015.11.040

14. Brady PG , Milligan FD.. Lymphangioma of the esophagus–diagnosis by endoscopic biopsy. *Am J Dig Dis* (1973) 18(5):423–5. doi: 10.1007/BF01071994

15. Perkins JA, Manning SC, Tempero RM, Cunningham MJ, Edmonds JL Jr., Hoffer FA, et al. Lymphatic malformations: current cellular and clinical investigations. *Otolaryngol Head Neck Surg* (2010) 142(6):789–94. doi: 10.1016/j.otohns.2010.02.025

16. Kang BH, Hur H, Joung YS, Kim DK, Kim YB, Ahn CW, et al. Giant mesenteric cystic lymphangioma originating from the lesser omentum in the abdominal cavity. *J Gastric Cancer* (2011) 11(4):243–7. doi: 10.5230/jgc.2011.11.4.243

17. van Oudheusden TR, Nienhuijs SW, Demeyere TB, Luyer MD, de Hingh IH. Giant cystic lymphangioma originating from the lesser curvature of the stomach. *World J Gastrointest Surg* (2013) 5(10):264–7. doi: 10.4240/wjgs.v5.i10.264

18. Cheng Y, Zhou X, Xu K, Huang Q. Esophageal lymphangioma: A case report and review of literature. *BMC Gastroenterol* (2019) 19(1):107. doi: 10.1186/s12876-019-1026-9

19. Ishikawa N, Fuchigami T, Kikuchi Y, Kobayashi H, Sakai Y, Nakanishi M, et al. EUS for gastric lymphangioma. *Gastrointest Endosc* (2000) 52(6):798–800. doi: 10.1067/mge.2000.108292

20. Haibin Z, Lingling W, Lexing Z, Xumin B, Yingyu W, Jianfeng Y, et al. Clinicopathological characteristics and prognosis of gastrointestinal vascular tumours. *Sci Rep* (2021) 11(1):16062. doi: 10.1038/s41598-021-94821-1

21. Qian W, Weishun C. Duodenal lymphangioma: one case report and literature review. *Chin J Gastroenterol Hepatol* (2019) 28(12):4.

22. Matsushita A, Yuasa N, Miyake H, Nagai H, Nagao T, Fujino M. Gastric lymphangioma coexisting with mucosal gastric cancer: A rare case report. *Clin J Gastroenterol* (2020) 13(1):46–9. doi: 10.1007/s12328-019-01013-6

23. Bai K, Dai Y, Jiang C, Lin S, Wang G. Gastric lymphangioma: A case report and review of literature. *BMC Gastroenterol* (2022) 22(1):407. doi: 10.1186/s12876-022-02431-6

24. Handra-Luca A, Montgomery E. Vascular malformations and hemangiolymphangiomas of the gastrointestinal tract: morphological features and clinical impact. *Int J Clin Exp Pathol* (2011) 4(5):430–43.

25. Luo D, Ye L, Wu W, Zheng H, Mao X. Huge lymphangioma of the esophagus resected by endoscopic piecemeal mucosal resection. *Case Rep Med* (2017) 2017:5747560. doi: 10.1155/2017/5747560

26. Nayak M, Purkait S, Sasmal PK, Singh PK. Cystic lymphangioma of the stomach with marked reactive changes: A rare cause of gastric outlet obstruction in adult. *BMJ Case Rep* (2020) 13(7):e233582. doi: 10.1136/bcr-2019-233582

27. Tanaka Y, Fujii S, Kusaka T, Kokuryu H. Effective use of EUS for diagnosing a jejunal lymphangioma accompanied with hemorrhage. *Gastrointest Endosc* (2020) 91(1):199–200. doi: 10.1016/j.gie.2019.08.009

28. Ghatak S, Ray S, Sanyal S, Sonar PK, Khamrui S, Basu K, et al. An unusual cause of acute abdomen in adults: giant cystic lymphangioma of the pancreatic head. *A Clin Case Literature Rev JOP* (2011) 12(3):266–70. doi: 10.6092/1590-8577/3295

29. Zhuang K, Jiang X, Huang S. A rare, giant, cystic, and cavernous lymphangioma originated from the stomach in A young woman. *J Gastrointest Surg* (2019) 23(6):1271–3. doi: 10.1007/s11605-018-3877-8

30. Matsushita M, Ueshima T, Nishimon S, Takahashi M, Asayama T, Shibatani N, et al. Unroofing technique: effective "incomplete" endoscopic resection of large esophageal lymphangiomas. *Endoscopy* (2020) 52(7):621. doi: 10.1055/a-1157-8888

31. Lawless ME, Lloyd KA, Swanson PE, Upton MP, Yeh MM. Lymphangiomatous lesions of the gastrointestinal tract: A clinicopathologic study and comparison between adults and children. *Am J Clin Pathol* (2015) 144 (4):563–9. doi: 10.1309/AJCPO8TW6EMAJSRP

32. Min M, Liu Y. Lymphangioma of the esophagus. *Am J Gastroenterol* (2018) 113(7):936. doi: 10.1038/s41395-018-0071-2

33. Tseng JJ, Chou MM, Ho ES. Fetal axillary hemangiolymphangioma with secondary intralesional bleeding: serial ultrasound findings. *Ultrasound Obstet Gynecol* (2002) 19(4):403–6. doi: 10.1046/j.1469-0705.2002.00633.x

34. Gomez-Galan S, Mosquera-Paz MS, Ceballos J, Cifuentes-Grillo PA, Gutierrez-Soriano L. Duodenal hemangiolymphangioma presenting as chronic anemia: A case report. *BMC Res Notes* (2016) 9(1):426. doi: 10.1186/s13104-016-2214-0

frontiers | Frontiers in Oncology

TYPE Methods
PUBLISHED 09 November 2022
DOI 10.3389/fonc.2022.939425

Check for updates

OPEN ACCESS

EDITED BY
Zhendong Jin,
Second Military Medical University, China

REVIEWED BY
Alfonso De Stefano,
G. Pascale National Cancer Institute Foundation, Scientific Institute for Research, Hospitalization and Healthcare (IRCCS), Naples, Italy
Govind Babu Kanakasetty,
HCG Cancer Hospital, India

*CORRESPONDENCE
Yoshito Komatsu
ykomatsu@ac.cyberhome.ne.jp

SPECIALTY SECTION
This article was submitted to Gastrointestinal Cancers: Colorectal Cancer, a section of the journal Frontiers in Oncology

RECEIVED 09 May 2022
ACCEPTED 21 October 2022
PUBLISHED 09 November 2022

CITATION
Nakatsumi H, Komatsu Y, Muranaka T, Yuki S, Kawamoto Y, Harada K, Dazai M, Tateyama M, Sasaki Y, Miyagishima T, Tsuji Y, Katagiri M, Nakamura M, Sogabe S, Hatanaka K, Meguro T, Kobayashi T, Ishiguro A, Muto O, Shindo Y, Kotaka M, Ando T, Takagi R, Sakamoto N and Sakata Y (2022) Study protocol for HGCSG1801: A multicenter, prospective, phase II trial of second-line FOLFIRI plus aflibercept in patients with metastatic colorectal cancer refractory to anti-EGFR antibodies.
Front. Oncol. 12:939425.
doi: 10.3389/fonc.2022.939425

Study protocol for HGCSG1801: A multicenter, prospective, phase II trial of second-line FOLFIRI plus aflibercept in patients with metastatic colorectal cancer refractory to anti-EGFR antibodies

Hiroshi Nakatsumi[1], Yoshito Komatsu[2*], Tetsuhito Muranaka[3], Satoshi Yuki[4], Yasuyuki Kawamoto[2], Kazuaki Harada[4], Masayoshi Dazai[5], Miki Tateyama[6], Yusuke Sasaki[7], Takuto Miyagishima[8], Yasushi Tsuji[9], Masaki Katagiri[10], Michio Nakamura[11], Susumu Sogabe[12], Kazuteru Hatanaka[13], Takashi Meguro[14], Tomoe Kobayashi[15], Atsushi Ishiguro[16], Osamu Muto[17], Yoshiaki Shindo[18], Masahito Kotaka[19], Takayuki Ando[20], Ryo Takagi[21], Naoya Sakamoto[4] and Yu Sakata[22]

[1]Department of Gastroenterology, National Hospital Organization Hokkaido Medical Center, Sapporo, Japan, [2]Division of Cancer Center, Hokkaido University Hospital, Sapporo, Japan, [3]Department of Internal Medicine, Wakkanai City Hospital, Wakkanai, Japan, [4]Department of Gastroenterology and Hepatology, Hokkaido University Hospital, Sapporo, Japan, [5]Department of Gastroenterology, Sapporo Medical Center NTT EC, Sapporo, Japan, [6]Department of Internal Medicine, Tomakomai Nissho Hospital, Tomakomai, Japan, [7]Department of Medical Oncology, Hakodate Central General Hospital, Hakodate, Japan, [8]Department of Medical Oncology, Kushiro Rosai Hospital, Kushiro, Japan, [9]Department of Medical Oncology, Tonan Hospital, Sapporo, Japan, [10]Department of Gastroenterology, Sapporo Hokuyu Hospital, Sapporo, Japan, [11]Department of Gastroenterology, Sapporo City General Hospital, Sapporo, Japan, [12]Department of Medical Oncology, KKR Sapporo Medical Center, Sapporo, Japan, [13]Department of Gastroenterology, Hakodate Municipal Hospital, Hakodate, Japan, [14]Department of Internal Medicine, Hokkaido Gastroenterology Hospital, Sapporo, Japan, [15]Department of Gastroenterology, Tomakomai City Hospital, Tomakomai, Japan, [16]Department of Medical Oncology, Teine Keijinkai Hospital, Sapporo, Japan, [17]Department of Medical Oncology, Japanese Red Cross Akita Hospital, Akita, Japan, [18]Department of Gastroenterological Surgery, Nakadori General Hospital, Akita, Japan, [19]General Cancer Center, Sano Hospital, Kobe, Japan, [20]The third department of Internal Medicine, University of Toyama, Toyama, Japan, [21]Clinical Research and Medical Innovation Center, Hokkaido University Hospital, Sapporo, Japan, [22]CEO, Misawa Municipal Misawa Hospital, Misawa, Japan

Background: The first-line chemotherapy for patients with *RAS* and *BRAF* wild-type metastatic colorectal cancer (mCRC) commonly involves cytotoxic regimens, such as FOLFOX and FOLFIRI, combined with epidermal growth factor receptor (EGFR) antibodies. When progression occurs following anti-EGFR antibody-combined chemotherapy, anti-angiogenic inhibitors can be used as second-line treatment. Although randomized controlled trials have

shown that anti-angiogenic inhibitors [bevacizumab, ramucirumab, and aflibercept (AFL)] carry survival benefit when combined with FOLFIRI as second-line chemotherapy, such trials did not provide data on patients with mCRC refractory to anti-EGFR antibody-combined chemotherapy. Therefore, our group planned a multicenter, nonrandomized, single-arm, prospective, phase II study to investigate the safety and efficacy of FOLFIRI plus AFL as a second-line chemotherapy for patients with mCRC refractory to oxaliplatin-based chemotherapy combined with anti-EGFR antibodies.

Methods: FOLFIRI (irinotecan 180 mg/m^2, *l*-leucovorin 200 mg/m^2, bolus 5-FU 400 mg/m^2, and infusional 5-FU 2400 mg/m^2/46 h) and AFL (4 mg/kg) will be administered every 2 weeks until progression or unacceptable toxicities occur. The primary endpoint will be the 6-month progression-free survival (PFS) rate, whereas the secondary endpoints will include overall survival, PFS, response rate, disease control rate, adverse events, and relative dose intensity for each drug. A sample size of 41 participants will be required. This study will be sponsored by the Non-Profit Organization Hokkaido Gastrointestinal Cancer Study Group and will be supported by a grant from Sanofi.

Discussion: There is only an observational study reporting data on FOLFIRI plus AFL for patients with mCRC who previously received anti-EGFR antibodies; therefore, a prospective clinical trial is needed. This study will prospectively evaluate the efficacy and safety of FOLFIRI plus AFL in patients with mCRC who are resistant to anti-EGFR antibodies and have limited data. Moreover, this study will reveal predictive biomarkers for AFL-based chemotherapy.

Clinical trial registration: Japan Registry of Clinical Trials, jRCTs011190006. Registered 19 November, 2019, https://jrct.niph.go.jp/latest-detail/jRCTs011190006.

KEYWORDS

colorectal cancer, chemotherapy, FOLFIRI, aflibercept, anti-EGFR antibodies

Introduction

The incidence of colorectal cancer (CRC) has increased over the decades and is the second most common cause of cancer-related death in Japan. Estimates in 2016 revealed 201,446 new CRC cases, with 50,099 deaths throughout Japan (1). Metastatic CRC (mCRC) carries a poor prognosis with no currently available cure. Chemotherapy remains the standard treatment for mCRC and aims to prolong survival and improve patients' quality of life. Nowadays, chemotherapy regimens, such as combinations of 5-fluorouracil (5-FU), leucovorin (LV), and oxaliplatin (FOLFOX) and 5-FU, LV, and irinotecan (FOLFIRI), have been recommended as first-line therapies usually in combination with monoclonal antibodies, such as an anti-vascular endothelial growth factor (VEGF)-A antibody [bevacizumab (BEV)] or anti-epidermal growth factor receptor (EGFR) antibodies (cetuximab or panitumumab) (2). Other studies have also recommended FOLFOXIRI, a combination chemotherapy comprising 5-FU, LV, oxaliplatin, and irinotecan (IRI), with or without BEV (3, 4). Chemotherapies comprising anti-EGFR antibodies have been recommended as the first-line chemotherapy for patients with *RAS* and *BRAF* wild-type mCRC. Indeed, a subgroup analysis of the FIRE-3 study showed that anti-EGFR antibody-based regimens promoted better survival outcomes than BEV-based regimens for left-sided mCRC (5), with several subgroup analyses of prospective clinical trials showing similar outcomes (6, 7). Nowadays, chemotherapy with anti-EGFR antibodies (cetuximab or panitumumab) has been the most recommended regimen in the ESMO-Asian consensus guidelines for patients with *RAS* wild-type left-sided mCRC (8).

Aflibercept (AFL) is a recombinant fusion protein containing portions of the extracellular domains of VEGF receptors 1 and 2 fused to the Fc portion of human immunoglobulin G1 (9). Interestingly, the VELOUR study, which compared FOLFIRI with or without AFL, showed that FOLFIRI plus AFL had better survival outcomes than FOLFIRI alone (median overall survival [OS]: 13.50 vs. 12.06 months, hazard ratio [HR] = 0.817, p = 0.0032) (9). Moreover, ML18147 (10) and RAISE (11) have found that BEV-based chemotherapy and FOLFIRI plus ramucirumab (RAM), a monoclonal antibody targeting VEGF receptor 2, were efficacious second-line therapies. ML18147 showed that continuous BEV plus second-line chemotherapy after progression with BEV plus first-line chemotherapy prolonged survival compared with second-line chemotherapy alone (median overall survival [OS]: 11.2 vs. 9.8 months, HR = 0.81, p = 0.0062) (10). RAISE also showed the efficacy of FOLFIRI plus RAM for patients with mCRC refractory to the first-line chemotherapy with BEV, oxaliplatin, and fluoropyrimidines compared with FOLFIRI plus placebo (median OS: 13.3 vs. 11.7 months, HR = 0.844, p = 0.0219) (11). Notably, ML18147 and RAISE have included participants who received BEV as their first-line chemotherapy, whereas VELOUR included those who received first-line chemotherapy without BEV. In the VELOUR study, the subgroup analysis defined by *RAS* or *BRAF* status showed that WT (all *RAS* wild-type and *BRAF* wild-type) and *BRAF* mutant-type (mut) tended to have better OS outcomes with FOLFIRI plus AFL (WT: HR = 0.76, 95% confidence interval [CI] 0.53–1.10; BRAF mut: HR = 0.42, 95% CI 0.16–1.09), which is a promising result for patients receiving first-line chemotherapy with anti-EGFR antibodies (12). However, the VELOUR study did not report results for patients who received first-line therapy with anti-EGFR antibodies, whereas little evidence regarding this population was presented. Therefore, no clinical studies have yet demonstrated the efficacy of adding a molecular-targeted agent to second-line chemotherapies for mCRC refractory to first-line treatment including anti-EGFR antibodies.

Considering the lack of evidence, second-line regimens have been selected based on physicians' discretion or patient preference. Therefore, this multicenter clinical study sought to investigate the efficacy and safety of FOLFIRI plus AFL for unresectable advanced or recurrent CRC refractory to combination therapy with oxaliplatin and panitumumab or cetuximab.

Materials and methods

Study design and treatment

This multicenter, nonrandomized, single-arm, prospective, phase II study was designed to investigate the safety and efficacy of FOLFIRI plus AFL as the second-line chemotherapy for patients with mCRC refractory to oxaliplatin-based chemotherapy combined with anti-EGFR antibodies (Figure 1). The inclusion and exclusion criteria are summarized in Table 1.

The treatment protocol starts 7 days after study registration; the treatment schedule is outlined in Figure 2. AFL (4 mg/kg) will be given as a continuous intravenous infusion over 60 min on day 1, followed by a continuous infusion of IRI (180 mg/m^2) over 90 min and *l*-leucovorin (200 mg/m^2) over 120 min. Immediately after completing the *l*-leucovorin infusion, 5-FU (400 mg/m^2) will be provided *via* rapid intravenous injection, followed by a continuous intravenous infusion of 5-FU (2400 mg/m^2) delivered over 46 h using an infusion pump. This 2-week treatment course will be repeated until disease progression or unacceptable toxicities occur.

This study will be conducted in accordance with the Declaration of Helsinki and Ethical Guidelines for Medical and Health Research Involving Human Subjects. HGCSG1801 received approval on October 9, 2019, by Hokkaido University Certified Review Board. All patients will be required to provide written informed consent before enrollment.

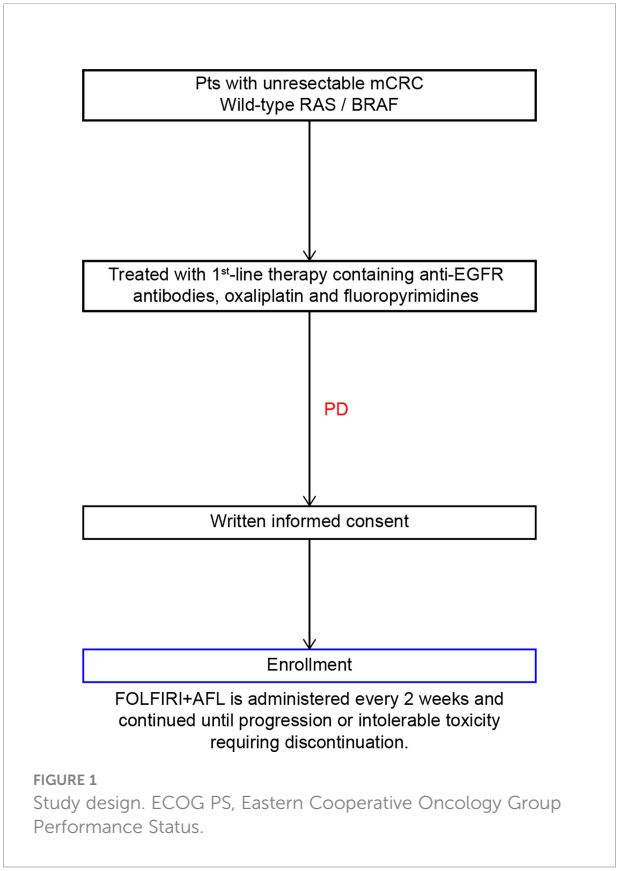

FIGURE 1
Study design. ECOG PS, Eastern Cooperative Oncology Group Performance Status.

TABLE 1 Eligibility criteria.

Inclusion criteria
1. Age 20–85 years
2. Histologically confirmed colorectal adenocarcinoma
3. ECOG PS 0 or 1
4. Documented disease progression 90 days or more after the start of first-line chemotherapy containing anti-EGFR antibodies, oxaliplatin, and fluoropyrimidines
5. Adequate major organ and hematologic functions 14 days before registration
Neutrophil ≥ 1500/mm^3
Platelet ≥ 100,000/mm^3
Hemoglobin ≥ 9.0 g/dL
AST ≤ 100 U/L (pts with liver metastases: ≤ 200 U/L)
ALT ≤ 100 U/L (pts with liver metastases: ≤ 200 U/L)
Total bilirubin ≤ 2.0 mg/dL
Creatinine ≤ 1.5× upper limit of normal
Urine protein (UP) ≤ 1+ or UP/creatinine ratio (UPCR) <2.0 without hematuria (pts with UP ≥2+ and UPCR > 1; UP ≤3.5 g in 24-h urine collection without hematuria)
6. Expected survival time ≥6 months upon registration
7. With documented informed consent
Exclusion criteria
1. Symptomatic CNS invasion and/or brain metastases
2. Uncontrollable infections
3. Uncontrollable diarrhea, anorexia, or nausea
4. Uncontrollable hypertension
5. Uncontrollable, symptomatic plural effusion, or ascites
6. Inability of oral intake
7. Radiation to all lesions
8. UGT1A1 *6 homo, *28 homo, or *6 and *28 double hetero
9. History of other malignancies within 5 years (except for curative resection of carcinoma in situ)
10. Pregnant women
11. Irinotecan-containing regimen as first-line therapy
12. Following status:
Gastrointestinal or abdominal inflammations
Gastrointestinal or other bleeding
Hemorrhagic diathesis, coagulopathy, or treated with anticoagulants
Thromboembolism
No wound healing from major surgery
13. Administration of aflibercept-containing medications
14. Dihydropyrimidine dehydrogenase deficiency
15. Interstitial pneumonia or pulmonary fibrosis
16. Participation in the clinical trial is determined as unsuitable

ALT, alanine aminotransferase; AST, aspartate aminotransferase; CNS, central nervous system; ECOG PS, Eastern Cooperative Oncology Group Performance Status; EGFR, endothelial growth factor receptor; UGT1A1, uridine diphosphate glucuronosyltransferase 1A1.

Endpoints and assessments

The primary endpoint will be the 6-month progression-free survival (PFS) rate, whereas the secondary endpoints will include OS, PFS, overall response rate (ORR), disease control rate (DCR), safety profile, and relative dose intensity.

The OS period will be defined as the duration from the first administration of the study treatment until death due to any cause. Surviving cases will be censored on the last confirmed survival day. The PFS period will be defined as the duration from the first administration of the study treatment until disease progression or death due to any cause, whichever comes first. Cases with no confirmed progression will be censored on the last confirmed PFS date. ORR and DCR will be evaluated based on the Response Evaluation Criteria in Solid Tumors version 1.1 (13). Regarding safety, the frequency of adverse events will be evaluated using the Common Terminology Criteria for Adverse Events v5.0.

The exploratory endpoint will indicate the relationship between primary/secondary endpoints and changes in the following biomarkers: placental growth factor (PlGF), hepatocyte growth factor (HGF), interleukin (IL)-6, IL-8, angiopoietin-2, neuropillin-1, tissue inhibitor of metalloproteinase-1 (TIMP-1), soluble intercellular adhesion molecule-1, soluble vascular cell adhesion molecule-1, thrombospondin-2 (TSP-2), osteopontin (OPN), sVEGFR1, sVEGFR2, sVEGFR3, VEGF-A, VEGF-D, interferon gamma, and transforming growth factor β1.

Biomarker analysis

Blood plasma will be collected three times (before study treatment initiation, before the fifth–sixth cycle, and after study discontinuation) to measure angiogenic factors mentioned earlier. These factors will be analyzed concurrently using the multiplex assay kit Ukit (G&G Science Co., Ltd.) from the MILLIPLEX® MAP multiplex assay kit lineup by Millipore (www.merckmillipore.jp/1milliplex-jp).

The MILLIPLEX® kit is a dedicated reagent for multiplex assay systems using Luminex xMAP® technology (https://www.merckmillipore.com/JP/en/life-science-research/protein-detection-quantification/Immunoassay-Platform-Solutions/luminex-instruments/xmap-technology/OUGb.qB.D_kAAAFB6sYRRk_Q,nav). Samples will be incubated with magnetic bead analytes (MILLIPLEX® MAP) stained stepwise with two fluorescent dyes to specifically bind the target protein to the magnetic bead analyte. Thereafter, the sample will be reacted with a biotin-labeled detection sample and fluorescently labeled with streptavidin-PE, followed by the identification of the magnetic bead analyte and fluorescence intensity quantification using two types of lasers. The analyses of these factors will be performed by GG.

Statistical analysis

The full analysis set (FAS) will include all enrolled patients. However, patients with serious protocol violations

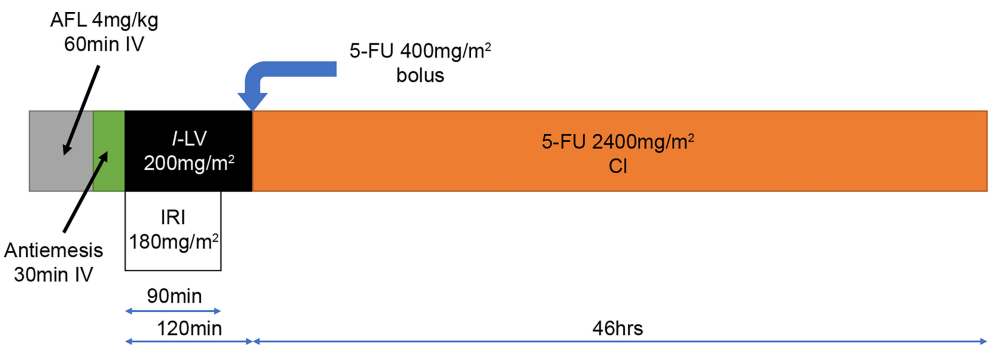

FIGURE 2
Treatment schedule for FOLFIRI+AFL. 5-FU, 5-fluorouracil; AFL, aflibercept beta; CI, continuous infusion; IRI, irinotecan; *l*-LV, *l*-leucovorin.

(no informed consent or serious violations of the study procedures) will be excluded. The safety analysis set (SAS) will include all enrolled patients who receive one dose of the study treatment. All efficacy analyses will be performed in the FAS population, whereas safety analysis will be performed in the SAS population.

The VELOUR study reported 6-month PFS rates of 38.9% and 58.4% for FOLFIRI and FOLFIRI + AFL, respectively, as second-line chemotherapy for mCRC refractory to first-line chemotherapy containing oxaliplatin and fluoropyrimidines, respectively (9). Based on the aforementioned results, we hypothesized a 6-month PFS rate of 58.4% for FOLFIRI plus AFL in patients previously treated and exhibited progression with anti-EGFR agents plus oxaliplatin-based first-line chemotherapy. Given the threshold and expected 6-month PFS rates of 38.9% and 58.4%, respectively, as well as a two-sided significance level (alpha error) of 0.1, a registration period of 2 years, and a follow-up period of 18 months, 37 cases will be required when the probability that the lower limit of the CI calculated using the Greenwood formula (14) exceeds the threshold is 80%. Consequently, the target number of cases will be set at 41 to account for ineligible cases.

This study primarily sought to evaluate the efficacy of FOLFIRI + AFL. The main analysis will utilize the Kaplan–Meier method (15) to evaluate the 6-month PFS rate (i.e., primary endpoint) in the FAS population. The 90% CI will be calculated using the Greenwood formula for the observed 6-month PFS rate, with significance being indicated when the lower limit of the 90% CI exceeds the threshold of 38.9%.

Secondary endpoints will be analyzed to supplement the main analysis results. OS and PFS will be evaluated using the Kaplan–Meier method, and the ORR and DCR will be calculated using the Clopper–Pearson 95% CI (16).

Discussion

Limited data have been available on the optimal second-line regimen for mCRC refractory to anti-EGFR antibodies. The QoLiTrap study reported promising data of FOLFIRI plus AFL for patients who previously received anti-EGFR antibodies (ORR 23.7%, median PFS 9.4 months and median OS 17.4 months); however, it is an observational study and included patients receiving FOLFIRI plus AFL as second- or later-line therapy (17). Therefore, a prospective clinical trial is needed.

The present study will evaluate the efficacy and safety of FOLFIRI plus AFL in patients who have progressed with EGFR inhibitors, as well as changes in angiogenesis-related biomarkers during FOLFIRI plus AFL chemotherapy, to identify predictive biomarkers for AFL-based chemotherapy.

Although no predictive markers for the efficacy of angiogenesis inhibitors, such as *RAS* or *BRAF*, in EGFR antibody therapy have previously been identified, some promising factors have been reported. Accordingly, PlGF and HGF were significantly increased during BEV-combined chemotherapy before imaging indicated progression, whereas VEGFR2 was significantly increased after BEV administration and then decreased at the time of progression (18). Moreover, patients with high IL-8 levels upon treatment initiation had a significantly shorter PFS versus those with low levels. A biomarker study in the CALGB80405 trial showed that low VEGF-D and low PlGF may indicate BEV effectiveness and that factors, including angiopoietin-2, HGF, ICAM-1, IL-6, OPN, TIMP-1, TSP-2, VCAM-1, VEGFR3, can be prognostic indicators (19).

The biomarker analysis in the VELOUR study (20, 21) revealed that high levels of VEGF-A, VEGFR2, PlGF, and VEGFR3 and low levels of IL-8 indicated the efficacy of FOLFIRI + AFL, with neuropilin-1 and angiopoietin-2 having been identified as prognostic factors.

The Angiogenesis Panel that will be used in the biomarker analysis of the present study is a kit that can simultaneously

measure 17 angiogenic factors. By evaluating changes in these factors before, during, and after study treatment administration, prognostic and prognostic factors can be identified.

The results of this study will elucidate the efficacy and safety of FOLFIRI plus AFL in mCRC refractory to anti-EGFR antibodies, as well as identify biomarkers for such a regimen.

Data availability statement

The original contributions presented in the study are included in the article/supplementary material. Further inquiries can be directed to the corresponding author.

Ethics statement

HGCSG1801 received approval on 9/Oct/2019 by Hokkaido University Certified Review Board. The patients/participants provided their written informed consent to participate in this study.

Author contributions

YoK, the chief investigator, designed and prepared the study protocol together with HN, TeM, and YaK. HN and TeM designed the biological specimen collection. HN, YoK, SY, YaK, KHar, MD, MT, YuSas, TMi, YT, MKa, MN, SS, KHat, TMe, TK, AI, OM, YoS, MKo, and TA will recruit and follow-up patients. RT is the chief statistician. NS and YuSaka will be coordinating the study. All authors contributed to the article and approved the submitted version.

Funding

This study is sponsored by the Non-Profit Organization Hokkaido Gastrointestinal Cancer Study Group and is supported by a grant from Sanofi (Grant no. SGZ-2017-11875).

Acknowledgments

We are grateful to all patients and investigators for their cooperation in the HGCSG1801 study. The authors would like to thank Enago (www.enago.jp) for the English language review.

Conflict of interest

HN has received honoraria from Takeda, Sanofi, and Taiho; YoK has received honoraria from Taiho, Yakult Honsha, Takeda, Pfizer, Daiichi Sankyo, Sanofi, and Nipro and has received research funding from Taiho, Yakult Honsha, Daiichi Sankyo, and Sanofi; SY has received honoraria from Takeda, Sanofi, Taiho, and Yakult Honsha; YaK has received honoraria from Takeda, Kyowa Kirin; YT has received honoraria from Taiho, Takeda, and Sawai; MN has received honoraria from Daiichi Sankyo, Taiho, Kyowa Kirin, Takeda and Mochida and has received research funding from Takeda; SS has received honoraria from Sanofi and Daiichi Sankyo; YoS has received honoraria from Yakult Honsha; MKo has received honoraria from Yakult Honsha, Takeda, Sanofi, and Taiho; TA has received honoraria from Takeda and Daiichi Sankyo; NS has received research funding from Takeda; YuSaka has received honoraria from Yakult Honsha and Taiho.

The remaining authors declare that the research was conducted in the absence of any commercial or financial relationships that could be construed as a potential conflict of interest.

Publisher's note

All claims expressed in this article are solely those of the authors and do not necessarily represent those of their affiliated organizations, or those of the publisher, the editors and the reviewers. Any product that may be evaluated in this article, or claim that may be made by its manufacturer, is not guaranteed or endorsed by the publisher.

References

1. *Cancer registry and statistics* . National Cancer Center, Japan: Cancer Information Service (Accessed May 7, 2020).

2. Hashiguchi Y, Muro K, Saito Y, Ito Y, Ajioka Y, Hamaguchi T, et al. Japanese Society for cancer of the colon and rectum (JSCCR) guidelines 2019 for the treatment of colorectal cancer. *Int J Clin Oncol* (2020) 25:1–42. doi: 10.1007/s10147-019-01485-z

3. Falcone A, Ricci S, Brunetti I, Pfanner E, Allegrini G, Barbara C, et al. Phase III trial of infusional fluorouracil, leucovorin, oxaliplatin, and irinotecan (FOLFOXIRI) compared with infusional fluorouracil, leucovorin, and irinotecan (FOLFIRI) as first-line treatment for metastatic colorectal cancer: the gruppo oncologico nord ovest. *J Clin Oncol* (2007) 25:1670–6. doi: 10.1200/JCO.2006.09.0928

4. Cremolini C, Loupakis F, Antoniotti C, Lupi C, Sensi E, Lonardi S, et al. FOLFOXIRI plus bevacizumab versus FOLFIRI plus bevacizumab as first-line treatment of patients with metastatic colorectal cancer: updated overall survival and molecular subgroup analyses of the open-label, phase 3 TRIBE study. *Lancet Oncol* (2015) 16:1306–15. doi: 10.1016/S1470-2045(15)00122-9

5. Heinemann V, Modest DP, von Weikersthal LF, Decker T, Kiani A, Vehling-Kaiser U, et al. Gender and tumor location as predictors for efficacy: influence on endpoints in first-line treatment with FOLFIRI in combination with cetuximab or bevacizumab in the AIO KRK 0306 (FIRE3) trial. *J Clin Oncol* (2014) 32:3600–6. doi: 10.1200/jco.2014.32.15_suppl.3600

6. Brulé SY, Jonker DJ, Karapetis CS, O'Callaghan CJ, Moore MJ, Wong R, et al. Location of colon cancer (right-sided versus left-sided) as a prognostic factor and a

predictor of benefit from cetuximab in NCIC CO. *17. Eur J Cancer* (2015) 51:1405–14. doi: 10.1016/j.ejca.2015.03.015

7. Arnold D, Lueza B, Douillard JY, Peeters M, Lenz HJ, Venook A, et al. Prognostic and predictive value of primary tumour side in patients with RAS wild-type metastatic colorectal cancer treated with chemotherapy and EGFR directed antibodies in six randomized trials. *Ann Oncol* (2017) 28:1713–29. doi: 10.1093/annonc/mdx175

8. Yoshino T, Arnold D, Taniguchi H, Pentheroudakis G, Yamazaki K, Xu RH, et al. Pan-Asian adapted ESMO consensus guidelines for the management of patients with metastatic colorectal cancer: a JSMO–ESMO initiative endorsed by CSCO, KACO, MOS, SSO and TOS. *Ann Oncol* (2018) 29:44–70. doi: 10.1093/annonc/mdx738

9. Van Cutsem E, Tabernero J, Lakomy R, Prenen H, Prausová J, Macarulla T, et al. Addition of aflibercept to fluorouracil, leucovorin, and irinotecan improves survival in a phase III randomized trial in patients with metastatic colorectal cancer previously treated with an oxaliplatin-based regimen. *J Clin Oncol* (2012) 30:3499–506. doi: 10.1200/JCO.2012.42.8201

10. Bennouna J, Sastre J, Arnold D, Österlund P, Greil R, Van Cutsem E, et al. Continuation of bevacizumab after first progression in metastatic colorectal cancer (ML18147): a randomised phase 3 trial. *Lancet Oncol* (2013) 14:29–37. doi: 10.1016/S1470-2045(12)70477-1

11. Tabernero J, Yoshino T, Cohn AL, Obermannova R, Bodoky G, Garcia-Carbonero R, et al. Ramucirumab versus placebo in combination with second-line FOLFIRI in patients with metastatic colorectal carcinoma that progressed during or after first-line therapy with bevacizumab, oxaliplatin, and a fluoropyrimidine (RAISE): a randomised, double-blind, multicentre, phase 3 study. *Lancet Oncol* (2015) 16:499–508. doi: 10.1016/S1470-2045(15)70127-0

12. Wirapati P, Pomella V, Vandenbosch B, Kerr P, Maiello E, Jeffery GM, et al. Velour trial biomarkers update: Impact of RAS, BRAF, and sidedness on aflibercept activity. *J Clin Oncol* (2017) 35:3538–46. doi: 10.1200/JCO.2017.35.15_suppl.3538

13. Eisenhauer EA, Therasse P, Bogaerts J, Schwartz LH, Sargent D, Ford R, et al. New response evaluation criteria in solid tumours: revised RECIST guideline (version 1. *1). Eur J Cancer* (2009) 45:228–47. doi: 10.1016/j.ejca.2008.10.026

14. Greenwood M. The errors of sampling of the survivorship tables. *Reports on Public Health and Medical Subjects*. London: Her Majesty's Stationery Office, Vol. 33 (1926).

15. Kaplan EL, Meier P. Nonparametric estimation from incomplete observations. *JASA* (1958) 53:457–81. doi: 10.1080/01621459.1958.10501452

16. Clopper CJ, Pearson ES. The use of confidence or fiducial limits illustrated in the case of the binomial. *Biometrika* (1934) 26:404–13. doi: 10.1093/biomet/26.4.404

17. Hofheinz RD, Anchisi S, Grünberger B, Derigs HG, Zahn MO, Geffriaud-Ricouard C, et al. Real-world evaluation of quality of life, effectiveness, and safety of aflibercept plus FOLFIRI in patients with metastatic colorectal cancer: the prospective QoLiTrap study. *Cancers* (2022) 14:3522. doi: 10.3390/cancers14143522

18. Kopetz S, Hoff PM, Morris JS, Wolff RA, Eng C, Glover KY, et al. Phase II trial of infusional fluorouracil, irinotecan, and bevacizumab for metastatic colorectal cancer: efficacy and circulating angiogenic biomarkers associated with therapeutic resistance. *J Clin Oncol* (2010) 28:453–9. doi: 10.1200/JCO.2009.24.8252

19. Nixon AB, Sibley A, Hatch AJ, Liu Y, Jiang C, Mulkey F, et al. Blood-based biomarkers in patients (pts) with metastatic colorectal cancer (mCRC) treated with FOLFOX or FOLFIRI plus bevacizumab (Bev), cetuximab (Cetux), or bev plus cetux: Results from CALGB 80405 (Alliance). *J Clin Oncol* (2016) 34:3597. doi: 10.1200/JCO.2016.34.15_suppl.3597

20. Sims TN, Gao B, Chiron M, Mancini P, Dochy E, Lowy I. Potential predictive and prognostic biomarkers identified in baseline plasma samples from the VELOUR trial. *J Clin Oncol* (2015) 33:638. doi: 10.1200/jco.2015.33.3_suppl.638

21. Van Cutsem E, Paccard C, Chiron M, Tabernero J. Impact of prior bevacizumab treatment on VEGF-a and PlGF levels and outcome following second-line aflibercept treatment: biomarker post hoc analysis of the VELOUR trial. *Clin Cancer Res* (2020) 26:717–25. doi: 10.1158/1078-0432.CCR-19-1985

COPYRIGHT

© 2022 Nakatsumi, Komatsu, Muranaka, Yuki, Kawamoto, Harada, Dazai, Tateyama, Sasaki, Miyagishima, Tsuji, Katagiri, Nakamura, Sogabe, Hatanaka, Meguro, Kobayashi, Ishiguro, Muto, Shindo, Kotaka, Ando, Takagi, Sakamoto and Sakata. This is an open-access article distributed under the terms of the Creative Commons Attribution License (CC BY). The use, distribution or reproduction in other forums is permitted, provided the original author(s) and the copyright owner(s) are credited and that the original publication in this journal is cited, in accordance with accepted academic practice. No use, distribution or reproduction is permitted which does not comply with these terms.

frontiers | Frontiers in Oncology

TYPE Original Research
PUBLISHED 11 November 2022
DOI 10.3389/fonc.2022.1003440

Check for updates

OPEN ACCESS

EDITED BY
Shantibhusan Senapati,
Institute of Life Sciences (ILS), India

REVIEWED BY
Lingying Wu,
Chinese Academy of Medical Sciences and Peking Union Medical College, China
Kotamballi N. Chidambara Murthy,
Neuberg Anand Academy of Laboratory Medicine Private Limited, India

*CORRESPONDENCE
Haixia Peng
phx1101@shtrhospital.com
Yimin Chu
yimin_chu@163.com

†These authors have contributed equally to this work and share first authorship

SPECIALTY SECTION
This article was submitted to Gastrointestinal Cancers: Colorectal Cancer, a section of the journal Frontiers in Oncology

RECEIVED 26 July 2022
ACCEPTED 24 October 2022
PUBLISHED 11 November 2022

CITATION
Sun W, Xu Y, Zhao B, Zhao M, Chen J, Chu Y and Peng H (2022) The prognostic value and immunological role of angiogenesis-related patterns in colon adenocarcinoma. *Front. Oncol.* 12:1003440. doi: 10.3389/fonc.2022.1003440

COPYRIGHT
© 2022 Sun, Xu, Zhao, Zhao, Chen, Chu and Peng. This is an open-access article distributed under the terms of the Creative Commons Attribution License (CC BY). The use, distribution or reproduction in other forums is permitted, provided the original author(s) and the copyright owner(s) are credited and that the original publication in this journal is cited, in accordance with accepted academic practice. No use, distribution or reproduction is permitted which does not comply with these terms.

The prognostic value and immunological role of angiogenesis-related patterns in colon adenocarcinoma

Weijie Sun[1†], Ying Xu[1†], Baolong Zhao[2†], Min Zhao[1], Jiaying Chen[1], Yimin Chu[1*] and Haixia Peng[1*]

[1]Digestive Endoscopy Center, Tongren Hospital, Shanghai Jiaotong University School of Medicine, Shanghai, China, [2]Qiqihar Medical University, Qiqihar, Heilongjiang, China

Colon adenocarcinoma (COAD) is a malignant tumor with a high mortality rate. Angiogenesis plays a key role in the development and progression of cancer. However, in COAD, studies between angiogenesis and prognosis, immune cell infiltration, and personalized treatment guidance are currently lacking. In the present study, we comprehensively assessed 35 angiogenesis-related genes (ARG) and identified key ARGs affecting OS in COAD patients. The ARG Prognostic Index (ARGPI) was constructed based on a univariate Cox regression model and its prognostic value was evaluated in TCGA-COAD, GSE39582, GSE161158 and TRSJTUSM Cohort. We constructed ARGPI as an independent risk factor for OS in COAD patients and combined with clinical parameters to further construct an ARGPI-based nomogram, which showed a strong ability to predict overall survival in COAD patients. High ARGPI is associated with cancer-related and immune-related biological processes and signaling pathways; high TP53 mutation rate; high infiltration of MSC, pericytes, and stromal cells; and more CMS4 subtype. And low ARGPI benefited more from immune checkpoint inhibitor treatment. In addition, we also predicted the sensitivity of different ARGPI groups to common chemotherapeutic and targeted agents. In conclusion, this study constructed an ARGPI based on ARG, which robustly predicted the OS of COAD patients and provided a possible personalized treatment regime for COAD patients.

KEYWORDS

COAD, angiogenesis, prognosis, drug sensitivity, immunotherapy

Introduction

According to the latest global cancer statistics, Colon adenocarcinoma (COAD) ranks among the highest in incidence and mortality (1). Patients with advanced colorectal cancer (CRC) have a very poor prognosis compared with those with early-stage colorectal cancer (2). At present, the main methods for the treatment of COAD are surgery, radiotherapy and chemotherapy, targeted therapy and immunotherapy. Although advances in understanding of the pathophysiology of COAD have led to increasingly individualized treatment regimens and have resulted in significantly improved overall survival in advanced stage patients, this is far from sufficient relative to early-stage patients (3). Since current treatments for COAD still have many limitations, it is imperative to develop biomarkers that can effectively predict disease progression and individualized treatment response.

Angiogenesis is one of the key conditions for a variety of physiological and pathological activities (4). Pathological angiogenesis in pathological diseases, including cancer, often results in abnormal vascular structure and function, which is one of the important factors in maintaining rapid growth of cancer (4). Because the oxygen, nutrients and growth factors needed to support the growth of cancer cells are all delivered by blood vessels. It is therefore not difficult to understand that tumor cells secrete a large number of pro-angiogenic factors to maintain the formation of vascular networks, albeit disorganized (5). Therefore, inhibition of angiogenesis is a good therapeutic option for the treatment of solid tumors (6, 7). However, current studies mostly target a certain gene or signaling pathway, such as vascular endothelial growth factor (VEGF), fibroblast growth factor and Notch signaling pathway, etc. (8). Unfortunately, anti-angiogenesis cannot completely eliminate tumor cells, which may also be one of the important reasons for cancer drug resistance (9). Therefore, the future will focus on the combination therapy of anti-angiogenic agents with chemotherapy, targeted therapy and immunotherapy (9–11). Current studies have focused on the value of angiogenesis-related genes in the prognosis and immunotherapy of gastric cancer (12). However, no studies have focused on the role of angiogenesis-related genes (ARG) in COAD, including the prognostic value and choice of combination therapy, especially immunotherapy.

Our study is the first to systematically explore the differential expression and prognostic value of angiogenesis-related genes in COAD and further explore the relationship with the immune microenvironment and the impact on the choice of chemotherapy, targeted therapy and immunotherapy. The 3-gene ARG Prognostic Index (ARGPI) was first identified by COAD. Next, we assessed the clinical value of ARGPI and its impact on the immune microenvironment, and finally assessed the clinical value of ARGPI for the effect of immunotherapy. We believe that this study has certain prognostic value and clinical treatment guiding significance for COAD patients.

Materials and methods

Patients and tissue samples

From March 2016 to December 2017, 77 surgical specimens after CRC resection were collected at Tongren Hospital, Shanghai Jiao Tong University School of Medicine (TRSJTUSM), immediately placed in liquid nitrogen, and stored at -80°C. This study was approved by the Ethics Committee of TRSJTUSM (No. 2017-003-01). All patients provided written informed consent and adhered to the Declaration of Helsinki.

Data collection

RNA-seq data for 33 cancers from TCGA were obtained from the University of California Santa Cruz (UCSC, https://xena.ucsc.edu/) xena, and clinical data for the TCGA-COAD dataset were obtained. Somatic mutation data in COAD patients were obtained from The Cancer Genome Atlas (TCGA, https://portal.gdc.cancer.gov/) database. The RNA-seq data and clinical data of GSE39582, GSE161158 and GSE78220 were obtained from the Gene Expression Omnibus (GEO, https://www.ncbi.nlm.nih.gov/geo/) database. Consensus molecular subtypes (CMS) of COAD patients in GSE39582 were obtained from data from previously published studies (13). RNA-seq data and matched clinical data from patients in the IMvigor210 cohort of advanced urothelial carcinoma treated with atezolizumab from previously published studies (14). All RNA-seq data were investigated in $\log_2$ (FPKM+1). Patients with an overall survival of less than 30 days were excluded from the prognostic correlation analysis.

Identification of key genes related to angiogenesis

The 36 ARG were obtained from h.all.v7.5.1.symbols.gmt (http://www.gsea-msigdb.org/gsea/msigdb/cards/HALLMARK_ANGIOGENESIS). Based on RNA-seq data of TCGA-COAD samples (471 tumors *vs.* 41 normal samples) obtained from UCSC xena, 35 ARG were identified using the limma package (PRG2 expression values with an average value of less than 0.2 were excluded) of differentially expressed genes ($P < 0.05$, $|\log_2 FC| > 1$). Key genes were then identified by a univariate Cox regression model.

ARGPI construction and verification

The ARGPI was constructed based on the results of the univariate Cox regression model. Briefly, the ARGPI for each sample is calculated by multiplying the expression values of key genes by their weight coefficient (coef values) in the Cox model and adding them together. Its ability to predict patient prognosis in the TCGA-COAD, GSE39582, GSE161158 and the TRSJTUSM Cohort. In addition, the prognostic value of ARGPI in 32 cancers was validated using the Kaplan-Meier survival curve analysis.

RNA extraction and qRT-PCR analysis

Related experiments were performed as previously described (15). Briefly, total RNA was extracted from frozen tissue using RNAiso Plus reagent (Takara Bio, Japan), and RNA was reverse transcribed to cDNA using PrimeScript™ RT Master Mix (Takara Bio, Japan). Quantification was performed by SYBR-Green qPCR Master Mix (Vazyme Bio, China) and normalized to β-actin. Relative quantification of PCR experimental data was performed using the 2−ΔΔCt method. PCR reaction program: preheat at 95°C for 30s, and then enter the amplification cycle. Denaturation at 95°C for 30s, renaturation at 55°C for 30s, and then maintained at 72°C for 60s to complete one cycle. The number of cycles was set to 40 times. Finally, the program was terminated after 5 minutes at 72°C.

The β-actin primer sequences are as follows, forward: CCCTGGAGAAGAGCTACGAG, reverse: GGAAGGAAGGCTGGAAGAGT.

The VEGFA primer sequences are as follows, forward: AGGGCAGAATCATCACGAAGT, reverse: AGGTCTCGATTGGATGGCA.

The JAG2 primer sequences are as follows, forward: AGCCATGCCTTAACGCTTTT, reverse: CACACACTGGTACCCGTTCA.

The TIMP1 primer sequences are as follows, forward: CGCAGCGAGGAGGTTTCTCAT, reverse: GGCAGTGATGTGCAAATTTCC.

Clinical significance of ARGPI and construction of nomogram

To determine whether ARGPI is an independent prognostic marker affecting OS in patients with COAD, we performed univariate and multivariate Cox regression analyses, respectively. Based on ARGPI, we combined multiple clinical indicators to construct a nomogram and used it to predict 1-, 3-, and 5-year OS in COAD patients. Calibration curve was used to evaluate the consistency between nomogram predictions and actual values, and ROC curve was used to evaluate the AUC value of the nomogram in predicting OS of COAD patients at 1-, 3-, and 5-year.

Gene set enrichment analysis

The TCGA-COAD samples were divided into high and low ARGPI groups by median ARGPI value. Based on the gene sets "c2.cp.kegg.v7.4.symbols.gmt" and "c5.go.v7.4.symbols.gmt", the biological processes (BP) and signaling pathways of different ARGPI groupings affecting COAD were analyzed by GSEA. GSEA is a classic tool for elucidating biological functions across different subgroups of patients through genomic expression data (16).

Immune cell infiltration analysis

xCell is a novel method to infer 64 immune and stromal cells based on gene signatures combined with gene set enrichment dominance and deconvolution methods (17). We calculated the infiltration levels of 64 immune and stromal cells in TCGA-COAD samples using xCell.

Mutation spectrum analysis

Somatic mutation data from TCGA-COAD patients were analyzed based on the maftools package (18). We first analyzed the mutational spectrum of angiogenesis-related genes in TCGA-COAD patients. Secondly, according to the median value of ARGPI, TCGA-COAD patients were divided into high ARGPI group and low ARGPI group, and the top 10 most easily mutated genes in different groups were discussed respectively. and calculated the tumor mutational burden (TMB) for each sample, TMB typically represents the number of nonsynonymous mutations per megabase in somatic cells (19).

Immunotherapy responsiveness and drug sensitivity analysis

We first analyzed the correlation of ARGPI with PDL1 and TMB. And use the TIDE algorithm to predict and predict cancer immunotherapy response (20), and analyze the difference of TIDE-related scores in different APGRI groups. Finally, the ability of ARGPI to predict immunotherapy response was validated using two immunotherapy cohorts (IMvigor210 cohort and the GSE78220 cohort). In this study, Immunotherapy efficacy indicators include complete remission (CR), partial remission (PR), stable disease (SD) and disease

progression (PD). CR and PR were classified as immunotherapy response, SD and PD as immunotherapy nonresponse.

The IC50 values of 88 common chemotherapy and targeted drugs were analyzed using the pRRophetic package to study the sensitivity of different APGPI groups to different drugs.

Statistical analysis

The TMB is obtained by processing the PERL programming language (v5.32.1). All data were analyzed in R language (R version 4.1.0). The Spearman method was used for correlation analysis, and the Wilcoxon test was used to analyze the differences between different ARGPI groups. Comparison of the distribution of CMS in different ARGPI groups by chi-square test. $P<0.05$ represents statistical significance.

Result

Construction and verification of ARGPI in COAD

First, we determined the somatic mutation of 35 ARG in COAD. As shown in Figure 1A, 167 of the 433 COAD samples had somatic mutations, of which VCAN was the ARG with the highest somatic mutation frequency (10%), followed by COLA5A and POSTN. Second, we obtained 471 COAD tissues and 41 normal tissues from TCGA, and identified 9 differentially expressed ARG (DEARG), including 8 up-regulated DEARG and 1 down-regulated DEARG. The associated heatmaps and volcano maps are shown in Figures 1B, C.

To identify prognostic genes affecting COAD survival, we performed a univariate Cox regression analysis of OS for 9 DEARGs. The results showed that only three genes (VEGFA, JAG2, and TIMP1) significantly affected OS in COAD patients (Figures 1D–G). We then constructed a prognostic index for all cancer samples based on the results of univariate Cox regression analysis (The detailed results of univariate Cox regression analysis are listed in Supplementary Table S1). ARGPI formula =coef of VEGFA*expression level of VEGFA+ coef of JAG2 * expression level of JAG2 + coef of TIMP1 * expression level of TIMP1. The COAD patients were divided into high ARGPI group and low ARGPI group by the median ARGPI value, and the results showed that the OS of the high ARGPI group was significantly lower than that of the low ARGPI group (Figure 1H).

The external cohort validation of ARGPI

In order to verify the stability and universality of ARGPI to guide prognosis. We first examined the expression of key ARGs using samples from the TRSJTUSM cohort. Univariate Cox regression model and Kaplan-Meier survival curve analysis showed that all three key ARGs significantly affected OS in CRC patients (Figures 2A–D). The ARGPI of the TRSJTUSM cohort was then constructed according to the above ARGPI formula. Similarly, CRC patients were divided into high-ARGPI group and low-ARGPI group according to the median ARGPI, and the results showed that the OS of the low-ARGPI group was significantly better than that of the high-ARGPI group (Figure 2E), which is consistent with the results of the TCGA-COAD dataset of. More importantly, consistent results were shown in GSE39582 and GSE161158, with significantly lower OS in the high ARGPI group than in the low ARGPI group (Figures 2F, G). Finally, we validated the prognostic value of ARGPI in 32 cancer types, and the results showed that ARGPI exhibits potential prognostic value in 22 cancer types (Supplementary Figure 1).

Construction of a nomogram to predict the prognosis of patients with COAD

First, we fitted into the clinicopathological features of COAD patients. Univariate Cox regression analysis showed that tumor stage and ARGPI were significantly associated with prognosis in COAD (Figure 3A). Multivariate Cox regression analysis confirmed that tumor stage and ARGPI were independent prognostic factors affecting COAD patients after adjusting for other clinicopathological factors (Figure 3B). Furthermore, we validated this conclusion in the TRSJTUSM cohort. Results show that tumor stage and ARGPI are independent prognostic factors for colorectal cancer patients (Supplementary Figures 2A, B). Due to the high correlation between ARGPI and patient prognosis, we constructed a nomogram combining clinical parameters. The nomograms we constructed were designed to assess 1-, 3-, and 5-year OS in COAD patients (Figure 3C). Calibration curves revealed a high consistency between the predicted values and actual values of nomograms for 1-, 3-, and 5-year OS in COAD patients (Figure 3D). In addition, we analyzed the AUC values of the nomogram for predicting OS at 1-, 3-, and 5-years by ROC curves. As shown in Figure 3E, the nomogram showed excellent predictive power for predicting the prognosis of COAD patients at 1, 3, and 5 years (AUC values of 0.794, 0.799, and 0.738, respectively).

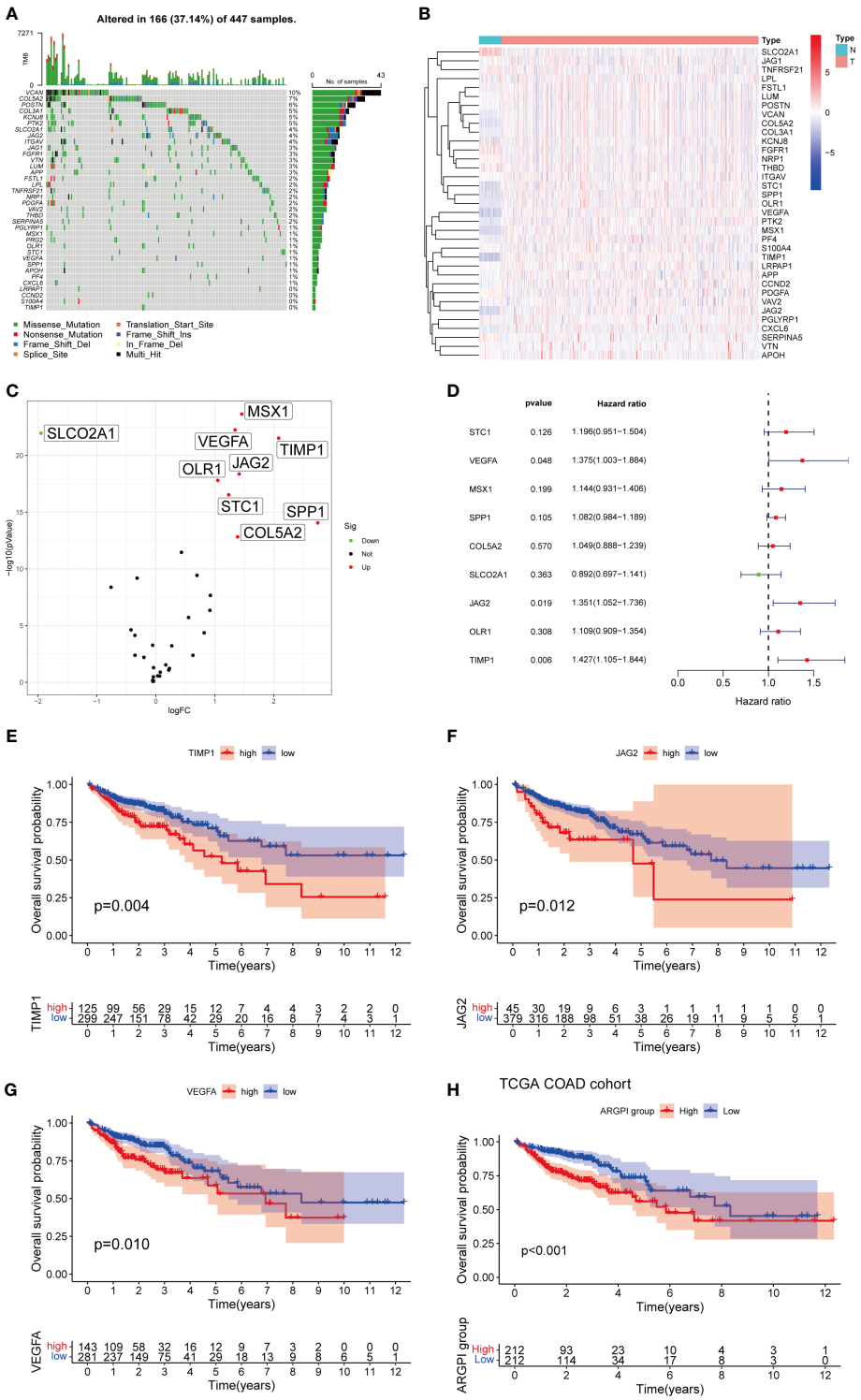

FIGURE 1
Construction of ARGPI. **(A)** 35 ARG mutation spectrum. **(B, C)** Heatmap and volcano plot of expression differences of 35 ARG between COAD and normal tissues. **(D)** Univariate Cox Analysis of 10 DEARG. **(E–G)** Kaplan-Meier survival analysis of three significant ARG in univariate Cox analysis. **(H)** Kaplan-Meier survival analysis of ARGPI subgroups in the TCGA-COAD cohort.

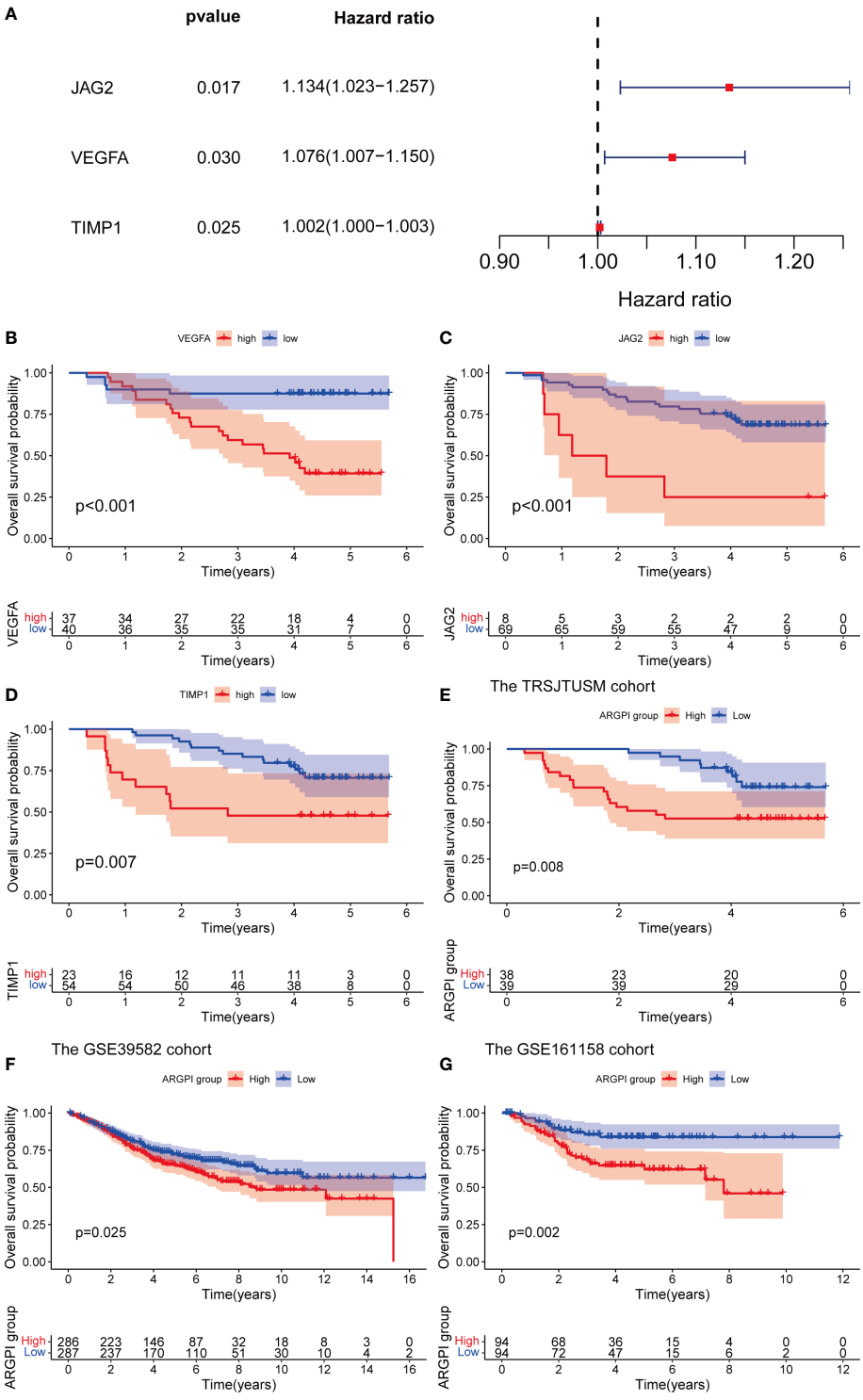

FIGURE 2
Verification of ARGPI. **(A)** Univariate Cox Analysis of JAG2, VEGFA and TIMP1 in TRSJTUSM Cohort. **(B–D)** Kaplan-Meier survival analysis of JAG2, VEGFA and TIMP1 in TRSJTUSM Cohort. **(E)** Kaplan-Meier survival analysis of ARGPI subgroups in the TRSJTUSM cohort. **(F)** Kaplan-Meier survival analysis of ARGPI subgroups in the GSE39582 cohort. **(G)** Kaplan-Meier survival analysis of ARGPI subgroups in the GSE161158 cohort.

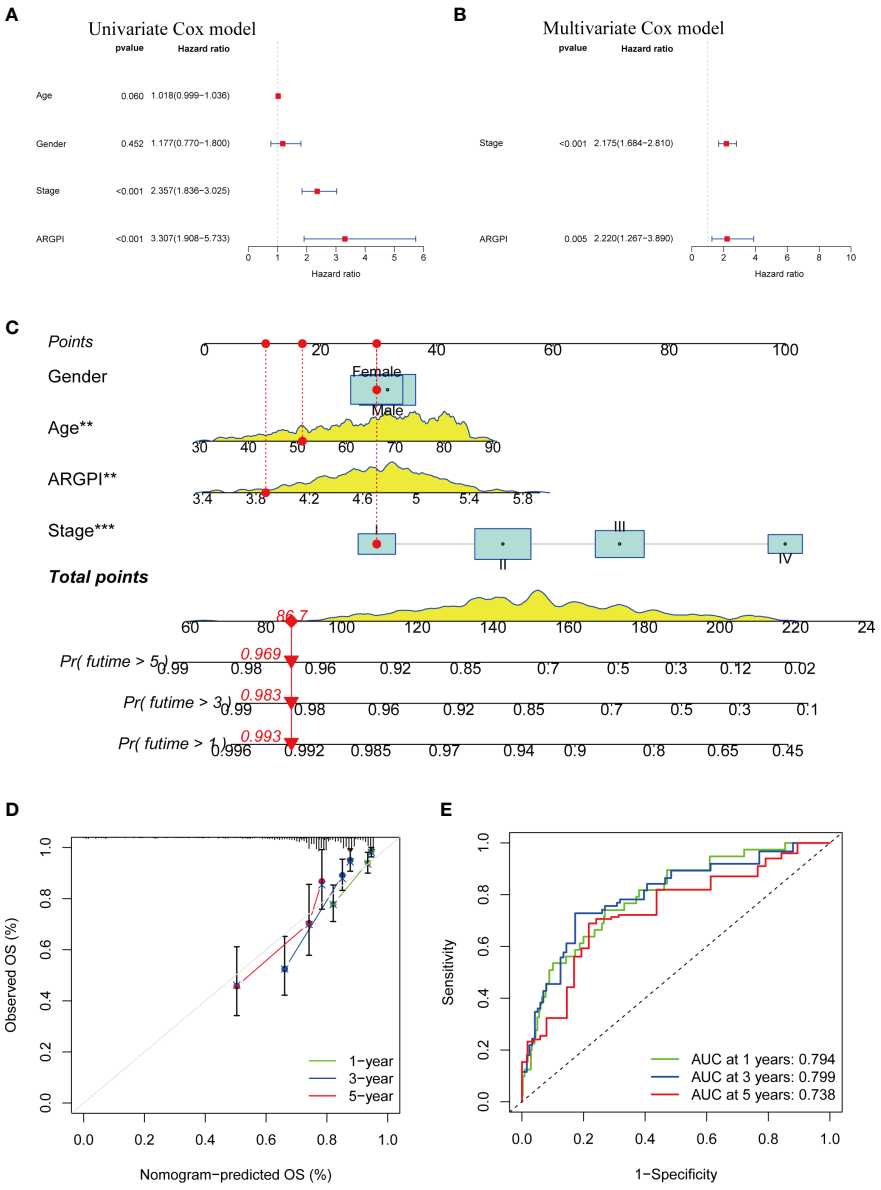

FIGURE 3
Construction of a nomogram. **(A, B)** Univariate and multivariate Cox analysis of clinicopathological factors and ARGPI in TCGA-COAD Cohort. **(C)** A nomogram based on ARGPI and clinicopathological factors to indicate OS in COAD patients. **(D, E)** Calibration curves and ROC curves were used to assess the robustness and accuracy of nomograms in predicting 1-, 3-, and 5-year OS in COAD patients. ** $p < 0.01$, and *** $p < 0.001$.

GSEA

To gain insight into the biological processes and signal transduction pathways that ARGPI may affect in COAD, we divided patients into high and low ARGPI groups with median ARGPI values and performed GSEA. First, we explored the biological process by which ARGPI might affect COAD, and the results showed that the BPs involved in the high ARGPI group were mainly enriched in GOBP ADAPTIVE IMMUNE RESPONSE, GOBP BLOOD VESSEL MORPHOGENESIS, GOBP CELL CHEMOTAXIS, GOBP CELL SUBSTRATE ADHESION, GOBP COLLAGEN FIBRIL ORGANIZATION (Figure 4A). The BPs involved in the low ARGPI group were mainly enriched in GOBP DNA CONFORMATION CHANGE, GOBP NUCLEOSOME ASSEMBLY, GOCC CHROMOSOMAL REGION, GOCC CHROMOSOME CENTROMERIC REGION, GOCC DNA PACKAGING COMPLEX (Figure 4B). Second, we explored the signaling pathways by which ARGPI may affect

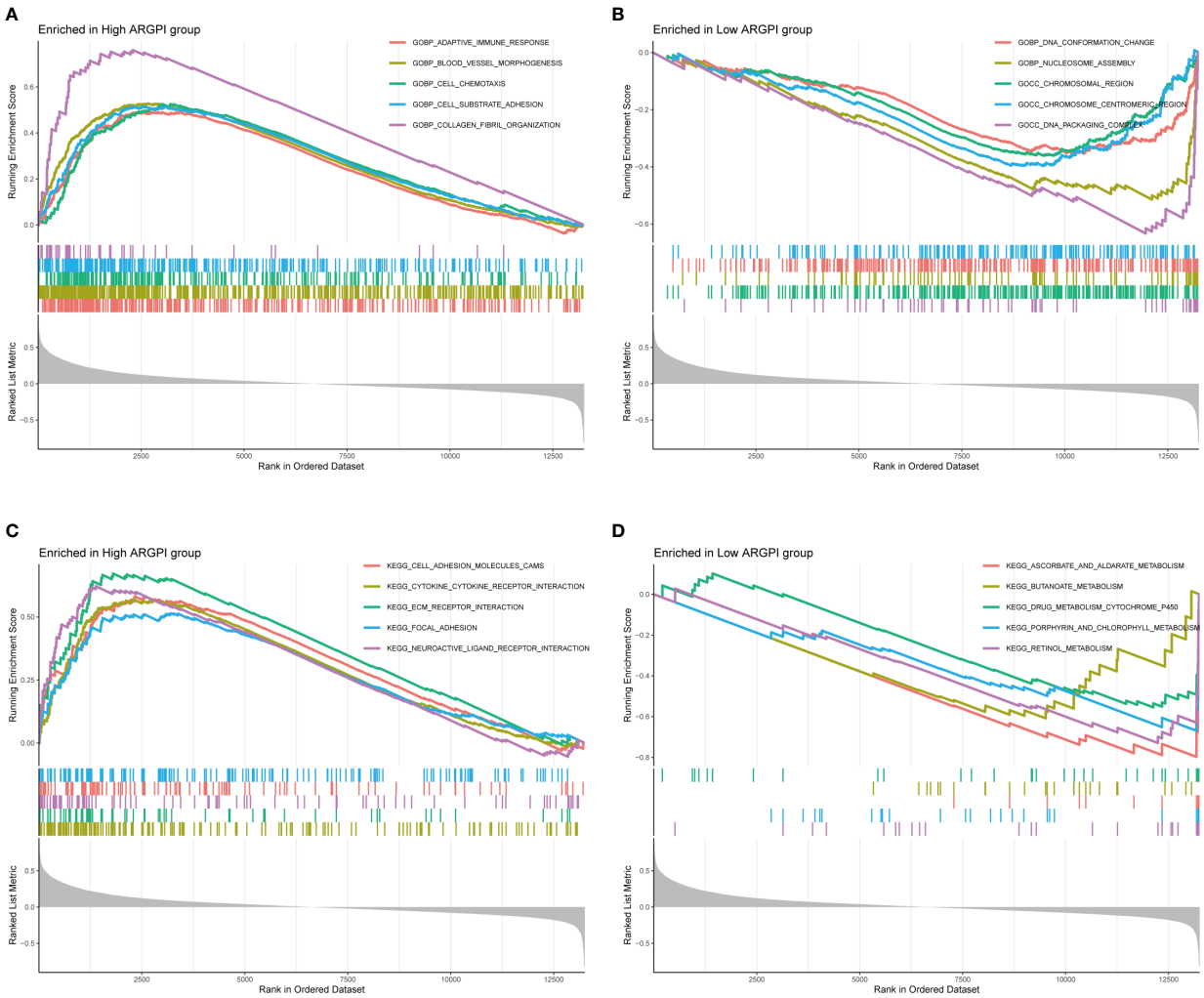

FIGURE 4
Gene Set Enrichment Analysis of ARGPI. **(A, B)** The 5 biological processes that were most significantly enriched in the high ARGPI group and the low ARGPI group, respectively. **(C, D)** The 5 signal pathways that were most significantly enriched in the high ARGPI group and the low ARGPI group, respectively.

COAD. The results showed that the signaling pathways affected by the high ARGPI group were mainly enriched in KEGG CELL ADHESION MOLECULES CAMS, KEGG CYTOKINE CYTOKINE RECEPTOR INTERACTION, KEGG ECM RECEPTOR INTERACTION, KEGG FOCAL ADHESION, KEGG NEUROACTIVE LIGAND RECEPTOR INTERACTION (Figure 4C). The signaling pathways affected by the low ARGPI group were mainly enriched in KEGG ASCORBATE AND ALDARATE METABOLISM, KEGG BUTANOATE METABOLISM, KEGG DRUG METABOLISM CYTOCHROME P450, KEGG PORPHYRIN AND CHLOROPHYLL METABOLISM, KEGG RETINOL METABOLISM (Figure 4D). Detailed results of GSEA are presented in Supplementary Table S2.

Correlation between ARGPI and immune cell infiltration

To determine whether ARGPI affects the level of immune cell infiltration in COAD samples, we assessed the infiltration levels of 64 immune-related cells in COAD samples using xCell. Using Spearman to analyze the correlation of ARGPI with immune cell infiltration, the results showed that ARGPI was associated with 45 out of 64 immune cell types ($p < 0.05$), including a positive correlation with 27 immune cell infiltration and 18 immune cell infiltration was negatively correlated (Figure 5A). Among them, Mesenchymal stem cell (MSC) were the immune cells with the strongest correlation with ARGPI (Figure 5B), followed by Pericytes (Figure 5C), mv

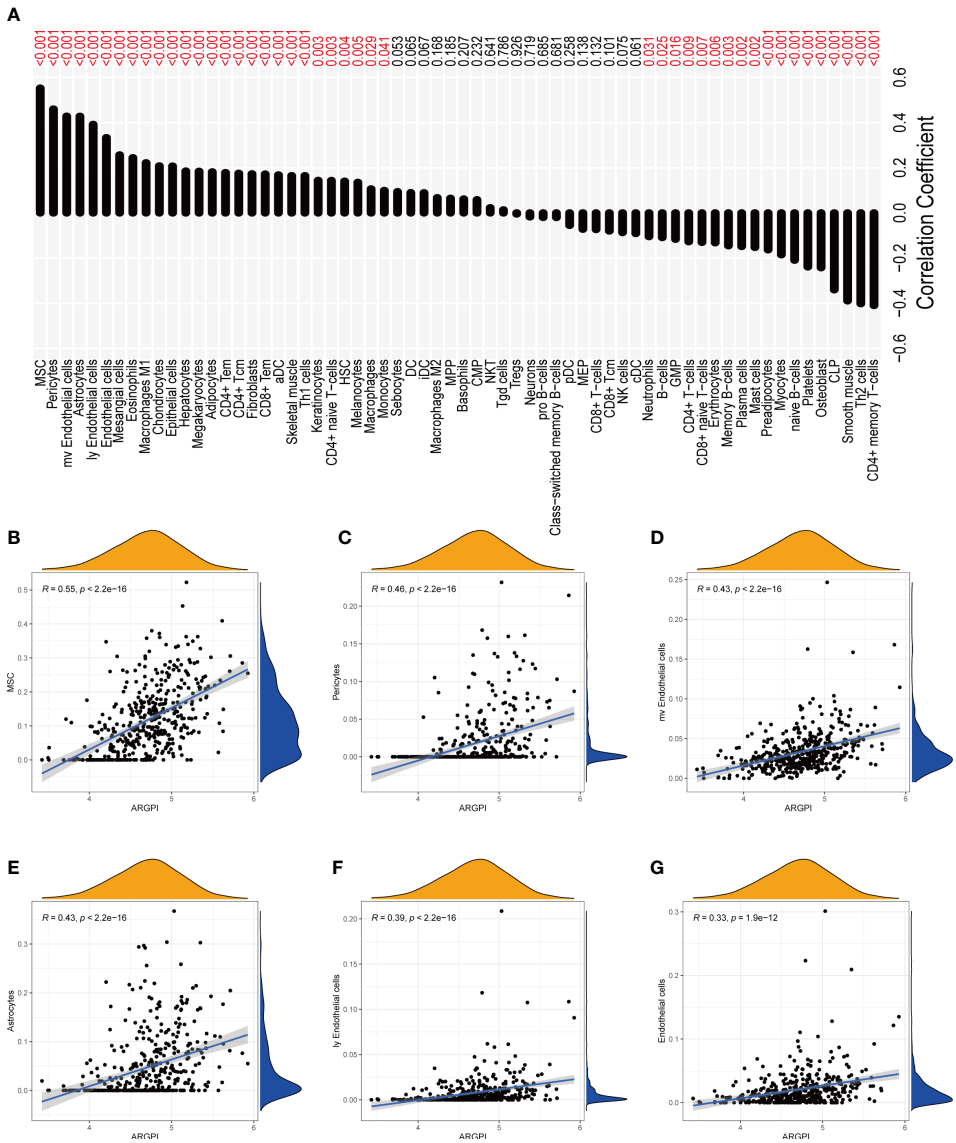

FIGURE 5
Correlation between ARGPI and immune cell infiltration. **(A)** Correlation histogram of ARGPI with 64 kinds of immune cells and stromal cells. **(B–G)** Scatter plot of 6 immune cell correlations most significantly associated with ARGPI.

Endothelial cells (Figure 5D), Astrocytes (Figure 5E), ly Endothelial cells (Figure 5F), Endothelial cells (Figure 5G).

Correlation between ARGPI and CMS

Previous studies have shown that COAD patients can be classified into 4 CMS. In short, CMS1 is known as the "MSI-like" subtype. CMS2 is known as the "Canonical" subtype. CMS3 is known as the "Metabolic" subtype. CMS4 is known as the "mesenchymal" subtype (13). We obtained the classification of consensus molecular subgroups of GSE39582 from previous studies, and further analyzed the distribution between ARGPI groupings and CMS, as shown in Figure 6A, there were significantly more CMS1 and CMS4 in the high ARGPI group than in the low ARGPI group, especially CMS4. While the low ARGPI group had significantly more CMS2 and CMS3 than the high ARGPI group. In addition, we also analyzed the prognosis in different CMS groups, and the results showed that the prognosis of the CMS4 phenotype

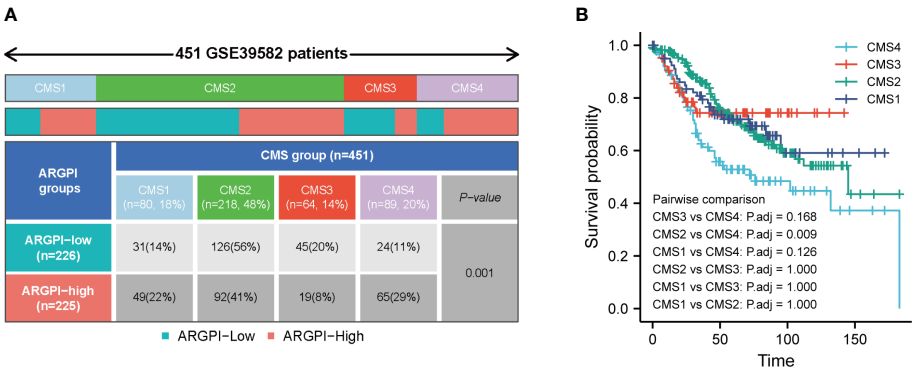

FIGURE 6
Distribution of consensus molecular subtypes (CMS) in different ARGPI subgroups **(A)** and prognostic analysis of CMS **(B)**.

was significantly worse, especially relative to the CMS2 phenotype (Figure 6B).

Association of ARGPI with PDL1, TMB, MSI and TIDE scores

Numerous studies have shown that PDL1, TMB and Microsatellite instability (MSI) are important predictors of immunotherapy response (21). First, we explored the gene mutation between different ARGPI groups, as shown in Figures 7A, B, we showed the 10 most easily mutated genes in different ARGPI groups. The mutation rates of APC, TP53, TTN and KRAS were higher than 40% in both groups. TP53, RYR2 and ZFHX4 were more common in the high ARGPI group. DNAH5 and OBSCN were more common in the low ARGPI group. We next discussed the association between ARGPI and PDL1 and TMB, and the results showed that ARGPI was not significantly correlated with neither PDL1 nor TMB (Figures 7C, D). Finally, we evaluated the potential clinical benefit of immunotherapy in different ARGPI groups by using TIDE. A lower TIDE score represents a lower possibility of immune evasion. That is, the lower the TIDE score, the greater the benefit of the patient from immune checkpoint inhibitor (ICI) treatment. In our results, the TIDE score in the low ARGPI group was significantly lower than that in the high ARGPI group (Figure 7E), implying that patients in the low ARGPI group had a higher clinical benefit from ICI than those in the high ARGPI group. In addition, compared with the high ARGPI group, patients in the low ARGPI group had higher MSI scores (Figure 7F) and lower cancer-associated fibroblasts (CAF), Exclusion, and Dysfunction (Figures 7G–I). However, there was no significant difference in Myeloid-derived suppressor cell (MDSC) between the two groups (Figure 7J).

Benefits of ICI therapy in different ARGPI subgroups

Inhibition of immune checkpoints using anti-PD1 and anti-CTLA4 monoclonal antibodies has become a mainstay option in anticancer therapy with unprecedented (22–24). Next, we explored the prognostic value of ARGPI for ICI therapy by combining the IMvigor210 and GSE78220 cohorts to assess clinical benefit. In the IMvigor210 cohort, the prognosis was worse in the high ARGPI group (Figure 8A), which is consistent with the results of the COAD cohort. The ROC curve of ARGPI in predicting OS of patients in IMvigor210 showed certain accuracy, with AUCs of 0.487, 0.571 and 0.600 for predicting OS at 6 months, 12 months and 18 months, respectively (Figure 8B). In addition, significantly more patients responded to ICI treatment in the low ARGPI group (Figure 8C). Likewise, the ARGPI was significantly lower in the ICI response group than in the ICI nonresponse group (Figure 8D). The results obtained based on IMvigor210 were further confirmed in GSE78220. First, patients in the high ARGPI group had a worse prognosis (Figure 8E), and the ROC curve for predicting patient OS in GSE78220 showed higher accuracy, with AUCs of 0.831, 0.699, and 0.761 for predicting OS at 6, 12, and 18 months, respectively (Figure 8F). Likewise, fewer patients responded to ICI treatment in the high ARGPI group (Figure 8G), and ARGPI was lower in the ICI response group (Figure 8H). Taken together, our data strongly suggests that ARGPI has a strong ability to assess response to ICI therapy.

Drug sensitivity analysis

Chemotherapy and targeted therapy are also important treatment strategies for patients with metastatic CRC (25, 26). Therefore, to understand whether ARGPI could serve as an

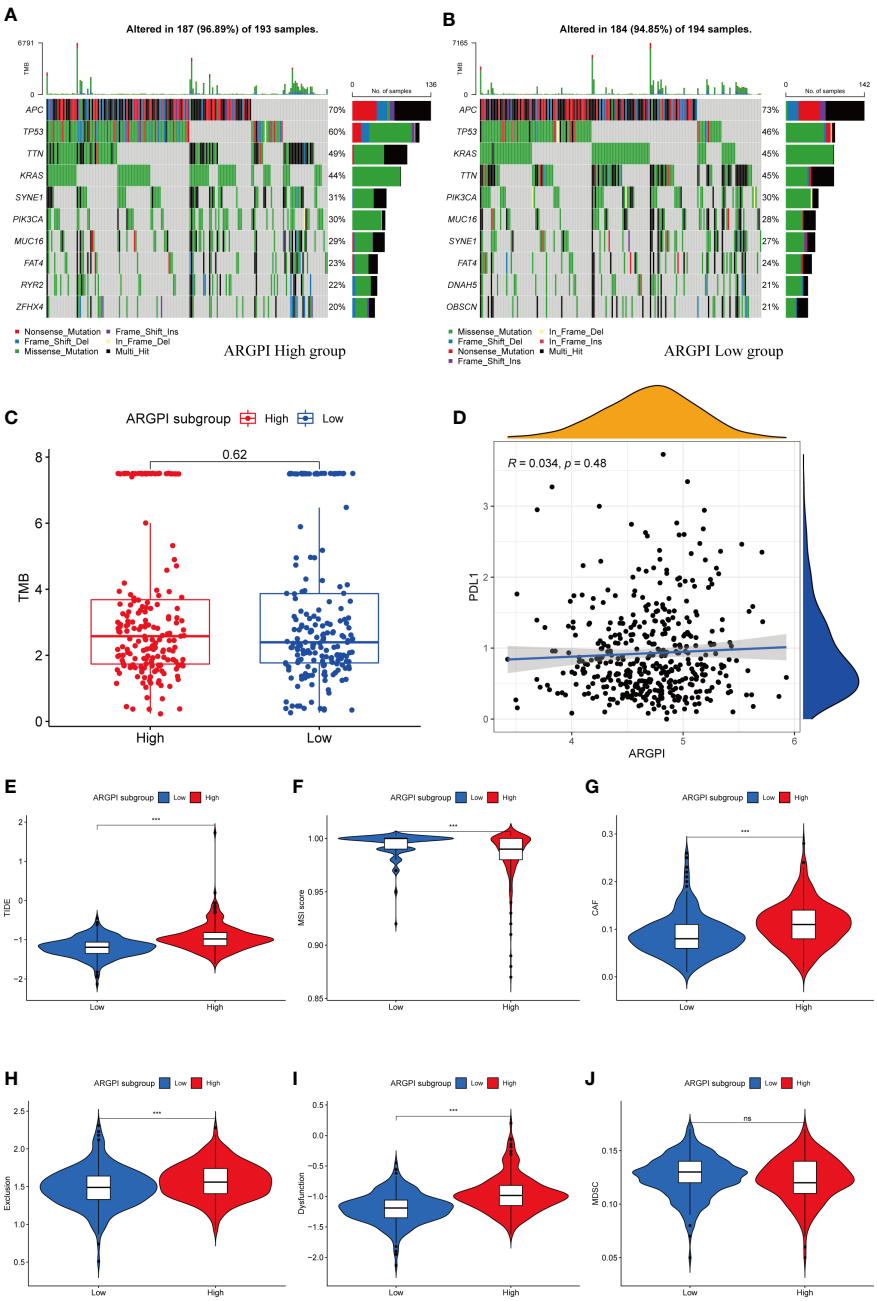

FIGURE 7
Association of ARGPI with markers for predicting ICI response. **(A, B)** The 10 most mutated genes in TCGA-COAD samples in the high and low ARGPI groups. **(C)** Differences in TMB in different ARGPI groups. **(D)** Correlation between ARGPI and PDL1 expression. **(E–J)** TIDE, MSI score, CAF, T-cell Exclusion and dysfunction scores, and MDSC in different ARGPI groups. "ns" represents not significant and "***" represents p < 0.001.

ability to predict sensitivity to chemotherapy and targeted therapy in COAD patients, we assessed IC50 values for 88 common drugs in TCGA-COAD patients using the pRRophetic package. We found that COAD patients with different ARGPI groups had significantly different IC50s for 51 drugs (Supplementary Table 3). We show differences in the sensitivity of 20 common chemotherapy/targeted agents across different ARGPI groups. The low ARGPI group may be more sensitive to drugs such as Cisplatin, Doxorubicin, Gemcitabine, Lapatinib and AKT.inhibitor.VIII (Figures 9A–E). The high ARGPI group may be more sensitive to drugs such as Imatinib, Dasatinib, Elesclomol, Docetaxel, Bosutinib,

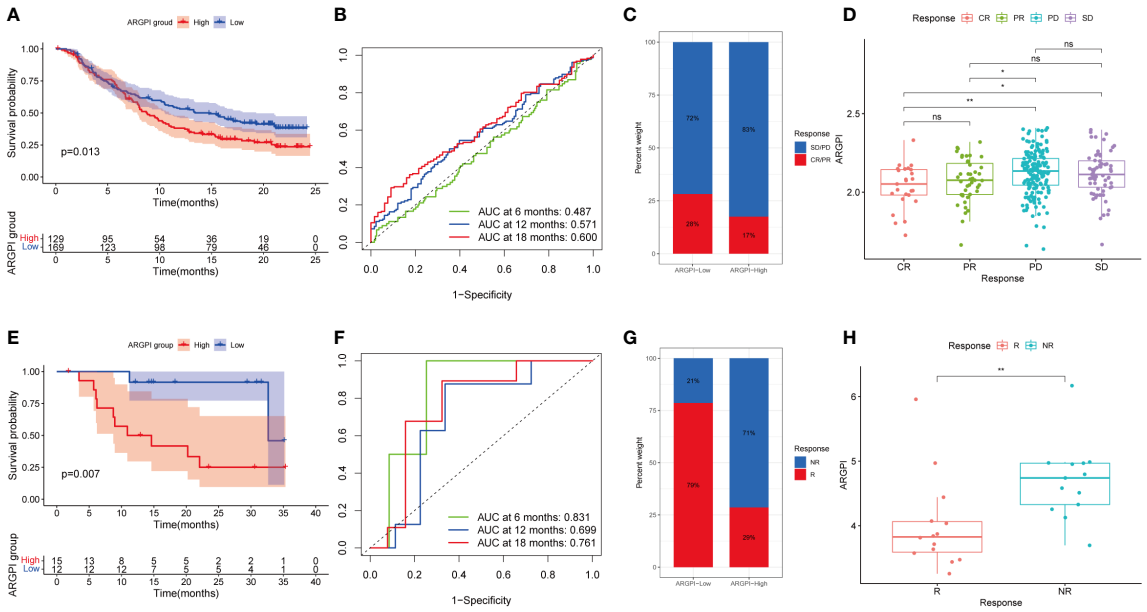

FIGURE 8
Validation of ARGPI ability to predict therapeutic benefit in ICI therapy. **(A)** Kaplan-Meier survival analysis of ARGPI subgroups in the IMvigor210 cohort. **(B)** ROC analysis of OS with ARGPI at 6-, 12- and 18-months follow-up in the IMvigor210 cohort. **(C)** Clinical response rates to ICI immunotherapy in the high and low ARGPI groups in the IMvigor210 cohort. **(D)** ARGPI distribution in different ICI immunotherapy clinical response status groups in the IMvigor210 cohort. **(E)** Kaplan-Meier survival analysis of ARGPI subgroups in the GSE78220 cohort. **(F)** ROC analysis of OS with ARGPI at 6-, 12- and 18-months follow-up in the GSE78220 cohort. **(G)** Clinical response rates to ICI immunotherapy in the high and low ARGPI groups in the GSE78220 cohort. **(H)** ARGPI distribution in different ICI immunotherapy clinical response status groups in the GSE78220 cohort. "ns" represents not significant, "*" represents $p < 0.05$ and "**" represents $p < 0.01$.

Paclitaxel, and PLX4720 (Figures 9F–L). Overall, ARGPIs were strongly associated with drug sensitivity.

Discussion

Current studies have fully demonstrated the critical role of angiogenesis in promoting tumor growth and metastasis (27, 28). Pro-angiogenic-related factors not only promote pathological angiogenesis in cancer, but also lead to immunosuppression (27). Conversely, innate and adaptive immune cells regulate angiogenesis in the tumor microenvironment (TME) by producing and releasing numerous pro-angiogenic factors (27, 29). Unfortunately, the clinical benefit of antiangiogenic agents alone in CRC patients is limited (30). Given that angiogenesis and immune microenvironment are closely related and cross-talk, combination therapy based on classical anti-angiogenic therapy and ICI therapy, which has achieved major breakthroughs in the field of cancer treatment, has received extensive clinical attention (31–34). At present, a small number of studies have begun to focus on the clinical application of anti-angiogenic agents and ICIs in CRC (35). However, effective predictive markers based on angiogenesis-related factors for treatment selection in patients with COAD have not yet been developed. Therefore, the necessity and urgency of exploring ARG as prognostic markers and therapeutic targets in COAD patients is more prominent. In this study, we analyzed the DEARG on the basis of the TCGA-COAD cohort, we obtained 9 DEARG, and further univariate Cox regression model determined that three genes were influencing prognostic factors for OS in COAD patients, and ARGPI was constructed based on these three genes. In the TCGA-COAD, GSE39582, GSE161158 and the TRSJTUSM cohorts, survival was lower in the high ARGPI group and higher in the low ARGPI group. Finally, we validated the prognostic value of ARGPI in 22 cancers by Kaplan-Meier survival curves, although it showed consistent prognostic value with COAD in 15 cancer types, which may suggest that ARGPI may play different roles in different tumors. In conclusion, ARGPI is a good prognostic marker for predicting COAD OS.

ARGPI consists of three genes, VEGFA, JAG2 and TIMP1. VEGFA is one of the main factors driving tumor vascular bed expansion and is significantly upregulated in hypoxia (36). In addition, VEGFA is also associated with antitumor immune responses. VEGFA induces T cell depletion in anti-PD-1-resistant microsatellite stable CRC patients (37). Meanwhile, the first approved angiogenesis inhibitor, bevacizumab, a

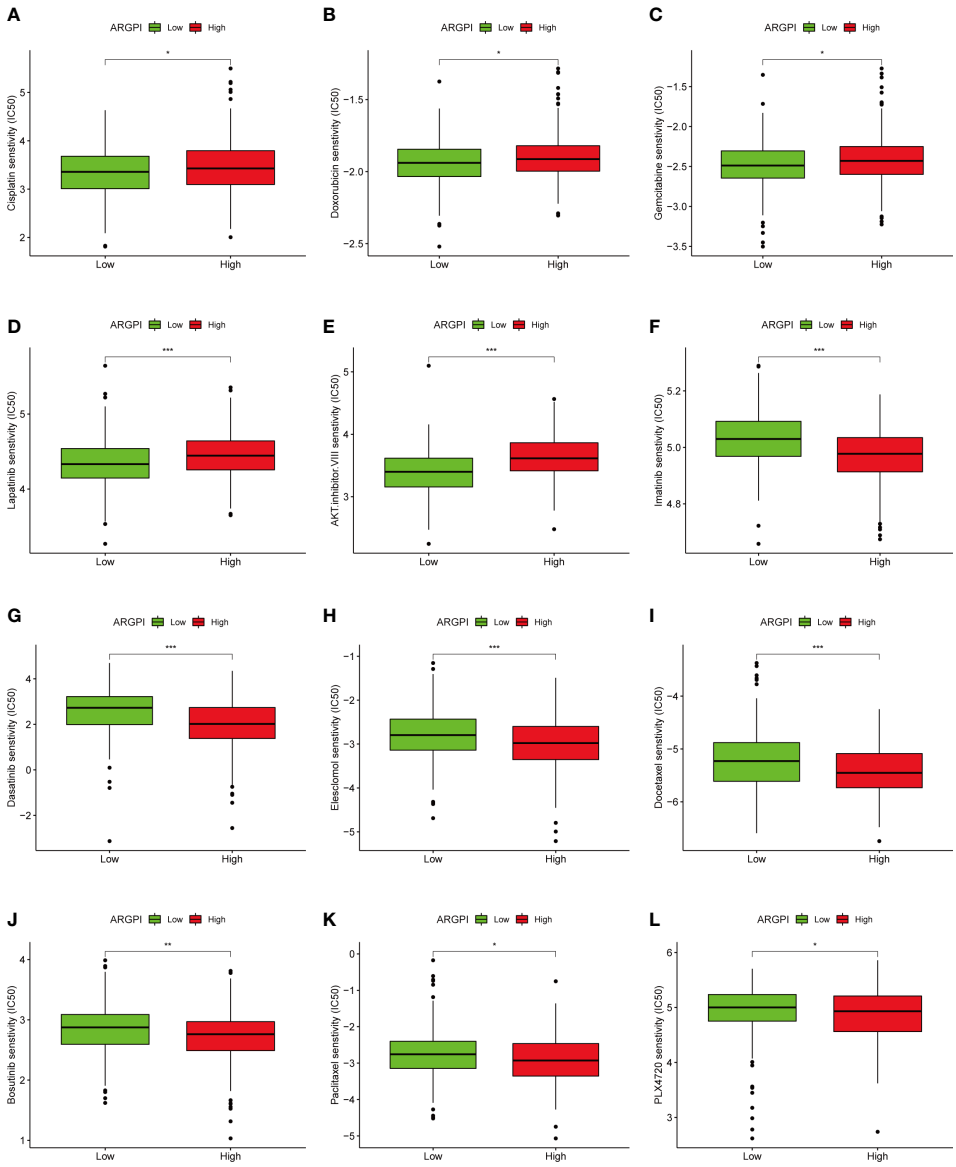

FIGURE 9
The relationship between ARGPI and treatment sensitivity. **(A–L)** Differences in sensitivity of 12 common drugs among different ARGPI groups. "*" represents $p < 0.05$, "**" represents $p < 0.01$, and "***" represents $p < 0.001$.

VEGFA-targeting monoclonal antibody, was initially approved in combination with chemotherapy for the treatment of metastatic CRC (38). Bevacizumab combined with ICI drugs has shown promising preliminary clinical benefits in RCC and NSCLC and is further suitable for patients with CRC with stable microsatellites (39). JAG2 is a transmembrane ligand of the Notch receptor and up-regulated activates the cancer-related Notch signaling pathway (40, 41). Notch signaling can promote and cancer stem cell (CSC) maintenance through crosstalk with VEGF receptors to regulate angiogenesis and influence the TME (41, 42). It has been shown that JAG2 acts as a prognostic factor for colon cancer (43) and is involved in regulating colon cancer cell migration and invasion (44). TIMP1 is a member of the TIMP family with multiple functions (45), and its role in cancer has been controversial (46). Studies have shown that TIMP1 can inhibit apoptosis and promote colon cancer occurrence and metastasis through FAK-PI3K/AKT and MAPK pathways (47). In the calculation formula of ARGPI, the coefficients of VEGFA, JAG2 and TIMP1 are all positive numbers, and ARGPI is positively correlated with VEGFA, JAG2 and TIMP1. In conclusion, ARGPI is closely related to angiogenesis and the immune microenvironment.

After controlling for clinical confounding parameters, ARGPI was shown to be an independent risk factor for OS in COAD patients. Based on ARGPI, combined with clinicopathological parameters, we established a nomogram to predict the prognosis of COAD patients. We validated its accuracy and robustness for 1-, 3-, and 5-year OS prediction with calibration curves and ROC curves. In addition, it is particularly important that we provide an excellent biomarker for predicting OS in COAD patients.

In order to understand the BP and signal transduction pathways in different ARGPI subgroups, it was shown by GSEA that the high ARGPI group mainly related to BP related to angiogenesis and adaptive immunity, and mainly affected cancer-related signaling pathways. This strongly suggests that ARGPI closely links angiogenesis and immunology in COAD. Understanding the TME can help us find new biomarkers for COAD treatment. We first estimated the infiltration levels of 64 immune and stromal cells using the Xcell algorithm. Another important advantage of xCell is the efficient classification of immune cells related to innate and adaptive immunity (17). We found that most immune cell infiltration levels were closely related to ARGPI. Remarkably, we found a significant positive correlation between ARGPI and MSC, pericytes and endothelial cells. Current studies suggest that MSC play an important role in promoting neovascularization (48) and can differentiate into CAF after interacting with cancer cells (49). CAF have been shown to imply a poor prognosis in CRC and promote CSC maintenance and chemoresistance (50, 51). Interaction between pericytes and endothelial cells is a central process regulating blood vessel formation (52). Studies have shown that Tie2 expressed by pericytes controls angiogenesis (53). Furthermore, tumor-associated endothelial cell proliferation-induced angiogenesis is a key factor in carcinogenesis, including CRC (54). Our results imply that ARGPI may affect COAD progression by affecting these immune cells. In terms of COAD immune subtype classification, the high ARGPI group had significantly more CMS4 subtypes than the low ARGPI group, and significantly fewer CMS2 and CMS3 patients. Moreover, the prognosis of patients in the CMS4 subgroup was significantly worse, which may be one of the reasons for the poor prognosis of the AGGPI high expression group. This is consistent with the analysis results obtained from the immune cell correlation analysis.

Next, we explored the relationship between ARGPI and known predictors of immunotherapy response. Such as PDL1, TMB and MSI. In general, PDL1 expression is an effective marker of response to ICI therapy in some tumors, such as non-small cell lung cancer and urothelial carcinoma (55, 56), but is not a good predictor of ICI response in CRC (57). MSI status has been shown to be a strong predictor of response to ICI in CRC patients, and MSI-High means better response to ICI therapy (57). Likewise, TMB may also serve as an emerging biomarker for predicting ICI response in CRC patients (58). MSI-High often means higher TMB, but there is no clear correlation between the two (58). In this study, we first investigated the gene mutation spectrum of different ARGPI groups, and we found that the gene with the largest mutation difference between groups was TP53. The TP53 mutation in the high ARGPI group was significantly higher than that in the low ARGPI group. TP53 is one of the most frequently mutated genes in CRC and is associated with poor prognosis (59). This is consistent with our survival results. Furthermore, we found that ARGPI was not significantly associated with neither PDL1 nor TMB. Therefore, we further used the TIDE score to predict the treatment response of COAD patients to ICI. Interestingly, the different ARGPI groups reflected differences in the clinical benefit of ICI therapy. The low ARGPI group may have a better response to ICI treatment (lower TIDE score). In contrast, the low ARGPI group had higher MSI scores. High MSI may be one of the reasons why the low ARGPI group benefited more from ICI therapy. In addition, the high ARGPI group had higher CAF content and higher T cell Exclusion and Dysfunction scores. Therefore, higher ARGPI-induced immunosuppression may be related to excess CAF or to T cell exclusion and dysfunction. More importantly, we confirmed this notion in two immunotherapy cohorts (IMvigor210 cohort and the GSE78220 cohort). We first analyzed the prognostic value of ARGPI in these two treatment cohorts, and as with COAD, the high ARGPI group implied a worse prognosis. And in the low ARGPI group, the patients with ICI response were significantly higher than those in the high ARGPI group. Likewise, ARGPI scores were significantly lower in the ICI response group. Taken together, our results implicate ARGPI as a promising biomarker for COAD predicting ICI response, offering new possibilities for improving the outcome of immunotherapy in CRC.

5-Fluorouracil-based chemotherapy is the first-line chemotherapy drug for CRC, but the problem of drug resistance has become increasingly serious (60). Reuse of old drugs is an important strategy in the development of anti-tumor drugs, which has the advantages of cost saving and drug safety. This study identified potentially sensitive drugs in patients in different ARGPI groups. The combination of these drugs with anti-vascular survival agents and ICI therapy may help to improve the efficacy of treatment and reduce the occurrence of drug resistance.

Although our model is beneficial for assessing patient prognosis and guiding clinical personalized treatment, there are still shortcomings. For example, TCGA-COAD has fewer clinical factors, and more clinical factors should be included in the future to fully explore the clinical value of ARGPI. It is necessary to conduct extensive prospective studies in the future to gain an in-depth understanding of the prognostic value and therapeutic guidance value of ARGPI in COAD.

Conclusions

In conclusion, for the first time, we have established a risk model of genetic angiogenesis that can accurately predict the prognosis of COAD patients and analyzed the correlation with TME. ARGPI may be a promising biomarker to guide personalized treatment of COAD. Furthermore, ARGPI consists of only three genes, making it easier to obtain and calculate.

Data availability statement

The original contributions presented in the study are included in the article/Supplementary Material. Further inquiries can be directed to the corresponding authors.

Ethics statement

The studies involving human participants were reviewed and approved by The Ethics Committee of Tongren Hospital, Shanghai Jiao Tong University School of Medicine. The patients/participants provided their written informed consent to participate in this study. Written informed consent was obtained from the individual(s) for the publication of any potentially identifiable images or data included in this article.

Author contributions

HP, YC, and WS were responsible for the design of the study. WS, YX, and BZ wrote and completed the manuscript. BZ, MZ, and JC were responsible for data download and analysis. All authors contributed to the article and agreed to the submitted version.

Funding

This study was funded by the Shanghai Natural Science Foundation (No. 21ZR1458600) and the Shanghai Jiaotong University Medical-Engineering Cross Research Fund (No. YG2022ZD031).

Conflict of interest

The authors declare that the research was conducted in the absence of any commercial or financial relationships that could be construed as a potential conflict of interest.

Publisher's note

All claims expressed in this article are solely those of the authors and do not necessarily represent those of their affiliated organizations, or those of the publisher, the editors and the reviewers. Any product that may be evaluated in this article, or claim that may be made by its manufacturer, is not guaranteed or endorsed by the publisher.

Supplementary material

The Supplementary Material for this article can be found online at: https://www.frontiersin.org/articles/10.3389/fonc.2022.1003440/full#supplementary-material

SUPPLEMENTARY FIGURE 1
Kaplan-Meier survival analysis of ARGPI in 32 cancer types.

SUPPLEMENTARY FIGURE 2
(A) Univariate Cox analysis of clinicopathological factors and ARGPI in TRSJTUSM Cohort. **(B)** Multivariate Cox analysis of clinicopathological factors and ARGPI in TRSJTUSM Cohort.

References

1. Sung H, Ferlay J, Siegel RL, Laversanne M, Soerjomataram I, Jemal A, et al. Global cancer statistics 2020: Globocan estimates of incidence and mortality worldwide for 36 cancers in 185 countries. *CA: Cancer J Clin* (2021) 71(3):209–49. doi: 10.3322/caac.21660

2. Brenner H, Kloor M, Pox CP. Colorectal cancer. *Lancet (London England)* (2014) 383(9927):1490–502. doi: 10.1016/s0140-6736(13)61649-9

3. Dekker E, Tanis PJ, Vleugels JLA, Kasi PM, Wallace MB. Colorectal cancer. *Lancet (London England)* (2019) 394(10207):1467–80. doi: 10.1016/s0140-6736(19)32319-0

4. Folkman J. Angiogenesis. *Annu Rev Med* (2006) 57:1–18. doi: 10.1146/annurev.med.57.121304.131306

5. Viallard C, Larrivée B. Tumor angiogenesis and vascular normalization: Alternative therapeutic targets. *Angiogenesis* (2017) 20(4):409–26. doi: 10.1007/s10456-017-9562-9

6. Wang Z, Dabrosin C, Yin X, Fuster MM, Arreola A, Rathmell WK, et al. Broad targeting of angiogenesis for cancer prevention and therapy. *Semin Cancer Biol* (2015) 35 Suppl(Suppl):S224–s43. doi: 10.1016/j.semcancer.2015.01.001

7. Jászai J, Schmidt MHH. Trends and challenges in tumor anti-angiogenic therapies. *Cells* (2019) 8(9):1102. doi: 10.3390/cells8091102

8. Al-Abd AM, Alamoudi AJ, Abdel-Naim AB, Neamatallah TA, Ashour OM. Anti-angiogenic agents for the treatment of solid tumors: Potential pathways, therapy and current strategies - a review. *J advanced Res* (2017) 8(6):591–605. doi: 10.1016/j.jare.2017.06.006

9. Ramjiawan RR, Griffioen AW, Duda DG. Anti-angiogenesis for cancer revisited: Is there a role for combinations with immunotherapy? *Angiogenesis* (2017) 20(2):185–204. doi: 10.1007/s10456-017-9552-y

10. Ansari MJ, Bokov D, Markov A, Jalil AT, Shalaby MN, Suksatan W, et al. Cancer combination therapies by angiogenesis inhibitors; a comprehensive review.

Cell communication Signaling CCS (2022) 20(1):49. doi: 10.1186/s12964-022-00838-y

11. Yi M, Zheng X, Niu M, Zhu S, Ge H, Wu K. Combination strategies with pd-1/Pd-L1 blockade: Current advances and future directions. *Mol Cancer* (2022) 21 (1):28. doi: 10.1186/s12943-021-01489-2

12. Qing X, Xu W, Liu S, Chen Z, Ye C, Zhang Y. Molecular characteristics, clinical significance, and cancer immune interactions of angiogenesis-associated genes in gastric cancer. *Front Immunol* (2022) 13:843077. doi: 10.3389/fimmu.2022.843077

13. Guinney J, Dienstmann R, Wang X, de Reyniès A, Schlicker A, Soneson C, et al. The consensus molecular subtypes of colorectal cancer. *Nat Med* (2015) 21 (11):1350–6. doi: 10.1038/nm.3967

14. Mariathasan S, Turley SJ, Nickles D, Castiglioni A, Yuen K, Wang Y, et al. Tgfβ attenuates tumour response to pd-L1 blockade by contributing to exclusion of T cells. *Nature* (2018) 554(7693):544–8. doi: 10.1038/nature25501

15. Sun W, Shen J, Liu J, Han K, Liang L, Gao Y. Gene signature and prognostic value of ubiquitin-specific proteases members in hepatocellular carcinoma and explored the immunological role of Usp36. *FBL* (2022) 27(6):190. doi: 10.31083/j.fbl2706190

16. Subramanian A, Tamayo P, Mootha VK, Mukherjee S, Ebert BL, Gillette MA, et al. Gene set enrichment analysis: A knowledge-based approach for interpreting genome-wide expression profiles. *Proc Natl Acad Sci USA* (2005) 102(43):15545–50. doi: 10.1073/pnas.0506580102

17. Aran D, Hu Z, Butte AJ. Xcell: Digitally portraying the tissue cellular heterogeneity landscape. *Genome Biol* (2017) 18(1):220. doi: 10.1186/s13059-017-1349-1

18. Mayakonda A, Lin DC, Assenov Y, Plass C, Koeffler HP. Maftools: Efficient and comprehensive analysis of somatic variants in cancer. *Genome Res* (2018) 28 (11):1747–56. doi: 10.1101/gr.239244.118

19. McNamara MG, Jacobs T, Lamarca A, Hubner RA, Valle JW, Amir E. Impact of high tumor mutational burden in solid tumors and challenges for biomarker application. *Cancer Treat Rev* (2020) 89:102084. doi: 10.1016/j.ctrv.2020.102084

20. Jiang P, Gu S, Pan D, Fu J, Sahu A, Hu X, et al. Signatures of T cell dysfunction and exclusion predict cancer immunotherapy response. *Nat Med* (2018) 24(10):1550–8. doi: 10.1038/s41591-018-0136-1

21. Rizzo A, Ricci AD, Brandi G. Pd-L1, tmb, msi, and other predictors of response to immune checkpoint inhibitors in biliary tract cancer. *Cancers (Basel)* (2021) 13(3):558. doi: 10.3390/cancers13030558

22. Curran MA, Montalvo W, Yagita H, Allison JP. Pd-1 and ctla-4 combination blockade expands infiltrating T cells and reduces regulatory T and myeloid cells within B16 melanoma tumors. *Proc Natl Acad Sci USA* (2010) 107 (9):4275–80. doi: 10.1073/pnas.0915174107

23. Duraiswamy J, Kaluza KM, Freeman GJ, Coukos G. Dual blockade of pd-1 and ctla-4 combined with tumor vaccine effectively restores T-cell rejection function in tumors. *Cancer Res* (2013) 73(12):3591–603. doi: 10.1158/0008-5472.can-12-4100

24. O'Donnell JS, Teng MWL, Smyth MJ. Cancer immunoediting and resistance to T cell-based immunotherapy. *Nat Rev Clin Oncol* (2019) 16(3):151–67. doi: 10.1038/s41571-018-0142-8

25. Aparicio J, Esposito F, Serrano S, Falco E, Escudero P, Ruiz-Casado A, et al. Metastatic colorectal cancer. first line therapy for unresectable disease. *J Clin Med* (2020) 9(12):3889. doi: 10.3390/jcm9123889

26. Ciombor KK, Bekaii-Saab T. A comprehensive review of sequencing and combination strategies of targeted agents in metastatic colorectal cancer. *oncologist* (2018) 23(1):25–34. doi: 10.1634/theoncologist.2017-0203

27. Albini A, Bruno A, Noonan DM, Mortara L. Contribution to tumor angiogenesis from innate immune cells within the tumor microenvironment: Implications for immunotherapy. *Front Immunol* (2018) 9:527. doi: 10.3389/fimmu.2018.00527

28. Hegde PS, Wallin JJ, Mancao C. Predictive markers of anti-vegf and emerging role of angiogenesis inhibitors as immunotherapeutics. *Semin Cancer Biol* (2018) 52(Pt 2):117–24. doi: 10.1016/j.semcancer.2017.12.002

29. Ribatti D, Crivellato E. Immune cells and angiogenesis. *J Cell Mol Med* (2009) 13(9a):2822–33. doi: 10.1111/j.1582-4934.2009.00810.x

30. Khan K, Cunningham D, Chau I. Targeting angiogenic pathways in colorectal cancer: Complexities, challenges and future directions. *Curr Drug Targets* (2017) 18(1):56–71. doi: 10.2174/1389450116666150325231555

31. Huinen ZR, Huijbers EJM, van Beijnum JR, Nowak-Sliwinska P, Griffioen AW. Anti-angiogenic agents - overcoming tumour endothelial cell anergy and improving immunotherapy outcomes. *Nat Rev Clin Oncol* (2021) 18(8):527–40. doi: 10.1038/s41571-021-00496-y

32. Khan KA, Kerbel RS. Improving immunotherapy outcomes with anti-angiogenic treatments and vice versa. *Nat Rev Clin Oncol* (2018) 15(5):310–24. doi: 10.1038/nrclinonc.2018.9

33. Hack SP, Zhu AX, Wang Y. Augmenting anticancer immunity through combined targeting of angiogenic and pd-1/Pd-L1 pathways: Challenges and opportunities. *Front Immunol* (2020) 11:598877. doi: 10.3389/fimmu.2020.598877

34. Song Y, Fu Y, Xie Q, Zhu B, Wang J, Zhang B. Anti-angiogenic agents in combination with immune checkpoint inhibitors: A promising strategy for cancer treatment. *Front Immunol* (2020) 11:1956. doi: 10.3389/fimmu.2020.01956

35. Kreidieh M, Mukherji D, Temraz S, Shamseddine A. Expanding the scope of immunotherapy in colorectal cancer: Current clinical approaches and future directions. *BioMed Res Int* (2020) 2020:9037217. doi: 10.1155/2020/9037217

36. Ferrara N. Vascular endothelial growth factor: Basic science and clinical progress. *Endocrine Rev* (2004) 25(4):581–611. doi: 10.1210/er.2003-0027

37. Kim CG, Jang M, Kim Y, Leem G, Kim KH, Lee H, et al. Vegf-a drives tox-dependent T cell exhaustion in anti-Pd-1-Resistant microsatellite stable colorectal cancers. *Sci Immunol* (2019) 4(41):eaay0555. doi: 10.1126/sciimmunol.aay0555

38. Garcia J, Hurwitz HI, Sandler AB, Miles D, Coleman RL, Deurloo R, et al. Bevacizumab (Avastin®) in cancer treatment: A review of 15 years of clinical experience and future outlook. *Cancer Treat Rev* (2020) 86:102017. doi: 10.1016/j.ctrv.2020.102017

39. Rahma OE, Hodi FS. The intersection between tumor angiogenesis and immune suppression. *Clin Cancer Res* (2019) 25(18):5449–57. doi: 10.1158/1078-0432.ccr-18-1543

40. Katoh M, Katoh M. Precision medicine for human cancers with notch signaling dysregulation (Review). *Int J Mol Med* (2020) 45(2):279–97. doi: 10.3892/ijmm.2019.4418

41. Pietras A, von Stedingk K, Lindgren D, Påhlman S, Axelson H. Jag2 induction in hypoxic tumor cells alters notch signaling and enhances endothelial cell tube formation. *Mol Cancer Res MCR* (2011) 9(5):626–36. doi: 10.1158/1541-7786.mcr-10-0508

42. Akil A, Gutiérrez-García AK, Guenter R, Rose JB, Beck AW, Chen H, et al. Notch signaling in vascular endothelial cells, angiogenesis, and tumor progression: An update and prospective. *Front Cell Dev Biol* (2021) 9:642352. doi: 10.3389/fcell.2021.642352

43. Yang X, Yan J, Jiang Y, Wang Y. An immune-related model based on inhba, Jag2 and Ccl19 to predict the prognoses of colon cancer patients. *Cancer Cell Int* (2021) 21(1):299. doi: 10.1186/s12935-021-02000-z

44. He W, Tang J, Li W, Li Y, Mei Y, He L, et al. Mutual regulation of Jag2 and Praf2 promotes migration and invasion of colorectal cancer cells uncoupled from epithelial-mesenchymal transition. *Cancer Cell Int* (2019) 19:160. doi: 10.1186/s12935-019-0871-5

45. Justo BL, Jasiulionis MG. Characteristics of Timp1, Cd63, and B1-integrin and the functional impact of their interaction in cancer. *Int J Mol Sci* (2021) 22 (17):9319. doi: 10.3390/ijms22179319

46. Grünwald B, Schoeps B, Krüger A. Recognizing the molecular multifunctionality and interactome of timp-1. *Trends Cell Biol* (2019) 29(1):6–19. doi: 10.1016/j.tcb.2018.08.006

47. Song G, Xu S, Zhang H, Wang Y, Xiao C, Jiang T, et al. Timp1 is a prognostic marker for the progression and metastasis of colon cancer through fak-Pi3k/Akt and mapk pathway. *J Exp Clin Cancer Res CR* (2016) 35(1):148. doi: 10.1186/s13046-016-0427-7

48. Guillamat-Prats R. The role of msc in wound healing, scarring and regeneration. *Cells* (2021) 10(7):1729. doi: 10.3390/cells10071729

49. Quante M, Tu SP, Tomita H, Gonda T, Wang SS, Takashi S, et al. Bone marrow-derived myofibroblasts contribute to the mesenchymal stem cell niche and promote tumor growth. *Cancer Cell* (2011) 19(2):257–72. doi: 10.1016/j.ccr.2011.01.020

50. Ren J, Ding L, Zhang D, Shi G, Xu Q, Shen S, et al. Carcinoma-associated fibroblasts promote the stemness and chemoresistance of colorectal cancer by transferring exosomal lncrna H19. *Theranostics* (2018) 8(14):3932–48. doi: 10.7150/thno.25541

51. Kobayashi H, Gieniec KA, Lannagan TRM, Wang T, Asai N, Mizutani Y, et al. The origin and contribution of cancer-associated fibroblasts in colorectal carcinogenesis. *Gastroenterology* (2022) 162(3):890–906. doi: 10.1053/j.gastro.2021.11.037

52. Armulik A, Abramsson A, Betsholtz C. Endothelial/Pericyte interactions. *Circ Res* (2005) 97(6):512–23. doi: 10.1161/01.RES.0000182903.16652.d7

53. Teichert M, Milde L, Holm A, Stanicek L, Gengenbacher N, Savant S, et al. Pericyte-expressed Tie2 controls angiogenesis and vessel maturation. *Nat Commun* (2017) 8:16106. doi: 10.1038/ncomms16106

54. Chen WZ, Jiang JX, Yu XY, Xia WJ, Yu PX, Wang K, et al. Endothelial cells in colorectal cancer. *World J gastrointestinal Oncol* (2019) 11(11):946–56. doi: 10.4251/wjgo.v11.i11.946

55. Reck M, Rodríguez-Abreu D, Robinson AG, Hui R, Csőszi T, Fülöp A, et al. Updated analysis of keynote-024: Pembrolizumab versus platinum-based chemotherapy for advanced non-Small-Cell lung cancer with pd-L1 tumor proportion score of 50% or greater. *J Clin Oncol* (2019) 37(7):537–46. doi: 10.1200/jco.18.00149

56. Powles T, Walker J, Andrew Williams J, Bellmunt J. The evolving role of pd-L1 testing in patients with metastatic urothelial carcinoma. *Cancer Treat Rev* (2020) 82:101925. doi: 10.1016/j.ctrv.2019.101925

57. Le DT, Uram JN, Wang H, Bartlett BR, Kemberling H, Eyring AD, et al. Pd-1 blockade in tumors with mismatch-repair deficiency. *New Engl J Med* (2015) 372 (26):2509–20. doi: 10.1056/NEJMoa1500596

58. Schrock AB, Ouyang C, Sandhu J, Sokol E, Jin D, Ross JS, et al. Tumor mutational burden is predictive of response to immune checkpoint inhibitors in msi-high metastatic colorectal cancer. *Ann Oncol* (2019) 30(7):1096–103. doi: 10.1093/annonc/mdz134

59. Schulz-Heddergott R, Stark N, Edmunds SJ, Li J, Conradi LC, Bohnenberger H, et al. Therapeutic ablation of gain-of-Function mutant P53 in colorectal cancer inhibits Stat3-mediated tumor growth and invasion. *Cancer Cell* (2018) 34(2):298–314.e7. doi: 10.1016/j.ccell.2018.07.004

60. Kishore C, Bhadra P. Current advancements and future perspectives of immunotherapy in colorectal cancer research. *Eur J Pharmacol* (2021) 893:173819. doi: 10.1016/j.ejphar.2020.173819

frontiers | Frontiers in Oncology

TYPE Original Research
PUBLISHED 15 November 2022
DOI 10.3389/fonc.2022.961653

Check for updates

OPEN ACCESS

EDITED BY
Zhendong Jin,
Second Military Medical University, China

REVIEWED BY
Huihui Cao,
Southern Medical University, China
Liu Wenlong,
(NIH), United States
Lianhua Cui,
Qingdao University, China
Lihong Zhou,
Shanghai University of Traditional Chinese Medicine, China

*CORRESPONDENCE
Shenglan Yang
yangshenglan005@163.com

†These authors have contributed equally to this work

SPECIALTY SECTION
This article was submitted to Gastrointestinal Cancers: Colorectal Cancer, a section of the journal Frontiers in Oncology

RECEIVED 05 June 2022
ACCEPTED 25 October 2022
PUBLISHED 15 November 2022

CITATION
Li J, Zhou F, Shang L, Liu N, Liu Y, Zhang M, Wang S and Yang S (2022) Integrated network pharmacology and experimental verification to investigate the mechanisms of YYFZBJS against colorectal cancer *via* CDK1/PI3K/Akt signaling. *Front. Oncol.* 12:961653. doi: 10.3389/fonc.2022.961653

COPYRIGHT
© 2022 Li, Zhou, Shang, Liu, Liu, Zhang, Wang and Yang. This is an open-access article distributed under the terms of the Creative Commons Attribution License (CC BY). The use, distribution or reproduction in other forums is permitted, provided the original author(s) and the copyright owner(s) are credited and that the original publication in this journal is cited, in accordance with accepted academic practice. No use, distribution or reproduction is permitted which does not comply with these terms.

Integrated network pharmacology and experimental verification to investigate the mechanisms of YYFZBJS against colorectal cancer *via* CDK1/PI3K/Akt signaling

Jinxiao Li[1†], Fangyuan Zhou[1†], Luorui Shang[1†], Na Liu[2†], Yuhan Liu[1], Mengqi Zhang[1], Shuhan Wang[1] and Shenglan Yang[1,3*]

[1]Department of Integrated Traditional Chinese and Western Medicine, Union Hospital, Tongji Medical College, Huazhong University of Science and Technology, Wuhan, Hubei, China, [2]Rehabilitation Department of traditional Chinese Medicine, Union Red Cross Hospital, Wuhan, China, [3]Department of Clinical Nutrition, Union Hospital, Tongji Medical College, Huazhong University of Science and Technology, Wuhan, Hubei, China

Background: Colorectal cancer (CRC) is a common digestive tract malignancy with rising incidence and morbidity worldwide during recent years. Yi-Yi-Fu-Zi-Bai-Jiang-San (YYFZBJS), a traditional Chinese medicine formula, has showed positive effects against cancers. However, the mechanisms underlying its anticancer effects requires investigation.

Methods: Information on bioactive compounds, potential YYFZBJS targets, and CRC-associated genes, was obtained from public databases. The key targets and ingredients as well their corresponding signaling pathways were identified using bioinformatic approaches, including Kyoto encyclopedia of genes and genomes (KEGG) analyses, gene ontology (GO), and protein–protein interaction (PPI). Subsequently, molecular docking was used to verify the main compounds-targets. Potential YYFZBJS therapeutic effects against CRC were validated *in vitro* and *in vivo*.

Results: Using pharmacological network analysis, 40 YYFZBJS active compounds and 21 potential anti-CRC targets were identified. YYFZBJS was an important regulator of CRC through various targets and signaling pathways, particularly the cell cycle and PI3K/AKT pathway. Additionally, YYFZBJS suppressed the proliferation of CRC cells. Flow cytometry showed that YYFZBJS induced apoptosis and cell cycle arrest in the G2/M phase. Western blotting analysis indicated that YYFZBJS reduced the protein levels of CDK1, p-AKT, and p-PI3K, without altering total PI3K and AKT protein levels. *In vivo* analysis found that YYFZBJS inhibited tumor growth and PI3K/AKT signaling in a mouse model of CRC.

Conclusion: As predicted by network pharmacology and validated by the experimental results, YYFZBJS inhibited proliferation, induced apoptosis and arrested cell cycle progression in CRC by modulating the CDK1/PI3K/Akt signaling pathway.

KEYWORDS

YYFZBJS, colorectal cancer, network pharmacology, PI3K/Akt pathway, apoptosis, cell cycle

Introduction

Ranked as the 3rd leading malignant tumor globally, colorectal cancer (CRC) is considered a fatal disease with mortality rates. Among the symptoms of CRC patients, the most common are abdominal pain, anemia, and rectal bleeding (1). CRC accounts for about 10% of annual cancer diagnoses and deaths (2). The rise of CRC incidence is attributed to risk factors like ageing populations, obesity, dietary habits, and limited physical activity (1). CRC is treated using surgery, chemotherapy, radiotherapy, and immunotherapy. However, these strategies are associated with disease recurrence, metastasis, and severe side effects. Thus, more effective treatments, without severe adverse effects should be developed.

Traditional Chinese medicine (TCM) is used as an adjunctive therapeutic option for preventing CRC metastasis, enhancing chemotherapeutic effects while minimizing toxicity, and increasing the patients' quality of life (3). Furthermore, due to its effectiveness and few side effects, the use of TCM for oncological applications has been rising in Western countries. Yi-Yi-Fu-Zi-Bai-Jiang-San (YYFZBJS), a classical TCM formula, was first described in Golden Chamber which was written by a TCM master, Zhang Zhong-Jing (Eastern Han Dynasty, A.D. 150–219). It's made up of three traditional Chinese medicines, Yi-yi-ren (Semen Coicis), Fu-Zi (monkshood), and Bai-jiang-cao (Herba Patriniae), which are combined at a 30:6:15 ratio. In China, this formula has historically been used to treat gastrointestinal disorders. Previous studies have shown that YYFZBJS markedly suppresses CRC progression in ApcMin/+ mice by remodeling the gut microbiota and inhibiting the generation of regulatory T cells (4). Another study found that YYFZBJS inhibits the development of ETBF-induced colorectal tumors in mice, as well as *in vitro* CRC cells proliferation through the regulation of ETBF primed Bone marrow-derived macrophages (5). Notably, the combination of Fuzi with radiotherapy exhibits significant anti-proliferative efficacy, strengthens immune response, suppresses immune escape, and weakens immune suppression in several types of human cancer cells (6, 7). Herba Patrinia ethanol extract (PE) triggers apoptosis of CRC cells and inhibits CRC tumor angiogenesis and proliferation (8). Like TCM formula, YYFZBJS contains several components and modulates several targets and cancer signaling pathways. Currently, the bioactive ingredients and mechanisms by which it inhibits CRC are not fully understood. Here, the inhibitory effects of YYFZBJS were explored to uncover its underlying mechanisms.

Network pharmacology combines systems biology, polypharmacology, and molecular networks to comprehensively describe the relationship between drugs, their targets, and diseases in terms of a visual active ingredients–targets–diseases network (9). Molecular docking involves modeling interactions between small molecules and proteins and its use in investigating the mechanisms of action of new drugs has markedly increased in recent years. Thus, network pharmacology and molecular docking offer unique advantages and have great potential in the study of TCM.

Here, the molecular mechanisms mediating the effects of YYFZBJS on CRC were elucidated (Figure 1).

Material and methods

Herbal data collection

Active YYFZBJS compounds were identified on the Traditional Chinese Medicine Systems Pharmacology (TCMSP) database (https://tcmsp-e.com) (10). In this study, oral bioavailability (OB) and drug-likeness (DL) were adopted to identify the bioactive ingredients of YYFZBJS. OB described the percentage of an oral dose capable of producing pharmacological activity. DL was applied to determine the similarity of a compound to conventional drugs and its physicochemical properties. Only compounds that had related targets and met the ADME criteria (ie, OB threshold≥30% and DL threshold≥0.18) were included in the study for subsequent research (11). Additionally, drug-related targets (DRTs) and their gene symbols were obtained from TCMSP and UniProt (https://www.uniprot.org), respectively.

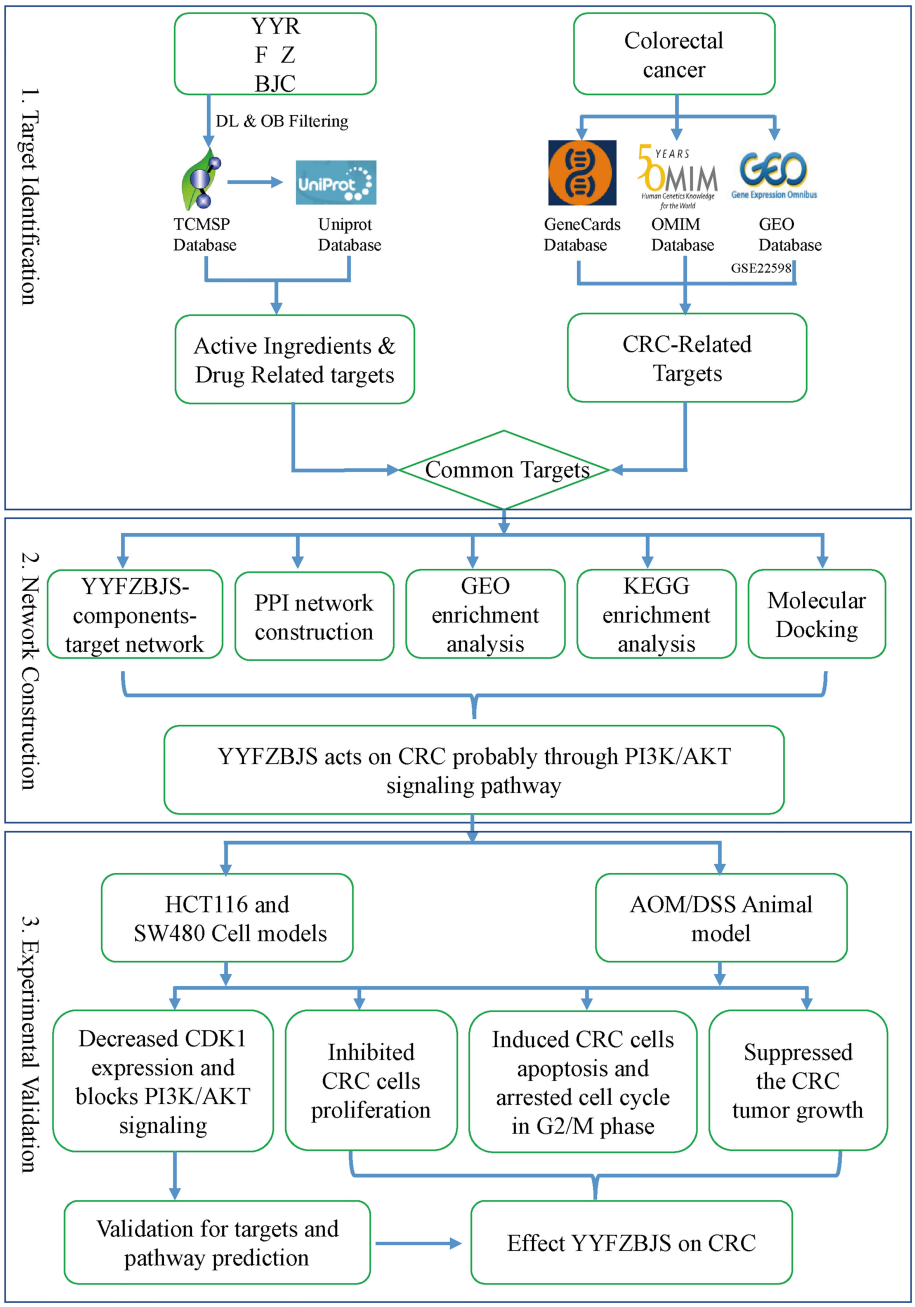

FIGURE 1
A flowchart of this study based on network pharmacology, molecular docking, and experimental validation of the mechanisms underlying the effects of YYFZBJS in colorectal cancer.

Related targets of CRC

Information on disease targets was obtained using datasets from GEO (https://www.ncbi.nlm.nih.gov/gds), Online Mendelian Inheritance in Man Database (OMIM, https://omim.org) and GeneCards (https://www.genecards.org). The term "Colorectal Cancer" was searched in OMIM and GeneCards to obtain all CRC targets, as well as in GEO to obtain dataset GSE22598 (Patient data) and GPL570 platform files. The R (version 3.6.0) package, LIMMA, was used to identify differentially expressed genes (DEGs) using $p \geq 0.05$ and log2 fold change (FC) ≥ 1 as cutoff thresholds. Finally, we

summarized the differentially expressed genes by taking the intersection of the DEGs identified from the GSE22598 and the CRC targets acquired from GeneCards and OMIM.

Construction of the YYFZBJS–targets–drug and protein–protein interaction networks

Using R (version 3.6.0), the drug-disease common targets were identified and visualized on a Venn diagram. Using Cytoscape (version 3.8.2), the protein–protein interaction (PPI) network between putative YYFZBJS targets was combined with that of the CRC-related targets. Next, the Cytoscape plugin, CytoNCA, was used to identify nodes with topological importance in the interaction network based on betweenness centrality (BC) and degree centrality (DC). These variables reflect the topological significance and their applications in systems pharmacology and network pharmacology have been previously described (12).

Gene ontology and Kyoto encyclopedia of genes and genomes analyses

Gene ontology (GO) biological process enrichment analysis was conducted for the common drug targets on R's bioconductor environment (http://www.bioconductor.org/) and used histograms and bubble charts to present the top 20 processes ($p < 0.05$). Kyoto encyclopedia of genes and genomes (KEGG) pathway enrichment analysis was done using the R packages "clusterProfiler" and "pathview" and the top 20 KEGG pathways visualized on heatmaps. The network of functional pathways was developed using Cytoscape.

Molecular docking

Molecular docking analysis was done using the molecular operating environment (MOE) v2015.10 in order to validate compound–target interactions. Protein 3D structures from the protein data bank (PDB, http://www.rcsb.org/) were imputed it into MOE to construct mating pockets of molecular docking after deleting water molecules, preparing protein structure, and minimizing energy. The structures of the compounds used for mating pocket construction and molecular docking analysis were downloaded from PubChem (https://pubchem.ncbi.nlm.nih.gov/) (13).

YYFZBJS preparation

The composition of YYFZBJS was 60g Yi-yi-ren (Semen Coicis), 12g Fu-Zi (monkshood), and 30g Bai-jiang-cao (Herba Patriniae) were purchased from Union hospital of Tongji Medical College, Huazhong University of Science and Technology under the guidance of Chinese Pharmacopeia 2020 edition. The extracts of the above variously prepared YYFZBJS were obtained by the following process. Firstly, all herbs were soaked for 30 min and decocted twice independently with the 8-fold volume of water, 1 h each time. Secondly, the decoction was collected and filtrated through filter paper. Thirdly, an 8-fold volume of 95% ethanol was added to the filtrate remains and reflux twice, 1 h each time. Next, these two parts of filtrates were combined, condensed to a density of 1.0 g/mL by rotary evaporation at 55°C and frozen at -80°C. Finally, it was converted into lyophilized powder by a freeze-drying machine (Cuddon; Blenheim, New Zealand). For *in vitro* assays, the YYFZBJS lyophilized powder was dissolved in culture media by ultra-sonication for 20 min, followed by centrifugation at 13,000 rpm for 5 min. The obtained supernatant was filtered with a 0.22 μm filter membrane as the extract solution. Before using, the extract solution was diluted to the desired concentrations. Culture media without YYFZBJS was used as negative control. For *in vivo* experiments, mice were intragastrically administered a YYFZBJS decoction.

Azoxymethane/dextran sulfate sodium induced CRC model and YYFZBJS treatment

Fifty male C57BL/6J (6–8 weeks) mice were obtained from the SPF (Beijing) biotechnology Co., Ltd. The animals were housed in pathogen-free conditions. CRC was induced using azoxymethane (AOM, Sigma Chemical Co) and dextran sulfate sodium (DSS, MP Biomedicals) as described before (14). Briefly, the mice were intraperitoneally (I.P.) injected with AOM (12 mg/kg) on day 1. After 1 week, they were administered 2.5% DSS in drinking water for 7 days and given tap water for 14 days to allow recovery. This cycle was repeated thrice and the mice sacrificed 2 weeks after the final DSS cycle. In the clinical practice of Chinese herbal medicine, YYFZBJS is usually prescribed at 51 mg daily. After converting the human dose into a mouse dose (assuming a person of 60 kg and a conversion factor of 9 between a person and a mouse), the equivalent mouse dose was 7.65 g/kg. Based on this human equivalent dose, the mice were administered YYFZBJS at 3.825 g/kg, 7.65 g/kg, and 15.3 g/kg once day from the second week for 10 weeks during the DSS treatment separately, with the control group receiving the same volume of sterile isotonic saline. The animals were provided normal drinking water. Mouse health and weight were monitored daily and weekly, respectively.

Cell culture and transfection

The human CRC cell lines, HCT116 and SW480, were purchased from the American Type Culture Collection (ATCC, Manassas, VA, United States) and confirmed to be mycoplasma-free using a LookOut mycoplasma PCR detection kit (Sigma Chemical Co). SW480 cells were cultured in DMEM/high glucose media (Gibco, USA). HCT116 cells were cultured in McCoy's 5A media (Gibco, USA) supplemented with 10% FBS (Gibco, USA) at 37 °C, 5% CO2.

HCT116 and SW480 cells (4×105 per well) were seeded in six-well plates and then transfected with a CDK1 overexpression plasmid (Guangzhou RiboBio Co., Ltd, Guangzhou, China) using Lipofectamine®2000 (Invitrogen, USA) according to manufacturer instructions. After 6 h, the transfection mixture was replaced with fresh growth media.

Histology

Mice were sacrificed and whole intestines collected and washed with ice-cold phosphate-buffered saline (PBS). To assess inflammation, the length of the whole colon was measured before and after being opened longitudinally (15). Adenoma incidence was determined by counting the number of tumors visible in the intestine. Tissues were fixed in 4% paraformaldehyde and embedded in paraffin. Next, the sections were stained with hematoxylin and eosin (HE) and examined by a pathologist who was blinded to the experimental groups.

Cell counting kit-8 assay

Cell proliferation was assessed using the cell counting kit-8 (CCK-8) assay (GLPBIO, Montclair, CA, USA). HCT116 and SW480 were seeded at 3 × 103 cells/well in 96 well plates and cultured to 80% confluence. They were then treated with YYFZBJS at 0, 30, 60 and 90 μg/mL for 24 h. Next, 10μL of CCK-8 solution was added into each well and the cells incubated for 90 min followed by absorbance (450 nm) reading on a microplate reader (Thermo Fisher, USA). The data are representative of three independent experiments in triplicate. IC50 values were calculated from the percent of viability reported to untreated cells using online tools https://www.xiantao.love/products.

Colony formation assays

HCT116 and SW480 cells were treated with 30, 60 and 90 μg/mL of YYFZBJS or PBS as a control for 24 h. The cells (3 × 103 per dish) were then cultured in 10 cm dish, and the medium was changed every 5 days for 14 days. Next, the colonies were fixed with 2% paraformaldehyde (Beyotime Biotechnology, Shanghai, China) for 30min and stained with 0.1% crystal violet (Beyotime Biotechnology, Shanghai, China) for 15min. They were then washed thrice, dried, and the number of positively stained colonies counted and imaged under a microscope (Leica, Germany).

Cell cycle analyses

HCT116 and SW480 cells were treated with YYFZBJS (30, 60 or 90 μg/mL) or PBS (negative control) for 24 h. The cells (1×106) were then collected, fixed in cold ethanol, and stored at 4°C overnight. The next day, they were washed twice with cold PBS and stained with 200μL PI/RNase staining buffer (BD Biosciences, USA) at 4 °C for 30 min in the dark. Measurements were taken using a flow cytometer (Beckman Coulter, USA) and the data analyzed using FlowJo 8.1 software.

Apoptosis analyses

Apoptotic cells were detected using an Annexin V-APC/7-ADD apoptosis detection kit (BD Biosciences, USA). Briefly, cells were detached using EDTA-free trypsin, centrifuged, and the supernatant discarded. They were then rinsed with ice-cold PBS, centrifuged, and the cell pellet resuspended in 200 μl of 1 × binding buffer. The cells were then transferred into a FACS tube and stained with Annexin V-APC and 7-AAD (5μL each) in the dark for 15 mins, at room temperature. Next, flow cytometry measurements were taken, and the data analyzed on FlowJo 8.1.

Western blot analysis

Total protein was extracted from the YYFZBJS-treated CRC cells or mouse CRC tissues using RIPA lysis buffer supplemented with a phosphatase and protease inhibitor cocktail. Protein concentration was then measured using a BCA assay kit according to manufacturer instructions. Next, 40μg of each sampled were resolved using 10% SDS-PAGE and transferred onto 0.45μm PVDF membranes (Millipore, USA). Membranes were then blocked using 5% skimmed milk in TBST for 1 h at room temperature, and then washed with TBST. The membranes were then incubated overnight (at 4°C) with antibodies against CDK1(1:1,000; Abcam), p-PI3K (1:1,000; CST), PI3K (1:1,000; CST), p-AKT (1:1,000; CST), AKT (1:1,000; CST) and β-actin (1:2000, ABclonal). The membranes were then washed and incubated with HRP-conjugated goat anti-mouse or anti-rabbit (1:1000) secondary

antibodies for 2 h, at room temperature. Signal was then developed using an ECL kit.

Statistical analysis

Statistical analysis was done using SPSS (version 26.0) and data plotted for visualization using GraphPad Prism (version 8). Data were expressed as mean ± SD. For normally distributed data, independent sample t test and one way ANOVA were used to statistically compare two groups and multiple groups, respectively. Non-normally distributed data were compared using nonparametric rank sum test. $p<0.05$ indicated statistically significant differences.

Result

YYFZBJS chemical compounds and targets

A total of 40 active YYFZBJS components were retrieved (oral bioavailability: ≥30%, drug likeness: ≥0.18) from TCMSP (Supplementary Table 1). The corresponding genes were then converted into gene symbols using Uniprot. Upon removal of duplicates and nonhuman targets, 197 drug targets were obtained.

Identification of candidate protein targets associated with CRC

Analysis of screening data from OMIM and GeneCards revealed 168 and 679 CRC-related targets respectively. After merging the results from OMIM and GeneCards, and duplicate removal, 760 targets were obtained. Analysis of colorectal cancer dataset GSE22598 from GEO and its associated platform file (GPL570), identified 1308 DEGs, which were visualized on heatmaps and volcano plots (Figures 2A, B). As shown in Figure 2C, we obtained 91 differentially expressed genes by taking the intersection of the DEGs identified from the GSE22598 and the CRC targets acquired from Genecards and OMIM using an online tool (http://bioinformatics.psb.ugent.be/webtools/Venn/) (Figure 2C).

Target protein–protein interaction network analysis

A total of 197 genes related to YYFZBJS, and 91 genes related to CRC were screened out. Next, Venn diagram analysis revealed 21 common targets between the YYFZBJS related genes and the CRC related genes (Figure 3A). We then used Cytoscape 3.8.2 to develop a CRC-target drug network based on the 21 common targets and 91 CRC-related active components of the 3 herbs (Figure 3B). The active components were presented as TCMSP MolIDs using different colors to indicate which herbs they belong to. The YYFZBJS active components with the most target genes were Mol000006 (luteolin), Mol000098 (quercetin), Mol000422 (kaempferol), MOL000359 (sitosterol), and MOL000449 (stigmasterol). Thus, we speculated that these active components may contribute to the effects of YYFZBJS against CRC.

Identification of candidate targets for YYFZBJS against CRC

To better understand the effects of YYFZBJS on CRC, we merged the PPI network of its putative targets and the PPI network of CRC-related targets in order to identify candidate YYFZBJS targets in CRC. This network contains 2,308 nodes and 64,565 edges (Figure 3C). Next, a subnetwork containing 283 nodes and 9,376 edges was obtained by selecting the top 30% based on degree centrality (DC, Figure 3D). After screening the

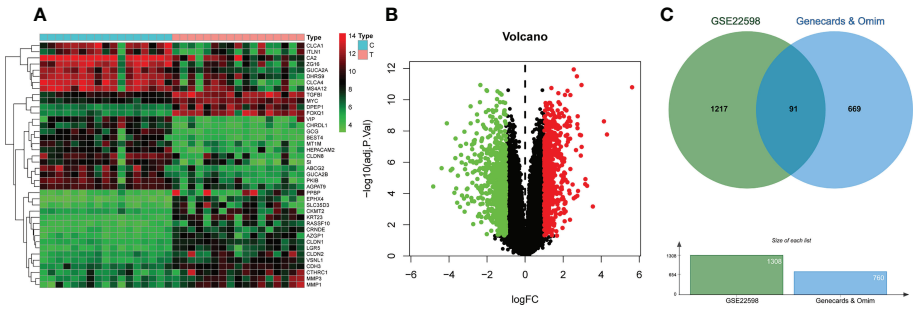

FIGURE 2
CRC-related differential gene analysis and CRC target collection. **(A)** Heatmap of differential gene analysis on dataset GSE22598. **(B)** Volcano plot of differential gene analysis on dataset GSE22598. **(C)** CRC common differentially expressed genes collection.

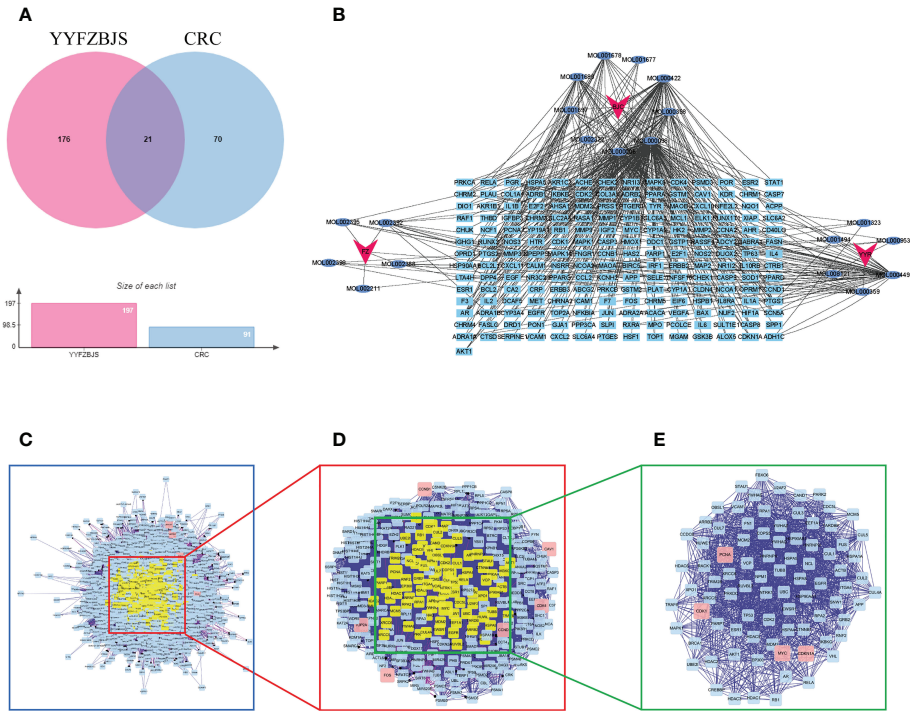

FIGURE 3
Identification of YYFZBJS's candidate targets in CRC. **(A)** Venn diagram showed 21 common targets of YYFZBJS in CRC. **(B)** "YYFZBJS-components-target" network (red V represents herbs; blue oval represents YYFZBJS compounds; sky blue rectangle represents compound targets). **(C)** An interactive PPI network of YYFZBJS-CRC target genes. **(D)** PPI network of significant proteins extracted from **(C, E)** PPI network of candidate YYFZBJS targets for CRC treatment extracted from **(D)**. DC, degree centrality; BC, betweenness centrality; CC, closeness centrality.

subnetwork's top 30% based on betweenness centrality (BC), a core network containing 85 nodes and 1516 edges was constructed (Figure 3E). Based on the core network, higher degrees indicated larger node sizes; magenta indicates the highest degree. The nodes with the top four degrees were CDKN1A, MYC, PCNA, and CDK1, which identified as critical genes in the PPI and subjected to further analysis.

GO enrichment analysis of YYFZBJS-CRC common targets

To determine the function of the identified protein targets, we performed functional enrichment analysis of the target genes. The R package, clusterProfiler, was used to annotate the biological process (BP), molecular function (MF), and cell composition (CC) of the 21 hub target proteins. The top 20 BP, CC, and MF terms (ranked based on their adjusted p value) are shown in Figures 4A–C. Low adjusted p values and red color indicated greater GO term enrichment. A total of 273 GO terms, including 252, 9, and 12 terms belonging to BP, CC, and MF, respectively, were identified. Most BP GO terms were associated with response to radiation, regeneration, response to light stimulus, cellular response to chemical stress, response to metal ions, response to oxidative stress, and response to xenobiotic stimulus. The main CC terms were associated with transferring phosphorus-containing groups, transferase complex, protein kinase complex, serine–threonine protein kinase complex, and cyclin-dependent protein kinase holoenzyme complex. MF terms were mainly enriched for kinase regulator activity, cyclin-dependent protein serine–threonine kinase regulator activity, protein kinase regulator activity, and endopeptidase activity.

Pathway enrichment and construction of the compound–target–pathway network

We used KEGG pathway analysis to identify potential pathways underlying the effects of YYFZBJS in CRC treatment. KEGG annotation revealed that 149 of the 163 target genes were enriched for 97 pathways ($p<0.001$). The top 20 significantly enriched pathways are shown. Furthermore, KEGG enrichment analysis showed that several target genes were closely associated with the cell cycle, cellular senescence, microRNAs in cancer, PI3K/Akt signaling, and p53 signaling pathway (Figure 4D). Among these pathways, PI3K/Akt

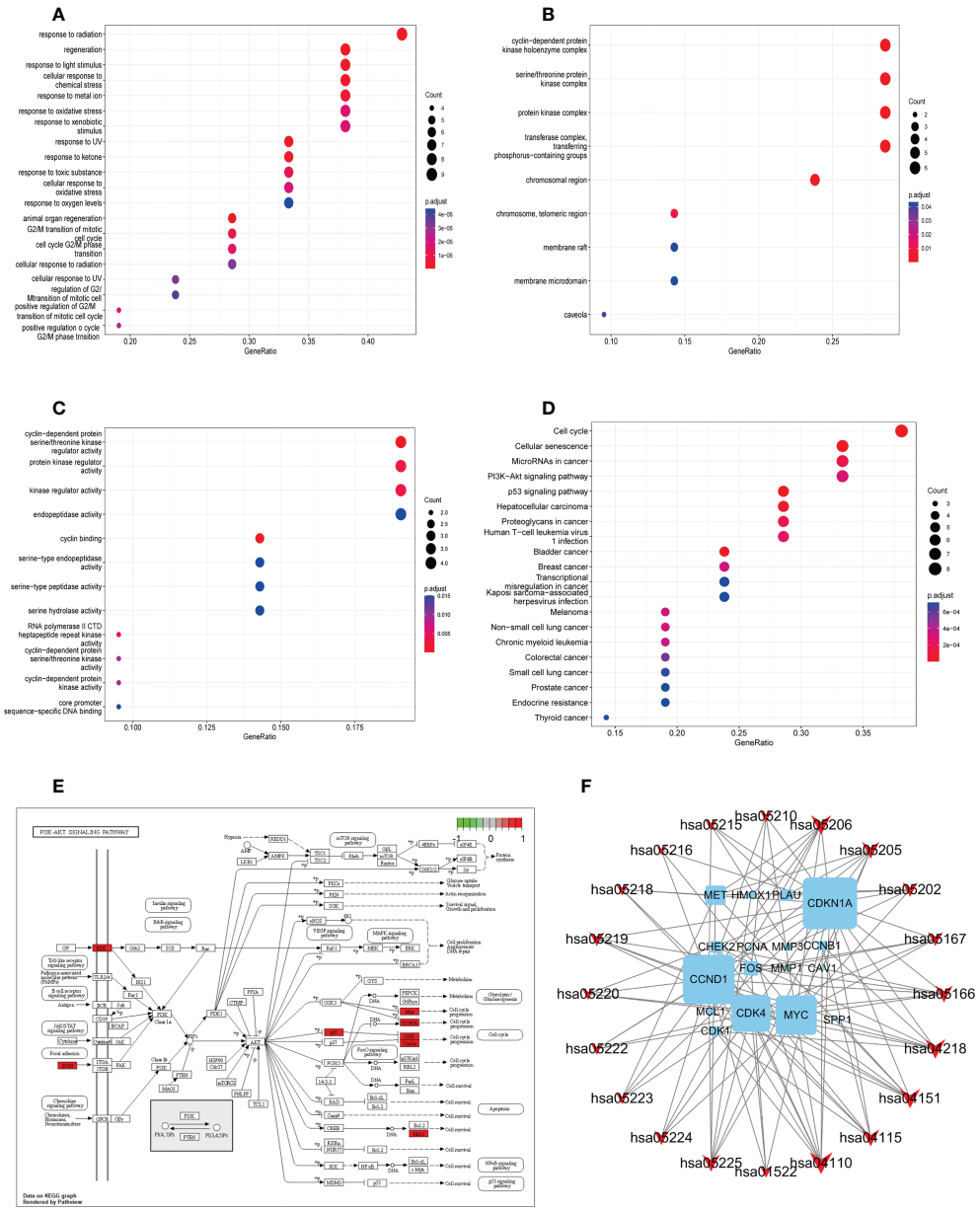

FIGURE 4
Gene ontology and KEGG pathway enrichment analysis of identified YYFZBJS-CRC common targets. **(A)** Biological processes. **(B)** Cellular components. **(C)** Molecular functions. **(D)** KEGG pathway enrichment analysis of key targets. The color scale indicates the p value, and the dot size indicates the gene count in each term. **(E)** Schematic of the PI3K/Akt signaling pathway. **(F)** Gene–pathway network of YYFZBJS against CRC. Sky blue squares represent target genes. Red V shapes represent pathways. Big size of the dot represents higher betweenness centrality.

signaling was the most prominent pathway based on the number of genes (Figure 4E), suggesting that YYFZBJS may activate P13K–Akt signaling in CRC. The PI3K/Akt pathway modulates cell proliferation, cell cycle, differentiation, apoptosis, and migration *via* multiple factors, including EGFR, BCL2, CCND1, CDK1, and CDK4. Next, a gene–pathway network was constructed using the significantly enriched pathways. Genes that influence these pathways are shown in Figure 4F.

Molecular docking verification of core targets and active ingredients

Five active ingredients (quercetin, luteolin, kaempferol, stigmasterol, and sitosterol) and ten potential target genes (CDKN1A, CCND1, CDK1, MYC, PLAU, FOS, MET, MCL1, HMOX1, and MMP3) were selected through network analysis, with high node scores and confidence. Molecular docking

studies were conducted to identify the interactions between the active YYFZBJS ingredients and CRC-related potential target genes at the molecular level. The 3D structures of the active ingredients and potential target genes were obtained from TCMSP and RCSB PDB, respectively. After dehydration and hydrogenation, we performed docking analysis using AutoDock tools and the AutoDock Vina software. The absolute binding energy value correlated positively with the connective stability of the ingredient molecule and target protein. The most stable connective patterns and binding energies are shown on Figures 5A, B.

According to the scoring results, quercetin-CDK1, kaempferol-CDK1, quercetin-CCND1, luteolin-CCND1, quercetin-PLAU, luteolin-MET had a strong correlation. Based on network analysis and molecular docking simulation, quercetin, which targets multiple CRC-related targets, with strong binding to the cell cycle factor, CDK1, was selected as candidate drug for *in vivo* analysis

Clinical significance of target hub genes in CRC

In total, 50 tumor samples and paired adjacent noncancerous tissue from TCGA (https://tcga-data.nci.nih.gov/tcga/) were analyzed. The publicly available data indicated that among the core target proteins, the levels of CDKN1A, CCND1, CDK1, MYC, PLAU, FOS, MET, MCL1, HMOX1, and MMP3 were significantly different in CRC tissues when compared with normal colorectal tissues (Figure 6). The levels of CDKN1A, FOS, MCL1, and HMOX1 were high in CRC tissue and low in normal colorectal tissue, while those of CCND1, CDK1, MYC,

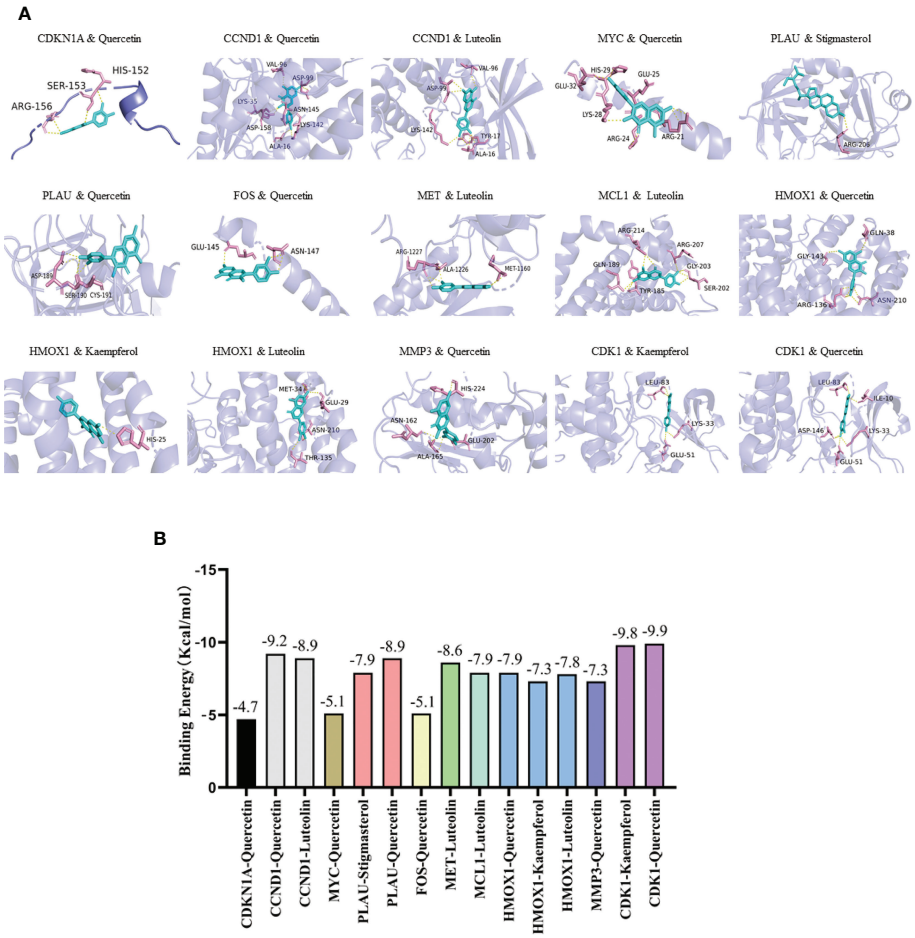

FIGURE 5
Molecular docking results. **(A)** Docking patterns of key targets genes (CDKN1A, CCND1, CDK1, MYC, PLAU, FOS, MET, MCL1, HMOX1, and MMP3) and specific active ingredients (quercetin, luteolin, kaempferol, stigmasterol, and sitosterol) of YYFZBJS. **(B)** Binding affinities (kcal/mol) of key targets and specific active ingredients of YYFZBJS.

PLAU, MET, and MMP3 were significantly higher in CRC tissues than in normal colorectal tissue.

YYFZBJS inhibits the proliferation of human CRC cells

To assess its effects on human CRC cells, cultured HCT116 and SW480 cells were treated with YYFZBJS at 0, 30, 60, and 90 μg/mL for 24 h and cell viability examined using CCK8 analysis. This analysis revealed that YYFZBJS significantly suppressed the viability of HCT116 and SW480 cells (Figures 7A, B). Colony formation assay, revealed that YYFZBJS suppressed colony formation by HCT116 and SW480 cells at all indicated concentrations (Figures 7C, D). Five active compounds including quercetin, kaempferol, beta-sitosterol, isorhamnetin, and stigmasterol were observed to inhibit SW480 and HCT116 proliferation in a concentration-dependent manner. The 24 h IC50 values of quercetin, luteolin, kaempferol, stigmasterol, and sitosterol in SW480 were 25.63, 85.89, 43.54,58.97, and 83.13μM; meantime the 24 h IC50 values of quercetin, kaempferol, beta-sitosterol, isorhamnetin, and stigmasterol in HCT116 were 27.58, 99.56, 41.28, 64.49, and 67.79μM. The cell viability curves were shown in Supplement Figure 1. These data indicate that YYFZBJS inhibits CRC cell viability and proliferation.

YYFZBJS induces apoptosis and arrests cell cycle progression in the G2/M phase by inhibiting CDK1/PI3K/AKT signaling

Next, we treated the CRC cells, HCT116 and SW480, with YYFZBJS at 0, 30, 60, and 90 μg/mL for 24 h and assessed the levels of CDK1 and PI3K/AKT using western blot analysis. This analysis revealed that YYFZBJS dose-dependently inhibited CDK1, p-PI3K and p-AKT expression in HCT116 and SW480 cells, which was reversed by CDK1 overexpression (Figures 8A–D). These results indicated that YYFZBJS could not only alter the expression of CDK1 and PI3K/AKT in colon cancer cells, but that it also has a regulatory relationship with CDK1. In addition, we performed different concentrations of YYFZBJC intervention in HCT116 and SW480, while overexpressing CDK1 in the 90μg/mL group. Then, the cell apoptosis and cell cycle distribution were investigated through flow cytometry. The results showed that administration of YYFZBJS at 30, 60, and 90μg/mL significantly increased the rate of apoptosis (Figures 8E, F). Moreover, YYFZBJS induced cell cycle arrest in HCT116 and SW480 cells (Figures 8G, H). Upon CDK1 overexpression, YYFZBJS's ability to induce apoptosis and cell cycle arrest in the tumor cells was weakened (Figures 8E–H). These results suggest that YYFZBJS induced apoptosis and cell cycle arrest in the G2/M phase by inhibiting CDK/PI3K/AKT signaling.

YYFZBJS inhibited tumor growth and PI3K/AKT signaling in a mouse model of CRC

To investigate the antitumor effects of YYFZBJS, we established a mouse model of CRC using AOM/DSS and treated the mice with YYFZBJS at 3.825 g/kg, 7.65 g/kg, and 15.3 g/kg using oral gavage. The mice were then sacrificed after 11 weeks and the entire colorectal tissue (from cecum to anus) collected. We then measured colon length and counted the number of tumors. Colon length shortening is regarded as a

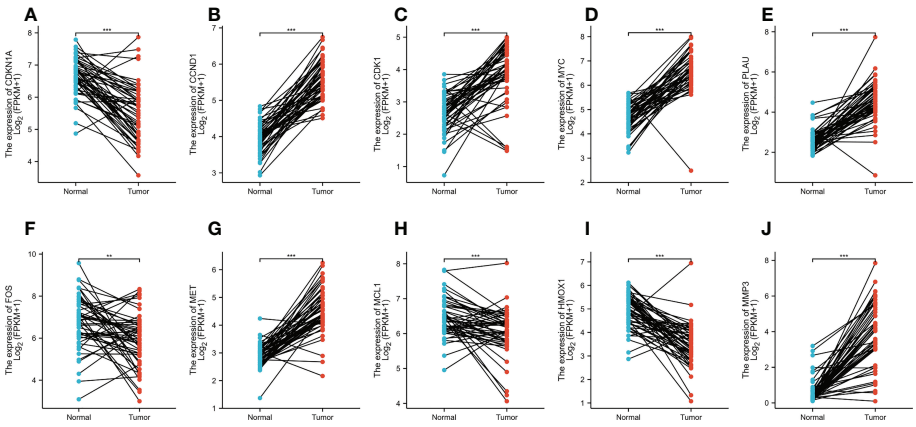

FIGURE 6
(A–J) The expression levels of CDKN1A, CCND1, CDK1, MYC, PLAU, FOS, MET, MCL1, HMOX1, and MMP3 in normal tissues versus CRC tissues based on the TCGA dataset. **p < 0.01, ***p < 0.001 versus the Normal.

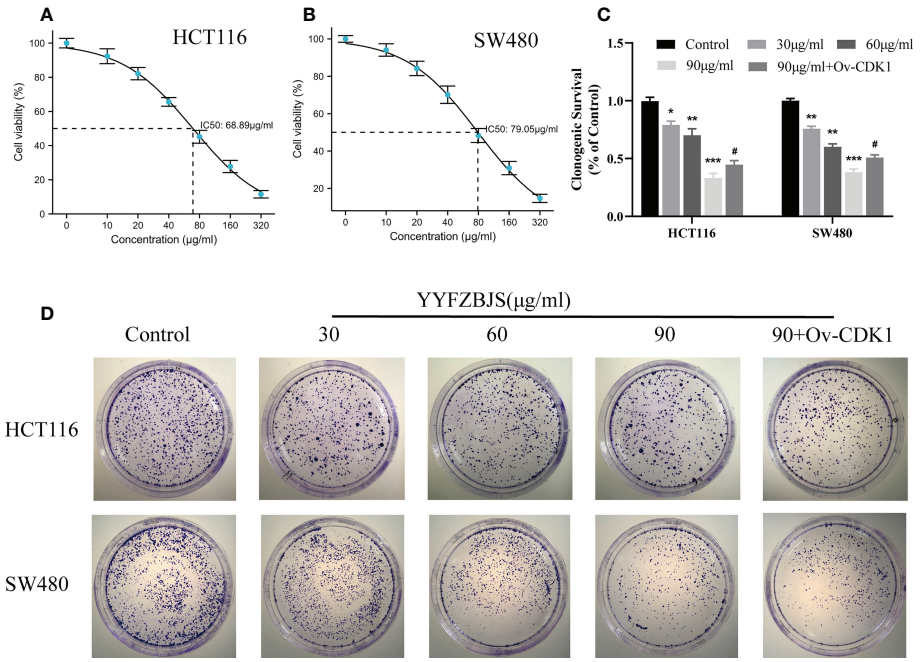

FIGURE 7
YYFZBJS inhibits cell viability. Viability of **(A)** HCT116 and **(B)** SW480 cells after treatment for 24 h with indicated doses of YYFZBJS. All data are presented as mean ± SD (n=3). **(C)** Colony formation assays were done using HCT116 and SW480 cells treated with YYFZBJS. A representative of three experiments is shown. **(D)** Colony formation is presented as mean ± SD (n=3), *$p < 0.05$, **$p < 0.01$, ***$p < 0.001$ versus the control group. #$p < 0.05$ versus the YYFZBJS 90 μg/ml group.

hallmark of inflammation upon DSS treatment (16). Here, we found that the mean colon length was significantly shorter in mice treated with AOM/DSS when compared to control mice ($p<0.01$), Notably, YYFZBJS markedly reversed the colon length changes triggered by AOM/DSS (Figures 9A, B). Tumor number and size is an indicator of the modeling efficiency and treatment efficacy. Here, we found that YYFZBJS significantly reduced the number of tumors dose-dependently (Figures 9C, D). In the model group, we found that mice that freely drank the DSS solution for seven consecutive days in the first, second, and third cycles, exhibited marked weight loss when compared with the controls. In contrast, significant improvement in weight loss was observed in mice treated with YYFZBJS after exposure to AOM/DSS (Figure 9E). Compared with the control group, Disease Activity Index (DAI) score was significantly decreased in the YYFZBJS treatment group (Figure 9F). Notably, the number of different tumor sizes was much less in all three different doses of YYFZBJS groups than that of the model group (Supplementary Figure 9J). These results suggest that YYFZBJS can effectively protect against AOM/DSS-induced tumorigenesis.

HE analysis of the colon tissues revealed that the model group lost normal tissue morphology, with intestinal villi exhibiting disruption, and tissue showing apparent nuclear enlargement, aggregation, and shrinkage. Treatment with YYFZBJS partially restored normal intestinal structure and improved the above pathological changes (Figure 9G). Network pharmacology analysis suggested that YYFZBJS may exert its effects on CRC *via* CDK1 and PI3K/AKT signaling. Thus, we examined protein levels of CDK1, PI3K, AKT, and p-AKT in colorectal tissues using western blotting. This analysis revealed that the expression of CDK1 was reduced upon treatment with YYFZBJS at 3.825, 7.65, and 15.3 mg/kg (Figure 8H). Next, western blot analysis of PI3K, p-PI3K, AKT, and p-AKT levels found that YYFZBJS significantly reduced the levels of p-PI3K and p-AKT without altering total PI3K and AKT levels (Figures 9H, I). These results are consistent with findings from network pharmacology analyses. Taken together, these results indicate that YYFZBJS exerts its effects on CRC *via* CDK1 and PI3K/AKT signaling.

Discussion

Using network pharmacology-based approach, experimental validation, and molecular docking tests, we explored bioactive components and the molecular mechanism of YYFZBJS for treating CRC. A YYFZBJS compound–target network constructed using 40 compounds and 197 compound targets suggested that most YYFZBJS compounds affect multiple targets. For example, luteolin, quercetin, and kaempferol affected 54,

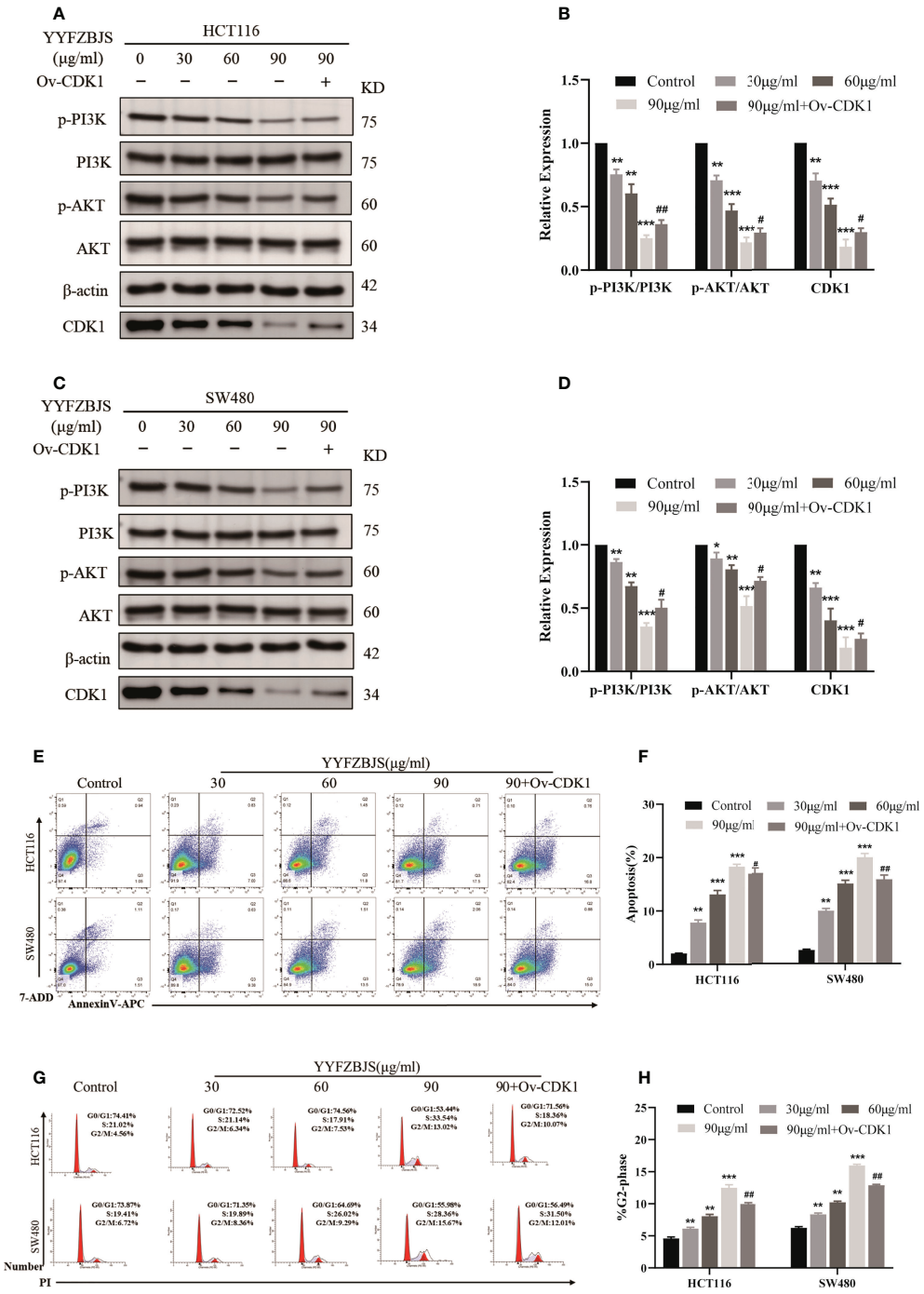

FIGURE 8
In HCT116 and SW480 cells, YYFZBJS induces apoptosis and cell cycle arrest in the G2/M phase, and inhibits CDK1/PI3K/AKT signaling. **(A–D)** Western blot analysis revealed that YYFZBJS (30, 60, and 90 μg/mL) dose dependently suppresses CDK1 expression and PI3K/AKT signaling in HCT116 and SW480 cells. Transfecting the cells with overexpressed CDK1 plasmid reversed YYFZBJS-induced PI3K/AKT expression in HCT116 and SW480 cell lines. **(E)** Flow cytometric analysis of Annexin V-APC/7-ADD double staining in HCT116 and SW480 cells treated with various concentrations of YYFZBJS for 24 h. **(F)** Statistical analysis of the apoptotic rate in HCT116 and SW480 cells. **(G)** Flow cytometric analysis of cell cycle arrest in HCT116 and SW480 cells treated with indicated doses of YYFZBJS for 24 h. **(H)** Quantification of cells in the G2/M phase of the cell cycle. All data are presented as mean ± SD (n=3). *$p < 0.05$, **$p < 0.01$, ***$p < 0.001$ versus the control group; $^{\#}p < 0.05$, $^{\#\#}p < 0.01$ versus the YYFZBJS 90 μg/ml group.

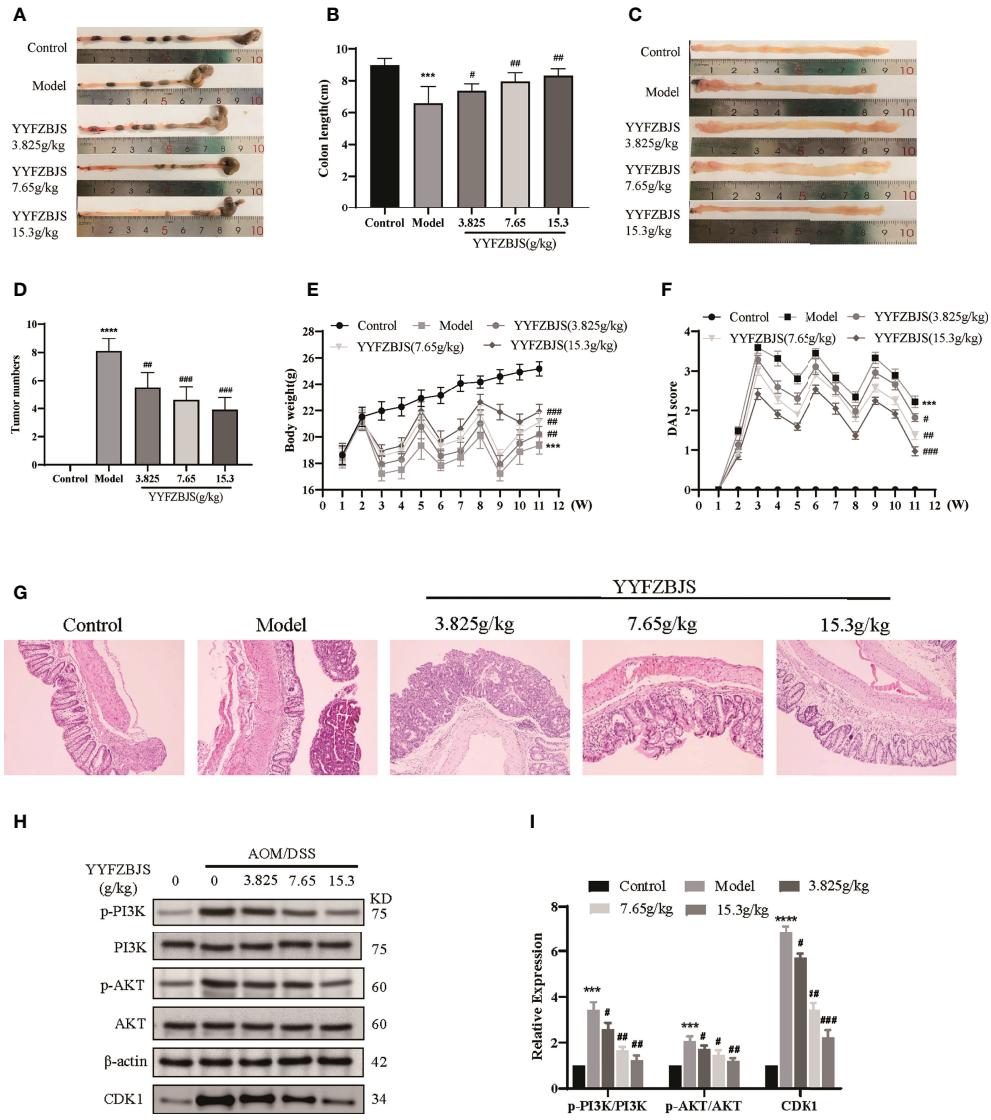

FIGURE 9
YYFZBJS inhibits colorectal cancer progression in mice through suppression of the CDK1/PI3K/Akt pathway. **(A, B)** YYFZBJS suppresses intestinal shortening in the mouse model of colon cancer (n=10). **(C, D)** YYFZBJS inhibits tumorigenesis in the mouse model of colon cancer (n=10). **(E)** YYFZBJS slowed weight loss in the mouse model of colon cancer (n=10). **(F)** YYFZBJS improved intestinal DAI score in the mouse model of colon cancer (n=10). **(G)** Hematoxylin and eosin staining (H&E; magnification: 100×) analysis confirmed that YYFZBJS improved intestinal morphology after disruption by AOM and DSS and inhibited tumorigenesis. **(H, I)** Western blot analysis confirmed that the effects of YYFZBJS on the mouse model of colon cancer was mediated *via* CDK1/PI3K/Akt signaling. All data are presented as mean ± SD (n=3), ***$p < 0.001$, ****$p < 0.0001$ versus the control group; $^{\#}p < 0.05$, $^{\#\#}p < 0.01$, $^{\#\#\#}p < 0.001$ versus the model group.

140, and 55 targets, respectively, suggesting that they pleiotropically mediate the effects of YYFZBJS. Although each herb showed distinct numbers of putative targets, there were many overlapping targets, indicating that multiple YYFZBJS compounds may modulate the same target, resulting in synergistic effects. Anticancer agents like luteolin induce apoptosis and arrest the cell cycle, thereby inhibiting metastasis and angiogenesis in multiple cancers (17). Quercetin inhibits tumors by regulating MAPK–ERK1/2, Wnt–β-catenin, and PI3K/Akt/mTOR pathways. Quercetin also affects cancer metabolism by inhibiting key glycolysis and glucose uptake enzymes (18). Kaempferol can restore cellular redox hemostasis by inhibiting the NF-κB pathway and upregulate the Nrf2 transcriptional pathway to control cancer through its antioxidative/antinitrosative and anti-inflammatory potential (19). Our findings indicate that YYFZBJS has

multitarget therapeutic effects. The role of these active compounds in CRC warrant further investigation.

We selected 40 bioactive compounds and 197 protein targets from public databases. PPI network analysis indicated that CDKN1A, CCND1, CDK1, MYC, PLAU, FOS, MET, MCL1, HMOX1, and MMP3 may be key mediators of the effects of YYFZBJS against CRC. CDK1 is a Ser/Thr protein kinase. Data indicates that CDK1–CCNB1 signaling regulates mitosis (20). CCNB1 is the main CDK1 activator and together with CDK1, promotes G2/M transition (20). Deregulated cell cycle results in formation of cancer stem cells, which drive tumorigenesis (21). CDK1 is upregulated in CRC (22). GO enrichment analysis revealed that YYFZBJS is associated with major biological processes (e.g., cyclin binding, regulator activity, protein kinase regulator, and cyclin-dependent protein serine/threonine kinase). KEGG pathway analysis revealed that multiple signaling pathways are involved in the treatment effects, including the cell cycle, cellular senescence, microRNAs in cancer, PI3K/Akt pathway, and p53 signaling. The PI3K/Akt pathway promotes cancer by influencing multiple biological processes, including cell survival, metabolism, proliferation, and cell growth (23). KEGG pathway analysis revealed that YYFZBJS's mechanisms of action in CRC involve the cell cycle and PI3K/AKT signaling. Together, these data suggest that YYFZBJS exerts anti-CRC effects through these signaling pathways, target genes, and active compounds.

The mechanisms through which YYFZBJS act against CRC were further investigated through molecular docking analysis. Molecular docking can efficiently predict the binding affinity between TCM components and their targets based on the spatial structure of ligands and receptors. Of the ten targets chosen for molecular docking analysis, CDKN1A, CDK1, MCL1, and MYC are known to be key factors in the cell cycle and PI3K/AKT signaling. Molecular docking analysis showed that quercetin, luteolin, kaempferol, stigmasterol, and sitosterol, can interact with CDKN1A, CDK1, MYC, PLAU and MCL1, etc. Previous studies have reported that quercetin-induced growth inhibition and cell death in prostatic carcinoma cells are associated with increased CDKN1A levels (24). Quercetin inhibits proliferation in endometriosis by regulating CCND1 (25). P21 (encoded by CDKN1A), is a cyclin-dependent kinase inhibitor that prevents the phosphorylation of key cyclin-dependent kinase substrates, thereby inhibiting cell cycle progression. MYC is a key proto-oncogene but currently, there are no therapies that directly target MYC (26).

Our data show that in the CRC cells, HCT116 and SW480, YYFZBJS inhibited CDK1 expression, induced cell cycle arrest at the G2/M phase, and activated apoptosis. Moreover, upregulation of phospho-Akt (p-Akt) and PI3K in the control group indicated PI3K/Akt signaling activation. Compared with the control group, p-Akt and PI3K were significantly suppressed in the YYFZBJS group while total Akt levels were unaffected, and these effects were YYFZBJS dose-dependent. These findings indicate that YYFZBJS's anti-CRC effects are mediated by PI3K/Akt signaling. The PI3K/Akt signaling pathway, which is dysregulated in many cancers, including CRC, may influence CRC invasion, migration, proliferation, and autophagy (27). It is also reported that CDK1/PI3K/AKT inhibitors may be effective adjuvants in CRC treatment (28).

There are several limitations to our study. Because the public databases utilized in this study are continuously updated, some bioactive ingredients and target genes may not have been included in our analysis. Additionally, other signaling pathways (e.g., P53 and cellular senescence) may be involved in the anti-tumor effects of YYFZBJS. Further research is needed to examine the potential involvement of such pathways. Moreover, YYFZBJS contains active components such as quercetin, luteolin, kaempferol, stigmasterol, and sitosterol by network pharmacology, however these are also widely distributed in many herbs/plants/fruits/vegetables and are not very specific. The aim of this paper is to investigate the effect of compound prescription on CRC. Later, we will find the unique active components of single herb and YYFZBJS in combination with high performance liquid chromatography, and further study its mechanism of action. Nonetheless, our findings provide important preliminary information on the role of YYFZBJS in CRC treatment and indicate that YYFZBJS may be a promising CRC therapeutic candidate.

Conclusion

Our results indicate that in CRC, YYFZBJS inhibited proliferation and induced apoptosis by modulating the CDK1/PI3K/Akt signaling pathway and highlight YYFZBJS as a promising adjuvant in CRC treatment.

Data availability statement

The datasets presented in this study can be found in online repositories. The names of the repository/repositories and accession number(s) can be found in the article/Supplementary Material.

Ethics statement

The animal study was reviewed and approved by Tongji Medical College, Huazhong University of Science and Technology.

Author contributions

SY and JL contributed to design of the study. JL, NL and FZ carried out the network pharmacology analyses. JL, LS and YL performed the experiments. JL and FZ wrote and the manuscript. LS, NL, MZ and SW contributed to manuscript revision. All authors contributed to the article and approved the submitted version.

Funding

This work was supported by the Natural Science Foundation of China (No: 81874397), and the Project of Key R&D Program of Hubei Province (No: 2020BCA065).

Acknowledgments

We thank all the individuals who contributed to study. We also would like to acknowledge the reviewers for their valuable comments and suggestions.

Conflict of interest

The authors declare that the research was conducted in the absence of any commercial or financial relationships that could be construed as a potential conflict of interest.

Publisher's note

All claims expressed in this article are solely those of the authors and do not necessarily represent those of their affiliated organizations, or those of the publisher, the editors and the reviewers. Any product that may be evaluated in this article, or claim that may be made by its manufacturer, is not guaranteed or endorsed by the publisher.

Supplementary material

The Supplementary Material for this article can be found online at: https://www.frontiersin.org/articles/10.3389/fonc.2022.961653/full#supplementary-material

References

1. Dekker E, Tanis PJ, Vleugels JLA, Kasi PM, Wallace MB. Colorectal cancer. *Lancet* (2019) 394(10207):1467–80. doi: 10.1016/S0140-6736(19)32319-0

2. Bray F, Ferlay J, Soerjomataram I, Siegel RL, Torre LA, Jemal A. Global cancer statistics 2018: GLOBOCAN estimates of incidence and mortality worldwide for 36 cancers in 185 countries. *CA Cancer J Clin* (2018) 68(6):394–424. doi: 10.3322/caac.21492

3. Sun Q, He M, Zhang M, Zeng S, Chen L , Zhao H, et al. Traditional Chinese medicine and colorectal cancer: Implications for drug discovery. *Front Pharmacol* (2021) 12:685002. doi: 10.3389/fphar.2021.685002

4. Sui H, Zhang L, Gu K, Chai N, Ji Q, Zhou L, et al. YYFZBJS ameliorates colorectal cancer progression in Apc(Min/+) mice by remodeling gut microbiota and inhibiting regulatory T-cell generation. *Cell Commun Signal* (2020) 18(1):113. doi: 10.1186/s12964-020-00596-9

5. Chai N, Xiong Y, Zhang Y, Cheng Y, Shi W, Yao Y, et al. YYFZBJS inhibits colorectal tumorigenesis by remodeling gut microbiota and influence on M2 macrophage polarization *in vivo* and *in vitro*. *Am J Cancer Res* (2021) 11 (11):5338–57. doi: 10.2139/ssrn.3837225

6. Hu Y, Zhou Q, Liu T, Liu Z. Coixol suppresses NF-kappaB, MAPK pathways and NLRP3 inflammasome activation in lipopolysaccharide-induced RAW 264.7 cells. *Molecules* (2020) 25(4):894. doi: 10.3390/molecules25040894

7. Zhang Q, Chen X, Luo Y, Ren H, Qiao T. Fuzi enhances anti-tumor efficacy of radiotherapy on lung cancer. *J Cancer* (2017) 8(19):3945–51. doi: 10.7150/jca.22162

8. Yang H, Cheung MK, Yue GG, Leung PC, Wong CK, Lau CB. Integrated network pharmacology analysis and *In vitro* validation revealed the potential active components and underlying mechanistic pathways of herba patriniae in colorectal cancer. *Molecules* (2021) 26(19):6032. doi: 10.3390/molecules26196032

9. Wang X, Wang ZY, Zheng JH, Li S. TCM network pharmacology: A new trend towards combining computational, experimental and clinical approaches. *Chin J Nat Med* (2021) 19(1):1–11. doi: 10.1016/S1875-5364(21)60001-8

10. Ru J, Li P, Wang J, Zhou W, Li B, Huang C, et al. TCMSP: a database of systems pharmacology for drug discovery from herbal medicines. *J Cheminform* (2014) 6:13. doi: 10.1186/1758-2946-6-13

11. Zhao L, Guo R, Cao N, Lin Y, Yang W, Pei S, et al. An integrative pharmacology-based pattern to uncover the pharmacological mechanism of ginsenoside h dripping pills in the treatment of depression. *Front Pharmacol* (2020) 11:590457. doi: 10.3389/fphar.2020.590457

12. Tang Y, Li M, Wang J, Pan Y, Wu FX. CytoNCA: a cytoscape plugin for centrality analysis and evaluation of protein interaction networks. *Biosystems* (2015) 127:67–72. doi: 10.1016/j.biosystems.2014.11.005

13. Huang S, Zhang Z, Li W, Kong F, Yi P, Huang J, et al. Network pharmacology-based prediction and verification of the active ingredients and potential targets of zuojinwan for treating colorectal cancer. *Drug Des Devel Ther* (2020) 14:2725–40. doi: 10.2147/DDDT.S250991

14. Parang B, Barrett CW, Williams CS. AOM/DSS model of colitis-associated cancer. *Methods Mol Biol* (2016) 1422:297–307. doi: 10.1007/978-1-4939-3603-8_26

15. De Santis S, Verna G, Serino G, Armentano R, Cavalcanti E, Liso M, et al. Winnie-APC(Min/+) mice: A spontaneous model of colitis-associated colorectal cancer combining genetics and inflammation. *Int J Mol Sci* (2020) 21(8):2972. doi: 10.3390/ijms21082972

16. Wang K, Hu Z, Zhang C, Yang L, Feng L, Yang P, et al. SIRT5 contributes to colorectal cancer growth by regulating T cell activity. *J Immunol Res* (2020) 2020:3792409. doi: 10.1155/2020/3792409

17. Imran M, Rauf A, Abu-Izneid T, Nadeem M, Shariati MA, Khan IA, et al. Luteolin, a flavonoid, as an anticancer agent: A review. *BioMed Pharmacother* (2019) 112:108612. doi: 10.1016/j.biopha.2019.108612

18. Reyes-Farias M, Carrasco-Pozo C. The anti-cancer effect of quercetin: Molecular implications in cancer metabolism. *Int J Mol Sci* (2019) 20(13):3177. doi: 10.3390/ijms20133177

19. Imran M, Salehi B, Sharifi-Rad J, Aslam Gondal T, Saeed F, Imran A, et al. Kaempferol: A key emphasis to its anticancer potential. *Molecules* (2019) 24 (12):2277. doi: 10.3390/molecules24122277

20. Alfonso-Perez T, Hayward D, Holder J, Gruneberg U, Barr FA. MAD1-dependent recruitment of CDK1-CCNB1 to kinetochores promotes spindle checkpoint signaling. *J Cell Biol* (2019) 218(4):1108–17. doi: 10.1083/jcb.201808015

21. Wu CX, Wang XQ, Chok SH, Man K, Tsang SHY, Chan ACY, et al. Blocking CDK1/PDK1/beta-catenin signaling by CDK1 inhibitor RO3306 increased the efficacy of sorafenib treatment by targeting cancer stem cells in a preclinical model of hepatocellular carcinoma. *Theranostics* (2018) 8(14):3737–50. doi: 10.7150/thno.25487

22. Li J, Wang Y, Wang X, Yang Q. CDK1 and CDC20 overexpression in patients with colorectal cancer are associated with poor prognosis: evidence from integrated bioinformatics analysis. *World J Surg Oncol* (2020) 18(1):50. doi: 10.1186/s12957-020-01817-8

23. Bahrami A, Khazaei M, Hasanzadeh M, ShahidSales S, Joudi Mashhad M, Farazestanian M, et al. Therapeutic potential of targeting PI3K/AKT pathway in treatment of colorectal cancer: Rational and progress. *J Cell Biochem* (2018) 119 (3):2460–9. doi: 10.1002/jcb.25950

24. Vijayababu MR, Kanagaraj P, Arunkumar A, Ilangovan R, Aruldhas MM, Arunakaran J. Quercetin-induced growth inhibition and cell death in prostatic carcinoma cells (PC-3) are associated with increase in p21 and hypophosphorylated retinoblastoma proteins expression. *J Cancer Res Clin Oncol* (2005) 131(11):765–71. doi: 10.1007/s00432-005-0005-4

25. Park S, Lim W, Bazer FW, Whang KY, Song G. Quercetin inhibits proliferation of endometriosis regulating cyclin D1 and its target microRNAs *in vitro* and *in vivo*. *J Nutr Biochem* (2019) 63:87–100. doi: 10.1016/j.jnutbio.2018.09.024

26. Fan JH, Xu MM, Zhou LM, Gui ZW, Huang L, Li XG, et al. Integrating network pharmacology deciphers the action mechanism of zuojin capsule in suppressing colorectal cancer. *Phytomedicine* (2022) 96:153881. doi: 10.1016/j.phymed.2021.153881

27. Wei R, Xiao Y, Song Y, Yuan H, Luo J, Xu W. FAT4 regulates the EMT and autophagy in colorectal cancer cells in part *via* the PI3K-AKT signaling axis. *J Exp Clin Cancer Res* (2019) 38(1):112. doi: 10.1186/s13046-019-1043-0

28. Mangiapane LR, Nicotra A, Turdo A, Gaggianesi M, Bianca P, Di Franco S, et al. PI3K-driven HER2 expression is a potential therapeutic target in colorectal cancer stem cells. *Gut* (2022) 71(1):119–28. doi: 10.1136/gutjnl-2020-323553

frontiers | Frontiers in Oncology

TYPE Review
PUBLISHED 22 November 2022
DOI 10.3389/fonc.2022.1061065

Check for updates

OPEN ACCESS

EDITED BY
Zhendong Jin,
Second Military Medical University, China

REVIEWED BY
Xiaoqun Dong,
Brown University, United States
Pixu Liu,
Dalian Medical University, China

*CORRESPONDENCE
Hui Yang
13938276142@163.com

SPECIALTY SECTION
This article was submitted to Gastrointestinal Cancers: Hepato Pancreatic Biliary Cancers, a section of the journal Frontiers in Oncology

RECEIVED 04 October 2022
ACCEPTED 07 November 2022
PUBLISHED 22 November 2022

CITATION
Ma X, Ding Y, Li W, Li Q and Yang H (2022) Diagnosis and management of gastroenteropancreatic neuroendocrine neoplasms by nuclear medicine: Update and future perspective. *Front. Oncol.* 12:1061065. doi: 10.3389/fonc.2022.1061065

COPYRIGHT
© 2022 Ma, Ding, Li, Li and Yang. This is an open-access article distributed under the terms of the Creative Commons Attribution License (CC BY). The use, distribution or reproduction in other forums is permitted, provided the original author(s) and the copyright owner(s) are credited and that the original publication in this journal is cited, in accordance with accepted academic practice. No use, distribution or reproduction is permitted which does not comply with these terms.

Diagnosis and management of gastroenteropancreatic neuroendocrine neoplasms by nuclear medicine: Update and future perspective

Xing Ma, Ying Ding, Wenliang Li, Qiang Li and Hui Yang*

Department of Nuclear Medicine, The Affiliated Cancer Hospital of Zhengzhou University & Henan Cancer Hospital, Zhengzhou, China

Gastrointestinal (GI) cancers are the second most common cause of cancer related deaths in the World. Neuroendocrine neoplasms (NENs) is a rare tumor that originated from peptidergic neurons and neuroendocrine cells. NENs occurs in all parts of the body, especially in stomach, intestine, pancreas and lung. These rare tumors are challenging to diagnose at earlier stages because of their wide anatomical distribution and complex clinical features. Traditional imaging methods including magnetic resonance imaging (MRI) and computed tomography (CT) are mostly of useful for detection of larger primary tumors that are 1cm in size. A new medical imaging specialty called nuclear medicine uses radioactive substances for both diagnostic and therapeutic purposes. Nuclear medicine imaging relies on the tissue-specific uptake of radiolabeled tracers. Nuclear medicine techniques can easily identify the NENs tissues for their ability to absorb and concentrate amine, precursors, and peptides, whereas the traditional imaging methods are difficult to perform well. The somatostatin receptor (SSTR) is a targetable receptor frequently expressed in the gastroenteropancreatic neuroendocrine neoplasms (GEP-NENs), and is a promising target for tumor-targeted therapies and radiography. SSTR based somatostatin receptor imaging and peptide receptor radionuclide therapy (PRRT) has emerged as a new hot subject in the diagnosis and treatment of GEP-NENs due to the rapid development of somatostatin analogues (SSAs) and radionuclide. This review aims to provide an overview of the current status of nuclear medicine imaging modalities in the imaging of GEP-NENs, and puts them in perspective of clinical practice.

KEYWORDS

nuclear medicine, positron emission tomography, neuroendocrine neoplasms, somatostatin receptor, gastrointestinal cancer

Introduction

Gastrointestinal (GI) cancers account for approximately 20% of all cancer and are responsible for 23% of cancer-related deaths worldwide (1). The GI epithelial tumors are more common compared to non-epithelial tumors and mainly found in the esophagus, stomach, liver, gallbladder, bile duct, pancreas, small intestine, colon, rectum and the anal region. A subset of GI epithelial lesions exhibits neuroendocrine differentiation and was known as neuroendocrine neoplasms (NENs). Gastroenteropancreatic neuroendocrine neoplasms (GEP-NENs) is one of the most common types of NENs and its incidence has been rising during the past three decades (2, 3). However, the clinical manifestations of NENs are mostly atypical (4). Examination techniques for early diagnosis of GEP-NENs are therefore urgently needed. The timely and accurate diagnosis of GEP-NENs remains challenging for clinicians. Endoscopy and endoscopic ultrasonography (EUS) maybe useful for visualizing tumors found in the stomach, duodenum, rectal and sigmoid. The diagnostic accuracy of traditional imaging techniques, including CT, MR, and US, has improved over the last few years (5, 6). However, traditional imaging techniques are unable to effectively diagnose the small primary tumors which have been metastasized. Additionally, primary midgut tumors that are common in jejunum, ileum, and proximal colon are challenging and difficult to diagnose by gastroscopy or EUS examination. With the extensive use of nuclear medicine in the early diagnosis of GEP-NENs, the clinical benefit for patients has improved widely. Nuclear medicine modalities have the benefit of showing the target tissues' morphological and functional condition. The tissue origin, cell type, benign or malignant status, level of differentiation, and anatomic placement are used to categorize tumors. Somatostatin receptors (SSTRs) are highly expressed in the GEP-NENs. SSTRs are overexpressed on well-differentiated GEP-NENs tumor cells, especially SSTR2. The exact detection or treatment of GEP-NENs can be accomplished by labeling somatostatin analogues (SSAs) with diagnostic radionuclides or therapeutic radionuclides based on the specificity of the SSTR (7). SSAs or peptide receptor radionuclide therapy (PRRT) can be used to diagnose, stage, and evaluate the effectiveness of the treatment. SSAs and radionuclides have continued to advance, and as a result, nuclear imaging and therapy are currently a popular topic in the field of GEP-NENs.

This review provides an overview of the currently used imaging modalities and ongoing developments in the imaging of GEP-NENs, with the emphasis on nuclear medicine and puts them in perspective of clinical practice.

Nuclear medical imaging

Routine imaging techniques such as CT and MRI, are the first line anatomic imaging modalities for the diagnosis of NENs. CT/MRI can provide detailed and accurate anatomic information in locating the primary tumor and identifying the local and distant metastases. However, the diagnostic sensitivity of these anatomical imaging techniques is not very high especially in the diagnosis of NENs. Nuclear imaging is a novel imaging technology which combines functional and morphologic techniques (8). This combination can provide more information for the better diagnosis and treatment guidance of NENs. Common nuclear imaging methods for NENs diagnosis include SRS and tumor metabolism imaging (9).

The appropriate use of imaging agents is very crucial for the management of NENs. Gallium-68 SSTR (^{68}Ga-SSTR) PET/CT and Fluorine-18-fluorodeoxyglucose (^{18}F-FDG) PET/CT are two most commonly used functional imaging for the diagnosis of NENs. Both can localize lesions that are difficult to be detected by traditional imaging techniques, as well as assess the function of the lesion and optimize treatment strategies. Most well-differentiated NENs highly express SSTR (10), which makes it possible to clinically apply SSTR-mediated radiographic imaging, including ^{99m}Tc-Octreotide SPECT-CT imaging and ^{68}Ga-SSTR PET/CT imaging.

Diagnostic role of nuclear medicine in GEP-NENs

^{18}F-FDG is the most popular molecular probe in nuclear medicine that reflects glucose metabolism *in vivo*. It is more sensitive to tumors with low differentiation and high malignancy, and its absorption and retention are mostly dependent on the expression and phosphorylation level of glucose transporters. According to the Ki-67 index for tumor grading, NEMs are divided into three grades: G1 (less than 2%), G2 (between 22% and 20%), and G3 (more than 20%) (11). Numerous investigations have demonstrated that ^{18}F-FDG PET-CT performs poorly in low-grade, well-differentiated GEP-NENs and performs well in high-grade, poorly differentiated GEP-NENs (12, 13). The SUV_{max} of ^{18}F-FDG PET/CT and Ki-67 expression are positively correlated as shown in several investigations (14, 15). This finding suggests that ^{18}F-FDG PET/CT has an important prognostic value in high grade GEP-NENs. Currently, guidelines published by both European Neuroendocrine Tumor Society (ENETS) and European Association of Nuclear Medicine (EANM) recommend the use of ^{18}F-FDG PET/CT to localize high-grade hypodifferentiated GEP-NENs for stratified analysis of patient prognosis prediction using semiquantitative parameters (16).

SSTR is an important target for molecular imaging diagnosis and radionuclide therapy of SSTR-positive tumors (17). GEP-NENs with varying degrees of grading express different amounts of SSTR on their surfaces. ^{111}In-Octreotide is the earliest SSTR agonist used in clinical practice and can be used for SPECT-CT,

but its low resolution affects its detection of microscopic lesions and metastases (18). Currently, SSTR agonists commonly used in clinical practice include ^{68}Ga-DOTATATE, ^{68}Ga-DOTATOC and ^{68}Ga-DOTANOC (19). ^{68}Ga is a positron radionuclide with a half-life of about 67 min. PET/CT imaging using ^{68}Ga-labeled SSTR agonists can substantially improve image quality and spatial resolution, compensating for the deficiency of ^{111}In-Octreotide (20). ^{68}Ga-DOTATATE PET/CT plays an important role in the detection, primary staging, restaging and efficacy assessment of SSTR-positive tumors. The guidelines published by the ENETS and the EANM both recommend the use of SSTR agonist PET/CT as the first-line imaging method for the diagnosis and staging of GEP-NENs.

However, the half-life and positron energy limit the utilization of ^{68}Ga SSTR scanning. Poorly differentiated GEP-NENs usually do not express or under-express SSTR, and therefore ^{68}Ga-DOTA-SSTR PET imaging is not effective in these tumors. These tumor cells usually have a higher glucose metabolism rate, so ^{18}F FDG-PET is more suitable in poorly differentiated GEP-NENs and has a higher sensitivity for metastatic lesions. ^{18}F-FDG PET/CT and ^{68}Ga-DOTATATE PET/CT have complementary effects. The combined detection of ^{18}F-FDG PET/CT and ^{68}Ga-DOTATATE PET/CT has better localization and diagnostic value for GEP-NENs than the two alone (21).

Advances in nuclear medicine diagnosis of GEP-NENs

In recent years, radionuclides with longer half-life and better imaging results have been gradually incorporated into clinical studies with great potential for development. ^{64}Cu-DOTATATE is the latest SSTR agonist approved by the FDA for localization of SSTR-positive NENs. ^{64}Cu has a longer half-life and better image resolution than conventional radionuclides, and is more sensitive for diagnosing SSTR-positive GEP-NENs. The long half-life of ^{64}Cu extends the time window for PET/CT imaging to 3 h, compensating for the shorter half-life of ^{68}Ga (22). Another more mature PET imaging agent for NENs is ^{18}F-FDOPA (23), which is a structural analogue of dopamine and can reflect the metabolism of dopamine in NENs. However, owing to the difficult synthesis and purification procedure and the early poor yield, it was not generally promoted in clinical practice. Its production has significantly increased in recent years due to improvements in chemical synthesis and labeling processes, and it has been promoted quickly with amazing results. In clinical research conducted abroad, ^{18}F-FDOPA has been extensively explored in the neurological, cardiac, and tumor domains, with the tumor study focusing primarily on medullary thyroid cancer and NENs (24). Currently, tumors with low or ambiguous SSTR expression are the key indications for NENs imaging with ^{18}F-FDOPA. Piccardo (25) et al. conducted a head-to-head ^{18}F-DOPA and SSTR agonists for PET/CT diagnostic meta-analysis, which showed that both examinations could accurately diagnose intestinal NENs, with a combined sensitivity of 95% for ^{18}F-DOPA in a lesion-based analysis, slightly higher than the combined sensitivity of 82% for SSTR agonists. Therefore, some studies (26, 27) have recommended ^{18}F-DOPA as a second-line screening method as complementary and alternative of SSTR-based imaging agents.

Therapeutic role of nuclear medicine in GEP-NENs

Surgery is still the preferred treatment for GEP-NENs (28), and systemic chemotherapy is an another option for individuals who are not candidates for surgery. Targeted therapy can be divided into non-radiolabeled SSA and PRRT. SSA has been applied in the clinical practice for more than 20 years. However, SSA has a relatively limited impact on establishing tumor biology and imaging remission, but it can successfully treat the clinical symptoms of hormone overproduction and stop NENs development (29). Since SSTR-targeted PRRT has been utilized in clinical settings in Europe and the US, it has proven to be an effective method for treating NENs and other SSTR-positive cancers, particularly GEP-NENs. PRRT utilizes therapeutic radionuclide ^{177}Lu and ^{90}Y-labeled SSTR agonists to deliver precise targeted internal radiotherapy to GEP-NENs.

SSA therapy is primarily indicated for the initial treatment of patients with carcinoid syndrome and unresectable tumors. In contrast, PRRT therapy is indicated for patients with SSTR-positive, G1/2 grade advanced GEP-NENs. The second-generation ^{90}Y-DOTA-TOC and the third-generation ^{177}Lu-DOTATATE are the most commonly used PPRT therapeutics. Several studies now confirm the safety and efficacy of ^{177}Lu-DOTATATE-mediated PRRT (30, 31). It is well tolerated by patients, has a low incidence of acute and long-term adverse effects, and is effective in reducing the specific symptoms of neuroendocrine syndrome, such as diarrhea, facial flushing, and cardiac dysfunction caused by right heart failure. In addition, PRRT has a significant analgesic effect, especially for bone pain caused by bone metastases from gastrointestinal or bronchial NENs.

Therapeutic advances in nuclear medicine of GEP-NENs

The results of combination therapy with PRRT showed the highest response rate for NENs with the combination of ^{90}Y-DOTA-TOC and ^{177}Lu-DOTA-TATE (38.1%), with a low rate

of tumor recurrence and mild adverse effects in most patients (32). There may be additional benefit from receiving a combination of both nuclides (33). The rationale for this treatment modality is to use the shorter tissue penetration of moderate-energy β-rays emitted by ^{177}Lu and the longer tissue penetration of high-energy β-rays emitted by ^{90}Y to achieve greater killing effect on both smaller and larger tumors when applied in combination.

In PRRT research, the results of animal experiments and clinical trials show that the antagonist probe ^{177}Lu-OPS201 has higher tumor radiation dose and better radiation safety than the agonist probe ^{177}Lu-DOTATATE, so it is more suitable for PRRT clinical research of NENs (34). Radionuclide labeled SSTR antagonist ^{177}Lu-DOTA-JR11 has a higher tumor uptake rate and a longer tumor retention time than SSTR agonist ^{177}Lu-DOTA-TOC, thereby increasing the radiation dose in the tumor by 1.7-10.6 times. The tumor growth delay time and the median survival time of patients were prolonged. Other studies have shown that after PRRT treatment of NENs patients with radionuclide labeled SSTR antagonist, it has a high uptake rate in all known lesion sites (liver, lymph node and bone) (35). Albrecht et al. (36) compared the efficacy of two cycles of PRRT with ^{177}Lu-DOTA-JR11, an antagonist of radionuclide labeled SSTR, and ^{177}Lu-DOTA-TOC, an agonist, in orthotopic NENs xenograft tumor mice. Mice treated with ^{177}Lu-DOTA-JR11 had significantly reduced tumor mass and almost no viable remaining tumor tissue 3 weeks after the end of two cycles of PRRT. In addition, the results of preclinical studies have shown that nuclide labeled SSTR antagonists induce more DNA double-strand breaks than agonists, resulting in better therapeutic effects (37). Therefore, it is of great significance to use radionuclide labeled SSTR antagonists as a neoadjuvant tool for PRRT in NENs patients. At present, a series of targeted imaging and therapeutic drugs based on radionuclide labeling are also being developed (38–40). It is believed that there will be major innovations in this field in the near future.

Conclusion and future perspective

GEP-NENs are challenging to diagnose and localize due to their wide anatomical distribution and complex clinical features. Although traditional techniques (CT, MRI) have significantly advanced during the last two decades, identification and detection of small primary GEP-NENs tumors still remains challenging. The staging and early identification of the disease is also very crucial for selection of the right treatment and effective management of the patients in timely manner. Using radionuclide-labeled SSTR analogues for nuclear medicine imaging of GEP-NENs shows superior imaging sensitivity and specificity as well as prognostic significance. At present, it serves as the gold standard for GEP-NENs diagnosis, localization, and staging. In future, with the improved technology and introduction of new tracers might further improve the sensitivity and specificity of these methods. Currently available and published data on tumor-targeted radioactive therapy is very encouraging. It has been acknowledged that PRRT has a therapeutic benefit in the management of advanced GEP-NENs and that it has significant potential for advancement as a first-line therapy. More individuals can now benefit from PRRT thanks to combination therapy and recent advances in pharmaceuticals. Nuclear medicine is now more useful in the diagnosis and treatment of GEP-NENs as a result of advancements in research on radionuclides and their ligands. However, it has to be further improved both in terms of dosages and patient's selection. We are aware that debates are still open in this area and will continue in the future. To get at a more compelling consensus, more assessments and thorough clinical investigations are required. However, it is important to stress that the role of nuclear medicine has grown over the last two decades, and its daily practice can confirm that these methods do offer many alternative valid solutions in the field of GEP-NENs diseases, as well as in other diseases.

Author contributions

HY and XM formulated the concept of this study; XM wrote the original manuscript draft; YD, WLL, QL provided the data and material support; HY and YD critically revised the manuscript. All authors contributed to the article and approved the submitted version.

Acknowledgments

We apologize to the authors whose study could not be cited for the limited spaces. We would like to thank Dr. Yang Shi and Dr. Yingying Zhang for their suggestions and comments on this manuscript.

Conflict of interest

The authors declare that the research was conducted in the absence of any commercial or financial relationships that could be construed as a potential conflict of interest.

Publisher's note

All claims expressed in this article are solely those of the authors and do not necessarily represent those of their affiliated organizations, or those of the publisher, the editors and the reviewers. Any product that may be evaluated in this article, or claim that may be made by its manufacturer, is not guaranteed or endorsed by the publisher.

References

1. Arnold M, Abnet CC, Neale RE, Vignat J, Giovannucci EL, McGlynn KA, et al. Global burden of 5 major types of gastrointestinal cancer. *Gastroenterology* (2020) 159(1):335–49.e15. doi: 10.1053/j.gastro.2020.02.068

2. Yao JC, Hassan M, Phan A, Dagohoy C, Leary C, Mares JE, et al. One hundred years after "Carcinoid": Epidemiology of and prognostic factors for neuroendocrine tumors in 35,825 cases in the United States. *J Clin Oncol* (2008) 26(18):3063–72. doi: 10.1200/JCO.2007.15.4377

3. Modlin IM, Oberg K, Chung DC, Jensen RT, de Herder WW, Thakker RV, et al. Gastroenteropancreatic neuroendocrine tumours. *Lancet Oncol* (2008) 9 (1):61–72. doi: 10.1016/S1470-2045(07)70410-2

4. Oronsky B, Ma PC, Morgensztern D, Carter CA. Nothing but net: A review of neuroendocrine tumors and carcinomas. *Neoplasia* (2017) 19(12):991–1002. doi: 10.1016/j.neo.2017.09.002

5. Gulpinar B, Peker E, Kul M, Elhan AH, Haliloglu N. Liver metastases of neuroendocrine tumors: Is it possible to diagnose different histologic subtypes depending on multiphasic ct features? *Abdominal Radiol* (2019) 44(6):2147–55. doi: 10.1007/s00261-019-01963-y

6. Baghdadi A, Ghadimi M, Mirpour S, Hazhirkarzar B, Motaghi M, Pawlik TM, et al. Imaging neuroendocrine tumors: Characterizing the spectrum of radiographic findings. *Surg Oncol* (2021) 37:101529. doi: 10.1016/j.suronc.2021.101529

7. Eriksson B, Öberg K. Summing up 15 years of somatostatin analog therapy in neuroendocrine tumors: Future outlook. *Ann Oncol* (1999) 10:S31–S8. doi: 10.1093/annonc/10.suppl_2.S31

8. Rowe SP, Pomper MG. Molecular imaging in oncology: Current impact and future directions. *CA: Cancer J Clin* (2022) 72(4):333–52. doi: 10.3322/caac.21713

9. Ambrosini V, Kunikowska J, Baudin E, Bodei L, Bouvier C, Capdevila J, et al. Consensus on molecular imaging and theranostics in neuroendocrine neoplasms. *Eur J Cancer* (2021) 146:56–73. doi: 10.1016/j.ejca.2021.01.008

10. Hankus J, Tomaszewska R. Neuroendocrine neoplasms and somatostatin receptor subtypes expression. *Nucl Med Rev* (2016) 19(2):111–7. doi: 10.5603/NMR.2016.0022

11. Kulke MH, Shah MH, Benson AB, Bergsland E, Berlin JD, Blaszkowsky LS, et al. Neuroendocrine tumors, version 1.2015. *J Natl Compr Cancer Network* (2015) 13(1):78–108. doi: 10.6004/jnccn.2012.0075

12. Rufini V, Baum RP, Castaldi P, Treglia G, De Gaetano AM, Carreras C, et al. Role of Pet/Ct in the functional imaging of endocrine pancreatic tumors. *Abdominal Imaging* (2012) 37(6):1004–20. doi: 10.1007/s00261-012-9871-9

13. Binderup T, Knigge U, Loft A, Mortensen J, Pfeifer A, Federspiel B, et al. Functional imaging of neuroendocrine tumors: A head-to-Head comparison of somatostatin receptor scintigraphy, 123i-mibg scintigraphy, and 18f-fdg pet. *J Nucl Med* (2010) 51(5):704–12. doi: 10.2967/jnumed.109.069765

14. Matsumoto T, Okabe H, Y-i Y, Yusa T, Itoyama R, Nakao Y, et al. Clinical role of fludeoxyglucose (18f) positron emission Tomography/Computed tomography (18f-fdg Pet/Ct) in patients with pancreatic neuroendocrine tumors. *Surg Today* (2019) 49(1):21–6. doi: 10.1007/s00595-018-1703-2

15. Abgral R, Leboulleux S, Deandreis D, Auperin A, Lumbroso J, Dromain C, et al. Performance of 18fluorodeoxyglucose-positron emission tomography and somatostatin receptor scintigraphy for high Ki67 (≥ 10%) well-differentiated endocrine carcinoma staging. *J Clin Endocrinol Metab* (2011) 96(3):665–71. doi: 10.1210/jc.2010-2022

16. Garcia-Carbonero R, Sorbye H, Baudin E, Raymond E, Wiedenmann B, Niederle B, et al. Enets consensus guidelines for high-grade gastroenteropancreatic neuroendocrine tumors and neuroendocrine carcinomas. *Neuroendocrinology* (2016) 103(2):186–94. doi: 10.1159/000443172

17. De Herder W, Hofland L, van der Lely A-J, Lamberts S. Somatostatin receptors in gastroentero-pancreatic neuroendocrine tumours. *Endocrine-Related Cancer* (2003) 10(4):451–8. doi: 10.1677/erc.0.0100451

18. Krausz Y, Keidar Z, Kogan I, Even-Sapir E, Bar-Shalom R, Engel A, et al. Spect/Ct hybrid imaging with 111in-pentetreotide in assessment of neuroendocrine tumours. *Clin Endocrinol* (2003) 59(5):565–73. doi: 10.1046/j.1365-2265.2003.01885.x

19. Yang J, Kan Y, Ge BH, Yuan L, Li C, Zhao W. Diagnostic role of gallium-68 dotatoc and gallium-68 dotatate pet in patients with neuroendocrine tumors: A meta-analysis. *Acta radiol* (2014) 55(4):389–98. doi: 10.1177/0284185113496679

20. Hope TA, Bergsland EK, Bozkurt MF, Graham M, Heaney AP, Herrmann K, et al. Appropriate use criteria for somatostatin receptor pet imaging in neuroendocrine tumors. *J Nucl Med* (2018) 59(1):66–74. doi: 10.2967/jnumed.117.202275

21. Chan DL, Pavlakis N, Schembri GP, Bernard EJ, Hsiao E, Hayes A, et al. Dual somatostatin Receptor/Fdg Pet/Ct imaging in metastatic neuroendocrine tumours: Proposal for a novel grading scheme with prognostic significance. *Theranostics* (2017) 7(5):1149. doi: 10.7150/thno.18068

22. Loft M, Carlsen EA, Johnbeck CB, Johannesen HH, Binderup T, Pfeifer A, et al. 64cu-dotatate pet in patients with neuroendocrine neoplasms: Prospective, head-to-Head comparison of imaging at 1 hour and 3 hours after injection. *J Nucl Med* (2021) 62(1):73–80. doi: 10.2967/jnumed.120.244509

23. Hoegerle S, Nitzsche E, Altehoefer C, Ghanem N, Manz T, Brink I, et al. Pheochromocytomas: Detection with 18f dopa whole-body pet–initial results. *Radiology* (2002) 222(2):507–12. doi: 10.1148/radiol.2222010622

24. Bozkurt MF, Virgolini I, Balogova S, Beheshti M, Rubello D, Decristoforo C, et al. Guideline for Pet/Ct imaging of neuroendocrine neoplasms with 68ga-Dota-Conjugated somatostatin receptor targeting peptides and 18f–dopa. *Eur J Nucl Med Mol Imaging* (2017) 44(9):1588–601. doi: 10.1007/s00259-017-3728-y

25. Piccardo A, Fiz F, Bottoni G, Ugolini M, Noordzij W, Trimboli P. Head-to-Head comparison between 18f-dopa Pet/Ct and 68ga-dota peptides Pet/Ct in detecting intestinal neuroendocrine tumours: A systematic review and meta-analysis. *Clin Endocrinol* (2021) 95(4):595–605. doi: 10.1111/cen.14527

26. Leroy-Freschini B, Amodru V, Addeo P, Sebag F, Vix M, Brunaud L, et al. Early 18f-fdopa Pet/Ct imaging after carbidopa premedication as a valuable diagnostic option in patients with insulinoma. *Eur J Nucl Med Mol Imaging* (2019) 46(3):686–95. doi: 10.1007/s00259-018-4245-3

27. Helali M, Addeo P, Heimburger C, Detour J, Goichot B, Bachellier P, et al. Carbidopa-assisted 18f-fluorodihydroxyphenylalanine Pet/Ct for the localization and staging of non-functioning neuroendocrine pancreatic tumors. *Ann Nucl Med* (2016) 30(9):659–68. doi: 10.1007/s12149-016-1110-y

28. Kulke MH, Siu LL, Tepper JE, Fisher G, Jaffe D, Haller DG, et al. Future directions in the treatment of neuroendocrine tumors: Consensus report of the national cancer institute neuroendocrine tumor clinical trials planning meeting. *J Clin Oncol* (2011) 29(7):934. doi: 10.1200/JCO.2010.33.2056

29. Modlin I, Pavel M, Kidd M, Gustafsson B. Somatostatin analogues in the treatment of gastroenteropancreatic neuroendocrine (Carcinoid) tumours. *Alimentary Pharmacol Ther* (2010) 31(2):169–88. doi: 10.1111/j.1365-2036.2009.04174.x

30. Kwekkeboom DJ, de Herder WW, Kam BL, van Eijck CH, van Essen M, Kooij PP, et al. Treatment with the radiolabeled somatostatin analog [177lu-Dota0, Tyr3] octreotate: Toxicity, efficacy, and survival. *J Clin Oncol* (2008) 26(13):2124–30. doi: 10.1200/JCO.2007.15.2553

31. Strosberg J, El-Haddad G, Wolin E, Hendifar A, Yao J, Chasen B, et al. Phase 3 trial of 177lu-dotatate for midgut neuroendocrine tumors. *N Engl J Med* (2017) 376(2):125–35. doi: 10.1056/NEJMoa1607427

32. Basu S, Parghane RV, Banerjee S. Availability of both [177lu] Lu-Dota-Tate and [90y] y-dotatate as prrt agents for neuroendocrine tumors: Can we evolve a rational sequential duo-prrt protocol for Large volume resistant tumors? *Eur J Nucl Med Mol Imaging* (2020) 47(4):756–8. doi: 10.1007/s00259-019-04546-7

33. de Jong M, Breeman WA, Valkema R, Bernard BF, Krenning EP. Combination radionuclide therapy using 177lu-and 90y-labeled somatostatin analogs. *J Nucl Med* (2005) 46(1 suppl):13S–7S.

34. Nicolas GP, Mansi R, McDougall L, Kaufmann J, Bouterfa H, Wild D, et al. Biodistribution, pharmacokinetics, and dosimetry of 177lu-, 90y-, and 111in-labeled somatostatin receptor antagonist Ops201 in comparison to the agonist 177lu-dotatate: The mass effect. *J Nucl Med* (2017) 58(9):1435–41. doi: 10.2967/jnumed.117.191684

35. Reidy-Lagunes D, Pandit-Taskar N, O'Donoghue JA, Krebs S, Staton KD, Lyashchenko SK, et al. Phase I trial of well-differentiated neuroendocrine tumors (Nets) with radiolabeled somatostatin antagonist 177lu-satoreotide Tetraxetan177lu-satoreotide tetraxetan in well-differentiated nets. *Clin Cancer Res* (2019) 25(23):6939–47. doi: 10.1158/1078-0432.CCR-19-1026

36. Albrecht J, Exner S, Grötzinger C, Prasad S, Konietschke F, Beindorff N, et al. Multimodal imaging of 2-cycle prrt with 177lu-Dota-Jr11 and 177lu-dotatoc in an orthotopic neuroendocrine xenograft tumor mouse model. *J Nucl Med* (2021) 62(3):393–8. doi: 10.2967/jnumed.120.250274

37. Dalm SU, Nonnekens J, Doeswijk GN, de Blois E, van Gent DC, Konijnenberg MW, et al. Comparison of the therapeutic response to treatment with a 177lu-labeled somatostatin receptor agonist and antagonist in preclinical models. *J Nucl Med* (2016) 57(2):260–5. doi: 10.2967/jnumed.115.167007

38. Morgenstern A, Apostolidis C, Kratochwil C, Sathekge M, Krolicki L, Bruchertseifer F. An overview of targeted alpha therapy with 225actinium and 213bismuth. *Curr radiopharmac* (2018) 11(3):200–8. doi: 10.2174/1874471011666180502104524

39. Chan HS, Konijnenberg MW, Daniels T, Nysus M, Makvandi M, de Blois E, et al. Improved safety and efficacy of 213bi-Dotatate-Targeted alpha therapy of somatostatin receptor-expressing neuroendocrine tumors in mice pre-treated with l-lysine. *EJNMMI Res* (2016) 6(1):1–11. doi: 10.1186/s13550-016-0240-5

40. Kratochwil C, Giesel F, Bruchertseifer F, Mier W, Apostolidis C, Boll R, et al. 213bi-dotatoc receptor-targeted alpha-radionuclide therapy induces remission in neuroendocrine tumours refractory to beta radiation: A first-in-Human experience. *Eur J Nucl Med Mol Imaging* (2014) 41(11):2106–19. doi: 10.1007/s00259-014-2857-9

frontiers | Frontiers in Oncology

TYPE Review
PUBLISHED 24 November 2022
DOI 10.3389/fonc.2022.1017692

Check for updates

OPEN ACCESS

EDITED BY
Zhendong Jin,
Second Military Medical University, China

REVIEWED BY
Yoshiaki Yura,
Osaka University, Japan
Giuseppe Portella,
University of Naples Federico II, Italy

*CORRESPONDENCE
Xiangjian Chen
wz1370@126.com
Linyong Du
dulinyong@qq.com

SPECIALTY SECTION
This article was submitted to Gastrointestinal Cancers: Gastric and Esophageal Cancers, a section of the journal Frontiers in Oncology

RECEIVED 12 August 2022
ACCEPTED 02 November 2022
PUBLISHED 24 November 2022

CITATION
Wang J, Du L and Chen X (2022) Oncolytic virus: A catalyst for the treatment of gastric cancer. *Front. Oncol.* 12:1017692. doi: 10.3389/fonc.2022.1017692

COPYRIGHT
© 2022 Wang, Du and Chen. This is an open-access article distributed under the terms of the Creative Commons Attribution License (CC BY). The use, distribution or reproduction in other forums is permitted, provided the original author(s) and the copyright owner(s) are credited and that the original publication in this journal is cited, in accordance with accepted academic practice. No use, distribution or reproduction is permitted which does not comply with these terms.

Oncolytic virus: A catalyst for the treatment of gastric cancer

Junqing Wang[1], Linyong Du[2*] and Xiangjian Chen[1*]

[1]School of the 1st Clinical Medical Sciences, Wenzhou Medical University, Wenzhou, Zhejiang, China, [2]Key Laboratory of Laboratory Medicine, Ministry of Education of China, School of Laboratory Medicine and Life Science, Wenzhou Medical University, Wenzhou, Zhejiang, China

Gastric cancer (GC) is a leading contributor to global cancer incidence and mortality. According to the GLOBOCAN 2020 estimates of incidence and mortality for 36 cancers in 185 countries produced by the International Agency for Research on Cancer (IARC), GC ranks fifth and fourth, respectively, and seriously threatens the survival and health of people all over the world. Therefore, how to effectively treat GC has become an urgent problem for medical personnel and scientific workers at this stage. Due to the unobvious early symptoms and the influence of some adverse factors such as tumor heterogeneity and low immunogenicity, patients with advanced gastric cancer (AGC) cannot benefit significantly from treatments such as radical surgical resection, radiotherapy, chemotherapy, and targeted therapy. As an emerging cancer immunotherapy, oncolytic virotherapies (OVTs) can not only selectively lyse cancer cells, but also induce a systemic antitumor immune response. This unique ability to turn unresponsive 'cold' tumors into responsive 'hot' tumors gives them great potential in GC therapy. This review integrates most experimental studies and clinical trials of various oncolytic viruses (OVs) in the diagnosis and treatment of GC. It also exhaustively introduces the concrete mechanism of invading GC cells and the viral genome composition of adenovirus and herpes simplex virus type 1 (HSV-1). At the end of the article, some prospects are put forward to determine the developmental directions of OVTs for GC in the future.

KEYWORDS

gastric cancer, oncolytic virus, adenovirus, herpes simplex virus type 1, tumor microenvironment, combination therapy

Abbreviations: MDSC, myeloid-derived suppressor cell; CAF, cancer-associated fibroblast; MSC, mesenchymal stem cell; PAMP, pathogen-associated molecular pattern; PRR, pattern-recognition receptor; TLR, Toll-like receptor; NLR, NOD-like receptor; RLR, RIG-I-like receptor; cGAS, cyclic GMP–AMP synthase; cGAMP, cyclic GMP–AMP; TBK1, TANKbinding kinase 1; IRF3, interferon regulatory factor 3; NF-κB, the nuclear factor-κB; IFN, interferon; RIG-I, retinoic acid-inducible gene I; MAVS, mitochondrial antiviral-signaling protein; ISG, interferon-stimulated gene; CAR, coxsackievirus adenovirus receptor; HVEM, herpesvirus-entry mediator; ICD, immunogenic cell death; TAA, tumor-associated antigen; DAMP, damage-associated molecular pattern; APC, antigen-presenting cell; RGD, arginine-glycine-aspartate; ITR, inverted terminal repetition; MHC, major histocompatibility complex; PTEN, phosphatase and tensin homolog; RNAi, RNA interference; CEA, carcinoembryonic antigen; ICP, infected cell protein; EMT, epithelial-mesenchymal transition; TSA, tumor-specific antigen.

1 Introduction

Gastric cancer (GC) is a common malignant tumor originating from gastric mucosa epithelial cells, and its onset is relatively insidious. In the early stage, there is generally no apparent symptom of discomfort or only indigestion-like clinical manifestations such as inappetence, gastroesophageal reflux, belching, and stomachache. However, as the disease progresses, hemorrhage, perforation, obstruction, cachexia, and other symptoms of advanced gastric cancer (AGC) gradually appear. Unfortunately, patients are already in the terminal stage at this time, and the cancer cells have already invaded the surrounding organs or metastasized far away, which leads to the loss of the curative chance for most patients (1). According to the GLOBOCAN 2020 estimates of incidence and mortality for 36 cancers in 185 countries produced by the International Agency for Research on Cancer (IARC), an estimated 19.3 million new cancer cases and almost 10.0 million cancer deaths occurred worldwide in 2020, and GC ranked fifth (5.6%) and fourth (7.7%), respectively (2). Therefore, accurately diagnosing early GC and effectively treating AGC patients who have lost the chance of radical surgical resection are two serious health problems worldwide.

Currently, therapeutic strategies for GC mainly incorporate surgical resection, radiotherapy, chemotherapy, targeted therapy, and immunotherapy. Among them, radical surgical resection is still the preferred and only method considered to cure GC. Endoscopic submucosal dissection (ESD) is recommended for early GC which is limited to the mucosa and without lymph node metastasis, and gastrectomy with D2 lymphadenectomy is recommended for AGC (3). Radiotherapy, chemotherapy, targeted therapy, and immunotherapy are basically intended to provide another choice for patients with post- or non-operative conditions. Chemotherapy, as the most common and indispensable adjuvant therapy, is updated constantly with advances in research. Recently, a randomized, open-label, phase 3 trial (NCT02322593) in 62 centers across Japan and South Korea showed that TAS-118 (S-1 (an oral anticancer agent comprising the 5-fluorouracil prodrug tegafur and targeted modulators, gimeracil and oteracil) plus leucovorin) plus oxaliplatin is more effective than S-1 plus cisplatin, and could be considered a new first-line treatment option for AGC in Asian patients (the median overall survival (OS) was 16.0 months (95% CI 13.8–18.3) in the TAS-118 plus oxaliplatin group and 15.1 months (95% CI 13.6–16.4) in the S-1 plus cisplatin group (hazard ratio 0.83, 95% CI 0.69–0.99; p=0.039)) (4). Furthermore, targeted therapy usually focuses on the human epidermal growth factor receptor 2 (HER2), because of its frequent amplification (5). In an open-label, randomized, phase 2 trial (NCT03329690), therapy with trastuzumab led to significant improvements in response and OS, compared with standard chemotherapy, among patients with HER2-positive GC (median, 12.5 vs. 8.4 months; hazard ratio for death, 0.59; 95% confidence interval, 0.39 to 0.88; P=0.01) (6). Although chemotherapy and targeted therapy have obtained satisfactory efficacy, resistance and fatal side effects gradually develop with the extension of exposure time. Thus, a new strategy is urgently needed to fill this gap.

With the exploration of the biological behavior and internal molecular mechanism of cancers, immunotherapy has become a novel, popular and promising treatment that can restore the ability of the immune system to respond to neoplasms, limiting their growth and killing malignant cells, ultimately achieving remission or even complete elimination (7). Existing cancer immunotherapies mainly include tumor vaccines (such as cervical cancer vaccine), immune checkpoint inhibitors (ICIs) (such as anti-PD-L1 antibody), adoptive immunotherapies (such as CAR T-cell) and OVTs (such as adenovirus) (8). OVTs are a safe and mature immunotherapy method because of their representative capacity to promote the infiltration of immune effector cells into the tumor microenvironment (TME) and have been favored by numerous researchers (9).

OVs, as their name implies, can specifically invade tumor cells and eventually lyse them. The first definitive record of OV was in 1904, when a 42-year-old leukemia patient was infected with influenza. Doctors were surprised to find a dramatic decrease in malignant cells in his blood. Recently, on January 2, 2021, Sarah Challenor also reported a 61-year-old patient with stage III Epstein–Barr virus (EBV)-positive classical Hodgkin lymphoma who was diagnosed with COVID-19, and four months later, the palpable lymphadenopathy had reduced and a fluorine-18 fluorodeoxyglucose positron emission tomography/CT (^{18}FDG-PET/CT) scan revealed widespread resolution of the lymphadenopathy and reduced metabolic uptake throughout (10). These miraculous phenomena about viruses "curing" cancers suggest that OVTs may be a promising cancer treatment. More notably, in 2015, the US Food and Drug Administration (FDA) approved the first OV (T-Vec, a HSV-1-based OV generated by deleting ICP47 gene and replacing ICP34.5 with GM-CSF gene) for the clinical treatment of malignant tumors by virtue of a randomized, open-label, phase 3 trial (NCT00769704); it can achieve a higher durable response rate (DRR) (26.4%; 95% CI, 21.4% to 31.5% vs. 5.7%; 95% CI, 1.9% to 9.5%) and longer OS (23.3 months; 95% CI, 19.5 to 29.6 months vs. 18.9 months; 95% CI, 16.0 to 23.7 months) in patients with unresectable stage IIIB to IV melanoma than subcutaneous injection of granulocyte macrophage colony-stimulating factor (GM-CSF) alone (11). In Japan, another single-arm, phase II clinical trial (UMIN000015995) was completed to test the efficacy of G47Δ (a HSV-1-based OV generated by deleting ICP47 and ICP34.5 genes and replacing

ICP6 gene with lacZ coding sequence) administered stereotactically in patients with residual or recurrent glioblastoma, and the results indicated that the 1-year- survival rate of 13 patients reached an astonishing 92.3% (12). Moreover, in a phase I/II, single-arm study (UMIN000002661) assessing the safety of G47Δ, the results revealed that G47Δ was safe for treating recurrent or progressive glioblastoma and warranted further clinical development (13). Based on these, G47Δ has received conditional approval from Japan's Ministry of Health, Labor and Welfare (MHLW) as an OVT for patients with malignant glioma. Furthermore, studies proving the ability of OVTs to rapidly eliminate cancer cells have led to approval of H101 in China and Rigvir in Latvia.

An increasing number of OVTs are being clinically approved, and trials of OVs for other malignancies have sprung up continually, including GC. As a malignant tumor with a poor prognosis, strong heterogeneity, and low immunogenicity, GC therapy may acquire a certain degree of breakthrough with the help of OV's exceptional function. Moreover, peritoneal metastasis is the most frequent form of distant metastasis and recurrence in GC, and the prognosis is extremely poor due to the resistance of systemic chemotherapy. OVTs for GC patients with peritoneal metastases *via* intraperitoneal injection not only act on the vast majority of metastases, but also activate the inherent immune cells in the abdominal cavity and recruit immune cells in the blood to exert corresponding antitumor functions. However, there is no systematic summary of OVTs for GC to date. In this review, we integrate most of the experimental studies and clinical trials of various OVs tested for the diagnosis and therapy of GC and meticulously discuss the mechanism of infection and the viral genome composition of adenovirus and HSV-1. Finally, we also put forward some prospects about the developmental directions of OVTs for GC in the future.

2 Mechanism of OVTs

According to existing experimental results on OVTs for cancers, a nonoptimal delivery route is one of the dominant reasons for treatment failure. Intravenous administration is a simple, common, and effective route for other cancer treatments, but when OVs are injected into the bloodstream, viral defense barriers such as the complement system, immunoglobulin and coagulation cascade will promptly inactivate the virus particles (14). Virions marked by natural immunoglobulin M (IgM) antibodies and coagulation factor X are captured and cleared by macrophages rapidly and efficiently in the liver, spleen, and lung, which probably trigger toxic reactions in the corresponding organs (15). Furthermore, during the process of rapid proliferation of cancer cells, a suitable environment for their survival called the tumor microenvironment (TME) is gradually established. Numerous mesenchymal cells such as myeloid-derived suppressor cells (MDSCs), cancer-associated fibroblasts (CAFs), mesenchymal stem cells (MSCs), and capillary endothelial cells, which are abundant in the TME, constitute a physical barrier in conjunction with the extracellular matrix (ECM). Even if OVs successfully escape the abovementioned clearance process and enter the TME, they will ultimately be captured or rejected by these "trap" cells, resulting in a further decrease in oncolytic effectiveness (16). Thus, intratumoral injection is still the optimal route of administration for solid tumors, including GC (17).

When OVs invade the interior of tumors, they mainly exert their antitumor function by selectively infecting and lysing the malignant cells locally (Figure 1) and stimulating the systemic adaptive antitumor immune response (Figure 2) (18):

2.1 Selectively infect and lyse the malignant cells locally

First, OVs infect host cells by recognizing and combining with relevant receptors or other special routes. Subsequently, they replicate and amplify by using nutrients from the host, similar to other viruses (18). After a certain period of proliferation, a small amount of new progeny virions, viral nucleic acids, and capsid protein accumulate inside the cell, which are known as pathogen-associated molecular patterns (PAMPs), and these products are identified by pattern-recognition receptors (PRRs, including Toll-like receptor (TLR), NOD-like receptor (NLR), and RIG-I-like receptor (RLR)) to initiate innate antiviral immune responses (19). In this review, we mainly highlight the two most acknowledged antiviral signal transduction pathways.

For a DNA virus, its gene fragments can activate the DNA sensor cyclic GMP–AMP synthase (cGAS) through direct binding, which triggers conformational changes that induce enzymatic activity (Figure 1A). Activated cGAS converts GTP and ATP into cyclic GMP–AMP (cGAMP), which is a unique endogenous second messenger. Then, the cGAMP product binds to STING, an endoplasmic reticulum (ER) -localized adaptor, and undergoes a conformational change to form dimers. Following the translocation of STING dimers to the Golgi apparatus, they interact with TANKbinding kinase 1 (TBK1) and IκB kinase (IKK), which phosphorylate interferon regulatory factor 3 (IRF3) and nuclear factor-κB (NF-κB), respectively. Activated IRF3 and NF-κB dimerize and translocate to the nucleus to regulate the transcription of type I interferon (IFN) and proinflammatory cytokines (20). In addition, other viral DNA sensors, such as IFI16, DAI and DDX41, can transmit antiviral immune signals through STING (21).

Retinoic acid-inducible gene I (RIG-I) is one of the primary originators of initiating infection signals of RNA virus, the other antiviral signal transduction pathway, along with melanoma

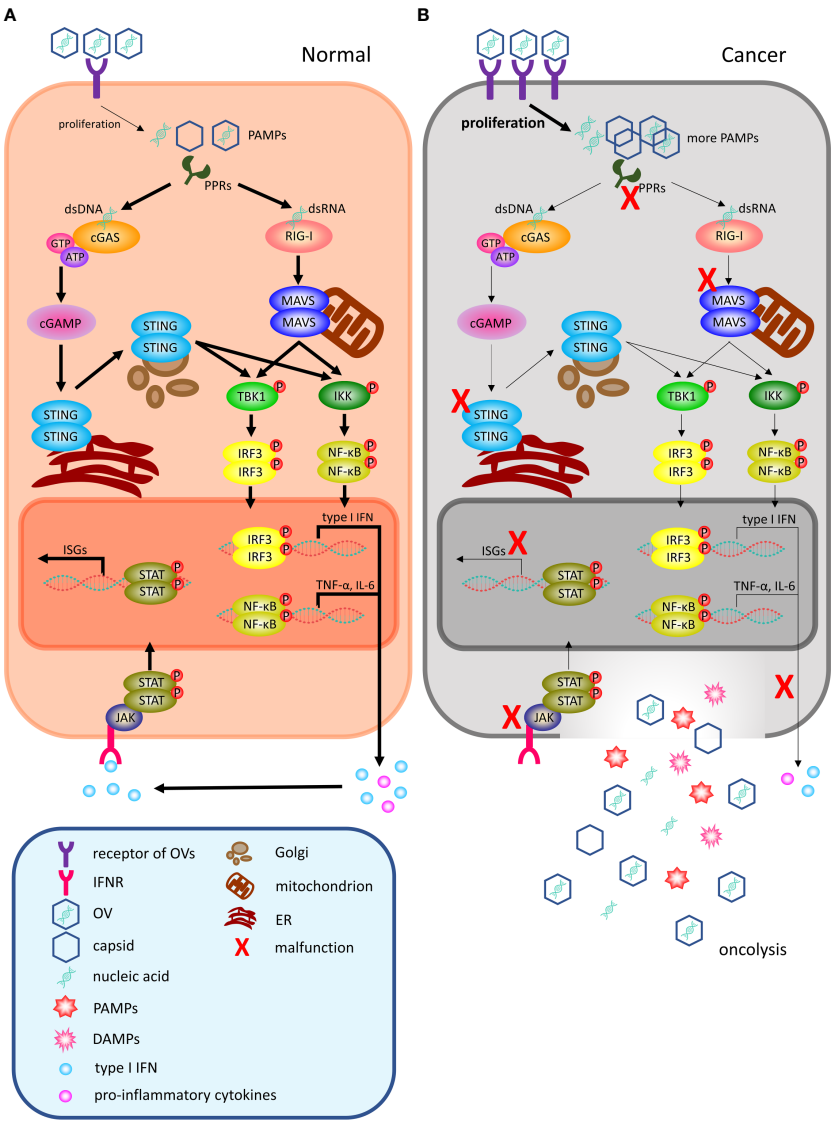

FIGURE 1
OVs can selectively infect and lyse cancer cells locally. **(A)** Following viral infection, most normal cells activate antiviral pathways against viral infections. The antiviral machinery can be triggered by viral PAMPs that activate PRRs (such as cGAS for DNA viruses and RIG-I for RNA viruses). Once PAMPs are detected, a signaling cascade through the adaptor molecule STING or MAVS phosphorylating IRF3 and NF-κB to dimerize and translocate to the nucleus to regulate the programmed transcription of type I IFN and proinflammatory cytokines. Among them, proinflammatory cytokines recruit immune cells to infiltrate the TME, and local IFN production can promote antiviral activity through IFNR. Upon type I IFN binding to receptors, the activated JAK-STAT signaling pathway leads to the rapid transcription of abundant ISGs to inhibit various stages of the viral lifecycle from invasion to release and can even target infected cells for apoptosis or necrosis. **(B)** In malignant cells, this process is disrupted. Cancer cells may increase the number of viral receptors or downregulate key signaling components within the innate antiviral signaling pathway, including PPRs, STING, MAVS, type I IFN and ISGs, thereby limiting their proapoptotic and cell cycle regulatory effects. Therefore, OVs can easily reach the critical value of viral load for oncolysis. OV, oncolytic virus; PAMPs, pathogen-associated molecular patterns; DAMPs, damage-associated molecular patterns; PRRs, pattern-recognition receptors; dsDNA, double-stranded linear DNA; dsRNA, double-stranded linear RNA; cGAS, cyclic GMP–AMP synthase; ATP, adenosine triphosphate; GTP, guanosine triphosphate; cGAMP, cyclic GMP–AMP; ER, endoplasmic reticulum; TBK1, TANK-binding kinase 1; IKK, IκB kinase; IRF3, interferon regulatory factor 3; NF-κB, nuclear factor-κB; RIG-I, retinoic acid-inducible gene I; TNF-α, tumor necrosis factor-α; IL-6, interleukin-6; ISGs, interferon-stimulated genes; IFN, interferon; IFNR, interferon receptor; JAK, Janus kinase; STAT, signal transducer and activator of transcription; TME, tumor microenvironment.

differentiation association gene 5 (MDA5) and laboratory of genetics and physiology 2 (LGP2) (22). In the absence of ligand, RIG-I exists in an autorepressed conformation wherein its helicase domain and repressor domain (RD) associate with its caspase activation and recruitment domains (CARDs), which precludes it from participating in signaling. It is only when RIG-I engages the appropriate PAMP RNA through the helicase and RD that the CARDs are released from autorepression to

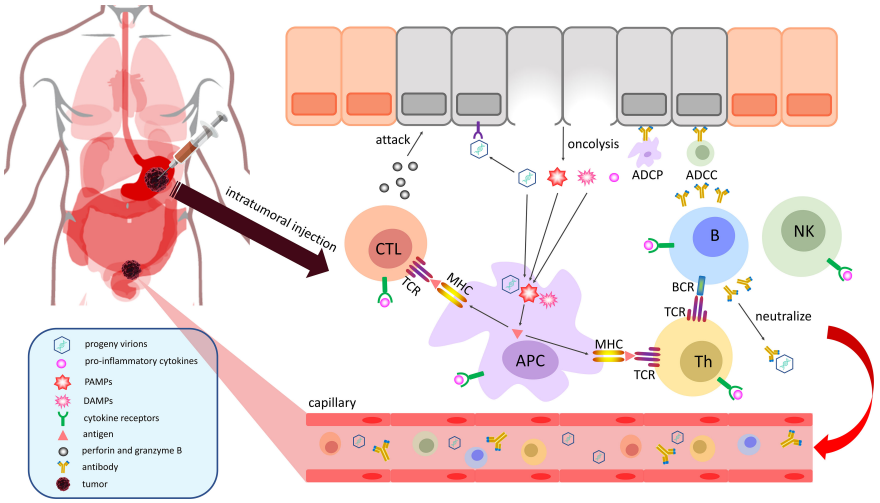

FIGURE 2
OVs can stimulate a systemic adaptive antitumor immune response. Cancer cells are lysed by mature OVs to release viral progeny, TAAs, PAMPs and DAMPs into the TME. Among them, progeny virions will ceaselessly infect the surrounding cancer cells to establish a cascade amplification reaction to eliminate malignancy. Infiltrative APCs can swallow and process TAAs, PAMPs, and DAMPs to present neoantigens by MHC molecules for the activation of immune cells. The sensitized CTLs attack the identified cancer cells by releasing perforin and granzyme B, and the activated Th cells can stimulate B cells to promote their activation and secrete neutralizing antibodies, which can mark malignant cells for ADCC by NK cells or ADCP by macrophages. Finally, immune effector cells, immune effector molecules and progeny virions will travel through the body with the blood to initiate a systemic adaptive antitumor immune response. APC, antigen-presenting cell; NK, natural killer cell; MHC, major histocompatibility complex molecule; CTL, cytotoxic T lymphocyte; Th, T helper cell; ADCC, antibody-dependent cellular cytotoxicity; ADCP, antibody-dependent cellular phagocytosis; PAMPs, pathogen-associated molecular patterns; DAMPs, damage-associated molecular patterns; TCR, T-cell receptor; BCR, B-cell receptor; TAA, tumor-associated antigen.

associate with the adaptor molecule mitochondrial antiviral-signaling protein (MAVS) on the membrane surface of mitochondria. MAVS assembles into aggregates that allow the ensuing signaling cascade to induce the phosphorylation and nuclear translocation of the key innate immune transcription factors IRF3 and NF-κB to drive the expression of downstream genes (23).

In summary, both DNA and RNA viruses can induce the production of type I IFN, which is released into the microenvironment surrounding infected cells. Upon type I IFN binding to receptors, a signal is transmitted by activating the Janus kinase signal transducer and activator of transcription (JAK-STAT) pathway in the cells, leading to the rapid transcription of abundant IFN-stimulated genes (ISGs), such as myxovirus resistance (Mx), viperin, and double-stranded RNA-dependent protein kinase (PKR), and they can inhibit various stages of the viral lifecycle from invasion to release (24). When normal cells are infected with OVs, the intact innate antiviral immune system responds quickly and eliminates internal immature virions, sometimes even inducing apoptosis of seriously infected cells to protect the other cells.

However, during the process of becoming cancerous, some aberrant changes enable OVs to survive and proliferate extensively in host cells (Figure 1B); for example, the number of viral receptors on the membrane surface increases dramatically. Adenovirus, as a familiar OV, mainly engages its receptor coxsackievirus adenovirus receptor (CAR) and coreceptor integrins to complete the invasion process (25), and the expression of CAR is significantly elevated in GC, lung cancer and female reproductive tumors (26, 27). Similarly, the herpes virus receptor, herpesvirus-entry mediator (HVEM), is also markedly increased in malignant melanoma, colorectal cancer, GC, and glioblastoma (28). The amplification of these receptors will facilitate an increasing number of virions entering the host cells and increase the basic level of OVs to obviously accelerate the multiplication rate. Moreover, PPRs act as viral sensors and cannot efficaciously activate their downstream signal of viral defense if their expression is reduced or their function is destroyed. In hepatocellular carcinoma (HCC), TLRs are downregulated to protect cancer cells from the apoptosis they trigger, likely linked to the occurrence and poor prognosis of HCC (29). Similarly, recent studies have demonstrated that NLRs function as intrinsic tumor suppressors in intestinal epithelial cells (IECs), by regulating their responses to proliferative signals following intestinal injury, but they are frequently deleted in colorectal cancer (30). Adaptors STING and MAVS are indispensable intermediate transducers of antiviral signals, and the existing data imply that the STING signaling pathway may be recurrently suppressed by multifarious mechanisms in a considerable variety of

malignant diseases and may be required for cellular transformation (31). To the best of our knowledge, cancers mainly acquire energy through glycolysis due to their rapid growth rate. Lactate serves as a key metabolite responsible for glycolysis-mediated RLR signaling inhibition by directly binding to the MAVS transmembrane domain and preventing MAVS aggregation, building a barrier to impede type I IFN production upon RLR activation (32). Hypoxia is also a common phenomenon in solid tumors and is strongly linked to hallmarks of cancers. This will lead to an overall downregulation of the type I IFN pathway to block the transcription of ISGs, due to repressed transcription and lower chromatin accessibility in a hypoxia-inducible factor 1/2α-independent manner (33). Cancer cells have a significantly weakened defense capability against OVs through the abovementioned various adaptive changes, which allow OVs to replicate and assemble, safely and quickly. Coupled with the silencing or mutation of genes that mediate apoptosis signals, infected tumor cells will not die immediately under normal circumstances (34, 35). Therefore, OVs can easily reach the critical value of viral load in tumor cells, eventually lysing them and releasing progeny viruses into the TME (34). Overall, OVs can take advantage of the differences in affinity and tolerance between normal and malignant cells for selectively infecting and lysing cancer cells.

2.2 Stimulate the systemic adaptive antitumor immune response

The immunogenicity of oncolysis caused by overloaded OVs significantly exceeds the process of apoptosis, which can stimulate a systemic antitumor immune response to a certain extent (Figure 2) (36). Findings from a phase II, multicenter, open-label study (NCT02366195) of patients with stage IIIB–IVM1c melanoma indicated that T-Vec had a significant therapeutic effect at the injection site of the tumor and it upregulated immune-cell populations in noninjected lesions, such as $CD8^+$ and $CD4^+$ T cells (37). When cancer cells cleaved by OVs undergo immunogenic cell death (ICD), a large number of progeny virions, tumor-associated antigens (TAAs), PAMPs and damage-associated molecular patterns (DAMPs) are released into the TME and blood circulation (18). Therefore, progeny virions will ceaselessly infect the surrounding cancer cells to establish a cascade amplification reaction, ultimately achieving the purpose of eliminating the malignancy. Proinflammatory cytokines produced by activated NF-κB can recruit antigen-presenting cells (APCs), B cells, T cells and natural killer (NK) cells and stimulate the activation of their relevant signaling pathways to perform antitumor functions (38). APCs, as specialized antigen-presenting cells, can take up and process the TAAs, PAMPs, and DAMPs produced by oncolysis and present these peptide antigens to T cells by major histocompatibility complex (MHC) molecules, ultimately activating $CD4^+$ T cells and $CD8^+$ T cells with the participation of costimulating molecules on the membrane surface (39). The sensitized cytotoxic T lymphocytes (CTLs) attack identified cancer cells by releasing perforin and granzyme B (18), and activated T helper (Th) cells offer costimulatory signals to B cells, thereby promoting their activation, causing them to secrete neutralizing antibodies, which can mark malignant cells for antibody-dependent cellular cytotoxicity (ADCC) by NK cells or antibody-dependent cellular phagocytosis (ADCP) by macrophages (40). In the end, immune effector cells, immune effector molecules and progeny virions generated in the TME will travel through the body with the blood and initiate a systemic adaptive antitumor immune response.

2.3 Two major therapeutic strategies of OVTs

The existing therapeutic strategies of OVTs are mainly divided into two categories, one is an oncolytic tool relies on its oncolysis, another is an exogenous gene delivery system relies on its selectivity for various cancers. As mentioned above, natural OVs can preferentially replicate and assemble in human cancer cells and inhibit tumor growth without specific deletion or modification to the genome. Multiple preclinical and clinical studies have demonstrated that OVTs have oncolytic properties and can stimulate antitumor immune responses against various malignancies (41). However, the two most challenging problems of OVTs in the process of application are as follows: (i) a significant reduction in the efficacy because of unsatisfactory oncolysis or the virions are eliminated by the body's strong immune system and (ii) OVs may infect and damage healthy tissues and cells with the increase of viral titer (42). For these two problems, on the one hand, the curative effects can be enhanced by further modification of their genome, which named armed OVs. Mechanistically, a variety of different armed oncolytic strategies have been explored, with particular success observed in strategies introducing immune-stimulating genes (such as T-Vec has an insertion of human GM-CSF in both copies of the ICP34.5 gene within HSV-1) and tumor-damaging genes (such as the insertion of tumor-suppressor genes or RNA interference to regulate oncogenes) (43–45). Although their efficacy is more favorable, the exogenous genes introduced by armed OVs have more unforeseen effects and potentially dangerous to normal cells than original OVs. On the other hand, the selectivity of the OVs also can be enhanced by further deletion of genes which essential for their proliferation in normal cells (42). For example, the deletion of E3 gene in adenovirus or ICP47 gene in HSV-1 can promote peptide loading of MHC-I molecules to encourage the elimination of virions by the immune system in normal cells (46). However,

these changes cannot affect the survival of OVs in cancer cells due to their antiviral immune responses are inherently defective. Nowadays, the third-generation adenovirus vector engineered by gene editing technology, which removes all of genes except inverted terminal repetitions (ITRs) and a packaging gene Ψ, only acts as an exogenous gene delivery system without the ability of self-replication (47, 48). Although the specificity and capacity of exogenous gene insertion are commendably increased, the absent replicative activity and low immunogenicity of virions can't activate the immune response or very poorly so that OVs lose the abilities of oncolysis and stimulating the systemic adaptive antitumor immune response (49). Therefore, it is indispensable that these engineered OVs treat cancer patients in combination with other antitumor agents, especially ICIs and adoptive immunotherapy.

3 Summary of OVTs for treating GC

3.1 Adenovirus

3.1.1 The internal structure and invasive process of adenovirus

Adenovirus is a nonenveloped double-stranded linear DNA virus with a nucleoprotein core encapsulated by an icosahedral protein capsid from which proteinaceous fibers protrude (50). It mainly initiates infection by high affinity binding of the fiber protein to CAR (Figure 3) or other receptors, such as CD46 and desmoglein (DSG)-2 (51). Upon cell binding, adenovirus typically requires a secondary receptor for endocytic uptake. This is usually mediated by the arginine-glycine-aspartate (RGD) sequence in an exposed loop of the penton base binding to active state αvβ3/αvβ5 integrins, followed by outside-in signals, which are critical for stimulating virion endocytosis to enter lysosomes. Because adenoviruses change the conformation of the protein capsid through a highly controlled process within lysosomes, the viral DNA are released from the lysosomes and transferred to the nucleus through nuclear pore complexes, and a series of complicated but regulated transcription and translation processes are carried out (52).

Adenoviruses contain a genome of approximately 36 kb with inverted terminal repetitions (ITRs) of ~100 bp at both ends, and on the inside of the left ITR (LITR), the signal Ψ is involved in viral packaging. Between the right ITR (RITR) and Ψ, early transcription units E1~E4 encode proteins that are required for viral replication, and all major late proteins are organized in the transcription units L1~L5, related to the assembly of adenovirus (53). E1A is the first gene that is transcribed during adenovirus infection to regulate the metabolism of host cells to make

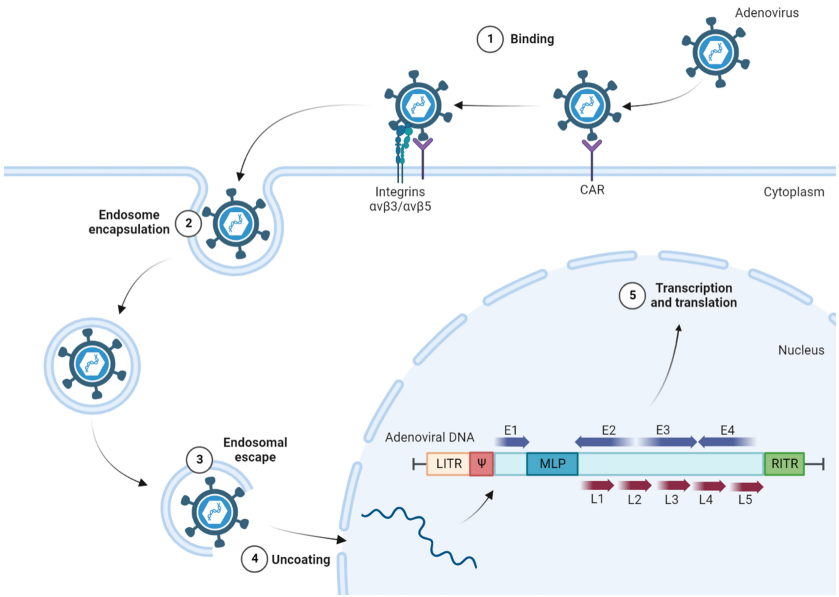

FIGURE 3
The internal structure and invasive process of adenovirus. Infection with adenovirus is mainly initiated by high affinity binding of fiber protein to CAR, with the participation of αvβ3/αvβ5 integrins as secondary receptors. Endocytic virions are released from lysosomes and transferred to the nucleus through nuclear pore complexes for transcription and translation. The adenoviral genome contains two ITRs at both ends, the packaging signal Ψ, and the major functional genes, such as early transcription units E1~E4 and late transcription units L1~L5. CAR, coxsackievirus adenovirus receptor; RGD, arginine-glycine-aspartate; LITR, left inverted terminal repetitions; RITR, right inverted terminal repetitions; Ψ, packaging signal; E1~E4, early transcription units; L1~L5, late transcription units; MLP, major late promoter.

replication easier, and E1A protein can also activate the promoters of other early transcription units (54). Replication requires a complex constructed by three viral proteins encoded by E2 genes: precursor terminal protein (pTP), DNA polymerase (DNA Pol), and the single-stranded DNA binding protein (ssDBP) (55). The E3 protein is a glycoprotein that can be transferred to the endoplasmic reticulum (ER) and then abrogate cell surface transport of MHC class I molecules to avoid the activation of CTLs (56). That, combined with the E4 gene, encodes at least 6 viral proteins that counteract host antiviral proteins during productive adenovirus infection (57). These products not only destroy the intracellular defensive capability of OVs but also block the signals of activating immune cells, ultimately promoting the proliferation of virions in host cells without restriction. When the early preparation for viral amplification is basically completed, the transcription and translation of the early transcription units are shut down, and the common major late promoter (MLP) begins to regulate the expression of late transcription units L1~L5 (58). With the participation of Ψ, mature progeny virions rush out of the tumor cells and enter the next round of lifecycle.

3.1.2 As an oncolytic tool

Oncolytic adenovirus therapy is gaining importance as a novel treatment option for the management of various cancers. As a well-known OV, oncolytic adenovirus has many studies and applications in treating GC, which can replicate in and kill tumor cells selectively (Table 1). Multiple studies have indicated

TABLE 1 Studies of various OVs for the treatment of GC.

Role	Virus	Modification	Detail	The route of administration	Combination	Effect	Reference
As an oncolytic tool	Adenovirus	Increase infection efficiency	the fiber is modified with an integrin-targeted motif	i.p.	None	benefit gene transfer efficiency and cell killing	(59)
			the fiber is modified with an IgG Fc-binding motif from the Staphylococcus protein A	i.p.	human anti-CEA monoclonal antibody	offer a therapeutic modality against CEA-producing GC	(60)
		Engineered	OBP-401	i.p.	paclitaxel	synergistic antitumor effect	(61)
			OBP-401	no animal research	None	detect GC cells from the peritoneal washes	(62)
	HSV-1	Engineered	NV1066	i.p.	None	induce apoptosis and inhibit metastasis	(63, 64)
			G47Δ	i.t.	None	decrease M2 macrophages while increasing M1 macrophages and NK cells in TME	(65)
			G207	i.p.	None	inhibit peritoneal metastasis	(66)
			G207	i.p.	5-fluorouracil and surgical resection	synergistic antitumor effect	(67)
	VSV	Original	VSV	no animal research	None	induce apoptosis	(68)
	VACV	Engineered	GLV-1h254	no animal research	None	detect circulating tumor cells	(69)
	NDV	Engineered	NDV(F3aa)	i.p.	None	inhibit peritoneal metastasis	(70)
	Measles virus	Engineered	rMV-Hu191	i.t.	cisplatin	synergistic antitumor effect	(71, 72)
	Reovirus	Original	reovirus	i.t.	trastuzumab	augment trastuzumab-induced cytotoxicity	(73)
			reovirus	i.p.	None	inhibit peritoneal metastasis	(74)
As an exogenous gene delivery system	Adenovirus	Insert exogenous genes	WT p53	i.t.	None	selective growth inhibition in mutated p53 GC	(44)
			dominant negative IGF-Ir	i.t.	None	suppress tumorigenicity and induce apoptosis	(75)
			Bax	i.t.	None	inhibit growth and induce apoptosis	(76)
			IRF-1	no animal research	None	induce apoptosis	(77)

(Continued)

TABLE 1 Continued

Role	Virus	Modification	Detail	The route of administration	Combination	Effect	Reference
			Flt-1	i.p.	None	suppress peritoneal dissemination	(78)
			UPRT	i.t.	5-fluorouracil	enhance the sensitivity of 5-fluorouracil	(79)
			ICAM-2	i.t.	None	enhance the adhesion and activation of NK cells	(80)
			TRAIL	i.t.	paclitaxel	synergistic antitumor effect	(81)
			XAF1	i.t.	None	induce autophagy	(82)
			cGMP-dependent PKG II	i.p. and i.t.	None	delay growth, induce apoptosis, and inhibit metastasis and angiogenesis	(83)
			DKK1	i.t.	None	suppress tumorigenicity of cancer stem cell *via* attenuating Wnt signaling	(84)
			p33	no animal research	None	inhibit growth and induce apoptosis	(85)
			anti-p21-Ras scFv	i.v.	CIK cells	synergistically kill tumor cells	(86)
			HER2-ECD	i.p.	Trastuzumab	inhibit peritoneal metastasis	(87)
			TIPE2	i.v.	None	inhibit migration, invasion, and metastasis *via* reversal of EMT	(88)
			ING4 and PTEN	i.t.	None	synergistically suppress tumor and induce apoptosis	(89)
			NK4	i.p.	None	prevent peritoneal dissemination	(90)
			B4GALNT2	i.p.	None	prevent peritoneal dissemination	(91)
			IL-10	i.p.	None	prevent peritoneal dissemination	(92)
			HSP-gp96	no animal research	None	promote T cell and DC response	(93)
			FasL and B7-1	i.t.	None	promote the activity of CTLs	(94)
		Knock down endogenous genes	Met	i.t.	None	inhibit growth	(45)
			Mcl-1	no animal research	5-fluorouracil and cisplatin	overcome chemotherapy resistance	(95)
			PAI-1	i.p.	None	inhibit peritoneal metastasis	(96)
			PGK1	no animal research	5-fluorouracil and mitomycin	synergistically kill tumor cells	(97)
			RhoA and RhoC	i.t.	None	inhibit growth and invasion	(98)
			PI3K	no animal research	None	inhibit proliferation and enhance apoptosis	(99)
		Replace promoters	CEA promoter	no animal research	5-fluorocytosine	enhance the sensitivity of 5-fluorocytosine	(100)
			CEA promoter	no animal research	ganciclovir	confer sensitivity to ganciclovir	(101)
			hTERT promoter	i.t.	None	eliminate quiescent cancer stem-like cells	(102)
			MK promoter and Cox-2 promoter	no animal research	None	show good selectivity and infectivity in GC	(103)
			a β-catenin/T-cell factor-responsive promoter	no animal research	None	improve efficacy and reduce toxicity	(104)

(Continued)

TABLE 1 Continued

Role	Virus	Modification	Detail	The route of administration	Combination	Effect	Reference
		others	induce MAGE-1 into DC vaccine	i.t.	None	stimulate anti-tumor immunity specific to GC	(105)
			induce L-PGDS into MSCs	i.t.	None	MSC-derived EVs to deliver L-PGDS to treat GC	(106)
	HSV-1	Insert exogenous genes	TSP-1	i.t.	None	enhance viral oncolysis with antiangiogenesis	(107)
		Replace promoters	hTERT promoter	no animal research	None	inhibit proliferation and enhance apoptosis	(108)
	VACV	Insert exogenous genes	survivin T34A and FilC	i.p.	None	synergistic antitumor effect	(109)
			hNIS	i.t.	None	image with (99m)Tc pertechnetate scintigraphy and PET/CT	(110)
	NDV	Insert exogenous genes	rL-RVG	i.t.	None	suppress migration	(111)
			IFN-λ1	no animal research	None	change Th1/Th2 response of TME	(112)
			GFP	no animal research	None	specifically detect the spread of intraperitoneal cancer	(113)

i.p., intraperitoneal injection; i.t., intratumoral injection; i.v., intravenous injection; IGF-Ir, insulin-like growth factor I receptor; IRF-1, interferon regulatory factor-1; Flt-1, a soluble form of VEGF receptor; UPRT, uracil phosphoribosyltransferase; hTERT, human telomerase reverse transcriptase; ICAM-2, intercellular adhesion molecule-2; MAGE-1, melanoma antigen gene-1; TRAIL, TNF-related apoptosis-inducing ligand; XAF1, XIAP-associated factor 1; cGMP, cyclic guanosine monophosphate; PKG, protein kinase; DKK1, Dickkopf-1; MK, midkine; Cox-2, cyclooxygenase-2; Mcl-1, myeloid cell leukemia-1; scFv, single-chain fragment variable; CIK; cytokine-induced killer; PAI-1, plasminogen activator inhibitor-1; HER2-ECD, HER2-extracellular domain; PGK1, phosphoglycerate kinase 1; TIPE2, tumor necrosis factor-alpha-induced protein 8-like 2; EMT, epithelial-mesenchymal transition; ING4, inhibitor of growth 4; PTEN, phosphatase and tensin homolog; B4GALNT2, β1,4N-acetylgalactosaminyltransferase 2; HSP-gp96, heat shock protein-glycoprotein96; Rho, Ras homolog gene family; PI3K, phosphoinositide 3-kinase; L-PGDS, lipocalin-type prostaglandin D2 synthase; EV extracellular vesicle; TSP-1, thrombospondin-1; VSV, vesicular stomatitis virus; hNIS, human sodium iodide symporter; IFN-λ1, interferon-λ1; GFP, green fluorescent protein.

that adenovirus possesses good selectivity and infectivity in GC cells to yield oncolysis (101, 103). According to the interpretation of the invasive process, Lotta Kangasniemi et al. incorporated an RGD-containing peptide into the HI loop of the fiber knob to preferably utilize αvβ-class integrins for binding and internalization, which significantly enhanced the transduction of target cells and oncolysis (59). However, it is worth noting that the modification of ligands also can promote more virions to enter normal cells, causing unwanted off-target and side effects. In addition, adenovirus can also increase the therapeutic effectiveness of peritoneal metastasis for GC patients. Peritoneal metastasis is the most frequent form of distant metastasis and recurrence of GC, and its prognosis is extremely poor due to its resistance to systemic chemotherapy. In an orthotopic human GC peritoneal dissemination mouse model, intraperitoneal administration of adenovirus (OBP-401) enhanced the accelerated autophagy and apoptosis of malignant cells and synergistically suppressed the peritoneal metastasis of GC in combination with paclitaxel (PTX) (61).

3.1.3 As an exogenous gene delivery system

Adenovirus vector is also a targeted, safe, and excellent gene delivery system, enables us to introduce exogenous genes into GC at will due to its selectivity for cancer cells (Table 1). P53 is a suppressor of carcinogenesis that plays a crucial role in a variety of cancers, including GC (114). *In vivo* studies showed that the growth of subcutaneous tumors of p53 mutant GC cells was significantly inhibited by intratumor injection of recombinant adenovirus encoding wild-type p53 (AdCAp53), but no significant growth inhibition was detected in the growth of p53 wild type GC (44). phosphatase and tensin homolog (PTEN) tumor-suppressor activity in the PI3K/Akt/mTOR pathway is essential to regulate many cellular processes of GC, including proliferation, survival, energy metabolism, and metastasis (115). Zhang, H. et al. revealed that a recombinant adenovirus co-expressing inhibitor of growth 4 (ING4) and PTEN (AdVING4/PTEN) could synergistically induce apoptosis of GC *via* enhancement of endogenous p53 responses (89). IFN regulatory factor-1 (IRF-1), XIAP-associated factor 1 (XAF1), and cGMP-dependent protein kinase (PKG) II, as tumor suppressor genes, also can inhibit proliferation and promote apoptosis of GC in a similar way (Table 1). Moreover, knocking down and out oncogenes possess the similar antitumor activity in the prolongation of GC patients' survival. The PI3K-serine/threonine kinase (AKT)-mammalian target of rapamycin (mTOR) pathway is an important cellular pathway involved in cell growth, tumorigenesis, cell invasion, and drug resistance. Bao-Song Zhu et al. constructed a recombinant adenovirus with RNA interference to silence PI3K gene. After the PI3K signaling pathway has been blocked

by siRNA, the proliferation of cells was inhibited and the apoptosis of GC cells was enhanced (99). In addition, myeloid cell leukemia-1 (Mcl-1) is an antiapoptotic protein that regulates apoptosis sensitivity in many cancers. When adenovirus-mediated RNAi technology was used to knockdown the expression of Mcl-1 in GC, $CD44^+$ cancer stem cell (CSC)-like cells became sensitized to chemotherapeutic agents such as 5-fluorouracil (5-FU) and cisplatin (CDDP) (95). More interestingly, a green fluorescent protein (GFP)-expressing adenovirus can detect malignant cells from the peritoneal washes of GC patients more sensitively and may thus be useful for both therapy stratification and precision medicine (62).

3.1.4 Relevant clinical trials

Based on previous studies, the Sidney Kimmel Cancer Center at Thomas Jefferson University is investigating the side effects of the Ad5. F35-hGCC-PADRE vaccine and determining how well it works in treating patients with gastrointestinal adenocarcinoma in a phase IIA trial (NCT04111172). The adenovirus 5/F35-human guanylyl cyclase C-PADRE (Ad5.F35-hGCC-PADRE) vaccine may help train the patient's own immune system to identify and kill tumor cells and prevent them from forming recurrences and metastases. In addition, a phase 1 trial that involves binary oncolytic adenovirus (CAdVEC) in combination with HER2-specific autologous CAR T-cells to treat advanced HER2-positive GC (NCT03740256) and a single arm phase 2 study of the combination of adenoviral p53 (Ad-p53) gene therapy administered intratumorally with approved ICIs in patients with recurrent or metastatic GC (NCT03544723) are underway.

3.2 Herpes simplex virus type 1

3.2.1 The internal structure and invasive process of HSV-1

Herpes virus is a round, enveloped double-stranded linear DNA virus with a core encapsulated by a protein capsid. The most common herpes virus, HSV-1, has a genome of 152 kb, but approximately 30 kb of these genes are not necessary for viral survival, which provides abundant space for the insertion of exogenous genes (116). Similar to most viral infection processes, HSV-1 entry into host cells requires viral binding to specific receptors to trigger membrane fusion, and multiple viral entry glycoproteins (gB, gC, gD, gH, and gL) on the surface of the virion play a coordinating role in this process (117). The direct fusion of HSV-1 with the plasma membrane of host cells involves three phases (Figure 4): (i) Virions attach to the membrane surface. gB and/or gC binds to heparan sulfate (HS) to facilitate viral adsorption to the cells. (ii) The host cell recognizes the virions. One of several entry receptors on the host cell surface, including HVEM, Nectin-1 or -2, and 3-O-sulfated heparan sulfate (3-OS HS), can bind to gD to stabilize the attachment between them and promote the formation of the gH-gL complex. (iii) Initiation of the fusion reaction of the viral envelope with the cytoplasmic membrane occurs. The gD, gB, and gH-gL complexes and their cognate receptors form the core fusion complex, which completes the fusion of the viral envelope with the host cell membrane (118).

Following the process of fusion, the nucleocapsid of HSV-1 is connected with the nuclear membrane to release DNA into the nucleus and activate its transcription and translation. The genomic DNA of HSV-1 is divided into long and short regions of unique sequences termed UL and US, respectively, which are flanked by regions of inverted internal and terminal repeats (119). Their expression of them is rigorous in chronological order and can be segmented into immediate-early (IE), early (E) and late (L) genes (also known as α, β, and γ). ICP0, ICP4 and ICP47 play an irreplaceable role in the early stage of infection as the expression products of IE genes. Among them, ICP0 is a multifunctional nonessential ubiquitin E3 ligase that targets a multitude of cellular proteins for proteasome-mediated degradation and counters intrinsic and IFN-related antiviral responses and epigenetic silencing of the viral genome (120). ICP4 is an essential transactivating factor that represses IE genes and activates E and L genes (120). Similar to the E3 gene in adenovirus, ICP47 can also block peptide loading of MHC-I molecules, encouraging the escape of detection by the immune system (46). The E genes include ICP6 and TK (thymidine kinase), which are mainly involved in viral DNA replication and nucleotide metabolism for amplification of HSV-1 (121). L gene expression occurs with the onset of viral DNA replication, and its products include capsid and DNA packaging proteins, glycoproteins, and tegument proteins (122). ICP34.5, one of the L genes, is the major viral neurovirulence factor, as well as a multifunctional protein that can bind phosphatase 1α (PP1α) to dephosphorylate eukaryotic translation initiation factor 2α (eIF2α) to prevent protein shutoff and bind TBK1 to block type 1 IFN induction to inhibit apoptosis of host cells (123). Thus, similar to adenovirus, we can modify the genetic composition of HSV-1 to make it more suitable for treating cancer in the clinic.

3.2.2 Relevant studies and clinical trials of HSV-1

HSV-1, as an OVT, plays a pioneering role in other cancer therapies, such as T-vec for melanoma or G47Δ for glioblastoma, but its application is relatively limited in GC (Table 1). Firstly, HSV-1 is a wonderful oncolytic tool. The existing results suggest that simply relying on the oncolytic ability of HSV-1 can induce apoptosis of infected GC cells and effectively treat disseminated peritoneal cancers (63, 66). More meaningfully, intratumoral HSV-1 injections markedly decreased M2 macrophages while increasing M1 macrophages and natural killer (NK) cells, which

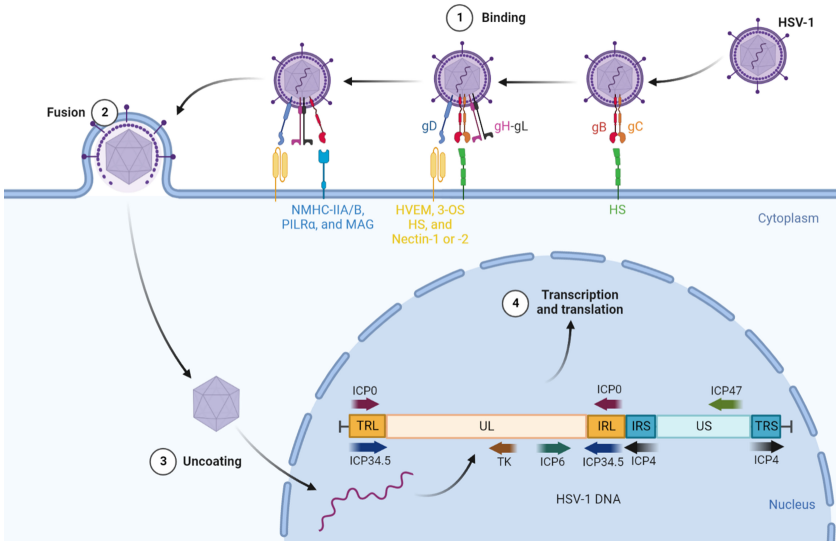

FIGURE 4
The internal structure and invasive process of HSV-1. HSV-1 requires viral binding to specific receptors to trigger membrane fusion to enter host cells. First, gB and/or gC binding to HS facilitates viral adsorption to the cells. Then, one of several entry receptors, including HVEM, Nectin-1 or -2, and 3-OS HS, can bind to gD to stabilize the attachment and promote the formation of the gH-gL complex. Subsequently, the gH–gL complex activates gB to interact with NMHC-IIA/B, PILRα or MAG. Finally, the gD, gB, and gH-gL complexes and their cognate receptors form the core fusion complex to initiate the fusion reaction of the viral envelope with the cytoplasmic membrane. The genomic DNA of HSV-1 is divided into UL, US, TRL, IRL, TRS, and IRS, which can be segmented into immediate-early (IE), early (E) and late (L) for their respective functions. HSV-1, herpes simplex virus type 1; gB, gC, gD, gH, and gL, viral entry glycoproteins; HS, heparan sulfate; HVEM, herpesvirus-entry mediator; 3-OS HS, 3-O-sulfated heparan sulfate; NMHC-IIA/B, non-muscle myosin heavy chain II A/B; PILRα, paired immunoglobulin-like receptor α; MAG, myelin-associated glycoprotein; UL/US, unique sequence of the long/short region; TRL/IRL, terminal/internal inverted repeat sequence of the long region; TRS/IRS, terminal/internal inverted repeat sequence of the short region; ICP, infected cell protein; TK, thymidine kinase.

means that the inherent immunosuppressive microenvironment of GC is destroyed by this method (65). Similar to adenovirus, HSV-1 can also be used to deliver exogenous genes. Thrombospondin-1 (TSP-1) suppresses tumor progression *via* multiple mechanisms, including antiangiogenesis. A novel armed oncolytic HSV-1 combined with TSP-1-mediated function, T-TSP-1, enhanced the therapeutic efficacy of GC by providing a combination of direct viral oncolysis with antiangiogenesis (107). Despite these successes in the laboratory, it is regrettable that few clinical trials using herpes virus for the treatment of GC has been conducted thus far. A phase I/II study (NCT03866525) evaluates the safety and efficacy of OH2 (an engineered recombinant herpes simplex virus) as single agent or in combination with HX008, an anti-PD-1 antibody, in patients with gastrointestinal cancers is underway.

3.3 Other OVs

In addition, others OVs also have corresponding therapeutic effects on GC (Table 1). As an oncolytic tool, Newcastle disease virus (NDV) was an effective antitumor treatment against peritoneal carcinomatosis from human GC in a xenograft model, correlated with viral replication and dosage (70, 111), and it can re-establish antitumor immunity in the suppressive TME (112). As an exogenous gene delivery system, Wang, M. et al. constructed a recombinant vaccinia virus (VACV) strain expressing mutant survivin T34A (SurT34A) and FilC and validated its strong replication and destruction ability in a murine GC model (109). In particular, due to its ability to selectively invade tumor cells, the therapeutic efficacy of a novel genetically engineered VACV carrying the human sodium iodide symporter (hNIS) gene, GLV-1 h153, was investigated in GC along with its potential utility for imaging with (99 m)Tc pertechnetate scintigraphy and ^{124}I positron emission tomography (PET) (110). Furthermore, tumor cell-specific recombinant VACV can accurately detect live metastatic tumor cells in blood samples from mice bearing human tumor xenografts, as well as in blood and cerebrospinal fluid samples from patients with GC (69). These data encourage the continued investigation of OVTs for the diagnosis and staging of GC in clinical settings.

4 Prospects

GC, as a malignant tumor with a poor prognosis, combines a variety of adverse factors, and once it progresses to an advanced stage, almost all existing methods cannot achieve the desired therapeutic effect. Therefore, it is urgent to provide new treatment options for these patients. OVs have attracted much attention since their discovery, and their special abilities, such as selectively lysing tumor cells, remodelling the inhibitory TME, and activating the systemic antitumor immune response, have made many researchers regard OVT as a promising strategy for the treatment of cancer, and several clinical trials have commendably confirmed this hypothesis. However, to date, research on GC is still quite limited, and the few experimental studies and clinical trials cannot promote the development of OVTs for GC. Thus, for better comprehension, we combined previous results in various cancers with our own insights to discuss the prospects of OVT.

4.1 OV is not only a killer but also a carrier

OVs are well known for their capacity for selective oncolysis, and it is almost effortless to obtain satisfactory positive results *in vitro*. However, during the actual usage process, due to the complex internal environment in the body, the interactions among various factors results in dissatisfactory oncolysis (124). If the dose is increased, adverse phenomena such as off-target infection of normal cells and unnecessary inflammatory responses will also appear (125). After continuous modification and development, their original oncolytic ability has been increasingly marginalized, and increasing attention has been given to selective infection, as an admirable exogenous gene delivery system (126, 127). Most related studies on the introduction of exogenous genes into GC cells have been enumerated (Table 1). However, one important point is that GC is a molecularly and phenotypically highly heterogeneous disease (128), and the previous studies basically selected meaningful genes from other cancers and stuck them into GC, which is unfavorable for further application of the technique in the clinic. The one-size-fits-all approach is one of the key reasons for the huge differences in therapeutic efficacy among patients, and the molecular typing of various tumors can make up for this deficiency to better guide the choice of clinical medication, including for GC (129).

The Asian Cancer Research Group (ACRG) previously performed whole-genome sequencing of GC and divided it into four subtypes: microsatellite instability (MSI); microsatellite stability/epithelial-mesenchymal transition (MSS/EMT); microsatellite stability/TP53 activation (MSS/TP53$^+$) and microsatellite stability/TP53 mutation (MSS/TP53$^-$) (130). For example, compared with MSS/TP53$^+$ GC, the MSS/TP53$^-$ subtype is undoubtedly more suitable for introducing the wild-type p53 gene by OVs to remedy the error. The mutated CDH1 gene is one of the indispensable drivers of EMT involved in GC invasion and metastasis (131), and the MSS/EMT subtype has the worst prognosis because of typical CDH1 loss of expression. Thus, recovering the original level of CDH1 by OVs may improve the prognosis of GC subtype patients. Furthermore, The Cancer Genome Atlas (TCGA) project classified GC as Epstein–Barr virus (EBV)-positive (EBV), microsatellite instability (MSI), genomically stable (GS) and chromosomal instability (CIN), by analyzing gastric adenocarcinoma primary tumor tissue from 295 patients not treated with prior chemotherapy or radiotherapy (132). Taking EBV-positive GC as an example, 80% of this subtype has a PIK3CA mutation, which can cause the continuous activation of phosphatidylinositol 3-kinase (PI3K) and enhance the transmission of intracellular signals, promoting the carcinogenesis of gastric epithelial cells (133). We can reverse this process by relying on the function of OV carriers. Currently, our understanding of molecular the classification of GC has substantially changed, and the capacity of OVs to deliver exogenous genes has also been significantly enhanced. Based on both, targeted correction of characteristic abnormally expressed genes of various subtypes by OVTs can overcome the heterogeneity of GC, benefiting each patient and fulfilling the concept of precision medicine.

4.2 Look for more suitable promoters

The dual safety valves constituted by OVs and tumor-specific promoters can preferably avoid the occurrence of "off-target" events, further improving the targeting and safety of OVTs. For some cancers, promoters that regulate the expression of tumor-specific antigens (TSAs) are optimal candidates for OVTs; for example, the alpha-fetoprotein (AFP) promoter for hepatocellular carcinoma (Figure 5A) and the prostate-specific antigen (PSA) promoter for prostate cancer (Figure 5B) (134, 135).

Unfortunately, no appropriate promoter with impressive sensitivity and specificity has been found in GC thus far. Notwithstanding the available biomarkers of CEA, cancer antigen 19-9 (CA19-9) and cancer antigen 72-4 (CA72-4) are frequently used to monitor GC in the clinic (136). Among them, CA19-9 and CA72-4, as carbohydrate antigens, do not require specific promoters to regulate their expression, and CEA is a broad-spectrum tumor antigen mainly associated with carcinoma of the colon, lung, breast, stomach, etc (137). (Figure 5C). Although previous studies have shown that CEA could participate in OVTs for GC (Table 1), its sensitivity is not satisfactory; in fact, it is only 4.3% for early GC and 24% for AGC (138, 139). Additionally, its slight but significant upregulation in GC in the context of some inflammatory diseases suggests that the CEA promoter is not an excellent option (140). In addition,

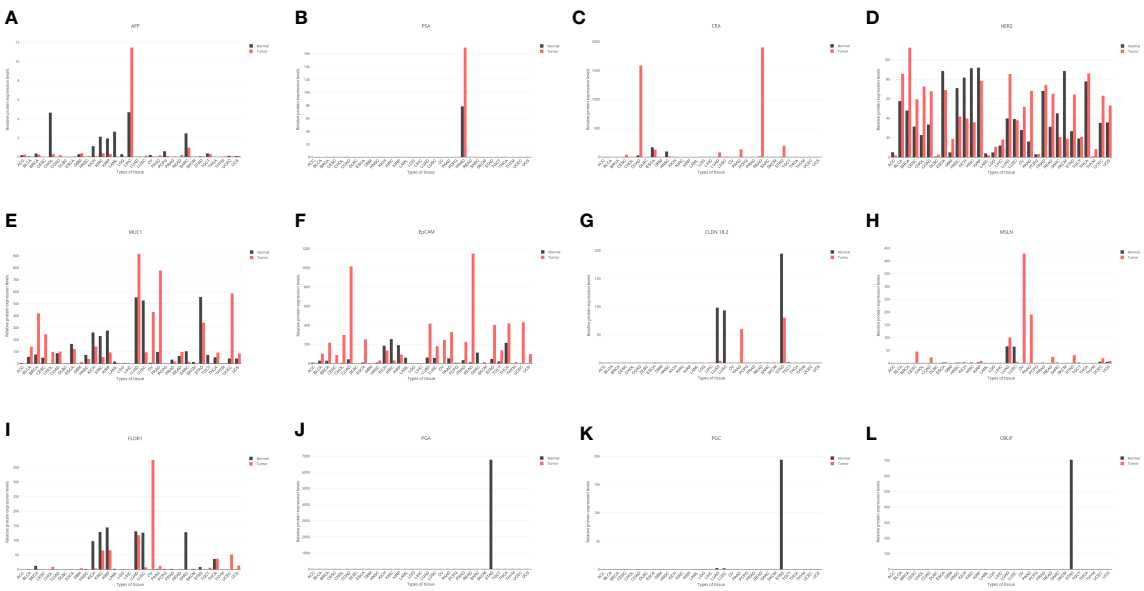

FIGURE 5
The expression levels of some genes in various tissues based on the GEPIA online database (http://gepia.cancer-pku.cn/index.html). AFP, alpha-fetoprotein; LIHC; liver hepatocellular carcinoma; PSA, prostate-specific antigen; PRAD, prostate adenocarcinoma; STAD, stomach adenocarcinoma; CEA, carcinoembryonic antigen; COAD, colon adenocarcinoma; READ, rectum adenocarcinoma; LUAD, lung adenocarcinoma; HER2, human epidermal growth factor receptor 2; MUC1, mucin 1; EpCAM, epithelial cell adhesion molecule; CLDN 18.2, claudin 18.2; MSLN, mesothelin; FOLR1, folate receptor 1; PGA, pepsinogen; PGC, gastricsin; CBLIF, cobalamin binding intrinsic factor.

some results also suggested that HER2, mucin 1 (MUC1), epithelial cell adhesion molecule (EpCAM), claudin 18.2 (CLDN 18.2), mesothelin (MSLN), and folate receptor 1 (FOLR1) are important targets in GC (141–143). After analysis, only EpCAM seems to be a candidate tumor-specific promoter for further research, while the other promoters have either low-level expression or poor specificity (Figures 5D-I).

The promoters of stomach-specific proteins are capable of becoming tumor-specific promoters similar to PSA in the prostate gland, such as pepsinogen (PGA), gastricsin (PGC), and cobalamin binding intrinsic factor (CBLIF). However, during the occurrence and development of GC, a large proportion of patients will experience a process of chronic atrophic gastritis, which can decrease the expression of these proteins by damaging the gastric mucosal epithelium, causing less expression in tumors than in normal tissue (Figures 5J-L) (144). In brief, finding a more suitable promoter than CEA to regulate the action of OVs will be a breakthrough in the treatment of GC.

4.3 Overcoming the deficiency of intravenous injection

One of the vital reasons for limiting the development of OVTs is the innate antiviral immune system. Due to a general history of previous infection in the population, such as adenovirus and HSV-1, pre-existing complement, immune cells, and corresponding antibodies will rapidly neutralize and inactivate OVs in the blood circulation (145, 146). Although intratumoral injection can avoid this problem to a certain extent, in the case of systemic multiorgan metastasis, peritoneal implantation and other special circumstances, intravenous injection is still the most appropriate way to obtain a better therapeutic effect. For this reason, it is also an attractive direction to explore how to treat GC by intravenous administration without disabling the OVTs.

The complement system constitutes a complex of heat labile serum proteins and cell surface proteins that act as an innate immune defense against invading pathogens, and intravenous injection of OVs with complement regulators can counteract inactivation mediated by complement to some extent (147). For immunoglobulin, using compound targeted mutagenesis of binding sites that mediate virus-immunoglobulin interactions, the engineered OVs resisted inactivation by the aforementioned factors, avoided sequestration in liver macrophages, and failed to trigger hepatotoxicity after intravenous delivery (15).

In addition to the above two strategies, a method such as the “Trojan horse” is generally recognized as a promising solution for intravenous injection. With the help of carrier cells which have a tropism toward the TME and are susceptible to OV infection, they can remain viable long enough to allow migration

and finally release OVs within the tumor bed (148). Due to their unique capability to specifically migrate to tumors, MSCs, MDSCs and tumor-infiltrating leukocytes (TILs) are universally regarded as candidates for carrying OVs, and their efficacy has been verified in glioma, colorectal cancer, and other malignancies (17, 149, 150). Moreover, angiogenesis plays an indispensable role in tumor proliferation, progression, and metastasis to supply sufficient nutrients for malignant tissues. Taking this into account, endothelial progenitor cells (EPCs) have stimulated worldwide interest as possible vehicles to perform autologous cell therapy of tumors because of their tumor-homing properties, and they may be a neotype of carriers for OVs (151).

OV delivery by carrier cells has attracted extensive attention, but there are still few studies on treating GC by this method. Only one study suggested that recombinant adenovirus KGHV500 carried by CIKs, which was equipped with a broad-spectrum anti-p21-Ras single-chain variable fragment antibody (scFv), could significantly infiltrate the TME to inhibit proliferation, migration, and invasiveness and promote cell apoptosis of GC (86). With the continuous innovation of material fabrication technology, the applications of new types of materials in cancer therapy is emerging, which can not only deliver therapeutic drugs efficiently by preventing them from being eliminated by the immune system but also target and transmit them into the tumor location relying on photodynamic therapy (PDT), magnetism, pH and so on (152–155). Therefore, using these emerging materials as carriers of OVs can be regarded as another approach to solving the problem of intravenous injection, but research on GC treatment is still lacking.

4.4 OVs are also diagnostic and staging tools

Diagnosing difficulty at an early stage leads to the poor prognosis of GC patients. The relevant data showed that the 5-year OS rate of patients who accepted radical surgical resection with early-stage localized GC is more than 60%, whereas that of patients with distant metastasis is less than 5% (156). In recent years, although endoscopic screening and pathological biopsy of patients with a high risk have greatly improved the diagnostic efficiency and slightly reduced the mortality of GC (157), it is undeniable that their accuracy is closely related to the technique and experience of the operators, and a number of patients are still missed due to various reasons. In addition, as an invasive operation, endoscopy also places a serious psychological burden on patients.

In summary, developing a technique with simple operation, high accuracy, and excellent patient compliance can become an important supplement to existing diagnostic methods for GC. OVs, as a tumor-targeting vector, can selectively introduce certain tagged protein genes, such as green fluorescent protein (GFP), into GC cells (62), and fluorescent endoscopy has been used in its diagnosis for a long time (158). Their combination may further improve the diagnostic sensitivity and specificity of early GC. It is widely known that therapeutic effects are closely related to the accurate staging of cancer, and patients with AGC in different stages need to receive the most appropriate therapeutic schedule to obtain the maximum benefit (159). Positron emission tomography with computed tomography (PET/CT), while currently the best method for evaluating systemic metastasis of malignant tumors, only had a sensitivity of 33% (95% CI, 17%-53%) for detecting distant metastases of GC in a multicenter prospective cohort study, which suggested it has limited additional value for GC staging (160). Based on the understanding of PET/CT imaging theory and the delivery ability of OVs, incorporating some transporter genes of radioactive substances used in PET/CT into cancer cells, such as human sodium iodide symporter (hNIS), can observably increase tracer uptake to improve the sensitivity of the examination, and this has been verified in pancreatic cancer and colon cancer (161, 162). Certainly, how to combine the advantages of OVs with existing examination methods to facilitate the diagnosis of GC is also a topic that needs additional study.

4.5 Destruction of the inhibitory TME by OVTs

The normal immune system possesses the function of recognizing, killing, and eliminating malignant cells in time to prevent the occurrence of cancers, which is called “immune surveillance”. However, under the selective pressure of immune surveillance, tumor cells undergo continuous remodeling at the genetic and epigenetic levels and develop a series of escape mechanisms; for example, by creating a suitable TME for growth or resisting apoptosis (163). In this long process, named “cancer immunoediting”, the immune system can both constrain and promote tumor development, which proceeds through three phases termed elimination, equilibrium, and escape to edit tumor immunogenicity and acquire immunosuppressive mechanisms (164). However, most existing immunotherapies are designed to damage the cancer cells themselves even though the dynamic and complex cell networks within the TME play a pivotal role in tumor progression and drug resistance, and it is possible to recover antitumor immunity by breaking negative and indulgent TME (165). For GC, the TME houses a variety of immunosuppressive cells, including regulatory T (Treg) cells, tumor-associated macrophages (TAMs), MSCs, MDSCs, and CAFs, which can promote tumor growth by releasing various molecules that directly activate cancer cell growth signals or reshape surrounding areas (166, 167). Accordingly, targeting

these "rebellious" cells will be a new concept for treating GC, and it has been verified in many aspects.

CAFs are one of the critical components in the GC mesenchyme and not only directly confer growth advantages to cancer cells *via* paracrine signaling with chemokines, cytokines, and growth factors, but they also play a critical role in migration through direct physical interactions between CAFs and cancer cells (168). Consequently, proliferation and invasion can be significantly inhibited when the interactions between them are blocked (169). Through study of GC clinical specimens, poor prognosis and resistance to cancer therapies are closely associated with the infiltration of MDSCs, and the higher the number of MDSCs in patients with late-stage III or IV GC, the worse the prognosis (170). Inhibiting the effects of MDSCs is beneficial to GC patients (171), as well as other immunosuppressive cells (172–174). Although OVs were initially known for their ability to lyse tumor cells, they can also invade nontumor cells (150, 175). Similarly, extending their oncolytic function to tumor stromal cells can destroy the inherently inhibitory TME to restore normal immune surveillance. Applying this theory, prostate cancer and glioblastoma have achieved great curative efficacy as expected, but no similar research has been conducted on GC (176, 177).

4.6 Combining OVTs with other cancer therapies

To date, adjuvant therapies such as chemoradiotherapy, targeted therapy and immunotherapy alone cannot achieve revolutionary curative effects in patients with AGC, which is probably closely related to its strong heterogeneity and low immunogenicity, as previously mentioned, and a combination of various methods, including OVT, assuredly maximizes its therapeutic effects and minimizes drug resistance (178, 179). Chemotherapy as the preferred choice for postoperative and AGC patients can indeed prolong survival, and the combination of various chemotherapy regimens with OVTs shows a certain additive effect for GC as well (61, 102). Most chemotherapeutic agents were developed through their direct cytotoxic effects without consideration of their major detrimental effects on the immune system, such as lymphodepletion, an antagonism for OVTs (180). Targeted therapy has no obvious overlap with OVTs in mechanism and leads to the fact that their combination cannot complement each other (181). In addition to direct oncolysis, OVTs possess a unique ability to indirectly induce innate and adaptive antitumor immunity, which can lead to effective infiltration of immune cells, converting a "cold" tumor with few immune cells into a "hot" one with increased immune cells (182). This is extremely meaningful and not available in other immunotherapies, which means the "soldiers" against cancer cells are prepared and then need to be equipped with "weapons" to further enhance their combat capabilities at present. ICIs have revolutionized medical oncology, although currently only a subset of patients have a response to such treatment (183), and the remaining tumors are nonresponsive, in part due to a lack of tumor-infiltrating immune cells (184). Therefore, OVTs can help increase their effectiveness as a supplement to synergistically enhance the antitumor effect of ICIs, and multiple completed or ongoing items have obtained remarkable results in numerous malignancies, but not in GC (185).

Despite the robust successes of ICIs, primary and acquired resistance is common and is attributable to several factors, including insufficient antitumor T cells, inadequate function of these cells, and the impaired formation of memory T cells. CAR T-cell therapy is another form of immunotherapy that havs strong potential to address many of the limitations of ICIs by its ability to augment the number, specificity, and reactivity of T cells against tumor tissue (186). Unlike hematopoietic tumors, a key limitation of CAR T-cell therapy in solid tumors is the immunosuppressive TME, which leads to T-cell hypofunction, restricting CAR T-cells persistence within the tumors (187). Fortunately, this "door" can be opened by the "key" of OVTs. This combinatorial approach improved antitumor efficacy and prolonged survival in mouse models of solid tumors when compared with monotherapies (188). Another important hurdle encountered with CAR T-cells is tumor immune evasion due to antigen loss (187). To overcome this challenge, OVTs can restore or overexpress absent original tumor antigens and provide tumor cells with unprecedented neoantigens and any other genes that can promote the effectiveness and targeting of CAR T-cell therapy, as a target for CAR (189), as well as CAR NK-cell therapy (190). In the same way, incorporating the content of OVs to damage the suppressive TME, a combination of CAR T-cell therapy and OVTs that deliver targets of inhibitory mesenchymal cells for CAR T-cells, can disrupt the TME more favorably and completely (191). In summary, OVTs may become the optimal companion for CAR T-cell therapy to achieve unprecedented progress in treating solid tumors, including GC; nevertheless, few researchers are currently exploring this avenue.

5 Conclusion

OVs have attracted extensive attention and exploration worldwide because of their abilities to selectively infect and lyse tumor cells. However, in the course of decades of research, scientists found that their selectivity is not absolute, which means they can replicate and proliferate inside nontumor cells as well. Furthermore, an increasing number of animal experiments and clinical trials have revealed that not all OVs can exert ideal oncolysis under safe virus titers, limiting the development of OVTs. Nonetheless, with the continuous decryption of relevant functions of the genes in OVs, coupled

with the rapid progress of gene editing technologies, artificial and purposeful modification of specific genes is possible. Currently, after varying degrees of transformation, the oncolysis of engineered OVs has been sidelined, and they are instead primarily regarded as excellent carriers of exogenous genes for targeting tumor cells. As a malignant tumor with a poor prognosis, strong heterogeneity, and low immunogenicity, how to effectively treat AGC patients has always been a worldwide problem. According to the characteristics of molecular typing in GC, engineered OVs can change their genetic and epigenetic expression levels by combining the introduction of exogenous genes and specific promoters to precisely destroy the malignancy of each subtype and preferably inform clinical medication choices. In addition, OVs can play a fascinating role in the diagnosis and staging of GC to better guide treatment in the clinic, but this needs further investigation. The TME, complicated but structured, plays an irreplaceable role in the occurrence and development of GC. By shifting the "spearhead" of OVs from tumor parenchymal cells to stromal cells, it is possible to break through this inhibitory mechanism to promote the infiltration of various immune effector cells and rebuild the function of immune surveillance against GC. For monotherapy, the crucial reasons for the poor response of various therapies are heterogeneity and resistance, so combination therapy definitely is the developmental direction of cancer treatment in the future, whether for GC or other malignancies. Specifically, the most meaningful function of OVTs is attracting immune cells into the TME to transform "cold" tumors into "hot" tumors, which will significantly improve the effect of immunotherapies for GC, such as ICIs and CAR T-cell therapy. Overall, OVTs can serve as powerful catalysts to assist other treatments, enabling GC patients to benefit more from cancer therapies.

Author contributions

JW: writing of original manuscript. LD: revision of the manuscript. XC: language modification of the manuscript. All authors contributed to the article and approved the submitted version. All authors contributed to the conception of the study and the preparation and approval of the paper.

Funding

This work was supported by Wenzhou Science & Technology Bureau Foundation (Grant No. Y2020144 to XC) and Zhejiang Provincial Natural Science Foundation (Grant No. LY22H160012 to LD).

Conflict of interest

The authors declare that the research was conducted in the absence of any commercial or financial relationships that could be construed as a potential conflict of interest.

Publisher's note

All claims expressed in this article are solely those of the authors and do not necessarily represent those of their affiliated organizations, or those of the publisher, the editors and the reviewers. Any product that may be evaluated in this article, or claim that may be made by its manufacturer, is not guaranteed or endorsed by the publisher.

References

1. Ansari S, Gantuya B, Tuan VP, Yamaoka Y. Diffuse Gastric Cancer: A summary of analogous contributing factors for its molecular pathogenicity. *Int J Mol Sci* (2018) 19(8):2424. doi: 10.3390/ijms19082424

2. Sung H, Ferlay J, Siegel RL, Laversanne M, Soerjomataram I, Jemal A, et al. Global cancer statistics 2020: Globocan estimates of incidence and mortality worldwide for 36 cancers in 185 countries. *CA Cancer J Clin* (2021) 71(3):209–49. doi: 10.3322/caac.21660

3. Smyth EC, Nilsson M, Grabsch HI, van Grieken NC, Lordick F. Gastric cancer. *Lancet* (2020) 396(10251):635–48. doi: 10.1016/s0140-6736(20)31288-5

4. Kang YK, Chin K, Chung HC, Kadowaki S, Oh SC, Nakayama N, et al. S-1 plus leucovorin and oxaliplatin versus s-1 plus cisplatin as first-line therapy in patients with advanced gastric cancer (Solar): A randomised, open-label, phase 3 trial. *Lancet Oncol* (2020) 21(8):1045–56. doi: 10.1016/s1470-2045(20)30315-6

5. Wiedermann U, Garner-Spitzer E, Chao Y, Maglakelidze M, Bulat I, Dechaphunkul A, et al. Clinical and immunologic responses to a b-cell epitope vaccine in patients with Her2/Neu-overexpressing advanced gastric cancer-results from phase ib trial Imu.Acs.001. *Clin Cancer Res* (2021) 27(13):3649–60. doi: 10.1158/1078-0432.Ccr-20-3742

6. Shitara K, Bang YJ, Iwasa S, Sugimoto N, Ryu MH, Sakai D, et al. Trastuzumab deruxtecan in previously treated Her2-positive gastric cancer. *N Engl J Med* (2020) 382(25):2419–30. doi: 10.1056/NEJMoa2004413

7. Zhou W, He X, Wang J, He S, Xie C, Fan Q, et al. Semiconducting polymer nanoparticles for photoactivatable cancer immunotherapy and imaging of immunoactivation. *Biomacromolecules* (2022) 23(4):1490–504. doi: 10.1021/acs.biomac.2c00065

8. Zhao Z, Zheng L, Chen W, Weng W, Song J, Ji J. Delivery strategies of cancer immunotherapy: Recent advances and future perspectives. *J Hematol Oncol* (2019) 12(1):126. doi: 10.1186/s13045-019-0817-3

9. Muscolini M, Tassone E, Hiscott J. Oncolytic immunotherapy: Can't start a fire without a spark. *Cytokine Growth Factor Rev* (2020) 56:94–101. doi: 10.1016/j.cytogfr.2020.07.014

10. Challenor S, Tucker D. Sars-Cov-2-Induced remission of Hodgkin lymphoma. *Br J Haematol* (2021) 192(3):415. doi: 10.1111/bjh.17116

11. Andtbacka RH, Kaufman HL, Collichio F, Amatruda T, Senzer N, Chesney J, et al. Talimogene laherparepvec improves durable response rate in patients with advanced melanoma. *J Clin Oncol* (2015) 33(25):2780–8. doi: 10.1200/jco.2014.58.3377

12. Zeng J, Li X, Sander M, Zhang H, Yan G, Lin Y. Oncolytic viro-immunotherapy: An emerging option in the treatment of gliomas. *Front Immunol* (2021) 12:721830. doi: 10.3389/fimmu.2021.721830

13. Todo T, Ino Y, Ohtsu H, Shibahara J, Tanaka M. A phase I/Ii study of triple-mutated oncolytic herpes virus G47Δ in patients with progressive glioblastoma. *Nat Commun* (2022) 13(1):4119. doi: 10.1038/s41467-022-31262-y

14. Maloney BE, Perera KD, Saunders DRD, Shadipeni N, Fleming SD. Interactions of viruses and the humoral innate immune response. *Clin Immunol* (2020) 212:108351. doi: 10.1016/j.clim.2020.108351

15. Atasheva S, Emerson CC, Yao J, Young C, Stewart PL, Shayakhmetov DM. Systemic cancer therapy with engineered adenovirus that evades innate immunity. *Sci Transl Med* (2020) 12(571):eabc6659. doi: 10.1126/scitranslmed.abc6659

16. Vähä-Koskela M, Hinkkanen A. Tumor restrictions to oncolytic virus. *Biomedicines* (2014) 2(2):163–94. doi: 10.3390/biomedicines2020163

17. Osali A, Zhiani M, Ghaebi M, Meymanat M, Esmaeilzadeh A. Multidirectional strategies for targeted delivery of oncolytic viruses by tumor infiltrating immune cells. *Pharmacol Res* (2020) 161:105094. doi: 10.1016/j.phrs.2020.105094

18. Kaufman HL, Kohlhapp FJ, Zloza A. Oncolytic viruses: A new class of immunotherapy drugs. *Nat Rev Drug Discovery* (2015) 14(9):642–62. doi: 10.1038/nrd4663

19. Yan N, Chen ZJ. Intrinsic antiviral immunity. *Nat Immunol* (2012) 13 (3):214–22. doi: 10.1038/ni.2229

20. Motwani M, Pesiridis S, Fitzgerald KA. DNA Sensing by the cgas-sting pathway in health and disease. *Nat Rev Genet* (2019) 20(11):657–74. doi: 10.1038/s41576-019-0151-1

21. Nie Y, Wang YY. Innate immune responses to DNA viruses. *Protein Cell* (2013) 4(1):1–7. doi: 10.1007/s13238-012-2122-6

22. Thoresen D, Wang W, Galls D, Guo R, Xu L, Pyle AM. The molecular mechanism of rig-I activation and signaling. *Immunol Rev* (2021) 304(1):154–68. doi: 10.1111/imr.13022

23. Chow KT, Gale MJr., Loo YM. Rig-I and other rna sensors in antiviral immunity. *Annu Rev Immunol* (2018) 36:667–94. doi: 10.1146/annurev-immunol-042617-053309

24. Schneider WM, Chevillotte MD, Rice CM. Interferon-stimulated genes: A complex web of host defenses. *Annu Rev Immunol* (2014) 32:513–45. doi: 10.1146/annurev-immunol-032713-120231

25. Burckhardt CJ, Suomalainen M, Schoenenberger P, Boucke K, Hemmi S, Greber UF. Drifting motions of the adenovirus receptor car and immobile integrins initiate virus uncoating and membrane lytic protein exposure. *Cell Host Microbe* (2011) 10(2):105–17. doi: 10.1016/j.chom.2011.07.006

26. Owczarek C, Ortiz-Zapater E, Kim J, Papaevangelou E, Santis G, Parsons M. Car Co-operates with integrins to promote lung cancer cell adhesion and invasion. *Front Oncol* (2022) 12:829313. doi: 10.3389/fonc.2022.829313

27. Reeh M, Bockhorn M, Görgens D, Vieth M, Hoffmann T, Simon R, et al. Presence of the coxsackievirus and adenovirus receptor (Car) in human neoplasms: A multitumour array analysis. *Br J Cancer* (2013) 109(7):1848–58. doi: 10.1038/bjc.2013.509

28. Demerlé C, Gorvel L, Olive D. Btla-hvem couple in health and diseases: Insights for immunotherapy in lung cancer. *Front Oncol* (2021) 11:682007. doi: 10.3389/fonc.2021.682007

29. Bonnin M, Fares N, Testoni B, Estornes Y, Weber K, Vanbervliet B, et al. Toll-like receptor 3 downregulation is an escape mechanism from apoptosis during hepatocarcinogenesis. *J Hepatol* (2019) 71(4):763–72. doi: 10.1016/j.jhep.2019.05.031

30. Lei A, Maloy KJ. Colon cancer in the land of nod: Nlrx1 as an intrinsic tumor suppressor. *Trends Immunol* (2016) 37(9):569–70. doi: 10.1016/j.it.2016.07.004

31. Konno H, Yamauchi S, Berglund A, Putney RM, Mulé JJ, Barber GN. Suppression of sting signaling through epigenetic silencing and missense mutation impedes DNA damage mediated cytokine production. *Oncogene* (2018) 37 (15):2037–51. doi: 10.1038/s41388-017-0120-0

32. Zhang W, Wang G, Xu ZG, Tu H, Hu F, Dai J, et al. Lactate is a natural suppressor of rlr signaling by targeting mavs. *Cell* (2019) 178(1):176–89.e15. doi: 10.1016/j.cell.2019.05.003

33. Miar A, Arnaiz E, Bridges E, Beedie S, Cribbs AP, Downes DJ, et al. Hypoxia induces transcriptional and translational downregulation of the type I ifn pathway in multiple cancer cell types. *Cancer Res* (2020) 80(23):5245–56. doi: 10.1158/0008-5472.Can-19-2306

34. Garg AD, Agostinis P. Cell death and immunity in cancer: From danger signals to mimicry of pathogen defense responses. *Immunol Rev* (2017) 280 (1):126–48. doi: 10.1111/imr.12574

35. Kesavardhana S, Malireddi RKS, Kanneganti TD. Caspases in cell death, inflammation, and pyroptosis. *Annu Rev Immunol* (2020) 38:567–95. doi: 10.1146/annurev-immunol-073119-095439

36. Weide B, Neri D, Elia G. Intralesional treatment of metastatic melanoma: A review of therapeutic options. *Cancer Immunol Immunother* (2017) 66(5):647–56. doi: 10.1007/s00262-016-1952-0

37. Malvehy J, Samoylenko I, Schadendorf D, Gutzmer R, Grob JJ, Sacco JJ, et al. Talimogene laherparepvec upregulates immune-cell populations in non-injected lesions: Findings from a phase ii, multicenter, open-label study in patients with stage iiib-Ivm1c melanoma. *J Immunother Cancer* (2021) 9(3):e001621. doi: 10.1136/jitc-2020-001621

38. Oosenbrug T, van de Graaff MJ, Ressing ME, van Kasteren SI. Chemical tools for studying tlr signaling dynamics. *Cell Chem Biol* (2017) 24(7):801–12. doi: 10.1016/j.chembiol.2017.05.022

39. Marelli G, Howells A, Lemoine NR, Wang Y. Oncolytic viral therapy and the immune system: A double-edged sword against cancer. *Front Immunol* (2018) 9:866. doi: 10.3389/fimmu.2018.00866

40. Hemminki O, Dos Santos JM, Hemminki A. Oncolytic viruses for cancer immunotherapy. *J Hematol Oncol* (2020) 13(1):84. doi: 10.1186/s13045-020-00922-1

41. Mondal M, Guo J, He P, Zhou D. Recent advances of oncolytic virus in cancer therapy. *Hum Vaccin Immunother* (2020) 16(10):2389–402. doi: 10.1080/21645515.2020.1723363

42. Cao GD, He XB, Sun Q, Chen S, Wan K, Xu X, et al. The oncolytic virus in cancer diagnosis and treatment. *Front Oncol* (2020) 10:1786. doi: 10.3389/fonc.2020.01786

43. Fukuhara H, Ino Y, Todo T. Oncolytic virus therapy: A new era of cancer treatment at dawn. *Cancer Sci* (2016) 107(10):1373–9. doi: 10.1111/cas.13027

44. Ohashi M, Kanai F, Ueno H, Tanaka T, Tateishi K, Kawakami T, et al. Adenovirus mediated P53 tumour suppressor gene therapy for human gastric cancer cells *in vitro* and *in vivo*. *Gut* (1999) 44(3):366–71. doi: 10.1136/gut.44.3.366

45. Shinomiya N, Gao CF, Xie Q, Gustafson M, Waters DJ, Zhang YW, et al. Rna interference reveals that ligand-independent met activity is required for tumor cell signaling and survival. *Cancer Res* (2004) 64(21):7962–70. doi: 10.1158/0008-5472.Can-04-1043

46. Cheng JT, Wang YY, Zhu LZ, Zhang Y, Cai WQ, Han ZW, et al. Novel transcription regulatory sequences and factors of the immune evasion protein Icp47 (Us12) of herpes simplex viruses. *Virol J* (2020) 17(1):101. doi: 10.1186/s12985-020-01365-3

47. Liao J, Xiao H, Dai G, He T, Huang W. Recombinant adenovirus (Adeasy system) mediated exogenous expression of long non-coding rna H19 (Lncrna H19) biphasic regulating osteogenic differentiation of mesenchymal stem cells (Mscs). *Am J Transl Res* (2020) 12(5):1700–13.

48. Wang TB, Huang WS, Lin WH, Shi HP, Dong WG. Inhibition of kit rnai mediated with adenovirus in gastrointestinal stromal tumor xenograft. *World J Gastroenterol* (2010) 16(40):5122–9. doi: 10.3748/wjg.v16.i40.5122

49. Aoki K, Barker C, Danthinne X, Imperiale MJ, Nabel GJ. Efficient generation of recombinant adenoviral vectors by cre-lox recombination *in vitro*. *Mol Med* (1999) 5(4):224–31.

50. Gresele P, Momi S, Marcucci R, Ramundo F, De Stefano V, Tripodi A. Interactions of adenoviruses with platelets and coagulation and the vaccine-induced immune thrombotic thrombocytopenia syndrome. *Haematologica* (2021) 106(12):3034–45. doi: 10.3324/haematol.2021.279289

51. Bieri M, Hendrickx R, Bauer M, Yu B, Jetzer T, Dreier B, et al. The rgd-binding integrins Avβ6 and Avβ8 are receptors for mouse adenovirus-1 and -3 infection. *PloS Pathog* (2021) 17(12):e1010083. doi: 10.1371/journal.ppat.1010083

52. Greber UF, Flatt JW. Adenovirus entry: From infection to immunity. *Annu Rev Virol* (2019) 6(1):177–97. doi: 10.1146/annurev-virology-092818-015550

53. Chang J. Adenovirus vectors: Excellent tools for vaccine development. *Immune Netw* (2021) 21(1):e6. doi: 10.4110/in.2021.21.e6

54. King CR, Zhang A, Tessier TM, Gameiro SF, Mymryk JS. Hacking the cell: Network intrusion and exploitation by adenovirus E1a. *mBio* (2018) 9(3):e00390–18. doi: 10.1128/mBio.00390-18

55. Hoeben RC, Uil TG. Adenovirus DNA replication. *Cold Spring Harb Perspect Biol* (2013) 5(3):a013003. doi: 10.1101/cshperspect.a013003

56. Sher YP, Lin SI, Chai KM, Chen IH, Liu SJ. Endoplasmic reticulum-targeting sequence enhanced the cellular immunity of a tumor-associated antigen L6-based DNA vaccine. *Am J Cancer Res* (2019) 9(9):2028–36.

57. Dybas JM, Lum KK, Kulej K, Reyes ED, Lauman R, Charman M, et al. Adenovirus remodeling of the host proteome and host factors associated with viral genomes. *mSystems* (2021):e0046821. doi: 10.1128/mSystems.00468-21

58. de Pablo PJ, San Martín C. Seeing and touching adenovirus: Complementary approaches for understanding assembly and disassembly of a complex virion. *Curr Opin Virol* (2022) 52:112–22. doi: 10.1016/j.coviro.2021.11.006

59. Kangasniemi L, Kiviluoto T, Kanerva A, Raki M, Ranki T, Sarkioja M, et al. Infectivity-enhanced adenoviruses deliver efficacy in clinical samples and orthotopic models of disseminated gastric cancer. *Clin Cancer Res* (2006) 12 (10):3137–44. doi: 10.1158/1078-0432.Ccr-05-2576

60. Tanaka T, Huang J, Hirai S, Kuroki M, Kuroki M, Watanabe N, et al. Carcinoembryonic antigen-targeted selective gene therapy for gastric cancer

through Fz33 fiber-modified adenovirus vectors. *Clin Cancer Res* (2006) 12 (12):3803–13. doi: 10.1158/1078-0432.Ccr-06-0024

61. Ishikawa W, Kikuchi S, Ogawa T, Tabuchi M, Tazawa H, Kuroda S, et al. Boosting replication and penetration of oncolytic adenovirus by paclitaxel eradicate peritoneal metastasis of gastric cancer. *Mol Ther Oncolytics* (2020) 18:262–71. doi: 10.1016/j.omto.2020.06.021

62. Watanabe M, Kagawa S, Kuwada K, Hashimoto Y, Shigeyasu K, Ishida M, et al. Integrated fluorescent cytology with nano-biologics in peritoneally disseminated gastric cancer. *Cancer Sci* (2018) 109(10):3263–71. doi: 10.1111/cas.13760

63. Stanziale SF, Petrowsky H, Adusumilli PS, Ben-Porat L, Gonen M, Fong Y. Infection with oncolytic herpes simplex virus-1 induces apoptosis in neighboring human cancer cells: A potential target to increase anticancer activity. *Clin Cancer Res* (2004) 10(9):3225–32. doi: 10.1158/1078-0432.ccr-1083-3

64. Stanziale SF, Stiles BM, Bhargava A, Kerns SA, Kalakonda N, Fong Y. Oncolytic herpes simplex virus-1 mutant expressing green fluorescent protein can detect and treat peritoneal cancer. *Hum Gene Ther* (2004) 15(6):609–18. doi: 10.1089/104303404323142051

65. Sugawara K, Iwai M, Yajima S, Tanaka M, Yanagihara K, Seto Y, et al. Efficacy of a third-generation oncolytic herpes virus G47δ in advanced stage models of human gastric cancer. *Mol Ther Oncolytics* (2020) 17:205–15. doi: 10.1016/j.omto.2020.03.022

66. Bennett JJ, Kooby DA, Delman K, McAuliffe P, Halterman MW, Federoff H, et al. Antitumor efficacy of regional oncolytic viral therapy for peritoneally disseminated cancer. *J Mol Med (Berl)* (2000) 78(3):166–74. doi: 10.1007/s001090000092

67. Nakano K, Todo T, Zhao G, Yamaguchi K, Kuroki S, Cohen JB, et al. Enhanced efficacy of conditionally replicating herpes simplex virus (G207) combined with 5-fluorouracil and surgical resection in peritoneal cancer dissemination models. *J Gene Med* (2005) 7(5):638–48. doi: 10.1002/jgm.700

68. Zeng D, Zhang T, Zhou S, Hu H, Li J, Huang K, et al. Proteomic analyses of gastric cancer cells treated with vesicular stomatitis virus matrix protein. *Protein J* (2011) 30(5):308–17. doi: 10.1007/s10930-011-9331-3

69. Wang H, Chen NG, Minev BR, Zimmermann M, Aguilar RJ, Zhang Q, et al. Optical detection and virotherapy of live metastatic tumor cells in body fluids with vaccinia strains. *PloS One* (2013) 8(9):e71105. doi: 10.1371/journal.pone.0071105

70. Song KY, Wong J, Gonzalez L, Sheng G, Zamarin D, Fong Y. Antitumor efficacy of viral therapy using genetically engineered Newcastle disease virus [Ndv (F3aa)-gfp] for peritoneally disseminated gastric cancer. *J Mol Med (Berl)* (2010) 88 (6):589–96. doi: 10.1007/s00109-010-0605-6

71. Lv Y, Zhou D, Hao XQ, Zhu MY, Zhang CD, Zhou DM, et al. A recombinant measles virus vaccine strain rmv-Hu191 has oncolytic effect against human gastric cancer by inducing apoptotic cell death requiring integrity of lipid raft microdomains. *Cancer Lett* (2019) 460:108–18. doi: 10.1016/j.canlet.2019.06.010

72. Lv Y, Zhang CD, Wang YL, Zhou DM, Zhu MY, Hao XQ, et al. Synergism of rmv-Hu191 with cisplatin to treat gastric cancer by acid sphingomyelinase-mediated apoptosis requiring integrity of lipid raft microdomains. *Gastric Cancer* (2021) 24(6):1293–306. doi: 10.1007/s10120-021-01210-8

73. Hamano S, Mori Y, Aoyama M, Kataoka H, Tanaka M, Ebi M, et al. Oncolytic reovirus combined with trastuzumab enhances antitumor efficacy through trail signaling in human Her2-positive gastric cancer cells. *Cancer Lett* (2015) 356(2Pt B):846–54. doi: 10.1016/j.canlet.2014.10.046

74. Kawaguchi K, Etoh T, Suzuki K, Mitui MT, Nishizono A, Shiraishi N, et al. Efficacy of oncolytic reovirus against human gastric cancer with peritoneal metastasis in experimental animal model. *Int J Oncol* (2010) 37(6):1433–8. doi: 10.3892/ijo_00000795

75. Min Y, Adachi Y, Yamamoto H, Imsumran A, Arimura Y, Endo T, et al. Insulin-like growth factor I receptor blockade enhances chemotherapy and radiation responses and inhibits tumour growth in human gastric cancer xenografts. *Gut* (2005) 54(5):591–600. doi: 10.1136/gut.2004.048926

76. Tsunemitsu Y, Kagawa S, Tokunaga N, Otani S, Umeoka T, Roth JA, et al. Molecular therapy for peritoneal dissemination of xenotransplanted human mkn-45 gastric cancer cells with adenovirus mediated bax gene transfer. *Gut* (2004) 53 (4):554–60. doi: 10.1136/gut.2003.021683

77. Gao J, Senthil M, Ren B, Yan J, Xing Q, Yu J, et al. Irf-1 transcriptionally upregulates puma, which mediates the mitochondrial apoptotic pathway in irf-1-Induced apoptosis in cancer cells. *Cell Death Differ* (2010) 17(4):699–709. doi: 10.1038/cdd.2009.156

78. Sako A, Kitayama J, Koyama H, Ueno H, Uchida H, Hamada H, et al. Transduction of soluble flt-1 gene to peritoneal mesothelial cells can effectively suppress peritoneal metastasis of gastric cancer. *Cancer Res* (2004) 64(10):3624–8. doi: 10.1158/0008-5472.Can-04-0304

79. Kanai F, Kawakami T, Hamada H, Sadata A, Yoshida Y, Tanaka T, et al. Adenovirus-mediated transduction of escherichia coli uracil phosphoribosyltransferase gene sensitizes cancer cells to low concentrations of 5-fluorouracil. *Cancer Res* (1998) 58(9):1946–51.

80. Tanaka H, Yashiro M, Sunami T, Sakate Y, Kosaka K, Hirakawa K. Icam-2 gene therapy for peritoneal dissemination of scirrhous gastric carcinoma. *Clin Cancer Res* (2004) 10(14):4885–92. doi: 10.1158/1078-0432.Ccr-0393-03

81. Chen L, Chen D, Gong M, Na M, Li L, Wu H, et al. Concomitant use of Ad5/35 chimeric oncolytic adenovirus with trail gene and taxol produces synergistic cytotoxicity in gastric cancer cells. *Cancer Lett* (2009) 284(2):141–8. doi: 10.1016/j.canlet.2009.04.026

82. Sun PH, Zhu LM, Qiao MM, Zhang YP, Jiang SH, Wu YL, et al. The Xaf1 tumor suppressor induces autophagic cell death *Via* upregulation of beclin-1 and inhibition of akt pathway. *Cancer Lett* (2011) 310(2):170–80. doi: 10.1016/j.canlet.2011.06.037

83. Wu Y, Yuan M, Su W, Zhu M, Yao X, Wang Y, et al. The constitutively active pkg ii mutant effectively inhibits gastric cancer development *Via* a blockade of Egf/Egfr-associated signalling cascades. *Ther Adv Med Oncol* (2018) 10:1758834017751635. doi: 10.1177/1758834017751635

84. Wang B, Liu J, Ma LN, Xiao HL, Wang YZ, Li Y, et al. Chimeric 5/35 adenovirus-mediated dickkopf-1 overexpression suppressed tumorigenicity of $Cd44^+$ gastric cancer cells *Via* attenuating wnt signaling. *J Gastroenterol* (2013) 48(7):798–808. doi: 10.1007/s00535-012-0711-z

85. Lv Y, Purbey BK, Huang Y, Li S, Radha G, Hao Z. Adenovirus-mediated expression of P33(Ing1b) induces apoptosis and inhibits proliferation in gastric adenocarcinoma cells *in vitro*. *Gastric Cancer* (2012) 15(4):355–62. doi: 10.1007/s10120-011-0123-4

86. Wang M, Hong Y, Feng Q, Pan X, Song S, Cui J, et al. Recombinant adenovirus Kghv500 and cik cells codeliver anti-P21-Ras scfv for the treatment of gastric cancer with wild-type ras overexpression. *Mol Ther Oncolytics* (2018) 11:90–101. doi: 10.1016/j.omto.2018.10.003

87. Ishida M, Kagawa S, Shimoyama K, Takehara K, Noma K, Tanabe S, et al. Trastuzumab-based photoimmunotherapy integrated with viral Her2 transduction inhibits peritoneally disseminated Her2-negative cancer. *Mol Cancer Ther* (2016) 15(3):402–11. doi: 10.1158/1535-7163.Mct-15-0644

88. Yin H, Huang X, Tao M, Hu Q, Qiu J, Chen W, et al. Adenovirus-mediated Tipe2 overexpression inhibits gastric cancer metastasis *Via* reversal of epithelial-mesenchymal transition. *Cancer Gene Ther* (2017) 24(4):180–8. doi: 10.1038/cgt.2017.3

89. Zhang H, Zhou X, Xu C, Yang J, Xiang J, Tao M, et al. Synergistic tumor suppression by adenovirus-mediated Ing4/Pten double gene therapy for gastric cancer. *Cancer Gene Ther* (2016) 23(1):13–23. doi: 10.1038/cgt.2015.59

90. Fujiwara H, Kubota T, Amaike H, Inada S, Takashima K, Atsuji K, et al. Suppression of peritoneal implantation of gastric cancer cells by adenovirus vector-mediated Nk4 expression. *Cancer Gene Ther* (2005) 12(2):206–16. doi: 10.1038/sj.cgt.7700782

91. Kawamura YI, Adachi Y, Curiel DT, Kawashima R, Kannagi R, Nishimoto N, et al. Therapeutic adenoviral gene transfer of a glycosyltransferase for prevention of peritoneal dissemination and metastasis of gastric cancer. *Cancer Gene Ther* (2014) 21(10):427–33. doi: 10.1038/cgt.2014.46

92. Tanaka F, Tominaga K, Shiota M, Ochi M, Kuwamura H, Tanigawa T, et al. Interleukin-10 gene transfer to peritoneal mesothelial cells suppresses peritoneal dissemination of gastric cancer cells due to a persistently high concentration in the peritoneal cavity. *Cancer Gene Ther* (2008) 15(1):51–9. doi: 10.1038/sj.cgt.7701104

93. Lu WW, Zhang H, Li YM, Ji F. Gastric cancer-derived heat shock protein-Gp96 peptide complex enhances dendritic cell activation. *World J Gastroenterol* (2017) 23(24):4390–8. doi: 10.3748/wjg.v23.i24.4390

94. Zheng SY, Li DC, Zhang ZD, Zhao J, Ge JF. Anti-gastric cancer active immunity induced by Fasl/B7-1 gene-modified tumor cells. *World J Gastroenterol* (2005) 11(21):3204–11. doi: 10.3748/wjg.v11.i21.3204

95. Akagi H, Higuchi H, Sumimoto H, Igarashi T, Kabashima A, Mizuguchi H, et al. Suppression of myeloid cell leukemia-1 (Mcl-1) enhances chemotherapy-associated apoptosis in gastric cancer cells. *Gastric Cancer* (2013) 16(1):100–10. doi: 10.1007/s10120-012-0153-6

96. Nishioka N, Matsuoka T, Yashiro M, Hirakawa K, Olden K, Roberts JD. Plasminogen activator inhibitor 1 rnai suppresses gastric cancer metastasis *in vivo*. *Cancer Sci* (2012) 103(2):228–32. doi: 10.1111/j.1349-7006.2011.02155.x

97. Schneider CC, Archid R, Fischer N, Bühler S, Venturelli S, Berger A, et al. Metabolic alteration–overcoming therapy resistance in gastric cancer *Via* pgk-1 inhibition in a combined therapy with standard chemotherapeutics. *Int J Surg* (2015) 22:92–8. doi: 10.1016/j.ijsu.2015.08.020

98. Sun HW, Tong SL, He J, Wang Q, Zou L, Ma SJ, et al. Rhoa and rhoc -sirna inhibit the proliferation and invasiveness activity of human gastric carcinoma by Rho/Pi3k/Akt pathway. *World J Gastroenterol* (2007) 13(25):3517–22. doi: 10.3748/wjg.v13.i25.3517

99. Zhu BS, Yu LY, Zhao K, Wu YY, Cheng XL, Wu Y, et al. Effects of small interfering rna inhibit class I phosphoinositide 3-kinase on human gastric

cancer cells. *World J Gastroenterol* (2013) 19(11):1760–9. doi: 10.3748/wjg.v19.i11.1760

100. Lan KH, Kanai F, Shiratori Y, Okabe S, Yoshida Y, Wakimoto H, et al. Tumor-specific gene expression in carcinoembryonic antigen–producing gastric cancer cells using adenovirus vectors. *Gastroenterology* (1996) 111(5):1241–51. doi: 10.1053/gast.1996.v111.pm8898638

101. Tanaka T, Kanai F, Okabe S, Yoshida Y, Wakimoto H, Hamada H, et al. Adenovirus-mediated prodrug gene therapy for carcinoembryonic antigen-producing human gastric carcinoma cells *in vitro*. *Cancer Res* (1996) 56(6):1341–5.

102. Yano S, Tazawa H, Hashimoto Y, Shirakawa Y, Kuroda S, Nishizaki M, et al. A genetically engineered oncolytic adenovirus decoys and lethally traps quiescent cancer stem-like cells in S/G2/M phases. *Clin Cancer Res* (2013) 19 (23):6495–505. doi: 10.1158/1078-0432.Ccr-13-0742

103. Ono HA, Davydova JG, Adachi Y, Takayama K, Barker SD, Reynolds PN, et al. Promoter-controlled infectivity-enhanced conditionally replicative adenoviral vectors for the treatment of gastric cancer. *J Gastroenterol* (2005) 40(1):31–42. doi: 10.1007/s00535-004-1490-y

104. Dvory-Sobol H, Sagiv E, Liberman E, Kazanov D, Arber N. Suppression of gastric cancer cell growth by targeting the beta-Catenin/T-Cell factor pathway. *Cancer* (2007) 109(2):188–97. doi: 10.1002/cncr.22416

105. He S, Wang L, Wu Y, Li D, Zhang Y. Ccl3 and Ccl20-recruited dendritic cells modified by melanoma antigen gene-1 induce anti-tumor immunity against gastric cancer ex vivo and *in vivo*. *J Exp Clin Cancer Res* (2010) 29(1):37. doi: 10.1186/1756-9966-29-37

106. You B, Jin C, Zhang J, Xu M, Xu W, Sun Z, et al. Msc-derived extracellular vesicle-delivered l-pgds inhibit gastric cancer progression by suppressing cancer cell stemness and Stat3 phosphorylation. *Stem Cells Int* (2022) 2022:9668239. doi: 10.1155/2022/9668239

107. Tsuji T, Nakamori M, Iwahashi M, Nakamura M, Ojima T, Iida T, et al. An armed oncolytic herpes simplex virus expressing thrombospondin-1 has an enhanced *in vivo* antitumor effect against human gastric cancer. *Int J Cancer* (2013) 132(2):485–94. doi: 10.1002/ijc.27681

108. Kato T, Nakamori M, Matsumura S, Nakamura M, Ojima T, Fukuhara H, et al. Oncolytic virotherapy with human telomerase reverse transcriptase promoter regulation enhances cytotoxic effects against gastric cancer. *Oncol Lett* (2021) 21 (6):490. doi: 10.3892/ol.2021.12751

109. Wang M, Luo Y, Sun T, Mao C, Jiang Y, Yu X, et al. The ectopic expression of Survivint34a and filc can enhance the oncolytic effects of vaccinia virus in murine gastric cancer. *Onco Targets Ther* (2020) 13:1011–25. doi: 10.2147/ott.S230902

110. Jun KH, Gholami S, Song TJ, Au J, Haddad D, Carson J, et al. A novel oncolytic viral therapy and imaging technique for gastric cancer using a genetically engineered vaccinia virus carrying the human sodium iodide symporter. *J Exp Clin Cancer Res* (2014) 33(1):2. doi: 10.1186/1756-9966-33-2

111. Bu X, Zhang A, Chen Z, Zhang X, Zhang R, Yin C, et al. Migration of gastric cancer is suppressed by recombinant Newcastle disease virus (Rl-rvg) *Via* regulating A7-nicotinic acetylcholine Receptors/Erk- emt. *BMC Cancer* (2019) 19 (1):976. doi: 10.1186/s12885-019-6225-9

112. Bu X, Li M, Zhao Y, Liu S, Wang M, Ge J, et al. Genetically engineered Newcastle disease virus expressing human interferon-Λ1 induces apoptosis in gastric adenocarcinoma cells and modulates the Th1/Th2 immune response. *Oncol Rep* (2016) 36(3):1393–402. doi: 10.3892/or.2016.4925

113. Wong J, Schulman A, Kelly K, Zamarin D, Palese P, Fong Y. Detection of free peritoneal cancer cells in gastric cancer using cancer-specific Newcastle disease virus. *J Gastrointest Surg* (2010) 14(1):7–14. doi: 10.1007/s11605-009-1071-8

114. Costa L, Corre S, Michel V, Le Luel K, Fernandes J, Ziveri J, et al. Usf1 defect drives P53 degradation during helicobacter pylori infection and accelerates gastric carcinogenesis. *Gut* (2020) 69(9):1582–91. doi: 10.1136/gutjnl-2019-318640

115. Zhu CH, Peng SQ, Cui LL, Cao W, Zhang LS, Zhao ZM, et al. Synergistic effects of rapamycin and fluorouracil to treat a gastric tumor in a pten conditional deletion mouse model. *Gastric Cancer* (2022) 25(1):96–106. doi: 10.1007/s10120-021-01229-x

116. Zhu H, Zheng C. The race between host antiviral innate immunity and the immune evasion strategies of herpes simplex virus 1. *Microbiol Mol Biol Rev* (2020) 84(4):e00099–20. doi: 10.1128/mmbr.00099-20

117. Connolly SA, Jardetzky TS, Longnecker R. The structural basis of herpesvirus entry. *Nat Rev Microbiol* (2021) 19(2):110–21. doi: 10.1038/s41579-020-00448-w

118. Huang Y, Song Y, Li J, Lv C, Chen ZS, Liu Z. Receptors and ligands for herpes simplex viruses: Novel insights for drug targeting. *Drug Discovery Today* (2022) 27(1):185–95. doi: 10.1016/j.drudis.2021.10.004

119. Whisnant AW, Jürges CS, Hennig T, Wyler E, Prusty B, Rutkowski AJ, et al. Integrative functional genomics decodes herpes simplex virus 1. *Nat Commun* (2020) 11(1):2038. doi: 10.1038/s41467-020-15992-5

120. Boutell C, Everett RD. Regulation of alphaherpesvirus infections by the Icp0 family of proteins. *J Gen Virol* (2013) 94(Pt 3):465–81. doi: 10.1099/vir.0.048900-0

121. Guo H, Gilley RP, Fisher A, Lane R, Landsteiner VJ, Ragan KB, et al. Species-independent contribution of Zbp1/Dai/Dlm-1-Triggered necroptosis in host defense against Hsv1. *Cell Death Dis* (2018) 9(8):816. doi: 10.1038/s41419-018-0868-3

122. Bommareddy PK, Peters C, Saha D, Rabkin SD, Kaufman HL. Oncolytic herpes simplex viruses as a paradigm for the treatment of cancer. *Annu Rev Cancer Biol* (2018) 2(1):155–73. doi: 10.1146/annurev-cancerbio-030617-050254

123. Manivanh R, Mehrbach J, Knipe DM, Leib DA. Role of herpes simplex virus 1 Γ34.5 in the regulation of Irf3 signaling. *J Virol* (2017) 91(23):e01156–17. doi: 10.1128/jvi.01156-17

124. Jin KT, Du WL, Liu YY, Lan HR, Si JX, Mou XZ. Oncolytic virotherapy in solid tumors: The challenges and achievements. *Cancers (Basel)* (2021) 13(4):588. doi: 10.3390/cancers13040588

125. Goradel NH, Baker AT, Arashkia A, Ebrahimi N, Ghorghanlu S, Negahdari B. Oncolytic virotherapy: Challenges and solutions. *Curr Prob Cancer* (2021) 45(1):100639. doi: 10.1016/j.currproblcancer.2020.100639

126. Hama S, Akita H, Iida S, Mizuguchi H, Harashima H. Quantitative and mechanism-based investigation of post-nuclear delivery events between adenovirus and lipoplex. *Nucleic Acids Res* (2007) 35(5):1533–43. doi: 10.1093/nar/gkl1165

127. Zhao Z, Anselmo AC, Mitragotri S. Viral vector-based gene therapies in the clinic. *Bioeng Transl Med* (2022) 7(1):e10258. doi: 10.1002/btm2.10258

128. Li B, Chen Y, Liang L, Wang Y, Huang W, Zhao K, et al. Tumor-derived extracellular vesicles shuttle c-myc to promote gastric cancer growth and metastasis *Via* the Kcnq1ot1/Mir-556-3p/Clic1 axis. *Cell Death Dis* (2022) 13(3):217. doi: 10.1038/s41419-021-04446-5

129. Wu P, Liu JL, Pei SM, Wu CP, Yang K, Wang SP, et al. Integrated genomic analysis identifies clinically relevant subtypes of renal clear cell carcinoma. *BMC Cancer* (2018) 18(1):287. doi: 10.1186/s12885-018-4176-1

130. Cristescu R, Lee J, Nebozhyn M, Kim KM, Ting JC, Wong SS, et al. Molecular analysis of gastric cancer identifies subtypes associated with distinct clinical outcomes. *Nat Med* (2015) 21(5):449–56. doi: 10.1038/nm.3850

131. Li M, Rao X, Cui Y, Zhang L, Li X, Wang B, et al. The keratin 17/Yap/Il6 axis contributes to e-cadherin loss and aggressiveness of diffuse gastric cancer. *Oncogene* (2022) 41(6):770–81. doi: 10.1038/s41388-021-02119-3

132. The Cancer Genome Atlas Research Network. Comprehensive molecular characterization of gastric adenocarcinoma. *Nature* (2014) 513(7517):202–9. doi: 10.1038/nature13480

133. Böger C, Krüger S, Behrens HM, Bock S, Haag J, Kalthoff H, et al. Epstein-Barr Virus-associated gastric cancer reveals intratumoral heterogeneity of Pik3ca mutations. *Ann Oncol* (2017) 28(5):1005–14. doi: 10.1093/annonc/mdx047

134. Yoon AR, Hong J, Kim M, Yun CO. Hepatocellular carcinoma-targeting oncolytic adenovirus overcomes hypoxic tumor microenvironment and effectively disperses through both central and peripheral tumor regions. *Sci Rep* (2018) 8 (1):2233. doi: 10.1038/s41598-018-20268-6

135. Wang L, Dong J, Wei M, Wen W, Gao J, Zhang Z, et al. Selective and augmented B-glucuronidase expression combined with dox-Ga3 application elicits the potent suppression of prostate cancer. *Oncol Rep* (2016) 35(3):1417–24. doi: 10.3892/or.2015.4454

136. Guo X, Lv X, Ru Y, Zhou F, Wang N, Xi H, et al. Circulating exosomal gastric cancer-associated long noncoding Rna1 as a biomarker for early detection and monitoring progression of gastric cancer: A multiphase study. *JAMA Surg* (2020) 155(7):572–9. doi: 10.1001/jamasurg.2020.1133

137. Das A, Barik S, Banerjee S, Bose A, Sarkar K, Biswas J, et al. A monoclonal antibody against neem leaf glycoprotein recognizes carcinoembryonic antigen (Cea) and restricts cea expressing tumor growth. *J Immunother* (2014) 37 (8):394–406. doi: 10.1097/cji.0000000000000050

138. Feng F, Tian Y, Xu G, Liu Z, Liu S, Zheng G, et al. Diagnostic and prognostic value of cea, Ca19-9, afp and Ca125 for early gastric cancer. *BMC Cancer* (2017) 17(1):737. doi: 10.1186/s12885-017-3738-y

139. Moriyama J, Oshima Y, Nanami T, Suzuki T, Yajima S, Shiratori F, et al. Prognostic impact of Cea/Ca19-9 at the time of recurrence in patients with gastric cancer. *Surg Today* (2021) 51(10):1638–48. doi: 10.1007/s00595-021-02248-y

140. Kelleher M, Singh R, O'Driscoll CM, Melgar S. Carcinoembryonic antigen (Ceacam) family members and inflammatory bowel disease. *Cytokine Growth Factor Rev* (2019) 47:21–31. doi: 10.1016/j.cytogfr.2019.05.008

141. Bębnowska D, Grywalska E, Niedźwiedzka-Rystwej P, Sosnowska-Pasiarska B, Smok-Kalwat J, Pasiarski M, et al. Car-T cell therapy-an overview of targets in gastric cancer. *J Clin Med* (2020) 9(6):1894. doi: 10.3390/jcm9061894

142. Cruz RGB, Madden SF, Brennan K, Hopkins AM. A transcriptional link between Her2, jam-a and Foxa1 in breast cancer. *Cells* (2022) 11(4):735. doi: 10.3390/cells11040735

143. Zhou PH, Zheng JB, Wei GB, Wang XL, Wang W, Chen NZ, et al. Lentivirus-mediated Rassf1a expression suppresses aggressive phenotypes of gastric cancer cells *in vitro* and *in vivo*. *Gene Ther* (2015) 22(10):793–801. doi: 10.1038/gt.2015.49

144. Bockerstett KA, Lewis SA, Noto CN, Ford EL, Saenz JB, Jackson NM, et al. Single-cell transcriptional analyses identify lineage-specific epithelial responses to inflammation and metaplastic development in the gastric corpus. *Gastroenterology* (2020) 159(6):2116–29.e4. doi: 10.1053/j.gastro.2020.08.027

145. Qiu Q, Xu Z, Tian J, Moitra R, Gunti S, Notkins AL, et al. Impact of natural igm concentration on gene therapy with adenovirus type 5 vectors. *J Virol* (2015) 89(6):3412–6. doi: 10.1128/jvi.03217-14

146. Raftery MJ, Wolter E, Fillatreau S, Meisel H, Kaufmann SH, Schönrich G. Nkt cells determine titer and subtype profile of virus-specific igg antibodies during herpes simplex virus infection. *J Immunol* (2014) 192(9):4294–302. doi: 10.4049/jimmunol.1300148

147. Rangaswamy US, Cotter CR, Cheng X, Jin H, Chen Z. Cd55 is a key complement regulatory protein that counteracts complement-mediated inactivation of Newcastle disease virus. *J Gen Virol* (2016) 97(8):1765–70. doi: 10.1099/jgv.0.000498

148. Reale A, Calistri A, Altomonte J. Giving oncolytic viruses a free ride: Carrier cells for oncolytic virotherapy. *Pharmaceutics* (2021) 13(12):2192. doi: 10.3390/pharmaceutics13122192

149. Chastkofsky MI, Pituch KC, Katagi H, Zannikou M, Ilut L, Xiao T, et al. Mesenchymal stem cells successfully deliver oncolytic virotherapy to diffuse intrinsic pontine glioma. *Clin Cancer Res* (2021) 27(6):1766–77. doi: 10.1158/1078-0432.Ccr-20-1499

150. Eisenstein S, Coakley BA, Briley-Saebo K, Ma G, Chen HM, Meseck M, et al. Myeloid-derived suppressor cells as a vehicle for tumor-specific oncolytic viral therapy. *Cancer Res* (2013) 73(16):5003–15. doi: 10.1158/0008-5472.Can-12-1597

151. Laurenzana A, Margheri F, Chillà A, Biagioni A, Margheri G, Calorini L, et al. Endothelial progenitor cells as shuttle of anticancer agents. *Hum Gene Ther* (2016) 27(10):784–91. doi: 10.1089/hum.2016.066

152. Zhang Y, Wu J, Zhang H, Wei J, Wu J. Extracellular vesicles-mimetic encapsulation improves oncolytic viro-immunotherapy in tumors with low coxsackie and adenovirus receptor. *Front Bioeng Biotechnol* (2020) 8:574007. doi: 10.3389/fbioe.2020.574007

153. Doswald S, Stark WJ, Beck-Schimmer B. Biochemical functionality of magnetic particles as nanosensors: How far away are we to implement them into clinical practice? *J Nanobiotech* (2019) 17(1):73. doi: 10.1186/s12951-019-0506-y

154. Lin D, Feng X, Mai B, Li X, Wang F, Liu J, et al. Bacterial-based cancer therapy: An emerging toolbox for targeted Drug/Gene delivery. *Biomaterials* (2021) 277:121124. doi: 10.1016/j.biomaterials.2021.121124

155. Liu Z, Xie Z, Li W, Wu X, Jiang X, Li G, et al. Photodynamic immunotherapy of cancers based on nanotechnology: Recent advances and future challenges. *J Nanobiotech* (2021) 19(1):160. doi: 10.1186/s12951-021-00903-7

156. Yuan L, Xu ZY, Ruan SM, Mo S, Qin JJ, Cheng XD. Long non-coding rnas towards precision medicine in gastric cancer: Early diagnosis, treatment, and drug resistance. *Mol Cancer* (2020) 19(1):96. doi: 10.1186/s12943-020-01219-0

157. Li WQ, Qin XX, Li ZX, Wang LH, Liu ZC, Fan XH, et al. Beneficial effects of endoscopic screening on gastric cancer and optimal screening interval: A population-based study. *Endoscopy* (2022) 54(9):848–58. doi: 10.1055/a-1728-5673

158. Nagaya T, Okuyama S, Ogata F, Maruoka Y, Choyke PL, Kobayashi H. Near infrared photoimmunotherapy using a fiber optic diffuser for treating peritoneal gastric cancer dissemination. *Gastric Cancer* (2019) 22(3):463–72. doi: 10.1007/s10120-018-0871-5

159. Badgwell B, Das P, Ajani J. Treatment of localized gastric and gastroesophageal adenocarcinoma: The role of accurate staging and preoperative therapy. *J Hematol Oncol* (2017) 10(1):149. doi: 10.1186/s13045-017-0517-9

160. Gertsen EC, Brenkman HJF, van Hillegersberg R, van Sandick JW, van Berge Henegouwen MI, Gisbertz SS, et al. 18f-Fludeoxyglucose-Positron emission Tomography/Computed tomography and laparoscopy for staging of locally advanced gastric cancer: A multicenter prospective Dutch cohort study (Plastic). *JAMA Surg* (2021) 156(12):e215340. doi: 10.1001/jamasurg.2021.5340

161. Zhang Z, Yang A, Chaurasiya S, Park AK, Kim SI, Lu J, et al. Pet imaging and treatment of pancreatic cancer peritoneal carcinomatosis after subcutaneous intratumoral administration of a novel oncolytic virus, Cf33-Hnis-Antipdl1. *Mol Ther Oncolytics* (2022) 24:331–9. doi: 10.1016/j.omto.2021.12.022

162. Wang J, Arulanandam R, Wassenaar R, Falls T, Petryk J, Paget J, et al. Enhancing expression of functional human sodium iodide symporter and somatostatin receptor in recombinant oncolytic vaccinia virus for *in vivo* imaging of tumors. *J Nucl Med* (2017) 58(2):221–7. doi: 10.2967/jnumed.116.180463

163. Zhang Z, Huang Q, Yu L, Zhu D, Li Y, Xue Z, et al. The role of mirna in tumor immune escape and mirna-based therapeutic strategies. *Front Immunol* (2021) 12:807895. doi: 10.3389/fimmu.2021.807895

164. O'Donnell JS, Teng MWL, Smyth MJ. Cancer immunoediting and resistance to T cell-based immunotherapy. *Nat Rev Clin Oncol* (2019) 16(3):151–67. doi: 10.1038/s41571-018-0142-8

165. Kubli SP, Berger T, Araujo DV, Siu LL, Mak TW. Beyond immune checkpoint blockade: Emerging immunological strategies. *Nat Rev Drug Discovery* (2021) 20(12):899–919. doi: 10.1038/s41573-021-00155-y

166. Zhao L, Liu Y, Zhang S, Wei L, Cheng H, Wang J, et al. Impacts and mechanisms of metabolic reprogramming of tumor microenvironment for immunotherapy in gastric cancer. *Cell Death Dis* (2022) 13(4):378. doi: 10.1038/s41419-022-04821-w

167. Anderson NM, Simon MC. The tumor microenvironment. *Curr Biol* (2020) 30(16):R921–r5. doi: 10.1016/j.cub.2020.06.081

168. Kobayashi H, Enomoto A, Woods SL, Burt AD, Takahashi M, Worthley DL. Cancer-associated fibroblasts in gastrointestinal cancer. *Nat Rev Gastroenterol Hepatol* (2019) 16(5):282–95. doi: 10.1038/s41575-019-0115-0

169. Bae CA, Ham IH, Oh HJ, Lee D, Woo J, Son SY, et al. Inhibiting the Gas6/Axl axis suppresses tumor progression by blocking the interaction between cancer-associated fibroblasts and cancer cells in gastric carcinoma. *Gastric Cancer* (2020) 23(5):824–36. doi: 10.1007/s10120-020-01066-4

170. Hsu HP, Wang CY, Hsieh PY, Fang JH, Chen YL. Knockdown of Serine/Threonine-protein kinase 24 promotes tumorigenesis and myeloid-derived suppressor cell expansion in an orthotopic immunocompetent gastric cancer animal model. *J Cancer* (2020) 11(1):213–28. doi: 10.7150/jca.35821

171. Tu SP, Jin H, Shi JD, Zhu LM, Suo Y, Lu G, et al. Curcumin induces the differentiation of myeloid-derived suppressor cells and inhibits their interaction with cancer cells and related tumor growth. *Cancer Prev Res (Phila)* (2012) 5 (2):205–15. doi: 10.1158/1940-6207.Capr-11-0247

172. Qu Y, Wang X, Bai S, Niu L, Zhao G, Yao Y, et al. The effects of tnf-A/Tnfr2 in regulatory T cells on the microenvironment and progression of gastric cancer. *Int J Cancer* (2022) 150(8):1373–91. doi: 10.1002/ijc.33873

173. Zhang H, Li R, Cao Y, Gu Y, Lin C, Liu X, et al. Poor clinical outcomes and immunoevasive contexture in intratumoral il-10-Producing macrophages enriched gastric cancer patients. *Ann Surg* (2022) 275(4):e626–e35. doi: 10.1097/sla.0000000000004037

174. Zhu T, Hu Z, Wang Z, Ding H, Li R, Wang J, et al. Microrna-301b-3p from mesenchymal stem cells-derived extracellular vesicles inhibits txnip to promote multidrug resistance of gastric cancer cells. *Cell Biol Toxicol* (2022). doi: 10.1007/s10565-021-09675-0

175. Seyed-Khorrami SM, Soleimanjahi H, Soudi S, Habibian A. Mscs loaded with oncolytic reovirus: Migration and *in vivo* virus delivery potential for evaluating anti-cancer effect in tumor-bearing C57bl/6 mice. *Cancer Cell Int* (2021) 21(1):244. doi: 10.1186/s12935-021-01848-5

176. Freedman JD, Duffy MR, Lei-Rossmann J, Muntzer A, Scott EM, Hagel J, et al. An oncolytic virus expressing a T-cell engager simultaneously targets cancer and immunosuppressive stromal cells. *Cancer Res* (2018) 78(24):6852–65. doi: 10.1158/0008-5472.Can-18-1750

177. Li M, Li G, Kiyokawa J, Tirmizi Z, Richardson LG, Ning J, et al. Characterization and oncolytic virus targeting of fap-expressing tumor-associated pericytes in glioblastoma. *Acta Neuropathol Commun* (2020) 8(1):221. doi: 10.1186/s40478-020-01096-0

178. Martin NT, Bell JC. Oncolytic virus combination therapy: Killing one bird with two stones. *Mol Ther* (2018) 26(6):1414–22. doi: 10.1016/j.ymthe.2018.04.001

179. Shi T, Song X, Wang Y, Liu F, Wei J. Combining oncolytic viruses with cancer immunotherapy: Establishing a new generation of cancer treatment. *Front Immunol* (2020) 11:683. doi: 10.3389/fimmu.2020.00683

180. Zhu S, Zhang T, Zheng L, Liu H, Song W, Liu D, et al. Combination strategies to maximize the benefits of cancer immunotherapy. *J Hematol Oncol* (2021) 14(1):156. doi: 10.1186/s13045-021-01164-5

181. Witt RG, Erstad DJ, Wargo JA. Neoadjuvant therapy for melanoma: Rationale for neoadjuvant therapy and pivotal clinical trials. *Ther Adv Med Oncol* (2022) 14:17588359221083052. doi: 10.1177/17588359221083052

182. Zuo S, Wei M, He B, Chen A, Wang S, Kong L, et al. Enhanced antitumor efficacy of a novel oncolytic vaccinia virus encoding a fully monoclonal antibody against T-cell immunoglobulin and itim domain (Tigit). *EBioMedicine* (2021) 64:103240. doi: 10.1016/j.ebiom.2021.103240

183. Huinen ZR, Huijbers EJM, van Beijnum JR, Nowak-Sliwinska P, Griffioen AW. Anti-angiogenic agents - overcoming tumour endothelial cell anergy and improving immunotherapy outcomes. *Nat Rev Clin Oncol* (2021) 18(8):527–40. doi: 10.1038/s41571-021-00496-y

184. Rosenbaum SR, Wilski NA, Aplin AE. Fueling the fire: Inflammatory forms of cell death and implications for cancer immunotherapy. *Cancer Discovery* (2021) 11(2):266–81. doi: 10.1158/2159-8290.Cd-20-0805

185. Sivanandam V, LaRocca CJ, Chen NG, Fong Y, Warner SG. Oncolytic viruses and immune checkpoint inhibition: The best of both worlds. *Mol Ther Oncolytics* (2019) 13:93–106. doi: 10.1016/j.omto.2019.04.003

186. Kirtane K, Elmariah H. Chung CH, abate-daga d. adoptive cellular therapy in solid tumor malignancies: Review of the literature and challenges ahead. *J Immunother Cancer* (2021) 9(7):e002723. doi: 10.1136/jitc-2021-002723

187. Wing A, Fajardo CA, Posey ADJr., Shaw C, Da T, Young RM, et al. Improving cart-cell therapy of solid tumors with oncolytic virus-driven production of a bispecific T-cell engager. *Cancer Immunol Res* (2018) 6(5):605–16. doi: 10.1158/2326-6066.Cir-17-0314

188. Evgin L, Kottke T, Tonne J, Thompson J, Huff AL, van Vloten J, et al. Oncolytic virus-mediated expansion of dual-specific car T cells improves efficacy against solid tumors in mice. *Sci Transl Med* (2022) 14(640):eabn2231. doi: 10.1126/scitranslmed.abn2231

189. Aalipour A, Le Boeuf F, Tang M, Murty S, Simonetta F, Lozano AX, et al. Viral delivery of car targets to solid tumors enables effective cell therapy. *Mol Ther Oncolytics* (2020) 17:232–40. doi: 10.1016/j.omto.2020.03.018

190. Ma R, Lu T, Li Z, Teng KY, Mansour AG, Yu M, et al. An oncolytic virus expressing Il15/Il15rα combined with off-the-Shelf egfr-car nk cells targets glioblastoma. *Cancer Res* (2021) 81(13):3635–48. doi: 10.1158/0008-5472.Can-21-0035

191. Sakemura R, Hefazi M, Siegler EL, Cox MJ, Larson DP, Hansen MJ, et al. Targeting cancer-associated fibroblasts in the bone marrow prevents resistance to cart-cell therapy in multiple myeloma. *Blood* (2022) 139(26):3708–21. doi: 10.1182/blood.2021012811

frontiers | Frontiers in Oncology

TYPE Original Research
PUBLISHED 29 November 2022
DOI 10.3389/fonc.2022.1068183

Check for updates

OPEN ACCESS

EDITED BY
Zhendong Jin,
Second Military Medical University, China

REVIEWED BY
Bin Zhang,
The Affiliated Hospital of Xuzhou Medical University, China
Hafiz Abdul Waqas Ahmed,
Lady Reading Hospital, Pakistan

*CORRESPONDENCE
Zhenzhen Liu
liuzhenzhen.zzu.edu@aliyun.com

SPECIALTY SECTION
This article was submitted to Gastrointestinal Cancers: Gastric and Esophageal Cancers, a section of the journal Frontiers in Oncology

RECEIVED 12 October 2022
ACCEPTED 24 October 2022
PUBLISHED 29 November 2022

CITATION
Zhao F, Liu Z, Wei A, Wang W, Xu N and Pu X (2022) Efficacy and feasibility of snare-assisted endoscopic resection of small submucosal gastric tumors: A retrospective analysis. *Front. Oncol.* 12:1068183. doi: 10.3389/fonc.2022.1068183

COPYRIGHT
© 2022 Zhao, Liu, Wei, Wang, Xu and Pu. This is an open-access article distributed under the terms of the Creative Commons Attribution License (CC BY). The use, distribution or reproduction in other forums is permitted, provided the original author(s) and the copyright owner(s) are credited and that the original publication in this journal is cited, in accordance with accepted academic practice. No use, distribution or reproduction is permitted which does not comply with these terms.

Efficacy and feasibility of snare-assisted endoscopic resection of small submucosal gastric tumors: A retrospective analysis

Fei Zhao, Zhenzhen Liu*, Anwei Wei, Wei Wang, Na Xu and Xuanmei Pu

Endoscopic Diagnosis and Treatment Center, The Affiliated Cancer Hospital of Zhengzhou University and Henan Cancer Hospital, Zhengzhou, China

Background and aim: The prevalence of small submucosal gastric tumors is rising. Despite the fact that high success rate of endoscopic resection of small submucosal gastric tumors originating from the muscularis propria has been reported, the procedure is technically challenging and has a high rate of complications. In this study, we investigated the efficacy and feasibility of a novel snare-assisted endoscopic resection technique for small submucosal gastric tumors.

Patients and methods: This is a single-center consecutive study of 50 patients who were diagnosed with small submucosal gastric tumors originating from the muscularis propria and who subsequently underwent snare-assisted endoscopic resection between January 2019 and January 2021 at our hospital. Data on the demographic characteristics, procedural success rate, complications, recurrence rate, and histopathology of the resected specimen were collected and analyzed retrospectively.

Results: The majority of the patient's population was male (66%) with the mean age of 48.4 ± 9 years (range, 20–70 years). The mean size of the tumor confirmed by endoscopic ultrasonography was 6.4 ± 1.6 mm (range, 3.1–9.8 mm). All the tumors were resected successfully using snare-assisted endoscopic resection technique. The mean procedure time was 22.8 ± 9.6 (range, 15–35 min). The technical (performed the procedure successfully without converting to surgery) and clinical (the patient fully recovered after the procedure without experiencing any complications) success rate of the procedure was 100%. Eighteen (24%) patients had very small amount of mucosal damage, and wound closure was not needed in these patients. During 6–24 months of follow-up, no recurrence or metastasis occurred. No adverse event was noted during the follow-up time.

Conclusion: The novel approach of snare-assisted endoscopic resection is simple, feasible, and effective for tumors with small size and originating from the gastric muscularis propria. In addition, it offers a better alternative therapy for the complete resection of small submucosal gastric tumors. Its advantages

compared with traditional endoscopic approaches such as endoscopic submucosal resection and endoscopic submucosal dissection include shorter procedure times, lesser cost, and a lower rate of complications (perforation, bleeding, and infection).

KEYWORDS

gastrointestinal tumors, submucosal gastric tumors, small gastric tumors, endoscopic resection, snare resection

Introduction

Gastrointestinal small submucosal tumors are prevalent and most often detected in the gastric cavity and are thought to have a high risk of malignancy (1, 2). Small gastric submucosal tumors are typically found accidentally during the routine upper gastrointestinal endoscopic examination (3). They may be asymptomatic or occasionally manifest with vague gastrointestinal symptoms. Recent improvements in endoscopic ultrasonography and the widespread use of digestive endoscopy have improved the frequency of diagnosing smaller submucosal gastric tumors, including tumors with malignant potential such as gastrointestinal stromal tumors (1, 4).

Traditionally, small submucosal gastric tumors are managed with laparoscopic surgery (5). However, with the revolution in interventional endoscopy, minimally invasive endoscopic resection techniques have become very popular for the removal of these small submucosal gastric tumors in complete and en bloc resection manner (6, 7). At present, endoscopic mucosal resection (EMR), endoscopic submucosal dissection (ESD), submucosal tunneling endoscopic resection (STER), and endoscopic full thickness resection (EFR) are the main endoscopic methods available for the resections of gastrointestinal tumors (8–10). None are completely satisfactory in that en bloc resection for relatively larger tumors cannot be consistently guaranteed by EMR technique. On the other hand, ESD offers complete en bloc resection of the relatively large tumors and a precise pathological diagnosis, but it carries a risk of perforation, bleeding, and abdominal infection. It is also associated with longer operation time and usually can only be performed by an expert endoscopist (11, 12). Small submucosal gastric tumors arising from the muscularis propria have been reported to have high (up to 50%) perforation rate following endoscopic submucosal dissection (13). If curative therapy is delayed after a perforation, the patient may probably have hemorrhagic shock or even death afterwards.

For this reason, a safe, simple, less expensive technique that could significantly lower the procedure-related complications such as gastric perforation rate is preferred. In this study, we share our experience with a cutting edge endoscopic resection technique using snare assistance for small submucosal gastric tumors. The aim of the study was to investigate the efficacy and feasibly of the snare-assisted endoscopic resection technique, and we suggest that snare-assisted endoscopic resection will provide an improved and effective alternative approach for the management of small submucosal gastric tumors.

Material and methods

Patients

Between January 2019 and January 2021, a total of 50 consecutive patients with small submucosal gastric tumors (<2 cm) were treated with snare-assisted endoscopic resections at our hospital. All tumors were defined by endoscopic ultrasonography (EUS) or computed tomography (CT) before the endoscopic resection. This is a retrospective analysis of consecutive patients based on the following inclusion criteria: 1) presence of small submucosal gastric tumors originating from the muscularis propria layer of the stomach without any sign of ulceration, 2) tumor diameter no more than 2 cm as measured by EUS or CT, 3) no evidence of distant metastasis, 4) no lymph node involvement, and 5) patients only managed by snare-assisted endoscopic resection. Exclusion criteria were as follows: 1) tumor diameter larger than 2 cm, 2) patients with severe bleeding or coagulation disorders, 3) patients under age of 18 or older than 75, 4) patients unable to bear general anesthesia, and 4) patients who refused to give consent for the procedure. All the procedures were performed by gastroenterologists with experience of approximately 200–300 therapeutic endoscopic procedures such as ESD.

Definitions

The technical success rate was defined as when the procedure was successfully performed and completed without

converting to surgery. The clinical success rate was defined as when the patient fully recovered after the procedure without any complications. The procedure time was defined as the time from endoscope entry into the gastric cavity to remove the lesion out. En bloc/complete resection was defined as the successful resection of the tumor in one piece.

Procedure

All the procedures were performed under general anesthesia in the endoscopy center of our institution. Prior to the procedure, routine bowel preparations were performed, and gastric cleansing was done using a saline solution. For the main procedure, a single-channel flexible endoscope (EVIS GIF-Q260J, Olympus, Tokyo, Japan) with transparent cap (Olympus, Model No. D-201-11804) and a snare (Boston Scientific, Ref; M00562650) attached on the tip was inserted into the gastric cavity. The lesion was examined carefully and sucked into the transparent cap. The snare was then used to ligate the base of the tumor. To resect the lesion completely, the wire of the snare was loosened to grasp the lesion from the base and then tightened. The high-frequency current was used to resect the lesion in one piece (Figure 1; Infographics). Hemostasis was achieved using electrocoagulation forceps (ICC 200 EA INT; ERBE, Tübingen, Germany) in case of bleeding. Finally, two to three endoclips depending on the resection size were used to close the wound site. The resected specimen was sent to the lab for histopathological diagnosis.

Follow-up

All patients were followed up after the resection of their tumors for healing of the wound, complications, and recurrence of the tumor. During the follow-up period, patients were advised to visit the hospital for evaluation if any discomfort, such as abdominal pain or other general gastrointestinal symptoms, occurred. Endoscopic examination was performed to follow up all the patients who visited the hospital. However, for those patients who were unable to come in for follow-up visit, telephone interviews were conducted, and records of their post-procedure health including the results of their check-up at local hospitals were collected and analyzed. Forty-four (88%) patients were followed up successfully; however, we lost contact with eight (12%) patients during the follow up period.

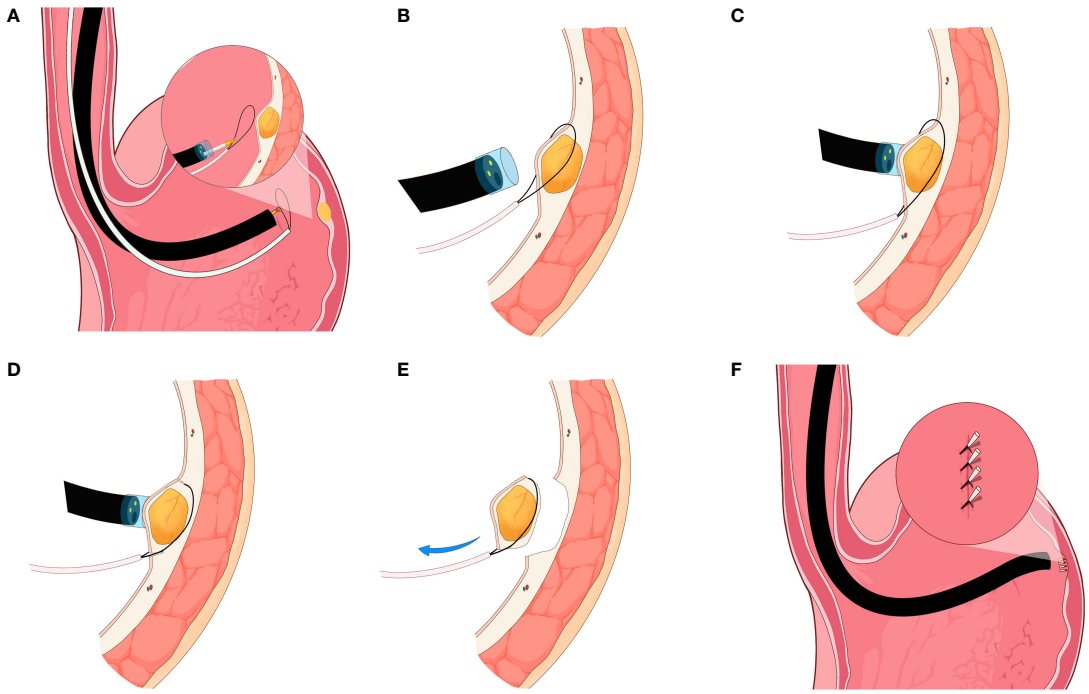

FIGURE 1
Infographics of snare-assisted endoscopic resection technique. **(A)** Endoscope attached with snare at the tip was inserted into the gastric cavity and view of the small submucosal gastric tumors. **(B)** Snare ligation around the base of the tumor. **(C)** Suction of the tumor into the transparent cap and snare tightening around the base of the tumor. **(D)** Complete resection of the small submucosal gastric tumors using snare assistance. **(E)** Resected tumor and view of the lesion resection site. **(F)** Endoscopic clipping to close the lesion resection site.

Results

This is a single-center analysis of 50 consecutive patients who were diagnosed with small submucosal gastric tumors and subsequently underwent snare-assisted endoscopic resection. The majority of the patient's population was male (66%) with the mean age of 48.4 ± 9 years (range, 20–70 years). The mean size of the tumor confirmed by endoscopic ultrasound was 6.4 ± 1.6 mm (range, 3.1–9.8 mm). The mean procedure time was 22.8 ± 9.6 (range, 15–35 min). In 47 (94%) patients, the procedure was completed in <25 min. The technical (performed the procedure successfully without converting to surgery) and clinical (the patient fully recovered after the procedure without experiencing any complications) success rate of the procedure was 100%. The endoscopic clipping to close the wound was required in 64% of the patients, and 24% patients had very small amount of mucosal damage during the procedure, in which wound closure was not needed in these patients.

Tumor location of the tumors were as follows: 25 (50%) in the body of the stomach, 22 (44%) in the fundus of the stomach near the cardia, and 3 (6%) were found in the antrum. During 6–24 months of follow up, no recurrence or metastasis was noted in any of the patient. No short- or long-term complication was observed in any of the patients. The most common tumor confirmed by histopathology examination was gastrointestinal stromal tumors (62%), leiomyoma (13%), schwannoma (4%), ectopic pancreas (4%), neurofibroma (2%), and neuroendocrine tumor (2%).

Discussion

During the routine upper gastrointestinal endoscopic examinations, a growing number of small submucosal gastric tumors, particularly those originating from the muscularis propria, are accidentally found (14). A variety of benign and malignant tumors, including gastrointestinal submucosal stromal tumors, leiomyoma, schwannoma, ectopic pancreas, neurofibroma, and neuroendocrine tumor are included in small submucosal gastric tumors (15). At present, the selection of which treatment strategy is used mainly depends on the tumor size. The American Society for Gastrointestinal Endoscopy (ASGE) guidelines in 2017 suggested endoscopic resection for tumors larger than 2 cm in size and periodic follow-up for tumors that are smaller than 2 cm in size and asymptomatic (15, 16). Contrarily, a number of recent studies suggested that small submucosal gastric tumors of smaller than 2 cm in size should also be resected endoscopically because they might be malignant.

There are several traditional endoscopic resection methods available for the resection of small submucosal gastric tumors such as EMR, ESD, and STER. However, EMR cannot perform complete en bloc resection of the lesion, and ESDs are crippled with serval complications such as perforations, bleeding, and infections (17–21). Therefore, a variety of advancements have been made in endoscopic resection techniques to reduce the complications rate and to prevent conversion rate to laparoscopic or open surgery during the procedure (22–24). In this study, we introduced a cutting edge snare-assisted endoscopic resection for small submucosal gastric tumors. The snare-assisted resection technique has several advantages over the traditional endoscopic resection techniques: (1) clear view of the dissection plane; (2) less procedure time; (3) lower cost; (4) reduced intra- and post-procedural complication rate (e.g., less bleeding); (5) shorter hospital stay duration and quick recovery after the procedure; (6) wound closure not necessary after the resection for tumors <1 cm in size; (7) stronger traction force for small submucosal gastric tumors, which is crucial for complete and smooth dissection of the tumor; and (8) endoscopic resection of small tumors using a snare assistance easy to master and perform.

As noted above, the snare-assisted resection method seems to be very crucial for the prompt removal of small submucosal gastric tumors, as the timely resection of these tumors reduces the patient's psychological stress and eliminates non-specific gastrointestinal symptoms. Therefore, this is an appropriate option for patients with small submucosal gastric tumors who choose to have their small gastric tumors removed rather than being followed up. Our study, to best of our knowledge, is the largest to assess the efficacy and feasibility of novel snare-assisted endoscopic resection of small submucosal gastric tumors arising from the muscularis propria layer of the stomach.

Nonetheless, the snare-assisted endoscopic resection method has several limitations/disadvantages: (1) tumors located in the gastric cardia cannot be effectively resected with the assistance of a snare, as there is limited space for the lesion resection and removal; (2) tumors larger than 2 cm cannot be dissected; (3) complications cannot be completely avoided as it still carries the risk of perforation, although it is very rare; and (4) dissection of gastric small submucosal gastric tumors with a wide base may cause a wide defect in the gastric wall, which may lead to bleeding and perforations.

This study has several limitations including single-center analysis, retrospective design of the study, small sample size, and absence of control group. Further studies especially prospective clinical trials comparing snare-assisted resection with the traditional endoscopic resection are needed before the final recommendations are made on the efficacy and feasibility of snare-assisted endoscopic resection technique.

Conclusion

Although traditional therapeutic endoscopic techniques such as EMR, ESD, STER, and EFTR are efficient and

frequently used for the resection of relatively larger size tumors, an alternative method that shortens surgery time, is affordable, has fewer complications, shortens hospital stay duration, results in fast patient recovery after the procedure, and is easy to perform would be desirable. This is an effective and feasible technique that has clinical success rates that are at par with or higher than those of other endoscopic resection methods (e.g., EMR and ESD). Further prospective multi-centered randomized-controlled studies are needed.

Data availability statement

The raw data supporting the conclusions of this article will be made available by the authors, without undue reservation.

Ethics statement

The studies involving human participants were reviewed and approved by The Affiliated Cancer Hospital of Zhengzhou University and Henan Cancer Hospital, Zhengzhou. The patients/participants provided their written informed consent to participate in this study.

Author contributions

Study Concept and Design: FZ, ZL. Manuscript Writing: FZ, ZL, AW, WW, NX, XP. Collection of Data and Data Analysis: AW, WW, NX, XP. Critical revision of the Manuscript: FZ, ZL. All authors contributed to the article and approved the submitted version.

Conflict of interest

The authors declare that the research was conducted in the absence of any commercial or financial relationships that could be construed as a potential conflict of interest.

Publisher's note

All claims expressed in this article are solely those of the authors and do not necessarily represent those of their affiliated organizations, or those of the publisher, the editors and the reviewers. Any product that may be evaluated in this article, or claim that may be made by its manufacturer, is not guaranteed or endorsed by the publisher.

References

1. Nishida T, Goto O, Raut CP, Yahagi N. Diagnostic and treatment strategy for small gastrointestinal stromal tumors. *Cancer* (2016) 122(20):3110–8. doi: 10.1002/cncr.30239

2. Adachi A, Hirata Y, Kawamura H, Harada T, Hattori R, Kumai D, et al. Efficacy of mucosal cutting biopsy for the histopathological diagnosis of gastric submucosal tumors. *Case Rep Gastroenterol* (2019) 13(1):185–94. doi: 10.1159/000499442

3. Kadkhodayan K, Rafiq E, Hawes RH. Endoscopic evaluation and management of gastric stromal tumors. *Curr Treat Options Gastroenterol* (2017) 15(4):691–700. doi: 10.1007/s11938-017-0160-0

4. Nishida T, Kawai N, Yamaguchi S, Nishida Y. Submucosal tumors: comprehensive guide for the diagnosis and therapy of gastrointestinal submucosal tumors. *Dig Endosc.* (2013) 25(5):479–89. doi: 10.1111/den.12149

5. Conrad C, Nedelcu M, Ogiso S, Aloia TA, Vauthey JN, Gayet B. Laparoscopic intragastric surgery for early gastric cancer and gastrointestinal stromal tumors. *Ann Surg Oncol* (2014) 21(8):2620. doi: 10.1245/s10434-013-3432-5

6. Zhang Y, Ye LP, Mao XL. Endoscopic treatments for small gastric subepithelial tumors originating from muscularis propria layer. *World J Gastroenterol* (2015) 21(32):9503–11. doi: 10.3748/wjg.v21.i32.9503

7. Zhu L, Khan S, Hui Y, Zhao J, Li B, Ma S, et al. Treatment recommendations for small gastric gastrointestinal stromal tumors: positive endoscopic resection. *Scand J Gastroenterol* (2019) 54(3):297–302. doi: 10.1080/00365521.2019

8. Nishizawa T, Yahagi N. Endoscopic mucosal resection and endoscopic submucosal dissection: technique and new directions. *Curr Opin Gastroenterol* (2017) 33(5):315–9. doi: 10.1097/MOG.0000000000000388

9. Schmidt A, Bauder M, Riecken B, von Renteln D, Muehleisen H, Caca K. Endoscopic full-thickness resection of gastric subepithelial tumors: a single-center series. *Endoscopy* (2015) 47(2):154–8. doi: 10.1055/s-0034-1390786

10. Ge N, Hu JL, Yang F, Yang F, Sun SY. Endoscopic full-thickness resection for treating small tumors originating from the muscularis propria in the gastric fundus: An improvement in technique over 15 years. *World J Gastrointest Oncol* (2019) 11(11):1054–64. doi: 10.4251/wjo.v11.i11.1054

11. Li P, Li S, Liu S, Zhang D. Risk factors for complications of therapeutic endoscopy for upper gastrointestinal subepithelial lesions. Zhong Nan Da Xue Xue Bao Yi Xue Ban. *English, Chinese* (2021) 46(3):278–82. doi: 10.11817/j.issn.1672-7347.2021

12. Natsagdorj E, Kim SG, Choi J, Kang S, Kim B, Lee E, et al. Clinical outcomes of endoscopic submucosal dissection for early gastric cancer in patients with comorbidities. *J Gastric Cancer.* (2021) 21(3):258–67. doi: 10.5230/jgc.2021.21.e25

13. Li S, Liang X, Zhang B, Tao X, Deng L. Novel endoscopic management for small gastric submucosal tumors: A single-center experience (with video). *Dig Liver Dis* (2021) 53(7):895–9. doi: 10.1016/j.dld.2021.02.014

14. Pimentel-Nunes P, Libânio D, Bastiaansen BAJ, Bhandari P, Bisschops R, Bourke MJ, et al. Endoscopic submucosal dissection for superficial gastrointestinal lesions: European society of gastrointestinal endoscopy (ESGE) guideline - update 2022. *Endoscopy* (2022) 54(6):591–622. doi: 10.1055/a-1811-7025

15. Esaki M, Ihara E, Gotoda T. Endoscopic instruments and techniques in endoscopic submucosal dissection for early gastric cancer. *Expert Rev Gastroenterol Hepatol* (2021) 15(9):1009–20. doi: 10.1080/17474124.2021.1924056

16. Akahoshi K, Oya M, Koga T, Shiratsuchi Y. Current clinical management of gastrointestinal stromal tumor. *World J Gastroenterol* (2018) 24(26):2806–17. doi: 10.3748/wjg.v24.i26.2806

17. Kahoshi K, Oya M, Koga T, Koga H, Motomura Y, Kubokawa M, et al. Clinical usefulness of endoscopic ultrasound-guided fine needle aspiration for gastric subepithelial lesions smaller than 2 cm. *J Gastrointestin Liver Dis* (2014) 23(4):405–12. doi: 10.15403/jgld.2014.1121.234.eug

18. Ye LP, Zhang Y, Mao XL, Zhu LH, Zhou X, Chen JY. Submucosal tunneling endoscopic resection for small upper gastrointestinal subepithelial tumors originating from the muscularis propria layer. *Surg Endosc.* (2014) 28(2):524–30. doi: 10.1007/s00464-013-3197-8

19. Cai MY, Zhu BQ, Xu MD, Qin WZ, Zhang YQ, Chen WF, et al. Submucosal tunnel endoscopic resection for extraluminal tumors: a novel endoscopic method for en bloc resection of predominant extraluminal growing subepithelial tumors or extra-gastrointestinal tumors (with videos). *Gastrointest Endosc.* (2018) 88(1):160–7. doi: 10.1016/j.gie.2018.02.032

20. Cai MY, Martin Carreras-Presas F, Zhou PH. Endoscopic full-thickness resection for gastrointestinal submucosal tumors. *Dig Endosc.* (2018) Suppl 1:17–24. doi: 10.1111/den.13003

21. Li B, Chen T, Qi ZP, Yao LQ, Xu MD, Shi Q, et al. Efficacy and safety of endoscopic resection for small submucosal tumors originating from the muscularis propria layer in the gastric fundus. *Surg Endosc.* (2019) 33(8):2553–61. doi: 10.1007/s00464-018-6549-6

22. Zhang Q, Cai JQ, Wang Z. Usefulness of tumor traction with a snare and endoclips in gastric submucosal tumor resection: a propensity-score-matching analysis. *Gastroenterol Rep (Oxf).* (2020) 9(2):125–32. doi: 10.1093/gastro/goaa050

23. Zhang Q, Lian ZY, Cai JQ, Bai Y, Wang Z. Safety and effectiveness of mucosal traction using a snare combined with endoclips to assist the resection of esophageal intraepithelial neoplasia: a propensity score matching analysis. *Dis Esophagus* (2022) 35(1):doab018. doi: 10.1093/dote/doab018

24. Zhang Q, Cai JQ, Wang Z, Xiao B, Bai Y. Snare combined with endoscopic clips in endoscopic resection of gastric submucosal tumor: a method of tumor traction. *Endosc Int Open* (2019) 7(9):E1150–62. doi: 10.1055/a-0849-9625

frontiers | Frontiers in Oncology

TYPE Original Research
PUBLISHED 08 December 2022
DOI 10.3389/fonc.2022.986762

Check for updates

OPEN ACCESS

EDITED BY
Zhendong Jin,
Second Military Medical University, China

REVIEWED BY
Antonino Maniaci,
University of Catania, Italy
Maikel Peppelenbosch,
Erasmus Medical Center, Netherlands

*CORRESPONDENCE
Ying He
heying2478@163.com
Ruijia Chen
ruijiachen503@163.com

†These authors have contributed equally to this work

SPECIALTY SECTION
This article was submitted to Gastrointestinal Cancers: Gastric and Esophageal Cancers, a section of the journal Frontiers in Oncology

RECEIVED 05 July 2022
ACCEPTED 15 November 2022
PUBLISHED 08 December 2022

CITATION
You M, Huang Y, Cai Z, Wu Q, Zhu W, He Y and Chen R (2022) Cost-effectiveness analysis of sintilimab plus chemotherapy for advanced or metastatic esophageal squamous cell carcinoma.
Front. Oncol. 12:986762.
doi: 10.3389/fonc.2022.986762

COPYRIGHT
© 2022 You, Huang, Cai, Wu, Zhu, He and Chen. This is an open-access article distributed under the terms of the Creative Commons Attribution License (CC BY). The use, distribution or reproduction in other forums is permitted, provided the original author (s) and the copyright owner(s) are credited and that the original publication in this journal is cited, in accordance with accepted academic practice. No use, distribution or reproduction is permitted which does not comply with these terms.

Cost-effectiveness analysis of sintilimab plus chemotherapy for advanced or metastatic esophageal squamous cell carcinoma

Maojin You[1†], Yufan Huang[1†], Zhongjie Cai[1], Qingfeng Wu[1], Wei Zhu[1], Ying He[2*] and Ruijia Chen[3*]

[1]Department of Pharmacy, Mindong Hospital Affiliated to Fujian Medical University, Ningde, Fujian, China, [2]Department of Emergency Medicine, Mindong Hospital Affiliated to Fujian Medical University, Ningde, Fujian, China, [3]Department of Pharmacy, Mengchao Hepatobiliary Hospital of Fujian Medical University, Fuzhou, Fujian, China

Background: Sintilimab plus chemotherapy (SIDCHM) is more effective than placebo plus chemotherapy (PLCHM) for advanced or metastatic esophageal squamous cell carcinoma (ESCC). However, considering the high cost of sintilimab, this study evaluated the cost-effectiveness of SIDCHM in comparison with PLCHM for advanced or metastatic ESCC from the Chinese healthcare system perspective.

Methods: Polymorphic Markov models were constructed to simulate the course and cost of SIDCHM. Treatment drug costs were calculated at national list prices and clinical data, other costs, and utility values were extracted from the reference literature. Primary outcomes included quality-adjusted life-years (QALYs) and incremental cost-effectiveness ratios (ICERs). The robustness of the model was verified by one-way sensitivity analysis and probabilistic sensitivity analysis (PSA).

Results: SIDCHM obtained 1.03 QALYs at $24,044.49, whereas the effectiveness and cost of PLCHM were 0.67 QALYs and $14,166.24, respectively. The ICER for SIDCHM versus PLCHM was $23,458.08/QALY. The utility of the PFS state was the parameter that had the greatest effect on the ICER. The PSA showed that SIDCHM had an 86% probability of being cost-effective at the willingness-to-pay threshold of 3* Chinese gross domestic product per capita ($37,653/QALY).

Conclusion: From the Chinese healthcare system perspective, SIDCHM is considered a cost-effective treatment option compared with PLCHM as first-line therapy for advanced or metastatic ESCC.

KEYWORDS

cost-effectiveness, sintilimab plus chemotherapy, esophageal squamous cell carcinoma, first-line treatment, placebo plus chemotherapy

Introduction

Esophageal cancer (EC) is one of the most frequently occurring malignancies of the digestive tract, ranking seventh in the incidence of malignant tumors worldwide; it is also a very aggressive and lethal disease (1, 2). In the histological subtype, the most common EC is squamous cell carcinoma (2), and the rate of esophageal squamous cell carcinoma (ESCC) is high in China, accounting for more than half of all patients with ESCC worldwide (3). Platinum drugs in combination with fluorouracil or paclitaxel are recommended as a standard first-line therapy currently for advanced or metastatic ESCC (4). In China, platinum plus paclitaxel is generally used, and platinum plus fluorouracil was chosen in preference in other countries (5). However, the median survival of patients with ESCC treated with standard first-line therapy is only 7.0–13.0 months, with very unsatisfactory results (6). The development of new therapy protocols for patients with advanced or metastatic ESCC, as a result, is an urgent matter.

Immune checkpoint inhibitor (ICI) which enhances the antitumor activity of T cells by blocking the programmed cell death protein 1 (PD-1) or cytotoxic T lymphocyte antigen 4 (CTLA-4) pathways, has shown breakthroughs in cancer therapy and has been effective in the treatment of EC in recent years (7, 8). The outcome of the phase II study by Xu et al. showed that the PD-1 inhibitor sintilimab significantly improved the overall survival of patients with advanced or metastatic ESCC after first-line chemotherapy compared to chemotherapy (9). A recent investigational phase III clinical study (ORIENT-15) evaluated the effect of sintilimab or placebo in combined chemotherapy (cisplatin plus paclitaxel or fluorouracil) as first-line therapy for unresectable locally advanced, recurrent, or metastatic ESCC. Sintilimab plus chemotherapy (SIDCHM) showed encouraging results with significant advantages in overall survival (OS, 16.7 vs 12.5 months, $P < 0.001$) and progression-free survival (PFS, 7.2 vs 5.7 months, $P < 0.001$) in comparison with placebo plus chemotherapy (PLCHM) (5).

Despite the significant advantages of sintilimab in the treatment of advanced or metastatic ESCC, we cannot ignore its high costs. Therefore, an economic evaluation of SIDCHM as a first-line treatment for advanced or metastatic ESCC based on the ORIENT-15 trial from the Chinese healthcare system perspective was designed.

Methods

Model structure

A Markov model was constructed to simulate the cost and effectiveness of SIDCHM, compared with PLCHM, as treatment in the first line for patients with advanced or metastatic ESCC in China. TreeAge Pro 2022 (TreeAge Software, LLC, USA) was used to develop the model and the R software (version 4.2.0) program was used for statistical analyses. Kaplan–Meier survival curves were numerically digitized to select the best-fit survival distribution. Finally, the Weibull survival distribution was used to generate the probability of metastasis for SIDCHM and PLCHM (Table 1). The model comprised three mutually exclusive health states: PFS, progressive disease (PD), and death (Figure 1) and has a run time of approximately 6 years (to be determined by the time at which 99% of the patients are assumed to die), and each cycle is 21 days long in this model. Through each cycle, patients either hold their assigned health status or advance to new health status and are not allowed to revert to their former health status. The background mortality rate in a Chinese context (10) was also calculated in the model. The output data we eventually had from the model was the total cost, quality-adjusted life-year (QALY), and incremental cost-effectiveness ratio (ICER). We set the willingness-to-pay (WTP) threshold at $37,653 (three times China's GDP in 2021 per capita), as recommended by the World Health Organization, and consider the treatment option cost-effective if the ICER is below our predefined WTP threshold.

Clinical data

Data on the clinical efficacy and adverse events were obtained from the ORIENT-15 trial (5). The trial screened patients of ESCC (Their inclusivity criteria were age≥18 years with histologically unresectable locally regionally advanced, recurrent, or metastatic ESCC; unsuitable for curative surgery or definitive concurrent chemoradiotherapy; no prior history of systemic therapy, etc.) and then randomized eligible ones to either the SIDCHM group or the PLCHM group. Sintilimab or placebo was administered per cycle (21 days) until disease progression or unacceptable toxicity developed. Chemotherapy drugs (cisplatin plus paclitaxel or fluorouracil) were also given once every 21 days, that is, cisplatin at 75 mg/m^2 per cycle, paclitaxel at 175 mg/m^2 per cycle, or fluorouracil at 800 mg/m^2 per cycle. Chemotherapy was provided for up to six cycles; thereafter, treatment was continued with sintilimab or placebo until disease progression or unendurable toxicity. Sintilimab or placebo lasted for a maximum of 24 months. If chemotherapy is not resistible, sintilimab or placebo was provided. Chemotherapy (cisplatin plus paclitaxel or fluorouracil) was not convertible during the study. We assumed that patients of the SIDCHM group received 200 mg of sintilimab and that patients in both arms received the best supportive care (BSC) after disease progression occurs.

Costs and utilities

We have only calculated direct medical costs, including costs of drugs, tests (e.g., laboratory tests and radiological tests),

TABLE 1 Relevant parameters of survival distribution.

Parameters	Value	Source
Weibull survival model of PFS		
SIDCHM	Scale = 0.039683, Shape = 1.101677	(5)
PLCHM	Scale = 0.031633, Shape = 1.437746	(5)
Weibull survival model of OS		
SIDCHM	Scale = 0.010568, Shape = 1.284650	(5)
PLCHM	Scale = 0.010993, Shape = 1.4354050	(5)

OS, overall survival; PFS, progression-free survival; PLCHM, placebo plus chemotherapy; SIDCHM, sintilimab plus chemotherapy.

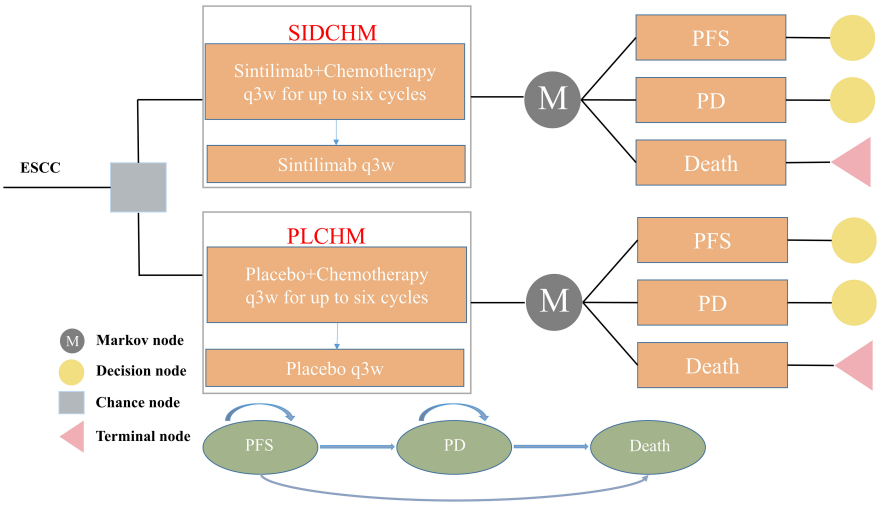

FIGURE 1
The Markov model simulates outcomes for the ORIENT-15 trial. All patients with ESCC started with PFS state and received treatment with SIDCHM or PLCHM. ESCC, esophageal squamous cell carcinoma; PD, progressive disease; PFS, progression-free survival; PLCHM, placebo plus chemotherapy; SIDCHM, sintilimab plus chemotherapy.

follow-up, end-of-life care, management of adverse events of severe grade >3, and BSC. Drug costs were based on national tender prices, and other costs were based on published publications. Prices were adjusted to 2021 prices using the China Statistics Bureau Medical Price Index. All costs were expressed in dollars and converted at the average of the 2021 exchange rate (1 dollar = 6.45 RMB). The utility values for PD and PFS were taken from the published literature (11) as there were no relevant quality-of-life data from the ORIENT-15 trial. Costs and utilities were discounted, and the discounted value was 3% per year.

Sensitivity analysis

To examine the robustness of the model, this study provides a sensitivity analysis of our model, including one-way sensitivity analysis and probabilistic sensitivity analysis (PSA). We adjusted all of the variables up or down within a specified range to establish the most economically influential parameters for the one-way sensitivity analysis. The final results were represented as a Tornado diagram. The maximum and minimum values of these variables were extracted from the literature, and in the presence of missing data the base value of ±20% was used, and the discount rate was used as the lower and upper limits of 0 and 5%, respectively (Table 2). The PSA was used to verify the effect of the factors on the uncertainty of the results, and we performed 1000 replications of Monte Carlo simulations with all parameters assigned with the distribution appropriate in the model (Table 2). The results were expressed as a probabilistic scatter plot and cost-effectiveness acceptability curves.

Subgroup analysis

We performed subgroup analyses of all patients by using subgroup-specific hazard ratios reported from the ORIENT-15 trial (5) based on the method of Hoyle et al. (18).

TABLE 2 The basic parameters of the input model and the range of sensitivity analyses.

Variables	Base value	Range		Distribution	Source
		Min	Max		
SIDCHM: incidence of AEs					
Anemia	0.125	0.100	0.150	Beta	(5)
Leukopenia	0.174	0.139	0.209	Beta	(5)
Nausea\vomiting	0.043	0.034	0.052	Beta	(5)
Neutropenia	0.300	0.240	0.360	Beta	(5)
Asthenia\decreased appetite	0.040	0.032	0.048	Beta	(5)
Thrombocytopenia	0.028	0.022	0.034	Beta	(5)
Febrile neutropenia	0.024	0.019	0.029	Beta	(5)
PLCHM: incidence of AEs					
Anemia	0.102	0.082	0.122	Beta	(5)
Leukopenia	0.223	0.178	0.268	Beta	(5)
Nausea\vomiting	0.033	0.026	0.040	Beta	(5)
Neutropenia	0.337	0.270	0.404	Beta	(5)
Asthenia\decreased appetite	0.045	0.036	0.054	Beta	(5)
Thrombocytopenia	0.030	0.024	0.036	Beta	(5)
Febrile neutropenia	0.018	0.014	0.022	Beta	(5)
Costs ($)					
Anemia	510.23	408.18	612.28	Gamma	(11)
Leukopenia	467.86	374.29	561.43	Gamma	(11)
Nausea\vomiting	49.42	39.54	59.30	Gamma	(12)
Neutropenia	84.21	67.37	101.05	Gamma	(12)
Asthenia\ decreased appetite	126.84	101.47	152.21	Gamma	(13)
Thrombocytopenia	1058.22	846.58	1269.86	Gamma	(14)
Febrile neutropenia	997.41	797.93	1196.89	Gamma	(15)
Paclitaxel (100 mg)	117.83	94.26	141.40	Gamma	#
Cisplatin (100 mg)	11.63	9.30	13.96	Gamma	#
Fluorouracil (100 mg)	1.86	1.49	2.23	Gamma	#
Sintilimab (100 mg)	167.44	133.95	200.93	Gamma	#
Routine follow-up cost per cycle	73.86	59.09	88.64	Gamma	(11)
Cost of laboratory tests and radiological examinations	358.03	286.42	429.63	Gamma	(11)
Cost of end-of-life care	1831.90	1465.52	2198.28	Gamma	(16)
Cost of best supportive care	167.96	134.37	201.55	Gamma	(11)
Utility value					
PFS	0.68	0.54	0.82	Beta	(11)
PD	0.42	0.34	0.50	Beta	(11)
Proportion					
Receiving cisplatin plus paclitaxel	0.93	0.74	1.12	Beta	(5)
Receiving cisplatin plus fluorouracil	0.07	0.056	0.084	Beta	(5)
Body surface area (m^2)	1.72	1.38	2.06	Normal	(11)
Discount rate (%)	3	0	5	Fixed	(17)

#, hospital charges; AE, adverse event; PD, progressive disease; PFS, progression-free survival; PLCHM, placebo plus chemotherapy; SIDCHM, sintilimab plus chemotherapy.

Results

Base-case analysis

The base case showed that the SIDCHM group achieved 1.03 QALYs at $24,044.49. The effectiveness was 0.67 QALYs at $14,166.24 in the PLCHM group. The incremental effect and cost of SIDCHM compared with PLCHM were 0.36 QALYs and $9878.25, respectively. The ICER for SIDCHM compared with PLCHM was $23458.08/QALY (Table 3). In China, SIDCHM is a cost-effective treatment strategy compared to PLCHM when the cost-effectiveness WTP threshold is $37,653/QALY.

TABLE 3 Effectiveness and costs in the model.

Regimen	PLCHM	SIDCHM	Incremental
Total QALYs	0.67	1.03	0.36
Total cost, $	14166.24	24044.49	9878.25
ICER, $			
Per QALY			23458.08

ICER, incremental cost-effectiveness ratio; PLCHM, placebo plus chemotherapy; QALY, quality-adjusted life year; SIDCHM, sintilimab plus chemotherapy.

Sensitivity analysis

In the one-way sensitivity analysis, results were presented in a Tornado diagram (Figure 2). The utility value of PFS and the cost of sintilimab (100 mg) had the most important influences on the results of the model, and the parameters that had relatively minor effects on the model were the cost of laboratory tests and radiological examinations, the utility value of PD, cost of follow-up, etc. However, even if the values of these variables were changed, the ICER was always below our predefined WTP threshold. The results of the PSA are expressed as a probabilistic scatter plot (Figure 3) and cost-effectiveness acceptance curve (Figure 4), with an 86% probability that the SIDCHM group was cost-effective compared with the PLCHM group when the WTP threshold was $37,653.

Subgroup analysis

For most subgroups, the ICER of SIDCHM compared with PLCHM was less than the WTP threshold of $37653/QALY, ranging from $26751.55/QALY (probabilities of cost-effectiveness, 87.1%) in patients with age ≥50 years to $335806.56/QALY (probabilities of cost-effectiveness, 53.6%) in patients with Eastern Cooperative Oncology Group performance status =0 (Table 4). Only in the subgroup of patients with programmed cell death ligand 1 expression (CPS)<1, the ICER of SIDCHM compared with PLCHM was higher than the WTP threshold of $37653/QALY (Table 4).

Discussion

In China, EC is the fourth most frequent cause of cancer death and the sixth most prevalent type of cancer, with 300,000 deaths and approximately 320,000 new cases in 2020 (19). ESCC histologically is more prevalent in China, accounting for 90% of all EC cases (20, 21). Palliative chemotherapy as first-line therapy for advanced or metastatic ESCC not only has a restricted survival advantage but also has a poor prognosis and a high number of adverse effects. ICI can significantly improve survival duration and quality of living in a variety of cancers through the inhibition of CTLA-4 or PD-1 pathways (22, 23). ICI plus chemotherapy has become the standard first-line therapeutic option for advanced or metastatic ESCC according to the 2022 guideline for EC treatment (24). Paclitaxel plus cisplatin in combination with camrelizumab is the first-line therapy choice for advanced or metastatic ESCC. The cisplatin plus fluorouracil chemotherapy regimen is combined with pembrolizumab as the first-line treatment for advanced or metastatic EC. Thus far, to the best of our knowledge, only two economic evaluations of camrelizumab or pembrolizumab plus chemotherapy as a first-line treatment option compared with chemotherapy alone for advanced or metastatic EC have been conducted, but neither is cost-effective

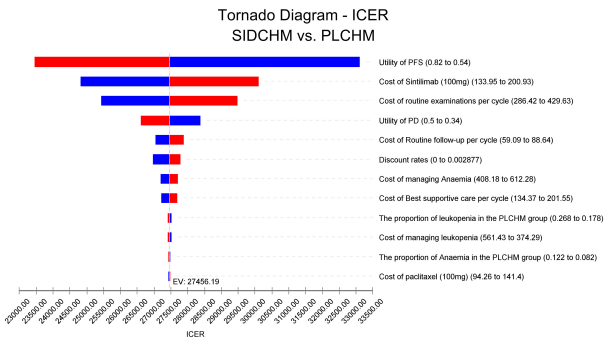

FIGURE 2
One-way sensitivity analyses of SIDCHM in comparison with PLCHM in China. BSA, body surface area; PD, progressive disease; PFS, progression-free survival; PLCHM, placebo plus chemotherapy; SIDCHM, sintilimab plus chemotherapy7.

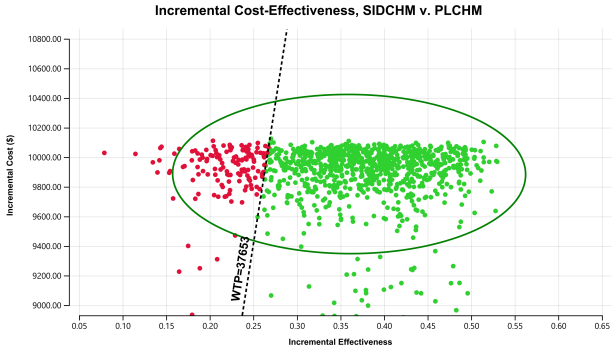

FIGURE 3
A probabilistic scatter plot of the ICER between the SIDCHM group and the PLCHM group. Each point means the ICER for 1 simulation. Ellipses are used to indicate 95% confidence intervals. Points that lie below the ICER threshold represent cost-effective simulations. ICER, incremental cost-effectiveness ratio; PLCHM, placebo plus chemotherapy; SIDCHM, sintilimab plus chemotherapy; WTP, willingness-to-pay.

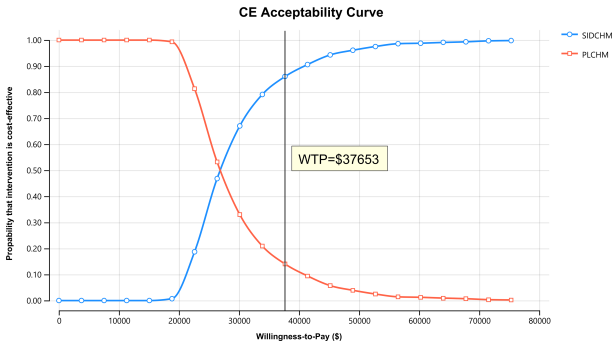

FIGURE 4
The cost-effectiveness acceptability curves for the SIDCHM treatment option compared to the PLCHM treatment option. PLCHM, placebo plus chemotherapy; QALY, quality-adjusted life year; SIDCHM, sintilimab plus chemotherapy; WTP, willingness-to-pay.

(11, 25). From a Chinese healthcare system perspective, Zhang et al. concluded that the probability of camrelizumab in addition to chemotherapy being cost-effective as a first-line treatment option for advanced or metastatic ESCC was lower than about 1% when compared with conventional chemotherapy at a cost-effectiveness threshold of $31,498.70, and the factor that had the greatest impact on the ICER was the cost of 200 mg of camrelizumab (11). The results of the economics study by Zhu et al. revealed that the first-line regimen of pembrolizumab plus fluorouracil and cisplatin for EC may not be as cost-effective as fluorouracil and cisplatin from a Chinese economic perspective, and the sensitivity analysis found that the price effect of pembrolizumab was the greatest (25). The high price of ICI will be a major constraint in making it a cost-effective solution. Therefore, searching for an ICI that is less expensive and has good results in treating advanced or metastatic ESCC is essential. Sintilimab is an ICI Self-developed in China and has a significant price advantage over other ICIs imported abroad. More promisingly, in the ORIENT-15 study, Lu et al. used SIDCHM for the first time to treat advanced or metastatic ESCC and showed that compared to chemotherapy, SIDCHM provided significantly better survival outcomes to patients with advanced or metastatic ESCC, with relative increases in median survival and PFS of 33.6% and 26.3%, respectively, with no obvious differences found in the incidence of adverse events (5). Undeniably, sintilimab may be an important option for immunotherapy in advanced or metastatic ESCC. However, the price of sintilimab is still high compared with chemotherapy, which may significantly increase healthcare expenditures, and previous economic analyses regarding the first-line treatment of advanced or metastatic ESCC with ICI have not been cost-effective from the Chinese healthcare system perspective (11, 25). Therefore, a cost-benefit analysis of sintilimab for advanced or metastatic ESCC is imperative.

Based on the ORIENT-15 trial (5), our economic analysis showed that compared with that of PLCHM, the ICER of SIDCHM as first-line therapy for advanced or metastatic ESCC

10.3389/fonc.2022.986762

TABLE 4 Results of subgroup analyses.

Subgroup	OS HR (95% CI)	PFS HR (95% CI)	ICER ($/QALY)	Cost-effectiveness probability (%)
Sex				
Men	0.64 (0.51 to 0.81)	0.56 (0.46 to 0.69)	32577.34	68.9
Women	0.57 (0.29 to 1.12)	0.60 (0.34 to 1.07)	33792.10	63.0
Age				
< 65 years	0.70 (0.54 to 0.92)	0.66 (0.52 to 0.84)	26751.55	87.1
≥ 65 years	0.54 (0.38 to 0.77)	0.45 (0.32 to 0.62)	28519.93	83.2
Weight(kg)				
< 60	0.67 (0.51 to 0.88)	0.59 (0.46 to 0.76)	34212.82	64.5
≥ 60	0.59 (0.41 to 0.83)	0.51 (0.38 to 0.69)	30547.14	74.7
Country or region				
China	0.63 (0.51 to 0.78)	0.56 (0.46 to 0.68)	32407.35	71.7
ECOG performance status				
0	0.59 (0.36 to 0.96)	0.68 (0.46 to 1.00)	35806.56	53.6
1	0.64 (0.50 to 0.81)	0.52 (0.42 to 0.65)	31302.74	75.8
Disease type				
Metastatic	0.62 (0.49 to 0.77)	0.57 (0.46 to 0.69)	32575.83	68.4
Local advanced	0.77 (0.41 to 1.44)	0.54 (0.29 to 1.00)	35678.27	58.0
Hepatic metastasis				
No	0.64 (0.50 to 0.82)	0.54 (0.43 to 0.67)	31975.12	69.9
Yes	0.60 (0.40 to 0.91)	0.63 (0.44 to 0.91)	34394.85	62.2
Chemotherapy				
cisplatin plus paclitaxel	0.65 (0.52 to 0.80)	0.55 (0.45 to 0.67)	32384.74	71.0
cisplatin plus 5-fluorouracil	0.31 (0.08 to 1.20)	0.55 (0.23 to 1.32)	29955.09	72.5
PD-L1 expression (CPS)				
CPS<10	0.62 (0.45 to 0.85)	0.53 (0.40 to 0.71)	31492.38	70.7
CPS ≥10	0.64 (0.48 to 0.85)	0.58 (0.45 to 0.75)	33326.68	65.3
CPS<5	0.56 (0.37 to 0.86)	0.51 (0.35 to 0.75)	30396.16	73.6
CPS ≥5	0.65 (0.51 to 0.83)	0.58 (0.47 to 0.73)	33428.42	65.3
CPS<1	1.32 (0.63 to 2.77)	0.76 (0.41 to 1.38)	107721.84	25.1
CPS ≥1	0.59 (0.47 to 0.74)	0.54 (0.44 to 0.66)	31270.97	75.6
PD-L1 expression (TPS) (%)				
TPS<10	0.67 (0.52 to 0.88)	0.56 (0.44 to 0.71)	33112.99	68.6
TPS ≥10	0.55 (0.38 to 0.78)	0.54 (0.39 to 0.74)	30951.88	71.7
TPS<5	0.61 (0.46 to 0.82)	0.57 (0.44 to 0.73)	32509.58	68.9
TPS ≥5	0.67 (0.49 to 0.92)	0.54 (0.40 to 0.73)	32524.29	68.7
TPS<1	0.71 (0.53 to 0.95)	0.52 (0.39 to 0.68)	30367.97	78.2
TPS ≥1	0.63 (0.51 to 0.78)	0.59 (0.46 to 0.77)	35057.11	58.7

CPS, combined positive score; ECOG, Eastern Cooperative Oncology Group; HR, hazard ratio; ICER, incremental cost-effectiveness ratio; OS, overall survival; PD-L1, programmed cell death ligand 1; PFS, progression-free survival; QALY, quality-adjusted life years; TPS, tumour proportion score.

in China was $23,458.08/QALY, and the probability of SIDCHM being cost-effective was 86% when the WTP threshold was set at $37,653/QALY. A major innovation in our study is the discovery of cost-effective first-line ICI therapeutic options for advanced or metastatic ESCC. The results of the subgroup analysis showed that most subgroups of patients preferred treatment with ADCHM owing to >50% probability of cost-effectiveness as compared to PLCHM, except for subgroups with programmed cell death ligand 1 expression (CPS)<1. A few pharmacoeconomic evaluations were conducted on sintilimab, with only three studies retrieved in PubMed, but their economic results were all cost-effective, which is consistent with our findings. Two economic studies using clinical data from the ORIENT-32 trial (26) demonstrated that compared with sorafenib, sintilimab plus bevacizumab may provide a cost-effective treatment for Chinese patients with unresectable hepatocellular carcinoma (14, 27). Rui et al. reported that sintilimab plus chemotherapy as a first-line therapeutic option for nonsquamous non-small-cell lung cancer of locally advanced or metastatic was more cost-effective in China in comparison with karilizumab plus chemotherapy (28). Therefore, to reduce the

economic burden of medical treatment and provide more accessibility to Chinese patients, more attention should be paid to whether to use SIDCHM as a first-line therapeutic option for advanced or metastatic ESCC compared to other ICIs from the perspective of policymaking in China. In other words, the present results have a significant reference value for the Chinese healthcare system in developing first-line therapeutic options for advanced or metastatic ESCC. We believe very strongly that SIDCHM has also the potential to become a cost-effective therapeutic option for other cancers because of its price advantage and positive anti-tumor effect, which needs more economic research.

Inevitably, this study has some limitations. First, given the shortage of long-term survival data, we must consider using the Weibull survival model to make inferences about survival outside of the follow-up time, which may not provide an accurate reflection of real-world conditions. We will update our cost-effectiveness analysis when longer-term data on survival becomes available. Second, in the setting of disease progression, we chose to offer BSC to all patients due to the absence of relevant survival datasets for the enrolled patients, which may not accurately represent clinical practice at this time. We will analyze this further when relevant treatment costs and survival data for patients after progression are available. Third, in the model, we considered only the most common serious adverse events (SAEs) of level 3 and higher. The sensitivity analyses showed that the economic results were insensitive to SAE-associated. Fourth, although 7% of the patients in the ORIENT-15 trial received chemotherapy that was different from the preferred regimen in China, which may affect the economic evaluation in China, the results of the sensitivity analysis do not support the finding that this affected the economic results. Fifth, we had assumed that all patients chose 200 mg of sintilimab in the model, which is different from the real clinical situation. However, this would strengthen our economic results rather than change them because it raises the cost of the SIDCHM group. Sixth, changes in exchange rates affect direct medical costs, but the results of the one-factor sensitivity analysis indicate that healthcare costs do not change the results of the model when they change within the range we set. Finally, given the lack of relevant survival utility values for China, the utility values in this present study were obtained from other countries, which may result in model outcome bias. However, the results of the sensitivity analysis suggest that this does not affect the results of our economic evaluation. Despite these limitations, which cannot be ignored, this study is important as an economic reference for Chinese decision-makers to decide whether SIDCHM can be used as a first-line therapeutic option for advanced or metastatic ESCC.

Conclusions

Current relevant guidelines for advanced or metastatic ESCC do not recommend SIDCHM as a first-line treatment option. However, the results of this study suggest that from the Chinese healthcare system perspective, SIDCHM is a cost-effective therapy choice for advanced or metastatic ESCC compared with conventional chemotherapy. Our findings will provide an important economic basis for the Chinese healthcare system to decide whether to use SIDCHM as a first-line treatment option for advanced or metastatic ESCC.

Data availability statement

The original contributions presented in the study are included in the article/Supplementary Material. Further inquiries can be directed to the corresponding authors.

Author contributions

Study design and supervision: MY, YHu, and ZC. Data analysis and interpretation: QW and WZ. Data collection: YHe and RC. Manuscript writing: MY. Final approval of the manuscript: All authors.

Funding

This study was supported in Social Development Project of Fuzhou Science and Technology Department (Grant number: 2021-S-108), Startup Fund for scientific research, Fujian Medical University (Grant number: 2019QH1301, 2021QH1203), and Mindong Hospital Science Fund (Grant number: 2022YN005). This study was not supported by any pharmaceutical company.

Conflict of interest

The authors declare that the research was conducted in the absence of any commercial or financial relationships that could be construed as a potential conflict of interest.

Publisher's note

All claims expressed in this article are solely those of the authors and do not necessarily represent those of their affiliated organizations, or those of the publisher, the editors and the reviewers. Any product that may be evaluated in this article, or claim that may be made by its manufacturer, is not guaranteed or endorsed by the publisher.

Supplementary material

The Supplementary Material for this article can be found online at: https://www.frontiersin.org/articles/10.3389/fonc.2022.986762/full#supplementary-material

SUPPLEMENTARY FIGURE

(A) Survival curves for model and the ORIENT-15 trial in the SIDCHM group. **(B)** Survival curves for model and the ORIENT-15 trial in the PLCHM group. OS, overall survival; PFS, progression-free survival; PLCHM, placebo plus chemotherapy.

References

1. Jiang Y, Zhang J, Zhao J, Li Z, Chen H, Qiao Y, et al. TOPK promotes metastasis of esophageal squamous cell carcinoma by activating the Src/GSK3β/STAT3 signaling pathway *via* γ-catenin. *BMC Cancer* (2019) 19:1264. doi: 10.1186/s12885-019-6453-z

2. Sung H, Ferlay J, Siegel RL, Laversanne M, Soerjomataram I, Jemal A, et al. Global cancer statistics 2020: GLOBOCAN estimates of incidence and mortality worldwide for 36 cancers in 185 countries. *CA Cancer J Clin* (2021) 71:209–49. doi: 10.3322/caac.21660

3. GBD 2017 Oesophageal Cancer Collaborators. The global, regional, and national burden of oesophageal cancer and its attributable risk factors in 195 countries and territorie-2017: A systematic analysis for the global burden of disease study 2017. *Lancet Gastroenterol Hepatol* (2020) 5:582–97. doi: 10.1016/S2468-1253(20)30007-8

4. Kitagawa Y, Uno T, Oyama T, Kato K, Kato H, Kawakubo H, et al. Esophageal cancer practice guidelines 2017 edited by the Japan esophageal society: part 2. *Esophagus* (2019) 16:25–43. doi: 10.1007/s10388-018-0642-8

5. Lu Z, Wang J, Shu Y, Liu L, Kong L, Yang L, et al. Sintilimab versus placebo in combination with chemotherapy as first line treatment for locally advanced or metastatic oesophageal squamous cell carcinoma (ORIENT-15): Multicentre, randomised, double blind, phase 3 trial. *BMJ (Clinical Res ed.)* (2022) 377:e068714. doi: 10.1136/bmj-2021-068714

6. Luo H, Lu J, Bai Y, Mao T, Wang J, Fan Q, et al. Effect of camrelizumab vs placebo added to chemotherapy on survival and progression-free survival in patients with advanced or metastatic esophageal squamous cell carcinoma: The ESCORT-1st randomized clinical trial. *JAMA* (2021) 326:916–25. doi: 10.1001/jama.2021.12836

7. Gandhi L, Rodríguez-Abreu D, Gadgeel S, Esteban E, Felip E, De Angelis F, et al. Pembrolizumab plus chemotherapy in metastatic non-Small-Cell lung cancer. *N Engl J Med* (2018) 378:2078–92. doi: 10.1056/NEJMoa1801005

8. Huang J, Xu J, Chen Y, Zhuang W, Zhang Y, Chen Z, et al. Camrelizumab versus investigator's choice of chemotherapy as second-line therapy for advanced or metastatic oesophageal squamous cell carcinoma (ESCORT): A multicentre, randomised, open-label, phase 3 study. *Lancet Oncol* (2020) 21:832–42. doi: 10.1016/S1470-2045(20)30110-8

9. Xu J, Li Y, Fan Q, Shu Y, Yang L, Cui T, et al. Clinical and biomarker analyses of sintilimab versus chemotherapy as second-line therapy for advanced or metastatic esophageal squamous cell carcinoma: A randomized, open-label phase 2 study (ORIENT-2). *Nat Commun* (2022) 13:857. doi: 10.1038/s41467-022-28408-3

10. Compiled by National Bureau of Statistics of China. (2021). Available at: http://www.stats.gov.cn/tjsj/ndsj/2021/indexch.htm (Accessed July 2, 2022).

11. Zhang Q, Wu P, He X, Ding Y, Shu Y. Cost-effectiveness analysis of camrelizumab vs. placebo added to chemotherapy as first-line therapy for advanced or metastatic esophageal squamous cell carcinoma in China. *Front Oncol* (2021) 11:790373. doi: 10.3389/fonc.2021.790373

12. Li M, Lin S, Wilson L, Huang P, Wang H, Lai S, et al. Cost-effectiveness analysis of hepatic arterial infusion of FOLFOX combined sorafenib for advanced hepatocellular carcinoma with portal vein invasion. *Front Oncol* (2021) 11:562135. doi: 10.3389/fonc.2021.562135

13. Li S, Peng L, Tan C, Zeng X, Wan X, Luo X, et al. Cost-effectiveness of ramucirumab plus paclitaxel as a second-line therapy for advanced gastric or gastro-oesophageal cancer in China. *PloS One* (2020) 15:e0232240. doi: 10.1371/journal.pone.0232240

14. Peng Y, Zeng X, Peng L, Liu Q, Yi L, Luo X, et al. Sintilimab plus bevacizumab biosimilar versus sorafenib as first-line treatment for unresectable hepatocellular carcinoma: A cost-effectiveness analysis. *Front Pharmacol* (2022) 13:778505. doi: 10.3389/fphar.2022.778505

15. Zhang PF, Xie D, Li Q. Cost-effectiveness analysis of nivolumab in the second-line treatment for advanced esophageal squamous cell carcinoma. *Future Oncol (London England)* (2020) 16:1189–98. doi: 10.2217/fon-2019-0821

16. Wu B, Li T, Cai J, Xu Y, Zhao G. Cost-effectiveness analysis of adjuvant chemotherapies in patients presenting with gastric cancer after D2 gastrectomy. *BMC Cancer* (2014) 14:984. doi: 10.1186/1471-2407-14-984

17. Insinga RP, Vanness DJ, Feliciano JL, Vandormael K, Traore S, Burke T. Cost-effectiveness of pembrolizumab in combination with chemotherapy in the 1st line treatment of non-squamous NSCLC in the US. *J Med Econ* (2018) 21:1191–205. doi: 10.1080/13696998.2018.1521416

18. Hoyle M, Green C, Thompson-Coon J, Liu Z, Welch K, Moxham T, et al. Cost-effectiveness of temsirolimus for first line treatment of advanced renal cell carcinoma. *Value Health* (2010) 13(1):61–68. doi: 10.1111/j.1524-4733.2009.00617.x

19. Cao W, Chen HD, Yu YW, Li N, Chen WQ. Changing profiles of cancer burden worldwide and in China: A secondary analysis of the global cancer statistics 2020. *Chin Med J* (2021) 134:783–91. doi: 10.1097/CM9.0000000000001474

20. Lin Y, Totsuka Y, He Y, Kikuchi S, Qiao Y, Ueda J, et al. Epidemiology of esophageal cancer in Japan and China. *J Epidemiol* (2013) 23:233–42. doi: 10.2188/jea.je20120162

21. He Y, Li D, Shan B, Liang D, Shi J, Chen W, et al. Incidence and mortality of esophagus cancer in chin-2012. *Chin J Cancer Res* (2019) 31:426–34. doi: 10.21147/j.issn.1000-9604.2019.03.04

22. Galluzzi L, Humeau J, Buqué A, Zitvogel L, Kroemer G. Immunostimulation with chemotherapy in the era of immune checkpoint inhibitors. *Nat Rev Clin Oncol* (2020) 17:725–41. doi: 10.1038/s41571-020-0413-z

23. Bagchi S, Yuan R, Engleman EG. Immune checkpoint inhibitors for the treatment of cancer: Clinical impact and mechanisms of response and resistance. *Annu Rev Pathol* (2021) 16:223–49. doi: 10.1146/annurev-pathol-042020-042741

24. *Notice of the general office of the national health and health commission on printing distributing the guidelines for the treatment of oncology and hematology-related diseases, (2022 edition)* (2022). Available at: http://www.nhc.gov.cn/yzygj/s2911/202204/a0e67177df1f439898683e1333957c74.shtml (Accessed July 2, 2022).

25. Zhu Y, Liu K, Ding D, Zhou Y, Peng L. Pembrolizumab plus chemotherapy as first-line treatment for advanced esophageal cancer: A cost-effectiveness analysis. *Adv Ther* (2022) 39:2614–29. doi: 10.1007/s12325-022-02101-9

26. Ren Z, Xu J, Bai Y, Xu A, Cang S, Du C, et al. Sintilimab plus a bevacizumab biosimilar (IBI305) versus sorafenib in unresectable hepatocellular carcinoma (ORIENT-32): A randomised, open-label, phase 2-3 study. *Lancet Oncol* (2021) 22:977–90. doi: 10.1016/S1470-2045(21)00252-7

27. Zhou T, Cao Y, Wang X, Yang L, Wang Z, Ma A, et al. Economic evaluation of sintilimab plus bevacizumab versus sorafenib as a first-line treatment for unresectable hepatocellular carcinoma. *Adv Ther* (2022) 39:2165–77. doi: 10.1007/s12325-022-02079-4

28. Rui M, Fei Z, Wang Y, Zhang X, Ma A, Sun H, et al. Cost-effectiveness analysis of sintilimab + chemotherapy versus camrelizumab + chemotherapy for the treatment of first-line locally advanced or metastatic nonsquamous NSCLC in China. *J Med Econ* (2022) 25:618–29. doi: 10.1080/13696998.2022.2071066

frontiers | Frontiers in Oncology

TYPE Original Research
PUBLISHED 20 December 2022
DOI 10.3389/fonc.2022.1065468

Check for updates

OPEN ACCESS

EDITED BY
Zhendong Jin,
Second Military Medical University, China

REVIEWED BY
Vincenzo Lizzi,
Azienda Ospedaliero-Universitaria Ospedali Riuniti di Foggia, Italy
Satya Ranjan Dash,
KIIT University, India

*CORRESPONDENCE
Quan Wang
wangquanjdyy@163.com

SPECIALTY SECTION
This article was submitted to Gastrointestinal Cancers: Colorectal Cancer, a section of the journal Frontiers in Oncology

RECEIVED 09 October 2022
ACCEPTED 05 December 2022
PUBLISHED 20 December 2022

CITATION
Qiu B, Su Xh, Qin X and Wang Q (2022) Application of machine learning techniques in real-world research to predict the risk of liver metastasis in rectal cancer.
Front. Oncol. 12:1065468.
doi: 10.3389/fonc.2022.1065468

COPYRIGHT
© 2022 Qiu, Su, Qin and Wang. This is an open-access article distributed under the terms of the Creative Commons Attribution License (CC BY). The use, distribution or reproduction in other forums is permitted, provided the original author(s) and the copyright owner(s) are credited and that the original publication in this journal is cited, in accordance with accepted academic practice. No use, distribution or reproduction is permitted which does not comply with these terms.

Application of machine learning techniques in real-world research to predict the risk of liver metastasis in rectal cancer

Binxu Qiu[1], Xiao hu Su[2], Xinxin Qin[1] and Quan Wang[1*]

[1]Department of Gastric and Colorectal Surgery, General Surgery Center, The First Hospital of Jilin University, Changchun, China, [2]Shanxi Bethune Hospital, Shanxi Academy of Medical Sciences, Tongji Shanxi Hospital, Third Hospital of Shanxi Medical University, Taiyuan, China

Background: The liver is the most common site of distant metastasis in rectal cancer, and liver metastasis dramatically affects the treatment strategy of patients. This study aimed to develop and validate a clinical prediction model based on machine learning algorithms to predict the risk of liver metastasis in patients with rectal cancer.

Methods: We integrated two rectal cancer cohorts from Surveillance, Epidemiology, and End Results (SEER) and Chinese multicenter hospitals from 2010-2017. We also built and validated liver metastasis prediction models for rectal cancer using six machine learning algorithms, including random forest (RF), light gradient boosting (LGBM), extreme gradient boosting (XGB), multilayer perceptron (MLP), logistic regression (LR), and K-nearest neighbor (KNN). The models were evaluated by combining several metrics, such as the area under the curve (AUC), accuracy score, sensitivity, specificity and F1 score. Finally, we created a network calculator using the best model.

Results: The study cohort consisted of 19,958 patients from the SEER database and 924 patients from two hospitals in China. The AUC values of the six prediction models ranged from 0.70 to 0.95. The XGB model showed the best predictive power, with the following metrics assessed in the internal test set: AUC (0.918), accuracy (0.884), sensitivity (0.721), and specificity (0.787). The XGB model was assessed in the outer test set with the following metrics: AUC (0.926), accuracy (0.919), sensitivity (0.740), and specificity (0.765). The XGB algorithm also shows a good fit on the calibration decision curves for both the internal test set and the external validation set. Finally, we constructed an online web calculator using the XGB model to help generalize the model and to assist physicians in their decision-making better.

Conclusion: We successfully developed an XGB-based machine learning model to predict liver metastasis from rectal cancer, which was also validated with a real-world dataset. Finally, we developed a web-based predictor to guide clinical diagnosis and treatment strategies better.

KEYWORDS

rectal cancer, machine learning, liver metastasis, web calculator, real-world research

Introduction

Rectal cancer is the eighth most common malignant tumor in the world, with a high mortality rate of about 340,000 lives yearly (1, 2). It has become one of the significant public health problems threatening human health. Patients with rectal cancer often have a poor prognosis due to liver metastasis and whose 5-year survival rate is less than 50% (3, 4). Previous studies have shown that 20-25% of patients with the initial diagnosis of rectal cancer develop liver metastasis. Even after radical resection, rectal cancers still have a 30% probability of liver metastasis (5, 6). Due to the poor prognosis and high prevalence of liver metastasis from rectal cancer, there is still more clinical concern about liver metastasis from rectal cancer (7, 8). Magnetic resonance imaging (MRI) and positron emission tomography/computed tomography (PET/CT) are standard techniques for screening patients with rectal cancer for distant metastasis. However, given the high cost of MRI and the disadvantages of PET-CT radiation damage, it is not recommended for all patients with rectal cancer to be screened for distant metastasis (9, 10). This imposes a high demand for the identification and rationalization of screening people at high risk of liver metastasis from rectal cancer. To address these issues, we used advanced machine learning algorithms to build a predictive model to predict liver metastasis in patients with rectal cancer.

Machine-Learning has become a new type of artificial intelligence that is beginning to be widely used in healthcare data analysis and is a powerful tool for improving clinical strategies (11–15). Machine-learning algorithms can automatically learn from input data to predict outcome values acceptable and identify patterns and trends in the data. A statistical and comprehensive review of machine learning in medical diagnosis by Bhavsar et al. shows that machine learning techniques help medical professionals reduce diagnostic errors, improve healthcare delivery and reduce treatment costs (16). Many scholars have achieved significant breakthroughs by using machine-learning algorithms in colorectal cancer, but machine-learning prediction models for liver metastasis in rectal cancer are not yet available (17, 18). Also, previous studies have limited constructing models only by using public databases, thus limiting the extrapolation of models. Therefore, involving real-world clinical datasets is essential for creating superior predictive models.

This study aims to develop machine-learning models that use clinicopathology features to predict the risk of liver metastasis from rectal cancer and suggest individual prevention strategies to help clinicians make treatment decisions.

Materials and methods

Study population

A retrospective analysis of the SEER (Surveillance, Epidemiology, and End Results) database and data from patients admitted to the First Affiliated Hospital of Jilin University and Shanxi Bethune Hospital was conducted. SEER is an authoritative source for cancer statistics in the United States. The Surveillance provides information on cancer statistics to reduce the cancer burden among the U.S. population. The inclusion criteria for the rectal cancer cohort from SEER were demonstrated as follows:(1) the primary pathological diagnosis was rectal cancer, (2) patients without concurrent malignancies, and (3) patients with complete clinical information, including age, gender, race, marital status, histological grade, tumor size, T-stage, N-stage, carcinoembryonic antigen (CEA), diagnostic information, and first site. In addition, the exclusivity criteria were shown as follows: (1) no complete clinical information, (2) another primary neoplastic disease, and (3) unknown liver metastatic status. The inclusion criteria for the external validation set were (1) metachronous liver metastasis (after diagnosis) and (2) patients not undergoing preoperative neoadjuvant therapy. All aspects of the clinical cohort study were approved for inclusion by the Institutional Ethics Committee of the First Hospital of Jilin University and Shanxi Bethune Hospital and were performed in adherence to the Declaration of Helsinki.

Data collection and data processing

SEER patient data were obtained from "SEER Research Plus Data, 18 Registries, Nov 2020 Sub (2000-2018)" and extracted using SEER * STAT (8.4.0) software. Patients diagnosed with rectal cancer from 2010-2017 were included in this study. Patients with rectal cancer from multiple centers in China were included in the external validation. The entire workflow is demonstrated in detail in Figure 1. In addition, patient data from multicenter hospitals were processed according to SEER database standards (Supplement Table 1). We transformed the clinical information into numbers to make it easy to compute in the model (Supplement Table 2).

Construction of the predictive model

In this study, we used six machine learning algorithms to predict liver metastasis of rectal cancer, including random forest (RF), Light Gradient Boosting (LGBM), extreme gradient boosting (XGB), multilayer perceptron (MLP), logistic regression (LR) and K-Nearest Neighbor (KNN). RF is a machine learning algorithm that deals with classification and regression problems by building multiple decision tree methods (19). LGBM is a gradient-boosting framework using a tree-based learning algorithm that has been successfully applied to the construction of medical models in recent years (20). XGB is a classical decision tree algorithm applied to classification or regression prediction models (21). MLP is a feedforward neural network model used in different prediction models (22). LR algorithm is a classification algorithm commonly used for dichotomous variables and is widely used in data mining due to its simplicity, parallelizability, and explanatory power (23). KNN algorithm is identified as an essential classification algorithm in the supervised machine-learning domain and is widely used in pattern recognition, data mining, and intrusion detection (24).

Patients from the SEER database were randomly partitioned into a training set and an internal test set using python with a ratio of 8:2. To improve the model's effectiveness while ensuring the data's authenticity, we use a synthetic minority oversampling technique (SMOTE) for the SEER database to solve the data imbalance problem (25). The training set was used to build the model, and the internal test set was used for model validation and evaluation. In the training set, k-fold cross-validation (k = 10) is performed, and a grid search is used to find the best combination of parameters. Subsequently, the model performance is initially evaluated in the internal test set. Finally, a rectal cancer cohort from two hospitals was used to validate the model's generalization capability and efficiency.

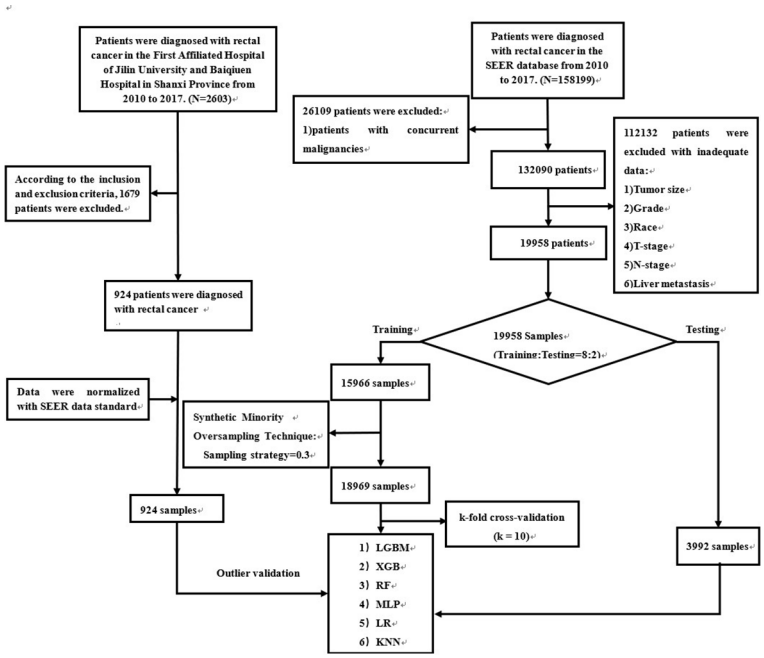

FIGURE 1
The workflow of the selection procedure for rectal cancer patients. Abbreviations: LGBM, light gradient boosting; XGB, extreme gradient boosting; RF, random forest; LR, logistic regression; KNN, K-nearest neighbor; MLP, multilayer perceptron.

Model performance and feature importance

Model performance is evaluated by area under the curve (AUC), predictive accuracy, sensitivity, specificity, and F1-score. Our primary evaluation metric for machine-learning models is AUC, calculated from ROC curves, which are graphical plots showing the diagnostic power of binary classifiers as their discriminative thresholds change (26). It is also combined with other metrics for a comprehensive evaluation to determine the best model. To further explore the degree of importance of incorporated features in all algorithms, we used the Permutation Importance principle for feature importance analysis of variables. The Permutation Importance approach assesses the effect of model construction on the remaining features by treating an incorporated feature as a random number. If the model performance decreases significantly, the feature is shown to have a more critical role (27). Finally, model performance was then further assessed by calibration curves.

Interpretability of the model and construction of the web calculator

The Shapley Additive explanation (SHAP) method is used in the article to interpret the constructed model. It allows for the calculation of precisely the contribution of each variable to the final prediction. In addition, each observation in the dataset can be interpreted by a specific set of SHAP values (28). We created a web calculator to make the model clinically easy to use and generalize.

Statistical analysis

All statistical analyses were performed in Python (version 3.8, Python Software Foundation) and R software (version 4.1.0). All machine learning algorithms were built based on scikit-learn (version 0.24.1). Categorical variables were expressed as totals and percentages, and differences between groups were compared using the $\chi 2$ test or Fisher's exact test. Continuous variables were expressed as median and Standard Deviation (SD), and the Wilcoxon rank sum test was used to compare groups. The results were considered statistically significant when the two-sided $P<0.05$.

Result

Patient components and clinical baseline information

Our study included rectal cancer data from the SEER database, ranging from 2010 to 2017. A total of 152,199 patients with rectal cancer were initially included. Based on established inclusion and exclusion criteria, the final number of patients included in the SEER database was 19,957, 1,712 patients (8.58%) had liver metastasis, and 18,246 patients (91.42%) had no liver metastasis. Outer validation was performed using a total of 924 patients from two centers in China. Patient data from SEER and the two centers in China are presented in Table 1.

Seven clinicopathological factors were included in our established model: age at diagnosis, gender, T-stage, N-stage, CEA, grade of differentiation, and tumor size (Table 2). Patients in the SEER database were divided into liver metastasis (LM) and non-liver metastasis groups (NLM). For age at diagnosis, we found that the mean age at diagnosis was significantly more extensive in the NLM group (58.89) than in the LM group (62.01; $P<0.001$). Notably, the proportion of male patients in the LM group (1119/1712;65.4%) was significantly higher than that in the NLM group (10762/18246; 59%; $P<0.001$). Unexpectedly, we found no difference between the two subgroups regarding race and married status. According to our assumptions, the LM group showed higher T-stage and N-stage patients ($P<0.001$). In terms of tumor progression, we found that patients in the LM group (5.70cm) had significantly larger tumor sizes than patients in the NLM group (4.25cm; $P<0.001$). In addition, we found that patients in the LM group (1070/1712;62.50%) had a higher percentage of positive CEA expression than the NLM group (4627/18246;25.40%;$P<0.001$).

Correlation of variables and feature importance of prediction

Seven selected variables were analyzed according to the spearman correlation test, and the heatmap results showed no significant correlation between the variables, and multicollinearity is unlikely (Figure 2). The importance ranking of features in the six machine-learning models is shown in Figure 3. The relative importance of the variables in the six machine learning models was analyzed using the permutation importance principle. Although the six machine learning algorithms ranked differently regarding the importance, CEA and tumor size ranked in the top two of most models. They may have a more critical predictive role for rectal cancer liver metastasis. In contrast, sex and grade ranked lower but contributed to rectal cancer liver metastasis. In the XGB model, the importance of features were ranked in descending order by tumor size, CEA, age, T-stage, N-stage, sex, and grade.

Model performance and model explainability

Ten-fold cross-validation of the training set data using six machine learning algorithms shows that the XGB model has an

10.3389/fonc.2022.1065468

TABLE 1 Clinical baseline features of SEER and multiple centers hospital database.

Variables	SEER database		Multiple centers
	Training set (N=15966)	Testing set (N=3992)	Outer validation set (N=924)
Age [mean (SD)]	61.74 (13.18)	61.72 (13.39)	61.72 (13.31)
Gender, n (%)			
Male	9471 (59.3)	2410 (60.4)	556 (60.2)
Female	6495 (40.7)	1582 (39.6)	368 (39.8)
Race, n (%)			
White	12969 (81.2)	3241 (81.2)	0
Black	1324 (8.3)	310 (7.8)	0
Asian or Pacific Islander	1532 (9.6)	402 (10.1)	924
American Indian/Alaska Native	141 (0.9)	39 (1.0)	0
T_stage, n (%)			
T1	2909 (18.2)	695 (17.4)	151 (16.3)
T2	2661 (16.7)	669 (16.8)	140 (15.2)
T3	8870 (55.6)	2236 (56.0)	509 (55.1)
T4	1526 (9.6)	392 (9.8)	124 (13.4)
N_ stage, n (%)			
N0	8604 (53.9)	2159 (54.1)	430 (46.5)
N1	5433 (34.0)	1372 (34.4)	376 (40.7)
N2	1929 (12.1)	461 (11.5)	118 (12.8)
Grade, n (%)			
Grade I	1380 (8.6)	344 (8.6)	53 (5.7)
Grade II	12393 (77.6)	3114 (78.0)	726 (78.6)
GradeI III	1926 (12.1)	471 (11.8)	109 (11.8)
GradeI IV	267 (1.7)	63 (1.6)	36 (3.9)
CEA, n (%)			
Negative	5763 (36.1)	1412 (35.4)	412 (44.6)
Borderline	61 (0.4)	15 (0.4)	75 (8.1)
Positive	4534 (28.4)	1163 (29.1)	242 (26.2)
Unknown	5608 (35.1)	1402 (35.1)	195 (21.1)
Marital, n (%)			
Married	9371 (58.7)	2381 (59.6)	622 (67.3)
Unmarried	4615 (28.9)	1151 (28.8)	231 (25.0)
Other	1980 (12.4)	460 (11.5)	71 (7.7)
Tumor. size (mean (SD))	4.37 (3.55)	4.38 (3.86)	4.34 (4.00)
Liver.Met, n (%)			
No	14592 (91.4)	3654 (91.5)	770 (83.3)
Yes	1374 (8.6)	338 (8.5)	154 (16.7)

10.3389/fonc.2022.1065468

TABLE 2 Distributions of clinicopathological characteristics in two groups.

Variables	LM	NLM	P value
	N=1712	N=18246	
Age [mean (SD)]	58.89 (12.99)	62.01 (13.21)	<0.001
Gender, n (%)			
Male	1119 (65.4)	10762 (59)	<0.001
Female	593 (34.6)	7484 (41.0)	
Race, n (%)			
White	14840 (81.3)	1370 (80.0)	0.080
Black	1466 (8.0)	168 (9.8)	
Asian or Pacific Islander	1774 (9.7)	160 (9.3)	
American Indian/Alaska Native	166 (0.9)	14 (0.8)	
T-stage (%)			
T1	246 (14.4)	3358 (18.4)	<0.001
T2	84 (4.9)	3246 (17.8)	
T3	1067 (62.3)	10039 (55.0)	
T4	315 (18.4)	1603 (8.8)	
N_ stage (%)			
N0	486 (28.4)	10277 (56.3)	<0.001
N1	811 (47.4)	5994 (32.9)	
N2	415 (24.2)	1975 (10.8)	
Grade			
Grade I	89 (5.2)	1635 (9.0)	<0.001
Grade II	1298 (75.8)	14209 (77.9)	
Grade III	280 (16.4)	2117 (11.6)	
Grade IV	45 (2.6)	285 (1.6)	
CEA			
Negative	232 (13.6)	6943 (38.1)	<0.001
Borderline	3 (0.2)	73 (0.4)	
Positive	1070 (62.5)	4627 (25.4)	
Unknown	407 (23.8)	6603 (36.2)	
Marital			
Married	965 (56.4)	10787 (59.1)	0.063
Unmarried	516 (30.1)	5250 (28.8)	
Other	231 (13.5)	2209 (12.1)	
Tumor size (mean (SD))	4.25 (3.46)	5.70 (4.84)	<0.001

CEA, carcinoembryonic antigen; LM, liver metastasis; NLM, non-liver metastasis.

FIGURE 2
Results of the correlation heatmap between all variables. The graph shows the correlations between all variables.

average AUC value of 0.993, indicating the best predictive power among all models (Figure 4). In the internal test set, XGB obtained an AUC of 0.918, an accuracy of 0.884, a sensitivity of 0.721, and a specificity of 0.787(Figure 5; Table 3). In the outer test set, the XGB model also showed excellent performance with an AUC of 0.926, an accuracy of 0.919, a sensitivity of 0.740, and a specificity of 0.765 (Figure 5; Table 3). The calibration curves for the internal and outer validation sets also demonstrate that the model has a reasonable degree of fit (Supplementary Table 3). Finally, to detect positive and negative correlations between characteristics and liver metastasis of rectal cancer, we used SHAP to reveal risk factors for liver metastasis of rectal cancer. The related results are presented in Figure 6.

Web predictor

Although XGB has shown excellent predictive ability in liver metastasis from rectal cancer, it is intricate and complex, which is not conducive to clinical dissemination. Therefore, this study developed an online web calculator for predicting liver metastasis risk in patients with rectal cancer. The calculator can be easily extended clinically and only requires inputting patient clinicopathological information to derive the probability of obtaining liver metastasis in patients with rectal cancer while stratifying patients into high and low risk. (https://share.streamlit.io/woshiwz/rectal_cancer/main/rectal.py) (Figure 7).

Discussion

In this study, we constructed a model for predicting liver metastasis from rectal cancer using popular machine-learning algorithms combining seven clinical and pathological features. To the best of our knowledge, this study is the first article on the prediction of liver metastasis in rectal cancer combined with machine learning algorithms while using real-world data for outer validation. The AUC performance of these models is mostly more extensive than 0.85 (Figure 5; Table 3), while the accuracy is mostly above 0.80 (Figure 5; Table 3); therefore, we

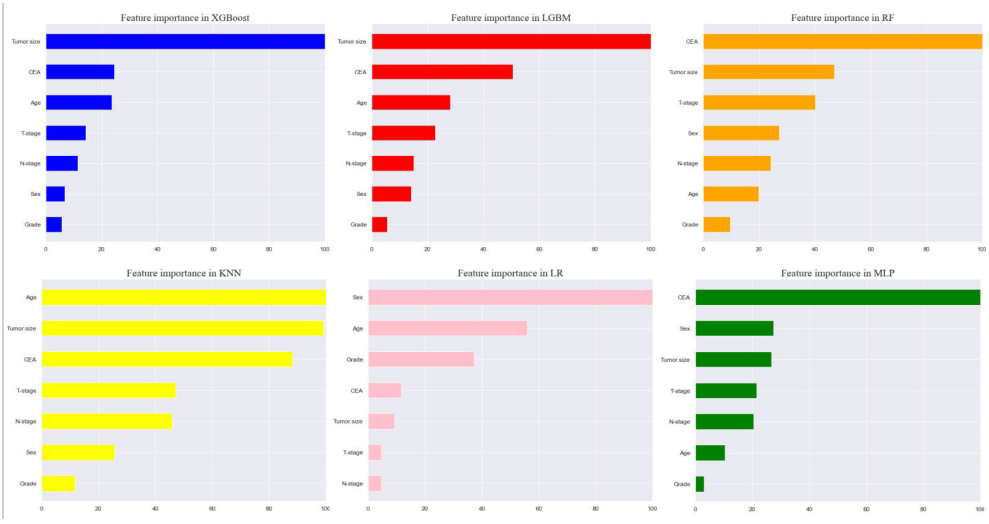

FIGURE 3
Feature importance of six models. The plot shows the ranking of six models' relevant volume of features. Abbreviations: LGBM, light gradient boosting; XGB, extreme gradient boosting; RF, random forest; LR, logistic regression; KNN, K-nearest neighbor; MLP, multilayer perceptron.

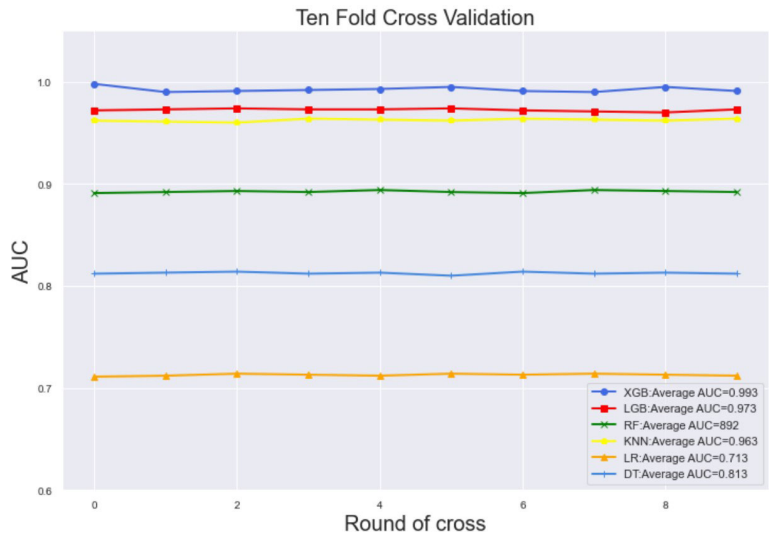

FIGURE 4
The training set has ten-fold cross-validation results of different machine learning models. Abbreviations: LGBM, light gradient boosting; XGB, extreme gradient boosting; RF, random forest; LR, logistic regression; KNN, K-nearest neighbor; MLP, multilayer perceptron.

believe that the developed models are robust and reliable while allowing for more significant clinical benefits. Comparing the prediction performance of six machine-learning algorithms, we found that the model based on the XGB algorithm performed the best. Finally, to make the model clinically applicable and generalizable, we developed an online web calculator based on the XGB model to calculate the probability of liver metastasis from rectal cancer and thus screen patients at high risk for liver metastasis.

In addition, machine learning's clinical importance is reflected in identifying important risk factors associated with liver metastasis from rectal cancer (29). In this study, tumor size, CEA, age, T-stage and N-stage were critical for liver metastasis from rectal cancer based on XGB algorithms' ranking of feature importance. In the present study, tumor size showed the best predictor in numerous models. Large tumor size indicates a long growth cycle, leading to a more proliferative and aggressive state of tumor cells, which increases liver metastasis (29, 30). CEA is the standard tumor

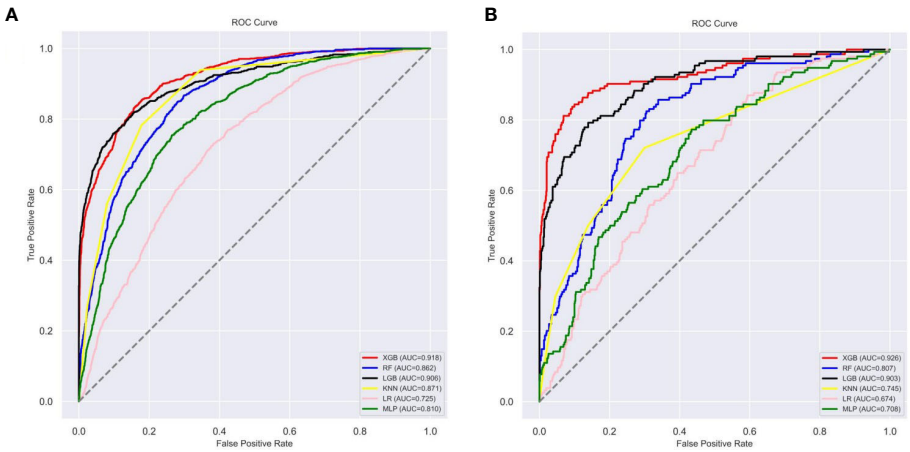

FIGURE 5
The roc curves of different machine learning models: **(A)** The roc curves of other machine learning models in the internal test set; **(B)** The roc curves of other machine learning models external test set. Abbreviations: LGBM, light gradient boosting; XGB, extreme gradient boosting; RF, random forest; LR, logistic regression; KNN, K-nearest neighbor; MLP multilayer perceptron; roc, receiver operating characteristic.

10.3389/fonc.2022.1065468

TABLE 3 Comparison prediction performances of different models for liver metastasis.

	model	AUC	Accuracy	Sensitivity	Speciality	F1-score
Internal test set						
	XGB	0.918	0.884	0.721	0.787	0.733
	LGBM	0.906	0.879	0.622	0.746	0.695
	RF	0.862	0.824	0.460	0.644	0.537
	KNN	0.871	0.840	0.561	0.665	0.608
	LR	0.725	0.774	0.081	0.440	0.137
	MLP	0.810	0.806	0.390	0.591	0.470
Outer validation set						
	XGB	0.926	0.919	0.740	0.765	0.752
	LGBM	0.903	0.903	0.610	0.758	0.676
	RF	0.807	0.825	0.318	0.462	0.377
	KNN	0.745	0.845	0.300	0.568	0.391
	LR	0.674	0.824	0.032	0.263	0.058
	MLP	0.708	0.803	0.156	0.316	0.209

LGBM, light gradient boosting; XGB, extreme gradient boosting; RF, random forest; LR, logistic regression; KNN, K-nearest neighbor; MLP, multilayer perceptron; AUC, area under the curve.

marker on colorectal cancer cell membranes and embryonic mucosal cells. An increasing number of studies have shown that pretreatment CEA levels are considered to be associated with tumor stage and metastasis, with studies showing that CEA is elevated in 45% of patients with stage B and 76% of patients with distal metastasis (31–34). Therefore, it is unsurprising that the preoperative serum CEA levels of patients with rectal cancer liver metastasis in this study were higher than those of non-liver metastasis. Although the proportion of young rectal cancer patients is increasing yearly, there is convincing evidence that younger people can achieve better outcomes than older patients (35).Interestingly, this study showed that the younger the patient, the higher the risk of liver metastasis from rectal cancer. The reason may be that younger patients' tumor cells often undergo mismatch repair and thus upregulate the tumor's aggressiveness (36–38). T-stage is an essential indicator of tumor progression and positively correlates with tumor metastasis in most tumors. Our results demonstrate that patients with rectal liver metastasis have a more advanced T-stage than those with non-rectal liver metastasis. Considerable research suggests that the reason may be due to the progressive increase in lymphatic vessels from the mucosal to the plasma layer of the rectal wall structure and the abundance of lymphatic reflux, which in turn increases the risk of liver metastasis from rectal cancer (39, 40). Several studies have shown that patients with regional lymph node metastasis are likelier to develop liver metastasis from rectal cancer (41–43). The liver is one of the organs with the most abundant lymphatic tissue in the body. Therefore, tumors are more likely to metastasize when local lymph nodes are metastatic. Although gender and differentiation grades did not perform well in the XGB model in this study, they still played a role in model construction. Tang et al. found that men and poorly differentiated patients were more likely to develop liver metastasis from rectal cancer, in concurrence with the results of this study (44, 45). Our model sufficiently integrates various risk factors that could affect liver metastasis from rectal cancer and achieves outstanding predictive performance.

FIGURE 6
The Shapley Additive explanation (SHAP) values.

Most traditional statistical methods are based on parametric regression models that assume a linear relationship between variables and outcomes (29, 46). However, we should know that

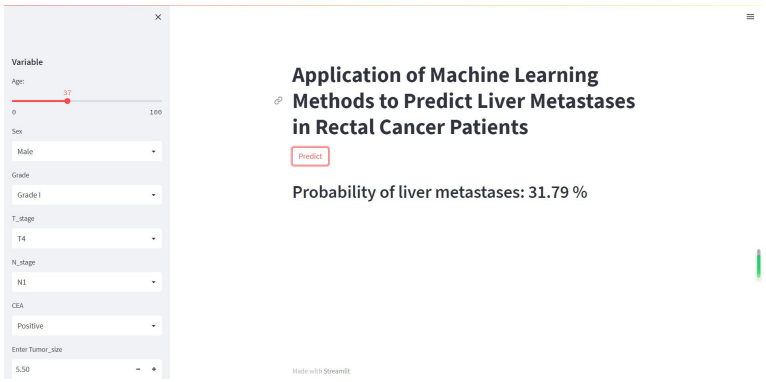

FIGURE 7
The machine learning model-based web predictor for predicting liver metastasis in rectal cancer patients.

most variables and results are more than just linearly related. With the rapid development of artificial intelligence, machine-learning algorithms play an increasing role in tumor diagnosis and prognosis assessment. Machine-learning algorithms have many advantages, including preventing overfitting and handling unbalanced data (47). In this study, XGB performed better than other algorithms because it added a regular term to the objective function to control the complexity of the model and avoid overfitting while supporting column sampling to enhance the stability of the model (21, 48).

Until now, only surgical resection has proven to be a curative treatment for patients with early resectable rectal cancer liver metastasis (49). Early systemic chemotherapy may improve prognosis and increase median survival in patients with undetectable rectal cancer liver metastasis (50). Combining all these results, we believe that further use of the rectal cancer liver metastasis model will aid clinical decision-making and improve the current treatment status.

The strengths of this study are the use of large-scale data from the SEER database for modeling and the use of real-world clinical data for outer validation, which prevents the overfitting of the data and ensures extrapolation of the model. However, this study also has some limitations. Firstly, the study is a retrospective study, and there may be selection bias in the sample selection. Secondly, there are limitations in the data available in the SEER database, such as the unavailability of crucial information on chemotherapy regimens, radiotherapy doses, and vascular infiltration, which limits the predictive value of our model. Finally, only two outer validation sets were used to validate the model, and further efforts are needed to validate the model's performance on a more diverse population. These reasons may lead to a limited verification effect of our model.

For future work, we will focus on prospective and diverse population validation of the models to verify their performance and stability. These models are then expected to be integrated into applications that assist clinicians in medical decision-making. This can be a step toward a semi-autonomous diagnostic system that can assist clinicians in making individualized diagnoses of liver metastasis for patients with rectal cancer.

Conclusion

In conclusion, we developed a prediction model for liver metastasis from rectal cancer, which uses machine-learning algorithms to predict liver metastasis from rectal cancer. A web calculator has also been designed to facilitate the screening of patients at high risk of liver metastasis from rectal cancer by inputting some parameters, which may help physicians to individualize the treatment of rectal cancer patients.

Data availability statement

The original contributions presented in the study are included in the article/Supplementary Material. Further inquiries can be directed to the corresponding author.

Ethics statement

Written informed consent was obtained from the individual(s), and minor(s)' legal guardian/next of kin, for the publication of any potentially identifiable images or data included in this article.

Author contributions

BQ and QW designed the study. BQ, XQ, and XS conducted data analysis. BQ conceived the project and wrote the manuscript. QW revised and approved the paper. All authors contributed to the article and approved the submitted version.

Funding

This study was supported by Beijing Xisike Clinical Oncology Research Foundation (Y-MSDPU2021-0281), the Bethune Medical Engineering and Instrument Center 2021 Project (BQEGCZX2021010) and the Jilin Provincial Science and Technology Department Science and Technology Program (20200802010GH).

Conflict of interest

The authors declare that the research was conducted in the absence of any commercial or financial relationships that could be construed as a potential conflict of interest.

Publisher's note

All claims expressed in this article are solely those of the authors and do not necessarily represent those of their affiliated organizations, or those of the publisher, the editors and the reviewers. Any product that may be evaluated in this article, or claim that may be made by its manufacturer, is not guaranteed or endorsed by the publisher.

Supplementary material

The Supplementary Material for this article can be found online at: https://www.frontiersin.org/articles/10.3389/fonc.2022.1065468/full#supplementary-material

References

1. Sung H, Ferlay J, Siegel RL, Laversanne M, Soerjomataram I, Jemal A, et al. Global cancer statistics 2020: GLOBOCAN estimates of incidence and mortality worldwide for 36 cancers in 185 countries. *CA Cancer J Clin* (2021) 71(3):209–49. doi: 10.3322/caac.21660

2. Wilkinson N. Management of rectal cancer. *Surg Clin North Am* (2020) 100 (3):615–28. doi: 10.1016/j.suc.2020.02.014

3. Chandra R, Karalis JD, Liu C, Murimwa GZ, Voth Park J, Heid CA, et al. The colorectal cancer tumor microenvironment and its impact on liver and lung metastasis. *Cancers (Basel).* (2021) 13(24):6206. doi: 10.3390/cancers13246206

4. Kawaguchi Y, Vauthey JN. The landmark series: Randomized control trials examining perioperative chemotherapy and postoperative adjuvant chemotherapy for resectable colorectal liver metastasis. *Ann Surg Oncol* (2020) 27(11):4263–70. doi: 10.1245/s10434-020-08777-z

5. Padmanabhan C, Nussbaum DP, D'Angelica M. Surgical management of colorectal cancer liver metastasis. *Surg Oncol Clin N Am* (2021) 30(1):1–25. doi: 10.1016/j.soc.2020.09.002

6. Rompianesi G, Pegoraro F, Ceresa CD, Montalti R, Troisi RI. Artificial intelligence in the diagnosis and management of colorectal cancer liver metastasis. *World J Gastroenterol* (2022) 28(1):108–22. doi: 10.3748/wjg.v28.i1.108

7. Tsilimigras DI, Ntanasis-Stathopoulos I, Bagante F, Moris D, Cloyd J, Spartalis E, et al. Clinical significance and prognostic relevance of KRAS, BRAF, PI3K and TP53 genetic mutation analysis for resectable and unresectable colorectal liver metastasis: A systematic review of the current evidence. *Surg Oncol* (2018) 27 (2):280–8. doi: 10.1016/j.suronc.2018.05.012

8. Vendrely V, Terlizzi M, Huguet F, Denost Q, Chiche L, Smith D, et al. Comment traiter un cancer du rectum avec métastases hépatiques synchrones? une question de stratégie thérapeutique [How to manage a rectal cancer with synchronous liver metastasis? a question of strategy]. *Cancer Radiother* (2017) 21(6-7):539–43. doi: 10.1016/j.canrad.2017.07.021

9. Brendle C, Schwenzer NF, Rempp H, Schmidt H, Pfannenberg C, la Fougère C, et al. Assessment of metastatic colorectal cancer with hybrid imaging: comparison of reading performance using different combinations of anatomical and functional imaging techniques in PET/MRI and PET/CT in a short case series. *Eur J Nucl Med Mol Imaging* (2016) 43(1):123–32. doi: 10.1007/s00259-015-3137-z

10. Suarez-Weiss KE, Herold A, Gervais D, Palmer E, Amorim B, King JD, et al. Hybridbildgebung bei abdominellen erkrankungen [Hybrid imaging of the abdomen and pelvis. *German version]. Radiol* (2020) 60(5):394–404. doi: 10.1007/s00117-020-00660-y

11. Li W, Huang Y, Zhuang BW, Liu GJ, Hu HT, Li X, et al. Multiparametric ultrasonics of significant liver fibrosis: A machine learning-based analysis. *Eur Radiol* (2019) 29(3):1496–506. doi: 10.1007/s00330-018-5680-z

12. Xiong H, Jin C, Alazab M, Yeh KH, Wang H, Gadekallu TRR, et al. On the design of blockchain-based ECDSA with fault-tolerant batch verication protocol for blockchain-enabled IoMT. *IEEE J BioMed Health Inform* (2021) 26(5):1977–86. doi: 10.1109/JBHI.2021.3112693

13. Wang W, Qiu C, Yin Z, Srivastava G, Gadekallu TR, Alsolami F, et al. Blockchain and PUF-based lightweight authentication protocol for wireless medical sensor networks. *IEEE Inter Thing J* (2021) 9:8883–91. doi: 10.1109/JIOT.2021.3117762

14. Wendi C, Mahboob K, Khalid Z, Javed AR, Rizwan M, Ghosh U, et al. Classification of COVID-19 individuals using adaptive neuro-fuzzy inference system. *Multimed Syst* (2021) 2021:151. doi: 10.1007/s00530-021-00774-w

15. Kutia S, Chauhdary SH, Iwendi C, Liu L, Yong W, Bashir AK. Socio-technological factors affecting user's adoption of ehealth functionalities: A case study of China and Ukraine health systems. *IEEE Access* (2019) 7:90777–88. doi: 10.1109/ACCESS.2019.292458415

16. Bhavsar KA, Singla J, Al-Otaibi YD, Song O-Y, Zikria YB, Bashir AK. Medical diagnosis using machine learning: a statistical review. *Comput Mater Continua.* (2021) 67:107–25. doi: 10.32604/cmc.2021.014604

17. Han T, Zhu J, Chen X, Chen R, Jiang Y, Wang S, et al. Application of artificial intelligence in real-world research for predicting the risk of liver metastasis in T1 colorectal cancer. *Cancer Cell Int* (2022) 22(1):28. doi: 10.1186/s12935-021-02424-7

18. Ahn JH, Kwak MS, Lee HH, Cha JM, Shin HP, Jeon JW, et al. Development of a novel prognostic model for predicting lymph node metastasis in early colorectal cancer: Analysis based on the surveillance, epidemiology, and end results database. *Front Oncol* (2021) 11:614398. doi: 10.3389/fonc.2021.614398

19. Breiman L. Random forests. *Mach Learn* (2010) 1(45):5–32. doi: 10.1023/A:1010933404324

20. Friedman JH. Greedy function approximation: a gradient boosting machine. *Ann Stat* (2001) 29:1189–232. doi: 10.1214/aos/1013203451

21. Ikram, Ikram ST, Cherukuri AK, Poorva B, Ushasree PS, Zhang Y, et al. Anomaly detection using XGBoost ensemble of deep neural network models. *Cybernetics Inf Technol* (2021) 21(3):175–88. doi: 10.2478/cait-2021-0037

22. Yao Y, Yang X, Lai SH, Chin RJ. Predicting tsunami-like solitary wave run-up over fringing reefs using the multi-layer perceptron neural network. *Natural Hazards.* (2021) 107(1):601–16. doi: 10.1007/s11069-021-04597-w

23. Levy JJ, O'Malley AJ. Don't dismiss logistic regression: the case for sensible extraction of interactions in the era of machine learning. *BMC Med Res Methodol* (2020) 20(1):171. doi: 10.1186/s12874-020-01046-3

24. Uddin S, Khan A, Hossain ME, Moni MA. Comparing different supervised machine learning algorithms for disease prediction. *BMC Med Inform Decis Mak.* (2019) 19(1):281. doi: 10.1186/s12911-019-1004-8

25. Janssen A, Hoogendoorn M, Cnossen MH, Mathôt RAAfor the OPTI-CLOT Study Group and SYMPHONY Consortium, , MH C, et al. Application of SHAP values for inferring the optimal functional form of covariates in pharmacokinetic modeling. *CPT Pharmacometrics Syst Pharmacol* (2022) 11 (8):1100–10. doi: 10.1002/psp4.12828

26. Muschelli J. ROC. And AUC with a binary predictor: a potentially misleading metric. *J Classif.* (2020) 37(3):696–708. doi: 10.1007/s00357-019-09345-1

27. Debeer D, Strobl C. Conditional permutation importance revisited. *BMC Bioinf* (2020) 21(1):307. doi: 10.1186/s12859-020-03622-2

28. Duan F, Zhang S, Yan Y, Cai Z. An oversampling method of unbalanced data for mechanical fault diagnosis based on MeanRadius-SMOTE. *Sensors (Basel).* (2022) 22(14):5166. doi: 10.3390/s22145166

29. Bai BL, Wu ZY, Weng SJ, Yang Q. Application of interpretable machine learning algorithms to predict distant metastasis in osteosarcoma. *Cancer Med* (2022) 9. doi: 10.1002/cam4.5225

30. Miller BA, Feuer EJ, Hankey BF. Recent incidence trends for breast cancer in women and the relevance of early detection: an update. *CA Cancer J Clin* (1993) 43 (1):27–41. doi: 10.3322/canjclin.43.1.27

31. Wu S, Gu W. Association of T stage and serum CEA levels in determining survival of rectal cancer. *Front Med (Lausanne).* (2020) 106:270. doi: 10.3389/fmed.2019.00270

32. Becerra AZ, Probst CP, Tejani MA, Aquina CT, González MG, Hensley BJ, et al. Evaluating the prognostic role of elevated preoperative carcinoembryonic antigen levels in colon cancer patients: Results from the national cancer database. *Ann Surg Oncol* (2016) 23(5):1554–61. doi: 10.1245/s10434-015-5014-1

33. Ogata Y, Murakami H, Sasatomi T, Ishibashi N, Mori S, Ushijima M, et al. Elevated preoperative serum carcinoembrionic antigen level may be an effective indicator for needing adjuvant chemotherapy after potentially curative resection of stage II colon cancer. *J Surg Oncol* (2009) 99(1):65–70. doi: 10.1002/jso.21161

34. Quah HM, Chou JF, Gonen M, Shia J, Schrag D, Landmann RG, et al. Identification of patients with high-risk stage II colon cancer for adjuvant therapy. *Dis Colon Rectum.* (2008) 51(5):503–7. doi: 10.1007/s10350-008-9246-z

35. Myers EA, Feingold DL, Forde KA, Arnell T, Jang JH, Whelan RL. Colorectal cancer in patients under 50 years of age: a retrospective analysis of two institutions' experience. *World J Gastroenterol* (2013) 19(34):5651–7. doi: 10.3748/wjg.v19.i34.5651

36. Law JH, Koh FH, Tan KK. Young colorectal cancer patients often present too late. *Int J Colorectal Dis* (2017) 32(8):1165–9. doi: 10.1007/s00384-017-2837-1

37. Brown G, Richards CJ, Bourne MW, Newcombe RG, Radcliffe AG, Dallimore NS, et al. Morphologic predictors of lymph node status in rectal cancer with use of high-spatial-resolution MR imaging with histopathologic comparison. *Radiology* (2003) 227(2):371–7. doi: 10.1148/radiol.2272011747

38. Suliman MS, Singh M, Ajmeri AN, Stuart DL, Teka ST. Virchow's node: a case report of an extremely rare presentation of metastasis of adenocarcinoma with mucinous features from the colon. *Int J Gen Med* (2019) 12:137–40. doi: 10.2147/IJGM.S201617

39. Chen Z, Liu Z, Deng X, Warden C, Li W, Garcia-Aguilar J. Chromosomal copy number alterations are associated with persistent lymph node metastasis after chemoradiation in locally advanced rectal cancer. *Dis Colon Rectum.* (2012) 55 (6):677–85. doi: 10.1097/DCR.0b013e31824f873f

40. Huang CM, Huang MY, Ma CJ, Yeh Y-, Tsai HL, Huang CW, et al. Neoadjuvant FOLFOX chemotherapy combined with radiotherapy followed by radical resection in patients with locally advanced colon cancer. *Radiat Oncol* (2017) 12(1):48. doi: 10.1186/s13014-017-0790-3

41. Liu H, Cui Y, Shen W, Fan X, Cui L, Zhang C, et al. Pretreatment magnetic resonance imaging of regional lymph nodes with carcinoembryonic antigen in prediction of synchronous distant metastasis in patients with rectal cancer. *Oncotarget* (2016) 7(19):27199–207. doi: 10.18632/oncotarget.7979

42. Liu LL, Sun JD, Xiang ZL. A nomogram to predict the prognosis of patients with unresected rectal adenocarcinoma undergoing chemoradiotherapy: a population-based study. *J Cancer* (2021) 12(16):4745–61. doi: 10.7150/jca.61642

43. Li J, Yi CH, Hu YT, Li JS, Yuan Y, Zhang SZ, et al. TNM staging of colorectal cancer should be reconsidered according to weighting of the T stage: Verification based on a 25-year follow-up. *Med (Baltimore)* (2016) 95(6):e2711. doi: 10.1097/MD.0000000000002711

44. Tang M, Wang H, Cao Y, Zeng Z, Shan X, Wang L. Nomogram for predicting occurrence and prognosis of liver metastasis in colorectal cancer: a population-based study. *Int J Colorectal Dis* (2021) 36(2):271–82. doi: 10.1007/s00384-020-03722-8

45. Kow AWC. Hepatic metastasis from colorectal cancer. *J Gastrointest Oncol* (2019) 10(6):1274–98. doi: 10.21037/jgo.2019.08.06

46. Sterne JA, White IR, Carlin JB, Spratt M, Royston P, Kenward MG, et al. Multiple imputation for missing data in epidemiological and clinical research: potential and pitfalls. *BMJ* (2009) 338:b2393. doi: 10.1136/bmj.b2393

47. Deo RC. Machine learning in medicine. *Circulation* (2015) 132(20):1920–30. doi: 10.1161/CIRCULATIONAHA.115.001593

48. Ogunleye A, Wang QG. XGBoost model for chronic kidney disease diagnosis. *IEEE/ACM Trans Comput Biol Bioinform* (2020) 17(6):2131–40. doi: 10.1109/TCBB.2019.2911071

49. Gallagher DJ, Kemeny N. Metastatic colorectal cancer: from improved survival to potential cure. *Oncology* (2010) 78(3-4):237–48. doi: 10.1159/000315730

50. Fong Y, Fortner J, RL S, MF B, Blumgart LH. Clinical score for predicting recurrence after hepatic resection for metastatic colorectal cancer: analysis of 1001 consecutive cases. *Ann Surg* (1999) 230(3):309–18. doi: 10.1097/00000658-199909000-00004

frontiers | Frontiers in Oncology

TYPE Review
PUBLISHED 22 December 2022
DOI 10.3389/fonc.2022.1062704

Check for updates

OPEN ACCESS

EDITED BY
Zhendong Jin,
Second Military Medical University, China

REVIEWED BY
Wendi Ma,
University of Miami Health System, United States
Muhammad Azhar Nisar,
Tulane University, United States

*CORRESPONDENCE
Yang Shi
doctorshi1990@gmail.com;
fccshiy@zzu.edu.cn
Jingjing Zhang
zhangjingjing107@sina.com
Xing Ma
fccmax@zzu.edu.cn

†These authors have contributed equally to this work

SPECIALTY SECTION
This article was submitted to Gastrointestinal Cancers: Colorectal Cancer, a section of the journal Frontiers in Oncology

RECEIVED 06 October 2022
ACCEPTED 12 December 2022
PUBLISHED 22 December 2022

CITATION
Shi Y, Wang M, Zhang J, Xiang Z, Li C, Zhang J and Ma X (2022) Tailoring the clinical management of colorectal cancer by ^{18}F-FDG PET/CT. *Front. Oncol.* 12:1062704. doi: 10.3389/fonc.2022.1062704

COPYRIGHT
© 2022 Shi, Wang, Zhang, Xiang, Li, Zhang and Ma. This is an open-access article distributed under the terms of the Creative Commons Attribution License (CC BY). The use, distribution or reproduction in other forums is permitted, provided the original author(s) and the copyright owner(s) are credited and that the original publication in this journal is cited, in accordance with accepted academic practice. No use, distribution or reproduction is permitted which does not comply with these terms.

Tailoring the clinical management of colorectal cancer by ^{18}F-FDG PET/CT

Yang Shi[1,2*†], Meiqi Wang[3†], Jiyu Zhang[1,2], Zheng Xiang[4], Can Li[5], Jingjing Zhang[6*] and Xing Ma[7*]

[1]Department of Gastroenterology, the First Affiliated Hospital of Zhengzhou University, Zhengzhou, China, [2]State Key Laboratory for the Prevention and Treatment of Esophageal Cancer, Zhengzhou University, Zhengzhou, China, [3]Academy of Medical Sciences, Zhengzhou University, Zhengzhou, China, [4]Department of Pathology, Henan Provincial People's Hospital, Zhengzhou University People's Hospital, Henan University People's Hospital, Zhengzhou, China, [5]Department of Administration, The Affiliated Cancer Hospital of Zhengzhou University & Henan Cancer Hospital, Zhengzhou, China, [6]Department of Nuclear Medicine, the First Affiliated Hospital of Zhengzhou University, Zhengzhou, China, [7]Department of Nuclear Medicine, The Affiliated Cancer Hospital of Zhengzhou University & Henan Cancer Hospital, Zhengzhou, China

Colorectal cancer (CRC) is among the most commonly diagnosed gastrointestinal malignancies worldwide. It is inadequate to handle in terms of staging and restaging only based on morphological imaging modalities and serum surrogate markers. And the correct and timely staging of CRC is imperative to prognosis and management. When compared to established sequential, multimodal conventional diagnostic methods, the molecular and functional imaging ^{18}F-FDG PET/CT shows superiorities for tailoring appropriate treatment maneuvers to each patient. This review aims to summarize the utilities of ^{18}F-FDG PET/CT in CRC, focusing on primary staging, follow-up assessment of tumor responses and diagnostic of recurrence. In addition, we also summarize the technical considerations of PET/CT and the conventional imaging modalities in those patients who are either newly diagnosed with CRC or has already been treated from this cancer.

KEYWORDS

FDG PET/CT, colorectal cancer, TNM staging, treatment monitoring, restaging

1 Introduction

Colorectal cancer (CRC) is the first most common and leading cause of gastrointestinal cancers (GI) worldwide, whose incidence and mortality rates accounted for 10% and 9.4%, respectively (1). Based on the statistics from International Researches Agency of Cancer (IRAC), the incidence and mortality of CRC would increase 40.1% and 43.4% by 2040 worldwide, respectively (2). Approximately 20% of CRC patients have initially diagnosed with metastases, mostly

depositing in regional lymph nodes, liver, lung, and peritoneum (3). And the overall survival rate of patients is closely associated with stage at presentation; the 5-year survival rate drops drastically decreases from stage I (93%) to stage IV (8%) (4). Therefore, the precise staging of the CRC is essential for prognosis and effective therapy. The curative surgery has been remained as the "workhorse" at the early stage of cancers, and part of patients only with isolated liver metastasis (5). Nowadays, the standard of care regimens tends to be multidisciplinary, consisting of surgery, 5-fluorouracil-based chemotherapy, radiotherapy, targeted therapies, and PD-1/PD-L1 blockade biotherapy (5). Accurate pre- and postoperative staging are pivotal to tailor treatment avenues, which unequivocally improving the survival and quality of life. Variety of imaging techniques have been introduced for this purpose, with varying degree of success.

In the routine clinical practice, colonoscopy continues to be the preferred method for the diagnosis of colon cancer, because it allows tissue biopsies (6). In addition, a number of non-invasive imaging modalities, including as morphologic imaging such as computed tomography (CT), magnetic resonance imaging (MRI), and metabolic imaging such as positron emission tomography (PET), are presently used for staging colon cancer (7–9). Conventional imaging modalities, CT or MRI, are only based on the modifications of morphology of lesions, which could be invalid for cases mainly with metabolic changes. And serial elevated serum carcinoembryonic antigen (CEA) is usually coupled with false positives and false negatives (10). Recent studies showed that the combined-imaging modality is preferable for the detection and characterization of different malignant lesions including colorectum when compared with traditional imaging techniques (11). PET with flourine-18 fluorodeoxyglucose (^{18}F-FDG PET/CT, hereafter refers as PET/CT) not only provides alternations of morphology, but also glycolytic metabolism changes based on glucose uptake, which increasing early diagnostic efficacy and visualize active tumor tissue (12). As for the molecular imaging, PET/CT represents a valuable ally for staging, therapeutic monitoring, and restaging for CRC patients (13, 14). However, the false positives were usually occurred when infection, inflammation, and other non-neoplastic conditions (15). Despite these drawbacks, PET/CT is irreplaceable in its ability to assess the abnormal metabolic activity precedes morphological change and to identify small sized malignant tumors in morphologically normal structures. This review attempts to discuss the role of PET/CT in the treatment of patients with CRC, which could pave the way for early accurate diagnosis and even individualized therapeutic strategies.

2 Evaluation of the preoperative TNM staging

Tumor-Node-Metastasis (TNM) staging system (AJCC) has provided the universal framework for optimal management of CRC patients since 1959 (16). The curative surgery is the mainstay of treatment based on accurate preoperative staging by the combination of T, N, and M indicators (Figure 1). Although the conventional imaging has served as the standard modality for this staging, PET/CT has been shown superior to

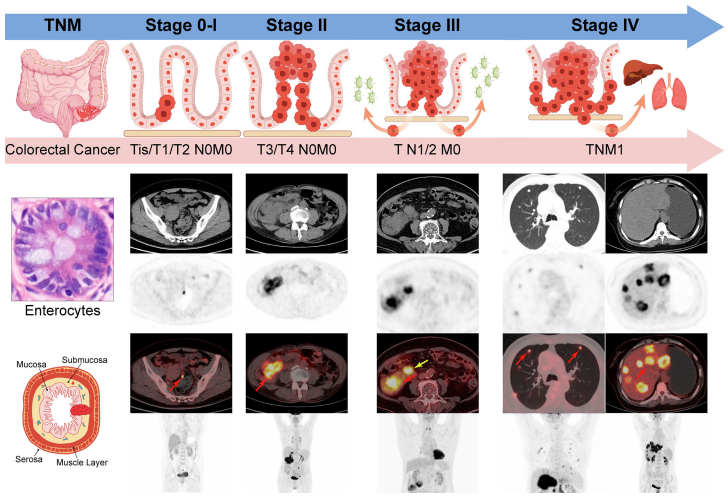

FIGURE 1
TNM stage of Colorectal cancer by AJCC 8th edition. Stage 0-I: Tumors spread within muscle layers without lymph nodes or distant deposits (Tis/T1/T2N0M0); Stage II: Tumors spread all layers or attached to nearby tissues without lymph nodes or distant deposits (T3/4N0M0); Stage III: Any T stage with the involvement of regional lymph nodes (TN1/2M0); Stage IV: Any T or N stage with distant metastasis (TNM1); Red arrow: the primary or metastatic tumors; yellow arrow: the metastatic lymph nodes.

evaluate the primary tumor, regional lymph nodes, and distant metastasis. Here we attempt to review and summarize the pros and cons of PET/CT in preoperative staging of CRC patients.

2.1 T-staging: The infiltration extent of primary tumor

Accurate preoperative evaluation of T-staging aids in selecting the related surgery approaches (17). Although limited spatial resolution of PET/CT confines its clinical application, there are still several strengths regarding preoperative assessment of T-staging. A meta-analysis including 2283 CRC patients from 28 studies shown the excellent performance for preoperative T-staging by PET/CT. The pooled specificity and AUC were 99% and 96%, respectively, which was significantly superior to CT (18). Other study demonstrated that the accurate preoperative T-staging was 94.3% except for only two tumors overestimation (19). As for the obstructive CRC, preoperative PET/CT colonography shows the particular advantages. Nagata K et al. demonstrated that PET/CT colonography could recognized all 13 primary CRC and 2 synchronous lesions proximal to the obstruction, while missed by other conventional imaging and optical colonoscopy more or less (20). Indeed, all lesions removed by single-stage procedure plays a vital role in the favorable outcomes of patients.

2.2 N-staging: Involvement of regional lymph nodes

Metastatic lymphadenopathy is indicated as a risk factor of recurrence and dismal survival in patients with CRC, which highlighting the merits of accurate detection and preoperative staging (21). The diagnosis of metastatic lymph nodes is generally based on a collection of morphological and density readout from the anatomic imaging techniques (CT & MRI). However, a plethora of positive lymph nodes tend to be not detected abnormality because of low density, small diameter, regular form and so on (22). Indeed, the overall accuracy of evaluation of N-staging by contrast enhanced CT (ceCT) has been reported merely from 59% to 71% (23, 24). Therefore, the alternative molecular imaging combined the morphological and functional techniques holds the promise for improving the diagnostic performance concerning metastatic deposits of CRC patients. Here we list several studies of the outstanding performance of PET/CT for this fields (Table 1) (22, 25–28).

For detection of regional lymph node metastasis, a retrospective study including 370 CRC patients showed superiority of PET/CT in specificity compared with CT (83.6% vs. 64.8%, $p = 0.000$), while inferiority in sensitivity (43.5% vs. 58.7%, $p = 0.029$) (25). Consistently, Kwak et al. also reported higher specificity of PET/CT, while the comparable sensitivity compared to CT (28). Absence of functional information from CT has been recognized as the main drawback responsible for the lower specificity, while the slightly higher sensitivity could be due to the limited spatial resolution of PET/CT (29). Besides, there are still several studies indicated the possible reasons of PET/CT fail to detect the metastatic lymph nodes (1): the interference from physiological uptake by bowel and bladder (2); the proximity to the primary tumor so as to interfere the diagnosis of regional lymph node (14, 30).

2.3 M-staging: Distant metastases

Life expectancy of CRC patients declines to 71% when local regional lymph nodes involved, while plummet to 17% in the case of distant metastases (31). Therefore, the clinical significance of tumor staging is particularly regarding the assessment of distant metastases. Although PET/CT has been suggested utilized in few circumstances, including metastatic synchronous adenocarcinoma, and metachronous metastases with elevated serial CEA but negative colonoscopy or CT,

TABLE 1 The comparison of diagnostic performance between CT and PET/CT for N-staging in CRC.

Ref.	Designs		Diagnostic Parameters (%)		
	Modality	No.	Sensitivity	Specificity	Accuracy
(22)	CT	220	58.7	64.8	62.3
	PET/CT		43.5	83.6	66.8
(23)	CT	473	87	29	59
	PET/CT		66	60	63
(25)	CT	370	38.4	95.5	65.0
	PET/CT		56.8	90.3	74.2
(26)	PET/CT	38	53.1	99.1	89.1
(27)	PET/CT	409	42.9	87.9	–

various clinical trials pertaining to PET/CT have shown advantages for M-staging. Given that liver metastasis is the main site of advanced CRC patients, ineligibility for curative hepatic resection is based on extrahepatic deposits except for few resectable lung metastases. Ruers et al. demonstrated that PET/CT could reduce the futile laparotomies concerning liver metastasis from 45% to 28%, which decreasing unnecessary procedures and economic burden to a large extent (32). Other retrospective study based on Korean population reported that PET/CT was superior to CT in specificity (94% vs. 87%) and accuracy (93% vs. 86%), which was accounted for the specific metabolic changes by the former (33). Therefore, more clinical trials pertaining to PET/CT should be performed in order to pave the way for clinical utilization.

3 Assessment of the response to targeted therapies

The developments of targeted therapies were renewed and have flourished in the past two decades (34). Recent applications of such treatments in CRC have been exemplified by the approval of oral kinase inhibitors or monoclonal antibodies, *e.g.*, anti-angiogenesis (VEGF) and targeting epidermal growth factor receptor (EGFR). However, given only part of patients respond to these targeted therapies, it has been highly recommended to early stratify patients in order to reduce unnecessary toxicity and economic burden. Generally, the anatomic imaging modalities based on RECIST criteria, CT or MRI, have been utilized to monitor the response of cytoreductive or cytotoxic chemotherapy, while shows inappropriate for evaluating the cytostatic effect by the above-mentioned targeted therapy (35, 36). It is a common knowledge that the alternations of glucose metabolism within tumor precede the morphological changes by several weeks (37). Within this framework, we review the most widely accepted PET tracer and the only licensed biomarker, ^{18}F-FDG (38), for assessing the responses to targeted therapies for patients with CRC.

Vascular endothelial growth factor (VEGF) targeted therapy disrupts tumor vasculature as well as inhibits angiogenesis, which have been exemplified by the first approved bevacizumab (Avastin) for metastatic colon cancer (mCRC) (39, 40). The semi-quantitative analysis of ^{18}F-FDG uptake compared to normal liver was demonstrated to be instrumental for pathologic response prediction to bevacizumab in mCRC (41). Because of the quantitative trait of PET, quantitative measurement for early treatment response shows more attraction. Standardized uptake value (SUV) is the widely accepted quantitative metric for assessing treatment response in clinical PET/CT utility (Figure 2) (42). For example, the reduction of maximum SUV (SUVmax) more than 50% showed predictive value for early response to Bevacizumab in mCRC patients, with the larger the decline, the greater the efficacy (43). And the relative decrease of SUVmax more than 15% presented highly predictive for non-responders detection after one cycle of Sorafenib combined with capecitabine in mCRC patients (44).

Dysregulations of EGFR pathway have been extensively involved in carcinogenesis of CRC, such as metastasis, proliferation, and resistant to apoptosis (45–47). The cetuximab-based regimens targeting EGFR signaling cascade is clinically utilized as the third-line therapy for mCRC patients without KRAS mutation (48). The PET Response Criteria in Solid Tumors (PERECIST) criterion was proposed for assessing the early therapy response by the relative change of SULpeak, *i.e.*, peak SUV normalized to lean body mass (SUL) in a spherical 1 cm^3 volume of interest (VOI) (49). Although treatment response using PERECIST predicted survival parameters (PFS & OS) at the end of

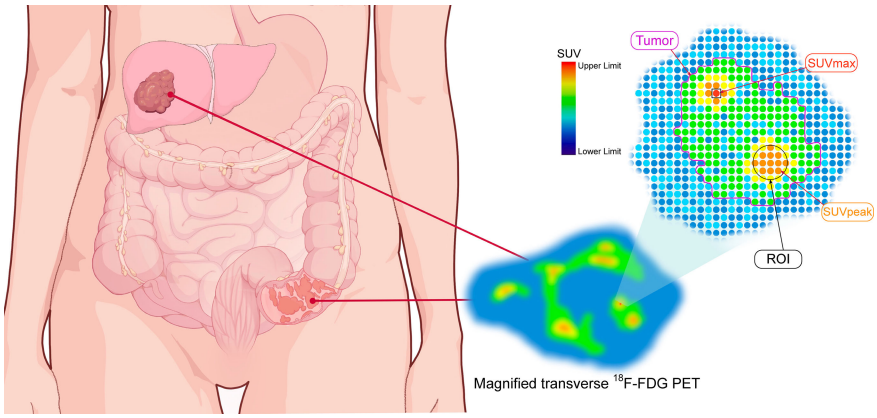

FIGURE 2
The schematic diagram of quantitative parameters of PET. The magnified transverse ^{18}F-FDG PET image of radiotracer uptake in tumor (purple outline). SUVmax: maximum standardized uptake value (red spot within black square); ROI: region of interest (black circle); SUVpeak: the average SUV obtained from a 1mL sphere within the tumor.

cetuximab-based therapy (4 week) for mCRC, the innovative principle based on any eligible VOI more than 2 could ahead of this schedule after one week (50). And the early metabolic response based on the reduction of SUVmax more than 20%, fitted with EORTC criteria (51), could serve as the surrogate parameter for early clinical response under cetuximab in CRC patients (52). All cases reviewed here are summarized in Table 2.

Therefore, detection of non-responders at early treatment stage could spare patients from the exposure of unnecessary toxicity and heavy economic burden.

4 Restaging of colorectal cancer

Most of CRC patients diagnosed at advanced staged would be suffered from recurrences, including liver, lung, and peritoneum metastases (21, 53). And serum markers and imaging modalities are utilized as the main examinations for those detection. Despite ceCT remains the clinical guideline recommendation, PET/CT is suggested in the workup of recurrent CRC patients with metachronous metastases, or elevated serial CEA but negative conventional imaging

TABLE 2 Evaluation of treatment response to targeted therapy by ^{18}F-FDG PET/CT.

Ref.	Designs			Patient Info.				Criteria			Results & Objectives
	Drug	Type	Target	Type	Traits	No. Patients	No. Lesions	Guideline	Aim	Cutoff	
(42)	Bevacizumab + Chemo	anti-VEGF	VEGF	mCRC	LM	7	17	Δ^{18}F-FDG uptake	CR	None uptake	Results: Response assessment = 70% Objectives: Pathologic outcome (% necrosis) prediction
(43)	Bevacizumab + Chemo	anti-VEGF	VEGF	mCRC	LM	11	–	–	Responders	ΔSUVmax >= -50%	Results: SUVmax from 8 (baseline) to 4 (after 1 cycle) Objectives: Early responders evaluation
(44)	Sorafenib + Chemo	VEGFR inhibitor	VEGF	mCRC	–	38	124	PERECIST adaptation	Responders	ΔSUVmax > -15%	Results: NPV of mR = 95%; PPV of mR = 72 % Objectives: Early non-responders detection
(50)	Cetuximab	anti-EGFR	EGFR	mCRC	*KRAS*-wt	27	85	–	Responders	(ΔSULpeak < 0 & SULpeak < 2)/VOI	Results: Favorable for PFS (p=0.001) & OS (p<0.001) Objectives: Early non-responders detection and survival prediction
(52)	Cetuximab	anti-EGFR	EGFR	mCRC	*KRAS*-wt	33	–	EORTC	Responders	ΔSUVmax > -20%	Results: Positive association: ΔSUVmax and ECR (OR=1.052, p=0.02) Objectives: Early non-responders detection

mCRC, metastatic colorectal cancer; LM, liver metastasis; Δ^{18}F-FDG uptake, relative change of ^{18}F-FDG uptake; CR, complete response; SUVmax, maximum standardized uptake value; ΔSUVmax = (SUVmax response - SUVmax baseline)/SUVmax baseline; NPV, negative predictive value; PPV, positive predictive value; mR, metabolic response; wt, wild type; SUL, SUV normalized to lean body mass; SULpeak, the average SUL within 1.2 cm diameter spheric VOI centered on the pixel with SULmax; ΔSULpeak, (SULpeak in S1 - SULpeak in S0)/(SULpeak in S0), S1, baseline of study, S1, study at the end of the first week; VOI, volume of interest; OS, overall survival; PFS, progression-free survival; ECR, early clinical response; OR, odds ratio.

modalities and optical colonoscopy. Besides, PET/CT also presents the unique strengths for those kinds of scenarios.

Distinction of recurrent lesions from postoperative scar tissues is the important superiority of PET/CT. FDG uptake within recurrences could significantly reduce false positives and false negatives as well (54). The sensitivity and specificity of serum surrogate marker CEA has been demonstrated elevated when combined with PET/CT. One of the retrospective studies including 112 patients showed the early detection of recurrent CRC was 71% compared with 55% of CT when CEA level greater than 13 ng/mL (55). Actually, the level of CEA less than 5 ng/mL also presented excellent performance by PET/CT (56). Besides, the diagnostic accuracy of PET/CT for recurrent cases with elevated CEA was moderate (65-75%) in the case of negative findings by conventional imaging modalities (57). Moreover, with the aim of assess the impact of PET/CT in tailoring management in CRC patients with proven or suspected recurrence, and further to evaluate the impact of different management on the prognosis of patients. Scott et al. reported that PET/CT modified the therapeutic strategies of 65.6% CRC patients with symptomatic or residual lesions suggestive of recurrence. And the treatment maneuvers of 43.9% patients with resectable metastatic deposits in lung or liver have also been changed. Besides, the additional lesions of those patients showed progressive disease in 60.5% and 65.9% in the above-mentioned two groups of patients compared with conventional imaging techniques (36.2% & 39.2%), which indicated the value of PET/CT regarding the stratification of patients into curative or palliative avenues (58). In addition, there are also plenty of studies demonstrated that the outstanding performance for recurrent lesions by PET/CT in comparison with CT or MRI, which was generally accounted for the combination with functional imaging (59–61).

5 Conclusion and perspective

Effective and precise pre- and postoperative staging is essential for the best and individualized management of CRC patients, especially for those with metastatic lesions. Nowadays, the conventional imaging modalities are still the mainstay for staging processes, while insensitivity to the monitor the treatment response of targeted therapy. Given that the single trait of morphological imaging techniques, the additional function of metabolic evaluation by PET/CT shows particular advantages, including early detection for tumors, sensitivity to the treatment response to cytostatic drugs, and evaluation numerous body regions in a single process. This makes PET/CT particularly helpful in the staging of patients to exclude the presence of distant metastases as well as in the restaging. However, more research is required to standardize the ideal PET/CT timing in relation to the chosen therapy (immunotherapy or chemotherapy). And there is still a dearth of information regarding the diagnostic potency of PET/CT in the evaluation of CRC. Given that anatomic imaging techniques are superior to detect small lesions because of the high resolution, the combined molecular and morphological imaging PET/CT would broaden its clinical utility. In conclusion, PET/CT adds value to the diagnosis of metastatic lesions and may aid patients with CRC in selecting more appropriate treatment modalities.

Author contributions

YS, XM, and JJZ formulated the design of this study; YS and XM wrote the manuscript; MW and CL revised the draft; JYZ drew the illustrations and figures; ZX assessed the histopathology of CRC. All authors contributed to the article and approved the submitted version.

Acknowledgments

We express our apology to the authors whose study could not be cited for the limited spaces. We would like to thanks Saif Ullah for his assistance in revising the manuscript.

Conflict of interest

The authors declare that the research was conducted in the absence of any commercial or financial relationships that could be construed as a potential conflict of interest.

Publisher's note

All claims expressed in this article are solely those of the authors and do not necessarily represent those of their affiliated organizations, or those of the publisher, the editors and the reviewers. Any product that may be evaluated in this article, or claim that may be made by its manufacturer, is not guaranteed or endorsed by the publisher.

References

1. Ferlay J, Colombet M, Soerjomataram I, Parkin DM, Piñeros M, Znaor A, et al. Cancer statistics for the year 2020: An overview. *Int J Cancer* (2021). doi: 10.1002/ijc.33588

2. Ferlay J, Laversanne M, Ervik M, Lam F, Colombet M, Mery L, et al. Global cancer observatory. In: *Cancer tomorrow Lyon*. France: International Agency for Research on Cancer (2020). Available at: https://gco.iarc.fr/tomorrow.

3. Van Cutsem E, Cervantes A, Nordlinger B, Arnold D. Metastatic colorectal cancer: Esmo clinical practice guidelines for diagnosis, treatment and follow-up. *Ann Oncol Off J Eur Soc Med Oncol* (2014) 25 Suppl 3::iii1–9. doi: 10.1093/annonc/mdu260

4. Diaz-Tasende J. Colorectal cancer screening and survival. *Rev Espanola Enfermedades Digestivas Organo Oficial la Sociedad Espanola Patologia Digestiva* (2018) 110(11):681–3. doi: 10.17235/reed.2018.5870/2018

5. Benson AB3rd, Venook AP, Cederquist L, Chan E, Chen YJ, Cooper HS, et al. Colon cancer, version 1.2017, nccn clinical practice guidelines in oncology. *J Natl Compr Cancer Netw JNCCN* (2017) 15(3):370–98. doi: 10.6004/jnccn.2017.0036

6. Zhang Q, Shen Y, Xu J, Gao P, Bing H. Clear colonoscopy as a surveillance tool in the prediction and reduction of advanced neoplasms: A randomized controlled trial. *Surg Endosc* (2021) 35(8):4501–10. doi: 10.1007/s00464-020-07964-z

7. Olsen ASF, Gundestrup AK, Kleif J, Thanon T, Bertelsen CA. Accuracy of preoperative staging with multidetector computed tomography in colon cancer. *Colorectal Dis Off J Assoc Coloproctol Great Britain Ireland* (2021) 23(3):680–8. doi: 10.1111/codi.15415

8. Chen SH, Miles K, Taylor SA, Ganeshan B, Rodriquez M, Fraioli F, et al. Fdg-Pet/Ct in colorectal cancer: Potential for vascular-metabolic imaging to provide markers of prognosis. *Eur J Nucl Med Mol Imag* (2021) 49(1):371–84. doi: 10.1007/s00259-021-05318-y

9. Nerad E, Lambregts DM, Kersten EL, Maas M, Bakers FC, van den Bosch HC, et al. Mri for local staging of colon cancer: Can mri become the optimal staging modality for patients with colon cancer? *Dis Colon Rectum* (2017) 60(4):385–92. doi: 10.1097/dcr.0000000000000794

10. Goldstein MJ, Mitchell EP. Carcinoembryonic antigen in the staging and follow-up of patients with colorectal cancer. *Cancer Invest* (2005) 23(4):338–51. doi: 10.1081/cnv-58878

11. Rodríguez-Fraile M, Cózar-Santiago MP, Sabaté-Llobera A, Caresia-Aróztegui AP, Delgado Bolton RC, Orcajo-Rincon J, et al. Fdg Pet/Ct in colorectal cancer. *Rev Espanola Medicina Nucl e Imagen Mol* (2020) 39(1):57–66. doi: 10.1016/j.remn.2019.09.009

12. Zhu A, Lee D, Shim H. Metabolic positron emission tomography imaging in cancer detection and therapy response. *Semin Oncol* (2011) 38(1):55–69. doi: 10.1053/j.seminoncol.2010.11.012

13. Almuhaideb A, Papathanasiou N, Bomanji J. 18f-fdg Pet/Ct imaging in oncology. *Ann Saudi Med* (2011) 31(1):3–13. doi: 10.4103/0256-4947.75771

14. Delbeke D, Martin WH. Pet and pet-ct for evaluation of colorectal carcinoma. *Semin Nucl Med* (2004) 34(3):209–23. doi: 10.1053/j.semnuclmed.2004.03.006

15. Hess S, Hansson SH, Pedersen KT, Basu S, Høilund-Carlsen PF. Fdg-Pet/Ct in infectious and inflammatory diseases. *PET Clinics* (2014) 9(4):497–519. doi: 10.1016/j.cpet.2014.07.002

16. Edge SB, Compton CC. The American joint committee on cancer: The 7th edition of the ajcc cancer staging manual and the future of tnm. *Ann Surg Oncol* (2010) 17(6):1471–4. doi: 10.1245/s10434-010-0985-4

17. Watanabe T, Muro K, Ajioka Y, Hashiguchi Y, Ito Y, Saito Y, et al. Japanese Society for cancer of the colon and rectum (Jsccr) guidelines 2016 for the treatment of colorectal cancer. *Int J Clin Oncol* (2018) 23(1):1–34. doi: 10.1007/s10147-017-1101-6

18. Ye Y, Liu T, Lu L, Wang G, Wang M, Li J, et al. Pre-operative tnm staging of primary colorectal cancer by (18)F-fdg pet-ct or pet: A meta-analysis including 2283 patients. *Int J Clin Exp Med* (2015) 8(11):21773–85.

19. Mainenti PP, Iodice D, Segreto S, Storto G, Magliulo M, De Palma GD, et al. Colorectal cancer and 18fdg-Pet/Ct: What about adding the T to the n parameter in loco-regional staging? *World J Gastroenterol* (2011) 17(11):1427–33. doi: 10.3748/wjg.v17.i11.1427

20. Nagata K, Ota Y, Okawa T, Endo S, Kudo SE. Pet/Ct colonography for the preoperative evaluation of the colon proximal to the obstructive colorectal cancer. *Dis Colon Rectum* (2008) 51(6):882–90. doi: 10.1007/s10350-008-9236-1

21. Riihimäki M, Hemminki A, Sundquist J, Hemminki K. Patterns of metastasis in colon and rectal cancer. *Sci Rep* (2016) 6:29765. doi: 10.1038/srep29765

22. Lee JY, Yoon SM, Kim JT, Kim KB, Kim MJ, Park JG, et al. Diagnostic and prognostic value of preoperative (18)F-fluorodeoxyglucose positron emission Tomography/Computed tomography for colorectal cancer: Comparison with conventional computed tomography. *Intestinal Res* (2017) 15(2):208–14. doi: 10.5217/ir.2017.15.2.208

23. Mainenti PP, Cirillo LC, Camera L, Persico F, Cantalupo T, Pace L, et al. Accuracy of single phase contrast enhanced multidetector ct colonography in the preoperative staging of colo-rectal cancer. *Eur J Radiol* (2006) 60(3):453–9. doi: 10.1016/j.ejrad.2006.08.001

24. Filippone A, Ambrosini R, Fuschi M, Marinelli T, Genovesi D, Bonomo L. Preoperative T and n staging of colorectal cancer: Accuracy of contrast-enhanced multi-detector row ct colonography–initial experience. *Radiology* (2004) 231(1):83–90. doi: 10.1148/radiol.2311021152

25. Sasaki K, Kawasaki H, Sato M, Koyama K, Yoshimi F, Nagai H. Impact of fluorine-18 2-Fluoro-2-Deoxy-D-Glucose uptake on preoperative positron emission Tomography/Computed tomography in the lymph nodes of patients with primary colorectal cancer. *Digest Surg* (2017) 34(1):60–7. doi: 10.1159/000448222

26. Kawashima K, Kato K, Tomabechi M, Matsuo M, Otsuka K, Ishida K, et al. Clinical evaluation of (18)F-fludeoxyglucose positron emission Tomography/Ct using point spread function reconstruction for nodal staging of colorectal cancer. *Br J Radiol* (2016) 89(1063):20150938. doi: 10.1259/bjr.20150938

27. Lu YY, Chen JH, Ding HJ, Chien CR, Lin WY, Kao CH. A systematic review and meta-analysis of pretherapeutic lymph node staging of colorectal cancer by 18f-fdg pet or Pet/Ct. *Nucl Med Commun* (2012) 33(11):1127–33. doi: 10.1097/MNM.0b013e328357b2d9

28. Kwak JY, Kim JS, Kim HJ, Ha HK, Yu CS, Kim JC. Diagnostic value of fdg-Pet/Ct for lymph node metastasis of colorectal cancer. *World J Surg* (2012) 36(8):1898–905. doi: 10.1007/s00268-012-1575-3

29. Dahmarde H, Parooie F, Salarzaei M. Is (18)F-fdg Pet/Ct an accurate way to detect lymph node metastasis in colorectal cancer: A systematic review and meta-analysis. *Contrast Media Mol Imaging* (2020) 2020:5439378. doi: 10.1155/2020/5439378

30. Kantorová I, Lipská L, Bêlohlávek O, Visokai V, Trubaĉ M, Schneiderová M. Routine (18)F-fdg pet preoperative staging of colorectal cancer: Comparison with conventional staging and its impact on treatment decision making. *J Nucl Med Off Publication Soc Nucl Med* (2003) 44(11):1784–8.

31. Maffione AM, Rubello D, Caroli P, Colletti PM, Matteucci F. Is it time to introduce Pet/Ct in colon cancer guidelines? *Clin Nucl Med* (2020) 45(7):525–30. doi: 10.1097/rlu.0000000000003076

32. Ruers TJ, Wiering B, van der Sijp JR, Roumen RM, de Jong KP, Comans EF, et al. Improved selection of patients for hepatic surgery of colorectal liver metastases with (18)F-fdg pet: A randomized study. *J Nucl Med Off Publication Soc Nucl Med* (2009) 50(7):1036–41. doi: 10.2967/jnumed.109.063040

33. Lee JY, Ock M, Jo MW, Son WS, Lee HJ, Kim SH, et al. Estimating utility weights and quality-adjusted life year loss for colorectal cancer-related health states in Korea. *Sci Rep* (2017) 7(1):5571. doi: 10.1038/s41598-017-06004-6

34. Lee YT, Tan YJ, Oon CE. Molecular targeted therapy: Treating cancer with specificity. *Eur J Pharmacol* (2018) 834:188–96. doi: 10.1016/j.ejphar.2018.07.034

35. Eisenhauer EA, Therasse P, Bogaerts J, Schwartz LH, Sargent D, Ford R, et al. New response evaluation criteria in solid tumours: Revised recist guideline (Version 1.1). *Eur J Cancer (Oxf Engl 1990)* (2009) 45(2):228–47. doi: 10.1016/j.ejca.2008.10.026

36. Skougaard K, Johannesen HH, Nielsen D, Schou JV, Jensen BV, Høgdall EV, et al. Ct versus fdg-Pet/Ct response evaluation in patients with metastatic colorectal cancer treated with irinotecan and cetuximab. *Cancer Med* (2014) 3(5):1294–301. doi: 10.1002/cam4.271

37. Lordick F, Ott K, Krause BJ, Weber WA, Becker K, Stein HJ, et al. Pet to assess early metabolic response and to guide treatment of adenocarcinoma of the oesophagogastric junction: The munich phase ii trial. *Lancet Oncol* (2007) 8(9):797–805. doi: 10.1016/s1470-2045(07)70244-9

38. Juweid ME, Cheson BD. Positron-emission tomography and assessment of cancer therapy. *New Engl J Med* (2006) 354(5):496–507. doi: 10.1056/NEJMra050276

39. Folkman J, Klagsbrun M. Angiogenic factors. *Sci (New York NY)* (1987) 235(4787):442–7. doi: 10.1126/science.2432664

40. Ferrara N, Hillan KJ, Gerber HP, Novotny W. Discovery and development of bevacizumab, an anti-vegf antibody for treating cancer. *Nat Rev Drug Discov* (2004) 3(5):391–400. doi: 10.1038/nrd1381

41. Goshen E, Davidson T, Zwas ST, Aderka D. Pet/Ct in the evaluation of response to treatment of liver metastases from colorectal cancer with bevacizumab

and irinotecan. *Technol Cancer Res Treat* (2006) 5(1):37–43. doi: 10.1177/153303460600500105

42. Kinahan PE, Fletcher JW. Positron emission tomography-computed tomography standardized uptake values in clinical practice and assessing response to therapy. *Semin Ultrasound CT MR* (2010) 31(6):496–505. doi: 10.1053/j.sult.2010.10.001

43. Malavasi N, Bagni B, Bertolini F, Dealis C, Depenni R, Cucca M, et al. Predictive role of fluorodeoxyglucose positron emission tomography (18 ff-fdg ct-pet) in early assessment of response to bevacizumab and folfox-6 combined neoadjuvant therapy for liver metastasis (Lm) from colorectal cancer (Crc). *J Clin Oncol* (2008) 26(15_suppl):15094–. doi: 10.1200/jco.2008.26.15_suppl.15094

44. Woff E, Hendlisz A, Garcia C, Deleporte A, Delaunoit T, Maréchal R, et al. Monitoring metabolic response using fdg pet-ct during targeted therapy for metastatic colorectal cancer. *Eur J Nucl Med Mol Imag* (2016) 43(10):1792–801. doi: 10.1007/s00259-016-3365-x

45. Ward WH, Cook PN, Slater AM, Davies DH, Holdgate GA, Green LR. Epidermal growth factor receptor tyrosine kinase. *Invest Catalytic Mechanism Structure Based Searching Discovery Potent Inhibitor Biochem Pharmacol* (1994) 48 (4):659–66. doi: 10.1016/0006-2952(94)90042-6

46. Huang SM, Harari PM. Epidermal growth factor receptor inhibition in cancer therapy: Biology, rationale and preliminary clinical results. *Invest New Drugs* (1999) 17(3):259–69. doi: 10.1023/a:1006384521198

47. Spano JP, Lagorce C, Atlan D, Milano G, Domont J, Benamouzig R, et al. Impact of Egfr Expression on Colorectal Cancer Patient Prognosis and Survival. *Annals of oncology : official journal of the European Society for Medical Oncology* (2005) 16(1):102–8. doi: 10.1093/annonc/mdi006

48. Chu E. An update on the current and emerging targeted agents in metastatic colorectal cancer. *Clin Colorectal Cancer* (2012) 11(1):1–13. doi: 10.1016/j.clcc.2011.05.005

49. Wahl RL, Jacene H, Kasamon Y, Lodge MA. From recist to percist: Evolving considerations for pet response criteria in solid tumors. *J Nucl Med Off Publication Soc Nucl Med* (2009) 50 Suppl 1(Suppl 1):122s–50s. doi: 10.2967/jnumed.108.057307

50. Liu FY, Yen TC, Wang JY, Yang TS. Early prediction by 18f-fdg Pet/Ct for progression-free survival and overall survival in patients with metastatic colorectal cancer receiving third-line cetuximab-based therapy. *Clin Nucl Med* (2015) 40 (3):200–5. doi: 10.1097/rlu.0000000000000693

51. Young H, Baum R, Cremerius U, Herholz K, Hoekstra O, Lammertsma AA, et al. Measurement of clinical and subclinical tumour response using [18f]-fluorodeoxyglucose and positron emission tomography: Review and 1999 eortc recommendations. European organization for research and treatment of cancer (Eortc) pet study group. *Eur J Cancer (Oxf Engl 1990)* (1999) 35(13):1773–82. doi: 10.1016/s0959-8049(99)00229-4

52. Berger AK, Lücke S, Abel U, Haag GM, Grüllich C, Stange A, et al. Early metabolic response in sequential fdg-Pet/Ct under cetuximab is a predictive marker for clinical response in first-line metastatic colorectal cancer patients: Results of the phase ii remotux trial. *Br J Cancer* (2018) 119(2):170–5. doi: 10.1038/s41416-018-0152-4

53. Dromain C, Caramella C, Dartigues P, Goere D, Ducreux M, Deschamps F. Liver, lung and peritoneal metastases in colorectal cancers: Is the patient still curable? what should the radiologist know. *Diagn Intervent Imag* (2014) 95(5):513–23. doi: 10.1016/j.diii.2014.03.011

54. O'Connor OJ, McDermott S, Slattery J, Sahani D, Blake MA. The use of pet-ct in the assessment of patients with colorectal carcinoma. *Int J Surg Oncol* (2011) 2011:846512. doi: 10.1155/2011/846512

55. Huang YY, Lee PI, Liu MC, Chen CC, Huang KC, Huang AT. A general cutoff level combined with personalized dynamic change of serum carcinoembryonic antigen can suggest timely use of fdg pet for early detection of recurrent colorectal cancer. *Clin Nucl Med* (2015) 40(10):e465–9. doi: 10.1097/rlu.0000000000000900

56. Sanli Y, Kuyumcu S, Ozkan ZG, Kilic L, Balik E, Turkmen C, et al. The utility of fdg-Pet/Ct as an effective tool for detecting recurrent colorectal cancer regardless of serum cea levels. *Ann Nucl Med* (2012) 26(7):551–8. doi: 10.1007/s12149-012-0609-0

57. Kalff V, Hicks RJ, Ware RE, Hogg A, Binns D, McKenzie AF. The clinical impact of (18)F-fdg pet in patients with suspected or confirmed recurrence of colorectal cancer: A prospective study. *J Nucl Med Off Publication Soc Nucl Med* (2002) 43(4):492–9.

58. Scott AM, Gunawardana DH, Kelley B, Stuckey JG, Byrne AJ, Ramshaw JE, et al. Pet changes management and improves prognostic stratification in patients with recurrent colorectal cancer: Results of a multicenter prospective study. *J Nucl Med Off Publication Soc Nucl Med* (2008) 49(9):1451–7. doi: 10.2967/jnumed.108.051615

59. Odalovic S, Stojiljkovic M, Sobic-Saranovic D, Pandurevic S, Brajkovic L, Milosevic I, et al. Prospective study on diagnostic and prognostic significance of postoperative fdg Pet/Ct in recurrent colorectal carcinoma patients: Comparison with mri and tumor markers. *Neoplasma* (2017) 64(6):954–61. doi: 10.4149/neo_2017_613

60. Caglar M, Yener C, Karabulut E. Value of ct, fdg pet-ct and serum tumor markers in staging recurrent colorectal cancer. *Int J Comput Assisted Radiol Surg* (2015) 10(7):993–1002. doi: 10.1007/s11548-014-1115-8

61. Uzun AK, Guveli TK, Ozulker F, Ozulker T. The efficacy of [Sup. 18] f-fdg Pet/Ct in detecting colorectal cancer recurrences. *Eur Arch Med Res* (2021) 37 (4):236–44. doi: 10.4274/eamr.galenos.2021.52533

frontiers | Frontiers in Oncology

TYPE Original Research
PUBLISHED 22 December 2022
DOI 10.3389/fonc.2022.1037783

Check for updates

OPEN ACCESS

EDITED BY
Zhendong Jin,
Second Military Medical University, China

REVIEWED BY
Xian-Shu Gao,
First Hospital, Peking University, China
Ruiguo Zhang,
Tianjin Medical University General Hospital, China
Raluca Mititelu,
Central University Emergency Military Hospital Bucharest Romania, Romania

*CORRESPONDENCE
Guiying Wang
wgywfp@126.com;
wfpzhj@126.com

†These authors have contributed equally to this work

SPECIALTY SECTION
This article was submitted to Gastrointestinal Cancers: Colorectal Cancer, a section of the journal Frontiers in Oncology

RECEIVED 06 September 2022
ACCEPTED 12 December 2022
PUBLISHED 22 December 2022

CITATION
Wu F, Zhang X, Yang C, Wang K, Xiao L, Zhou C, Zhao X and Wang G (2022) The reduction of ^{18}F-FDG uptake ability of tumor tissue after neoadjuvant chemoradiotherapy in locally advanced rectal cancer can effectively reflect the degree of tumor regression.
Front. Oncol. 12:1037783.
doi: 10.3389/fonc.2022.1037783

COPYRIGHT
© 2022 Wu, Zhang, Yang, Wang, Xiao, Zhou, Zhao and Wang. This is an open-access article distributed under the terms of the Creative Commons Attribution License (CC BY). The use, distribution or reproduction in other forums is permitted, provided the original author(s) and the copyright owner(s) are credited and that the original publication in this journal is cited, in accordance with accepted academic practice. No use, distribution or reproduction is permitted which does not comply with these terms.

The reduction of ^{18}F-FDG uptake ability of tumor tissue after neoadjuvant chemoradiotherapy in locally advanced rectal cancer can effectively reflect the degree of tumor regression

Fengpeng Wu[1†], Xiaoxiao Zhang[1,2†], Congrong Yang[1], Kanghua Wang[1,3], Linlin Xiao[1], Chaoxi Zhou[4], Xinming Zhao[5†] and Guiying Wang[2,6*†]

[1]Department of Radiation Oncology, Fourth Hospital of Hebei Medical University, Shijiazhuang, China, [2]Department of Radiation Oncology, Hebei Cancer Hospital Chinese Academy of Medical Sciences, Langfang, China, [3]Department of Medical Oncology, Affiliated Hospital Of Hebei University, Baoding, China, [4]Department of General Surgery, Fourth Hospital of Hebei Medical University, Shijiazhuang, China, [5]Department of Nuclear Medicine, Fourth Hospital of Hebei Medical University, Shijiazhuang, China, [6]Department of General Surgery, Second Hospital of Hebei Medical University, Shijiazhuang, China

Introduction: To evaluate the predictive value of ^{18}F-fluorodeoxyglucose positron emission tomography–computed tomography (^{18}F-FDG PET-CT) imaging parameters for the response to neoadjuvant chemoradiotherapy (nCRT) in locally advanced rectal cancer (LARC).

Methods: From January 2016 to March 2020, 52 LARC patients who underwent ^{18}F-FDG PET-CT scans within 1 week before and 8-9 weeks after nCRT, were enrolled in this study according to a pre-designed screening criteria. After total mesorectal excision (TME) surgery, we assessed tumor response to treatment and analyzed the correlation between imaging parameters obtained from two PET-CT scans and tumor regression status.

Results: Tumor response assessment showed that 13 of 52 patients received good response (GR), including 9 cases with pathological complete regression (pCR) and 4 cases with near-pathological complete regression (near-pCR). We also found that the maximum standard uptake value after nCRT (post-SUVmax), the response index (RI), the mean standard uptake values after nCRT (post-SUVmean), and the ratio of tumor SUVmean to liver SUVmean after nCRT (post-Ratio), were correlated with GR and pCR. Among these parameters, post-SUVmax and RI had a near-strong correlation with pCR (r_s= -0.58 and 0.59, respectively), and also had a strong correlation with GR (r_s = -0.7 and 0.63, respectively). Further ROC analysis showed that post-SUVmax and RI had

higher values in predicting whether patients could achieve GR and pCR after nCRT, and the area under the curve (AUC) of both were greater than 0.9. The positive predictive values (PPVs) and negative predictive values (NPVs) of post-SUVmax for GR were 80.01% and 97.3%, and for pCR were 66.68% and 97.5%, respectively. The PPVs and NPVs of the RI values for GR were 84.61% and 94.87%, and for pCR were 69.24% and 100%, respectively.

Conclusion: For LARC patients, the analysis of imaging parameters such as post-SUVmax and RI, which can reflect the changes of ^{18}F-FDG uptake capacity of tumor tissues before and after nCRT, is of great value for predicting the response of patients to neoadjuvant therapy and guiding the selection of subsequent treatment strategies.

KEYWORDS

locally advanced rectal cancer, neoadjuvant chemoradiotherapy (NACRT), 18F-FDG PET-CT, pathological complete regression, near-pathological complete regression, clinical complete regression

Introduction

Neoadjuvant chemoradiotherapy (nCRT) combined with total mesorectal excision (TME) has been widely used as a standard treatment for locally advanced rectal cancer (LARC) patients. However, the follow-up treatment strategy for patients with good response (GR) after nCRT is still controversial. From the perspective of local radical treatment, TME is undoubtedly the most thorough treatment. However, there are some unavoidable problems with this treatment, especially for patients whose primary lesion is adjacent to the anorectal ring plane, even though clinical complete regression (cCR) is obtained, it is difficult to avoid the implementation of Miles operation. In addition, postoperative complications such as intestinal leakage, sepsis, abscess, wound healing difficulties, and cardiopulmonary complications usually increase significantly in patients who have received radical radiotherapy.

At present, the concept of personalized therapy is receiving more and more attention, and the method of screening the group suitable for sphincter retention therapy from the patients with GR after nCRT is increasingly emerging. Watch and Wait (W&W) strategy and local excision (LE) strategy are the focus of subsequent treatment of patients with cCR and near clinical complete response (near-cCR). However, clinical data show that the local recurrence rate of patients with "W & W" is still 21-25% within 2 years (1–3), and 7% of patients with LE strategy have local recurrence within 5 years (4). Therefore, whether cCR can be used as the standard to determine the treatment strategy of patients with LARC after nCRT is still debatable. Currently, it is indisputable that pCR is the best endpoint of nCRT, Pang's meta-analysis showed that patients with pCR were superior to cCR patients in 2-year LR (0.568% *vs.* 9.82%) and 5-year prognosis (DFS: 86.86% *vs.* 73.33%, OS: 91.92% *vs.* 80%) (5). However, patients who have obtained pCR after nCRT must be confirmed by pathology after surgery, so it is necessary to find an effective method to evaluate whether patients have achieved pCR before surgery.

^{18}F-fluorodeoxyglucose positron emission tomography–computed tomography (^{18} F-FDG PET-CT) can not only distinguish benign and malignant lesions accurately through the uptake of ^{18}F-FDG by cells, but also has important significance in evaluating the therapeutic response of tumors. However, due to the high cost of examination, PET-CT is still mainly used in the differential diagnosis of newly diagnosed patients, and its application in evaluating the efficacy of cancer patients is relatively rare. For LARC patients, although the value of PET-CT imaging parameters in the evaluation of nCRT reactivity has been reported, due to the different intervals between the second PET-CT scaning and nCRT in these studies, the significant evaluation parameters and their optimal cut-off values are different (6–8).

In this study, we screened 52 LARC patients who had performed PET-CT scans within 1 week before nCRT and 8-9 weeks after nCRT (shortly before TME surgery) from previous clinical data, and analyzed the predictive values of PET-CT imaging parameters for GR and pCR patients. The purpose is to provide a basis for the selection of individualized treatment options for LARC patients with GR after nCRT.

Materials and methods

Patients

LARC patients who completed neoadjuvant therapy combined with TME surgery, and performed PET-CT scans before and after neoadjuvant therapy in the Fourth Hospital of Hebei Medical University from January 2016 to March 2020, were included in this study. The inclusion criteria were as follows: (1) Histopathology confirmed rectal adenocarcinoma before neoadjuvant therapy; (2) T3-4, N0/N+, and M0 were diagnosed by imaging examination (Chest CT, Abdominal and Pelvic MRI) at initial diagnosis; (3) Neoadjuvant therapy and TME surgery were completed before entering this study; (4)The mode of neoadjuvant therapy was long- course concurrent chemoradiotherapy recommended by NCCN guidelines; (5) Before entering this study, two PET-CT examinations were completed, and the first PET-CT was performed within 1 week before nCRT, and the second PET-CT was performed within 8-9 weeks after nCRT. The exclusion criteria included: (1) Patients with other malignancies besides rectal cancer; (2) Patients with primary tumor baseline assessment of T1-2 before nCRT; (3) The timing of PET-CT scan was not within the period required for enrollment in this study; (4) SUVmax value of the primary lesion <2.0 in the first PET-CT; (5) The neoadjuvant therapy was chemotherapy alone, short-course radiotherapy (SCRT) or induction chemotherapy before radiotherapy; (6) The second PET-CT scan revealed distant metastasis. The collection of clinical data was approved by the ethics committee of the fourth hospital of Hebei Medical University (Number: 2021104). The data are anonymous, and the requirement for informed consent was therefore waived.

Treatment procedures

The treatment plan was determined by a multidisciplinary team consisting of gastrointestinal surgeons, medical oncologists, medical imaging specialists, and radiation oncologists. The neoadjuvant regimen was long-course concurrent chemoradiotherapy, and TME surgery was performed 9-10 weeks after nCRT. The prescription dose of radiotherapy was implemented in two phases: the first phase was 45Gy/25 fractions (45Gy/25F), 1.8Gy/1F, 5F/W, and the dose was received by planning target volume (PTV); the second phase was 5.4Gy/3F, 1.8Gy/1F, 5F/W, and the dose was received by clinical target volume-high (CTV-H). The radiotherapy targets were defined on the basis of the International Commission on Radiation Units and Measurements report no. 83 (2010) and the recommendations by Nancy in his academic writings (9). All patients received capecitabine (825 mg m^{-2}) bid by oral concurrently with RT, and suspended drug use when RT was disrupted every weekend.

PET-CT scans and image parameter analysis

The baseline PET-CT was completed within 1 week before nCRT, and the second PET-CT scan was completed within 8-9 weeks after radiotherapy. Patients were fasting for at least 6 hours before injection of ^{18}F-FDG (2.6-3.7 MBq/kg), and fasting blood glucose was required to be less than 12mg/dl. PET-CT scans (GEMINI GXL-16 PET-CT scanner, Philips, Netherlands) was performed after one hour of calm rest post-injection. All scans were performed on the same scanner with the same acquisition and reconstruction protocols. Each patient was asked to empty as much urine as possible before the scan. Patient was supine with arms raised during the scan. Spiral CT scan from the top of the head to the mid-thigh. PET scanning parameters were as follows: ube voltage, 120kV; tube current, 160 mAs; matrix, 512×512; pitch 0.813, slice thickness, 5mm; and rotation time, 0.5s. The PET image was acquired at 2.5min/bed using a three-dimensional model. PET and CT images were fused with syntegra software and transmitted to the Philips service workstation.

The PET-CT images were read by two experienced radiology and nuclear medicine physicians, and the imaging parameters for the efficacy assessment of patients were as follows: SUVmax (incl. pre-SUVmax, post-SUVmax); SUVmean (incl. pre-SUVmean, post-SUVmean); metabolic tumor volume (MTV), (incl. pre-MTV, post-MTV); response index (RI), RI=[(pre-SUVmax−post-SUVmax)/pre-SUVmax]×100%; total lesion glycolysis (TLG) (incl. pre-TLG, post-TLG), TLG=SUVmean×MTV; Ratio of tumor SUVmean to liver SUVmean×100% (incl. pre-Ratio, post-Ratio).

Pathological response evaluation

The efficacy of nCRT was evaluated by two pathologists according to the tumor regression grading (TRG) of mDworak standard, which was established by Kim (10) based on the standard of Dworak (11). The mDworak TRG standard is as follows: TRG 1 (minimal regression), defined as a dominant tumor mass encompassing more than 50% of the primary tumor and/or regional lymph node (LN) metastase; TRG 2 (moderate regression), defined as dominant fibroinflammatory changes with vasculopathy encompassing more than 50% of the entire tumor, including the tumor, regional LN metastases, and perirectal tumor deposits; TRG 3 (near complete regression), defined as one or two microscopic foci (each< 0.5 cm in

diameter) of residual tumor cells or groups in the primary tumor and regional LNs; TRG 4 (complete regression), defined as no residual tumor cells in the primary tumor and regional LNs (ypT0N0). In this study, we defined TRG 3 as near-pCR, TRG 4 as pCR, TRG 3 and TRG 4 as good response (GR).

Statistical analysis

Statistical analysis was performed using SPSS software 22.0 (SPSS, Inc., Chicago, IL, USA) and MedCalc Version 16.2. Quantitative data that conform to normal distribution were described in the form of $x \pm SD$, while those that do not conform to normal distribution were described in the form of median (quaternary interval), i.e. M (Q_R). Comparison of differences among quantitative data: T test was used for those meeting normal distribution and homogeneity of variance, while Wilcoxon rank sum test was used for those not meeting normal distribution. Spearman method was used to analyze the correlation between imaging parameters and tumor regression. The correlation coefficient was expressed by r_s, $0.2< r_s \leq 0.4$ means weak correlation, $0.4\leq r_s <0.6$ means moderate correlation, $0.6 \leq r_s \leq 1.0$ means a strong correlation. Receiver operating characteristic (ROC) curve analysis was used to evaluate the diagnostic performance of significant imaging parameters. In this study, $P < 0.05$ was considered statistically significant.

Results

Characteristics of enrolled patients

From January 2016 to March 2020, there were 174 LARC patients who completed two PET-CT scans before and after neoadjuvant treatment were found in our center, of which 52 patients met the screening criteria of this study (Figure 1). The median age of these patients (42 males and 10 females) was 53.2 years (36-77.6), and the clinical stage was as follows: 36 patients had cT3, 16 had cT4 tumors; 4 patients had cN0, 7 had cN1 and 41 had cN2 diseases. In terms of the efficacy evaluation of nCRT, according to the mDworak standard, pathology experts identified 13 of 52 cases with TRG 1, 26 with TRG 2, 4 with TRG 3, and 9 with TRG 4. In our study, patients with TRG 1-2 status were defined as non-GR, TRG 3-4 status as GR, TRG3 status as near-pCR, TRG 4 status as pCR, and patients without TRG 4 status were defined as non-pCR. The main clinical characteristics of the patients and their response status to nCRT were listed in Table 1.

PET/CT imaging parameters of pCR and non-pCR patients

After analyzed the difference of PET-CT parameters between pCR and non-pCR patients by Wilcoxon rank sum test, we found that there were statistically significant differences in post-SUVmax, RI, post-SUVmean and post-Ratio between the two groups ($P < 0.05$). RI in pCR group was significantly higher than that in non-PCR group, while post-SUVmax, post-SUVmean and post-Ratio were significantly lower than those in non-pCR group. Spearman correlation analysis showed that RI ($r_s = 0.59$, $P < 0.001$) and post-SUVmax ($r_s= -0.58$, $P < 0.001$) were near-strongly correlated with pCR, post-SUVmean ($r_s = -0.43$, $P=0.001$), was moderately negatively correlated with pCR, while post-Ratio ($r_s=-0.36$, $P=0.009$) was weakly negatively correlated with pCR, as shown in Table 2. ROC curve analysis showed that the area under curve (AUC) of post-SUVmax, RI, post-SUVmean and post-Ratio were 0.939, 0.951, 0.831 and 0.775, respectively. Using post-SUVmax ≤ 2.5, RI > 0.67, post-SUVmean ≤ 2.2 and post-Ratio ≤ 1.39 as cut-off values, the sensitivity of these parameters to pCR diagnosis were 88.89%, 100%, 100% and 100%, the specificity were 90.7%, 90.7%, 65.12% and 55.81%, the positive predictive values (PPVs) were 66.68%, 69.24%, 37.51% and 32.14%, and the negative predictive values (NPVs) were 97.5%, 100%, 100% and 100%, respectively, as shown in Figure 2 and Table 3.

PET/CT imaging parameters of GR and non-GR patient

The differential analysis for PET-CT parameters between GR and non-GR patients showed that there were statistically significant differences in post-SUVmax, RI, post-SUVmean, post-TLG, post-Ratio between the two groups ($P< 0.05$). RI in

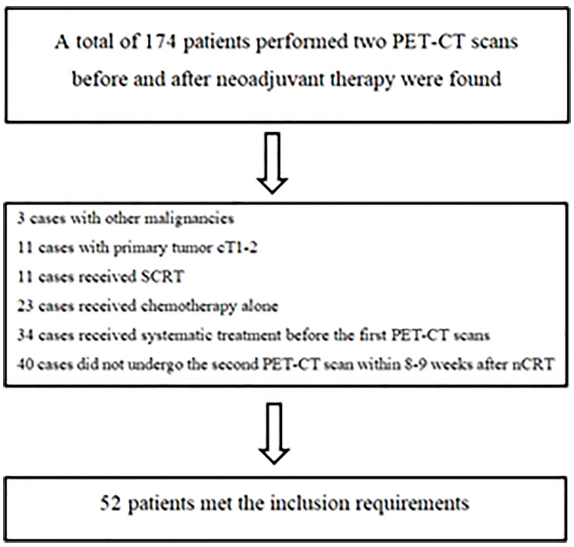

FIGURE 1
Screening process of selected patients.

10.3389/fonc.2022.1037783

TABLE 1 Characteristics of patients and tumor response to nCRT (N, %).

Characteristic	near-pCR	pCR	non-pCR	GR	non-GR
Gender					
Male	3 (7.14%)	7 (16.67%)	35 (83.33%)	10 (23.81%)	32 (76.19%)
Female	1 (10.00%)	2 (20.00%)	8 (80.00%)	3 (30.00%)	7 (70.00%)
Age					
<53.2Y	2 (7.69%)	6 (23.08%)	20 (76.92%)	8 (30.77%)	18 (69.23%)
>53.2Y	2 (7.69%)	3 (11.54%)	23 (88.46%)	5 (19.23%)	21 (80.77%)
Distance to anal verge					
≤5cm	2 (10.00%)	4 (20.00%)	16 (80.00%)	6 (30.00%)	14 (70.00%)
>5cm	2 (6.25%)	5 (15.63%)	27 (84.37%)	7 (21.88%)	25 (78.12%)
T-stage					
cT_3	2 (5.56%)	5 (13.89%)	31 (86.11%)	7 (19.44%)	29 (80.56%)
cT_4	2 (12.50%)	4 (25.00%)	12 (75.00%)	6 (37.50%)	10 (62.50%)
N-stage					
cN_0	0 (0.00%)	1 (25.00%)	3 (75.00%)	1 (25.00%)	3 (75.00%)
cN_1	2 (28.57%)	1 (14.29%)	6 (85.71%)	3 (42.86%)	4 (57.14%)
cN_2	2 (4.88%)	7 (17.07%)	34 (82.93%)	9 (21.95%)	32 (78.05%)
Total	4 (7.69%)	9 (17.31%)	43 (82.69%)	13 (25.00%)	39 (75.00%)

nCRT, neoadjuvant chemoradiotherapy; pCR, pathological complete regression; GR, good response.

TABLE 2 Correlation analysis of parameters of ^{18}F-FDG PET-CT in pCR and non-pCR.

Parameters	Wilcoxon			Spearman	
	pCR, M(Q_R)	non-pCR,M(Q_R)	*P* value	r_s	*P* value
Pre-SUVmax	8.50 (7.55)	7.78 (6.80)	0.371	0.13	0.367
post-SUVmax	2.10 (0.55)	6.10 (4.52)	<0.001	-0.58	<0.001
RI	0.75(0.09)	0.41(0.47)	<0.001	0.59	<0.001
pre-SUVmean	5.56(2.09)	4.52 (3.82)	0.371	0.13	0.376
post-SUVmean	1.53(0.61)	2.91(2.48)	0.002	-0.43	0.001
pre-MTV	22.00 (28.00)	28.00(22.00)	0.377	-0.12	0.382
post-MTV	4.00(12.00)	5.00(5.00)	0.567	-0.08	0.572
ΔMTV	0.77(0.18)	0.77(0.22)	0.856	0.07	0.641
pre-TLG	109.46(109.09)	139.02(140.46)	0.781	-0.04	0.784
post-TLG	6.60 (18.04)	17.25 (20.24)	0.137	-0.21	0.138
ΔTLG	0.92(0.05)	0.88(0.18)	0.064	0.03	0.821
pre-Ratio	2.79 (2.26)	2.44 (1.47)	0.461	0.10	0.466
post-Ratio	0.79 (0.50)	1.59 (1.47)	0.010	-0.36	0.009

pCR, pathological complete regression; SUVmax, the maximum standard uptake value; SUVmean, the mean standard uptake values; MTV, metabolic tumor volume; TLG, total lesion glycolysis; RI, response index; rs, Spearman's correlation coefficient; pre-, Before neoadjuvant therapy; post-, After neoadjuvant therapy; Ratio, Tumor SUVmean/ liver SUVmean.

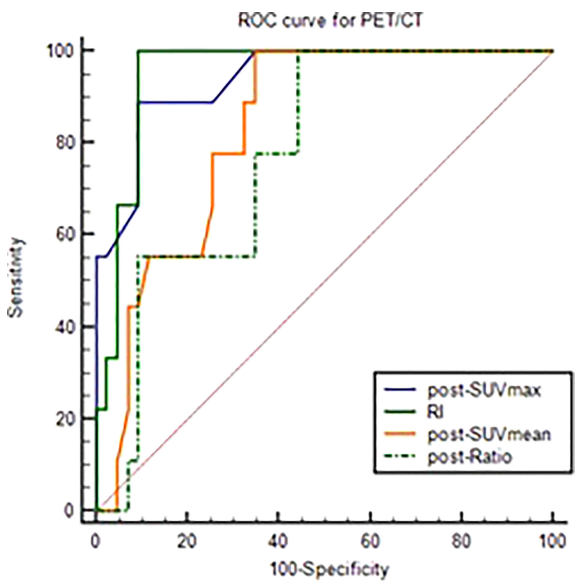

FIGURE 2
ROC curve of post-SUVmax, RI, post-SUVmean and post-Ratio using the pCR as test variable.

GR group was not only significantly higher than that in non-GR group, but also had a strong positive correlation with GR (r_s=0.63, P< 0.001). The values of post-SUVmax, post-SUVmean, post-TLG and post-Ratio were significantly lower than those in non-GR group. Post-SUVmax was strongly negatively correlated with GR (r_s=-0.70, P < 0.001), post-SUVmean and post-Ratio were moderately negatively correlated with GR (r_s=-0.48, P< 0.001; r_s=-0.46, P=0.009), and post-TLG was weakly negatively correlated with GR (r_s=-0.30, P=0.032), as shown in Table 4. In the analysis of ROC curve, we found that AUCs of post-SUVmax, RI, post-SUVmean, post-TLG, post-Ratio were 0.966, 0.921, 0.821, 0.698 and 0.805, respectively. Using post-SUVmax≤ 2.6, RI> 0.67, post-SUVmean≤ 2.2, post-TLG≤ 11.88 and post-Ratio≤ 1.39 as cut-off values, the sensitivity of these parameters to GR diagnosis were 92.31%, 84.66%, 100%, 84.62%, and 100%, the specificity were 92.31%, 94.87%, 71.79%, 64.1%, and 61.54%, the PPVs were 80.01%, 84.61%, 54.16%, 44%, and 46.43%, and the NPVs were 97.3%, 94.87%, 100%, 92.59%, and 100%, respectively, as shown in Figure 3 and Table 5.

Discussion

Currently, as the standard treatment for LARC patients, nCRT has been widely used in clinical practice. However, not all patients can benefit from this treatment. Studies show that only about 20% of patients can achieve pCR efficacy (12–15). In this study, we evaluated the efficacy of 52 patients, and found that 17.31% of patients obtained pCR and 25.00% obtained GR (pCR + near-pCR). As we all know, the ideal goal of tumor treatment is to enable patients to obtain “no evidence of disease” status (NED) and long-term survival. The complete response (CR) status is the assessment of good therapeutic efficacy of tumor patients and is the interpretation of NED, including clinical complete response (cCR) and pCR. For LARC patients, cCR is a dynamic concept with time limit, obtained based on enteroscopy, imaging and other data, since the results of cCR obtained through existing examination methods may be denied by a more advanced examination result in the future. Studies have shown that the local recurrence rate of two years of LARC patients obtained cCR is still over 20% after “W&W” strategy was adopted (1–3). However, pCR and near-pCR are postoperative pathological results, which are outcome concepts and have a more critical impact in prognosis. Studies have shown that only 36% patients assessed as cCR in LARC patients after completing nCRT can be verified for pCR (16). Therefore, exploring a method that can accurately predict the responsiveness of LARC patients to neoadjuvant therapy is of great significance for guiding clinicians to choose the follow-up treatment after neoadjuvant therapy.

It is well known that ^{18}F-FDG PET-CT has high sensitivity and specificity in the diagnosis of malignant tumors. Up to now, a number of studies have reported the significance and application value of PET-CT imaging parameters in predicting LARC patients after receiving nCRT. However, due to the inconsistency of PET-CT scanning timing after nCRT, the predicted values of various imaging parameters are not

TABLE 3 ROC analysis of PET-CT parameters to pCR.

Parameters	AUC	95%CI	Cut-off	Sensitivity	Specificity	PPV	NPV
post-SUVmax	0.939	0.836-0.987	≤2.5	88.89%	90.7%	66.68%	97.5%
RI	0.951	0.853-0.992	≥0.67	100%	90.7%	69.24%	100%
post-SUVmean	0.831	0.701-0.920	≤2.2	100%	65.12%	37.51%	100%
post-Ratio	0.775	0.638-0.879	≤1.392	100%	55.81%	32.14%	100%

pCR, pathological complete regression; SUVmax, the maximum standard uptake value; SUVmean, the mean standard uptake values; RI, response index; pre-, Before neoadjuvant therapy; post-, After neoadjuvant therapy; Ratio, Tumor SUVmean/ liver SUVmean; PPV, positive predictive value; NPV, negative predictive value.

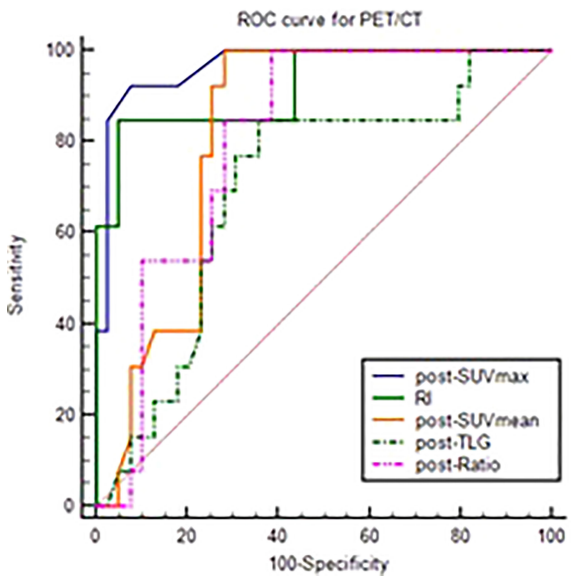

FIGURE 3
ROC curve of post-SUVmax, RI, post-SUVmean, post-TLG, post-Ratio using the GR as test variable.

consistent in clinical application. In our study, the timing of the second PET-CT scan was set within 1 week before surgery, that is, 8-9 weeks after nCRT, to better reflect the tumor status pre-operation. And our results show that post-SUVmax, RI, post-SUVmean and post-TLG are of high value in evaluating the status of pCR status of LARC patients, and post-ratio was also a good predictor of GR in addition to the above indicators.

Post-SUVmax and post-SUVmean are parameters that reflect the uptake capacity of ^{18}F-FDG by tumor cells after receiving nCRT. In this study, we found that these two parameters were significantly lower in patients who obtained pCR than in non-pCR patients. When the Cut-off values of post-SUVmax ≤2.5, its NPV was as high as 97.5%, that is, only 2.5% of the patients who obtained pCR using this parameter might be mistaken for non-pCR. Similarly, when the Cut-off values of post-SUVmean ≤2.2, its NPV was up to 100%. For GR and non-GR, these two parameters also had a good exclusion diagnostic advantage, with a NPV of 97.3% for post-SUVmax at Cut-off ≤2.6, and 100% for post-SUVmean at Cut-off ≤ 2.2. The NPV and PPV of post-SUVmax obtained by Mafione et al. in predicting GR were 69.56% and 91.30%, respectively (we obtained by further calculations based on the information provided in the original paper). This result is somewhat different from our study, which may be due to the fact that Maffione's second PET-CT was performed 4.6-17.4 weeks after nCRT (17). In another study (18), the researchers set the timing of the second PET-CT at 6-7 weeks after the completion of nCRT and found that the sensitivity, specificity, PPV and NPV of post-SUVmax in predicting pCR were 87.5%, 34.4%, 25% and 91.7% respectively. The advantage of this result in negative predictive value was similar to our results, which also reflected the advantage of post-SUVmax in excluding false-positive patients.

MTV and TLG are two parameters that reflect the overall glucose metabolism of tumor. MTV mainly reflects tumor

TABLE 4 Correlation analysis of parameters of PET-CT in GR and non-GR.

Parameters	Wilcoxon			Spearman	
	GR, M(Q_R)	non-GR,M(Q_R)	*P* value	r_s	*P* value
Pre-SUVmax	8.50(7.45)	7.78(6.70)	0.767	0.04	0.771
post-SUVmax	2.40(0.45)	6.20(4.50)	<0.001	-0.70	<0.001
RI	0.75(0.10)	0.38(0.45)	<0.001	0.63	<0.001
pre-SUVmean	5.56(2.58)	4.52(2.99)	0.583	0.08	0.588
post-SUVmean	1.75(0.52)	3.45(2.37)	0.001	-0.48	<0.001
pre-MTV	22.00(19.50)	28.00(21.00)	0.139	-0.21	0.140
post-MTV	4.00(2.50)	5.00(5.00)	0.282	-0.15	0.287
ΔMTV	0.77(0.28)	0.77(0.21)	0.711	0.13	0.362
pre-TLG	86.80(52.78)	144.04(169.83)	0.180	-0.19	0.182
post-TLG	7.00(6.43)	17.40(21.84)	0.034	-0.30	0.032
ΔTLG	0.92(0.06)	0.88(0.20)	0.089	0.11	0.459
pre-Ratio	2.67(2.25)	2.44(1.48)	0.4907	-0.02	0.909
post-Ratio	0.83(0.31)	1.62(1.52)	0.001	-0.46	0.001

GR, good response; SUVmax, the maximum standard uptake value; SUVmean, the mean standard uptake values; MTV, metabolic tumor volume; TLG, total lesion glycolysis; RI, response index; rs, Spearman's correlation coefficient; pre-, Before neoadjuvant therapy; post-, After neoadjuvant therapy; Ratio, Tumor SUVmean/ liver SUVmean.

TABLE 5 ROC analysis of PET-CT parameters to GR.

	AUC	95%CI	Cut-off	Sensitivity	Specificity	PPV	NPV
post-SUVmax	0.966	0.875-0.997	≤2.6	92.31%	92.31%	80.01%	97.3%
RI	0.921	0.812-0.978	≥0.67	84.62%	94.87%	84.61%	94.87%
post-SUVmean	0.821	0.689-0.913	≤2.2	100%	71.79%	54.16%	100%
post-TLG	0.698	0.555-0.818	≤11.88	84.62%	64.10%	44%	92.59%
post-Ratio	0.805	0.671-0.902	≤1.392	100%	61.54%	46.43%	100%

GR, good response; SUVmax, the maximum standard uptake value; SUVmean, the mean standard uptake values; RI, response index; TLG, total lesion glycolysis; pre-, Before neoadjuvant therapy; post-, After neoadjuvant therapy; Ratio, Tumor SUVmean/ liver SUVmean; PPV, positive predictive value; NPV, negative predictive value.

metabolic volume, which is a direct parameter obtained after PET-CT scanning, while TLG is an indirect parameter obtained by MTV and SUVmean, which reflects both metabolic volume and metabolic activity of tumor cells (19). It is found that TLG is of great value in the prognosis of patients with non-small cell lung cancer, renal cell carcinoma, head and neck cancer, ovarian cancer and soft tissue sarcoma (20–24). In this study, we found that post-TLG had a negative predictive value of 92.59% for GR status in LARC patients, but did not show a predictive advantage in pCR status. In previous studies, there have been meaningful reports about MTV, ΔMTV and ΔTLG in predicting the responsiveness of LARC patients to nCRT (8, 25–27). However, in our study, none of these three parameters was found to have meaningful predictive value in our study. Therefore, the predictive value of these parameters needs to be further explored.

The RI value reflects the change of an ability of tumor to uptake ^{18}F-FDG before and after therapy, which is also described as ΔSUVmax, Δ%SUV or ΔSUVmax% in some literatures. Murcia et al. found that the RI value was 79.9±4.69% in the responders, significantly higher than 60.3±4.6% in the non-responders, suggesting that this parameter has important value in differentiating the response ability of LARC patients to nCRT (28). In the study of leccisotti et al., patients received three time PET-CT scans in different timing (before nCRT, at the end of the second week of nCRT, and shortly before surgery), obtained early RI and late RI, and found that the early RI had a high predictive value for the pCR status. When the cut-off value was 61.2%, the sensitivity, specificity, PPV and NPV were 85.4%, 65.2%, 90% and 56%, respectively (7). In terms of predicting GR status, Capirci's study showed that when cut-off value was 63.4%, the predictive sensitivity, specificity, PPV, NPV and overall accuracy of RI for GR were 84.5%, 80%, 81.4%, 84.2% and 81% respectively, and the AUC of ROC curve was 0.862 (29). Caruso et al. found that when cut-off values were 70%, the sensitivity, specificity, PPV and NPV of Δ%SUV for GR prediction were 84.4%, 80%, 81.4% and 84.2%, respectively (30). In this study, we conducted ROC analysis on the predictive value of RI and found that AUCs obtained by pCR and GR were 0.951 and 0.921, respectively. When cut-off values were 67%, the sensitivity, specificity, PPV and NPV for pCR were 100%, 90.7%, 69.24% and 100%, respectively, and 84.62%, 94.87%, 84.61% and 94.87% for GR. It can be seen from previous results and our study that RI value is of high value in predicting whether LARC patients can obtain pCR and GR after receiving nCRT, and RI value of 60-70% or higher indicates high reactivity of patients to nCRT.

In this study, the timing of two PET-CT scans was strictly limited when the patients were enrolled. In particular, the time of the second scans were limited to in the 8 to 9 weeks after the completion of nCRT. This is exactly coincided with the timing of TME surgery recommended by the current diagnosis and treatment guidelines, and also reflects the status of the specimens *in vivo* to the greatest extent. However, this also leads to the limitation of number of cases in this study. Therefore, in subsequent clinical practice, we will increase the sample size to verify our results. In addition, as most patients receiving neoadjuvant therapy in our center chose a long course of nCRT in terms of treatment mode, we did not analyze patients receiving SCRT in this study, which might also be a limitation. Furthermore, in the inclusion criteria, the number of chemotherapy cycles between long-course nCRT and TME surgery was not limited, so the relationship between whether patients were treated with total neoadjuvant therapy (TNT) mode and the tumor reactivity of patients' PET-CT imaging parameters was not analyzed. Due to the TNT treatment model has been preferentially recommended by the NCCN guidelines since 2022, the prediction of efficacy by PET-CT has not yet been reported. It will be a new direction to study the prediction of tumor reactivity in TNT mode.

Under the premise of strictly limiting the inclusion criteria, this study obtained the predictive value of ^{18}F-FDG PET-CT imaging parameters such as post-SUVmax, post-suvmean, RI, post-Ratio and post-TLG for the tumor pathological status of LARC patients before surgery. Among these indicators, post-SUVmax and RI, which can reflect the change of the maximum uptake capacity of ^{18}F-FDG by tumor tissue, are of great value in predicting the GR and pCR status of patients. The application of

these parameters will provide an important reference for the selection of subsequent treatment strategies for patients with high response to nCRT.

Data availability statement

The original contributions presented in the study are included in the article/supplementary material. Further inquiries can be directed to the corresponding author.

Ethics statement

The studies involving human participants were reviewed and approved by the fourth hospital of Hebei Medical University. Written informed consent for participation was not required for this study in accordance with the national legislation and the institutional requirements.

Author contributions

Conceived and designed the study: GW, XMZ. Performed the study and analyzed the data: FW, XXZ, KW, CY, CZ. Wrote the paper: XXZ, FW, LX. Supervised the entire study and review the final paper: GW, XMZ, XXZ, FW, KW, CZ, CY, LX. All authors contributed to the article and approved the submitted version.

Funding

This study was funded by the Hebei Provincial Department of Bureau of Science and Technology (22377733D).

Conflict of interest

The authors declare that the research was conducted in the absence of any commercial or financial relationships that could be construed as a potential conflict of interest.

Publisher's note

All claims expressed in this article are solely those of the authors and do not necessarily represent those of their affiliated organizations, or those of the publisher, the editors and the reviewers. Any product that may be evaluated in this article, or claim that may be made by its manufacturer, is not guaranteed or endorsed by the publisher.

References

1. van der Valk MJM, Hilling DE, Bastiaannet E, Meershoek-Klein, Kranenbarg E, Beets GL, et al. Long-term outcomes of clinical complete responders after neoadjuvant treatment for rectal cancer in the international watch & wait database (IWWD): an international multicentre registry study. *Lancet.* (2018) 391 (10139):2537–45. doi: 10.1016/S0140-6736(18)31078-X

2. Chadi SA, Malcomson L, Ensor J, Riley RD, Vaccaro CA, Rossi GL, et al. Factors affecting local regrowth after watch and wait for patients with a clinical complete response following chemoradiotherapy in rectal cancer (InterCoRe consortium): an individual participant data meta-analysis. *Lancet Gastroenterol Hepatol* (2018) 3(12):825–36. doi: 10.1016/S2468-1253(18)30301-7

3. Smith JJ, Strombom P, Chow OS, Roxburgh CS, Lynn P, Eaton A, et al. Assessment of a watch-and-wait strategy for rectal cancer in patients with a complete response after neoadjuvant therapy. *JAMA Oncol* (2019) 5(4):e185896. doi: 10.1001/jamaoncol.2018.5896

4. Rullier E, Vendrely V, Asselineau J, Rouanet P, Tuech JJ, Valverde A, et al. Organ preservation with chemoradiotherapy plus local excision for rectal cancer: 5-year results of the GRECCAR 2 randomised trial. *Lancet Gastroenterol Hepatol* (2020) 5(5):465–74. doi: 10.1016/S2468-1253(19)30410-8

5. Pang K, Rao Q, Qin S, Jin L, Yao H, Zhang Z. Prognosis comparison between wait and watch and surgical strategy on rectal cancer patients after treatment with neoadjuvant chemoradiotherapy: a meta-analysis. *Therap Adv Gastroenterol* (2019) 12:1756284819892477. doi: 10.1177/1756284819892477

6. Koç M, Kaya GÇ, Demir Y, Sürücü E, Sarioğlu S, Obuz F, et al. The value of liver-based standardized uptake value and other quantitative 18F-FDG PET-CT parameters in neoadjuvant therapy response in patients with locally advanced rectal cancer: correlation with histopathology. *Nucl Med Commun* (2015) 36 (9):898–907. doi: 10.1097/MNM.0000000000000342

7. Leccisotti L, Gambacorta MA, de Waure C, Stefanelli A, Barbaro B, Vecchio FM, et al. The predictive value of 18F-FDG PET/CT for assessing pathological response and survival in locally advanced rectal cancer after neoadjuvant radiochemotherapy. *Eur J Nucl Med Mol Imaging.* (2015) 42(5):657–66. doi: 10.1007/s00259-014-2820-9

8. Avallone A, Aloj L, Pecori B, Caracò C, De Stefano A, Tatangelo F, et al. (18) F-FDG PET/CT is an early predictor of pathologic tumor response and survival after preoperative radiochemotherapy with bevacizumab in high-risk locally advanced rectal cancer. *J Nucl Med* (2019) 60(11):1560–8. doi: 10.2967/jnumed.118.222604

9. Nancy YL, Jiade JL. *Target volume delineation and field setup: a practical guide for conformal and intensity-modulated radiation therapy*. Berlin, Heidelberg: Springer-Verlag (2013) p. 161–8. doi: 10.1007/978-3-642-28860-9

10. Kim SH, Chang HJ, Kim DY, Park JW, Baek JY, Kim SY, et al. What is the ideal tumor regression grading system in rectal cancer patients after preoperative chemoradiotherapy? *Cancer Res Treat* (2016) 48(3):998–1009. doi: 10.4143/crt.2015.254

11. Dworak O, Keilholz L, Hoffmann A. Pathological features of rectal cancer after preoperative radiochemotherapy. *Int J Colorectal Dis* (1997) 12(1):19–23. doi: 10.1007/s003840050072

12. Ferrari L, Fichera A. Neoadjuvant chemoradiation therapy and pathological complete response in rectal cancer. *Gastroenterol Rep (Oxf).* (2015) 3(4):277–88. doi: 10.1093/gastro/gov039

13. Tawfik B, Mokdad AA, Patel PM, Li HC, Huerta S. The neutrophil to albumin ratio as a predictor of pathological complete response in rectal cancer patients following neoadjuvant chemoradiation. *Anticancer Drugs* (2016) 27 (9):879–83. doi: 10.1097/CAD.0000000000000411

14. Maas M, Nelemans PJ, Valentini V, Das P, Rödel C, Kuo LJ, et al. Long-term outcome in patients with a pathological complete response after chemoradiation for rectal cancer: a pooled analysis of individual patient data. *Lancet Oncol* (2010) 11(9):835–44. doi: 10.1016/S1470-2045(10)70172-8

15. Martin ST, Heneghan HM, Winter DC. Systematic review and meta-analysis of outcomes following pathological complete response to neoadjuvant

chemoradiotherapy for rectal cancer. *Br J Surg* (2012) 99(7):918–28. doi: 10.1002/bjs.8702

16. Cercek A, Roxburgh CSD, Strombom P, Smith JJ, Temple LKF, Nash GM, et al. Adoption of total neoadjuvant therapy for locally advanced rectal cancer. *JAMA Oncol* (2018) 4(6):e180071. doi: 10.1001/jamaoncol.2018.0071

17. Maffione AM, Ferretti A, Grassetto G, Bellan E, Capirci C, Chondrogiannis S, et al. Fifteen different 18F-FDG PET/CT qualitative and quantitative parameters investigated as pathological response predictors of locally advanced rectal cancer treated by neoadjuvant chemoradiation therapy. *Eur J Nucl Med Mol Imaging.* (2013) 40(6):853–64. doi: 10.1007/s00259-013-2357-3

18. Martoni AA, Di Fabio F, Pinto C, Castellucci P, Pini S, Ceccarelli C, et al. Prospective study on the FDG–PET/CT predictive and prognostic values in patients treated with neoadjuvant chemoradiation therapy and radical surgery for locally advanced rectal cancer. *Ann Oncol* (2011) 22(3):650–6. doi: 10.1093/annonc/mdq433

19. Larson SM, Erdi Y, Akhurst T, Mazumdar M, Macapinlac HA, Finn RD, et al. Tumor treatment response based on visual and quantitative changes in global tumor glycolysis using PET-FDG imaging. *Visual response score Change total lesion glycolysis. Clin Positron Imaging.* (1999) 2:159–71. doi: 10.1016/S1095-0397(99)00016-3

20. Akhurst T, Ng V, Larson SM, O'Donoghue JA, O'Neel J, Erdi Y, et al. T Tumor burden assessment with positron emission tomography with [18-f] 2-fluoro 2-deoxyglucose (FDG PET) modeled in metastatic renal cell cancer. *Clin Positron Imaging.* (2000) 3(2):57–65. doi: 10.1016/s1095-0397(00)00041-8

21. Zhang H, Wroblewski K, Liao S, Kampalath R, Penney BC, Zhang Y, et al. Prognostic value of metabolic tumor burden from (18)FFDG PET in surgical patients with non-small-cell lung cancer. *Acad Radiol* (2013) 20:32–40. doi: 10.1016/j.acra.2012.07.002

22. La TH, Filion EJ, Turnbull BB, Chu JN, Lee P, Nguyen K, et al. Metabolic tumor volume predicts for recurrence and death in headand-neck cancer. *Int J Radiat Oncol Biol Phys* (2009) 74:1335–41. doi: 10.1016/j.ijrobp.2008.10.060

23. Chung HH, Kwon HW, Kang KW, Park NH, Song YS, Chung JK, et al. Prognostic value of preoperative metabolic tumor volume and total lesion glycolysis in patients with epithelial ovarian cancer. *Ann Surg Oncol* (2012) 19:1966–72. doi: 10.1245/s10434-011-2153-x

24. Choi ES, Ha SG, Kim HS, Ha JH, Paeng JC, Han L. Total lesion glycolysis by 18F-FDG PET/CT is a reliable predictor of prognosis in soft-tissue sarcoma. *Eur J Nucl Med Mol Imaging.* (2013) 40(12):1836–42. doi: 10.1007/s00259-013-2511-y

25. Deantonio L, Caroli A, Puta E, Ferrante D, Apicella F, Turri L, et al. Does baseline [18F] FDG-PET/CT correlate with tumor staging, response after neoadjuvant chemoradiotherapy, and prognosis in patients with rectal cancer? *Radiat Oncol* (2018) 13(1):211. doi: 10.1186/s13014-018-1154-3

26. Fernando S, Lin M, Pham TT, Chong S, Ip E, Wong K, et al. Prognostic utility of serial 18F-FDG-PET/CT in patients with locally advanced rectal cancer who underwent tri-modality treatment. *Br J Radiol* (2020) 93(1105):20190455. doi: 10.1259/bjr.20190455

27. Pyo DH, Choi JY, Lee WY, Yun SH, Kim HC, Huh JW, et al. A nomogram for predicting pathological complete response to neoadjuvant chemoradiotherapy using semiquantitative parameters derived from sequential PET/CT in locally advanced rectal cancer. *Front Oncol* (2021) 11:742728. doi: 10.3389/fonc.2021.742728

28. Murcia Duréndez MJ, Frutos Esteban L, Luján J, Frutos MD, Valero G, Navarro Fernández JL, et al. The value of 18F-FDG PET/CT for assessing the response to neoadjuvant therapy in locally advanced rectal cancer. *Eur J Nucl Med Mol Imaging.* (2013) 40(1):91–7. doi: 10.1007/s00259-012-2257-y

29. Capirci C, Rubello D, Pasini F, Galeotti F, Bianchini E, Favero GD, et al. The role of dual-time combined 18-fluorodeoxyglucose positron emission tomography and computed tomography in the staging and restaging workup of locally advanced rectal cancer, treated with preoperative chemoradiation therapy and radical surgery. *Int J Radiat Oncol Biol Phys* (2009) 74(5):1461–9. doi: 10.1016/j.ijrobp.2008.10.064

30. Caruso R, Vicente E, Quijano Y, Duran H, Fabra I, Diaz E, et al. Role of 18F –PET–CT to redict pathological response after neoadjuvant treatment of rectal cancer. *Discovery Oncol* (2021) 12(1):16. doi: 10.1007/s12672-021-00405-w

frontiers | Frontiers in Oncology

TYPE Original Research
PUBLISHED 22 December 2022
DOI 10.3389/fonc.2022.1021625

Check for updates

OPEN ACCESS

EDITED BY
Zhendong Jin,
Second Military Medical University, China

REVIEWED BY
Yosuke Tsuji,
The University of Tokyo, Japan
Gang Sun,
The first affiliated hospital of People's Liberation Army General Hospital, China
Zhen Li,
Qilu Hospital, Shandong University, China

*CORRESPONDENCE
Xiao jun Huang
huangxj@lzu.edu.cn

SPECIALTY SECTION
This article was submitted to Gastrointestinal Cancers: Gastric and Esophageal Cancers, a section of the journal Frontiers in Oncology

RECEIVED 17 August 2022
ACCEPTED 05 December 2022
PUBLISHED 22 December 2022

CITATION
Feng J, Yu Sr, Zhang Yp, Qu L, Wei L, Wang Pf, Zhu Lj, Bao Y, Lei Xg, Gao Ll, Feng Yh, Yu Y and Huang Xj (2022) A system based on deep convolutional neural network improves the detection of early gastric cancer. *Front. Oncol.* 12:1021625. doi: 10.3389/fonc.2022.1021625

COPYRIGHT
© 2022 Feng, Yu, Zhang, Qu, Wei, Wang, Zhu, Bao, Lei, Gao, Feng, Yu and Huang. This is an open-access article distributed under the terms of the Creative Commons Attribution License (CC BY). The use, distribution or reproduction in other forums is permitted, provided the original author(s) and the copyright owner(s) are credited and that the original publication in this journal is cited, in accordance with accepted academic practice. No use, distribution or reproduction is permitted which does not comply with these terms.

A system based on deep convolutional neural network improves the detection of early gastric cancer

Jie Feng[1,2], Shang rui Yu[1], Yao ping Zhang[1,2], Lina Qu[1,2], Lina Wei[1], Peng fei Wang[1], Li juan Zhu[3], Yanfeng Bao[3], Xiao gang Lei[4], Liang liang Gao[5], Yan hu Feng[1], Yi Yu[1] and Xiao jun Huang[1,2]*

[1]Department of Gastroenterology, Lanzhou University Second Hospital, Lanzhou, Gansu, China, [2]Technology Research and Development Department, Digestive Endoscopy Engineering Research and Development Center of Gansu Province, Lanzhou, Gansu, China, [3]Department of Sciences and Technology, Beijing Huag gen Anbang Technology Technology Company Limited, Beijing, China, [4]Department of Gastroenterology, Lanzhou Cheng guan District People's Hospital, Lanzhou, Gansu, China, [5]Department of Gastroenterology, Min County People's Hospital, Ding Xi, Gansu, China

Background: Early gastric cancer (EGC) has a high survival rate, but it is difficult to diagnosis. Recently, artificial intelligence (AI) based on deep convolutional neural network (DCNN) has made significant progress in the field of gastroenterology. The purpose of this study was to establish a DCNN assist system to improve the detection of EGC.

Methods: 3400 EGC and 8600 benign images were collected to train the DCNN to detect EGC. Subsequently, its diagnostic ability was compared to that of endoscopists using an independent internal test set (ITS, including 1289 images) and an external test set (ETS, including 542 images) come from three digestive center.

Results: The diagnostic time of DCNN and endoscopists were 0.028s, 8.05 ± 0.21s, 7.69 ± 0.25s in ITS, and 0.028s, 7.98 ± 0.19s, 7.50 ± 0.23s in ETS, respectively. In ITS, the diagnostic sensitivity and accuracy of DCNN are 88.08%(95% confidence interval,95%CI,85.24%-90.44%), 88.60% (95% CI,86.74%-90.22%), respectively. In ETS, the diagnostic sensitivity and accuracy are 92.08% (95%CI, 87.91%- 94.94%),92.07%(95%CI, 89.46%-94.08%), respectively. DCNN outperformed all endoscopists in ETS, and had a significantly higher sensitivity than the junior endoscopists(JE)(by18.54% (95% CI, 15.64%-21.84%) in ITS, also higher than JE (by21.67%,95%CI, 16.90%-27.32%) and senior endoscopists (SE) (by2.08%, 95%CI, 0.75%-4.92%)in ETS. The accuracy of DCNN model was higher (by10.47%,95%CI, 8.91%-12.27%) than that of JE in ITS, and also higher (by14.58%,95%CI, 11.84%-17.81%; by 1.94%,95%CI,1.25%-2.96%, respectively) than JE and SE in ETS.

Conclusion: The DCNN can detected more EGC images in a shorter time than the endoscopists. It will become an effective tool to assist in the detection of EGC in the near future.

KEYWORDS

deep convolutional neural network, early gastric cancer, diagnosis rate, sensitivity, accuracy, false positive, false negative

Introduction

According to the 2020 Global Cancer Statistics, Gastric cancer is the third most lethal and the fifth most common malignancy from a global perspective, and Asia remains the region with a high incidence of cancer, with a cancer incidence rate of 49.3% and a mortality rate of 58.3%, with 719524 new cases of gastric cancer (1). The survival rate of patients with stage IA was 91%, Whereas the patients with stage IV less than 17% (2) Therefore, the early detection of gastric cancer is particularly important. However, the diagnosis of early gastric cancer (EGC) is difficult and often be ignored, especially in countries with large populations, such as China: the detection rate of EGC in China is only 10%, much lower than that in South Korea (50%) and Japan (70%) (3, 4), the diagnosis rate of EGC has great room for improvement. However, the large number of patients, insufficient diagnostic knowledge and experience of physicians, lack of advanced endoscopic equipment, and shortage of endoscopists have seriously affected the improvement of the diagnostic level of EGC in China. These problems are particularly prominent in primary medical institutions (5).

Some studies have reported a false negative rate of 4.6-25.8% in the detection of gastric cancer by esophagogastroduodenoscopy (EGD) (6–14), 71.4% of gastric cancer patients were initially diagnosed with gastritis, ulcers or "suspicious lesions", with the majority (73%) of errors made by endoscopists (9), technical factors and subjective cognition have significant influence on the screening of EGC (15). The detection of EGC requires not only well-trained endoscopists but also comprehensive knowledge (16), secondly, it is also necessary for endoscopists to avoid the influence of subjective factors, which limit the detection of EGC (17). Therefore, it is very important to develop a tool that has good detection ability and will not be affected by subjective factors to assist endoscopists in the detection of EGC. In recent years, artificial intelligence (AI) based on deep convolutional neural deep learning (DCNN) has come into being, and DCNN has made remarkable progress in various fields, including medicine. In the field of digestive endoscopy, it has been applied to the detection of colonic polyps (18) and the diagnosis of auxiliary capsule endoscopy (19). Based on the above reasons, we constructed an auxiliary diagnosis system for EGC base on DCNN, and tested the diagnostic efficiency of DCNN, aiming to improve the diagnostic efficiency of EGC.

Methods

Training dataset preparation

The DCNN was trained using EGD images obtained from the digestive center of Lanzhou University Second Hospital, total 12000 images were selected from the database from January, 2013 to December 2019, including 3400 images of EGC, 8600 images of benign lesions and normal images. All the lesions included in the study were confirmed by biopsy or surgical pathology and the lesion scope was clear, the patient and lesion characteristics of EGC in training set was shown in Supplementary Material 1. Postoperative pathological diagnosis included high-grade intraepithelial neoplasia and carcinoma confined to mucosa or submucosa. The equipment for endoscopic images was standard GIF-GIF-260/H290Z, Olympus Medical Systems, Co., Ltd., Tokyo, Japan) and a standard endoscopic video system (EVIS LUCERA ELITE CV-290/CLV-290SL; Olympus Medical Systems), and all images were white light endoscopes without magnification. Images containing poor inflation, halo, blur, defocus or mucus, and post-biopsy bleeding were excluded from the training dataset.

DCNN training

According to the outcome of pathology, the EGD images were labeled as EGC and other benign lesions, computer engineers will be annotated images for unified clipping, color space transformation, denoising, image morphology operations and normalization of a series of processing, eliminate human and environmental interference, better display image features, enhance the robustness of the algorithm. Algorithm engineers used the DCNN module to test multiple computer models such as DLA34 and Swim Transformer Tiny, and put the training set into the model for training. Through observation and comparison, the 18-layer convolutional neural network model

with the optimal accuracy and speed was determined. Input resolution: 512 × 512, batch-size: 32, initial learning rate: 1.25e-4, optimization: Adam

DCNN testing

We used standard EGC images independent of the training set to verify the accuracy of DCNN (From January 2020 to October 2020). Our test set was divided into internal test set (ITS) and external test set (ETS). The images of the ETS were from Wuwei Cancer Hospital and Minxian People's Hospital. The test set excluded postoperative gastric images, magnification, staining endoscopy, mucus and halo images. The patient and lesion characteristics of EGC in ITS and ETS set was shown in Table 1. The ITS contains 1289 images (604 EGC) and the ETS contains 542 images (240 EGC). Non-cancer images include ulcers, polyps and chronic gastritis. We identified each lesion area by comparing endoscopic images with the extent of the lesion in the excised specimen, and manually annotated all gastric cancer lesions in the test data set by two experienced endoscopists (L.W and P.W) using a true red rectangular border.

TABLE 1 Patient and lesion characteristics of EGC in Internal test set and External test set.

Patient characteristics	Internal test set (n=134)	External test set (n=48)
Age (years), Mean (range)	60 (27–79)	65 (35-84)
Sex, Number (%)		
Male	92 (68.66)	38 (79.17)
Female	42 (31.34)	10 (20.83)
Size of lesion (mm), Median (range)	15 (4-48.5)	17.4 (6-40.2)
Tumor location, Number (%)		
Cardia, Fundus of the stomach,	18 (13.43)	3 (6.25)
Number (%)		
Body	58 (43.28)	13 (27.08)
Angle	28 (20.90)	12 (25)
Antrum	30 (22.39)	20 (41.67)
Macroscopic type, Number (%)		
0-1	8 (5.97)	1 (2.08)
O-IIa	33 (24.63)	9 (18.75)
O-IIb	7 (5.22)	2 (4.17)
O-IIc	9 (6.72)	0 (0)
0-IIa+O-IIc	47 (35.07)	22 (45.83)
0-Hc+O-IIa	18 (13.43)	10 (20.83)
0-IIb+O-Hc	12 (8.96)	3 (6.25)
O-III	0 (0)	1 (2%)
Differentiation status, Number (%)		
Differentiated	124 (92.54)	41 (85.42)
Undifferentiated	2 (1.49)	1 (2.08)
Mixed	8 (5.97)	6 (12.5)
Depth of tumor, Number (%)		
Tla	128 (95.52)	44 (91.67)
Tlb	6 (8.96)	4 (8.33)

Tla, mucosa; Tlb, submucosa.

Comparison between the performance of DCNN and endoscopists

Eight endoscopists were selected from two hospitals and divided into the primary group and the expert group. Junior endoscopists (JE) with 2 years of operation experience and less than 1000 cases of EGD operation experience, respectively. Senior endoscopists(SE) have more than 10 years of endoscopic diagnosis and treatment experience, and each of them independently completed at least 80 cases of EGC ESD treatment; the images of the test set are arranged in a random order. Endoscopists individually read the images from the test set and recorded the time required to read the images. At the same time, DCNN recognizes the test set images and records the results.

Outcome measures and data statistics

The DCNN showed a 0–100% continuous variable number, which represented a probability score for gastric cancer in each image. Definition of correct answer, for EGC: the correct marking is the red rectangle (according to the results of the ESD postoperative pathology), the yellow rectangle is the DCNN marking and the blue rectangle is the endoscopists marking. When the yellow and red marking overlap is more than 50%, or blue and red marking overlap is greater than 50% is correct (Figure 1A); Non-cancerous lesions: The yellow rectangle box is not displayed and the word "cancer" is not displayed.95% confidence intervals (95% CI) using the modified Wald method: Agresti and Coull (The American Statistician. 52:119-126, 1998) Two-tailed unpaired Student's T-test (chi-square test)

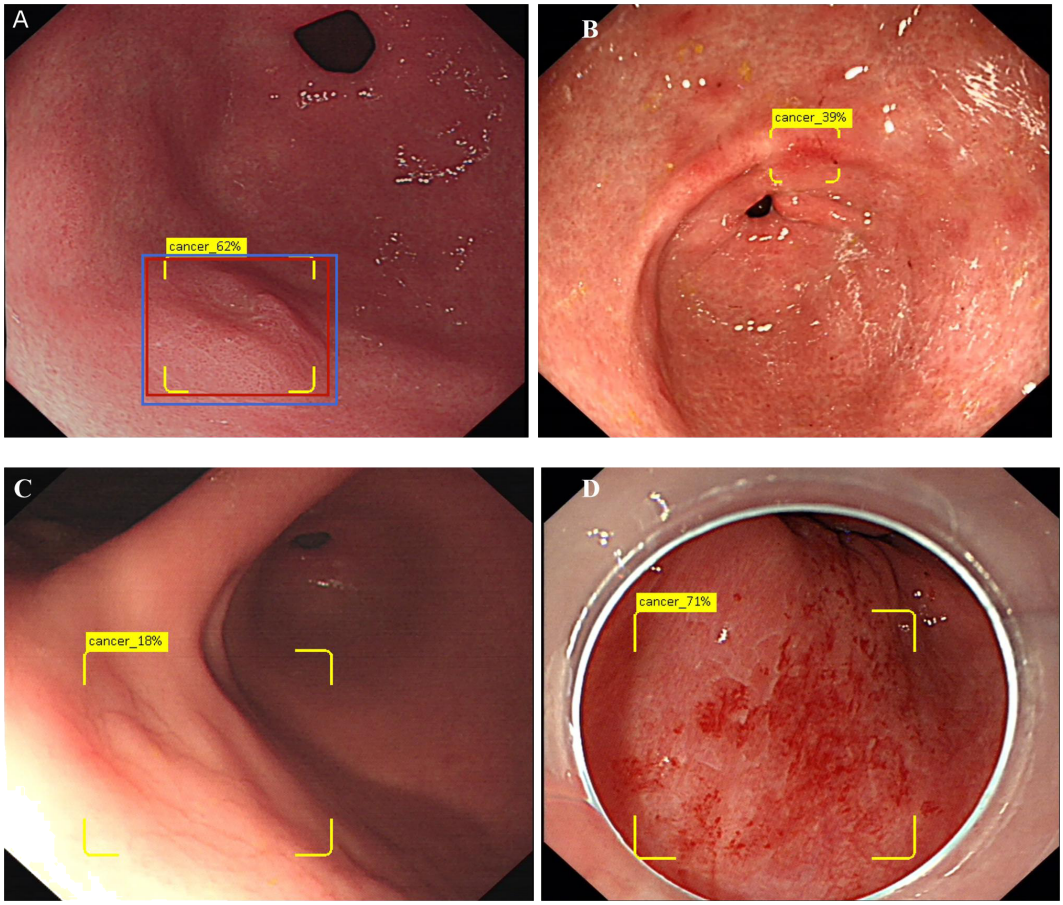

FIGURE 1
Show the concept of correctly identifies and diagram of DCNN producing false positives. **(A)** Show 0-IIa lesion in the anterior wall of gastric antrum, the red rectangle is the correct marking, the yellow box is the DCNN marking, and the blue rectangle is the endoscopist's marking. Only when the overlap reaches 50% or more, the diagnosis is correct. The yellow logo shows "Cancer 62%", indicating that DCNN predicts that the probability of EGC for this lesion is 62%. **(B)** Show an image of falsely diagnosing inflammation as EGC. **(C)** Show an image of DCNN diagnosed the normal mucosa in the reflective area as EGC. **(D)** Show an image of DCNN diagnosed the bleeding mucosa in the reflective area as EGC.

was used, with a significance level of 0.05. The accuracy, sensitivity, specificity, positive and negative predictive values (PPV and NPV, respectively) were compared. Interobserver used Cohen's Kappa coefficient (Kappa value) to assess intra-observer consistency for endoscopists. SPSS 26 (IBM, Chicago, IL, USA) was used to complete all calculations.

Ethics

The study was approved by the Ethics Committee of the Lanzhou University Second Hospital (No.2022A-004).

Results

Characteristics of patients and lesions in the test data set

The characteristics of patients and lesions in the test data set are summarized in Table 1, 95.52%patients were mucosal cancer (T1a), 4.48% patients were submucosal cancer(T1b) in ITS, and 91.67%patients were mucosal cancer (T1a), 8.33% patients were submucosal cancer(T1b) in ETS. In terms of histopathological types, 124 (92.54%) patients were differentiated gastric cancer, 10(7.46%) patients were undifferentiated gastric cancer in ITS. Differentiated cancers accounted for 41 (85.42%), and undifferentiated and mixed cancers accounted for 7 (14.58%). The cancer diameter ranged from 4mm to 48.5mm, with a median size of 15mm in ITS, and 6-40.2mm in ETS. The most common Macroscopic type was 0-IIa+IIc, accounting for 35.07% in ITS and 45.83% in ETS, respectively.

Performance of DCNN model and endoscopists for ITS and ETS

DCNN performance

The performances of DCNN model and endoscopist are summarized in Table 2. The sensitivity, specificity, accuracy, PPV and NPV of DCNN model in ITS was 88.08%,95% confidence interval (95% CI), (85.24%-90.44%); 89.05%(95% CI, 86.48%-91.19%), 88.60%(95%CI,86.74%-90.22%), 87.64% (95%CI,84.78%-90.04%),89.44%(95%CI,86.90%-91.54%), respectively.And 92.08% (95% CI,87.91%- 94.94%),92.05%(95% CI,88.40%-94.65%), 92.07%(95%CI,89.46%-94.08%), 90.2% (95%CI, 85.79%-93.38%), 93.60(95%CI,90.17%-95.92%) in ETS. The performance of DCNN model in ETS is obviously higher than that in ITS. The average time for DCNN model analysis of each image in ITS and ETS was 0.028s.

Endoscopists performance

The endoscopist's diagnostic performances are summarized in Table 2. The diagnostic time of each image was 8.05 ± 0.21s and 7.69 ± 0.25s for the JE group and SE group in ITS, and there was no significant difference in the diagnostic time between the

TABLE 2 The performances of DCNN and endoscopist in internal test set and external test set.

Competitors	Sensitivity, % (95%CI)	Specificity, % (95%CI)	Accuracy, % (95%CI)	PPV, % (95%CI)	NPV, % (95% CI)	DT(s)
Internal test set						
DCNN	88.08	89.05	88.60	87.64	89.44	0.028s
	(85.24-90.44)	(86.48-91.19)	(86.74-90.22)	(84.78-90.04)	(86.90-91.54)	
JE group	69.54[a]	85.69	78.12[s]	81.08	76.13	8.05±0.21[a]
	(66.88-72.07)	(83.74-87.45)	(75.78-80.30)	(78.58-83.35)	(73.94-78.20)	
SE group	89.57[a]	90.00	89,73[a]	88.76	90.73	7.69±0.25[a]
	(87.71-91.17)	(88.29-91.48)	(86.79-92.08)	(86.86-90.42)	(89.07-92.16)	
External test set						
DCNN model	92.08	92.05	92.07	90.2	93.60	0.028s
	87.91-94.94	88.40-94.65	89.46-94.08	85.79-93.38	90.17-95.92	
JE group	70.42[a]	82.95	77.40[a]	76.64	77.92	7.98±0.19[a]
	66.18-74.33	79.73-85.74	74.81-79.79	72.47-80.36	74.54-80.96	
SE group	90[b]	90.23	90.13[c]	87.98	91.91	7.50±0.23[a]
	86.97-92.39	87.59-92.36	88.20-91.77	84.79-90.58	89.41-93.86	

a: P<0.01; b: P=0.02; c: P > 0.05. JE(juniorendoscopists); SE(seniorendoscopists); PPV (positive predictive value); NPV(negative predictive value); DT(diagnostic time).

two, respectively. In ITS,the sensitivity, specificity, accuracy, PPV and NPV of JE group were as follows: 69.54%(95% CI,66.88%-72.07%) 85.69%(95%CI, 83.74%-87.45%) 78.12% (95%CI, 75.78%-80.30%),81.08%(95%CI, 78.58%-83.35%) 76.13%(95%CI, 73.94%-78.20%); SE group has a better performance, 89.57(95%CI, 87.71%-91.17%) of sensitivity,90.00%(95%CI, 88.29%-91.48%)of specificity,89.73% (95%CI,86.79%-92.08%) for accuracy,88.76% (95%CI, 86.86%-90.42%)for PPV and 90.73%(95%CI, 89.07%-92.16%) for NPV. The sensitivity and accuracy of the SE group were significantly higher than those of the JE group(P<0.01), The sensitivity of SE group was higher (by20.03%95%CI, 17.03%-23.42%,P<0.01) than JE group, and the accuracy of SE group was higher (by11.61%,95%CI, 10%-13.51%,P<0.01) than JE group. In the ETS, the diagnostic time for each image in the JE and SE groups was 7.98 ± 0.19s and 7.50 ± 0.23s, respectively, and there was no significant difference in diagnostic time between the two group, the performance of SE group was significantly higher than that of JE group, the sensitivity of SE group was higher (by19.58%,95%CI, 15.04%-25.09%,P<0.01) than that of JE group, and the accuracy of SE group was higher (by12.73%,95%CI, 10.17%-15.81%, P<0.01) than that of JE group. In terms of the ITS and the ETS, the diagnostic efficacy of endoscopists in the ETS was higher than that in the ITS.

In terms of diagnostic consistency, in the ITS, the DCNN model and endoscopist's pairwise Kappa values ranged from 0.765 to 0.913, while the endoscopist's diagnostic Kappa values ranged from 0.735 to 0.959. The diagnostic consistency was reasonable. The mean value of Kappa between DCNN model and endoscopist was 0.8794, JE-1 was 0.8424, JE-2 was 0.871, SE-1 was 0.8868, and SE-2 was 0.878. In the ETS, the Kappa values of DCNN model and endoscopists ranged from 0.676 to 0.981, while the diagnostic Kappa values of endoscopist ranged from 0.682 to 0.950. The mean value of Kappa between DCNN model and endoscopist's was 0.8638, JE-3 was 0.8106, JE-4 was 0.8418, SE-3 was 0.8832, and SE-4 was 0.8686.

Comparison of DCNN and endoscopist performance

The receiver operating characteristic (ROC) curve of DCNN model and endoscopist's diagnostic effectiveness is shown in Figure 2. In ITS, the area under ROC curve (AUC) of the DCNN model, JE group and SE group were 0.8857 (95%CI,0.8655-0.9058),0.7710 (95%CI,0.7443-0.7978) and 0.8890(95% CI,0.8690-0.9091),respectively. In ETS, AUC of the DCNN model, JE group and SE group were 0.9207 (95%CI,0.9020-0.9394), 0.7668(95%CI,0.7372-0.7964) and 0.9012 (95% CI,0.8805-0.9218), respectively. DCNN model was significantly faster than all endoscopists in test sets. The sensitivity of the DCNN model was 18.54% (95%CI, 15.64%-21.84%,P<0.01) higher than that of the JE group and 0.33%(95%CI, 0.06%-1.05%, P>0.05) lower than that of the SE group in the ITS. In the ETS, it was 21.67% (95%CI, 16.90%-27.32%, P<0.01) higher than

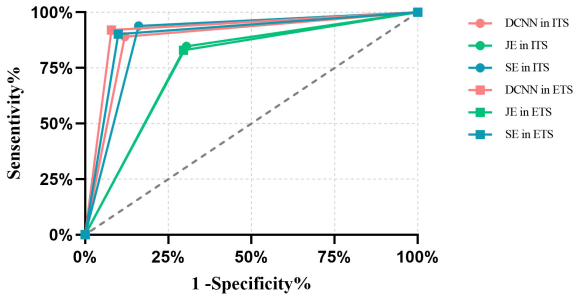

FIGURE 2
ROC curve of DCNN model and endoscopists in internal test sets and external test sets.

that in the JE group and 2.08%(95%CI, 0.75%-4.92%, P>0.05) higher than that in the SE group. In terms of accuracy, DCNN model was 10.47%(95%CI, 8.91-12.27%,P<0.05) higher than that of JE group, and 1.16% (95%CI, 0.69%-1.93%,P > 0.05) lower than that of SE group in the ITS; In the ETS, it was 14.58%(95% CI, 11.84%-17.81%, P<0.01) higher than JE group and 1.94% (95%CI,1.25%-2.96%,P > 0.05)higher than SE group.

Cause of false positives and false negatives

In order to further analyze the causes of false positives and false negatives produced by DCNN model and endoscopists, we summarized it in Tables 3, 4. The first cause for false positive of DCNN model is Gastritis (redness, atrophy, intestinal metaplasia)(44% and 62.5%,respectively),which were also the most reasons for endoscopists(59.29% and 68.52%).Mucus (10.67%) was the secondary cause of in the ITS, while ulcer (12.5%) was the secondary cause in the ETS, which we found that the surface appearance of ulcers were very similar to that of gastric cancer. The third false-positive factor was folding and foam (9.33% in the ITS) and blood (8.33% in the ETS). For endoscopists, ulcer was the second reason (11.43% and 18.52%). However, compared with the DCNN model, endoscopists rarely mistake mucus, foam, and folding for EGC.

Table 4 summarizes the causes of false negatives, the first reason for the false negative in DCNN model was that the diameter of the lesions was less than 10mm (38.88% and 21.05%, respectively). And the 32 images were from 14 patients respectively, DCNN model could identify some of the images in these cases, however the long shooting distance combined with the small diameter of the lesions was the biggest reason for the error recognition of DCNN model. The second factor was visual angle (25% in the ITS), distance and ulcers (15.79% in the ETS, respectively). Different shooting angles resulted in incomplete identification of multiple images of the same

TABLE 3 Details of DCNN model and false positive images of endoscopists.

Cause	Internal test set		External test set	
	DCNN, n (%)	Endoscopists, Total n (%)	DCNN,n (%)	Endoscopists, Total n (%)
Total number	75	280	24	162
Gastritis (redness, atrophy, intestinal metaplasia)	33 (44)	166 (59.29)	15 (62.5)	111 (68.52)
Mucus	8 (10.67)	2 (0.71)	1 (4.17)	4 (2.47)
Fold	7 (9.33)	11 (3.93)	0 (0)	7 (4.32)
Foam	7 (9.33)	4 (1.43)	1 (4.17)	0 (0)
Halation	5 (6.67)	5 (1.79)	0 (0)	0 (0)
Blood	4 (5.33)	8 (2.86)	2 (8.33)	4 (2.47)
blood vessel	4 (5.33)	0 (0)	0 (0)	0 (0)
Ulcer	3 (4)	32 (11.43)	3 (12.5)	30 (18.52)
Xanthoma	2 (2.67)	11(3.93)	1 (4.17)	3 (1.85)
Normal anatomical structure (cardia, pylorus, angulus)	1 (1.33)	0 (0)	0 (0)	0 (0)
Hyperplastic polyp	1 (1.33)	30(10.71)	0 (0)	2 (1.23)
Scar	0 (0)	11(3.93)	1 (4.17)	1 (0.62)

lesion, some lesions in these unrecognized images were relatively flat (type 0-IIb), some of the light increased as the shooting angle changed. The third factor of false negative was distant (16.67% in ITS), tangential line and inflammation-like(10.53%, respectively). For endoscopists, the biggest factor of false negative is inflammation-like (32.74% and 56.84%). Examples of false positive and false negative by DCNN model was shown in Figures 1B–D, 3A–D.

Discussion

In the world, only Japan and South Korea have relatively high diagnosis rate of EGC, while European and American countries have not carried out large-scale endoscopic screening of EGC. China has a large population, and the incidence of gastric cancer accounts for 1/4 of the world, but the diagnosis rate of EGC is only 10% (3, 4), it is far behind Japan and South

TABLE 4 Details of false negative images by DCNN model and endoscopists.

Cause	Internal test set		External test set	
	DCNN, n (%)	Endoscopists, total n (%)	DCNN, n (%)	Endoscopists, totaln (%)
Total number	72	562	19	190
Small (< 10mm)	28 (38.88)	112 (19.93)	4 (21.05)	16 (8.42)
visual angle	18 (25)	50 (8.90)	1 (5.3)	2 (1.05)
Distant	12 (16.67)	90 (16.01)	3 (15.79)	12 (6.32)
Tangential Line	5 (6.94)	12 (2.14)	2 (10.53)	4 (2.1)
Ulcer	4 (5.56)	91 (16.19)	3 (15.79)	28 (14.74)
Adenoma-like	2 (2.78)	16 (2.85)	1 (5.3)	4 (2.1)
Inflammation-like	2 (2.78)	184 (32.74)	2 (10.53)	108 (56.84)
Blood	1 (1.39)	2 (0.36)	1 (5.3)	6 (3.16)
Scar-like	0 (0)	5 (0.89)	0 (0)	5 (2.63)
Others	0 (0)	0 (0)	2 (10.53)	5 (2.63)

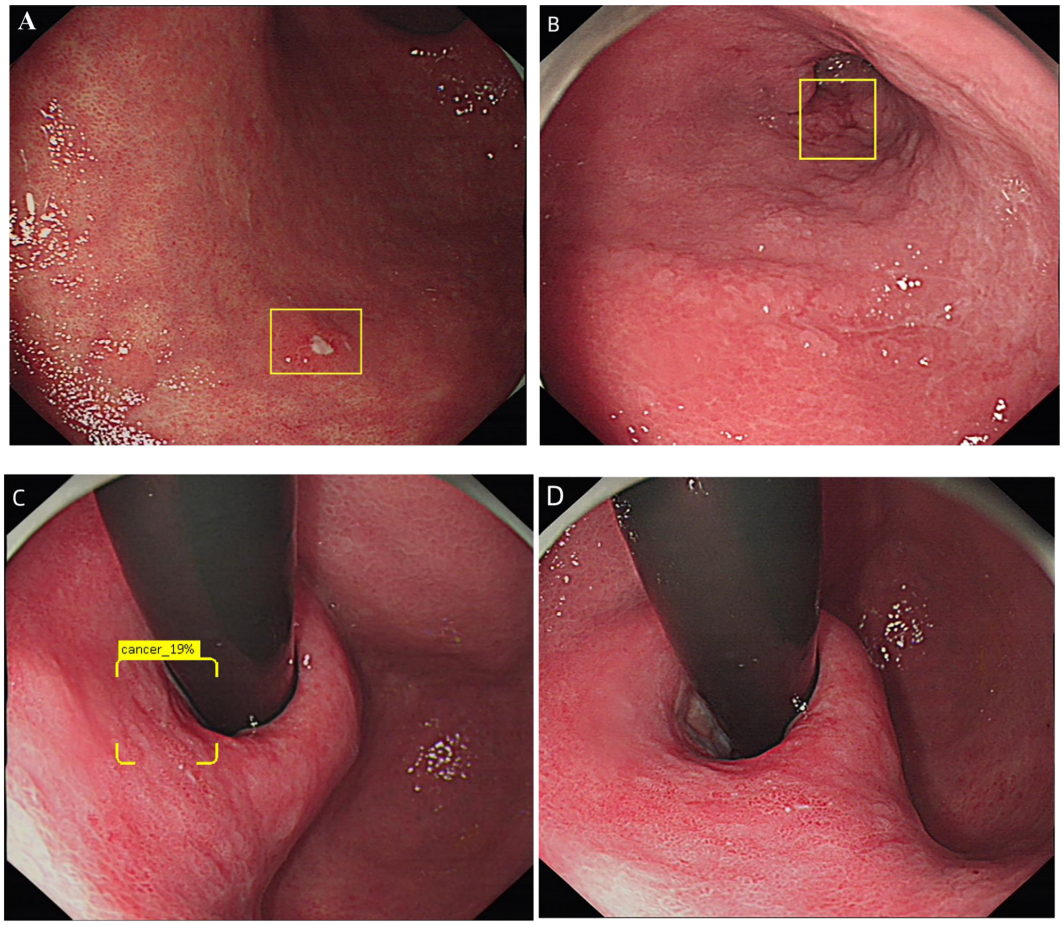

FIGURE 3
Diagram of DCNN producing false negatives. **(A)** Show an image that the lesions were too small to be recognized by DCNN. **(B)** Show an image of the lesions were too far to be recognized by DCNN. **(C, D)** Shows images taken from different shooting angles of the same lesion. **(C)** was effectively recognized as EGC by DCNN, while **(D)** was not recognized by DCNN.

Korea. The difficulty in treatment of EGC lies in early detection. EGD is the only effective tool to identify EGC. Although standardized training of EGD can improve the diagnosis rate, However, the time of training curve is long, and the scope of standardized training is limited (20, 21), in addition, there is a serious shortage of specialized endoscopists in China, the overall level of diagnosis rate in EGC is low, and it is difficult to improve the diagnosis rate of EGC in a short period of time. Therefore, how to quickly shorten endoscopists training time and improve the level of diagnosis rate of EGC is an urgently problem for us to solve.

Although various image enhancement techniques have been developed and applied, white light imaging(WLI) is the first step in standard EGD (16), The use of image enhancement technology is considered only after suspicious lesion under WLI. It has been reported that the sensitivity of WLI for EGC is 33%-75% (22), On the other hand, diagnosis depends on the experience and subjective awareness of the EGD operator (17). Therefore, through the training of images, we developed the DCNN system to assist the diagnosis of EGC in WLI. The sensitivity of DCNN model is 88.08% and 92.08%, which was significantly higher than that of all endoscopists, and its recognition time was significantly shorter than that of all endoscopists.

We found that ulcers (11.43% and 18.52%) were an important cause of false positives produced by endoscopists, as well as a cause of missed diagnosis (16.19% and 14.74%), which means that endoscopists have difficulty in distinguishing ulcers from EGC. Ulcers were included as negative controls in our DCNN model training. Therefore, compared with endoscopists, the proportion of false positives in DCNN model due to ulcers was lower than that of endoscopists (4%-12.5% vs.11.43%-18.52%). This means that our DCNN model can help endoscopists reduce the incidence of such errors. Of course, our DCNN model also has a certain false negative rate. Among them, 38.88% and 21.05% are lesions smaller than 10mm.

Considering that it is difficult for even experienced endoscopists to diagnose small lesions, the development time of intratumoral cancer is 2-3 years, we speculate that this limitation can be confirmed by annual upper gastrointestinal endoscopy and biopsy (23), and for the update iteration of DCNN, we will also increase the training of small lesions. 25% and 5.3% false negatives are difficult to identify because of different angles of view. However, DCNN can identify at least two images of a patient from different angles, therefore, we speculate that the retention of suspicious lesions from multiple locations and angles can make up for this defect of DCNN. The lesion distance is the third major reason leading to false negative of DCNN. Although the morphology of these lesions is prominent, but the images were taken as a far distance, and the color, texture and other features of the lesions were not obvious, therefore it is easy to be ignored by the DCNN. Another rare reason for false negatives in DCNN is that lesions are similar to inflammatory changes, but they are the most common cause for endoscopists. This finding suggests that endoscopists may misdiagnose inflammation, but DCNN does not miss lesions (2.78% vs. 32.74% in ITS, 10.53% vs.56.84% in ETS).

The most common causes of false positives are mucosal redness, atrophy, and intestinal degeneration. Even experienced endoscopists can hardly distinguish these lesions by a single WLI without magnifying endoscopy. 29.33% and 8.34% of false positives are due to mucus, foam and folding. DCNN is more likely to be affected by the above factors, while endoscopists are less affected by these factors, which means that DCNN may be more affected by the background in the stomach in the actual application process. However, as demonstrated by Mori et al. (24) these limitations can be reduced by mucosal irrigation, the use of antifoaming agents and adequate gas injection, as well as the application of a large number of images for training in the real process of EGD.

For specificity and PPV, Although SE performed better on specificity and PPV in ITS, the DCNN model was higher than that of JE, our image of training set goes through carefully selected, excluded those poor quality of the image images, containing mucus, bubble, folding and dizzy light images, We believe that if we strengthen the training of false positive images, these problems will be solved (25). DCNN is more sensitive and can identify more EGCs than experienced endoscopists, especially for JE. In addition, the sensitivity and PPV of expert endoscopists are significantly higher than those of JE, so DCNN may be more helpful to those endoscopists with limited experience.

We reviewed the relevant literature and found that some AI have a sensitivity of up to 90% (26–28). However, the control groups in these studies only included normal or chronic gastritis, not ulcerative lesions that endoscopists are more likely to confuse. and there studies focused on the sensitivity of detecting gastric cancer as a whole, including advanced gastric cancer, and were not compared with endoscopists. Moreover, most studies did not analyze the causes of false positive and false negative for endoscopists and DCNN, so as to carry out targeted strengthening training. The sensitivity found in this study appears to be lower in ITS than those studies for the following reasons: first, only EGC images were included in this study, and intermediate and advanced gastric cancer were not included. Second, sensitivity was calculated per lesion, not per image in those studies, that is, if at least one image of gastric cancer is recognized in multiple images of the same lesion, the diagnosis is considered correct. Third, in these studies, the concept of correct diagnosis is that if the image area identified by DCNN overlaps slightly with that of EGC, it is considered correct. However, in our study, only the image range identified by DCNN overlapped by more than 50% with the image range marked by endoscopist was considered correct, while occasionally marked or not marked enough, we considered it incorrect. Recently, A multicenter study reported (29) that DCNN assisted diagnosis of upper gastrointestinal tumors, including gastric cancer shows diagnostic accuracy of DCNN was up to 90%, and the sensitivity was comparable with that of expert endoscopists. However, in this study, the rate of advanced gastric cancer was relatively higher, while the early gastric cancer was only 18.6%. Our research aims to find more EGC that endoscopists are prone to misdiagnose.

In terms of stability evaluation, SE group with higher diagnostic accuracy has better diagnostic consistency than JE group. According to the general guidelines of ICC standard (30), there are considerable differences in the diagnosis consistency among endoscopists, which is not clearly related to professional knowledge and experience. Due to the subjective interpretation of the characteristics of EGC and the different learning curve in the diagnosis of EGC, objective diagnosis is very necessary (9). The DCNN system achieves perfect observer protocol (Kappa 1.0) without interference of subjective judgment. The EGC detection system based on the DCNN has sufficient and consistent diagnostic performance, eliminating some diagnostic subjectivity. Moreover, the DCNN system is very helpful for JE, this is consistent with the research of Ikenoyama et al. (31) DCNN may be a powerful tool to assist endoscopists, especially JE in detecting EGC. The shorter screening time and fatigue free DCNN may enable rapid surveillance of EGC. More importantly, the diagnosis of EGC by DCNN can be fully automated and online, which may facilitate the development of telemedicine and thereby alleviate the problem of a shortage of endoscopists.

Yet, the study has several limitations, first of all, our DCNN only trained WLI images, it can provides the first step of EGC detection, which is also the most important step, but it did not trained narrow-band images (NBI) and the magnifying endoscopy (ME). However. in past research report, endoscopic image enhancement is rarely used, unless there is a suspicious lesion found in the WLI (32). In addition, a multicenter study showed no significant difference in the diagnostic efficacy of nonamplified NBI and WLI in EGC (33). Moreover, in reality,

unless use the NBI routinely in esophageal observation, It is generally not used in endoscopic examination unless suspicious lesions are found under WLI (32). Secondly, we only use Olympus 260 or 290 series gastroscope system, without other brands of endoscopes such as Fuji Endoscope, this may reduce the efficiency of DCNN. Third, in the control group of gastric cancer detection dataset, we eliminated most of the images containing mucus and halo, and the diagnostic sensitivity of DCNN may be lower in the real world. Fourth, static images are used in the training and testing sets of this study, and video images can improve the performance and present the real scene, we plan to use video as a validation set in the future, which will be used as another separate study. Fifth, in this study, DCNN model missed diagnosis of small lesions, increasing the number of training of small lesions and flat lesions, as well as the number of negative control images will help improve the diagnostic efficiency of the model.

In conclusion, we constructed an assist EGC detection system based on DCNN and compared the diagnostic ability of DCNN and endoscopists. It has excellent diagnostic sensitivity, fast diagnostic characteristics, achieved a perfect observer protocol. It can help endoscopists (especially JE) to find more EGC. We believe that DCNN will contribute to the overall improvement of the diagnosis rate of EGC, and serve as an assisting work to help improve the diagnosis rate of EGC.

Data availability statement

The original contributions presented in the study are included in the article/Supplementary Material. Further inquiries can be directed to the corresponding author.

Ethics statement

Written informed consent was obtained from the individual(s) for the publication of any potentially identifiable images or data included in this article.

Author contributions

JF designed the experiment and drafted this article. SY and YZ were responsible for the collection of training set images. LQ was responsible for the submission of ethical approval documents. YF nd YY were responsible for the annotation of the images. LG, XL, WL and PW were responsible for the recognition of the test set images. YB and LZ were responsible for the algorithm training of DCNN. XH was responsible for the project coordination. All authors contributed to the article and approved the submitted version.

Funding

This work was supported by the Cuiying Scientific and Technological Innovation Program of Lanzhou University Second Hospital (2020QN-12), the Program of Gansu Youth Science and Technology(21JR1RA155). Science and Technology Department of Gansu(20YF8FA076). the Program of Gansu Youth Science and Technology(22JR5RA1000).

Acknowledgments

We thank all the authors for their contributions to this article.

Conflict of interest

The authors declare that the research was conducted in the absence of any commercial or financial relationships that could be construed as a potential conflict of interest.

Publisher's note

All claims expressed in this article are solely those of the authors and do not necessarily represent those of their affiliated organizations, or those of the publisher, the editors and the reviewers. Any product that may be evaluated in this article, or claim that may be made by its manufacturer, is not guaranteed or endorsed by the publisher.

Supplementary material

The Supplementary Material for this article can be found online at: https://www.frontiersin.org/articles/10.3389/fonc.2022.1021625/full#supplementary-material

References

1. Sung H, Ferlay J, Siegel RL, Laversanne M, Soerjomataram I, Jemal A, et al. Global cancer statistics 2020: GLOBOCAN estimates of incidence and mortality worldwide for 36 cancers in 185 countries. *CA: Cancer J Clin* (2021) 71(3):209–49. doi: 10.3322/caac.21660

2. Katai H, Ishikawa T, Akazawa K, Isobe Y, Miyashiro I, Oda I, et al. Five-year survival analysis of surgically resected gastric cancer cases in Japan: a retrospective analysis of more than 100,000 patients from the nationwide registry of the Japanese gastric cancer association (2001-2007). *Gastric Cancer.* (2018) 21(1):144–54. doi: 10.1007/s10120-017-0716-7

3. Baptista V, Singh A, Wassef W. Early gastric cancer: an update on endoscopic management. *Curr Opin gastroenterology.* (2012) 28(6):629–35. doi: 10.1097/MOG.0b013e328358e5b5

4. Bu Z, Ji J. Controversies in the diagnosis and management of early gastric cancer. *Chin J Cancer Res = Chung-kuo yen cheng yen chiu.* (2013) 25(3):263–6. doi: 10.3978/j.issn.1000-9604.2013.06.15

5. Asaka M, Mabe K. Strategies for eliminating death from gastric cancer in Japan. *Proc Japan Acad Ser B Phys Biol Sci* (2014) 90(7):251–8. doi: 10.2183/pjab.90.251. Cited in: Pubmed

6. Amin A, Gilmour H, Graham L, Paterson-Brown S, Terrace J, Crofts TJ. Gastric adenocarcinoma missed at endoscopy. *J R Coll Surgeons Edinburgh.* (2002) 47(5):681–4. doi: 10.1055/s-2004-825853

7. Hosokawa O, Tsuda S, Kidani E, Watanabe K, Tanigawa Y, Shirasaki S, et al. Diagnosis of gastric cancer up to three years after negative upper gastrointestinal endoscopy. *Endoscopy.* (1998) 30(8):669–74. doi: 10.1055/s-2007-1001386

8. Menon S, Trudgill N. How commonly is upper gastrointestinal cancer missed at endoscopy? A meta-analysis. *Endoscopy Int Open* (2014) 2(2):E46–50. doi: 10.1055/s-0034-1365524

9. Yalamarthi S, Witherspoon P, McCole D, Auld CD. Missed diagnoses in patients with upper gastrointestinal cancers. *Endoscopy.* (2004) 36(10):874–9. doi: 10.1055/s-2004-825853

10. Suvakovic Z, Bramble MG, Jones R, Wilson C, Idle N, Ryott J. Improving the detection rate of early gastric cancer requires more than open access gastroscopy: a five year study. *Gut.* (1997) 41(3):308–13. doi: 10.1136/gut.41.3.308

11. Voutilainen ME, Juhola MT. Evaluation of the diagnostic accuracy of gastroscopy to detect gastric tumours: clinicopathological features and prognosis of patients with gastric cancer missed on endoscopy. *Eur J Gastroenterol hepatology.* (2005) 17(12):1345–9. doi: 10.1097/00042737-200512000-00013

12. Raftopoulos SC, Segarajasingam DS, Burke V, Ee HC, Yusoff IF. A cohort study of missed and new cancers after esophagogastroduodenoscopy. *Am J gastroenterology.* (2010) 105(6):1292–7. doi: 10.1038/ajg.2009.736

13. Vradelis S, Maynard N, Warren BF, Keshav S, Travis SP. Quality control in upper gastrointestinal endoscopy: detection rates of gastric cancer in Oxford 2005-2008. *Postgraduate Med J* (2011) 87(1027):335–9. doi: 10.1136/pgmj.2010.101832

14. Hosokawa O, Hattori M, Douden K, Hayashi H, Ohta K, Kaizaki Y. Difference in accuracy between gastroscopy and colonoscopy for detection of cancer. *Hepato-gastroenterology.* (2007) 54(74):442–4. doi: 10.1055/s-2001-13685

15. Rutter MD, Senore C, Bisschops R, Domagk D, Valori R, Kaminski MF, et al. The European society of gastrointestinal endoscopy quality improvement initiative: developing performance measures. *United Eur Gastroenterol J* (2016) 4 (1):30–41. doi: 10.1177/2050640615624631

16. Yao K, Uedo N, Muto M, Ishikawa H. Development of an e-learning system for teaching endoscopists how to diagnose early gastric cancer: basic principles for improving early detection. *Gastric Cancer.* (2017) 20(Suppl 1):28–38. doi: 10.1007/s10120-016-0680-7

17. Scaffidi MA, Grover SC, Carnahan H, Khan R, Amadio JM, Yu JJ, et al. Impact of experience on self-assessment accuracy of clinical colonoscopy competence. *Gastrointestinal endoscopy.* (2018) 87(3):827–36. doi: 10.1016/j.gie.2017.10.040

18. Wang KW, Dong M. Potential applications of artificial intelligence in colorectal polyps and cancer: Recent advances and prospects. *World J gastroenterology.* (2020) 14 26(34):5090–100. doi: 10.3748/wjg.v26.i34.5090

19. Xia J, Xia T, Pan J, Gao F, Wang S, Qian YY, et al. Use of artificial intelligence for detection of gastric lesions by magnetically controlled capsule endoscopy. *Gastrointestinal endoscopy.* (2021) 93(1):133–139.e4. doi: 10.1016/j.gie.2020.05.027

20. Yamazato T, Oyama T, Yoshida T, Baba Y, Yamanouchi K, Ishii Y, et al. Two years' intensive training in endoscopic diagnosis facilitates detection of early gastric cancer. *Internal Med (Tokyo Japan).* (2012) 51(12):1461–5. doi: 10.2169/internalmedicine.51.7414

21. Zhang Q, Chen ZY, Chen CD, Liu T, Tang XW, Ren YT, et al. Training in early gastric cancer diagnosis improves the detection rate of early gastric cancer: An observational study in China. *Medicine.* (2015) 94(2):e384. doi: 10.1097/md.0000000000000384

22. Ezoe Y, Muto M, Uedo N, Doyama H, Yao K, Oda I, et al. Magnifying narrowband imaging is more accurate than conventional white-light imaging in diagnosis of gastric mucosal cancer. *Gastroenterology.* (2011) 141(6):2017–2025.e3. doi: 10.1053/j.gastro.2011.08.007

23. Fujita S. Biology of early gastric carcinoma. *Pathology Res practice.* (1978) 163(4):297–309. doi: 10.1016/s0344-0338(78)80028-4

24. Mori Y, Kudo SE, Mohmed HEN, Misawa M, Ogata N, Itoh H, et al. Artificial intelligence and upper gastrointestinal endoscopy: Current status and future perspective. *Dig Endosc.* (2019) 31(4):378–88. doi: 10.1111/den.13317

25. Gotoda T, Uedo N, Yoshinaga S, Tanuma T, Morita Y, Doyama H, et al. Basic principles and practice of gastric cancer screening using high-definition white-light gastroscopy: Eyes can only see what the brain knows. *Dig Endosc.* (2016) 28 Suppl 1:2–15. doi: 10.1111/den.12623

26. Hirasawa T, Aoyama K, Tanimoto T, Ishihara S, Shichijo S, Ozawa T, et al. Application of artificial intelligence using a convolutional neural network for detecting gastric cancer in endoscopic images. *Gastric Cancer.* (2018) 21(4):653–60. doi: 10.1007/s10120-018-0793-2

27. Luo H, Xu G, Li C, He L, Luo L, Wang Z, et al. Real-time artificial intelligence for detection of upper gastrointestinal cancer by endoscopy: a multicentre, case-control, diagnostic study. *Lancet Oncol* (2019) 20(12):1645–54. doi: 10.1016/s1470-2045(19)30637-0

28. Wu L, Zhou W, Wan X, Zhang J, Shen L, Hu S, et al. A deep neural network improves endoscopic detection of early gastric cancer without blind spots. *Endoscopy.* (2019) 51(6):522–31. doi: 10.1055/a-0855-3532

29. Luo H, Xu G, Li C, He L, Luo L, Wang Z, et al. Real-time artificial intelligence for detection of upper gastrointestinal cancer by endoscopy: A multicentre, case-control, diagnostic study. *Lancet Oncol* (2019) 20(12):1645–54. doi: 10.1016/s1470-2045(19)30637-0

30. Koo TK, Li MY. A guideline of selecting and reporting intraclass correlation coefficients for reliability research. *J chiropractic Med* (2016) 15(2):155–63. doi: 10.1016/j.jcm.2016.02.012

31. Ikenoyama Y, Hirasawa T, Ishioka M, Namikawa K, Yoshimizu S, Horiuchi Y, et al. Detecting early gastric cancer: Comparison between the diagnostic ability of convolutional neural networks and endoscopists. *Dig Endosc.* (2021) 33(1):141–50. doi: 10.1111/den.13688

32. Uedo N, Gotoda T, Yoshinaga S, Tanuma T, Morita Y, Doyama H, et al. Differences in routine esophagogastroduodenoscopy between Japanese and international facilities: A questionnaire survey. *Dig Endosc.* (2016) 28 Suppl 1:16–24. doi: 10.1111/den.12629

33. Ang TL, Pittayanon R, Lau JY, Rerknimitr R, Ho SH, Singh R, et al. A multicenter randomized comparison between high-definition white light endoscopy and narrow band imaging for detection of gastric lesions. *Eur J Gastroenterol hepatology.* (2015) 27(12):1473–8. doi: 10.1097/meg.0000000000000478

frontiers | Frontiers in Oncology

TYPE Original Research
PUBLISHED 22 December 2022
DOI 10.3389/fonc.2022.1050288

Check for updates

OPEN ACCESS

EDITED BY
Zhendong Jin,
Second Military Medical University, China

REVIEWED BY
Hailin Tang,
Sun Yat-sen University Cancer Center (SYSUCC), China
Yi Jia,
Guizhou Medical University, China

*CORRESPONDENCE
Jianguo Zeng
zengjianguo@hunau.edu.cn
Xinhua Xia
xiaxinhua001@hnucm.edu.cn

†These authors have contributed equally to this work

SPECIALTY SECTION
This article was submitted to Gastrointestinal Cancers: Gastric and Esophageal Cancers, a section of the journal Frontiers in Oncology

RECEIVED 21 September 2022
ACCEPTED 26 October 2022
PUBLISHED 22 December 2022

CITATION
Yang J, Wu Z, Wu X, Chen S, Xia X and Zeng J (2022) Constructing and validating of m6a-related genes prognostic signature for stomach adenocarcinoma and immune infiltration: Potential biomarkers for predicting the overall survival. *Front. Oncol.* 12:1050288. doi: 10.3389/fonc.2022.1050288

COPYRIGHT
© 2022 Yang, Wu, Wu, Chen, Xia and Zeng. This is an open-access article distributed under the terms of the Creative Commons Attribution License (CC BY). The use, distribution or reproduction in other forums is permitted, provided the original author(s) and the copyright owner(s) are credited and that the original publication in this journal is cited, in accordance with accepted academic practice. No use, distribution or reproduction is permitted which does not comply with these terms.

Constructing and validating of m6a-related genes prognostic signature for stomach adenocarcinoma and immune infiltration: Potential biomarkers for predicting the overall survival

Jing Yang[1,2], Zixuan Wu[2], Xiaoxi Wu[3], Siya Chen[2], Xinhua Xia[2*†] and Jianguo Zeng[1*†]

[1]Hunan Agricultural University, Changsha, China, [2]School of Pharmacy, Hunan University of Chinese Medicine, Changsha, China, [3]The Second Affiliated Hospital of Guangzhou University of Chinese Medicine, Guangzhou, China

Background: Stomach adenocarcinoma (STAD) arises from the mutations of stomach cells and has poor overall survival. Chemotherapy is commonly indicated for patients with stomach cancer following surgical resection. The most prevalent alteration that affects cancer growth is N6-methyladenosine methylation (m6A), although the possible function of m6A in STAD prognosis is not recognized.

Method: The research measured predictive FRGs in BLCA samples from the TCGA and GEO datasets. Data on the stemness indices (mRNAsi), gene mutations, copy number variations (CNV), tumor mutation burden (TMB), and corresponding clinical characteristics were obtained from TCGA and GEO. STAD from TCGA and GEO at 24 m6A was investigated. Lasso regression was used to construct the prediction model to assess the m6A prognostic signals in STAD. In addition, the correlation between m6a and immune infiltration in STAD patients was discussed using GSVA and ssGSEA analysis. Based on these genes, GO and KEGG analyses were performed to identify key biological functions and key pathways.

Result: A significant relationship was discovered between numerous m6A clusters and the tumor immune microenvironment, as well as three m6A alteration patterns with different clinical outcomes. Furthermore, GSVA and ssGSEA showed that m6A clusters were significantly associated with immune infiltration in the STAD. The low-m6Ascore group had a lower immunotherapeutic response than the high-m6Ascore group. ICIs therapy was more effective in the group with a higher m6Ascore. Three writers (VIRMA, ZC3H13, and METTL3) showed significantly lower expression, whereas five

authors (METTL14, METTL16, WTAP, RBM15, and RBM15B) showed considerably higher expression. Three readers (YTHDC2, YTHDF2, and LRPPRC) had higher levels of expression, whereas eleven readers (YTHDC1, YTHDF1, YTHDF3, HNRNPC, FMR1, HNRNPA2B1, IGFBP1, IGFBP2, IGFBP3, and RBMX) had lower levels. As can be observed, the various types of m6 encoders have varied ramifications for STAD control.

Conclusion: STAD occurrence and progression are linked to m6A-genes. Corresponding prognostic models help forecast the prognosis of STAD patients. m6A-genes and associated immune cell infiltration in the tumor microenvironment (TME) may serve as potential therapeutic targets in STAD, which requires further trials. In addition, the m6a-related gene signature offers a viable alternative to predict bladder cancer, and these m6A-genes show a prospective research area for STAD targeted treatment in the future.

KEYWORDS

stomach adenocarcinoma (STAD), M6A, predicting model, immunity, SNP, CNV

Introduction

Gastric cancer (GC) is the fifth most frequent cancer and the third major cause of cancer-related deaths globally. Stomach adenocarcinoma (STAD) is the most frequent histologic form of GC with rapid progression, and malignant GC accounts for 95 percent of all gastric tumors. Research has discovered that Helicobacter pylori infection is responsible for 90% of STAD cases (1). Many researchers have proposed that STAD could also be triggered by autoimmunity, bacteria, and their metabolites (2). STAD is now considered a collection of uncommon illnesses that risk human health (3), underlining the timely intervention of STAD (4). Chemotherapy is an important part of tumor treatment, but their cytotoxicity and potential adverse effects after long-term use will pose considerable issues for patients. Recurring usage of chemotherapy drugs is associated with tumor cell resistance, thereby compromising the curative impact (5). Moreover, the lack of precise biomarkers for early tumor diagnosis and restricted preclinical models result in unsatisfactory STAD therapeutic outcomes (6, 7). Therefore, there is a pressing need to identify novel and reliable biomarkers for the early identification and diagnosis of STAD.

There are 172 identified forms of RNA alterations, and the most common chemical modifications are m6A, m1A, and m5C. m6A is one of the most prevalent eukaryotic mRNA modifications (8). The m6A modification involves the methylation of adenosine's sixth nitrogen atom, with Sadenosylmethionine, a cellular methyltransferase substrate, functioning as the methyl donor (9). Epigenetic regulation of cell development and differentiation has been linked to m6A and post-translational histone changes (10). m6A was the most prevalent internal epistemic RNA modification, and it was implicated with several biological functions such as RNA splicing, export, and translation (11, 12). M^6A regulators, such as methyltransferases complex ("writers"), signal transducers ("readers"), and demethylases ("erasers"), control the m^6A alterations (13). Different levels of m^6A are associated with tumor stem cell self-renewal, cancer cell proliferation, and chemotherapy sensitivity in numerous studies (14, 15). Tumor stem cell self-renewal is stimulated by aberrant m^6A, which contributes to tumor growth (16). Thus, a novel anticancer method based on restoring RNA methylation equilibrium in tumor cells was created (17, 18).

Numerous studies have shown that m6A regulators play an important role in tumor immune microenvironment control. FTO has a comparable antitumor effect on melanoma as a factor in anti-PD-1 resistance. The researchers expected that combining FTO inhibitors with anti-PD-1 inhibition would aid in the reduction of treatment resistance in melanoma patients. m6A alteration, as a reversible epigenetic change, should be addressed in the context of tumor therapy.

Abbreviations: STAD, Stomach adenocarcinoma; m6A, N6-methyladenosine methylation; CNV, copy number variations; MF, molecular functions; ICIs, immune checkpoint inhibitors; TML, Tumor mutation load; GSEA, gene set enrichment analyses; TCGA, The Cancer Genome Atlas; SNP, simple nucleotide variation; BP, Biological processes; CC, cellular components; OS, overall survival; GEO, Gene Expression Omnibus; DEGs, differentially expressed genes; KEGG, Kyoto Encyclopedia of Genes and Genomes.

Materials and methods

We used the approaches proposed by Zi-Xuan Wu, et al. 2021 (19).

Datasets and PRGs

The TCGA was used to collect STAD gene and clinical data (20). 375 STADs and 32 normal data were registered in the TCGA on September 6, 2022. The GEO was searched for mRNA expression on September 6, 2022. Series: GSE84437. Platform: GPL6947-13512. The GEO was used to maintain 433 STAD cases (21) (Table 1). 24 m6A regulators were identified (22) (Table S1).

DEGs and mutation rates

Perl matched and sorted transcription data to acquire exact mRNA data. The IDs were converted into gene names. FDR<0.05 and |log2FC|≥1 were utilized to assess a substantial change in m6a-genes expression. The relevance of differentially expressed m6a-genes was investigated (DEGs). Data on the simple nucleotide variation (SNP) and copy number variations (CNV) were obtained from TCGA. The R maftools package was used to evaluate and visualize the SNP mutation. The SNP2APA database was created to investigate the impact of SNPs and give OS across various cancer types. The EDGs and GEO data were subsequently merged from TCGA and matched to obtain m6a-genes. We examined this database for particular SNPs with predictive significance in STAD and investigated the connection between these SNPs and critical m6A-genes.

Tumor m6a classification based on the DEGs

Cluster analysis was performed using the Limma and ConsensusClusterPlus package, and the prognosis-related m6a-genes were separated into three clusters: clusters A, B and C. Survminer was used to study the survivability of m6a-genes, and survival was used to evaluate the predictive utility of m6a-genes. The limma was utilized to discover changes in particular genes between subtypes and tissue types.

GSEA analysis and cluster DEGs

GSEA was done in GEO and TCGA groups to compare the median level of three clusters' expression to explore the biological signaling route. NES, gene ratio, and P-value were used to identify KEGG pathways with significant enrichment data. The enriched values (ssGSEA) of immune cells in both the 3 cohorts and the PCA methods were investigated. To test whether or not the prognosis model successfully divided patients into three groups. To assess a substantial change in m6a-genes expression, FDR<0.001 and |log2FC|≥1 were utilized. The relevance of differentially expressed m6a-genes was Cluster DEGs.

GO and KEGG analysis

Using GO and KEGG, the biological function and pathways linked with the DEGs were investigated. BP, MF, and CC regulated by differentially expressed m6a-genes were explored using R.

TABLE 1 Patient clinical features.

TCGA		GEO	
Variable	**Number of samples**	**Variable**	**Number of samples**
Gender		Gender	
Male/Female	285/158	Male/Female	296/137
Age at diagnosis		Age at diagnosis	
≤65/>65/NA	197/241/5	≤65/>65	283/150
Grade		Grade	
G1/G2/G3/G4/NA	Unknown	G1/G2/G3/G4/NA	Unknown
Stage		Stage	
I/II/III/IV/NA	59/130/183/44/27	I/II/III/IV/NA	Unknown
T		T	
T1/T2/T3/T4/NA	23/93/198/119/10	T1/T2/T3/T4	11/38/92/292
M		M	
M0/M1/NA	391/30/22	M0/M1/NA	Unknown
N		N	
N0/N1/N2/N3/NA	132/119/85/88/19	N0/N1/N2/N3	80/188/132/33

Prognostic signature and cluster

Every STAD patient's risk score was evaluated. Lasso regression was associated with prognostic genes. These prognostic genes were subjected to cluster analysis to assess their respective expression in different clusters. Accordingly, the m6a-genes associated with prognosis were obtained after matching. M6a-DEGs were classified under two categories: low- or high-risk. Survival curves for the 2 categories were evaluated. To confirm the impact of clinical variables on this model, a nurse independent prediction analysis was performed. Risk and clinical interaction studies were made available.

Prognostic m6a-genes and immune cell infiltration

Tumor mutation load (TML) is a good predictor of immunotherapy response that count the amount of mutations per DNA megabase and detect alterations such as nucleotide insertions, base substitutions, and deletions. MSI is a molecular tumor characteristic that is distinguished by spontaneous nucleotide loss or gain from short tandem repeat DNA sequences. The association between m6a-genes Expression and TMB and MSI was explored.

Results

The m6A regulator landscape

M6A regulator mRNA expression changed between STAD and normal tissues (Figure 1A). The expression of each eraser (FTO, ALKBH5) was considerably increased in STAD tissues. Three writers (VIRMA, ZC3H13, and METTL3) revealed noticeably reduced expressions, whereas five writers (METTL14, METTL16, WTAP, RBM15, and RBM15B) displayed conspicuously high expressions. Three readers (YTHDC2, YTHDF2, and LRPPRC) were expressed at greater levels, while ten readers (YTHDC1, YTHDF1, YTHDF3, HNRNPC, FMR1, HNRNPA2B1, IGFBP1, IGFBP2, IGFBP3, and RBMX) were expressed at lower levels. The CNVs of the 23 m6A regulators were then summarized in STAD (Figure 1B). The results of the SNV analysis are shown as a circle graph (Figure 1C; Table S2). The m6A regulatory network represents an investigation into the expression correlation and prognostic significance of the 24 m6A regulators in STAD patients (Figure 1D; Table S3). To determine the hazard ratios (HRs) and PFS for the m6A regulators, a univariate Cox regression model was employed (Table S1). Consequently, ZC3H13, FTO, IGFBP1, IGFBP2, and IGFBP3 were identified as risk factors, whereas RBM15, HNRNPC, and HNRNPA2B1 were identified as protective factors. Furthermore, the frequency of m6A regulator mutations was lower than 7% (Figure 1E), indicating no relationship to tumor growth. Low expression of erasers, as prognostic variables, revealed that a reduction in m6A demethylation can inhibit the development of STAD. Upregulation of three STAD readers (YTHDC2, YTHDF2, and LRPPRC) is associated with poor prognosis. Table S2 contains a complete study of RNA expression and CNV.

Mutation and expression correlation, m6A survival analysis

ZC3H13 is the gene with the highest mutation rate (Figure 1E), based on which grouping analysis was performed. There was significant variability in four genes (HNRNPC, YTHDC2, YTHDF3 and ZC3H13) (Figure 2A). In terms of survival analysis, all these m6a-genes correlated with the prognosis of STAD, suggesting a strong relationship between m6a-genes on the progression of STAD and the survival status of patients (Figure 2B).

Tumor classification and immune cells

When k was 3, intraorganizational links were strongest and intergenerational connections were weakest (Figure 3A). The PCA efficiently classified STAD's individuals with various dangers into three basic categories (Figure 3B). A heatmap reflects both the m6a genes and clinical characteristics (Figure 3C). M6a Clusters were employed in survival research to investigate PRG predictive capacity, and Cluster C had a greater survival rate (P=0.005; Figure 3D; Table S4). The enriched values of immune cells in both 3 cohorts were studied. The variability between the three groups was highly significant except for two cells(CD56dim.natural.killer.cell and Eosinophil) (Figure 3E). The functional enrichment of m6a-genes was determined using GSEA (Figures 4A, B). These genes were associated with RNA and Methylation.

Cluster variance analysis and differential gene identification

To further analyse the differential expression of the m6a gene in these clusters, a differential analysis (Figures 5A, B) was performed. When k was 3, intraorganizational links were strongest and intergenerational connections were weakest (Figure 5C). DEGs were employed in survival research to investigate Cluster DEGs' predictive potential, and Cluster B had a greater survival rate (P=0.004; Figure 5D). A heatmap reflects both the Cluster DEGs and clinical characteristics (Figure 5E).

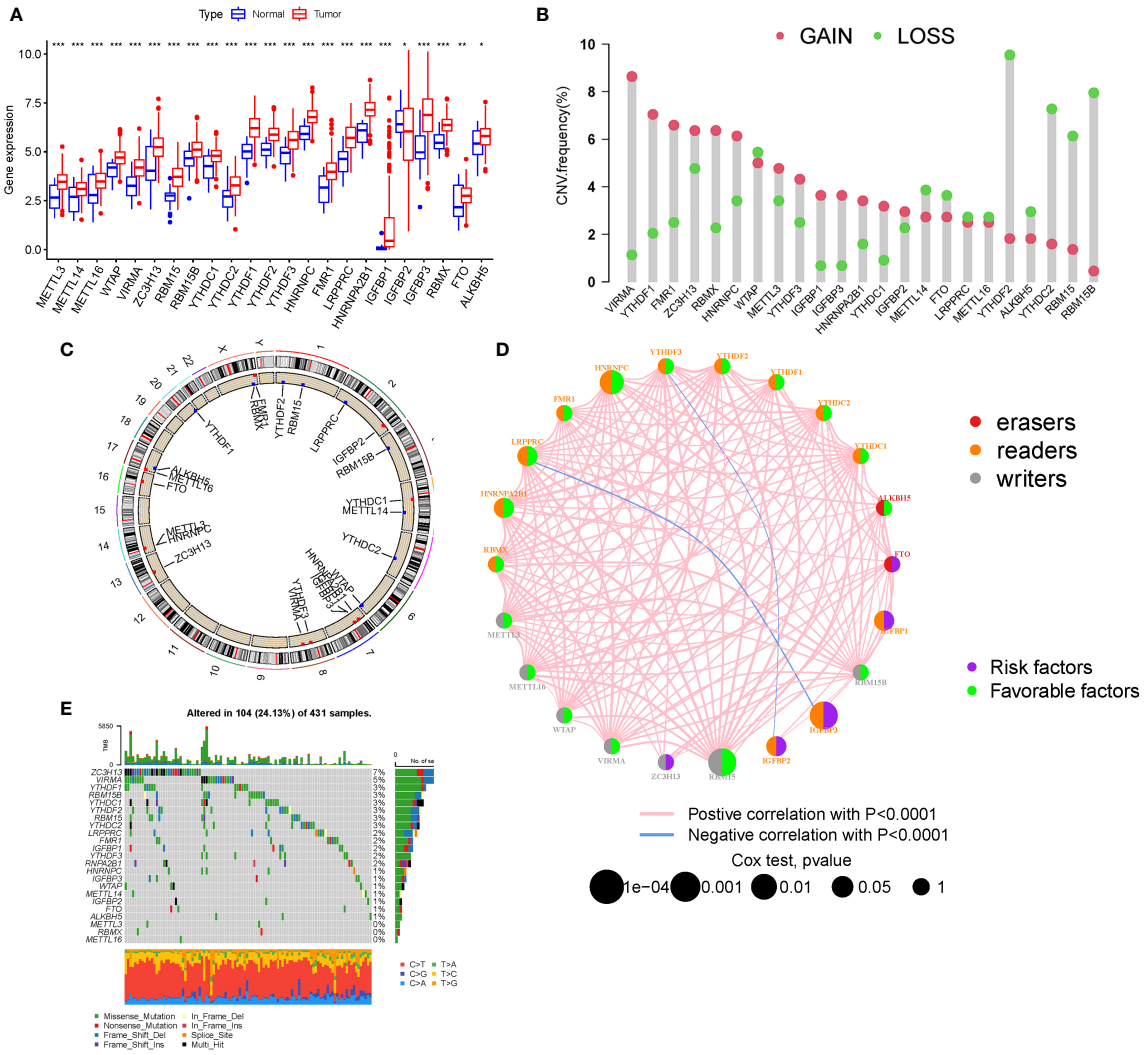

FIGURE 1
Landscape of genetic and expression variation. **(A)** The expression of m6A regulators. **(B)** The CNV variation frequency. **(C)** CNV Analysis (M6a shows a significant association with CNV in STAD). **(D)** The interaction between m6A regulators (The m6A regulatory network is a study of the expression correlation and prognostic importance of the 24 m6A regulators in STAD patients). **(E)** Waterfall plot of TMB (the frequency of m6A regulator mutations was lower than 7%). (*P < 0.05; **P < 0.01; ***P < 0.001).

GO and KEGG analysis

GO analysis revealed 707 core targets. The MF mainly involves signaling transcription coregulator activity (GO:0003712), ATPase activity (GO:0016887), catalytic activity, and acting on RNA (GO:0140098). The CC mainly involves the mitochondrial inner membrane (GO:0005743), mitochondrial matrix (GO:0005759), nuclear envelope (GO:0005635). The BP mainly involves the regulation of cellular amide metabolic process (GO:0034248), LncRNA metabolic process (GO:0034660), organelle fission (GO:0048285). Furthermore, KEGG analysis was used to identify the primary signaling pathways, which indicated that Cluster DEGs were mostly engaged in the Amyotrophic lateral sclerosis (hsa05014), Spliceosome (hsa03040), Cell cycle (hsa04110) (Figure 6; Tables S5, 6).

m6A score construction

We created the m6Ascore, a set of scoring methods for assessing the m6A modification pattern of individual STAD patients, in response to the demand for more reliable and clear models for immunotherapy prediction based on these phenotype-related genes. Although survival analysis indicated two distinct prognoses, the cluster of m6A regulators and CEGs were separated into three groups. As a consequence, CEG PCA

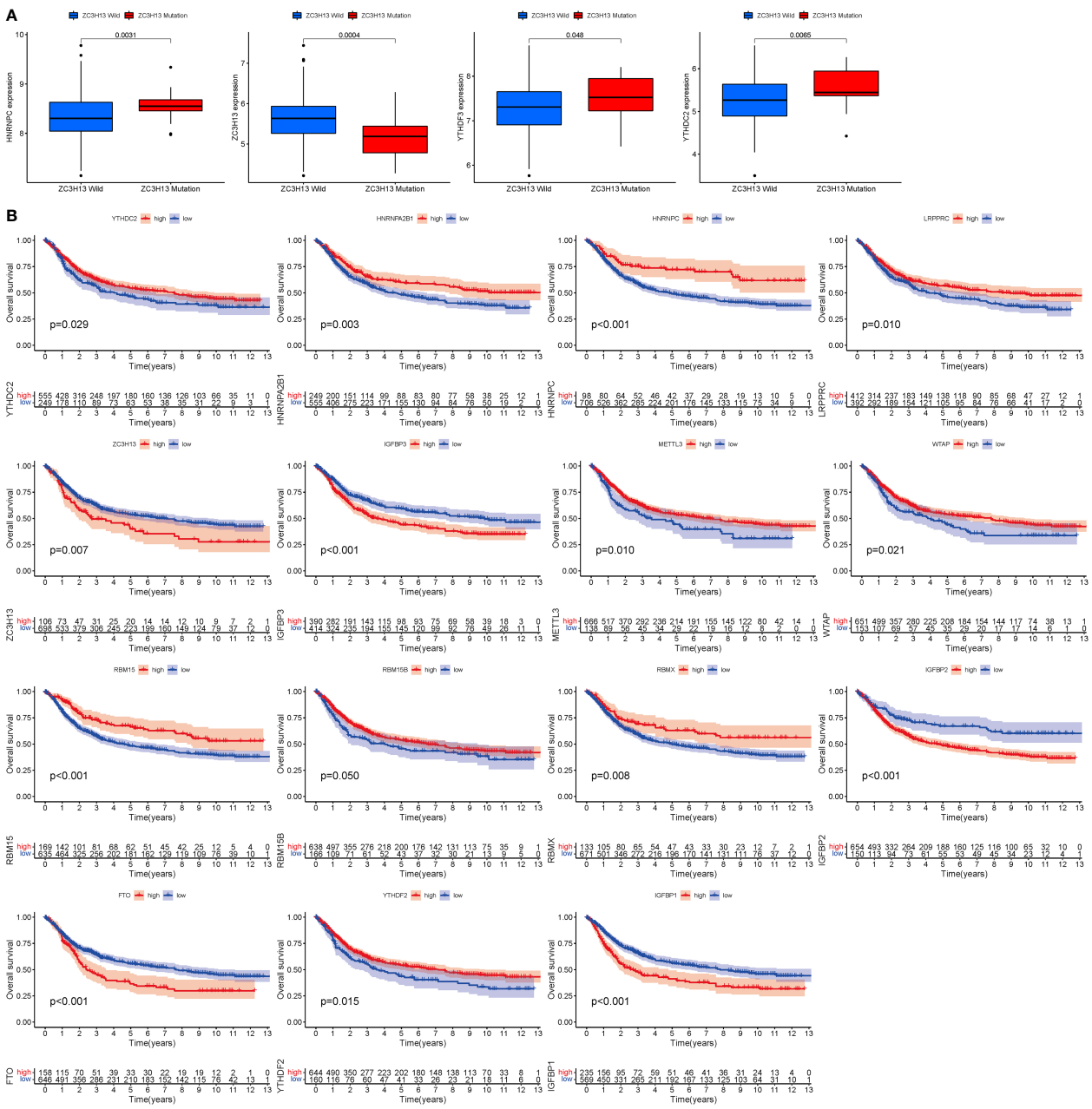

FIGURE 2
Mutation and expression correlation. **(A)** Mutation and expression (There was considerable variation in four genes (HNRNPC, YTHDC2, YTHDF3, and ZC3H13). **(B)** m6A survival analysis (All of these m6a-genes were associated with STAD prognosis.).

was used to distinguish between high and low m6Ascores. The high-m6Ascore group had a better prognosis than the low-m6Ascore group based on the results of the Kaplan-Meier survival analysis (Figure 7A). The relationships between m6A regulator clusters, immunological clusters, gene clusters, and m6Ascore groups were studied. It is evident that the relationships between the different m6a and gene clusters are intricate and their correspondence with survival states is not one-to-one. Cluster B has a higher probability of survival state (Figure 7B). In addition, as seen in the figure, multiple m6A-genes in STAD were significantly correlated with T and B cells, suggesting that m6A-genes affect immune cells and thus the development of STAD (Figure 7C). The greatest m6Ascore was found in m6A regulators cluster B, whereas the lowest m6Ascore was found in m6A regulators cluster A. (Figure 7D). Gene cluster C had the highest m6Ascore (Figure 7E).

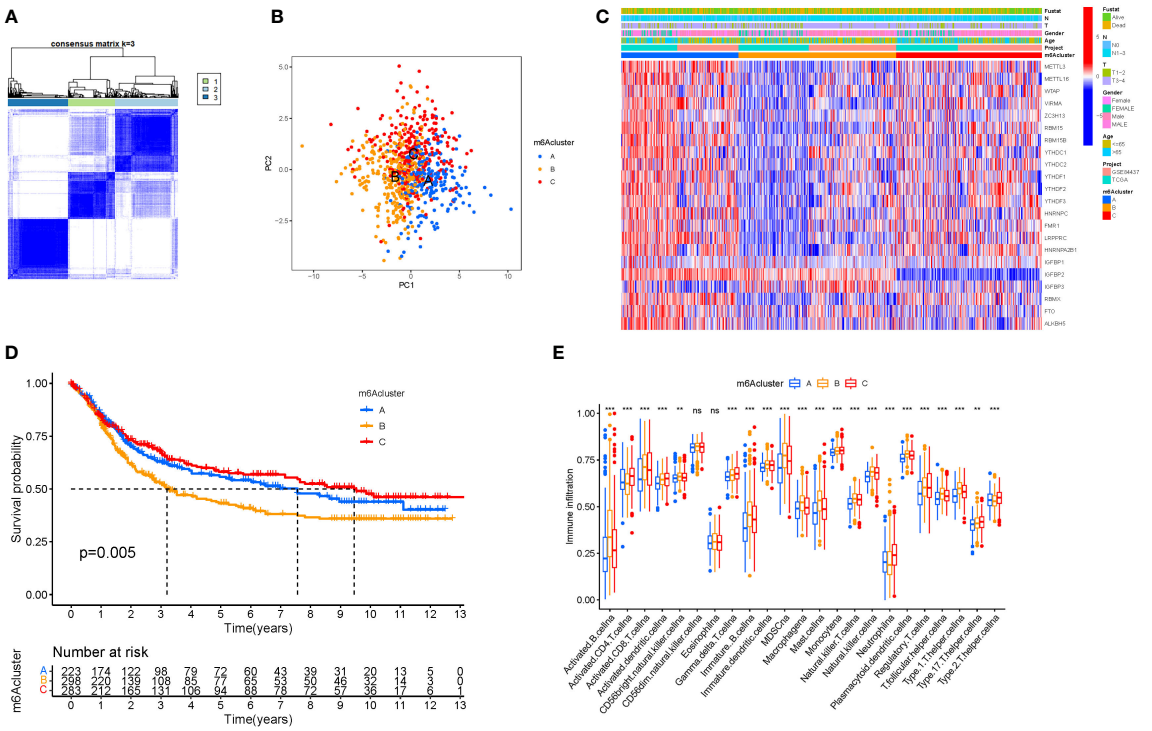

FIGURE 3
Tumor classification and Immune cells. **(A)** The consensus (When k was 3, intraorganizational ties were the greatest and intergenerational relationships were the lowest). **(B)** PCA (The patients were separated into three groups based on their level of risk). **(C)** Heatmap. **(D)** Kaplan-Meier OS curves (Cluster C had a greater survival rate). **(E)** Enriched values of immune cells (Except for CD56dim.natural.killer.cell and Eosinophil, the variability across the three groups was extremely significant). (na P > 0.05; **P < 0.01; ***P < 0.001).

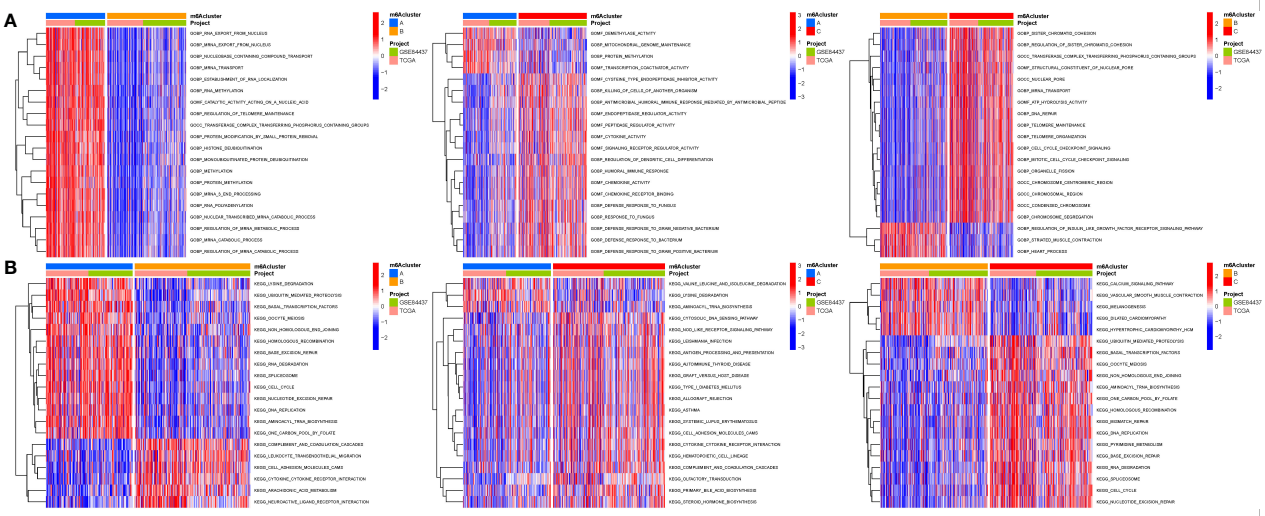

FIGURE 4
GSEA. **(A)** GO. **(B)** KEGG. These genes were associated with RNA and Methylation.

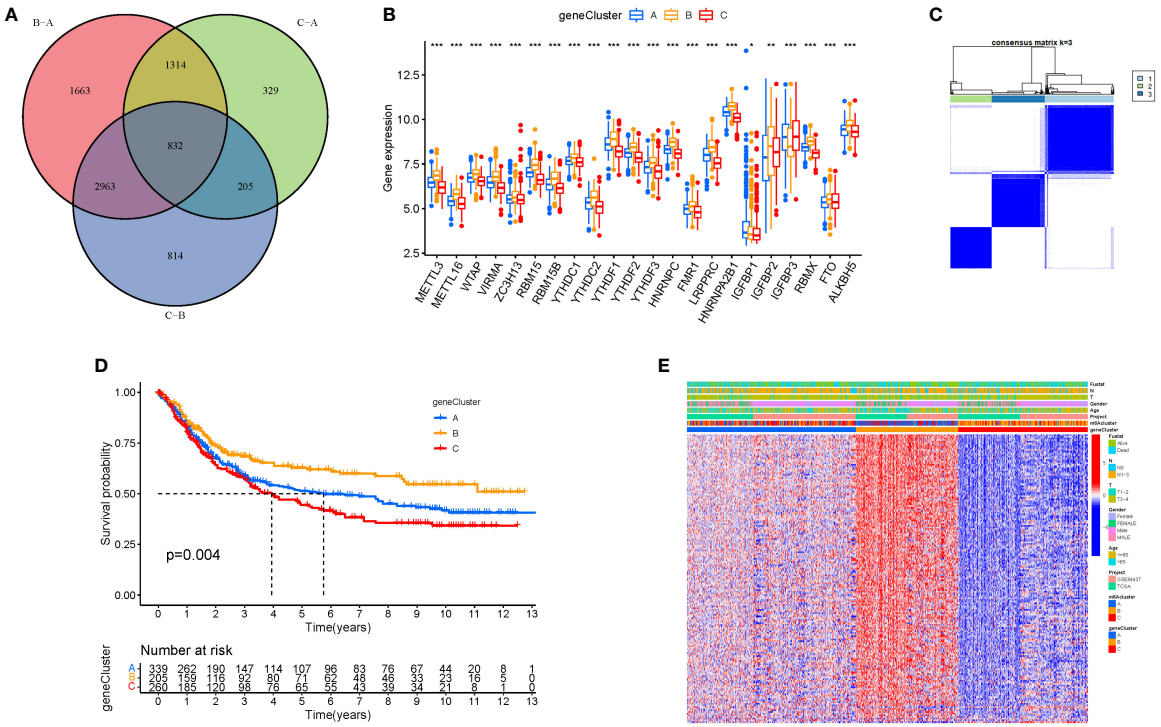

FIGURE 5
Cluster variance analysis and DEGs. **(A)** VNN (Correlation of differential expression of m6a gene among the three clusters). **(B)** Boxplot. **(C)** The consensus (When k was 3, intraorganizational links were strongest and intergenerational connections were weakest). **(D)** Kaplan-Meier OS curves (Cluster B had a greater survival rate). **(E)** Heatmap.

TMB score construction

We also created the TMBscore, a set of scoring methods for measuring the pattern of gene mutations in specific STAD patients. The greater Tumor Burden Mutation was found in low in m6Ascore.group (Figure 8A). Tumor Burden Mutation is negatively correlated with m6Ascore. It can be seen that m6Ascore is not a good predictor of gene mutations in STAD patients (Figure 8B). To test the predictability of TMB, a survival investigation was performed, and H-TMB had a greater chance of survival (Figure 8C). However, there was no difference in the survival analysis between TMB and m6Ascore (Figure 8D). Furthermore, separate analyses were carried out for high and low mutations based on the three groups of mutated genes. The gene mutation status was shown with a waterfall plot. The overall average mutation frequency of DEGs in the prognostic model ranged from 20 to 55% and 10 to 44%, suggesting that STAD mutations might be associated with the deregulation of critical genes (Figures 8E, F). The clinical data were incorporated to predict survival for the grouping of mutations. Mortality was higher and significantly different when the m6ascore increased. In addition, according to the risk assessment of survival, the survival rate was 51% in the low risk group compared to 41% in the high scoring risk group (Figures 8G, H).

M6A regulation and immunotherapy

Immunotherapy is a significant advancement in cancer treatment. The correlation of m6A modification with the impact of tumor immunotherapy based on the association between m6A alteration and immune cell infiltration in STAD was evaluated. There was no difference in tumor staging between T1-T2, while the difference between T3-4 was significant (Figures 9A, B). Anti-PD-1/L1 immunotherapy provided substantial therapeutic benefits and clinical response in individuals with two m6Ascore compared. Furthermore, patients with a low m6Ascore had considerably higher CD274 expression, indicating a possible successful response to anti-PD-1/L1 immunotherapy (Figure 9C). Significant difference in the analysis of immunotherapy results when ctla4 is positive and pd1 is negative or ctla4 is negative and pd1 is positive (Figures 9D–G). MSI demonstrates that m6Ascore expression is highest in MSS at both high and low risk groups (Figures 9H, I). The tumor composed of a complicated TME. New data

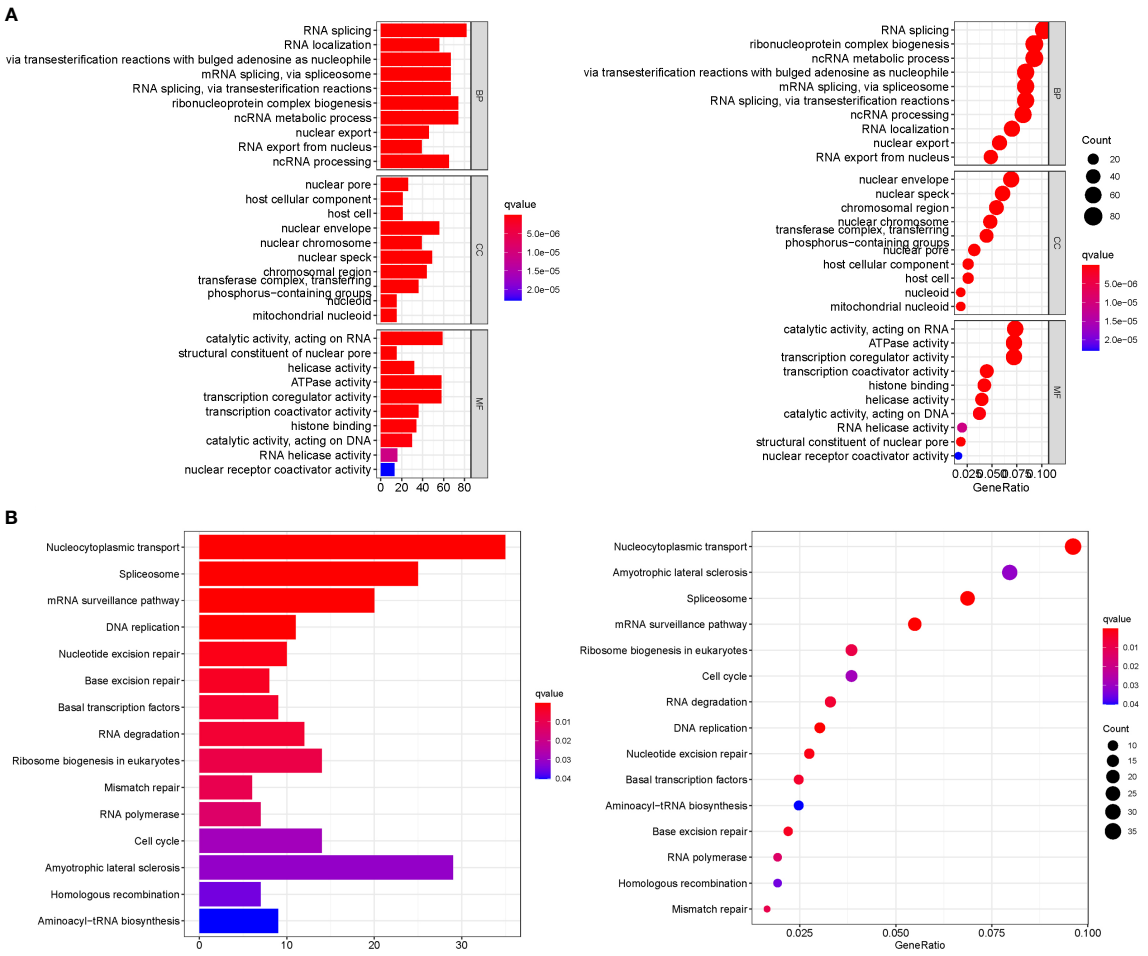

FIGURE 6
Enrichment analysis. **(A)**: GO. **(B)**: KEGG.

demonstrates its crucial involvement in tumor development, immune escape, and immunotherapy response. We found several various tumor immune phenotypes in this study by parsing the TME landscape heterogeneity and complexity, which will also increase the capacity of the results of this investigation to advise and forecast immunotherapy reactivity.

Discussion

The clinical management of STAD is a serious clinical concern due to rapid disease progression and poor prognosis. The level of precision medicine for STAD is hampered by a lack of effective tumor-killing initiators and selective tumor-targeting therapeutic medicines (23). A recent study found that alterations of the mechanism of programmed tumor cell death may potentiate the targeted therapeutic impact of STAD (24). Thus, early identification and diagnosis of the illness are essential. m6A is the most common internal alteration of mRNAs in all higher eukaryotes, and it is methodically regulated by a slew of 'writers,' 'erasers,' and 'readers.' (15) The alteration of m6A affects cancer processing. m6A controls cellular proliferation and maturation, both of which are linked to cancer genesis (13). Evidence shows that abnormal m6A methylation may promote cancer development by upregulating oncogenes and suppressing tumor suppressor genes and that m6A RNA methylation can be altered by the expression of m6A regulators and the activity of m6A enzymes, further impacting tumor progression (25). Based on the interactions of m6A regulators in STAD, the tendencies of m6A readers, writers, and erasers were determined. All erasers' expression levels were reduced, whereas the majority of readers' expression levels were considerably increased. This pattern shows that STAD aided in the methylation of m6A RNA. Furthermore, these variables control immune cell infiltration in STAD (26).

Two "writer" genes, METTL3 and METTL14, were shown to have opposing expression patterns in cancers compared to

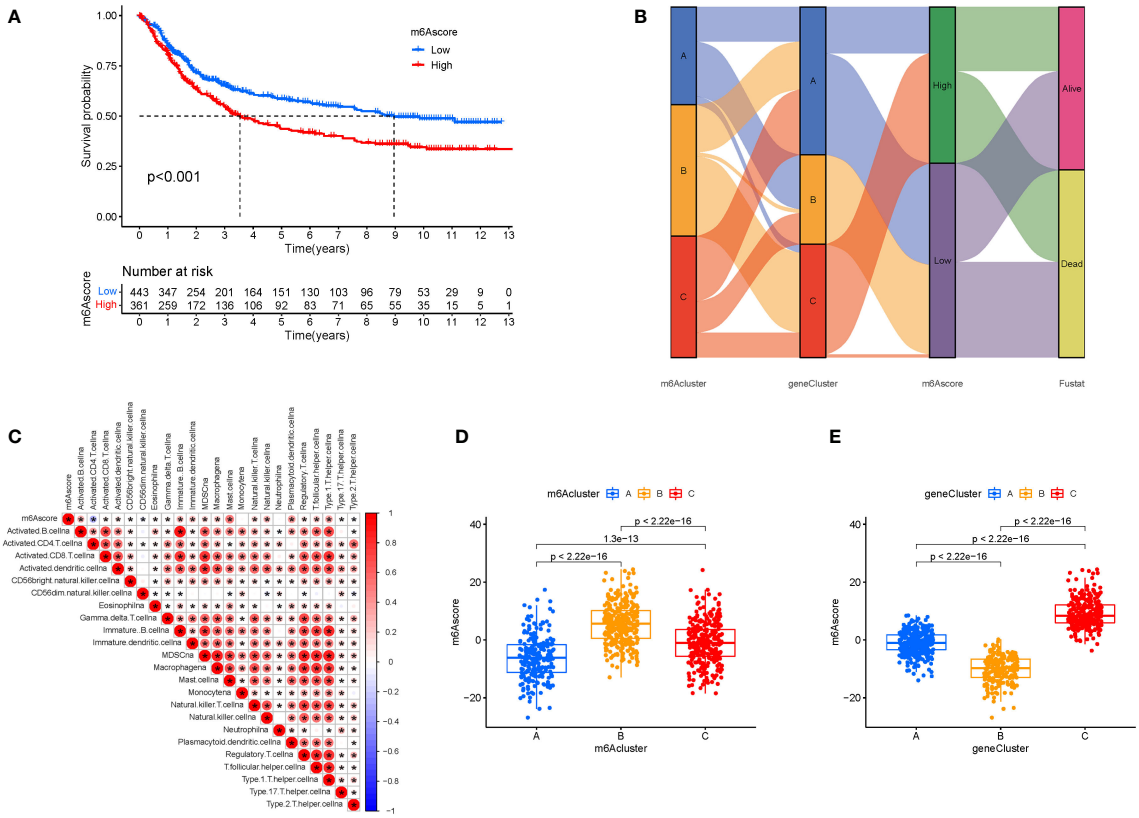

FIGURE 7
M6A Score Construction. **(A)** Survival (The high-m6Ascore group fared better than the low-m6Ascore group). **(B)** Ggalluvial plot. **(C)** Immune cells and prognosis m6A-genes. **(D)** m6A regulators cluster (The highest m6Ascore was discovered in the m6A regulators cluster B, whereas the lowest m6Ascore was discovered in the m6A regulators cluster A). **(E)** Gene cluster.

normal indicating that METTL3 and METTL14 functioned as a complex regulator in STAD. Furthermore, the link between m6a-genes, immune cell infiltration and immune checkpoint therapy was investigated. Recent studies have discovered a relationship between RNA modifications mechanisms and anticancer immunity (27). In the last decade, immune checkpoint inhibitors (ICIs) have revolutionized cancer treatment. In ICI-resistant cancers, activation of pyroptosis, ferroptosis, and necroptosis resulted in synergistically improved anticancer efficiency (28). However, there are few studies on the impact of m6a on ICIs. Many patients are resistant to immune checkpoint blockade (ICB) therapy, and multiple pathologic processes are regulated by m6A in RNA (29). According to Na Li's findings, tumors are more susceptible to cancer immunotherapy in the absence of the m6A demethylase Alkbh5. The inhibitor of Alkbh5 has been shown to improve the effectiveness of cancer immunotherapy (30). Anti-PD-1/L1 immunotherapy offers significant therapeutic benefits and clinical response in persons with two m6Ascores assessed in the present study. Furthermore, patients with a low m6Ascore had significantly increased CD274 expression, indicating that anti-PD-1/L1 immunotherapy might be effective. According to a recent study, METTL3 plays a critical role in several forms of cancer. The abnormal m6A mutation in large intestine cancer was shown to be induced by overexpression of METTL3, which has been linked to tumor spread (31), and METTL3 was downregulated in STAD tissues in this investigation. Moreover, METTL3 has been shown to be oncogenic in the majority of malignancies and to be a tumor suppressor in RCC, bladder cancer, and glioblastoma stem cell (32). Diverse groups have demonstrated that METTL3 has either oncogenic or tumor-suppressive properties, which may be explained by tumor heterogeneity and/or diverse model systems used in the study, and further research is required to gain a better understanding.

KEGG analysis found that the genes were primarily involved in the mRNA surveillance pathway. The NMD mRNA surveillance pathway downregulates aberrant E-cadherin transcripts in gastric cancer cells and in CDH1 mutation carriers. In GSVA, the hedgehog signaling pathway was the most significantly enriched pathway. Smo and Gli1 genes are components of the hedgehog signaling pathway, and their over-

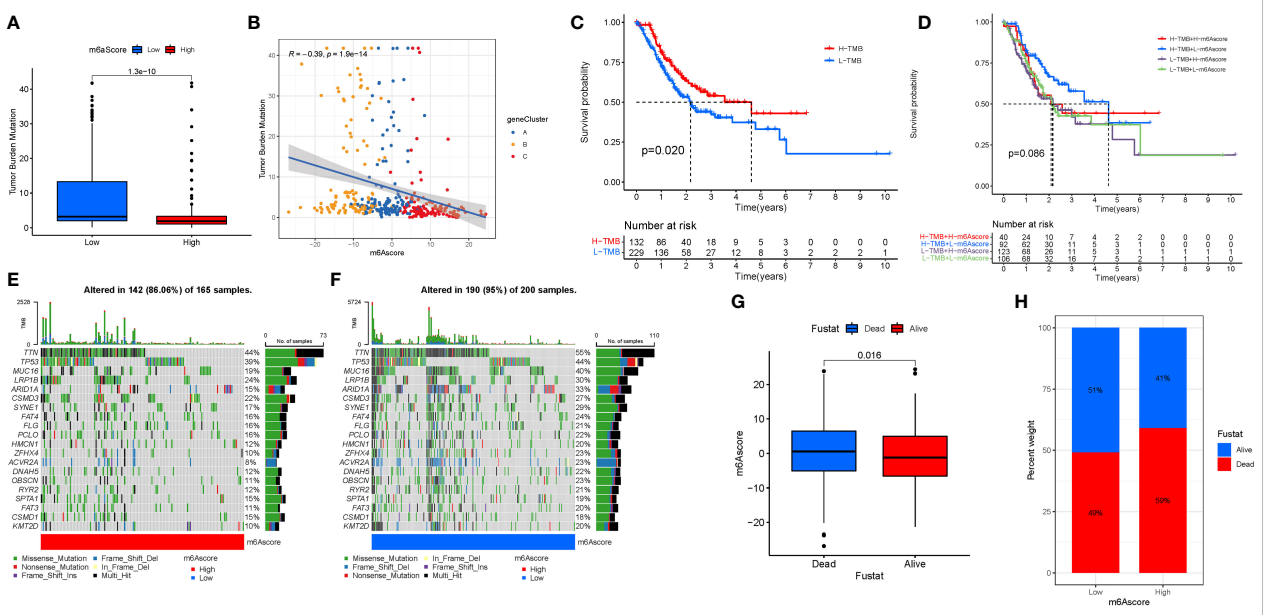

FIGURE 8
TMB Score Construction. **(A)** TMB of m6Ascore.group. **(B)** Tumor Burden Mutation with m6Ascore. **(C)** TMB.survival. **(D)** TMB-score.survival. **(E)** High mutations. **(F)** Low mutations. **(G, H)** Survival investigation.

expression may trigger STAD. The degree of expression is linked to the stage and severity of STAD (33). Furthermore, studies have shown that Hedgehog-interacting protein (HHIP) may inhibit the growth and proliferation of STAD cell lines by blocking Hedgehog signal transduction, which may serve as a new biological marker for STAD and a new approach for STAD treatment by targeting the drug target of HHIP formation (34). Overactivation of the hedgehog pathway is linked to the occurrence and progression of STAD, and specific targeted therapy targeting this pathway shows good potential as an effective measure for the clinical management of STAD (35).M6A genes may influence STAD cell migration and proliferation *via* modulating the nod like receptor signaling pathway.

This study examined numerous features of STAD using cluster analysis. The expression of 24 m6A regulators was divided into three unique patterns. Interactions between m6A regulators might result in m6A methylation or demethylation. The m6A regulator clusters indicated that tumor cells control their activity by different RNA regulation patterns. Survival disparities in diverse patterns suggest that m6A regulatory patterns have a major influence on STAD patients' survival. However, classification of m6A regulators into three categories is insufficient to accurately reflect patient prognosis. As a result, the m6Ascore was developed to differentiate the m6A expression patterns and directly predict prognosis. In our investigation, the m6Ascore was linked to the impact of immunotherapy. Individuals with a low m6Ascore had a better prognosis than those who did not get immunotherapy. The higher mutation rate of the low m6Ascore group, along with the release of SNV neoantigens and ITH, might explain this result. The higher the mutation rate in tumor tissue, the more immunogenicity that has been stored is released, and treatment efficacy improves. As a result of the discovery of novel ICIs targeting CTLA4 and PD1, which are generated by activated T cells, neoantigens have emerged as important tumor antigens for the human immune system. However, other researchers observed an inverse association between ITH and the immune checkpoint response in liver cancer. Patients with significant tumor heterogeneity responded favorably to immunotherapy. The reason may be that tumor heterogeneity reacts differently to immunoreactivity, whereas tumor heterogeneity does not necessarily determine immunotherapy response.

The tumor part was composed of a complex TME. As the understanding of the diversity and complexity of the tumor microenvironment deepens, emerging evidence reveals its critical role in the tumor progression, immune escape, and its effect on response to immunotherapy (36). Based on the link between m6A change and immune cell infiltration in STAD, the correlation of m6A modification with the impact of tumor immunotherapy was investigated. Patients with a low m6Ascore had significantly increased CD274 expression, indicating the effectiveness of anti-PD-1/L1 immunotherapy. There is a significant difference in immunotherapy outcomes when ctla4 is positive and pd1 is negative or when ctla4 is negative and pd1 is positive. According to MSI, m6Ascore

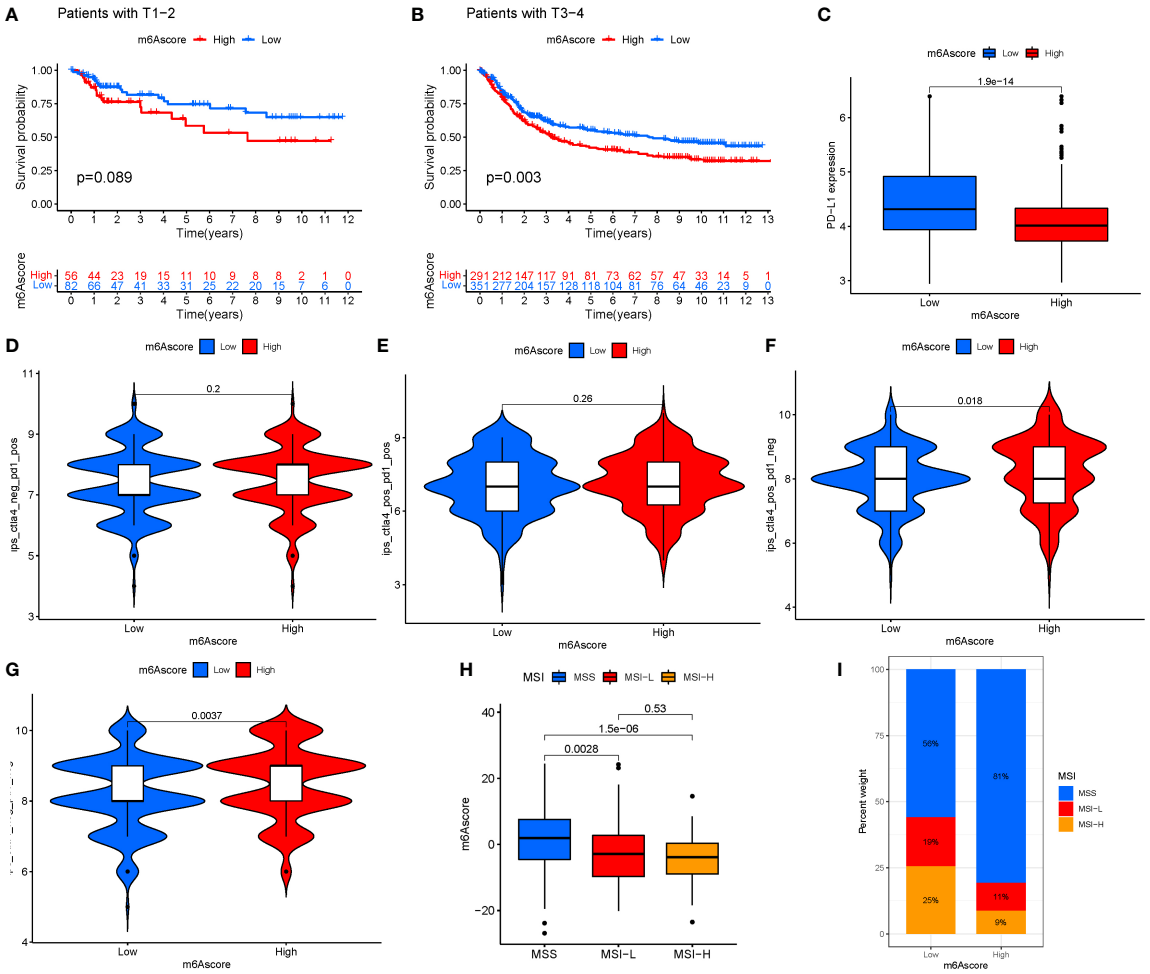

FIGURE 9
(A) T1-T2. **(B)** T3-4. **(C)** Anti-PD-1/L1 immunotherapy. **(D)** ips_ctla4_neg_pd1_neg. **(E)** ips_ctla4_neg_pd1_pos. **(F)** ips_ctla4_pos_pd1_neg. **(G)** ips_ctla4_pos_pd1_pos. **(H, I)** MSI analysis.

expression is the greatest in MSS at both high and low risk. Therefore, this study comprehensively through parsing the TME landscape heterogeneity and complexity, we identified some different tumor immune phenotypes, which may also provide benefits to guide and predict the reactivity of immunotherapy.

The relationship between m6a and STAD has been marginally explored. Currently, four papers have used bioinformatics analysis to explore the relationship between m6a and STAD (37–40). Yao Qi et al. observed the expression of METTL14 in STAD by bioinformatics and immunohistochemistry assays. METTL14 expression was substantially downregulated in STAD, reflecting the contribution of major tumors in STAD, progression of TNM staging and poor OS. Furthermore, the inhibitory effects of METTL14 on STAD cell proliferation, migration and invasion have been demonstrated in *in vitro* experiments. Na Luo et al. identified a 10-gene signature based on probable predictive m6a regulatory genes, and these genes (METTL3, WTAP, RBM15, RBM15B, YTHDC2, YTHDF2, HNRNPC, FMR1, LRPPRC, and RBMX) were found to be negatively associated with STAD clinical stage. 23 m6a genes were found in STAD Prognosis by Zhang Meijing et al.

The uniqueness of the study is as follows. First, the current study complemented prior papers with additional FRG data from the TCGA database, which is constantly updated. Second, TCGA data were used as the primary analysis, with GEO data included into the common pattern for model validation. Third, to strengthen the credibility of the results, several databases were employed to measure immune cells and function.

Our analysis has the following limitations: (1) the present study did not obtain sufficient different data sources from other publicly available sites to validate the model's trustworthiness. (2) The functional enrichment processes at work in the regulatory networks of various risk groups were explored, but their specific mechanisms in permitting m6A require more investigation to

confirm the current findings. (3) The prediction model created in this study must be externally and practically validated.

Conclusions

We discovered three distinct m6A regulatory patterns for STAD, as well as transcriptome and immune infiltration characteristics in distinct m6A regulatory patterns. The current study specifies the functions of m6A regulators and explains the underlying causes of different clinical outcomes and immunotherapy responses in different m6A regulatory patterns. A detailed investigation of individual m6A regulation patterns will contribute to the formulation of personalized immunotherapy treatments for STAD patients and provide a better understanding of STAD immune-cell characterization.

Furthermore, the goal of this work is to discover and thoroughly profile the gene signatures of m6A-related regulators in STAD. The many m6A alteration patterns contributed significantly to the TME's variety and complexity. A predictive model was also created based on the m6a gene signature, which might predict the clinical course of STAD. Our findings suggest that the m6A genes are promising prognostic markers that might give new insights into STAD treatment options and guide successful immunotherapy.

Data availability statement

The original contributions presented in the study are included in the article/Supplementary Material. Further inquiries can be directed to the corresponding authors.

Author contributions

JY and ZW drafted and revised the manuscript. JY and XW revised the manuscript. SC and XW were in charge of data collection. JZ and XX conceived and designed this article, in charge of syntax modification and revised of the manuscript. All authors contributed to the article and approved the submitted version.

Funding

1. Hunan Province Traditional Chinese Medicine Research Program (NO.2021211); 2. First-class Discipline Project on Chinese Pharmacology of Hunan University of Chinese Medicine (No. 201803).

Acknowledgments

Thanks for your thoughtful remarks, reviewers and editors.

Conflict of interest

The authors declare that the research was conducted in the absence of any commercial or financial relationships that could be construed as a potential conflict of interest.

Publisher's note

All claims expressed in this article are solely those of the authors and do not necessarily represent those of their affiliated organizations, or those of the publisher, the editors and the reviewers. Any product that may be evaluated in this article, or claim that may be made by its manufacturer, is not guaranteed or endorsed by the publisher.

Supplementary material

The Supplementary Material for this article can be found online at: https://www.frontiersin.org/articles/10.3389/fonc.2022.1050288/full#supplementary-material

References

1. Aydin E. M, Demir TD, Seymen N, Said SS, Oktem-Okullu S, Tiftikci A, et al. The crosstalk between h. pylori virulence factors and the PD1:PD-L1 immune checkpoint inhibitors in progression to gastric cancer. *Immunol Lett* (2021) 239:1–11. doi: 10.1016/j.imlet.2021.06.009

2. Mimura K, Kua LF, Xiao JF, Asuncion BR, Nakayama Y, Syn N, et al. Combined inhibition of PD-1/PD-L1, lag-3, and Tim-3 axes augments antitumor immunity in gastric cancer-T cell coculture models. *Gastric Cancer* (2021) 24(3). doi: 10.1007/s10120-020-01151-8

3. Yee NS, Lengerich EJ, Schmitz KH, Maranki JL, Gusani NJ, Tchelebi L, et al. Frontiers in gastrointestinal oncology: Advances in multi-disciplinary patient care. *Biomedicines* (2018) 6(2):611–23. doi: 10.3390/biomedicines6020064

4. Lee HE, Smyrk TC, Zhang L. Histologic and immunohistochemical differences between hereditary and sporadic diffuse gastric carcinoma. *Hum Pathol* (2018) 74. doi: 10.1016/j.humpath.2017.12.023

5. Schinzari G, Cassano A, Orlandi A, Basso M, Barone C. Targeted therapy in advanced gastric carcinoma: the future is beginning. *Curr Med Chem* (2014) 21 (8):1026–38. doi: 10.2174/09298673216613129124054

6. Machlowska J, Baj J, Sitarz M, Maciejewski R, Sitarz R. Gastric cancer: Epidemiology, risk factors, classification, genomic characteristics and treatment strategies. *Int J Mol Sci* (2020) 21(11). doi: 10.3390/ijms21114012

7. Bizzaro N, Antico A, Villalta D. Autoimmunity and gastric cancer. *Int J Mol Sci* (2018) 19(2). doi: 10.3390/ijms19020377

8. Xu Z, Chen Q, Shu L, Zhang C, Liu W, Wang P. Expression profiles of m6A RNA methylation regulators, PD-L1 and immune infiltrates in gastric cancer. *Front Oncol* (2022) 12. doi: 10.3389/fonc.2022.970367

9. Chen S, Su X, Wang J, Zheng N, Tang Y, Peng G, et al. Identification and validation of METTL3-related molecules for predicting prognosis and efficacy of immunotherapy in gastric cancer based on m6A methylome and transcriptome sequencing analysis. *Front Oncol* (2022) 12. doi: 10.3389/fonc.2022.935239

10. Yu J, Mao W, Sun S, Hu Q, Wang C, Xu Z, et al. Identification of an m6A-related lncRNA signature for predicting the prognosis in patients with kidney renal clear cell carcinoma. *Front Oncol* (2021) 11:663263. doi: 10.3389/fonc.2021.663263

11. Nian L, Tao P. N6-methyladenosine-encoded epitranscriptomics. *Nat Struct Mol Biol* (2016) 23:98–102. doi: 10.1038/nsmb.3162

12. Zhao BS, Roundtree IA, He C. Post-transcriptional gene regulation by mRNA modifications. *Nat Rev Mol Cell Biol* (2017) 18(1):31–42. doi: 10.1038/nrm.2016.132

13. Zaccara S, Ries RJ, Jaffrey SR. Reading, writing and erasing mRNA methylation. *Nat Rev Mol Cell Biol* (2019) 20(10):608–24. doi: 10.1038/s41580-019-0168-5

14. Zheng J, Guo J, Cao B, Zhou Y, Tong J. Identification and validation of lncRNAs involved in m6A regulation for patients with ovarian cancer. *Cancer Cell Int* (2021) 21(1):363. doi: 10.1186/s12935-021-02076-7

15. Wang T, Kong S, Tao M, Ju S. The potential role of RNA N6-methyladenosine in cancer progression. *Mol Cancer* (2020) 19(1):88. doi: 10.1186/s12943-020-01204-7

16. Ma JZ, Yang F, Zhou CC, Liu F, Yuan JH, Wang F, et al. METTL14 suppresses the metastatic potential of hepatocellular carcinoma by modulating N6-methyladenosine-dependent primary MicroRNA processing. *Hepatology* (2017) 65 (2):529–43. doi: 10.1002/hep.28885

17. Wang S, Chai P, Jia R, Jia R. Novel insights on m6A RNA methylation in tumorigenesis: A double-edged sword. *Mol Cancer* (2018) 17(1):101. doi: 10.1186/s12943-018-0847-4

18. He L, Li J, Wang X, Ying Y, Xie H, Yan H, et al. The dual role of N6-methyladenosine modification of RNAs is involved in human cancers. *J Cell Mol Med* (2018) 22(10):4630–39. doi: 10.1111/jcmm.13804

19. Wu ZX, Huang X, Cai MJ, Huang PD, Guan Z. Development and validation of a prognostic index based on genes participating in autophagy in patients with lung adenocarcinoma. *Front Oncol* (2021) 11:799759. doi: 10.3389/fonc.2021.799759

20. Wang Z, Jensen MA, Zenklusen JC. A practical guide to the cancer genome atlas (TCGA). *Methods Mol Biol* (2016) 1418:111–41. doi: 10.1007/978-1-4939-3578-9_6

21. Barrett T, Wilhite SE, Ledoux P, Evangelista C, Kim IF, Tomashevsky M, et al. NCBI GEO: archive for functional genomics data sets–update. *Nucleic Acids Res* (2013) 41(Database issue):D991–5. doi: 10.1093/nar/gks1193

22. Xu D, Ji Z, Qiang L. Molecular characteristics, clinical implication, and cancer immunity interactions of pyroptosis-related genes in breast cancer. *Front Med (Lausanne)* (2021) 8:702638. doi: 10.3389/fmed.2021.702638

23. Wang X, Xu K, Liao X, Rao J, Huang K, Gao J, et al. Construction of a survival nomogram for gastric cancer based on the cancer genome atlas of m6A-related genes. *Front Genet* (2022) 13. doi: 10.3389/fgene.2022.936658

24. Xie Y-H, Chen Y-X, Fang J-Y. Comprehensive review of targeted therapy for colorectal cancer. *Signal Transduct Target Ther* (2020) 5(1):22. doi: 10.1038/s41392-020-0116-z

25. Huang J, Song J, Li X, Liu S, Huang W, Shen Z, et al. Analysis and prognostic significance of tumour immune infiltrates and immune microenvironment of m6A-related lncRNAs in patients with gastric cancer. *BMC Med Genomics* (2022) 15(1):164. doi: 10.1186/s12920-022-01318-5

26. Dai D, Wang H, Zhu H, Jin L, Wang X. N6-methyladenosine links RNA metabolism to cancer progression. *Cell Death Dis* (2018) 9(2):124. doi: 10.1038/s41419-017-0129-x

27. Li X, Ma S, Deng Y, Yi P, Yu J. Targeting the RNA m(6)A modification for cancer immunotherapy. *Mol Cancer* (2022) 21(1):76. doi: 10.1186/s12943-022-01558-0

28. Hsu SK, Li CY, Lin IL, Syue WJ, Chen YF, Cheng KC, et al. Inflammation-related pyroptosis, a novel programmed cell death pathway, and its crosstalk with immune therapy in cancer treatment. *Theranostics* (2021) 11(18):8813–35. doi: 10.7150/thno.62521

29. Yan G, An Y, Xu B, Wang N, Sun X, Sun M. Potential impact of ALKBH5 and YTHDF1 on tumor immunity in colon adenocarcinoma. *Front Oncol* (2021) 11:670490. doi: 10.3389/fonc.2021.670490

30. Li N, Kang Y, Wang L, Huff S, Tang R, Hui H, et al. ALKBH5 regulates anti-PD-1 therapy response by modulating lactate and suppressive immune cell accumulation in tumor microenvironment. *Proc Natl Acad Sci USA* (2020) 117 (33):20159–70. doi: 10.1073/pnas.1918986117

31. Raj N, Wang M, Seoane JA, Zhao RL, Kaiser AM, Moonie NA, et al. The Mettl3 epitranscriptomic writer amplifies p53 stress responses. *Mol Cell* (2022) 82 (13):2370–84. doi: 10.1016/j.molcel.2022.04.010

32. Ye H, Chen T, Zeng Z, He B, Yang Q, Pan Q, et al. The m6A writers regulated by the IL-6/STAT3 inflammatory pathway facilitate cancer cell stemness in cholangiocarcinoma. *Cancer Biol Med* (2022) 19(03):343–57. doi: 10.20892/j.issn.2095-3941.2020.0661

33. Abdel-Rahman O. Hedgehog pathway aberrations and gastric cancer; evaluation of prognostic impact and exploration of therapeutic potentials. *Tumor Biol* (2015) 36(3):1367–74. doi: 10.1007/s13277-015-3216-6

34. Xu Y, Song S, Wang Z, Ajani JA. The role of hedgehog signaling in gastric cancer: molecular mechanisms, clinical potential, and perspective. *Cell Commun Signaling* (2019) 17(6):157. doi: 10.1186/s12964-019-0479-3

35. Akyala AI, Peppelenbosch MP. Gastric cancer and hedgehog signaling pathway: emerging new paradigms. *Genes Cancer* (2018) 9(1-2):1–10. doi: 10.18632/genesandcancer.168

36. Zhang B, Wu Q, Li B, Wang D, Wang L, Zhou YL. M(6)A regulator-mediated methylation modification patterns and tumor microenvironment infiltration characterization in gastric cancer. *Mol Cancer* (2020) 19(1):53. doi: 10.1186/s12943-020-01170-0

37. Yao Q, He L, Gao X, Tang N, Lin L, Yu X, et al. The m6A methyltransferase METTL14-mediated N6-methyladenosine modification of PTEN mRNA inhibits tumor growth and metastasis in stomach adenocarcinoma. *Front Oncol* (2021) 11:699749. doi: 10.3389/fonc.2021.699749

38. Jiang L, Li Y, He Y, Wei D, Yan L, Wen H. Knockdown of m6A reader IGF2BP3 inhibited hypoxia-induced cell migration and angiogenesis by regulating hypoxia inducible factor-1alpha in stomach cancer. *Front Oncol* (2021) 11:711207. doi: 10.3389/fonc.2021.711207

39. Luo N, Fu M, Zhang Y, Li X, Zhu W, Yang F, et al. Prognostic role of M6A-associated immune genes and cluster-related tumor microenvironment analysis: A multi-omics practice in stomach adenocarcinoma. *Front Cell Dev Biol* (2022) 10:935135. doi: 10.3389/fcell.2022.935135

40. Meijing Z, Tianhang L, Biao Y. N6-methyladenosine modification patterns and tumor microenvironment immune characteristics associated with clinical prognosis analysis in stomach adenocarcinoma. *Front Cell Dev Biol* (2022) 10:913307. doi: 10.3389/fcell.2022.913307

frontiers | Frontiers in Oncology

TYPE Original Research
PUBLISHED 04 January 2023
DOI 10.3389/fonc.2022.1075974

Check for updates

OPEN ACCESS

EDITED BY
Zhendong Jin,
Second Military Medical University, China

REVIEWED BY
Zhen Li,
Qilu Hospital, Shandong University, China
Gang Sun,
The first affiliated hospital of People's Liberation Army General Hospital, China

*CORRESPONDENCE
Zhigang Jie
jiezg123@126.com
Zhengrong Li
lzr13@foxmail.com

†These authors have contributed equally to this work

SPECIALTY SECTION
This article was submitted to Gastrointestinal Cancers: Gastric and Esophageal Cancers, a section of the journal Frontiers in Oncology

RECEIVED 21 October 2022
ACCEPTED 08 December 2022
PUBLISHED 04 January 2023

CITATION
Zhang G, Song J, Feng Z, Zhao W, Huang P, Liu L, Zhang Y, Su X, Wu Y, Cao Y, Li Z and Jie Z (2023) Artificial intelligence applicated in gastric cancer: A bibliometric and visual analysis *via* CiteSpace. *Front. Oncol.* 12:1075974. doi: 10.3389/fonc.2022.1075974

COPYRIGHT
© 2023 Zhang, Song, Feng, Zhao, Huang, Liu, Zhang, Su, Wu, Cao, Li and Jie. This is an open-access article distributed under the terms of the Creative Commons Attribution License (CC BY). The use, distribution or reproduction in other forums is permitted, provided the original author(s) and the copyright owner(s) are credited and that the original publication in this journal is cited, in accordance with accepted academic practice. No use, distribution or reproduction is permitted which does not comply with these terms.

Artificial intelligence applicated in gastric cancer: A bibliometric and visual analysis *via* CiteSpace

Guoyang Zhang[1,2†], Jingjing Song[3†], Zongfeng Feng[1,2†], Wentao Zhao[4], Pan Huang[1], Li Liu[1], Yang Zhang[1], Xufeng Su[1], Yukang Wu[1], Yi Cao[1], Zhengrong Li[1*] and Zhigang Jie[1*]

[1]Department of General Surgery, The First Affiliated Hospital of Nanchang University, Nanchang, China, [2]Medical Innovation Center, The First Affiliated Hospital of Nanchang University, Nanchang, China, [3]Jiangxi Med College of Nanchang University, Nanchang, China, [4]The Third Clinical Department of China Medical University, Shenyang, China

Objective: This study aimed to analyze and visualize the current research focus, research frontiers, evolutionary processes, and trends of artificial intelligence (AI) in the field of gastric cancer using a bibliometric analysis.

Methods: The Web of Science Core Collection database was selected as the data source for this study to retrieve and obtain articles and reviews related to AI in gastric cancer. All the information extracted from the articles was imported to CiteSpace to conduct the bibliometric and knowledge map analysis, allowing us to clearly visualize the research hotspots and trends in this field.

Results: A total of 183 articles published between 2017 and 2022 were included, contributed by 201 authors from 33 countries/regions. Among them, China (47.54%), Japan (21.86%), and the USA (13.11%) have made outstanding contributions in this field, accounting fsor 82.51% of the total publications. The primary research institutions were Wuhan University, Tokyo University, and Tada Tomohiro Inst Gastroenterol and Proctol. Tada (n = 12) and Hirasawa (n = 90) were ranked first in the top 10 authors and co-cited authors, respectively. Gastrointestinal Endoscopy (21 publications; IF 2022, 9.189; Q1) was the most published journal, while Gastric Cancer (133 citations; IF 2022, 8.171; Q1) was the most co-cited journal. Nevertheless, the cooperation between different countries and institutions should be further strengthened. The most common keywords were AI, gastric cancer, and convolutional neural network. The "deep-learning algorithm" started to burst in 2020 and continues till now, which indicated that this research topic has attracted continuous attention in recent years and would be the trend of research on AI application in GC.

Conclusions: Research related to AI in gastric cancer is increasing exponentially. Current research hotspots focus on the application of AI in

gastric cancer, represented by convolutional neural networks and deep learning, in diagnosis and differential diagnosis and staging. Considering the great potential and clinical application prospects, the related area of AI applications in gastric cancer will remain a research hotspot in the future.

KEYWORDS

gastric cancer, bibliometric analysis, CiteSpace, research trends, Web of Science, artificial intelligence

1 Introduction

Gastric cancer (GC) is one of the most important members of the global cancer burden (1). According to the 2018 Global Cancer Statistics Report, the number of GC cases has exceeded 1,034,000, and it has become the fifth most common cancer (5.6%) except breast (11.7%), lung (11.4%), colorectal (10.0%), and prostate cancer (7.3%) (2, 3). Due to its frequently advanced stage at diagnosis, gastric cancer is with high mortality. Additionally, it was estimated as responsible for about 783,000 deaths worldwide in 2018 and was the third leading cause of cancer death worldwide (4).

Endoscopic ultrasound (EUS), MRI, computed tomography (CT), positron emission computed tomography (PET-CT), and other imaging examinations recommended by the guidelines for GC of the Chinese Society of Clinical Oncology (CSCO) in 2021 played an important role in the clinical diagnosis, therapeutic evaluation, and prognosis prediction of GC (5). The majority of early gastric cancer (EGC) can be cured by endoscopic resection, and the 5-year survival rate can reach more than 90%. In addition, comprehensive surgical treatment is the main treatment for advanced GC; the 5-year survival rate of advanced GC is <30%. It can be concluded that early detection, early diagnosis, and treatment of GC is the main strategy to reduce the mortality and improve the survival rate. Significantly, the rapid development of endoscopy has increased the detection rate, diagnosis, and treatment rate of EGC, and increased the incidence postoperative quality of life (6, 7). However, the professional knowledge and experience of the endoscopist and complex factors of the gastrointestinal (GI) tract determine the accuracy of detection (8). At the same time, with the era of individualized treatment of GC, the obvious deficiency of biological information such as morphology, size, and enhancement of the lesion of traditional imaging examination reflecting tumor heterogeneity is gradually exposed (9–11). Every area and industry, including healthcare, has been influenced by digital transformation as a result of the synchronous maturation of several significant digital innovations in information and communications technology that developed at an unprecedented rate this new century. Meanwhile, a remarkable ecosystem for new opportunities in healthcare and other industries has been created by digital innovations including the further consolidation of tele-health, the evolution of fifth generation wireless networks (5G), artificial intelligence (AI) approaches such as machine learning (ML) and deep learning (DL), and the Internet of Things (IoT), and digital security capabilities such as blockchain (12). The concept of AI was first proposed in 1956 and has developed rapidly in the past 10 years. The intersection of medical and engineering disciplines resulted in the development of AI-based radiomics and deep-learning technology, which can overcome the limitation of conventional imaging that depends on visual judgment, convert images into massive data features that can be mined, and objectively and quantitatively represent the heterogeneity and microenvironment within tumors. Therefore, AI technology has shown great advantages in the clinical diagnosis, therapy, and prognosis prediction of GC, which is a hotspot of research at present (13). Pathology, endoscopy, and computed tomography (CT) were mainly included in AI-assisted diagnosis, while prognosis researchers concentrated on recurrence, metastasis, and survival prediction (14).

In this study, scientometric analysis is mainly reflected in bibliometric and manual analysis. Bibliometric analysis is a new tool for exploring patterns and trends of a filed or subject at a high rate of speed using statistical methods and visualization (15). Moreover, CiteSpace, a Java-based application, uses metrology, co-authorship, co-citation, and co-occurrence analyses between countries, institutions, journals, authors, references, and keywords to quantitatively and qualitatively analyze and visualize the current research status and research frontiers in a certain field (16, 17). In the past few years, relatively many researchers and institutions have focused on the research of AI in the field of GC. Based on the core collection database of Web of Science, this study adopts CiteSpace knowledge graph software technology to understand and compare the basic situation, research hotspots, and development trends of AI in the field of GC from the perspective of visualization, so as to provide new ideas and clues for related research work.

2 Methods

2.1 Data source

With the availability of bibliometric indicators and more than 12,000 significant high-quality journals from nations throughout the world, Web of Science (WoS), one of the most comprehensive, systematic, and authoritative databases, is widely used for bibliometrics analysis and visualization of scientific literature (18). Significantly, the data collected from WoS could directly provide reference files that satisfy the specific format requirements set by bibliometric software CiteSpace. Otherwise, if data were downloaded from other databases, an additional procedure for file format conversion should be required (19). In addition, the accuracy, reliability, and representativeness of a certain dataset rely on the authority of the database, so the Science Citation Index Expanded (SCI-Expanded) of Web of Science Core Collection (WoSCC) database was chosen as the data source in this study. With allowing us to extract the relevant publications using an appropriate retrieval strategy, the majority of publications on AI applicated in GC are included in the WoS online database.

2.2 Retrieval strategies

A flow chart of literature selection included in this study is shown in Figure 1. Publications were retrieved from the Science Citation Index (SCI) Expanded of the WoSCC database from 2017 to 2022 and were downloaded within 1 day on 6 October 2022 in order to reduce bias due to daily updates of the database. The search terms were as follows: (((((TS=("Stomach Neoplasm")) OR TS=("Cancer of Stomach")) OR TS=("Stomach Cancers")) OR TS=("Gastric Cancer")) OR TS=("Gastric Neoplasm")) AND (TS=("Computational Intelligence") OR TS=("artificial intelligence")). In addition, to ensure the accuracy and objectivity of the analysis, only articles and reviews written in English were included, and other types of publications, such as meeting abstract and editorial material, were excluded. Finally, there remained a total of 183 publications related to this field, and then they were exported as "full records and references." All records, including the titles, authors, abstracts, keywords, etc., were imported to CiteSpace to summarize and visualize scientific literature.

2.3 Analysis tool

The records retrieved and downloaded from the WoSCC were converted into plain text format for export, which was named download_ XXX.txt, including complete records and references. Finally, all valid data retrieved from the WoSCC was imported into Microsoft Excel and CiteSpace to perform a bibliometric and visual analysis.

CiteSpace, an interactive visualization analysis software developed by Professor Chen Chaomei of Drexel University using Java language based on scientometrics and data visualization, cannot only analyze the distribution of countries/regions, authors and co-cited authors, journals and co-cited journals, co-cited references, keyword cluster analysis, and timelines but also support structural and temporal analyses of a variety of networks derived from scientific literature, including collaboration networks, co-occurrence networks, co-citation networks, and networks of hybrid node types such as terms, authors, and countries (20–22). Additionally, burst detection is also one of the functions of CiteSpace, which can be used for detecting sharp increases of interest in a certain field (23). The results of the bibliometric analysis were displayed as knowledge network maps created by CiteSpace, and knowledge network maps is a growing field motivated by digital technology to easily understand the research hotspots and evolution process of different fields in the knowledge system and predict the development trend of various fields (24). As a consequence, we can concentrate on examining patterns and dynamic changes in scientific research publications and try to identify key points in a certain field to evaluate the current research hotspots and development tendency in a certain filed through the distribution and structure of scientific knowledge presented by knowledge map. In addition, the obtained data were exported into R Studio (Bibliometrix: An R-tool version 3.2.1) and VOSviewer (version 1.6.17) to draw scientific knowledge maps visually.

3 Results

3.1 Trends of publication outputs

As shown in Figure 2A, the data of a total of 183 publications in this research field from 2017 to 2022 were retrieved and plotted *via* WoS database, and the earliest literature on the application of AI in the field of GC in the database was published in 2017, but the number of publications was only 1. The change trend in number and the annual number of publications related to the research on AI and AI applicated in medicine are displayed in Figure 2B, and we can observe that it has been a stage of rapid development of AI since the 1990s. Especially, the number of relevant publications has shown a rapid increase since 2016, and the annual growth rate of the number of publications from 2016 to 2017 was the highest, reaching 49.20%. At the same time, the application of AI in the field of medicine has also developed accordingly, and the number of publications has also increased year by year. Similarly, AI also shows great application prospects in transportation, education, finance, and other fields. Since 2017, research on AI in the field of GC has also received corresponding attention, and the number of relevant articles has been increasing annually. Particularly in 2021, the annual average growth rate reached 264.11%. However, the overall base of research on the application of AI in the field of GC

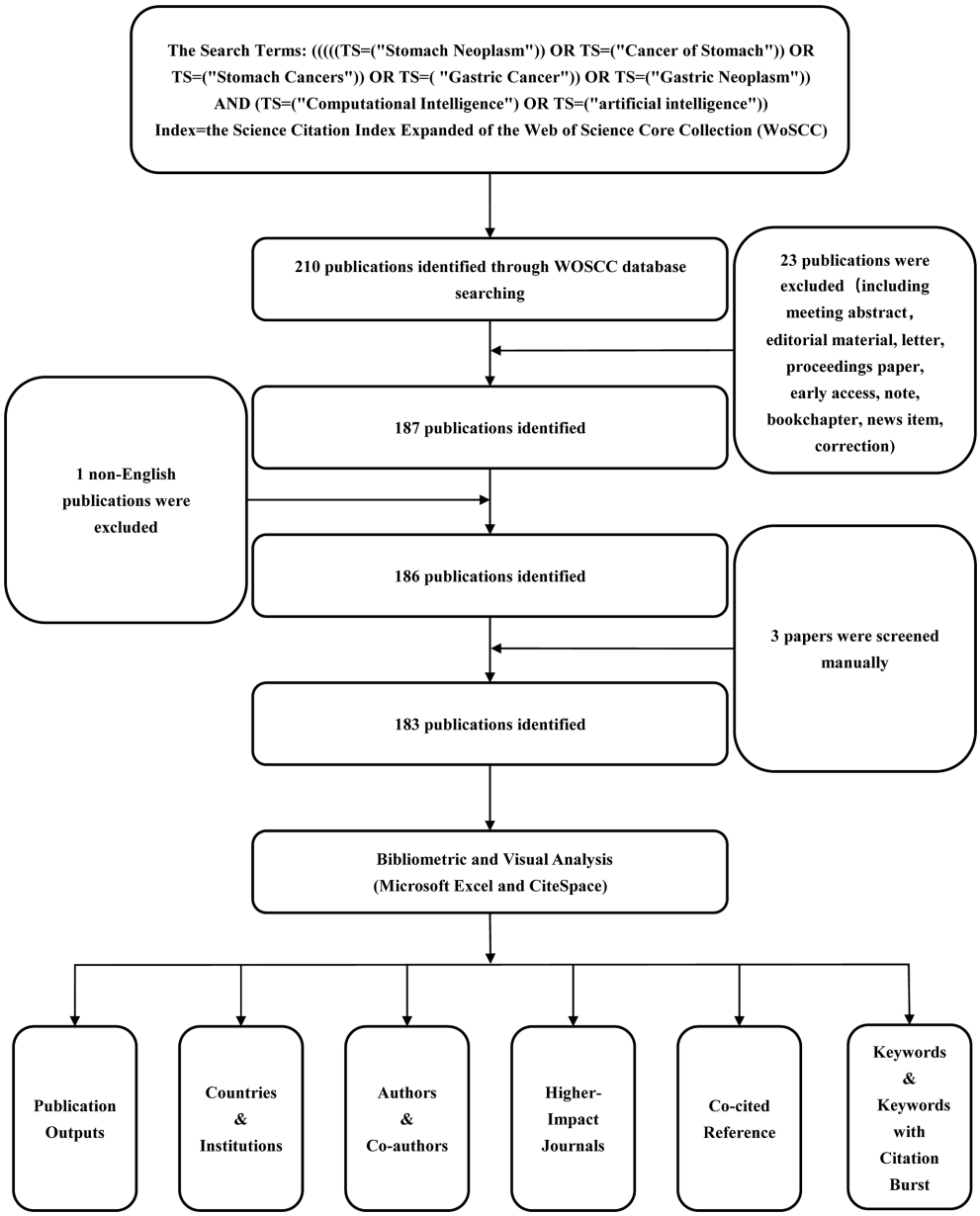

FIGURE 1
Flowchart of literature selection and the steps of bibliometric analysis included in this study.

was small, which indicated that there were still few relevant studies in this field.

3.2 Quantitative and cooperation analysis

3.2.1 Bibliometric analysis of countries and institutions

In the cooperative network map created by CiteSpace software, the larger the size of the node that represents research items such country/region, institution, and author, the more frequently the item appears or is cited. In addition, a series of citation tree-rings across a number of time slices are used to describe each node. The lines between nodes represent a co-occurrence or a co-citation between these nodes, and the thicker the line, the closer is the connection between them (25). The distinction of different years is represented by different colors. Moreover, the outermost layer of the node is surrounded by a purple circle, and the size of this purple proportion represents the centrality of each item. In CiteSpace, the term

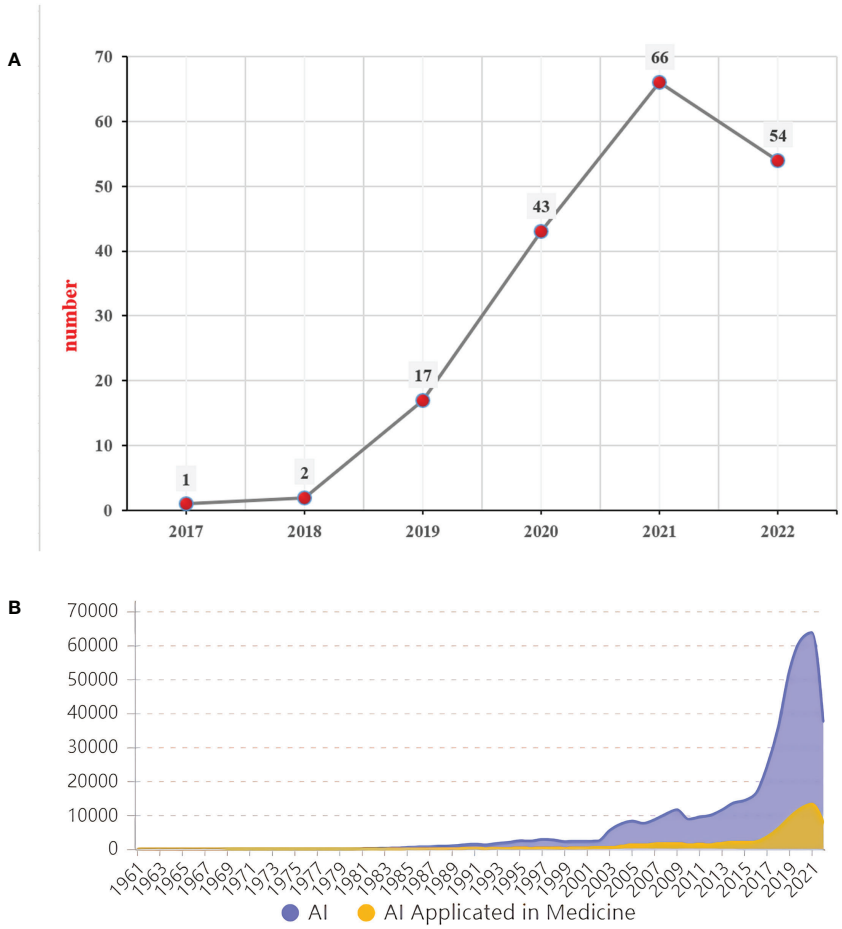

FIGURE 2
(A) Change trend of annual number of publications related to the research on AI applicated in gastric cancer, 2017–2022. **(B)** Change trend of number and the annual number of publications related to the research on AI and AI applicated in medicine, 1961–2022.

"centrality" refers to intermediary centrality and is an indicator to assess the significance of each network node (26). CiteSpace uses this index to evaluate and reveal the importance of the literature in a certain field, and if node-intermediary centrality with purple is not <0.1, then such node will be applied a purple circle for emphasis.

A total of 33 countries/regions contributed to the research on the application of AI on GC; Figure 3A and Supplementary Figure S1A show that there were 34 nodes and 106 connections in the cooperation network between countries/regions, with a density of 0.1889. As shown in Table 1 and Figure 4A, China (87, 47.54%) ranked first in the number of articles published, followed by Japan (n=40, 21.86%), the USA (n=24, 13.11%), South Korea (13, 7.10%), and Italy (n=12, 6.56%). China collaborated with Sudan and Cameroon in 2022 and also with Japan, the USA, Norway, Italy, Germany, and the United Kingdom in 2021. Furthermore, we created a world map that displayed the contribution to this field of each country in Figure 4B, using color gradients to show how many publications that these countries have published, and it is clear that most of the articles are published by researchers in East Asia, North America, and other regions.

H-index is frequently used as a quantitative and qualitative indicator of academic output and allows us to have an assessment of the quality and quantity of publications of a nation, a journal, or an institution (27). As shown in Table 1 and Figure 4A, research related to this field in China started later compared with Japan, but the output of articles and the number of achievements in China were much higher than in any other countries, and Chinese centrality was with the highest strength, reaching 0.4. However, the H-index of China (n=16) ranked third, lower than Japan (n=18.17) or the USA (n=16.3), and the average citation of China (n=11.59) was also lower than Japan (14), which indicated that the quality and quantity of output should be enhanced.

Using CiteSpace for organization co-occurrence analysis, we set the node type to Organization, and then the result is shown in

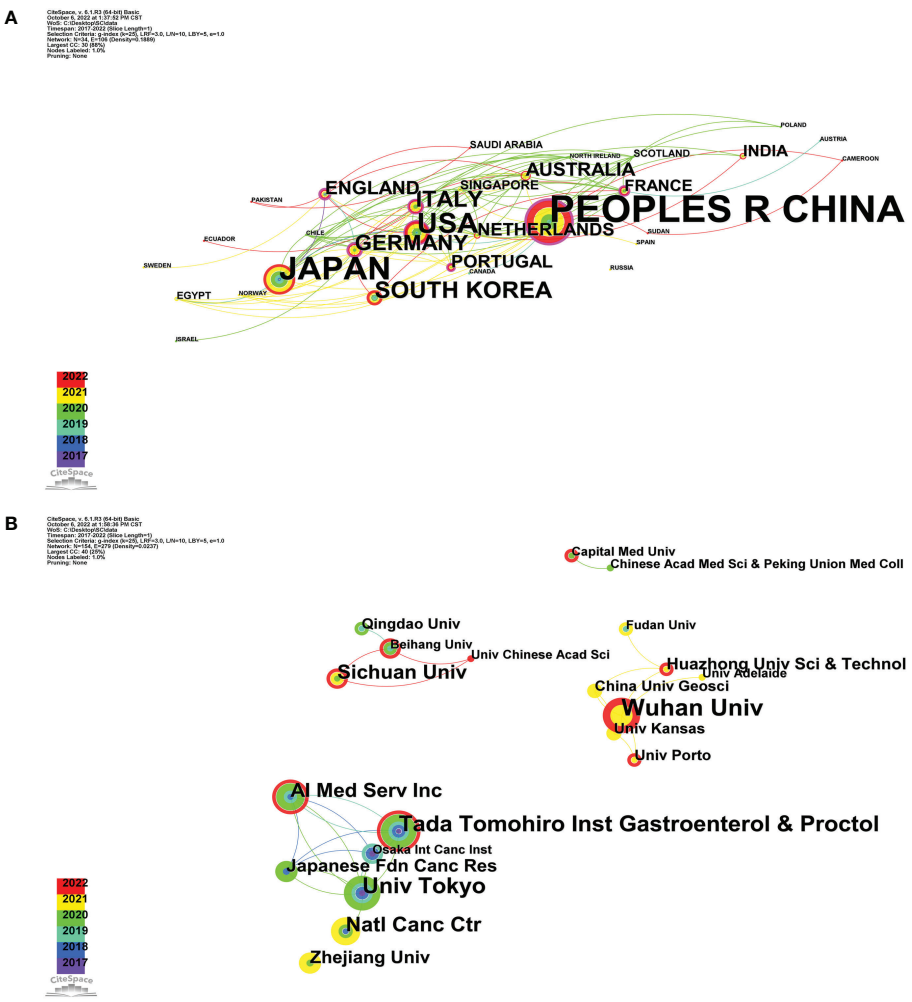

FIGURE 3
(A) Map of a subset of cooperative relations among countries, 2017–2022. **(B)** Map of a subset of cooperative relations among institutions, 2017–2022.

Figure 3B. We can learn that the cooperation between institutions was roughly divided into four groups. In addition, as presented in Table 1, Wuhan University published the largest number of articles among all institutions (13 publications), followed by The University of Tokyo (11 publications) and Tada Tomohiro Inst Gastroenterol and Proctol (11 publications). Furthermore, Wu et al. from Wuhan University, University of Bologna (Italy), University of Oslo (Norway), University of Porto (Portugal), Showa University (Japan), and University of Kansas (USA) conducted a collaborative study to assess the accuracy of endoscopists who use AI validation research framework to identify upper gastrointestinal tumors (UGINs), which demonstrated that the accuracy of endoscopists in identifying UGIN is poor even in frameworks with high prevalence and disease awareness. Future research on AI validation can represent a framework for assessing endoscopist capabilities (28). Then, in a paper published in *Lancet Gastroenterology and Hepatology*, Wu et al. conducted a single-center, tandem, randomized controlled trial to evaluate the effect of AI systems for detecting focal lesions and diagnosing gastric tumors on decreasing the rate of missed gastric tumor diagnoses in clinical practice, and the results showed that the use the AI system during upper gastrointestinal endoscopy significantly reduced the rate of missed diagnosis of gastric tumors. As a result, AI-assisted endoscopy may enhance the detection rate of gastric tumors by endoscopists (29). In a recent study, Wu et al. later proposed a deep-learning-based system, called Endoangel-ME, for diagnosing EGC in magnified image-enhanced endoscopy (M-IEE). Through a multicenter diagnostic study, the results showed that Endoangel-ME could be well applied in clinical settings (30–32). As mentioned above, Japan was the first country to start research in this field, publishing the first research publication in University of Tokyo on AI in GC in 2017. Shichijo Satoki et al. (University of Tokyo) built a convolutional neural network (CNN) and evaluated its capacity to diagnose *Helicobacter pylori* infection, since AI endoscope image in

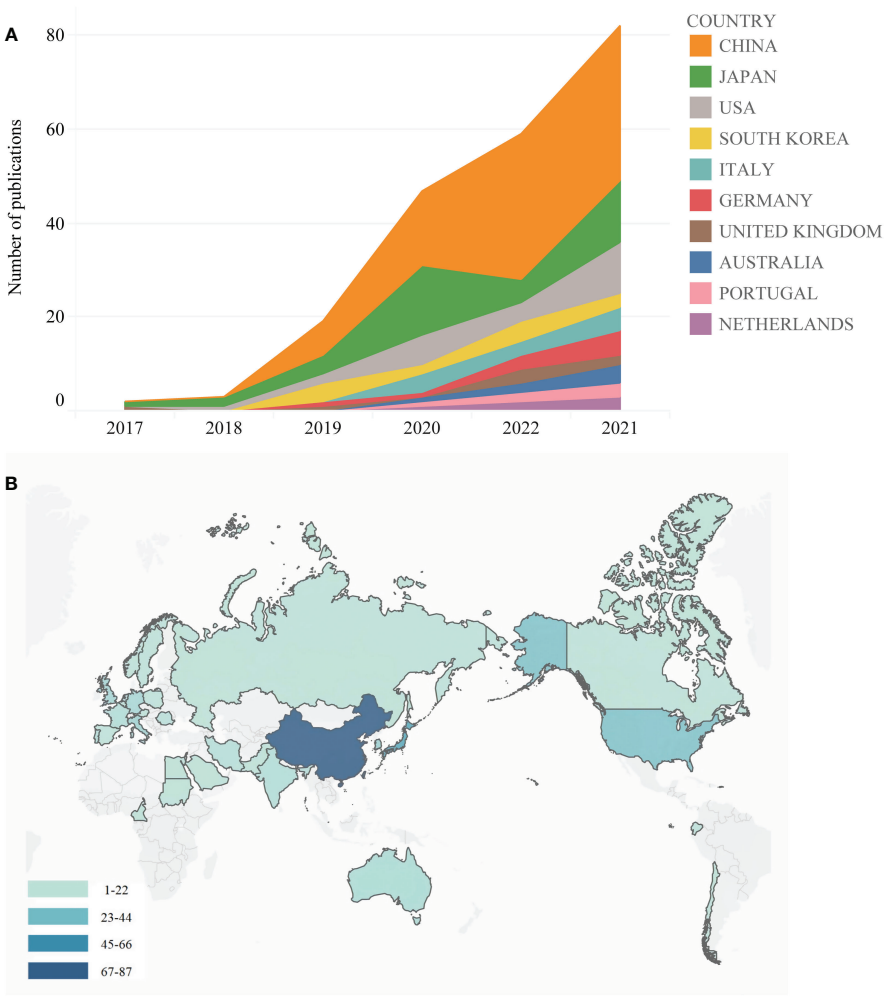

FIGURE 4
(A) The annual number of publications in the top 10 most productive countries from 2017 to 2022. **(B)** A world map displaying the contribution of each country based on publication counts.

the diagnosis of *H. pylori* gastritis has not been evaluated. Additionally, the findings demonstrated that *H. pylori* gastritis can be diagnosed based on endoscopic image diagnosis to CNN, and this method is time saving and more accurate than the artificial diagnostic endoscopy doctors (33). Background image recognition can be performed by CNN for AI, and deep learning has been significantly improved and increasingly applied to diagnostic imaging in the medical field. Hirasawa Toshiaki et al. (University of Tokyo) thus developed a CNN that can automatically detect GC in endoscopic images, which showed that the constructed CNN system for GC detection can process a large amount of stored endoscopic images in a very short time and has clinically relevant diagnostic capability. Moreover, it may be well adapted to everyday clinical practice to reduce the burden on endoscopists (34). The paper published by Hirasawa Toshiaki et al. has become a highly cited paper with 308 citations. Ryota Niikura, Satoki Shichijo, Toshiaki Hirasawa et al. (University of Tokyo) demonstrated the advantage of AI in the diagnosis of GC by comparing the diagnostic rate of endoscopic GC imaging with that of AI and professional endoscopists, but it did not prove its superiority (35).

3.2.2 Bibliometric analysis of authors and co-authors

The quantity and quality of publications can represent the level of research and contribution of the author in this field. Totally, 201 authors participated in a total of 183 publications. From the perspective of publication count (Table 2), Tada (12 publications) had the largest number of articles, followed by Li (10 publications), Yu (10 publications), and Wang (9 publications). Tada from Japan graduated from the University of Tokyo. He is the founder and CEO of AI Medical Service and also serves as the CEO of Tada Tomohiro Inst Gastroenterol and

10.3389/fonc.2022.1075974

TABLE 1 The top 10 prolific countries/regions and corresponding institutions.

Ranking	Country	Centrality	Frequency/ N (%)	H-index	Average Citation	Institution	Centrality	Frequency/ N (%)
1	People's R China	0.4	87/47.54	16	11.59	Wuhan Univ	0.06	13/7.10
						Sichuan Univ	0.02	8/4.37
						Zhejiang Univ	0	6/3.28
2	Japan	0.09	40/21.86	18.17	14	Univ Tokyo	0.07	11/6.01
						Tada Tomohiro Inst Gastroenterol & Proctol	0.01	11/6.01
						AI Med Serv Inc	0.01	8/4.37
3	USA	0.12	24/13.11	16.3	9	Univ Kansas	0	4/2.19
						Harvard Med Sch	0	2/1.09
						Microsoft Ltd Co	0	2/1.09
4	South Korea	0	13/7.10	13.43	8	Chuncheon Sacred Heart Hosp	0.01	2/1.09
						Gachon Univ	0	2/1.09
						Sungkyunkwan Univ	0	2/1.09
5	Italy	0.18	12/6.56	10.5	8	Nuovo Regina Margherita Hosp	0	2/1.09
						Sapienza Univ Rome	0	2/1.09
						Univ Bologna	0	2/1.09
6	Germany	0.3	10/5.46	8.9	5	Univ Klinikum Augsburg	0	2/1.09
						Alfred Wegener Inst Helmholtz Zentrum Polar & Mee	0	1/0.55
						Berlin Inst Hlth BIH	0	1/0.55
7	England	0.3	7/3.83	38	3	Imperial Coll London	0	1/0.55
						Kings Coll Hosp NHS Fdn Trust	0	1/0.55
8	Australia	0.05	7/3.83	4.86	4	Univ Adelaide	0	3/1.64
						Alfred Hosp	0	1/0.55
						Griffith Univ	0	1/0.55
9	Portugal	0.11	6/3.28	7.83	3	Univ Porto	0	4/2.19
						Portuguese Oncol Inst Porto	0	2/1.09
10	Netherlands	0.07	6/3.28	8.33	3	Eindhoven Univ Technol	0	2/1.09
						Amsterdam UMC Locat Vrije Univ Amsterdam	0	1/0.55
						Amsterdam UMC	0	1/0.55

Proctol. Additionally, he had an H-index of 26 and 2,146 citations. We can learn from Table 1 that these three institutions mentioned above were the top 3 institutions in Japan in terms of the number of articles related on AI applicated in GC. Tada participated in the first research applying AI to GC in 2017 (33) and co-published the highly cited paper (mentioned above in *Section 3.2.1*), with the lead author Hirasawa (34). This highly cited paper has attracted much attention in the field of AI research and has been cited over 337 times up to now. The key authors in a co-citation network of a certain field can be identified by the author co-citation analysis (36). The author with the highest total citations was Hirasawa from the Japan Cancer Research Foundation with 90 total citations, working at the Tomohiro Inst Gastroenterol and Proctol Tada from 2018 to 2021. The major areas of his research were Stomach Cancer, Renal Oncocytoma, Esophageal

TABLE 2 The top 10 most productive authors and top 10 co-cited authors.

Ranking	Author	Count	Centrality	H-index	Country	Co-cited author	Count	Centrality	H-index	Country
1	Tada T	12	0.01	26	Japan	Hirasawa T	90	0.03	26	Japan
2	Li Y	10	0.05	25	People's R China	Bray F	61	0	108	France
3	Yu H	10	0.01	33	People's R China	Zhu Y	59	0.03	12	People's R China
4	Wang Y	9	0.02	14	People's R China	Wu LL	56	0.04	15	People's R China
5	Wu L	8	0.01	15	People's R China	Horiuchi Y	46	0.03	17	Japan
6	He X	8	0.01	11	People's R China	Li L	43	0.01	15	People's R China
7	Zhang Y	7	0.06	12	People's R China	Mori Y	42	0.01	29	Norway
8	Liu J	7	0.1	16	People's R China	Shichijo S	39	0.11	21	Japan
9	Fujisaki J	6	0.01	28	Japan	Horie Y	39	0.04	17	Japan
10	Kim J	6	0.01	18	South Korea	Kanesaka T	39	0.07	/	/

Cancer, and *Campylobacter* Infection, and his latest findings were mentioned above in *Section 3.2.1* (35). Bray, with the second highest number of co-citations, was also a key author in this field, and he was branch head cancer surveillance in the International Agency for Research on Cancer with specialist in descriptive epidemiology of cancer, time trends and predictions, and cancer registries.

Researchers that focus on research have abundant and unique professional knowledge, and cooperation between them can enhance communication and productivity of a certain research subject. In addition, researchers can learn existing partnerships and develop potential cooperative subjects by analyzing the co-authorship of authors. Therefore, we used CiteSpace to make a network diagram of author cooperation, from which we can observe that author cooperation was roughly divided into two groups. The smaller group included Japanese authors and was mainly led by Tada and Hirasawa, while the larger group included Chinese authors led by Li, Yu, Wang et al. (Figure 5).

3.2.3 Bibliometric analysis of the higher-impact journals

In this study, all these publications related to AI applicated in GC were distributed in 94 academic journals and co-cited journals. Table 3 summarizes the basic information on the top 20 journals and co-cited journals. The impact factor (IF) is frequently used as an indicator of the significance of a journal to its field of a 2-year moving average citation of a journal, which was first introduced by Eugene Garfield, the founder of the Institute for Scientific Information (37). As shown in Table 3, we can learn that 45% of journals and 55% of co-cited journals belong to Q1. The journal *Gastrointestinal Endoscopy* (21 publications; IF 2022, 9.189; Q1) with the second highest number of citations (115 citations, 11.5%) had the highest number of outputs on AI applicated in GC, followed by *World Journal of Gastroenterology* (13 publications, 7.1%; IF 2022, 5.715; Q2) and *Digestive Endoscopy* (12 publications, 6.6%; IF 2022, 5.779; Q2). In addition, the journal *Gastric Cancer* (133 citations; IF 2022, 8.171; Q1) had the highest citations among them, followed by *Gastrointestinal Endoscopy* (115 citations; IF 2022, 9.189; Q1), *Gut* (109 citations; IF 2022,27.827; Q1), and *Endoscopy* (106 citations; IF 2022, 9.508; Q1). The frequency of being co-cited, which reflects whether a journal has a huge impact on a particular research field, determines the influence of journals. Therefore, the main research direction of these journals was *Gastrointestinal Endoscopy*, *Gastric Cancer*, and *Endoscopy*. Furthermore, it is worth mentioning that *Gastrointestinal Endoscopy* ranked first in journal and second in co-cited journal, which indicated that it had an absolute influence on AI applicated in GC.

3.2.4 Analysis of co-cited reference

It is an efficient method to assess the progress and trace the developmental frontiers of any research field using reference co-citation analysis (38). The top 10 co-cited references related to our research are presented in Table 4. The paper titled "Application of AI using a convolutional neural network for detecting gastric cancer in endoscopic images" published by

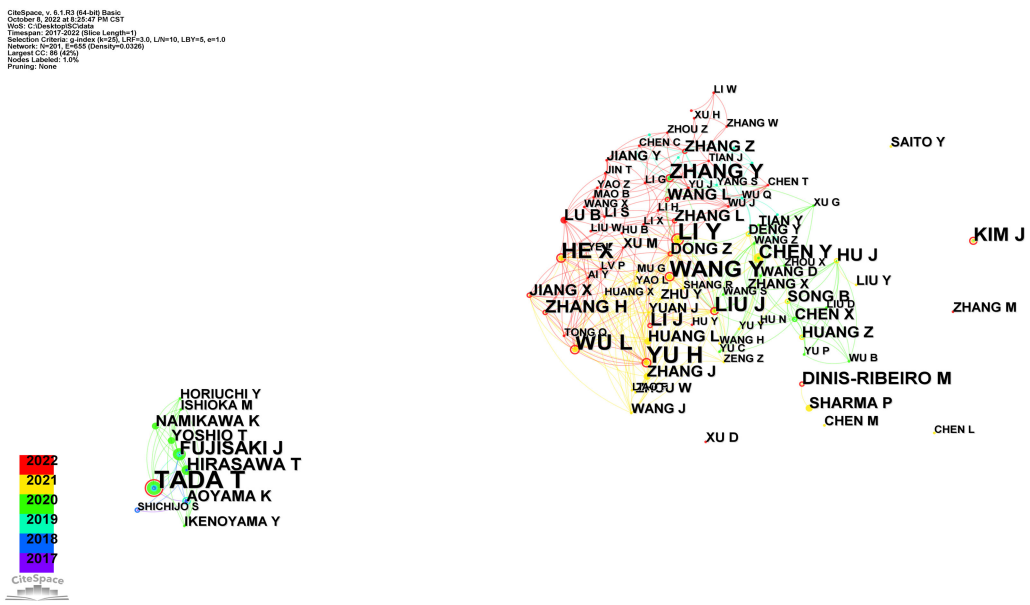

FIGURE 5
The network of authors, 2017–2022.

Hirasawa in *Gastric Cancer* in 2018 ranked first with a total number of citations of 89. The second is "Global cancer statistics 2018: GLOBCAN estimates of incidence and mortality worldwide for 36 satellites in 185 countries" published by Bray in *CA—Cancer J Clin* (60 citations), followed by "Application of convolutional neural network in the diagnosis of the invasion depth of gastric cancer based on conventional endoscopy" (57 citations). Four of the top 5 papers were highly cited, which showed that there was a certain relationship between citation times and co-citation times.

3.3 Research topic and hotspots analysis—analysis of keywords and keywords with citation burst

Keywords are the crystallization of the text content of an article, which is with a high generalization and reflection ability in a research field and can directly point to the center of the text. Therefore, keywords with high frequency are often used to present the hot issues in a research field and reflect the research hotspots in a certain period of time from a macroperspective. In order to describe the research status and hotspots of AI in the field of GC, the knowledge map of keyword co-occurrence was obtained using CiteSpace (Figure 6). The knowledge map of keyword co-occurrence was obtained through CiteSpace analysis and presented in two forms: Cluster View (Figure 7A) and Timeline View (Figure 7B).

Centrality represents the degree of importance of the node in the network co-occurrence, so keywords with high centrality may be regarded as the research hotspots in a certain field over a period of time (24). As mentioned above, the larger the node is in the keyword visualization map, the more frequent the keyword co-occurrence is. Additionally, the thickness of the lines represents the co-occurrence intensity between nodes, and the thicker the line is, the greater the co-occurrence intensity is. Therefore, the higher the co-occurrence frequency and centrality of node are, the more important the keyword in the research field is. The node of "AI" is the largest, followed by "gastric cancer," "convolutional neural network," and "deep learning" through CiteSpace and VOSviewer (Figure 6; Supplementary Figure S1B). According to the data in Table 5, the number of their appearances is 118, 101, 61, 48, 29, and 28, respectively.

Finally, we gained the clustering function in Figure 7A. It is worth mentioning that the modularity value (Q-value) and mean silhouette value (S-value) are two important indicators to evaluate the significance of community structure, and a clustering with a $Q > 0.3$ and $S > 0.7$ is significant. There were 16 different clusters in the network map, and the Q-value (0.8239) and weighted mean silhouette (0.9487) demonstrated the reasonableness of this network (39). From Figure 7A and Table 6, it can be observed that "upper gastrointestinal endoscopy" #0 and "*Helicobacter pylori* infection" #1 were the largest cluster, followed by "conventional histopathology" #2, "retrospective study genomics" #3, and "current application" #4.

In order to further analyze the keywords of AI applicate in GC, a Timeline View analysis was conducted. For time clustering, click "Find Clusters," then "LLR," and select "Timeline View" in Layout last, and the result is finally shown in Figure 7B. The evolution pace

TABLE 3 The top 20 journals and co-cited journals.

Ranking	Journal	Output	IF	JCR	Co-cited journal	Citation	IF	JCR
1	Gastrointestinal Endoscopy	21	9.189	Q1	Gastric Cancer	133	8.171	Q1
2	World Journal of Gastroenterology	13	5.715	Q2	Gastrointestinal Endoscopy	115	9.189	Q1
3	Digestive Endoscopy	12	5.779	Q2	Gut	109	27.827	Q1
4	Diagnostics	9	4.129	Q2	Endoscopy	106	9.508	Q1
5	Frontiers in Oncology	8	6.122	Q2	Gastroenterology	97	29.175	Q1
6	Endoscopy	7	9.508	Q1	Digestive Endoscopy	91	5.779	Q2
7	Cancers	5	6.886	Q1	CA—A Cancer Journal for Clinicians	90	334.259	Q1
8	Frontiers in Medicine	5	5.493	Q2	World Journal of Gastroenterology	89	5.715	Q2
9	Gastric Cancer	5	8.171	Q1	Scientific Reports	82	5.516	Q2
10	BMC Gastroenterology	4	3.23	Q4	Journal of Gastroenterology and Hepatology	65	4.319	Q2
11	Computational and Mathematical Methods in Medicine	4	2.887	Q2	Endoscopy International Open	65	0.77	Q2
12	Journal of Gastroenterology and Hepatology	4	4.319	Q2	eBioMedicine	65	10.481	Q1
13	Journal of Medical Internet Research	4	7.69	Q1	Nature	59	63.58	Q1
14	Surgical Endoscopy and Other Interventional Techniques	4	3.796	Q2	Lancet Oncology	59	49.204	Q1
15	Best Practice Research Clinical Gastroenterology	3	4.875	Q4	PLOS One	58	4.069	Q2
16	eBioMedicine	3	10.481	Q1	Digestive Diseases and Sciences	57	3.522	Q3
17	Journal of Clinical Oncology	2	38.801	Q1	Surgical Endoscopy and Other Interventional Techniques	54	3.796	Q2
18	Annals of Translational Medicine	2	4.263	Q3	JAMA—Journal of the American Medical Association	53	101.13	Q1
19	Archives of Computational Methods in Engineering	2	8.967	Q1	New England Journal of Medicine	49	125.115	Q1
20	Chinese Medical Journal	2	3.81	Q1	Journal of Clinical Medicine	45	5.098	Q2

of each cluster by time could be observed to further explore the key research contents in this field from a microperspective. In Figure 7B, there remained a total of 16 clustering, numbered from 0 to 15. Moreover, the distance from left to right or from top to bottom of every clustering and the size of the color line load point represent the appearing time and end time of each clustering, and color curve represents cluster label word co-occurrence relation between the different colors. We can see that the research focus has shifted from "genomics" (5), "utilizing AI" (11), and "world health organization classification" (12) to "upper gastrointestinal endoscopy" (1), "*Helicobacter pylori* infection" (2), "conventional histopathology" (3), "retrospective study" (4), "current application" (5), "Kyoto classification" (6), and "predicting bleeding" (7).

Additionally, burst detection, an algorithm developed by Kleinberg (40), is an effective analytical tool for capturing the turning point in keywords or references popularity over a specified period. Figure 8 shows the top 7 keywords with the strongest keyword outbreak. The blue line represents the time interval, and the red line represents the duration of the outbreak. The first six keywords started to break out in 2019, and the end time was 2020, while the "deep-learning algorithm" started to break out in 2020 and continues till now, which indicated that this research topic has attracted continuous attention in recent years and might be the trend of research on AI application in GC.

4 Discussion

4.1 General information

In the present study, we performed a systematic literature search of the WoS databases for articles published from 2017 to

TABLE 4 The top 10 co-cited reference.

Ranking	Title	Journal	First Author	Publication year	Total citations
1	Application of AI using a convolutional neural network for detecting gastric cancer in endoscopic images	*GASTRIC CANCER*	Hirasawa T	2018	89
2	Global cancer statistics 2018: GLOBCAN estimates of incidence and mortality worldwide for 36 cancers in 185 countries	*CA-CANCER J CLIN*	Bray F	2018	60
3	Application of convolutional neural network in the diagnosis of the invasion depth of gastric cancer based on conventional endoscopy	*GASTROINTEST ENDOSC*	Zhu Y	2019	57
4	Convolutional neural network for the diagnosis of early gastric cancer based on magnifying narrow band imaging	*GASTRIC CANCER*	Li L	2020	43
5	A deep neural network improves endoscopic detection of early gastric cancer without blind spots	*ENDOSCOPY*	Wu LL	2019	41
6	The diagnostic outcomes of esophageal cancer by AI using convolutional neural networks	*GASTROINTEST ENDOSC*	Horie Y	2019	39
7	Computer-aided diagnosis for identifying and delineating early gastric cancers in magnifying narrow-band imaging	*GASTROINTEST ENDOSC*	Kanesaka T	2018	38
8	Convolutional Neural Network for Differentiating Gastric Cancer from Gastritis Using Magnified Endoscopy with Narrow Band Imaging	*DIGEST DIS SCI*	Horiuchi Y	2020	35
9	Real-time AI for detection of upper gastrointestinal cancer by endoscopy: a multicentre, case-control, diagnostic study	*LANCET ONCOL*	Luo HY	2019	34
10	Application of Convolutional Neural Networks in the Diagnosis of Helicobacter pylori Infection Based on Endoscopic Images	*EBIOMEDICINE*	Shichijo S	2017	32

2022 about AI applicated in GC, a total of 183 publications in this research field was retrieved and plotted. As shown in Figure 2B, due to the accelerated development and research of machine learning and artificial neural networks, great breakthroughs have taken place in AI in the 1990s. Meanwhile, the number of publications on AI has been gradually increasing, and the application of AI in medicine has also increased, but it is still relatively small. The publication of

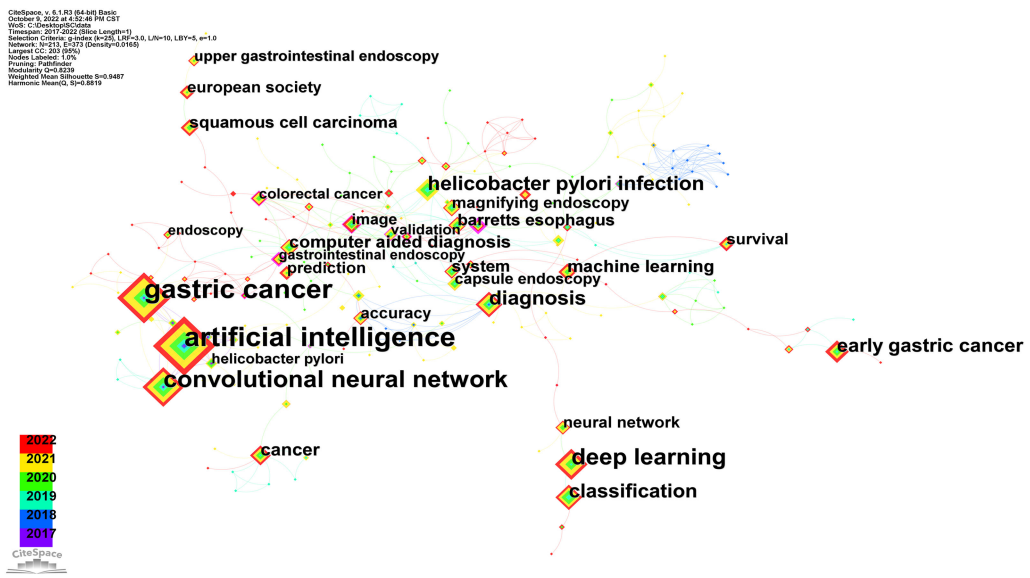

FIGURE 6
The keyword visualization map.

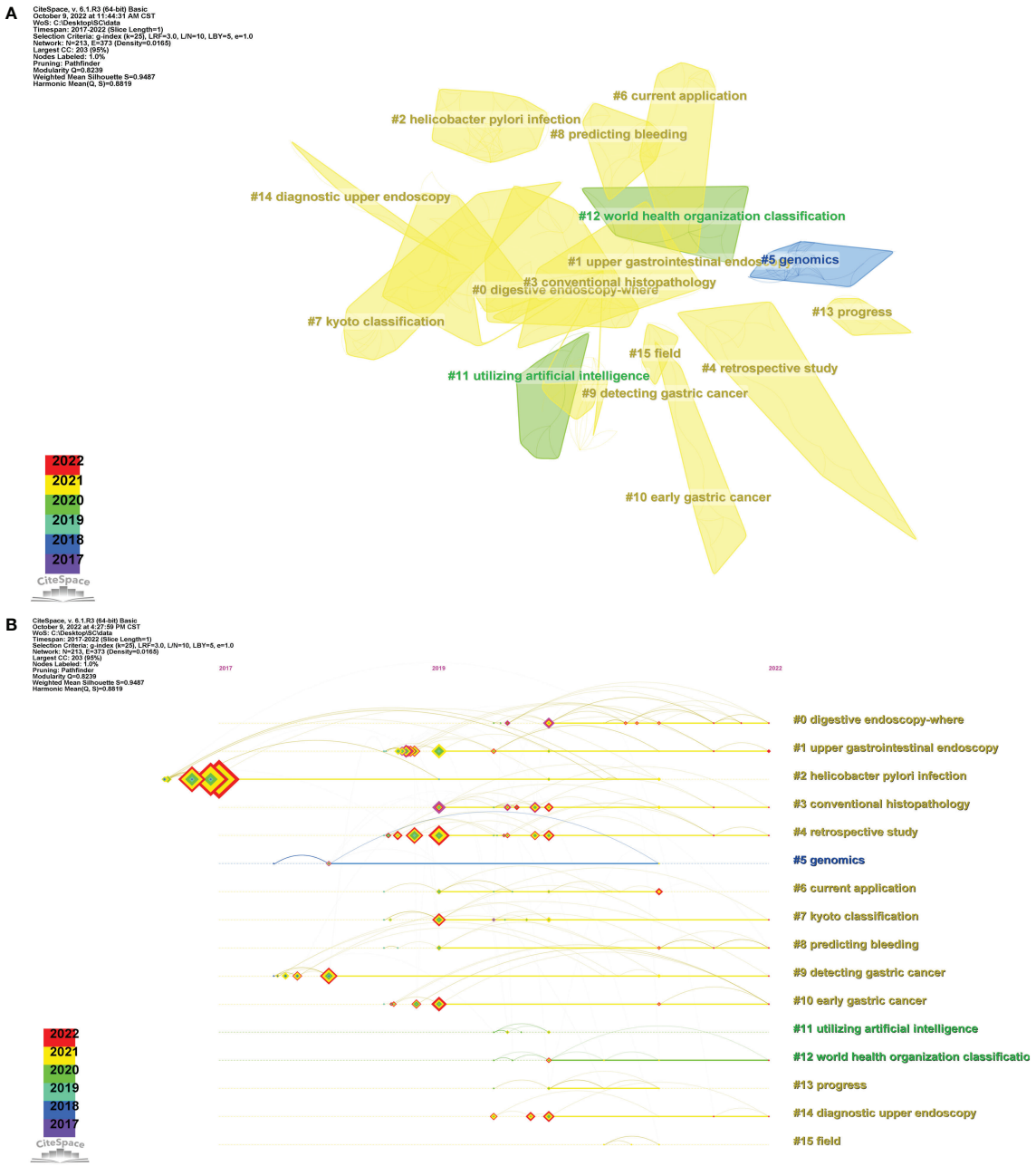

FIGURE 7
(A) The cluster view map of keyword. **(B)** The cluster timeline view map of keywords analysis.

the relevant papers was an important inflection point in 2016, the annual growth rate from 2016 to 2017 was the highest, and the first application of AI in the field of GC in the database was published in 2017. Because an important event occurred in this year, Alpha Go defeated the world Go master Lee Sedol, pushing the high tide of AI development to a new level (41). Meanwhile, the world's major economic powers have accelerated the deployment of AI, which laid a firm foundation for new breakthroughs in the field of AI on a global scale causing the increase in investment in the AI industry and various policies to encourage the development of AI. The application of AI in the field of medicine has also developed accordingly, and the number of publications has increased annually, indicating that this topic has received significant attention. Additionally, 2017 was the year when AI was first universally recognized in the world. In this year, Alpha Go Zero achieved self-renewal and

10.3389/fonc.2022.1075974

TABLE 5 Top 20 keywords.

Ranking	Keyword	Count	Centrality	Year
1	AI	118	0	2017
2	gastric cancer	101	0.14	2017
3	convolutional neural network	61	0.05	2017
4	deep learning	48	0.05	2019
5	Diagnosis	29	0.11	2018
6	*Helicobacter pylori* infection	28	0.06	2019
7	classification	27	0.04	2019
8	early gastric cancer	23	0.02	2019
9	cancer	18	0.12	2019
10	machine learning	17	0	2020
11	computer aided diagnosis	16	0.14	2019
12	Barrett's esophagus	14	0.14	2019
13	system	14	0.19	2019
14	squamous cell carcinoma	14	0.05	2020
15	magnifying endoscopy	13	0	2019
16	European Society	13	0.04	2020
17	neural network	13	0.09	2020
18	prediction	13	0	2020
19	accuracy	13	0.1	2018
20	survival	13	0.12	2019

upgrading through deep learning, constantly surpassing itself and beating Alpha Go (42). Moreover, Watson, an AI developed by IBM, analyzes and interprets massive medical data and literature through machine learning and then proposes treatment plans, which highly coincide with doctors' treatment recommendations (retrieved 14 October 2022, https://en.wikipedia.org/wiki/IBM_Watson). Xiaoice is an AI system developed by Microsoft, and through self-study on modern poetry, the first AI-authored collection of poems—The Sunshine Lost Windows—was published by Xiaoice in May 2017 (retrieved 14 October 2022, https://en.wikipedia.org/wiki/Xiaoice). Research on AI in the field of GC has also received corresponding attention; the annual average growth rate of relevant articles reached 264.11% particularly in 2021 (Figure 2A). Although the overall research base of AI in the field of GC is relatively small, according to the current trend, it indicates that it will be a research hotspot in the future and will continue to receive attention.

Using visual analysis of the distribution of countries and institutions enables us to better understand which countries and institutions are the main contributors to this field. As shown in Table 1 and Figure 4A, we could see that China ranked first in the number of articles published. Moreover, institutional distribution was generally consistent with the country distribution, and the institution with the largest output of publications was Wuhan University, while University of Tokyo and Tada Tomohiro Inst Gastroenterol and Proctol followed. The explanation for this could be due to the fact that East Asia is a region with highest incidence of GC (3). Although China has made a late start in this field compared with Japan, but its pace of development is staggering. In addition, Chinese centrality was with the highest strength, reaching 0.4. The above results were attributed to the Chinese government's significant support for AI applications. Unfortunately, when the theme distribution of the H-index and the average citation were examined, China ranked third and second, respectively, indicating that the impact of output should be improved. However, with the rapid development, China will potentially take the leading and dominant position in this field. As shown in Figures 3A, B, although countries possess their cooperation networks, the connection between countries is sparse. From the perspective of research institutions, we could learn that the cooperation between institutions was roughly divided into four groups; there is substantially less collaboration and exchange of achievements across groups. Nevertheless, the

10.3389/fonc.2022.1075974

TABLE 6 The clusters information of keywords.

ClusterID	Label	Size	Silhouette	Mean(year)
#0	upper gastrointestinal endoscopy	22	0.948	2021
#1	helicobacter pylori infection	22	0.925	2020
#2	conventional histopathology	18	0.958	2019
#3	retrospective study	16	0.891	2020
#4	Genomics	16	0.924	2020
#5	current application	16	0.93	2018
#6	Kyoto classification	13	0.936	2020
#7	predicting bleeding	12	0.981	2019
#8	detecting gastric cancer	12	0.954	2020
#9	early gastric cancer	11	0.994	2019
#10	utilizing AI	10	1	2020
#11	World Health Organization classification	9	0.958	2020
#12	progress	8	0.977	2020
#13	diagnostic upper endoscopy	7	0.972	2020
#14	field	6	0.955	2020
#15	upper gastrointestinal endoscopy	5	0.985	2021

objective situation is that relatively few countries are currently involved in research related to the application of AI in GC worldwide. These situations hinder the development of this research area. Meanwhile, this also means that there is a large research gap that could be further explored and paid more attention in this field. Therefore, it is strongly suggested to strengthen the international exchanges and collaborations between countries and institutions to promote the research and development of AI in GC.

The emergence of academic journals always plays a significant role not only in the presentation of research results and science communication of scientists but also in our demand for academic knowledge. Publications serve as carriers for achievements in scientific research, and effective scientific communication requires the research results in an international peer-reviewed journal. Therefore, through the analysis of the distribution of journal sources, researchers can rapidly locate the most appropriate journals for their papers (43). Journals and Co-cited Journals Analysis (Table 3) showed that 45% of journals and 55% of co-cited journals were located in the Q1 JCR region. The journal *Gastrointestinal Endoscopy* had the highest number of outputs and the second highest number of citations for AI applied to GC, indicating that the journal has a significant influence in the field of AI in GC. In addition, the top journal in the field of gastric cancer,

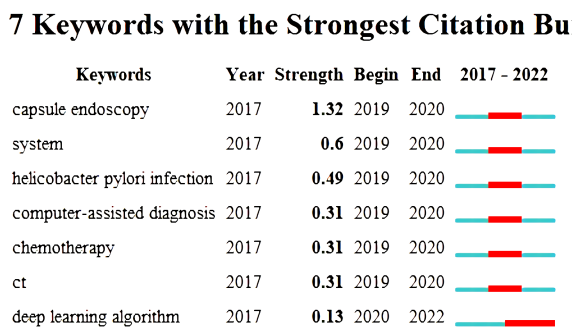

FIGURE 8
The top 7 keywords with the strongest citation burst.

Gastric Cancer, had the highest citations among them. The IF of these journals could reflect the importance and priority of AI to some extent. These high-quality journals have a significant influence on their respective academic fields, which further indicate AI applicated in GC as an important research direction for GC. In terms of the category of subject distribution, besides medical-related journals, it also includes one journal of engineering and technical, *Archives of Computational Methods In Engineering*. This indicates that the application of AI in GC is an interdisciplinary field, and its development requires multidisciplinary cooperation.

Generally, the authors who are frequently cited are regarded to have more impact than those who are less cited, and authors who are jointly cited probably focus on the relevant research field. From the perspectives of author contributions and co-cited authors (Table 2), the author with the most published articles in this field was Tada with 12 published articles, whose research focused on AI Medical Service. Moreover, Tada participated in the first research applying AI to GC in 2017 [26]. When co-cited authors were taken into account, Hirasawa was the most frequently co-cited author at 90 times, while Shichijo had the highest centrality. It should be noted that almost all of the top 10 active and co-cited authors were from Asia, implying that Asian researchers have played an important role and made significant contributions to AI in GC research. Furthermore, after comprehensive analysis of the data of the network diagram of author cooperation, we found that the author cooperation can be roughly divided into two groups, represented by Tada, Hirasawa, and Li, Yu, and Wang, respectively (Figure 5). The results indicate that Tada, Hirasawa, and Li are accomplished authors in this field and have a significant influence on other authors, and their teams would be excellent potential collaborators for researchers.

4.2 Knowledge base

Reference co-citation analysis is a valuable technique to assess the evolution and trace the developmental frontiers of a research field (38). The knowledge base is a collection of co-cited references (21). The top 10 co-cited references related to our research are presented in Table 4, which includes nine clinical trials and one epidemiological study. Four of the top 5 papers were highly cited papers, which showed that there was a certain relationship between citation times and co-citation times.

Almost all clinical trials were focused on the diagnosis and differential diagnosis of AI in GC, with the exception of one study of CNNs in the endoscopic imaging diagnosis of *H. pylori* infection. Shichijo (33) first constructed a CNN in 2017 to evaluate its ability to diagnose *H. pylori* infection. Compared with the artificial diagnostic endoscopists, the accuracy is higher, and it takes less time. Among the most frequently co-cited references related to application of AI in GC was a paper published by Hirasawa in *Gastric Cancer* in 2018, which was the most cited paper (89 citations). The authors constructed a CNN-based diagnostic system and used it for an independent test set of 2,296 gastric images collected from 69 consecutive patients with 77 GC lesions. The results showed that the CNN system could be used to detect GC with a clinically relevant diagnostic ability (34). Simultaneously, another clinical trial conducted by Kanesaka et al. developed a computer-aided diagnosis (CAD) system to assist endoscopists in identifying and diagnosing EGCs (44). The diagnostic performance revealed high sensitivity and accuracy, illustrating the great potential in real-time diagnosis and delineation of EGCs in M-NBI images. One year later, Zhu et al. published the results of a clinical trial using a CNN-CAD system to determine the invasion depth of GC with high accuracy and specificity and thereby could reduce unnecessary gastrectomy (45). Similarly, Wu et al. presented the results of a novel deep convolution neural network (DCNN) to detect EGCs. Compared to endoscopists, the system could detect and localize EGC more accurately. Moreover, it could significantly actively track suspected cancerous lesions and monitor blind spots during esophagogastroduodenoscopy (46). Another clinical trial published by Horie et al. evaluated the sensitivity and accuracy of the CNN system in detecting esophageal cancer. The results showed that 1,118 test images were analyzed in 27 s, with a sensitivity of 98% in detecting esophageal cancer cases and an accuracy of 98% in identifying superficial esophageal cancer and advanced esophageal cancer (47). The only one multicenter case–control diagnostic study was published in *Lancet Oncol* by Luo's group (48). The authors successfully constructed the Gastrointestinal Artificial Intelligence Diagnostic System (GRAIDS), and the result proved that GRAIDS achieved high diagnostic accuracy and sensitivity in upper gastrointestinal cancers. The two clinical studies published in 2020 focused on CNN system in the diagnosis of EGC and in the differential diagnosis of gastritis and GC observed by magnifying endoscopy with narrow band imaging(M-NBI) (49, 50). Bray et al. reported on cancer incidence and mortality of 36 cancers in 185 countries/regions worldwide in *CA—A Cancer Journal for Clinicians*, which contributed notable epidemiological data on GC (3).

In summary, there is no doubt that the top 10 most co-cited references provide an important foundation for the development of this field. The emphasis of these studies mainly includes the application of AI in the early diagnosis and differential diagnosis of GC to provide accurate guidance and support for clinical therapy. It is gratifying to see that some breakthroughs have been achieved in the research of the application of AI in GC. The analysis of co-cited reference allows us to better understand the evolution of the application of AI in GC.

4.3 The analysis of research hotspots

Keywords with high frequency are often used to present the hot issues in a research field and reflect the research hotspots in a

certain period of time from a macroperspective. To understand the research hotspots and frontiers of AI in GC, we visualized the keywords in Figure 6. The more representative keywords include AI, gastric cancer, convolutional neural network, deep learning, diagnosis, *Helicobacter pylori* infection, which indicate that these topics are research hotspots in this field. Currently, the application of AI in GC is mainly for diagnostic and differential diagnosis, and convolutional neural networks and deep learning are the most commonly used methods.

Furthermore, the knowledge map of keyword co-occurrence was obtained through CiteSpace analysis. With the help of the clustering function, the whole network map could be sorted into some different clusters, and studies in the same cluster might have similar research themes. The clusters were named by extracting nominal terms as labels from the titles of the cited articles, and the log-likelihood ratio (LLR) algorithm is applied as the extraction method. As shown in Figure 7A and Table 6, the cluster view of the keywords revealed that "upper gastrointestinal endoscopy" #0 and "helicobacter pylori infection" #1 were the largest cluster, indicating that the application of AI in endoscopy may be a mature and important theme in the AI research field. Simultaneously, a Timeline View analysis was conducted to observe the evolution pace of each cluster by time and to further explore the key research contents in this field from a microperspective. We can clearly observe in Figure 7B that the research focus has shifted; after a period of technical reserve based on theoretical research and basic applications, AI-related research in GC has gradually shifted toward clinical applications. AI has been widely applied in the field of endoscopy, pathology, and radiomics, achieving inspiring results and providing accurate guidance and support for clinical therapy decisions.

Additionally, since burst detection was an effective analytic tool to capture the dramatic increases in references or keywords popularity within a specified period, it therefore served as an important indicator of research hotspots or research frontiers over time. The evolution of the burst keywords over the last 5 years is shown in Figure 8. According to the ranking by burstiness strength, we observed that the top 6 keywords started to burst in 2019, and the end time was 2020. More importantly, the "deep-learning algorithm" started to burst in 2020 and continues till now, which indicated that this research topic has attracted continuous attention in recent years and might be the trend of research on AI application in GC. More importantly, the "deep-learning algorithm" started to burst in 2020 and continues till now. Deep learning was widely applied in the clinical diagnosis, therapy, and prognosis prediction of GC (9, 51–54). In a retrospective multi-institutional study enrolling 2,320 patients, Jiang et al. developed a multitask deep-learning model that could accurately predict peritoneal recurrence and survival in GC patients by using preoperative CT images (51). Another retrospective multicenter cohort study suggested that deep-learning-based classifiers for microsatellite instability and EBV-positive detection could be used as convenient and inexpensive predictive biomarkers for immunotherapy in GC, which has significant implications for the comprehensive therapy of GC (52). Moreover, a deep learning radiomic nomogram (DLRN) was built to determine the number of lymph node metastasis (LNM) in the locally advanced gastric cancer (LAGC). The results showed its excellent predictive value and provide baseline information for individualized treatment of LAGC (9). These studies illustrated that this research topic has attracted continuous attention in recent years and might be the trend of research on AI application in GC.

AI approaches such as machine learning and deep learning allows extracting quantitative features non-invasively from digital medical image for histological classification, tumor staging, therapy response, and prognosis. With the digital innovations including tele-health and 5G, AI application will become an integral part of GC research. However, the development of AI in GC is limited by issues such as the generality of models built by AI technology and the security of AI system data, which is the future direction of AI in GC.

According to the above analysis, our bibliometric study conducted a systematic analysis of the basic situation, research hotspots, and trends in AI in the field of GC from a visualization perspective. Therefore, the results of the bibliometric study were objective and accurate, which could provide a comprehensive guide for clinicians and academics working in this field. Given the important role of AI technology in GC and its significant advantages in the clinical diagnosis, therapy, and prognosis prediction of GC, without a doubt, the application of AI in the field of GC is a current research hotspot and will be a major research direction for scholars in the following years.

4 Limitation

The bibliometric analysis yielded a great deal of valuable information but inevitably had some limitations. Although the WoSCC database is one of the most comprehensive, systematic, and authoritative databases widely used for bibliometric analysis and visualization of scientific literature, we only used data from the WoSCC database and excluded data from other databases, which may have affected the results of the study. Additionally, the rigorous retrieval strategy and the restriction to articles published in English can also result in the loss of some data. Nevertheless, most of the publications on AI applied to GC are included in this study and can represent the actual research hotspots, evolutionary processes, and trends in this field.

5 Conclusion

AI possesses essential research value and application prospects in GC, especially showing great advantages in the clinical diagnosis, therapy, and prognosis prediction of GC. Research on AI in GC is increasing exponentially, highlighted by the outstanding contributions

of China, Japan, and the USA to the development of this field. Current research hotspots focus on the application of AI in the diagnosis and differential diagnosis and staging to provide accurate guidance and support for clinical treatment, and convolutional neural networks and deep learning are the most commonly used methods. Meanwhile, deep-learning algorithm has attracted continuous attention in recent years and will serve as the focus of future research. Therefore, it is urgent to strengthen the cooperation and communication between countries and institutions to promote development in this field and benefit more patients with GC.

Data availability statement

The original contributions presented in the study are included in the article. Further inquiries can be directed to the corresponding authors.

Author contributions

ZJ and ZL designed this study. GZ, JS and ZF performed the search and prepared the paper. WZ, PH, LL, YZ, XS and YW re-checked data. YC, ZJ and ZL revised and reviewed the manuscript analysis. All authors contributed to the article and approved the submitted version.

Funding

This study was supported by the National Natural Science Foundation of China (Nos. 81960503 and 81860428), the Leading Talents Program of Jiangxi (20213BCJL22050), and the Youth Science Foundation of Jiangxi Province (No. 20212BAB216036).

Conflict of interest

The authors declare that the research was conducted in the absence of any commercial or financial relationships that could be construed as a potential conflict of interest.

Publisher's note

All claims expressed in this article are solely those of the authors and do not necessarily represent those of their affiliated organizations, or those of the publisher, the editors and the reviewers. Any product that may be evaluated in this article, or claim that may be made by its manufacturer, is not guaranteed or endorsed by the publisher.

Supplementary material

The Supplementary Material for this article can be found online at: https://www.frontiersin.org/articles/10.3389/fonc.2022.1075974/full#supplementary-material

SUPPLEMENTARY FIGURE 1
(A) Pictorial representation of countrywide collaboration using the country collaboration map.(**B**) The keyword visualization map by VOSviewer.

References

1. Van Cutsem E, Sagaert X, Topal B, Haustermans K, Prenen H. Gastric cancer. *Lancet (London England)* (2016) 388(10060):2654–64. doi: 10.1016/s0140-6736(16)30354-3

2. GBD 2017 Stomach Cancer Collaborators. The global, regional, and national burden of stomach cancer in 195 countries, 1990-2017: a systematic analysis for the global burden of disease study 2017. *Lancet Gastroenterol Hepatol* (2020) 5(1):42–54. doi: 10.1016/s2468-1253(19)30328-0

3. Bray F, Ferlay J, Soerjomataram I, Siegel RL, Torre LA, Jemal A. Global cancer statistics 2018: GLOBOCAN estimates of incidence and mortality worldwide for 36 cancers in 185 countries. *CA: Cancer J Clin* (2018) 68(6):394–424. doi: 10.3322/caac.21492

4. Sung H, Ferlay J, Siegel RL, Laversanne M, Soerjomataram I, Jemal A, et al. Global cancer statistics 2020: GLOBOCAN estimates of incidence and mortality worldwide for 36 cancers in 185 countries. *CA: Cancer J Clin* (2021) 71(3):209–49. doi: 10.3322/caac.21660

5. Wang FH, Zhang XT, Li YF, Tang L, Qu XJ, Ying JE, et al. The Chinese society of clinical oncology (CSCO): Clinical guidelines for the diagnosis and treatment of gastric cancer, 2021. *Cancer Commun (London England)* (2021) 41(8):747–95. doi: 10.1002/cac2.12193

6. Oda I, Oyama T, Abe S, Ohnita K, Kosaka T, Hirasawa K, et al. Preliminary results of multicenter questionnaire study on long-term outcomes of curative endoscopic submucosal dissection for early gastric cancer. *Digestive Endoscopy Off J Japan Gastroenterological Endoscopy Soc* (2014) 26(2):214–9. doi: 10.1111/den.12141

7. Katai H, Ishikawa T, Akazawa K, Isobe Y, Miyashiro I, Oda I, et al. Five-year survival analysis of surgically resected gastric cancer cases in Japan: a retrospective analysis of more than 100,000 patients from the nationwide registry of the Japanese gastric cancer association (2001-2007). *Gastric Cancer Off J Int Gastric Cancer Assoc Japanese Gastric Cancer Assoc* (2018) 21(1):144–54. doi: 10.1007/s10120-017-0716-7

8. Ajani JA, D'Amico TA, Bentrem DJ, Chao J, Cooke D, Corvera C, et al. Gastric cancer, version 2.2022, NCCN clinical practice guidelines in oncology. *J Natl Compr Cancer Network JNCCN* (2022) 20(2):167–92. doi: 10.6004/jnccn.2022.0008

9. Dong D, Fang MJ, Tang L, Shan XH, Gao JB, Giganti F, et al. Deep learning radiomic nomogram can predict the number of lymph node metastasis in locally advanced gastric cancer: an international multicenter study. *Ann Oncol Off J Eur Soc Med Oncol* (2020) 31(7):912–20. doi: 10.1016/j.annonc.2020.04.003

10. Seevaratnam R, Cardoso R, McGregor C, Lourenco L, Mahar A, Sutradhar R, et al. How useful is preoperative imaging for tumor, node, metastasis (TNM) staging of gastric cancer? a meta-analysis. *Gastric Cancer Off J Int Gastric Cancer Assoc Japanese Gastric Cancer Assoc* (2012) 15 Suppl 1:S3–18. doi: 10.1007/s10120-011-0069-6

11. Lee DH, Kim SH, Joo I, Han JK. CT perfusion evaluation of gastric cancer: correlation with histologic type. *Eur Radiol* (2018) 28(2):487–95. doi: 10.1007/s00330-017-4979-5

12. Ting DSW, Carin L, Dzau V, Wong TY. Digital technology and COVID-19. *Nat Med* (2020) 26(4):459–61. doi: 10.1038/s41591-020-0824-5

13. Bi WL, Hosny A, Schabath MB, Giger ML, Birkbak NJ, Mehrtash A, et al. Artificial intelligence in cancer imaging: Clinical challenges and applications. *CA: Cancer J Clin* (2019) 69(2):127–57. doi: 10.3322/caac.21552

14. Liu DY, Gan T, Rao NN, Xing YW, Zheng J, Li S, et al. Identification of lesion images from gastrointestinal endoscope based on feature extraction of combinational methods with and without learning process. *Med image Anal* (2016) 32:281–94. doi: 10.1016/j.media.2016.04.007

15. Dracos A, Cognetti G. [Scientific literature: bibliometric and bibliographic indicators as integrative criteria for an objective evaluation of research activity]. *Annali dell'Istituto superiore di Sanita* (1995) 31(3):381–90.

16. Chen C. Searching for intellectual turning points: progressive knowledge domain visualization. *Proc Natl Acad Sci United States America* (2004) 101 Suppl 1 (Suppl 1):5303–10. doi: 10.1073/pnas.0307513100

17. Chen CM. CiteSpace II: Detecting and visualizing emerging trends and transient patterns in scientific literature. *J Am Soc Inf Sci Technol* (2006) 57(3):359–77. doi: 10.1002/asi.20317

18. Wu H, Wang Y, Tong L, Yan H, Sun Z. Global research trends of ferroptosis: A rapidly evolving field with enormous potential. *Front Cell Dev Biol* (2021) 9:646311. doi: 10.3389/fcell.2021.646311

19. Wu H, Zhou Y, Xu L, Tong L, Wang Y, Liu B, et al. Mapping knowledge structure and research frontiers of ultrasound-induced blood-brain barrier opening: A scientometric study. *Front Neurosci* (2021) 15:706105. doi: 10.3389/fnins.2021.706105

20. Synnestvedt MB, Chen C, Holmes JH. CiteSpace II: visualization and knowledge discovery in bibliographic databases. AMIA. Annual symposium proceedings. *AMIA Symposium* (2005) 2005:724–8.

21. Ma D, Guan B, Song L, Liu Q, Fan Y, Zhao L, et al. A bibliometric analysis of exosomes in cardiovascular diseases from 2001 to 2021. *Front Cardiovasc Med* (2021) 8:734514. doi: 10.3389/fcvm.2021.734514

22. Yuan G, Shi J, Jia Q, Shi S, Zhu X, Zhou Y, et al. Cardiac rehabilitation: A bibliometric review from 2001 to 2020. *Front Cardiovasc Med* (2021) 8:672913. doi: 10.3389/fcvm.2021.672913

23. Xiao F, Li C, Sun J, Zhang L. Knowledge domain and emerging trends in organic photovoltaic technology: A scientometric review based on CiteSpace analysis. *Front Chem* (2017) 5:67. doi: 10.3389/fchem.2017.00067

24. Ma D, Yang B, Guan B, Song L, Liu Q, Fan Y, et al. A bibliometric analysis of pyroptosis from 2001 to 2021. *Front Immunol* (2021) 12:731933. doi: 10.3389/fimmu.2021.731933

25. Chen C, Hu Z, Liu S, Tseng H. Emerging trends in regenerative medicine: a scientometric analysis in CiteSpace. *Expert Opin Biol Ther* (2012) 12(5):593–608. doi: 10.1517/14712598.2012.674507

26. Wang ZY, Ma DB, Pang R, Xie F, Zhang JX, Sun DQ. Research progress and development trend of social media big data (SMBD): Knowledge mapping analysis based on CiteSpace. *ISPRS Int J Geo-Inf.* (2020) 9(11):16. doi: 10.3390/ijgi9110632

27. Hirsch JE. An index to quantify an individual's scientific research output. *Proc Natl Acad Sci United States America* (2005) 102(46):16569–72. doi: 10.1073/pnas.0507655102

28. Frazzoni L, Arribas J, Antonelli G, Libanio D, Ebigbo A, van der Sommen F, et al. Endoscopists' diagnostic accuracy in detecting upper gastrointestinal neoplasia in the framework of artificial intelligence studies. *Endoscopy* (2022) 54 (4):403–11. doi: 10.1055/a-1500-3730

29. Wu L, Shang R, Sharma P, Zhou W, Liu J, Yao L, et al. Effect of a deep learning-based system on the miss rate of gastric neoplasms during upper gastrointestinal endoscopy: a single-centre, tandem, randomised controlled trial. *Lancet Gastroenterol Hepatol* (2021) 6(9):700–8. doi: 10.1016/s2468-1253(21)00216-8

30. Wu L, Wang J, He X, Zhu Y, Jiang X, Chen Y, et al. Deep learning system compared with expert endoscopists in predicting early gastric cancer and its invasion depth and differentiation status (with videos). *Gastrointestinal Endoscopy* (2022) 95(1):92–104.e3. doi: 10.1016/j.gie.2021.06.033

31. Wu L, Xu M, Jiang X, He X, Zhang H, Ai Y, et al. Real-time artificial intelligence for detecting focal lesions and diagnosing neoplasms of the stomach by white-light endoscopy (with videos). *Gastrointestinal Endoscopy* (2022) 95(2):269–280.e6. doi: 10.1016/j.gie.2021.09.017

32. He X, Wu L, Dong Z, Gong D, Jiang X, Zhang H, et al. Real-time use of artificial intelligence for diagnosing early gastric cancer by magnifying image-enhanced endoscopy: a multicenter diagnostic study (with videos). *Gastrointestinal Endoscopy* (2022) 95(4):671–678.e4. doi: 10.1016/j.gie.2021.11.040

33. Shichijo S, Nomura S, Aoyama K, Nishikawa Y, Miura M, Shinagawa T, et al. Application of convolutional neural networks in the diagnosis of helicobacter pylori infection based on endoscopic images. *EBioMedicine* (2017) 25:106–11. doi: 10.1016/j.ebiom.2017.10.014

34. Hirasawa T, Aoyama K, Tanimoto T, Ishihara S, Shichijo S, Ozawa T, et al. Application of artificial intelligence using a convolutional neural network for detecting gastric cancer in endoscopic images. *Gastric Cancer Off J Int Gastric Cancer Assoc Japanese Gastric Cancer Assoc* (2018) 21(4):653–60. doi: 10.1007/s10120-018-0793-2

35. Niikura R, Aoki T, Shichijo S, Yamada A, Kawahara T, Kato Y, et al. Artificial intelligence versus expert endoscopists for diagnosis of gastric cancer in patients who have undergone upper gastrointestinal endoscopy. *Endoscopy* (2022) 54(8):780–4. doi: 10.1055/a-1660-6500

36. Wu H, Li Y, Tong L, Wang Y, Sun Z. Worldwide research tendency and hotspots on hip fracture: a 20-year bibliometric analysis. *Arch osteoporosis* (2021) 16(1):73. doi: 10.1007/s11657-021-00929-2

37. Garfield E. The history and meaning of the journal impact factor. *Jama* (2006) 295(1):90–3. doi: 10.1001/jama.295.1.90

38. Wu H, Zhou Y, Wang Y, Tong L, Wang F, Song S, et al. Current state and future directions of intranasal delivery route for central nervous system disorders: A scientometric and visualization analysis. *Front Pharmacol* (2021) 12:717192. doi: 10.3389/fphar.2021.717192

39. Li KL, Chen YM, Wang XQ, Hu HY. Bibliometric analysis of studies on neuropathic pain associated with depression or anxiety published from 2000 to 2020. *Front Hum Neurosci* (2021) 15:729587. doi: 10.3389/fnhum.2021.729587

40. Kleinberg J. Bursty and hierarchical structure in streams. *Data Min Knowl Discovery* (2003) 7(4):373–97. doi: 10.1023/a:1024940629314

41. Silver D, Huang A, Maddison CJ, Guez A, Sifre L, van den Driessche G, et al. Mastering the game of go with deep neural networks and tree search. *Nature* (2016) 529(7587):484–9. doi: 10.1038/nature16961

42. Silver D, Schrittwieser J, Simonyan K, Antonoglou I, Huang A, Guez A, et al. Mastering the game of go without human knowledge. *Nature* (2017) 550 (7676):354–9. doi: 10.1038/nature24270

43. Butt NS, Malik AA, Shahbaz MQ. Bibliometric analysis of statistics journals indexed in web of science under emerging source citation index. *SAGE Open* (2021) 11(1):8. doi: 10.1177/2158244020988870

44. Kanesaka T, Lee TC, Uedo N, Lin KP, Chen HZ, Lee JY, et al. Computer-aided diagnosis for identifying and delineating early gastric cancers in magnifying narrow-band imaging. *Gastrointestinal Endoscopy* (2018) 87(5):1339–44. doi: 10.1016/j.gie.2017.11.029

45. Zhu Y, Wang QC, Xu MD, Zhang Z, Cheng J, Zhong YS, et al. Application of convolutional neural network in the diagnosis of the invasion depth of gastric cancer based on conventional endoscopy. *Gastrointestinal Endoscopy* (2019) 89 (4):806–815.e1. doi: 10.1016/j.gie.2018.11.011

46. Wu L, Zhou W, Wan X, Zhang J, Shen L, Hu S, et al. A deep neural network improves endoscopic detection of early gastric cancer without blind spots. *Endoscopy* (2019) 51(6):522–31. doi: 10.1055/a-0855-3532

47. Horie Y, Yoshio T, Aoyama K, Yoshimizu S, Horiuchi Y, Ishiyama A, et al. Diagnostic outcomes of esophageal cancer by artificial intelligence using convolutional neural networks. *Gastrointestinal Endoscopy* (2019) 89(1):25–32. doi: 10.1016/j.gie.2018.07.037

48. Luo H, Xu G, Li C, He L, Luo L, Wang Z, et al. Real-time artificial intelligence for detection of upper gastrointestinal cancer by endoscopy: a multicentre, case-control, diagnostic study. *Lancet Oncol* (2019) 20(12):1645–54. doi: 10.1016/s1470-2045(19)30637-0

49. Li L, Chen Y, Shen Z, Zhang X, Sang J, Ding Y, et al. Convolutional neural network for the diagnosis of early gastric cancer based on magnifying narrow band imaging. *Gastric Cancer Off J Int Gastric Cancer Assoc Japanese Gastric Cancer Assoc* (2020) 23(1):126–32. doi: 10.1007/s10120-019-00992-2

50. Horiuchi Y, Aoyama K, Tokai Y, Hirasawa T, Yoshimizu S, Ishiyama A, et al. Convolutional neural network for differentiating gastric cancer from gastritis using magnified endoscopy with narrow band imaging. *Digestive Dis Sci* (2020) 65 (5):1355–63. doi: 10.1007/s10620-019-05862-6

51. Jiang Y, Zhang Z, Yuan Q, Wang W, Wang H, Li T, et al. Predicting peritoneal recurrence and disease-free survival from CT images in gastric cancer with multitask deep learning: a retrospective study. *Lancet Digital Health* (2022) 4 (5):e340–50. doi: 10.1016/s2589-7500(22)00040-1

52. Muti HS, Heij LR, Keller G, Kohlruss M, Langer R, Dislich B, et al. Development and validation of deep learning classifiers to detect Epstein-Barr virus and microsatellite instability status in gastric cancer: a retrospective multicentre cohort study. *Lancet Digital Health* (2021) 3(10):e654–64. doi: 10.1016/s2589-7500(21)00133-3

53. Wang X, Chen Y, Gao Y, Zhang H, Guan Z, Dong Z, et al. Predicting gastric cancer outcome from resected lymph node histopathology images using deep learning. *Nat Commun* (2021) 12(1):1637. doi: 10.1038/s41467-021-21674-7

54. Rasmussen SA, Arnason T, Huang WY. Deep learning for computer-assisted diagnosis of hereditary diffuse gastric cancer. *J Pathol Trans Med* (2021) 55(2):118–24. doi: 10.4132/jptm.2020.12.22

frontiers | Frontiers in Oncology

TYPE Original Research
PUBLISHED 09 January 2023
DOI 10.3389/fonc.2022.1007317

Check for updates

OPEN ACCESS

EDITED BY
Zhendong Jin,
Second Military Medical University, China

REVIEWED BY
Philipp Stroebel,
University Medical Center Göttingen, Germany
Francesco Panzuto,
Sapienza University of Rome, Italy

*CORRESPONDENCE
Qiaofei Liu
qfliu@aliyun.com
Quan Liao
lqpumc@126.com

†These authors have contributed equally to this work and share first authorship

SPECIALTY SECTION
This article was submitted to Gastrointestinal Cancers: Colorectal Cancer, a section of the journal Frontiers in Oncology

RECEIVED 30 July 2022
ACCEPTED 08 December 2022
PUBLISHED 09 January 2023

CITATION
Song H, Yang S, Zhang Y, Hua Y, Kleeff J, Liu Q and Liao Q (2023) Comprehensive analysis of mixed neuroendocrine non-neuroendocrine neoplasms (MiNENs): A SEER database analysis of 767 cases.
Front. Oncol. 12:1007317.
doi: 10.3389/fonc.2022.1007317

COPYRIGHT
© 2023 Song, Yang, Zhang, Hua, Kleeff, Liu and Liao. This is an open-access article distributed under the terms of the Creative Commons Attribution License (CC BY). The use, distribution or reproduction in other forums is permitted, provided the original author(s) and the copyright owner(s) are credited and that the original publication in this journal is cited, in accordance with accepted academic practice. No use, distribution or reproduction is permitted which does not comply with these terms.

Comprehensive analysis of mixed neuroendocrine non-neuroendocrine neoplasms (MiNENs): A SEER database analysis of 767 cases

Huixin Song[1,2†], Sen Yang[1†], Yalu Zhang[1], Yuze Hua[1], Jorg Kleeff[3], Qiaofei Liu[1*] and Quan Liao[1*]

[1]Department of General Surgery, State Key Laboratory of Complex Severe and Rare Diseases, Peking Union Medical College Hospital, Chinese Academy of Medical Science and Peking Union Medical College, Beijing, China, [2]Department of Gastroenterology, Beijing Friendship Hospital, Capital Medical University, Beijing, China, [3]Department of Visceral, Vascular and Endocrine Surgery, Martin-Luther-University Halle-Wittenberg, Halle (Saale), Germany

Background: Mixed neuroendocrine non-neuroendocrine neoplasm (MiNEN) is an extremely rare entity, consisting of neuroendocrine and non-neuroendocrine components. It can occur in various organs throughout the body, with a rising incidence. Its clinical management is a rapidly growing field of interest; however, large-scale patient cohorts are still missing to guide clinical practice.

Patients and methods: The demographic, clinicopathological, and survival information of all patients diagnosed with MiNEN in the national Surveillance, Epidemiology, and End Results (SEER) program database (2000–2017) were extracted and further analyzed. The information of the patients before and after 2010 was compared to understand the epidemiological changes of MiNEN. The characteristics of MiNEN originating in different organs were compared. The clinical significance of surgical resection for metastatic MiNENs was also analyzed.

Results: A total of 1081 patients were screened, and after applying the exclusion criteria, 767 patients were finally analyzed. There was no obvious sex preference (49.2% vs 50.8%, p>0.05) and the majority of the patients were Caucasians (n=627, 81.7%). A total of 88.3% of the patients were older than 50 years old, and the median age was 60 years. 79.3% of the tumors are located in the distal digestive tract, and 67.7% were grade 3/4. Distant metastasis was presented in 33.9% of the patients at diagnosis. A total of 88% of the patients underwent surgical treatments. The number of patients increased 10-fold between 2000 and 2017. There was no significant difference in sex, race, stage, or surgical treatments among the patients diagnosed before and after 2010. More patients older than 60 years were diagnosed after 2010 (p=0.009). The median survival was 61.0 ± 9.8 months for the whole cohort. After multivariate analysis, older age (>60 years, p<0.01), more advanced stage (p<0.01), grade 3/4 (p<0.01), and non-surgical treatment (p<0.01) were

independent risk factors for poorer survival. The appendiceal MiNENs showed the best prognosis. A total of 260 metastatic MiNENs were further analyzed. Only patients with metastatic MiNENs originating from the appendix had a potential benefit from surgical resection, compared to other sites (p=0.05).

Conclusion: This study provides the epidemiological, clinicopathological, and survival information of the largest number of MiNEN patients. Although MiNEN is an extremely rare malignant neoplasm, its incidence increases rapidly. The majority of the patients suffered from advanced-stage disease, which highlights the need for improvement of early detection in the future. The appendix is the most common primary site of MiNEN, and surgical resection for selected metastatic MiNEN originating in the appendix has favorable survival outcomes.

KEYWORDS

surveillance, epidemiology, risk factor, SEER (surveillance epidemiology and end results) database, mixed neuroendocrine non-neuroendocrine neoplasms, MiNEN

Introduction

Mixed adeno-neuroendocrine carcinoma (MANEC) was first reported by Oberndorfer et al. in 1907 and classified by the World Health Organization (WHO) in 2010. Before 2010, composite carcinoid was the most commonly used name to describe MANEC. It is an extremely rare neoplasm containing at least 30% of both exocrine and endocrine components (1). It has been reported that MANEC can involve multiple organs, including the gastrointestinal (2), respiratory, and urogenital tract (3, 4). Due to its specific architecture and unspecific clinical manifestations, it is always very difficult to have a definitive diagnosis of MANEC before surgery, and under most circumstances, it was diagnosed after surgical resection by a combination of cytological morphologies and immunohistochemical staining. In the WHO classification (2019), the nomenclature of mixed neuroendocrine non-endocrine neoplasms (MiNENs) was proposed to describe a wider range of these mixed neuroendocrine neoplasms in the digestive system (5, 6).

The majority of the published reports about MiNENs are small retrospective case series, with significant drawbacks in summarizing the clinicopathological characteristics. Recently, a population-level analysis of digestive MiNENs showed a sustained and rapid increase in incidence and mortality from 2010 to 2016 (7). Brathwaite et al. (8) reported a study of the surveillance, epidemiology, and end results (SEER) of appendiceal MiNENs. They found that the overall survival for appendiceal MiNENs was much shorter than of carcinoid tumors but better than that of signet ring cell carcinomas. In addition, several published case series reported that MiNENs in the duodenum (9), gallbladder (10), and liver 11 had extremely poor survival. Similar to other solid neoplasms, radical surgical resection may offer a cure for MiNENs, however, its rapid progression and atypical symptoms in early stages result in a high rate of advanced stages at diagnosis in most patients.

In this study, we utilized the SEER program database from 2000 to 2017 to comprehensively generate evidence for MiNENs patients to better guide clinical practice.

Patients and methods

Mining the SEER database

The clinicopathological, surgical, and survival information of the MiNEN patients were extracted from the SEER database (2000–2017) by using the SEER* Stat 8.3.6.1 software. The inclusion criteria were as follows: (1) patients were pathologically diagnosed with MiNENs from January 1, 2000, to December 31, 2017; (2) patients had an active follow-up and did not suffer any other kind of malignant tumor. The exclusion criteria were as follows: (1) patients died from any other cause other than MiNENs; (2) patients whose cause of death was missing or unknown; (3) patients with other malignant tumors.

The setting of mining strategies of the SEER database was as follows: “cases in research database”, “year of diagnosis = 2000–2017”, “diagnostic confirmation = microscopically confirmed”, and “ICD-O-3 code:8244”. Details of the data extraction are presented in Figure 1.

The following variables were extracted: patient ID, age recorded with exact age and 85+, sex, race recode, year of diagnosis, site according to ICD-O-3/WHO 2008, vital status, survival months, COD to the site, SEER cause-specific death classification, survival months, grade of differentiation, summary

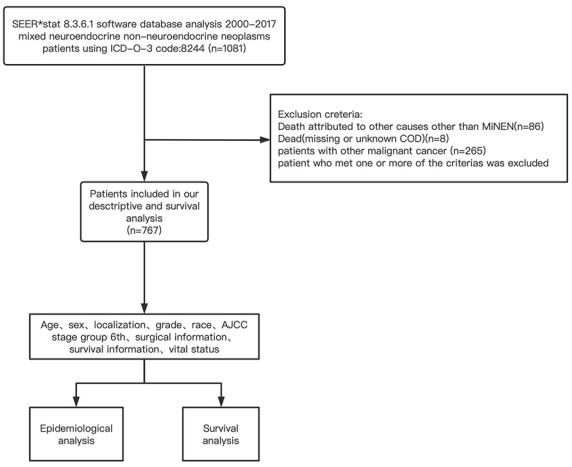

FIGURE 1
Flow diagram of SEER database mining strategy.

stage 2000 (1998+), derived AJCC Stage Group, 6th ed (2004-2015), derived AJCC T, 6th ed (2004-2015), derived AJCC N, 6th ed (2004-2015), derived AJCC M, 6th ed (2004-2015), the reason for no cancer-directed surgery, SEER cause-specific death classification, SEER other cause of death classification, COD to site and the total number of in situ/malignant tumors per patient.

Statistical analysis

Continuous variables were presented as mean± SD, with analysis using a t-test, analysis of variance (ANOVA), or Mann-Whitney U test. Categorical variables were compared using the Chi-squared test and survival information was analyzed with Kaplan–Meier plotting. The 1-year, 2-year, 3-year, and 5-year mortality ratios were estimated by Kaplan-Meier curves in consideration of sex, age, tumor localization, differentiation stage, AJCC staging group, ethnic origin, surgical information, and summary stage. Univariate and multivariate analysis were performed with a logistic regression model. All tests were two-tailed and a p-value of less than 0.05 was considered statistically significant. The analyses mentioned above were performed using GraphPad Prism 8.2.0 and IBM SPSS statistics 21 (SPSS Statistics V21, IBM Corporation, New York).

Data availability

Primary data is available online and from the corresponding author (QFL) upon reasonable request.

End points

The main endpoint was cancer-specific mortality (CSM) according to the data in the SEER database. CSM refers to deaths from MiNENs according to the recorded cause of death. Survival time was the duration from the initial diagnosis to death from cancer or to the last follow-up.

Results

General characteristics of the study population

There were 1081 individuals diagnosed with MiNENs in the database from 2000 to 2017, of which 767 were eligible for the study. In the analyzed cohort, 376 (49.2%) were female and 390 (50.8%) were male. The patients enrolled were largely Caucasians (n=627, 81.7%). MiNENs were mainly diagnosed between the ages of 50 and 70 (425, 55.4%), with a median age of 60 years. The number of patients below 50 (n=163, 21.3%) and above 70 (n=179, 23.3%) were similar. Only 3.8% of the tumors occurred in the small intestine, followed by 9.3% in the organs derived of foregut(respiratory, esophagus, stomach, hepato-biliary-pancreatic), 26.4% in the colon-rectum, and 52.9% in the appendix.

Of all included patients, 8.3% of patients (n=64) had well-differentiated tumors, 14.3% of patients (n=110) had moderately differentiated tumors, and 39.6% of patients (n=304) had poorly differentiated tumors. 8% of patients (n=61) had undifferentiated tumors, and the grade information was missing in 29.7% of the patients. Only 49 patients (6.4%) were diagnosed with early-stage of MiNENs. Stage II, III, and IV of the AJCC staging had similar proportions (17.7%, 13.3%, 19.3%). The 6th AJCC staging information was unknown in 332 cases (43.3%). Localized, regional, and distant stage accounted for 22.7%, 38.6% and 33.9% of patients, respectively. Only a small proportion of patients (n=92, 12%) did not receive surgery after being diagnosed with MiNENs. Chemotherapy information was largely missing or incomplete and was therefore not further analyzed. Detailed information was shown in Table 1.

Patients diagnosed with MiNENs before 2010 versus after 2010

The number of patients diagnosed with MiNENs significantly increased from 2000 to 2017 (Figure 2). To evaluate the effect of the year of diagnosis, we separated the 767 patients into two groups: diagnosed 20 from 00 to 2010

TABLE 1 Comparison of demographic and clinical information between patients diagnosed with MiNENs before and after 2010.

Classification	Variables	Total		≤2010		>2010		p-value
		N	%	N	%	N	%	
Sex	Female	377	49.2	123.0	51.5	254.0	48.1	0.40
	Male	390	50.8	116.0	48.5	274.0	51.9	
Age	<60 years	373	48.6	133.0	55.7	240.0	45.5	0.009
	≥60 years	394	51.4	106.0	44.4	288.0	54.6	
Race	White	627	82.1	191.0	80.6	436.0	82.7	0.48
	Non-white	137	17.9	46.0	19.4	91.0	17.3	
AJCC staging (6th)	I+II	183	42.3	69.0	43.7	114.0	41.5	NA
	III+IV	250	57.7	89.0	56.3	161.0	58.6	
Differentiation grade	Grade 1-2	174	32.3	50.0	39.7	124.0	30.0	0.04
	Grade 3-4	365	67.7	76.0	60.3	289.0	70.0	
Summary stage	Localized	174	23.8	67.0	29.4	107.0	21.3	0.06
	Regional	296	40.5	87.0	38.2	209.0	41.6	
	Distant	260	35.7	74.0	32.5	186.0	37.1	
Surgical information	Surgery performed	675	88.0	217.0	90.8	458.0	86.7	0.11
	No surgery	92	12.0	22.0	9.2	70.0	13.3	

NA, not available.

(group 1, n=239, 31.2%)and from 2011 to 2017 (group 2, n=528, 68.8%) (Table 1). There was no significant difference in sex, race, surgery and summary stage between these two groups. There were more patients over 60 years old in group 2 (54.4%) than in the other group (44.4%) (p= 0.009). Causations took the most part in both groups, with no significant difference (group 1:80.6%, n=191; group2:82.7%, n=436; p=0.5). A higher rate of grade 3/4 MiNENs was observed in group 2 (60.3% vs 70.0%, p=0.04). There was also a lower rate of localized MiNENs in this group (29.4% vs 21.3%, p=0.06).

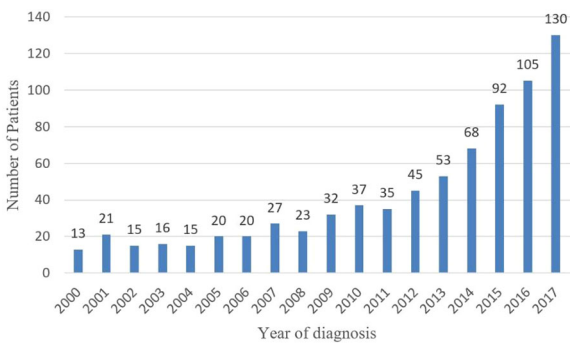

FIGURE 2
Number of patients diagnosed with MiNENs during 2000-2017.

Survival analysis for MiNEN patients

The estimated median survival time of these 767 patients was 61.0 ± 9.8 months. The estimated 1-year, 2-year, 3-year, and 5-year survival rate was, 79.4%, 66.2%, and 58.6%, respectively. The estimated 1-year, 2-year, 3-year, and 5-year survival rate of each variable are presented in Table 2. Non-appendical site (p<0.001), Older age (p<0.001), advanced AJCC staging (p<0.0001), grade 3/4 (p<0.0001), summary stage (p<0.0001), non-surgical treatment (p<0.0001) and distant metastasis (p<0.0001) were shown to be independent risk factors for shorter survival (Figure 3).The sex and race of the patients did not correlate with survival (Figure 3, Table 3) Multivariate analysis of factors associated with mortality in MiNEN patients revealed that age, localization, AJCC staging, differentiation, summary stage and surgical choice were independent factors associated with prognosis (Table 4).

Surgical treatment for metastatic MiNEN patients

A total of 260 metastatic MiNEN patients were enrolled in this study, 199 of whom (76.5%) underwent surgical resection. The elder patients with metastatic tumors over 60 years old had a lower rate of surgical resection (29.6% vs 16.8%, p=0.02). After

TABLE 2 Survival regarding different variables.

Classification	Variables	1 year survival rate (%)	2 year survival rate (%)	3 year survival rate (%)	5 year survival rate (%)
Sex	Female	79.1	65.3	57.4	51.8
	Male	79.7	67.0	59.6	48.9
Age	10-49 years	89.2	76.9	68.9	64.5
	50-59 years	86.7	71.2	63.1	53.1
	60-69 years	76.6	64.8	58.5	NA
	70-85+ years	64.3	51.2	42.7	34.3
Localization	Respiratory system	59.2	48.6	NA	NA
	Stomach	68.5	35.8	26.2	NA
	Hepatobiliary and pancreatic system	59.3	NA	14.2	NA
	Small intestine	75.3	62.7	NA	35.7
	Appendix	88.9	75.1	68.9	60.2
	Colorectum	67.4	58.9	49.5	41.7
	Other	71.0	NA	39.9	NA
Differentiation	Grade1	91.9	89.9	85.8	80.3
	Grade 2	90.7	81.6	72.6	65.3
	Grade 3	73.7	56.2	46.4	35.1
	Grade 4	66.2	60.9	48.8	39.9
AJCC staging (6^{th})	I	95.6	93.4	91.1	91.1
	II	97.8	94.0	92.2	84.3
	III	85.1	70.8	56.3	42.3
	IV	54.7	33.8	19.7	12.1
Race	White	79.2	65.8	57.9	50.2
	Non-white	80.3	68.1	61.1	51.8
Surgical information	Surgery performed	83.9	71.4	64.2	55.7
	No surgery	44.4	25.3	14.7	11.1
Summary stage	Localized	97.5	94.5	92.9	88.8
	Regional	87.7	76.9	69.0	57.0
	Distant	59.8	37.3	23.3	14.2

NA, not available.

2010, the rate of non-surgical choice in metastatic MiNEN patients was 27.4%, in comparison to 13.5% before 2010 (p=0.02). Surgery significantly improved the survival of the patients with metastatic MiNENs (19.0 ± 2.2 months vs 7.0 ± 2.3 months, p<0.001). Further, metastatic MiNENs in organs derived from the foregut (respiratory, upper gastrointestinal, and hepatobiliary-pancreatic), small intestine, and colon-rectum did not have survival benefit from surgical resection, in contrary, surgical resection improved the survival time of metastatic MiNENs originating from appendix (22.0 ± 3.3 months vs 14.0 ± 0.7 months, p=0.05) (Figure 4).

Discussion

The rarity of MiNENs makes it difficult to get high quality evidence from prospective randomized controlled trials to optimize its clinical care. Therefore, retrospective studies at a

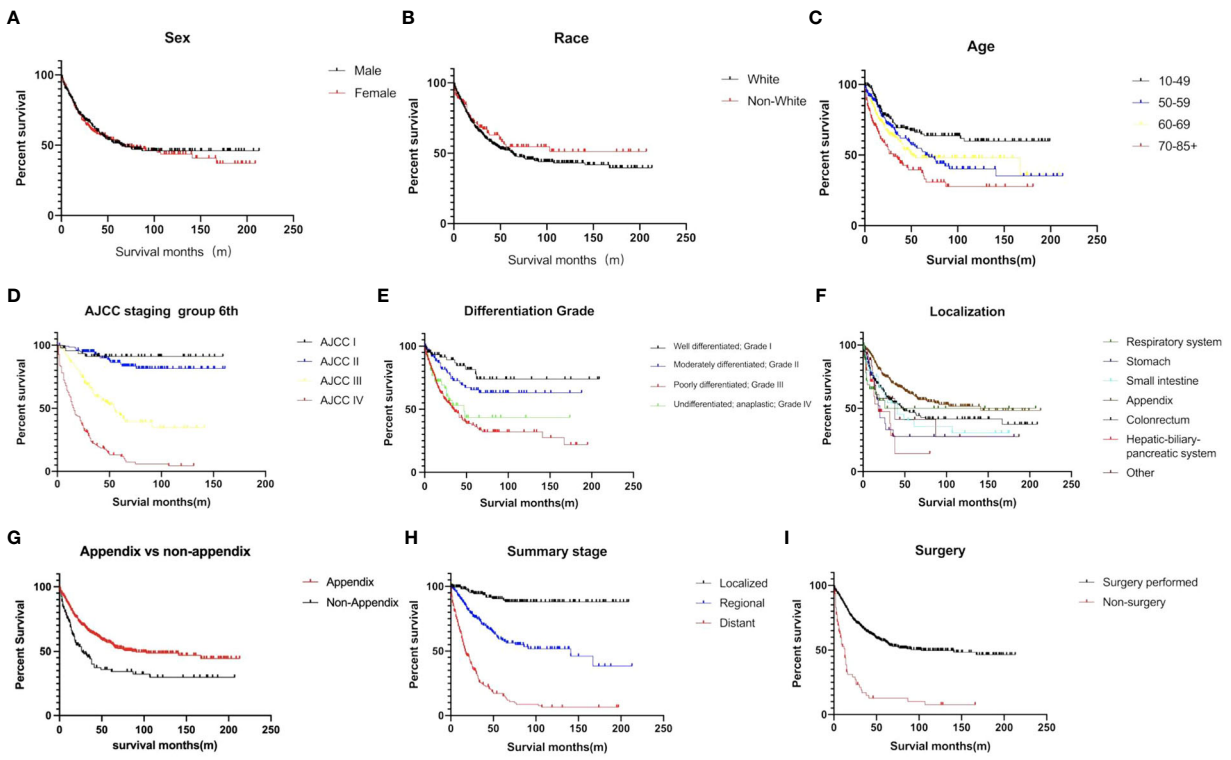

FIGURE 3
Survival curves of MiNENs depending on **(A)** sex (p>0.05), **(B)** age (p<0.001), **(C)** race (p>0.05), **(D)** AJCC staging group (p < 0.001), **(E)** differentiation (p < 0.001), **(F)** tumor localization (p < 0.001), **(G)** appendix vs non-appendix (p < 0.001), **(H)** summary stage (p < 0.001), and **(I)** surgical information (p < 0.001).

population-level are an alternative to provide solid evidence to help guiding the clinical management of this rare malignant neoplasm. As the largest cancer registration program, the SEER database covers approximately 30% of the United States population, which is a powerful resource for retrospective studies at a population- level. Previously, only two SEER analyses for MiNENs were conducted. Brathwaite et al. (8) compared the characteristics of appendiceal MiNEN (n=249), with goblet cell carcinoids (n= 944), signet ring cell carcinoma (n=579), and carcinoid (n=960). It was shown that median overall survival for MiNEN was 6.5 years, which was significantly shorter in comparison to 13.8 years for goblet cell tumors, 39.4 years for carcinoids, but longer in comparison to 2.4 years for signet ring carcinoma. However, in their study, MiNENs originating from other digestive organs was not analyzed. Later, Wang et al. (7) analyzed the epidemiological trend of gastrointestinal MiNENs. In their study, 518 cases of gastrointestinal MiNENs were analyzed, and they found that a sustained and rapid increase both in incidence and mortality of MiNENs from 2000 to 2016. Further, appendiceal MiNENs had better median survival, compared to cecal MiNENs (115 months vs 31 months, p<0.001). The details of MiNENs in other gastrointestinal organs, such as stomach, small intestine, esophagus, hepato-biliary-pancreatic systems, was not analyzed. Herein, we further comprehensive analyzed all of the pathologically diagnosed MiNENs throughout the SEER database from 2000 to 2017, to provide the strongest retrospective evidence to improve the clinical care of this rare entity. In this study, we mainly focused on three issues. The first one was epidemiology differences before and after 2010, when MaNEC was officially named by the WHO. The second one was the differences in clinicopathological characteristics and prognosis of MiNENs originating in different organs. The third one was the clinical significance of surgical treatment for metastatic MiNENs.

Increasing reports of MiNENs have been published during the last 20 years, however, the majority of them were small retrospective studies from singe centers, which likely did not show the real epidemiological trend of all of the diagnosed MiNENs (10–13). Our study showed that in 2000, only 13 cases of MiNEN (composite carcinoid) were found in the SEER database, however, by 2017, it increased ten-fold. The incidence of MiNENs showed a substantially increase during the last 20 years. However, similar to other malignancies, such as thyroid carcinoma, lung cancer, breast cancer (14), pancreatic cystic neoplasm (15–17), which also showed rapid increases in

TABLE 3 Univariate analyses of risk factors for survival.

Classification	Variables	Median survival(m)	SE(m)	Univariate analysis	
		61.0	9.8	95%CI	p-value
Sex	Female	62.0	15.3	32.00-92.00	0.84
	Male	52.0	12.2	32.15-79.86	
Age	<60 years	107.0	NA	26.51-49.49	<0.01
	≥60 years	38.0	5.9	41.74-80.26	
Race	White	61.0	8.4	44.5-77.5	0.52
	Non-white	103.0	NA	NA	
Localization	Appendix	141.0	NA	NA	<0.001
	Colorectum	41.0	13.1	15.4-66.6	
	Small intestine	36.0	8.3	19.8-52.2	
	Others	26.0	6.4	13.4-38.6	
AJCC staging (6^{th})	I	NA	NA		<0.001
	II	NA	NA		
	III	54.0	9.5	35.3-72.7	
	IV	14.0	1.7	10.5-17.5	
Differentiation	G1-G2	NA	NA	NA	<0.001
	G3-G4	33.0	3.8	25.5-40.5	
Summary stage	Localized	NA	NA	NA	<0.001
	Regional	141.0	46.6	49.7-232.3	
	Distant	16.0	1.4	13.2-18.8	
Surgical information	Surgery performed	86.0	NA	3.3-14.7	<0.001
	No surgery	9.0	2.9	41.7–80.3	

NA, not available.

incidence during the last 20 years, it is difficult to say that whether the increasing incidence is attributed to real higher tumor occurrence or to more clinical detections due to the wide use of more accurate imaging modalities.

Although MiNENs can occur throughout the human body, much more reports of MiNENs with larger number of patients in distal digestive tract were published than other organs, indicating its anatomical site preferences (7, 18, 19). In a systematic review of lower digestive tract MiNENs, Grossi et al. (20) reported that 60.3% of them were in the appendix, 29.3% were in the colon, and 10.4% were in the anorectum. In this study, we found the majority of the cases in midgut and hindgut organs, and only 13.1% of them were located in organs derived from the foregut, including the respiratory system, esophagus, stomach, and hepato-biliary-pancreatic system. The most common site was appendix (52.9%), followed by colorectum (26.4%). It is worth noting that neuroendocrine neoplasm is a relative common tumor in appendix which has malignant potential. Brighi et al. (21) reported that tumor size larger than 15.5 mm, G2, and presence of lymphovascular infiltration were predictive factors for nodal metastasis.

MiNENs mainly occurred in patients over 50 years, and there was no race and gender preference. The majority of the MiNENs were grade 3/4, and diagnosed at an advanced stage. It should be stated that in the SEER database, the detail of the grading of the MiNENs was missing. The authors did not know how the tumors were graded exactly. Since there were two components in the tumor, theoretically, both of them should be graded. In the WHO (2019) guidelines and the ENETS guidelines, the grading criteria of GEP-NENs was clearly defined according to the mitotic count and ki-67 index. In the guidelines, it was mentioned that both of the two components in the majority of the MiNENs are poorly differentiated, and the proliferation index for the neuroendocrine components was consistent with other NENs. However, if the differentiation of these two components were not consistent, they should be

10.3389/fonc.2022.1007317

TABLE 4 Multivariate analyses of risk factors for survival.

Classification	Variables	HR	Multivariate	
			95%CI	p-value
Age	<60 years	1.0	1.1-2.0	0.02
	≥60 years	1.5		
Localization	Appendix	1.0		
	Colon-rectum	1.4	0.74-2.5	0.3
	Respiratory/ upper gastrointestinal/hepatobiliary-pancreatic organs	1.6	1.2-2.3	0.004
	Small intestine	1.3	0.77-2.1	0.4
Differentiation grade	G1-G2	1.0		
	G3-G4	1.9	1.3-2.7	0.001
Summary stage	Localized	1.0		
	Regional	5.8	2.8-12.1	<0.0001
	Distant	16.7	8.0-34.8	<0.001
Surgical information	Surgery performed	1.0		
	No surgery	2.7	1.7-4.7	<0.001

separately graded (6, 22). A total of 33.9% of the patients presented with metastasis when diagnosed. It is worth noting that only 12% of the patients did not undergo surgical resection, thus, most of the patients with metastatic MiNENs in the SEER database underwent surgical resection. However, it does not mean that in the real world, majority of the metastatic MiNENs were surgically resected; on the contrary, it is possible that many of the patients with metastatic MiNENs who did not undergo surgery died without a definitive pathological diagnosis. Generally, the survival of MiNENs was comparable or worse

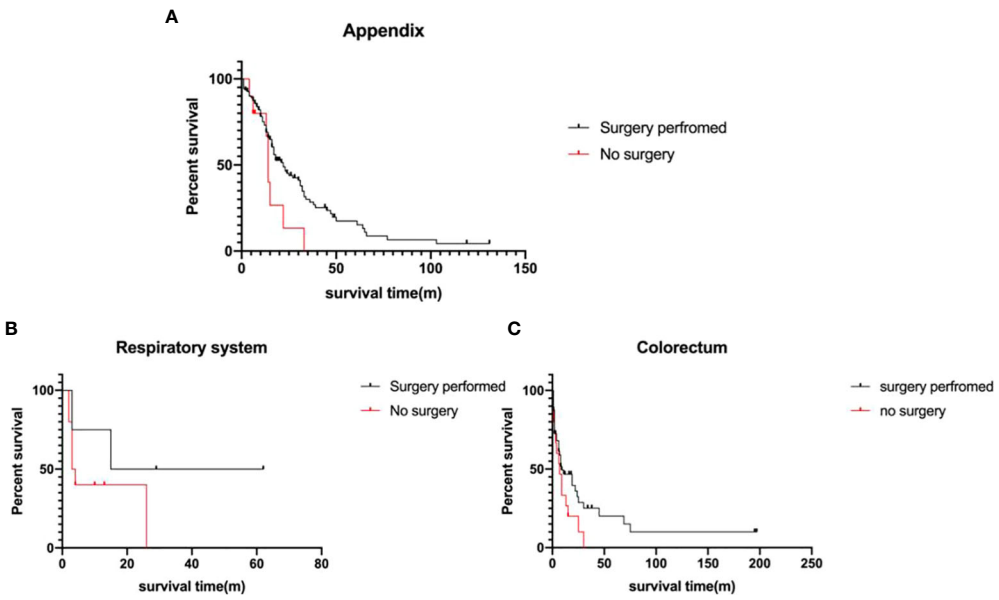

FIGURE 4
Survival analysis of the metastatic MiNEN Patients **(A)** appendix (p=0.05), **(B)** respiratory system (p>0.05), and **(C)** colorectum(p>0.05), depending on surgical information.

to adenocarcinoma of the involved organs (8, 13, 23). MiNENs of the appendix showed the best survival, followed by colon-rectum, whereas foregut MiNENs had the poorest survival. Multivariate analysis showed that non-appendiceal site, older age, higher grade of differentiation, advanced stage were independent risk factors for survival.

Due to the substantial improvements of multimodal therapies, several metastatic neoplasms can be treated by surgery. For example, resections have been successful to improve the survival of metastatic colorectal carcinoma and neuroendocrine neoplasms in selected patients (24–26). However, the benefit of surgery for metastatic MiNENs is unknown. In this study, 260 metastatic MiNENs were analyzed. The patients with metastatic MiNENs were younger and had a higher ratio of resection. Generally, surgery substantially improved the survival of these patients (86.0 months vs 9.0 months, $p<0.001$), however, further analyses showed that only appendiceal MiNENs patients had a survival benefit from surgical resection. Due to the incomplete information of the burden of metastatic lesions in liver and the general status of the patients who underwent surgery or not, there were potential selective biases which may have impact on the interpretation of the results. The patients who underwent surgical resection may have better general status and lower metastatic burden in liver.

Neoadjuvant chemotherapy and adjuvant chemotherapy significantly improve survival of several cancers, and the immunotherapies by targeting immune check points, are successfully used in certain cancers (27–29). In this study, we could not analyze these important aspects of multimodal and novel therapies, as there was not sufficient information available.

The mixed neuroendocrine and non-neuroendocrine components make the biological behaviors of MiNENs more complicated. Genetics analysis have shown that this two components share the same clonal origin (5, 30, 31). However, adjuvant treatments for these two components are largely different (31). In addition, although some molecular targeted drugs and immunotherapies have been preliminary used to treat MiNENs, the evidence of efficacy is limited, and therefore, their roles in MiNENs need further exploration which is beyond the scope of this study (32).

Limitations of this study

Although this is the largest retrospective study of MiNENs, it has limitations due to its retrospective registration study in nature. Several important information is missing, such as the ki-67 index, mitotic count, immunohistochemical markers, metastatic tumor burden, general status of the patients, adjuvant treatments, et al. In addition, compared to other malignant tumors, such as adenocarcinoma, squamous carcinoma neuroendocrine neoplasm, it can be very difficult to get a definitive diagnosis of MiNEN by fine needle or cord needle biopsy, therefore, in the real world, a large number of metastatic MiNEN patients who did not undergo surgical resection may die without a definitive diagnosis. Although majority of MiNENs are MANECs, there is a very minor proportion of mixed neuroendocrine non-adenocarcinoma neoplasms (e.g., squamous or sarcomatoid phenotypes), which was not included in this study.

Conclusion

MiNEN is a rare malignant neoplasm with a rising incidence, which can affect multiple organs throughout the body. MiNEN has an anatomical preference in the distal digestive tract, and the appendix is the most common site. MiNEN shows high heterogeneity of aggressiveness: appendiceal MiNEN has the best survival, followed by colon-rectum. The majority of MiNENs are diagnosed at an advanced stage, therefore, early detection should be improved in the future. Generally, distant MiNENs have a dismal prognosis, and surgical treatment only for selected metastatic MiNENs originating in appendix may be feasible. Currently, there is only sparse data on multimodal, treatment options for this disease.

Data availability statement

The original contributions presented in the study are included in the article/Supplementary Material. Further inquiries can be directed to the corresponding authors.

Author contributions

QFL and QL designed and supervised the study. HS, SY, YZ, YH, and QFL searched and analyzed the data. HS, JK, and QFL interpreted the data and wrote the paper. All authors contributed to the article and approved the submitted version.

Funding

This study was supported by the National High Level Hospital Clinical Research Funding (2022-PUMCH-A-053), the CAMS Innovation Fund for Medical Sciences (CIFMS, 2021-I2M-1-002), National Natural Science Foundation of China (82172765, 81872501, and 81673023), The Seed program of Beijing Friendship Hospital (YYZZ202104)and Youth Foundation of Peking Union Medical College Hospital (pumch201911866).

Conflict of interest

The authors declare that the research was conducted in the absence of any commercial or financial relationships that could be construed as a potential conflict of interest.

Publisher's note

All claims expressed in this article are solely those of the authors and do not necessarily represent those of their affiliated organizations, or those of the publisher, the editors and the reviewers. Any product that may be evaluated in this article, or claim that may be made by its manufacturer, is not guaranteed or endorsed by the publisher.

Supplementary material

The Supplementary Material for this article can be found online at: https://www.frontiersin.org/articles/10.3389/fonc.2022.1007317/full#supplementary-material

References

1. Frizziero M, Chakrabarty B, Nagy B, Lamarca A, Hubner RA, Valle JW, et al. Mixed neuroendocrine non-neuroendocrine neoplasms: A systematic review of a controversial and underestimated diagnosis. *J Clin Med* (2020) 9:273. doi: 10.3390/jcm9010273

2. Kim KH, Lee HJ, Lee SH, Hwang SH. Mixed adenoneuroendocrine carcinoma in the stomach: a case report with a literature review. *Ann Surg Treat Res* (2018) 94:270–3. doi: 10.4174/astr.2018.94.5.270

3. Nishimura C, Naoe H, Hashigo S, Tsutsumi H, Ishii S, Konoe T, et al. Pancreatic metastasis from mixed adenoneuroendocrine carcinoma of the uterine cervix: a case report. *Case Rep Oncol* (2013) 6:256–62. doi: 10.1159/000351308

4. Raison N, McGovern U, Hines J, Volanis D. Mixed adenoneuroendocrine carcinoma of the urethra. *BMJ Case Rep* (2019) 12:e227948. doi: 10.1136/bcr-2018-227948

5. Nagtegaal ID, Odze RD, Klimstra D, Paradis V, Rugge M, Schirmacher P, et al. The 2019 WHO classification of tumours of the digestive system. *Histopathology* (2020) 76:182–8. doi: 10.1111/his.13975

6. Wu W, Chen J, Bai C, Chi Y, Du Y, Feng S, et al. The Chinese guidelines for the diagnosis and treatment of pancreatic neuroendocrine neoplasms (2020). *J Pancreatology* (2021) 4:1–17. doi: 10.1097/JP9.0000000000000064

7. Wang J, He A, Feng Q, Hou P, Wu J, Huang Z, et al. Gastrointestinal mixed adenoneuroendocrine carcinoma: a population level analysis of epidemiological trends. *J Transl Med* (2020) 18:128. doi: 10.1186/s12967-020-02293-0

8. Brathwaite S, Yearsley MM, Bekaii-Saab T, Wei L, Schmidt CR, Dillhoff ME, et al. Appendiceal mixed adeno-neuroendocrine carcinoma: A population-based study of the surveillance, epidemiology, and end results registry. *Front Oncol* (2016) 6:148. doi: 10.3389/fonc.2016.00148

9. Maeda Y, Nakahara O, Tamaoki Y, Saito S, Hasuta S, Nasu J, et al. [A case of mixed adenoneuroendocrine Carcinoma(MANEC)of the duodenum with rapid liver metastases after pancreatoduodenectomy]. *Gan To Kagaku Ryoho* (2018) 45:1747–50.

10. Zhang Z, Zhong D, Feng T, Yao Y, Huang X. Mixed adenoneuroendocrine carcinoma of the gallbladder. *J Gastrointest Surg* (2022) 26:503–6. doi: 10.1007/s11605-021-05139-2

11. Costa AC, Cavalcanti CLC, Coelho HGB, Leao LHA, Soares DTC, Santa-Cruz F, et al. Rare mixed adenoneuroendocrine carcinoma of the gallbladder: Case report and review of literature. *Am J Case Rep* (2021) 22:e929511. doi: 10.12659/AJCR.929511

12. Liu S, Zhong Z, Xiao M, Song Y, Zhu Y, Hu B, et al. Mixed adenoneuroendocrine carcinoma of the hepatic bile duct: a case report and review of the literature. *BMC Gastroenterol* (2020) 20:399. doi: 10.1186/s12876-020-01550-2

13. Lin J, Zhao Y, Zhou Y, Tian Y, He Q, Lin J, et al. Comparison of survival and patterns of recurrence in gastric neuroendocrine carcinoma, mixed adenoneuroendocrine carcinoma, and adenocarcinoma. *JAMA Netw Open* (2021) 4:e2114180. doi: 10.1001/jamanetworkopen.2021.14180

14. Du XL, Song L. Breast cancer incidence trends in Asian women aged 20 or older as compared to other ethnic women in the united states from 2000 to 2018 by time period, age and tumor stage. *Cancer Epidemiol* (2022) 76:102076. doi: 10.1016/j.canep.2021.102076

15. Cong L, Wu W, Lou W, Wang J, Gu F, Qian J, et al. Gastroenteropancreatic neuroendocrine tumor registry study in China. *J Pancreatology* (2018) 1:35–8. doi: 10.1097/JP9.0000000000000005

16. Xiao SY, Ye Z. Pancreatic cystic tumors: An update. *J Pancreatology* (2018) 1:2–18. doi: 10.1097/JP9.0000000000000003

17. Lee AW, Mendoza RA, Aman S, Hsu R, Liu L. Thyroid cancer incidence disparities among ethnic Asian American populations, 1990-2014. *Ann Epidemiol* (2022) 66:28–36. doi: 10.1016/j.annepidem.2021.11.002

18. Tian F, Dai MH, Jia CW, Liu ZW, Li BL. Retrospective analysis of seven cases of pancreatic mixed adenoneuroendocrine carcinoma from a high-volume center and review of the literature. *BMC Surg* (2019) 19:89. doi: 10.1186/s12893-019-0546-0

19. Harada K, Sato Y, Ikeda H, Maylee H, Igarashi S, Okamura A, et al. Clinicopathologic study of mixed adenoneuroendocrine carcinomas of hepatobiliary organs. *Virchows Arch* (2012) 460:281–9. doi: 10.1007/s00428-012-1212-4

20. Grossi U, Bonis A, Carrington EV, Mazzobel E, Santoro GA, Cattaneo L, et al. Mixed adenoneuroendocrine carcinoma (MANEC) of the lower gastrointestinal tract: A systematic review with Bayesian hierarchical survival analysis. *Eur J Surg Oncol* (2021) 47:2893–9. doi: 10.1016/j.ejso.2021.05.021

21. Brighi N, La Rosa S, Rossi G, Grillo F, Pusceddu S, Rinzivillo M, et al. Morphological factors related to nodal metastases in neuroendocrine tumors of the appendix: A multicentric retrospective study. *Ann Surg* (2020) 271:527–33. doi: 10.1097/SLA.0000000000002939

22. de Mestier L, Cros J, Neuzillet C, Hentic O, Egal A, Muller N, et al. Digestive system mixed neuroendocrine-Non-Neuroendocrine neoplasms. *Neuroendocrinology* (2017) 105:412–25. doi: 10.1159/000475527

23. Wu W, Jin G, Wang C, Miao Y, Wang H, Lou W, et al. The current surgical treatment of pancreatic cancer in China: A national wide cross-sectional study. *J Pancreatology* (2019) 2:16–21. doi: 10.1097/JP9.0000000000000012

24. Liu Q, Zhang R, Michalski CW, Liu B, Liao Q, Kleeff J, et al. Surgery for synchronous and metachronous single-organ metastasis of pancreatic cancer: a SEER database analysis and systematic literature review. *Sci Rep* (2020) 10:4444. doi: 10.1038/s41598-020-61487-0

25. Wu W, Chen J, Bai C, Chi Y, Du Y, Feng S, et al. The Chinese guidelines for the diagnosis and treatment of pancreatic neuroendocrine neoplasms (2020). *J Pancreatology* (2021) 4:1–17. doi: 10.1097/JP9.0000000000000064

26. Arhin ND, Shen C, Bailey CE, Matsuoka LK, Hawkins AT, Holowatyj AN, et al. Surgical resection and survival outcomes in metastatic young adult colorectal cancer patients. *Cancer Med* (2021) 10:4269–81. doi: 10.1002/cam4.3940

27. Lee JH, Long GV, Boyd S, Lo S, Menzies AM, Tembe V, et al. Circulating tumour DNA predicts response to anti-PD1 antibodies in metastatic melanoma. *Ann Oncol* (2017) 28:1130–6. doi: 10.1093/annonc/mdx026

28. Zhang X, Cai X, Zheng H. Anti-PD1 or anti-PD-L1 antibodies alone or in combination with chemotherapy first-line treatment of advanced non-small cell lung cancer. *Thorac Cancer* (2022) 13:1104–5. doi: 10.1111/1759-7714.14358

29. Zhang C, Li D, Xiao B, Zhou C, Jiang W, Tang J, et al. B2M and JAK1/2-mutated MSI-h colorectal carcinomas can benefit from anti-PD-1 therapy. *J Immunother* (2022) 45:187–93. doi: 10.1097/CJI.0000000000000417

30. Jesinghaus M, Konukiewitz B, Keller G, Kloor M, Steiger K, Reiche M, et al. Colorectal mixed adenoneuroendocrine carcinomas and neuroendocrine carcinomas are genetically closely related to colorectal adenocarcinomas. *Mod Pathol* (2017) 30:610–9. doi: 10.1038/modpathol.2016.220

31. Jacob A, Raj R, Allison DB, Soares HP, Chauhan A. An update on the management of mixed neuroendocrine-non-neuroendocrine neoplasms (MiNEN). *Curr Treat Options Oncol* (2022) 23:721–35. doi: 10.1007/s11864-022-00968-y

32. Ricco B, Salati M, Reggiani Bonetti L, Dominici M, Luppi G. PD-1 blockade in deficient mismatch repair mixed adenoneuroendocrine carcinoma of the stomach: new hope for an orphan disease. *Tumori* (2020) 106:NP57–62. doi: 10.1177/0300891620952845

frontiers | Frontiers in Oncology

TYPE Original Research
PUBLISHED 18 January 2023
DOI 10.3389/fonc.2023.995618

Check for updates

OPEN ACCESS

EDITED BY
Imayavaramban Lakshmanan,
University of Nebraska Medical Center,
United States

REVIEWED BY
Aruna Prabhu,
Thangam Cancer Center, India
Alessio Vagliasindi,
Santa Maria delle Croci Hospital, Italy

*CORRESPONDENCE
Yantao Tian
tyt67@163.com
Jing Zhang
13436383665@163.com

SPECIALTY SECTION
This article was submitted to Gastrointestinal Cancers: Gastric and Esophageal Cancers, a section of the journal Frontiers in Oncology

RECEIVED 16 July 2022
ACCEPTED 03 January 2023
PUBLISHED 18 January 2023

CITATION
Zhong Y, Kang W, Hu H, Li W, Zhang J and Tian Y (2023) Lobaplatin-based prophylactic hyperthermic intraperitoneal chemotherapy for T4 gastric cancer patients: A retrospective clinical study. *Front. Oncol.* 13:995618. doi: 10.3389/fonc.2023.995618

COPYRIGHT
© 2023 Zhong, Kang, Hu, Li, Zhang and Tian. This is an open-access article distributed under the terms of the Creative Commons Attribution License (CC BY). The use, distribution or reproduction in other forums is permitted, provided the original author(s) and the copyright owner(s) are credited and that the original publication in this journal is cited, in accordance with accepted academic practice. No use, distribution or reproduction is permitted which does not comply with these terms.

Lobaplatin-based prophylactic hyperthermic intraperitoneal chemotherapy for T4 gastric cancer patients: A retrospective clinical study

Yuxin Zhong[1], Wenzhe Kang[1], Haitao Hu[1], Weikun Li[1], Jing Zhang[2*] and Yantao Tian[1*]

[1]Department of Pancreatic and Gastric Surgery, National Cancer Center/National Clinical Research Center for Cancer/Cancer Hospital, Chinese Academy of Medical Sciences and Peking Union Medical College, Beijing, China, [2]Department of Surgery, Huanxing Cancer Hospital, Beijing, China

Objective: To explore the clinical efficacy of lobaplatin-based prophylactic hyperthermic intraperitoneal chemotherapy (HIPEC) for patients with T4 gastric cancer after surgery and to evaluate its impact on survival.

Materials and methods: Data on patients with T4 gastric cancer who underwent radical gastric resection between March 2016 and August 2017 were collected from the National Cancer Center and Huangxing Cancer Hospital. Enrolled patients were divided into two groups according to receiving or not receiving HIPEC.

Results: A total of 106 patients were included in this study; among them, 51 patients underwent radical gastric resection plus prophylactic HIPEC, and 55 patients underwent radical gastric resection only. The baseline characteristics were well balanced between the two groups. The postoperative platelet counts in the HIPEC group were significantly lower than those in the non-HIPEC group ($P < 0.05$); however, we did not observe any occurrences of serious bleeding in the HIPEC group. There were no significant differences in the postoperative complication rates between the two groups ($P > 0.05$). The postoperative (1 month) CEA, CA19-9, and CA72-4 levels in the HIPEC group were significantly decreased in the HIPEC group ($P < 0.05$). At a median follow-up of 59.3 months, 3 (5.5%) patients in the HIPEC group experienced peritoneal recurrence, and 10 (18.2%) patients in the non-HIPEC group experienced peritoneal recurrence ($P < 0.05$). Both groups had comparable 5-year overall survival (OS) rates (41.1% HIPEC group *vs*. 34.5% non-HIPEC group, $P = 0.118$). The 5-year disease-free survival was significantly higher in the HIPEC group than in the non-HIPEC group (28.6% versus 39.7%, $p = 0.046$).

Conclusions: Lobaplatin-based prophylactic HIPEC is feasible and safe for patients with T4 gastric cancer and does not increase postoperative adverse effects. The

use of HIPEC showed a significant decrease in the incidence of local recurrence rates and blood tumor marker levels. The 5-year disease-free survival was significantly higher in the HIPEC group; however, the 5-year OS benefit was not found in T4 stage patients.

KEYWORDS

gastric cancer, lobaplatin, hepatic intraperitoneal chemotherapy, prognosis, advanced

1 Introduction

According to the 2020 Global Cancer Statistics Report, gastric cancer (GC) has become the fifth most common cancer worldwide and has the fourth highest mortality rate. It is estimated that there were over one million new gastric cancer cases and approximately 770,000 gastric cancer deaths in 2020 (1). In China, nearly 78% of the cases are diagnosed as advanced gastric cancer at the time of the initial clinical visit (2). Surgical resection combined with chemotherapy is the primary treatment for advanced gastric cancer, but the therapeutic effect is not satisfactory (3). Peritoneal metastasis is one of the most common and important causes of poor prognosis for gastric cancer patients with serosal involvement (T4), and it accounts for nearly half of the postoperative relapses (4).

Metastasis to the peritoneum can lead to several complications, such as ascites, bowel obstruction, and hydronephrosis, all of which worsen the patient's condition and quality of life (5–7).

In recent years, HIPEC has been used as one form of treatment for patients with advanced gastrointestinal cancers (8, 9). Compared with conventional intravenous chemotherapy, HIPEC has significant advantages (10). It increases the amount of chemotherapeutics within the tumor cells and, coupled with thermal effects, can kill tumor cells (11). Lobaplatin, as a third generation platinum-based anticancer agent, exerts stronger antitumor activity, with lower toxicity and higher solubility and stability in water (12). Lobaplatin-based HIPEC has been gradually applied to treat advanced gastric cancer after radical surgery to reduce peritoneal metastasis (13). To determine the safety and efficacy of radical surgery with prophylactic lobaplatin-based HIPEC, especially its effect on peritoneum metastasis and long-term survival, we retrospectively analyzed the clinical data of patients with T4 gastric cancer admitted to the National Cancer Center and Huangxing Cancer Hospital.

2 Materials and methods

2.1 Study population and grouping

We retrospectively reviewed the clinical data of patients with gastric cancer who underwent radical surgical resection at the National Cancer Center and Huangxing Cancer Hospital between March 2016 and August 2017. The surgeon explained the possible benefits and risks to the cT4 gastric cancer patients to obtain their informed consent, and the patients decided whether or not receiving HIPEC by themselves. Before surgery, hematological examination, contrast-enhanced computed tomography (CT), gastroscopy were routinely performed on all patients for tumor staging. And If lymph node metastasis was suspected based on preoperative imaging, neoadjuvant chemotherapy was performed. The patients were divided into two groups according to whether prophylactic HIPEC was performed. This study was conducted following the ethical standards of the Declaration of Helsinki and within the national and international guidelines. The study was performed with ethics approval from the Ethics Committee of National Cancer Center, Chinese Academy of Medical Sciences (NCC2017-YZ-026). Due to the retrospective nature of this study, consent of the patients to review their medical records was not required by the Institutional Review Board (IRB). The inclusion criteria were as follows: 1. Pathologically diagnosed as gastric adenocarcinoma; 2. The postoperative pathological stage was T4, with or without lymph node metastasis; 3. Absence of distant metastasis (M0); 4. Age between 18 and 75 years old; 5. The laboratory examinations had to meet the following conditions: white blood cells ≥ 4.0×109/L; neutrophil counts ≥ 2.0×109/L; platelets ≥ 100×109/L; hemoglobin≥90 g/L; serum total bilirubin ≤ 17.1 μmol/L; serum alanine aminotransferase ≤ 1.5×ULN; serum creatinine ≤ 1.5×ULN; creatinine clearance ≥ 60 ml/min (Cockcroft-Gault formula). The exclusion criteria included the following: 1. Tumor located at esophagogastric junction, and thoracotomy was needed; 2. Distant metastasis (M1), including peritoneal metastasis; 3. Patients with severe complications who could not tolerate or who refused prophylactic HIPEC; 4. Patients with previous or coexisting other malignant diseases; 5. Patients who had a history of neurological or psychiatric disease and who were unable to complete the follow-up evaluation. Finally, 106 patients with gastric cancer met the inclusion criteria. Among them, 51 patients were included in the radical surgery plus prophylactic HIPEC group, and 56 patients underwent radical surgery.

2.2 Treatment method

The patients in the two groups underwent laparoscopic-assisted radical gastrectomy. The patients were placed under general anesthesia with orotracheal intubation. The patients were placed in a supine position with their legs split, the surgeon operated from the right side,

Abbreviations: HIPEC, hyperthermic intraperitoneal chemotherapy; GC, gastric cancer; CT, computed tomography; DFS, disease free survival; OS, overall survival; SPSS, Statistical Package for the Social Sciences.

the assistant was on the left side and the camera assistant was between the patients' legs. Laparoscopic radical surgery was performed with a five-hole approach. Based on the tumor location, total or distal subtotal gastrectomy with D2 lymphadenectomy was performed. After transection, a 5-7 cm long incision was made in the mid-upper abdomen, the specimen was removed, and extracorporeal digestive tract reconstruction was performed through the incision. Reconstruction of the digestive tract included Billroth-I, Billroth-II, and Roux-en-Y after gastrectomy.

In the HIPEC group, lobaplatin-based prophylactic HIPEC was performed under general anesthesia after closure of the incision. Two inlet pipes and two outlet pipes were installed. Lobaplatin (50mg/m^2) was diluted in heated 5% glucose solution and then was circulated for 60 min. The perfusion rate was 400-500 ml/min. The circulating temperature was maintained at 42.5-43°C. After HIPEC, at least 90% of the perfusion fluid was removed. The patient's vital signs and color of drainage were observed carefully during HIPEC. All patients received adjuvant chemotherapy after radical surgical resection.

2.3 Postoperative follow-up

The first day after surgery represented the beginning of the follow-up period. According to the NCCN gastric cancer guidelines, the patients were followed every 3 months for the first two years, then every 6 months for the next three years and then once a year after five years. The follow-up examinations included biochemical tests, tumor marker examination, and computed tomography (CT). The last date of follow-up was April 7th, 2022. Disease-free survival (DFS) was defined as the time from surgery to recurrence, while overall survival (OS) was defined as the time from surgery to all deaths.

2.4 Statistical analysis

Data statistics and analysis were conducted using Statistical Package for the Social Sciences (SPSS) version 23.0 for Windows (IBM Corp, Armonk, NY, United States) and GraphPad Prism (version 8, GraphPad Prism Software Inc.). Continuous data are expressed as the mean ± SD and were analyzed by a t test. Categorical data are shown as frequencies and percentages and were analyzed by the chi-squared test or Fisher's exact test. Ranked and abnormally distributed quantitative data were assessed by the Mann–Whitney test. Survival analysis was performed using Kaplan–Meier curves and the log-rank test. Differences were considered significant when the P value was less than 0.05.

3 Results

3.1 Patient characteristics

A total of 106 patients met our inclusion criteria, and they had a mean age of 54.2 ± 10.3 years. Of these patients, 51 (48.1%) patients were in the HIPEC group, and 55 (52.9%) patients were in the non-HIPEC group. These two groups of patients were well balanced in terms of age, sex, ASA score, BMI, gastrectomy, tumor grade and pathological N staging (Table 1). The mean operation time in the HIPEC group was significantly longer than that in the non-HIPEC group (206 ± 35.6 min *vs.* 164 ± 34.3 min, p = 0.034). There were no significant differences in conversion to open surgery, estimated blood loss or hospital stay after the operations. Similarly, the postoperative gastrointestinal recovery was not significantly different between the two groups regarding the time to first flatus (2.3 ± 1.6 days versus 2.2 ± 1.2 days, p = 0.744) and time to regular diet (5.4 ± 2.2 days versus 5.2 ± 2.9 days, p = 0.649). Five (9.8%) patients in the HIPEC group had abnormal liver function (elevated ALT level), and 2 (3.6%) patients in the non-HIPEC group had abnormal liver function. All patients recovered to have a normal liver function after being given liver protection drugs. Nine (17.6%) patients in the HIPEC group suffered a decline in their peripheral platelet count (less than 150,000 platelets per microliter), which included 2 (3.6%) patients in the non-HIPEC group (p = 0.026); however, none of the patients in either of the groups experienced major bleeding events leading to anemia. There were no cases of 30-day postoperative mortality in either group (Table 2).

The CEA positive rate, CA199 positive rate and CA724 positive rate 1 month after surgery in the HIPEC group were significantly lower than those in the non-HIPEC group (23.53% versus 47.27%, p = 0.044; 23.50% versus 43.64%, p = 0.049; 31.37% versus 52.73%, p = 0.025). There were no significant differences in terms of the CA125 positive rate between the two groups (21.57% versus 32.73%, p = 0.063) (Table 3).

3.2 Survival analysis

The mean follow-up time was 59.3 months. All patients underwent postoperative adjuvant chemotherapy (oxaliplatin plus capecitabine for 6 cycles). During the follow-up period, 3 (5.5%) patients in the HIPEC group experienced peritoneal recurrence, and 10 (18.2%) patients in the non-HIPEC group experienced recurrence (p < 0.05) (Table 2). Both groups had comparable 5-year overall survival (OS) rates (41.1% HIPEC group *vs.* 34.5% non-HIPEC group, P = 0.118) (Figure 1A). The 5-year disease-free survival was significantly higher in the HIPEC group than in the non-HIPEC group (39.7% versus 28.6%, p = 0.046) (Figure 1B). A multivariable analysis was performed using logistic regression to determine factors associated with disease-free survival. The results showed that poorly differentiated, mucinous or signet cell adenocarcinoma, pathological positive lymph nodes and no neoadjuvant chemotherapy were significantly associated with poor disease-free survival. On the other hand, patients who underwent radical surgery plus HIPEC were less likely to have tumor recurrence (Table 4).

4 Discussion

In this double-center retrospective observational study, we found that in patients with T4 gastric cancer, prophylactic HIPEC was a strong independent positive predictor of DFS. Patients who underwent prophylactic HIPEC had a lower peritoneal recurrence rate. The results also indicated that the expression of tumor markers 1

10.3389/fonc.2023.995618

TABLE 1 Baseline characteristics of the T4 gastric cancer patients.

Characteristics	All patients (n = 106)	HIPEC (n = 51)	Non-HIPEC (n = 55)	*P value*
Age at diagnosis, year, (n%)	54.2 ± 10.3	53.5 ± 10.5	55.1 ± 10.9	0.252
21-49	22 (20.8%)	12 (23.5%)	10 (18.2%)	
50-75	71 (67.0%)	34 (66.7%)	37 (67.3%)	
76-96	13 (10.2%)	5 (9.8%)	8 (14.5%)	
Sex, n (%)				0.748
Female	49 (46.2%)	24 (47.1%)	25 (45.5%)	
Male	57 (53.8%)	27 (52.9%)	30 (54.5%)	
ASA score				0.275
I	34 (32.1%)	16 (31.4%)	18 (32.7%)	
II	68 (64.2%)	33 (64.7%)	35 (63.6%)	
III	4 (3.7%)	2 (3.9%)	2 (3.6%)	
BMI, kg/m2 (mean ± SD)	24.2 ± 2.5	23.6 ± 2.4	25.5 ± 2.7	0.334
Gastrectomy				0.438
Proximal	18 (17.0%)	10 (19.7%)	8 (14.5%)	
Distal	72 (67.9%)	33 (64.7%)	39 (71.0%)	
Total	16 (15.1%)	8 (15.6%)	8 (14.5%)	
Tumor grade				0.458
Poor or moderately	67 (63.2%)	33 (64.7%)	34 (61.8%)	
Mucinous or signet cell	39 (36.8%)	18 (35.3%)	21 (38.2%)	
Neoadjuvant CHT				
Yes	82 (77.4%)	39 (76.5%)	43 (78.2%)	0.347
No	24 (22.6%)	12 (23.5%)	12 (21.8%)	
Pathological N staging				0.354
N0	10 (9.4%)	5 (9.8%)	6 (10.9%)	
N1	39 (36.8%)	18 (35.3%)	21 (38.2%)	
N2	46 (43.4%)	24 (47.1%)	22 (40%)	
N3	11 (10.4%)	5 (9.8%)	6 (10.9%)	

TABLE 2 Perioperative data of the patients.

Characteristics	HIPEC (n = 51)	Non-HIPEC (n = 55)	*P value*
Conversion to open, n (%)	2 (3.9%)	3 (5.5%)	1
Operation time in min, mean ± SD	206 ± 35.6	164 ± 34.3	0.034
Estimated blood loss in mL, mean ± SD	85.2 ± 23.6	77.9 ± 25.8	0.553
Hospital stay after operation (d, mean ± SD)	7.1 ± 1.3	7.7 ± 0.9	0.386
30 d post-operative mortality, n (%)	0	0	N/A
Time to first flatus, day (mean±SD)	2.3 ± 1.6	2.2 ± 1.2	0.744
Time to Regular diet, day (mean±SD)	5.4 ± 2.2	5.2 ± 2.9	0.649
Postoperative complications (grades III, IV)			
Anastomotic Leakage	2 (3.9%)	1 (1.8%)	0.704
Bowel Obstruction	2 (3.9%)	2 (3.6%)	1
Surgical Wound Infection	5 (9.8%)	6 (10.9%)	0.833
Bleeding	2 (3.9%)	3 (5.5%)	0.936
Delayed gastric emptying	5 (9.8%)	7 (12.7%)	0.557
Lung infection	1 (2.0%)	0	1
Fever	6 (11.8%)	3 (5.5%)	0.129
Abnormal blood routine tests	9 (17.6%)	2 (3.6%)	0.026
Abnormal renal function	1 (2.0%)	1 (1.8%)	0.957
Abnormal liver function	5 (9.8%)	2 (3.6%)	0.068
Severe neurotoxicity	0	0	N/A
Peritoneal recurrence	3 (5.5%)	10 (18.2%)	0.037

month after surgery was decreased significantly in the HIPEC group. However, these advantages did not translate into an OS benefit.

Whether prophylactic PIPEC in patients with T4 gastric cancer affords a survival advantage is still controversial, and research in this area has remained rather limited. There is still a lack of a unified treatment strategy, and no consensus is available regarding this topic. Radical surgery and HIPEC were first described in 1980 (14), and some of the previous studies and meta-analyses reported that the incidence of postoperative complications was higher in the HIPEC group (15–17) (18–21). In 2000, Samel et al. (18) reported 9 patients with advanced gastric cancer who underwent gastrectomy plus intraoperative HIPEC. The results showed that 6 of the patients (66%) developed postoperative complications, including anastomotic leakage, pancreatic fistula, pancreatitis and renal failure, indicating that intraoperative HIPEC was associated with a high risk of perioperative complications. French researchers (19) conducted a retrospective multicenter study of 159 patients from 15 institutions. A total of 10 (6.5%) patients died after surgery. The causes of death included multiple organ failure (2 patients), septic shock (2 patients), respiratory complications (2

TABLE 3 Comparison of the tumor markers positive rates between the two groups before surgery and 1 month after surgery.

Characteristics	HIPEC (n = 51)	Non-HIPEC (n = 55)	*P value*
CEA positive rate, (n%)			0.044
Before surgery	90.20%	89.10%	
1month after surgery	23.53%	47.27%	
CA199 positive rate, (n%)			0.049
Before surgery	88.00%	85.45%	
1month after surgery	25.50%	43.64%	
CA724 positive rate, (n%)			0.025
Before surgery	86.37%	87.27%	
1month after surgery	31.37%	52.73%	
CA125 positive rate, (n%)			0.063
Before surgery	84.31%	81.82%	
1 month after surgery	21.57%	32.73%	

patients), peritonitis caused by anastomotic leakage (1 patient), thromboembolic events (1 patient), cardiac arrhythmia (1 patient), and hematological toxicity (1 patient). The postoperative grade 3-4 morbidity rate was 27.8%. Fourteen percent of the patients required surgery. They concluded that for patients with gastric cancer, surgery with HIPEC may achieve long-term survival in a selected group of patients. Because of its high mortality rate, a stringent screening process should be employed and should be reserved for experienced institutions. The high overall complication rate in the past was probably due to the immature method of implementation of HIPEC, technological imperfections, and inaccurate temperature and may also be related to the general physical conditions of patients (20–22).

With the continuous exploration of HIPEC and improvement of its instruments, the application of HIPEC in gastrointestinal tumors has been quite mature (23). In recent years, a number of studies have suggested that HIPEC does not increase the incidence of postoperative complications (24–28). Beeharry et al. (29) conducted a randomized case–control study in 2019, and 80 patients with locally advanced gastric cancer were randomly divided into two groups: the HIPEC group (curative resection plus intraoperative HIPEC) and the control group (curative resection only). Their results indicated that faster recovery of bowel function (43 ± 5 h *vs.* 68 ± 7, $P < 0.05$) and shorter postoperative stay (8 d *vs.* 14 d, $P < 0.05$) were noted in the HIPEC group. Mild renal dysfunction, mild liver dysfunction and hyperbilirubinemia were recorded in the HIPEC group, but their incidences were found to be statistically insignificant when compared with the control group ($P > 0.05$). The prophylactic HIPEC group had a higher DFS rate and a lower peritoneal recurrence rate. These conclusions are similar to our conclusions.

Our conclusion demonstrated that thrombocytopenia occurred in 9 (17.6%) patients in the HIPEC group, which was significantly higher than that in the non-HIPEC group (n = 2, 3.6%). However, no severe bleeding events occurred in either group. Even then, liver and renal function, as well as routine blood tests, must be closely monitored in patients who undergo HIPEC after surgery. Our results also showed that there were no significant differences between the two groups in terms of complications and adverse events; this result is consistent with recent research.

Our results also indicated that after one month of treatment, the positive rates of tumor markers (CEA, CA199, CA724) were significantly lower in the HIPEC plus surgery group than in the CRS alone group. Both treatment strategies are helpful to reduce the level of serum tumor markers, while HIPEC plus surgery is more effective.

In this study, the results showed that patients with T4 gastric cancer who had HIPEC after surgery had better DFS and a lower peritoneal recurrence rate but showed no significant benefit in OS. The multivariable analysis confirmed that HIPEC had a significant and positive impact on DFS. At present, some studies are consistent with this result. Desiderio et al. (30) published a meta-analysis in 2017, and a total of 32 trials (2520 patients) were included. The analysis showed that HIPEC had advantages in preventing peritoneal metastasis, and the 3-year OS rate and 5-year OS rate in the HIPEC group were significantly higher than those in the non-HIPEC group (29).

This study has several limitations. First, even though the clinicopathological characteristics of the two groups were balanced, the

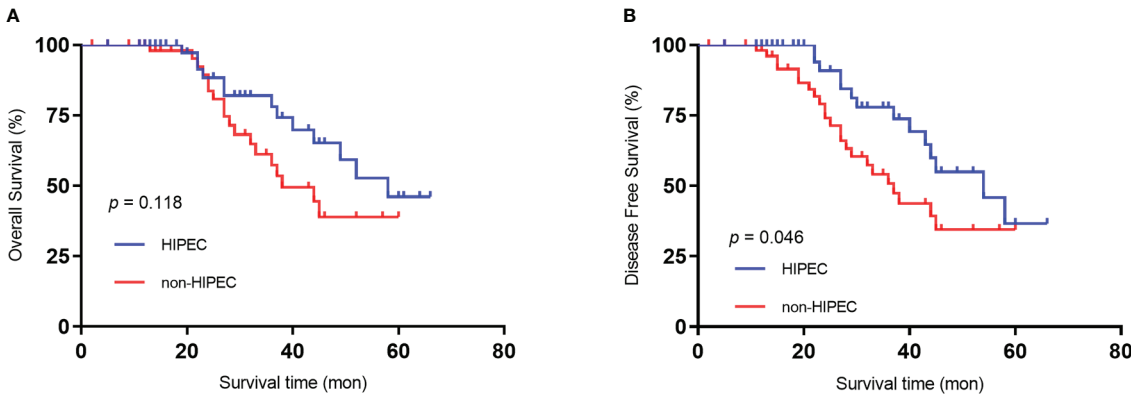

FIGURE 1
Kaplan–Meier survival curves depicting the survival in patients with T4 gastric cancer. **(A)** Patient OS based on whether HIPEC was performed. **(B)** Patient DFS based on whether HIPEC was performed..

TABLE 4 Multivariable analysis of the prognostic factors influencing DFS.

Characteristics	OR (95% CI)	*P* value
Age at diagnosis, year		
21-49	1 [Reference]	
50-75	0.933 (0.723-1.235)	0.527
76-96	0.622 (0.378-1.254)	0.054
Sex		
Female	1 [Reference]	
Male	1.216 (0.873-1.345)	0.343
ASA score		
I	1 [Reference]	
II	0.733 (0.485-1.176)	0.14
III	1.340 (0.842-1.875)	0.31
Gastrectomy		
Proximal	1 [Reference]	
Distal	0.777 (0.581-1.040)	0.09
Total	0.850 (0.642-1.125)	0.255
Tumor grade		
Poor or moderately	1 [Reference]	
Mucinous or signet cell	1.521 (1.113-2.124)	0.005
Pathological N staging		
N0	1 [Reference]	
N1/N2/N3	1.347 (1.054-1.674)	0.038
Neoadjuvant chemotherapy		
Yes	1 [Reference]	
No	1.467 (1.026-1.772)	0.024
Treatment modality		
Surgery	1 [Reference]	
Surgery plus prophylactic HIPEC	0.584 (0.348-0.837)	0.046
Preoperative abnormal tumor markers level		
CEA levels	1.207 (0.984-1.326)	0.674
CA199 levels	1.237 (1.014-1.528)	0.437
CA125 levels	1.207 (0.835-1.429)	0.348
CA724 levels	1.372 (0.934-1.539)	0.332

retrospective nature of this study may have led to selection bias, and there might be unknown confounders that could have affected the results of this study. Second, this was a double-center study, and the sample size was relatively small. Multicenter, large-scale, randomized studies are needed to further confirm the survival benefits provided by lobaplatin-based prophylactic HIPEC in patients with T4 gastric cancer.

In conclusion, our study shows that lobaplatin-based prophylactic HIPEC is feasible and safe for patients with T4 gastric cancer and does not increase postoperative adverse effects. The use of HIPEC was associated with a significantly decreased incidence of peritoneal recurrence rates and blood tumor marker levels. The 5-year disease-free survival was significantly higher in the HIPEC group; however, a 5-year OS benefit was not found in T4 stage patients.

Data availability statement

The raw data supporting the conclusions of this article will be made available by the authors, without undue reservation.

Author contributions

YZ and WK: acquisition of data. YZ: analysis and interpretation of data. YZ, HH and WL: drafted the manuscript. JZ and YT: critical revision of the manuscript. All authors contributed to the article and approved the submitted version.

Funding

This work was supported by the Beijing Hope Run Special Fund of Cancer Foundation of China (NO. LC2020A25) and the CAMS Innovation Fund for Medical Sciences (No. 2021-12 M-1-022).

Conflict of interest

The authors declare that the research was conducted in the absence of any commercial or financial relationships that could be construed as a potential conflict of interest.

Publisher's note

All claims expressed in this article are solely those of the authors and do not necessarily represent those of their affiliated organizations, or those of the publisher, the editors and the reviewers. Any product that may be evaluated in this article, or claim that may be made by its manufacturer, is not guaranteed or endorsed by the publisher.

References

1. Sung H, Ferlay J, Siegel RL, Laversanne M, Soerjomataram I, Jemal A, et al. Global cancer statistics 2020: GLOBOCAN estimates of incidence and mortality worldwide for 36 cancers in 185 countries. *CA Cancer J Clin* (2021) 71:209–49. doi: 10.3322/caac.21660

2. Qiu H, Cao S, Xu R. Cancer incidence, mortality, and burden in China: a time-trend analysis and comparison with the united states and united kingdom based on the global epidemiological data released in 2020. *Cancer Commun (Lond)* (2021) 41:1037–48. doi: 10.1002/cac2.12197

3. Smyth EC, Nilsson M, Grabsch HI, van Grieken NC, Lordick F. Gastric cancer. *Lancet* (2020) 396:635–48. doi: 10.1016/s0140-6736(20)31288-5

4. Tustumi F, Bernardo WM, Dias AR, Ramos MF, Cecconello I, Zilberstein B, et al. Detection value of free cancer cells in peritoneal washing in gastric cancer: a systematic review and meta-analysis. *Clinics (Sao Paulo)* (2016) 71:733–45. doi: 10.6061/clinics/2016(12)10

5. Song H, Wang T, Tian L, Bai S, Chen L, Zuo Y, et al. Macrophages on the peritoneum are involved in gastric cancer peritoneal metastasis. *J Cancer* (2019) 10:5377–87. doi: 10.7150/jca.31787

6. Saito H, Kono Y, Murakami Y, Kuroda H, Matsunaga T, Fukumoto Y, et al. Gross appearance and curability are predictive factors of a better prognosis after gastrectomy in gastric cancer patients with metastasis to the adjacent peritoneum of the stomach. *Yonago Acta Med* (2017) 60:174–8. doi: 10.33160/yam.2017.09.006

7. Seshadri RA, Glehen O. Cytoreductive surgery and hyperthermic intraperitoneal chemotherapy in gastric cancer. *World J Gastroenterol* (2016) 22:1114–30. doi: 10.3748/wjg.v22.i3.1114

8. Granieri S, Bonomi A, Frassini S, Chierici AP, Bruno F, Paleino S, et al. Prognostic impact of cytoreductive surgery (CRS) with hyperthermic intraperitoneal chemotherapy (HIPEC) in gastric cancer patients: A meta-analysis of randomized controlled trials. *Eur J Surg Oncol* (2021) 47:2757–67. doi: 10.1016/j.ejso.2021.05.016

9. Gurusamy K, Vale CL, Pizzo E, Bhanot R, Davidson BR, Mould T, et al. Cytoreductive surgery (CRS) with hyperthermic intraoperative peritoneal chemotherapy (HIPEC) versus standard of care (SoC) in people with peritoneal metastases from colorectal, ovarian or gastric origin: protocol for a systematic review and individual participant data (IPD) meta-analyses of effectiveness and cost-effectiveness. *BMJ Open* (2020) 10:e039314. doi: 10.1136/bmjopen-2020-039314

10. Koemans WJ, van der Kaaij RT, Boot H, Buffart T, Veenhof A, Hartemink KJ, et al. Cytoreductive surgery and hyperthermic intraperitoneal chemotherapy versus palliative systemic chemotherapy in stomach cancer patients with peritoneal dissemination, the study protocol of a multicentre randomised controlled trial (PERISCOPE II). *BMC Cancer* (2019) 19:420. doi: 10.1186/s12885-019-5640-2

11. Yu P, Ye Z, Dai G, Zhang Y, Huang L, Du Y, et al. Neoadjuvant systemic and hyperthermic intraperitoneal chemotherapy combined with cytoreductive surgery for gastric cancer patients with limited peritoneal metastasis: a prospective cohort study. *BMC Cancer* (2020) 20:1108. doi: 10.1186/s12885-020-07601-x

12. Lv X, Cao X, Xia WX, Liu KY, Qiang MY, Guo L, et al. Induction chemotherapy with lobaplatin and fluorouracil versus cisplatin and fluorouracil followed by chemoradiotherapy in patients with stage III-IVB nasopharyngeal carcinoma: an open-label, non-inferiority, randomised, controlled, phase 3 trial. *Lancet Oncol* (2021) 22:716–26. doi: 10.1016/s1470-2045(21)00075-9

13. Yin CY, Lin XL, Tian L, Ye M, Yang XY, Xiao XY. Lobaplatin inhibits growth of gastric cancer cells by inducing apoptosis. *World J Gastroenterol* (2014) 20:17426–33. doi: 10.3748/wjg.v20.i46.17426

14. Spratt JS, Adcock RA, Muskovin M, Sherrill W, McKeown J. Clinical delivery system for intraperitoneal hyperthermic chemotherapy. *Cancer Res* (1980) 40:256–60.

15. Yonemura Y, de Aretxabala X, Fujimura T, Fushida S, Katayama K, Bandou E, et al. Intraoperative chemohyperthermic peritoneal perfusion as an adjuvant to gastric cancer: final results of a randomized controlled study. *Hepatogastroenterology* (2001) 48:1776–82.

16. Xu Y, Zhang R, Li C, Sun Z, Deng J, Wang X, et al. Intraperitoneal chemotherapy using fluorouracil implants combined with radical resection and postoperative adjuvant chemotherapy for stage III gastric cancer: A multi-center, randomized, open-label, controlled clinical study. *Front Oncol* (2021) 11:670651. doi: 10.3389/fonc.2021.670651

17. Fujimura T, Yonemura Y, Nakagawara H, Kitagawa H, Fushida S, Nishimura G, et al. Subtotal peritonectomy with chemohyperthermic peritoneal perfusion for peritonitis carcinomatosa in gastrointestinal cancer. *Oncol Rep* (2000) 7:809–14. doi: 10.3892/or.7.4.809

18. Samel S, Singal A, Becker H, Post S. Problems with intraoperative hyperthermic peritoneal chemotherapy for advanced gastric cancer. *Eur J Surg Oncol* (2000) 26:222–6. doi: 10.1053/ejso.1999.0780

19. Glehen O, Gilly FN, Arvieux C, Cotte E, Boutitie F, Mansvelt B, et al. Peritoneal carcinomatosis from gastric cancer: a multi-institutional study of 159 patients treated by cytoreductive surgery combined with perioperative intraperitoneal chemotherapy. *Ann Surg Oncol* (2010) 17:2370–7. doi: 10.1245/s10434-010-1039-7

20. Otani S, Maeta M, Oka A, Hirooka Y, Tsujitani S, Ikeguchi M, et al. Long-term survival of 5 years following initial surgery for gastric cancer and simultaneous disseminated peritoneal metastasis: report of a case. *Surg Today* (1995) 25:959–61. doi: 10.1007/bf00312381

21. Ikeguchi M, Maeta M, Kaibara N. Therapeutic value of intraperitoneal hyperthermic peritoneal perfusion for patients with gastric cancer. *Int J Oncol* (1997) 11:1081–5. doi: 10.3892/ijo.11.5.1081

22. Bozzetti F, Vaglini M, Deraco M. Intraperitoneal hyperthermic chemotherapy in gastric cancer: rationale for a new approach. *Tumori* (1998) 84:483–8. doi: 10.1177/030089169808400409

23. Prabhu A, Mishra D, Brandl A, Yonemura Y. Gastric cancer with peritoneal metastasis-a comprehensive review of current intraperitoneal treatment modalities. *Front Oncol* (2022) 12:864647. doi: 10.3389/fonc.2022.864647

24. Reutovich MY, Krasko OV, Sukonko OG. Efficacy of adjuvant systemic chemotherapy combined with radical surgery and hyperthermic intraperitoneal chemotherapy in gastric cancer treatment. *Indian J Surg Oncol* (2020) 11:337–43. doi: 10.1007/s13193-020-01102-w

25. Zhu ZG, Tang R, Yan M, Chen J, Yang QM, Li C, et al. Efficacy and safety of intraoperative peritoneal hyperthermic chemotherapy for advanced gastric cancer patients with serosal invasion. *A long-term follow-up study Dig Surg* (2006) 23:93–102. doi: 10.1159/000093778

26. Kang LY, Mok KT, Liu SI, Tsai CC, Wang BW, Chen IS, et al. Intraoperative hyperthermic intraperitoneal chemotherapy as adjuvant chemotherapy for advanced gastric cancer patients with serosal invasion. *J Chin Med Assoc* (2013) 76:425–31. doi: 10.1016/j.jcma.2013.04.004

27. Sun J, Song Y, Wang Z, Gao P, Chen X, Xu Y, et al. Benefits of hyperthermic intraperitoneal chemotherapy for patients with serosal invasion in gastric cancer: a meta-analysis of the randomized controlled trials. *BMC Cancer* (2012) 12:526. doi: 10.1186/1471-2407-12-526

28. Mi DH, Li Z, Yang KH, Cao N, Lethaby A, Tian JH, et al. Surgery combined with intraoperative hyperthermic intraperitoneal chemotherapy (IHIC) for gastric cancer: a systematic review and meta-analysis of randomised controlled trials. *Int J Hyperthermia* (2013) 29:156–67. doi: 10.3109/02656736.2013.768359

29. Beeharry MK, Zhu ZL, Liu WT, Yao XX, Yan M, Zhu ZG. Prophylactic HIPEC with radical D2 gastrectomy improves survival and peritoneal recurrence rates for locally advanced gastric cancer: personal experience from a randomized case control study. *BMC Cancer* (2019) 19:932. doi: 10.1186/s12885-019-6125-z

30. Desiderio J, Chao J, Melstrom L, Warner S, Tozzi F, Fong Y, et al. The 30-year experience-a meta-analysis of randomised and high-quality non-randomised studies of hyperthermic intraperitoneal chemotherapy in the treatment of gastric cancer. *Eur J Cancer* (2017) 79:1–14. doi: 10.1016/j.ejca.2017.03.030

frontiers | Frontiers in Oncology

TYPE Original Research
PUBLISHED 02 March 2023
DOI 10.3389/fonc.2023.1049787

Check for updates

OPEN ACCESS

EDITED BY
Recep Avci,
The University of Auckland, New Zealand

REVIEWED BY
Abraham A. Pouliakis,
National and Kapodistrian University of Athens Medical School, Greece
Wen Wei,
Arizona State University, United States

*CORRESPONDENCE
Jeongseon Kim
jskim@ncc.re.kr

SPECIALTY SECTION
This article was submitted to Gastrointestinal Cancers: Gastric and Esophageal Cancers, a section of the journal Frontiers in Oncology

RECEIVED 03 October 2022
ACCEPTED 20 January 2023
PUBLISHED 02 March 2023

CITATION
Tran TT, Lee J, Gunathilake M, Kim J, Kim S-Y, Cho H and Kim J (2023) A comparison of machine learning models and Cox proportional hazards models regarding their ability to predict the risk of gastrointestinal cancer based on metabolic syndrome and its components. *Front. Oncol.* 13:1049787. doi: 10.3389/fonc.2023.1049787

COPYRIGHT
© 2023 Tran, Lee, Gunathilake, Kim, Kim, Cho and Kim. This is an open-access article distributed under the terms of the Creative Commons Attribution License (CC BY). The use, distribution or reproduction in other forums is permitted, provided the original author(s) and the copyright owner(s) are credited and that the original publication in this journal is cited, in accordance with accepted academic practice. No use, distribution or reproduction is permitted which does not comply with these terms.

A comparison of machine learning models and Cox proportional hazards models regarding their ability to predict the risk of gastrointestinal cancer based on metabolic syndrome and its components

Tao Thi Tran[1], Jeonghee Lee[2], Madhawa Gunathilake[2], Junetae Kim[1], Sun-Young Kim[1], Hyunsoon Cho[1] and Jeongseon Kim[2]*

[1]Department of Cancer Control and Population Health, Graduate School of Cancer Science and Policy, Goyang-si, Gyeonggi-do, Republic of Korea, [2]Department of Cancer Biomedical Science, Graduate School of Cancer Science and Policy, Goyang-si, Gyeonggi-do, Republic of Korea

Background: Little is known about applying machine learning (ML) techniques to identify the important variables contributing to the occurrence of gastrointestinal (GI) cancer in epidemiological studies. We aimed to compare different ML models to a Cox proportional hazards (CPH) model regarding their ability to predict the risk of GI cancer based on metabolic syndrome (MetS) and its components.

Methods: A total of 41,837 participants were included in a prospective cohort study. Incident cancer cases were identified by following up with participants until December 2019. We used CPH, random survival forest (RSF), survival trees (ST), gradient boosting (GB), survival support vector machine (SSVM), and extra survival trees (EST) models to explore the impact of MetS on GI cancer prediction. We used the C-index and integrated Brier score (IBS) to compare the models.

Results: In all, 540 incident GI cancer cases were identified. The GB and SSVM models exhibited comparable performance to the CPH model concerning the C-index (0.725). We also recorded a similar IBS for all models (0.017). Fasting glucose and waist circumference were considered important predictors.

Conclusions: Our study found comparably good performance concerning the C-index for the ML models and CPH model. This finding suggests that ML models may be considered another method for survival analysis when the CPH model's conditions are not satisfied.

KEYWORDS

metabolic syndrome, gastrointestinal cancer, machine learning, prospective cohort study, Korea

Introduction

Gastrointestinal (GI) cancer refers to cancers affecting the digestive system. Gastric cancer, colorectal cancer, liver cancer, esophageal cancer, and pancreatic cancer are recognized as common GI cancers (1). According to an estimate in 2018, GI cancer accounted for 26% of new cancer cases and 35% of deaths related to cancer worldwide (1). The trend of GI cancers varies geographically by specific types; for instance, the highest rates of liver cancer, esophageal cancer, and gastric cancer are found in Asia (2). Although the trend has been upwards for colorectal and pancreatic cancer, the remaining cancers have experienced a downwards trend since 1999; GI cancer remains one of the most common cancers in Korea (3).

Although risk factors for specific types of GI cancer vary, lifestyle-related factors contribute significantly to the development of GI cancer (2). Specifically, a Western lifestyle has been documented to be associated with a higher prevalence of GI cancer (2). Notably, metabolic syndrome (MetS), which has been reported to be a global epidemic, might be considered an important mediator of the effect of a Western lifestyle on GI cancer development (2). MetS has been described as a group of conditions including obesity, hypertension, high blood sugar, and dyslipidemia (4). Currently, there are three definitions used for MetS diagnosis, namely, the WHO 1999, the National Cholesterol Education Program (NCEP) Adult Treatment Panel III (ATP III) 2005, and the International Diabetes Federation 2006 definitions. Although MetS definitions are modified by health care organizations for different regions, MetS remains a significant and alarming global public health problem (5).

Existing evidence from epidemiological studies has revealed that MetS may be an etiologic factor for GI cancer development. For example, a previous study of large-scale molecular data for 366,016 participants reported a potential link between MetS and an elevated risk of GI cancer regardless of the MetS definition used (6). Similarly, an increased risk of colorectal cancer, liver cancer, and gastric cancer was found in participants with MetS in other cohort studies (7–11). Notably, Cox proportional hazards (CPH) model was used in these studies; a CPH model is a linear regression with good interpretability (12). CPH model is known to be a semiparametric method in which survival times are assumed in relation to predictor variables in a particular way and proportional hazards (13).

To date, attention has been drawn to the application of machine learning (ML) to cancer prediction. In particular, the application of ML in survival analysis has been indicated in recent years (14, 15). However, the value of ML models compared to CPH model is ambiguous due to inconsistent results in previous studies (15–18). For example, an ML model outperformed a CPH model in predicting breast cancer survival in a previous study (16). In contrast, a comparably good performance was observed to predict survival in patients with oral and pharyngeal cancer in another study (17). Thus, the value of ML approaches compared to CPH model in survival analysis is still debatable.

To our knowledge, little is known about the application of ML techniques in epidemiological studies to identify important predictors affecting GI cancer development. In addition, no study has compared the accuracy of ML and CPH models for predicting GI cancer. Therefore, our study aimed to examine whether MetS and its components are related to GI cancer prediction and whether ML models outperform a CPH model in predicting GI cancer based on MetS and other confounders.

Abbreviations: ATP III, Adult Treatment Panel III; BMI, body mass index; CI, confidence interval; CPH, Cox proportional hazards; EST, extra survival trees; GB, gradient boosting; GI, gastrointestinal; HDL cholesterol, high-density lipoprotein cholesterol; HR, hazard ratio; IBS, integrated Brier score; MetS, metabolic syndrome; ML, machine learning; NCEP, National Cholesterol Education Program; RSF, random survival forest; SSVM, survival support vector machine; ST, survival trees.

Methods

Study population

The Cancer Screenee Cohort Study was established in 2002 to explore the association of risk factors with cancer development in South Korea. The information of this cohort has been described (19). In brief, we recruited 41,837 participants aged 16 and older who visited the Center for Cancer Prevention and Detection at the National Cancer Center in South Korea for health examinations between August 2002 and December 2014. We required participants to complete baseline questionnaires and identified incident cancer cases by following up with participants until December 2019. Our final analysis included 24,139 participants after exclusion of 1,754 participants with incomplete questionnaires, 2,100 participants with a diagnosis of any cancer before recruitment, 6 participants aged <20 years, and 13,122 participants who lacked information on individual characteristics (Figure 1). We obtained written informed consent from all participants and approval for the study protocol from the institutional review board of the National Cancer Center (No. NCCNCS-07-077).

Outcome and predictor measurement

Potential incident GI cancer cases were obtained by linking to the 2019 Korea National Cancer Incidence Database of the Korea Central Cancer Registry. We used the following International Classification of Diseases, 10th Revision codes to identify common incident GI cancers: gastric cancer (C16), colorectal cancer (C18-C20), liver cancer (C22), esophageal cancer (C15), gallbladder cancer (C23), and pancreatic cancer (C25). We identified 540 incident GI cancer cases, namely, 242 (44.8%) incident cases of gastric cancer, 123 (22.8%) incident cases of colorectal cancer, 102 (18.9%) incident cases of liver cancer, 41 (7.6%) incident cases of pancreatic cancer, 16 (3.0%) incident cases of gallbladder cancer, and 16 (3.0%) incident cases of esophageal cancer.

Currently, the MetS definition in Korea is based on the criteria of the ATP III of the NCEP and specific values of waist circumference from the World Health Organization and the Korean Society for the Study of Obesity. MetS was identified among those who met 3 or more of the following criteria (20):

1. Waist circumference: males ≥ 90 cm and females ≥85 cm

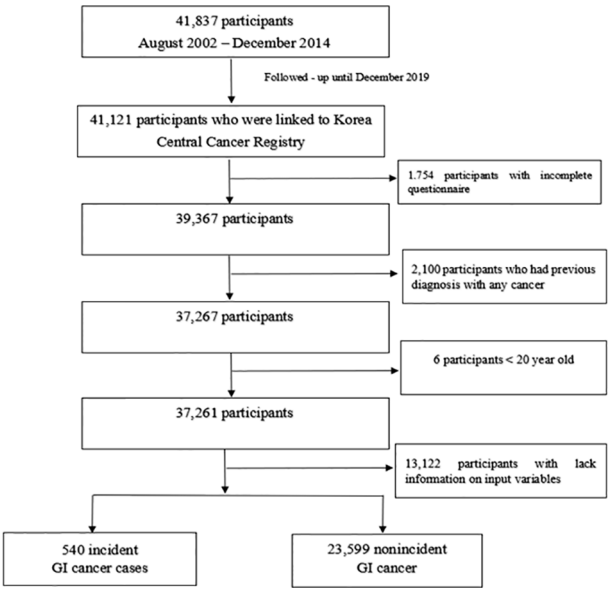

FIGURE 1
Flow chart of the study participants. Among 41,837 participants recruited, 41,121 participants were linked to the Korea Central Cancer Registry. Our final analysis included 24,139 participants after exclusion of 1,754 participants with incomplete questionnaires, 2,100 participants with a diagnosis of any cancer before recruitment, 6 participants aged <20 years, and 13,122 participants who lacked information on individual characteristics.

2. Blood pressure: ≥130/85 mmHg
3. Triglycerides: ≥150 mg/dL
4. High-density lipoprotein cholesterol (HDL cholesterol): males <40 mg/dL and females <50 mg/dL
5. Fasting glucose: ≥100 mg/dL or a history of diabetes.

We collected venous blood samples from participants at baseline after they had fasted for 8 hours to determine the blood-related components of MetS. Height (m) and weight (kg) were measured with InBody 3.0 (Biospace, Seoul, Korea) or automatic height and weight measurements (DS-102, Dong Shin Jenix Co., Ltd., Seoul, Korea). The measurement of waist circumference was performed with a tape measure 1 cm above the umbilicus with minimal respiration. A chemistry analyzer (TBA-200FR, Toshiba, Tokyo, Japan) was used to measure fasting glucose, triglyceride, and HDL cholesterol levels. Blood pressure was measured by trained personnel with an automatic blood pressure monitor (FT-200S, Jawon Medical, Kyungsan, Korea) after the patients had 15 minutes of rest (21). In addition, a self-administered questionnaire regarding information on baseline characteristics was completed by participants.

Predictors of GI cancer incidence in our study included MetS and its individual components (waist circumference, HDL, triglycerides, blood pressure, and fasting glucose). In addition, sociodemographic variables included age, sex, educational level (high school graduate or less and college or higher), marital status (married or cohabitating and others), monthly income (10,000 Korean won/month) (<200, 200-400, and >400), and first-degree family history of cancer (yes, no). Lifestyle factors included smoking status (nonsmoker, ex-smoker and current-smoker), alcohol consumption (nondrinker, former drinker and current-drinker), and physical activity (yes, no). These sociodemographic and lifestyle characteristics may be confounders for the association between MetS and GI cancer (6).

Models and evaluation

We used a CPH model and ML survival models, including random survival forest (RSF), survival trees (ST), gradient boosting (GB), survival support vector machine (SSVM), and extra survival trees (EST), to predict GI cancer. The ability of these ML models to predict an outcome in right-censored time-to-event data has been documented in the literature as follows:

Random forest is an ML model that is most frequently used to solve problems in relation to classification and regression by constructing ensembles from decision trees and combining results to give a final decision. RSF extends random forest to censored lifetime data (22).

ST is another forest approach that has been widely used to handle time-to-event data. The implementation of ST is as follows: data partitioning is performed based on a criterion for splitting, and objects with similar events are grouped as the same node. (23).

Similar to RSF, the GB model is an ensemble model that combines the predictions of multiple base learners to improve the prediction of the overall model. However, RSF averages predictions from independent trees to obtain the overall prediction, while the GB model is additive (24).

Support vector machine aims to find a hyperplane to maximize the margin between classes. SSVM is an extension of the support vector machine to handle time-to-event data (16).

The EST model is a slightly different version of RSF (25). In comparison with RSF, the splitting criteria of EST are more random (26).

We used the following two evaluation metrics, which have been widely used in survival analyses in the literature, to compare the performance of the regression models (15, 22, 23, 26). The concordance index (C-index) is a rank order statistic for

predictions against true outcomes and is defined as the ratio of the concordant pairs to the total comparable pairs (23); the closer the C-index is to 1, the better the model performs (15, 26). The integrated Brier score (IBS) reflects calibration over all time points, with a smaller value indicating greater accuracy (22). Furthermore, we evaluated the models based on the time-dependent area under the curve (AUC).

Statistical analysis

We calculated person-years from baseline to the date of cancer diagnosis, death, or end of follow-up (December 31, 2019), whichever came first. We used chi-square tests and Wilcoxon rank-sum tests to compare the baseline characteristics between the incident GI cancer cases and nonincident GI cancer.

There were several steps for model development. First, we used an 80:20 ratio to randomly split the data into training and testing datasets. The purposes of the training and testing datasets were to fit the model and evaluate the final model, respectively. Second, a grid search was utilized to search hyperparameters for C-index maximization with 10-fold cross validation. We found the following optimal hyperparameters: n_estimators=400, max_depth=4 for RSF, max_depth=4 for ST, learning_rate=1 and max_depth=1 for GB, alpha=0.0002 for SSVM, and n_estimators=500, max_depth=4 for EST. Third, we fit the models using the training dataset based on selected input variables, the optimal hyperparameters, and default values of other hyperparameters. Fourth, the testing dataset was used to evaluate and compare model performance. Then, the ELI5 package was used to explore the contribution of predictors to the models, which calculates important variables based on the permutation important method by identifying the weight of variables (26). We used bootstrapping and 10-fold cross validation to assess the robustness of the models.

Furthermore, we used the CPH model to explore the specific associations of MetS and its components with incident GI cancer after adjusting for the aforementioned confounding factors. We performed statistical analyses by using Python software (version 3.7.9) with the scikit-survival library (26) and SAS software (version 9.4, SAS Institute, Cary, NC, USA) with a two-sided *P* value less than 0.05 was considered statistically significant.

Results

Characteristics of the participants

A total of 540 incident GI cancer cases were identified among 24,139 participants during the follow-up period (mean, 10.7 years), among which gastric cancer accounted for the highest number of cases (44.8%), followed by colorectal cancer (22.8%). Compared with the nonincident GI cancer group, the incident GI cancer group comprised older patients (54.7 ± 8.9 years old vs. 49.2 ± 9.1 years old, P<0.001) and patients who exhibited higher proportions of a low education level (49.4% vs. 44.1%, P=0.013), a low income level (23.9% vs. 15.0%, P<0.001), being married or cohabitating (93.7% vs. 90.6%, P=0.015), a first-degree family history of cancer (49.6% vs. 44.3%, P=0.014), and BMI≥25 (44.3% vs. 33.5%, P<0.001). In addition, this group tended to be current smokers (30.0% vs. 25.0%, P<0.001) and current drinkers (67.8% vs. 65.4%, P<0.001). With regard to MetS, incident GI cancer cases accounted for a higher proportion of MetS than those without incident GI cancer (26.3% vs. 18.2%, P<0.001). Similarly, the proportions of central obesity, elevated blood pressure, and high fasting glucose levels tended to be higher in incident GI cancer cases than in nonincident GI cancer (45.2% vs. 34.6%, P<0.001, 48.5% vs. 37.5%, P<0001, and 32.2% vs. 19.2%, P<0.001, respectively) (Table 1).

Model performance

The C-index and IBS were used to compare the performance of the models. Table 2 presents these metrics for the CPH and ML models based on the testing dataset. Comparably good performance was recorded for the GB, SSVM, and CPH models, with a C-index value of 0.725. The RSF and EST models exhibited a lower performance than the CPH model (0.699 vs. 0.725 and 0.671 vs. 0.725, respectively). IBS was not estimated for SSVM because it is applicable for models that can estimate a survival function. A similar value of IBS was found for the remaining models (0.017). Furthermore, comparably good discrimination was found for the ML and CPH models concerning the time-dependent AUC (Figure 2).

Importance of predictors of GI cancer

Table 3 presents the top five most important predictors of incident GI cancer based on the ML models. Notably, among the predictors related to MetS, fasting glucose was indicated as an important predictor for the occurrence of GI cancer across models. Furthermore, according to the GB model, waist circumference was one of the five important predictors contributing to incident GI cancer.

We then determined the specific relationships between MetS and its components and GI cancer development by using the CPH model. Notably, the important predictors were identified by the CPH model, which were similar to those of the ML models. In detail, a higher risk of GI cancer was found for participants with high waist circumference in both the crude model and adjusted model; the HRs (95% CIs) were 1.56 (1.32-1.85) for the former and 1.36 (1.15-1.62) for the latter. Similarly, high fasting glucose was observed in relation to an increased GI cancer risk in the crude model [HR=2.05 (1.71-2.46)], and this significance remained unchanged in the adjusted model [HR=1.41 (1.17-1.69)]. Furthermore, participants with MetS exhibited a significantly higher risk of GI cancer than those without MetS, and the HRs (95% CIs) were 1.64 (1.35-1.98) in the crude model and 1.29 (1.06-1.56) in the adjusted model (Table 4).

Discussion

In this study, we constructed five ML models and compared them with a conventional CPH model to predict incident GI cancer and

10.3389/fonc.2023.1049787

TABLE 1 Characteristics of the study subjects.

Characteristics	Total		
	Nonincident GI cancer (n=23,599)	Incident GI cancer (n=540)	*P* value[a]
Age[b]	49.2 ± 9.1	54.7 ± 8.9	<0.001
Follow-up duration (year)[b]	10.8 ± 3.8	6.1 ± 4.5	<0.001
Sex (n, %)			
Male	12971 (55.0)	400 (74.1)	<0.001
Female	10628 (45.0)	140 (25.9)	
Educational level (n, %)			
High school graduate or less	10405 (44.1)	267 (49.4)	0.013
College or higher	13194 (55.9)	273 (50.6)	
Household income (10,000 won/month) (n, %)			
<200	3539 (15.0)	129 (23.9)	<0.001
200-400	7747 (32.8)	171 (31.7)	
>400	12313 (52.2)	240 (44.4)	
Marital status (n, %)			
Married or cohabitating	21390 (90.6)	506 (93.7)	0.015
Others	2209 (9.4)	34 (6.3)	
First-degree family history of cancer (n, %)			
Yes	10457 (44.3)	268 (49.6)	0.014
No	13142 (55.7)	272 (50.4)	
Smoking status (n, %)			
Nonsmokers	12217 (51.8)	200 (37.0)	<0.001
Ex-smokers	5472 (23.2)	178 (33.0)	
Current smokers	5910 (25.0)	162 (30.0)	
Alcohol consumption (n, %)			
Nondrinkers	6986 (29.6)	126 (23.3)	<0.001
Ex-drinkers	1175 (5.0)	48 (8.9)	
Current drinkers	15438 (65.4)	366 (67.8)	
Regular exercise (n, %)			
Yes	13342 (56.5)	329 (60.9)	0.042
No	10257 (43.5)	211 (39.1)	
BMI (kg/m^2)			
<23	9377 (39.7)	141 (26.1)	<0.001
23-25	6321 (26.8)	160 (29.6)	
≥25	7901 (33.5)	239 (44.3)	
Metabolic syndrome (n, %)			
No	19305 (81.8)	398 (73.7)	<0.001
Yes	4294 (18.2)	142 (26.3)	
Waist circumference (n, %)			
Men <90 cm and women<85 cm	15439 (65.4)	296 (54.8)	<0.001
Men ≥90 cm and women≥85 cm	8160 (34.6)	244 (45.2)	

(Continued)

TABLE 1 Continued

Characteristics	Total		
	Nonincident GI cancer (n=23,599)	Incident GI cancer (n=540)	*P* value[a]
HDL (n, %)			
Men ≥40 mg/dL and women ≥50 mg/dL	19778 (83.8)	440 (81.5)	0.147
Men <40 mg/dL and women <50 mg/dL	3821 (16.2)	100 (18.5)	
Triglycerides (n, %)			
<150 mg/dL	17791 (75.4)	403 (74.6)	0.686
≥150 mg/dL	5808 (24.6)	137 (25.4)	
Blood pressure (n, %)			
<130/85 mmHg	14757 (62.5)	278 (51.5)	<0.001
≥130/85 mmHg	8842 (37.5)	262 (48.5)	
Fasting glucose (n, %)			
<100 mg/dL or no history of diabetes	19069 (80.8)	366 (67.8)	<0.001
≥100 mg/dL or history of diabetes	4530 (19.2)	174 (32.2)	

[a]Chi-square tests. We used chi-square tests and Wilcoxon rank-sum tests to compare the baseline characteristics between the incident GI cancer cases and nonincident GI cancer.
[b]values are presented as the mean ± SD.

identify whether MetS and its components are potential predictors of GI cancer development. Our findings identified a comparably good performance concerning the C-index for the GB, SSVM, and CPH models. High fasting glucose was found to be a predictor for GI cancer development across six models. However, the important predictor was not restricted to high fasting glucose, and the importance of high waist circumference emerged in the GB and CPH models.

To date, attention has been drawn to the application of ML models to time-to-event data. As a result, many studies have been conducted to compare the predictive performance of ML models against CPH models. For example, based on a previous study, an extreme gradient boosting model outperformed a CPH model in predicting breast cancer survival based on C-index values (0.73 vs. 0.63) (16). Similar results were obtained in other studies comparing RSF models and CPH models for survival prediction in patients with liver transplantation or oral squamous cell carcinoma (18, 27). The C-index values obtained in these studies were 0.622/0.620 and 0.764/0.694 for the RSF and CPH models, respectively (18, 27). However,

TABLE 2 C-index and integrated Brier score for the testing dataset.

Models	C-index on testing dataset	IBS
Cox	0.725 (0.723-0.727)	0.017
Random survival forest	0.699 (0.697-0.701)	0.017
Survival support vector machine	0.725 (0.723-0.727)	–
Survival trees	0.721 (0.719-0.723)	0.017
Gradient boosting	0.723 (0.721-0.725)	0.017
Extra survival trees	0.671 (0.668-0.673)	0.017

The C-index was estimated based on 100 bootstrapped data samples. The integrated Brier score (IBS) applies to models that can estimate a survival function. Thus, it is impossible to estimate the IBS for the survival support vector machine.

the value of ML models against CPH model is still open to discussion because inconsistent results have been obtained in other studies. Specifically, a comparably good performance was recorded for RSF, conditional inference forest, and CPH models in predicting the survival of patients with oral and pharyngeal cancer (17). Similarly, a CPH model showed better performance in another study conducted in China, where CPH and RSF models were used to predict the progression of high-grade glioma after proton and carbon ion radiotherapy (15).

To our knowledge, our study is the first attempt to use ML and CPH models for the prediction of GI cancer development based on MetS and other confounders. CPH model has been widely applied to investigate the impact of risk factors on incident cancers due to its simple, fast computation and meaningful outputs; however, its limitations need to be clarified (16). First, the proportional hazard assumption must be satisfied in the model. Survival curves for different strata need to have hazard functions that are proportional over time. Second, there is a linear relationship between log hazards and covariates (28). Thus, CPH model may not be appropriate for a dataset with nonlinearity due to a decreased accuracy in prediction (12, 17). To date, the development of ML has been documented to address the limitations of conventional statistical analysis in cancer prediction (16). The self-study, classification, prediction, and feature selection abilities of ML have been well recognized. ML methods can be adapted to deal with data with nonlinearity and high-dimensional covariates (22, 29). However, we found comparable performance for the CPH and ML models. This finding is consistent with some previous studies (17, 30) and may be explained as follows. First, a CPH model tries to fit the data to a specific model and tests the proportional hazards assumptions to examine the influence of predictors on an outcome (17). Thus, the proportional hazards assumption of CPH was

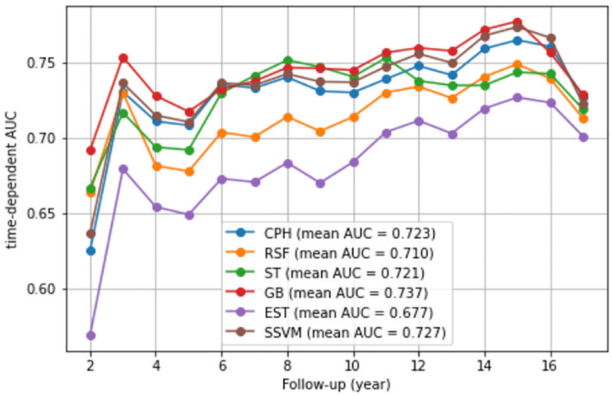

FIGURE 2
Time-dependent AUC. We presented the time-dependent AUC of the CPH model and five ML models, namely, the random survival forest, survival trees, gradient boosting, extra survival trees, and survival support vector machine models. The vertical axis is the time-dependent AUC. The horizontal axis is follow-up (year).

satisfied in our data, which may be a potential explanation. Second, complex associations and interactions seem to be unimportant in our data. Third, a small number of predictors were used in our study. Overall, it is important to realize that the superiority of ML models is found only when a CPH model meets its limitations (17). Notably, we evaluated the models based on the C-index, which can account for censoring and does not depend on a single fixed evaluation time (27). Taken together, a CPH model should be considered a method in epidemiological studies when its conditions are satisfied. Additionally, a combination of ML and CPH models could be used to provide further insight into predictors; specifically, nonlinear interactions may be obtained using ML models, whereas a CPH model is used to summarize the risk in a dataset that is not suitable for CPH model analysis (14, 17).

Among the variables related to MetS, the importance of high fasting glucose as a predictor for GI cancer development was found across all models. This finding is consistent with the results of a previous study, where diabetes mellitus was documented to be associated with elevated GI cancer (31). Notably, a consistent association was also found for specific types of GI cancer. For instance, high fasting glucose was demonstrated to play an important role in gastric cancer development in our previous study (32). Similarly, we identified a positive association for colorectal cancer (11). Our finding was reinforced by the conclusions of other studies (33, 34). For example, a higher risk of colorectal cancer was observed in participants with type II diabetes in two large prospective cohorts in the U.S (33). Additionally, a higher risk of primary liver cancer and pancreatic cancer may be attributed to increased fasting glucose (35–37). Our study suggests that greater emphasis must be placed on participants with high fasting glucose, including those with prediabetes (100 mg/dL-125 mg/dL) and diabetes (≥126 mg/dL or a history of diabetes). Prediabetes may have a potential link to GI cancer development (32). Several biological mechanisms may be involved in the effect of high fasting glucose on GI cancer development. First, hyperglycemia could provide nutrients for tumor cells, which has certain effects on the proliferation of these cells. For example, epidermal growth factor expression and epidermal growth factor receptor transactivation may be induced by high glucose, which can contribute to promoting cell proliferation in pancreatic cancer (38). Second, there is a positive association between hyperglycemia and proinflammatory factor production; proinflammatory factors are known to stimulate the expression of oncogenes, regulate the cell cycle, promote the proliferation of tumor cells, inhibit apoptosis, and even induce the epithelial-to-mesenchymal transition (38). Third, insulin-like growth factor 1 (IGF-1) bioavailability could be promoted by insulin, which could inhibit apoptosis, stimulate cellular proliferation, and induce carcinogenesis (39).

TABLE 3 Top 5 most important predictors for incident GI cancer based on the ML models.

Rank	RSF model		SSVM model		ST model		GB model		EST model.	
	Variables	Weight	Variables	Weight	Variables	Weight	Variables	Weight	Variables	Weight
1	Age	0.0975 ± 0.0365	Age	0.1472 ± 0.0494	Age	0.1822 ± 0.0614	Age	0.1784 ± 0.0531	Age	0.0562 ± 0.0214
2	Sex	0.0213 ± 0.0293	Sex	0.0158 ± 0.0197	Sex	0.0459 ± 0.0232	Sex	0.0336 ± 0.0217	Sex	0.0243 ± 0.0371
3	Smoking status	0.0029 ± 0.0059	First degree family history of cancer	0.0067 ± 0.0095	**Fasting glucose**	**0.0065 ± 0.0055**	**Fasting glucose**	**0.0030 ± 0.0065**	**Fasting glucose**	**0.0106 ± 0.0138**
4	**Fasting glucose**	**0.0029 ± 0.0104**	Smoking status	0.0054 ± 0.0091	Education	0.0037 ± 0.0068	**Waist circumference**	**0.0011 ± 0.0032**	Income	0.0045 ± 0.0068
5	First degree family history of cancer	0.0015 ± 0.0034	**Fasting glucose**	**0.0037 ± 0.0075**	Smoking status	0.0020 ± 0.0027	–	–	First degree family history of cancer	0.0012 ± 0.0045

Bold text indicates the predictors related to metabolic syndrome.

10.3389/fonc.2023.1049787

TABLE 4 Hazard ratios and 95% confidence intervals of incident GI related to metabolic syndrome and its components.

Exposure	Total			
	GI cancer cases	Person years	HR (95% CI) (Model 1)	HR (95% CI) (Model 2)
Waist circumference				
Men <90 cm, women <85 cm	296	168927.01	1.00	1.00
Men ≥90 cm, women ≥85 cm	244	89300.40	1.56 (1.32-1.85)	1.36 (1.15-1.62)
HDL				
Men ≥40 mg/dL, women ≥50 mg/dL	440	214258.72	1.00	1.00
Men <40 mg/dL, women <50 mg/dL	100	43968.68	1.10 (0.89-1.37)	1.11 (0.89-1.38)
Triglycerides				
<150 mg/dL	403	195275.75	1.00	1.00
≥150 mg/dL	137	62951.66	1.06 (0.87-1.28)	0.89 (0.73-1.09)
Blood pressure				
<130/85 mmHg	278	164464.34	1.00	1.00
≥130/85 mmHg	262	93763.07	1.65 (1.40-1.96)	1.26 (1.06-1.50)
Fasting glucose				
<100 mg/dL or no history of diabetes	366	209775.34	1.00	1.00
≥100 mg/dL or history of diabetes	174	48452.06	2.05 (1.71-2.46)	1.41 (1.17-1.69)
Metabolic syndrome				
No	398	212086.40	1.00	1.00
Yes	142	46141.00	1.64 (1.35-1.98)	1.29 (1.06-1.56)

HR, hazard ratio; CI, confidence interval.
Model 1: crude model; Model 2: adjusted for age, sex, education, alcohol consumption, marital status, smoking status, regular exercise, monthly income, and first-degree family history of cancer.

Furthermore, high waist circumference was considered an important predictor of the occurrence of GI cancer in the CPH model and GB model in our study. Overall obesity has received more attention in previous studies than central obesity. However, central obesity may have more influence on cancer risk than overall obesity because metabolic derangement is reflected by insulin and IGF levels (40). This hypothesis was supported by a conclusion drawn from a previous study, which emphasized the stronger influence of waist circumference on colon cancer risk than BMI (41). Furthermore, the adverse effect of central obesity on GI cancer development was reinforced by evidence from two meta-analyses of prospective studies (42, 43). The pathophysiological mechanisms can be explained as follows. First, insulin resistance is an important mediator of the link between central obesity and cancer. In detail, high insulin levels lead to IGF activation, promote cellular proliferation, and inhibit apoptosis (44). Second, sex hormones may be a possible mechanism because they are related to a relationship between body size and shape. The pathogenesis of the link between body size and shape and cancer may include obesity-induced hypoxia, genetic susceptibility, and adipose stromal cell migration (44). Notably, MetS was demonstrated to be associated with GI cancer development in the CPH model. However, it was not indicated as the top five important variables in the ML models. A possible reason may be the stronger effects of high fasting glucose and waist circumference. These components are implied to be central factors for the causal link between MetS and GI cancer.

Notably, with regard to variable importance, CPH model exhibits a straightforward interpretation as an HR, whereas a large important variable has more influence on the transition to predict an outcome, and ML models do not provide the sign of the prediction (negative or positive effect) (45). To date, the direct comparison of CPH with ML models regarding interpretation is limited due to the lack of a common metric. Thus, it is necessary to address this limitation in further studies (18).

There are several strengths in our study. First, this is the first attempt to use an ML approach to predict and identify the adverse effects of high fasting glucose and central obesity on GI development with time-to-event data. Second, our study has a relatively large sample size with a long follow-up time, accurately identifying incident cases by linking to the national cancer registry using a high-quality database. Third, we used standardized operating procedures to perform the laboratory tests with standardized equipment and trained personnel. However, there are some limitations in our study. First, we used a small number of predictors. Second, the predictive power may be affected by a low proportion of incident cases in our study. Thus, further studies with a larger number of incident cases and predictors may be warranted to clarify the value of ML models against CPH model. Third, information on medication and dietary factors was not available to consider in our models.

In conclusion, our study found comparably good performance according to the C-index for the ML and CPH models. This finding

suggested that ML models may be considered another method for survival analysis when a CPH model has limitations. However, further studies with a larger number of predictors are necessary to clarify the value of ML models. Furthermore, our study indicated that preventing high fasting glucose and central obesity could be expected to reduce GI cancer development.

Data availability statement

The raw data supporting the conclusions of this article will be made available by the authors, without undue reservation.

Ethics statement

The studies involving human participants were reviewed and approved by institutional review board of the National Cancer Center (No. NCCNCS-07-077). Written informed consent to participate in this study was provided by the participants' legal guardian/next of kin.

Author contributions

Formal analysis, TT, JL. Preparation of original draft, TT. Writing-review and editing, JSK, S-YK, HC, JTK, MG. Data curation, JL, JSK. Investigation, JL. Methodology, JL, JSK. Funding acquisition, JSK. Project administration, JSK. Supervision, JSK. All authors contributed to the article and approved the submitted version.

Funding

This work was supported by International Cooperation & Education Program (NCCRI•NCCI 52210-52211, 2020) of National Cancer Center, Korea and National Research Foundation of Korea (2021R1A4A1032861)

Conflict of interest

The authors declare that the research was conducted in the absence of any commercial or financial relationships that could be construed as a potential conflict of interest.

Publisher's note

All claims expressed in this article are solely those of the authors and do not necessarily represent those of their affiliated organizations, or those of the publisher, the editors and the reviewers. Any product that may be evaluated in this article, or claim that may be made by its manufacturer, is not guaranteed or endorsed by the publisher.

References

1. Arnold M, Abnet CC, Neale RE, Vignat J, Giovannucci EL, McGlynn KA, et al. Global burden of 5 major types of gastrointestinal cancer. *Gastroenterology* (2020) 159:335–49. doi: 10.1053/j.gastro.2020.02.068

2. Lu L, Mullins CS, Schafmayer C, Zeißig S, Linnebacher M. A global assessment of recent trends in gastrointestinal cancer and lifestyle-associated risk factors. *Cancer Commun (Lond)* (2021) 41:1137–51. doi: 10.1002/cac2.12220

3. Hong S, Won YJ, Lee JJ, Jung KW, Kong HJ, Im JS, et al. Cancer statistics in Korea: Incidence, mortality, survival, and prevalence in 2018. *Cancer Res Treat* (2021) 53:301–15. doi: 10.4143/crt.2021.291

4. Yoo H, Kim H, Lee JH, Lee KS, Choi MJ, Song HR, et al. Study on the relevance of metabolic syndrome and incidence of gastric cancer in Korea. *Int J Environ Res Public Health* (2019) 16:1101. doi: 10.3390/ijerph16071101

5. Saklayen MG. The global epidemic of the metabolic syndrome. *Curr Hypertens Rep* (2018) 20:12. doi: 10.1007/s11906-018-0812-z

6. Rothwell JA, Jenab M, Karimi M, Truong T, Mahamat-Saleh Y, Ferrari P, et al. Metabolic syndrome and risk of gastrointestinal cancers: an investigation using large-scale molecular data. *Clin Gastroenterol Hepatol* (2022) 20:e1338–e52. doi: 10.1016/j.cgh.2021.10.016

7. Jimba T, Kaneko H, Yano Y, Itoh H, Yotsumoto H, Seki H, et al. Relation of the metabolic syndrome to incident colorectal cancer in young adults aged 20 to 49 years. *Am J Cardiol* (2021) 158:132–8. doi: 10.1016/j.amjcard.2021.07.049

8. Ku MS, Chiu SY, Chien KL, Lee YC, Chen SL, Chen CD. Gender difference in metabolic syndrome and incident colorectal adenoma: A prospective observational study (KCIS No.42). *Medicine* (2021) 100:e26121. doi: 10.1097/MD.0000000000026121

9. Xia B, Peng J, Enrico DT, Lu K, Cheung EC, Kuo Z, et al. Metabolic syndrome and its component traits present gender-specific association with liver cancer risk: A prospective cohort study. *BMC Cancer* (2021) 21:1084. doi: 10.1186/s12885-021-08760-1

10. Lin Y, Ness-Jensen E, Hveem K, Lagergren J, Lu Y. Metabolic syndrome and esophageal and gastric cancer. *Cancer Causes Control* (2015) 26:1825–34. doi: 10.1007/s10552-015-0675-4

11. Tran TT, Gunathilake M, Lee J, Kim J. Association between metabolic syndrome and its components and incident colorectal cancer in a prospective cohort study. *Cancer* (2022) 128:1230–41. doi: 10.1002/cncr.34027

12. Liu P, Fu B, Yang SX, Deng L, Zhong X, Zheng H. Optimizing survival analysis of XGBoost for ties to predict disease progression of breast cancer. *IEEE Trans BioMed Eng* (2021) 68:148–60. doi: 10.1109/TBME.2020.2993278

13. Kartsonaki C. Survival analysis. *Diagn Histopathol* (2016) 22:263–70. doi: 10.1016/j.mpdhp.2016.06.005

14. Aivaliotis G, Palczewski J, Atkinson R, Cade JE, Morris MA. A comparison of time to event analysis methods, using weight status and breast cancer as a case study. *Sci Rep* (2021) 11:14058. doi: 10.1038/s41598-021-92944-z

15. Qiu X, Gao J, Yang J, Hu J, Hu W, Kong L, et al. A comparison study of machine learning (Random survival forest) and classic statistic (Cox proportional hazards) for predicting progression in high-grade glioma after proton and carbon ion radiotherapy. *Front Oncol* (2020) 10:551420. doi: 10.3389/fonc.2020.551420

16. Moncada-Torres A, van Maaren MC, Hendriks MP, Siesling S, Geleijnse G. Explainable machine learning can outperform cox regression predictions and provide insights in breast cancer survival. *Sci Rep* (2021) 11:6968. doi: 10.1038/s41598-021-86327-7

17. Du M, Haag DG, Lynch JW, Mittinty MN. Comparison of the tree-based machine learning algorithms to cox regression in predicting the survival of oral and pharyngeal cancers: Analyses based on SEER database. *Cancers* (2020) 12:2802. doi: 10.3390/cancers12102802

18. Kantidakis G, Putter H, Lancia C, de Boer J, Braat AE, Fiocco M. Survival prediction models since liver transplantation - comparisons between cox models and machine learning techniques. *BMC Med Res Methodol* (2020) 20:277. doi: 10.1186/s12874-020-01153-1

19. Kim J. Cancer screenee cohort study of the national cancer center in south Korea. *Epidemiol Health* (2014) 36:e2014013. doi: 10.4178/epih/e2014013

20. Lee SH, Tao S, Kim HS. The prevalence of metabolic syndrome and its related risk complications among koreans. *Nutrients* (2019) 11:1755. doi: 10.3390/nu11081755

21. Cho YA, Kim J, Cho ER, Shin A. Dietary patterns and the prevalence of metabolic syndrome in Korean women. *Nutr Metab Cardiovasc Dis* (2011) 21:893–900. doi: 10.1016/j.numecd.2010.02.018

22. Liu Y, Zhou S, Wei H, An S. A comparative study of forest methods for time-to-event data: Variable selection and predictive performance. *BMC Med Res Methodol* (2021) 21:193. doi: 10.1186/s12874-021-01386-8

23. Wang P, Li Y, Reddy CK. Machine learning for survival analysis: A survey. *ACM Comput Surv* (2019) 51:1–36. doi: 10.1145/3214306

24. Natekin A, Knoll A. Gradient boosting machines, a tutorial. *Front Neurorobot* (2013) 7:21. doi: 10.3389/fnbot.2013.00021

25. Dey AK, Suhas N, Teja TS, Juneja A. *Some variations on ensembled random survival forest with application to cancer research* . Available at: https://www.arxiv-vanity.com/papers/1709.05515/ (Accessed 04 February 2022).

26. Pölsterl S. Scikit-survival:a library for time-to-event analysis built on top of scikit-learn. *J Mach Learn Res* (2020) 21:1–6.

27. Kim DW, Lee S, Kwon S, Nam W, Cha I-H, Kim HJ. Deep learning-based survival prediction of oral cancer patients. *Sci Rep* (2019) 9:6994. doi: 10.1038/s41598-019-43372-7

28. Hashim D, Weiderpass E. Cancer survival and survivorship. In: *Encyclopedia of cancer*, *3rd ed.* Elsevier (2019). p. 250–59.

29. Ryo M, Rillig MC. Statistically reinforced machine learning for nonlinear patterns and variable interactions. *Ecosphere* https://www.sciencedirect.com/science/article/pii/B9780128012383651024?via%3Dihub (2017) 8:e01976. doi: 10.1002/ecs2.1976

30. Datema FR, Moya A, Krause P, Bäck T, Willmes L, Langeveld T, et al. Novel head and neck cancer survival analysis approach: Random survival forests versus cox proportional hazards regression. *Head Neck* (2012) 34:50–8. doi: 10.1002/hed.21698

31. Luo J, Chlebowski R, Liu S, McGlynn KA, Parekh N, White DL, et al. Diabetes mellitus as a risk factor for gastrointestinal cancers among postmenopausal women. *Cancer Causes Control* (2013) 24:577–85. doi: 10.1007/s10552-012-9996-8

32. Tran TT, Lee J, Gunathilake M, Cho H, Kim J. Influence of fasting glucose level on gastric cancer incidence in a prospective cohort study. *Cancer Epidemiol Biomarkers Prev* (2022) 31:254–61. doi: 10.1158/1055-9965.EPI-21-0670

33. Ma Y, Yang W, Song M, Smith-Warner SA, Yang J, Li Y, et al. Type 2 diabetes and risk of colorectal cancer in two large U.S. prospective cohorts. *Br J Cancer* (2018) 119:1436–42. doi: 10.1038/s41416-018-0314-4

34. Ali Khan U, Fallah M, Sundquist K, Sundquist J, Brenner H, Kharazmi E. Risk of colorectal cancer in patients with diabetes mellitus: A swedish nationwide cohort study. *PloS Med* (2020) 17:e100343. doi: 10.1371/journal.pmed.1003431

35. Feng X, Wang G, Li N, Lyu Z, Chen S, Wei L, et al. The association between fasting blood glucose and the risk of primary liver cancer in Chinese males: A population-based prospective study. *Br J Cancer* (2017) 117:1405–11. doi: 10.1038/bjc.2017.296

36. Rapp K, Schroeder J, Klenk J, Ulmer H, Concin H, Diem G, et al. Fasting blood glucose and cancer risk in a cohort of more than 140,000 adults in Austria. *Diabetologia* (2006) 49:945–52. doi: 10.1007/s00125-006-0207-6

37. Jee SH, Ohrr H, Sull JW, Yun JE, Ji M, Samet JM. Fasting serum glucose level and cancer risk in Korean men and women. *Jama* (2005) 293:194–202. doi: 10.1001/jama.293.2.194

38. Li W, Zhang X, Sang H, Zhou Y, Shang C, Wang Y, et al. Effects of hyperglycemia on the progression of tumor diseases. *J Exp Clin Cancer Res* (2019) 38:327. doi: 10.1186/s13046-019-1309-6

39. Kwon HJ, Park MI, Park SJ, Moon W, Kim SE, Kim JH, et al. Insulin resistance is associated with early gastric cancer: A prospective multicenter case control study. *Gut Liver* (2019) 13:154–60. doi: 10.5009/gnl17556

40. Lee KR, Seo MH, Do Han K, Jung J, Hwang IC. Waist circumference and risk of 23 site-specific cancers: a population-based cohort study of Korean adults. *Br J Cancer* (2018) 119:1018–27. doi: 10.1038/s41416-018-0214-7

41. Moore LL, Bradlee ML, Singer MR, Splansky GL, Proctor MH, Ellison RC, et al. BMI and waist circumference as predictors of lifetime colon cancer risk in framingham study adults. *Int J Obes* (2004) 28:559–67. doi: 10.1038/sj.ijo.0802606

42. Du X, Hidayat K, Shi BM. Abdominal obesity and gastroesophageal cancer risk: Systematic review and meta-analysis of prospective studies. *Biosci Rep* (2017) 37. doi: 10.1042/BSR20160474

43. Aune D, Greenwood DC, Chan DS, Vieira R, Vieira AR, Navarro Rosenblatt DA, et al. Body mass index, abdominal fatness and pancreatic cancer risk: A systematic review and non-linear dose-response meta-analysis of prospective studies. *Ann Oncol* (2012) 23:843–52. doi: 10.1093/annonc/mdr398

44. Barberio AM, Alareeki A, Viner B, Pader J, Vena JE, Arora P, et al. Central body fatness is a stronger predictor of cancer risk than overall body size. *Nat Commun* (2019) 10:383. doi: 10.1038/s41467-018-08159-w

45. Kim J, Lee S, Hwang E, Ryu KS, Jeong H, Lee JW, et al. Limitations of deep learning attention mechanisms in clinical research: empirical case study based on the Korean diabetic disease setting. *J Med Internet Res* (2020) 22:e18418–e. doi: 10.2196/18418

frontiers | Frontiers in Oncology

TYPE Original Research
PUBLISHED 16 March 2023
DOI 10.3389/fonc.2023.1064790

Check for updates

OPEN ACCESS

EDITED BY
Zhendong Jin,
Second Military Medical University, China

REVIEWED BY
Yizhuo Wang,
University of Texas MD Anderson Cancer Center, United States
Ziv Radisavljevic,
Harvard Medical School, United States

*CORRESPONDENCE
Guanhua Wang
nywgh@163.com
Wenjun Yang
ywj007@yeah.net

†These authors have contributed equally to this work

SPECIALTY SECTION
This article was submitted to Gastrointestinal Cancers: Gastric and Esophageal Cancers, a section of the journal Frontiers in Oncology

RECEIVED 08 October 2022
ACCEPTED 06 March 2023
PUBLISHED 16 March 2023

CITATION
Li X, Chen Z, Zhang Y, Zhang H, Niu H, Zheng C, Jing X, Qiao H, Wang G and Yang W (2023) Effect of multimodal chemotherapy on survival of gastric cancer with liver metastasis – a population based analysis.
Front. Oncol. 13:1064790.
doi: 10.3389/fonc.2023.1064790

COPYRIGHT
© 2023 Li, Chen, Zhang, Zhang, Niu, Zheng, Jing, Qiao, Wang and Yang. This is an open-access article distributed under the terms of the Creative Commons Attribution License (CC BY). The use, distribution or reproduction in other forums is permitted, provided the original author(s) and the copyright owner(s) are credited and that the original publication in this journal is cited, in accordance with accepted academic practice. No use, distribution or reproduction is permitted which does not comply with these terms.

Effect of multimodal chemotherapy on survival of gastric cancer with liver metastasis – a population based analysis

Xinghui Li[1†], Zhiqiang Chen[2†], Yue Zhang[1†], Hong Zhang[1], Haiyan Niu[3], Cheng Zheng[1], Xiaoying Jing[1], Hui Qiao[1], Guanhua Wang[1*] and Wenjun Yang[1,2,3*]

[1]Cancer Institute of the General Hospital, School of Public Health and Management, Ningxia Medical University, Yinchuan, Ningxia, China, [2]Department of Radiology, The First Affiliated Hospital, Hainan Medical University, Haikou, China, [3]Department of Pathology, The First Affiliated Hospital, Hainan Medical University, Haikou, China

Objectives: Limited efforts have been made to evaluate the effect of multimodal chemotherapy on the survival of gastric cancer patients with liver metastases (LMGC). This study aimed to identify prognostic factors in LMGC patients and the superiority of multimodal chemotherapy with respect to overall survival (OS) in these patients.

Methods: We conducted a retrospective cohort study of 1298 patients with M1 stage disease between January 2012 and December 2020. The effects of clinicopathological variables and preoperative chemotherapy (PECT), postoperative chemotherapy (POCT), and palliative chemotherapy on survival in patients with liver metastases (LM group) and non-liver metastases (non-LM group) were compared.

Results: Of the 1298 patients analysed, 546 (42.06%) were in the LM group and 752 (57.94%) were in the non-LM group. The median (interquartile range) age was 60 (51–66) years. The 1-year, 3-year and 5-year overall survival (OS) rates in the LM group were 29.3%, 13.9%, and 9.2%, respectively, and those in the non-LM group were. 38.2%, 17.4%, and 10.0%, respectively ($P < 0.05$, > 0.05, and > 0.05, respectively.) The Cox proportional hazards model revealed that palliative chemotherapy was a significant independent prognostic factor in both the LM and non-LM groups. Age ≥55 years, N stage, and Lauren classification were also independent predictors of OS in the LM group ($P < 0.05$). Palliative chemotherapy and POCT were associated with improved OS compared with PECT in the LM group (26.3% vs. 36.4% vs. 25.0%, $P < 0.001$).

Conclusion: LMGC patients had a worse prognosis than non- LMGC. Number of metastatic sites more than 1, liver and other metastatic sites, no CT treatment and HER2-negative had a poor prognosis. LMGC patient may benefit more from palliative chemotherapy and POCT than from PECT. Further well-designed, prospective studies are needed to validate these findings.

KEYWORDS

gastric cancer, liver metastases, preoperative chemotherapy, postoperative chemotherapy, palliative chemotherapy, overall survival, prognosis

1 Introduction

Gastric cancer (GC) is the fourth most common cause of cancer-related death worldwide, accounting for nearly 800,000 deaths in 2020; approximately 50% of these deaths (an estimated 373,789) occurred in China (1). The poor prognosis of GC is related to local recurrence, gross peritoneal dissemination, invasion of other organs, and extensive distant metastasis (2). With current treatment strategies, patients with localised disease usually have a good prognosis, but metastatic cancers are generally incurable because of their spread to distant locations, leaving patients with no chance of radical resection and only conservative medical treatment to control the progression of the disease (3). The median survival of Chinese patients with metastatic GC varies from 3.9 months to 18.4 months based on the metastatic location (4–8). Therefore, identifying the optimal therapies for patients with metastatic GC is still needed.

The liver is a frequent site of distant metastasis in GC, with an incidence of 5–34% (9, 10). Despite significant efforts to improve survival of patients with liver metastasis (LM), the prognosis remains poor. Therapeutic surgery provides a potential cure for liver metastasis from gastric cancer (LMGC); however, surgery is currently not a standard treatment option for patients with advanced GC other than palliative surgery for bleeding, obstruction, or perforation caused by the tumour. Therefore, palliative chemotherapy is still regarded as the standard treatment modality for patients with metastatic GC (11–13). The SOPP trial showed that S-1 plus oxaliplatin (SOX) regimen can be recommended as a first-line treatment for metastatic or recurrent GC, and the median OS can be extended to12.9 months (14). According to recent studies (15–17), the median survival of patients with LMGC who undergo systemic chemotherapy is between 7 and 14 months. However, there are currently no internationally approved standard adjuvant or palliative chemotherapy regimens for patients with advanced GC. The MAGIC trial explored the preoperative administration of epirubicin, cisplatin, and infused fluorouracil (ECF) in patients with resectable GC in the United Kingdom (18) and showed that patients receiving preoperative ECF had reduced tumour size and stage and improved overall survival (OS) compared to patients treated with surgery alone (5-year OS: 36.3% vs. 23.0%, P = 0.009). Therefore, perioperative chemotherapy (PECT) is the standard treatment strategy for patients with advanced GC in Europe and the United States. The CLASSIC trial conducted at 37 centres in South Korea, China, and Taiwan showed that postoperative capecitabine plus oxaliplatin (XELOX) regimen led to better disease-free survival (DFS) than gastrectomy alone (3-year DFS, 74.0% vs. 59.0%; P < 0.001) (19), which reinforces the efficacy of POCT in GC patients in East Asia (20, 21). SOX or XELOX regimen has been recommended as one of the standard perioperative chemotherapy regimens for advanced gastric cancer in China (22–24). Nevertheless, studies on PECT and PORT in Chinese GC patients with LM was limitied.

Multimodal chemotherapy is the preferred treatment for LMGC to improve survival. However, most studies have focused on the prognosis of patients with LMGC who also undergo hepatectomy, and there are no clinical trials or cohort studies on multimodal chemotherapy in LMGC. Therefore, predicting the prognosis of LMGC patients is difficult. We retrospectively analysed the clinicopathological and survival data of LMGC patients in the Ningxia region in China, which has a high incidence of GC. We aimed to assess the clinical features and prognostic factors of LMGC to aid in identifying the optimal chemotherapy treatment timing for these patients.

2 Materials and methods

2.1 Patient population

This retrospective study enrolled 1298 patients with metastatic GC from the General Hospital of Ningxia Medical University of Northwest China. The inclusion criteria were as follows (1): age ≥18 years (2) M1 stage GC diagnosed between 2012 and 2020, (3) diagnosed based on baseline radiological staging investigations, including computed tomography, performed following the initial diagnosis of GC by endoscopic biopsy and confirmed histologically, and (4) complete follow-up information. The exclusion criteria were as follows: (1) patients with duplicate numbers, (2) history of malignancy or complicating other tumours, (3) the site of metastasis was unknown. A flowchart of the patient selection

process is illustrated in Figure 1. The study protocol was approved by the Ethical Committee of Ningxia Medical University, and informed consent was obtained from all the patients.

2.2 Variables

The demographic variables included age at diagnosis, sex, occupation, ethnicity, medical insurance, smoking history, alcohol consumption, family history, and blood type. Clinicopathologic variables included TN stage, primary tumour site, tumour size, differentiation, pathological type, Lauren classification, number of metastatic sites, human epidermal growth factor receptor 2 (HER2) status, serum carcinoembryonic antigen (CEA), treatment method, and survival time in months. Ethnicity was classified as Han, Hui, or others; sex was recorded as male or female; and age was grouped as <55 years and ≥55 years. The primary tumour site was classified as the upper, middle, or lower stomach. The tumour size was classified as <7 cm or ≥7 cm. The differentiation was classified into three grades: high, medium, and low. The pathological type was classified as mucinous adenocarcinoma, glandular cancer, signet-ring cell carcinoma, or other. The Lauren classification was classified as intestinal, diffuse, or mixed type. HER2 status was assessed using *in situ* hybridisation (ISH) and immunohistochemistry (IHC). HER2 was considered positive if the IHC score was 3+ and negative if the score was 0 or 1+. IHC scores of 2+ were categorised as missing if ISH was not used to confirm the result. Treatment therapies were grouped as no chemotherapy (CT), preoperative chemotherapy (PECT), postoperative chemotherapy (POCT), and palliative chemotherapy (palliative CT). The cohort was divided into two metastatic groups based on the sites of metastasis at the initial presentation: the liver metastases (LM) group (n = 546) and the no liver metastases (non-LM) group (n = 752).

2.3 Follow-up

All data were obtained from the patients' medical records at the hospital. The survival information included survival status, date of death, and cause of death and was collected by telephone calls or text messages to patients or their family members. All cases were followed up in April 2021 within 2 weeks. Patients who could not be contacted after three tries or who had with incorrect phone numbers were considered lost to follow-up. Those who were lost to follow-up, alive, or died of other diseases at the end of follow-up were censored. The primary endpoint of this study was OS, which was defined as the time from the diagnosis of metastatic GC until death or the time of the last follow-up visit. Survival data were available for 558 (43.0%) patients, and follow-up information was available for 991 (76.3%) patients.

2.4 Statistical analysis

Descriptive statistics are presented as percentages and numerical statistics as medians. One-way analysis of variance and chi-square tests were used to compare differences in categorical variables between the groups. The Kaplan–Meier method was used to estimate OS, and the log-rank test was used to compare OS between groups. Cox regression analysis was used to calculate the hazard ratios and 95% confidence intervals (CIs) of covariates associated with OS. Factors with $P < 0.05$ in the univariate analysis were used to select covariates for the final multivariate models. Statistical significance was set at $P < 0.05$. Survival curves were plotted using GraphPad Prism (version 6.0; San Diego, California, USA). Forest plots were generated using the RMS package of R (version 4.1.0; R Foundation, Vienna, Austria). All other analyses were performed using SPSS statistical package (version 25.0; IBM Corporation, Armonk, NY, USA).

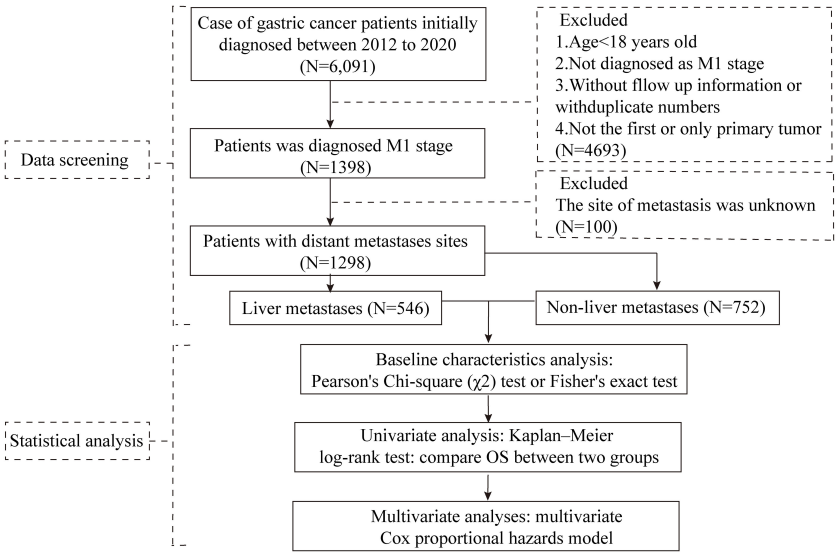

FIGURE 1
Schematic representation of the research process.

3 Results

3.1 Patient characteristics

The demographic and clinical characteristics of the patients are shown in Table 1.

A total of 1298 patients with M1 stage GC were selected according to the predefined inclusion and exclusion criteria, including 956 men (73.7%) and 342 women (23.6%). The median age was 60 years (interquartile range [IQR] 51-66) and the median follow-up time was 42 months (IQR 24-61). The main histological subtype is glandular cancer (88.6%). T3 and T4 is the most common clinical stage (92.9%), and most tumours have low differentiation (70.0%). 624 (48.1%) patients have a single organ site of metastases while 674 patients (51.9%) patients have multi-organ metastases. A total of 622 patients HER2 status was assessed, including 73 (11.1%) positive patients and 549 (88.3%) negative patients. Most patients received chemotherapy (63.4%), and 34.5% of patients received surgery plus chemotherapy. Among the patients who received chemotherapy (N = 823), 57 (4.4%), 391 (30.1%), and 375 (28.9%) received PECT, POCT, and palliative CT, respectively.

To explore the relationship between metastatic patterns and survival, we divided the patients based on the presence of LM, regardless of the number of metastatic sites. Of the 1298 patients, 546 had LM and 752 had non-LM. There are 404 (74.0%) patients aged >55 years in the LM group and 456 (60.6%) patients aged >55 years in the non-LM group. There are 449 (82.2%) men in the LM group and 507 (67.4%) men in the non-LM group. There are statistically significant differences in the distributions of age and sex between the LM and non-LM groups (all $P < 0.001$): patients in the LM group are more likely to be older and male than those in the non-LM group. In the LM group, 16 patients (2.9%) were treated with PECT, 140 (25.6%) were treated with POCT, and 196 (35.9%) were treated with palliative CT.

TABLE 1 Baseline patient characteristics.

Variables	No. (%) (n=1298)	LM (%) (n=546)	Non-LM (%) (n=752)	χ^2	*P*
Age (years)				25.232	<0.001
<55	438 (33.7)	142 (26.0)	296 (39.4)		
≥55	860 (66.3)	404 (74.0)	456 (60.6)		
Sex				35.773	<0.001
Male	956 (73.7)	449 (82.2)	507 (67.4)		
Female	342 (26.3)	97 (17.8)	245 (32.6)		
Ethnicity				15.967	<0.001
Han	1017 (78.4)	399 (73.1)	618 (82.2)		
Hui	265 (20.4)	140 (25.6)	125 (16.6)		
Others	16 (1.2)	7 (1.3)	9 (1.2)		
Occupation				5.853	0.119
Peasant	544 (41.9)	244 (44.7)	300 (39.9)		
Worker	322 (24.8)	140 (25.6)	182 (24.2)		
Others	168 (12.9)	61 (11.2)	107 (14.2)		
Unemployed	264 (20.3)	101 (18.5)	163 (21.7)		
BMI				15.450	<0.001
<18.5	205 (17.6)	72 (14.4)	133 (20.1)		
18.5~23	554 (47.6)	225 (44.9)	329 (49.6)		
≥23	405 (34.8)	204 (40.7)	201 (30.3)		
Cigarette smoking				4.954	0.026
No	784 (63.0)	310 (59.4)	474 (65.6)		
Yes	461 (37.0)	212 (40.6)	249 (34.4)		
Alcohol drinking				0.224	0.636
No	994 (79.9)	413 (79.3)	581 (80.4)		
Yes	250 (20.1)	108 (20.7)	142 (19.6)		
Family history				1.164	0.281

(Continued)

TABLE 1 Continued

Variables	No. (%) (n=1298)	LM (%) (n=546)	Non-LM (%) (n=752)	χ^2	*P*
No	1168 (94.1)	485 (93.3)	683 (94.7)		
Yes	73 (5.9)	35 (6.7)	38 (5.3)		
Blood type				0.368	0.947
A	260 (29.7)	106 (29.9)	154 (29.6)		
B	269 (30.7)	106 (29.9)	163 (31.3)		
AB	87 (9.9)	34 (9.6)	53 (10.2)		
O	259 (29.6)	108 (30.5)	151 (29.0)		
T Stage				3.498	0.174
T1~T2	43 (4.0)	21 (4.6)	22 (3.5)		
T3~T4	1011 (92.9)	421 (91.3)	590 (94.1)		
Tx	34 (3.1)	19 (4.1)	15 (2.4)		
N Stage				0.882	0.643
N0	55 (5.3)	23 (5.3)	32 (5.3)		
N1~ N3	618 (59.5)	252 (57.9)	366 (60.7)		
Nx	365 (35.2)	160 (36.8)	205 (34.0)		
Differentiation				23.170	<0.001
Low	691 (70.0)	268 (62.6)	423 (75.7)		
Medium	246 (24.9)	127 (29.7)	119 (21.3)		
High	50 (5.1)	33 (7.7)	17 (3.0)		
Pathological diagnosis				29.795	<0.001
Glandular cancer	900 (88.6)	392 (91.0)	508 (86.8)		
Mucinous adenocarcinoma	27 (2.7)	5 (1.2)	22 (3.8)		
Signet-ring cell carcinoma	52 (5.1)	9 (2.1)	43 (7.4)		
Others	37 (3.6)	25 (5.8)	12 (2.1)		
Primary tumor size				1.839	0.175
<7cm	206 (45.3)	77 (49.7)	129 (43.0)		
≥7cm	249 (54.7)	78 (50.3)	171 (57.0)		
Primary tumor site				3.340	0.188
Upper	277 (26.4)	121 (27.4)	156 (25.7)		
Middle	366 (34.9)	140 (31.7)	226 (37.2)		
Lower	406 (38.7)	180 (40.8)	226 (37.2)		
Lauren's type				12.131	0.002
Intestinal	122 (33.7)	67 (43.8)	55 (26.3)		
Diffuse	123 (34.0)	45 (29.4)	78 (37.3)		
Mixed	117 (32.3)	41 (26.8)	76 (36.4)		
Borrmann's type				7.762	0.051

(Continued)

TABLE 1 Continued

Variables	No. (%) (n=1298)	LM (%) (n=546)	Non-LM (%) (n=752)	χ^2	*P*
I	47 (8.2)	17 (7.9)	30 (8.5)		
II	48 (8.4)	19 (8.8)	29 (8.2)		
III	202 (35.4)	91 (42.1)	111 31.4)		
IV	273 (47.9)	89 (41.2)	184 (52.0)		
HER2				3.649	0.056
Negative	549 (88.3)	207 (85.2)	342 (90.2)		
Positive	73 (11.7)	36 (14.8)	37 (9.8)		
CEA				0.750	0.386
Negative	155 (26.7)	63 (28.8)	92 (25.5)		
Positive	425 (73.3)	156 (71.2)	269 (74.5)		
P53				2.046	0.153
Negative	108 (32.3)	44 (37.3)	64 (29.6)		
Positive	226 (67.7)	74 (62.7)	152 (70.4)		
Ki67				4.772	0.029
Low-expression	239 (40.4)	77 (34.7)	162 (43.8)		
High-expression	353 (59.6)	145 (65.3)	208 (56.2)		
EGFR				0.030	0.863
Low-expression	72 (29.1)	28 (29.8)	44 (28.8)		
High-expression	175 (70.9)	66 (70.2)	109 (71.2)		
VEGF				0.468	0.494
Low-expression	73 (31.1)	30 (33.7)	43 (29.5)		
High-expression	162 (68.9)	59 (66.3)	103 (70.5)		
Hp				0.933	0.334
Negative	213 (70.8)	105 (73.4)	108 (68.4)		
Positive	88 (29.2)	38 (26.6)	50 (31.6)		
Treatment				27.173	<0.001
No	475 (36.6)	194 (35.5)	281 (37.4)		
PECT	57 (4.4)	16 (2.9)	41 (5.5)		
POCT	391 (30.1)	140 (25.6)	251 (33.4)		
Palliative CT	375 (28.9)	196 (35.9)	179 (23.8)		
Number of metastasis sites				6.420	0.011
1	624 (48.1)	285 (52.2)	339 (45.1)		
>1	674 (51.9)	261 (47.8)	413 (54.9)		

GC, gastric cancer; LM, liver metastasis; PECT, preoperative chemotherapy; POCT, postoperative chemotherapy; CT, chemotherapy.

3.2 Survival analysis

The median OS of all patients was 12.0 months (95% CI 10.5–13.5) and the 1-year, 3-year and 5-year OS rates were 34.4%, 15.9% and 9.6%; the survival curves are shown in Figure 2A. The OS rates were 25.2% and 31.4% in the LM and non-LM groups, respectively ($P < 0.05$), and the corresponding median OS were 11.0 months (95% CI 9.2–12.8) and 14.0 months (95% CI 12.0–16.0),

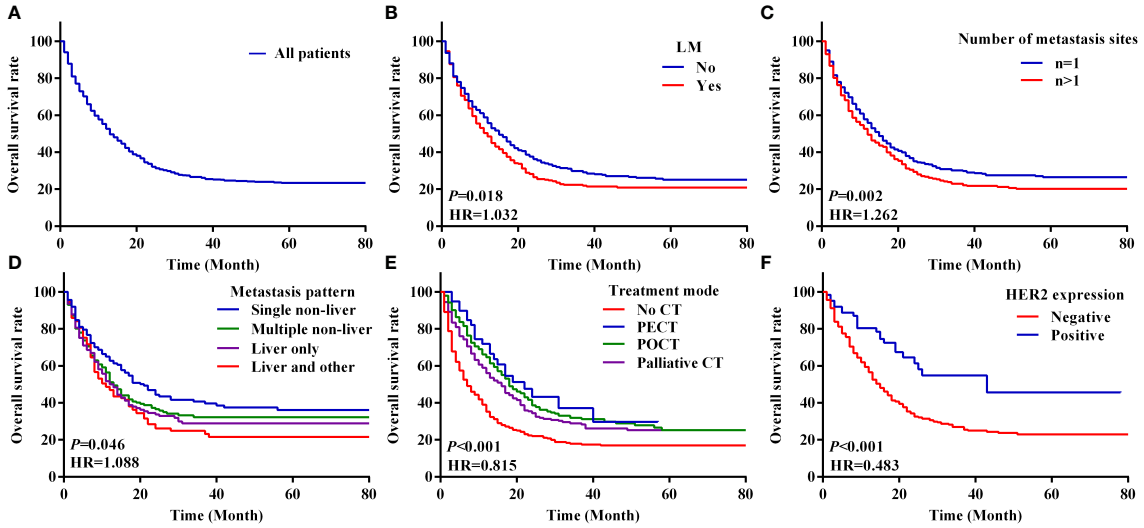

FIGURE 2
Kaplan–Meier analysis of survival curves based on clinical features with metastasis GC patients. **(A–F)** The overall survival curves of 1298 patients with M1 stage GC **(A)**, overall survival curves between the LM and non-LM groups **(B)**, number of metastasis sites of total patients **(C)**, metastasis pattern of total GC patients **(D)**, four modes of treatment **(E)**, overall survival curves between the HER2 negative and HER2 positive groups of metastasis GC patients **(F)**. LM, liver metastasis; PECT, preoperative chemotherapy; POCT, postoperative chemotherapy; CT, chemotherapy.

respectively (Figure 2B). The 1-year, 3-year and 5-year OS rates in the LM group were 29.3%, 13.9%, and 9.2%, respectively, and the corresponding rates in the non-LM group were 38.2%, 17.4%, and 10.0%, respectively ($P < 0.05$, > 0.05, and > 0.05, respectively) (Table 2). Patients with single-site metastases had better survival than those with multiple-site metastases ($P < 0.05$; Figure 2C). In the entire cohort, 282, 264, 339, and 413 patients have liver only, liver and other, single non-liver, and multiple non-liver metastases, respectively. The OS rates were 29.4% and 23.5% for the liver only and liver and other metastases groups, respectively, both of which were significantly lower than those of the single non-liver and multiple non-liver metastases groups (39.1% and 33.2%, respectively). Figure 2D shows the survival curves based on the metastatic pattern.

3.3 Effect of multimodal chemotherapy on survival in patients with LMGC

We analysed the survival of patients with metastatic GC based on their characteristics and treatment modality. The survival of patients with metastatic GC was significantly different based on the chemotherapy modality. The median OS of patients who received no CT, PECT, POCT, and palliative CT were 6.0 months (95% CI 4.7–7.3), 22.0 months (95% CI 13.4–30.6), 18.0 months (95% CI 15.0–21.0), and 15.0 months (95% CI 12.4–17.6), respectively ($P < 0.001$; Figure 2E). In the LM group, patients who underwent POCT had the highest survival rate (36.4%). However, in the non-LM group, patients who underwent PECT had the highest survival rate (51.9%), the survival curves are shown in Figure 3. Notably, HER2 positivity was associated with better OS than HER2 negativity; the corresponding median OS were 43.0 months (95% CI 13.1–72.9) and 14.0 months (95% CI 12.1–16.0), respectively (Figure 2F). The HER2 positivity rates were 6.6% (36/546) in the LM group and 4.9% (37/752) in the non-LM group. The OS of patients with HER2 positivity were 51.7% and 68.6% in the LM and non-LM groups, respectively ($P < 0.05$), the survival curves are shown in Figure S1.

3.4 Prognostic factors for OS in patients with LMGC

The results of the univariate analyses are shown in Table S1. Age, N stage, Lauren classification, and treatment mode are significant prognostic factors for OS in the LM group (all $P < 0.05$; Table S1). Age, HER2 expression, treatment mode, and number of metastatic sites are significant prognostic factors for OS in the non-LM group (all $P < 0.05$; Table S1). Significant variables ($P < 0.05$) associated with survival in the univariate analysis included in the multivariate Cox proportional hazards model. The results of the multivariate analyses are shown in Figure 4. The multivariate Cox proportional hazards model revealed that palliative CT is a significant independent prognostic factor in both the LM and non-LM groups; age ≥ 55 years, POCT, Nx stage, and mixde Lauren classification were independent predictors in the LM group, whereas PECT and HER2 positivity are independent predictors in the non-LM group. Receiver operating characteristic (ROC) was used to evaluate the accuracy of survival model, AUC=0.723, shown in Figure S2.

4 Discussion

In the present study, we retrospectively collected data of 1298 patients with M1 stage GC: 546 (42.06%) in the LM group and 752 (57.94%) in the non-LM group. All patients were from the Ningxia

TABLE 2 The OS of the LM and Non-LM of GC patients.

OS	LM (%)	Non-LM (%)	*P*
1-year	29.3	38.2	0.022
3-year	13.9	17.4	0.145
5-year	9.2	10.0	0.289
Total	25.2	31.4	0.015

GC, gastric cancer; LM, liver metastasis; OS, overall survival.

region in northwest China, which has a high incidence of GC. The median OS of all patients was 12 months, which was consistent with data from previous reports (median OS of 3.9–18.4 months) (4–8). Our analysis further showed that the 5-year survival rate (5ySR) of the LM group was slightly lower than that of the non-LM group (9.2% vs. 10.0%), whereas the median survival time was much lower in the LM group than in the non-LM group (11 months vs. 14 months). The 5ySR of patients with LMGC in our study is much lower than that observed in previous studies examining LMGC patients from Beijing or Japan (9.2%, 12.2%, and 31.1%, respectively) (25, 26).

Several reports, including ours, have demonstrated that old age, Lauren classification, submucosal invasion, vascular involvement, lymph node metastasis, tumour differentiation, the number of LMs, and tumour size are significant factors influencing the prognosis of patients with LMGC (27–30). In the present study, we also identified POCT and palliative chemotherapy as independent prognostic factors for patients with LMGC. Compared with those receiving PECT, GC patients with LM who received POCT and palliative chemotherapy had improved survival outcomes (25.0% vs. 36.4% vs. 26.3%, $P < 0.001$). Palliative chemotherapy is currently the most common treatment option for LMGC, and the global standard for first-line chemotherapy is 5-fluorouracil- and cisplatin-based combinations. These chemotherapies have response rates of approximately 30-40% and a median OS of 9-11 months (31), which is lower than the median OS of 15 months in LMGC patients who received palliative chemotherapy in our study. The MAGIC trial included 503 GC patients and showed that POCT after R0 resection reduced tumour size and stage, significantly improved progression-free survival and OS, and increased the 5ySR by 13%. Therefore, POCT has been clinically considered for patients with advanced GC (32). In our study, the proportions of patients receiving PECT, POCT, and palliative chemotherapy were 3.9%, 20.4%, and 34.6%, respectively. All three modes of chemotherapy improved survival in patients with LMGC compared with those who did not receive chemotherapy, and those who received POCT had the best OS (36.4%). Moreover, with the exception of palliative chemotherapy and PECT, there was no effect on the outcomes of patients without LM, which may be due to the large proportion of patients (15.2%) with more severe peritoneal metastases, which offset the effects of chemotherapy in the non-LM group. Therefore, further prospective controlled trials are needed to investigate whether palliative chemotherapy and POCT have a survival advantage in patients with metastatic GC, especially LMGC.

Some studies have demonstrated that PECT can reduce the staging of the primary tumour, increase the possibility and efficacy of radical resection, eliminate micrometastases, and prevent or reduce tumour recurrence and metastasis in GC patients (33–35). However, the survival time of patients with LMGC did not increase with PECT in our study. The reasons for the ineffectiveness of PECT in patients with LMGC are manifold. First, gastrointestinal cancers are drained by the enterohepatic circulation, reaching the liver first, which provides a rich vascular system and sufficient nutrients for the expansive growth of tumour cells (36–38). However, the majority of chemotherapeutic drugs enter the liver through the portal vein, and liver metastases affect local drug metabolism (39). Second, LMGC patients may be less responsive to chemotherapy due to the prolonged doubling time of tumour cells, and they may be unable to tolerate adequate amounts of chemotherapy drugs (40). Last, the liver microenvironment triggers inflammation, promotes angiogenesis, and enhances permeability; therefore, PECT may not be a safe and effective intervention (41). However, these speculations are based on results derived from retrospective dataset analyses involving patients with LMGC and need to be confirmed prospectively.

The results of this study support the addition of adjuvant chemotherapy to improve OS in patients with LMGC. However, this is limited to POCT, as PECT had no survival benefit. We hope that adjuvant chemotherapy can be considered as an additional

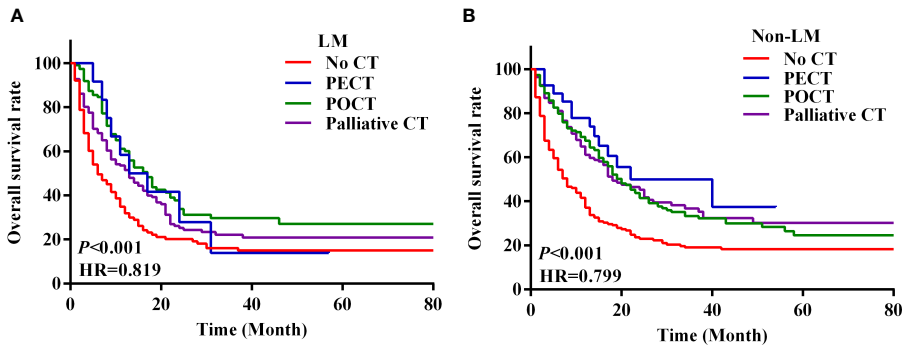

FIGURE 3
Survival curves of LM and non-LM patients with four treatment modalities. **(A, B)** Survival curves of 546 LM patients with four modes of treatment **(A)**, survival curves of 752 non-LM patients with four modes of treatment **(B)**. PECT, preoperative chemotherapy; POCT, postoperative chemotherapy; CT, chemotherapy.

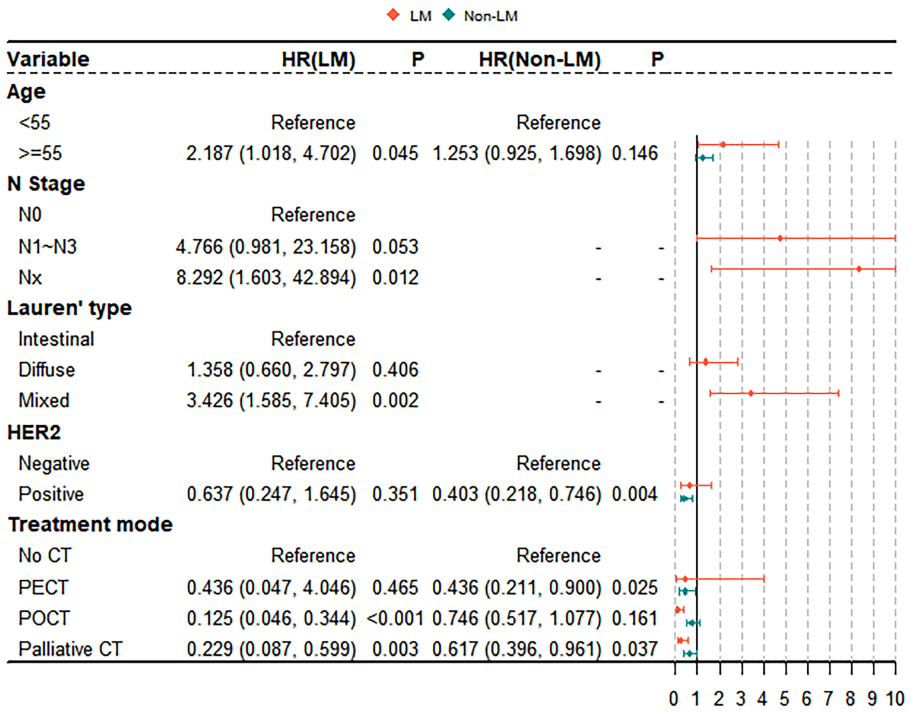

FIGURE 4
Multivariable Cox proportional hazards model for analyzing the prognostic factors for metastasis GC patients.

therapy for patients with LMGC in the hands of rigorous surgeons and wise oncologists. Our findings, while not prospective, provide compelling motivation to explore the potential benefits of multimodal chemotherapy in patients with LMGC in randomised clinical trials.

The limitations of this study should be considered when interpreting the results. First, all participants came from one region, and the cohort may not be representative of all GC patients in China. Second, the study reviewed eight years of clinical data on patients with LMGC who received any combination of chemotherapy (administered orally, intravenously, or intraperitoneally). Patients were given SOX or XELOX perioperative chemotherapy regiments, which was divided into 2–4 cycles, the evaluation results may be biased. Therefore, further investigation in multiple populations is required. Third, the results are dependent on the quality of data collection. In addition, there were only 57 LMGC patients in the PECT group, and the conclusion that PECT has no prognostic significance in patients with LMGC needs to be verified in larger studies.

In conclusion, this study collected 1298 patients with metastatic GC from a high GC incidence area in China, examined a variety of clinical characteristics to construct a Cox proportional hazards model, and systematically evaluated the prognostic factors that may affect patients with LMGC. Our study revealed that LMGC patients had a worse prognosis than non- LMGC. Number of metastatic sites more than 1, liver and other metastatic sites, no CT treatment and HER2-negative were all unfavorable factors to the survival of LMGC. LMGC patients who received palliative chemotherapy and POCT had significantly better survival than those who received PECT. These prognostic factors can help clinicians and patients quantify the benefits of adjuvant therapy for LMGC and make individualised treatment recommendations and decisions.

Data availability statement

The original contributions presented in the study are included in the article/Supplementary Material. Further inquiries can be directed to the corresponding authors.

Ethics statement

The studies involving human participants were reviewed and approved by Ningxia Medical University. The patients/participants provided their written informed consent to participate in this study.

Author contributions

All the authors were involved in the design of the study or in the explanation of the data. XL, ZC and YZ together collected the data of the patients, and sorted out, analyzed and evaluated the quality of the data, which was checked by GW and WY. ZC and YZ contributed to the analysis and write-up of findings. XL wrote the first draft of the manuscript. CZ and HZ contributed to the methodology. HN, HQ and XJ contributed to proofread the article. All authors contributed to the article and approved the submitted version.

Funding

This work was supported by grants from National Natural Science Foundation of China (No. 82160535 and 81760525), National Natural Science Foundation of Ningxia (No. 2022AAC03544 and 2022AAC03130), and partly from Hainan Province Clinical Medical Center.

Conflict of interest

The authors declare that the research was conducted in the absence of any commercial or financial relationships that could be construed as a potential conflict of interest.

Publisher's note

All claims expressed in this article are solely those of the authors and do not necessarily represent those of their affiliated organizations, or those of the publisher, the editors and the reviewers. Any product that may be evaluated in this article, or claim that may be made by its manufacturer, is not guaranteed or endorsed by the publisher.

Supplementary material

The Supplementary Material for this article can be found online at: https://www.frontiersin.org/articles/10.3389/fonc.2023.1064790/full#supplementary-material

References

1. Sung H, Ferlay J, Siegel RL, Laversanne M, Soerjomataram I, Jemal A, et al. Global cancer statistics 2020: GLOBOCAN estimates of incidence and mortality worldwide for 36 cancers in 185 countries. *CA Cancer J Clin* (2021) 71(3):209–49. doi: 10.3322/caac.21660

2. Global Burden of Disease Cancer C, Fitzmaurice C, Allen C, Barber RM, Barregard L, Bhutta ZA, et al. Global, regional, and national cancer incidence, mortality, years of life lost, years lived with disability, and disability-adjusted life-years for 32 cancer groups, 1990 to 2015: A systematic analysis for the global burden of disease study. *JAMA Oncol* (2017) 3(4):524–48. doi: 10.1001/jamaoncol.2016.5688

3. Stoletov K, Beatty PH, Lewis JD. Novel therapeutic targets for cancer metastasis. *Expert Rev Anticancer Ther* (2020) 20(2):97–109. doi: 10.1080/14737140.2020.1718496

4. Yang LP, Wang ZX, He MM, Wu HX, Yuan SQ, Wang W, et al. A real-world evidence of efficacy of palliative gastrectomy plus chemotherapy in metastatic gastric cancer patients. *Cancer Manag Res* (2019) 11:3993–4003. doi: 10.2147/CMAR.S197052

5. Zheng H, Zhao Y, He Q, Hao H, Tian Y, Zou B, et al. Multi-institutional development and validation of a nomogram to predict recurrence after curative resection of gastric neuroendocrine/mixed adenoneuroendocrine carcinoma. *Gastric Cancer.* (2021) 24(2):503–14. doi: 10.1007/s10120-020-01119-8

6. Zhao L, Li J, Bai C, Nie Y, Lin G. Multi-modality treatment for patients with metastatic gastric cancer: A real-world study in China. *Front Oncol* (2019) 9:1155. doi: 10.3389/fonc.2019.01155

7. Song JC, Ding XL, Zhang Y, Zhang X, Sun XH. Prospective and prognostic factors for hepatic metastasis of gastric carcinoma: A retrospective analysis. *J Cancer Res Ther* (2019) 15(2):298–304. doi: 10.4103/jcrt.JCRT_576_17

8. Hu HM, Tsai HJ, Ku HY, Lo SS, Shan YS, Chang HC, et al. Survival outcomes of management in metastatic gastric adenocarcinoma patients. *Sci Rep* (2021) 11 (1):23142. doi: 10.1038/s41598-021-02391-z

9. Ohno S, Fujii T, Ueda S, Nakamoto T, Kinugasa S, Yoshimura H, et al. Predictive factors and timing for liver recurrence after curative resection of gastric carcinoma. *Am J Surg* (2003) 185(3):258–63. doi: 10.1016/s0002-9610(02)01377-6

10. Kawahara K, Makino H, Kametaka H, Hoshino I, Fukada T, Seike K, et al. Outcomes of surgical resection for gastric cancer liver metastases: A retrospective analysis. *World J Surg Oncol* (2020) 18(1):41. doi: 10.1186/s12957-020-01816-9

11. Joshi SS, Badgwell BD. Current treatment and recent progress in gastric cancer. *CA Cancer J Clin* (2021) 71(3):264–79. doi: 10.3322/caac.21657

12. Fokter-Dovnik N, Smyth EC. More is not always better: Triplet chemotherapy and advanced gastric cancer. *Lancet Gastroenterol Hepatol* (2019) 4(7):490–1. doi: 10.1016/S2468-1253(19)30145-1

13. Tokunaga M, Sato Y, Nakagawa M, Aburatani T, Matsuyama T, Nakajima Y, et al. Perioperative chemotherapy for locally advanced gastric cancer in Japan: current and future perspectives. *Surg Today* (2020) 50(1):30–7. doi: 10.1007/s00595-019-01896-5

14. Lee KW, Chung IJ, Ryu MH, Park YI, Nam BH, Oh HS, et al. Multicenter phase III trial of s-1 and cisplatin versus s-1 and oxaliplatin combination chemotherapy for first-line treatment of advanced gastric cancer (SOPP trial). *Gastric Cancer.* (2021) 24 (1):156–67. doi: 10.1007/s10120-020-01101-4

15. Kang YK, Boku N, Satoh T, Ryu MH, Chao Y, Kato K, et al. Nivolumab in patients with advanced gastric or gastro-oesophageal junction cancer refractory to, or intolerant of, at least two previous chemotherapy regimens (ONO-4538-12, ATTRACTION-2): a randomised, double-blind, placebo-controlled, phase 3 trial. *Lancet* (2017) 390(10111):2461–71. doi: 10.1016/S0140-6736(17)31827-5

16. Koizumi W, Narahara H, Hara T, Takagane A, Akiya T, Takagi M, et al. S-1 plus cisplatin versus s-1 alone for first-line treatment of advanced gastric cancer (SPIRITS trial): a phase III trial. *Lancet Oncol* (2008) 9(3):215–21. doi: 10.1016/S1470-2045(08)70035-4

17. Granieri S, Altomare M, Bruno F, Paleino S, Bonomi A, Germini A, et al. Surgical treatment of gastric cancer liver metastases: Systematic review and meta-analysis of long-term outcomes and prognostic factors. *Crit Rev Oncol Hematol* (2021) 163:103313. doi: 10.1016/j.critrevonc.2021.103313

18. Smyth EC, Wotherspoon A, Peckitt C, Gonzalez D, Hulkki-Wilson S, Eltahir Z, et al. Mismatch repair deficiency, microsatellite instability, and survival: An exploratory analysis of the medical research council adjuvant gastric infusional chemotherapy (MAGIC) trial. *JAMA Oncol* (2017) 3(9):1197–203. doi: 10.1001/jamaoncol.2016.6762

19. Bang YJ, Kim YW, Yang HK, Chung HC, Park YK, Lee KH, et al. Adjuvant capecitabine and oxaliplatin for gastric cancer after D2 gastrectomy (CLASSIC): a phase 3 open-label, randomised controlled trial. *Lancet* (2012) 379(9813):315–21. doi: 10.1016/S0140-6736(11)61873-4

20. Pavel M, Oberg K, Falconi M, Krenning EP, Sundin A, Perren A, et al. Gastroenteropancreatic neuroendocrine neoplasms: ESMO clinical practice guidelines for diagnosis, treatment and follow-up. *Ann Oncol* (2020) 31(7):844–60. doi: 10.1016/j.annonc.2020.03.304

21. Ajani JA, D'Amico TA, Almhanna K, Bentrem DJ, Chao J, Das P, et al. Gastric cancer, version 3.2016, NCCN clinical practice guidelines in oncology. *J Natl Compr Canc Netw* (2016) 14(10):1286–312. doi: 10.6004/jnccn.2016.0137

22. Cunningham D, Starling N, Rao S, Iveson T, Nicolson M, Coxon F, et al. Capecitabine and oxaliplatin for advanced esophagogastric cancer. *N Engl J Med* (2008) 358(1):36–46. doi: 10.1056/NEJMoa073149

23. Li T, Chen L. [Efficacy and safety of SOX regimen as neoadjuvant chemotherapy for advanced gastric cancer]. *Zhonghua Wei Chang Wai Ke Za Zhi.* (2011) 14(2):104–6.

24. Wang FH, Shen L, Li J, Zhou ZW, Liang H, Zhang XT, et al. The Chinese society of clinical oncology (CSCO): clinical guidelines for the diagnosis and treatment of gastric cancer. *Cancer Commun (Lond).* (2019) 39(1):10. doi: 10.1186/s40880-019-0349-9

25. Li J, Zhang K, Gao Y, Xi H, Cui J, Liang W, et al. Evaluation of hepatectomy and palliative local treatments for gastric cancer patients with liver metastases: A propensity score matching analysis. *Oncotarget* (2017) 8(37):61861–75. doi: 10.18632/oncotarget.18709

26. Kinoshita T, Kinoshita T, Saiura A, Esaki M, Sakamoto H, Yamanaka T. Multicentre analysis of long-term outcome after surgical resection for gastric cancer liver metastases. *Br J Surg* (2015) 102(1):102–7. doi: 10.1002/bjs.9684

27. Lin Z, Wang R, Zhou Y, Wang Q, Yang CY, Hao BC, et al. Prediction of distant metastasis and survival prediction of gastric cancer patients with metastasis to the liver, lung, bone, and brain: Research based on the SEER database. *Ann Transl Med* (2022) 10 (1):16. doi: 10.21037/atm-21-6295

28. Uggeri F, Ripamonti L, Pinotti E, Scotti MA, Famularo S, Garancini M, et al. Is there a role for treatment-oriented surgery in liver metastases from gastric cancer? *World J Clin Oncol* (2020) 11(7):477–94. doi: 10.5306/wjco.v11.i7.477

29. Kiyasu Y. Long-term recurrence-free survival after metachronous surgery of the stomach and liver for gastric adenocarcinoma and multiple, synchronous liver metastases: a case report and review of literature. *Int Surg* (2013) 98(3):241–6. doi: 10.9738/INTSURG-D-12-00015.1

30. Koemans WJ, Luijten J, van der Kaaij RT, Grootscholten C, Snaebjornsson P, Verhoeven RHA, et al. The metastatic pattern of intestinal and diffuse type gastric carcinoma - a Dutch national cohort study. *Cancer Epidemiol.* (2020) 69:101846. doi: 10.1016/j.canep.2020.101846

31. Kataoka K, Kinoshita T, Moehler M, Mauer M, Shitara K, Wagner AD, et al. Current management of liver metastases from gastric cancer: what is common practice? new challenge of EORTC and JCOG. *Gastric Cancer* (2017) 20(5):904–12. doi: 10.1007/s10120-017-0696-7

32. Smyth EC, Fassan M, Cunningham D, Allum WH, Okines AF, Lampis A, et al. Effect of pathologic tumor response and nodal status on survival in the medical research council adjuvant gastric infusional chemotherapy trial. *J Clin Oncol* (2016) 34 (23):2721–7. doi: 10.1200/JCO.2015.65.7692

33. Markar SR, Mackenzie H, Mikhail S, Mughal M, Preston SR, Maynard ND, et al. Surgical resection of hepatic metastases from gastric cancer: Outcomes from national series in England. *Gastric Cancer.* (2017) 20(2):379–86. doi: 10.1007/s10120-016-0604-6

34. Brodt P. Role of the microenvironment in liver metastasis: From pre- to prometastatic niches. *Clin Cancer Res* (2016) 22(24):5971–82. doi: 10.1158/1078-0432.CCR-16-0460

35. Zhang F, Huang X, Song Y, Gao P, Zhou C, Guo Z, et al. Conversion surgery for stage IV gastric cancer. *Front Oncol* (2019) 9:1158. doi: 10.3389/fonc.2019.01158

36. Fujitani K, Kurokawa Y, Takeno A, Kawabata R, Omori T, Imamura H, et al. Prospective multicenter interventional study of surgical resection for liver metastasis from gastric cancer: R0 resection rate, and operative morbidity and mortality. *Ann Surg Oncol* (2022) 29(2):924–32. doi: 10.1245/s10434-021-10750-3

37. Sugawara K, Kawaguchi Y, Seto Y, Vauthey JN. Multidisciplinary treatment strategy for locally advanced gastric cancer: A systematic review. *Surg Oncol* (2021) 38:101599. doi: 10.1016/j.suronc.2021.101599

38. Obenauf AC, Massague J. Surviving at a distance: Organ-specific metastasis. *Trends Cancer.* (2015) 1(1):76–91. doi: 10.1016/j.trecan.2015.07.009

39. Schuhmacher C, Gretschel S, Lordick F, Reichardt P, Hohenberger W, Eisenberger CF, et al. Neoadjuvant chemotherapy compared with surgery alone for locally advanced cancer of the stomach and cardia: European organisation for research and treatment of cancer randomized trial 40954. *J Clin Oncol* (2010) 28(35):5210–8. doi: 10.1200/JCO.2009.26.6114

40. Cunningham D, Allum WH, Stenning SP, Thompson JN, Van de Velde CJ, Nicolson M, et al. Perioperative chemotherapy versus surgery alone for resectable gastroesophageal cancer. *N Engl J Med* (2006) 355(1):11–20. doi: 10.1056/NEJMoa055531

41. Chambers AF, Groom AC, MacDonald IC. Dissemination and growth of cancer cells in metastatic sites. *Nat Rev Cancer.* (2002) 2(8):563–72. doi: 10.1038/nrc865

frontiers | Frontiers in Oncology

TYPE Original Research
PUBLISHED 17 March 2023
DOI 10.3389/fonc.2023.1062142

Check for updates

OPEN ACCESS

EDITED BY
Zhendong Jin,
Second Military Medical University, China

REVIEWED BY
Arda Isik,
Istanbul Medeniyet University, Türkiye
Yu Fan,
Jiangsu University Affiliated People's Hospital, China

*CORRESPONDENCE
Xiao Chen
chenxiaomd@163.com
Wenjie Wang
sciencedoctor@126.com

†These authors have contributed equally to this work and share first authorship

SPECIALTY SECTION
This article was submitted to Gastrointestinal Cancers: Gastric and Esophageal Cancers, a section of the journal Frontiers in Oncology

RECEIVED 05 October 2022
ACCEPTED 06 March 2023
PUBLISHED 17 March 2023

CITATION
Li J, Cui T, Huang Z, Mu Y, Yao Y, Xu W, Chen K, Liu H, Wang W and Chen X (2023) Analysis of risk factors for lymph node metastasis and prognosis study in patients with early gastric cancer: A SEER data-based study.
Front. Oncol. 13:1062142.
doi: 10.3389/fonc.2023.1062142

COPYRIGHT
© 2023 Li, Cui, Huang, Mu, Yao, Xu, Chen, Liu, Wang and Chen. This is an open-access article distributed under the terms of the Creative Commons Attribution License (CC BY). The use, distribution or reproduction in other forums is permitted, provided the original author(s) and the copyright owner(s) are credited and that the original publication in this journal is cited, in accordance with accepted academic practice. No use, distribution or reproduction is permitted which does not comply with these terms.

Analysis of risk factors for lymph node metastasis and prognosis study in patients with early gastric cancer: A SEER data-based study

Jinzhou Li[1†], Ting Cui[1†], Zeping Huang[2†], Yanxi Mu[1], Yalong Yao[1], Wei Xu[1], Kang Chen[2], Haipeng Liu[2], Wenjie Wang[2*] and Xiao Chen[2*]

[1]The Second Clinical Medical College, Lanzhou University, Lanzhou, China, [2]Department of General Surgery, The Second Hospital of Lanzhou University, Lanzhou, China

Background: Lymph node status is an important factor in determining the prognosis of patients with early gastric cancer (EGC) and preoperative diagnosis of lymph node metastasis (LNM) has some limitations. This study explored the risk factors and independent prognostic factors of LNM in EGC patients and constructed a clinical prediction model to predict LNM.

Methods: Clinicopathological data of EGC patients was collected from the public Surveillance, Epidemiology, and End Results (SEER) database. Univariate and multivariate logistic regression was used to identify risk factors for LNM in EGC patients. The performance of the LNM model was evaluated by C-index, calibration curve, receiver operating characteristic (ROC) curve, decision curve analysis (DCA) curve, and clinical impact curve (CIC) based on the results of multivariate regression to develop a nomogram. An independent data set was obtained from China for external validation. The Kaplan-Meier method and Cox regression model were used to identify potential prognostic factors for overall survival (OS) in EGC patients.

Results: A total of 3993 EGC patients were randomly allocated to a training cohort (n=2797) and a validation cohort (n=1196). An external cohort of 106 patients from the Second Hospital of Lanzhou University was used for external validation. Univariate and multivariate logistic regression showed that age, tumor size, differentiation, and examined lymph nodes count (ELNC) were independent risk factors for LNM. Nomogram for predicting LNM in EGC patients was developed and validated. The predictive model had a good discriminatory performance with a concordance index (C-index) of 0.702 (95% CI: 0.679-0.725). The calibration plots showed that the predicted LNM probabilities were the same as the actual observations in both the internal validation cohort and external validation cohort. The AUC values for the training cohort, internal validation cohort and external validation cohort were 0.702 (95% CI: 0.679-0.725), 0.709 (95% CI: 0.674-0.744) and 0.750(95% CI: 0.607-0.892), respectively, and the DCA curves and CIC showed good clinical applicability. The Cox regression model identified age, sex, race, primary site, size, pathological type, LNM, distant metastasis, and ELNC were prognostic factors for OS in EGC patients, while a year at diagnosis, grade, marital status, radiotherapy, and chemotherapy were not independent prognostic factors.

Conclusion: In this study, we identified risk factors and independent prognostic factors for the development of LNM in EGC patients, and developed a relatively accurate model to predict the development of LNM in EGC patients.

KEYWORDS

early gastric cancer, lymph node metastasis, prognosis, nomogram, SEER

1 Introduction

Gastric cancer remains important cancer worldwide and is responsible for over one million new cases in 2020 and an estimated 769,000 deaths, ranking fifth for incidence and fourth for mortality globally (1). In recent years, the diagnosis of early gastric cancer (EGC) has rapidly increased due to improvements in universal screening and endoscopic techniques. According to the staging manual jointly developed by the American Joint Committee on Cancer (AJCC) and the International Union Against Cancer (UICC), EGC is defined as a superficial gastric lesion confined to the mucosa (T1a) and submucosa (T1b), regardless of the lymph node status (2). EGC accounts for more than 50% of total cases in Japan and Korea, whereas in Western countries, it accounts for only about 20% (3).

In general, endoscopic resections, such as endoscopic mucosal resection (EMR) and endoscopic submucosal dissection (ESD), can be performed when the likelihood of lymph node metastasis (LNM) is minimal and the size and location of the lesion allow for whole-block resection (4). Lesions are considered absolute indications for endoscopic therapy if they are presupposed to have a <1% risk of LNM (5). EGC progresses slowly, but approximately 20% of patients with EGC develop LNM (6). LNM is an independent risk factor affecting the prognosis of patients with EGC and determining the extent of lymph node dissection (7). The 2018 edition of the Chinese guidelines for the management of gastric cancer states that gastrectomy combined with lymph node dissection remains the primary treatment for patients with EGC with LNM (8). However, in some cases, the occurrence of LNM in EGC patients cannot be identified, resulting in receiving unreasonable endoscopic treatment. For patients with EGC who develop distant metastases, the Japanese guidelines for gastric cancer recommend systemic therapy (9). However, due to the limited number of cases, the main risk factors and prognostic factors for LNM in EGC patients have not been well studied. Therefore, the prediction of the risk of LNM in EGC and the identification of prognostic factors are important prerequisites and bases to guide the rational clinical selection of treatment modalities and improve survival.

To date, several studies have identified some clinicopathological features of EGC as risk factors for predicting LNM, such as age, tumor size, lymphatic invasion, depth of invasion, grade, and intestinal type associated with LNM (10–13), and corresponding predictive models, including nomograms and scoring systems, have been developed to provide evidence for clinical decision-making, but there is still no consensus on their applicability to the clinic.

The nomogram is widely used for cancer prognosis, mainly because of its ability to reduce statistical prediction models to single-digit estimates of the probability of an event (death or recurrence) (14). Therefore, a nomogram for preoperative assessment of the risk of LNM in EGC can help clinicians choose appropriate treatment modalities. Cox regression analysis can identify risk factors associated with prognosis and may help patients and physicians in various aspects of decision-making.

In this study, using the SEER database, the clinicopathological characteristics of EGC patients with and without LNM were first compared. Logistic regression analysis was then used to identify risk factors associated with LNM. A Cox proportional hazards model was further employed to identify risk factors associated with the prognosis of EGC patients. The results of this population-based study will help improve the management of patients with EGC.

2 Methods

2.1 Ethics approval and consent to participate

The study was a retrospective study based on the SEER database. The authors obtained authorization to exact and analyze the research data stored in the SEER program from the National Cancer Institute, USA (reference number 19369-Nov2021). All procedures followed were in accordance with the Declaration of Helsinki and subsequent versions, and were approved by the Ethics Committee of the Second Hospital of Lanzhou University (approval number: 2022A-623).

2.2 Data sources and population selection

Clinical data of EGC patients in the SEER database were collected using SEER*Stat software (version 8.3.9; www.seer.cancer.gov) and using personal ID (account number: 12145-Nov2020). Since the SEER database is public, informed consent is not required, therefore, this study was exempted from review by the ethics committee of our institution (15).

Gastric cancer (C16.0-16.9) patients were identified from the SEER database according to the website recoding classification. And 106 patients from the Second Hospital of Lanzhou University who

underwent gastric surgery from January 2015 to December 2017. The inclusion criteria used in this study were as follows: (1) Year of diagnosis: January 2004 to December 2015; (2) Histopathologically confirmed and only one primary tumor was gastric cancer; (3) Age > 18 years old; (4) The postoperative pathological stage was: T1N0-3M0-1. Exclusion criteria: (1) unknown ethnicity; (2) unknown tumor size; (3) unknown degree of differentiation; (4) ELNC was not recorded or unclear; (5) survival time was not recorded or survival time after diagnosis was less than 1 month. The process of patient screening is shown in Figure 1 and Figure 2. Patients from the SEER database were randomized into a training cohort and an internal validation cohort. The training cohort included 2,797 patients, while the internal validation cohort included 1,196 patients and 106 patients (the Second Hospital of Lanzhou University). The primary clinical endpoint was OS.

This study was based on public data from the SEER database without interacting with human subjects or using personal identifying information. This research was therefore exempted from review by the Human Subjects Committee of Institutional Review Board of the Second Hospital of Lanzhou University.

2.3 Variables and outcomes

The following variables were collected: year at diagnosis (2004-2007, 2008-2011, 2012-2015), age (≤70 years, >70 years), sex, marital status (married, other), race (white, black, other races), tumor size (1-10mm, 11-20mm, 21-30mm, >30mm). Histological types were classified using the coding pattern of the ICD-O-3 (International Classification of Diseases in Oncology, Third Edition) (16), adenocarcinomas (8140, 8143-8144, 8210-8211, 8255, 8260-8263, 8310, 8323, 8480-8481, 8574, 8576), signet ring cell carcinoma (8490) and others. Grade (grade I: well differentiated, grade II: moderately differentiated, grade III: poorly differentiated, grade IV: undifferentiated), primary site (cardia: C16.0-cardia; non-cardia: C16.1-stomach bottom, C16.2-body, C16.3-gastric antrum, C16.4-pylorus, C16.5-lesser curvature, C16.6-lesser curvature, C16.8-overlapping lesions of the stomach). The optimal cut-off value of the ELNC by X-tile software (≤11, >11), and the TNM staging were restaged according to the 8th edition of the AJCC/UICC guidelines (N0, non-N0: N1, N2, N3). Treatment-related included radiotherapy (yes, no/unknown), chemotherapy (yes, no/unknown), and surgery (yes, no/unknown). Overall survival (OS) was interpreted as the period from the date of diagnosis to the last follow-up or death from any cause.

2.4 Statistical methods

The patients in the database were randomly divided into the training cohort and validation cohort in a ratio of 7:3. The training cohort is used for model development, and the validation cohort is used for evaluation and validation. The optimal cutoff value of ELNC associated with LNM was calculated using X-tile software. The basic characteristics of the included patients were described by number and percentage (n, %). Each variable's contribution in predicting LNM of EGC in the training cohort was tested by univariate logistic analysis. Variables that were statistically significant were further analyzed by multivariate logistic regression. The odds ratios (OR) with corresponding 95% confidence interval (CI) was calculated. Risk factors which were statistically significant in the multivariate analysis were used to construct a predictive nomogram to predict the LNM. Nomogram performance was evaluated with respect to discrimination and calibration. For discrimination ability, the nomogram was evaluated using the area under the receiver operating characteristic (ROC) curve (AUC). Calibration curves were plotted to verify the accuracy and reliability of the nomogram. Internal and external validations were performed to validate the nomogram. Moreover, decision curve analysis (DCA) was plotted to measure the applicability of the nomogram to clinical practice. After exploring the

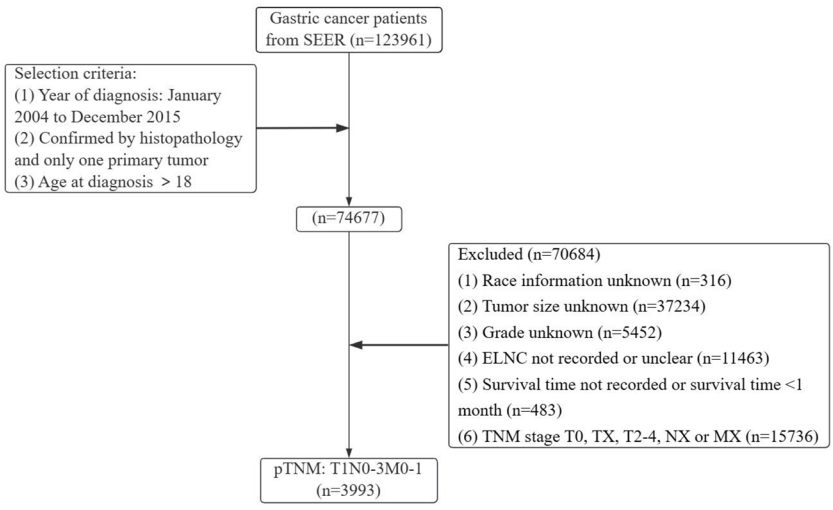

FIGURE 1
Flow chart of the patient screening process in the Surveillance, Epidemiology, and End Results.

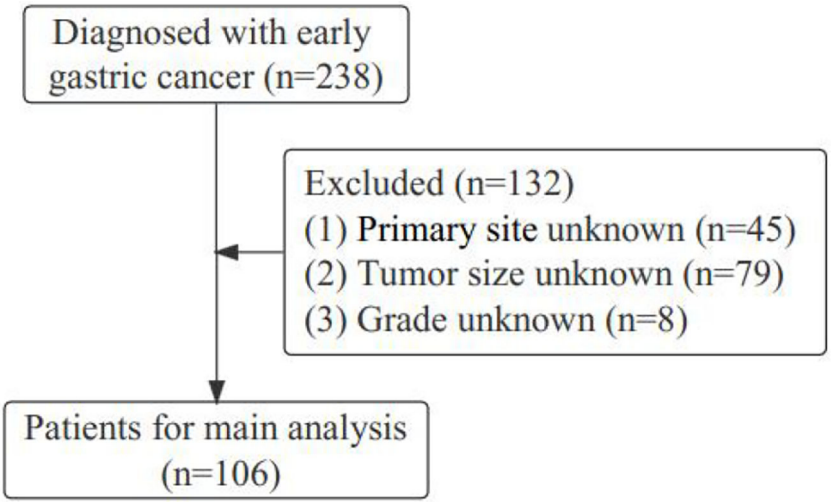

FIGURE 2
The diagram of the patient screening process in the Second Hospital of Lanzhou University.

risk factors of LNM in EGC patients, we also used the Kaplan-Meier method and Cox regression model to analyze the prognosis of EGC patients. All statistical analyses were performed with v SPSS 25.0 and R software v4.0.3 (https://www.r-project.org/). Two-sided p-values were considered statistically significant.

3 Results

3.1 Patient baseline characteristics

According to the inclusion and exclusion criteria, a total of 3993 EGC patients were identified, with an overall LNM rate of 20.84% and an overall distant metastasis rate of 1.53%. The R language random number method was used to divide the research subjects according to the ratio of 7:3, including 2797 cases in the training cohort and 1196 cases in the validation cohort. The optimal cutoff value of ELNC associated with LNM was calculated using X-tile software as 11. The demographic and clinicopathological characteristics of the training cohort and the validation cohort are shown in Table 1. The two groups of patients were diagnosed in a year, age, sex, race, pathological type, primary site, tumor size, grade, marital status, ELNC, and LNM. There was no significant difference between radiotherapy and chemotherapy (P>0.05). The overall division of the two groups conformed to simple randomization and was comparable.

TABLE 1 Demographic and clinicopathologic variables in the training and validation cohort.

Variables	All patients	Training cohort, n (%)	Validation cohort, n (%)	χ^2	*p* value
Total	3993	2797	1196		
Year of diagnosis				0.139	0.933
2004-2007	1271	887(31.70)	384(32.10)		
2008-2011	1390	972(34.70)	418(34.90)		
2012-2015	1332	938(33.60)	394(32.90)		
Age at diagnosis				0.088	0.767
≤70	2069	1445(51.70)	624(52.20)		
>70	1924	1352(48.30)	572(47.80)		
Gender				0.002	0.962
Male	2445	1712(61.20)	733(61.30)		
Female	1548	1085(38.80)	463(38.70)		
Race				0.753	0.686
White	2528	1781(63.70)	747(62.50)		

(Continued)

TABLE 1 Continued

Variables	All patients	Training cohort, n (%)	Validation cohort, n (%)	χ^2	*p* value
Black	466	327(11.70)	139(11.60)		
Other	999	689(24.60)	310(25.90)		
Primary site				0.442	0.506
Cardia	1113	771(27.60)	342(28.60)		
Non-cardia	2880	2026(72.40)	854(71.40)		
Tumor size (mm)				5.927	0.115
1-10	946	652(23.30)	294(24.60)		
11-20	1201	870(31.10)	331(27.70)		
21-30	824	580(20.70)	244(20.40)		
>30	1022	695(24.80)	327(27.30)		
Histology				0.008	0.996
Adenocarcinoma	3125	2188(78.20)	937(78.30)		
SRC	636	446(15.90)	190(15.90)		
Others	232	163(5.80)	69(5.80)		
Grade				2.622	0.454
Grade I	557	376(13.40)	181(15.10)		
Grade II	1509	1073(38.40)	436(36.50)		
Grade III	1864	1305(46.70)	559(46.70)		
Grade IV	63	43(1.50)	20(1.70)		
Marital status				1.284	0.257
Married	2246	1557(55.70)	689(57.60)		
Others	1747	1240(44.30)	507(42.40)		
ELNC				0.157	0.692
≤11	1725	1214(43.40)	511(42.70)		
>11	2268	1583(56.60)	685(57.30)		
N Stage				1.078	0.299
N0	3161	2202(78.70)	959(80.20)		
N1/N2/N3	832	595(21.30)	237(19.80)		
M Stage				0.849	0.357
M0	3932	2751(98.40)	1181(98.70)		
M1	61	46(1.60)	15(1.30)		
Chemotherapy				0.672	0.412
Yes	708	505(18.10)	203(17.00)		
None/Unknown	3285	2292(81.90)	993(83.00)		
Radiation				0.197	0.657
Yes	478	339(12.10)	139(11.60)		
None/Unknown	3515	2458(87.90)	1057(88.40)		

P value was calculated by $\chi 2$ test; EGC: early gastric cancer; SRC, signet ring cell carcinoma; ELNC, examined lymph node count.
As for the external validation cohort, 106 patients from our center were included in this study. In the external validation cohort, the mean value of age was 57.6 ± 8.6, the mean value of tumor size was 2.1 ± 1.3 cm, and the average number of ELNC removed during surgery was 17.7 ± 8.7. Continuous variables were converted to categoric variables. The clinicopathological characteristics in the Second Hospital of Lanzhou University are listed in Table 2.

TABLE 2 The clinicopathological characteristics in the Second Hospital of Lanzhou University.

Variables	No. of patients (%), n=106
Age at diagnosis	
≤70	97(91.5%)
>70	9(8.5%)
Gender	
Male	72(67.9)
Female	34(32.1)
Primary site	
Cardia	10(9.4)
Non-cardia	96(90.6)
Tumor size (mm)	
1-10	30(28.3)
11-20	38(35.8)
21-30	23(21.7)
>30	15(14.2)
Grade	
Grade I	20(18.9)
Grade II	60(56.6)
Grade III	24(22.6)
Grade IV	2(1.9)
ELNC	
≤11	24(22.6)
>11	82(77.4)
N Stage	
N0	92(86.8)
N1/N2/N3	14(13.2)

3.2 Analysis of risk factors for LNM in EGC patients

3.2.1 Univariate logistic regression analysis

To identify risk factors for LNM in EGC patients. We performed univariate logistic regression and multivariate logistic regression to adjust for confounders. Univariate logistic regression results (Table 3) showed that age, tumor size, grade, histology, and ELNC were related to LNM.

3.2.2 Multivariate logistic regression analysis

Factors with P<0.1 in univariate logistic regression were included in multivariate logistic regression, and four significant risk factors for LNM were finally included: age at diagnosis, tumor size, grade, and ELNC (Table 3). In terms of age, older patients had a lower risk of developing LNM (OR=0.847, 95%CI=0.698-1.026, P=0.090). In terms of tumor size, larger patients had an increased risk of developing LNM, 11-20mm compared with EGC patients with size 1-10mm (OR=1.556, 95%CI=1.132-2.140, P=0.006), 20-30mm (OR=2.946, 95%CI=2.138-4.061, P<0.001), greater than 30mm (OR=4.258, 95%CI=3.135-5.782, P<0.001), compared with well-differentiated EGC cancer, moderately differentiated (OR=2.523, 95%CI=1.654-3.850, P<0.001), poorly differentiated (OR=4.078, 95%CI=2.700-6.159, P<0.001) and undifferentiated (OR=2.907, 95%CI=1.270-6.652, P=0.012) patients had a higher risk of LNM. The risk of LNM increased when the ELNC was higher (OR=1.586, 95%CI=1.310-1.934, P<0.001).

3.2.3 Establish a nomogram of LNM

Based on the results of univariate logistic regression, we established a nomogram plot including age, tumor size, grade, and ELNC for examination to predict the probability of LNM in EGC patients (Figure 3). In this model, tumor size and grade were the biggest predictors of LNM. The resampling method was used for internal validation of the nomogram model, and the ROC curve and C-Index were used to evaluate the accuracy of the model; the calibration curve was used to evaluate the consistency of the predicted value with the actual survival situation; the DCA curve and the CIC were used to evaluate the net benefit of constructing the model.

The training cohort ROC (Figure 4A) showed great discrimination against the nomogram, with an AUC value of 0.702 and a model C-index of 0.702 (95% CI=0.679-0.25). The calibration curve showed high accuracy (Figure 5A). In addition, DCA and CIC showed that the nomogram showed a threshold probability of 0.2-0.6 with good gain (Figures 6A and 7A). Also in the internal validation cohort, the AUC value of the ROC curve was 0.709 (Figure 4B) and the C-index was 0.709 (95% CI=0.674-0.744). The calibration curve showed high accuracy (Figure 5B). In addition, DCA and CIC showed that the nomogram showed a threshold probability of 0.2-0.6 with good gain (Figures 6B and 7B). The evaluation effect of the external validation cohort is essentially the same as the internal validation cohort (Figures 4C, 5C, 6C, 7C).

3.3 Survival analysis of EGC patients

After exploring the risk factors of LNM in EGC patients, we also used the Kaplan-Meier method and Cox regression model to analyze the prognosis of EGC patients. Risk factors related to survival in EGC patients were analyzed by Cox proportional hazards regression model. Both univariate and multivariate results showed that age, gender, race, primary site, tumor size, pathological type, LNM, ELNC, and distant metastasis were significantly associated with tumor OS, while the year of diagnosis, grade, radiotherapy, and chemotherapy were not associated with OS (Table 4).

10.3389/fonc.2023.1062142

TABLE 3 Univariate and multivariate logistic regression analysis to identify risk factors for LNM in EGC patients.

Variable	Univariate analysis		Multivariate analysis	
	OR (95% CI)	*P* value	OR (95% CI)	*P* value
Year of diagnosis				
2004-2007	Ref			
2008-2011	0.884(0.709-1.102)	0.272		
2012-2015	0.856(0.685-1.07)	0.173		
Age at diagnosis				
≤70	Ref		Ref	
>70	0.796(0.663-0.955)	0.014	0.847(0.698-1.026)	0.090
Gender				
Male	Ref			
Female	0.932(0.773-1.123)	0.459		
Race				
White	Ref			
Black	1.046(0.787-1.389)	0.758		
Other	0.911(0.733-1.133)	0.403		
Primary site				
Cardia	Ref			
Non-cardia	0.919(0.752-1.123)	0.409		
Tumor size (mm)				
1-10	Ref		Ref	
11-20	1.717(1.255-2.35)	0.001	1.556(1.132-2.140)	0.006
21-30	3.294(2.403-4.515)	<0.001	2.946(2.138-4.061)	<0.001
>30	4.643(3.438-6.271)	<0.001	4.258(3.135-5.782)	<0.001
Histology				
Adenocarcinoma	Ref		Ref	
SRC	1.129(0.883-1.443)	0.333	0.839(0.637-1.105)	0.211
Others	1.679(1.182-2.384)	0.004	1.182(0.810-1.726)	0.386
Grade				
Grade I	Ref		Ref	
Grade II	2.778(1.8344.206)	<0.001	2.523(1.654-3.850)	<0.001
Grade III	4.753(3.1747.116)	<0.001	4.078(2.700-6.159)	<0.001
Grade IV	3.766(1.6838.428)	0.001	2.907(1.270-6.652)	0.012
Marital status				
Married	Ref			
Others	1.046(0.8721.255)	0.628		
ELNC				
≤11	Ref		Ref	
>11	1.734(1.4342.097)	<0.001	1.586(1.310-1.934)	<0.001

10.3389/fonc.2023.1062142

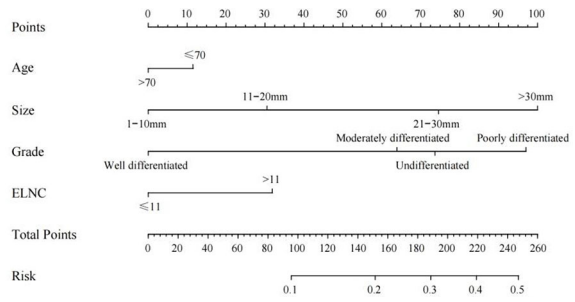

FIGURE 3
Nomogram for predicting the LNM.

4 Discussion

EGC is defined by the Japanese Society for Gastrointestinal Endoscopy as an invasive gastric cancer that does not invade deeper than the submucosa and is not associated with LNM. Currently, only South Korea and Japan have relatively complete gastric cancer prevention and screening systems in the world (17). In recent years, with the gradual popularization and application of endoscopic EMR and ESD surgery, the clinical diagnosis and treatment of patients with EGC have developed from a simple surgical operation to a two-way choice of endoscopic resection or surgical treatment. The advantages of endoscopic resection of EGC are less trauma, quick postoperative recovery, high quality of life, and long-term efficacy comparable to surgery. According to the Japanese gastric cancer treatment guidelines, the absolute indications for endoscopic resection are differentiated adenocarcinoma of cT1a without ulceration or differentiated adenocarcinoma of cT1a with ulceration diameter ≤ 3cm. Endoscopic resection of undifferentiated cT1a carcinomas ≤ 2 cm in diameter without ulcerative manifestations is considered an expanded indication (9). However, even with strict adherence to the indications for endoscopic therapy, at least 1.9 percent of cases recur after resection of the lesion, with intervals ranging from 4 months to more than 10 years (18). One of the important risk factors for recurrence is LNM. However, the main drawback of endoscopic resection is that it cannot achieve perigastric lymph node dissection. For patients with EGC with LNM, surgery is

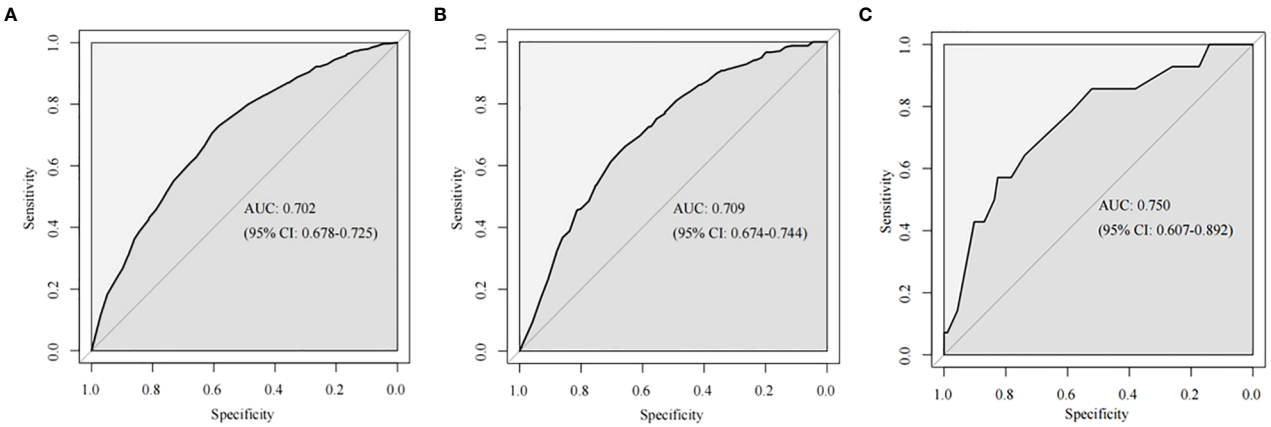

FIGURE 4
The ROC curves of the nomogram for predicting LNM in the training cohort **(A)**, internal validation cohort **(B)** and external validation **(C)**.

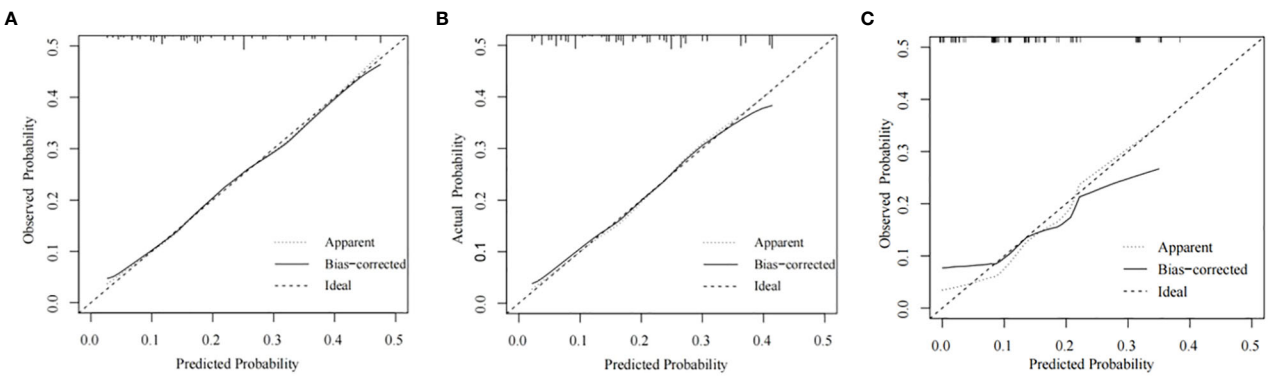

FIGURE 5
Calibration plots for the nomogram. Calibration plots for the nomogram in the training cohort **(A)**, the internal validation cohort **(B)**, and the external validation cohort **(C)**.

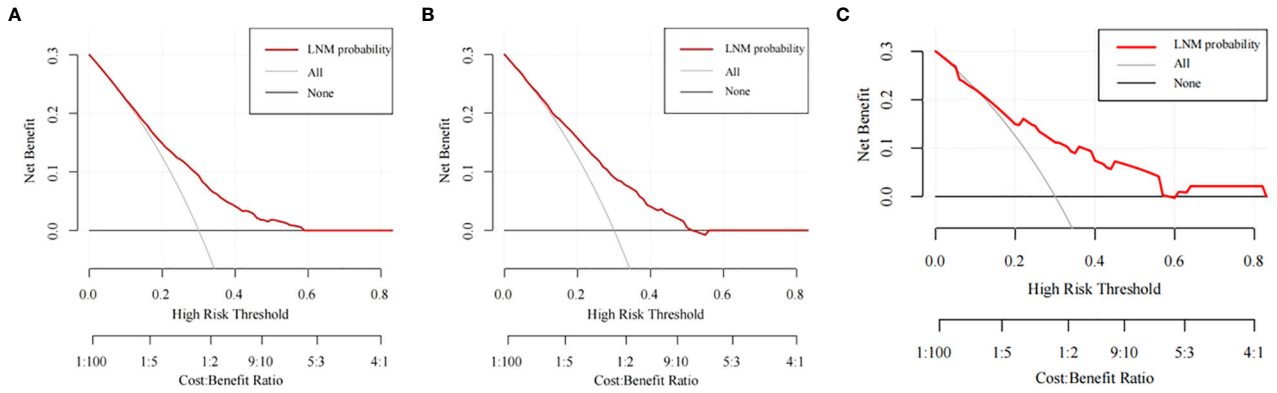

FIGURE 6
The DCA curves of the nomogram for predicting the LNM in the training cohort **(A)**, the internal validation cohort **(B)**, and the external validation cohort **(C)**.

still required to achieve radical tumor resection. Previous studies have shown that preoperative diagnosis of lymph node status still has certain limitations. Therefore, effective prediction and accurate prognostic assessment of LNM in EGC are the premises to guide the rational choice of clinical treatment.

There are several articles reported on studies of lymph node metastasis in EGC, which fall into two main categories, one being studies based on the SEER database with a large amount of data but lacking data from other institutions for external validation (10, 19). The other category is that of single-center-based studies, which included many study variables but had a small overall sample size and lacked external validation (20–24). The models constructed in the above two types of studies failed to be further validated in terms of clinical generalizability. Our study, with the addition of our center's data as external validation after this revision, confirmed that the model is still applicable in our center's cohort, and the addition of the clinical impact curve as an indicator in the method of assessing the model compared with previous studies allowed for a more comprehensive assessment of the model.

In our study, the LNM rate of EGC was 20.84%, which was consistent with the results reported in the previous study by Wang et. al (12), but higher than the 12.3-15.5% in the previous study and 2.5-8.6% in the Japanese scholar's study (25), which may be due to Japan's early cancer screening policy and high-grade intraepithelial neoplasia defined as EGC in Japanese diagnostic criteria. Using the population-based SEER database, first, multiple clinicopathological factors associated with an increased risk of LNM were identified by univariate logistic regression: age, tumor size, grade, and ELNC. The study by Lin et al. showed that female gender, tumor diameter >20 mm, submucosal invasion, and undifferentiated tumor histology were independent risk factors with an area under the curve of 0.694 (95% CI: 0.659-0.730) (26). In addition, studies have shown that age, Lauren classification, and lymphatic and perineural invasion are closely related to LNM, and T1b is more prone to LNM than T1a (27, 28). Yin et al. established a first nomogram to identify EGC patients at high risk for LNM using preoperative indicators, the model incorporated 6 independent predictors including tumor size, gross features, histological differentiation, P53, CA19-9, and lymph node status reported by computed tomography, the model has a C-index of 0.82 (95% CI: 0.78-0.86), which has a high clinical value (22), but due to the relatively small number of included studies. Less, the convincing power of the results is limited.

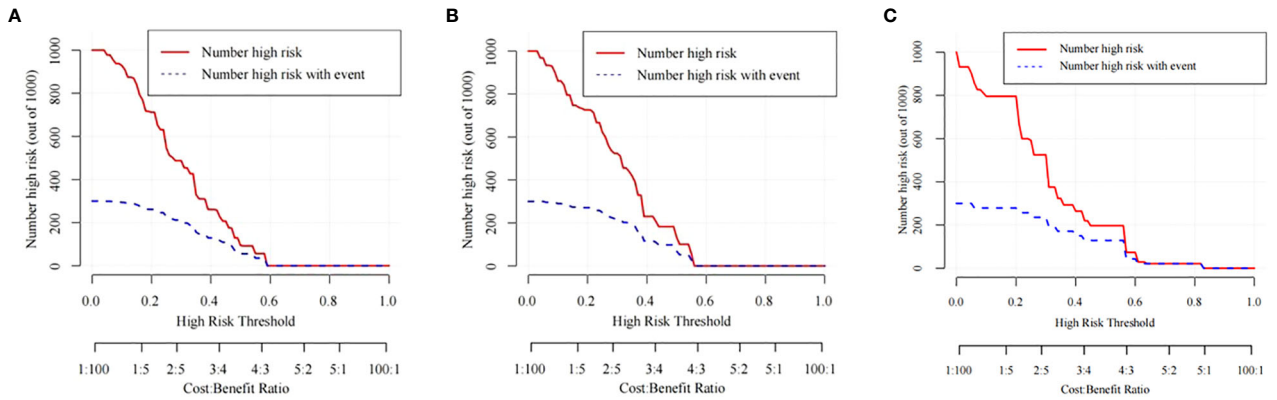

FIGURE 7
The CIC curves of the nomogram for predicting the LNM in the training cohort **(A)**, the internal validation cohort **(B)**, and the external validation cohort **(C)**.

10.3389/fonc.2023.1062142

TABLE 4 Cox regression of univariate and multivariate analysis associated with OS of EGC.

Variable	Univariate analysis		Multivariate analysis	
	HR (95% CI)	P value	HR (95% CI)	P value
Year of diagnosis				
2004-2007	Ref		Ref	
2008-2011	0.901(0.807-1.006)	0.063	0.973(0.870-1.087)	0.624
2012-2015	0.814(0.713-0.929)	0.002	0.900(0.787-1.029)	0.124
Age				
≤70	Ref		Ref	
>70	2.260(2.051-2.492)	<0.001	2.356(2.130-2.607)	<0.001
Gender				
Male	Ref		Ref	
Female	0.780(0.707-0.861)	<0.001	0.763(0.689-0.845)	<0.001
Race				
White	Ref		1.170(1.008-1.358)	0.039
Black	0.997(0.863-1.151)	0.964	0.784(0.691-0.890)	<0.001
Other	0.679(0.603-0.766)	<0.001	0.775(0.691-0.870)	<0.001
Primary site				
Cardia	Ref			
Non-cardia	0.820(0.741-0.908)	<0.001	0.775(0.691-0.870)	<0.001
Tumor size (mm)				
1-10	Ref			
11-20	1.175(1.024-1.348)	0.022	1.106(0.963-1.270)	0.153
21-30	1.465(1.268-1.693)	<0.001	1.242(1.073-1.438)	0.004
>30	1.563(1.363-1.793)	<0.001	1.338(1.160-1.542)	<0.001
Histology				
Adenocarcinoma	Ref		0.832(0.718-0.964)	0.014
SRC	0.660(0.572-0.761)	<0.001	0.852(0.679-1.071)	0.170
Others	0.712(0.569-0.890)	0.003		
Grade				
Grade I	Ref			
Grade II	1.080(0.934-1.250)	0.300		
Grade III	0.968(0.839-1.118)	0.658		
Grade IV	0.801(0.518-1.239)	0.319		
Marital status				
Married	Ref			
Others	1.077(0.980-1.183)	0.122		
ELNC				
≤11	Ref			
>11	0.693(0.631-0.762)	<0.001	0.717(0.650-0.790)	<0.001

(Continued)

TABLE 4 Continued

Variable	Univariate analysis		Multivariate analysis	
	HR (95% CI)	P value	HR (95% CI)	P value
N Stage				
N0	Ref			
N1/N2/N3	1.624(1.459-1.807)	<0.001	1.670(1.492-1.869)	<0.001
M Stage				
M0	Ref			
M1	2.360(1.738-3.207)	<0.001	1.914(1.401-2.615)	<0.001
Chemotherapy				
Yes	Ref			
None/Unknown	0.953(0.842-1.078)	0.445		
Radiation				
Yes	Ref			
None/Unknown	0.879(0.765-1.011)	0.072		

In this study, we found that, as in many previous studies, a nomogram of constructed logistic regression showed that age, tumor size, grade, and ELNC were risk factors for LNM, and tumor location was not associated with LNM, consistent with previous findings (22, 29). The AUC value of the model was 0.698 (95%CI: 0.679-0.717), The correction effect of the calibration was satisfactory and the DCA decision curve analysis showed strong clinical practicability. The pathological type in this study is not a risk factor for LNM, which is still controversial in several current studies (25, 30), which may be related to the difference in the included study population and the number of cases. Lymphovascular invasion and depth of tumor invasion have also been shown to be risk factors for the development of LNM in EGC, possibly due to the abundance of lymphatic vessels in the lamina propria and submucosa (25, 31). Unfortunately, due to the limitations of the SEER database, these two indicators were not included in our study. It is worth mentioning that ELNC was associated with LNM in this study, which may be closely related to the presence of lymphatic micrometastases (32), and examining more NLNCs can improve the detection rate of potentially metastatic-positive lymph nodes (33). Lou et al. explored the significance of lymph node micrometastasis (LNMM) in T1N0 EGC, and LNMM may be a key mechanism of recurrence after surgical treatment in T1N0 EGC patients (34). Therefore, establishing a risk model for predicting LNM can help improve the risk stratification of patients with EGC and improve the accuracy of diagnosis.

In the analysis of the prognosis of EGC patients, the 3-year and 5-year OS of EGC patients were 77.6% and 68.0%, respectively, which is much lower than that of most Japanese studies reporting that the 5-year and 10-year survival rates of EGC patients were both above 90%. In Western studies, 5-year survival rates ranged from 68.0% to 92.0%. The difference in survival may be due to the higher incidence of diffuse histotype in Western countries and less advanced endoscopic procedures, where surgical resection and D2 lymphadenectomy are considered the gold standard of care (18). Multivariate Cox regression results showed that LNM was a significantly poor prognostic factor (HR: 1.786, 95%CI: 1.512-2.111, P<0.001). In addition, age, gender, race, primary site, tumor size, distant metastasis, and whether surgery and ELNC were independent prognostic factors, while radiotherapy, chemotherapy, and pathological type and grade were not associated with prognosis. ELNC is not only a risk factor for LNM but also an independent prognostic factor. The 8th edition of the AJCC guidelines does not clearly define the minimum number of lymph nodes to be dissected in patients with T1 gastric cancer undergoing surgical treatment, but our study shows that the ELNC is more than 11. Lymph nodes showed a better prognosis than ≤11 (HR: 1.786, 95%CI: 1.512-2.111, P<0.001), so for EGC patients undergoing surgical treatment, we recommend that the total number of lymph nodes to be dissected should be at least 11. Sun et al. fit a β-binomial model of the number of lymph nodes to be examined for different primary tumor stages. The study concluded that examining 11 lymph nodes could reduce the probability of missing positive lymph nodes to <10%, which is required for patients with EGC. At least six lymph nodes were dissected (35). Population-based results showed no effect of chemotherapy on prognosis in EGC, but a previous analysis of patients with pT1 GC showed that curative surgery alone is sufficient for patients with pT1N0 and pT1N1. Xelox showed no survival advantage in pT1N2 patients. If adverse reactions are considered, S-1 is the best choice for pT1N2 patients. Xelox is recommended for pT1N3 patients (36). Minerva Chirurgica et al. evaluated the prognostic significance of preoperative serum albumin values and metastatic lymph node ratios in patients with gastric cancer. The results confirm that with albumin, age, resection type, perineural invasion, and ratio of metastatic lymph nodes, T and TNM stages were significant predictors of cancer-specific survival (CSS) (37). In addition, some studies have reported the prognostic value of CD44 Variant 9, Ki-67, and microsatellite

instability in EGC, but these conclusions need to be confirmed by more future studies (38, 39).

This study has several limitations. First, this is a retrospective analysis and may be subject to data selection bias. Second, our study lacked serum pepsinogen (PG), serum gastrin-17 (gastrin-17, G-17), Hp infection detection, tumor markers, preoperative imaging, and related ESD or EMR treatment data. Finally, the study population is derived from the SEER database, which mainly reflects the data of Western countries. Although validation of the nomogram with an external cohort may help avoid overfitting of the model, the number of cases in the external validation cohort may have been insufficient. The clinical practices of Eastern and Western countries in the treatment of EGC are very different, so the data of the Eastern population will be required for external validation in the future.

5 Conclusions

In summary, we established a nomogram for predicting LNM in EGC patients through logistic regression, and internal validation showed that the model had a good discriminative ability, accuracy, and clinical applicability. Independent prognostic factors were identified by Cox regression, and the results showed that EGC patients had better prognoses when the number of dissected lymph nodes exceeded 11. It is hoped that our results can help clinicians make individualized clinical decisions for EGC patients and facilitate the process of individualized treatment.

Data availability statement

The original contributions presented in the study are included in the article/supplementary material. Further inquiries can be directed to the corresponding authors.

Ethics statement

Written informed consent was not obtained from the individual (s) for the publication of any potentially identifiable images or data included in this article.

Author contributions

JL, TC, and ZH contributed to the study design and wrote the article. YM and WX completed the data analysis. YY and WX generated and improved the figures and tables. KC and HL proofread the manuscript. XC and WW reviewed the article. All authors contributed to the article and approved the submitted version.

Funding

Science and Technology Foundation Program for Young Scientists of Gansu Province, China (No.21JR7RA424), Science and Technology Program of Lanzhou (No.2022-ZD-107), Cuiying Scientific and Technological Innovation Program of Lanzhou University Second Hospital (CY2021-QN-A04). Natural Science Foundation of Gansu Province, China (Grant No.21JR11RA126).

Acknowledgments

The authors are grateful to all the patients, researchers, and institutions that participated in the SEER database.

Conflict of interest

The authors declare that the research was conducted in the absence of any commercial or financial relationships that could be construed as a potential conflict of interest.

Publisher's note

All claims expressed in this article are solely those of the authors and do not necessarily represent those of their affiliated organizations, or those of the publisher, the editors and the reviewers. Any product that may be evaluated in this article, or claim that may be made by its manufacturer, is not guaranteed or endorsed by the publisher.

References

1. Sung H, Ferlay J, Siegel RL, Laversanne M, Soerjomataram I, Jemal A, et al. Global cancer statistics 2020: GLOBOCAN estimates of incidence and mortality worldwide for 36 cancers in 185 countries. *CA Cancer J Clin* (2021) 71(3):209–49. doi: 10.3322/caac.21660

2. Sano T, Aiko T. New Japanese classifications and treatment guidelines for gastric cancer: revision concepts and major revised points. *Gastric Cancer.* (2011) 14(2):97–100. doi: 10.1007/s10120-011-0040-6

3. Hamashima C. Update version of the Japanese guidelines for gastric cancer screening. *Jpn J Clin Oncol* (2018) 48(7):673–83. doi: 10.1093/jjco/hyy077

4. Bourke MJ, Neuhaus H, Bergman JJ. Endoscopic submucosal dissection: Indications and application in Western endoscopy practice. *Gastroenterology* (2018) 154(7):1887–1900.e5. doi: 10.1053/j.gastro.2018.01.068

5. Ono H, Yao K, Fujishiro M, Oda I, Uedo N, Nimura S, et al. Guidelines for endoscopic submucosal dissection and endoscopic mucosal resection for early gastric cancer (second edition). *Dig Endosc.* (2021) 33(1):4–20. doi: 10.1111/den.13883

6. Hanada Y, Choi AY, Hwang JH, Draganov PV, Khanna L, Sethi A, et al. Low frequency of lymph node metastases in patients in the united states with early-stage gastric cancers that fulfill Japanese endoscopic resection criteria. *Clin Gastroenterol Hepatol* (2019) 17(9):1763–9. doi: 10.1016/j.cgh.2018.11.031

7. Asakawa Y, Ohtaka M, Maekawa S, Fukasawa M, Nakayama Y, Yamaguchi T, et al. Stratifying the risk of lymph node metastasis in undifferentiated-type early gastric cancer. *World J Gastroenterol* (2015) 21(9):2683–92. doi: 10.3748/wjg.v21.i9.2683

8. China NHCOTPRO. Chinese Guidelines for diagnosis and treatment of cervical cancer 2018 (English version). *Chin J Cancer Res* (2019) 31(2):295–305. doi: 10.21147/j.issn.1000-9604.2019.02.04

9. Japanese Gastric Cancer Association. Japanese Gastric cancer treatment guidelines 2018 (*5th* edition). *Gastric Cancer* (2021) 24(1):1–21. doi: 10.1007/s10120-020-01042-y

10. Kim SM, Min BH, Ahn JH, Jung SH, An JY, Choi MG, et al. Nomogram to predict lymph node metastasis in patients with early gastric cancer: A useful clinical tool to reduce gastrectomy after endoscopic resection. *Endoscopy* (2020) 52(6):435–43. doi: 10.1055/a-1117-3059

11. Tang CT, Chen SH. Higher lymph node metastasis rate and poorer prognosis of intestinal-type gastric cancer compared to diffuse-type gastric cancer in early-onset early-stage gastric cancer: A retrospective study. *Front Med (Lausanne).* (2021) 8:758977. doi: 10.3389/fmed.2021.758977

12. Wang J, Wang L, Li S, Bai F, Xie H, Shan H, et al. Risk factors of lymph node metastasis and its prognostic significance in early gastric cancer: A multicenter study. *Front Oncol* (2021) 11:649035. doi: 10.3389/fonc.2021.649035

13. Eom BW, Joo J, Park B, Jo MJ, Choi SH, Cho SJ, et al. Nomogram incorporating CD44v6 and clinicopathological factors to predict lymph node metastasis for early gastric cancer. *PloS One* (2016) 11(8):e0159424. doi: 10.1371/journal.pone.0159424

14. Iasonos A, Schrag D, Raj GV, Panageas KS. How to build and interpret a nomogram for cancer prognosis. *J Clin Oncol* (2008) 26(8):1364–70. doi: 10.1200/JCO.2007.12.9791

15. Cronin KA, Ries LA, Edwards BK. The surveillance, epidemiology, and end results (SEER) program of the national cancer institute. *Cancer* (2014) 120 Suppl 23:3755–7. doi: 10.1002/cncr.29049

16. Fritz A, Percy C, Jack A, Shanmugaratnam K, Sobin, Leslie H, et al. International classification of diseases for oncology. *3rd* ed. *World Health Organization* (2000) https://apps.who.int/iris/handle/10665/42344.

17. Goto R, Hamashima C, Mun S, Lee WC. Why screening rates vary between Korea and Japan–differences between two national healthcare systems. *Asian Pac J Cancer Prev* (2015) 16(2):395–400. doi: 10.7314/APJCP.2015.16.2.395

18. Chiarello MM, Fico V, Pepe G, Tropeano G, Adams NJ, Altieri G, et al. Early gastric cancer: A challenge in Western countries. *World J Gastroenterol* (2022) 28(7):693–703. doi: 10.3748/wjg.v28.i7.693

19. Yang B, Sun K, Hui Y, Zhu L, Wang S, Ma S, et al. Large Population-based study using the SEER database: is endoscopic resection appropriate for early gastric cancer patients in the united states. *Scand J Gastroenterol* (2020) 55(7):834–42. doi: 10.1080/00365521.2020.1786158

20. Zhang M, Ding C, Xu L, Feng S, Ling Y, Guo J, et al. A nomogram to predict risk of lymph node metastasis in early gastric cancer. *Sci Rep* (2021) 11(1):22873. doi: 10.1038/s41598-021-02305-z

21. Mu J, Jia Z, Yao W, Song J, Cao X, Jiang J, et al. Predicting lymph node metastasis in early gastric cancer patients: development and validation of a model. *Future Oncol* (2019) 15(31):3609–17. doi: 10.2217/fon-2019-0377

22. Yin XY, Pang T, Liu Y, Cui HT, Luo TH, Lu ZM, et al. Development and validation of a nomogram for preoperative prediction of lymph node metastasis in early gastric cancer. *World J Surg Oncol* (2020) 18(1):2. doi: 10.1186/s12957-019-1778-2

23. Zhang Y, Liu Y, Zhang J, Wu X, Ji X, Fu T, et al. Construction and external validation of a nomogram that predicts lymph node metastasis in early gastric cancer patients using preoperative parameters. *Chin J Cancer Res* (2018) 30(6):623–32. doi: 10.21147/j.issn.1000-9604.2018.06.07

24. Wang Z, Liu J, Luo Y, Xu Y, Liu X, Wei L, et al. Establishment and verification of a nomogram for predicting the risk of lymph node metastasis in early gastric cancer. *Rev Esp Enferm Dig.* (2021) 113(6):411–7. doi: 10.17235/reed.2020.7102/2020

25. Li X, Liu S, Yan J, Peng L, Chen M, Yang J, et al. The characteristics, prognosis, and risk factors of lymph node metastasis in early gastric cancer. *Gastroenterol Res Pract* (2018) 2018:6945743. doi: 10.1155/2018/6945743

26. Lin JX, Wang ZK, Wang W, Desiderio J, Xie JW, Wang JB, et al. Risk factors of lymph node metastasis or lymphovascular invasion for early gastric cancer: a practical and effective predictive model based on international multicenter data. *BMC Cancer.* (2019) 19(1):1048. doi: 10.1186/s12885-019-6147-6

27. Zhao X, Cai A, Xi H, Chen L, Peng Z, Li P, et al. Predictive factors for lymph node metastasis in undifferentiated early gastric cancer: a systematic review and meta-analysis. *J Gastrointest Surg* (2017) 21(4):700–11. doi: 10.1007/s11605-017-3364-7

28. Kim DG, An JY, Kim H, Shin SJ, Choi S, Seo WJ, et al. Clinical implications of microsatellite instability in early gastric cancer. *J Gastric Cancer.* (2019) 19(4):427–37. doi: 10.5230/jgc.2019.19.e38

29. ZeLong Y, ZhenYu C, JianHai L, MingHua Z, KeCheng Z, ChunXi W. Influence of tumor location on lymph node metastasis and survival for early gastric cancer: a population-based study. *J Gastrointest Surg* (2020) 24(9):1978–86. doi: 10.1007/s11605-019-04367-x

30. Kim YI, Lee JH, Kook MC, Lee JY, Kim CG, Ryu KW, et al. Lymph node metastasis risk according to the depth of invasion in early gastric cancers confined to the mucosal layer. *Gastric Cancer.* (2016) 19(3):860–8. doi: 10.1007/s10120-015-0535-7

31. Kanda Y. Investigation of the freely available easy-to-use software 'EZR' for medical statistics. *Bone Marrow Transplant.* (2013) 48(3):452–8. doi: 10.1038/bmt.2012.244

32. Kim JJ, Song KY, Hur H, Hur JI, Park SM, Park CH. Lymph node micrometastasis in node negative early gastric cancer. *Eur J Surg Oncol* (2009) 35(4):409–14. doi: 10.1016/j.ejso.2008.05.004

33. Yamashita H, Deng J, Liang H, Seto Y. Re-evaluating the prognostic validity of the negative to positive lymph node ratio in node-positive gastric cancer patients. *Surgery* (2017) 161(6):1588–96. doi: 10.1016/j.surg.2016.12.018

34. Lou GC, Dong J, Du J, Chen WY, He XL. Clinical significance of lymph node micrometastasis in T1N0 early gastric cancer. *Math Biosci Eng.* (2020) 17(4):3252–9. doi: 10.3934/mbe.2020185

35. Sun L, Liu Q, Ren H, Li P, Liu G, Sun L. Nodes staging score to quantify lymph nodes for examination in gastric cancer. *Med (Baltimore).* (2020) 99(33):e21085. doi: 10.1097/MD.0000000000021085

36. Mei Y, Feng T, Yan M, Zhu Z, Zhu Z. Is adjuvant chemotherapy necessary for early gastric cancer. *Cancer Biol Med* (2021) 19(4):518–32. doi: 10.20892/j.issn.2095-3941.2020.0636

37. Isik A, Okan I, Firat D, Yilmaz B, Akcakaya A, Sahin M. A new prognostic strategy for gastric carcinoma: albumin level and metastatic lymph node ratio. *Minerva Chir.* (2014) 69(3):147–53.

38. Go SI, Ko GH, Lee WS, Lee JH, Jeong SH, Lee YJ, et al. The use of CD44 variant 9 and ki-67 combination can predicts prognosis better than their single use in early gastric cancer. *Cancer Res Treat* (2019) 51(4):1411–9. doi: 10.4143/crt.2018.663

39. Zhu X, Wang Y, Li H, Xue W, Wang R, Wang L, et al. Deficiency of hMLH1 and hMSH2 expression is a poor prognostic factor in early gastric cancer (EGC). *J Cancer.* (2017) 8(8):1477–83. doi: 10.7150/jca.18487

frontiers | Frontiers in Oncology

TYPE Brief Research Report
PUBLISHED 27 March 2023
DOI 10.3389/fonc.2023.1036871

Check for updates

OPEN ACCESS

EDITED BY
Zhendong Jin,
Second Military Medical University, China

REVIEWED BY
Linda Erlina,
University of Indonesia, Indonesia
Helmout Modjathedi,
Kingston University, United Kingdom

*CORRESPONDENCE
Peh Yean Cheah
cheah.peh.yean@sgh.com.sg

†These authors share first authorship

‡Senior author

§PRESENT ADDRESSES
Yee Syuen Low,
Department of Pathology and Molecular Medicine, Wellington School of Medicine and Health Sciences, University of Otago, Wellington, New Zealand
Michelle Wong,
Department of Plastic Reconstructive and Aesthetic Surgery, Singapore General Hospital, Singapore, Singapore

SPECIALTY SECTION
This article was submitted to Gastrointestinal Cancers: Colorectal Cancer, a section of the journal Frontiers in Oncology

RECEIVED 05 September 2022
ACCEPTED 27 February 2023
PUBLISHED 27 March 2023

CITATION
Lam KK, Low YS, Lo M, Wong M, Leong Tang C, Tan E, Chok AY, Seow-En I, Wong SH and Cheah PY (2023) KRAS-specific antibody binds to KRAS protein inside colorectal adenocarcinoma cells and inhibits its localization to the plasma membrane. *Front. Oncol.* 13:1036871. doi: 10.3389/fonc.2023.1036871

COPYRIGHT
© 2023 Lam, Low, Lo, Wong, Leong Tang, Tan, Chok, Seow-En, Wong and Cheah. This is an open-access article distributed under the terms of the Creative Commons Attribution License (CC BY). The use, distribution or reproduction in other forums is permitted, provided the original author(s) and the copyright owner(s) are credited and that the original publication in this journal is cited, in accordance with accepted academic practice. No use, distribution or reproduction is permitted which does not comply with these terms.

KRAS-specific antibody binds to KRAS protein inside colorectal adenocarcinoma cells and inhibits its localization to the plasma membrane

Kuen Kuen Lam[1†], Yee Syuen Low[1†§], Michelle Lo[1], Michelle Wong[1§], Choong Leong Tang[1], Emile Tan[1], Aik Yong Chok[1], Isaac Seow-En[1], Siew Heng Wong[2‡] and Peh Yean Cheah[1,3,4*]

[1]Department of Colorectal Surgery, Singapore General Hospital, Singapore, Singapore, [2]JW Bioscience Pte. Ltd., Singapore, Singapore, [3]Saw Swee Hock School of Public Health, National University of Singapore, Singapore, Singapore, [4]Duke-NUS Medical School, National University of Singapore, Singapore, Singapore

Colorectal cancer (CRC) is the third highest incidence cancer and a leading cause of cancer mortality worldwide. To date, chemotherapeutic treatment of advanced CRC that has metastasized has a dismayed success rate of less than 30%. Further, most (80%) sporadic CRCs are microsatellite-stable and are refractory to immune checkpoint blockade therapy. KRAS is a gatekeeper gene in colorectal tumorigenesis. Nevertheless, KRAS is 'undruggable' due to its structure. Thus, focus has been diverted to develop small molecule inhibitors for its downstream effector such as ERK/MAPK. Despite intense research efforts for the past few decades, no small molecule inhibitor has been in clinical use for CRC. Antibody targeting KRAS itself is an attractive alternative. We developed a transient *ex vivo* patient-derived matched mucosa-tumor primary culture to assess whether anti-KRAS antibody can be internalized to bind and inactivate KRAS. We showed that anti-KRAS antibody can enter live mucosa-tumor cells and specifically aggregate KRAS in the cytoplasm, thus hindering its translocation to the inner plasma membrane. The mis-localization of KRAS reduces KRAS dwelling time at the site where it tethers to activate downstream effectors. We previously showed that expression of SOX9 was KRAS-mutation-dependent and possibly a better effector than ERK in CRC. Herein, we showed that anti-KRAS antibody treated tumor cells have less intense SOX9 cytoplasmic and nuclear staining compared to untreated cells. Our results demonstrated that internalized anti-KRAS antibody inhibits KRAS function in tumor. With an efficient intracellular antibody delivery system, this can be further developed as combinatorial therapeutics for CRC and other KRAS-driven cancers.

KEYWORDS

KRAS, antibody therapeutics, metastatic colorectal cancer, SOX9, *ex vivo* culture

1 Introduction

Colorectal cancer (CRC) is one of the leading cancers in the developed world with almost 900,000 deaths annually (1, 2). The 5-year age-standardized observed survival is only 60% and 10% for lymph-node-involved Stage III and distal organ-involved Stage IV CRC respectively (3). Currently, the success rate of first line chemotherapy of 5-Fluorouracil and oxaliplatin for metastatic CRC is less than 30% (4, 5). Patients who do not respond to this first line therapy and have wild-type *KRAS* gene are sometimes given the anti-EGFR (epidermal growth factor receptor) therapy, Cetuximab or Panitumumab. However, the overall survival is only 4.6% to 12.3% for Cetuximab monotherapy and 6.9% to 18.9% for Cetuximab in combination with chemotherapy for colorectal cancer, and almost all therapy recipients eventually develop resistance to this second line therapy due to the selective pressure for activating mutation of proto-oncogene *KRAS*, downstream of the EGFR signaling pathway (6–8). Although immune checkpoint blockade therapy has some success with microsatellite-unstable CRCs, most (80%) sporadic CRCs are microsatellite-stable and refractory to such therapy (9). There is thus an urgent need to develop better therapeutics for this deadly cancer. Oncogenic RAS has been shown to be essential for tumor maintenance and KRAS mutation in CRC is associated with metastasis and poor prognosis (10–13).

Despite KRAS displaying a central role in CRC tumorigenesis and possibly metastasis, direct inhibition of KRAS is exceptionally challenging as it is not receptive to inhibitor docking (14–16). Approximately 50% of CRC harbors KRAS oncogenic mutations and our unpublished findings show that *KRAS* mutations is associated with metastasis (17). To date, the only approved direct KRAS inhibitor is Sotorasib (AMG 510) which specifically targets KRAS p.Gly12Cys in non-small-cell lung carcinoma by forming a covalent bond with the 12-cysteine (18). Nevertheless, KRAS p.Gly12Cys mutations are rare in CRC. Alternative strategies like inhibition of farnesyl transferase which prevents KRAS C-terminal prenylation, required for inner plasma membrane localization where KRAS functions, were unsuccessful as farnesyl transferase are functionally replaced by geranylgeranyl transferase (19, 20). Efforts were then diverted to inhibit KRAS downstream targets Raf/MEK/ERK, also known as mitogen-activated protein kinase (MAPK) and PI3K/Akt (21, 22). Despite extensive efforts in research and clinical trials over the past three decades, none of these inhibitors have progressed to clinical use for CRC. In fact, to date, only one clinical trial (NCT02788279) has progressed past Phase 2 [reviewed by Xie, Chen (23)]. Our recent study also reported the absence of MAPK and PI3K/Akt pathways activation in CRC tumors compared to matched normal mucosa indicating that phosphorylated ERK/AKT may not be the appropriate downstream effectors to repress *KRAS* signaling (24).

Antibody targeted therapy has much reduced toxicity than small-molecule therapies (25). However, as KRAS is an intracellular protein, it is a challenge to transport the antibody into the cells. Nonetheless, there are several reports of autoantibodies that can naturally penetrate into cells as reviewed by Ruiz–Arguelles and Alarcon–Segovia (26). These autoantibodies can be found in the serum of autoimmune patients which likely contribute to disease progression, for instance Anti-U1snRNP IgG penetrate into subsets of human T lymphocytes, anti-dsDNA (double stranded DNA) IgG penetrate into human lymphocytes and kidney glomerular cells, both trigger active cell death and tissue damage (27–31). Anti-dsDNA 3E10 IgG from systemic lupus erythematosus-prone mice can also be internalized into the cytosol, and its derivatives like TMab4 have shown cell-penetrating properties (32–34).

We needed a model for the preliminary study of anti-KRAS antibody internalization. While CRC cell lines are the most common experimental model, most cell lines are highly culture adapted thus often do not reflect biological characteristics of CRC in patients. Ronen, Hayat (35) reported that many commonly used CRC cell lines (e.g., HT-29 and LOVO) failed to cluster with human CRC tissue based on multi-omics studies (copy number alterations, transcriptome, somatic mutations, gene methylation), indicating their divergence from CRC in biological characteristics. *In vivo* studies of animal models, mostly mouse models of CRC may not mimic the human disease process and requires a long time, and hence not ideal for proof-of-concept studies (36). While patient-derived xenograft models consider patient-to-patient tumor variation, the environment for the tumor growth is from the mice rather than human, and further differences in environment is contributed by heterotopic models, and similarly requires a long lead time to propagate. Patient-derived organoids are decent models for CRC but is technically challenging and time consuming, thus not suitable for preliminary screening tests, like our current proof-of-concept study. Organoids have other disadvantages like accessibility of cells to treatment due to their three-dimensional structure, the need to start from stem cells and failure of the stem cells to terminally differentiate in the organoid (37).

In this study, we developed an *ex vivo* cell culture of crypt epithelial cells derived from patients' CRC tumor and matched mucosa tissues. In this *ex vivo* culture system, the culture is transient, viable for 3 days. This minimizes culture adaptation such that cells largely retain their original biological characteristics, thus a more accurate representation of human CRC. Both the tumor and matched mucosa crypt epithelial live cells were treated with anti-KRAS antibodies. The 2-dimensional nature of this culture system allows us to clearly visualize the internalization of anti-KRAS antibodies by confocal microscopy. The data can be correlated to the patient's clinicopathological features (such as age, gender, tumor stage, site, and differentiation). The availability of archived human matched mucosa-tumor tissues of the same patients would enable us to profile the genomics, transcriptomics and metabolomics, whenever necessary to elucidate the pathways involved and better understand

Abbreviations: CRC, Colorectal cancer; DMEM, Dulbecco`s Modified Eagle Media; dsDNA, double stranded DNA; DTT, Dithiothreitol; FBS, Fetal bovine serum; kDa, kilo Dalton; MAPK, Mitogen-activated protein kinase; PBS, Phosphate buffered saline; PBSCM, PBS with calcium and magnesium; PBSCM-T, PBSCM with Triton-X-100; SMI, Small molecule inhibitor; WT, Wild type.

the biology. The histology of the tumor can also be studied to correlate KRAS internalization and effect on cell viability and KRAS downstream pathway activation. Hitherto, tumor heterogeneity has hampered therapeutics considerably. The availability of samples that are simultaneously cultured and archived would enable more systematic experimentation that could potentially throw more light on inter-tumor heterogeneity and genetic variability of disease subgroups that would no doubt contribute eventually to therapy.

Herein, we showed that anti-KRAS antibodies can be internalized in the *ex vivo* cultured matched mucosa-tumor cells. We showed that most of the internalized anti-KRAS antibodies are localized in the cytoplasm and not endosomes, and that the antibody altered endogenous KRAS localization from the inner plasma membrane to the cytoplasm in tumor cells harboring KRAS p.Gly12Val mutation. As expected, the treatment of mucosa and tumor cells with anti-KRAS antibodies led to a decrease in SOX9 expression.

2 Materials and methods

2.1 Colon crypts isolation and culture

All colorectal cancer tissue samples were collected from freshly resected colon or rectum. A piece of 1 x 1 cm tumor and a strip of 5-10 x 1 cm of mucosa samples were cut using a scalpel blade and a pair of dissection scissors, respectively. The mucosa sampled is as far from the tumor as allowed by internal guidelines, 2 cm from the resection margin (Supplementary Figure 1A). The tissues were transported in phosphate-buffered saline (PBS; 10 mM sodium phosphates, 2.68 mM KCl, 140 mM NaCl) back to the laboratory. Any tumor sample with diameter 2 cm or greater, collected within an hour of surgery from consented patients is included in the study. Tumor tissue which is 2 cm or less in diameter and/or is necrotic is excluded. The study methodologies follow guidelines set by the Human Biomedical Research Act, Ministry of Health, Singapore. The study was also approved by the SingHealth Centralised Institutional Review Board (CIRB project number 2018/2837) and conform to the standards set by the Declaration of Helsinki.

The extraction of crypts from the colorectal tissues for cell culture was adapted from the protocol by Booth, Dove (38). The tumor and mucosa tissues were washed with PBS for 3 times and sterilized in bleach (Clorox, 5.25% sodium hypochlorite) diluted to 0.09% (~0.005% sodium hypochlorite) in PBS at room temperature for 20 min. The tumor and matched mucosa tissues were washed with PBS 3 times. To dislodge crypts of the tissues, the tumor and matched mucosa tissues were first incubated in chelating buffer composed of 0.5 mM EDTA and 0.05 mM DTT in PBS, for 15 minutes in 37°C, then washed with PBS. The debris and top crypts were dislodged by shaking the tissues in PBS vigorously for 15 s, 2 times, and were then discarded. This chelation-dislodging process was repeated for 2 more times in increasing strengths of chelating buffer of 1 mM EDTA with 0.05 mM DTT, then finally 3 mM EDTA with 0.5 mM DTT in PBS for mucosa; and only one more time using the latter buffer for tumor as tumor crypts are easier to dislodge (Supplementary Figure 1B). The dislodged crypts were passed through a 40 μm cell strainer (SPL Life Sciences, Gyeonggi-do, Korea) which traps the crypts while allowing single cells to flow through. The crypts were then recovered from the cell strainer in cell culture medium consisting of DMEM (Dulbecco`s Modified Eagle Media; Lonza, Basel, Switzerland) supplemented with 10% FBS (fetal bovine serum; Hyclone, UT, USA) and 2X Pen-Strep (Penicillin-Streptomycin; Thermo Fisher Scientific, MA, USA), then pelleted down by centrifugation at 200x g, 5 min. The pelleted tumor and mucosa crypts were resuspended in cell culture medium and seeded onto coverslips coated with Matrigel (Corning, NY, USA) diluted 1:10 in DMEM with 2X Pen-Strep for 1 hour at 37°C, 5% CO_2 prior to seeding.

2.2 Fixation, permeabilization and immunofluorescent staining

The cells attached to coverslips were fixed with pre-chilled methanol for 5 minutes at -20°C. Cells were washed with cold PBS with calcium and magnesium (PBSCM; PBS with 0.5 mM $MgCl_2$ and 0.5 mM $CaCl_2$) 5 times for 5 minutes each wash, then permeabilized with PBSCM with 0.1% Triton-X-100 (PBSCM-T) for 30 min at room temperature. The cells were then blocked-in blocking buffer (5% Goat Serum, 5% FBS, 3% BSA in PBSCM) for 1 h at room temperature. Thereafter, they were incubated with primary rabbit polyclonal anti-KRAS antibody (Thermo Fisher Scientific, cat# PA5-27234) at 20 μg/mL, mouse anti-EEA1 antibody (ab70521, Abcam) at 1:200 dilution or anti-SOX9 antibody (Sigma-Aldrich cat# AMAB90795) at 1:200 in blocking buffer at 4°C overnight. After incubation, cells were washed with PBSCM-T for 3 times with 5 minutes interval each. The cells were then incubated in secondary antibodies: FITC conjugated goat anti-rabbit IgG, (Thermo Fisher Scientific cat# 31583) at 1:50, Alexa Fluor 488 conjugated goat anti-rabbit IgG (Cell Signaling Technology, MA, USA, cat# 4412) at 1:500 or Alexa Fluor 555 conjugated goat anti-mouse IgG at 1:500 (Cell Signaling Technology cat# 4409) diluted in blocking buffer. Coverslips were mounted with ProLong™ Gold Antifade mounting medium with DAPI (Thermo Fisher Scientific) or VECTASHIELD® PLUS antifade mounting medium with DAPI (Vector Laboratories, CA, USA) onto microscope glass slides.

2.3 Treatment of *ex vivo* culture cells with anti-KRAS antibodies

Rabbit polyclonal anti-KRAS (Thermo Fisher Scientific cat# PA5-27234), rabbit monoclonal anti-Ras (Cell Signaling Technology cat# E4K9L) or mouse monoclonal anti-KRAS (Thermo Fisher Scientific cat# 415700) antibodies were diluted to 20 μg/ml in antibody incubation buffer (DMEM + 1% FBS + 25 mM HEPES + 2X Pen-Strep), or vice versa. Rabbit anti-KRAS polyclonal IgG antibody (dialyzed) and rabbit monoclonal anti-Ras IgG antibody (in PBS without preservatives). The cells attached onto coverslips were washed with 2 ml of cell culture medium for 3 times, with 200 rpm, 5 min of shaking on an orbital shaker each time to

thoroughly remove cell debris and sticky dead cells. 80 µl of diluted antibody was added to the center of each well of a new 6-well culture plate, then the coverslip with cells facing downward is placed atop of the diluted antibody, allowing the latter to spread, and come in contact with the cells. The samples were incubated at 33°C, 10% CO_2 for 16 h. For co-localization experiments, coverslips were processed as in sn2.2< h>ectio above. The epitopes of the anti-KRAS and anti-Ras antibodies are listed in Supplementary Table 1.

2.4 Confocal microscopy imaging and image processing

Brightfield and phase contrast images were taken with Nikon (Tokyo, Japan) Eclipse Ti inverted microscope. Confocal fluorescence microscope images were acquired with the Nikon A1 Confocal Microscope. Z-stacks of the cell images were acquired; the optical slices in which the DAPI is most conspicuous (indicating slices at the intracellular level) were selected for analysis. The optical thickness for each slice was 2.51 µm and 0.47 µm for 20X and 60X magnification, respectively. Images were processed using the Nikon-Elements Advance Software or ImageJ (39, 40).

The methods for KRAS sequencing and rabbit polyclonal anti-KRAS antibody dialysis is in the Supplementary Methods.

3 Results

3.1 Establishment of transient *ex vivo* culture of CRC tumor and matched mucosa tissues

To establish an *ex vivo* primary culture of both tumor and mucosa epithelial cells derived from freshly resected colorectal tissues of CRC patients, we first dislodged whole crypts from the tumor and matched mucosa tissues. The dislodged mucosa crypts appear to have a consistent elongated shaped ~200-300 µm (Supplementary Figure 1C) while the tumor crypts appear to be clumps of irregular shapes with varying sizes (Supplementary Figure 1D). This matches the common histological observation of mucosa having defined, organized and elongated crypts, while tumor having disorganized, often convoluted and irregularly shaped crypts (Supplementary Figure 2). Furthermore, the number of full complete crypts in tumor is visibly lower as compared to its' matched mucosa (Supplementary Figure 1). To culture crypts epithelial cells, isolated crypts were seeded onto Matrigel-coated coverslips and incubated in cell culture medium supplemented with FBS without additional growth factors. The tumor and matched mucosa crypts epithelial cells were observed to be able to attach and spread on Matrigel-coated coverslips a day after seeding (Figures 1A–D). The mucosa crypt epithelial cells appear flatter, more widespread (Figures 1A–C) while the tumor epithelial crypt cells appear more tightly packed (Figures 1B–D). The *KRAS* mutation status of all *ex vivo* cultured specimens (n=70) are listed in Supplementary Table 2.

3.2 KRAS membrane localization observed in ex. vivo cultured and post-fixed KRAS p.Gly12Val tumors

We first determined the subcellular localization of KRAS in the *ex vivo* tumor and matched mucosa cells. Immunofluorescence (IF) staining revealed that KRAS localized predominantly to the cytoplasm in the matched mucosa (Figure 1E) and KRAS wild-type (WT) tumor (Supplementary Figure 3). However, KRAS were shown to localize largely at the inner plasma membrane resembling a net-like pattern in the KRAS p.Gly12Val (G12V) tumor (Figure 1F). Activated KRAS is expected to be tethered to the inner plasma membrane to activate downstream targets (e.g. BRAF), thus higher pools of inner membrane localized-KRAS indicates higher activation (41). This corroborates with the concept that KRAS oncogenic mutants (but not WT) are constitutively activated. KRAS inner plasma membrane localization in tumor with *KRAS* mutation is also consistent with the observation in *KRAS* mutated CRC cell lines like SW480 [Figure 6C of Zhang, Jiang (42)].

3.3 Anti-KRAS antibody can be internalized into live colon mucosa and tumor cells and form punctate structures

Since KRAS proteins are inside the cancer cells, anti-KRAS antibodies must be able to enter the cytoplasm to bind to the KRAS molecules. Thus, we assessed whether anti-KRAS antibody can be internalized into live *ex-vivo* cultured mucosa-tumor pairs. Live *ex vivo* cultured cells were treated with rabbit anti-KRAS IgG antibody, rabbit IgG isotype control, or antibody diluent for 16 h at 33°C, fixed and counterstained with FITC-conjugated secondary antibodies. As shown in Figure 2 (Panel C and F), anti-KRAS antibody was internalized into the cytoplasm and formed punctate structures in both the mucosa and tumor. No punctate structures could be observed in the untreated (Figures 2A–D) and rabbit IgG control antibody-treated (Figures 2B–E) live mucosa-tumor cells. The punctate staining indicates that the anti-KRAS antibody was internalized into both the mucosal and tumor cells. These punctate staining were not observed in cells treated with Rabbit IgG isotype control, further supporting that the punctate structures were likely due to KRAS-specific antibody-protein complexes formation. Co-localization of two different anti-KRAS antibodies in the same structures provided additional evidence that the aggregates were KRAS-antibody complexes (Supplementary Figure 4).

3.4 The internalized anti-KRAS antibodies were not accumulated in the endosomes

It is possible that a significant pool of anti-KRAS antibody molecules internalized *via* the fluid-phase endocytosis pathway and thus may be trapped in endosomes. For the anti-KRAS antibodies to

10.3389/fonc.2023.1036871

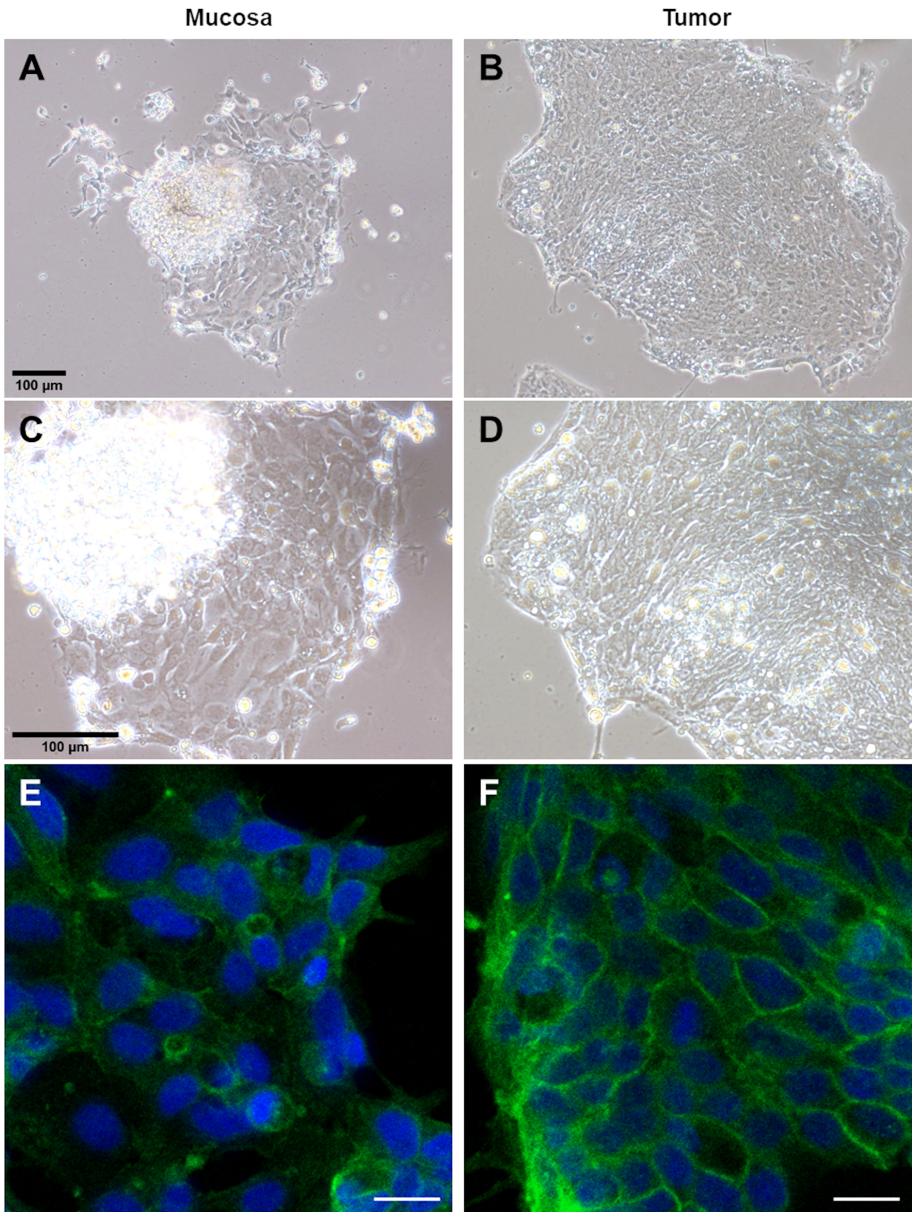

FIGURE 1
Crypt epithelial cells from patient-derived CRC matched mucosa and tumor tissues can be maintained and immunoassayed in *ex vivo* culture. Phase contrast images of a patient's matched mucosa **(A, C)** and tumor **(B, D)** crypt epithelial cells at 10X **(A, B)** and 20X **(C, D)** magnification. Confocal imaging for *ex vivo* cultured colorectal mucosa **(E)** and tumor **(F)** cells which were fixed and immunostained for KRAS. KRAS is more evenly distributed in the cytoplasm in fixed *ex vivo* cultured mucosa cells **(E)** while localized more to the plasma membrane in tumor cells **(F)**. The tumor in **(F)** harbors a KRAS p.Gly12Val somatic mutation. The scale bar in **(A)** is applicable to **(A, B)** and in **(C)** is applicable to **(C, D)**. The scale bar in **(E, F)** is 20 µm.

be able to bind to and sequester endogenous KRAS, they must be localized to the cytoplasm. However, endosomal escape is usually inefficient, leading to most cargoes end up being degraded in the lysosomes. It is possible that the punctate structures that we observed in Figure 2 were due to accumulation of internalized anti-KRAS antibodies in the endosomes. To exclude this possibility, we treated live *ex vivo* cultured colon tumor cells with rabbit anti-KRAS antibodies. At 16 h after treatment, the cells were permeabilized and immunostained for early endosomal marker EEA1. Confocal imaging showed that most of the anti-KRAS antibody-positive punctate structures did not co-localize with EEA1 (Supplementary Figure 5A-C), excluding the possibility that the internalized antibodies were accumulated in the endosomes.

3.5 Tumor cells with KRAS p.Gly12Val mutation showed reduced KRAS membrane localization after anti-KRAS antibody treatment

We hypothesize that treatment of *ex vivo* cultured tumor with anti-KRAS antibody can reduce the membrane localization of

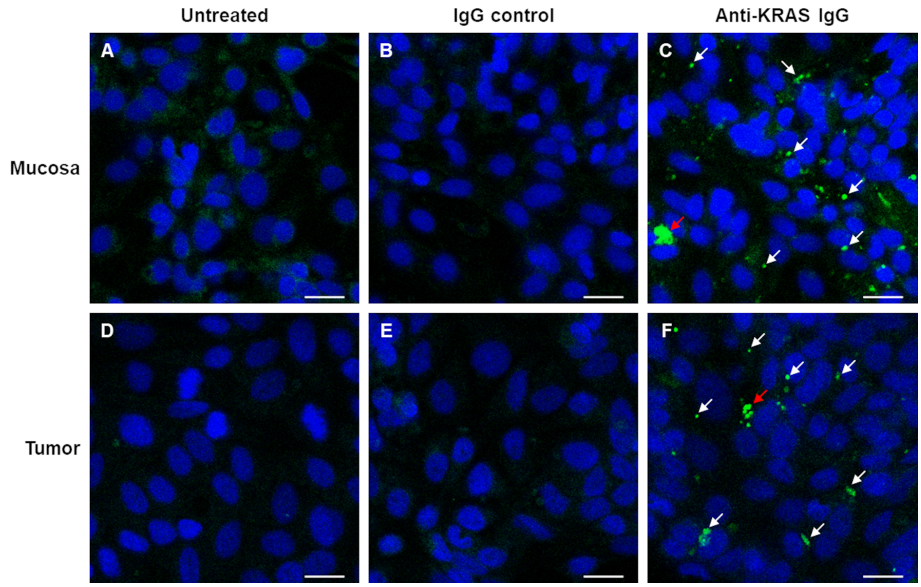

FIGURE 2
Confocal imaging shows internalization of anti-KRAS antibodies into *ex vivo* cultured mucosa and tumor cells. Live *ex vivo* cultured matched mucosa **(A–C)** and tumor **(D–F)** cells were untreated **(A–D)**, treated with Rabbit IgG Isotype control **(B–E)** or Rabbit anti-KRAS antibody **(C–F)** for 16 h, then fixed and counterstained with FITC-conjugated anti-rabbit IgG secondary antibody. The arrows in **(C)** and **(F)** point to the aggregates of anti-KRAS antibodies; the red arrows point to larger aggregates. Scale bar = 20 μm.

KRAS by aggregating KRAS in the cytoplasm. We treated the KRAS p.Gly12Val tumor cells with mouse anti-KRAS antibody, then fixed and immunostained for KRAS using rabbit anti-KRAS antibodies. Compared to untreated tumor control (Figure 3A), treated tumor cells has reduced KRAS plasma membrane localization (Figure 3B). Meanwhile, KRAS wild-type tumor cells do not show obvious alterations in KRAS localization (data not shown).

3.6 *Ex vivo* cultured tumor treated with anti-KRAS antibodies displayed decreased SOX9 expression and nuclear localization

While treatment of tumor cells with anti-KRAS antibodies led to an observable change of localization of KRAS from inner plasma membrane to cytoplasm, its effect on downstream signaling remains to be confirmed. Phospho-ERK1/2 and phospho-Akt1/2/3 are known downstream effectors of KRAS in the MAPK signaling in cancer cell lines (21). However, we previously reported that phospho-ERK1/2 or phospho-Akt1/2/3 were not upregulated in CRC tumor compared to matched mucosa tissues, and in fact in most cases, downregulated in tumor (24). Instead, most CRC tumor tissues displayed upregulation of SOX9 compared to matched normal mucosa. Furthermore, SOX9 were previously reported to be able to promote cancer cell proliferation and tumor progression by directly activating stem cell-like signaling and inhibit cell differentiation (43). Since we showed previously that the expression of SOX9 proteins in CRC was KRAS-mutant-dependent (24), treatment of CRC with anti-KRAS antibodies is expected to downregulate SOX9 protein expression. Thus, we counterstained the tumor cells for SOX9 after treatment with anti-KRAS antibodies. Compared to untreated cells (Figure 3C) or tumor cells treated with rabbit IgG negative control (Figure 3D), tumor cells treated with anti-KRAS antibody showed weaker SOX9 cytoplasmic staining and less nuclear localization (Figure 3E).

4 Discussion

Direct inhibition of KRAS has been a longstanding challenge, due to its structure being impermissible to pharmacological targeting. While it is largely believed that macromolecules above 1 kDa cannot penetrate the cell membrane, the existence of cell-penetrating autoantibodies of ~150 kDa contradicted this concept (26, 44). We thus speculated that anti-KRAS antibodies can similarly penetrate cells and inhibit endogenous KRAS.

In this study, we developed a transient *ex vivo* culture from CRC patients' tumor and matched mucosa tissues (Figures 1A–D) as a model to test for anti-KRAS antibody internalization. We first characterized the localization of endogenous KRAS in fixed and permeabilized *ex vivo* cultured CRC matched mucosa-tumor pair which revealed that tumors with somatic KRAS p.Gly12Val activating mutations show higher inner plasma membrane KRAS localization (net-like pattern) compared to its matched mucosa (where KRAS was wild-type) (Figures 1E, F). This is possibly contributed by increased KRAS activation hence increase membrane dwell time which is essential for KRAS effector function (41). Interestingly, the net-like pattern is less prominent

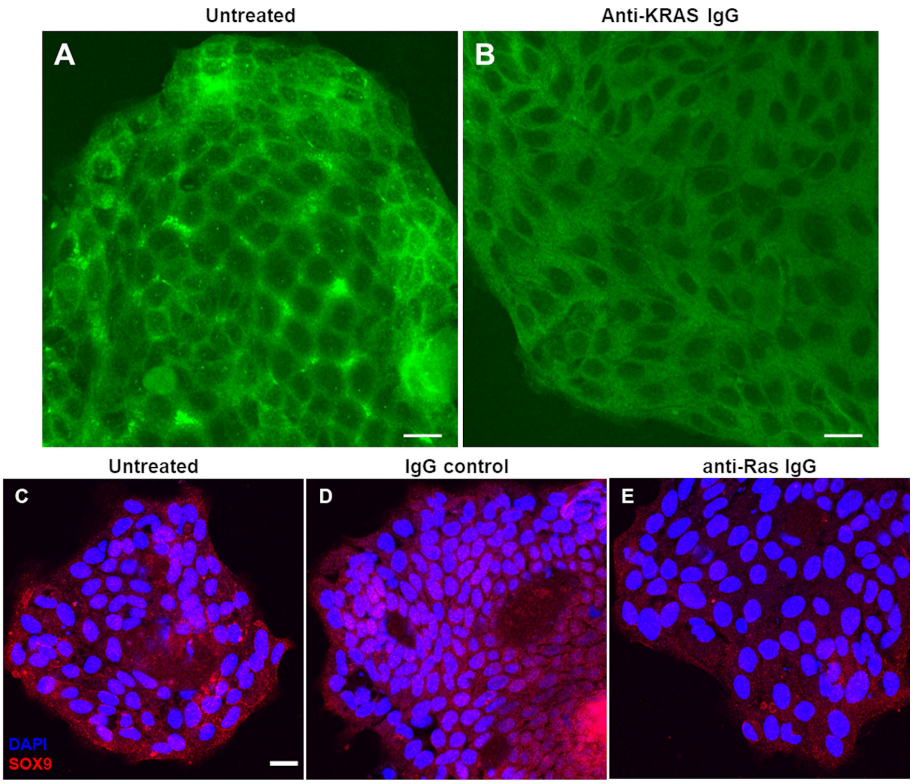

FIGURE 3
Decreased KRAS inner membrane localization and reduced SOX9 immunostaining after treatment of live *ex vivo* cultured tumor cells with anti-KRAS antibody observed by confocal imaging. Live *ex vivo* cultured tumor cells were untreated (negative control) **(A)** or treated with mouse anti-KRAS antibody **(B)**, fixed and immunostained with rabbit-anti-KRAS antibody then counterstained with FITC-conjugated anti-rabbit IgG secondary antibody. Live *ex vivo* cultured tumor cells were untreated **(C)** or treated with rabbit IgG isotype control **(D)** or rabbit anti-Ras IgG antibody **(E)**, fixed and immunostained with mouse anti-SOX9 antibody then counterstained with Alexa Fluor 555-conjugated anti-mouse IgG secondary antibody. The tumor in **(A, B)** harbors a KRAS p.Gly12Val mutation. The scale bar in **(A–C)** are equivalent to 20 μm. The scale bar in **(C)** is applicable to **(C–E)**.

in other KRAS activating mutation tumors, which may be due to different plasma membrane anchoring properties of the mutants.

We next hypothesized that anti-KRAS antibodies can penetrate cells and enter the cytosol to sequester endogenous KRAS, preventing its plasma membrane localization. Our results show that anti-KRAS antibody can indeed be internalized into both *ex vivo* cultured matched mucosa and tumor cells (Figures 2C–F). We observed that the internalized anti-KRAS antibodies form aggregates (punctate structures) in the cells (Figures 2C–F), but not in untreated (Figures 2A–D) or cells treated with rabbit IgG isotype control (Figures 2B–E), showing that the aggregates are not due to fortuitous antibody aggregation but possibly aggregation of endogenous KRAS by anti-KRAS antibodies. The aggregates were confirmed to be KRAS-antibody complexes with co-localization of two different anti-KRAS antibodies (Supplementary Figure 4).

These antibodies are largely localized in the cytoplasm with little trapped in endosomes as observed from minimal co-localization of the internalized anti-KRAS antibody with early endosome marker EEA1 (Supplementary Figure 5). The internalized anti-KRAS antibodies binds to and aggregates endogenous KRAS in the cytoplasm. Shin, Choi (45) and Shin, Kim (46) has claimed that entry of anti-Ras antibody into cell line was mainly by endocytosis with endosomal escape efficiency at only 4-5% and 13-16% respectively while most antibodies are trapped in endosomes. Our results may be attributed to different cells, different antibodies, or HEPES in our antibody dilution medium which has been reported to drive protein transduction, or components from the Matrigel that may mediate alternative non-endocytic entry (47).

Treatment of live *ex vivo* cultured tumor cells harboring p.Gly12Val somatic mutations with anti-KRAS antibodies reduced inner plasma membrane localization of KRAS where it must tether to function (Figure 1F). Live tumor cells treated with anti-KRAS antibody also showed less intense cytoplasmic and less nuclear staining for SOX9, thus providing further evidence that SOX9, a cancer stem cell marker and potential driver in CRC (43, 48), is a downstream effector of KRAS signaling (Figures 3C–E). These differential phenotypes of anti-KRAS antibody-treated tumor cells indicated that the internalized antibody is functional and could potentially be developed into novel antibody therapeutics for CRC.

We propose a mode of action of anti-KRAS antibody in inhibition of KRAS signaling and inner plasma membrane localization (Figure 4). Anti-KRAS antibodies must first be internalized and localized to the cytoplasm, either by fluid-phase endocytosis then endosomal escape or by direct penetration

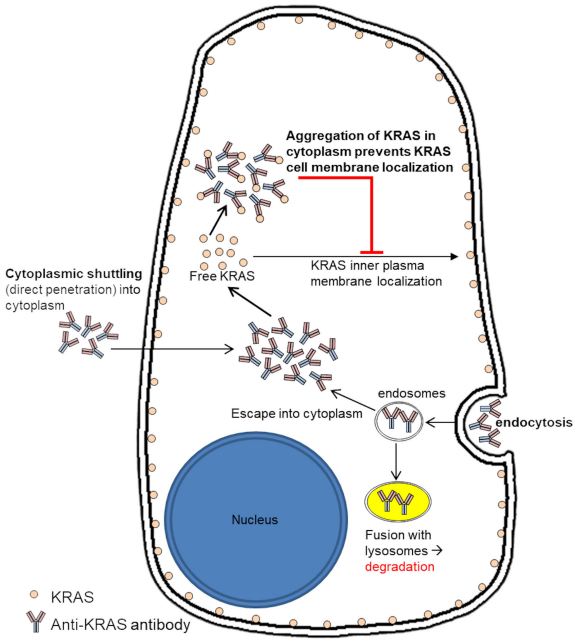

FIGURE 4
Proposed mode of action of anti-KRAS antibody treatment on sequestering endogenous KRAS in the cytoplasm to inhibit them from localizing to the inner plasma membrane. We propose that anti-KRAS antibodies taken up by the cells enters the cytoplasm and binds to endogenous KRAS, preventing KRAS from localizing to the inner plasma membrane where it activates downstream effectors.

through the plasma membrane lipid bilayer. The antibodies then bind to endogenous KRAS in the cytoplasm and prevent KRAS from being translocated to the inner plasma membrane where it functions.

While small molecules are the major trend in therapeutics due to their small size, thus easy entry into cells, macromolecule biologics like antibodies have several advantages. Small molecules tend to have off-target pleiotropic effects, whereas antibodies, a type of biologics, are more specific for their target due to a higher structure complexity (49). While monobodies can also target internal proteins, they lack the Fc domain of intracellular antibodies which can be recognized by cytosolic Fc receptor to activate the intracellular immunity through TRIM21 and targets the antibody-protein complex for degradation (50–52). Since IgG antibodies are naturally occurring, toxicity usually associated with small molecule inhibitors and monobodies is minimized. Moreover, if the mode of action is mislocalization rather than altered expression of the protein, therapy-induced secondary mutations and resistance can conceivably be reduced.

The long-term goal is to produce antibodies that specifically target mutant KRAS. The antibodies should be further optimized for more efficient internalization by tumor cells, with the aim of eventually proceeding to clinical trials. Anti-KRAS antibodies can be used in combination with anti-EGFR antibody (Cetuximab) in *KRAS* wildtype advanced colorectal cancer (CRC) patients to concurrently kill tumor cells that has developed resistance to anti-EGFR therapy due to acquired KRAS mutation. For patients who are already *KRAS* mutation-positive, anti-KRAS antibody targeting the hot-spots codons-12 and -13, will be the therapy of choice. Furthermore, majority of pancreatic ductal adenocarcinoma (PDAC), another common fatal cancer, is initiated by *KRAS* mutation and hence overexpression of the KRAS protein (53). Thus, the successful production of the anti-KRAS antibody targeting the mutational hot spots will potentially be a useful alternative therapy for PDAC as well.

Data availability statement

The raw data supporting the conclusions of this article will be made available by the authors, without undue reservation.

Ethics statement

The studies involving human participants were reviewed and approved by Singhealth Centralized Review Board. The patients/participants provided their written informed consent to participate in this study.

Author contributions

PC and SW contributed to the concept and study design. KL and YL contributed to the experimental planning and the acquisition, analysis, and interpretation of data. CT, ET, AC and IS-E contributed to the tissue collection, clinical data and administration. ML and MW contributed to the tissue collection process and ML contributed to execution of certain experimental procedures. KL, YL and PC drafted the manuscript. KL, PC and SW contributed to the critical revision of the manuscript. All authors contributed to the article and approved the submitted version.

Funding

We acknowledge grant funding from National Medical Research Council (NMRC) Singapore grant (OFIRG-0004-2016) and Singapore General Hospital Cancer Peak Research Seed Grant to PC.

Acknowledgments

We would like to thank Dr. Michelle Tan from Department of Clinical Research, Singapore General Hospital and Mr. Ernest Cheah from Nikon Imaging Centre for providing support on confocal imaging.

Conflict of interest

The authors declare that the research was conducted in the absence of any commercial or financial relationships that could be construed as a potential conflict of interest.

Publisher's note

All claims expressed in this article are solely those of the authors and do not necessarily represent those of their affiliated organizations, or those of the publisher, the editors and the reviewers. Any product that may be evaluated in this article, or claim that may be made by its manufacturer, is not guaranteed or endorsed by the publisher.

Supplementary material

The Supplementary Material for this article can be found online at: https://www.frontiersin.org/articles/10.3389/fonc.2023.1036871/full#supplementary-material

References

1. Noone AM, Howlader N, Krapcho M, Miller D, Brest A, Yu M, et al. *Seer cancer statistics review (Csr)* (2018). Available at: https://seer.cancer.gov/csr/1975_2015/.

2. Sung H, Ferlay J, Siegel RL, Laversanne M, Soerjomataram I, Jemal A, et al. Global cancer statistics 2020: Globocan estimates of incidence and mortality worldwide for 36 cancers in 185 countries. *CA Cancer J Clin* (2021) 71(3):209–49. doi: 10.3322/caac.21660

3. *Singapore Cancer registry, annual registry report, trends in cancer incidence in Singapore 2010 – 2014*. Singapore: National Registry of Diseases Office (2015). Available at: https://www.nrdo.gov.sg/docs/librariesprovider3/default-document-library/cancer-trends-report-2010—2014_web.pdf?sfvrsn=0.

4. Goyle S, Maraveyas A. Chemotherapy for colorectal cancer. *Dig Surg* (2005) 22 (6):401–14. doi: 10.1159/000091441

5. Bleiberg H. Adjuvant treatment of colon cancer. *Curr Opin Oncol* (2005) 17 (4):381–5. doi: 10.1097/01.cco.0000166648.92674.4c

6. Misale S, Yaeger R, Hobor S, Scala E, Janakiraman M, Liska D, et al. Emergence of kras mutations and acquired resistance to anti-egfr therapy in colorectal cancer. *Nature* (2012) 486(7404):532–6. doi: 10.1038/nature11156

7. Diaz LAJr., Williams RT, Wu J, Kinde I, Hecht JR, Berlin J, et al. The molecular evolution of acquired resistance to targeted egfr blockade in colorectal cancers. *Nature* (2012) 486(7404):537–40. doi: 10.1038/nature11219

8. Gomez D, De Rosa A, Addison A, Brooks A, Malik HZ, Cameron IC. Cetuximab therapy in the treatment of metastatic colorectal cancer: The future frontier? *Int J Surg* (2013) 11(7):507–13. doi: 10.1016/j.ijsu.2013.04.014

9. Le DT, Uram JN, Wang H, Bartlett BR, Kemberling H, Eyring AD, et al. Pd-1 blockade in tumors with mismatch-repair deficiency. *N Engl J Med* (2015) 372 (26):2509–20. doi: 10.1056/NEJMoa1500596

10. Chin L, Tam A, Pomerantz J, Wong M, Holash J, Bardeesy N, et al. Essential role for oncogenic ras in tumour maintenance. *Nature* (1999) 400(6743):468–72. doi: 10.1038/22788

11. Rui Y, Wang C, Zhou Z, Zhong X, Yu Y. K-Ras mutation and prognosis of colorectal cancer: A meta-analysis. *Hepatogastroenterology* (2015) 62(137):19–24.

12. Huang D, Sun W, Zhou Y, Li P, Chen F, Chen H, et al. Mutations of key driver genes in colorectal cancer progression and metastasis. *Cancer Metastasis Rev* (2018) 37 (1):173–87. doi: 10.1007/s10555-017-9726-5

13. Ottaiano A, Normanno N, Facchini S, Cassata A, Nappi A, Romano C, et al. Study of ras mutations' prognostic value in metastatic colorectal cancer: Storia analysis. *Cancers* (2020) 12(7):1919. doi: 10.3390/cancers12071919

14. Stephen AG, Esposito D, Bagni RK, McCormick F. Dragging ras back in the ring. *Cancer Cell* (2014) 25(3):272–81. doi: 10.1016/j.ccr.2014.02.017

15. Cox AD, Fesik SW, Kimmelman AC, Luo J, Der CJ. Drugging the undruggable ras: Mission possible? *Nat Rev Drug Discov* (2014) 13(11):828–51. doi: 10.1038/nrd4389

16. Wang W, Fang G, Rudolph J. Ras inhibition *Via* direct ras binding–is there a path forward? *Bioorg Med Chem Lett* (2012) 22(18):5766–76. doi: 10.1016/j.bmcl.2012.07.082

17. Prior IA, Hood FE, Hartley JL. The frequency of ras mutations in cancer. *Cancer Res* (2020) 80(14):2969–74. doi: 10.1158/0008-5472.CAN-19-3682

18. Ostrem JM, Peters U, Sos ML, Wells JA, Shokat KM. K-Ras(G12c) inhibitors allosterically control gtp affinity and effector interactions. *Nature* (2013) 503 (7477):548–51. doi: 10.1038/nature12796

19. Rowell CA, Kowalczyk JJ, Lewis MD, Garcia AM. Direct demonstration of geranylgeranylation and farnesylation of ki-ras in vivo. *J Biol Chem* (1997) 272 (22):14093–7. doi: 10.1074/jbc.272.22.14093

20. Whyte DB, Kirschmeier P, Hockenberry TN, Nunez-Oliva I, James L, Catino JJ, et al. K- and n-ras are geranylgeranylated in cells treated with farnesyl protein transferase inhibitors. *J Biol Chem* (1997) 272(22):14459–64. doi: 10.1074/jbc.272.22.14459

21. Fang JY, Richardson BC. The mapk signalling pathways and colorectal cancer. *Lancet Oncol* (2005) 6(5):322–7. doi: 10.1016/S1470-2045(05)70168-6

22. Drosten M, Barbacid M. Targeting the mapk pathway in kras-driven tumors. *Cancer Cell* (2020) 37(4):543–50. doi: 10.1016/j.ccell.2020.03.013

23. Xie YH, Chen YX, Fang JY. Comprehensive review of targeted therapy for colorectal cancer. *Signal Transduct Target Ther* (2020) 5(1):22. doi: 10.1038/s41392-020-0116-z

24. Lam KK, Tang CL, Tan E, Wong SH, Cheah PY. Kras mutation-independent downregulation of Mapk/Pi3k signaling in colorectal cancer. *Mol Oncol* (2022) 16 (5):1171–83. doi: 10.1002/1878-0261.13163

25. Imai K, Takaoka A. Comparing antibody and small-molecule therapies for cancer. *Nat Rev Cancer* (2006) 6(9):714–27. doi: 10.1038/nrc1913

26. Ruiz-Arguelles A, Alarcon-Segovia D. Penetration of autoantibodies into living cells, 2000. *Isr Med Assoc J* (2001) 3(2):121–6.

27. Alarcon-Segovia D, Ruiz-Arguelles A, Llorente L. Broken dogma: Penetration of autoantibodies into living cells. *Immunol Today* (1996) 17(4):163–4. doi: 10.1016/s0167-5699(96)90258-3

28. Alarcon-Segovia D, Llorente L, Ruiz-Arguelles A. The penetration of autoantibodies into cells may induce tolerance to self by apoptosis of autoreactive lymphocytes and cause autoimmune disease by dysregulation and/or cell damage. *J Autoimmun* (1996) 9(2):295–300. doi: 10.1006/jaut.1996.0038

29. Alarcon-Segovia D, Llorente L, Ruiz-Arguelles A, Richard-Patin Y, Perez-Romano B. Penetration of anti-DNA antibodies into mononuclear cells causes apoptosis. *Arthritis Rheum* (1995) 3:S179.

30. Ruiz-Arguelles A, Perez-romano B, Llorente L, Alarcon-Segovia D, Castellanos JM. Penetration of anti-DNA antibodies into immature live cells. *J Autoimmun* (1998) 11(5):547–56. doi: 10.1006/jaut.1998.0216

31. Madaio MP, Yanase K. Cellular penetration and nuclear localization of anti-DNA antibodies: Mechanisms, consequences, implications and applications. *J Autoimmun* (1998) 11(5):535–8. doi: 10.1006/jaut.1998.0217

32. Gordon RE, Nemeth JF, Singh S, Lingham RB, Grewal IS. Harnessing sle autoantibodies for intracellular delivery of biologic therapeutics. *Trends Biotechnol* (2021) 39(3):298–310. doi: 10.1016/j.tibtech.2020.07.003

33. Jang JY, Jeong JG, Jun HR, Lee SC, Kim JS, Kim YS, et al. A nucleic acid-hydrolyzing antibody penetrates into cells via caveolae-mediated endocytosis, localizes in the cytosol and exhibits cytotoxicity. *Cell Mol Life Sci* (2009) 66(11-12):1985–97. doi: 10.1007/s00018-009-9179-2

34. Choi DK, Bae J, Shin SM, Shin JY, Kim S, Kim YS. A general strategy for generating intact, full-length igg antibodies that penetrate into the cytosol of living cells. *MAbs* (2014) 6(6):1402–14. doi: 10.4161/mabs.36389

35. Ronen J, Hayat S, Akalin A. Evaluation of colorectal cancer subtypes and cell lines using deep learning. *Life Sci Alliance* (2019) 2(6):e201900517. doi: 10.26508/lsa.201900517

36. Mittal VK, Bhullar JS, Jayant K. Animal models of human colorectal cancer: Current status, uses and limitations. *World J Gastroenterol* (2015) 21(41):11854–61. doi: 10.3748/wjg.v21.i41.11854

37. Hofer M, Lutolf MP. Engineering organoids. *Nat Rev Mater* (2021) 6(5):402–20. doi: 10.1038/s41578-021-00279-y

38. Booth C, Dove WF, Gordon JI, Halberg RB, O'Shea JA, Stappenbeck TS, et al. *Techniques for modeling human intestinal cancer in mice*. Wisconsin, USA: The Jackson Laboratory, University of Wisconsin-Madison (2000).

39. Schindelin J, Arganda-Carreras I, Frise E, Kaynig V, Longair M, Pietzsch T, et al. Fiji: An open-source platform for biological-image analysis. *Nat Methods* (2012) 9 (7):676–82. doi: 10.1038/nmeth.2019

40. Rueden CT, Schindelin J, Hiner MC, DeZonia BE, Walter AE, Arena ET, et al. Imagej2: Imagej for the next generation of scientific image data. *BMC Bioinf* (2017) 18 (1):529. doi: 10.1186/s12859-017-1934-z

41. Martin EW, Mittag T. Dwelling at membranes promotes decisive signaling. *Science* (2019) 363(6431):1036–7. doi: 10.1126/science.aaw6434

42. Zhang J, Jiang X, Yin J, Dou S, Xie X, Liu T, et al. Rnf141 interacts with kras to promote colorectal cancer progression. *Oncogene* (2021) 40(39):5829–42. doi: 10.1038/s41388-021-01877-4

43. Liang X, Duronio GN, Yang Y, Bala P, Hebbar P, Spisak S, et al. An enhancer-driven stem cell-like program mediated by Sox9 blocks intestinal differentiation in colorectal cancer. *Gastroenterology* (2022) 162(1):209–22. doi: 10.1053/j.gastro.2021.09.044

44. Matsson P, Kihlberg J. How big is too big for cell permeability? *J Med Chem* (2017) 60(5):1662–4. doi: 10.1021/acs.jmedchem.7b00237

45. Shin SM, Choi DK, Jung K, Bae J, Kim JS, Park SW, et al. Antibody targeting intracellular oncogenic ras mutants exerts anti-tumour effects after systemic administration. *Nat Commun* (2017) 8:15090. doi: 10.1038/ncomms15090

46. Shin SM, Kim JS, Park SW, Jun SY, Kweon HJ, Choi DK, et al. Direct targeting of oncogenic ras mutants with a tumor-specific cytosol-penetrating antibody inhibits ras mutant-driven tumor growth. *Sci Adv* (2020) 6(3):eaay2174. doi: 10.1126/sciadv.aay2174

47. Chen SH, Chao A, Tsai CL, Sue SC, Lin CY, Lee YZ, et al. Utilization of hepes for enhancing protein transfection into mammalian cells. *Mol Ther Methods Clin Dev* (2019) 13:99–111. doi: 10.1016/j.omtm.2018.12.005

48. Aguilar-Medina M, Avendano-Felix M, Lizarraga-Verdugo E, Bermudez M, Romero-Quintana JG, Ramos-Payan R, et al. Sox9 stem-cell factor: Clinical and functional relevance in cancer. *J Oncol* (2019) 2019:6754040. doi: 10.1155/2019/6754040

49. Buvailo A. *Will biologics surpass small molecules in the pharmaceutical race?* London, United Kingdom: BiopharmaTrend.com (2022). Available at: https://BiopharmaTrend.com.

50. Teng KW, Tsai ST, Hattori T, Fedele C, Koide A, Yang C, et al. Selective and noncovalent targeting of ras mutants for inhibition and degradation. *Nat Commun* (2021) 12(1):2656. doi: 10.1038/s41467-021-22969-5

51. Khan I, Koide A, Zuberi M, Ketavarapu G, Denbaum E, Teng KW, et al. Identification of the nucleotide-free state as a therapeutic vulnerability for inhibition of selected oncogenic ras mutants. *Cell Rep* (2022) 38(6):110322. doi: 10.1016/j.celrep.2022.110322

52. Mallery DL, McEwan WA, Bidgood SR, Towers GJ, Johnson CM, James LC. Antibodies mediate intracellular immunity through tripartite motif-containing 21 (Trim21). *Proc Natl Acad Sci USA* (2010) 107(46):19985–90. doi: 10.1073/pnas.1014074107

53. Eser S, Schnieke A, Schneider G, Saur D. Oncogenic kras signalling in pancreatic cancer. *Br J Cancer* (2014) 111(5):817–22. doi: 10.1038/bjc.2014.215

frontiers | Frontiers in Oncology

TYPE Brief Research Report
PUBLISHED 28 March 2023
DOI 10.3389/fonc.2023.1062926

Check for updates

OPEN ACCESS

EDITED BY
Zhendong Jin,
Second Military Medical University, China

REVIEWED BY
Akanksha Bhargava,
Johns Hopkins Medicine, United States
Kohei Togami,
Hokkaido University of Science, Japan

*CORRESPONDENCE
Jeroen Hagendoorn
j.hagendoorn-3@umcutrecht.nl

SPECIALTY SECTION
This article was submitted to Gastrointestinal Cancers: Hepato Pancreatic Biliary Cancers, a section of the journal Frontiers in Oncology

RECEIVED 06 October 2022
ACCEPTED 06 March 2023
PUBLISHED 28 March 2023

CITATION
Frenkel N, Poghosyan S, van Wijnbergen JW, van den Bent L, Wijler L, Verheem A, Borel Rinkes I, Kranenburg O and Hagendoorn J (2023) Tissue clearing and immunostaining to visualize the spatial organization of vasculature and tumor cells in mouse liver.
Front. Oncol. 13:1062926.
doi: 10.3389/fonc.2023.1062926

COPYRIGHT
© 2023 Frenkel, Poghosyan, van Wijnbergen, van den Bent, Wijler, Verheem, Borel Rinkes, Kranenburg and Hagendoorn. This is an open-access article distributed under the terms of the Creative Commons Attribution License (CC BY). The use, distribution or reproduction in other forums is permitted, provided the original author(s) and the copyright owner(s) are credited and that the original publication in this journal is cited, in accordance with accepted academic practice. No use, distribution or reproduction is permitted which does not comply with these terms.

Tissue clearing and immunostaining to visualize the spatial organization of vasculature and tumor cells in mouse liver

Nicola Frenkel, Susanna Poghosyan, Jan Willem van Wijnbergen, Lotte van den Bent, Liza Wijler, André Verheem, Inne Borel Rinkes, Onno Kranenburg and Jeroen Hagendoorn*

Laboratory for Translational Oncology, University Medical Center Utrecht, Utrecht, The Netherlands

The liver has a complex and hierarchical segmental organization of arteries, portal veins, hepatic veins and lymphatic vessels. In-depth imaging of liver vasculature and malignancies could improve knowledge on tumor micro-environment, local tumor growth, invasion, as well as metastasis. Non-invasive imaging techniques such as computed tomography (CT), magnetic resonance imaging (MRI) and positron-emission transmission (PET) are routine for clinical imaging, but show inadequate resolution at cellular and subcellular level. In recent years, tissue clearing – a technique rendering tissues optically transparent allowing enhanced microscopy imaging – has made great advances. While mainly used in the neurobiology field, recently more studies have used clearing techniques for imaging other organ systems as well as tumor tissues. In this study, our aim was to develop a reproducible tissue clearing and immunostaining model for visualizing intrahepatic blood microvasculature and tumor cells in murine colorectal liver metastases. CLARITY and 3DISCO/iDISCO+ are two established clearing methods that have been shown to be compatible with immunolabelling, most often in neurobiology research. In this study, CLARITY unfortunately resulted in damaged tissue integrity of the murine liver lobes and no specific immunostaining. Using the 3DISCO/iDISCO+ method, liver samples were successfully rendered optically transparent. After which, successful immunostaining of the intrahepatic microvasculature using panendothelial cell antigen MECA-32 and colorectal cancer cells using epithelial cell adhesion molecule (EpCAM) was established. This approach for tumor micro-environment tissue clearing would be especially valuable for allowing visualization of spatial heterogeneity and complex interactions of tumor cells and their environment in future studies.

KEYWORDS

tissue clearing, liver vasculature, CLARITY, 3DISCO, iDISCO, tumor micro environment, colorectal cancer, liver metastasis

Introduction

The liver consists of a complex and hierarchical segmental organization of arteries, portal veins, hepatic veins, and lymphatic vessels. These are also a crucial component of the liver-tumor micro-environment and play an important role in processes such as local tumor growth, invasion, as well as onward metastasis. For visualization of the three-dimensional (3D) liver vessel organization and malignancies, imaging techniques such as computed tomography (CT), magnetic resonance imaging (MRI) and positron-emission transmission (PET) are used clinically. However, for fundamental and translational research, these imaging techniques lack the appropriate cellular resolution for three-dimensional imaging at tissue level (1, 2).

Traditionally, histological techniques such as immunohistochemistry can provide excellent cellular and subcellular resolution. However, they require thin tissue sections ranging in thickness between 3 and 5 µm due to imaging depth constraints. 3D renderings can be constructed by means of serial sectioning and post-image reconstruction, a labor intensive and therefore inefficient process. Moreover, sectioning causes tissue damage, distortion and artifacts (1–6). Therefore, tissue clearing, an approach clarifying tissues by reducing light scattering and absorption hereby improving high resolution imaging depth, provides a promising alternative to visualize liver vasculature and malignancies. The first attempts at tissue clearing were performed over 100 years ago (7, 8). Since then, various tissue clearing methods have been devised, adjusted, and optimized. Clearing agents improve the trajectory of light through tissues by eliminating certain biomolecules such as lipids and light-absorbing pigments, hereby homogenizing the refractive index of the tissue, rendering the tissue "transparent" (1–6). (Figure 1A) The ideal method should yield excellent clearing while also maintaining native tissue architecture, preserve endogenous fluorescent proteins, and allowing specific immunolabeling. Generally, three groups of current clearing methods exist: 1) Organic-solvent based (such as 3DISCO, iDISCO, BABB) 2) aqueous-based (such as CLEAR, Scale, SeeDB, CUBIC, FRUIT), and 3) hydrogel embedding (such as CLARITY, PACT, PARS). Compared to thin tissue sections of only several micrometres used for histological techniques, successful clearing and imaging has been established for thick tissue sections and even whole mouse organs, reaching excellent imaging depths of several millimetres (1–6).

While some tissue clearing methods have been shown to render liver tissue reasonably optically transparent, liver tissue clearing is generally hampered by its high content of light-absorbing heme (9–15). Moreover, optimal tissue clearing involves the use of strong organic solvents or detergents which affect native biomolecules and tissue architecture to the point of them being severely altered, damaged or lost (2, 3, 6, 16). Here, our aim was to develop a robust and reproducible murine tissue clearing and immunostaining model for the visualization of intrahepatic blood microvasculature, as well as tumor cells in murine colorectal cancer (CRC) metastases. As the clearing methods CLARITY and 3DISCO/iDISCO+ are well established for compatibility with immunolabelling, albeit mainly in the neurobiology field, these methods were investigated for clearing and immunolabelling liver tissue and CRC metastasis samples. We showed that the hydrogel-based CLARITY with passive clearing method in liver tissue resulted in tissue integrity unsuitable for immunolabelling. Using 3DISCO/iDISCO+, we could successfully render liver and CRC tumor samples optically transparent and immunolabel the intrahepatic endothelial system as well as CRC metastases, making this approach a suitable technique for future studies of intrahepatic vasculature as well as the spatial heterogeneity and interactions of tumor cells and their environment in future studies.

Materials and methods

Tumor organoid culture

From a previously described transgenic mouse model with conditional activation of the Notch1 receptor as well as a p53 deletion in the digestive tract (17), organoids were derived from spontaneously formed colon tumors. All of the derived tumors showed mutations of either Ctnnb1 or Apc genes, implicating classical Wnt pathway activation (17). Organoids were FACS-sorted after being transduced using a lentiviral vector expressing luciferase and tdTomato (pUltra-Chili-Luc, Addgene #48688). Culturing was done at 37°C in a humidified atmosphere containing 5% CO2 using a 3D matrix structure (droplets of Growth Factor Reduced Basement Membrane Extract (BME; Amsbio) and Advanced DMEM/F12 (Thermo Fisher Scientific) medium which was supplemented with 1% Penicillin-Streptomycin (Gibco), 1% HEPES buffer, 2 mM Glutamax (Invitrogen), 2% B27 supplement (Invitrogen), 100 ng/ml Noggin (produced by lentiviral transfection), 10 nM murine recombinant FGF (PeproTech) and 1 mM n-Acetylcysteine (Sigma-Aldrich). Passaging was done weekly using TrypLE Express (Gibco) and medium was refreshed biweekly or earlier if needed based on organoid density.

Animals

Male C57BL/6 (for non-tumor optical clearing experiments) and C57BL/6NCrl mice (for colorectal (CRC) tumor inoculation experiments), aged 8-10 weeks, were housed in groups of maximum 5 animals per cage in open cages with tissues and contact bedding. The animals were kept on a 12:12 h light (7AM)/dark (7PM) cycle at 20-24° C, 45-60% humidity and received water and AIN-93M pellets (Ssniff Spezialdiäten GmbH) ad libitum. Mice were acclimated for minimally 1 week before tumor inoculation. All mice were assessed biweekly for body weight and physical tumor progression. Bioluminescent imaging was performed *in vivo* weekly to monitor tumor progression and metastasis formation. Mice were anesthetized using isoflurane 4% for induction and 2% for maintenance, with 1.6 l/min oxygen. They received an intraperitoneal injection with 100 µL of D-luciferin (VivoGloTM Luciferin, Promega) in PBS. Mice were then imaged at 1s exposure/image for 5min, using the PhotonIMAGERTM RT system (Biospace Lab, Paris, France) an d M3 Vision software (Biospace Lab).

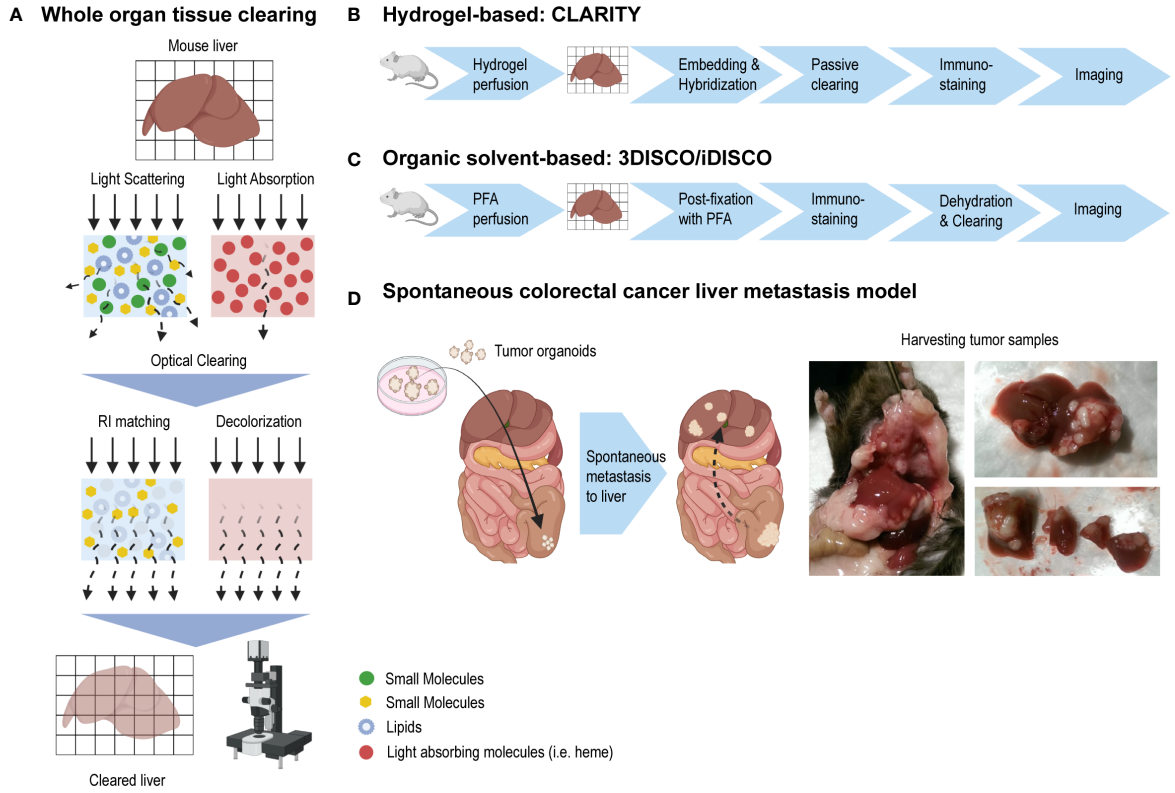

FIGURE 1
Whole organ tissue clearing using CLARITY and 3DISCO/iDISCO methods. **(A)** A tissue's opacity is mainly caused by light scattering (due to the heterogeneity of the tissue components optical characteristics or refractive indexes) and light-absorbing compounds such as heme. Light scattering and light absorption hinder the light as it travels through a tissue. By using tissue clearing techniques, lipids are extracted and refractive indexes are better matched. Steps to remove light absorbing compounds are taken. The result is a "transparent" tissue in which microscopy imaging depth has greatly been improved. **(B)** CLARITY is a tissue clearing method which uses a tissue-gel hybrid to support and maintain the tissue's architecture. **(C)** 3DISCO and iDISCO methods do not make use of a hydrogel scaffold like CLARITY, but use organic solvents instead for optical tissue clearing. **(D)** In a murine model, colorectal cancer organoids were implanted into the mouse cecum, after which the tumor cells spontaneously metastasized to the liver. Liver tumor samples were harvested and used to establish a tumor tissue clearing protocol.

In vivo surgical inoculation of colorectal cancer organoids

Mice were anesthetized using isoflurane and analgesic buprenorphine (0.1 mg/kg) was administered subcutaneously. Colorectal cancer organoids were dissociated using TrypLE (Gibco). A total of 250.000 single cells were embedded in 6µL of 75% Rat Tail Type I Collagen (Corning) droplets and 25% neutralization buffer; AlphaMEM powder (Life Technology), 1 M HEPES buffer pH 7.5 (Invitrogen) and NaHCO3 (Sigma). The organoids were left to recover overnight. The next day, the cecum was exposed by median laparotomy. A small 2mm incision was made into the cecum using a scalpel and bleeding was stemmed using cotton tips. The collagen drops containing 1-day old CRC organoids were shortly air-dried and gently pushed into the incision site, and afterwards sealed by placing Seprafilm (Genzyme) over the incision site. The peritoneum wall and skin were then sutured. Mice were monitored closely for 2 days to ensure proper incision closure. Upon signs of tumor growth and metastasis formation, determined clinically and by bioluminescence imaging, mice were sacrificed and samples were harvested as stated below.

Tissue clearing method: CLARITY

The CLARITY method has been previously described (18). To form the hydrogel monomer (HM) solution, the following were combined cold and kept on ice: (in total volume 400ml) 4% acrylamide (BioRad), 1x TBS, 4% PFA, 0.25% VA-044 (FujiFilm), in 220ml dH2O. HM solution was stored in 50ml Falcon tubes at -20°C. On the day of the experiment, the HM solution was thawed on ice and gently mixed by inverting. A dedicated mouse surgery room was used. All operations were performed during the afternoon. After anesthesia, mice were given Temgesic (0,3mg/ml, Indivior Europe Limited) by subcutaneous injection preoperatively at 0.05 mg/kg. Median laparotomy was performed, the diaphragm was cut, the xiphoid was lifted and held in place with a clamp and the heart was exposed. A 23G needle was inserted into the left ventricle and the right atrium was opened with a small cut. Transcardial perfusion was performed using an infusion pump to infuse first 20ml ice-cold PBS and 20ml ice-cold HM solution immediately afterwards. Liver lobes were harvested and were placed in a 50ml Falcon tube containing ice-cold 30ml HM solution. Murine liver lobes differ in size (as seen in Figure 2). The liver lobe samples had a maximum length of 30mm and maximum width of 20mm, with a maximum thickness of 10mm. The liver lobes were

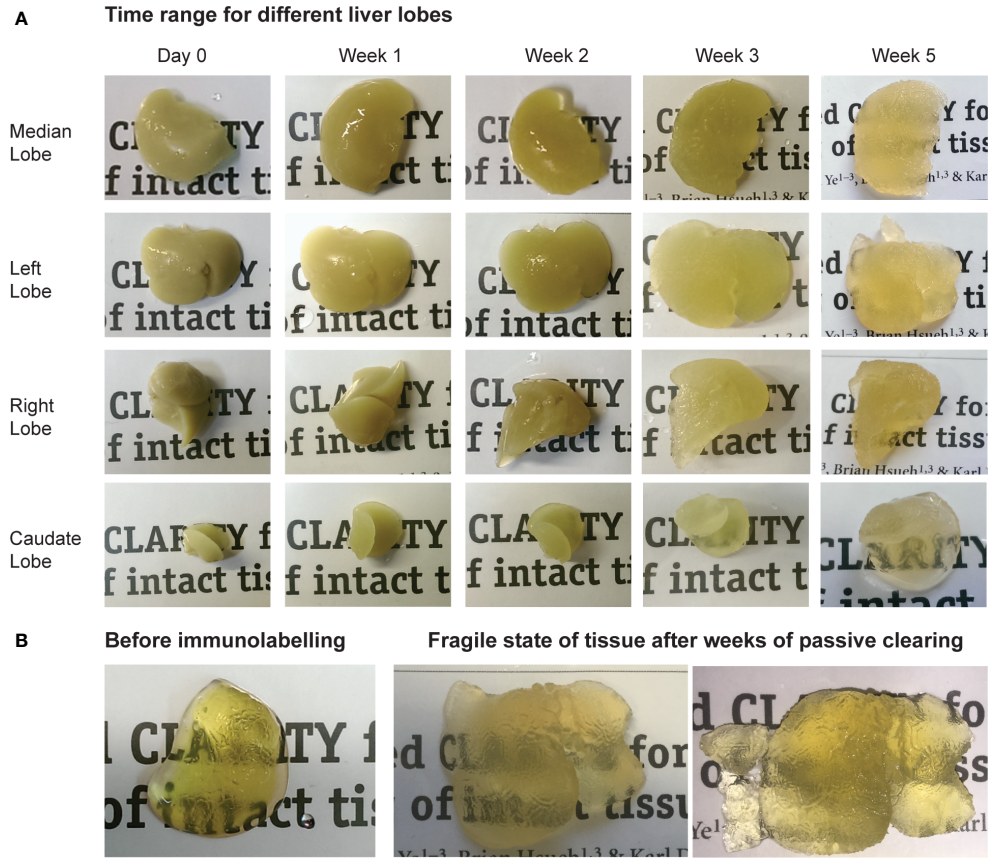

FIGURE 2
Tissue clearing using hydrogel-based CLARITY method. **(A)** Time range showing the passive clearing process for different liver lobes. **(B)** Before immunolabeling, adequate transparency of tissue was reached for the liver lobes. As passive clearing required several weeks of the tissues being in contact with strong detergent solutions before they were rendered adequately transparent for imaging, the samples became extremely fragile and would easily fragment during experimental handling.

incubated at 4°C for 12hrs. As preparation for tissue embedding, oxygen must be removed from sample tubes as oxygen inhibits hydrogel polymerization. A layer of mineral oil of 5mm thick was placed on top of the HM solution. The falcon tube was then placed in a 37°C water bath for 3-4 hrs. The liver lobes were extracted carefully from the solidified hydrogel and the hydrogel was removed from the sample surfaces using gentle rubbing motion with disposable Kimwipes (Kim Tech). Liver lobes samples were washed 2x for 24hrs in 50ml SDS/Boric Acid clearing solution (SBC) solution (stock solution: 20% SDS (Roche) and 1M boric acid buffer (Sigma) in H2O (pH adjusted using NaOH to pH 8.5). Final clearing solution was freshly prepared each time by diluting stock solution fivefold in H2O). The sample was then incubated at 37°C on a swivel platform in SBC solution for several weeks (for the complete liver lobes incubation time of 5-6 weeks was used). Fresh clearing solution was added 2x a week. Afterwards, samples were washed 2x with PBST (PBS + 0.1% Triton X-100 (Sigma)) at 37°C on a swivel platform for 24hrs each wash. Samples were incubated with primary antibodies in PBST for 7 days at 37°C on a swivel platform. To the Ab/PBST solution, 0.01% sodium azide (Merck) was added to prevent microbial growth. Samples were washed for 2-3 days in PBST buffer at 37°C on a swivel platform. Fresh buffer was added every 4-6hrs. Then samples were incubated with secondary antibodies and DAPI in PBST buffer for 2-3 days at 37°C on a swivel platform. Antibodies used were (at 1:50) Phalloidin-Actin Alexa 488 (A12379, Life Technology), Phalloidin-Actin Alexa 568 (A12380, Life Technology), CD31 (01951D Pharmingen, sc-1505 Santa Cruz), vWF, panendothelial marker MECA-32 (120502, Biolegend). Secondary antibodies (1:200): Goat anti-Rat Alexa 488, Donkey anti-Goat Alexa 488, Donkey anti-Sheep Alexa 647 (Invitrogen). DAPI (Biolegend) was used at 1:100. After immunolabelling, samples can be stored in PBST with 0.01% sodium azide at 4°C. For refractive index homogenization, before imaging, samples were submerged in glycerol for 24hrs in the dark at room temperature. Once the tissues are cleared, imaging with Ultramicroscope II (LaVision BioTec) lightsheet microscope or confocal microscopy (Zeiss LSM700) was performed. Imaging analysis was performed using Imaris software (Version 8.4, Bitplane).

Tissue clearing method: 3DISCO/iDISCO+

The 3DISCO/iDISCO+ method has been described previously (3, 19–21). Mouse transcardial perfusion and sample harvesting were performed as described above using ice-cold PBS and 4% PFA (Sigma). Liver lobes were extracted. The liver lobes had a maximum length of 30mm and maximum width of 20mm, with a maximum thickness of 10mm. The median, left and right lobes were

cut into smaller samples with a maximum length of 20mm and maximum width of 10mm, maximum thickness of 10mm. The smaller caudate lobes were cut in half (maximum length 5mm x width 5mm, maximum thickness 3-4mm) and used for antibody validation (after antibodies had been tested in immunolabeling on immunohistochemistry (IHC) and frozen sections, see Figures 3E, G). Liver samples were incubated in 50ml Falcon tubes in ice-cold 4% PFA for 12hrs. The next day, samples were left for 1hr at RT on a roller bank and washed 3x with PBS for 30min. Samples were dehydrated using MeOH (Merck)/PBS: 50-80-100% MeOH, 1,5hr for each step at RT with agitation. Samples were then transferred to a solution of MeOH and 6% H2O2 (Merck) for bleaching and left to incubate overnight at 4°C, protected from light. Afterwards, samples were rehydrated in 100% MeOH (2x), 80% and 50% MeOH in PBS, 1,5hrs at RT with agitation for each step. Samples were then incubated in PBSGT (0.2% gelatin (Sigma, from porcine skin) and 0.5% Triton X-100 (Sigma) in PBS) at RT for 24hrs – 4 days depending on sample size. Samples were incubated with primary antibodies in PBSGT + 0.1% saponin (ThermoFisher) for 7 - 14 days depending on sample size at 37°C on swivel platform. Samples sized 20mm x 10mm were incubated for 14 days, while smaller samples (caudate lobes) sized 10mm x 10mm were incubated for 7 days. After washing 6x with PBSGT at RT with agitation, samples were incubated with secondary antibodies and DAPI in PBSGT and 0.1% saponin overnight – 2 days depending on sample size at 37°C on swivel platform. Smaller samples of 5x5mm were incubated overnight, while the larger samples of 20x10mm were incubated for 2 days. To avoid precipitates, secondary antibody solutions were passed through 0.22µm filter. Antibodies used (1:500): Epcam (SinoBiological, 50591-R002) and Panendothelial marker MECA-32 (120502, Biolegend). Secondary antibodies (1:500) were Goat anti-Rat Alexa 568 and Goat anti-rabbit Alexa 647 (Invitrogen). DAPI (Biolegend) was used at 1:100. Samples were washed 6x with PBSGT at RT with agitation. Samples could be stored at 4°C until clearing. Clearing step: 20-40-60-80-100% MeOH/PBS, 1 hr for each step at RT under agitation, protected from light. Then incubation for 3hrs – overnight in 2/3 DCM (ThermoFisher) + 1/3 MeOH, protected from light. Then samples were incubated in 100% DCM 30min and transferred to 100% DBE (Sigma) until cleared. Sample can be kept in DBE at RT protected from light, in glass vial. Once the tissues were cleared, imaging with light sheet microscopy (Ultramicroscope II, LaVision BioTec) or confocal microscopy (Zeiss LSM700) was immediately performed. When using the light sheet microscope, the imaging chamber was filled with DBE containing the sample. Due to tissue shrinkage inherent during this clearing protocol, final tissue thickness when used for imaging was a maximum of 5-6mm where an imaging depth of 5mm was reached. Imaging analysis was performed using Imaris software (Version 8.4, Bitplane).

Ethical guidelines

This research was approved by the National Competent Authority (Licence number AVD115002016614), which is advised by the Animal Ethics Committee, and conducted in accordance with institutional guidelines for the care and use of laboratory animals as well as the Dutch Law on Animal Experiments and the European Directive 2010/63/EU.

Results

Tissue integrity hindering immunolabelling using hydrogel-based CLARITY

Using the hydrogel-based clearing method called CLARITY(20), tissue-gel hybrid samples of liver tissue were created. (Figure 1B) While liver samples could be made optically transparent, unfortunately the passive clearing took several weeks for obtaining adequate tissue transparency, which caused the tissues to become extremely fragile. (See Figures 2A, B) Samples were immunolabeled with Phalloidin-Actin and DAPI to evaluate immunolabeling, tissue structure and integrity after the CLARITY process. Unfortunately, this resulted in epitope damaging and non-specific labelling (data not shown). Because of the tissues' fragile state, the samples were extremely difficult to handle and would fragment easily. Further rounds of adjusted experimental procedures could not improve either the immunolabeling or tissue integrity.

Improved tissue integrity using organic-solvent based 3DISCO/iDISCO+

Different from CLARITY, this method does not make use of hydrogel embedding and hybridization, but uses organic solvents to clear tissues. (Figure 1C). Liver samples were cleared rapidly while maintaining tissue integrity. (Figure 3A).

Immunolabelling intrahepatic vasculature using 3DISCO/iDISCO+

Liver tissue consists of remarkably organized and structured vasculature comprising bile ducts, portal veins, central veins, hepatic arteries, sinusoids and lymphatic vessels. (Figures 3B, C) To visualize intrahepatic endothelial vasculature, firstly CD31 (cluster of differentiation 31, also known as platelet endothelial cell adhesion molecule PECAM-1) was used. While sinusoids and larger vessels could be distinguished (Supplementary Figure 1A), CD31 showed no specific staining as it strongly resembled controls using only the secondary antibody (data not shown). In contrast, immunostaining with MECA-32 (a panendothelial cell antigen on murine endothelium) showed specific labelling of the liver sinusoidal and larger endothelial structures. (Figure 3F) Before usage in the clearing and immunolabelling protocol, immunofluorescent MECA-32 blood vasculature labelling was validated on liver and colon tissue sections. (Figures 3D, E)

To visualize intrahepatic lymphatic vessels, antibodies targeting established lymphatic markers such as PROX-1 (Prospero homeobox protein 1), LYVE-1 (Lymphatic Vessel Endothelial Receptor 1) and Podoplanin were used. Unfortunately, none of the lymphatic marker antibodies showed specific staining. (Supplementary Figure 1B) Further optimizing and validation of lymphatic marker antibodies will be pursued.

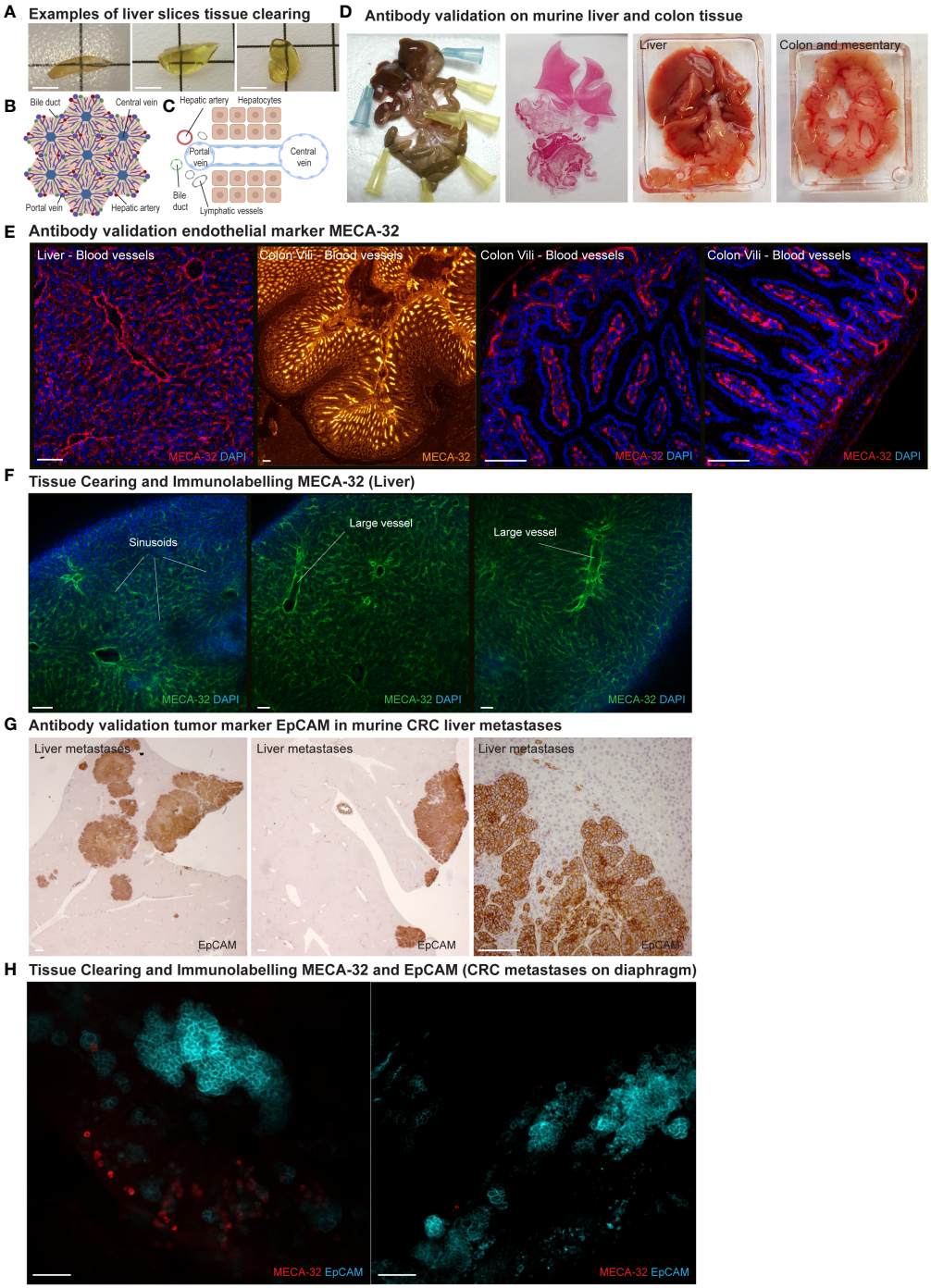

FIGURE 3
Tissue clearing: Vasculature and CRC tumor cells using 3DISCO/iDISCO. **(A)** Examples of transparency of liver samples after tissue clearing with the 3DISCO/iDISCO method. Scale bar = 5 mm **(B, C)** Structural organization of liver tissue and vasculature. **(D)** Tissue samples of murine liver and colon, used for antibody validation on tissue sections. **(E)** Antibody validation on liver and colon (vili) sections of pan-endothelial marker MECA-32 for blood vessel immunolabelling. DAPI (blue), MECA-32 (red and orange) Scale bar = 100µm **(F)**. Visualization of blood endothelial microvasculature of the liver using endothelial marker MECA-32 (green). (DAPI in blue). MECA-32 showed specific staining of the liver sinusoids and larger vessels. Scale bar = 100µm **(G)** Antibody validation of tumor marker EpCAM in murine CRC liver metastases. Scale bar = 100µm. **(H)** To use the model for tumor micro-environment imaging, a robust tumor marker is needed. EpCAM (turquoise) showed strong specific staining of tumor cells in a metastatic lesion on diaphragm tissue. MECA-32 (red) Scale bar = 100µm.

Immunolabelling tumor cells using 3DISCO/iDISCO+

To investigate tissue clearing compatibility with immunolabeling of colorectal cancer tumor cell markers, we used a murine model in which colorectal cancer organoids were inoculated into the murine cecum. In this model, tumor cells spontaneously metastasize to the liver. (Figure 1D) Samples of tumor-bearing liver tissue were harvested. To identify a reliable tumor marker, antibodies against CD44 (a glycoprotein overexpressed in various cancers) and HES (mammalian Hairy enhance of split-1) were used. However, no specific staining was seen. (Supplementary Figure 1C) Using a tissue sample of the diaphragm with macroscopic tumor lesions, another possible tumor marker, EpCAM (Epithelial adhesion molecule), was evaluated. This tumor marker showed specific staining of the CRC tumor cells on the diaphragm tissue. (Figure 3H) Before usage in the clearing and immunolabelling protocol, EpCAM labelling was validated on murine colorectal liver metastases immunohistochemistry (IHC) sections. (Figures 3D, G)

Discussion

In this study, we investigated methods for murine liver tissue clearing to visualize the intrahepatic microvasculature as well as tumor cells in murine colorectal metastases. The field of tissue clearing offers a wide variety of clearing techniques, each with their own advantages and drawbacks (the discussion of which is beyond the scope of this paper). Most tissue clearing research has focused on neurobiology as well as made use of endogenous fluorescence while imaging. For the aim of this study to visualize intrahepatic microvasculature and tumor cells, a clearing technique was needed that could 1) adequately render liver tissue transparent (hampered by the liver's high heme content) and 2) was compatible with immunolabelling vasculature and CRC tumor cells.

At the time, CLARITY and especially 3DISCO/iDISCO+ had shown immunolabelling compatibility for many antibodies in the neurobiology field, as well as proven capable of liver clearing. Therefore, for this study these clearing techniques were chosen. Unfortunately, in this study CLARITY using passive clearing did not allow suitable immunolabelling due to tissue integrity difficulties. While CLARITY is designed to embed samples into a polymer scaffold, hereby providing support to better preserve tissue structure (5, 18), as passive clearing of liver lobes took several weeks, the extended chemical exposure damaged the hydrogel-supported tissue structure. The active clearing CLARITY approach which is used to great effect in many studies (2, 3, 18, 22, 23), uses an electrochemical gradient which results in fast clearing. However, this requires specific equipment that was not available for us at this time. Molina et al. (24) showed an adjusted version of active CLARITY with immunolabelling to visualise liver bile ducts. Therefore, active CLARITY techniques with liver-focused antibody labelling could still provide an interesting clearing technique for imaging the liver (tumor) micro-environment.

Most optical clearing methods aim to preserve endogenous fluorescent proteins and counteract fluorescence quenching. The 3DISCO method created by Ertürk et al. (19) was further adapted by Renier et al. (20) to especially focus on whole-mount immunolabeling and imaging of large-volume samples. This method, dubbed iDISCO (immunolabeling-enabled 3D imaging of solvent-cleared organs), was then further adjusted by Chédotal and colleagues (3, 21). In this study, the 3DISCO/iDISCO+ approach successfully cleared liver tissue while maintaining tissue integrity and allowed immunolabeling of intrahepatic vasculature and CRC tumor cell markers (MECA-32 and EpCAM, respectively).

Currently, more clearing techniques are developed or adjusted to suit other organ systems besides the neurobiology field and better suit immunolabelling. Therefore, in the future more immunolabelling clearing options will be available for tumor micro-environment imaging in various organ systems. However, for specifically investigating the spatial organization of such tissues, maintaining tissue integrity is crucial. In many clearing protocols, such as iDISCO+, the solvents result in the expansion or shrinkage of the tissue samples (1). While some studies report shrinkage in all dimensions hereby maintaining similar spatial distribution, others suggest different amounts of shrinkage for different tissues, which could warp the original tissue and organ structure (19, 25, 26). On the other hand, tissue shrinkage can also benefit imaging depth as it renders larger samples smaller. In future studies, the influence of solvents on tissue dimensions and integrity should be considered when studying tissue spatial organization. Further investigation is needed to elucidate the reaction of different tissue components to the clearing solvents.

To our knowledge, only three other studies attempted to visualize both the liver's endothelial and lymphatic structures. Oren et al. (23) made use of transgenic mice with a tdTomato fluorescent marker under the Vecad promotor to visualize blood vessels. In this study LYVE-1 was used as a lymphatic endothelial cell marker, however, it is not specific for liver lymphatic vessels as the sinusoidal endothelial cells also express LYVE-1 (27). Bobe et al. (28), in addition to LYVE-1 used co-stainings with PROX-1, VEGFR-3, and podoplanin for visualizing intrahepatic lymphatic embryonic development. Future studies will need to determine whether this method can be used to study the lymphatic vessels of the intrahepatic tumor micro-environment. Messal et al. (29) developed the FLASH method which was used to clear and label many organ tissues, such as the liver. In liver tissue, they labelled structures as bile ducts, smooth muscle cell markers for vasculature as well as PROX-1 for lymphatic vasculature. Moreover, they imaged *in vitro* tumor organoids in matrigel as well as pancreatic cancer tissue. It would be interesting to use this method for further imaging of the liver tumor-microenvironment, especially using other lymphatic markers such as podoplanin.

Validation of antibodies is a vital step of clearing methods. As tissue clearing protocols make use of harsh chemicals, such as methanol, many antibodies are not compatible. While time consuming and often costly, to be able to specifically label

proteins of interest, an evaluation of various antibodies, different dilutions and incubation times is needed for immunolabelling optimization (1, 2, 4). Various tissue clearing methods have dedicated online databases documenting which antibodies were tested. As we currently used smaller samples for establishing this method, further optimization will be needed when we broaden the method to whole liver imaging. One of the major challenges is adequate antibody penetration into whole-organ samples. Recently, to improve antibody penetration the use of high-pressure delivery systems for antibodies as well as the use of nanobodies have been reported (6).

In this study, the approach to immunolabel the intrahepatic blood vasculature was chosen. To visualize blood vessels, intravenous injection of fluorescent agents such as fluorescently-labelled lectin can be used (15, 22). As this offers a strong fluorescent signal in for instance the 488 nm laser range, it might offer an alternative to blood vessel staining within a laser range that is often excluded due to strong autofluorescence. Moreover, many research groups visualize their protein of interest using transgenic fluorescent reporter mice. However, this offers a new set of challenges concerning creating transgenic mice and the quenching of endogenous fluorescence during the harsh chemical process of tissue clearing. Recently, Stamatelos et al. (30) and Ehling et al. (31) used micro-CT imaging to study tumor microvasculature, blood flow, and angiogenesis in murine xenografts. Moreover, Bhargava et al. (32) developed a comprehensive approach named VascuViz combining micro-MRI and micro-CT with possible optical clearing and imaging to visualize whole-organ and tumor microvasculature. To image blood vasculature, fluorescent CT and MRI contrast agents were combined for intracardial perfusion, after which tissue samples were collected, fixed and imaged by micro-MRI and micro-CT. Then tissue samples were used for IHC immunolabelling or for tissue clearing and imaging of endogenous fluorescent proteins and the fluorescent contrast agents. Afterwards, all data was integrated. This technique would require access to micro-MRI and micro-CT equipment as well as data integration expertise. In future studies, it would be fascinating to use this VascuViz technique to combine micro-MRI and micro-CT imaging with immunolabelling of various tumor micro-environment cell types such as cancer cells, immune cells and cancer-associated fibroblasts.

Whole organ clearing has also been used to investigate cancer metastasis evolution in a variety of murine tumor models (22, 33–35). Regarding post-mortem human tumor tissue, small sections used for tissue clearing have been performed on breast neoplasms (34, 36), prostate cancer (37), microvasculature in colorectal cancer (38), as well as lymphatic vasculature of bladder cancers (39). Tanaka et al. used tissue clearing to study patterns of cancer heterogeneity in both a murine bladder model as well as in biopsy samples of human ovarian, pancreas, colon, head and neck, and lung cancers (40). Three-dimensional tumor micro-environment tissue clearing would be valuable as it would allow visualization of the spatial heterogeneity and interactions of tumor cells and other components such as immune cells, endothelial cells or cancer-associated fibroblasts (CAFs) (14, 36, 41–43). Where the question can be posed whether 2D immunohistochemistry can truly adequate and representatively capture tumor heterogeneity, whole-organ tissue clearing could offer a more comprehensive approach. In fact, Cuccarese et al. studied the spatial distribution of tumor-associated macrophages in murine pulmonary carcinoma and their response to drug delivery (44). In future studies, we expect the use of tissue clearing in evaluating drug penetration, distribution, accumulation, tissue retention and any therapeutic treatment effect to intensify (2, 42, 45, 46). Interestingly, whereas most clearing protocols target proteins of interest, recently combining whole-mount *in situ* hybridization techniques such as smFISH techniques with tissue clearing have been attempted successfully (47–49). While this development is very recent and needs further enhancement, it offers the interesting possibility of studying both proteins and RNA simultaneously in the 3D tumor micro-environment structure.

In conclusion, we used the 3DISCO/iDISCO+ method to successfully render murine liver tissue optically transparent and immunolabel intrahepatic vasculature using MECA-32 as well as colorectal tumor cells using EpCAM. Further optimization of immunolabelling intrahepatic lymphatic vasculature is needed. Moreover, the immunolabeling of tumor cells, which was successful in a tumor lesion on the diaphragm, will need to be optimized for liver tissue. Imaging intrahepatic blood and lymphatic vasculature as well as tumor cells would be an especially valuable technique for allowing visualization of the spatial heterogeneity and complex interactions of tumor cells and their environment in future studies.

Data availability statement

The raw data supporting the conclusions of this article will be made available by the authors, without undue reservation.

Ethics statement

The animal study was reviewed and approved by the National Competent Authority (Licence number AVD115002016614) and Animal Ethics Committee (UMC Utrecht).

Author contributions

NF, SP, OK, IR, JH were involved in study concept and design. NF, LB, SP, JW, LW in acquisition of data. NF, SP, OK, JH in analysis and interpretation of data. NF, LB, JH in drafting of the manuscript. IR, OK, JH in critical revision of the manuscript. NF, SP OK, JH in statistical analysis. JH, OK, IR obtained funding. All authors contributed to the article and approved the submitted version.

Funding

This work was supported by the Dutch Cancer Society/ Koningin Wilhelmina Fonds (grant no. UU2014-6904 to JH) and the Alexandre Suerman Young Talent Stipend (NF).

Conflict of interest

The authors declare that the research was conducted in the absence of any commercial or financial relationships that could be construed as a potential conflict of interest.

Publisher's note

All claims expressed in this article are solely those of the authors and do not necessarily represent those of their affiliated organizations, or those of the publisher, the editors and the reviewers. Any product that may be evaluated in this article, or claim that may be made by its manufacturer, is not guaranteed or endorsed by the publisher.

Supplementary material

The Supplementary Material for this article can be found online at: https://www.frontiersin.org/articles/10.3389/fonc.2023.1062926/full#supplementary-material

SUPPLEMENTARY FIGURE 1
(A) Immunolabelling intrahepatic vasculature with CD31 (red) showed no specific staining. DAPI (blue) Scale bar = 100mm **(B)** Lymphatic endothelial markers PROX-1 (nuclear staining, green), LYVE-1 (green) and Podoplanin (green) showed no specific staining. DAPI (red). Scale bar = 100mm **(C)** Moreover, tumor markers CD44 and HES (both in turquoise) also showed no specific staining for labelling colorectal cancer cells. DAPI (red), CRC tumor liver metastasis (*). Scale bar = 100mm.

References

1. Gómez-Gaviro MV, Sanderson D, Ripoll J, Desco M. Biomedical applications of tissue clearing and three-dimensional imaging in health and disease. *iScience* (2020) 23 (8):101432. doi: 10.1016/j.isci.2020.101432

2. Tian T, Yang Z, Li X. Tissue clearing technique: Recent progress and biomedical applications. *J Anat* (2021) 238:489–507. doi: 10.1111/joa.13309

3. Vigouroux RJ, Belle M, Chédotal A. Neuroscience in the third dimension: shedding new light on the brain with tissue clearing. (2017) 10(1):33. doi: 10.1186/s13041-017-0314-y

4. Susaki EA, Ueda HR. Whole-body and whole-organ clearing and imaging techniques with single-cell resolution: Toward organism-level systems biology in mammals. *Cell Chem Biol* (2016) 23:137–57. doi: 10.1016/j.chembiol.2015.11.009

5. Seo J, Choe M, Kim SY. Clearing and labeling techniques for large-scale biological tissues. *Molecules Cells* (2016) 39:439–46. doi: 10.14348/molcells.2016.0088

6. Ueda HR, Ertürk A, Chung K, Gradinaru V, Chédotal A, Tomancak P, et al. Tissue clearing and its applications in neuroscience. *Nat Rev Neurosci* (2020) 21:61–79. doi: 10.1038/s41583-019-0250-1

7. Spalteholz W. *Uüber das durchsichtigmachen von menschlichen und tierischen Praüparaten und seine theoretischen bedingungen, nebst anhang: Uüber Knochenfaürbung*. Leipzig: S. Hirzel (1911).

8. Spalteholz W. *Uüber das durchsichtigmachen von menschlichen und tierischen Praüparaten und seine theoretischen bedingungen, nebst anhang: Uüber Knochenfaürbung*. Leipzig: S. Hirzel (1914).

9. Susaki EA, Tainaka K, Perrin D, Yukinaga H, Kuno A, Ueda HR. Advanced CUBIC protocols for whole-brain and whole-body clearing and imaging. *Nat Protoc* (2015) 10(11):1709–27. doi: 10.1038/nprot.2015.085

10. Ren Z, Wu Y, Wang Z, Hu Y, Lu J, Liu J, et al. CUBIC-plus: An optimized method for rapid tissue clearing and decolorization. *Biochem Biophys Res Commun* (2021) 568:116–23. doi: 10.1016/j.bbrc.2021.06.075

11. Chen L, Li G, Li Y, Li Y, Zhu H, Tang L, et al. UbasM: An effective balanced optical clearing method for intact biomedical imaging. *Sci Rep* (2017) 7(1):12218. doi: 10.1038/s41598-017-12484-3

12. Tainaka K, Kubota SI, Suyama TQ, Susaki EA, Perrin D, Ukai-Tadenuma M, et al. Whole-body imaging with single-cell resolution by tissue decolorization. *Cell* (2014) 159(4):911–24. doi: 10.1016/j.cell.2014.10.034

13. Jing D, Zhang S, Luo W, Gao X, Men Y, Ma C, et al. Tissue clearing of both hard and soft tissue organs with the pegasos method. *Cell Res* (2018) 28(8):803–18. doi: 10.1038/s41422-018-0049-z

14. Hofmann J, Gadjalova I, Mishra R, Ruland J. Efficient tissue clearing and multi- organ volumetric imaging enable quantitative visualization of sparse immune cell populations during in fl ammation. *Front Immunol* (2021) 11:1–17. doi: 10.3389/fimmu.2020.599495

15. Feuchtinger A, Walch A, Dobosz M. Deep tissue imaging: a review from a preclinical cancer research perspective. *Histochem Cell Biol* (2016) 146:781–806. doi: 10.1007/s00418-016-1495-7

16. Azaripour A, Lagerweij T, Scharfbillig C, Jadczak AE, Willershausen B, Van Noorden CJ. A survey of clearing techniques for 3D imaging of tissues with special reference to connective tissue. *Prog Histochem Cytochem* (2016) 51(2):9–23. doi: 10.1016/j.proghi.2016.04.001

17. Chanrion M, Kuperstein I, Barrière C, El Marjou F, Cohen D, Vignjevic D, et al. Concomitant notch activation and p53 deletion trigger epithelial-to-mesenchymal transition and metastasis in mouse gut. *Nat Commun* (2014) 5:5005. doi: 10.1038/ncomms6005

18. Tomer R, Ye L, Hsueh B, Deisseroth K. Advanced CLARITY for rapid and high-resolution imaging of intact tissues. *Nat Protoc* (2014) 9:1682–97. doi: 10.1038/nprot.2014.123

19. Ertürk A, Becker K, Jährling N, Mauch CP, Hojer CD, Egen JG, et al. Three-dimensional imaging of solvent-cleared organs using 3DISCO. *Nat Protoc* (2012) 7 (11):1983–95. doi: 10.1038/nprot.2012.119

20. Renier N, Wu Z, Simon DJ, Yang J, Ariel P, Tessier-Lavigne M. iDISCO : A simple, rapid method to immunolabel Large tissue samples for volume imaging. *Cell* (2014) 159(4):896–910. doi: 10.1016/j.cell.2014.10.010

21. Belle M, Godefroy D, Couly G, Malone SA, Collier F, Giacobini P, et al. Tridimensional visualization and analysis of early human development resource tridimensional visualization and analysis of early human development. (2017) 169 (1):161–73.e12. doi: 10.1016/j.cell.2017.03.008

22. Lagerweij T, Dusoswa SA, Negrean A, Hendrikx EML, de Vries HE, Kole J, et al. Optical clearing and fluorescence deep-tissue imaging for 3D quantitative analysis of the brain tumor microenvironment. *Angiogenesis* (2017) 20(4):533–46. doi: 10.1007/s10456-017-9565-6

23. Oren R, Fellus-Alyagor L, Addadi Y, Bochner F, Gutman H, Blumenreich S, et al. Whole organ blood and lymphatic vessels imaging (WOBLI). *Sci Rep* (2018) 8 (1):1–9. doi: 10.1038/s41598-018-19663-w

24. Molina LM, Krutsenko Y, Jenkins NEC, Smith MC, Tao J, Wheeler TB, et al. LiverClear: A versatile protocol for mouse liver tissue clearing. *STAR Protoc* (2022) 3 (1):101178. doi: 10.1016/j.xpro.2022.101178

25. Pan C, Cai R, Quacquarelli FP, Ghasemigharagoz A, Lourbopoulos A, Matryba P, et al. Shrinkage-mediated imaging of entire organs and organisms using uDISCO. *Nat Methods* (2016) 13(10):859–67. doi: 10.1038/nmeth.3964

26. Vulders RCM, van Hoogenhuizen RC, van der Giessen E, van der Zaag PJ. Clearing-induced tisssue shrinkage: A novel observation of a thickness size effect. *PloS One* (2021) 16:e0261417. doi: 10.1371/journal.pone.0261417

27. Mouta Carreira C, Nasser SM, di Tomaso E, Padera TP, Boucher Y, Tomarev SI, et al. LYVE-1 is not restricted to the lymph vessels: Expression in normal liver blood sinusoids and down-regulation in human liver cancer and cirrhosis. *Cancer Res* (2001) 61(22):8079–84.

28. Bobe S, Beckmann D, Klump DM, Dierkes C, Kirschnick N, Redder E, et al. Volumetric imaging reveals VEGF-c-dependent formation of hepatic lymph vessels in mice. *Front Cell Dev Biol* (2022) 10:949896. doi: 10.3389/fcell.2022.949896

29. Messal HA, Almagro J, Zaw Thin M, Tedeschi A, Ciccarelli A, Blackie L, et al. Antigen retrieval and clearing for whole-organ immunofluorescence by FLASH. *Nat Protoc* (2021) 16(1):239–62. doi: 10.1038/s41596-020-00414-z

30. Stamatelos SK, Bhargava A, Kim E, Popel AS, Pathak AP. Tumor ensemble-based modeling and visualization of emergent angiogenic heterogeneity in breast cancer. *Sci Rep* (2019) 9:5276. doi: 10.1038/s41598-019-40888-w

31. Ehling J, Theek B, Gremse F, Baetke S, Möckel D, Maynard J, et al. Micro-CT imaging of tumor angiogenesis: quantitative measures describing micromorphology and vascularization. *Am J Pathol* (2014) 184(2):431–41. doi: 10.1016/j.ajpath.2013.10.014

32. Bhargava A, Monteagudo B, Kushwaha P, Senarathna J, Ren Y, Riddle RC, et al. VascuViz: a multimodality and multiscale imaging and visualization pipeline for vascular systems biology. *Nat Methods* (2022) 19(2):242–54. doi: 10.1038/s41592-021-01363-5

33. Kubota SI, Takahashi K, Nishida J, Morishita Y, Ehata S, Tainaka K, et al. Whole-body profiling of cancer metastasis with single-cell resolution. *Cell Rep* (2017) 20(1):236–50. doi: 10.1016/j.celrep.2017.06.010

34. Rios AC, Capaldo BD, Vaillant F, Pal B, van Ineveld R, Dawson CA, et al. Intraclonal plasticity in mammary tumors revealed article intraclonal plasticity in mammary tumors revealed through Large-scale single-cell resolution 3D imaging. (2019) 35(4):618–32.e6. doi: 10.1016/j.ccell.2019.02.010

35. Lin PY, Peng SJ, Shen CN, Pasricha PJ, Tang SC. PanIN-associated pericyte, glial, and islet remodeling in mice revealed by 3D pancreatic duct lesion histology. *Am J Physiol - Gastrointest Liver Physiol* (2016) 311:G412–22. doi: 10.1152/ajpgi.00071.2016

36. Sabdyusheva Litschauer I, Becker K, Saghafi S, Ballke S, Bollwein C, Foroughipour M, et al. 3D histopathology of human tumours by fast clearing and ultramicroscopy. *Sci Rep* (2020) 10(1):17619. doi: 10.1038/s41598-020-71737-w

37. van Royen ME, Verhoef EI, Kweldam CF, van Cappellen WA, Kremers GJ, Houtsmuller AB, et al. Three-dimensional microscopic analysis of clinical prostate specimens. *Histopathology* (2016) 69(6):985–92. doi: 10.1111/his.13022

38. Liu YA, Pan ST, Hou YC, Shen MY, Peng SJ. 3-d visualization and quantitation of microvessels in transparent human colorectal carcinoma. (2013) 8(11):e81857. doi: 10.1371/journal.pone.0081857

39. Tanaka N, Kaczynska D, Kanatani S, Sahlgren C, Mitura P, Stepulak A. Mapping of the three-dimensional lymphatic microvasculature in bladder tumours using light-sheet microscopy. *Br J Cancer* (2018) 118(7):995–9. doi: 10.1038/s41416-018-0016-y

40. Tanaka N, Kanatani S, Tomer R, Sahlgren C, Kronqvist P, Kaczynska D, et al. Whole-tissue biopsy phenotyping of three-dimensional tumours reveals patterns of cancer heterogeneity. *Nat Biomed Eng* (2017) 1(10):796–806. doi: 10.1038/s41551-017-0139-0

41. Hofmann J, Keppler SJ. Tissue clearing and 3D imaging – putting immune cells into context. *J Cell Sci* (2021) 134(15):jcs258494. doi: 10.1242/jcs.258494

42. Lee SS, Bindokas VP, Kron SJ, Biology C, Facility LM. Multiplex three-dimensional mapping of macromolecular drug distribution in the tumor microenvironment. *Mol Cancer Ther* (2019) 18:213–26. doi: 10.1158/1535-7163.MCT-18-0554

43. Almagro J, Messal HA, Zaw Thin M, van Rheenen J, Behrens A. Tissue clearing to examine tumour complexity in three dimensions. *Nat Rev Cancer* (2021) 21:718–30. doi: 10.1038/s41568-021-00382-w

44. Cuccarese MF, Dubach JM, Pfirschke C, Engblom C, Garris C, Miller MA, et al. Heterogeneity of macrophage infiltration and therapeutic response in lung carcinoma revealed by 3D organ imaging. *Nat Commun* (2017) 8:14293. doi: 10.1038/ncomms14293

45. Dobosz M, Ntziachristos V, Scheuer W, Strobel S. Multispectral fluorescence Ultramicroscopy : Three- dimensional visualization and automatic quantification of tumor morphology, drug penetration, and antiangiogenic treatment response. *Neoplasia* (2014) 16:1–13. doi: 10.1593/neo.131848

46. Kingston BR, Muhammad A, Ngai J, Sindhwani S. Assessing micrometastases as a target for nanoparticles using 3D microscopy and machine learning. *Proc Natl Acad Sci USA* (2019) 116:14937–46. doi: 10.1073/pnas.1907646116

47. Sylwestrak EL, Rajasethupathy P, Wright MA, Jaffe A, Deisseroth K. Multiplexed intact-tissue transcriptional analysis at cellular resolution. *Cell* (2016) 164:792–804. doi: 10.1016/j.cell.2016.01.038

48. Yang B, Treweek JB, Kulkarni RP, Deverman BE, Chen CK, Lubeck E, et al. Single-cell phenotyping within transparent intact tissue through whole-body clearing. *Cell* (2014) 158(4):945–58. doi: 10.1016/j.cell.2014.07.017

49. Shah S, Lubeck E, Schwarzkopf M, He TF, Greenbaum A, Sohn CH, et al. Single-molecule RNA detection at depth by hybridization chain reaction and tissue hydrogel embedding and clearing. *Development* (2016) 143:2862–7. doi: 10.1242/dev.138560

frontiers | Frontiers in Oncology

TYPE Original Research
PUBLISHED 27 April 2023
DOI 10.3389/fonc.2023.1065744

Check for updates

OPEN ACCESS

EDITED BY
Zhendong Jin,
Second Military Medical University, China

REVIEWED BY
Zhi Yang,
Beijing Cancer Hospital, Peking University, China
Changjing Zuo,
Second Military Medical University, China

*CORRESPONDENCE
Li Zhang
zhangli96nuclear@126.com.s
Wei Cao
caowei@hust.edu.cn

SPECIALTY SECTION
This article was submitted to Gastrointestinal Cancers: Colorectal Cancer, a section of the journal Frontiers in Oncology

RECEIVED 10 October 2022
ACCEPTED 30 January 2023
PUBLISHED 27 April 2023

CITATION
Zhang L, Liu Y, Ding Y, Deng Y, Chen H, Hu F, Fan J, Lan X and Cao W (2023) Predictive value of intratumoral-metabolic heterogeneity derived from ^{18}F-FDG PET/CT in distinguishing microsatellite instability status of colorectal carcinoma. *Front. Oncol.* 13:1065744. doi: 10.3389/fonc.2023.1065744

COPYRIGHT
© 2023 Zhang, Liu, Ding, Deng, Chen, Hu, Fan, Lan and Cao. This is an open-access article distributed under the terms of the Creative Commons Attribution License (CC BY). The use, distribution or reproduction in other forums is permitted, provided the original author(s) and the copyright owner(s) are credited and that the original publication in this journal is cited, in accordance with accepted academic practice. No use, distribution or reproduction is permitted which does not comply with these terms.

Predictive value of intratumoral-metabolic heterogeneity derived from ^{18}F-FDG PET/CT in distinguishing microsatellite instability status of colorectal carcinoma

Li Zhang[1,2]*, Yu Liu[1,2], Ying Ding[1,2], Yinqian Deng[1,2], Huanyu Chen[1,2], Fan Hu[1,2], Jun Fan[3], Xiaoli Lan[1,2] and Wei Cao[1,2]*

[1]Department of Nuclear Medicine, Union Hospital, Tongji Medical College, Huazhong University of Science and Technology, Wuhan, China, [2]Hubei Key Laboratory of Molecular Imaging, Wuhan, China, [3]Department of Pathology, Union Hospital, Tongji Medical College, Huazhong University of Science and Technology, Wuhan, China

Purpose/background: Microsatellite instability (MSI) status is a significant biomarker for the response to immune checkpoint inhibitors, response to 5-fluorouracil-based adjuvant chemotherapy, and prognosis in colorectal carcinoma (CRC). This study investigated the predictive value of intratumoral-metabolic heterogeneity (IMH) and conventional metabolic parameters derived from ^{18}F-FDG PET/CT for MSI in patients with stage I–III CRC.

Methods: This study was a retrospective analysis of 152 CRC patients with pathologically proven MSI who underwent ^{18}F-FDG PET/CT examination from January 2016 to May 2022. Intratumoral-metabolic heterogeneity (including heterogeneity index [HI] and heterogeneity factor [HF]) and conventional metabolic parameters (standardized uptake value [SUV], metabolic tumor volume [MTV], and total lesion glycolysis [TLG]) of the primary lesions were determined. MTV and SUV_{mean} were calculated on the basis of the percentage threshold of SUVs at 30%–70%. TLG, HI, and HF were obtained on the basis of the above corresponding thresholds. MSI was determined by immunohistochemical evaluation. Differences in clinicopathologic and various metabolic parameters between MSI-High (MSI-H) and microsatellite stability (MSS) groups were assessed. Potential risk factors for MSI were assessed by logistic regression analyses and used for construction of the mathematical model. Area under the curve (AUC) were used to evaluate the predictive ability of factors for MSI.

Results: This study included 88 patients with CRC in stages I–III, including 19 (21.6%) patients with MSI-H and 69 (78.4%) patients with MSS. Poor differentiation, mucinous component, and various metabolic parameters including $MTV_{30\%}$, $MTV_{40\%}$, $MTV_{50\%}$, and $MTV_{60\%}$, as well as $HI_{50\%}$, $HI_{60\%}$, $HI_{70\%}$, and HF in the MSI-H group were significantly higher than those in the MSS group (all $P < 0.05$). In multivariate logistic regression analyses, post-standardized $HI_{60\%}$ by Z-score ($P = 0.037$, OR: 2.107) and mucinous component ($P < 0.001$, OR:11.394) were independently correlated with MSI. AUC of $HI_{60\%}$ and our model of the $HI_{60\%}$ + mucinous component was 0.685 and 0.850, respectively ($P = 0.019$), and the AUC of $HI_{30\%}$ in predicting the mucinous component was 0.663.

Conclusions: Intratumoral-metabolic heterogeneity derived from ^{18}F-FDG PET/CT was higher in MSI-H CRC and predicted MSI in stage I–III CRC patients preoperatively. $HI_{60\%}$ and mucinous component were independent risk factors for MSI. These findings provide new methods to predict the MSI and mucinous component for patients with CRC.

KEYWORDS

microsatellite instability, positron emission tomography/computed tomography, metabolic parameter, heterogeneity, colorectal carcinoma, immune-checkpoint inhibitors

Introduction

The world's second leading cause of cancer death is colorectal cancer (CRC), which is the third most common cancer (1). While surgery and adjuvant chemotherapy are currently the main treatments for CRC, immunotherapy has emerged as a new therapeutic strategy for cancer treatment. The programmed cell death 1 (PD-1)/programmed death-ligand 1 (PD-L1) axis is a critical immune response. Anti-PD-1/anti-PD-L1 blockade therapy enhances the antitumor activity of T cells by blocking the binding of PD-L1 on tumor cells and PD-1 on immune T cells, representing a key anticancer strategy. Blocking these pathways effectively reduces tumor growth and improves survival in most solid tumors (2), especially in microsatellite instability-high (MSI-H) CRC (3). Nivolumab and pembrolizumab, PD-1 inhibitors, were officially approved by the FDA in 2017 for the treatment of MSI-H solid tumors (4), ushering in a new era of immunotherapy.

Under proficient mismatch repair (pMMR) conditions, errors in the replication of microsatellites are repaired by MMR proteins. Mismatch repair deficiency (MMR-D) can lead to errors beyond repair normally and has been detected in endometrial cancer, CRC, and gastric cancer (5). MSI results from errors in the DNA replication of microsatellites and is observed in approximately 12%–15% of localized CRC cases and 4% of stage IV CRC cases (2, 6). The accumulation of MSI eventually leads to development of MSI-H. MSI status has been regarded as an important prognostic biomarker for patients with CRC and affects the selection of adjuvant 5-fluorouracil-based chemotherapy or immune checkpoint inhibitors. Studies showed that 5-fluorouracil-based adjuvant chemotherapy had limited therapeutic effect for patients with MSI-H CRC (7, 8). MSI tumors have large proportions of mutant neoantigens and tumor-infiltrating lymphocytes (TILs) (2, 6, 9) and a high tumor mutational burden (TMB) that promotes the infiltration of immune cells; therefore, MSI plays a significant role in long-term durable immunotherapy (10, 11).

CRC, especially CRC with MSI-H, exhibits significant heterogeneity, which refers to the different characteristics within a tumor in regard to genomics, histopathologic features, tumor microenvironment, T-cell infiltrate, and response to therapies (9, 12, 13). MSI is generally determined by evaluation of MMR proteins including MLH1, PMS2, MSH2, and MSH6 using immunohistochemical (IHC) or by PCR testing and next-generation sequencing to test MMR genes. However, the above methods are usually invasive and may be affected by intratumoral heterogeneity. Therefore, it is meaningful to screen tumors for MSI status to avoid unnecessary inspections and promote the immunotherapy of early-stage CRC patients.

PET/CT is a systemic examination that can detect the distant metastasis of tumors. In recent years, ^{18}F-FDG PET/CT has demonstrated efficiency in staging, predicting prognosis, assessing treatment response, and determining gene mutational status in patients with CRC (14–17). MSI-H CRCs have higher intratumoral heterogeneity compared with microsatellite stability (MSS) CRCs (9, 12, 13, 18). ^{18}F-FDG PET/CT can reflect the intratumoral-metabolic heterogeneity (IMH) by the heterogeneity index (HI) and the heterogeneity factor (HF). These two quantitative indicators reflect IMH and have already been shown to predict survival outcomes in epithelial ovarian cancer, gastric cancer, and oral cavity squamous cell carcinoma (19–21). However, the role of IMH derived from ^{18}F-FDG PET/CT in predicting MSI in CRC patients is unknown (22, 23). Therefore, we aimed to explore the ability of IMH and conventional metabolic parameters (standardized uptake value [SUV], metabolic tumor volume [MTV], and total lesion glycolysis [TLG]) derived from ^{18}F-FDG PET/CT for the prediction of MSI status in patients with stage I–III CRC.

Materials and methods

Patient inclusion and exclusion

This study included patients who underwent ^{18}F-FDG-PET/CT in Wuhan Union Hospital from January 2016 to May 2022. The inclusion criteria were as follows: patients with (a) colorectal lesions diagnosed as colorectal adenocarcinoma with or without a mucinous component (part of the tumor volume with mucin associated likely produced by malignant glands or forming mucin pools, which account for 5%–100% of the tumor volume) by pathology; (b) complete ^{18}F-FDG PET/CT images before surgery within 1 month of surgery; and (c) IHC staining evaluated MMR protein expression status.

The exclusion criteria were as follows: (a) patients who received neoadjuvant chemoradiotherapy or surgery before ^{18}F-FDG PET/CT examination (n = 41); (b) the primary lesion did not show metabolism on PET/CT (n = 3); (c) the presence of other tumors that interfered

with the measurement of the CRC primary tumor (n = 2); and (d) CRC patients in stage IV (n = 18). The flowchart is shown in Figure 1.

PET/CT imaging acquisition protocol

All patients got whole-body imaging (from the cranium to the upper third of the thighs) by ^{18}F-FDG PET/CT scans with a dedicated PET/CT system (GE Healthcare, Milwaukee, WI, USA; Discovery VCT and Discovery LS). An intravenous injection of 3.7–4.4 MBq/kg ^{18}F-FDG was administered, after at least 6 h of fasting and a blood glucose level drops below 200 mg/dl. The examination was performed approximately 60 min after the injection of ^{18}F-FDG. A slice spiral CT scan was first performed. The PET imaging was collected in three-dimensional mode at 2 min per frame for a total of seven to eight frames. PET data were reconstructed on the basis of ordered-subset expectation maximization. The reconstructed images were processed on a workstation (Xeleris Workstation, GE Healthcare).

Measurement of PET metabolic parameters

The PET/CT image was evaluated in a blind manner by two nuclear medicine doctors, each with more than 6 years of clinical experience. The ROI of the primary lesions of CRC patients was delineated in the workstation. The quadrate working frame was placed on the primary lesion, and if necessary, areas of physiologic uptake or nearby lymph node metastasis were manually excluded. The SUV_{max} of the primary lesion was measured automatically by the workstation (AW4.6; GE Healthcare). The SUV_{mean} and MTV were obtained by the percent threshold of SUV_{max} in the working frame. $MTV_{30\%–70\%}$ were calculated with 30%–70% of SUV_{max} as the percent threshold,

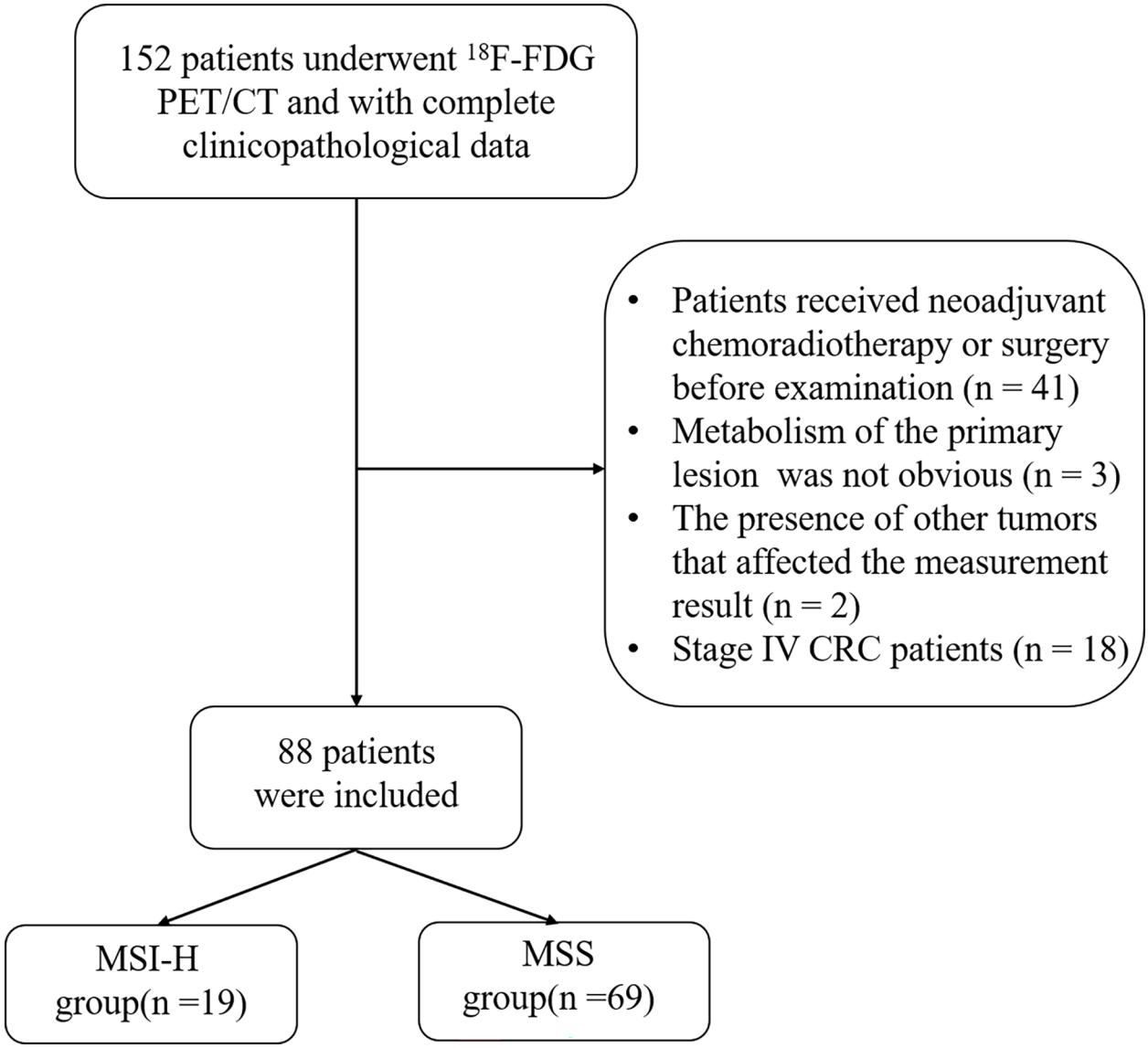

FIGURE 1
Flowchart of patient selection.

respectively (23). SUV_{mean} was obtained from the corresponding MTV. TLG = MTV × SUV_{mean}. IMH contains the HI and HF. HI = SUV_{max}/SUV_{mean}. $HI_{30\%–70\%}$ was determined from the primary tumors. In addition, the HF was the absolute value of the linear regression slope calculated by the least square method from the different threshold of the ROI (Figure 2) (21).

Immunohistochemical evaluation

Clinicopathological data, including differentiation grade, mucinous component, TN stages, tumor deposit, lymphovascular invasion, perineural invasion, and IHC results for four MMR proteins (MLH1, MSH2, MSH6, PMS2), were evaluated by pathologists. The absence of any MMR protein was defined as MMR-D, also known as MSI-H. The expression of all four MMR proteins was defined as pMMR, characterized as MSS. All patients in stage I–III CRC had undergone surgery within 1 month after the PET/CT scan.

Statistical analysis

The quantitative variable distribution was analyzed between groups. Following the distribution of data, data were expressed by mean ± standard deviation or median (interquartile range) and analyzed by T-test or Mann–Whitney U test, respectively. The categorical data were examined using the Fisher's exact test. Various metabolic parameters were standardized by Z-score normalization before performing logistic regression analysis, as the significant differences in various metabolic parameter values. The mathematical model was built, as described in the study by Wang et al. (24). The ROC curve was used to estimate the predictive value of different metabolic parameters for MSI. The DeLong test was used to assess the variation in AUC values. All data were analyzed by SPSS software version 23 (IBM Corp, Armonk, NY, USA) and MedCalc software (version 19.7.2). Statistical significance was defined as a two-sided *P* value less than 0.05.

Results

Patient characteristics

This study included 88 patients, including 59 male patients (70.2%) and 29 female patients (29.8%). The average age was 65 years (range 28–89 years). Among the total 88 patients, 19 (21.6%) patients were categorized into the MSI-H group and 69 (78.4%) patients were categorized into the MSS group. Patients and tumor characteristics are summarized in Table 1. The MSI-H CRC group tended to have a mucinous component, poor differentiation, and a larger maximum tumor diameter, with a higher frequency of male patients compared with the MSS CRC group, with statistical significance (all $P < 0.05$). Age, primary tumor location, TN stage, AJCC-TNM stage, tumor deposit, lymphovascular invasion, and perineural invasion were not significantly different between the MSI-H group and the MSS group (all $P > 0.05$).

Differences in PET/CT metabolic parameters between the MSI-H group and the MSS group

In terms of conventional metabolic parameters, the MSI-H group tended to have higher $MTV_{30\%}$, $MTV_{40\%}$, $MTV_{50\%}$, and $MTV_{60\%}$ compared with the MSS group, with significant differences (all $P < 0.05$). Regarding IMH, $HI_{60\%}$, $HI_{70\%}$, and HF were significantly higher (all $P < 0.05$) in the MSI-H group compared with the MSS group. No

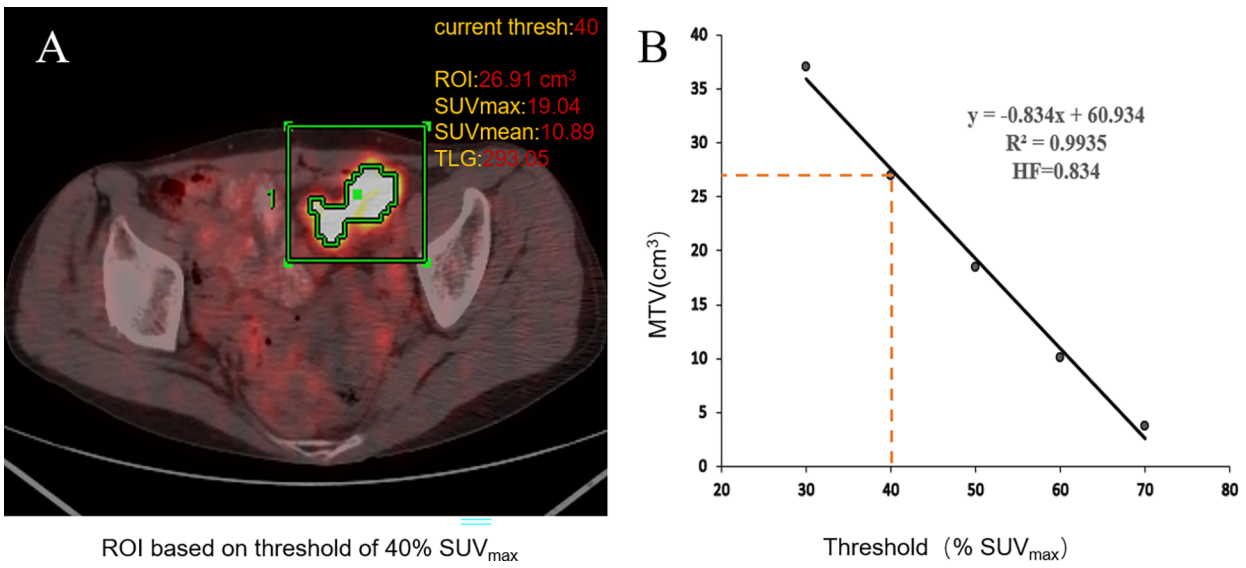

FIGURE 2
Workflow of ^{18}F-FDG PET/CT metabolic parameter measurements. When using the percent threshold of 40%, SUV_{max} was 19.04, the volume of ROI was 26.91 cm^3, SUV_{mean} was 10.98, and TLG was 293.05. HI = SUV_{max}/SUV_{mean} = 1.75 **(A)**. The HF is the absolute value of the linear regression slope calculated by the least square method from the different threshold of the ROI; the threshold of tumor volumes ranged from 30% to 70% of SUV_{max} **(B)**.

TABLE 1 Clinicopathologic characteristics of patients.

Characteristics	Number	MSI-H (n = 19)	MSS (n = 69)	*P* value
Age				0.282*
<60	28	8	20	
≥60	60	11	49	
Gender				0.026*
Male	59	17	42	
Female	29	2	27	
Primary tumor location				0.405*
Left	35	6	29	
Right	34	10	24	
Rectum	19	3	16	
Differentiation				0.019*
Poor	12	6	6	
Well or moderate	76	13	63	
Mucinous component				<0.001*
Positive	16	10	6	
Negative	72	9	63	
Maximum tumor diameter (cm)		4.98±1.29	4.19±1.73	0.037#
T stage				1*
T1-T2	12	2	10	
T3-T4	76	17	59	
N stage				0.276*
0	59	15	44	
1-2	29	4	25	
AJCC-TNM stage				0.328*
I	10	2	8	
II	49	13	36	
III	29	4	25	
Tumor deposit				0.11*
Negative	78	19	59	
Positive	10	0	10	
Lymphovascular invasion				1*
Negative	68	15	53	
Positive	20	4	16	
Perineural invasion				0.138*
Negative	66	17	49	
Positive	22	2	20	

MSI, microsatellite instability; MSS, microsatellite stability; AJCC, American Joint Committee on Cancer; TNM, tumor–node–metastasis. P values were calculated using the *Fisher's exact test and #T-test.

significant difference was found in SUV_{max} and other metabolic parameters between the groups. Details of IMH and conventional metabolic parameters in the MSS group and MSI-H group are listed in Table S1.

Independent predictive indicators of PET/CT parameters and clinical parameters for MSI

The aforementioned significant characteristics were included into logistic analysis. Univariate logistic analysis showed that the expression of MSI in CRC was associated with mucinous component, differentiation, and standardized parameters Z-$HI_{50\%}$ and Z-$HI_{60\%}$ (all $P < 0.05$) (Table 2). Multivariate logistic regression analysis showed that mucinous component and Z-$HI_{60\%}$ were the independent predictive indicators for MSI of the CRC (Table 3).

Model establishment and mucinous composition exploration

MSI-H CRC had higher IMH and MTV values in preoperative PET/CT examination and were more prone to exhibit a mucinous component than MSS CRC (Figures 3, 4). A model of the $HI_{60\%}$+ mucinous component was established, and the formula was as follows: $y = \exp(x)/[1+\exp(x)]$, $x = -2.083 + 2.114 \times$ Z-$HI_{60\%}$+ $13.32 \times$ mucinous component (the "-" or "+" of mucinous component was defined as "0" or "l"). The cutoff value determined by ROC analysis was $y = 0.1432$, when $y > 0.1432$ was considered as MSI-H CRC, while $y < 0.1432$ was considered as MSS CRC. The AUC of $HI_{60\%}$ and the mathematical model were 0.685 and 0.85, with a sensitivity of 0.579 and 0.842 and specificity of 0.826 and 0.768, respectively. There was a significant difference in AUC between $HI_{60\%}$ and our model ($Z = 2.339$, $P = 0.019$). The predictive ability of ROC curves is illustrated in Figure 5.

The Mann–Whitney U test was used to further evaluate the connection between mucinous components and various metabolic parameters. $HI_{30\%}$ was significantly higher in CRC with mucinous component than in CRC without mucinous component. The AUC of $HI_{30\%}$ was 0.663, with sensitivity of 0.875 and specificity 0.5, respectively. The cutoff value was 1.974. The performance of PET/CT parameters is illustrated in Table S2.

Discussion

Our study examined the value of ^{18}F-FDG PET/CT imaging parameters in identifying MSI in stage I–III CRC and explored the intratumoral heterogeneity. As we know, this is the first study examining the utility of IMH determined by PET/CT to predict MSI of CRC. Our results showed that $HI_{60\%}$ and the mucinous component were independent prediction factors for MSI status in stage I–III CRC.

TABLE 2 Univariate regression analyses for predicting MSI in CRC patients.

Factors	*P* value	Odds ratio	95% CI
Differentiation	0.016	0.206	0.06-0.74
Mucinous component	<0.001	11.70	3.41-39.90
Maximum tumor diameter (cm)	0.074	1.332	0.97-1.83
Z-$MTV_{30\%}$	0.136	1.404	0.90-2.19
Z-$MTV_{40\%}$	0.150	1.384	0.89-2.15
Z-$MTV_{50\%}$	0.173	1.360	0.87-2.12
Z-$MTV_{60\%}$	0.221	1.316	0.85-2.04
Z-$HI_{50\%}$	0.039	1.747	1.03-2.98
Z-$HI_{60\%}$	0.042	2.105	1.03-4.31
Z-$HI_{70\%}$	0.059	2.590	0.96-6.97
Z-HF	0.133	1.414	0.90-2.22

Z-, processed by Z-score standardization method; MTV, metabolic tumor volume; TLG, total lesion glycolysis; HI, heterogeneity index; HF, heterogeneity factor; CI, confidence interval.

CRC is tumor with high glucose metabolism that rapidly converts glucose to lactate (known as the "Warburg effect") (25, 26). Other effects include m6A modifications (27), glycolysis-associated lncRNA of colorectal cancer (GLCC1) (28), and insulin-like growth factor 1 (IGF-1) signaling (29), which could also enhance glycolysis in different paths. SUV_{max}, as a semiquantitative parameter in the ^{18}F-FDG uptake of lesions, is considered to be an auxiliary index for judging benign and malignant tumors and a general prognostic factor in malignancies (30). The limitation of SUV_{max} is that it only reflects a single voxel value and cannot reflect the characteristics of the entire ROI. MTV is an indicator usually based on a fixed SUV threshold of 2.5 or percentage SUV_{max} threshold of 40%–42% (30), reflecting the tumor burden of the tumor; it plays an important role in predicting prognosis (30) and even target volume delineation before radiotherapy (31). TLG can reflect both volume and metabolic activity of lesions, which can reflect the advantage of PET/CT better. While SUV_{max}, MTV, and TLG are established as parameters to assess for diagnosis, efficacy, prognosis, tumor burden, and TMB in cancer (32, 33), they have limited value in judging IMH.

IMH is one of the characteristics of solid tumors. The measurement of tumor heterogeneity is of great significance to the drug resistance, tumor invasion, and prognosis of patients (33, 34). The difference in proliferation, receptor expression, necrosis, hypoxia, energy metabolites, micro-vessel density, protein expression, and gene expression in tumors may lead to uncertainties in therapeutic effects (9, 18, 35, 36). ^{18}F-FDG PET/CT can reflect tumor metabolic heterogeneity through different parameters, including HI (21, 33), HF (19), coefficient of variation (19, 20, 33), and texture parameters (34). In our research, HI was calculated by dividing SUV_{max} by SUV_{mean} for the tumor, which reflects not only the ^{18}F-FDG metabolism in the ROI of tumors but also the average of metabolic activity. Research showed that higher $HI_{30\%}$ levels were related to poorer overall survival in patients with oral cavity squamous cell carcinoma (21). In the study by Kim et al. (37), a lower HI based on a threshold of 2.5 of the primary tumors was associated with better prognosis in locally advanced nasopharyngeal carcinoma. Compared with calculation of the HI, calculation of the HF is more complicated and determined by linear regressions of MTVs under different SUV thresholds, determined by two methods (percentage threshold method and fixed threshold method). In general, the percentage threshold method is suitable for lesions with high SUV_{max}, which avoids interference with the surrounding normal tissue metabolism (21). The fixed threshold method is more suitable for tumors with a low ^{18}F-FDG uptake (38). For this reason, we selected the percentage threshold method in our study. In a study of 55 patients with advanced gastric cancer (19), HF (SUV threshold based on 2.5–3.5) was significantly associated with TNM stage and overall survival.

In our study, several conventional metabolic parameters were significant predictors of MSI, which was similar to previous findings (23, 39). Song et al. (39) retrospectively analyzed the relationship between conventional metabolic parameters based on the threshold of 40% SUV_{max} in 420 CRC patients. The results proved that MTV ≥32.19 cm^3 of CRC was linked to the presence of MSI-H and the increased density of TILs in MSI-H CRC may lead to higher TMB. The result was consistent with the previous study of Liu et al. (23) and our results (Table 4). Moreover, our analysis further proved the existence of IMH of CRC. The HI is the ratio of the highest ^{18}F-FDG uptake and the average ^{18}F-FDG uptake of the lesions. MSI-H CRCs showed a higher HI compared with MSS CRC even though SUV_{max} and SUV_{mean} were not statistically different in the two groups, which might be caused by the larger proportion of mutant neoantigens increasing glucose metabolism and upregulated immune checkpoints of MSI-H CRC that preserve MSI-H CRC from the pernicious immune microenvironment (2). Therefore, $HI_{60\%}$ could make up for the limitation of conventional metabolic parameters in predicting MSI. HF reflects the metabolic changes in tumors under different thresholds. In our research, MSI-H CRC had a higher HF than MSS CRC, which indicated a higher heterogeneity in MSI-H CRC.

MSI-H CRC is a tumor with higher heterogeneity and increased TMB and tumor burden compared with MSS CRC. MSI-H CRC has more TILs in both tumor and tumor-adjacent tissues. The higher CD3+ and CD8 T lymphocyte densities are associated with higher tumor size and MTV value (9, 12, 39). The consumption of glucose by

TABLE 3 Multivariate regression analyses for predicting MSI in CRC.

Factors	*P* value	Odds ratio	95% CI	*P* value	Odds ratio	95% CI
Differentiation	0.090	0.260	0.06-1.24	0.113	0.278	0.06-1.35
Mucinous component	0.001	9.348	2.53-34.51	<0.001	11.394	2.96-43.89
Z-$HI_{50\%}$	0.057	1.717	0.98-3.0			
Z-$HI_{60\%}$				0.037	2.107	1.05-4.25

Z-, processed by Z-score standardization method; HI, heterogeneity index; CI, confidence interval.

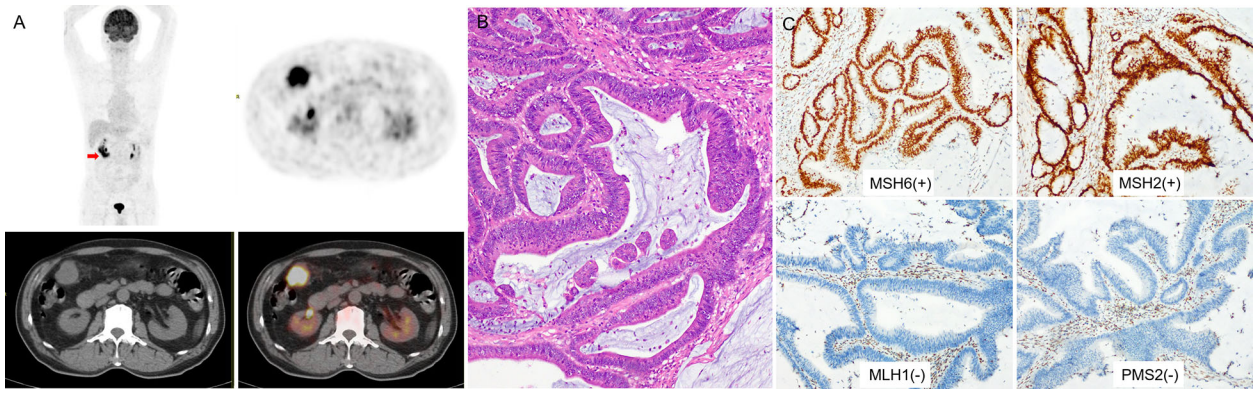

FIGURE 3
(A) a 73-year-old man with right colon cancer. PET/CT showed high ^{18}F-FDG accumulate in the colon of hepatic flexure (arrow; SUV_{max} 10.8; $HI_{60\%}$ 1.43). **(B)** Pathological analysis revealed well-differentiated carcinoma; in H&E, the bulk of the malignant glands produced visible mucin. **(C)** IHC analysis demonstrated MSI-H, MMR proteins showed as MSH6(+), MSH2(+), MLH1(-), PMS2(-).

tumor limits T-cell metabolism, leading to the dampened glycolytic capacity, mTOR activity, and IFN-γ production, representing the adaptation of resistance to the MSI-induced immunoreactive microenvironment and thereby allowing tumor progression. Due to the inhibition of TIL metabolism, the insignificant change of SUV_{mean} in $HI_{60\%}$ can be explanted. Checkpoint blockade antibodies against PD-1, PD-L1, and CTLA-4 can restore glycolysis, IFN-γ production, and immune responses in T cells (36, 40) and lead to an insignificant decrease of SUV_{mean} in MSI-H solid tumors in the early stage of immunotherapy.

Mucins are highly O-glycosylated glycoproteins that are essential for a variety of biological processes. Tumor growth results in an unfavorable microenvironment; however, mucins help to evade acidity, hypoxia, and other inhospitable conditions that block drug delivery and promote cancer progression. Mucin is classified into more than 20 subtypes, and the functions are not fully understood (41). MUC2 and MUC5AC mucins produced by colonic goblet cells tend to overexpress in mucinous CRC and MSI-H CRC (42). The EGFR pathway substantially leads to the formation of CRC with the mucinous component, regardless of the percentage (43). Additionally, the mutation rate of RAS/RAF/MAPK and PI3K/AKT pathways in mucinous adenocarcinoma (with more than 50% of mucinous component) is higher than that in non-mucinous adenocarcinoma (42). Our study revealed a higher $HI_{30\%}$ in CRC with a mucinous component than in CRC without a mucinous component. Therefore, ^{18}F-FDG PET/CT may contribute to detect the existence of a mucinous component in CRC and help to predict MSI of CRC.

Multivariate logistic regression analysis demonstrated that Z-$HI_{60\%}$ and mucinous component were independent risk factors of MSI in stage I–III CRC. These results indicate that more attention should be given to heterogeneity of tumors in the early stage. MSI-H in CRC is associated with pathological features such as mucinous carcinoma, proximal colon, poorly differentiation, lymphatic invasion, tumor staging, tumor size, KRAS mutation, and BRAFV600E mutation (2, 6); some results of our study are consistent with these findings. CRC with MSI-H more frequently appears in stage II cases (approximately 20%) compared with stage III (approximately 12%) and is relatively uncommon among stage IV CRC (around 4%) (6). Compared with pMMR/MSI tumors, stage I–III CRC with MSI-H generally have a better prognosis. Stage IV CRC has significant heterogeneity compared

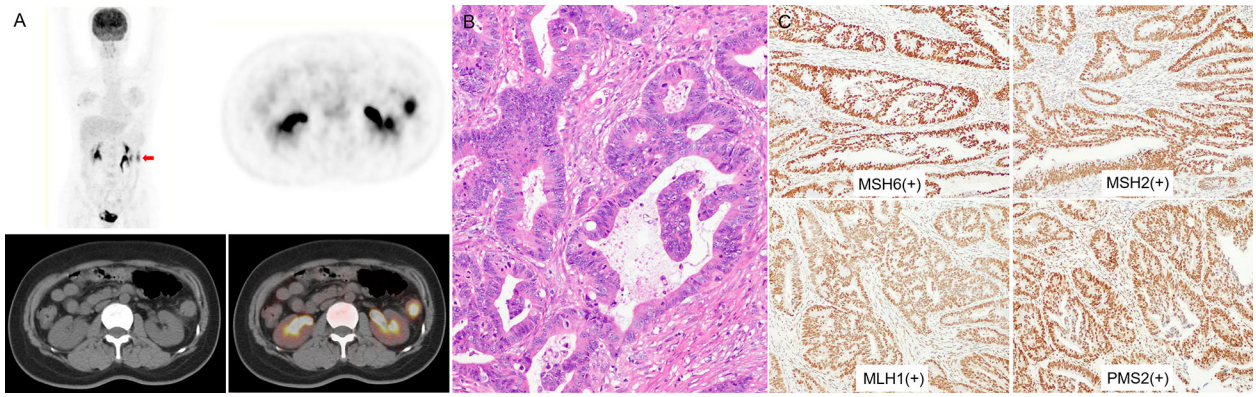

FIGURE 4
(A) a 48-year-old woman with left colon cancer. ^{18}F-FDG PET/CT showed hypermetabolism in the descending colon (arrow; SUV_{max} 9.86; $HI_{60\%}$ 1.38). **(B)** The pathological diagnosis was moderately differentiated CRC, without mucinous component. **(C)** IHC analysis results for MMR proteins were MSH6 (+), MSH2(+), MLH1(+), and PMS2(+), indicating MSS.

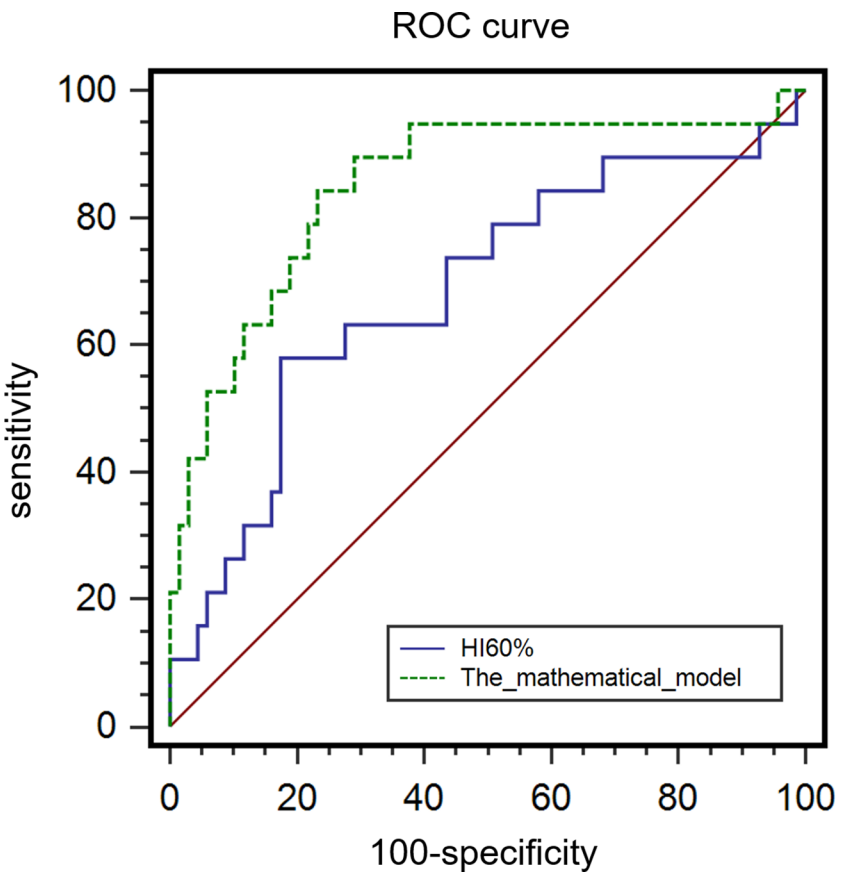

FIGURE 5
ROC curve for $HI_{60\%}$ and the mathematical model in predicting MSI.

with stage I–III CRC, especially between the metastasis and primary tumors (35). The assessment of M staging is one of the most obvious advantages of PET/CT examination. Early detection of intratumoral heterogeneity may be helpful for the formulation of clinical treatment decisions; to avoid the influence of the differences of intertumoral heterogeneity, we selected stage I–III CRC into our research.

The proportion of MSI-H in our study (21.6%) was higher than that in epidemiological reports (12%–15%), which may be because MSI-H CRC is more common in hypermetabolic CRC and makes it easier to be found by PET/CT. In addition, our research object was stage I–III CRC, while MSI-H CRC accounts for only 4% of stage IV CRC (6), which implied that many MSS CRC patients were not included in this study. Although we had built a mathematical model, the limitations of our study include the limited number of cases and the absence of a validation cohort to support, and thus further data validation is required. As a retrospective study, selective bias was inevitable. In our research, imaging data were obtained from two different equipment. While monthly quality control was routinely performed and the same workstation was used, there may still be some uncontrollable differences in the measurement of metabolic parameters by the two devices. Finally, our research was based on a single center, and therefore data from more centers need to be included to validate the utility of IMH and conventional metabolic parameters for predicting MSI in patients with CRC.

TABLE 4 PET/CT for predicting MSI.

	Sensitivity	Specificity	AUC	Stage (I–IV)	Sample size (MSI-H/MSS)	Location
$HI_{60\%}$ our model	0.579 0.842	0.826 0.768	0.658 0.850	I–III	88 (19/69)	Colorectal
Li's model (22)	0.833	0.763	0.828	I–IV	173 (13/160)	Colorectal
Liu's result (23)	0.929	0.667	0.805	I–IV	44 (14/30)	Colorectal
Song's result (39)	0.523	0.766	0.633	II–IV	420 (44/376)	Colorectal

Related parameters: our model: $HI_{60\%}$ and mucinous component; Li's model: CEA, one PET feature (wavelet-LHH_firstorder_Skewness_PET) and one CT feature (wavelet-HHL_firstorder_RootMeanSquared_CT); Liu's result: $MTV_{50\%}$; Song's result: age, primary lesion located, and $MTV_{40\%}$.

Conclusion

This study not only demonstrated that MSI-H CRCs have a higher tumor metabolic burden than MSS CRCs but also revealed a higher IMH in MSI-H CRCs compared with MSS CRCs. The $HI_{60\%}$ derived from ^{18}F-FDG PET/CT and mucinous component were the independent risk factors for MSI in CRC. The mathematical model from $HI_{60\%}$+ mucinous component demonstrated the highest predictive performance. PET/CT is a non-invasive approach to evaluate MSI and the mucinous component in CRC and will help in guiding immunotherapy in CRC patients.

Data availability statement

The raw data supporting the conclusions of this article will be made available by the authors, without undue reservation.

Ethics statement

The studies involving human participants were reviewed and approved by the Institutional Review Board of Union Hospital, Tongji Medical College, Huazhong University of Science and Technology. Written informed consent from the participants' legal guardian/next of kin was not required to participate in this study in accordance with the national legislation and the institutional requirements. Patient consent was waived due to the retrospective design.

Author contributions

Conceptualization, LZ, YD, and WC; formal analysis, WC; investigation, YL, YQD, and HC; resources, XL, JF, WC, and FH.; writing—original draft preparation, LZ; writing—review and editing, LZ, YL, YQD, and HC; funding acquisition, WC. All authors contributed to the article and approved the submitted version.

Funding

This research was funded by National Key R&D Program of China, grant mumber 2017YFC0113302, and thanks to the Open Foundation of Hubei Provincial Key Laboratory of Molecular Imaging, grant number 2021fzyx0013.

Conflict of interest

The authors declare that the research was conducted in the absence of any commercial or financial relationships that could be construed as a potential conflict of interest.

Publisher's note

All claims expressed in this article are solely those of the authors and do not necessarily represent those of their affiliated organizations, or those of the publisher, the editors and the reviewers. Any product that may be evaluated in this article, or claim that may be made by its manufacturer, is not guaranteed or endorsed by the publisher.

Supplementary material

The Supplementary Material for this article can be found online at: https://www.frontiersin.org/articles/10.3389/fonc.2023.1065744/full#supplementary-material

References

1. Sung H, Ferlay J, Siegel RL, Laversanne M, Soerjomataram I, Jemal A, et al. Global cancer statistics 2020: GLOBOCAN estimates of incidence and mortality worldwide for 36 cancers in 185 countries. *CA Cancer J Clin* (2021) 71(3):209–49. doi: 10.3322/caac.21660

2. Cohen R, Pudlarz T, Delattre JF, Colle R, André T. Molecular targets for the treatment of metastatic colorectal cancer. *Cancers (Basel)* (2020) 12(9):2350. doi: 10.3390/cancers12092350

3. de Vicente JC, Rodríguez-Santamarta T, Rodrigo JP, Blanco-Lorenzo V, Allonca E, García-Pedrero JM. PD-L1 expression in tumor cells is an independent unfavorable prognostic factor in oral squamous cell carcinoma. *Cancer Epidemiol Biomarkers Prev* (2019) 28(3):546–54. doi: 10.1158/1055-9965.EPI-18-0779

4. Lemery S, Keegan P, Pazdur R. First FDA approval agnostic of cancer site - when a biomarker defines the indication. *N Engl J Med* (2017) 377(15):1409–12. doi: 10.1056/NEJMp1709968

5. Bonneville R, Krook MA, Kautto EA, Miya J, Wing MR, Chen HZ, et al. Landscape of microsatellite instability across 39 cancer types. *JCO Precis Oncol* (2017) 17:73. doi: 10.1200/PO.17.00073

6. Kawakami H, Zaanan A, Sinicrope FA. Microsatellite instability testing and its role in the management of colorectal cancer. *Curr Treat Options Oncol* (2015) 16(7):30. doi: 10.1007/s11864-015-0348-2

7. Jover R, Zapater P, Castells A, Llor X, Andreu M, Cubiella J, et al. Gastrointestinal oncology group of the spanish gastroenterological association. the efficacy of adjuvant chemotherapy with 5-fluorouracil in colorectal cancer depends on the mismatch repair status. *Eur J Cancer* (2009) 45(3):365–73. doi: 10.1016/j.ejca.2008.07.016

8. Benatti P, Gafà R, Barana D, Marino M, Scarselli A, Pedroni M, et al. Microsatellite instability and colorectal cancer prognosis. *Clin Cancer Res* (2005) 11(23):8332–40. doi: 10.1158/1078-0432.CCR-05-1030

9. Yoon HH, Shi Q, Heying EN, Muranyi A, Bredno J, Ough F, et al. Intertumoral heterogeneity of CD3+ and CD8+ T-cell densities in the microenvironment of DNA mismatch-repair-deficient colon cancers: Implications for prognosis. *Clin Cancer Res* (2019) 25(1):125–33. doi: 10.1158/1078-0432.CCR-18-1984

10. Le DT, Uram JN, Wang H, Bartlett BR, Kemberling H, Eyring AD, et al. PD-1 blockade in tumors with mismatch-repair deficiency. *N Engl J Med* (2015) 372(26):2509–20. doi: 10.1056/NEJMoa1500596

11. Le DT, Durham JN, Smith KN, Wang H, Bartlett BR, Aulakh LK, et al. Mismatch repair deficiency predicts response of solid tumors to PD-1 blockade. *Science* (2017) 357 (6349):409–13. doi: 10.1126/science.aan6733

12. Sagaert X, Vanstapel A, Verbeek S. Tumor heterogeneity in colorectal cancer: What do we know so far? *Pathobiol* (2018) 85(1-2):72–84. doi: 10.1159/000486721

13. Möller K, Blessin NC, Höflmayer D, Büscheck F, Luebke AM, Kluth M, et al. High density of cytotoxic T-lymphocytes is linked to tumoral PD-L1 expression regardless of the mismatch repair status in colorectal cancer. *Acta Oncol* (2021) 60(9):1210–7. doi: 10.1080/0284186X.2021.1933585

14. He P, Zou Y, Qiu J, Yang T, Peng L, Zhang X. Pretreatment ^{18}F-FDG PET/CT imaging predicts the KRAS/NRAS/BRAF gene mutational status in colorectal cancer. *J Oncol* (2021) 18:6687291. doi: 10.1155/2021/6687291

15. Shamim SA, Kumar R, Shandal V, Halanaik D, Kumar G, Bal CS, et al. FDG PET/CT evaluation of treatment response in patients with recurrent colorectal cancer. *Clin Nucl Med* (2011) 36(1):11–6. doi: 10.1097/RLU.0b013e3181feeb48

16. Monteil J, Le Brun-Ly V, Cachin F, Zasadny X, Seitz JF, Mundler O, et al. Comparison of ^{18}FDG-PET/CT and conventional follow-up methods in colorectal cancer: A randomised prospective study. *Dig Liver Dis* (2021) 53(2):231–7. doi: 10.1016/j.dld.2020.10.012

17. Yang Z, Liu Z. The efficacy of ^{18}F-FDG PET/CT-based diagnostic model in the diagnosis of colorectal cancer regional lymph node metastasis. *Saudi J Biol Sci* (2020) 27 (3):805–11. doi: 10.1016/j.sjbs.2019.12.017

18. Wu W, Liu Y, Zeng S, Han Y, Shen H. Intratumor heterogeneity: the hidden barrier to immunotherapy against MSI tumors from the perspective of IFN-γ signaling and tumor-infiltrating lymphocytes. *J Hematol Oncol* (2021) 14(1):160. doi: 10.1186/s13045-021-01166-3

19. Liu G, Yin H, Cheng X, Wang Y, Hu Y, Liu T, et al. Intra-tumor metabolic heterogeneity of gastric cancer on ^{18}F-FDG PETCT indicates patient survival outcomes. *Clin Exp Med* (2021) 21(1):129–38. doi: 10.1007/s10238-020-00659-8

20. Lee M, Lee H, Cheon GJ, Kim HS, Chung HH, Kim JW, et al. Prognostic value of preoperative intratumoral FDG uptake heterogeneity in patients with epithelial ovarian cancer. *Eur Radiol* (2017) 27(1):16–23. doi: 10.1007/s00330-016-4368-5

21. Kimura M, Kato I, Ishibashi K, Shibata A, Nishiwaki S, Fukumura M, et al. The prognostic significance of intratumoral heterogeneity of ^{18}F-FDG uptake in patients with oral cavity squamous cell carcinoma. *Eur J Radiol* (2019) 114:99–104. doi: 10.1016/j.ejrad.2019.03.004

22. Li J, Yang Z, Xin B, Hao Y, Wang L, Song S, et al. Quantitative prediction of microsatellite instability in colorectal cancer with preoperative PET/CT-based radiomics. *Front Oncol* (2021) 11:702055. doi: 10.3389/fonc.2021.702055

23. Liu H, Ye Z, Yang T, Xie H, Duan T, Li M, et al. Predictive value of metabolic parameters derived from ^{18}F-FDG PET/CT for microsatellite instability in patients with colorectal carcinoma. *Front Immunol* (2021) 12:724464. doi: 10.3389/fimmu.2021.724464

24. Wang L, Chen Y, Tang K, Lin J, Zhang H. The value of 18F-FDG PET/CT mathematical prediction model in diagnosis of solitary pulmonary nodules. *BioMed Res Int* (2018) 2018:9453967. doi: 10.1155/2018/9453967

25. Warburg O. On the origin of cancer cells. *Science* (1956) 123(3191):309–14. doi: 10.1126/science.123.3191.309

26. Koppenol WH, Bounds PL, Dang CV. Otto Warburg's contributions to current concepts of cancer metabolism. *Nat Rev Cancer* (2011) 11(5):325–37. doi: 10.1038/nrc3038

27. Shen C, Xuan B, Yan T, Ma Y, Xu P, Tian X, et al. m6A-dependent glycolysis enhances colorectal cancer progression. *Mol Cancer* (2020) 19(1):72. doi: 10.1186/s12943-020-01190-w

28. Tang J, Yan T, Bao Y, Shen C, Yu C, Zhu X, et al. LncRNA GLCC1 promotes colorectal carcinogenesis and glucose metabolism by stabilizing c-myc. *Nat Commun* (2019) 10(1):3499. doi: 10.1038/s41467-019-11447-8

29. Kasprzak A. Insulin-like growth factor 1 (IGF-1) signaling in glucose metabolism in colorectal cancer. *Int J Mol Sci* (2021) 22(12):6434. doi: 10.3390/ijms22126434

30. Hwang SH, Jung M, Jeong YH, Jo K, Kim S, Wang J, et al. Prognostic value of metabolic tumor volume and total lesion glycolysis on preoperative ^{18}F-FDG PET/CT in patients with localized primary gastrointestinal stromal tumors. *Cancer Metab* (2021) 9 (1):8. doi: 10.1186/s40170-021-00244-x

31. Fonti R, Conson M, Del Vecchio S. PET/CT in radiation oncology. *Semin Oncol* (2019) 46(3):202–9. doi: 10.1053/j.seminoncol.2019.07.001

32. Haghighat Jahromi A, Barkauskas DA, Zabel M, Goodman AM, Frampton G, Nikanjam M, et al. Relationship between tumor mutational burden and maximum standardized uptake value in 2-[^{18}F]FDG PET (positron emission tomography) scan in cancer patients. *EJNMMI Res* (2020) 10(1):150. doi: 10.1186/s13550-020-00732-z

33. Zhao Y, Liu C, Zhang Y, Gong C, Li Y, Xie Y, et al. Prognostic value of tumor heterogeneity on ^{18}F-FDG PET/CT in HR+HER2- metastatic breast cancer patients receiving 500 mg fulvestrant: a retrospective study. *Sci Rep* (2018) 8(1):14458. doi: 10.1038/s41598-018-32745-z

34. Martin-Gonzalez P, de Mariscal EG, Martino ME, Gordaliza PM, Peligros I, Carreras JL, et al. Association of visual and quantitative heterogeneity of 18F-FDG PET images with treatment response in locally advanced rectal cancer: A feasibility study. *PloS One* (2020) 15(11):e0242597. doi: 10.1371/journal.pone.0242597

35. Li C, Sun YD, Yu GY, Cui JR, Lou Z, Zhang H, et al. Integrated omics of metastatic colorectal cancer. *Cancer Cell* (2020) 38(5):734–747.e9. doi: 10.1016/j.ccell.2020.08.002

36. Chang CH, Qiu J, O'Sullivan D, Buck MD, Noguchi T, Curtis JD, et al. Metabolic competition in the tumor microenvironment is a driver of cancer progression. *Cell* (2015) 162(6):1229–41. doi: 10.1016/j.cell.2015.08.016

37. Yang Z, Shi Q, Zhang Y, Pan H, Yao Z, Hu S, et al. Pretreatment (^{18})F-FDG uptake heterogeneity can predict survival in patients with locally advanced nasopharyngeal carcinoma–a retrospective study. *Radiat Oncol* (2015) 10:4. doi: 10.1186/s13014-014-0268-5

38. Kim YI, Kim YJ, Paeng JC, Cheon GJ, Lee DS, Chung JK, et al. Heterogeneity index evaluated by slope of linear regression on ^{18}F-FDG PET/CT as a prognostic marker for predicting tumor recurrence in pancreatic ductal adenocarcinoma. *Eur J Nucl Med Mol Imaging* (2017) 44(12):1995–2003. doi: 10.1007/s00259-017-3755-8

39. Song J, Li Z, Yang L, Wei M, Yang Z, Wang X. Metabolic activity *via* ^{18}F-FDG PET/CT is predictive of microsatellite instability status in colorectal cancer. *BMC Cancer* (2022) 22(1):808. doi: 10.1186/s12885-022-09871-z

40. Shao Q, Wang L, Yuan M, Jin X, Chen Z, Wu C. TIGIT induces (CD3+) T cell dysfunction in colorectal cancer by inhibiting glucose metabolism. *Front Immunol* (2021) 12:688961. doi: 10.3389/fimmu.2021.688961

41. Wi DH, Cha JH, Jung YS. Mucin in cancer: a stealth cloak for cancer cells. *BMB Rep* (2021) 54(7):344–55. doi: 10.5483/BMBRep.2021.54.7.064

42. Hugen N, Simons M, Halilović A, van der Post RS, Bogers AJ, Marijnissen-van Zanten MA, et al. The molecular background of mucinous carcinoma beyond MUC2. *J Pathol Clin Res* (2014) 1(1):3–17. doi: 10.1002/cjp2.1

43. Li X, Sun K, Liao X, Gao H, Zhu H, Xu R. Colorectal carcinomas with mucinous differentiation are associated with high frequent mutation of KRAS or BRAF mutations, irrespective of quantity of mucinous component. *BMC Cancer* (2020) 20(1):400. doi: 10.1186/s12885-020-06913-2

Frontiers in Oncology

Advances knowledge of carcinogenesis and tumor progression for better treatment and management

The third most-cited oncology journal, which highlights research in carcinogenesis and tumor progression, bridging the gap between basic research and applications to imrpove diagnosis, therapeutics and management strategies.

Discover the latest Research Topics

See more →

Frontiers

Avenue du Tribunal-Fédéral 34
1005 Lausanne, Switzerland
frontiersin.org

Contact us

+41 (0)21 510 17 00
frontiersin.org/about/contact